

**Groundwater Hydrology and Modelling of the
Jemalong and Lake Cowal Aquifer Systems,
Lachlan Catchment, NSW**

Rubenito M. Lampayan

June 2001

**A thesis submitted for the degree of Doctor of Philosophy of
The Australian National University**

ACKNOWLEDGMENTS

DECLARATION

I would like to sincerely thank the following people and organizations for their invaluable contributions and for strong support during the course of my PhD.

My former official supervisor Dr Ferdinand (Fido) Gonzalez, for his guidance and support throughout the course of my study. Fido continued to be my mentor until the submission of

This thesis contains no material that has been accepted for the award of any other degree or diploma in any university or institution and, to the best of the author's knowledge and belief, contains no material previously written or published by any other person except where due reference is made in the text.

All staff and fellow students in CREB for making my life enjoyable in CREB, especially to the Director, Professor Robert Warren and former Director, Professor Henry Cox for their support. Valde Santa, Mark Greenway, Phil Genova, Allan Maruya and Kirby Mackie for their administrative support, current and former PhD students Nina Pascual, Jane Magina, Erlinda Lacerda, Dennis Nolasco, Robin Connor, Ross Lumbao, Andre Lopez, Caribart Wolfgang, Wendy Manik, Luchita Nolasco, Phil Gibbons, Sir William, Lino Pardo and others for the friendship and support.

Members of the Club of ANU Filipino Students and to all members of the ANU Filipino Community, especially the members of Association of Filipino Students (AFS), Philippine Cultural Society (PCS), Philippine-Australian Association (PAA), and Filipino Student Group (FSG).

My special friends Peter and Elizabeth van der Horst, Felice Dumlao, Jerson Aguilan, Mags Yasin, Ian McLean, Nita Mediano, Dedee Gonzalez, Yvonne Manalo, Eulene Tapan, Sarah Doreana, and the Family, 1997 Filipino Interns especially the late Mrs. Vi Chato, May Dama, Mel Pacifico and Pope Valera for their friendship.

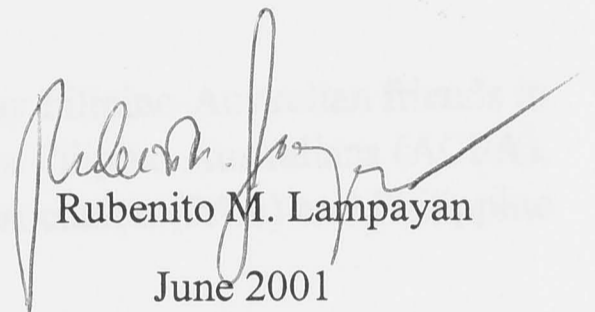
The Australian Government through AusAID for providing me an Australian Development Cooperation Scholarship (ADCOS) to pursue my PhD at ANU.

The International Rice Research Institute (IRRI) in the Philippines for granting my study leave to do my PhD at ANU. Thanks to my former IRRI supervisor Dr Sergio Angeles and my current IRRI supervisor Dr Ben Bonanza for their support and encouragement, my current and former colleagues at the Water Science Section especially Domingo Tabala, Leo Ferrero, Licio Camalitan, Perito Capellan, Lizard Lierra, Mary Susan, Betty Calumpang and Anido Balang for their encouragement.

My research work was also supported by the Department of Land and Water Conservation (DLWC) and Jernidang Irigapan Ltd. Special appreciation goes to the following individuals: Greg Bratton at DLWC, Dunbo Office; Martin O'Hanrahan, Anahane Galat and Ken Brennan at DLWC, Perth Office; Gail McGrath, Andrew Glavin and Neil Hamilton at the Jernidang Irigapan Ltd in Perth.

The DLWC Water Management, Field and the Water Research Foundation of Australia provided financial assistance for completion of my research work.

Special thanks to my parents, brother and sisters for their prayers, trust and love, and to Mary Reyes for her love, prayers, support and inspiration. Finally, thanks to my beloved Lord Jesus Christ, for His blessings and grace, and for giving me wisdom to bravely pursue this work.



Rubenito M. Lampayan
June 2001

ACKNOWLEDGMENTS

I would like to sincerely thank the following people and organisations for their invaluable contributions and for strong support during the course of my PhD:

- My former official supervisor Dr Fereidoun (Fred) Ghassemi, for his guidance and support throughout the course of my study. Fred continued to be my mentor until the submission of this thesis.
- My supervisor Professor Ian White for his guidance, support and for taking over as my formal supervisor after Fred's retirement. My other supervisor Professor Tony Jakeman for his support and assistance.
- All staff and fellow students in CRES for making my life enjoyable in CRES, especially to the Director, Professor Robert Wasson and former Director, Professor Henry Nix for their support; Valda Semets, Mark Greenway, Phil Greaves, Alan Martyn and Kathy Hicks for their administrative support; current and former PhD students Nina Pangahas, Jane Mogina, Rebecca Letcher, Donna Nunnan, Robin Connor, Ross Lambie, Andre Zerger, Carolann Wolfgang, Wendy Merrit, Lachlan Newham, Phil Gibbons, Su Wildriver, Jason Evans and others for the friendship and support.
- Members of the Club of ANU Filipino Students; and to all my Filipino-Australian friends in Canberra, especially the members of Association of Canberra Filipino-Australians (ACFA), Philippine Cultural Society (PCS), Philippine-Australian Association (PAA) and Philippine Studies Group (PSG).
- My special friends: Peter and Elizabeth van den Heuvel, Feding Donaghue, Burton Aggabao, Mayo Yanilla, Ian McLean, Nilo Mordeno, Dedette Gonzales, Vanessa Manalo, Fatchie Tepora, Sarah Bernasor, and my January 1997 Filipino batchmates especially Au dela Rea, Vi Chato, May Batas, Med Panlilio and Peps Veloria for their friendship.
- The Australian Government through AusAID for providing me an Australian Development Cooperation Scholarship (ADCOS) to pursue my PhD at ANU.
- The International Rice Research Institute (IRRI) in the Philippines for granting my study leave to do my PhD at ANU. Thanks to my former IRRI supervisor Dr Sadiq Bhuiyan and my current IRRI supervisor Dr Bas Bouman for their support and encouragement, my current and former colleagues at the Water Science Section especially Doming Tabbal, Lou Herrero, Lucio Caramihan, Ferdie Corquera, Lizzel Llorca, Mary Burac, Romy Cabangon and Annie Boling for their encouragement.
- My research work was also supported by the Department of Land and Water Conservation (DLWC) and Jemalong Irrigation Ltd. Special appreciation goes to the following individuals: Greg Brereton at DLWC, Dubbo Office; Martin O'Rourke, Antoinette Carter and Rei Breumer at DLWC, Forbes Office; Sally McGrath, Andrew Glasson and Ned Hamilton at the Jemalong Irrigation Ltd in Forbes.

The DLWC Water Management Fund and the Water Research Foundation of Australia provided financial assistance for completion of this research work.

Special thanks to my parents, brothers and sisters for their prayers, trust and love, and to Daisy Reyes for her love, prayers, support and inspiration. Finally, thanks to my Saviour and Lord, Jesus Christ, for His blessings and graces, and for giving me wisdom to humbly finish this work.

DEDICATION

Water resource management in NSW has undergone a rapid transition in recent years. The State has been set on a course towards sustainable use of all water resources, including groundwater with explicit provision of water for environment. The capacity of surface water in most major rivers has reached its limit and increasing pressure is being placed on the State's aquifers. In 1994 the Council of Australian Governments developed a National Water Reform Agreement which provides a strategic national framework for water reform. As part of this strategy the States give a commitment to implement management policies for natural resources based on Ecologically Sustainable Development principles.

The Jerrilder and Wyllie Plains Irrigation District is a critical one in the Lachlan catchment, New South Wales. The area was first developed in the 1940's. While various natural resource management issues exist in the area, groundwater level and water sustainability is considered the most pressing. The irrigation district and Lake Copal area are characterised with rising water table and salinisation. Management of these areas and their adjacent in proximity of the aquifer and surface water requires that the identification of all processes governing the groundwater dynamics and salinisation be clearly identified.

The present study aims to review the state of knowledge on water resources and related land resources of the Lachlan catchment. It also aims to investigate the groundwater systems and salinisation processes in the Jerrilder and Wyllie Plains Irrigation District, Lake Copal and Broad Creek catchment and to profile potential areas of salinisation. Specific objectives are:

1. Review the existing information on land and water resources of the Lachlan catchment and the study area.
2. Investigate the hydrogeological features of the aquifer system in the study area and to identify the recharge and discharge areas.
3. Investigate the interaction of the aquifer system with the Lake Copal, Lake Copal, Broad Creek and the irrigation system.
4. Investigate the spatial and temporal distribution of ground water salinity.
5. Develop and calibrate a numerical model of the aquifer system.
6. Use the calibrated model to examine water table fluctuations between aquifer, surface water and the irrigation system and to quantify the water balance of the groundwater system.
7. Develop management strategies and options in order to minimise the risk of salinisation.

The study identifies some water changes observed in the study area over the past century. The study also identifies some water changes observed in the study area over the past century. The study also identifies some water changes observed in the study area over the past century. The study also identifies some water changes observed in the study area over the past century.

This work is dedicated to my family particularly:

My parents Papa Tiyong and Mama Nading

My brothers Kuya Jelly, Manong Nelly and Jun

And my sisters Ate Vic, Susan and Arlene

ABSTRACT

Water resource management in NSW has undergone a rapid transition in recent years. The State has been set on a course towards sustainable use of all water resources, including groundwater with explicit provision of water for environment. The capacity of surface water to meet usage needs has reached its limit and increasing pressure is being placed in the State's aquifers. In 1994 the Council of Australian Governments developed a National Water Reform Agreement which provides a strategic national framework for water reform. As part of this strategy the States gave a commitment to implement management policies for natural resources based on Ecologically Sustainable Development principles.

The Jemalong and Wyldes Plains Irrigation District is a critical area in the Lachlan catchment, New South Wales. The area was first developed in the 1940's. While various natural resource management issues exist in the area, increasing land and water salinisation is considered the most pressing. The irrigation district and Lake Cowal area are threatened with rising watertables and salinisation. Management of these areas and land salinisation occurring on its western part requires that the contribution of all processes impacting on groundwater dynamics and salinisation be clearly identified.

The present study aims to review the state of knowledge on water resources and related land resources of the Lachlan catchment. It also aims to investigate the groundwater systems and salinisation processes in the Jemalong and Wyldes Plains Irrigation District, Lake Cowal and Bland Creek catchment and to predict potential areas of salinisation. Specific objectives are to:

- Review the existing information on land and water resources of the Lachlan catchment and the study area;
- Investigate the hydrogeological features of the aquifer system in the study area, and to identify the recharge and discharge areas;
- Investigate the interaction of the aquifer system with the Lachlan River, lake Cowal, Bland Creek and the irrigation system;
- Investigate the spatial and temporal distribution of groundwater salinity;
- Develop and calibrate a numerical model of the aquifer systems;
- Use the calibrated model to examine watertable rise, interactions between aquifers, surface water and the irrigation system and to quantify various components of the groundwater balance;
- Develop management strategies and options in order to minimise the risk of salinisation.

The study identified some major changes occurring in the Lachlan catchment over the past century. The seasonality of streamflow has been significantly altered due to river regulation and water abstraction. The volume of water reaching the lower Lachlan has been greatly reduced. Water quality is poor and stream salinity levels in the Lachlan River are increasing. The incidence of dryland salinity is also increasing and groundwater levels are generally rising.

Groundwater investigations in the study area indicated an average rise of 2.5 m of groundwater level in the irrigation district between March 1969 and October 1990. Periodic major floods have a clear and enormous influence of watertable heights. A major flood in 1990 resulted in the

watertable in the irrigation district rising close to the ground surface. After the 1990 flood, the groundwater level declined up to 2 m between October 1990 and July 1997. However, near Lake Cowal, the watertable has continued to rise. Groundwater salinity is high and not suitable for consumptive use of surface and groundwater.

Groundwater modelling in the study area has provided a better understanding of the aquifer's behaviour and its interaction with the irrigation system and surface water resources. A numerical three-dimensional groundwater flow model has been developed for the area using Visual MODFLOW. The modelled domain which extends approximately 45 km from east to west and 66 km from north to south covers an area of about 170,000 ha and consists of 4 layers. Horizontally, the aquifer system has been discretised by a uniform grid of 500 m x 500 m and in vertical direction in such a way to represent 4 layers of the aquifer system. The model has been calibrated in steady-state for April 1988, and in transient mode for the period of May 1988 to July 1997 with 111 monthly timesteps.

Calibration of the model has revealed unsuspected leakage from the lower aquifer into the fractured basement rocks. These leakages have a significant contribution to the overall groundwater balance of the area and explain why the rate of watertable rise and land salinisation has been relatively low in spite of the long history of irrigation in the area since 1944. The calibrated model indicates that heavy rainfall which caused flooding in the irrigation district. This is a major source of recharge in the area, accounting for about 72% of the total annual volume of recharge during the period of calibration. Irrigation water constituted 16% ($2.2 \times 10^6 \text{ m}^3 \text{ yr}^{-1}$) of the total volume of recharge, and 80% of this has been recharged around the Warroo Channel. The constant head boundary along the Lachlan River provided an average annual inflow from the upper reach of the river of about $4.2 \times 10^6 \text{ m}^3$. The volume of outflow from the aquifer into the lower reach of the Lachlan river is about $3.0 \times 10^6 \text{ m}^3$.

Because groundwater is saline in a large part of the area, pumping is not a management option due to the fact that there are no opportunities to dispose saline groundwater. Even conjunctive use of surface and groundwater in the narrow strip close to the river is not a feasible option because in the long term, it will cause northward as well as upward movement of saline groundwater. Improved irrigation efficiency and a partial area tree plantation strategy provide better groundwater management options. The model predicted that by sealing of the Warroo Channel watertable will drop by more than 1 m in this area. Another simulation indicated that 20 percent tree plantation above Dog Kennel Hill to partially intercept groundwater flow towards Bogandillon area will lower the watertable by over 0.5 m in the salt affected areas in Bogandillon creek. Finally, on the southern part of the study area where a continuous watertable rise has been observed, simulation indicated that modest tree planting in three locations will lower watertable depths by more than 1 m. It is concluded that improved irrigation efficiency and partial tree plantation in a small portion of the area will reverse the current trend in watertable rise.

TABLE OF CONTENTS

Declaration	i
Acknowledgments	ii
Dedication	iii
Abstract	iv
Table of Contents	vi
List of Tables	xii
List of Figures	xv
List of Appendices	xxiv
CHAPTER 1 INTRODUCTION	1-1
1.1. Background	1-1
1.2. Importance of the research	1-2
1.3. Objectives and scope of the research	1-3
1.4. Organisation of the thesis	1-3
CHAPTER 2 OVERVIEW OF THE LACHLAN RIVER VALLEY	2-1
2.1. Physiography	2-1
2.2. Socio-economic characteristics	2-1
2.3. Geology	2-2
2.3.1. Consolidated sediments	2-4
2.3.2. Unconsolidated sediments	2-4
2.3.2.1 Lachlan Formation	2-4
2.3.2.2 Cowra Formation	2-5
2.4. Soils	2-5
2.5. Climate	2-6
2.5.1. Rainfall	2-6
2.5.1.1. Rainfall stations and data	2-6
2.5.1.2. Rainfall distribution	2-6
2.5.1.3. Rainfall and southern oscillation index	2-9
2.5.2. Temperature, sunshine duration and wind speeds	2-12
2.5.3. Evaporation	2-16
2.6. Hydrology	2-17
2.6.1. Average runoff	2-17
2.6.2. Stream gauging	2-17
2.6.3. Streamflow characteristics	2-17
2.6.3.1. Annual streamflows	2-17
2.6.3.2. Monthly streamflows	2-20
2.6.4. Flood and drought	2-23
2.6.5. Hydraulic structures	2-24
2.6.5.1. Headwater storage	2-24
2.6.5.2. Diversion weirs	2-25
2.6.5.3. Enroute storages	2-26
2.6.6. Surface water usage	2-26
2.6.7. Surface water quality	2-28
2.6.7.1. Stream salinity	2-28
2.6.7.2. Turbidity, SAR and nutrients	2-35

2.7.	Hydrogeology	2-37
2.7.1.	Exploration and extraction wells	2-37
2.7.2.	Test drilling	2-37
2.7.3.	Characteristics of various aquifer systems	2-38
2.7.4.	Piezometric surface and groundwater trends	2-38
	2.7.4.1. Headwaters	2-38
	2.7.4.2. Young district	2-39
	2.7.4.3. Upper Lachlan	2-39
	2.7.4.4. Lower Lachlan	2-39
2.7.5.	Recharge of the aquifer systems	2-41
2.7.6.	Groundwater availability, extraction and usage	2-42
2.7.7.	Groundwater salinity	2-44
2.8.	Land salinisation	2-45
2.9.	Flora and Fauna	2-45
2.9.1.	Vegetation at the riparian zone	2-45
2.9.2.	Floodplain vegetation	2-45
2.9.3.	Fauna	2-47
2.10.	Wetlands	2-50
2.10.1.	Present condition of the wetlands	2-50
2.10.2.	Water regime and quality in the wetland areas	2-51
2.11.	Provision of environmental flow	2-52
2.11.1.	Contingency allocations	2-52
2.11.2.	Sharing of unregulated flows	2-53
2.11.3.	Minimum target flows	2-53
2.12.	Land use	2-53
2.13.	Irrigation	

CHAPTER 3 DESCRIPTION OF THE JEMALONG AND BLAND CREEK STUDY AREA **3-1**

3.1.	Location and topographic features	3-1
3.2.	Climate	3-1
3.2.1.	Rainfall	3-1
3.2.2.	Temperature, relative humidity, potential evapotranspiration, solar radiation and wind speed	3-4
3.3.	Soils	3-10
3.3.1.	Soil types	3-12
3.3.2.	Soil-water characteristics	3-14
3.4.	Hydrology	3-14
3.4.1.	Runoff and drainage	3-15
3.4.2.	Stream gauging	3-16
3.4.3.	Streamflow characteristics	3-16
	3.4.3.1. Lachlan River at Jemalong Weir	3-16
	3.4.3.2. Manna Creek, near Lake Nerang Cowal	3-16
	3.4.3.3. Bland Creek at Morangarell	3-16
	3.4.3.4. Bogandillon Creek at Birrack Bridge	3-19
3.4.4.	Surface water quality	3-19

3.4.4.1.	Irrigation water	3-19
3.4.4.2.	Bogandillon creek	3-22
3.4.4.3.	Lake Cowal	3-25
3.4.4.4.	Bland creek area	3-25
3.5.	Irrigation	3-25
3.5.1.	Irrigation system facilities	3-26
3.5.2.	System operation	3-26
3.5.3.	Water supply	3-28
3.5.4.	Irrigation system efficiency and losses	3-29
3.6.	Land use	3-31
3.7.	Wetlands	3-31
CHAPTER 4 GEOLOGY		4-1
4.1.	Structural geology	4-1
4.2.	Stratigraphy	4-2
4.2.1.	Consolidated sediments	4-2
4.2.1.1.	Ordovician	4-2
4.2.1.2.	Silurian	4-4
4.2.1.3.	Devonian	4-4
4.2.1.4.	Tertiary	4-4
4.3.	Unconsolidated sediments	4-4
4.3.1.	Geological history and mode of deposition	4-5
4.4.	Geological cross sections	4-5
4.4.1.	Geological cross-section A-A'	4-6
4.4.2.	Geological cross-section B-B'	4-7
4.4.3.	Geological cross-section C-C'	4-9
4.4.4.	Geological cross-section D-D'	4-10
4.4.5.	Geological cross-section E-E'	4-10
4.4.6.	Geological cross-section F-F'	4-11
4.4.7.	Geological cross-section G-G'	4-12
4.4.8.	Geological cross-section H-H'	4-14
4.4.9.	Geological cross-section I-I'	4-15
4.5.	Contour map of the basement	4-15
4.6.	Isopach of the unconsolidated sediments	4-17
4.7.	Local geology of Lake Cowal	4-17
CHAPTER 5 HYDRODYNAMICS		5-1
5.1.	Groundwater environment	5-1
5.2.	Groundwater monitoring system	5-1
5.3.	Watertable aquifer	5-5
5.3.1.	Watertable fluctuations versus rainfall	5-7
5.3.2.	Watertable fluctuations versus Lachlan River stage	5-7
5.3.3.	Watertable elevation	5-7
5.3.4.	Watertable depth below ground surface	5-12
5.3.5.	Watertable rise	5-12
5.3.6.	Recharge-discharge area	5-12
5.4.	Groundwater in sand and gravel lenses	5-16

5.4.1.	Bland creek area	5-16
5.4.2.	Lake Cowal and JWPID area	5-18
5.4.3.	Lachlan area	5-19
5.5.	Hydrodynamic parameters of the aquifer	5-20
CHAPTER 6 GROUNDWATER SALINITY AND CHEMISTRY		6-1
6.1.	Groundwater salinity	6-1
6.1.1.	Salinity of the watertable aquifer	6-2
6.1.2.	Salinity of the sand and gravel lenses	6-6
6.1.3.	Salinity of fractured rock aquifers	6-8
6.2.	Chemical composition of groundwater	6-8
6.2.1.	Chemical composition of groundwater in the Lachlan Formation	6-8
6.2.2.	Chemical composition of groundwater in the Cowra Formation	6-12
6.2.3.	Chemical composition of rainfall and surface water components	6-13
6.2.4.	Major ion-TDS relationship	6-13
6.2.5.	Major ion-chloride relationship	6-13
6.2.6.	Hydrochemical types	6-17
CHAPTER 7 GROUNDWATER FLOW MODELLING AND MODEL SET-UP OF THE STUDY AREA		7-1
7.1.	Introduction	7-1
7.2.	Groundwater models – a review	7-1
7.3.	Model formulation	7-2
7.4.	MODFLOW, Visual MODFLOW, and PEST	7-3
7.5.	Previous modelling exercises in the study area	7-3
7.5.1.	Groundwater model for JWPID	7-3
7.5.2.	Proposed gold mine dewatering project	7-6
7.6.	Groundwater model set-up of the study area	7-6
7.6.1.	Definition of model objectives	7-6
7.6.2.	Characterisation of the aquifer system	7-7
7.6.3.	Geometry of the modelled domain	7-7
7.6.4.	Conceptual model of the aquifer	7-9
7.6.5.	Discretisation of the aquifer system	7-9
7.6.6.	Boundary conditions	7-9
7.6.7.	Initial conditions and simulation period	7-15
7.6.8.	Parameterisation of the aquifer system	7-15
CHAPTER 8 STEADY-STATE CALIBRATION		8-1
8.1.	Introduction	8-1
8.2.	Hydraulic conductivity	8-1
8.2.1.	Calibration of <i>K</i> values using PEST software	8-6
8.3.	Recharge from rainfall and irrigation	8-6
8.4.	Recharge due to flooding	8-8
8.5.	Recharge from channel seepage	8-8
8.6.	Recharge from lakes	8-10
8.7.	Constant head cell boundary	8-11
8.8.	Evapotranspiration	8-11
8.9.	Inflow and outflow across aquifer boundaries	8-11

8.10.	Leakages through the basement's fractures	8-13
8.11.	Drainage of the system by the Gilmore Fault	8-13
8.12.	Results of the steady-state calibration	8-13
	8.12.1. Observed versus computed piezometric heads	8-13
	8.12.2. Vertical distribution of piezometric heads	8-17
	8.12.3. Direction of groundwater flow	8-19
	8.12.4. Groundwater balance	8-19
	8.12.4.1. Inputs	8-19
	8.12.4.2. Outputs	8-23
CHAPTER 9 TRANSIENT CALIBRATION		9-1
9.1.	Introduction	9-1
9.2.	Hydraulic conductivity	9-1
9.3.	Storage coefficients	9-1
9.4.	Recharge due to rainfall and irrigation	9-2
9.5.	Recharge due to flooding	9-2
9.6.	Recharge due to seepage at the Warroo Channel	9-4
9.7.	Constant head cell boundary	9-6
9.8.	Evapotranspiration	9-6
9.9.	Inflow and outflow across aquifer boundaries	9-6
9.10.	Leakages through the basement's fractures	9-7
9.11.	Drainage of the system through Gilmore Fault	9-7
9.12.	Results of the transient simulation	9-7
	9.12.1. Match between measured and computed heads over the period of simulation at selected observation wells	9-7
	9.12.2. Match between measured and computed head contours at three selected stress periods	9-7
	9.12.3. Statistical analysis of the degree of match between the measured and computed heads	9-16
	9.12.4. Groundwater balance	9-16
	9.12.4.1. Inputs	9-16
	9.12.4.2. Outputs	9-21
	9.12.4.3. Change in groundwater storage	9-22
9.13.	General comments on PEST software	9-23
CHAPTER 10 SENSITIVITY ANALYSES		10-1
10.1.	Introduction	10-1
10.2.	Hydraulic conductivity	10-1
10.3.	Storage coefficients	10-6
10.4.	Recharge	10-18
10.5.	Evapotranspiration	10-19
10.6.	ET extinction depth	10-35
10.7.	Summary	10-44

CHAPTER 11	SIMULATION OF MANAGEMENT OPTIONS	11-1
11.1.	Introduction	11-1
11.2.	Model scenarios	11-1
11.3.	The 'average/no change' scenario	11-2
	11.3.1. Data used and assumptions	11-2
	11.3.2. Results and discussion	11-2
11.4.	Reduced recharge by improving irrigation and drainage efficiency	11-7
	11.4.1. Data used and assumptions	11-7
	11.4.2. Results and discussion	11-7
	11.4.2.1. Option A	11-7
	11.4.2.2. Option B	11-12
	11.4.2.3. Option C	11-12
11.5.	Partial area tree-planting strategy	11-12
	11.5.1. Results and discussion	11-22
	11.5.1.1. Tree plantation above Dog Kennel Hill (Area A)	11-22
	11.5.1.2. Tree-planting at the southern part of the study area (Areas B1, B2 and B3)	11-27
11.6.	Summary	11-28
CHAPTER 12	SUMMARY AND CONCLUSIONS	12-1
12.1.	Summary	12-1
	12.1.1. Lachlan River Valley	12-1
	12.1.2. The Jemalong and Bland creek study area	12-2
	12.1.3. Groundwater flow modelling	12-4
12.2.	Conclusions	12-5
12.3.	Future research recommendations	12-5
REFERENCES		13-1

LIST OF TABLES

CHAPTER 2 OVERVIEW OF THE LACHLAN RIVER VALLEY

Table 2.1:	Comparison of the mean annual rainfall between the periods pre-1946 and post 1946 at the selected meteorological stations in the Lachlan River Valley.	2-8
Table 2.2:	Seasonal comparison of rainfall for the periods pre-1946 and post 1946 at five meteorological stations in the Lachlan River Valley.	2-11
Table 2.3:	Mean annual streamflow characteristics for selected stream gauging stations at the Lachlan River.	2-21
Table 2.4:	Dams in the Lachlan Valley.	2-25
Table 2.5:	Water supply schemes serving the Lachlan Valley.	2-27
Table 2.6:	Annual estimated trend in salinity increase at the selected gauging stations along the Lachlan River.	2-35
Table 2.7:	Annual mean water and salt balances (1985-1994) at the selected gauging stations along the Lachlan River Valley.	2-36
Table 2.8:	Groundwater use in GMA 011 from 1986/87 to 1992/93.	2-42
Table 2.9:	Electrical conductivities for selected observation wells in GMA 011.	2-44
Table 2.10:	General status of the State Forests of the Lachlan River downstream of Cowra.	2-48
Table 2.11:	Irrigated crop areas and methods for regulated Lachlan system in 1995/1996 water year.	2-54

CHAPTER 3 DESCRIPTION OF THE JEMALONG AND BLAND CREEK STUDY AREA

Table 3.1:	Changes in rainfall at 13 meteorological stations in the study area.	3-8
Table 3.2:	Soil types of the Land and Water Management Plan Area.	3-10
Table 3.3:	Hydraulic characteristics of floodway (Figure 3.16) soils.	3-14
Table 3.4:	Hydrological characteristics of Lake Cowal.	3-15
Table 3.5:	Available stream gauging stations in the study area.	3-15
Table 3.6:	Ion composition of the irrigation water diverted at Jemalong Weir (1976-1981).	3-21
Table 3.7:	Water quality indices of the irrigation water diversion at Jemalong Weir (1976-1981).	3-22
Table 3.8:	Distribution of water usage along main channels.	3-29
Table 3.9:	Channel diversions, deliveries and losses.	3-30
Table 3.10:	Diversions, deliveries and losses at Cadow/Waroo and Jemalong main channels during 1994/95 water year .	3-30
Table 3.11:	Land use in the dryland and irrigated areas of the Jemalong and Wyldes Plains Irrigation District (JWPID) and the Land and Water Management Plan (LWMP) area in hectares.	3-32
Table 3.12:	Classification of wetland areas in the Jemalong and Wyldes Plains Irrigation District.	3-36

CHAPTER 4 GEOLOGY

Table 4.1:	Stratigraphic units of the study area.	4-2
Table 4.2	Number of bores and wells in the study area (including bores in the basement rocks).	4-6
Table 4.3:	Number of bores and wells in the alluvial part of the study area.	4-6

CHAPTER 5 HYDRODYNAMICS

Table 5.1	Transmissivity values of the selected regional observation wells in the study area.	5-21
-----------	---	------

CHAPTER 6 GROUNDWATER SALINITY AND CHEMISTRY

Table 6.1:	Change of electrical conductivity (EC) values between July 1994 and May 1997 at the selected DLWC piezometers in the Lake Cowal and Lake Nerang Cowal areas.	6-4
Table 6.2:	Groundwater salinity of the upper watertable aquifer at the proposed Lake Cowal Gold Mine.	6-4
Table 6.3:	Concentrations of major ions at different levels of TDS.	6-14

CHAPTER 8 STEADY-STATE CALIBRATION

Table 8.1:	The initial and the calibrated hydraulic conductivity (K) values.	8-4
Table 8.2:	Example of K values estimation at well no. 36523.	8-4
Table 8.3:	Hydraulic conductivity values for upper aquitard or Layer 1.	8-6
Table 8.4:	Initial and calibrated recharge values for the modelled area.	8-8
Table 8.5:	Steady-state groundwater balance of the modelled area.	8-22
Table 8.6:	Total recharge rate at each recharge zone in the modelled domain.	8-23

CHAPTER 9 TRANSIENT CALIBRATION

Table 9.1:	Calibrated storage coefficients	9-2
Table 9.2:	Recharge factors assigned to recharge zones 1 to 8 of the modelled area.	9-4
Table 9.3:	Calibrated recharge at the floodway during flooding events from May 1988 to July 1997.	9-5
Table 9.4:	Statistical indicators of the errors for all timesteps in transient simulation.	9-17

CHAPTER 10 SENSITIVITY ANALYSIS

Table 10.1:	Sensitivity of the average annual groundwater balance due to changes in hydraulic conductivity (K) values for the period May 1988 to July 1997.	10-10
Table 10.2:	Sensitivity of the average annual groundwater balance due to changes in storage coefficient (S) values for the period May 1988 to July 1997.	10-18
Table 10.3:	Sensitivity of the average annual groundwater balance due to changes in recharge for the period May 1988 to July 1997.	10-27
Table 10.4:	Sensitivity of the average annual groundwater balance due to changes in evapotranspiration (ET) rates for the period May 1988 to July 1997.	10-36

Table 10.5: Sensitivity of the average annual groundwater balance due to changes in ET extinction depth for the period May 1988 to July 1997.	10-44
---	-------

CHAPTER 11 SIMULATION OF MANAGEMENT OPTIONS

Table 11.1: Comparison of annual groundwater balance for the transient calibration, and 'average/no change' scenario.	11-6
Table 11.2: Mean annual groundwater balance components under 'average/no change' scenario and options A, B, and C.	11-11
Table 11.3: Assumed rate of groundwater extraction per tree from 1 to 6 years after planting for <i>E. camaldulensis</i> (from Morris and Collopy; and others).	11-21
Table 11.4: Annual groundwater balance under 'average' scenario and alley farming for Plantation area A.	11-21
Table 11.5: Annual groundwater balance components under 'average/no change' scenario and tree-planting strategy (alley farming) at the southern part of the study area (Plantation areas B1, B2 and B3 on Figure 11.13).	11-27

LIST OF FIGURES

CHAPTER 2 OVERVIEW OF THE LACHLAN RIVER VALLEY

Figure 2.1: Murray Darling Drainage Basin sub-catchments.	2-2
Figure 2.2: River network, selected meteorological stations and annual rainfall and evaporation.	2-3
Figure 2.3: Geological cross-sections A-A' and B-B' through Lachlan River Valley.	2-5
Figure 2.4: Annual (bar) and 10-year moving average (line) rainfall at five meteorological stations in the Valley.	2-7
Figure 2.5: Comparison of mean annual rainfall between pre- and post 1946 data.	2-8
Figure 2.6: Mean monthly rainfall at five selected meteorological stations in the Valley.	2-9
Figure 2.7: Monthly comparison of average rainfall between pre-1946 and post 1946 data at 5 stations in the Lachlan Valley.	2-10
Figure 2.8: Comparison of seasonal mean rainfall between pre-1946 and post 1946 data at 5 stations in the Lachlan Valley.	2-10
Figure 2.9: Annual southern oscillation index (SOI) and annual rainfall at five stations in the Lachlan Valley.	2-13
Figure 2.10: Relationship between southern oscillation index and annual rainfall at five stations in the Lachlan Valley.	2-14
Figure 2.11: Monthly mean daily air temperature in the selected at Cowra, Condobolin and Hillston stations.	2-15
Figure 2.12: Mean monthly pan evaporation at the Cowra, Condobolin and Hillston.	2-16
Figure 2.13: Comparison of mean monthly pan evaporation and mean monthly rainfall at Cowra.	2-16
Figure 2.14: Line diagram of the Lachlan River.	2-18
Figure 2.15: Annual streamflow (lines) and rainfall (bars) at the selected gauging stations along the Lachlan River.	2-19
Figure 2.16: Distribution of mean monthly streamflows (1973-1997) at selected gauging stations along the Lachlan River.	2-20
Figure 2.17: Extent of flooding in the Lachlan River Valley.	2-22
Figure 2.18: Areas of flood liable in various parts of the Lachlan River Valley.	2-23
Figure 2.19: Irrigation water use and irrigated area in the regulated Lachlan System, 1983-1996.	2-28
Figure 2.20: Mean annual streamflow, mean daily EC, salt loads and mean daily salt load per volume of streamflow at the selected gauging station along the Lachlan River.	2-29
Figure 2.21: Electrical conductivity, salt load and streamflow at gauging station 412002- Lachlan River at Cowra.	2-31
Figure 2.22: Electrical conductivity, salt load and streamflow at gauging station 412004- Lachlan River at Forbes.	2-32
Figure 2.23: Electrical conductivity, salt load and streamflow at gauging station 412006- Lachlan River at Condobolin.	2-33
Figure 2.24: Electrical conductivity, salt load and streamflow at gauging station 412039- Lachlan River at Hillston.	2-34
Figure 2.25: Subdivision of the Groundwater Management Area (GMA) 011.	2-40

Figure 2.26: Irrigation water use (bars) and irrigated area (line) from high yield bores.	2-41
Figure 2.27: Groundwater salinity in the Lachlan River Valley.	2-43
Figure 2.28: Salinity in the Lachlan River Valley.	2-46
Figure 2.29: Wetlands of the Lachlan River Valley floodplain.	2-49

CHAPTER 3 DESCRIPTION OF THE JEMALONG AND BLAND CREEK STUDY AREA

Figure 3.1: Location of the study area.	3-2
Figure 3.2: Spatial distribution of the long-term mean annual rainfall in the study area.	3-3
Figure 3.3: Annual and mean monthly rainfall at Grenfell Post Office (073014).	3-5
Figure 3.4: Annual and mean monthly rainfall at Greenthorpe (073017).	3-5
Figure 3.5: Annual and mean monthly rainfall at Wombat (073041).	3-5
Figure 3.6: Annual and mean monthly rainfall at Stockinbingal (073036).	3-5
Figure 3.7: Annual and mean monthly rainfall at Temora, Barmedman Road (073037).	3-6
Figure 3.8: Annual and mean monthly rainfall at Temora Agricultural Research Station (073038).	3-6
Figure 3.9: Annual and mean monthly rainfall at Quandialla Post Office (073032).	3-6
Figure 3.10: Annual and mean monthly rainfall at Wyalong Post Office (073054).	3-6
Figure 3.11: Annual and mean monthly rainfall at West Wyalong (050044).	3-7
Figure 3.12: Annual and mean monthly rainfall at Bumbaldry (073100).	3-7
Figure 3.13: Annual and mean monthly rainfall at Caragabal (073008).	3-7
Figure 3.14: Annual and mean monthly rainfall at Warroo (050020).	3-7
Figure 3.15: Monthly potential evapotranspiration (Etp) and solar radiation at JWPID.	3-9
Figure 3.16: Monthly potential evapotranspiration (Etp) and wind speed at JWPID.	3-9
Figure 3.17: Soil classes map of the Land and Water Management Plan (LWMP) area.	3-11
Figure 3.18: Drainage basins and floodway of the Jemalong and Wyldes Plains Irrigation District.	3-13
Figure 3.19: (a) Annual streamflow, (b) mean monthly streamflow, (c) daily streamflow and (d) daily flow duration curve for gauging station 412036 – Lachlan River at Jemalong Weir.	3-17
Figure 3.20: (a) Annual streamflow, (b) mean monthly streamflow, (c) daily streamflow and (d) daily flow duration curve for gauging station 412009 – Manna Creek, near Lake Nerang Cowal.	3-18
Figure 3.21: (a) Annual streamflow, (b) mean monthly streamflow, (c) daily streamflow and (c) daily flow duration curve for gauging station 412103 – Bland Creek (Morangarell).	3-20
Figure 3.22: Daily streamflow for gauging station 412142 – Bogandillon Creek at Birrack Bridge (1993-1996).	3-21
Figure 3.23: Locations of EC gauging stations along the Bogandillon Creek.	3-23
Figure 3.24: Salinity data in the Bogandillon area.	3-24
Figure 3.25: Salinity data at Lake Cowal.	3-25
Figure 3.26: Irrigation supply system of the Jemalong and Wyldes Plains Irrigation Districts.	3-27
Figure 3.27: Historical water deliveries from the Jemalong Weir.	3-28
Figure 3.28: Monthly diversions for the 2 main channels (Cadow/Warroo and Jemalong) for 1994/1995 water year.	3-30

Figure 3.29: Irrigated and non-irrigated areas of the Land and Water Management Plan (LWMP) area.	3-33
Figure 3.30: Land use map of the Land and Water Management Plan (LWMP) area in 1996	3-34
Figure 3.31: Classification of wetlands in the Land and Water Management Plan (LWMP) area.	3-35

CHAPTER 4 GEOLOGY

Figure 4.1: Structural units of New South Wales.	4-1
Figure 4.2: Geological map of the study area and locations of cross-sections.	4-3
Figure 4.3: Geological cross-section A-A'.	4-7
Figure 4.4: Geological cross-section B-B'.	4-8
Figure 4.5: Geological cross-section C-C'.	4-9
Figure 4.6: Geological cross-section D-D'.	4-10
Figure 4.7: Geological cross-section E-E'.	4-11
Figure 4.8: Geological cross-section F-F'.	4-12
Figure 4.9: Geological cross-section G-G'.	4-13
Figure 4.10: Geological cross-section H-H'.	4-14
Figure 4.11: Geological cross-section I-I'.	4-15
Figure 4.12: Topography of the paleochannel basement.	4-16
Figure 4.13: Isopach of the unconsolidated sediments.	4-18

CHAPTER 5 HYDRODYNAMICS

Figure 5.1: Location of monitoring wells in the study area.	5-2
Figure 5.2: Shallow observation wells in the JWPID.	5-3
Figure 5.3: Distribution of the regional observation wells in the study area.	5-4
Figure 5.4: Difference of mean groundwater levels between watertable wells (W) and piezometers (P) at 26 sites in the JWPID.	5-5
Figure 5.5: Hydrographs of the W (Watertable) and P (Piezometer) observation wells at sites 10, 33 and 35.	5-6
Figure 5.6: Effect of rainfall on the watertable elevation at sites 1W, 9W and 50W.	5-8
Figure 5.7: Effect of the variations of the Lachlan River stage (solid line) on the watertable elevation (dots) at sites 8W, 13W and 43W.	5-9
Figure 5.8: Watertable elevation map of the JWPID in March 1969.	5-10
Figure 5.9: Watertable elevation map of the JWPID in October 1990.	5-10
Figure 5.10: Watertable elevation map of the JWPID in July 1997.	5-11
Figure 5.11: Map of watertable depth below ground surface map of the JWPID in March 1969.	5-13
Figure 5.12: Map of watertable depth below ground surface of the JWPID in October 1990.	5-13
Figure 5.13: Map of watertable depth below ground surface of the JWPID in July 1997.	5-14
Figure 5.14: Changes in watertable levels between March 1969 and October 1990.	5-14
Figure 5.15: Changes in watertable levels between October 1990 and July 1997.	5-15
Figure 5.16: Changes in watertable levels between March 1969 and July 1997.	5-15
Figure 5.17: Total thickness of sand and gravel in the study area.	5-17
Figure 5.18 Hydrodynamic parameters at sites A, B and C (Figure 5.2) in the JWPID.	5-21

CHAPTER 6 GROUNDWATER SALINITY AND CHEMISTRY

- Figure 6.1: Relationship between electrical conductivity (EC) and total dissolved solids (TDS) in the study area (number of measurements = 160). 6-1
- Figure 6.2: Groundwater electrical conductivity (EC) of the JWPID watertable aquifer in February 1997 at the depth of 0-8 m. 6-3
- Figure 6.3: Groundwater electrical conductivity (EC) of the JWPID watertable aquifer in February 1997 at the depth of 8-20 m. 6-3
- Figure 6.4: Plots of electrical conductivity (EC) measured from piezometers 1 to 22 at the southern part of the JWPID and around lakes Cowal and Nerang Cowal areas from July 1994 to May 1997. 6-5
- Figure 6.5: Relationship between groundwater electrical conductivity (EC) and depth to watertable (based on 1863 observations). 6-6
- Figure 6.6: Variations of EC values with depth in observation well number 36551 and 36528. 6-7
- Figure 6.7: Groundwater electrical conductivity (EC) of the JWPID at the depth of 40 m. 6-9
- Figure 6.8: Groundwater electrical conductivity (EC) of the JWPID at the depth of 60 m. 6-9
- Figure 6.9: Groundwater electrical conductivity (EC) of the JWPID at the depth of 80 m. 6-10
- Figure 6.10: Groundwater electrical conductivity (EC) of the JWPID at the depth of 100 m. 6-10
- Figure 6.11: Piper diagram of the 410 groundwater samples in the JWPID. 6-11
- Figure 6.12: Piper diagram of 46 groundwater samples of the Lachlan Formation. 6-11
- Figure 6.13: Piper diagram of 61 groundwater samples of Cowra Formation. 6-12
- Figure 6.14: Relationship between ion concentrations and ranges of TDS in the study area. 6-13
- Figure 6.15: Plot of sodium (Na^+) versus chloride (Cl^-) for the JWPID and Bland Creek groundwater samples. 6-14
- Figure 6.16: Plot of Na^+/Cl^- versus electrical conductivity (EC) for EC range of 0-2,000 $\mu\text{S cm}^{-1}$. 6-15
- Figure 6.17: Plot of Na^+/Cl^- versus electrical conductivity (EC) for EC range of 2,000-60,000 $\mu\text{S cm}^{-1}$. 6-16
- Figure 6.18: Plot of calcium (Ca^{2+}) versus chloride (Cl^-) for the JWPID and Bland Creek groundwater samples. 6-16
- Figure 6.19: Plot of magnesium (Mg^{2+}) versus chloride (Cl^-) for the JWPID and Bland Creek groundwater samples. 6-17
- Figure 6.20: Plot of potassium (K^+) versus chloride (Cl^-) for the JWPID and Bland Creek groundwater samples. 6-17

CHAPTER 7. GROUNDWATER FLOW MODELLING AND MODEL SET-UP OF THE STUDY AREA

- Figure 7.1: A typical cross-section of the aquifer system. 7-4
- Figure 7.2: Computed and observed groundwater levels for the JWPID in 1992. 7-5
- Figure 7.3: Boundary conditions and elements for the proposed Gold Mine Dewatering Project. 7-7
- Figure 7.4: Land surface elevation contours of the modelled area in m AHD and locations of three cross-sections of the aquifer system. 7-8

Figure 7.5:	Selected cross-sections of the modelled area showing the aquifer system.	7-10
Figure 7.6:	Isopach of the upper aquifer (Layer 2) in metres.	7-11
Figure 7.7:	Isopach of the lower aquifer (Layer 4) in metres.	7-12
Figure 7.8:	Boundary conditions and discretisation of model grids for the top aquifer.	7-13
Figure 7.9:	Boundary conditions and model grids for the lower aquifer.	7-14
Figure 7.10:	Diagram of the steady-state and transient calibration with monthly timesteps from April 1988 to July 1997.	7-15

CHAPTER 8 STEADY-STATE CALIBRATION

Figure 8.1:	Distribution of hydraulic conductivity zones for the upper aquifer or Layer 2 of Figure 7.5.	8-2
Figure 8.2:	Distribution of hydraulic conductivity zones for the lower aquifer or Layer 4 of Figure 7.5.	8-3
Figure 8.3:	Distribution of hydraulic conductivity zones for the upper aquitard or Layer 1 of Figure 7.5.	8-5
Figure 8.4:	Distribution of recharge zones in the modelled area	8-7
Figure 8.5:	Comparison of observed and computed piezometric head distributions along Warroo channel without considering the channel seepage for April 1988.	8-9
Figure 8.6:	Distribution of observed and calibrated seepage rates for the Warroo Channel.	8-10
Figure 8.7:	Distribution of flow rates at each cell of the inflow (A) and outflow (B) boundaries.	8-12
Figure 8.8:	Distribution of computed piezometric heads for April 1988 in the modelled area without leakage through in the basement.	8-14
Figure 8.9:	Distribution of drain cells along the Gilmore Fault in the western side of the modelled domain.	8-15
Figure 8.10:	Computed versus observed piezometric head distribution of the top aquifer for April 1988.	8-16
Figure 8.11:	Plot of the computed versus observed piezometric heads at 88 observation points together with statistical indicators of the errors.	8-17
Figure 8.12:	Vertical distribution of the piezometric heads in three selected cross-sections of the modelled domain.	8-18
Figure 8.13:	Computed piezometric heads and direction of groundwater flow for the upper aquifer in April 1988.	8-20
Figure 8.14:	Computed piezometric heads and direction of groundwater flow for the lower aquifer in April 1988.	8-21

CHAPTER 9 TRANSIENT CALIBRATION

Figure 9.1:	Monthly rainfall and evapotranspiration in the modelled area from 1988 to 1997.	9-3
Figure 9.2:	Monthly delivered irrigation water in the modelled area from 1988 to 1997.	9-3
Figure 9.3:	Lachlan River water level at the Jemalong Weir gauging station.	9-5
Figure 9.4:	Recharge rates in high and low seepage sections of the Warroo channel.	9-6

Figure 9.5:	Location of the selected observation wells used to check the match between measured and computed heads for transient calibration.	9-8
Figure 9.6a:	Comparison between measured and computed heads in transient simulation at observation wells 1W, 9W, 13W and 16W for 1 st May 1988 to 31 st July 1997.	9-9
Figure 9.6b:	Comparison between measured and computed heads in transient simulation at observation wells 24 W, 32W, 40P and 44W for 1 st May 1988 to 31 st July 1997.	9-10
Figure 9.6c:	Comparison between measured and computed heads in transient simulation at observation wells 45W, 46W, 48W and 52W for 1 st May 1988 to 31 st July 1997.	9-11
Figure 9.6d:	Comparison between measured and computed heads in transient simulation at observation wells 56W, 58P, 91P and 6 for 1 st May 1988 to 31 st July 1997.	9-12
Figure 9.7:	Measured and computed piezometric heads in transient simulation for the flood period of October 1990 (timestep 30).	9-13
Figure 9.8:	Measured and computed piezometric heads in transient simulation for October 1994 representing a period of low groundwater levels (timestep 78).	9-14
Figure 9.9:	Measured and computed piezometric heads in transient simulation for July 1997 representing the end of the period of simulation (timestep 111).	9-15
Figure 9.10:	Comparison of computed versus measured piezometric heads and statistical indicators of the errors in transient simulation for timesteps 30, 78 and 111.	9-19
Figure 9.11:	Monthly total volume of inflow and outflow components of the groundwater balance for the period May 1988 to July 1997.	9-20
Figure 9.12:	Monthly total volume of recharge components for the period May 1988 to July 1997.	9-22
Figure 9.13:	Cumulative volume of change in storage for the entire transient simulation period of May 1988 to July 1997.	9-23

CHAPTER 10 SENSITIVITY ANALYSIS

Figure 10.1a:	Comparison between measured and computed heads at observation wells 1W, 9W, 13W and 16W with respect to changes in hydraulic conductivity.	10-2
Figure 10.1b:	Comparison between measured and computed heads at observation wells 24W, 32W, 40W and 44W with respect to changes in hydraulic conductivity.	10-3
Figure 10.1c:	Comparison between measured and computed heads at observation wells 45W, 46W, 48W and 52W with respect to changes in hydraulic conductivity.	10-4
Figure 10.1d:	Comparison between measured and computed heads at observation wells 56W, 58P, 91P and 6 with respect to changes in hydraulic conductivity.	10-4

Figure 10.2a: Sensitivity of the computed heads due to the changes in the assigned hydraulic conductivity for the flood period of October 1990 (timestep 30). 10-7

Figure 10.2b: Sensitivity of the computed heads due to the changes in the assigned hydraulic conductivity for October 1994 representing a period of low groundwater levels (timestep 78). 10-8

Figure 10.2c: Sensitivity of the computed heads due to the changes in the assigned hydraulic conductivity for July 1997 representing the end of the period of simulation (timestep 111). 10-9

Figure 10.3a: Comparison between measured and computed heads at observation wells 1W, 9W, 13W and 16W with respect to 50% and 100% increase in storage coefficient. 10-11

Figure 10.3b: Comparison between measured and computed heads at observation wells 24W, 32W, 40W and 44W with respect to 50% and 100% increase in storage coefficient. 10-12

Figure 10.3c: Comparison between measured and computed heads at observation wells 45W, 46W, 48W and 52W with respect to 50% and 100% increase in storage coefficient. 10-13

Figure 10.3d: Comparison between measured and computed heads at observation wells 56W, 58P, 91P and 6 with respect to 50% and 100% increase in storage coefficient. 10-14

Figure 10.4a: Sensitivity of the computed heads due to the changes in the storage assigned coefficient for the flood period of October 1990 (timestep 30). 10-15

Figure 10.4b: Sensitivity of the computed heads due to the changes in the assigned storage coefficient for October 1994 representing a period of low groundwater levels (timestep 78). 10-16

Figure 10.4c: Sensitivity of the computed heads due to the changes in the assigned storage coefficient for July 1997 representing the end of the period of simulation (timestep 111). 10-17

Figure 10.5a: Comparison between measured and computed heads at observation wells 1W, 9W, 13W and 16W with respect to $\pm 20\%$ change in recharge values. 10-20

Figure 10.5b: Comparison between measured and computed heads at observation wells 24W, 32W, 40W and 44W with respect to $\pm 20\%$ change in recharge values. 10-21

Figure 10.5c: Comparison between measured and computed heads at observation wells 45W, 46W, 48W and 52W with respect $\pm 20\%$ change in recharge values. 10-22

Figure 10.5d: Comparison between measured and computed heads at observation wells 56W, 58P, 91P and 6 with respect $\pm 20\%$ change in recharge values. 10-23

Figure 10.6a: Sensitivity of the computed heads due to $\pm 20\%$ change in recharge values for the flood period of October 1990 (timestep 30). 10-24

Figure 10.6b: Sensitivity of the computed heads due to $\pm 20\%$ change in recharge values for October 1994 representing a period of low

	groundwater levels (timestep 78).	10-25
Figure 10.6c:	Sensitivity of the computed heads due to $\pm 20\%$ change in recharge values for July 1997 representing the end of the period of simulation (timestep 30).	10-26
Figure 10.7a:	Comparison between measured and computed heads at observation wells 1W, 9W, 13W and 16W with respect to 25% and 50% increase in evapotranspiration rates.	10-28
Figure 10.7b:	Comparison between measured and computed heads at observation wells 24W, 32W, 40W and 44W with respect to 25% and 50% increase in evapotranspiration rates.	10-29
Figure 10.7c:	Comparison between measured and computed heads at observation wells 45W, 46W, 48W and 52W with respect to 25% and 50% increase in evapotranspiration rate.	10-30
Figure 10.7d:	Comparison between measured and computed heads at observation wells 56W, 58P, 91P and 6 with respect to 25% and 50% increase in evapotranspiration rate.	10-31
Figure 10.8a:	Sensitivity of the computed heads due to changes in evapotranspiration rate for the flood period of October 1990 (timestep 30).	10-32
Figure 10.8b:	Sensitivity of the computed heads due to changes in Evapotranspiration rate for October 1994 representing the period of low groundwater levels (timestep 78).	10-33
Figure 10.8c:	Sensitivity of the computed heads due to changes in evapotranspiration rate for July 1997 representing the end of the period of simulation (timestep 111).	10-34
Figure 10.9a:	Comparison between measured and computed heads at observation wells 1W, 9W, 13W and 16W with 2 m and 4 m ET extinction depth.	10-37
Figure 10.9b:	Comparison between measured and computed heads at observation wells 24W, 32W, 40W and 44W with 2 m and 4 m ET extinction depth.	10-38
Figure 10.9c:	Comparison between measured and computed heads at observation wells 45W, 46W, 48W and 52W with 2 m and 4 m ET extinction depth.	10-39
Figure 10.9d:	Comparison between measured and computed heads at observation wells 56W, 91P and 6 with 2 m and 4 m ET extinction depth.	10-40
Figure 10.10a:	Sensitivity of the computed heads due to changes in ET extinction depth for the flood period of October 1990 (timestep 30).	10-41
Figure 10.10b:	Sensitivity of the computed heads due to changes in ET extinction depth for October 1994 representing a period of low groundwater levels (timestep 78).	10-42
Figure 10.10c:	Sensitivity of the computed heads due to changes in ET extinction depth for July 1997 representing the end of the period of simulation (timestep 111).	10-43

CHAPTER 11 SIMULATION OF MANAGEMENT OPTIONS

Figure 11.1:	Computed watertable depth map of July 1997.	11-3
Figure 11.2:	Computed watertable depth map for year 2020 with ' <i>average/no change</i> ' scenario.	11-4

Figure 11.3:	Computed piezometric head distribution for year 2020 under the ' <i>average/no change</i> ' scenario.	11-5
Figure 11.4:	Piezometric head distribution under 'sealing of Warroo Channel' (Option A) in year 2020.	11-8
Figure 11.5:	Watertable depths under 'sealing of Warroo Channel' (Option A) in year 2020.	11-9
Figure 11.6:	Decline in watertable depths for year 2020 due to Option A as compared with the ' <i>average/no change</i> ' scenario.	11-10
Figure 11.7:	Piezometric head distribution under Option B in year 2020.	11-13
Figure 11.8:	Watertable depths under Option B for year 2020.	11-14
Figure 11.9:	Decline in watertable depths for year 2020 due to Option B as compared with the ' <i>average/no change</i> ' scenario.	11-15
Figure 11.10:	Piezometric head distribution under Option C in year 2020.	11-16
Figure 11.11:	Watertable depths under Option C in year 2020.	11-17
Figure 11.12:	Decline in watertable depths in year 2020 due to Option C as compared with the ' <i>average/no change</i> ' scenario.	11-18
Figure 11.13:	Location of plantation areas under tree-planting strategy.	11-20
Figure 11.14:	Piezometric head distribution due to tree plantation above Dog Kennel Hill in year 2020.	11-23
Figure 11.15:	Watertable depths in year 2020 under tree-planting strategy above Dog Kennel Hill (Area A).	11-24
Figure 11.16:	Decline in watertable depths in year 2020 due to tree-planting (area A).	11-25
Figure 11.17:	Decline in watertable depth at three observation wells (wells 34P, 35P and 98W) in the alley farmed area A.	11-26
Figure 11.18:	Piezometric head distribution in year 2020 under the tree-planting strategy in the southern part of the study area.	11-29
Figure 11.19:	Watertable depths under the tree-planting strategy in the southern part of the study area in year 2020.	11-30
Figure 11.20:	Decline in watertable depths in year 2020 due to tree-planting strategy in the southern part of the study area, as compared with the ' <i>average/no change</i> ' scenario.	11-31
Figure 11.21:	Decline in watertable depth at three observation wells (5n, 8n and 15n) in the southern part of the study area.	11-32

LIST OF APPENDICES

Appendix A: List of active meteorological stations in the Lachlan River Valley with at least 50 years of records.	A-1
Appendix B: Wells used in preparation of the geological cross-sections A-A' to I-I'.	B-1
Appendix C: Shallow observation wells in the JWPID.	C-1
Appendix D: Regional observation wells in the study area.	D-1
Appendix E: Hydrographs of the shallow observation wells in the JWPID.	E-1
Appendix F: Regional observation wells hydrographs in the study area.	F-1
Appendix G: Thickness of sand and gravel at the different wells in the study area.	G-1
Appendix H: Plots of electrical conductivity (EC) monitored at the shallow observation wells at the Jemalong and Wyldes Plains Irrigation District.	H-1
Appendix I: Comparison of electrical conductivity (EC) values between watertable and piezometric wells in the Jemalong and Wyldes Plains Irrigation District.	I-1
Appendix J: Plots of groundwater electrical conductivity (EC) for regional observation wells in the study area.	J-1
Appendix K: Hydrochemical types of groundwater samples at the selected observation wells.	K-1
Appendix L: Statistical indicators of errors.	L-1
Appendix M: Dates and length of timesteps in transient model.	M-1
Appendix N: Groundwater balance of the modelled area for May 1988 to July 1997.	N-1
Appendix O: Volume of recharge components and leakages through the basement rocks.	O-1

CHAPTER 1

INTRODUCTION

1.1. Background

Australia is a dry continent in which water scarcity is intensified by climate variability, including periodic drought and flood. The unique conditions in Australia make water an important issue. In the past, water has not been treated as an economic resource. Instead it has been used to promote regional development and settlement in semi-arid inland areas through the introduction of irrigation schemes (AATSE, 1999). Governments provided the capital needed for irrigation infrastructure development. Water charges paid by irrigators, however, were often unable to meet the costs of delivery of services. The full cost of urban water, sewerage services and rural domestic, irrigation and livestock supplies were not recovered from users.

A major change in water policies occurred in Australia in the 1990s. The emphasis of water policies has shifted in most jurisdictions from infrastructure development to sustainability (AATSE, 1999). The Council of Australian Governments (COAG) developed a National Water Reform Agenda in 1994. The Agenda combines elements of ecologically sustainable development and the National Competition Policy and is to be implemented by 2001 (Prime Minister's Science and Engineering Council, 1996). It covers, among other water related issues, major areas including water pricing, water allocation or entitlements, trading in water, institutional reform consultation and public education and environmental considerations (COAG, 1994).

One of the major highlights of this shift in water policy is the interstate agreement to cap total water diversions from all sources in the Murray Darling Basin at 1994 levels (Murray-Darling Basin Ministerial Council, 1996a). The introduction of the Cap was seen as an essential first step in establishing management systems to achieve healthy rivers and sustainable consumptive use. Similarly, in the Great Artesian Basin, the Department of Land and Water Conservation has declared an embargo in the Great Artesian Basin in New South Wales following a recommendation from the Great Artesian Basin Advisory Committee. This prevents the issuing of new high yield industrial and irrigation bore licenses, but does not apply to new stock and domestic bore licenses (Department of Land and Water Conservation, 2001). However, the natural resource and environmental aspirations of the COAG Agenda are yet to be realised (AATSE, 1999). Environmental water allocation, although incorporated in State plans, is accompanied by varying statutory force, and the cap on Murray-Darling Basins diversions is yet to be implemented in all states. Even the nationwide State of the environment reporting lacks the detail to establish current status and trend in water resources (AATSE, 1999).

The Lachlan catchment is part of the Murray-Darling Basin. The Murray Darling Basin Commission is guided by the decisions and priorities established by the Murray-Darling Ministerial Council, which consists of relevant State and Federal Ministers. Appropriate policies and plans include the: Salinity and Drainage Strategy; Natural Resources Management Strategy; Fish Management Plan; and Ministerial Council Interim Cap on Water Extractions (Department of Land and Water Conservation, 1998).

Strategic catchment planning and management for the Lachlan Valley has been in progress for about 9 years. The Lachlan Catchment Management Committee (LCMC), which is composed of representatives from the regional community and representatives, has prepared a community strategy for natural resources management in the Lachlan catchment in 1993 (Lachlan Catchment Management Committee, 1993). This is currently being reviewed and updated.

NSW Government has established the Lachlan River Management Committee as part of the August 1997 Water Reform Package. One of the roles of the committee is to prepare action plans for river flow, water quality and groundwater management to achieve the environmental objectives set by the NSW Government in the Lachlan Catchment (NSW Govt, 1997).

1.2. Importance of the research

Increasing land salinisation and stream salinity in the Murray Darling Basin is a great concern to the Australian community. The need to investigate and understand the processes involved to ensure that both land and water resources remain sustainable for future generations is widely acknowledged. In response to worsening salinity in the Basin, the Murray-Darling Basin Commission formulated the Salinity and Drainage Strategy (Murray-Darling Basin Management Commission, 1987). Numerous studies suggest that stream and dryland salinity will increase dramatically in the Basin (e.g. Jolly, *et al.*, 1997a and 1997b; Walker, *et al.*, 1998; Williamson, *et al.*, 1997). Much of this projected increase is the result of increased recharge due to land clearing in the past 200 years and development of irrigation systems without drainage and disposal facilities throughout the Basin.

The Jemalong and Wyldes Plains Irrigation District, Lake Cowal and Bland Creek sub-catchments are threatened with rising watertable and salinisation (Williams, 1993; van der Lely, 1993). These areas are located within the Lachlan River Valley, a sub-basin of the Murray Darling Basin. In order to address this threat it is necessary to elucidate the contributions of various natural and anthropogenic processes contributing to salinisation. Several studies have been undertaken in the area with conflicting conclusions about the contributions of irrigation to groundwater recharge. Many farmers argue that periodic flooding of the Lachlan River accounts for watertable rise and expansion of salinity.

Management of this irrigation area and the salinisation occurring in its western part requires that the contributions of all processes impacting on the groundwater dynamics be clearly identified. These processes include the impact of flow from the south towards Lake Cowal which is an important issue not considered in previous investigations.

A numerical groundwater flow model covering the Jemalong and Wyldes Plains Irrigation District, Lake Cowal and Bland Creek is developed in this work using Visual MODFLOW package. The modelled area extends from the Lachlan River in the north and Bland Creek to the south of the Lake Cowal. Lack of groundwater data has been the main reason for excluding the Bland Creek catchment from the modelled area.

1.3. Objectives and scope of the research

This research aims to: review the state of knowledge on water resources and related land resources of the Lachlan River Valley; investigate the groundwater systems and salinisation processes in the research area; and predict potential areas of salinisation. Specific objectives are to:

- Review the existing information on land and water resources of the Lachlan catchment and the study area.
- Investigate the hydrogeological features of the aquifer systems in the study area, and identify the recharge and discharge areas.
- Investigate the interaction of the aquifer system with the Lachlan River, Lake Cowal, Bland Creek and the irrigation system.
- Investigate the spatial and temporal distribution of groundwater salinity.
- Develop and calibrate a numerical model of the aquifer systems.
- Use the calibrated model to examine watertable rise, interactions between aquifers, surface water and the irrigation system and to quantify various components of recharge and discharge terms of the groundwater balance.
- Develop management strategies and options in order to minimise the risk of salinisation.

1.4. Organisation of the thesis

This thesis consists of 12 chapters. Apart from the current chapter, the contents of this thesis are as follows:

Chapter 2 provides an overview of the Lachlan River Valley. In this Chapter, the state of knowledge about the Valley's climatic changes, land and water resources, their historical and current status, and the associated problems are provided. An approximately 50 years cyclic pattern of annual rainfall variation has recurred in the catchment since the last century. Based on the time series of annual rainfall, the most widespread change occurred around 1945-1946. The median annual rainfall before 1946 at Cowra was about 554 mm. This is about 101 mm lower than the post 1946 median annual rainfall of 655 mm. There is a weak correlation of about 30% between rainfall and Southern Oscillation Index in the catchment has been observed.

Chapter 3 describes the Jemalong and Wyldes Plains Irrigation District, Lake Cowal and Bland Creek study area. The location and physiographic features, climatic and soils characteristics and land use are discussed. In addition, hydrological characteristics including runoff, streamflow characteristics and surface water quality issues are described. Another important section in this Chapter is the description of the irrigation district, its facilities, efficiency, operation and management.

Chapter 4 examines the surface and sub-surface geological features of the study area. It describes particularly the characteristics and extent of the Cowra and Lachlan Formations encountered in each geological cross-section across the alluvial area.

In Chapter 5, the hydrodynamic characteristics of the groundwater system in the study area are investigated. The historical changes in groundwater movement and level, aquifer transmissivity, and identification of recharge-discharge areas are examined in this Chapter.

Chapter 6 presents an analysis of groundwater salinity and chemistry in the study area. Groundwater salinity levels at the watertable aquifer and sand lenses are described and specific areas affected and under threat of salinisation are identified. The chemical composition of the groundwater in the Lachlan and Cowra formations are described based on the analysis undertaken by Anderson *et al.* (1993). The relationship between major ions and total dissolved solids (TDS) are also analysed and reported in this chapter.

Chapter 7 provides a review of groundwater models, including Visual MODFLOW. It also describes the development of the three-dimensional numerical model of the study area. The three-dimensional groundwater model consisted of 4 layers (two aquifers and two aquitards), and horizontally discretised into 500 m x 500 m grids covering the groundwater system within the Jemalong and Wyldes Plains Irrigation District and Lake Cowal area.

Chapter 8 discusses the results of the steady-state model calibration and the adjustment of the initial values of parameters hydraulic conductivity values, recharge rates, initial boundary conditions. Volumes of inflow and outflow components for steady-state groundwater balance of the modelled area based on April 1988 data is presented. During the the steady-state calibration, possible leakages into the basement's rocks were identified which appear to have helped in preventing the watertable in the system from rising dramatically.

Chapter 9 presents the results of transient calibration undertaken in the period between May 1988 and July 1997, in which major floodings and droughts occurred. The simulation period is divided into monthly timesteps which generates 111 timesteps for the entire calibration period. Rainfall provides the major source of recharge into the system, accounting for about 72% of the mean annual volume of recharge for the entire transient simulation period. Mean annual recharge due to irrigation accounts only about 16% of the total volume of recharge, and 80% of this is recharged from the Warroo Channel. The average recharge rate due to irrigation losses at the Warroo Channel is about $3,900 \text{ m}^3 \text{ d}^{-1}$ in the high seepage sections of the channel. Mean annual inflow from the constant head boundary along the Lachlan River near the Jemalong Gap is about $4.2 \times 10^6 \text{ m}^3 \text{ yr}^{-1}$ and accounts for 23% of the mean annual total inflow to the system. On the other hand, mean annual volume of outflow to the constant head boundary is about $3 \times 10^6 \text{ m}^3 \text{ yr}^{-1}$ which is 17% of the mean annual total volume of outflow from the system. Groundwater evaporation is the major source of outflow in the system, accounting for about 65% of the mean annual total volume of outflow.

Chapter 10 examines the sensitivity of the model to changes in various parameters. Parameters tested include hydraulic conductivity, storage coefficient, evapotranspiration, extinction depth of evapotranspiration, and recharge. Of the five parameters tested, the model is most sensitive to changes in ET extinction depth. The model is also sensitive to changes in storage coefficients but less sensitive to hydraulic conductivity values.

The results of the simulation of the management options are presented in Chapter 11. Three options were evaluated by the groundwater flow model over 23-year period from 1988 to 2020 including: 'average recharge' scenario; reduced recharge through improved irrigation and drainage efficiency; and alley farming. The results indicated that improvement of irrigation and drainage efficiency through sealing off the Warroo Channel leakage is a viable alternative in lowering watertables in the irrigation district. A corresponding decline of mean watertable

depths in the order 1 to 3 m has been computed for the Warroo Channel area, while the change in aquifer's storage has been reduced by 62%. Alley cropping in selected regions near the salt-affected areas in the western part of the model along the Bogandillon Creek provides a promising result in delaying salinisation expansion. Mean watertable depths in this area are effectively lowered to about 5 to 6 m at the end of year 2020.

The final chapter (Chapter 12) in this thesis provides a summary and concluding note on the major findings of this study. An important conclusion that may be drawn from this research is that the reclamation of existing saline land, the prevention of further land salinisation relies on redressing the hydrogeological imbalance by either reducing recharge, increasing evapotranspiration by tree-planting or both.

CHAPTER 2

OVERVIEW OF THE LACHLAN RIVER VALLEY

2.1. Physiography

The Lachlan River Valley is the third largest valley in the Murray-Darling Basin and lies in the Central West of New South Wales (Figure 2.1). It covers an area of 84,700 km², about 10.5% of the whole New South Wales (Department of Water Resources, 1989). It is a narrow, 550 km long Valley lying between Macquarie and Darling River valleys to the north and Murrumbidgee River Valley to the south. On the east, the Valley is separated from the adjoining coastal valley of the Hawkesbury River by the Great Dividing Range. The river eventually discharges into the Great Cumbung Swamp (Figure 2.2) and except during times of flood little, if any, flow enters the junction with Murrumbidgee River, 20 km downstream of Oxley via the main channel (Fleming, 1982).

About 75% of the Valley is flat, with slopes less than 3 degrees and the remaining is undulating to hilly terrain rising to elevations of between 1,000 m and 1,400 m on the eastern boundary of the Valley (Department of Water Resources, 1989). The major tributaries of the Lachlan River are Abercrombie; Crookwell; Boorowa and Belubula rivers which join the Lachlan upstream of Forbes, in the top third of the Valley (Figure 2.2). The Valley has four principal water storage facilities, namely: Wyangala Dam; Carcoar Dam; Lake Cargelligo; and Lake Brewster.

The central part of the Valley has a series of north-south trending ranges through which the river has cut a path. The constrictions produced by these ranges are in part responsible for the formation of the Brewster, Cargelligo and Cowal lakes. Downstream of Forbes the river system is characterised by a number of anabranches (channels which leave the mainstream and rejoins it further downstream). Towards the end of the Valley the stream gradient becomes smaller, being on average 1:3,000 between Forbes and Condobolin, and 1:2,000 between Oxley and the junction with the Murrumbidgee River (Department Water Resources, 1989). This flattening out has an obvious effect on flood patterns. Approximately one-third of the basin being flood prone. The upper portion of the Valley is not affected by flooding.

Significant alluvial flats in the Valley commence about 13 km upstream of Cowra. The alluvium within the Upper Lachlan River Valley (area between Lake Cargelligo, Forbes and Cowra) occupies over 4,000 km² (Bish and Williams, 1994), while downstream of the Lake Cargelligo, the alluvium is extensive (Williamson, 1986).

2.2. Socio-economic characteristics

The Valley has a population of about 106,000 people (Australian Bureau of Statistics, 1997) and is made up of 24 local councils. The main contributors to the employment in the Lachlan are agriculture, forestry, community services, and wholesale and retail trade. Mining and tourism have also contributed to the economy in the Valley. Some professional fishing is undertaken at Lakes Cowal, Cargelligo and Brewster (Department of Land and Water Conservation, 1998).

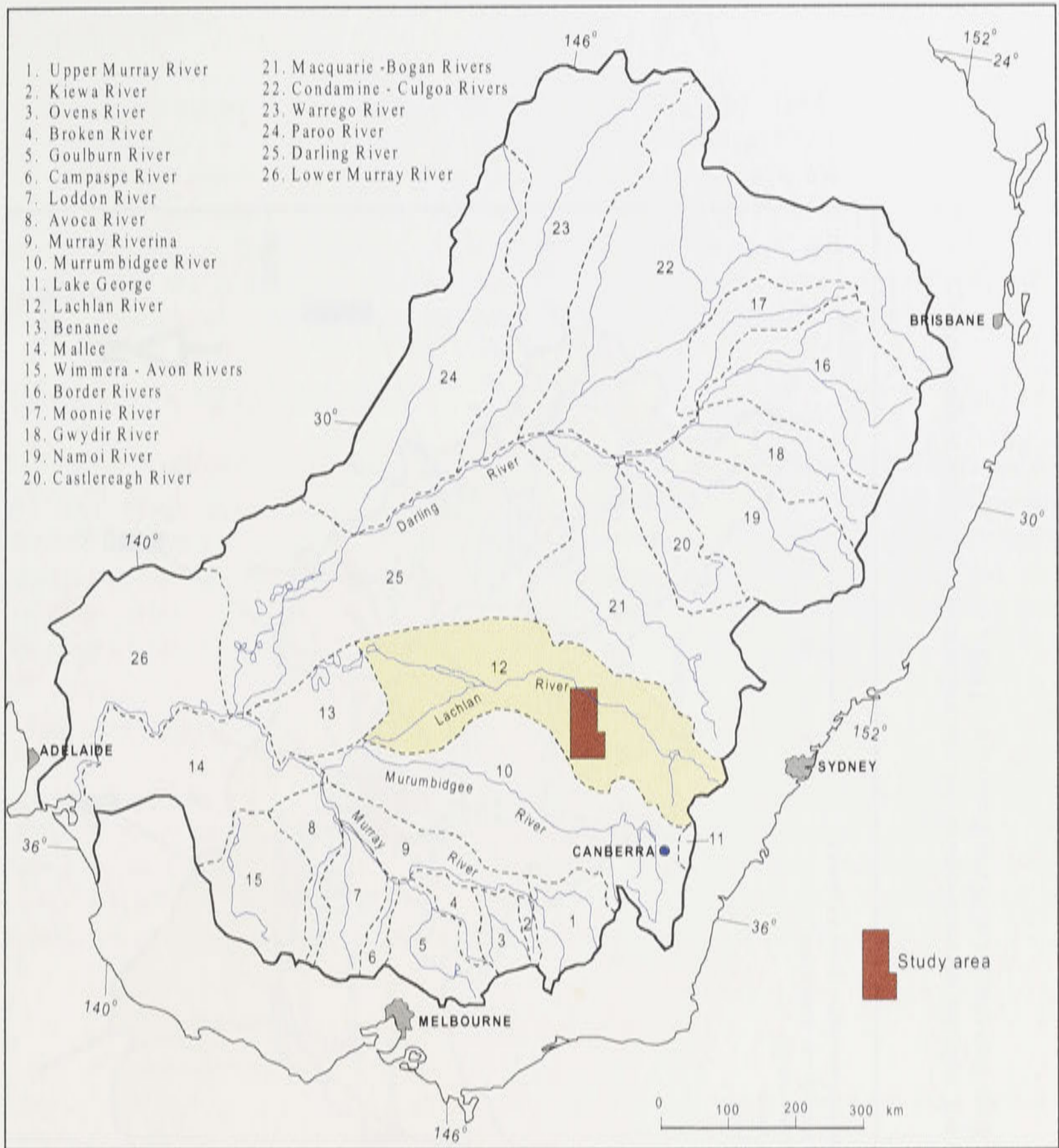


Figure 2.1: Murray Darling Drainage Basin sub-catchments (modified from Fleming, 1982).

The Lachlan Region is an important agricultural area in New South Wales. In 1993, the agricultural production was about \$821 million which is 14% of the total agricultural production in NSW (Australian Bureau of Statistics, 1996). There were some 83,700 ha of crops under irrigation in 1995/96 (Department of Land and Water Conservation, 1998). Lucerne, pasture and winter cereals constitute the major crops under irrigation.

2.3. Geology

The geology of the Valley is dominated by ancient fractured crystalline rocks. Any of these rocks that are now exposed are the remnants of high mountain ranges. The erosion of these ranges which started 10.5 to 23.5 million years ago has led to the infilling of the Valley with alluvial

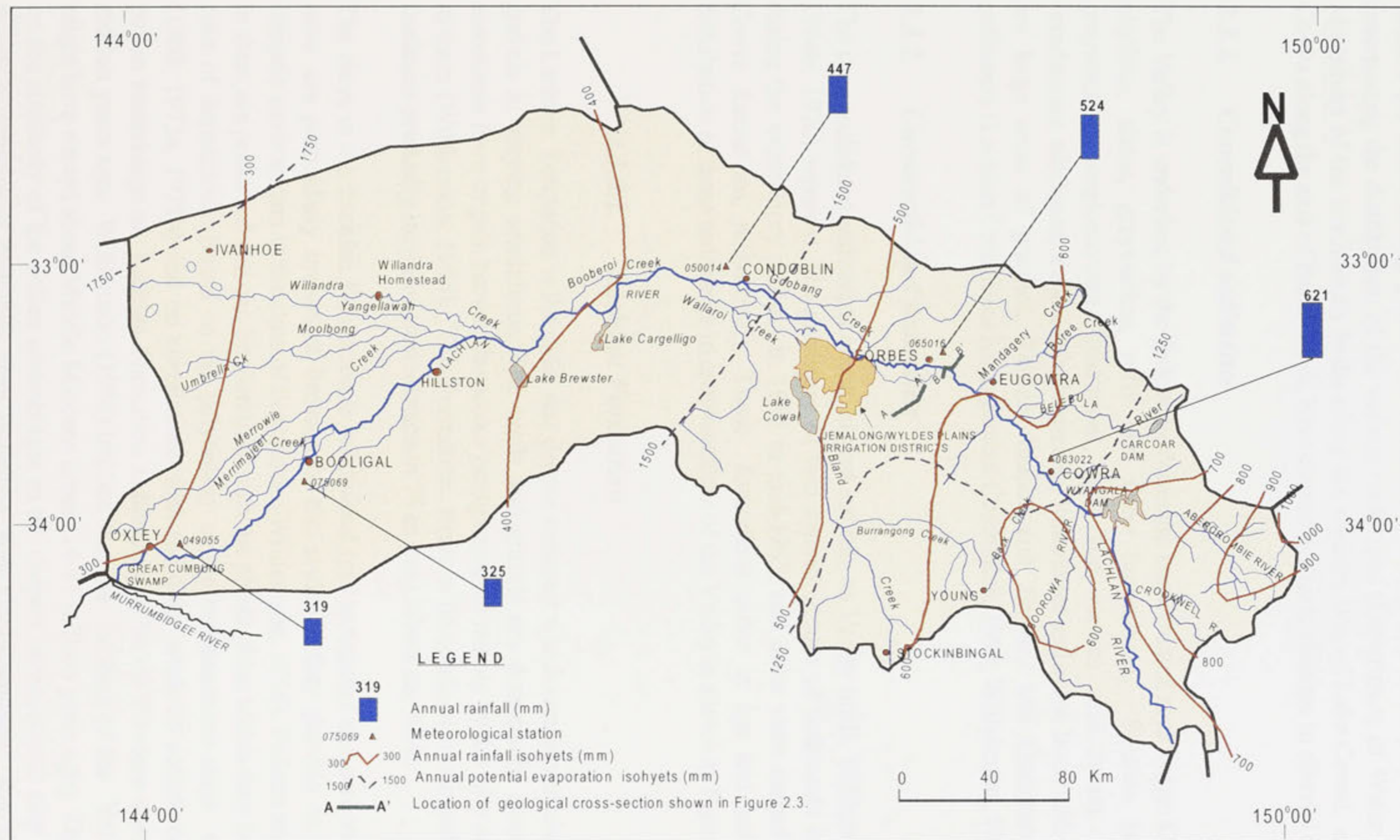


Figure 2.2: River network, selected meteorological stations and annual rainfall and evaporation (modified from Department of Water Resources, 1989).

sediment (Department of Water Resources, 1989; Anderson *et al.*, 1993; Bish and Williams, 1994). During that time the river channel meandered over the flood plain, depositing sand, gravel and clay. Sedimentary deposition, volcanic and major tectonic activities have folded and faulted the strata during periods of mountain building and have played the primary role in determining the distribution of the various rock types (Department of Water Resources, 1989). Movement of the north-south faults along the western side of Lake Cowal, and downstream of Cowra along the axis of Back Creek, have caused dramatic changes in alluvial thickness.

2.3.1. Consolidated sediments

The Valley is underlain by the following dominant consolidated rock types: Ordovician (schists, phyllites, slates, greywackes, tuffs and some limestones), Silurian (slates, sandstones, greywackes, conglomerates, limestones, tuffs and various acid lavas), and Devonian (sandstones, siltstones, shales, conglomerates, limestones and some lavas and tuffs). Also, there are large areas of granites, Tertiary basalts and Tertiary and Quaternary unconsolidated sediments (Lachlan Catchment Management Committee, 1993; Williamson, 1986).

2.3.2. Unconsolidated sediments

The unconsolidated sediments occur almost entirely as Valley infill. Williamson (1961; 1964a; 1964b; 1970) reported the discovery of two distinct groups of sediments infilling the Valley during the exploratory drilling in 1957 to mid-1965, and these were named the Lachlan and Cowra formations, respectively. These formations differ in age and composition and the distribution of these sediments in cross-sections of the Valley is shown in Figure 2.3.

2.3.2.1. Lachlan Formation

The Lachlan Formation is the older and deeper sediment which consists of clays, silts, sands and gravels in varying admixtures. The sands and gravels are dominantly grey or off-white, but sometimes fawn or pale brown, the colour being imparted mainly by the silty and clayey fractions in them (Williamson, 1986). This Formation tends to be confined to the paleochannels and its thickness gradually increases downstream to 75 m near Jemalong Weir.

The clays in the Lachlan Formation is subdivided into variegated and carbonaceous clays. The latter are particularly important because of the evidence they provide on their age and the climatic environment at the time of deposition (Williamson, 1986). Pollens and spores entrapped in them are preserved and can be identified with the plants from which they had been shed at the time of deposition. Based on the palynology of the carbonaceous clays detailed by Martin (1969, 1973a, 1973b) and on correlations with the older work on sedimentary sequences, the pollen assemblage of Lachlan Formation indicates it to be of Pliocene age, which is 1.8 to 5 million years ago. Williamson (1986) implied that the infilling of the Valley with sediments might have started about Middle Miocene times (14-17 million years ago). The estimate is based on the similarity of the pollen assemblages in the deepest carbonaceous clay near Forbes to the pollen in samples of diatomite from Bulgaldie, near Coonabarabran. But because of renewed erosion and downcutting in the late Miocene, most of these sediments were removed and only a small amount of Middle Miocene sediments are recorded in the geological record (Anderson *et al.*, 1993).

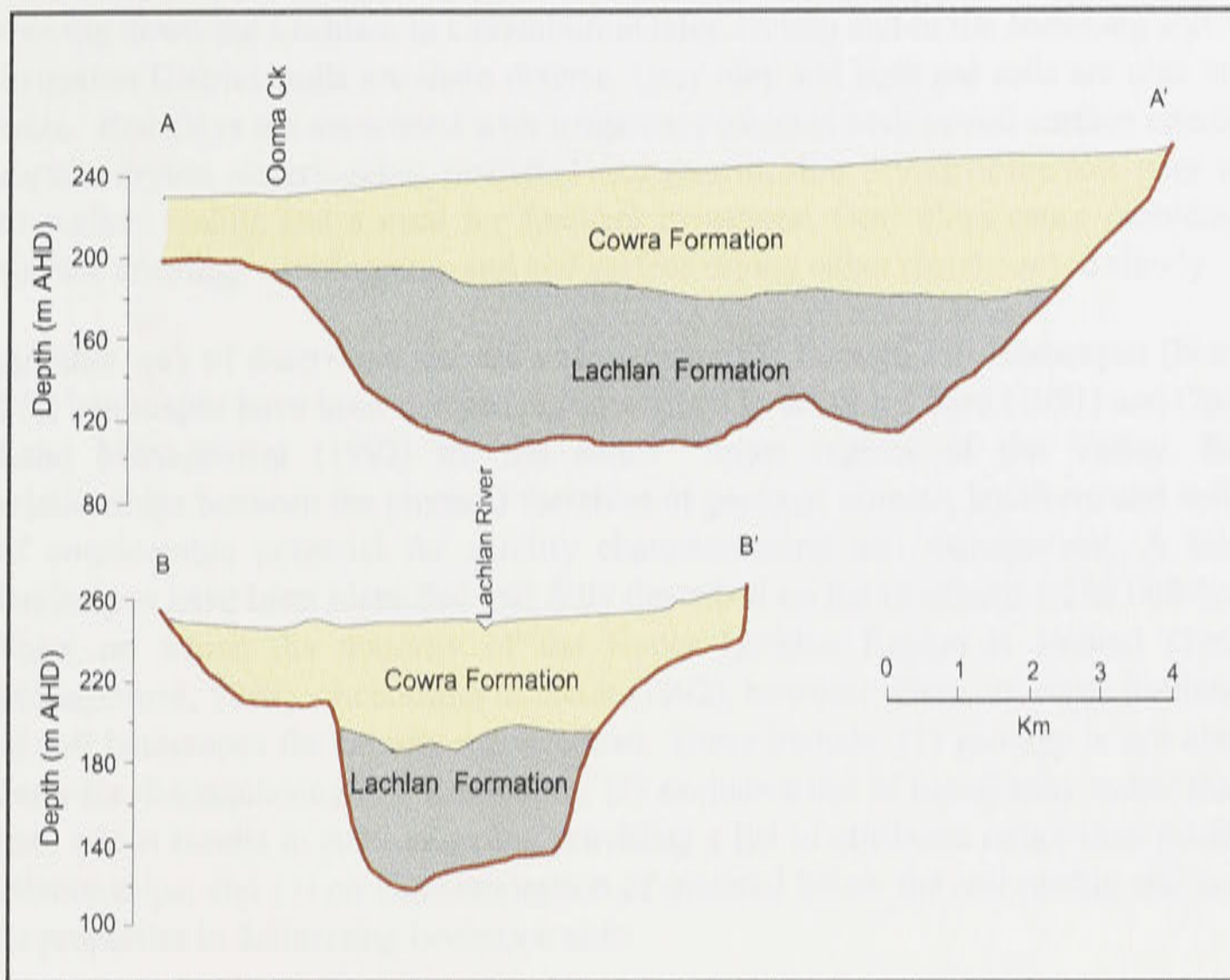


Figure 2.3: Geological cross-sections A-A' and B-B' through Lachlan River Valley (modified from Williamson, 1986).

2.3.2.2. Cowra Formation

The younger Cowra Formation unconformably overlies the Lachlan Formation and basement rocks. It is generally around 30-40 m thick in Cowra and gradually becomes thicker downstream reaching a thickness of 64 m in the Forbes area. The Formation consists of moderately well sorted sand and gravel with interbedded clays, which are predominantly brown in colour as opposed to dominant greys of sand and gravels of the Lachlan Formation (Williamson, 1986).

The Cowra Formation has been deposited since the Pleistocene (up to 1.8 million years). This estimate is based on the analysis of the few pollens found in a limited number of samples by Martin (1973b) as cited by Williamson (1986).

2.4. Soils

Some of the alluvial soils in the floodplain have excellent characteristics and possess natural fertility. Away from the floodplain, soil types include: the granite and basalts derived soils of the higher slopes; the red duplex loam over a clay sub-soil; and heavy sodic clays. In conventional agriculture systems, all soils except alluvial soils and some basalt soils require additional phosphates.

Ross *et al.* (1992) categorised the soil types under irrigation in the Valley according to the terminology used by the local farmers into the following: deep alluvial; grey clay; light red; red clay; and loams. Deep alluvial is the major soil type from Wyangala Dam to Condobolin. Irrigators preferred to irrigate this soils because they were the most productive and caused very few management problems. However, the frequency of occurrence of these soils decreases

moving down the Lachlan. In Condobolin-Oxley section and in the Jemalong and Wylde Plains Irrigation District, soils are more diverse. Grey clay and light red soils are also major irrigation soils. Red clays are associated with irrigation problems such as soil surface crusting, rapid soil surface drying, waterlogging, restricted root growth, slow drying of the soil, poor infiltration due to surface sealing and a need for frequent irrigations. Grey clays cause problems such as soil surface crusting, waterlogging, and soil surface drying either rapidly or too slowly.

Another way of describing the soil characteristics is through soil landscapes (Northcote, 1979). Soil landscapes have been mapped and described in detail by Hird (1991) and Conservation and Land Management (1992) for the entire upper regions of the Valley. Information on relationships between the physical variables of geology, climate, landform and soil landscapes is of considerable potential for salinity characterisation and management. A total of 58 soil landscapes have been identified and fully described on the Goulburn 1:250 000 Soil Landscapes Sheet on which the majority of the Upper Lachlan Region is located (Total Catchment Management, 1993). According to Hook (1992), however, there are some limitations in the use of soil landscapes for salinity management. These include: (1) geology is not always used as a basis for distinguishing soil landscapes; (2) exclusive use of topography rather than geomorphic data which results in static mapping providing a list of attributes rather than possibly indicating relationships; and (3) no characterisation of material below the soil profile and consideration of its properties in delineating landscape units.

2.5. Climate

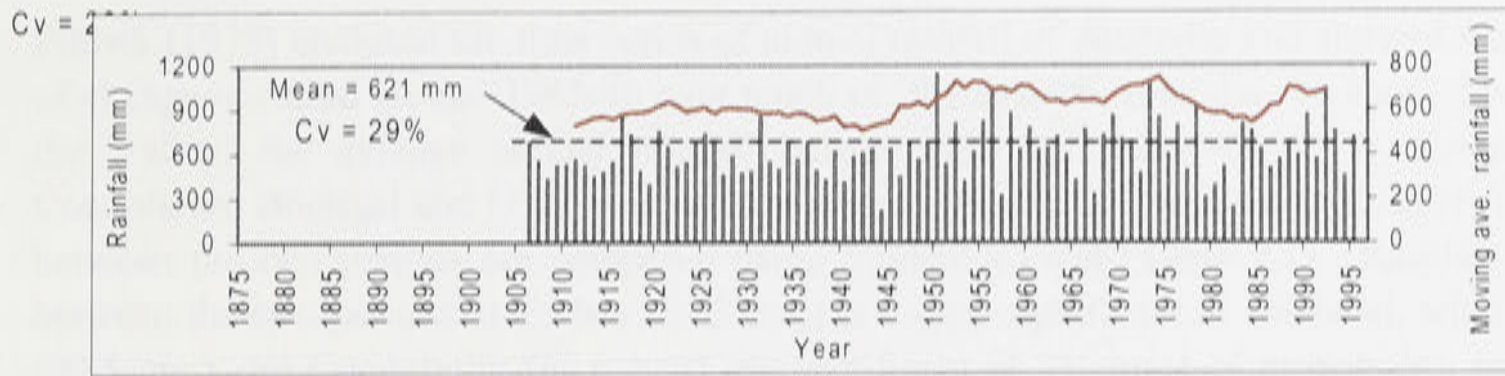
2.5.1 Rainfall

2.5.1.1. Rainfall stations and data

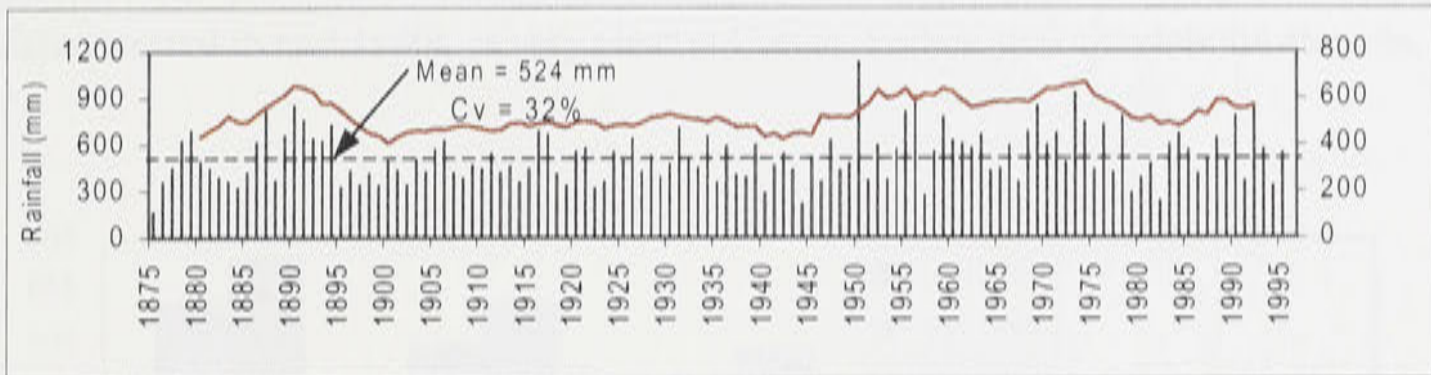
Long term rainfall data in the Valley were obtained from the Bureau of Meteorology for active meteorological stations with rainfall records of at least 50 years (Appendix A). The longest rainfall record available in the Valley is 130 years for station 050007 at Borambil Park, Condobolin. In the succeeding rainfall analysis, five rainfall stations with at least 73 years of records were selected because of their strategic representations of the important sections along the Lachlan River. These are station 063022 (Cowra) for the upper section, 065016 (Forbes) and 050014 (Condobolin) for the mid section, and 075069 (Booligal) and 049055 (Oxley) for the lower sections of the Valley, respectively (Figure 2.2).

2.5.1.2. Rainfall distribution

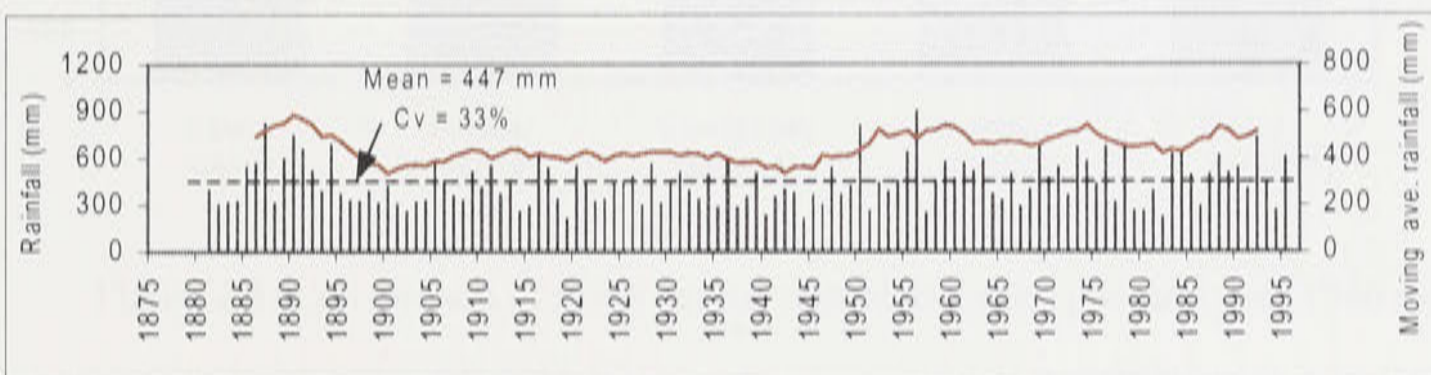
The upper region of the Valley receives up to 1000 mm of rainfall per year on average. This drops to around 500 mm and 300 mm in the middle and lower regions of the Valley, respectively (Figure 2.2). Rainfall is generally distributed evenly throughout the year, but can vary dramatically from year to year. Figure 2.4 shows these annual variations expressed as coefficient of variation (Cv) using the long term records of the selected stations. At station 063022 in Cowra which has the highest mean annual rainfall of about 621 mm, the Cv is about 29%. Coefficient of variation increases progressively towards the lower rainfall areas downstream of the Valley. For example, station 065016 in Forbes whose mean annual rainfall is 524 mm, has a Cv of 32% and at station 049055 in Oxley, the Cv is 39.5%, 10% more than Cowra station.



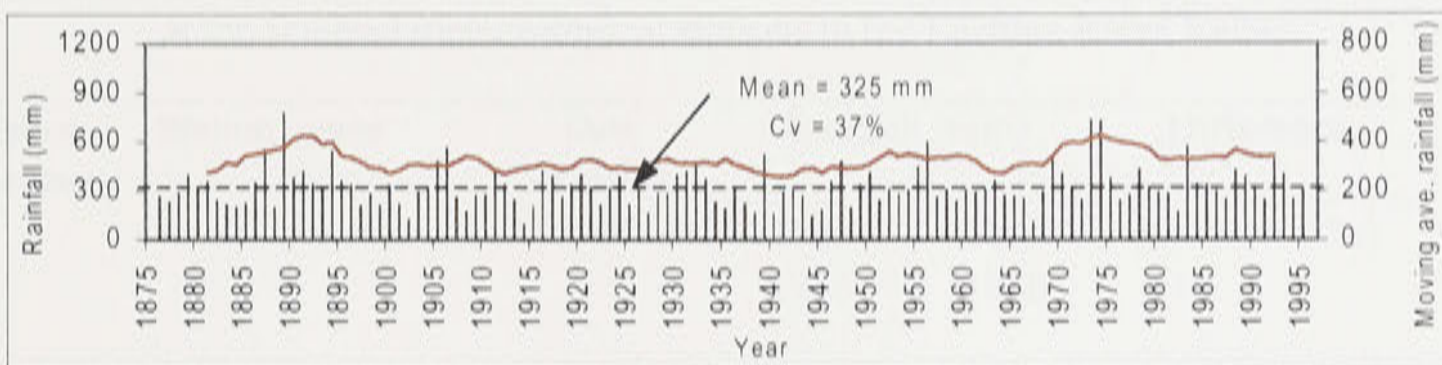
(a) Cowra (063022)



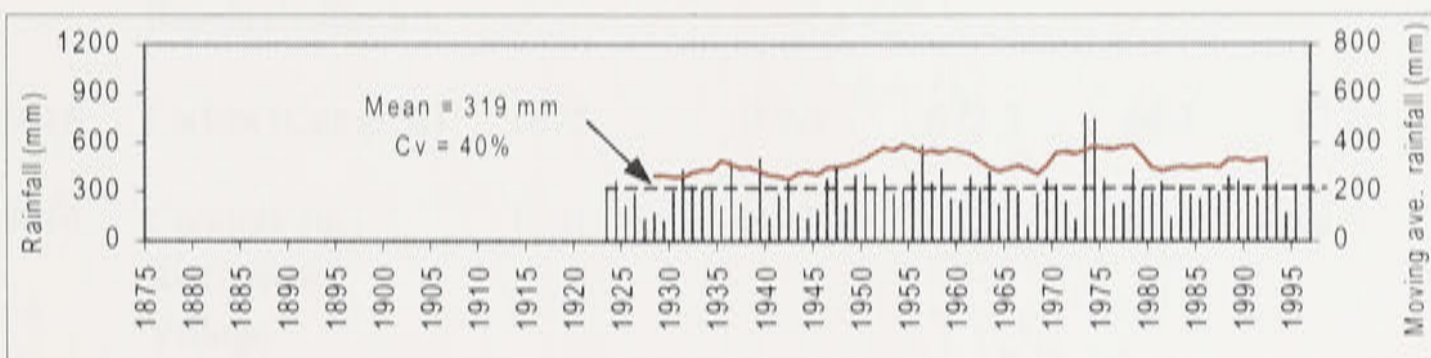
(b) Forbes (065016)



(c) Condobolin (050014)



(d) Booligal (075069)



(e) Oxley (049055)

Figure 2.4: Annual (bar) and 10-year moving average (red line) rainfall at five meteorological stations in the Valley.

Pittock (1975) analysed the time series of annual rainfall of Australia and showed that a pattern of change occurred around 1945-46 over much of the eastern Australia. To show this change at the Valley, the average annual rainfall before 1946 and after 1946 at Cowra, Forbes, Condobolin, Booligal and Oxley stations are plotted (Figure 2.5) and the difference of the mean between the two periods are compared using Student's t-test (Table 2.1). Rainfall difference between the two periods at Forbes (84.3 mm) is highly significant at 1% level, whereas Cowra (90.5 mm) and Condobolin (62.6 mm) are significant at 5% level of probability, respectively. The pattern of change of annual rainfall occurred around 1945-46 is also well illustrated in Figure 2.4 using the 10-year moving average at the five stations selected. This change of trend which occurred in mid 1940s is very clear at Cowra, Forbes, and Condobolin stations.

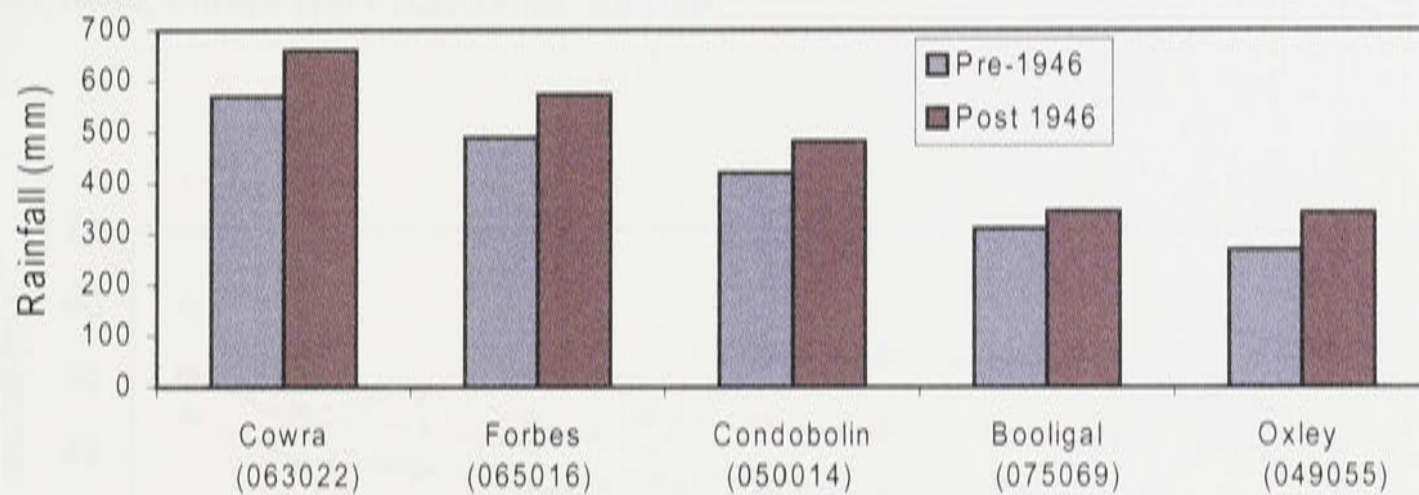


Figure 2.5: Comparison of mean annual rainfall between pre- and post 1946 data.

Table 2.1: Comparison of the mean annual rainfall between the periods pre-1946 and post 1946 at the selected meteorological stations in the Lachlan River Valley.

Station number	Station name	Data available since	Rainfall (mm)		Difference		Level of Significance* (%)
			Pre-1946	Post 1946	(mm)	(%)	
063022	Cowra Agricultural Research Station	1905	570.6	661.1	90.5	13.7	5
065016	Forbes (Camp St)	1875	489.4	573.7	84.3	17.2	1
050014	Condobolin Retirement Village	1881	419.7	482.3	62.6	14.9	5
075069	Booligal (Ulonga)	1876	310.4	345.2	34.8	11.2	10
049055	Oxley (Walmer Downs)	1923	268.8	342.2	73.4	27.3	3

*Level of significance is estimated using Student's t-test.

The Valley is also characterised by winter and/or spring low rainfall (Bish and Gates, 1991). Mean monthly rainfalls for Cowra, Forbes and Condobolin (Figure 2.6) reflect this pattern and show low rainfall during winter and early spring, followed by slightly higher rainfall during late spring and summer. On average, October and January are the wettest months of the year. Figure 2.7 shows the mean monthly comparison of rainfall between pre 1946 and post 1946 rainfall data series. With the exception of June, the average monthly rainfalls after 1946 are higher than the average monthly rainfalls before 1946. The difference of the monthly rainfalls is very much pronounced during spring and summer months. Figure 2.8 shows the seasonal plot of the average rainfalls categorised into pre 1946 and post 1946 data. Comparing the means of the seasonal rainfalls between the two periods of summer (December, January and February) and spring (September, October and November) seasons exhibited a highly significant difference of mean seasonal rainfall between the periods considered (Table 2.2). This difference is again pronounced in Cowra, Forbes and Condobolin stations.

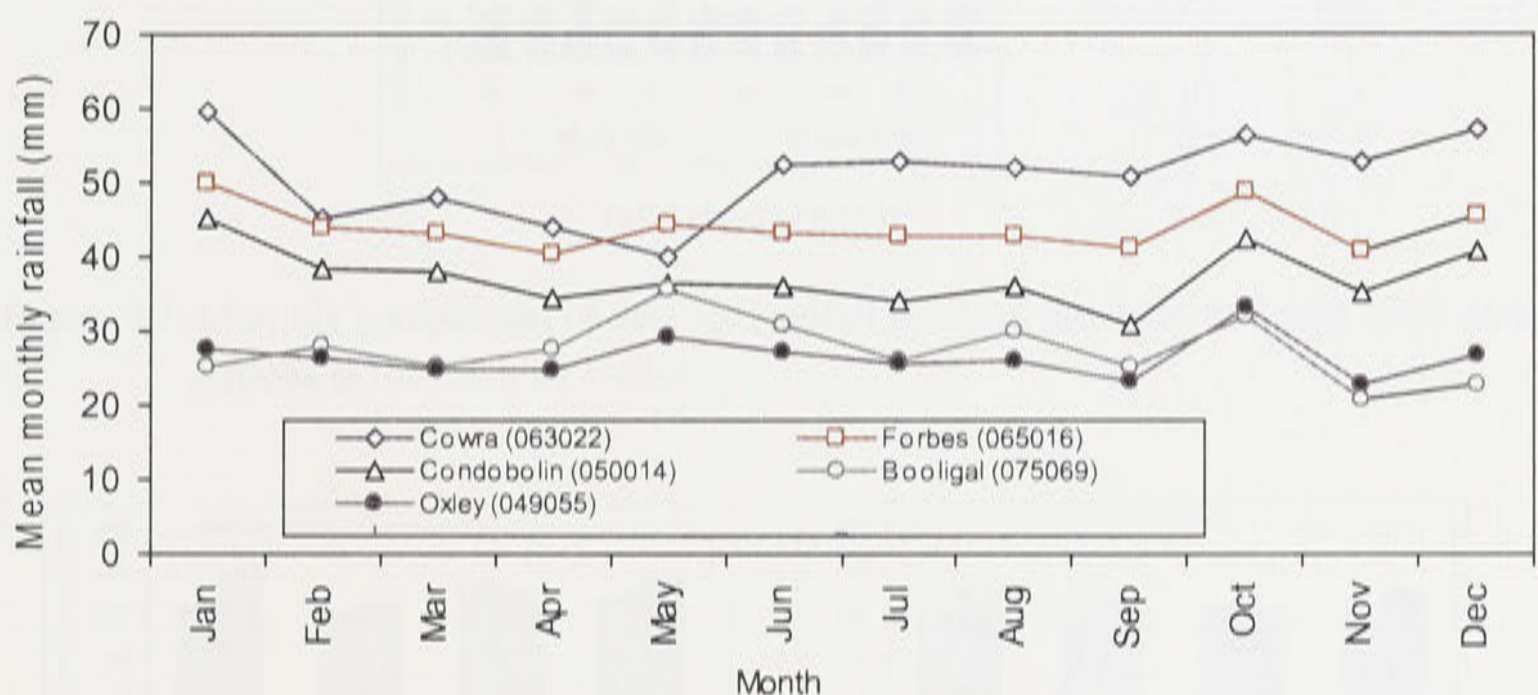


Figure 2.6: Mean monthly rainfall at five selected meteorological stations in the Valley.

2.5.1.3. Rainfall and southern oscillation index

Elements of the global-scale climate phenomenon now referred to as the El Nino/Southern Oscillation (ENSO) began to be noted toward the end of the 19th century (Nicholls, 1992). El Nino is an unusual warming of the normally cool near-surface waters off the west coast of South America and was so named by the inhabitants of northern Peru in reference to the Christ-child, because it typically appears as an enhancement to the annual onset of a warm, southward setting current that occurs there around the Christmas season. Beginning with the work of Bjerknes (1966a,b and 1969) it is now recognised that the El Nino phenomenon of South America is a regional manifestation of ocean-atmospheric interactions on a much larger scale. During El Nino, the equatorial zone and much of the tropical belt are anomalously warm across the breadth of the Pacific and are characterised by strong perturbations in the currents and deeper thermal structure as well (Enfield, 1992).

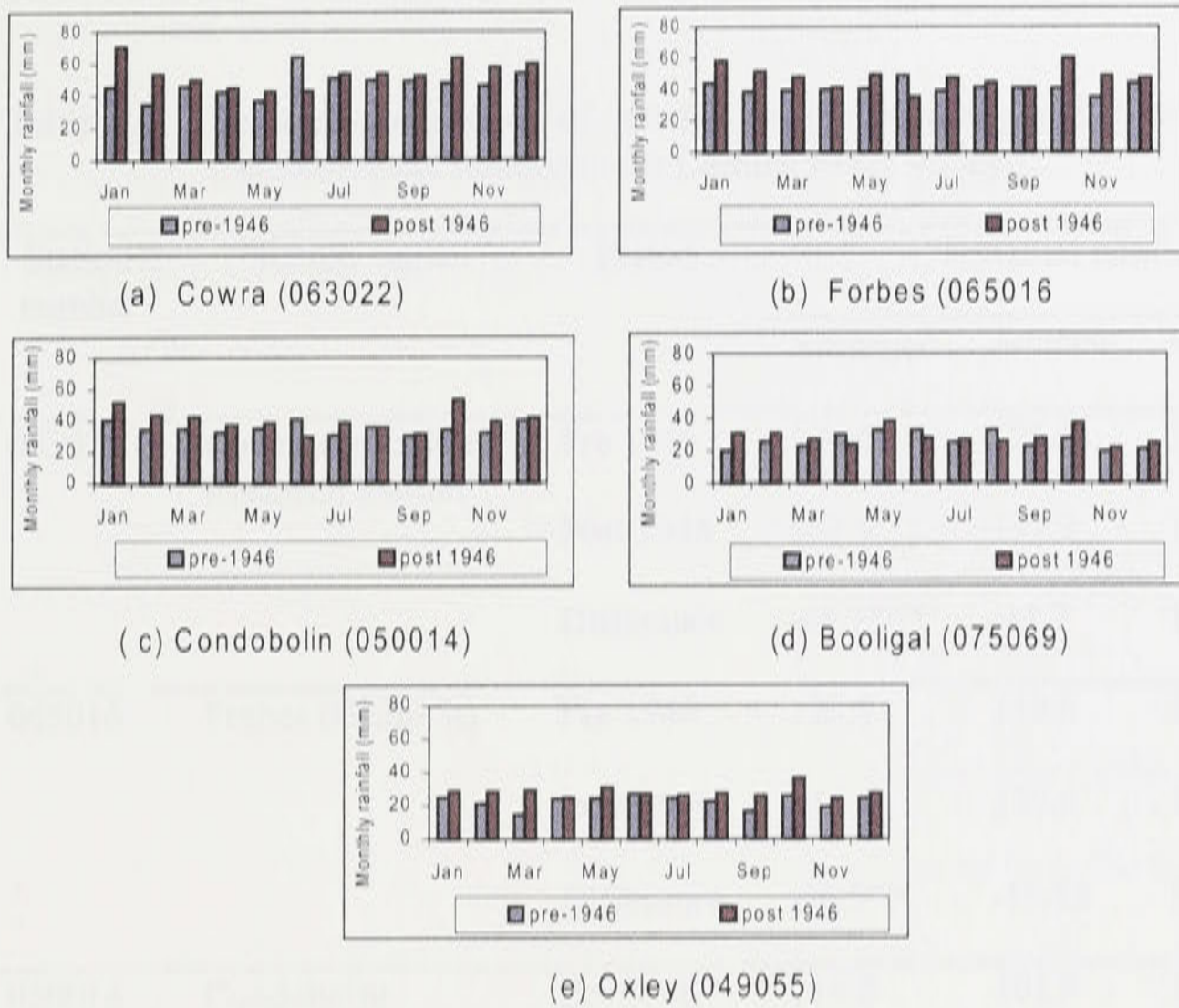


Figure 2.7: Monthly comparison of average rainfall between pre-1946 and post 1946 data at 5 stations in the Lachlan Valley

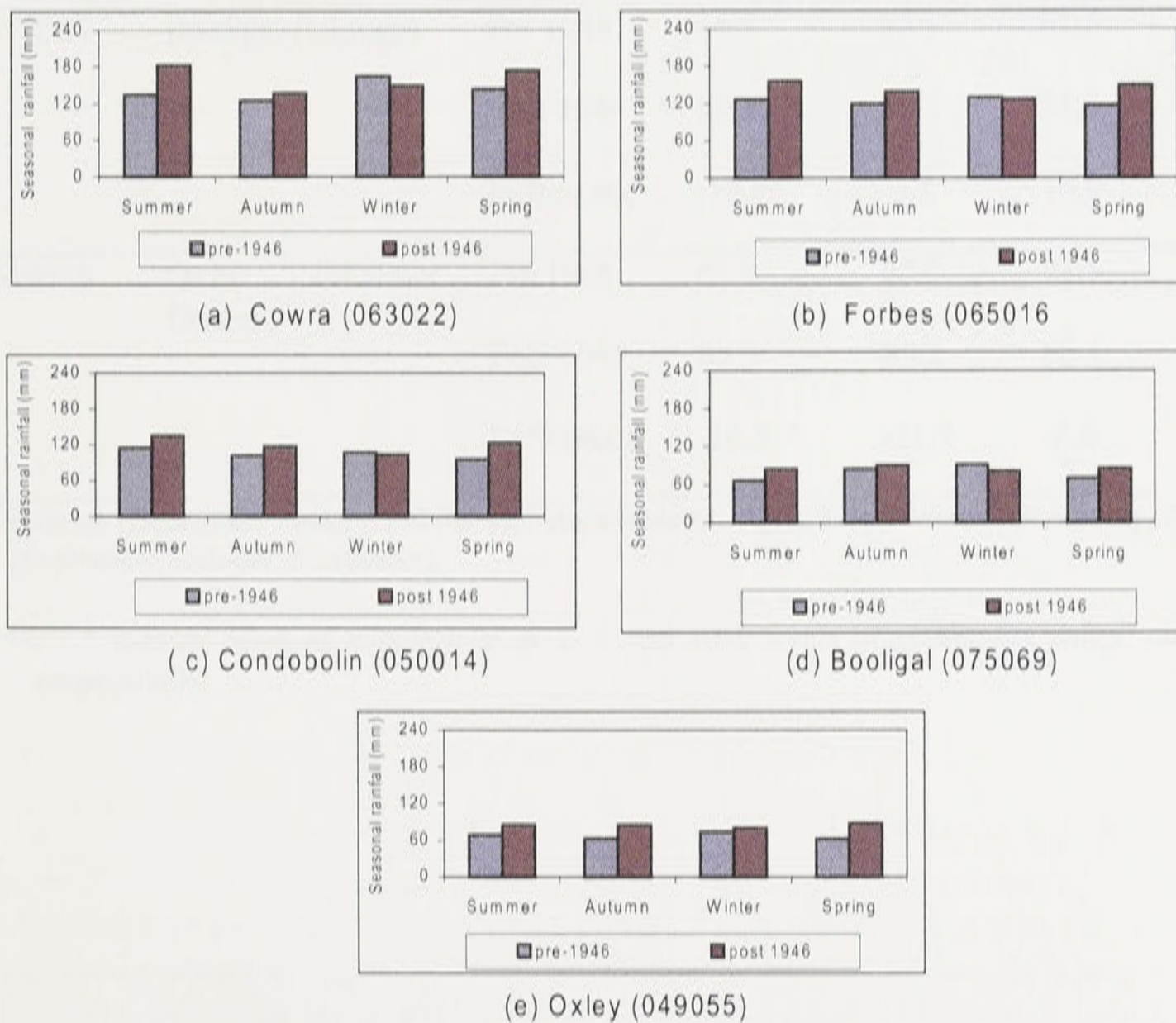


Figure 2.8: Comparison of seasonal mean rainfall between pre-1946 and post 1946 data at 5 stations in the Lachlan Valley.

Table 2.2: Seasonal comparison of rainfall for the periods pre-1946 and post 1946 at five meteorological stations in the Lachlan River Valley.

Station number	Station name	Period	Seasonal rainfall (mm) ¹			
			Summer	Autumn	Winter	Spring
063022	Cowra Agricultural Research Station	Pre 1946	134.6	125.5	164.2	143.8
		Post 1946	182.9	137.2	149.4	174.2
		Difference	-48.3***	-11.7	14.8	-30.4**
065016	Forbes (Camp St)	Pre 1946	126.9	119.8	130.0	117.3
		Post 1946	156.8	139.6	127.5	149.9
		Difference	-29.9**	-19.82	2.5	-32.6***
050014	Condobolin Retirement Village	Pre 1946	114.8	101.8	107.2	95.8
		Post 1946	135.3	117.6	103.7	123.5
		Difference	-20.5	-15.8	3.5	-27.7**
075069	Booligal (Ulonga)	Pre 1946	66.5	85.1	91.5	70.3
		Post 1946	85.1	90.2	81.5	85.5
		Difference	-18.6*	-5.1	10.0	-15.2*
049055	Oxley (Walmer Downs)	Pre 1946	68.8	63.5	74.5	62.0
		Post 1946	85.3	85.2	80.1	87.8
		Difference	-16.5	-21.7	-5.6	-25.8**

¹ Summer (December, January, February); autumn (March, April, May); winter (June, July, August); spring (September, October, November).

***,**, * indicate level of significance at 1, 5 and 10% levels of probability using Student's t-test, respectively.

Southern Oscillation (SO) is the atmospheric counterpart to El Nino and recognised by Walker (1923) and Walker and Bliss (1932) as a coherent variation of barometric pressures at interannual intervals. The state of the SO pressure system is characterised by the Southern Oscillation Index (*SOI*), and defined by Troup (1965) as:

$$SOI = \frac{PA(Tahiti) - PA(Darwin) \times 10}{Std. Dev. Difference} \quad (2.1)$$

where:

PA (Tahiti) = Atmospheric pressure anomaly at Tahiti

PA (Darwin) = Atmospheric pressure anomaly at Darwin

Std. Dev. Difference = Standard deviation of the atmospheric pressure difference

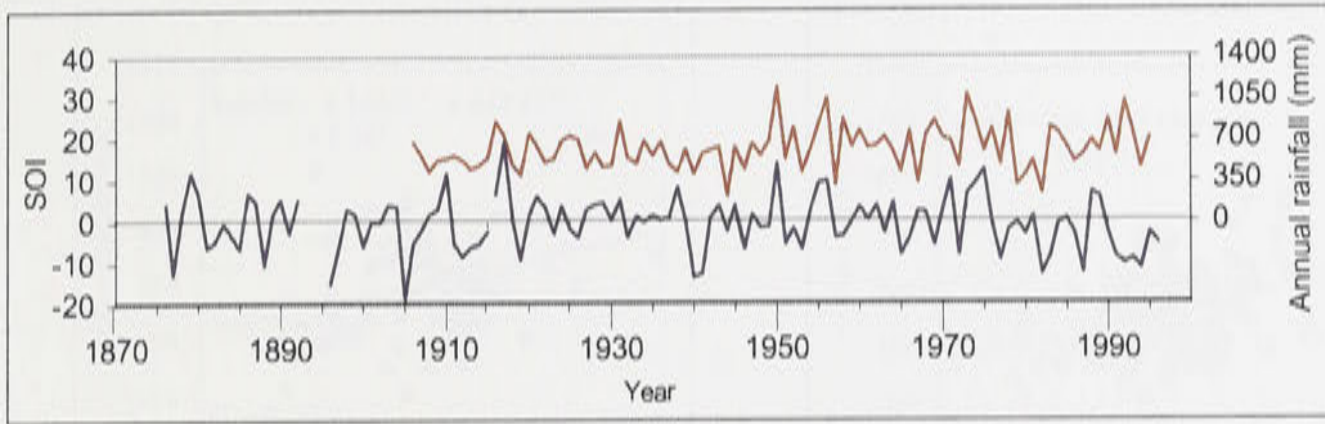
Atmospheric pressure anomaly is computed as the monthly mean minus the long term mean of the atmospheric pressure. An *SOI* of -10 means that the *SOI* is 1 standard deviation on the negative side of the long-term mean for that month.

The ENSO phenomenon is obviously a major reason for eastern Australian rainfall fluctuations, but the lack of major mountain ranges also contributes (Nicholls, 1992). The parts of eastern Australia where the influence of ENSO is weakest lie around the coastal fringe, where the Great Dividing Range can produce local rainfall effects. This complicates the large-scale influence of ENSO (Nicholls, 1992). Inland of the coastal mountains, however, there is little orography to differentiate the reaction to the broad-scale influence of ENSO leading to widespread, coherent rainfall fluctuations. Ropelewski and Halpert (1986) examined the relationship between El Nino episodes and Australian rainfall. They concluded that rainfall was deficient from about February of an El Nino year through to the following February for much of eastern Australia.

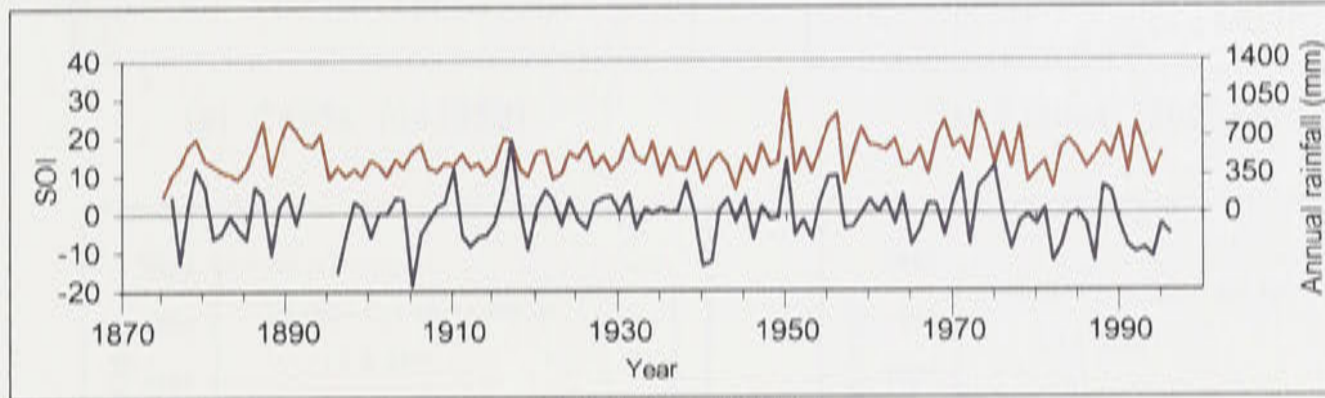
As shown in Figure 2.9, rainfall variations in the Lachlan River Valley are only slightly correlated with the ENSO phenomenon. The linear relationship between the annual *SOI* and rainfall is very weak (Figure 2.10) with low correlation coefficients of about 0.25, 0.20, 0.33, 0.37 and 0.33 at Oxley, Booligal, Condobolin, Forbes and Cowra stations, respectively. These explain only about 10% of the variance.

2.5.2. *Temperature, sunshine duration and wind speeds*

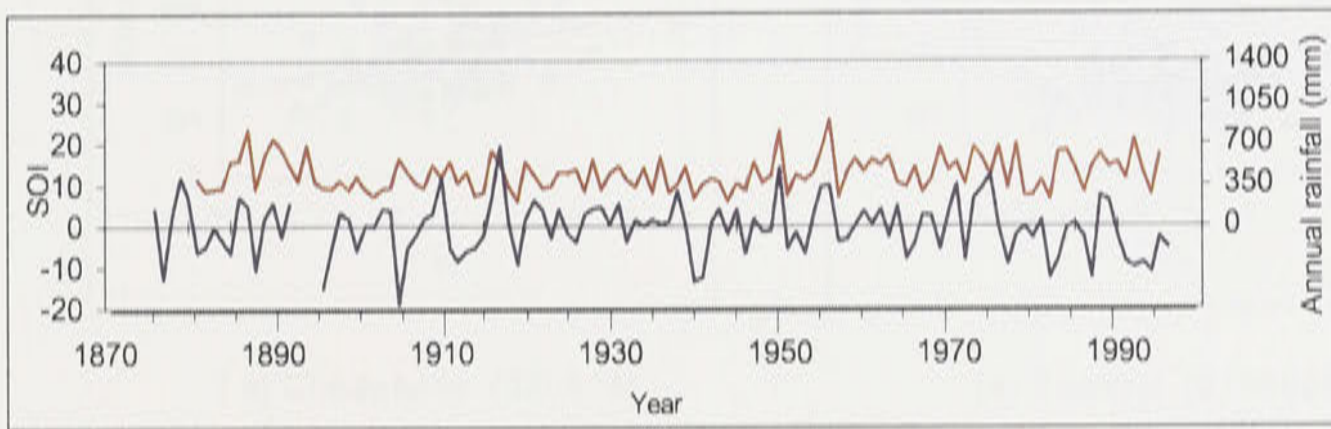
Climatic features in the Valley differ from the eastern to the western end. At higher elevations, upstream of Cowra, temperatures vary from a winter average minimum of 0°C to a summer average maximum of 27°C (Department of Water Resources, 1989). Below Cowra temperatures vary from a winter average minimum of 2°C, to a summer average maximum of 35°C (Figure 2.11), with individual daily minimum of less than -6°C and maximum of more than 48°C, respectively. Frost also occurs during the cooler months of the year, usually from May through September with frequencies ranging from more than 80 occurrences per year over the highlands to about 10 per year over the western section of the Valley.



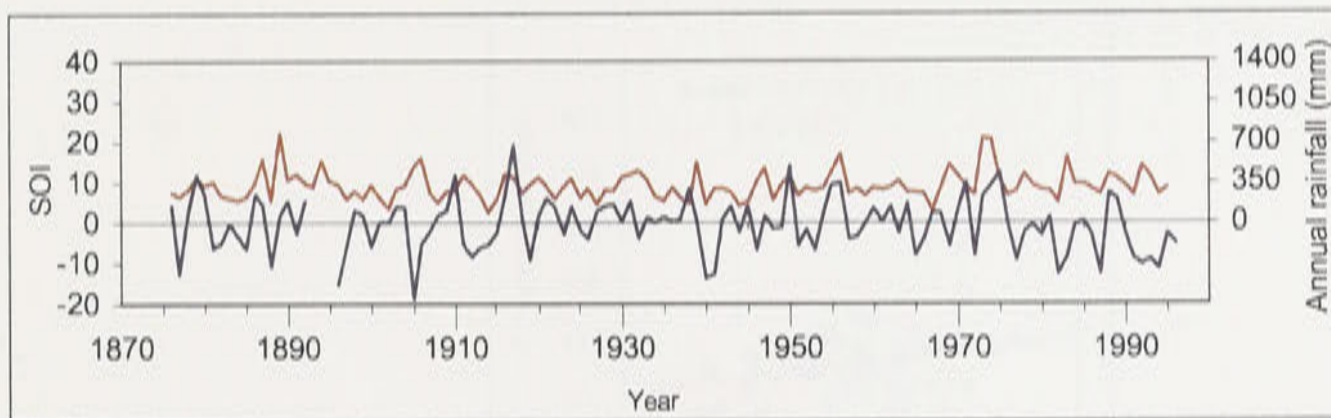
(a) Cowra (063022)



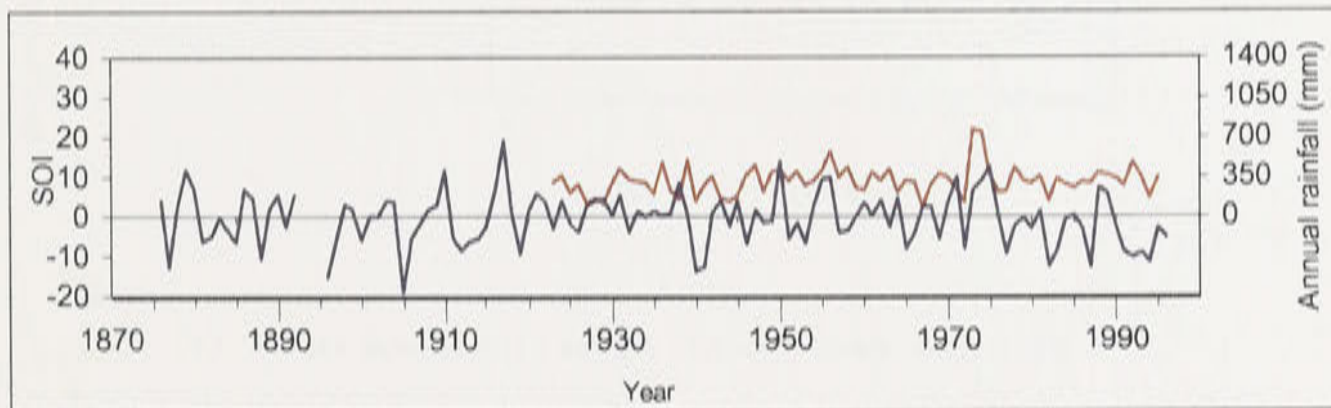
(b) Forbes (065016)



(c) Condobolin (050014)

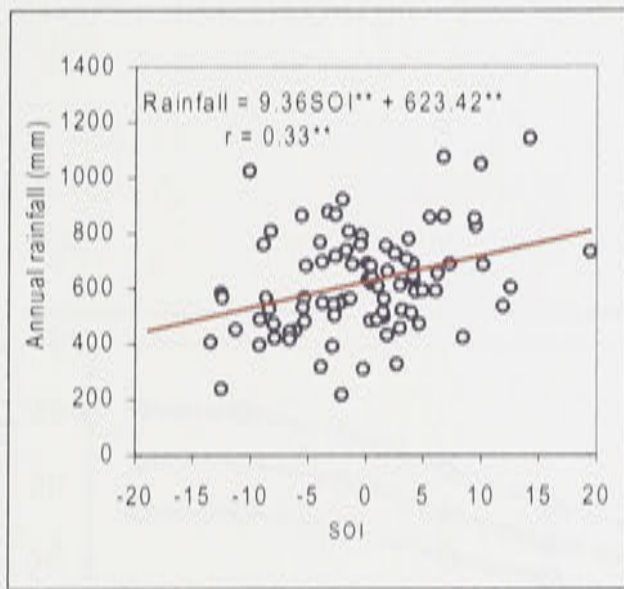


(d) Booligal (075069)

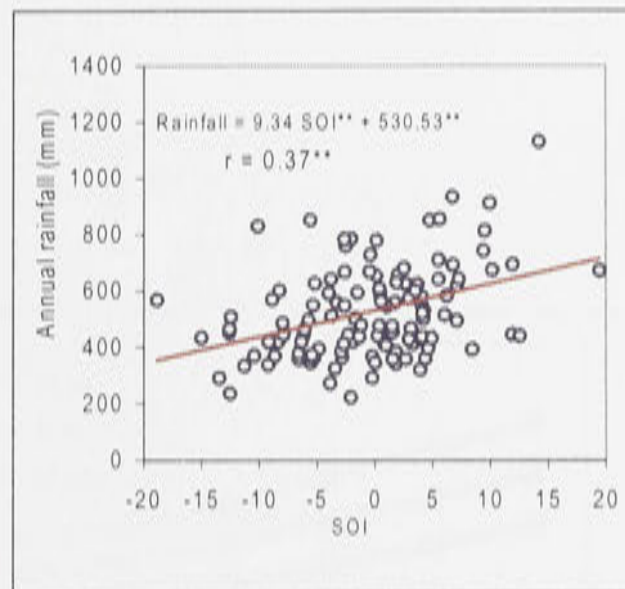


(e) Oxley (049055)

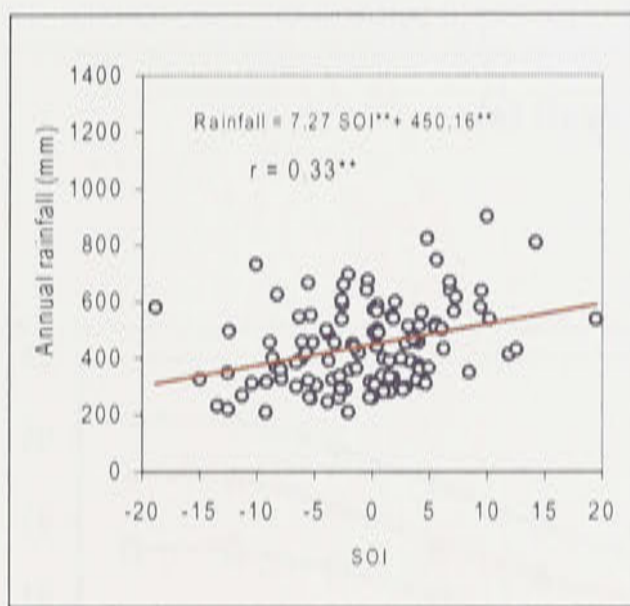
Figure 2.9: Annual southern oscillation index (*SOI*) and annual rainfall at five stations in the Lachlan Valley.



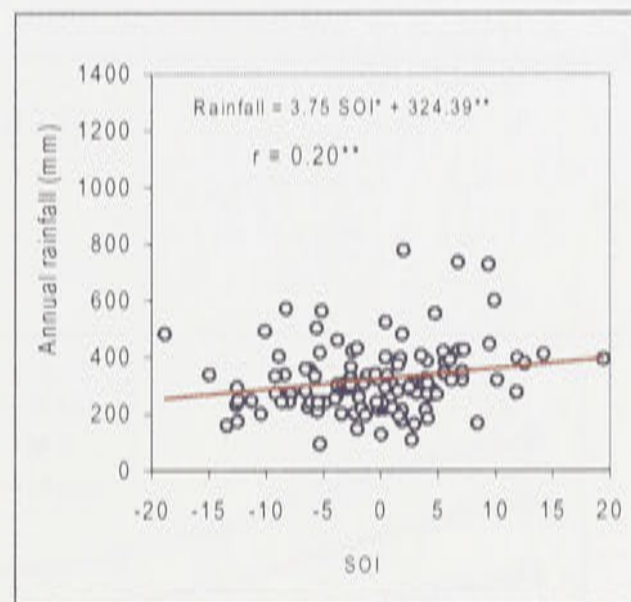
(a) Cowra (063022)



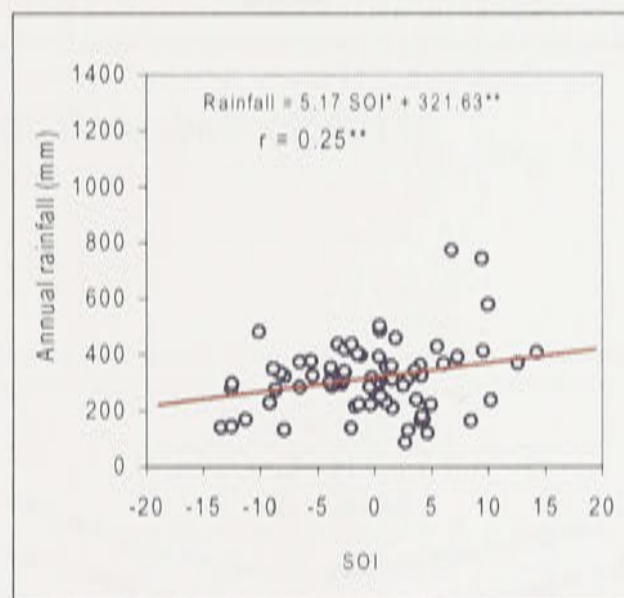
(b) Forbes (065016)



(c) Condobolin (050014)



(d) Booligal (0750069)

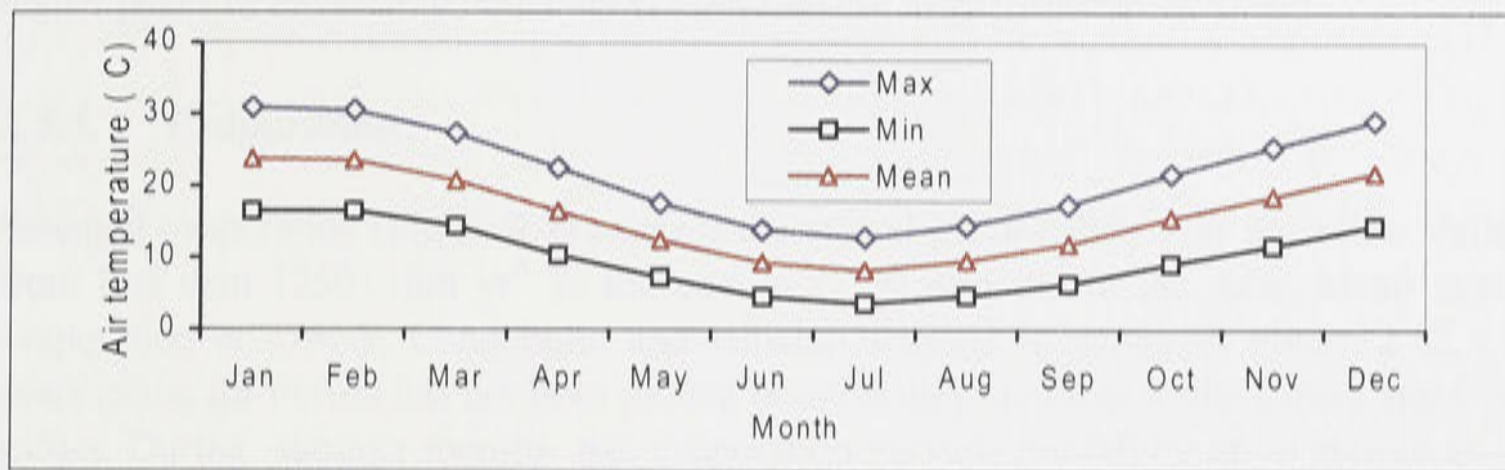


(e) Oxley (049055)

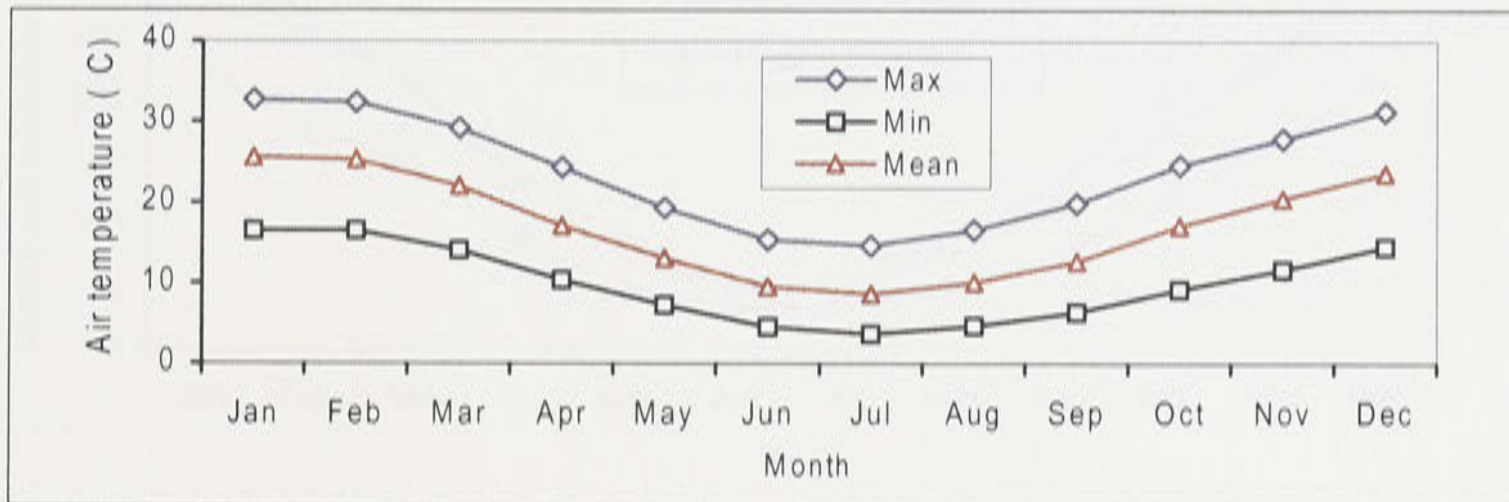
Note:

**,* means significant at 1 and 5% probability levels, respectively.

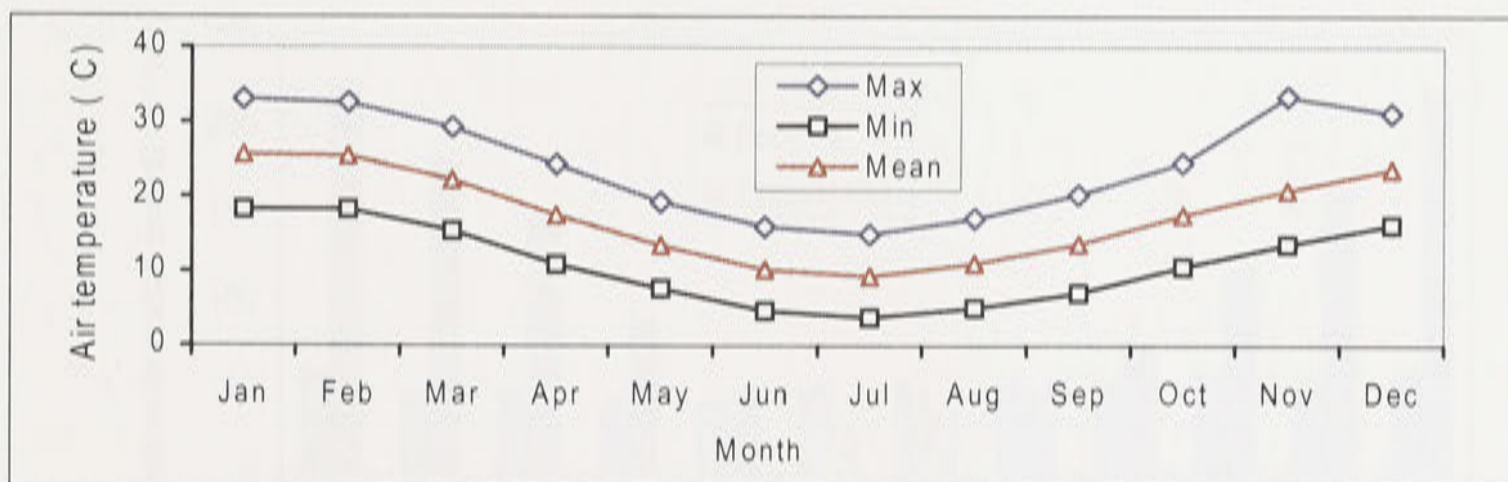
Figure 2.10: Relationship between southern oscillation index and annual rainfall at five stations in the Lachlan River Valley.



(a) Cowra (063022)



(b) Condobolin (050014)



(c) Hillston (075032)

Figure 2.11: Monthly mean daily air temperature at Cowra, Condobolin and Hillston stations.

The average sunshine duration in the Valley ranges from 5 to 6 hr d⁻¹ in June, and from 9.7 to 11.4 hr d⁻¹ in January (Department of Water Resources, 1989). Wind speeds over the Valley are mainly light to moderate, but higher wind speeds (about 65 km hr⁻¹) may be experienced over the higher peaks of the eastern boundary (Department of Water Resources, 1989).

2.5.3. Evaporation

Potential evaporation (Figure 2.2) exceeds the annual precipitation over the entire Valley, rising from less than 1250 mm yr⁻¹ in the east to 1,750 mm yr⁻¹ in the west. Mean monthly pan evaporation at Cowra, Condobolin and Hillston stations is shown in Figure 2.12. Potential evaporation for Forbes has not been plotted because they are close to the Cowra and Condobolin values. During summer months pan evaporation exceeds rainfall by up to sixfold as shown in Figure 2.13 for Cowra.

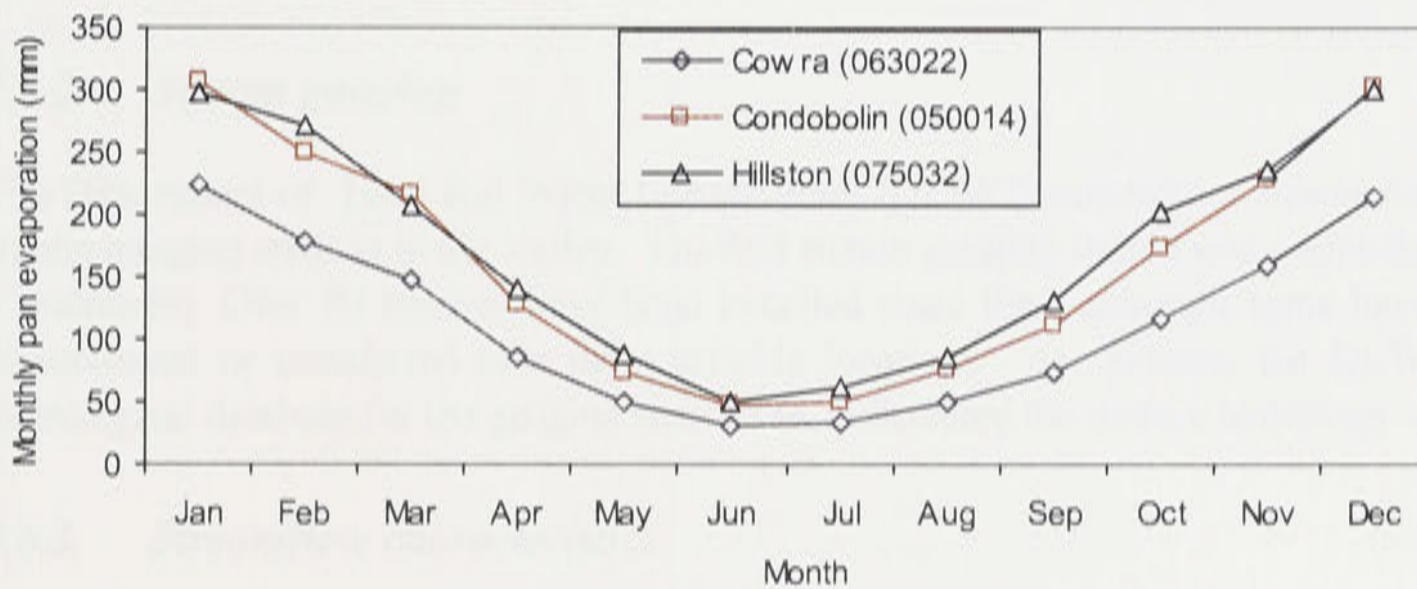


Figure 2.12: Mean monthly pan evaporation at Cowra, Condobolin and Hillston.

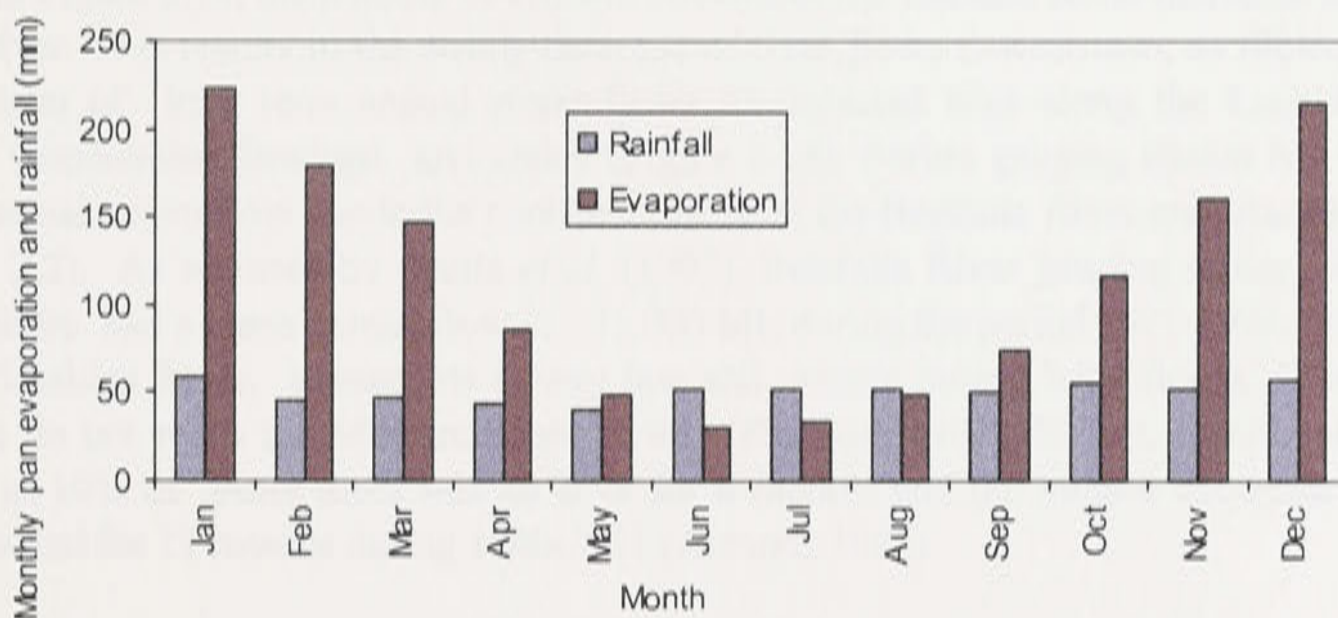


Figure 2.13: Comparison of mean monthly pan evaporation and mean monthly rainfall at Cowra.

2.6 Hydrology

2.6.1. Average runoff

The significant runoff sources in the Valley come from the 20% of the Valley upstream of Mandagery Creek confluence near Eugowra (Figure 2.2), with little contribution from the flat plains west of Condobolin. According to the Department Water Resources (1989), the average annual runoff in the Valley which appears in stream channels after losses due to evaporation, transpiration and deep seepage is about 1,325,000 ML. This is approximately 4 % of the annual rainfall over the entire Valley.

In a recent study of the Lachlan hydrology by Panta *et al.* (1997), the estimated average annual inflow for the entire reach of the Lachlan River was 2,500,000 ML. Of this, 44% is from the Wyangala Dam, 36% from the gauged tributaries and 20% from the ungauged tributaries. Only 283,000 ML yr⁻¹ of streamflow passes beyond Booligal due to irrigation water diversions, evaporation, groundwater recharge and diversion into the effluent creeks.

2.6.2. Stream gauging

The Department of Land and Water Conservation (DLWC) maintains a substantial network of stream gauging stations in the Valley. The first stream gauging station was established in 1891 at Condobolin. Over 90 stations have been installed since then, although some have either been discontinued or transferred to a more suitable locations. At present, the DLWC maintains hydrological database for the gauging stations to understand the surface hydrology of the Valley.

2.6.3. Streamflow characteristics

2.6.3.1 Annual streamflows

The waterway area of the main channel of the Lachlan River tends to progressively decrease downstream. This is very similar to all major western flowing rivers in eastern Australia. As shown in Figure 2.14, the number of effluent streams of the Lachlan River increases downstream of the river. This results in the steady decrease of river flows downstream, as illustrated by the comparison of long term annual streamflows for selected sites along the Lachlan River at Forbes, Condobolin, Booligal and Oxley (Figure 2.15). Forbes gauging station has the highest mean annual streamflow due to the contributions from the Belebula River and Mandagery Creek (Figure 2.2). As reported by Panta *et al.* (1997), Belebula River gauging station 412009 at Canowindra had a mean annual flow of 195,000 ML during the period 1971-1994. Downstream of the Lachlan River, streamflow is very low and except during large floods, flows from the Lachlan do not reach the Murrumbidgee River (Fleming, 1982). In fact, records show that at Oxley, in 10% of years there was no flow for 6 months and the longest continual no flow at Oxley lasted for 11 months during 1940-1941 (Alvarez, 1982).

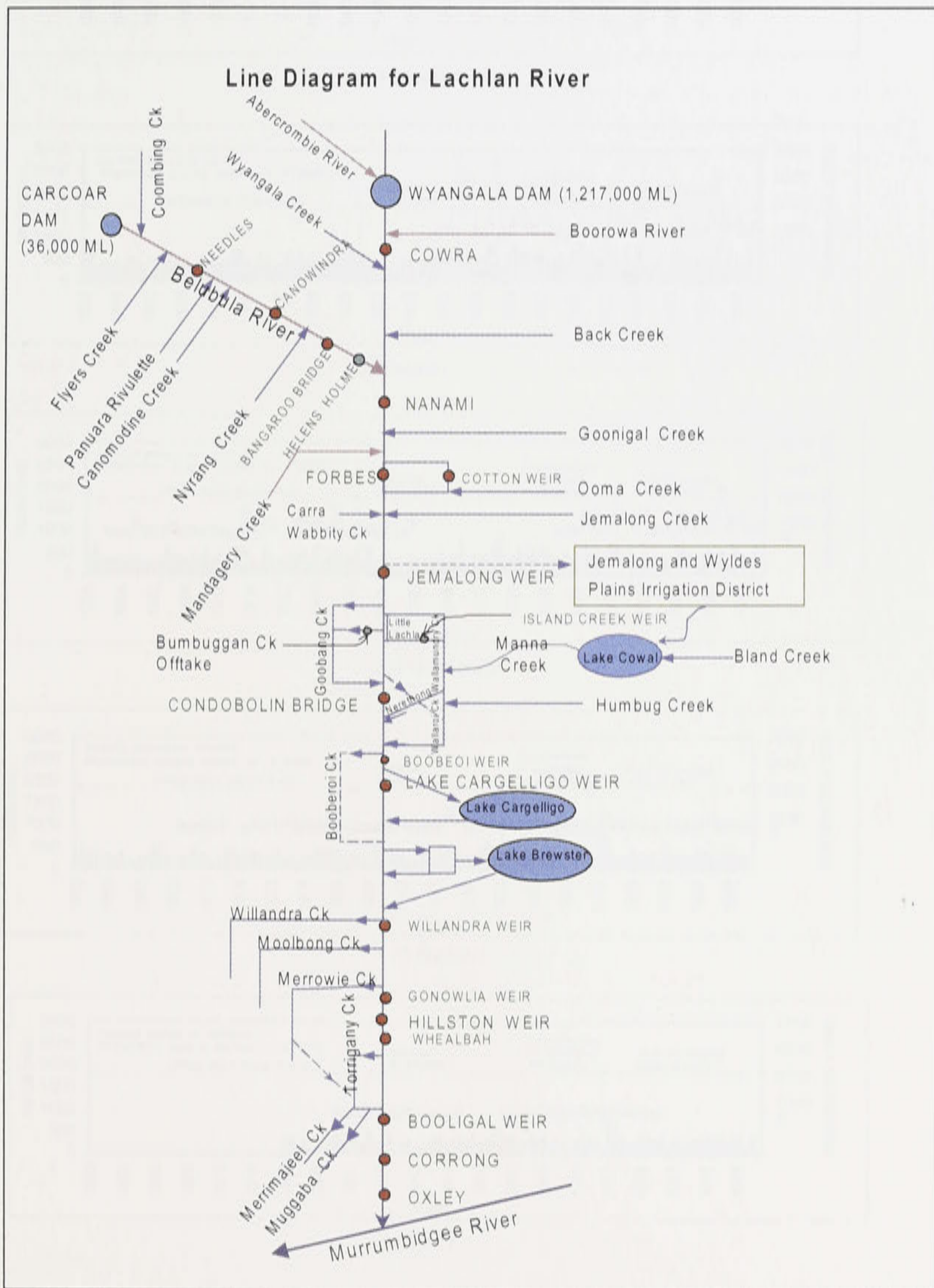
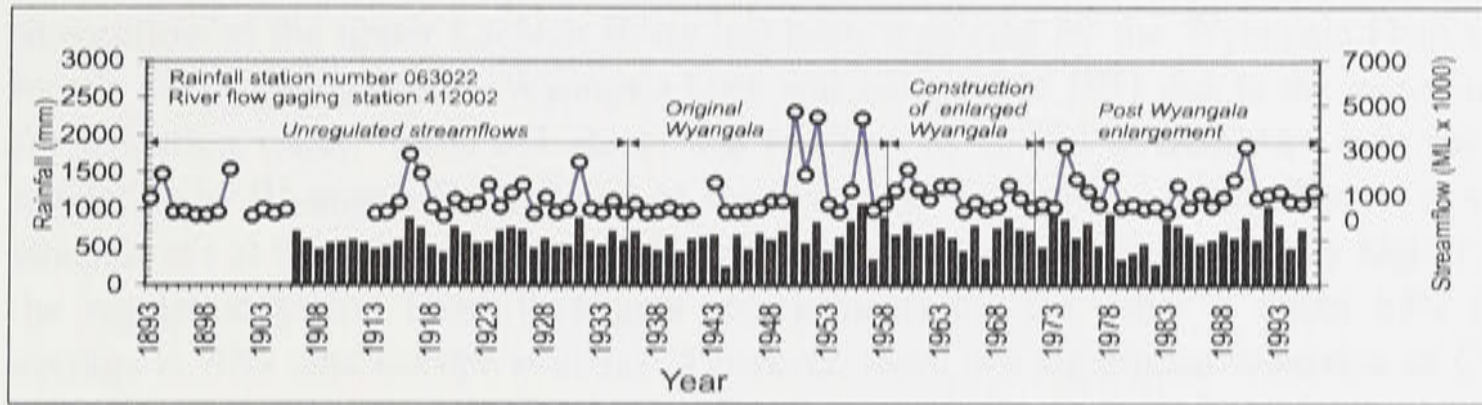
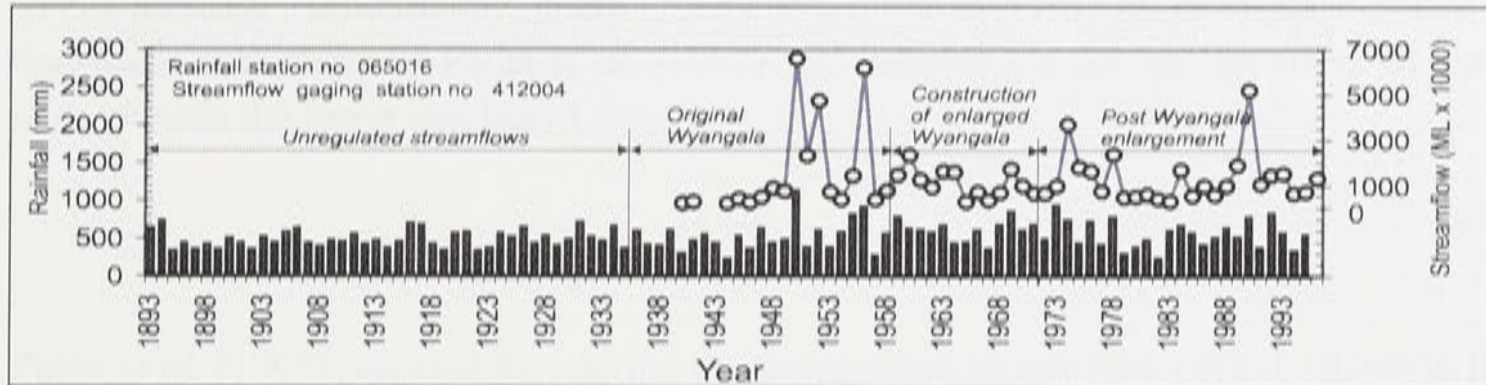


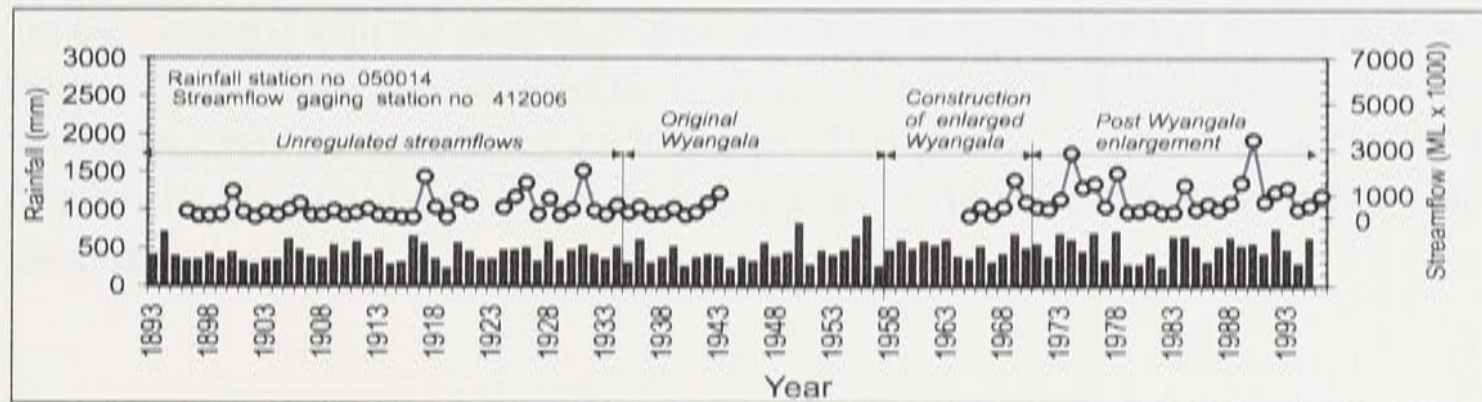
Figure 2.14: Line diagram of the Lachlan River (modified from Department of Land and Water Conservation, unpublished).



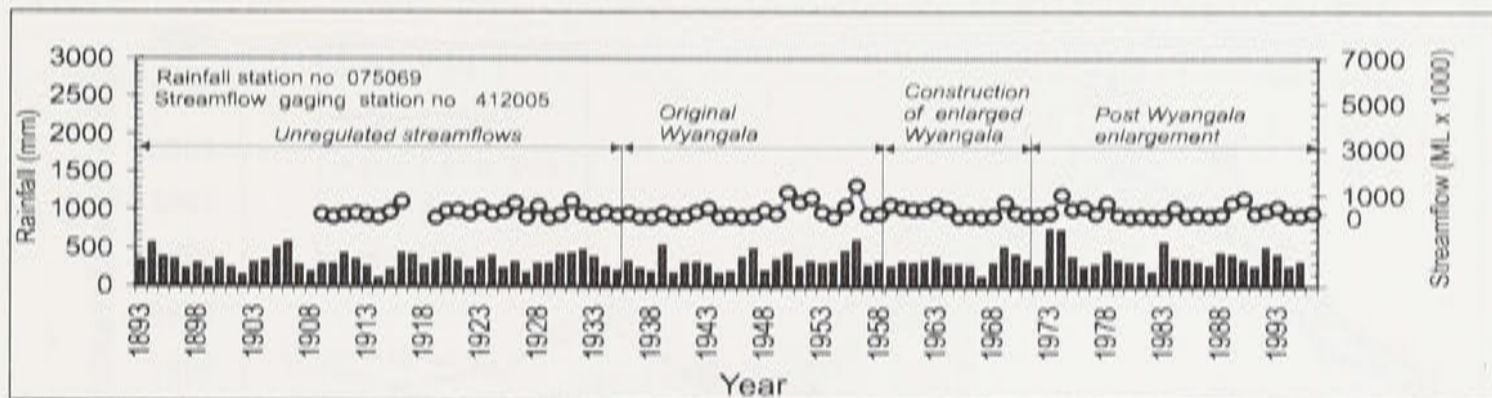
(a) Cowra



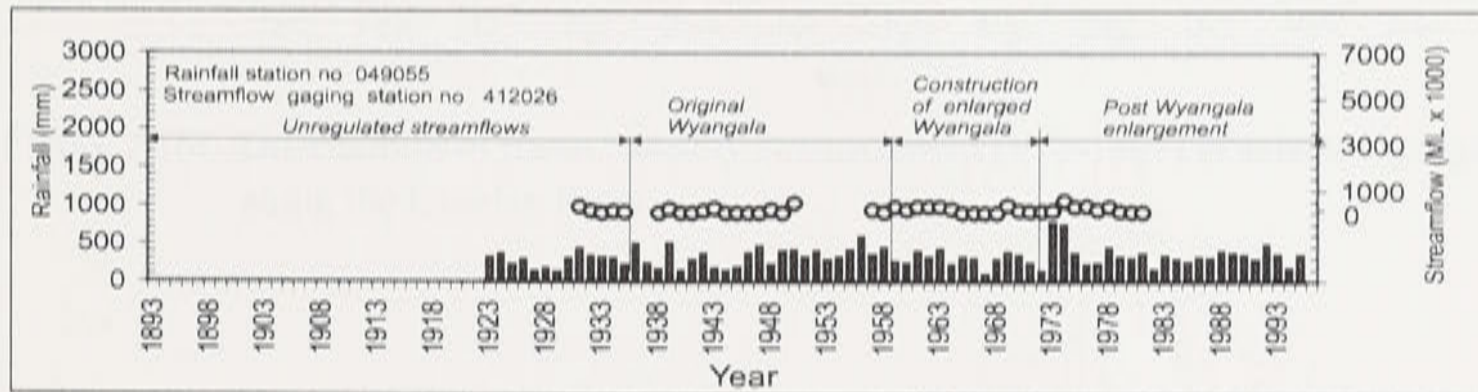
(b) Forbes



(c) Condobolin



(d) Booligal



(e) Oxley

Figure 2.15: Annual streamflow (circles) and rainfall (bars) at the selected gauging stations along the Lachlan River.

Streamflow at the upper Lachlan River has been regulated by the Wyangala Dam since 1936, mostly for irrigation needs. Wyangala Dam was enlarged in 1971 due to the increasing demand for irrigation water. Table 2.3 shows the analysis of annual streamflows over the period of regulation by Wyangala Dam. Based on the results of the analysis, the coefficient of variation of streamflows at the selected gauging stations in the Lachlan River is relatively high. Even during the regulation period (post Wyangala enlargement) the Cv value is about 85% (Australian average is 70% and Europe is 20%). However, there is a significant reduction of Cv by about 29% at Cowra and 25% at Condobolin gauging stations, respectively between pre-regulation and post Wyangala enlargement periods. The Cv values during the post Wyangala enlargement (after 1972) increase downstream from 75 % at Cowra to 97% at Booligal. These results are consistent with those of Panta *et al.* (1997) and indicate the decreasing effect of the Wyangala dam towards the lower reaches of the river.

2.6.3.2 Monthly streamflows

Panta *et al.* (1997) reported that during the unregulated streamflow period, flows in the Lachlan River are very seasonal. Natural streamflows are high from June through October, and lowest in late summer. As a result of streamflow regulation, this pattern has been altered slightly as flows are less seasonal with the peak discharge occurring in September and a secondary peak in April (Figure 2.16). The secondary peak in April is the result of the release of water from the Wyangala Dam for summer crops irrigation. This pattern is observed in Cowra, Forbes and Condobolin gauging stations. No secondary peak in April was observed at Booligal and Oxley gauging stations.

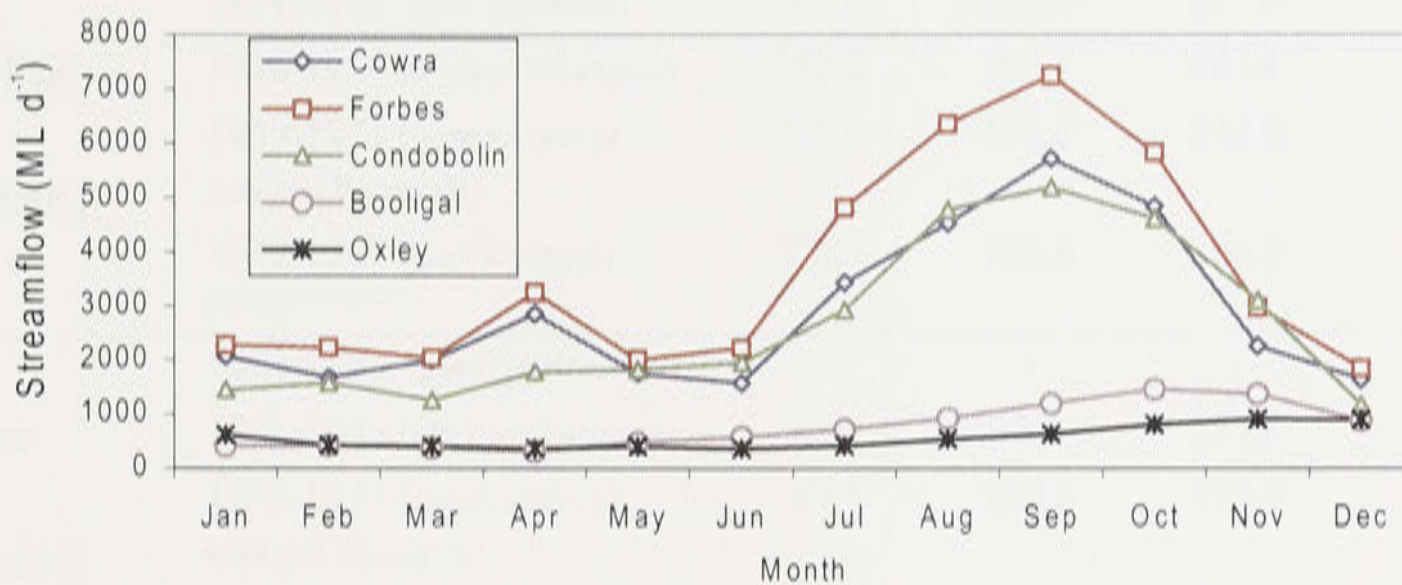


Figure 2.16: Distribution of mean monthly streamflows (1973-1997) at selected gauging stations along the Lachlan River.

Table 2.3: Mean annual streamflow characteristics for selected stream gauging stations at the Lachlan River.

Station and its number	Period	Mean (GL)	Median (GL)	Standard deviation (GL)	Coefficient of variation (%)
Cowra (412002)	1894-1935 ¹ (pre-regulation)	696.7	394.3	738.5	106
	1936-1958 (original Wyangala)	1275.5	601.2	1567.3	123
	1959-1971 (construction of enlarged Wyangala)	964.2	845.0	545.0	56
	1972-1997 (post Wyangala enlargement)	1034.9	837.0	774.2	75
Forbes (412004)	1894-1935 ² (pre-regulation)	-	-	-	-
	1936-1958 (original Wyangala)	1584.3	711.8	2126.7	134
	1959-1971 (construction of enlarged Wyangala)	1121.6	984.1	603.2	54
	1972-1997 (post Wyangala enlargement)	1323.6	996.5	1084.5	82
Condobolin (412006)	1894-1935 ³ (pre-regulation)	423.2	247.7	492.9	116
	1936-1958 ² (original Wyangala)	-	-	-	-
	1959-1971 ² (construction of enlarged Wyangala)	-	-	-	-
	1972-1997 (post Wyangala enlargement)	937.7	626.1	812.6	87
Booligal (412005)	1894-1935 ⁴ (pre-regulation)	245.0	174.0	217.0	89
	1936-1958 (original Wyangala)	362.0	190.7	402.4	110
	1959-1971 (construction of enlarged Wyangala)	308.0	370.0	232.0	75
	1972-1997 (post Wyangala enlargement)	273.7	162.8	266.8	97
Oxley (412045)	1894-1935 ² (pre-regulation)	-	-	-	-
	1936-1958 (original Wyangala)	99.0	33.3	127.8	129
	1959-1971 (construction of enlarged Wyangala)	167.5	165.6	126.0	75
	1972-1997 ⁵ (post Wyangala enlargement)	-	-	-	-

¹ Three years of missing data (1906-1908)

² Not calculated because of many missing data

³ Five years missing data (1901, 1916, 1917, 1922, 1923)

⁴ Four years of missing data

⁵ Gauging station discontinued

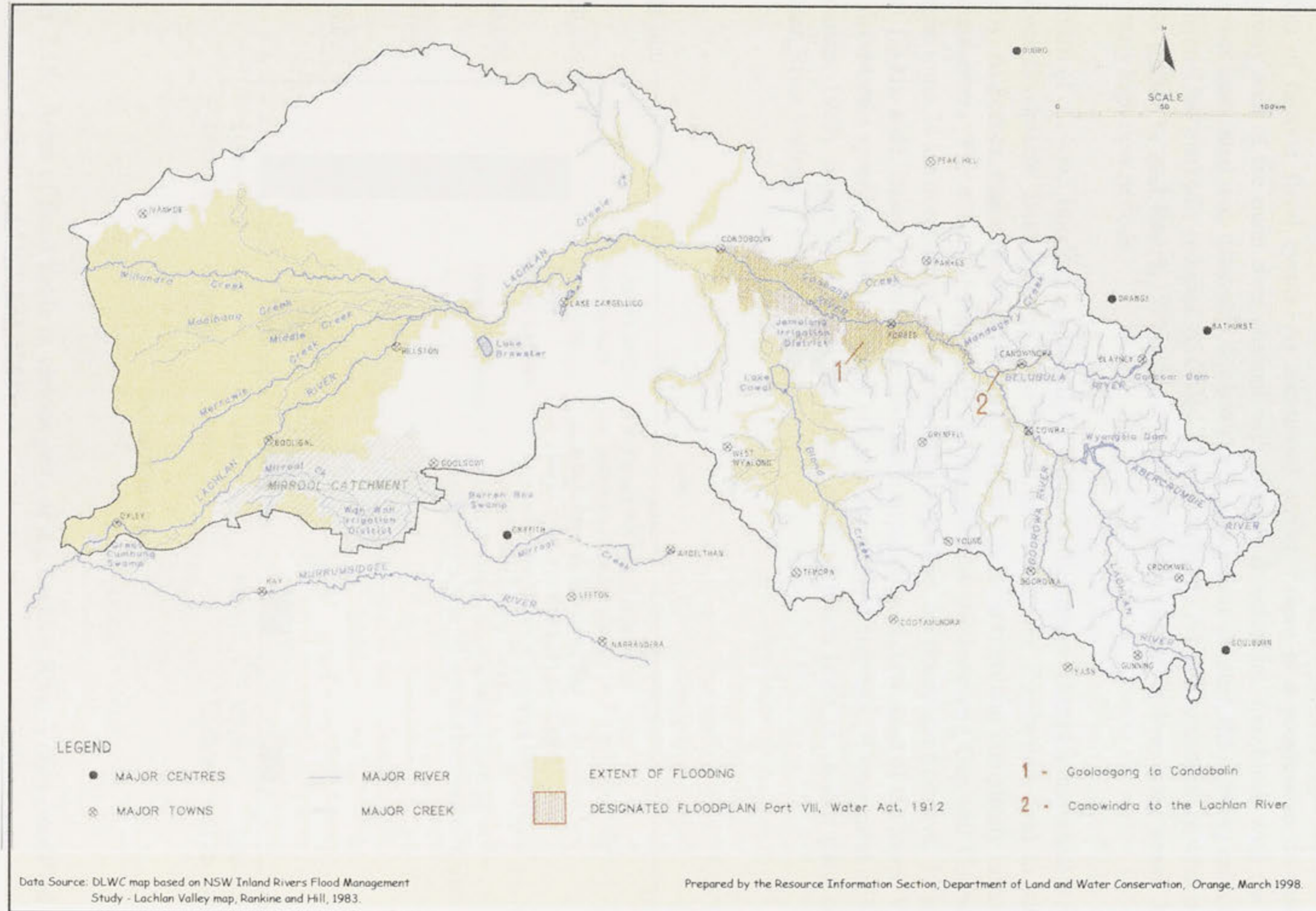


Figure 2.17: Extent of flooding in the Lachlan River Valley (modified from Department of Land and Water Conservation, 1998).

2.6.4 Flood and drought

About one third of the Valley is flood-prone (Figure 2.17) due to the characteristics of the Lachlan River. A floodplain management study of the Lachlan River Valley by Rankine and Hill Pty Ltd (1983) estimated the flood-labile area in the Valley to about 28,440 km², of which 19,300 km² (68% of the flood-labile area) was in the lower Lachlan below Hillston. This was based on studies of historic flood events. As mentioned earlier, there is a progressive decrease of waterway area of the main river channel with distance downstream. Combined with the slow velocities associated with extremely flat bed slopes of the river channel, the carrying capacity of the channel has markedly reduced. At Oxley, channel capacity is barely one-tenth of what it is in Forbes (Solomon and Roberts, 1997). As a result flooding occurs in low lying areas during extremely high flow periods.

Upstream of Cowra, flooding is generally confined to the stream channels and small areas of adjacent floodplains. Below Cowra, the terrain moderates, and floodwaters tend to subside quickly. At Forbes, major floods divide the town into three sections and completely isolate the business centre. The effects of big floods are increased by the Jemalong Gap and Corradgery Ranges, some 24 km downstream of Forbes, which constrict the floodplain from over 11 km to about 1.5 km wide. Below Hillston, the floodplain expands to occupy most of the lower Valley and floodwaters spread out through many effluent streams and channels (Department of Water Resources, 1989). Figure 2.18 shows the extent of flood prone lands in various parts of the Lachlan River Valley.

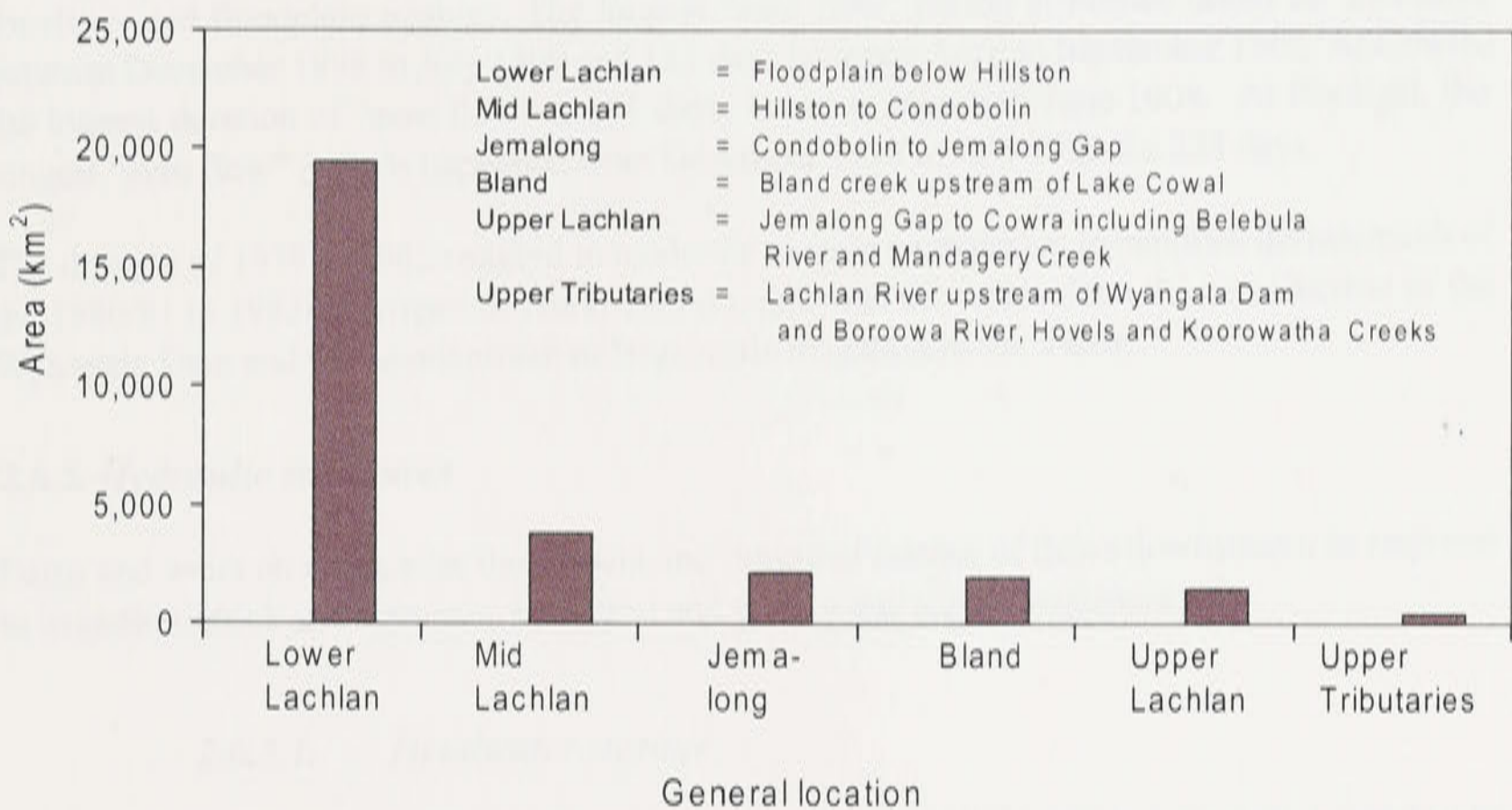


Figure 2.18: Areas of flood liable in various parts of the Lachlan River Valley (modified from Rankine and Hill Ltd, 1983).

Flood data are available from the Department of Land and Water Conservation, the Bureau of Meteorology and the New South Wales State Emergency Services. Measurement of stream heights in the Lachlan River Valley commenced in December, 1891 following the establishment of a gauging station at Condobolin on the Lachlan River. The history of Lachlan River Valley flooding commences with a flood in 1870 which would have reached 10.62 m on the Forbes Iron Bridge gauge (Rankine and Hill, 1979). This record stood until 18th June 1952, when a height of 10.78 m was recorded. Figure 2.15 shows the recorded annual streamflows at several gauging stations along the Lachlan River .

Following major flooding during 1974 and 1975, many residents of the Lachlan Valley pressed for greater use to be made of Wyangala Dam for flood mitigation (Water Resources Commission, undated). Study of flood mitigation options in the Lachlan River Valley was also undertaken by Rankine and Hill Ltd (1979). Options included flood mitigation dams, off-river storages, channel improvements, defined floodways, and non-structural mitigation measures (zoning ordinances, land use conversions, permanent evacuation, insurance, flood forecasting and warning).

Panta *et al.* (1997) examined the effect of Wyangala Dam on the magnitude of floods on the immediate downstream using flood frequency analysis. They found that the dam has reduced the magnitude of once in 10 year flood by about 40% in peak daily discharge. However, it has a little effect on smaller floods.

When Wyangala Dam, Lake Brewster and Lake Cargelligo are full, there is adequate stored water to supply a full year's irrigation demand without endangering towns and other users whose access to water supply must be protected (Department of Water Resources, 1989).

Droughts are as natural as floods for inland river valleys in semi-arid areas and equally important for rivers and floodplain ecology. The longest "zero flow" period at Forbes lasted for 224 days between December 1898 to July 1899 and 183 days between April to September 1902. At Cowra, the longest duration of "zero flow" is 111 days, between March to June 1908. At Booligal, the longest "zero flow" periods happened from December 1919 to July 1920 for 228 days.

The drought of 1979 to 1982 resulted in moderate to severe restriction to supplies during much of the 1980/81 to 1983/84 irrigation years. This drought was the worst since the construction of the Wyangala Dam and the development of large-scale irrigation in the Valley.

2.6.5. Hydraulic structures

Dams and weirs on rivers alter the amount and timing of release of flows downstream in response to irrigation, stock and domestic, industrial and town water supply requirements.

2.6.5.1. Headwater storage

Table 2.4 lists the dams of the Lachlan River Valley which had undergone special scrutiny by the Dam Safety Committee NSW (1995).

The Wyangala Dam, constructed between 1928-1935 and enlarged between 1961-1971, is the major headwater storage in the Valley with a maximum storage capacity of 1,217,000 ML. It is located approximately 50 km upstream from Cowra and is fed by Abercrombie and Lachlan Rivers. The dam is a concrete gravity structure with eight large radial spillway gates. When the

Table 2.4. Dams in the Lachlan Valley.

Dam	River/ Watercourse	Storage (ML)	Owner
1. Bergalia	Bergalia Creek	480	Parkes Shire Council
2. Bogolong	Bogolong Creek	360	Central Tablelands County Council
3. Boorowa	Boorowa River	180	Boorowa Council
4. Carcoar	Belebula River	36,000	DLWC
5. Company	Un-named	113	Weddin Council
6. Crookwell	Kentgrove Creek	450	Crookwell Council
7. Junction Reef	Belebula	7,300	DLWC (State Lands)
8. Endeavour	Billabong Creek	2,400	Parkes Shire Council
9. Rowlands	Coombing Creek	4,690	Central Tablelands County Council
10. Wyangala	Lachlan and Abercrombie	1,217,000	DLWC

Source: Dams and Safety Committee, NSW (1995).

dam is full, the impoundment extends 35 km up to Abercrombie River and 42 km up the Lachlan River. The dam services properties as far downstream as Hillston which is 633 km downstream of the dam.

Carcoar Dam, completed in 1970 as the second headwater storage, is a double-curvature concrete arch dam located on the Belebula River. It has a storage capacity of 36,000 ML with a maximum crest length of about 268 m and maximum height of 52 m.

2.6.5.2. *Diversion weirs*

Jemalong Weir (Figure 2.14) was constructed in 1940 to provide a pool level suitable for diversion of water to the Jemalong and Wyldes Plains Irrigation District (Department of Water Resources, 1989). The active weir pool capacity of 1,600 ML also permits minor short-term re-regulation of the Lachlan River flow. Water can be supplied to the irrigation district at a rate of 800 ML d⁻¹ (Department of Water Resources, 1989). The weir was made of concrete with 3 vertical lift steel gates each 12.2 m wide by 5.5 m high. A slide gate by-pass, 1.8 m x 1.4 m, is provided in each abutment. The offtake regulation for Jemalong supply channel located outside the left abutment is controlled by a 4.1 m wide and 1.5 m high radial gate.

Booberoi Weir (Figure 2.14) was completed in 1913 and diverts water into Booberoi Creek. Other weirs capable of diverting flows during the autumn/spring period for stock and domestic use along the Lachlan River are :

- Willandra Weir, constructed in 1891 on the Lachlan, serving landholders in Willandra Creek.
- Gonowlia Weir, constructed in 1957 on the Lachlan, serving the Merrowie Creek Water Trust District.
- Torriganny Weir, originally built in 1933 and replaced in 1961 on the Torriganny Creek, and anabranch of the Lachlan to serve the Muggabah, Torriganny and Merrimajeel Water Trust Districts.

2.6.5.3. Enroute storages

Lakes Cargelligo and Brewster are the two large enroute storages that permit re-regulation of flows to the Lower Lachlan. Situated 40 km apart and with no significant catchment of their own, the storages are replenished from surplus flows in the Lachlan (Department of Water Resources, 1989). Inlet and outlet channels, and diversion and regulation structures have been provided for each storage. Lake Cargelligo has a total storage capacity of 36,000 ML and useable capacity of 23,000 ML. Lake Brewster has a storage capacity of 153,000 ML with 133,000 ML useable.

2.6.6. Surface water usage

The current total surface water allocation from the Lachlan system for irrigation, town water supply, stock and domestic and industrial uses is approximately 600,000 ML per annum (Department of Water Resources, 1989).

Surface water usage in the Valley is influenced by seasonal irrigation demands and water availability. Figure 2.19 shows the irrigation usage and area within the regulated Lachlan system. Based on this figure, annual irrigation water use per hectare ranges from 5 to 10 ML ha⁻¹. (500 to 1000 mm). Irrigation is the greatest user of surface water, accounting for approximately 93% of all surface water used in 1993/94 (Department of Water Resources, 1994).

No accurate data on water usage is available on unregulated streams. However, there are some evidences that a number of unregulated streams such as the Boorowa River, Mandagery Creek, Goobang Creek and Burrangong Creek have a relatively high level of extraction (Department of Land and Water Conservation, 1998).

Data on trends and actual domestic/urban use of water is very limited owing to the disparate nature of available data (Department of Land and Water Conservation, 1998). A summary of water supply schemes operating in the Lachlan Valley is shown in Table 2.5.

Table 2.5: Water supply schemes serving the Lachlan Valley.

Water supply schemes and towns supplied	Estimated population supplied	Local government	Source of supply
<i>Condobolin</i>	3,500	Lachlan	Lachlan River/Goobang Creek
<i>Cowra Villages</i> Bendick Murrel, Crowther, Greenthorpe, Koorawatha, Noonbinna, Wattamondara, Warrangong, Wirrimah	650	Cowra	Lachlan River
<i>Cowra</i>	8500	Cowra	Lachlan River
<i>Crookwell</i>	2500	Crookwell	Kentgrove Creek
<i>Dalton</i>	130	Gunning	Golong Creek Borefield
<i>Euabalong</i> Euabalong, Euabalong West	300	Cobar	Lachlan River
<i>Forbes</i>	7000	Forbes	Lachlan River/ Grawlin Borefield
<i>Forbes-Tottenham</i> Albert, Bogan Gate, Gunningland, Tottenham, Trundle, Tullamore	2000	Forbes	Lachlan River
<i>Lake Cargelligo</i> Lake Cargelligo, Tullibigeal	1200	Lachlan	Lake Cargelligo
<i>Rankin Springs</i>	100	Carrathool	Myall Park Channel/Murrumbidgee River
<i>Wyangala</i>	140	Cowra	Lachlan River
<i>Boorowa</i>	1200	Boorowa	Boorowa River
<i>Central Tablelands</i> Blayney, Carcoar, Cargo, Canowindra, Cudal, Eugowra, Grenfell, Gooloogong, Lyndhurst, Mandurama, Manildra, Millthorpe, Morbel, Somers, Woodstock	11,000	Blayney, Cabonne, Weddin, Cowra	Lake Rowlands (Cumbung Rivulet)
<i>Gunning</i>	500	Gunning	Lachlan River
<i>Hillston</i>	1100	Carrathool	Groundwater at Hillston
<i>Ivanhoe</i>	500	Central Darling	Willandra Creek (Turkeys Nest Dam)
<i>Nymagee</i>	40	Cobar	Ground Tank
<i>Parkes</i> Cookamidgera, Muginconble, North Parkes Mine, Parkes, Peak Hill, Tomingley	10,000	Parkes	Billabong Creek/Lachlan Borefield, Beargamil Creek (Lake Endeavour Dam, Beargamil Dam)
<i>Quandialla</i>	170	Weddin	Ground Tank
<i>Riverina Water</i> Temora, Ungarie, Naradhan, Weethalle, West Wyalong, Stockinbingal, Barmedman, Tallimba	10,000	Cootamun- dra, Temora, Bland	Murrumbidgee River and Gumly Gumly Bores

Source of data: Department of Water Resources (1994).

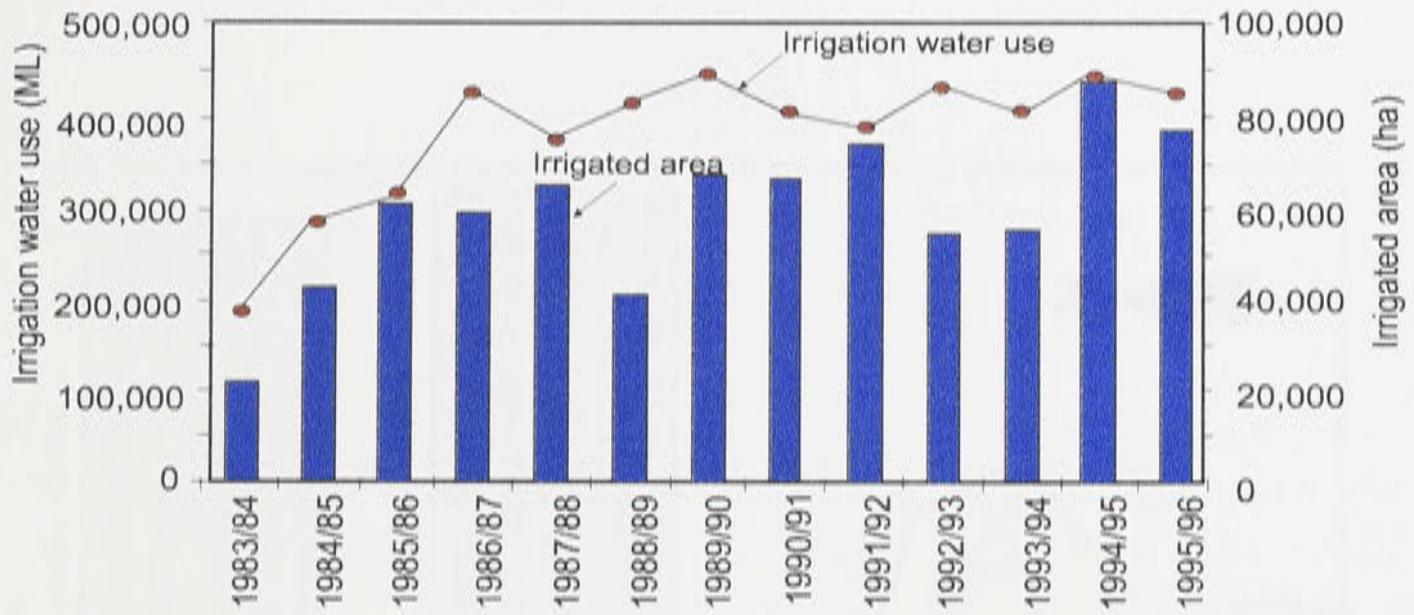


Figure 2.19: Irrigation water use and irrigated area in the regulated Lachlan System, 1983-1996 (modified from Department of Land and Water Conservation, 1998).

2.6.7. Surface water quality

Water quality has been a critical issue throughout the Valley (Sainty and Roberts, 1997; Department of Land and Water Conservation, 1998). It is commonly believed that the water quality in the Valley has deteriorated over time. Though scientific data is deficient, there is an indication of the rise of saline inflows, turbidity due to siltation, water-borne diseases, nutrients from farm animal sources carried by runoff and impact of industries and urban communities (Total Catchment Management, 1993).

The Department of Land and Water Conservation (1996c) has developed broad water quality ratings based on the national and state water quality guidelines for the Key Sites Monitoring Program. The Key Sites Water Quality Monitoring Program monitors water quality at 11 sites (Figure 2.20) evenly distributed throughout the Lachlan River Valley. Monitoring sites have been also established at the main water storages of Carcoar and Wyangala Dam, and Lake Cargelligo and Brewster. The key sites program is designed to detect long term trends in quality of surface water using turbidity, total phosphorus and electrical conductivity as the primary indicators.

2.6.7.1. Stream salinity

Salinity levels in the Lachlan River are normally in the medium range, that is, the river water has an electrical conductivity between 300 and 800 $\mu\text{S cm}^{-1}$ (Department of Water Resources, 1989). The level of electrical conductivity gradually increases downstream from an average of 410 $\mu\text{S cm}^{-1}$ in gauging station 412002 at Cowra to 550 $\mu\text{S cm}^{-1}$ in gauging station 412045 at Oxley (Figure 2.20). Mean daily salt load which is the product of electrical conductivity, streamflow and 0.64 is highest in gauging station 412004 at Forbes with a value of 665 t day^{-1} . This is because of the largest mean annual streamflow discharge is largest at Forbes. As streamflow reduces downstream, salt load also decreases. However, mean daily salt load per volume ($\text{t d}^{-1} \text{ML}^{-1}$) in the River increases downstream from 0.26 at Cowra to 0.35 $\text{t day}^{-1} \text{ML}^{-1}$

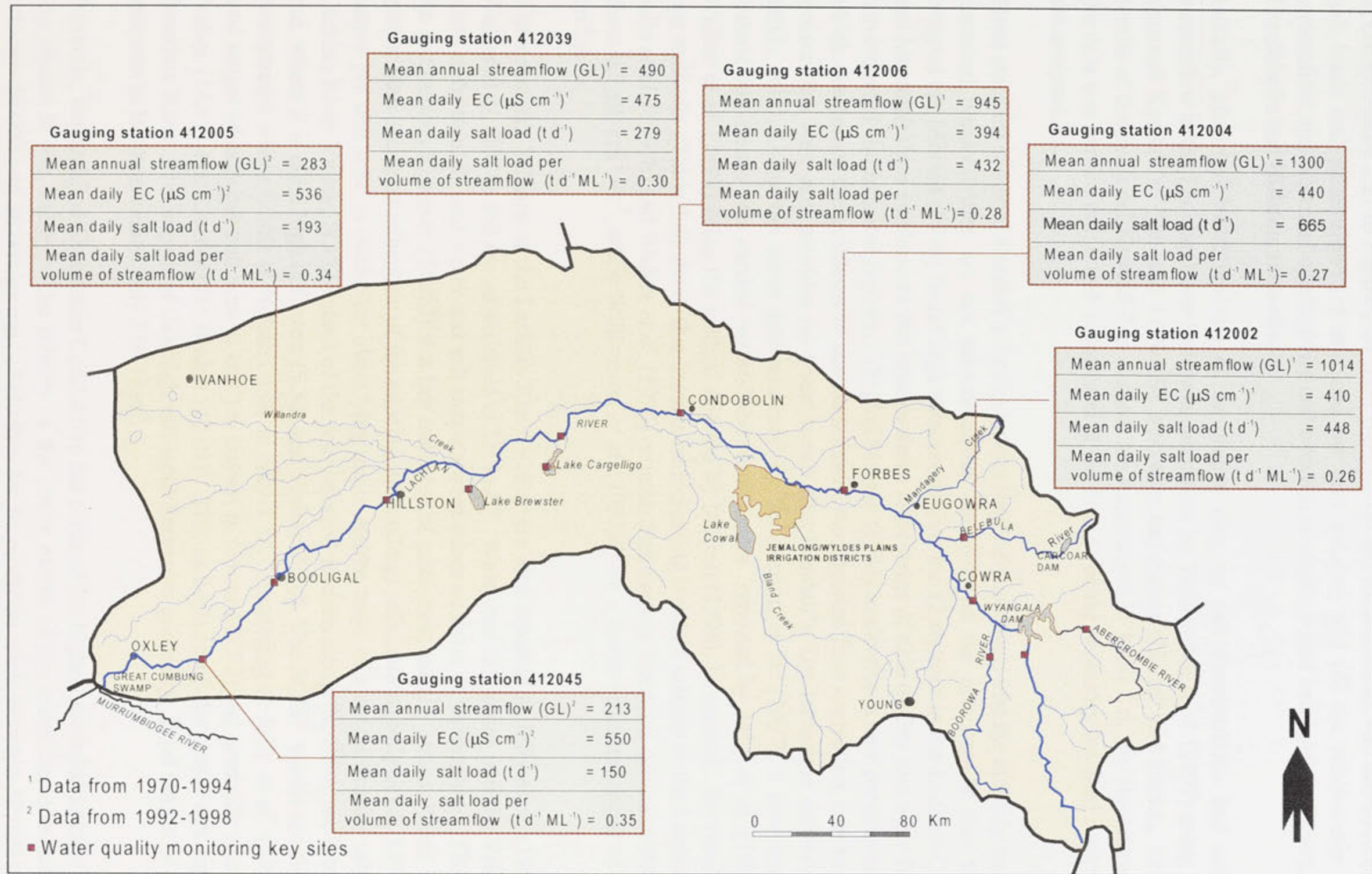


Figure 2.20: Mean annual streamflow, mean daily EC, salt loads and mean daily salt load per volume of streamflow at the selected gauging stations along the Lachlan River.

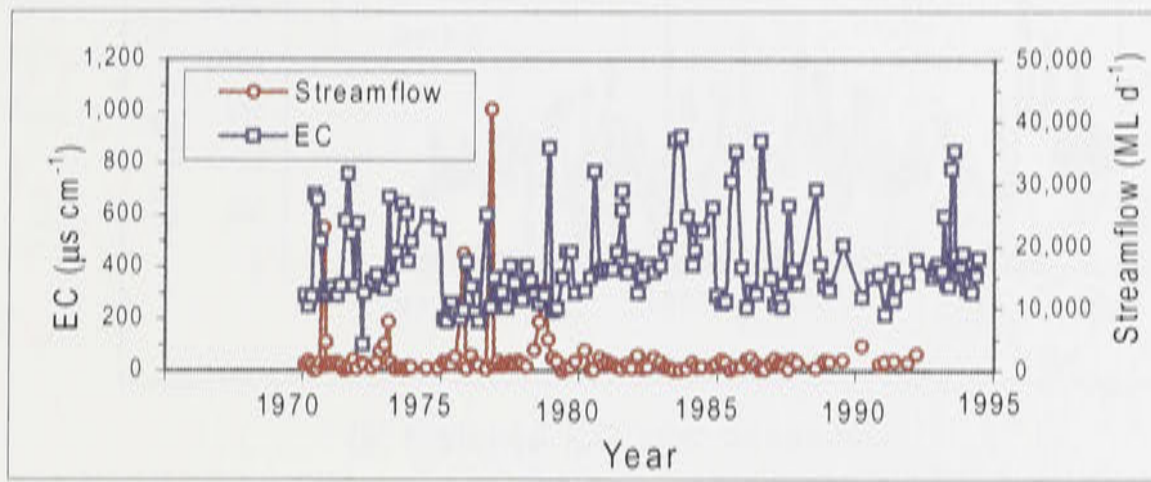
at Oxley. Figure 2.21 to Figure 2.24 show plots of: (a) electrical conductivity and streamflow; (b) salt loads and streamflow; (c) salt load per unit volume; and (d) the relationship between streamflow and electrical conductivity and between streamflow and salt loads at Cowra, Forbes, Condobolin and Hillston, respectively.

Initially, historical trend analysis of the sparse data on salt concentration and saltload of streamflow at the Lachlan River had been carried out by Williamson *et al.* (1997) using standard seasonal Kendall's Tau and LOWESS smoother techniques (Helsel and Hirsch, 1992). The results of the Seasonal Kendall Tau analysis are summarised in Table 2.6. No flow correction of the data was carried out; a task recognised at the time as being necessary for final completion of the analyses.

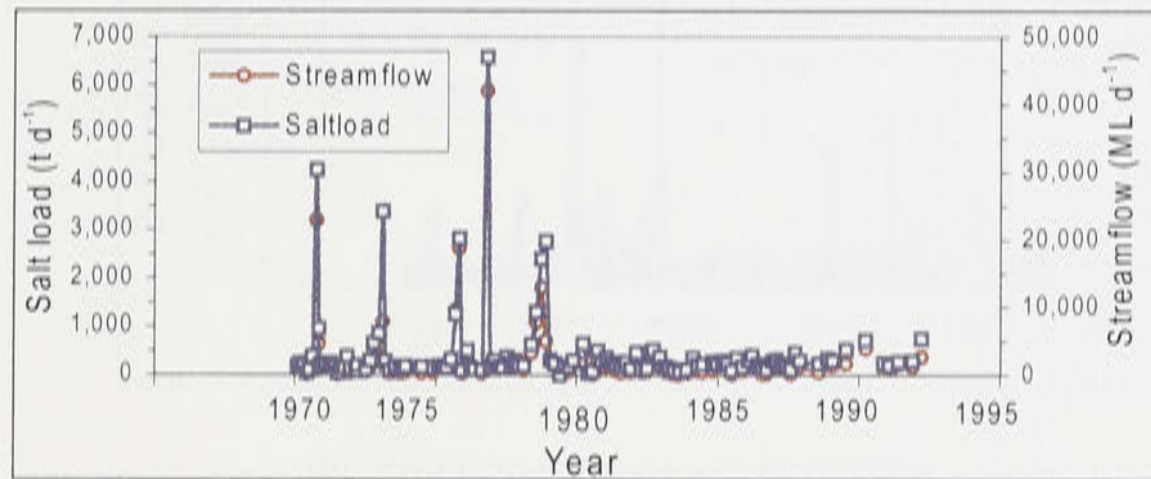
Since standard seasonal Kendall's Tau technique implicitly assumed that the monthly readings of electrical conductivities are not autocorrelated, concerns on the accuracy of this technique cropped up. Morton (1996) found high autocorrelations for 12 stations in the Loddon-Campaspe and Murrumbidgee catchments that encompassed wide range of data quality and were from both non-irrigated and irrigated regions. This led Morton (1996) to develop a new parametric method which overcomes the problems of autocorrelation, incorporates flow correction, can be used on sparser data sets, and provides no linear trends (the Kendall's Tau technique estimates linear trends only). Using the same data sets used by Williamson *et al.* (1997), a new analysis of historic salt trends was carried out and the results were reported by Jolly *et al.* (1997b) and Walker *et al.* (1998) using the method developed by Morton (1996). In general, the results of the two methods (Table 2.6) show that there is an increasing trend of salinity in the Lachlan River. Jolly *et al.* (1997b) and Walker *et al.* (1998) estimated an average electrical conductivity trend of about $6.2 \mu\text{S cm}^{-1} \text{ yr}^{-1}$, while Williamson *et al.* (1997) have a lower estimated trend of $4.8 \mu\text{S cm}^{-1} \text{ yr}^{-1}$.

Water and salt balance of the Lachlan River Valley are also reported in Jolly *et al.* (1997a) and Walker *et al.* (1998) and are summarised in Table 2.7. Water and salt inputs into the Valley were taken to be rainfall, and water and salt outputs were taken as those in streamflow. The ratio of the salt outputs to inputs (SO/SI) is a key indicator of catchment salinity status. A salt O/I ratio greater than one is an indication of the existing (impending) salinisation (Jolly *et al.*, 1997a). Salt output per unit area is useful for identifying major source areas of a catchment for salt. In the Lachlan River Valley, SO/SI values of the four selected stations along the River are greater than one, where it is quite high at Cowra (5.38) and Forbes (4.56). The SO/SI values are decreasing downstream where SO/SI at Hillston weir is only 1.19. According to Jolly *et al.* (1997a), the total output of salts per unit area (t km^{-2}) is highest in Cowra (17.72) and gradually decreases in Forbes (14.67) and Condobolin Bridge (12.01). This is because of the major salt input from Boroowa River. The impact of this high salt input decreases gradually. Total output of salts per unit area in Hillston weir is only 3.04 t km^{-2} .

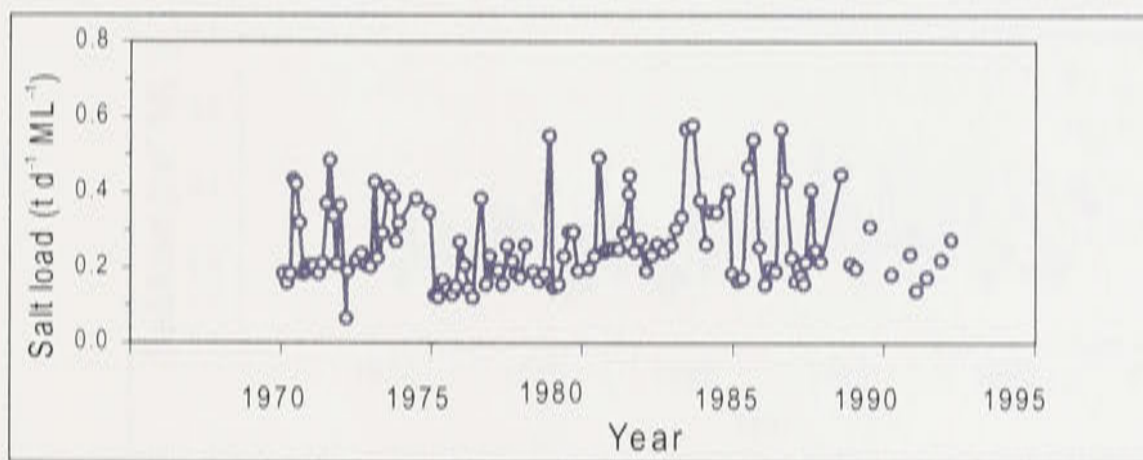
Presently, Bogandillon Creek near Condobolin has some of the highest recorded salinity levels of any stream in the Valley. The salinity of the lower extent of the creek has commonly been between 10,000 and 20,000 $\mu\text{S cm}^{-1}$. Salinities for Bogandillon creek between 30,000 to 50,000 $\mu\text{S cm}^{-1}$ was recorded at Birrack Bridge in the summer of 1994 (Department of Land and Water Conservation, 1998).



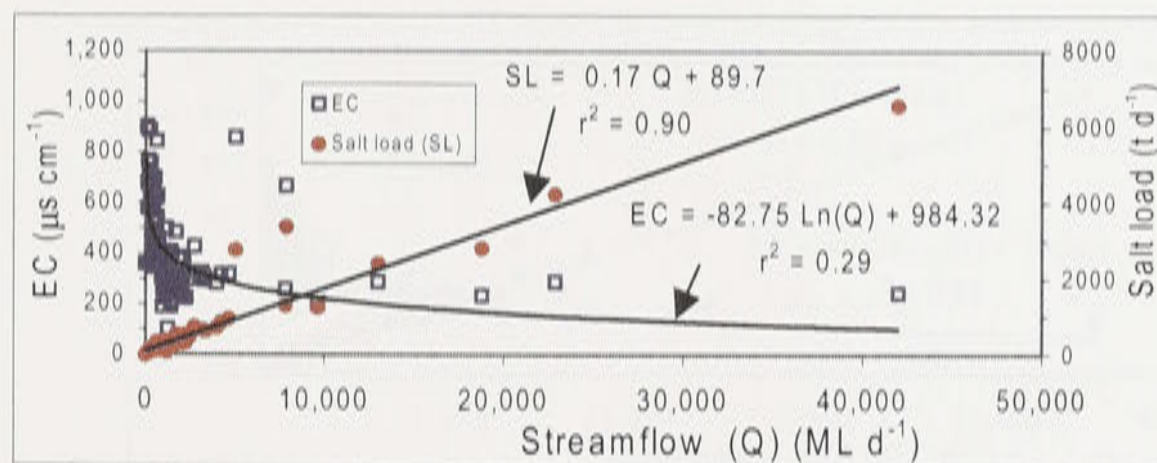
(a) Historical EC and streamflow



(b) Historical salt load and streamflow

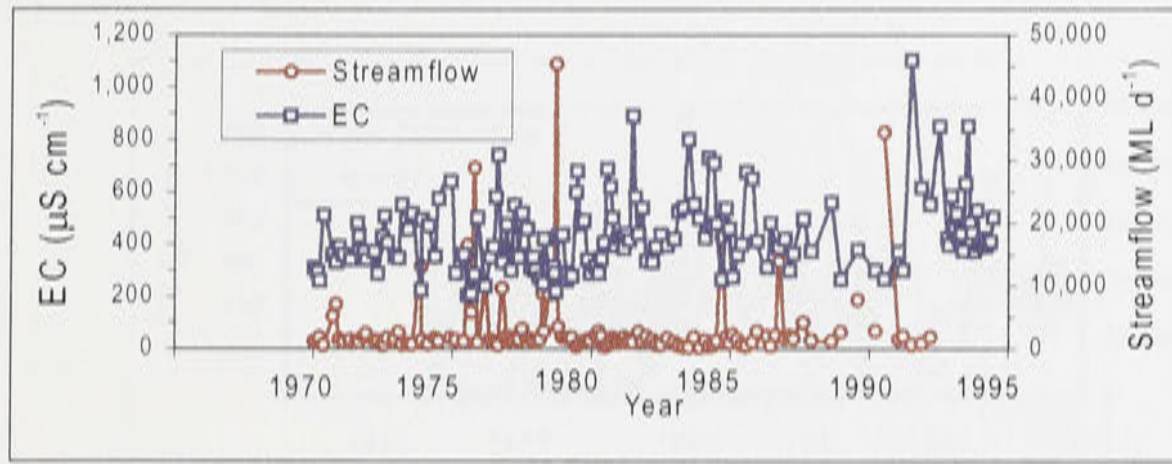


(c) Computed salt load per unit volume

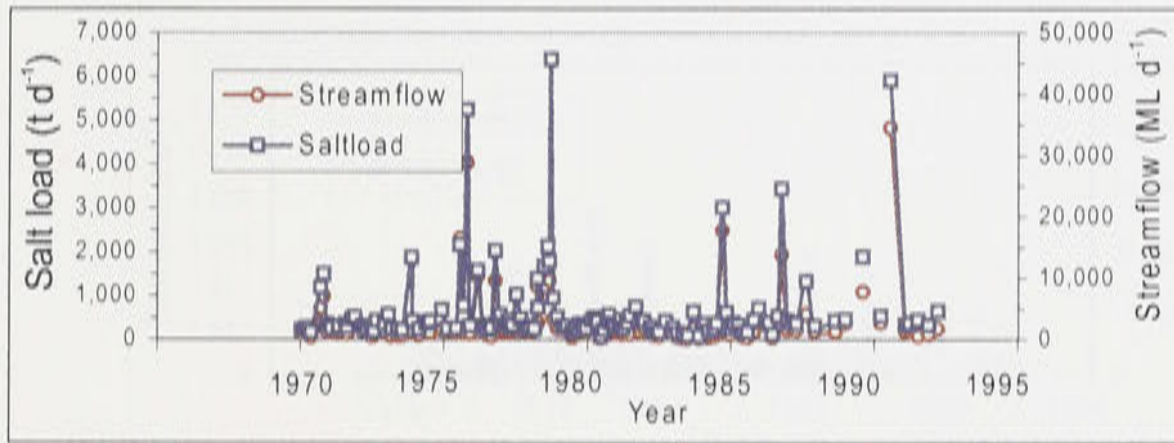


(d) EC and salt load vs streamflow

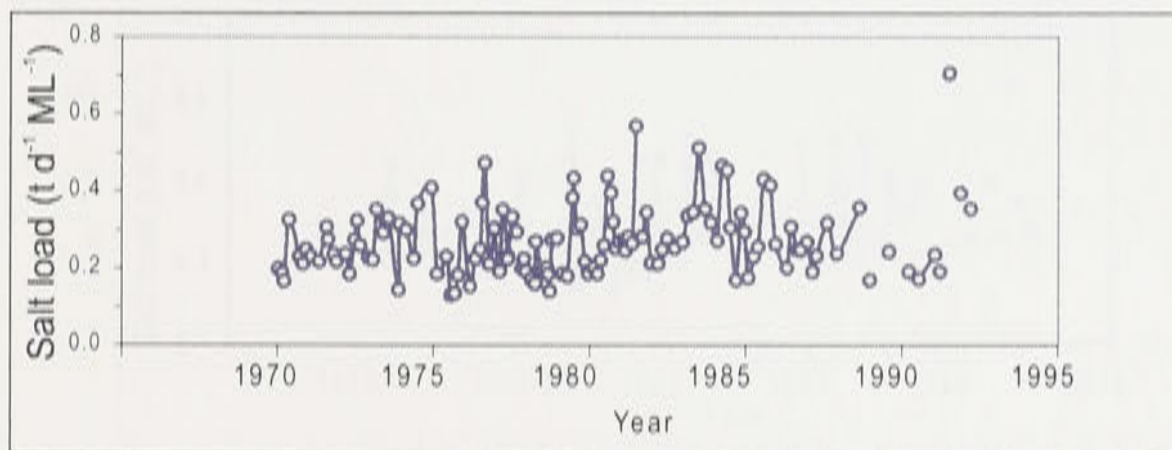
Figure 2.21: Electrical conductivity, salt load and streamflow at gauging station 412002-Lachlan River at Cowra.



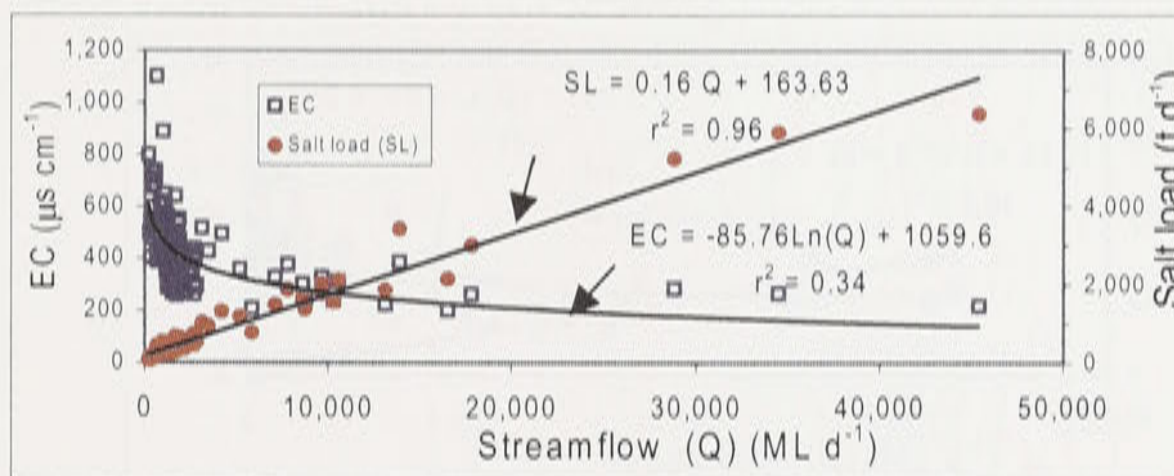
(a) Historical EC and streamflow



(b) Historical salt load and streamflow

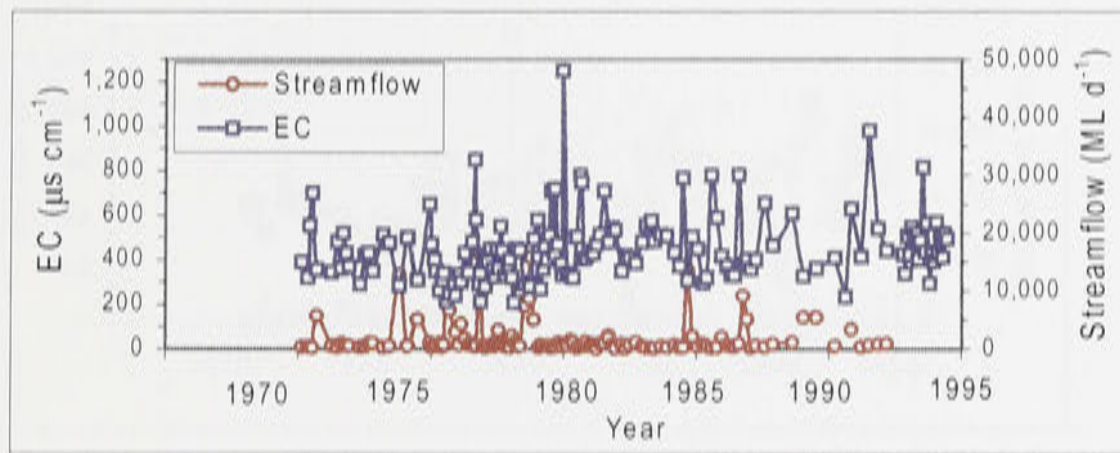


(c) Computed salt load per unit volume

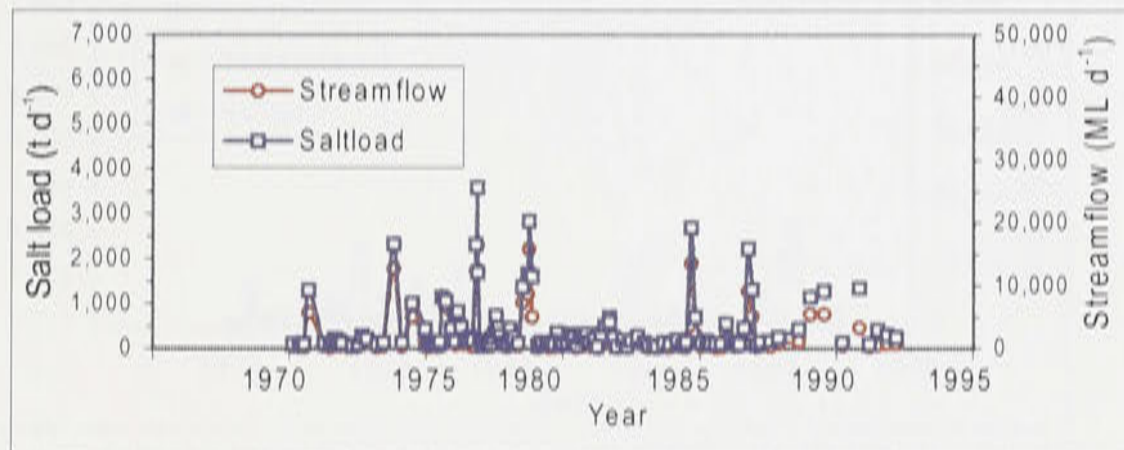


(d) EC and salt load vs streamflow

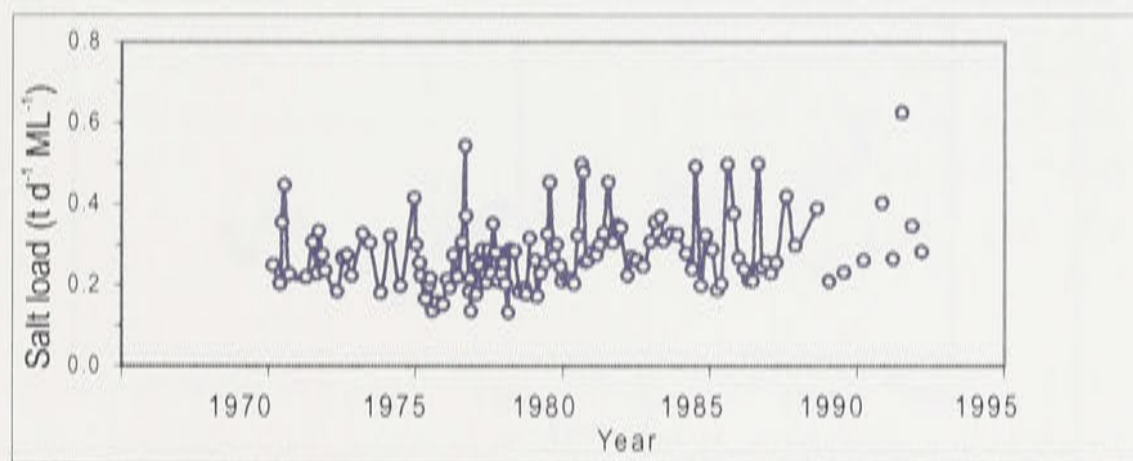
Figure 2.22: Electrical conductivity, salt load and streamflow at gauging station 412004- Lachlan River at Forbes.



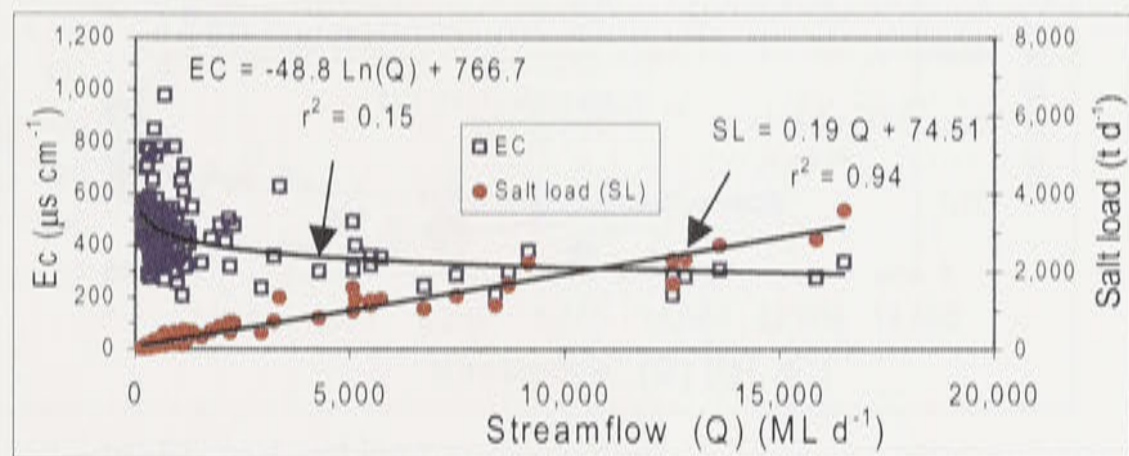
(a) Historical EC and streamflow



(b) Historical salt load and streamflow

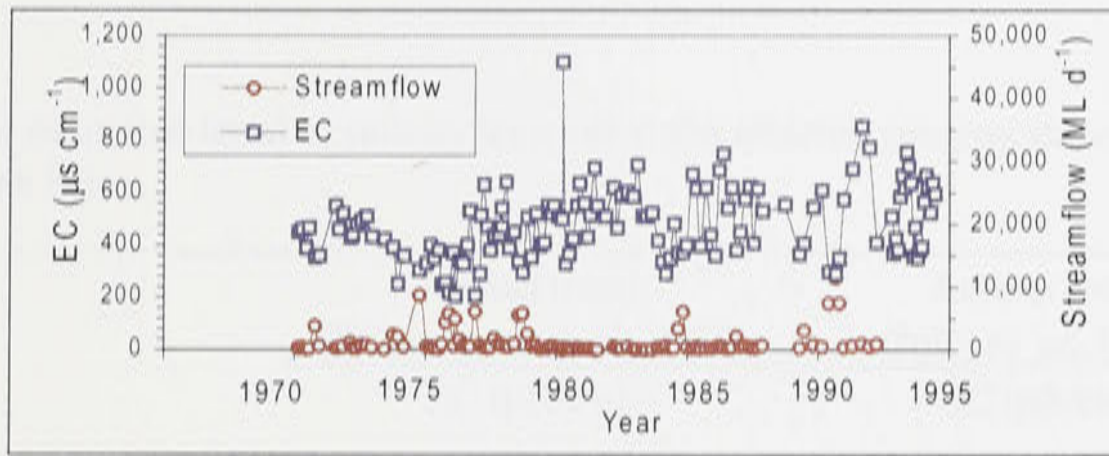


(c) Computed salt load per unit volume

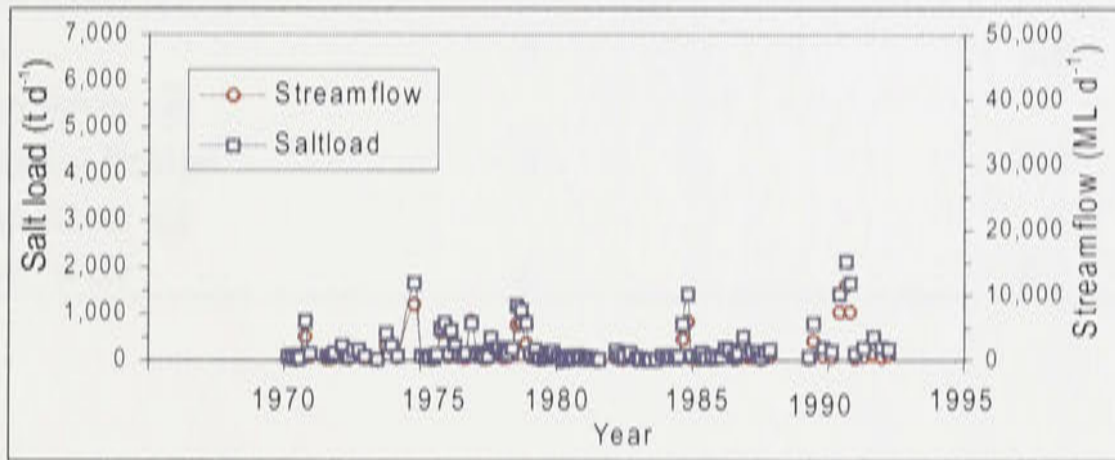


(d) EC and salt load vs streamflow

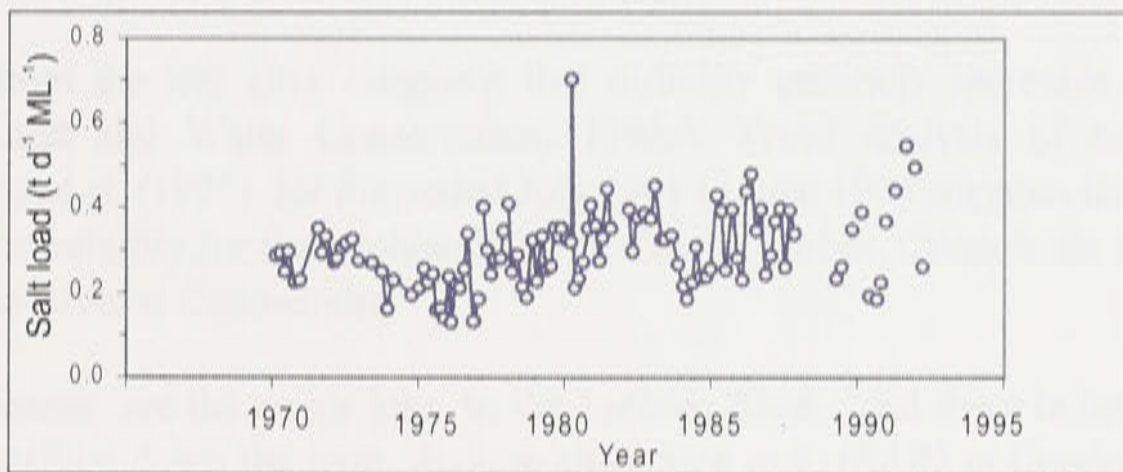
Figure 2.23: Electrical conductivity, salt load and streamflow at gauging station 412006- Lachlan River at Condobolin.



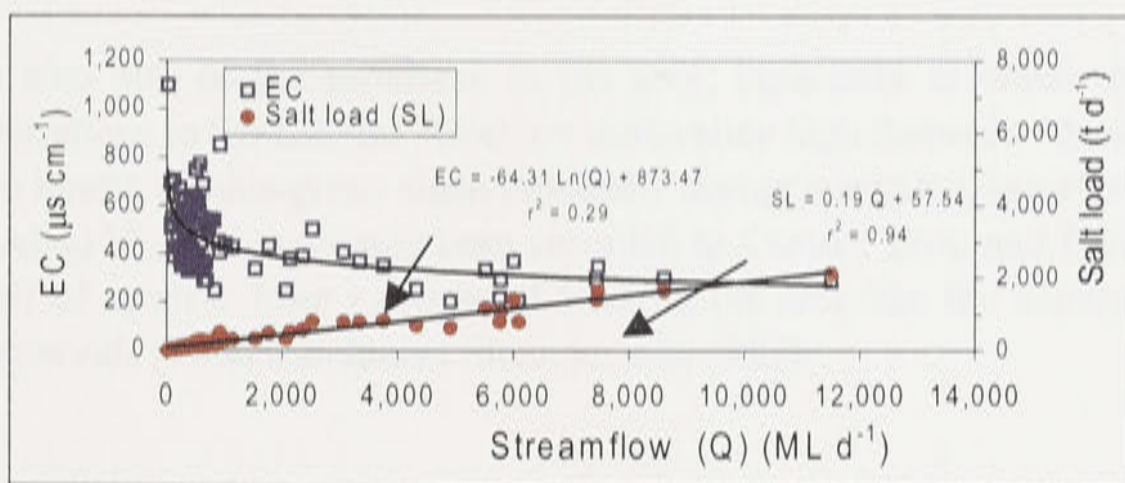
(a) Historical EC and streamflow



(b) Historical salt load and streamflow



(c) Computed salt load per unit volume



(d) EC and salt load vs streamflow

Figure 2.24: Electrical conductivity, salt load and streamflow at gauging station 412039- Lachlan River at Hillston.

Table 2.6: Annual estimated trend in salinity increase at the selected gauging stations along the Lachlan River.

Station number	Name	Annual trend	Annual trend
		(Williamson <i>et.al.</i> 1997) EC ($\mu\text{S/cm}$)	(Jolly <i>et al.</i> , 1997). EC ($\mu\text{S/cm}$)
412002	Lachlan River @ Cowra	3	4.9
412004	Lachlan River @ Forbes	5	5.6
412006	Lachlan River @ Condobolin Bridge	4	6.2
412039	Lachlan River @ Hillston Weir	6	8.2

2.6.7.2. *Turbidity, SAR and nutrients*

Analysis of data from the key sites suggests that turbidity generally increases downstream (Department of Land and Water Conservation, 1996c). Trend analysis of turbidity data conducted by Preece *et al.* (1997) for the period July 1991 to June 1996 suggests that there is no detectable change in turbidity for the Lachlan River at Cowra, Forbes, Condobolin and Hillston, and for the Belebula River at Canowindra.

Sodium and bicarbonate are the major ions in the Lachlan River, and there is little change in their relative composition down the river. Sodium absorption ratio (SAR) at Condobolin ranges from 1.07 to 1.60, and at Whealbah 1.19 to 1.82, which are below the critical levels of 8 to 18 (Department of Water Resources, 1989).

Eutrophication is also one of the problems in the area, especially in water storages. The phosphorous concentrations in the Lachlan River are moderately high (between 30 and 100 $\mu\text{g L}^{-1}$) resulting in massive bloom of blue-green algae especially during summer (Department of Water Resources, 1989). Algal bloom has already been recorded in Carcoar Dam and Lake Cargelligo caused by the runoff of nutrient from agricultural lands in the area into the storages especially during the flooding periods (Total Catchment Management, 1993).

Table 2.7: Annual mean water and salt balances (1985-1994) at the selected gauging stations along the Lachlan River Valley.

Station number	Name	Contributing area	Rainfall	Rainfall water input ¹	Rainfall salt input ²	Streamflow water output ³	Streamflow salt output ⁴	Diversion water ⁵	Diversion salt ⁶	Total water output ⁷	Total salt output ⁸	Total WO/WI ⁹	Total SO/SI ¹⁰	Total salt output/area ¹¹
		(km ²)	(mm)	(GL)	(t)	(GL)	(t)	(GL)	(t)	(GL)	(t)			(t km ⁻²)
412002	Lachlan R. @ Cowra	11100	746	8284	35621	1122	195985	4	706	1126	196691	0.13	5.38	17.72
412004	Lachlan R. @ Forbes	19000	717	13621	58571	1494	271028	43	7653	1537	278681	0.11	4.56	14.67
412006	Lachlan R. @ Condobolin Bridge	25200	673	16952	72894	1031	199397	149	28732	1181	228130	0.07	2.99	12.01
412039	Lachlan R. @ Hillston Weir	54100	577	31189	134111	548	124438	203	39781	751	164219	0.02	1.19	3.04

2-36

- 1 Rainfall water input (GL) = Rainfall x contributing area.
- 2 Rainfall salt input (tonnes) = Rainfall x contributing area x saltfall concentration. Saltfall station is based at Cowra with an estimated saltfall concentration of 4.3 mg L⁻¹.
- 3 Streamflow water output is the total streamflow (GL) from the catchment.
- 4 Streamflow salt output is the total salt output (tonnes) in streamflow from the catchment
- 5 Diversion water is the total streamflow (GL) diverted from or to streams within the contributing area.
- 6 Diversion salt is the total saltload (tonnes) diverted from or to streams within the contributing area.
- 7 Total Water Output (WO) from the catchment. When diversion data is present, it is calculated as Streamflow water output + Diversion Water, otherwise the same as Streamflow Water Output.
- 8 Total salt output (tonnes) from the catchment. When diversion data is present, it is calculated as Streamflow Salt Output + Diversion Water, otherwise the same as Streamflow Salt Output.
- 9 Water output (WO) to input (WI) ratio calculated as Total Water Output/Rainfall Water Input.
- 10 Salt output (SO) to input (SI) ratio calculated as Total Salt Output/Rainfall Salt Input.
11. Salt output per unit area of the catchment (t km²) calculated as Total Salt Output/Contributing Area.

Source: Jolly *et al.* (1997a).

2.7. Hydrogeology

2.7.1. Exploration and extraction wells

The first publication indicating that there are substantial groundwater resources in the Lachlan River Valley was in relation to deep alluvial leads being worked for gold in the Forbes area (Williamson, 1986). Most of the early publications are in annual reports of the then New South Wales Department of Mines, in the 1870's and 1880's. They are well summarised by Andrews (1910). Test drilling for more recent investigations began in 1957 and the results are reported and updated from time to time (Williamson, 1961; 1964a, 1964b; 1968a; 1968b; 1970). The findings are also incorporated in more general publications of the then Water Conservation and Irrigation Commission (1971; 1972), the Australian Water Resources Council (1975), and the Water Resources Commission (1984).

Within the then Water Resources Commission, further reports were published on particular aspects of investigations such as: Megalla and Kalf (1973) concerning the buried valley of the ancient Lachlan River between Cowra and Forbes; Odins (1975), concerning application of seismic refraction geophysical methods; and Ross (1982), on an interim report on the drilling and the observation bore network.

In recent years, additional test drillings were also conducted in specific areas vulnerable to groundwater level rise, especially in the Jemalong and Wyldes Plains Irrigation District.

The systematic recording of water well data in New South Wales was taken up by the then Water Conservation and Irrigation Commission when it commenced operations in 1913. At present the records are stored in the DLWC computer system and the data processing and retrieval is operated by the Department of Land and Water Conservation as the Groundwater Data Bank.

2.7.2. Test drilling

Initially, groundwater investigations were limited only to the specific information required for licensing water wells in New South Wales. At that stage (1957) there were numerous wells recorded in the Valley, however, they were shallow (up to about 20 m) and almost entirely for stock and domestic purposes. The objective of the test boring program was to gain a broad picture of the groundwater conditions from the beginning of the alluvial deposits, about 13 km upstream of Cowra, down to Jemalong Weir, and including major enroute tributaries. The test drilling program, summarised by Williamson (1986), was divided into three phases.

The first phase was undertaken from 1957 to mid-1965 upstream of Jemalong Weir. It involved a total of 131 bores in 14 representative cross sections. With the continued development of groundwater resources in the area, a second phase drilling was undertaken to cover that part of the Valley extending upstream from Condobolin to Cowra. The third phase of investigation involved drilling to bedrock in areas where information was limited and where wells drilled in the second phase failed to reach bedrock. As the time went on and the results of the investigation became known in the Valley, more landholders attempted to obtain irrigation water supplies by tapping the groundwater resources (Williamson, 1986).

During the 1960's, a number of seismic profiles were acquired across the alluvium of the upper Lachlan Valley to supplement the earlier drilling. A total of 240 km were shot in 45 spreads, which included around 150 km between Jemalong Gap and Condobolin. The interpretation of these seismic data in most cases provided reasonable correlation with depth to bedrock where drilling data was available (Anderson *et al.*, 1993).

2.7.3. Characteristics of various aquifer systems

Both the Lachlan and Cowra Formations are considered productive aquifers (see section 2.3.2 for the description of these Formations) in the Lachlan Valley. The Lachlan Formation are the most productive aquifers in the area investigated with yields of up to 200 L s⁻¹ (Williamson, 1986). The sands and gravels in this formation are well sorted, more permeable and thicker, both in individual layers and in aggregate thickness, than those in the overlying Cowra Formation. There is a general trend of increasing maximum thickness of sands and gravels in the Lachlan Formation within distance down from the Valley. This is not pronounced in the Cowra Formation.

The Cowra Formation is widespread in the alluvial infill of the Valley. Unfortunately, the groundwater potential of the Cowra Formation is much more limited than the Lachlan Formation. In the upper part of the Valley, the gravels are mainly medium to coarse. With distance downstream sands predominate and are usually silty and clayey.

2.7.4. Piezometric surface and groundwater trends

Historical trend analysis of groundwater levels in the Valley are limited and at best localised to a few intensively studied areas. Some investigations were carried out at the headwaters; Young district groundwater areas; upper Lachlan between Cowra to Condobolin; Jemalong and Wyldes Plains Irrigation District and Bland Creek catchment; between Condobolin and Cargelligo and Lower Lachlan. Highlights of the findings of these investigations are discussed below.

2.7.4.1. Headwaters

In the headwaters region, Gates and Williams (1988) analysed the groundwater level behaviour over a 60 year period from 1915 to 1974. Average increase of groundwater level over this period was estimated at 4 m. The Change in level varied between a rise of 24.4 m and a fall of 7.5 m. The median increase was 2.9 m.

2.7.4.2. Young district

Williams (1990) investigated the rise of the groundwater levels in three rock provinces in the Young district, namely: igneous (granite), sedimentary rock and alluvial over the period 1979-1988. Groundwater levels in igneous rock province were rising at a rate of 0.5 m per year. In the sedimentary rock province, the rise was of up to 0.15 m per year at Bendick Murrell between Young and Cowra. In the alluvial flats, the average rise was less than 0.1 m per year.

2.7.4.3. Upper Lachlan

The alluvial system in the Valley has been divided into four groundwater management areas (Department of Land and Water Conservation, 1996a; 1997). The groundwater systems of the upper Lachlan belong to Groundwater Management Area (GMA) 011. Analysis of the groundwater levels at GMA 011 has been carried out by Bish and Williams (1994). The alluvium of the upper Lachlan Valley is divided into 8 zones according to the similarity of hydrogeological units shown in Figure 2.25. Analysis of the representative hydrographs from key observation wells from Zone 1 to 8 are presented by Bish and Williams (1994). They concluded that there was an apparent, considerable rise in water levels over the entire management area during the high recharge events in April 1990. Between Cowra and Back creek (Zone 1), the overall increase was approximately 0.5 m between 1977 to 1993 with an apparent response to fluctuations in river levels. In Zone 2 (Cowra to Gooloogong), groundwater level was generally steady and a rise of 1-2 m was observed in 1990 as a result of flooding, but dissipated in 1992/1993. Within the Gooloogong to Jemalong Gap (Zone 3) water levels are impacted generally by pumping and the aquifer shows large fluctuations in response to groundwater extraction. In the alluvial area near Eugowra (Zone 4), water levels were relatively static since 1976 with the exception of significant short term rise in 1990 due to rainfall and flooding. In Zone 5 (Jemalong Gap to Condobolin), the estimated water level rise was about 2-3 m between 1968 to 1993, and changes in the hydrographic records were generally related to seasonal events. In the Jemalong and Wyldes Plains Irrigation District area (Zone 6), there was a dramatic rise in the watertable level in the early 1950's, which coincided with a period of major flooding. Watertable rises of between 2-4 m were observed between 1944-1994 (Williams, 1993) and the current water level mound appears to be centred on the prior stream formation. High water levels in Zone 6 resulted in salinisation of arable land and local surface water bodies. In Zone 7 which occupies the area from Lake Cowal to the highland extremities of the Bland Creek, groundwater level was quite steady with negligible response to seasonal variations or pumping. In Zone 8 which extends from Condobolin to Lake Cargelligo, a significant rise of groundwater level occurred following the 1990 flood event. Groundwater levels declined steadily following the major recharge events (Sturgess, 1994).

2.7.4.4. Lower Lachlan

The Water Resource Commission (1986) reported that data collected in the area of major pumping north of Hillston indicated a cycle of water level rises and falls due to ongoing pumping and recovery.

2.7.5. Recharge of the aquifer systems

Recharge of the alluvial aquifers of the Valley occurs from rainfall, streams (during high flow stages), overbank flooding events (Williamson, 1986) and irrigation. Discharge occurs by natural flow to the stream, extraction from bores and wells, and evapotranspiration when the watertable is close to the ground surface. The degree of hydraulic connection between the aquifers controls the extent to which recharge can reach deeper aquifers. The analysis of the well hydrographs by Williamson (1986) has concluded that a significant degree of hydraulic connection between the shallow and deep aquifers exists throughout the system.

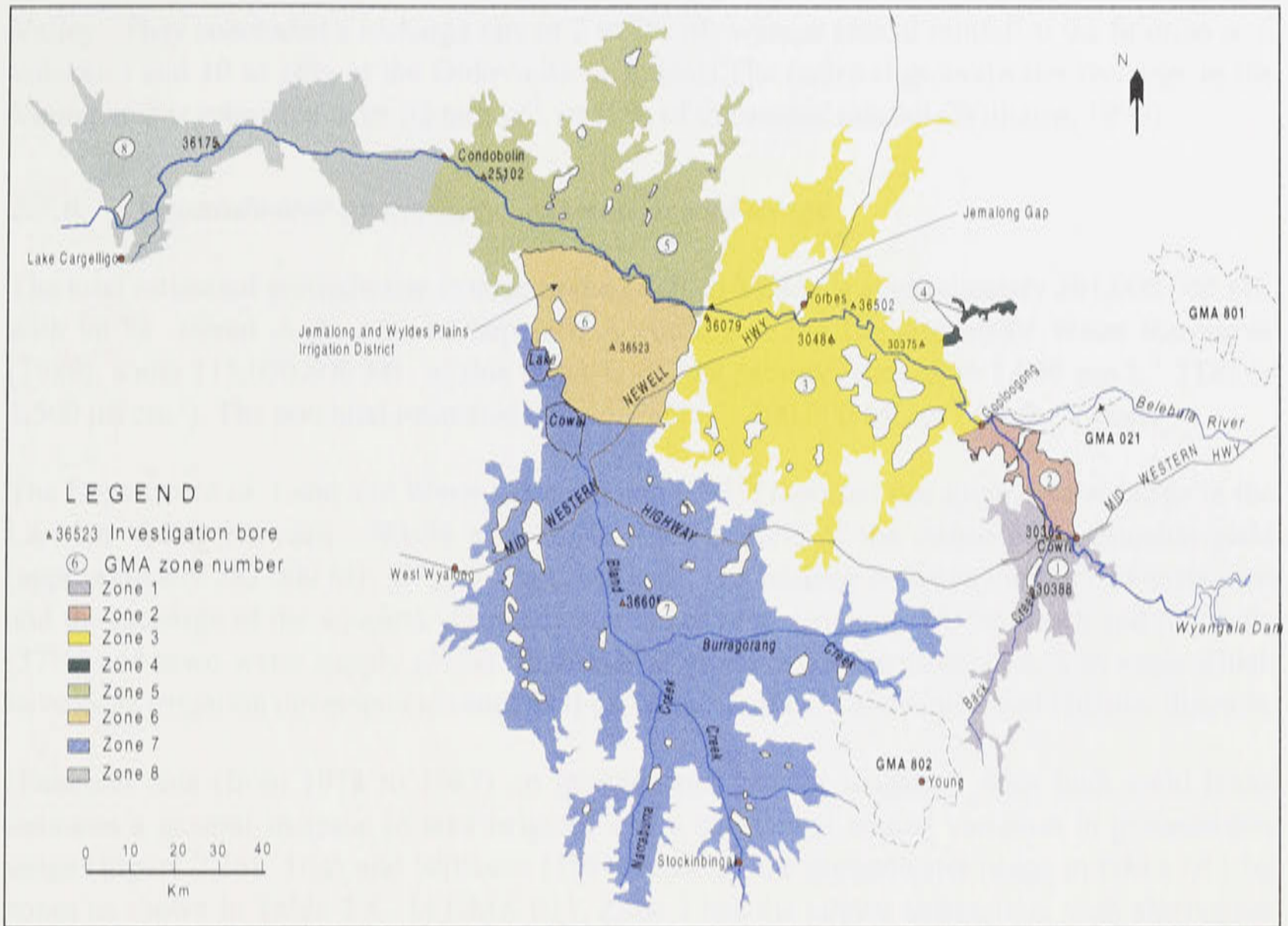


Figure 2.25: Subdivision of the Groundwater Management Area (GMA) 011 (modified from Bish and Williams, 1994).

Panta *et al.* (1997) estimated an annual recharge of about 750,000 ML from the Lachlan River. This is equivalent to about 30% of the total annual flow of the Lachlan River. About 45% of the total annual recharge from the River occurs between Jemalong and Lake Cargelligo reach. It should be noted that the recharge estimated by Panta *et al.* (1997) seems high and unrealistic.

Based on the observed rate of groundwater rise from 1969 to 1992, Williams (1993) has estimated a total accessions to the groundwater system of at least 8,000 ML yr⁻¹ and may be as high as 30,000 ML yr⁻¹ in the Jemalong and Wyldes Plains Irrigation District (JWPID). Anderson *et al.* (1993) have calculated an annual recharge of 32,000 ML day⁻¹ from the Warroo Paleochannel in the JWPID. This does not include the vertical infiltration from flood events nor constant inputs from the Lachlan River near Jemalong Gap.

At the headwaters region in the Lachlan Valley, information on groundwater recharge rate is unknown. However, Barnett (1994) suggested the use of recharge rate information available at the adjacent Yass River Valley. A study of the relationship between surface infiltration rates and geology in the Boorowa region conducted by Bush (1994) correlates well with recharge in Yass River Valley. Since the Lachlan headwaters region and the Yass River Valley share similar lithology and climate, the groundwater recharge is also thought to be similar. At Williams Creek, a sub-catchment of the Yass River Valley, Bradd *et al.* (1991) calculated an average long term recharge rate of between 42 mm and 65 mm yr⁻¹ for the lower side slopes. In high recharge areas, it was estimated that recharge was at least 97 mm yr⁻¹. Nicoll and Scown (1993) have also calculated the current groundwater recharge rates for various lithologies in the Yass River

Valley. They concluded a recharge rate of 2 to 8% of average annual rainfall at the Silurian acid volcanics and 10 to 38% at the Ordovician sediments. The regional groundwater recharge in the Young area is estimated to be 82 mm yr⁻¹, or 12% of the annual rainfall (Williams, 1990).

2.7.6. Groundwater availability, extraction and usage

The total estimated groundwater storage in the Lachlan Valley is approximately 291,000,000 ML with 98 % stored in the alluvial deposits. According to the Department of Water Resources (1989), some 115,000,000 ML of this water is of low salinity (less than 1,000 mg L⁻¹ TDS or 1,500 µS cm⁻¹). The potential estimated annual yield is 1,200,000 ML yr⁻¹ for the Valley.

The Department of Land and Water Conservation (1995) reported that groundwater usage in the Lachlan Valley between 1993-94 was 62,000 ML, or 22% of the estimated sustainable yield (approximately 283,000 ML yr⁻¹). Sustainable yield is a balance between the rates of extraction and the recharge of the aquifers. Groundwater is used for irrigation (47%), stock and domestic (37%) and town water supply (16%). Substantial groundwater demands occurs in areas which have large irrigation developments such in the Cowra, Forbes, Canowindra and Hillston districts.

Historical data (from 1978 to 1987) on groundwater use for irrigation from high yield bores indicates a general increase in area irrigated and a substantial annual variation in groundwater usage (Figure 2.26). Bish and Williams (1994) reported the groundwater usage in GMA 011 by zones as shown in Table 2.8. In GMA 011, Zone 3 has the largest abstraction, with abstraction from zone 2 providing most of the remaining high yield use. Usage in Zones 1 4 and 5 are minor but may be locally significant. Zone 5 has declining usage over the period of record, although it is understood that the area has reasonable level of pumping capacity (Bish and Williams, 1994). Zone 7 has a very low level of development and Zone 8 has none.

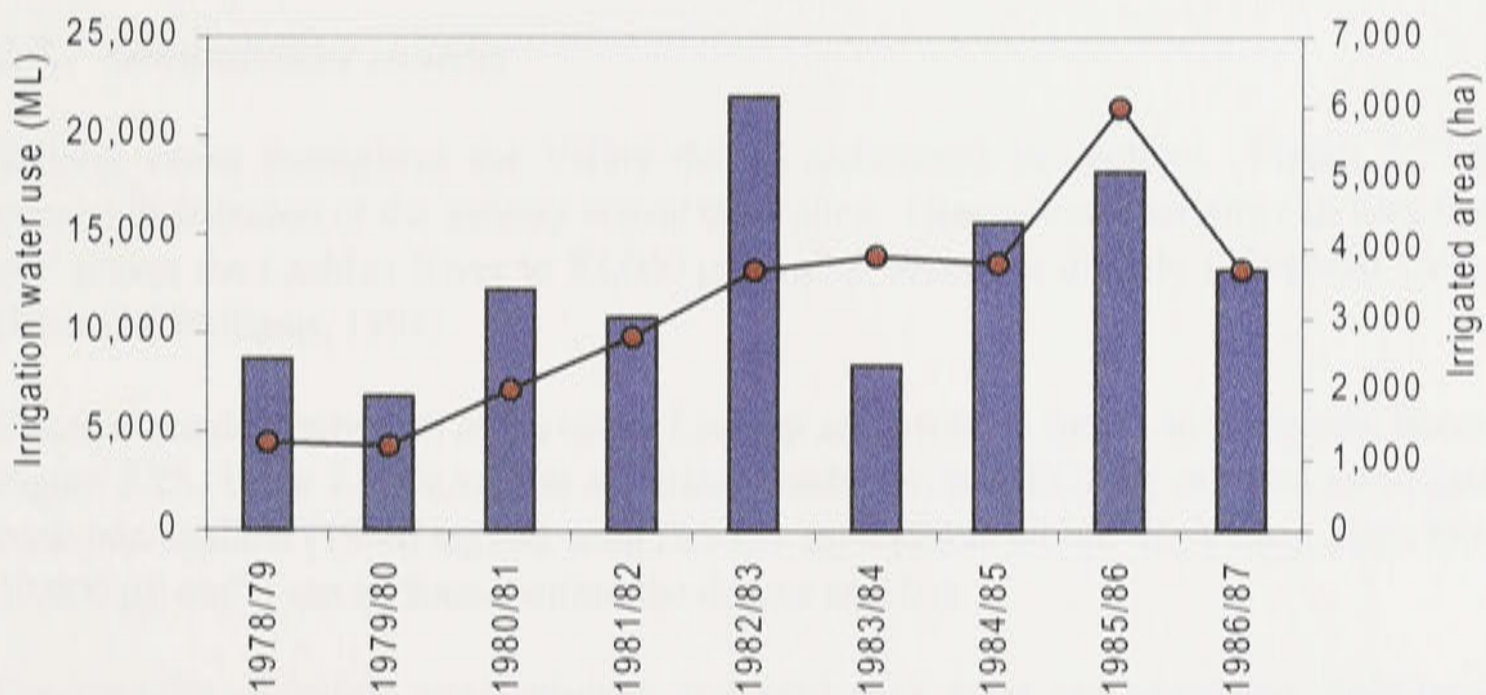


Figure 2.26: Irrigation water use (bars) and irrigated area (line) from high yield bores (modified from Department of Water Resources, 1989).

Table 2.8: Groundwater use in GMA 011 from 1986/87 to 1992/93.

Water year	Usage (ML)								Total
	Zone 1	Zone 2	Zone 3	Zone 4	Zone 5	Zone 6	Zone 7	Zone 8	
1986/87	46	1098	4135	7	247	210	5	0	5748
1987/88	60	870	3841	8	196	602	3	0	5580
1988/89	41	501	2462	0.1	165	78	0	0	3247
1989/90	72	587	2730	16	29	140	0	0	3574
1990/91	101	1787	3004	22	9	93	90	0	5106
1991/92	38	691	1919	3	0	90	0	0	2741
1992/93	49	301	1615	11	0	35	0.05	0	2011

Source: Bish and Williams (1994).

According to Department of Land and Water Conservation (1998), there are about 3,099 licensed bores in the Lachlan River Valley. The relative number of bores grouped by dominant use are: stock and domestic (2,340); irrigation (455); test bores (111); farming (81); industrial (330); town water supply (33); mining (15); recreation (10); drainage (9); monitoring (7); conservation of water (2); commercial (10); aquaculture (1); and grape vines (1). A proportion of bores in the Valley are registered but not licensed, such as DLWC monitoring and observation bores, and abandoned bores and wells. The estimated number of bores in the catchment is 12,000.

2.7.7 Groundwater salinity

Salinity varies throughout the Valley due to differences in geology. Figure 2.27 shows the general distribution of the salinity across the Valley. Groundwater salinity can vary from 800 $\mu\text{S cm}^{-1}$ nearer the Lachlan River to 32,000 $\mu\text{S cm}^{-1}$ in areas not directly influenced by the streams (Bish and Williams, 1994).

Electrical conductivity data in the upper Lachlan are available for the investigation bores shown in Figure 2.25. Table 2.9 shows the electrical conductivities (EC) for selected investigation bores sunk into shallow (18-40 m) and deep (80-131 m) aquifers within the Valley. High EC values ($> 10,000 \mu\text{S cm}^{-1}$) can be found within the deeper aquifers.

Geologically, electrical conductivities and hard rock areas are correlated. Salinisation in the Boorowa-Yass area is most pronounced in the area underlain by Ordovician slates and siltstones (Scott, 1991). Bish and Gates (1991) conducted a study on dryland salinisation which concentrated on the groundwater level changes within the hard rock formations in the upper Lachlan River Valley. A major finding of this study was that areas underlain by metamorphic rocks such as slate were the most at risk from salinity outbreaks, as these units experienced the largest mean water level rise over the period of record.

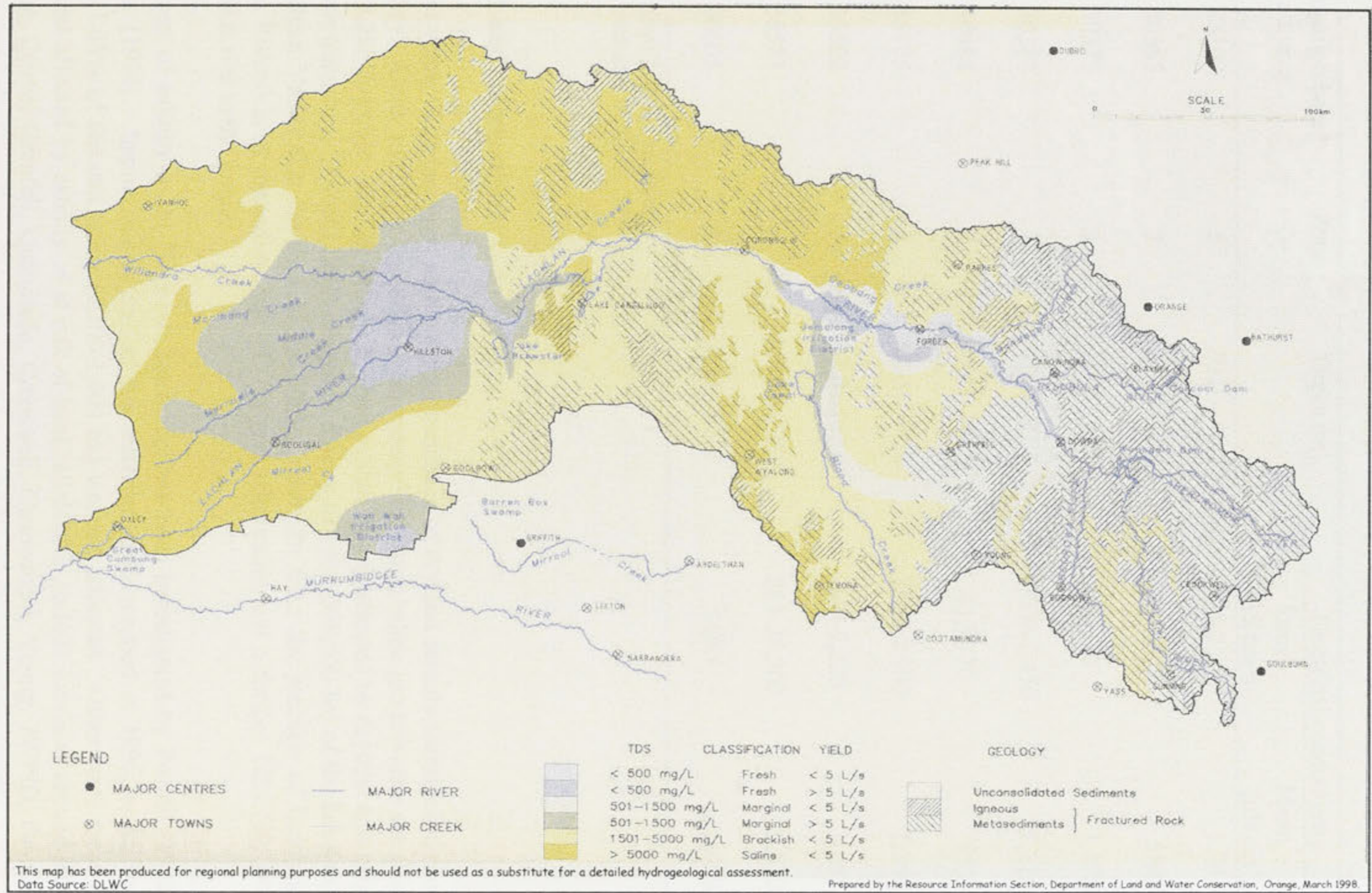


Figure 2.27: Groundwater salinity in the Lachlan River Valley (modified from Department of Land and Water Conservation, 1998).

Table 2.9: Electrical conductivities for selected observation wells in GMA 011:

Investigation bore* number	Zone	Depth (m)	Electrical conductivity	
			Range ($\mu\text{S cm}^{-1}$)	Mean ($\mu\text{S cm}^{-1}$)
25102	5	39.0 – 40.2	895-2,250	1,742
30365	2	32.0 – 39.6	370-845	584
30375	3	18.2 – 19.8	1,170	1,170
30388	1	31.4 – 37.5	1,000-1,450	1,218
30484	3	99.1 – 107.7	415-770	525
36175	8	68.5 – 71.6	1000-2,900	1,850
36502	3	97.0 – 102.0	369-2,220	1,155
36523	6	128.0 – 131.0	283-24,300	5,310
36605	7	80.0 – 86.0	1680	1,680

* See Figure 2.25 for locations.
Source: Bish and Williams (1994).

2.8. Land salinisation

In recent years, there has been an increasing incidence of dryland salinity identified throughout the Valley. Areas in the Valley currently threatened by rising saline groundwater are shown in Figure 2.28. However, the exact area of the Lachlan Valley affected by dryland and irrigation salinity is unknown. Barnet (1994) suggested that up to 19% (308,000 ha) of the headwaters of the Lachlan Valley (i.e. the area of the Valley upstream from the junction of Belebula and Lachlan Rivers) is at immediate risk of dryland salinisation and a further 12% (205,000 ha) could be at risk in the future.

The extent of salinity in the Boorowa catchment has been investigated by Powell (1992) and Hayman (1996). Approximately half of the catchment was mapped in 1996, indicating that around 1.65% of the catchment (1,300-1,400 ha) was salt affected. Other rural areas of the catchment affected by salinity or at risk of land salinisation include localities around Blayney, Gunning, Cowra, Grenfell, Quandialla, Crookwell, Canowindra, Young, JWPID, Condobolin, Hillston and Lake Cargelligo (Department of Land and Water Conservation, 1998).

Urban salinity has also been a major issues in large part of New South Wales. In 1996, the Australian Geological Survey Organisation prepared an incomplete lists of 20 inland New South Wales regional towns affected by urban salinity. Eight of these affected towns summarised in Debashish *et al.* (1996) are in the Lachlan River Valley, namely: Condobolin, Parkes, Forbes, Lake Cargelligo, Blaney, Cowra, Grenfell, and Boorowa.

2.9. Flora and Fauna

2.9.1. *Vegetation at the riparian zone*

Riparian vegetation is a vegetation which is dependent upon the stream and grows on the exposed stream bed, on the stream banks and on the land adjacent to the stream. This area is also known as riparian zone. The riparian vegetation of the upper Lachlan River and major tributaries typically consists of grasses, river she-oaks (*Casuarina cunninghamiana*), river red gums (*Eucalyptus camaldulenses*) and willow (*Salix spp.*). White gum (*Eucalyptus viminalis*) and Stringybark (*Eucalyptus cinerea*) are also found in the riparian zone of the Abercrombie catchment (Togher, 1996).

River red gums are the dominant vegetation of the riparian zone along the lower reaches of the Lachlan River. River cooba (*Acacia stenophylla*) and Cooba (*Acacia saligna*) also occur in association with river red gum between Gooloogong and Hillston (Sivertsen and Metcalfe, 1995). Black box (*Eucalyptus largiflorens*), lignum (*Muehlenbeckia florulenta*) and river cooba are common plant species along the ephemeral and effluent creeks of the lower Lachlan floodplains, with river red gums appearing nearer the confluence with the Lachlan River (Massey, 1997).

2.9.2. *Floodplain vegetation*

The floodplain of the Lachlan River typically consists of tall open river red gum forests along the banks of the river with black box woodlands covering the floodplains adjacent to the banks and in depressions. Low shrublands of lignum and tall shrublands of myall occur between the black box woodlands and the billabongs, lagoons and swamps of the floodplains, which are often vegetated by sedges and reeds.

There are nine State forests on the Lachlan River or its adjacent waterbodies downstream of Cowra. The location and condition of these forests is summarised in Table 2.10. The condition of these forests provides a measure of the extent of impacts and threats on their values and the effectiveness of current management policies. The Lachlan River has a dominant effect on the ecosystem of these forests, particularly water supply, sediments/nutrient supply and microclimate (Department of Land and Water Conservation, 1998). These forests are significant given their semi-natural state and the extent of past clearing of the vegetation of the floodplain and riparian zone.

Mapping and surveys of the natural vegetation covered by the Forbes and Cargelligo 1:250,000 map sheet by Sivertsen and Metcalfe (1995), provides some indication of the diversity and condition of the vegetation in the Lachlan floodplain. The survey indicates that 16% (376,800 ha) of the study area remains under native vegetation. Of the remaining native vegetation, 21% (79,035) is classified as riparian and floodplain vegetation.

2.9.3. *Fauna*

A detailed list of all known native animal species of the Lachlan floodplain is available from the Atlas of New South Wales Wildlife (Ellis and Etheridge, 1993).

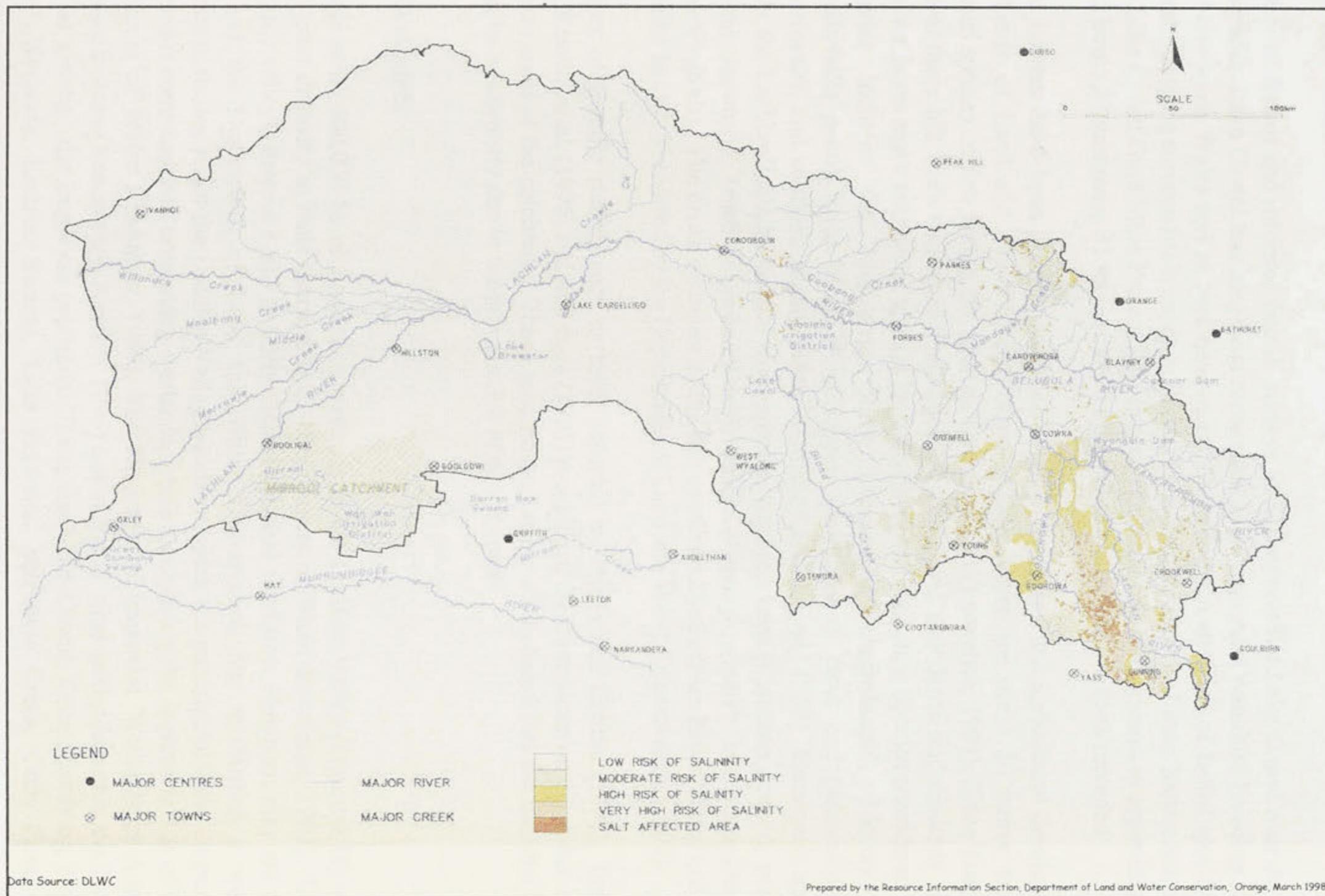


Figure 2.28: Salinity in the Lachlan River Valley (modified from Department of Land and Water Conservation, 1998).

Extensive habitat alteration brought about by European settlement has reduced the diversity of native fauna and favoured the spread of feral animal, including fox, rabbit and pig. Possums, small ground mammals and birds which occur in the wooded Valley areas are rare, although wallabies and kangaroos are more abundant (Department of Water Resources, 1989).

A number of formal and informal faunal surveys have conducted at Lake Cowal over the past three decades. Lake Cowal has long been recognised as an important waterbird breeding site in inland New South Wales and as such has naturally attracted the attention of faunal specialists. The results of these surveys has been compiled by Fanning (1995) in the Fauna Impact Statement for the Lake Cowal Gold Mine Project. The importance of the wetland systems is apparent given that 222 birds, 29 mammals, 31 reptiles and 11 amphibians species have been recorded.

Aquatic habitats have been greatly modified by flow regulation and agricultural development (Department of Land and Water Conservation, 1998). There are some 30 native and 11 introduced species of fish within the Murray Darling Basin (Lawrence, 1991). Since European settlement there has been widespread reduction of the natural abundance and diversity of the native river fauna and a number of species have become locally extinct. Species considered to be endangered include: the Macquarie perch (*Macquaria australasica*); Murray Cod (*Maccullochella peeli*); river blackfish (*Gadopsis marmoratus*); trout cod (*Maccullochella macquariensis*); and southern pigmy perch (Goldney and Bowie, 1996). Introduced species found in the Lachlan include: several trout species; common carp (*Cyprinus carpio*); goldfish (*Carassius auratus*); tench (*Cyprinus tinca*); redbfin (*Perca fluviatilis*); and mosquito fish (*Gambusia affinis*). The broad overview of the fish species in the Lachlan River Valley and their distribution has been reported by the Department of Land and Water Conservation (1998).

A number of specific studies such as those reported by Harris and Gehrke (1997), Tougher (1996), Keenan *et al.* (1996) and McBryde (1995) provide useful information on the status of fish in discrete areas of the catchment. These specific studies have concluded that the Lachlan River is losing its biodiversity due to the introduction of new species.

2.10. Wetlands

There are some 400,000 ha of floodplain wetlands in the Lachlan Valley (Figure 2.29) which display great diversity in their characteristics (Department of Water Resources, 1990). Unlike many other valleys, these are still in fairly natural physical condition. However, they are under threat and the Department of Land and Water Conservation has established a wetland management strategies for the Lachlan Valley which will seek the participation and cooperation of the wider community in conserving wetlands, while recognising the legitimate use of water (Department of Water Resources, 1989). The Directory of Important Wetlands in Australia (Australian Nature Conservation Agency, 1996) has included nine wetlands within the Lachlan Valley as among the important wetlands. These are Lake Cowal, Great Cumbung Swamp, Booligal Wetlands, Lachlan Swamp, Lake Brewster, Merrowie Creek, Cuba Dam, Lake Merrimajeel/Murrumbidgee Swamp and Lower Mirrool Creek.

Wetlands are also common along many of the streams and depressions of the headwaters and tablelands of the Valley. However these wetlands have not been systematically mapped to date (Department of Land and Water Conservation, 1998).

Table 2.10: State Forests of the Lachlan River downstream of Cowra.

State Forest	General location	Area (ha)	Dominant forest type	Condition	Threats
Cumbijowa	Forbes	271	River red gum	Regrowth with scattered large trees amongst younger red gum regrowth. Weeds are a serious problem.	River regulation; fire; and weeds.
Towyal	Warroo	140	River red gum	Regrowth with scattered large trees amongst younger red gum regrowth. Weeds are a serious problem.	River regulation; and changed flooding regime.
Cadow	Island Creek-Condobolin	263	River red gum	Regrowth with scattered large trees amongst younger red gum regrowth. Weeds are a serious problem	River regulation and changed flooding regime.
Kiacatoo	Kiacatoo	134	River red gum	Regrowth with scattered large trees amongst younger red gum regrowth. Weed are a serious problem.	River regulation and changed flooding regime.
Hillston	Hillston	2198	River red gum with some box trees. Grassy understorey and some lignum	Most of the red gums are old trees. Some younger trees which appear to be slow growing probably due to a poor water regime.	River regulation and changed flooding regime; fire; and weeds.
Quandong	One Tree	494	River red gum with grassy understorey	Trees are low height and slow growth suggesting inadequate flooding.	River regulation and changed flooding regime; and Mirrol creek drainage.
Moon Moon	Whealbah	514	River red gum with grassy understorey	Some older trees and few younger trees/regeneration.	River regulation and changed flooding regime.
McFarlands	Corrong	709	River red gum, Black box and grassy understorey	Health of trees appears reasonable. Trees on high country (less frequently watered) are stressed. Slow overall growth rates. Regeneration not prolific.	River regulation and changed flooding regime. Irrigation drainage.
Oxley	Oxley	1212	River gum with fringe of Black box on western side	Dense woodland structure. Thick pockets of healthy regeneration.	Unnatural wetting and drying cycles; fire and weeds.

Source: Department of Land and Water Conservation (1998).

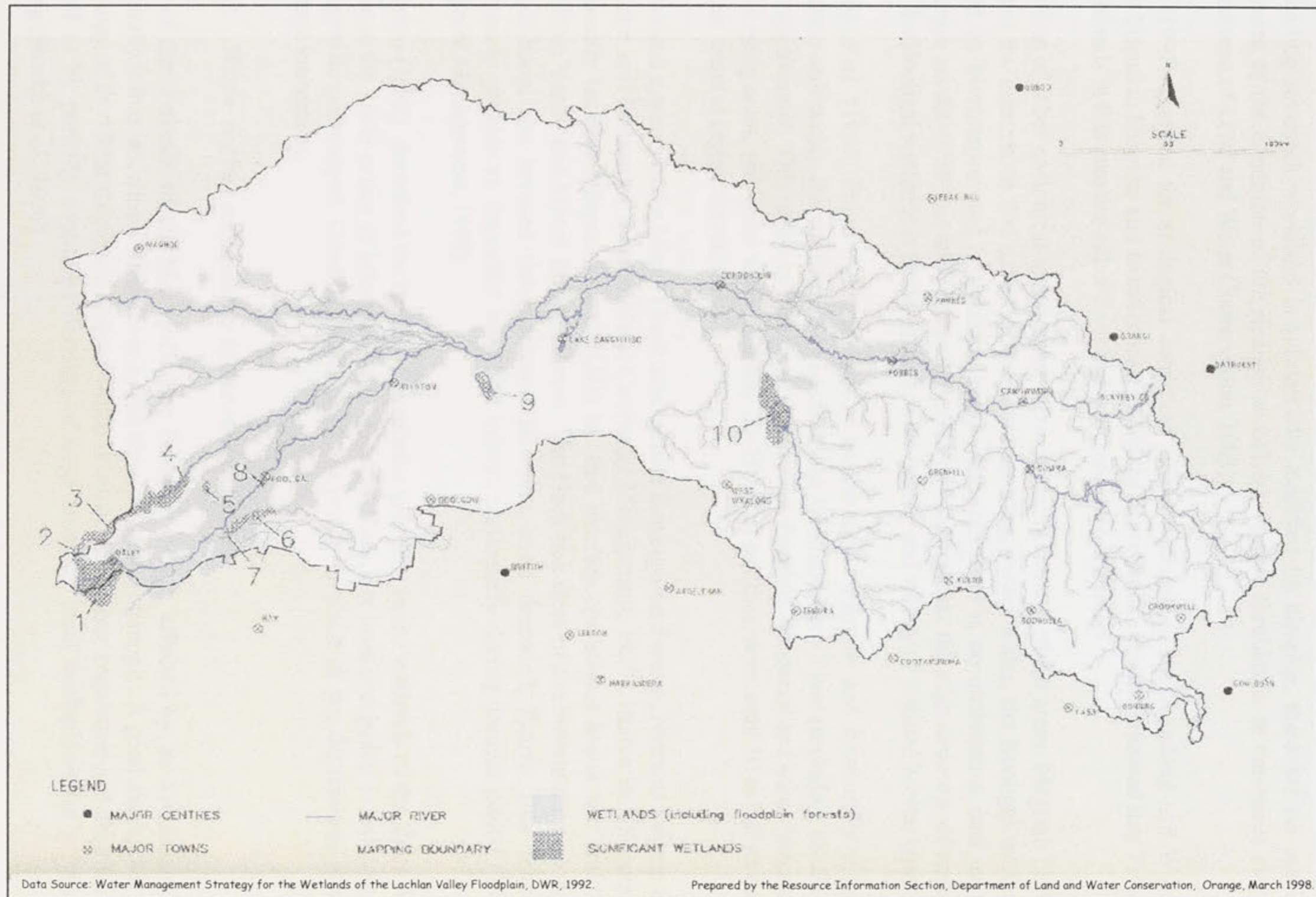


Figure 2.29: Wetlands of the Lachlan River Valley floodplain (modified from Department of Land and Water Conservation, 1998).

2.10.1. Present condition of the wetlands

The inventory of the Lachlan wetlands was undertaken by the then Department of Water Resources between 1986-88 (Department of Water Resources, 1990 and 1992). The classification of the wetlands were undertaken according to vegetation types and hydrological conditions in the respective wetland areas (Department of Water Resources, 1990).

Hatton (1991) described the wetland habitats within the Lake Cowal system. While the surrounding savannah woodland is substantially modified by clearing, there are no specific references to the condition of the riparian woodland, lignum shrublands or canegrass swamp (Department of Land and Water Conservation, 1998).

King (1997) assessed the ecological conditions of the wetlands of the Jemalong and Wyldes Plains Irrigation Districts and found at least 10,600 ha of wetlands. It was estimated that 71% of the wetlands in this area are either degraded or in moderate condition.

A number of other ecological assessments were carried in other wetland areas. Magrath (1992) reported the occurrence and extent of waterbird breeding events within the Booligal wetlands located on Merrimajeel and Muggabah Creeks. Although there is no quantitative data on the vegetation condition in this area, Magrath (1992) pointed out that the high diversity of species using the Booligal wetlands is the testimony to the quality and variety of wetland habitat types.

Pressey *et al.* (1984) found river red gum to be the most intensive and structurally diverse vegetation unit within the confluence of Lachlan and Murrumbidgee River (including the Great Cumbung Swamp). This is due to variations in elevation, flooding frequency and other factors. In the low lying areas, red gums were generally 20-25 m tall but they were only 10 m tall in some marginal areas at higher elevations.

The wetland systems in the Mirrol Creek area include Benangerine Swamp, Narrabri Swamp and Dry Lake and BarrenBox Swamp (Total Catchment Management, 1993). Barren Box Swamp is permanently inundated depressions of 3,200 ha that receives operational losses and drainage water from Yanco and Mirrol Irrigation areas. The black box trees of the swamp are now dead and cumbungi has invaded the perimeter. However, even degraded, Barren Box Swamp continues to provide an important waterbird habitat, particularly during drought period (Total Catchment Management, 1993).

Shepherd (1992) described the health of vegetation growing in the wetlands of the Wah Wah District at the lower extent of Mirrol Creek. Healthy black box trees dominated in only one of the depressions surveyed. Cumbungi dominates the centre of some of the depressions due to persistent inundation.

2.10.2. Water regime and quality in the wetland areas

Most of the wetlands of the Murray-Darling Basin have been affected by an insufficient or unnaturally infrequent supply of water or by the changed timing of supply. A good example is the hydrology of the Great Cumbung Swamp which is impacted by river regulation and abstraction, as well as by partially controlled flooding of large areas by local landholders for enhanced grazing (Shaikh *et al.*, 1996).

Rural development such as construction of levees has the potential to significantly alter the inundation patterns of some wetlands within the Lachlan River Valley. Most levee development occurs on the Belebula River, downstream of Canowindra and the Lachlan River between

Gooloogong and Condobolin (Department of Land and Water Conservation, 1998). Levees also occur along the Lachlan River around Hillston and within the Great Cumbung Swamp. The impacts of past development works on the inundation patterns of wetlands has often not been thoroughly investigated. More recent flood mitigation proposals and development have undergone some form of environmental assessment (Department of Land and Water Conservation, 1998).

The quality of water in some of the wetlands is constantly deteriorating. Wetlands located on tributaries such as Bogandillon Creek and Mirrol Creek are subjected to salinity and other pollutants. The Bogandillon Swamp which serves as one of the terminal basins to the surface drainage systems of the Jemalong and Wyldes Plains Irrigation Districts has been severely degraded as a result of saline surface water inflows and saline groundwater recharge (Williams, 1993).

2.11. Provision of environmental flow

Provision of environmental flow for ecosystems in the Lachlan River Valley was implemented as a response to obvious degradation of the wetlands as a consequence of land and water resources development. Provisions began in 1989 as a result of major flooding in 1989 and 1990 that brought large colonies of waterbirds to wetlands in the Lachlan Region (Allan and Lovett, 1997).

In both 1989 and 1990, the New South Wales Department of Land and Water Conservation released 15,000 ML from Lake Brewster to ensure successful completion of bird breeding activity (Magrath, 1992). Other actions (unregulated flow access rules) were also implemented to ensure continuous flooding. In 1992, the concept of Environmental Contingency Allowances (ECA) was introduced by the then Department of Water Resources and a 5 year trial program developed for the Lachlan Valley (Allan and Lovett, 1997).

An Environmental Flows Management Committee comprising of representatives from the then Department of Water Resources, the Lachlan River Advisory Committee, National Parks and Wildlife Service, Environmental Protection Agency and an environmental nominee was formed to deal with the management of ECA trials, determination of all environmental flow and monitoring procedures (Department of Water Resources, 1993). The Environmental Flow Management Committee produced an Environmental Flow Package for the Lachlan Valley with three major elements, namely: environmental contingency allowance, sharing of unregulated flows, and minimum target flows. Specific issues addressed by the Lachlan environmental flow package include blue-green algal control; salinity dilution; extension of high flow recessions to ensure completion of bird breeding events or fish migration and spawning; and wetting of wetlands and riparian areas following prolonged dry periods as a result of regulation (Department of Water Resources, 1993).

In late 1997, the Lachlan River Management Committee (LRMC) was established to draft environmental flow rules for 1998/99. The LRMCs indicative flow rules in the Lachlan have been based on the eleven interim State-wide river flow objectives (RFOs) established by Government for all major NSW rivers. These objectives, which are currently subject to broad community consultation are summarised in Lachlan River Management Committee (1998). The objectives are:

1. Protect natural water levels in river pools and wetlands during periods of no flow;
2. Protect natural low flows

3. Protect or restore a portion of freshes and high flows;
4. Maintain or restore the natural inundation patterns and distribution of floodwaters supporting natural wetland and floodplain ecosystems;
5. Mimic the natural frequency, duration and seasonal nature of drying periods in naturally temporary streams;
6. Maintain or mimic natural flow variability in all streams;
7. Maintain the rates of rise and fall of river heights within natural bounds;
8. Maintain groundwater within natural levels and variability, critical to surface flows or ecosystem;
9. Minimise the impact of in-stream structures;
10. Minimise downstream water quality impacts of storage releases;
11. Ensure that the management of river flows provides the necessary means to address contingent environmental and water quality events.

2.11.1 Contingency allocations

A Contingency Allowance (CA) of 100,000 ML has been allocated for the Lachlan River Valley, of which 30,000 ML is for high security and 70,000 ML for normal security (Allan and Lovett, 1997). The CAs have been targeted in: bird breeding sites; areas affected by algal blooms; native fish habitats; and streams with salinity problems (Allan and Lovett, 1997; Department of Water Resources, 1993).

Booligal rookery on Merrimajeel Creek has a CA of 11,000 ML, Lake Tarwong on Merrowie Creek has 9,000 ML (Department of Water Resources, 1993). The CA for Booligal was called upon in 1992-93, to a very limited extent in 1993-94 (due to extensive unregulated flows), and in 1996 (Allan and Lovett, 1997).

Contingency allocation has also been set at 6,000 ML for algal bloom suppression and 9,000 ML for salinity dilution in the Lower Lachlan (below Lake Cargelligo), both of these have high security status (Allan and Lovett, 1997).

2.11.2 Sharing of unregulated flows

Unregulated flows are simply the natural flows of the rivers. They are tremendously important in maintaining the overall health of rivers, wetlands and floodplains. Unregulated flow policy has been in place in Lachlan regulated system since 1992/93 water year and involves a number of strategies. Restrictions have been introduced that view unregulated flow as a resource to be shared between users and the environment. Previously, unregulated flows were deemed to be surplus water and irrigators gained first access to this water through the declaration of off-allocation flows (Allan and Lovett, 1997).

The Lachlan unregulated flow policy has a set of access rules to achieve periodic wetting of effluent streams and fish passage over structures to antecedent threshold conditions. The priorities for commitment of the water resource governing these rules summarised in Allan and Lovett (1997) and Department of Water Resources (1993) are as follows::

- The first flush remains in the river to maintain the in-stream environment and water quality;
- water is provided for stock on regulated, effluent streams;
- water is provided for native fish (16,000 ML.d⁻¹ at Booligal for 7 days after a suitable flow

event) and wetland requirements (based on assessments made when unregulated water becomes available). Defined plans are in place for the management of Booligal Swamp and draft plans have been issued for the wetlands of the Merrowie Creek and Willandra Creek systems;

- flows are made available for storage; and
- after the previous needs are satisfied, unregulated flows are regarded as available to irrigators.

The main focus of the unregulated flow policy is on the current flow regime and the protection of natural flow variability. The limit of off-allocation extraction set by Lachlan River Management Committee for the 1998/99 water year was 30,000 ML. This limit assisted the prevention of further loss of variability and improvement of water quality (Lachlan River Management Committee, 1998).

2.11.3 Minimum target flows

Minimum flows are maintained within the 80th percentile range to meet ecosystem needs (Allan and Lovett, 1997). Minimum flow targets are also set to meet water quality objectives. For example, a minimum flow of 250 ML d⁻¹ at Cowra is based on the need to mitigate saline inflows, while the minimum at Booligal is based on eutrophication concerns. The Lachlan River Management Committee (1998) has recommended a minimum flow of 50 ML d⁻¹ at Booligal to allow more drying of some portions of the Great Cumbung Swamp wetland which have been receiving too much water.

2.12. Land use

The dominant landuses in the Lachlan Valley Region is agriculture and pastoral industry. Both dryland and irrigated farming are practised. Wool, wheat, and meat production from sheep or cattle are the traditional industries on broadacre farms, however recent instabilities and declining profits in these areas has resulted in a greater diversity of rural ventures, especially into winter cash crops such as wheat, canola, etc. (Lachlan River Management Committee, 1993).

Lucerne and pastures are currently the predominant crops grown under irrigation upstream of Condobolin, and in the Jemalong and Wyldes Plains Irrigation Districts,. Notable recent developments have been the increased irrigated area of maize (for feed lots) and soybeans. Asparagus is also significant irrigated crop in the upper Lachlan, with the crop being processed at Cowra. Pastures are the predominant user of the irrigation water downstream of Condobolin. However, in the Hillston area more intense development has resulted in a variety of cropping enterprises, including cereals, coarse grains, oil seeds, vegetables and citrus. A significant recent development in the Lachlan has been the growing of cotton on a commercial scale (Department of Water Resources, 1989; Lachlan Catchment Management Committee, 1993) and rice.

Intensive livestock systems such as housed piggeries and cattle feedlots are scattered throughout the Valley and are becoming an increasingly significant industry.

2.13. Irrigation

Ross *et al.* (1992) conducted a survey of irrigators in the Lachlan Valley in 1988-89 to determine the amount of land developed for irrigation, the present use of irrigation water and land, the

current techniques used by irrigators to apply water and the range of soil types being irrigated. To facilitate the interpretation of the results of the survey, the Valley was arbitrarily divided into four sections: (1) Wyangala Dam to Gooloogong; (2) Gooloogong to Condobolin; (3) Condobolin to Oxley; and (4) Jemalong-Wyldes Plains Scheme. Based on the result of the survey, most water supplied for irrigation in the Lachlan Valley was by direct pumping from the river (and creeks) systems for section 1, 2, and 3 and by diversion of water river in section 4. A few irrigators in section 3 (3%) had access only to water from Lake Cargelligo, and 9% of irrigators on the Jemalong-Wyldes Plain Irrigation Scheme had access only to river and creek systems. Bores were an alternative supply of water for some irrigators in each section.

According to Department of Water Resources (1989), the total area authorised for irrigation is around 90,000 ha, however, Ross *et al.* (1992) estimated the total area that can be irrigated was around 102,772 ha with riparian irrigators. The Valley has 457 irrigation licenses. Since most of the irrigation systems in the Valley are old and poorly designed, most field irrigation problems were related to flood irrigation layouts and designs.

Table 2.11 shows the crops and area under irrigation in the irrigated areas in the Lachlan during the 1995/96 cropping season. Winter cereals accounted for about 26% of the total area under irrigation on that season. Lucerne (23%) and winter pasture (18%) were the other major crops grown under irrigation (Department of Land and Water Conservation, 1996b).

Table 2.11: Irrigated crop areas and methods for regulated Lachlan system in 1995/1996 water year.

Crop type	Crop area (ha) in:				Total areas
	Belebula River	Wyangala Dam to Lake Cargelligo	Lake Cargelligo to Oxley	JWPID	
Lucerne	725	12,030	2,259	4,040	19,054
Summer Pasture	35	3,781	2,815	1,429	8,060
Winter Pasture	104	7,083	4,390	3,452	15,029
Forage crops	16	1,582	240	44	1,882
Winter cereals	351	11,160	7,678	2,521	21,710
Oilseeds	52	647	2,170	984	3,853
Grain and legumes	31	320	1,112	29	1,492
Summer cereals	16	3,064	2,338	837	6,255
Vegetables	173	1,074	14	0	1,261
Fruit	4	509	512	0	1,025
Grapes	25	501	108	0	634
Other crops	120	2,857	428	58	3,463
Totals	1,652	44,608	24,064	13,394	83,718

Source: Department of Land and Water Conservation (1996b).

According to Ross *et al.* (1992), the allocation of irrigation water per ha showed that riparian irrigators (sections 1, 2, 3) had a mean annual allocation of 6.7 ML ha⁻¹ and section 4 had a mean annual allocation of 4.1 ML ha⁻¹. The median area for irrigation per farm did not vary greatly between sections 1, 2, and 3 (102, 93, 123 ha, respectively) while section 4 was higher than those of the other sections (275 ha). The main proportion of total farm area that was irrigated decreased with distance down the river from 58% in section 1, to 46% in section 2, 30% in section 3. Section 4 reversed the trend with 44%.

Irrigation water is applied by flood and spray systems in the Lachlan Valley (Ross *et al.* 1992). Spray irrigation is dominant in section 1 while flood irrigation in the other sections.

A detailed description of the Jemalong and Wyldes Plains study area is now presented.

CHAPTER 3

DESCRIPTION OF THE JEMALONG AND BLAND CREEK STUDY AREA

3.1. Location and topographic features

The study area includes the Jemalong and Wyldes Plains Irrigation District (JWPID) and the alluvial area of the Bland Creek catchment (Figure 3.1).

The topography of the JWPID is flat with floodplain elevations ranging from 205 to 225 m Australian Height Datum (AHD) (Kelly 1988; Anderson *et al.*, 1993). The ridges that form the boundaries of the Jemalong District have elevations of up to 480 m AHD, and characteristic slopes of 12 to 15 degrees. Lithology is the main topographic control of the district, being characterised by a series of resistant rock ridges with a north-south trend (see Chapter 4). Natural depressions range in size from major features such as Lake Cowal (13,200 ha), through medium sized depressions of 500 ha, to smaller depressions of less than 100 ha (Forbes Rigby Pty Ltd, 1996). The JWPID is managed by the corporatised Jemalong Irrigation Ltd (JIL). It has a total area of 93,123 ha (McGrath, 1997) with water for the irrigation district diverted from the Lachlan River at Jemalong Weir and fed by gravity through some 306 km of earthen supply and drainage channels.

The Lachlan River flows from the Jemalong Weir, between the Jemalong and Corradgery Ranges, north-westwards past the northern end of the Manna Range. The stream gradient over this reach is approximately 1:3000. The river system in this area is characterised by a number of anabranches which include the Wallamundry Creek, Island Creek and Bomobbin Creek.

The Manna Range which forms the western boundary of the irrigation district restricts any westward surface and subsurface water flow and is responsible, in part, for the formation of Lake Cowal and the adjoining Lake Nerang Cowal.

The Bland Creek catchment extends to the hills surrounding Temora at an elevation of 350 m, Young at 550 m and Grenfell at about 600 m. The alluvial plain is bisected by the Bland Creek. Flat floodplains encompass many towns in the middle of the catchment.

3.2. Climate

3.2.1. Rainfall

As mentioned in Chapter 2, rainfall in the Lachlan River Valley decreases from east to west. In the study area, mean annual rainfalls are higher at the southern and southeastern sides (Figure 3.2).

The mean annual rainfall at Grenfell (073014) is about 633 mm, while at Greenthorpe (093017) south of Grenfell is about 581 mm. Further south from Grenfell, mean annual rainfalls are higher with 698 mm at Wombat (073041) near Young and 587 mm at Stockinbingal (073036). Rainfall in these 4 stations are distributed almost uniformly throughout the year with slightly higher rainfalls

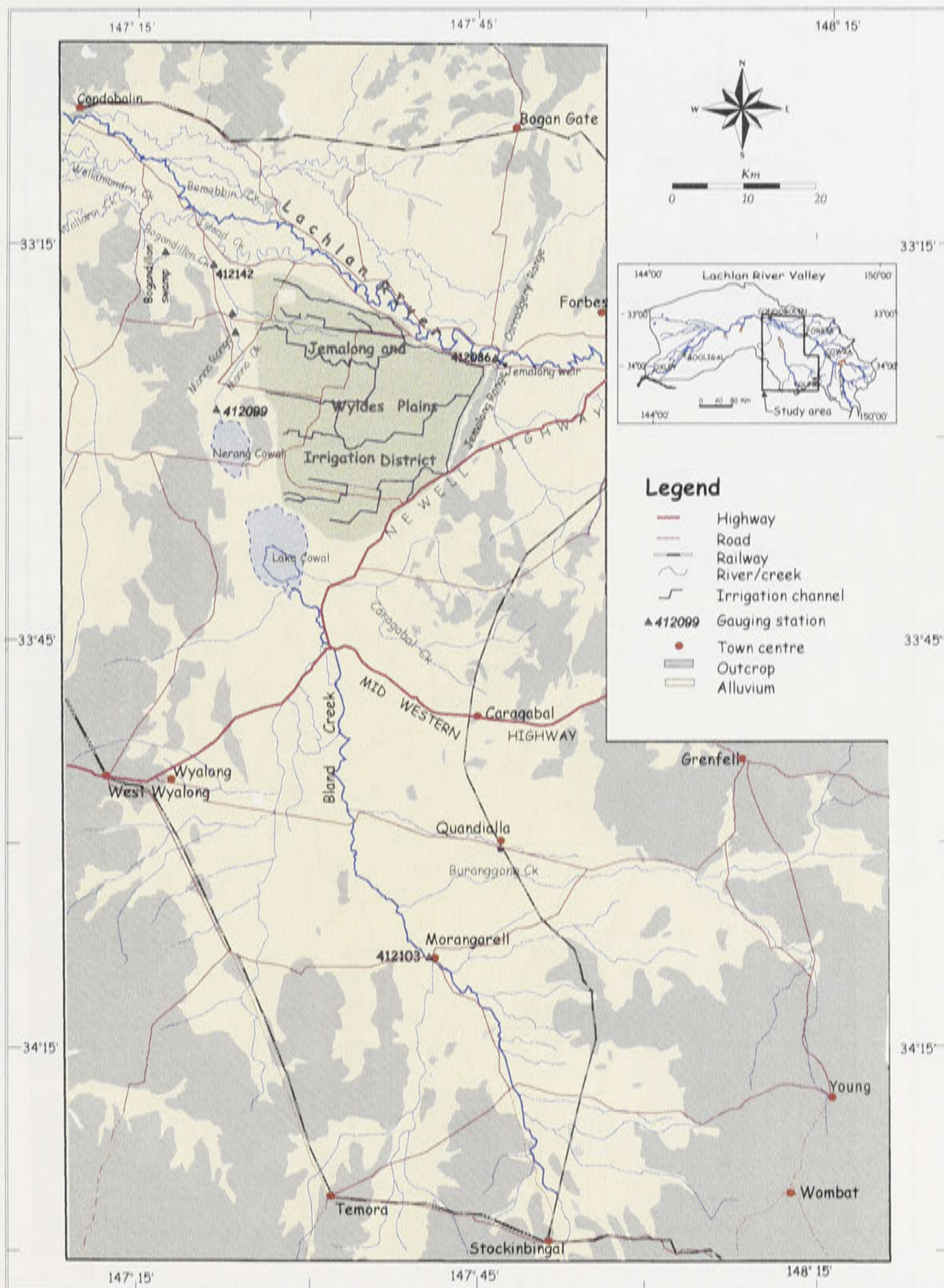


Figure 3.1: Location of the study area.

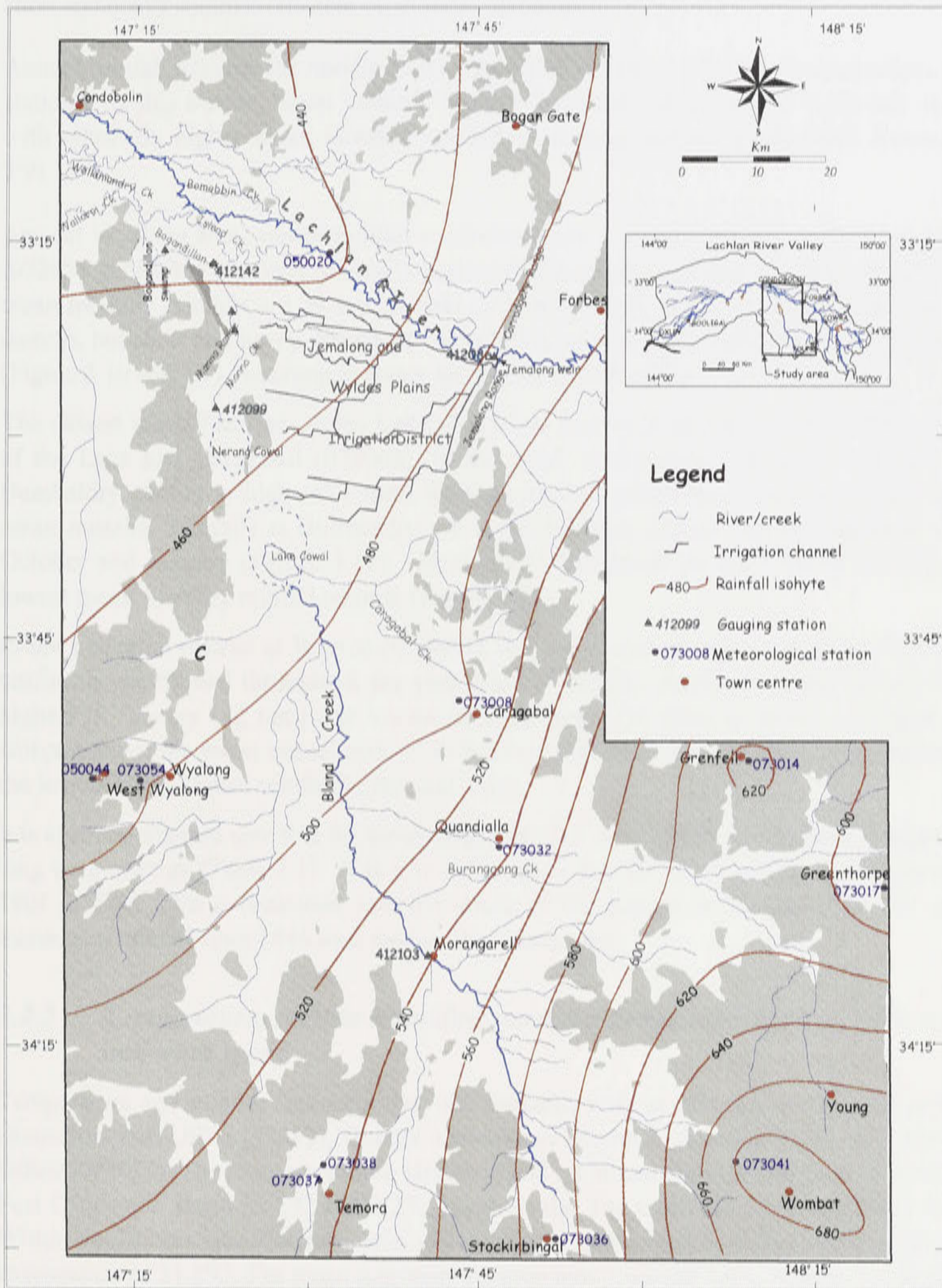


Figure 3.2: Spatial distribution of the long-term mean annual rainfall in the study area.

during winter months (Figure 3.3 to 3.6). In the Temora area, the mean of annual rainfalls at stations 073037 and 073038 are 530 and 534 mm respectively. Also, the long term mean monthly rainfalls for these two stations is about 45 mm (Figure 3.7 and 3.8). However, October and January have slightly higher mean monthly rainfalls at both stations. The Temora area also experiences short and heavy summer falls that often cause flooding.

Annual rainfall towards the middle of the study area is between 533 mm at Quandialla (073032) station. At this station, mean monthly rainfall is 44 mm and is almost uniformly distributed, with relatively higher mean monthly rainfalls occurring during October and January (Figure 3.9).

Around Wyalong area, annual rainfall is relatively low. Annual rainfall at Wyalong Post Office (073054) and West Wyalong (050044) stations are about 480 mm and 460 mm respectively, while mean monthly rainfalls are 39 mm at both stations. Slightly higher rainfalls occur during winter months, but short and heavy downpours of rainfalls are also observed during October and January (Figure 3.10 and 3.11) resulting in minor local short term flooding.

The closest rainfall stations to the Lake Cowal are located at Bumbaldry (073100) to the south of the Lake and Caragabal (073008) on the south eastern side. The mean annual rainfall at Bumbaldry station is high (674 mm) whereas at Caragabal station is lower (493 mm). The mean monthly rainfalls at Bulmandry are slightly higher during winter months as well as in October and January (Figure 3.12). However in Caragabal station, winter months have the lowest mean monthly rainfall records (Figure 3.13).

In the irrigation district at Warroo (050020), the mean annual rainfall is about 434 mm and is uniformly distributed throughout the year with an average monthly rainfall of about 37 mm, highest in January (42 mm) and lowest in September (32 mm) as shown in Figure 3.14. A comparison of the mean annual rainfall in Warroo with other stations shows that this station has the lowest mean annual rainfall in the study area.

It is also important to note that the mean annual rainfall since 1946 in all stations is higher than the long term average (Table 3.1). It is 5 to 23% higher than the mean annual rainfall for the period 1901 to 1945. This is consistent with the results of the analysis in Chapter 2 for the significant increase of rainfall since 1946 over the Lachlan Catchment.

3.2.2 *Temperature, relative humidity, potential evapotranspiration, solar radiation and wind speed*

Temperature and relative humidity data are available only at meteorological stations located at Quandialla Post Office (73032), Temora Agricultural Research Station (073038) and Wyalong Post Office (073054). The mean maximum (January) and minimum (July) temperature at the Quandialla Post Office are about 32.6°C and 2.2°C, respectively. The mean relative humidity is about 69%. Within the Temora area, the mean relative humidity is approximately 69% and the mean maximum temperature of 31.5°C. The mean minimum temperature is around 1.6°C in July. In Wyalong area, the mean relative humidity is around 53% and mean maximum temperature of 32.2°C. The mean minimum temperature is about 2.3°C in July.

Daily pan evaporation (E_p), wind speed and solar radiation at the JWPID have been monitored by the Jemalong Irrigation Ltd since April 1995. Monthly solar radiation, the principal driver of ET, shows the expected seasonal sinusoidal pattern (Figure 3.15). The average solar radiation from May 1, 1995 to May 1, 1997 is about 17 MJ m⁻² and summer and winter seasons averages are 25 and 9 MJ m⁻², respectively for the period 1995 to 1997.

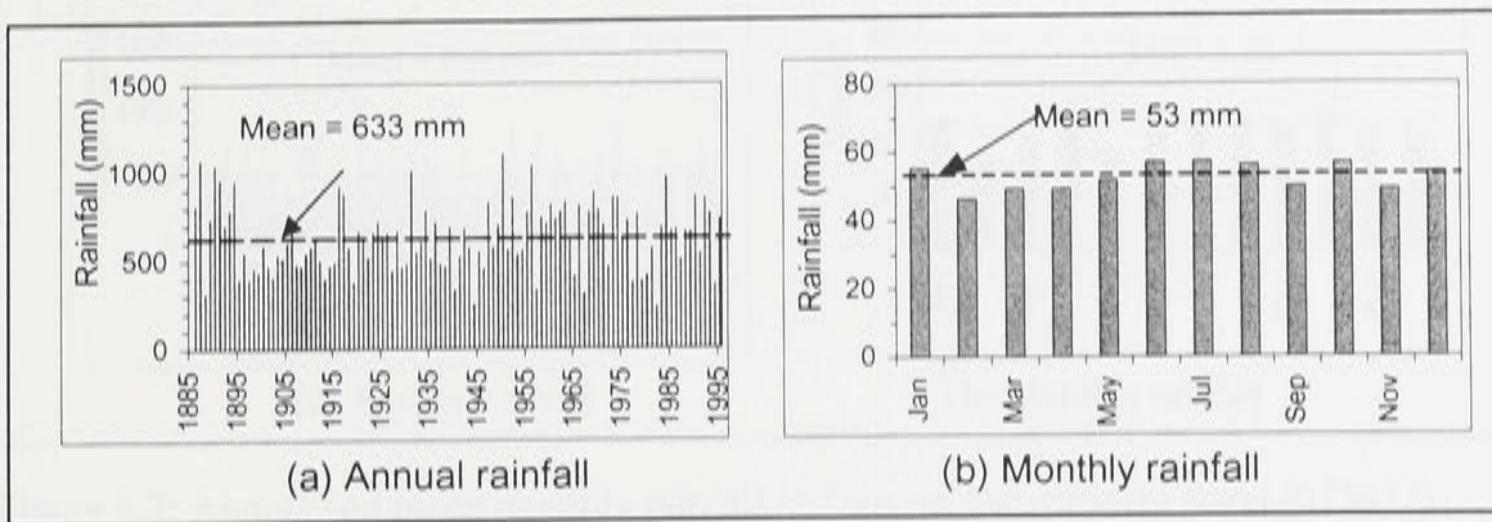


Figure 3.3: Annual and mean monthly rainfall at Grenfell Post Office (073014).

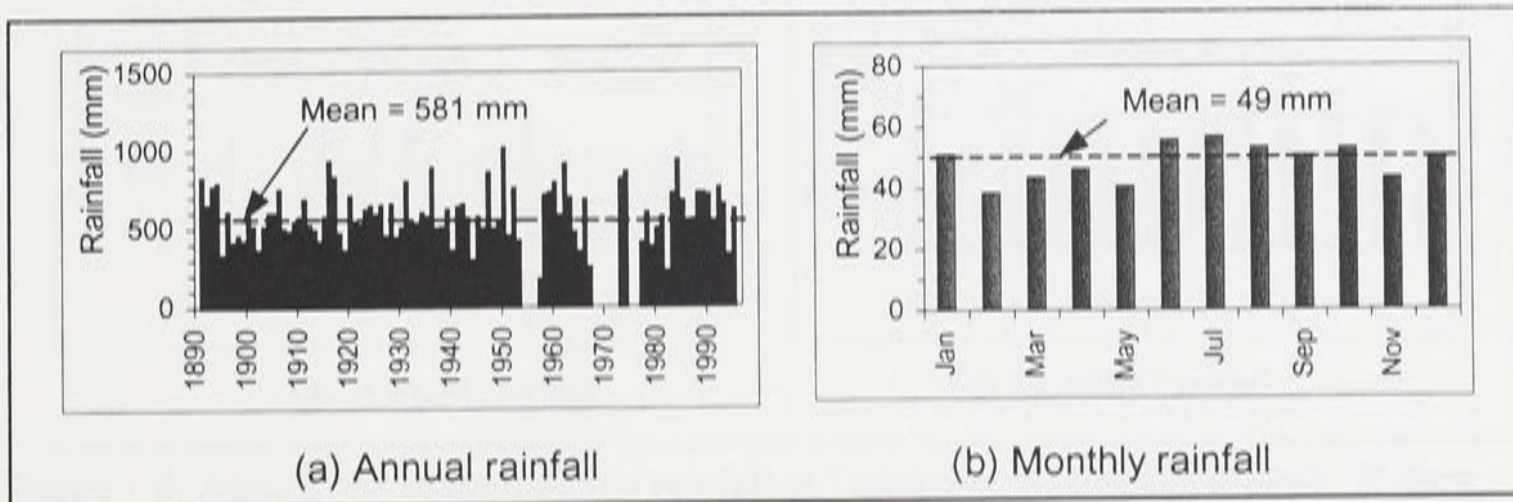


Figure 3.4: Annual and mean monthly rainfall at Greenthorpe (073017).

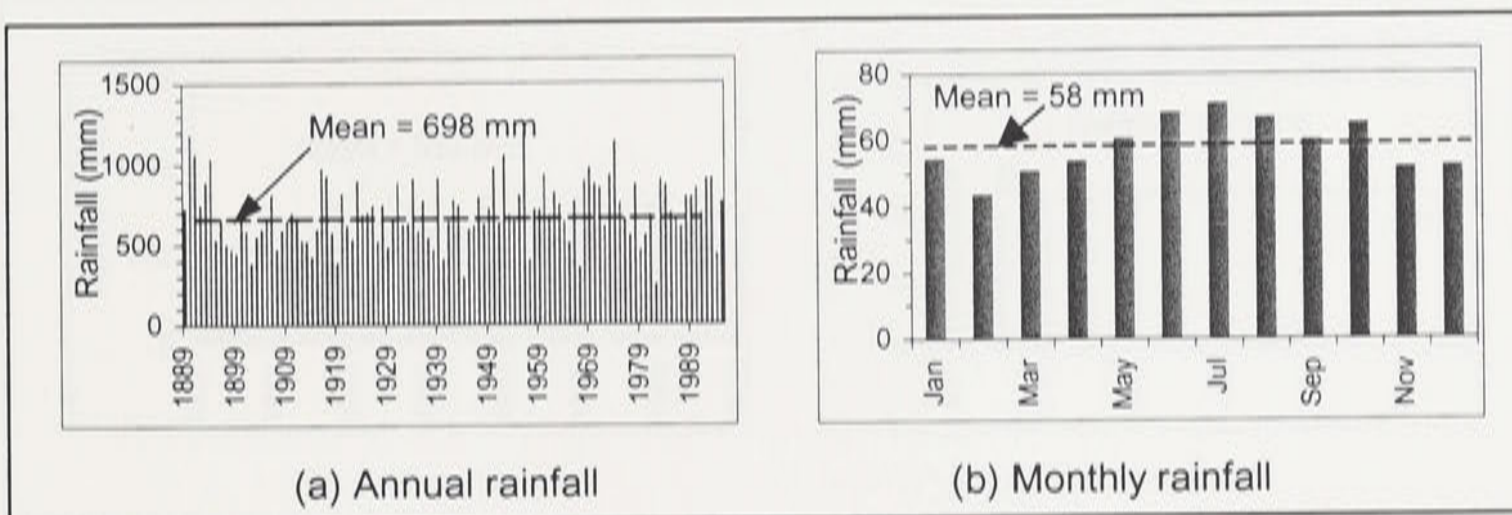


Figure 3.5: Annual and mean monthly rainfall at Wombat (073041).

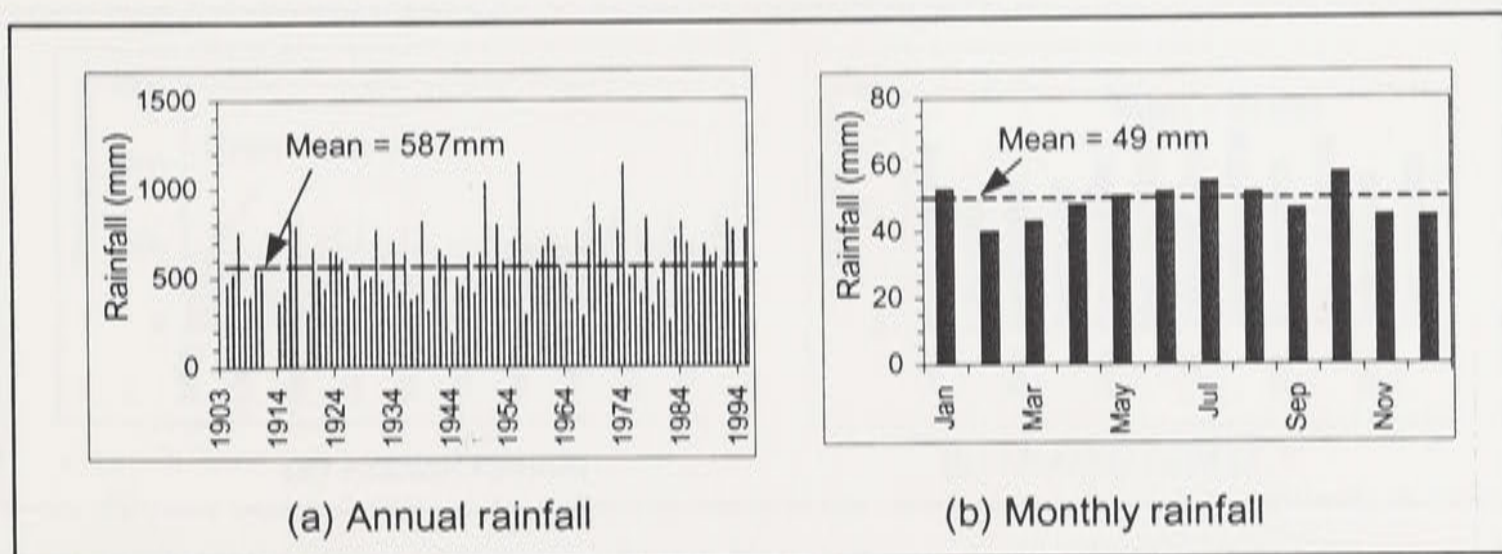


Figure 3.6: Annual and mean monthly rainfall at Stockinbingal (073036).

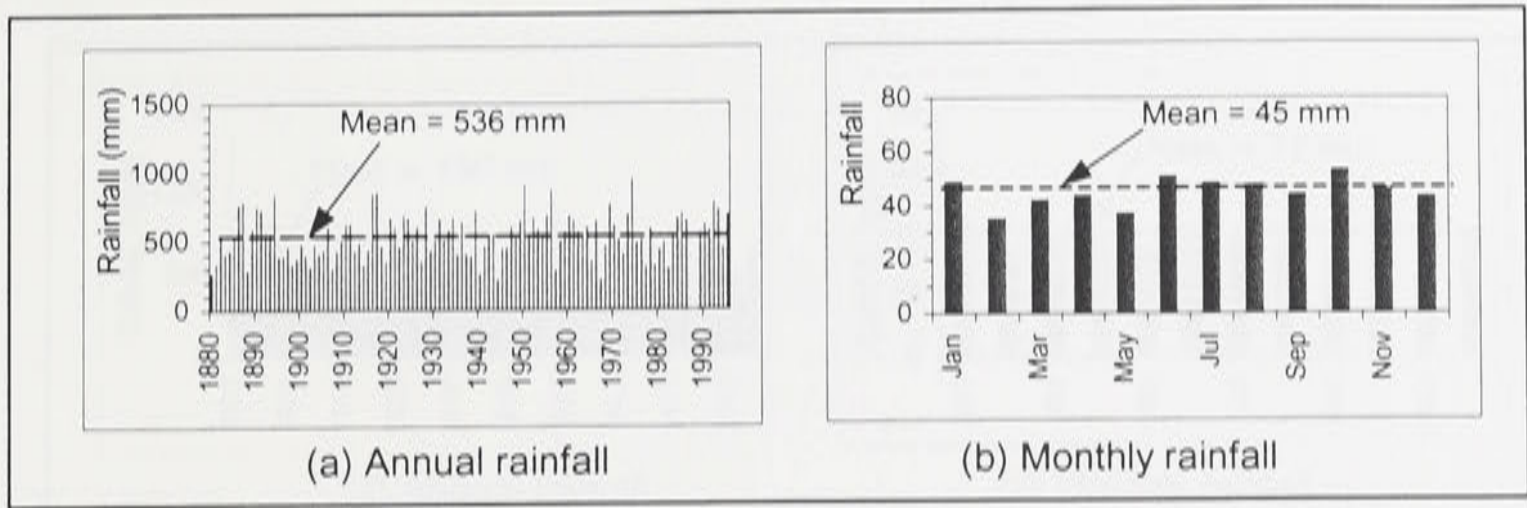


Figure 3.7: Annual and mean monthly rainfall at Temora, Barmedman Road (073037).

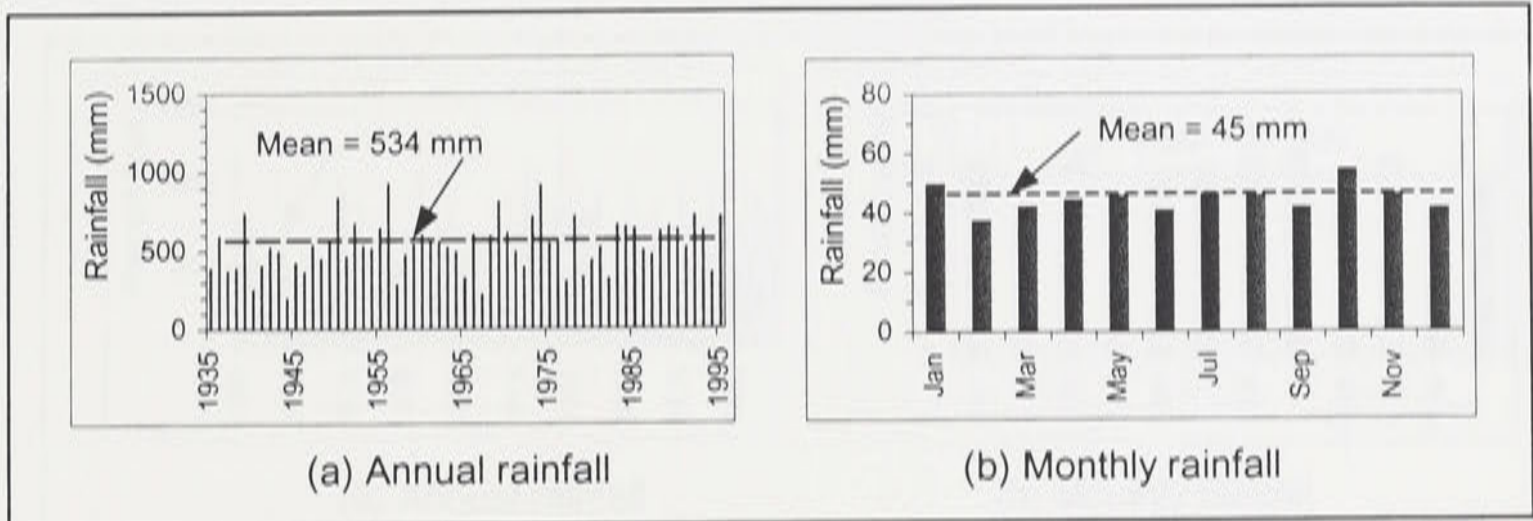


Figure 3.8: Annual and mean monthly rainfall at Temora Agricultural Research Station (073038).

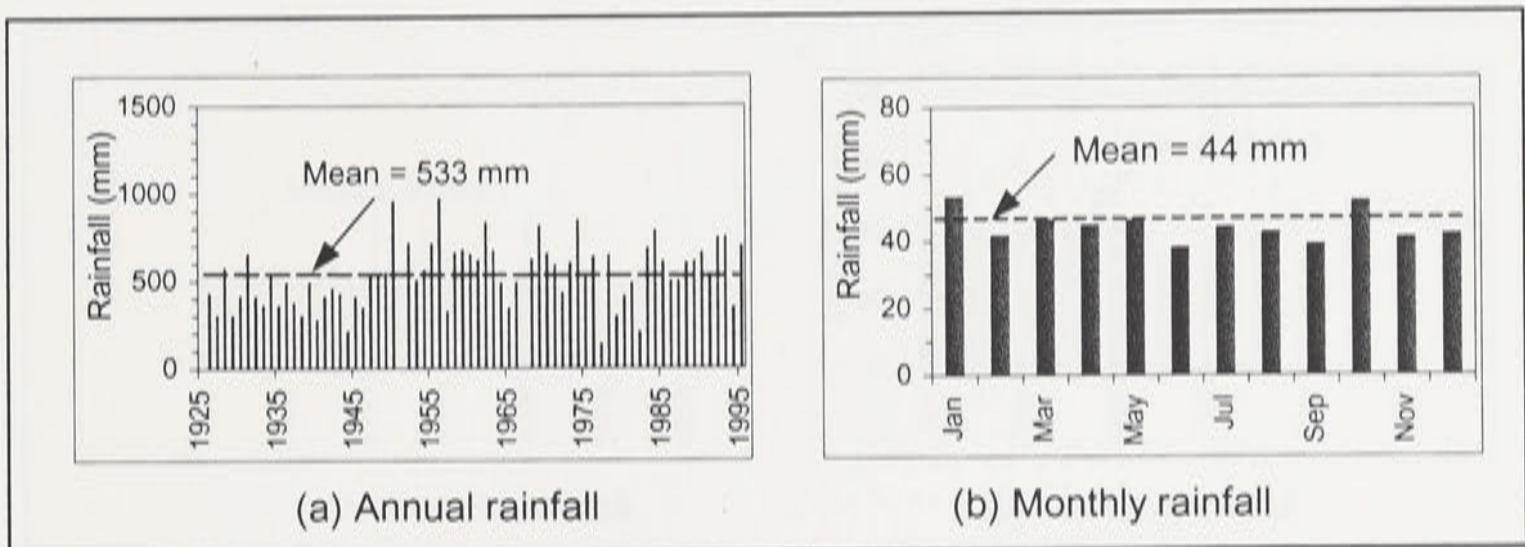


Figure 3.9: Annual and mean monthly rainfall at Quandialla Post Office (073032).

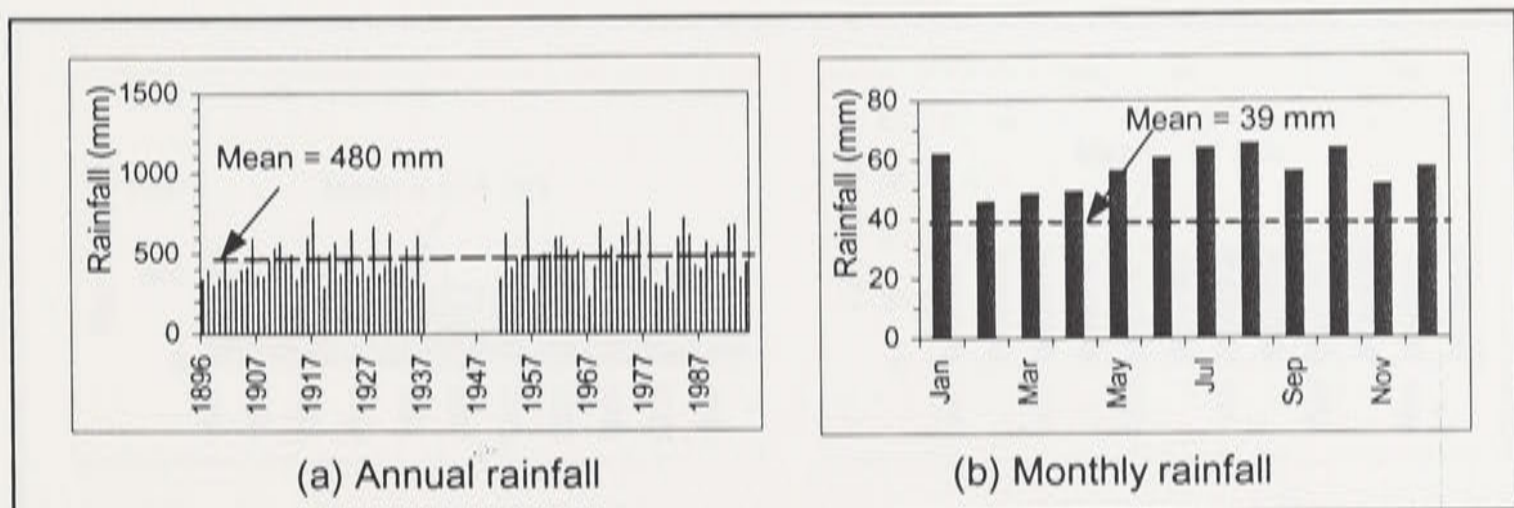


Figure 3.10: Annual and mean monthly rainfall at Wyalong Post Office (073054).

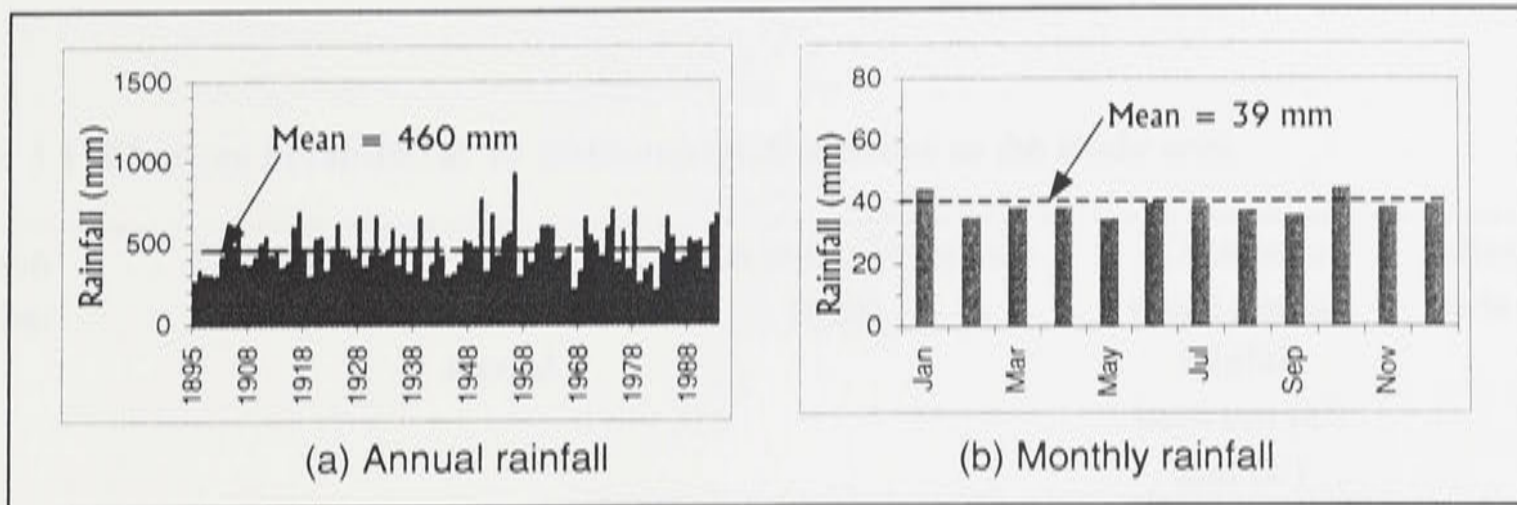


Figure 3.11: Annual and mean monthly rainfall at West Wyalong (050044).

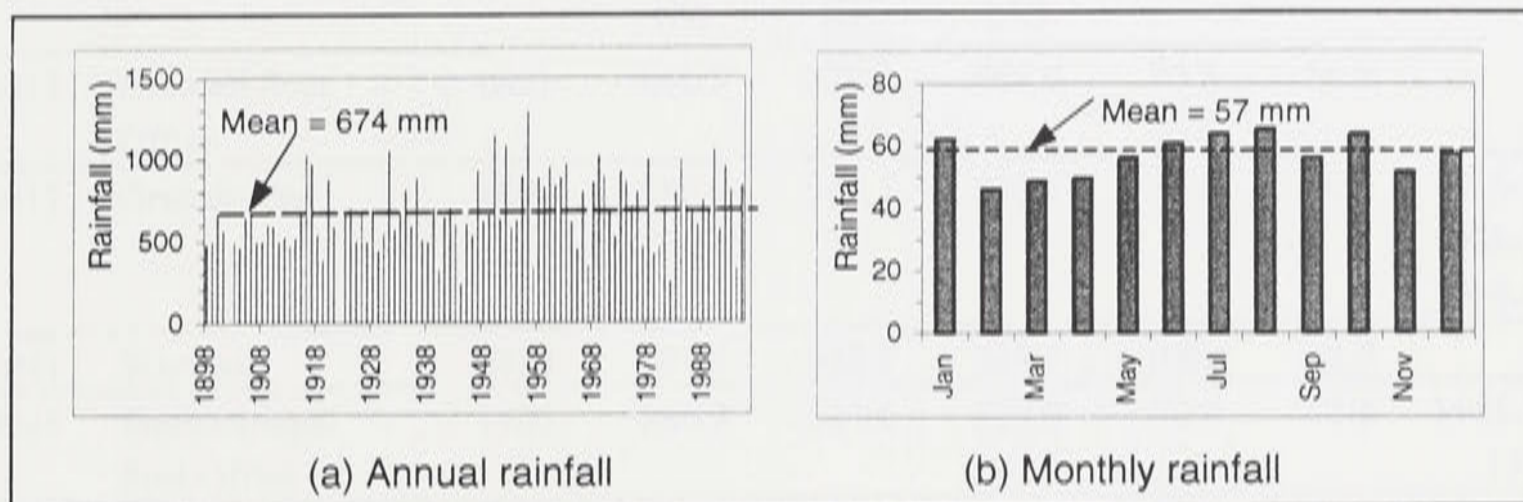


Figure 3.12: Annual and mean monthly rainfall at Bumbaldry (073100).

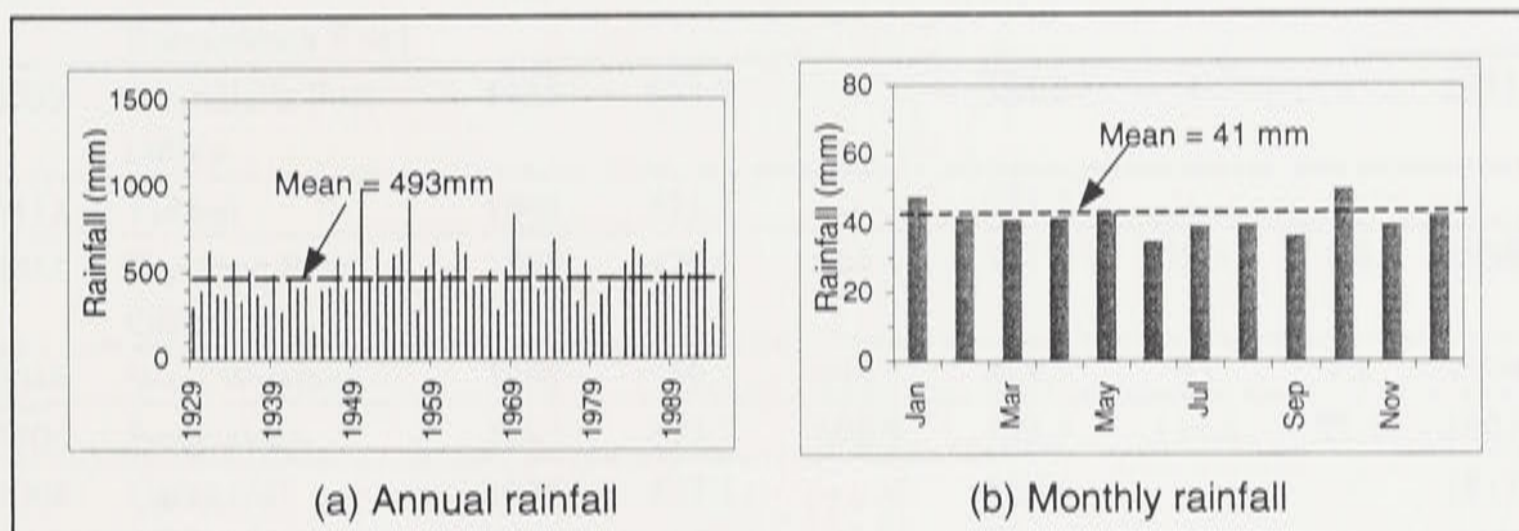


Figure 3.13: Annual and mean monthly rainfall at Caragabal (073008).

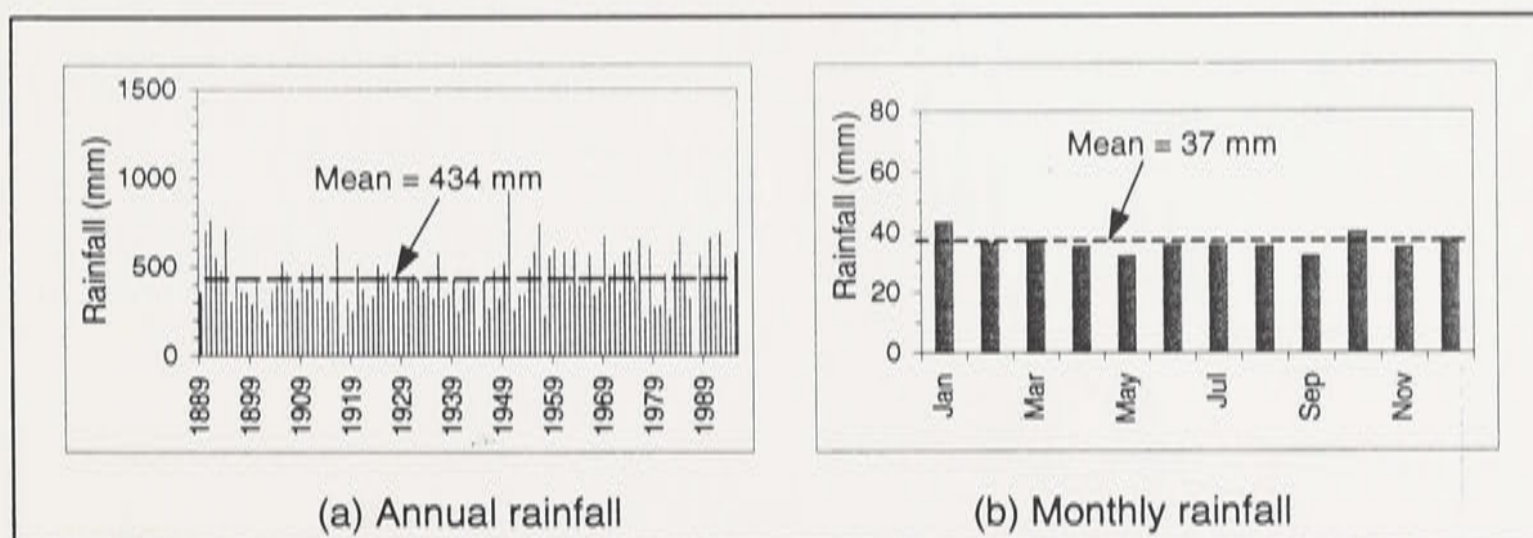


Figure 3.14: Annual and mean monthly rainfall at Warroo (050020).

Table 3.1 Changes in rainfall at 13 meteorological stations in the study area.

Station number	Station name	Year start of record	Mean annual rainfall (mm)			Change in mean annual rainfall between (C) and (B)		Missing data in:
			Whole record (A)	1901-1945 (B)	1946-1995 (C)	mm	%	
073014	Grenfell Post Office	1885	632.5	575.7	669.0	93.3	16.0	
073017	Greenthorpe	1890	580.5	565.2	596.8	31.6	5.5	1955-1956, 1968-1972, 1975-1976,
073041	Wombat	1888	697.6	638.5	739.1	100.6	15.7	
073036	Stockinbingal Post Office	1903	586.9	533.0	627.9	94.9	17.8	1911-1913, 1918
073038	Temora Agric. Research Station	1934	534.1	-	555.4	-	-	
073037	Temora, Barmedman Road	1880	535.6	508.69	570.5	61.81	5.3	1987-1988
073032	Quandialla Post Office	1925	533.3	-	584.5	-	-	1951, 1967
073113	Tubbul	1968	571.2	-	571.2	-	-	
073054	Wyalong Post Office	1895	479.6	464.1	503.0	38.9	8.4	1938-1950
050044	West Wyalong	1895	459.6	446.7	481.7	35	7.8	1994-1995
073100	Bumbaldry	1897	673.5	608.9	743.7	134.8	22.1	1902, 1922
073008	Caragabal	1916	493.1	-	525.6	-	-	1917-1928, 1982
050020	Warroo	1889	434.4	381.66	471.3	89.64	23.4	

Potential ET also reflects the sinusoidal variation in solar radiation (Figure 3.15). The mean daily evapotranspiration for the two summer seasons for the period 1995 to 1997 is about 6.6 mm d^{-1} and the mean for 3 winter seasons from 1995 to 1997 is about 1.3 mm d^{-1} . Mean daily evapotranspiration from 1st May 1995 to 1st May 1997 is about 3.8 mm d^{-1} . The mean daily wind speed has also a sinusoidal distribution throughout the year (Figure 3.16). The average wind speed from March 14, 1995 to September 29, 1997 is about 5.6 km hr^{-1} .

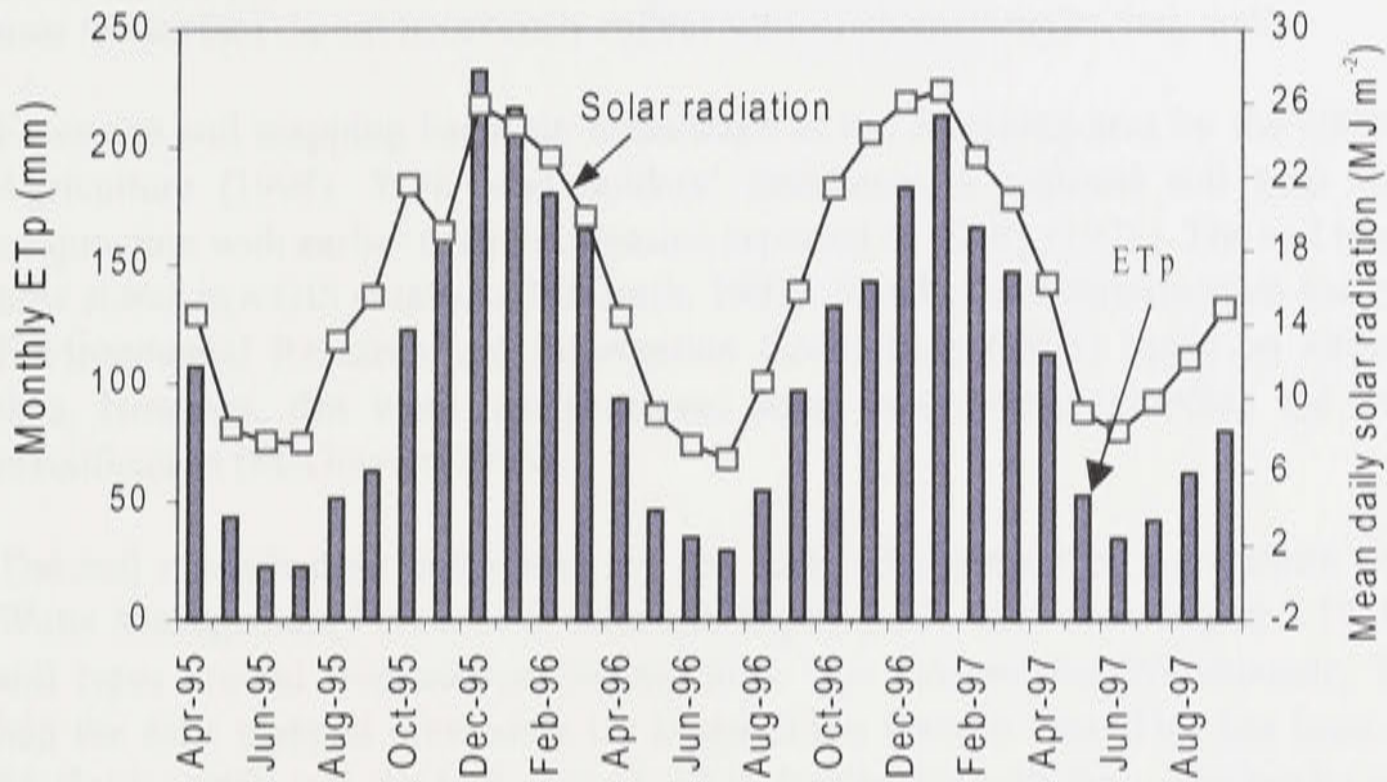


Figure 3.15: Monthly potential evapotranspiration (ETp) and solar radiation at JWPID.

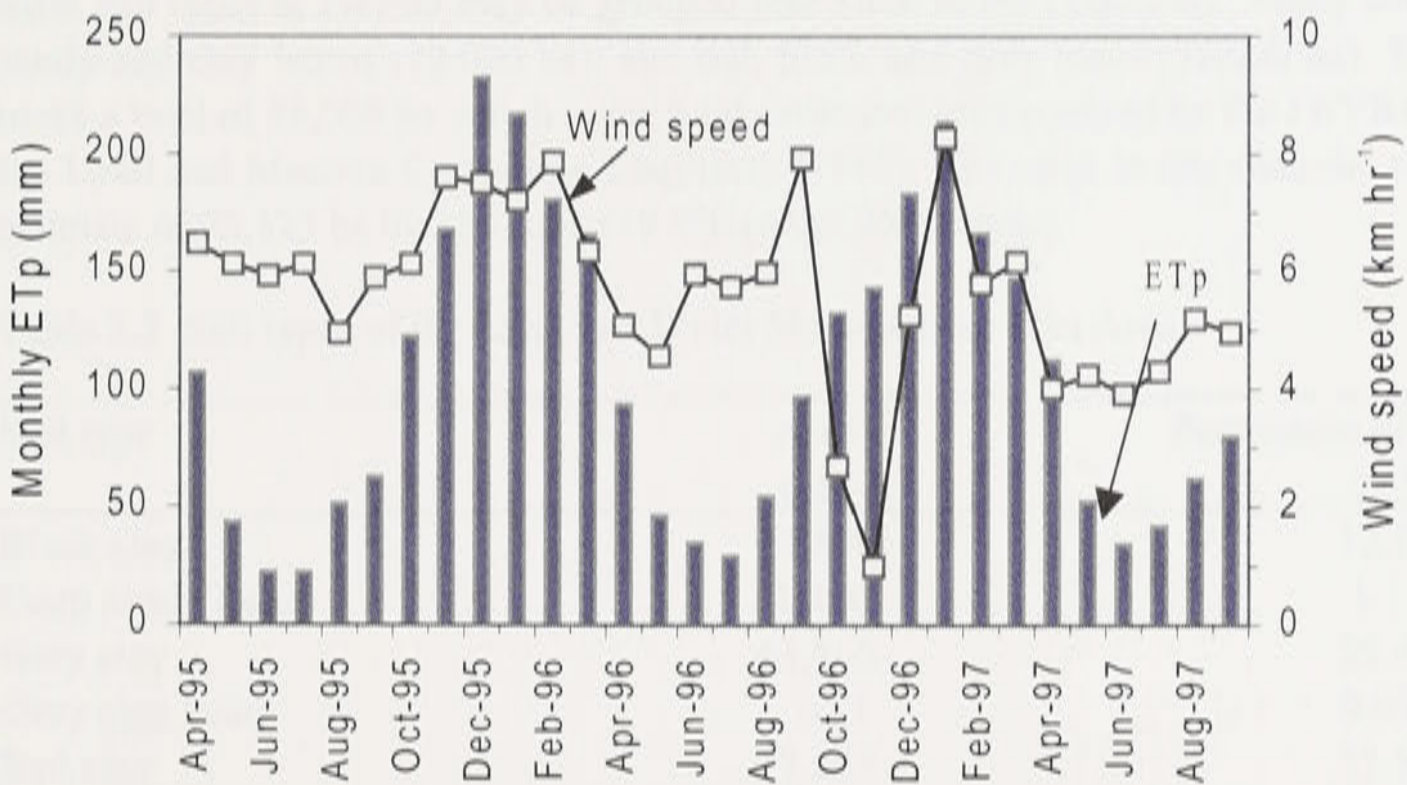


Figure 3.16: Monthly potential evapotranspiration (ETp) and wind speed at JWPID.

3.3. Soils

3.3.1. Soil types

Soils at the JWPID are a complex mixture of soils derived from fluvial processes (Forbes Rigby Pty Ltd, 1996). Distribution of the soil types across the district is complex and very variable as a result of the period over which the sediments have been deposited. Soil characteristics at or near the surface do not necessarily reflect subsoil characteristics very well.

Extensive soil mapping has been undertaken at the Jemalong area by the NSW Department of Agriculture (1994). With land holders' assistance, a regional soil map was produced in conjunction with earlier soils information reported in Kelly (1971). The soil type information is now stored in a GIS database (McGrath, 1997). Another soil classification has been done by the Environmental Research and Information Consortium (1995) based on airborne radiometric data. However, this work has generated some controversy regarding the usefulness of the classification (McGowen, 1996).

The soil classification undertaken by the NSW Department of Agriculture for the Land and Water Management Plan area is shown in Figure 3.17. However, Figure 3.17 doesn't show the soil types around Bogandillon Swamp area. The Bogandillon/Wallamundry Landcare Group had the soils mapped previously for Bogandillon Swamp area. This has been incorporated by McGrath (1997) into the GIS of the LWMP landholder soils map. The predominant soil type is grey clay covering 43,865 ha (Table 3.2), however red clay, red clay loam, black clay, sandy loam, and red loam are also relatively dominant. Grey and red clays are found on the lower parts of the districts particularly in floodways and Lake Cowal area. These soils have voids filled with fine clays. This has caused their poor internal drainage characteristics. Areas of grey soils are generally where waterlogging presents a potential problem (Maunsell and Partners, 1986). According to Lyall and Macoun Consulting Engineers (1995), from the hydrologic viewpoint, main soil types at JWPID may be grouped into three broad classes as : sandy soils (16,000 ha); sandy and clay loams (22,000 ha); and red, black and grey clays (50,000 ha). These soil types make a total of 88,000 ha which is the total estimated area covered by the JWPID as reported by the Lyall and Macoun Consulting Engineers (1995). This area is less than the reported current estimate of 93,123 ha by McGrath (1997) using GIS analysis.

Table 3.2 Soil types of the Land and Water Management Plan Area.

Soil type	Area (ha)	Percentage of total area (%)
Black clay	14,890	12.0
Deep sandy loam	1,406	1.1
Grey clay	43,865	35.4
Grey clay loam	751	0.61
Red clay	17,235	13.9
Red clay loam	17,144	13.8
Red loam	11,551	9.3
Rock	647	0.52
Sand	3,600	2.9
Sandy loam	12,803	10.3
Total	123,892	100

Source: Mc Grath (1997).

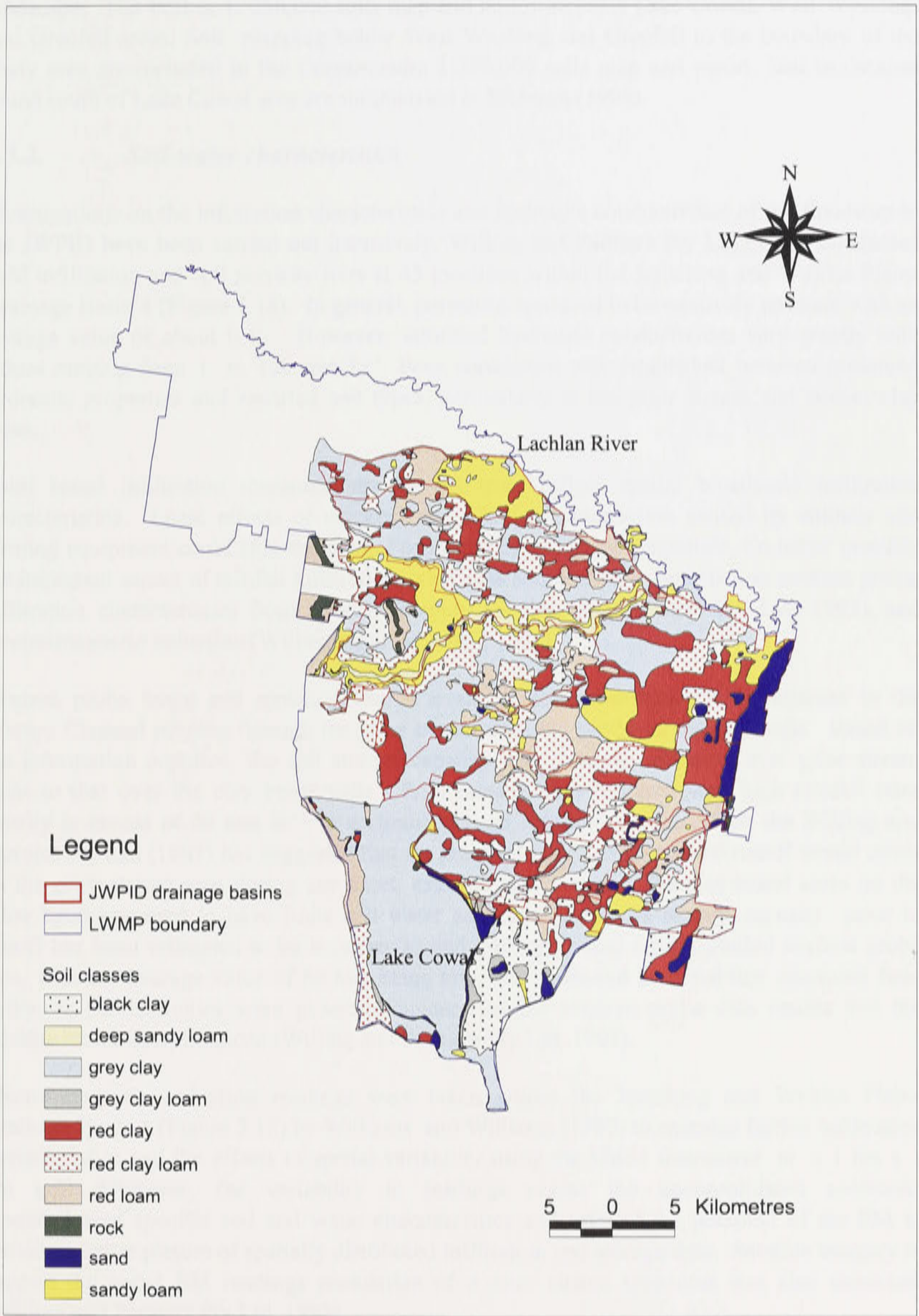


Figure 3.17: Soil classes map of the Land and Water Management Plan (LWMP) area (Source of data: McGrath, 1997).

The soil mapping at the southern part of the study area below Lake Cowal covering the Bland creek catchment is not as detailed as in Jemalong area and mapping units are according to soil landscape. The Forbes 1: 250,000 soils map and report includes Lake Cowal, West Wyalong, and Grenfell areas. Soil mapping below West Wyalong and Grenfell to the boundary of the study area are included in the Cootamundra 1:250,000 soils map and report. Soil landscapes found south of Lake Cowal area are summarised in McInnes (1995).

3.3.2. *Soil-water characteristics*

Investigations on the infiltration characteristics and hydraulic conductivities of the floodway in the JWPID have been carried out intensively. Willing and Partners Pty Ltd (1993) conducted field infiltration and soil porosity tests at 45 locations within the Jemalong and Wyldes Plains Drainage Basin 4 (Figure 3.18). In general, porosities appeared to be relatively constant with an average value of about 0.45. However, saturated hydraulic conductivities vary greatly with values ranging from 1 to 100 mm hr⁻¹. Poor correlation was established between measured hydraulic properties and reported soil types, particularly at the prior stream and stream clay areas.

Point based infiltration measurements do not truly reflect spatial broadscale infiltration characteristics. Local effects of cracking and localised compaction caused by animals and farming equipment could alter the natural condition by orders of magnitude. To better quantify the important aspect of rainfall infiltration, other data sources were used such as neutron probe, infiltration characteristics from satellite imagery (Willing and Partners Pty Ltd, 1993), and electro-magnetic induction (Williams and Williams, 1992).

Neutron probe based soil moisture data is available from transects mainly adjacent to the Warroo Channel running through the prior stream area and partly on the clay soils. Based on the information supplied, the soil storage capacity was distinctly different over prior stream areas to that over the clay based soils. Prior stream areas required very high rainfall rates usually in excess of 20 mm hr⁻¹ to accumulate even localised runoff. Thus, the Willing and Partners Pty Ltd (1993) has suggested that for practical purposes no surface runoff would occur on the prior stream area during any short, extreme storm event. The clay-based areas on the other hand appeared to have finite soil water capacity. Soil water storage capacity prior to runoff has been estimated to be between 20 and 140 mm based on the limited neutron probe data, with an average value of 80 mm being adopted. It should be noted that measured field hydraulic conductivities were generally higher than the neutron probe data results and the satellite based interpretations (Willing and Partners Pty Ltd, 1993).

Electro-magnetic induction readings were taken across the Jemalong and Wyldes Plains Drainage Basin 4 (Figure 3.18) by Williams and Williams (1992) to examine further infiltration characteristics and the effects of spatial variability using the EM31 instrument at a 1 km x 1 km grid. However, the variability in readings across the unconsolidated sediments overshadowed specific soil and water characteristics and masked the potential of the EM to provide a better picture of spatially distributed infiltration and storage data. Satellite imagery to support the aerial EM readings postulation of a prior stream type area was also examined (Willing and Partners Pty Ltd, 1993).

Based on the above investigations by Willing and Partners Pty Ltd (1993) and Williams and Williams (1992), sand to sandy loam soils in the Jemalong and Wyldes Plains Irrigation District floodways have high infiltration rates and saturated hydraulic conductivities whereas the clay to

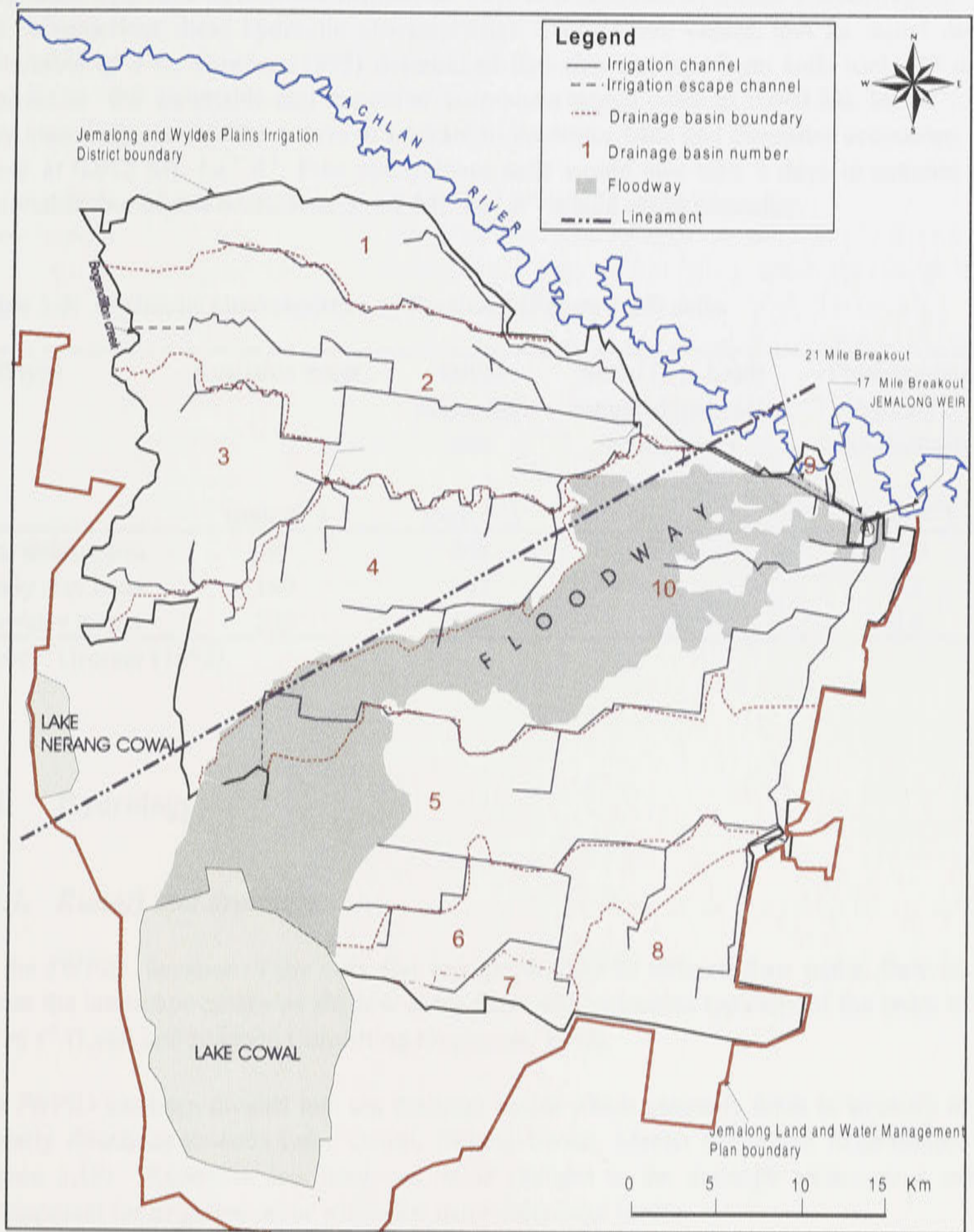


Figure 3.18: Drainage basins and floodway of the Jemalong and Wyldes Plains Irrigation District (modified from Lyall and Macoun Consulting Engineers, 1995).

clay loam type soils have lower infiltration rates and saturated hydraulic conductivities. Table 3.3 summarises these hydraulic characteristics. Using these values, and an initial depth to watertable of 3 m, Gromer (1992) determined that clay to clay loam soils took 28 days to saturate to the watertable and thereafter accessions would occur at 0.006 ML ha⁻¹ d⁻¹. Sandy clay loam soils would take 4 days to saturate to the water table and thereafter accessions would occur at 0.012 ML ha⁻¹ d⁻¹. Fine sandy loam soils would also take 4 days to saturate to the watertable, but higher accessions of 1.2 ML ha⁻¹ d⁻¹ would occur thereafter.

Table 3.3. Hydraulic characteristics of floodway (Figure 3.16) soils.

Soil type	Available water (mm m ⁻¹)	Initial infiltration rate (mm d ⁻¹)	Initial (3 m head) saturated hydraulic conductivity (mm d ⁻¹)	Final saturated hydraulic conductivity (mm d ⁻¹)
Fine sandy loam	60	600	360	120
Sandy clay loam	140	192	60	1.2
Clay/clay loams	200	120	24	0.6

Source: Gromer (1992).

3.4. Hydrology

3.4.1. Runoff and drainage

At the JWPID, because of the very flat topography and ill defined flow paths, flow of water across the landscape occurs as shallow sheet flow with velocities typically of the order of 0.05-0.2 m s⁻¹ (Lyall and Macoun Consulting Engineers, 1995).

The JWPID has been divided into ten drainage basins which generally drain in westerly or south westerly directions towards Lake Cowal, Nerang Cowal, Manna Creek and Bogandillon Creek (Figure 3.18). Except in few instances, most changes to the drainage pattern as a result of development for irrigation occur within the natural drainage basins.

Flood breakouts provide significant source of groundwater recharge for the district. Floodwaters have been confined to the floodway in all but the wettest of years. Willing and Partners Pty Ltd (1993) modelled the 1990 flood event in the Jemalong area which resulted from approximately 280 mm of rain occurring over a 3 week period during April. The model has estimated that the volume of standing surface water ponding in the modelled area (Basin 4) was in excess of 2,000 ML, with spilling volume of 6,500 ML occurring during the storm peak at the end of April. Water ponding lasted for 6 to 7 months due partly to low seepage loss averaging 1.5 mm d⁻¹.

Bland creek and its tributaries, at the southern part of the JWPID drain northward discharging into Lake Cowal. Lake Cowal also receives flood runoff from the Lachlan River through the floodway. This flood water is the major recharge source for Lake Cowal. The flood water flows south-west along the leveed Main Floodway from the "17 and 21 Mile breakouts" on the Lachlan River, through the JWPID (Figure 3.1). The flood water enters Lake Cowal in the area immediately north of Bogeys Island through swampy depressions. When Lake Cowal is full,

floodwater begins to fill Lake Nerang Cowal by flowing across the intervening saddle. Once filled to capacity the overflow from the Lake Cowal system ultimately discharges to the Lachlan River through the Manna and Bogandillon Creek complex (Coffey Partners International Pty Ltd, 1994). Lake Cowal has a local catchment of 700 km². When it is full, it has a storage capacity of 194,000 ML (Department of Water Resources, 1992).

Table 3.4 indicates that the frequency of partial inundation is approximately 50% (31 out of 64 years from 1930 to 1994). Once full the Lake system takes approximately two to three years to be depleted depending on the size of the preceding flood, evaporation, and extraction by farmers for irrigation.

Table 3.4: Hydrological characteristics of Lake Cowal.

Period of record	Capacity (ML)	Source of water supply	Inundation years	Duration of inundation	Land title and use
1930-1994	194,000	Lachlan River and Bland Creek	1931, 1939, 1950-1959, 1960, 1962, 1963, 1964, 1966, 1968, 1969, 1970, 1974-1976, 1978, 1983, 1984, 1990, 1991-1994	2-3 years after filling. Last dry in 1986-1989	Freehold, limited area of game reserve. Mostly grazing, and some cropping.

Source: Coffey Partners International Pty Ltd (1995b).

3.4.2. Stream gauging

Stream gauging data at four gauging stations in the study area are summarised in Table 3.5. Active gauging stations are available at the Lachlan River at Jemalong Weir (412036), Manna Creek near Lake Nerang Cowal (412099), Bogandillon Creek at Birrack Bridge (412142) and Bland Creek at Morangarell (412103). Apart from these stations, there are four other stations without number shown on Figure 3.1.

Table 3.5. Available stream gauging stations in the study area.

Station number*	Station name	Date of establishment
412036	Lachlan River at Jemalong Weir	?
412099	Manna Creek at near Lake Nerang Cowal	21 Oct 1975
412142	Bogandillon Creek at Birrack Bridge	19 Nov 1992
412103	Bland Creek at Morangarell	28 Oct 1976

* see Figure 3.1 for locations.

3.4.3. *Streamflow characteristics*

3.4.3.1. *Lachlan River at Jemalong Weir*

Water level in the Lachlan River at the Jemalong Weir (station no. 412036) has been recorded since 1941 and is generally about 3 m above an arbitrary datum, but rises up to 8 m during periods of high river flow. During the major flood event in 1990, water levels remained at about 8 m for approximately four months. The mean annual streamflow at this station is 1,204,000 ML between 1941 to 1995 (Figure 3.19), with missing records from 1983 to 1989. Between 1972 to 1997 (post Wyangala Dam enlargement), mean annual streamflow is about 1,155,000 ML and is about 169,000 ML lower than the average annual streamflow that passes through Forbes gauging station 412004 (see Table 2.3). This is partly due to the diversion of water for irrigation and stock use at the Jemalong Weir, 50 m above the gauging station. On average, Jemalong Weir water diversion is about 70,000 ML yr⁻¹ from 1986/87 to 1996/97 water year. Monthly streamflow characteristics at this station are generally similar to the other gauging stations along the Lachlan River (Cowra, Forbes and Condobolin stations) as discussed in Chapter 2. In general, streamflows are high during winter months due to release for winter crops and low during summer months. The average streamflow in August is the highest at 228,000 ML whereas January streamflow is the lowest at 53,000 ML.

The daily flow duration curve for the period of 1990-1998 (Figure 3.19d) shows that about 10% of the samples equalled or exceeded 10,000 ML d⁻¹. It should be noted that 48% of the samples that equalled or exceeded 10,000 ML d⁻¹ are from the 1990 daily streamflow records (Figure 3.19c). The highest recorded daily streamflow is about 102,000 ML d⁻¹ in 7 August 1990. No cease-flow conditions occurred at this station between 1990 to 1997, and the lowest daily streamflow is about 21 ML d⁻¹ recorded in 26 July 1993.

3.4.3.2. *Manna Creek, near Lake Nerang Cowal*

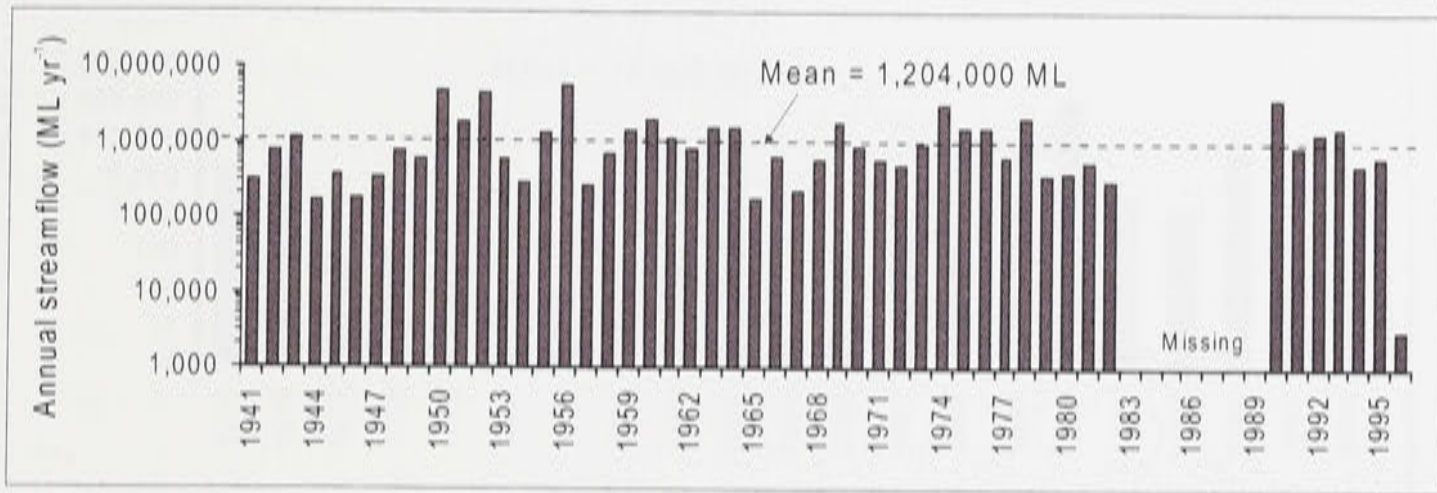
Recording of streamflow at this station (412099) commenced in 1975 with a maximum gauged stage at 4.12 m on 17 August 1990. The average annual streamflow is about 76,000 ML, with the highest annual streamflow of 1,290,000 ML recorded in 1990 (Figure 3.20a). The lowest annual streamflow is recorded in 1985 (0.46 ML) which is considered one of the driest years.

Monthly streamflow is high from July to September, with the highest in August at 29,000 ML (Figure 3.20b) as a result of major spilling of flood water from Lake Cowal especially during the major flood events in 1990. Very little flows at the Manna Creek during summer months with the lowest monthly value of 366 ML recorded in January.

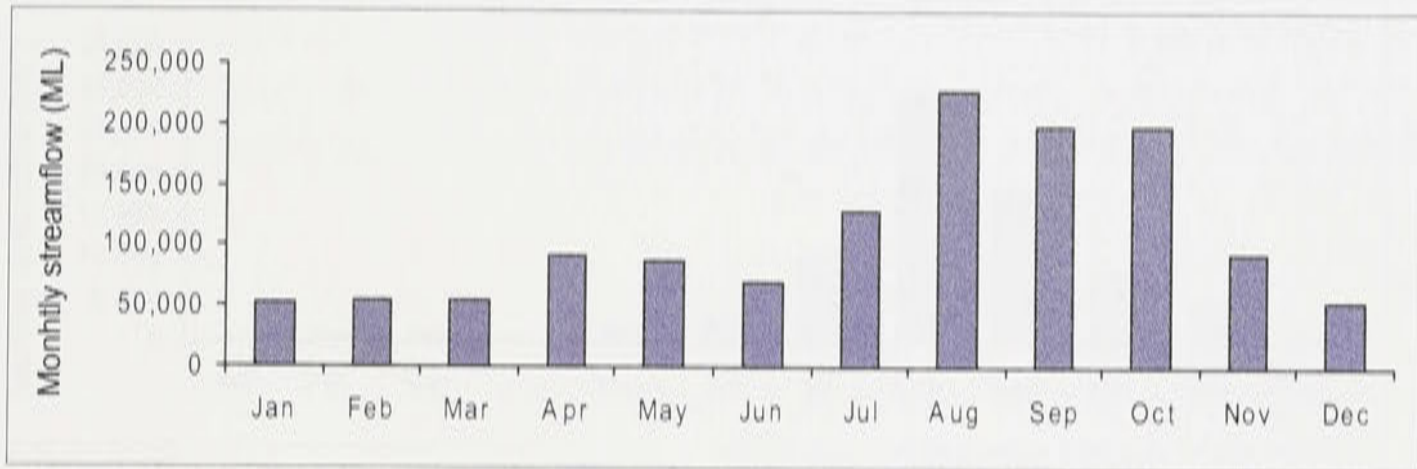
Daily streamflows from 1990 to 1995 at the creek are shown in Figure 3.20c where water was continuously flowing in the creek from 7 February 1990 to 2 March 1993. The daily flow duration analysis using the streamflow data from 1975 to 1995 shows that in about 60% of the cases, no flow conditions occurred at the creek (Figure 3.20d).

3.4.3.3. *Bland Creek at Morangarell*

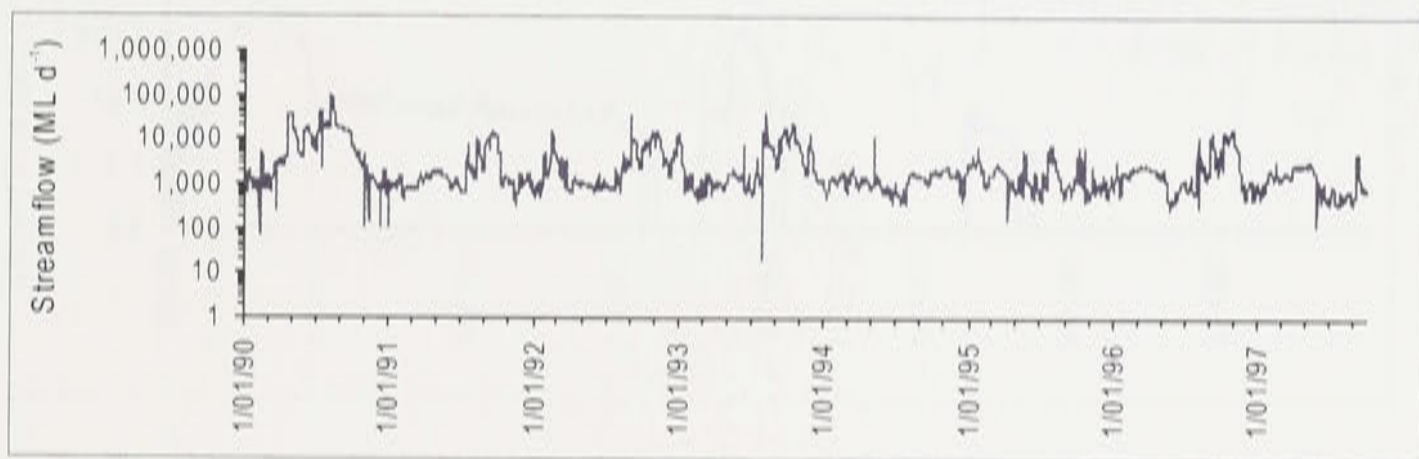
Gauging station 412103 has been installed in 1976 to monitor the runoff of the Bland Creek catchment. The maximum gauged stage is about 5.585 m recorded in 29 August 1983.



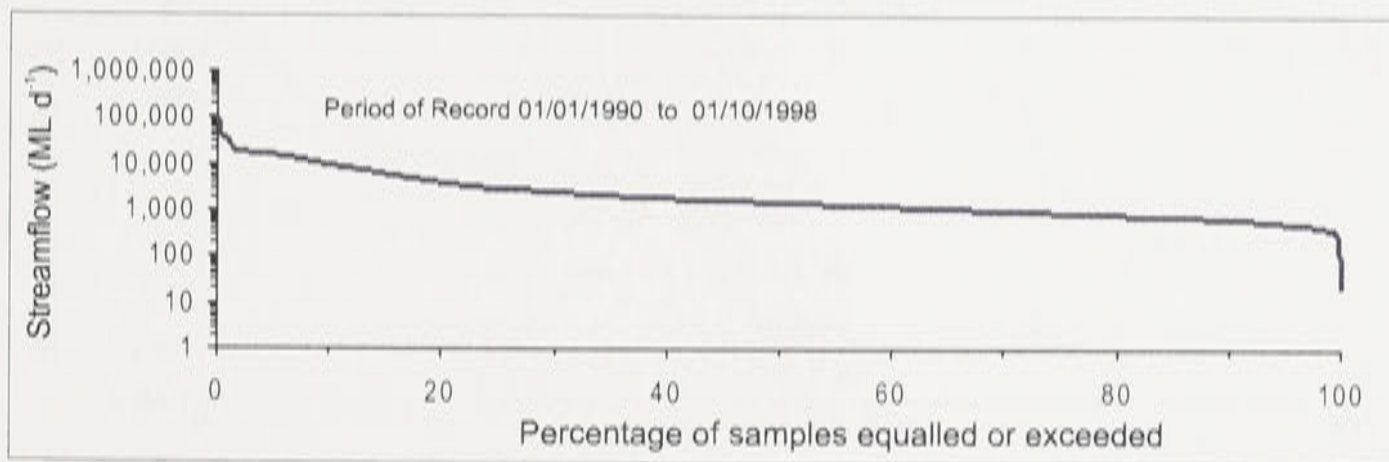
(a) Annual streamflow



(b) Mean monthly streamflow (1990-1996)

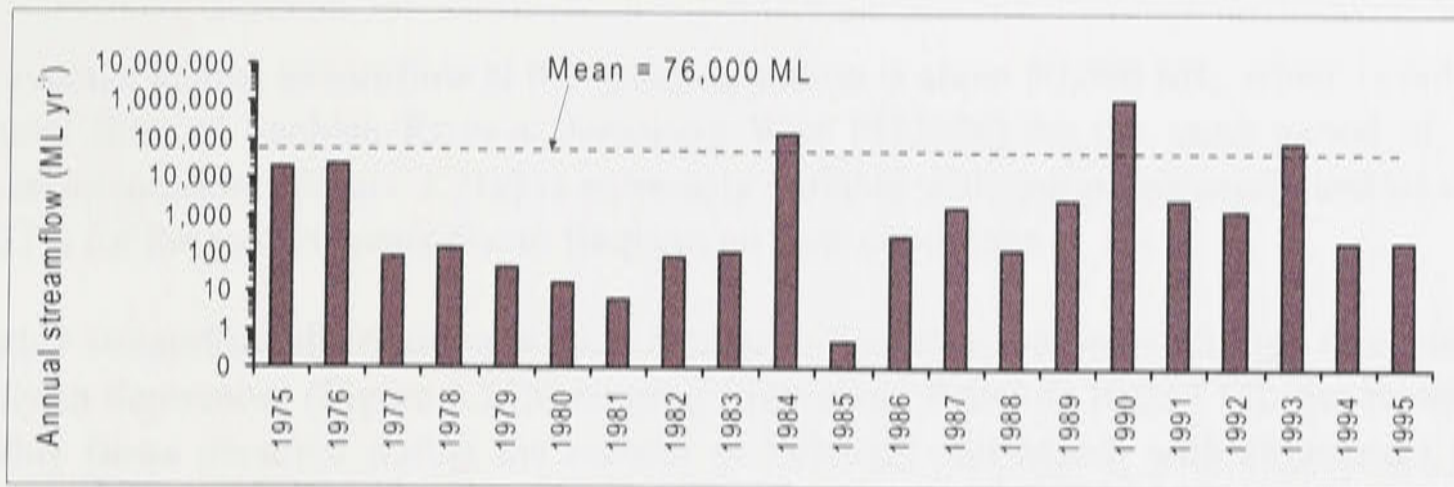


(c) Daily streamflow (1990-1996)

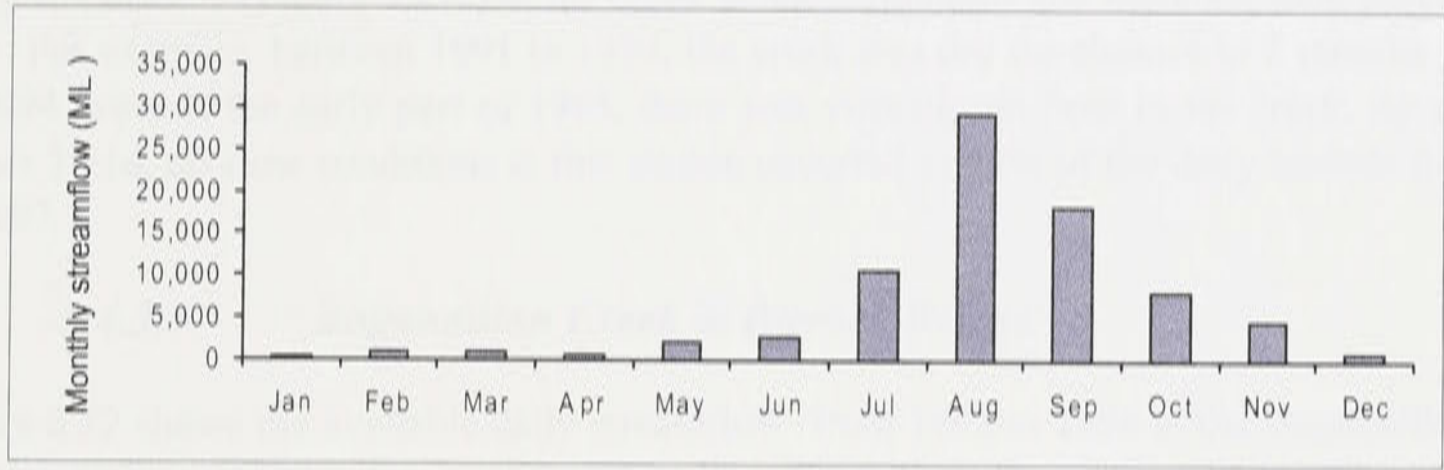


(d) Daily flow duration curve

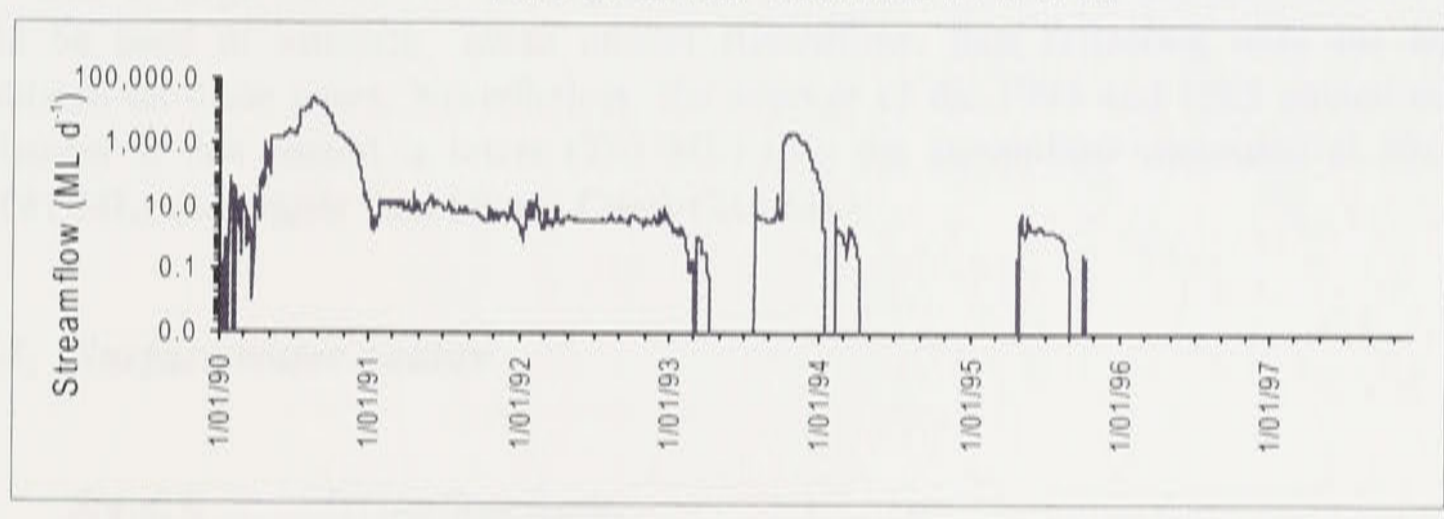
Figure 3.19: (a) Annual streamflow, (b) mean monthly streamflow, (c) daily streamflow and (d) daily flow duration curve for gauging station 412036 – Lachlan River at Jemalong Weir.



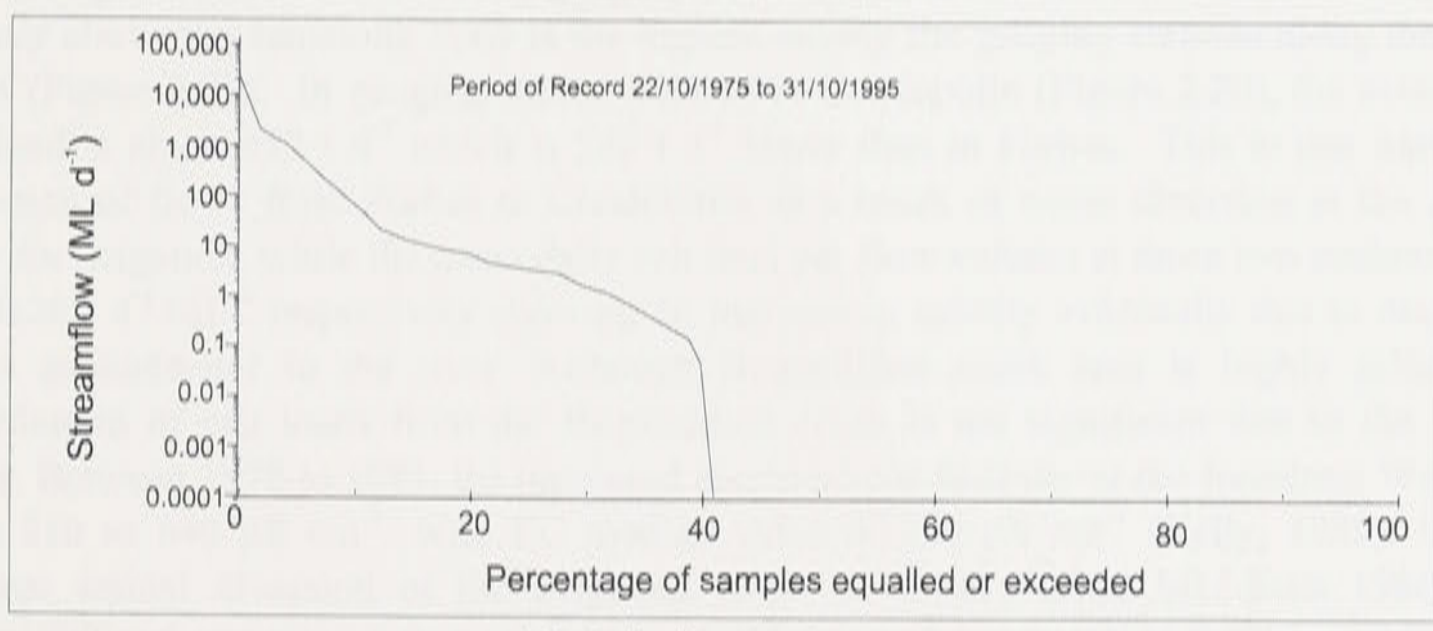
(a) Annual streamflow



(b) Mean monthly streamflow (1975-1995)



(c) Daily streamflow (1990-1995)



(d) Daily flow duration curve

Figure 3.20: (a) Annual streamflow, (b) mean monthly streamflow, (c) daily streamflow and (d) daily flow duration curve for gauging station 412009 – Manna Creek, near Lake Nerang Cowal.

The average annual streamflow at this gauging station is about 50,000 ML, which is only 5% of the total flow of Lachlan River at Jemalong Weir (412036) for the same period of records. Annual streamflow (Figure 3.21a) is extremely variable with computed coefficient of variation of 127% for the past 20 years due to frequent no flow conditions.

Monthly streamflow distribution is quite similar to the other stations with high flows occurring in July to September (Figure 3.21b) ranging from about 8,600 to 10,257 ML per month. Low monthly flows occurred during the months of February and March with an average monthly flow of 628 and 527 ML, respectively.

Daily streamflow (Figure 3.21c) at the creek is not continuous and there are long periods of no flow. For example, between 1991 to 1994, the creek was dry for about 4 to 5 months per year. In 1994 towards the early part of 1995, there was virtually no flow in the creek. As shown in Figure 3.21d, no flow conditions at this station occurred in 55% of the daily records from 1976 to 1997.

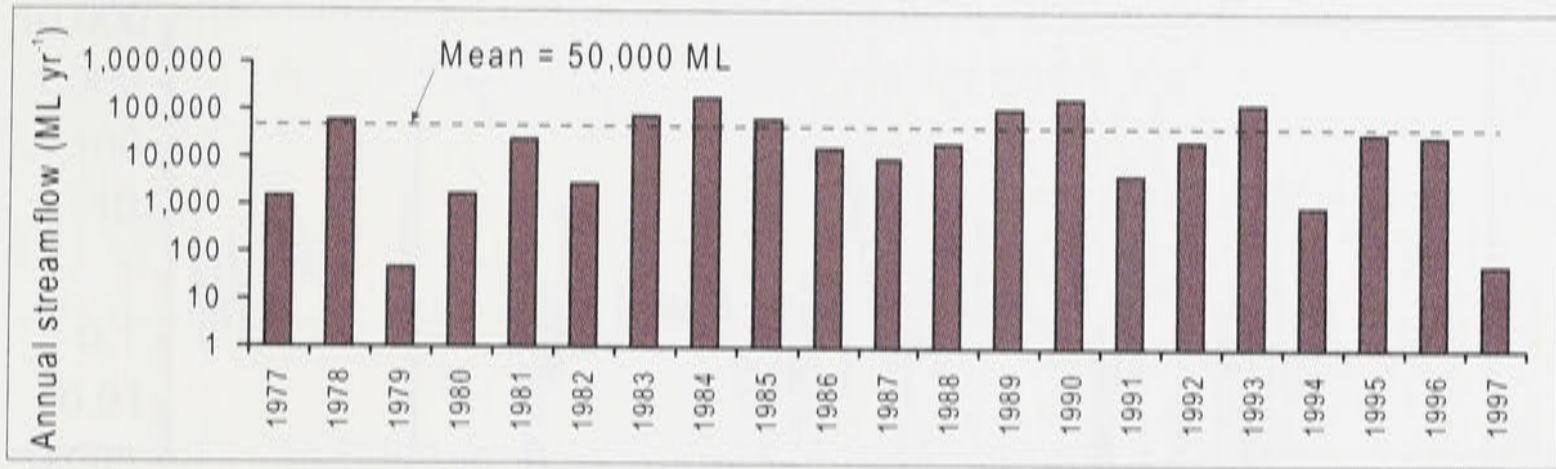
3.4.3.4. Bogandillon Creek at Birrack Bridge

Figure 3.22 shows the available daily streamflow from 1993 to 1996 at the Bogandillon Creek gauging station 412142. The average daily flow for the whole duration of record is about 93 ML. Due to large number of missing data in 1993 and 1996, only the data in 1994 and 1995 could be used to estimate mean annual streamflow, thus reflecting only the streamflow conditions on these years. Nevertheless, the average of the 1994 and 1995 annual streamflow discharges at this station is lower (780 ML) than the streamflow measured at Bland Creek (18,081 ML) and higher than Manna Creek (213 ML).

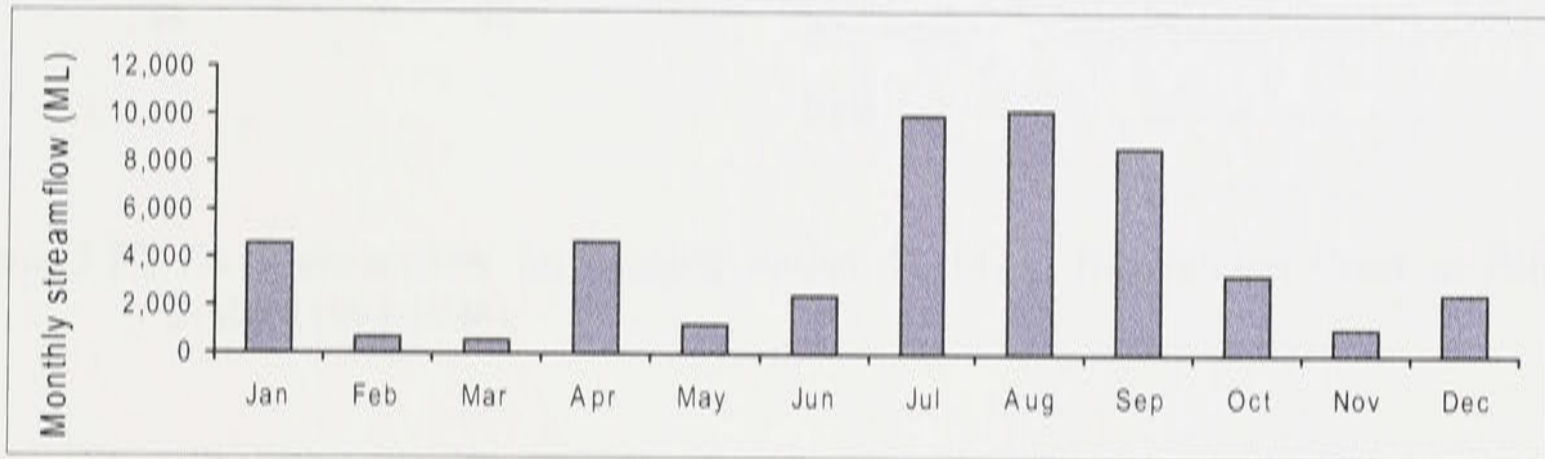
3.4.4. Surface water quality

3.4.4.1. Irrigation water

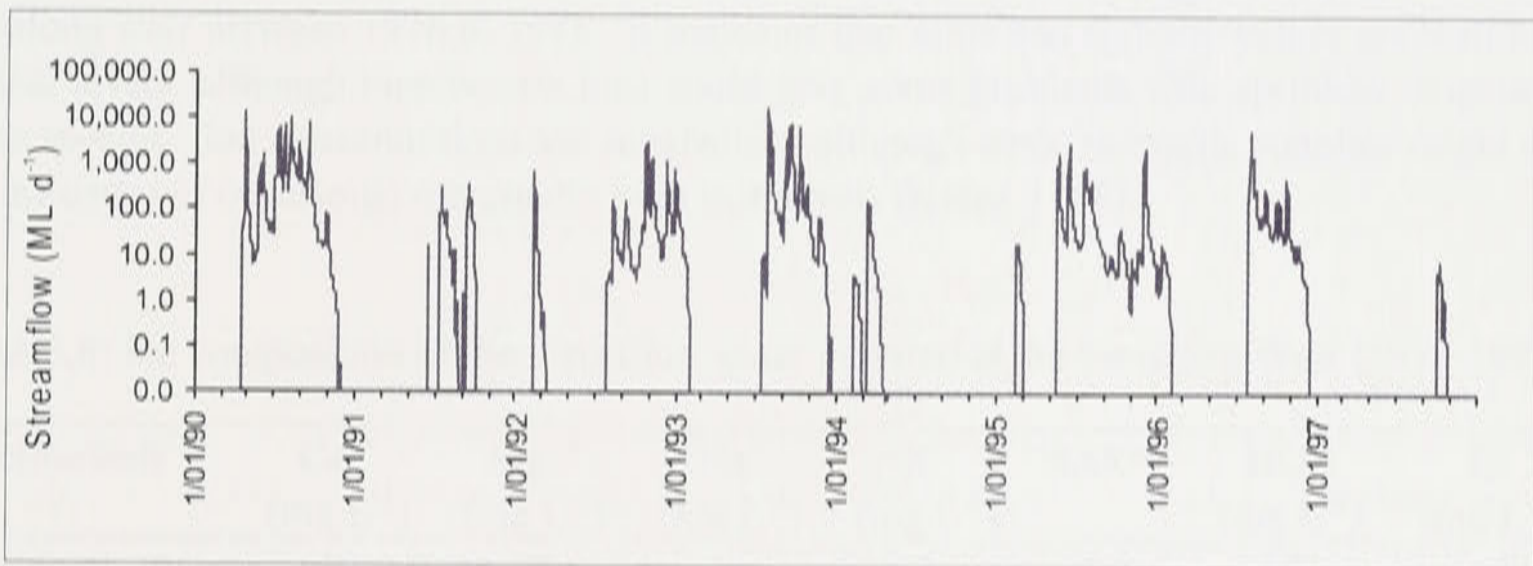
The average salt load of 665 t d^{-1} at gauging station 412004 at Forbes (see Figure 2.20) which is directly above the Jemalong Weir is the highest among the gauging stations along the Lachlan River (Figure 2.20). In gauging station 412006 at Condobolin (Figure 2.20), the average daily salt load is about 432 t d^{-1} which is 233 t d^{-1} lower than in Forbes. This is due partly to the reduction of flows from Forbes to Condobolin as a result of water diversion at the Jemalong Weir for irrigation, while the mean daily salt load per flow volume at these two stations are 0.27 and $0.28 \text{ t d}^{-1} \text{ ML}^{-1}$ respectively showing an increase in salinity eventually due to discharge of saline groundwater to the river. Although Bogandillon creek area is highly salinised, the contribution of salt loads from the Bogandillon creek is not significant due to the very low flows. Between 1970 to 1981, the measured electrical conductivity at the Jemalong Weir ranged from 210 to $640 \mu\text{S cm}^{-1}$ with EC median value of $350 \mu\text{S cm}^{-1}$ (Kelly, 1988). Using the average annual diversion of the irrigation water of about 70,000 ML from 1986/1987 to 1996/1997 and assuming a mean daily EC of $400 \mu\text{S cm}^{-1}$ (mean EC at Forbes is 440 and 394 $\mu\text{S cm}^{-1}$ at Condobolin), and a conversion factor of 0.64, the average daily salt load into the irrigation district is estimated to be about 50 t d^{-1} .



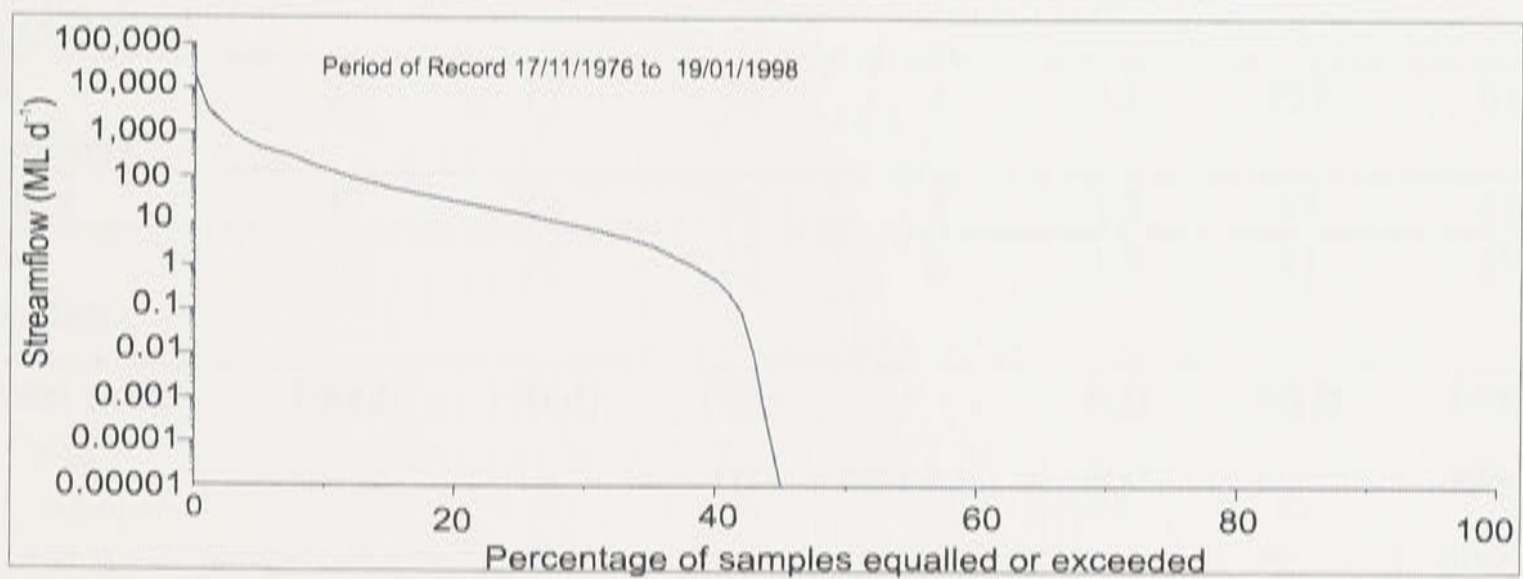
(a) Annual streamflow



(b) Mean monthly streamflow (1977-1997)



(c) Daily streamflow (1990-1997)



(d) Daily flow duration curve

Figure 3.21: (a) Annual streamflow, (b) mean monthly streamflow, (c) daily streamflow and (d) daily flow duration curve for gauging station 412103 – Bland Creek (Morangarell).

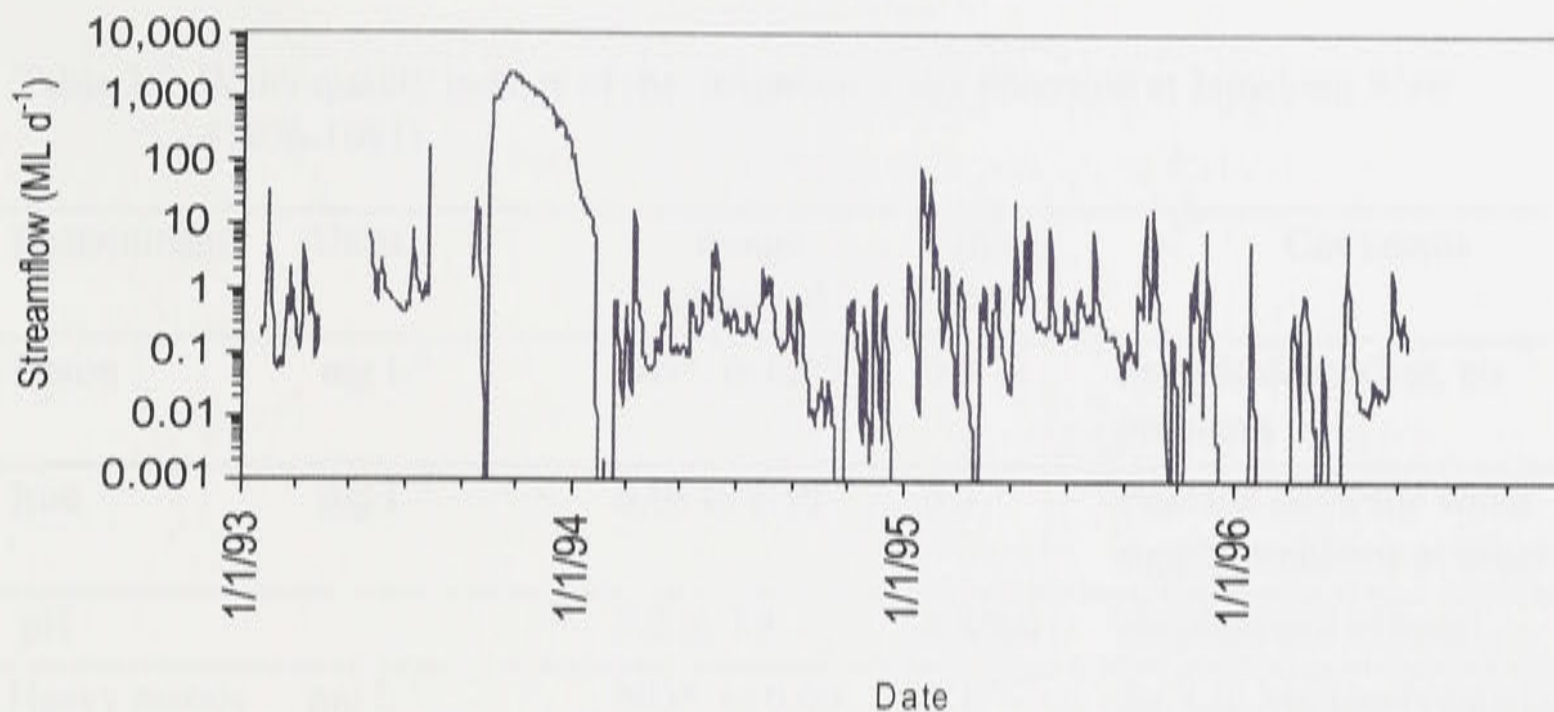


Figure 3.22: Daily streamflow for gauging station 412142 – Bogandillon Creek at Birrack Bridge (1993-1996).

Tables 3.6 and 3.7 show the other water quality indices for the irrigation water diversion at Jemalong weir between 1976 to 1981. It indicates that ionic and sodicity values are well below critical levels, although bicarbonate ions could give some problems with sprinkler irrigation of some species. Ion concentrations are satisfactory although some domestic supplies might show the influence of occasional marginally high iron levels (Kelly, 1988).

Table 3.6: Ion composition of the irrigation water diverted at the Jemalong Weir (1976-1981).

Determinants	Ca ⁺⁺ (mg L ⁻¹)	Mg ⁺⁺ (mg L ⁻¹)	Na ⁺ (mg L ⁻¹)	K ⁺ (mg L ⁻¹)	SAR**	HCO (mg L ⁻¹)	Cl ⁻ (mg L ⁻¹)
Maximum recorded	29	23	36	3	2.3	142	65
Minimum recorded	14	12	20	1	0.8	79	36
90% exceedance	23	17	32	2	2.1	132	61
Median	17	14	25	2	1.5	93	41
10% exceedance	13	12	22	2	1.2	83	39
Critical value*	200(d)	150(d)	70(f) (r)		6(f) 6(s)	90(f)	140(f) 100(f) 600(d)

* Critical value is lower threshold when effects may become increasingly significant for: d=domestic; f=foliar; r=root; and s=soil physical properties.

** adjusted for the bicarbonate ion.

Source: Kelly (1988).

Table 3.7. Water quality indices of the irrigation water diversion at Jemalong Weir (1976-1981).

Determinants	Units	Range observed	Critical value	Comments
Boron	mg L ⁻¹	ND* to 0.09	0.5	Species dependent, no problems
Iron	mg L ⁻¹	0.08 to 1.10	0.3	Possible domestic water supply problems at times
pH		7.2 to 7.8	6.8/8.0	No plant/soil effects
Heavy metals	mg L ⁻¹	ND* to 0.09	0.1	Zn, Cu, Mn levels satisfactory
Turbidity		3 to 30	-	Only limited problems for domestic supply
Phosphorus (P)	mg L ⁻¹ Total P	0.04 to 0.09	0.03	No algal problem generally
Hardness	mg L ⁻¹ CaCO ₃	84 to 123	1.5	No problem with domestic supply

* ND = non detectable

Source: Kelly (1988).

3.4.4.2. *Bogandillon creek*

Regular salinity readings in Bogandillon area have been recorded by the Department of Land and Water Conservation at five stations (Figures 3.23). Electrical conductivity measurements were relatively continuous for the Bogandillon gauge from January 1969 to March 1994, with a number of significant gaps. Readings for the other stations were patchy or non-existent until 1980's or 1990's, where they were measured more regularly. For comparison, only data since 1991 are plotted.

The readings in Glencoe gauge since 1991 indicate a general increase of EC from autumn to late summer, then fall at late summer or early autumn (Figure 3.24a). This is due to late summer heavy rain events that diluted the creek water. Salinity data at the Driftway Bridge since 1991 (Figure 3.24b) has similar trend but slightly higher in concentration compared to Glencoe Gauge readings. At Birrack Bridge, high EC readings were observed with the highest recorded EC value of 39,000 $\mu\text{S cm}^{-1}$ in October 1994 (Figure 3.24c). About 34% of the recorded data at this station are highly saline (above 15,000 $\mu\text{S cm}^{-1}$) and 52% falls in brackish to saline category (1,500-15,000 $\mu\text{S cm}^{-1}$). At the Bogandillon Gauge (Figure 3.24d), the 1991 to present readings show similar pattern to the other upstream stations. Fresh to saline concentrations of stream water were found at this station, with the majority of the measurements ranging from brackish to saline. At the Bogandillon Swamp (Figure 3.24e), there is a somewhat similar trend with the other stations, although there is a major gap in data.

Based on the above data, salinity concentrations appear to have fluctuated over time. This fluctuation is likely due to changes in flow, with increased flow reducing salt concentration as expected.

Assessment of the spatial salinity changes in the Bogandillon creek has also been conducted by Sturgess *et al.* (1993) using the data taken from the two surveys completed in early January and early March 1993. The first survey was extended from just upstream of Glencoe Homestead

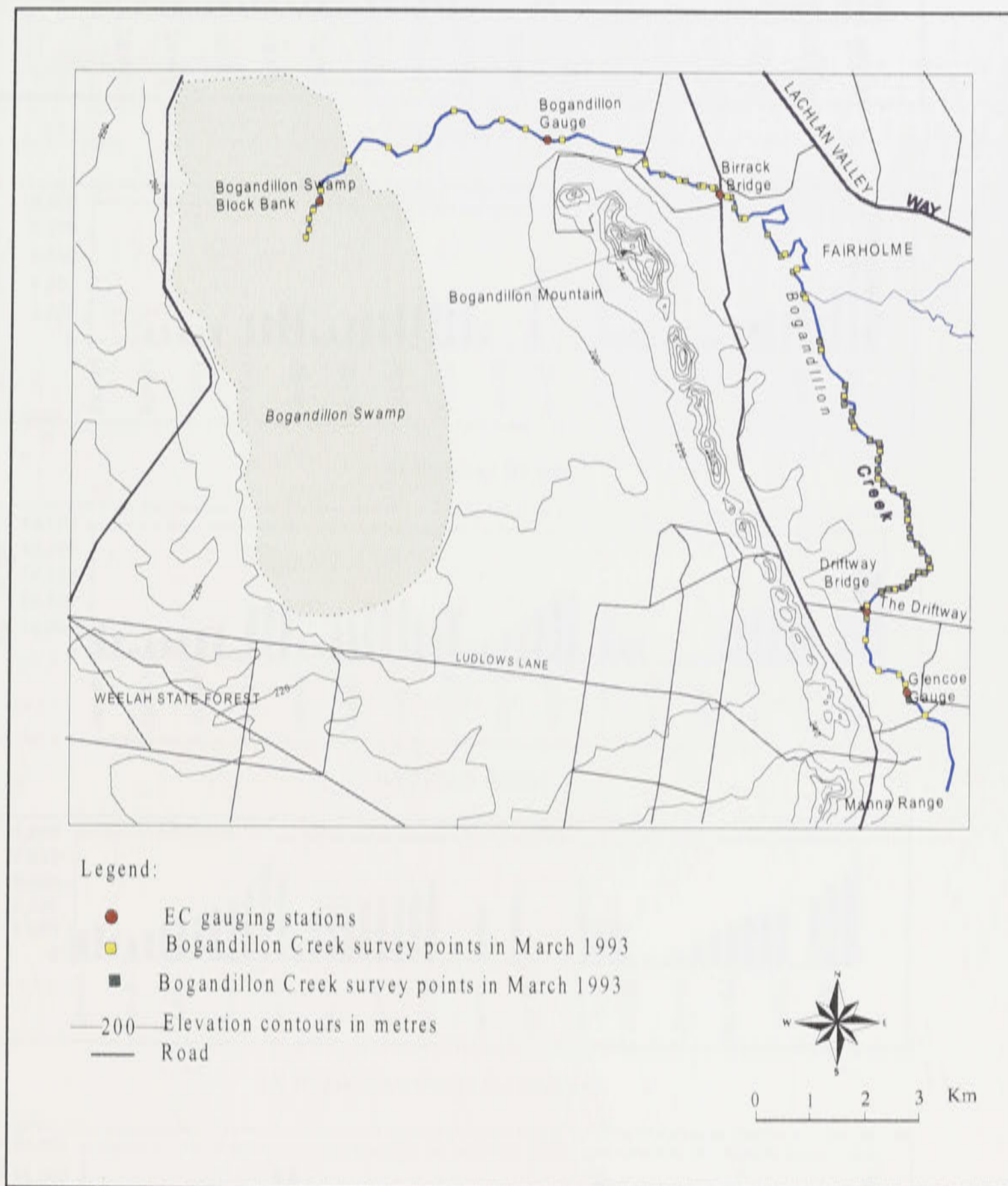
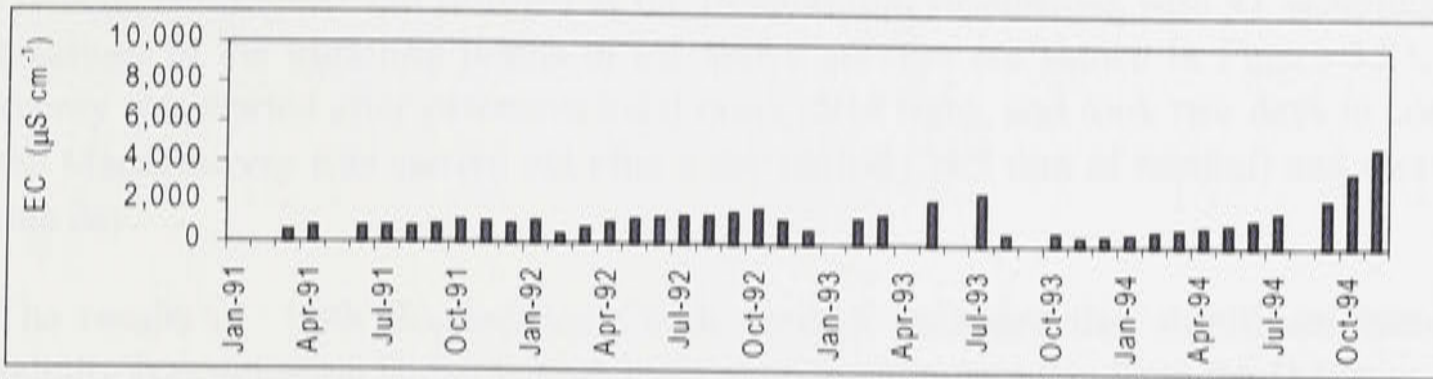
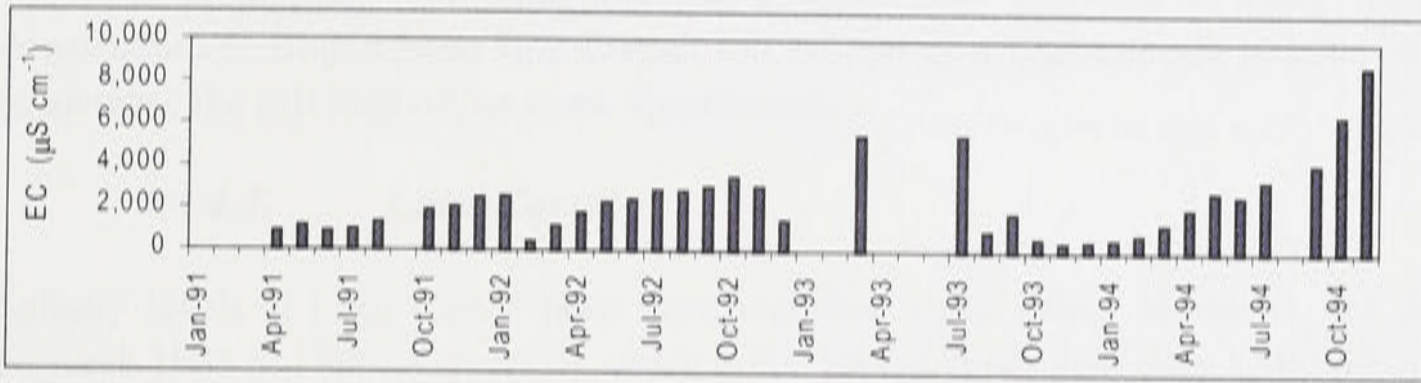


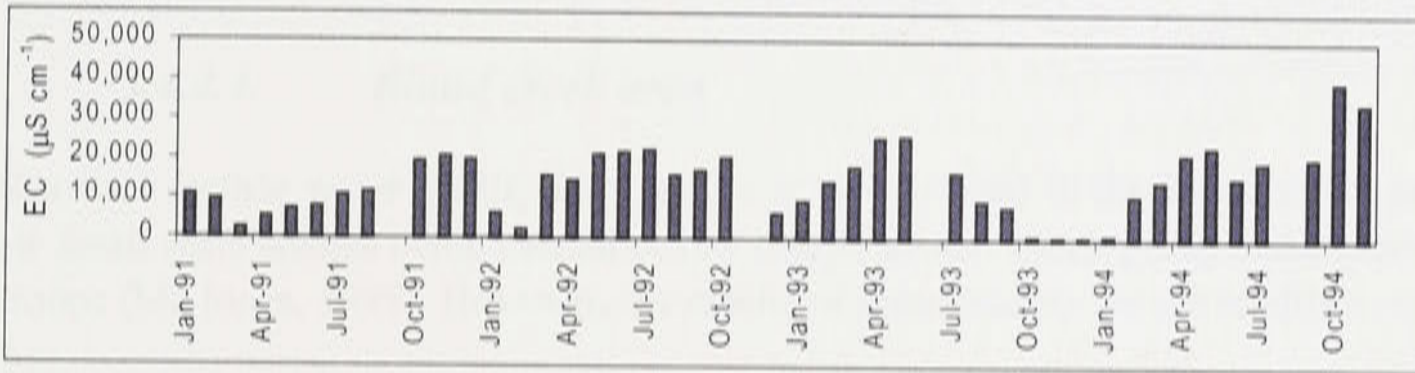
Figure 3.23: Locations of EC gauging stations along the Bogandillon Creek (modified from Sturgess *et al.*,1993).



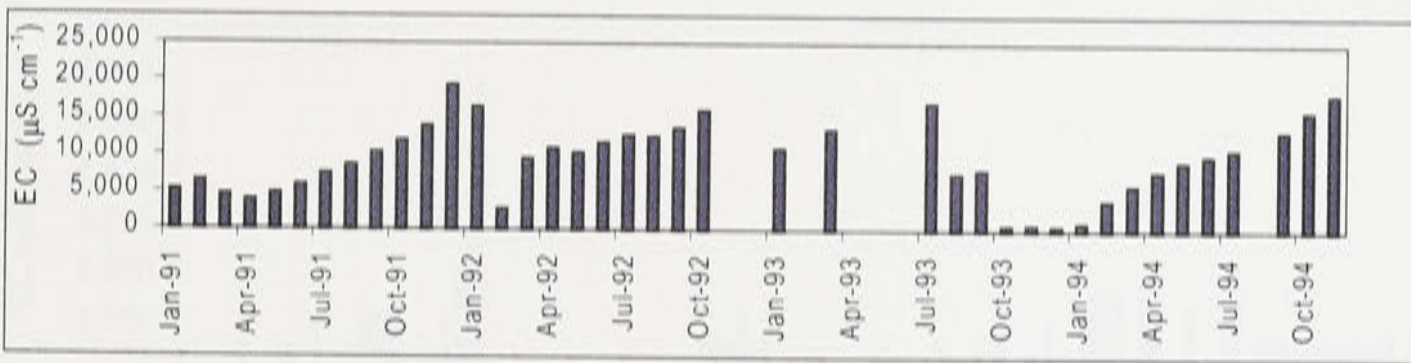
(a) Glencoe Gauge



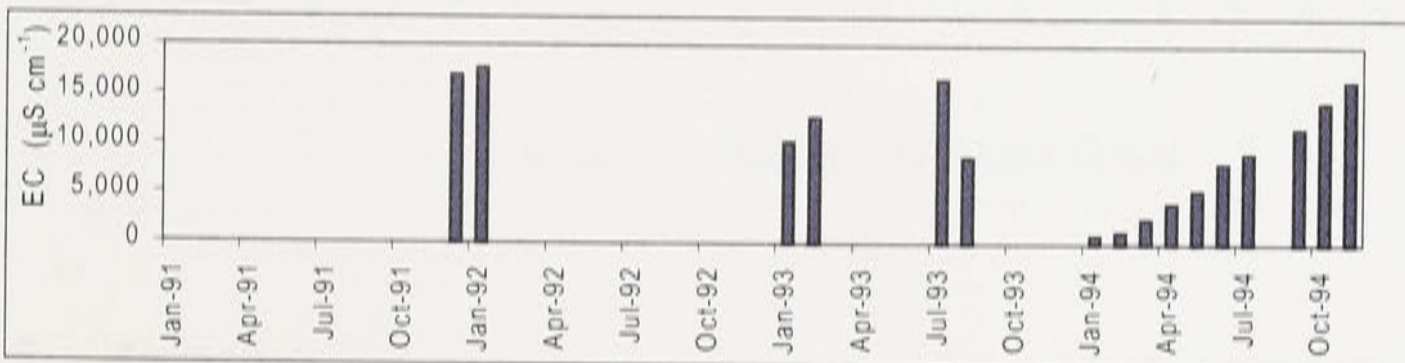
(b) Driftway Bridge



(c) Birrack Bridge



(d) Bogandillon Gauge (homestead)



(e) Bogandillon Swamp (Block bank)

Figure 3.24: Salinity data in the Bogandillon area.

and finished at the Bogandillon Homestead with 36 sampling points. The second began at the Glencoe Homestead and finished at the Bogandillon Homestead with 41 sampling points. The locations of the sampling points of the above surveys are shown in Figure 3.23. The January survey was started after extensive local rain (150.8 mm), and took two days to complete, while the March survey was carried out after a dry period (34.3 mm of rainfall) and was completed in one day.

The results of both Bogandillon Creek surveys indicated that significant increase in creek salinity concentration began approximately 1.5 km downstream from the Driftway Bridge. This is likely to be due to flow of local saline groundwaters to the creek at this point (Sturgess et al. 1993). It is thought that these shallow groundwaters continue to enter the creek system downstream to Bogandillon Homestead, but are not of a high enough volume or concentration to increase the salt load of the creek significantly.

3.4.4.3. *Lake Cowal*

Salinity levels at Lake Cowal have been recorded since 1986. However, the data are patchy between 1988 to 1990. Generally, water in the lake is fresh (less than 1,500 $\mu\text{S cm}^{-1}$) with 89% of the recorded data belong to this category. The highest recorded EC is only about 6,000 $\mu\text{S cm}^{-1}$ and was measured in February 1988 (Figure 3.25).

3.4.4.4. *Bland creek area*

Historical surface water quality information is very limited in the Bland creek area. There are few small scale studies being carried out by school stream watch group and concerned Landcare Groups (Mc Innes, 1995). However, the results of these studies are not readily available.

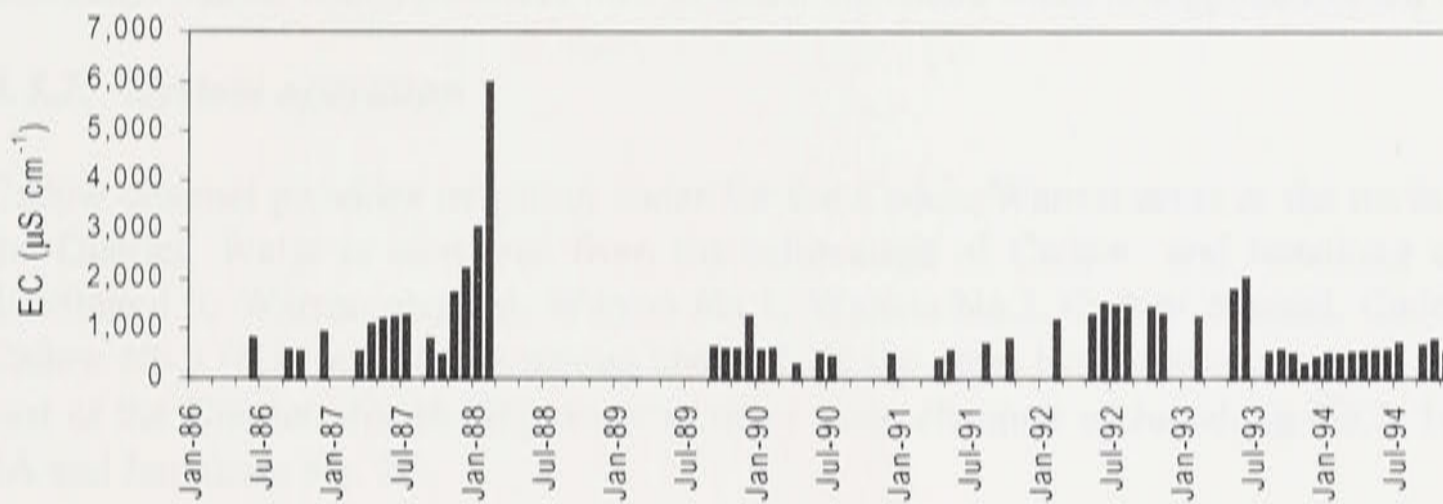


Figure 3.25: Salinity data at Lake Cowal.

3.5. Irrigation

The Jemalong and Wyldes Plains Irrigation District (JWPID) is the only area irrigated in the study area. The District comprises 155 properties on 94,000 hectares. The ownership and management of all water supply and drainage infrastructure has recently been transferred from the Government in 1994 to the newly corporatised Jemalong Irrigation Ltd (JIL). JIL is run by, and acts on behalf of the irrigators and is responsible for the management of water supplies and associated delivery and drainage infrastructure. The irrigation district has an annual allocation

of 100,054 ML plus any subsequent addition for contract sales or transfers into the district. However, the average annual delivery has been about 70,000 ML since 1986 (see section 3.5.3 for details). The extent of irrigation within the district may vary considerably from year to year. Typically between 12,000 and 20,000 ha of land are irrigated within the district in any one year, primarily for purposes of cropping and grazing activities. Water usage is between 300 to 450 mm yr⁻¹.

3.5.1. Irrigation system facilities

The irrigation supply channel system for the JWPID (Figure 3.26) is split into two main branches approximately 2 km downstream of the Jemalong Weir. The upper branch of the system known as Cadow Channel supplies irrigation water to Cadow and Warroo regions, while the lower branch (Jemalong) supplies irrigation water to the Jemalong area located to the south and east of the district.

Originally constructed with a trapezoidal earthen channel, some locations within the channels are becoming rectangular and parabolic due to scouring. Channel depth varies from more than 2 m, at the upstream section of the system, to 0.5-1 m at the downstream (Lyall and Macoun Consulting Engineers, 1995), with top widths between 2 and 20 m depending on channel capacity with larger dimensions at the upstream section. The majority of the channels which can supply peak demands of 100-200 ML d⁻¹, generally have a typical top width of about 10m. In general, the channels have the capacity to convey the peak demands to the corresponding locations. Figure 3.26 shows the decreasing peak demands from the upstream to the downstream end of the channels.

Various hydraulic structures are located on the channel system which include: drainage subways; siphons; check drops to control water level in the channels; flow regulators; and Dethridge outlets which monitors flow at locations where water is supplied to each farm.

3.5.2. System operation

Cadow channel provides irrigation water for the Cadow/Warroo areas at the north and west of the District. Water is conveyed from the bifurcation of Cadow and Jemalong channels and distributed to Warroo channel, Warroo No.1, Warroo No.2, Cadow channel, Cadow No.2 and Cadow No.3 (Figure 3.26). Jemalong channel, on the other hand, transport water into south and east of the District, distributing water to other main channels of Jemalong No.2, Jemalong No. 2A and Jemalong No. 2D.

Usually irrigation water takes 1 to 2 days to travel from the top to the bottom of the system for both divisions. Thus, farmers are required to place their orders for water 4 days in advance with notification 24 hours in advance if changes to current order are required (Lyall and Macoun Consulting Engineers, 1995).

Shutdown procedures to stop the flow of water in the irrigation channels in the event of rain involve closing the check drop/gate structures along the channels. The whole system can be shut down by the closure of all drop structures within about 24 hours in the event of heavy rainfall which causes farmers to cancel water orders (Lyall and Macoun Consulting Engineers, 1995).

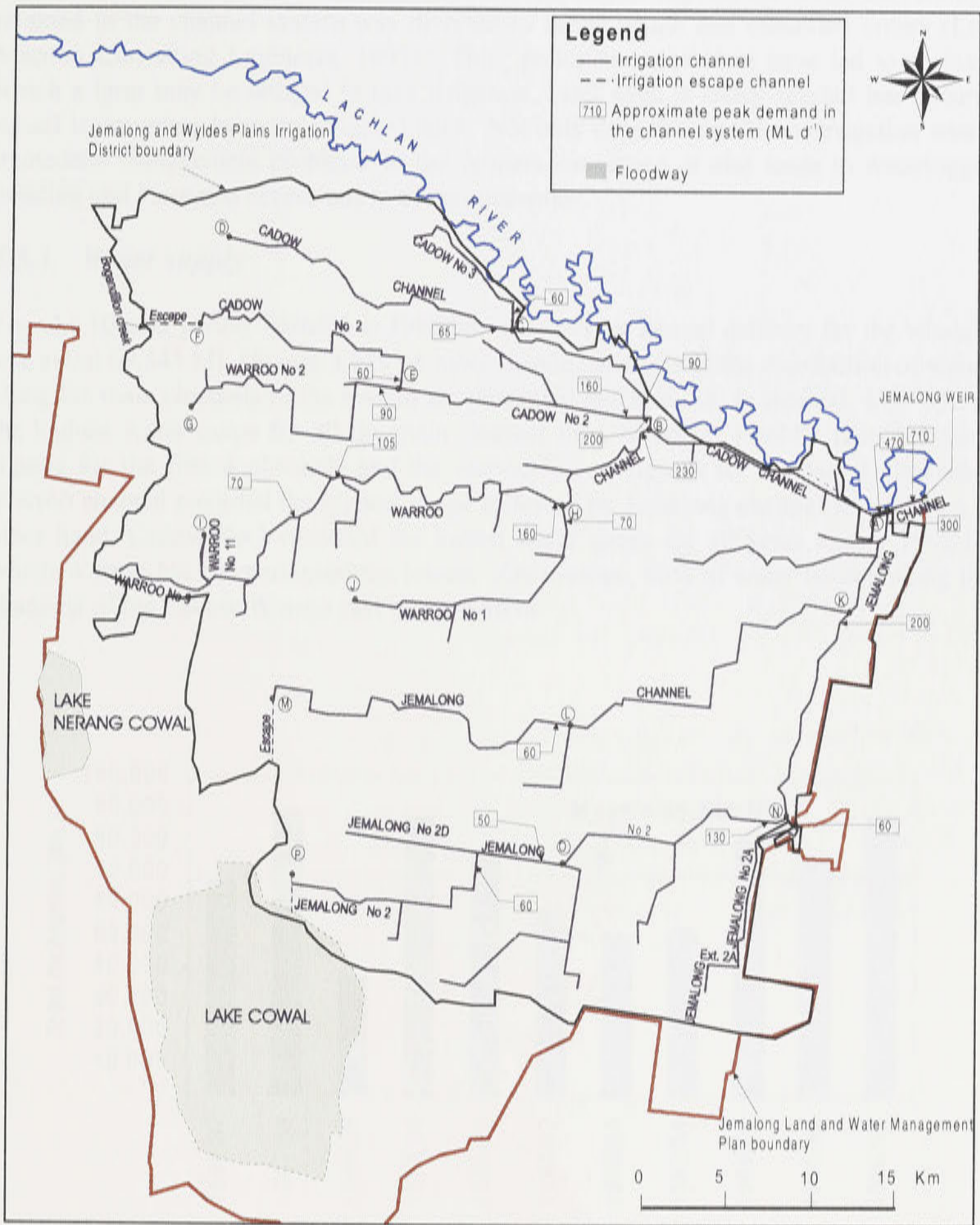


Figure 3.26: Irrigation supply system of the Jemalong and Wyldes Plains Irrigation District (modified from Lyall and Macoun Consulting Engineers, 1995).

Prior to 1991, any excess flow was allowed to flow out of the district via escape channels at the end of all the major supply canals. This operational policy was revised in 1991 to ensure that no water was diverted into the escape channels. Instead any excess water that could not be retained in the channel system was diverted to farms which had cancelled orders (Lyall and Macoun Consulting Engineers, 1995). This policy is reported to have led to a situation in which a farm may be obliged to take irrigation water even if heavy rainfall has occurred and runoff is occurring from the irrigated land. Not only does this additional irrigation water cause immediate management problems to the farmers concerned, it also leads to waterlogging and ponding and increased accessions to the groundwater.

3.5.3. Water supply

For the 10 year period 1986/87 to 1997/98, the average annual delivery for the whole system was about 69,545 ML (Figure 3.27). A more detailed analysis of the distribution of water usage along the main channels of the system are presented in Table 3.8. In general, 1994/95 recorded the highest water usage for all the main channel lines whereas 1992/93 recorded the lowest figures for the first 4 channels and the second lowest figures for the last 3 channels listed. Warroo channel recorded the highest usage followed by Jemalong channel for all years. On the other hand, Cadow No.2 recorded the lowest water usage for all years except 1992/1993, in which Warroo No.2 experienced the lowest. On average, 63% of water is used along the main channels of the Cadow/Warroo part of the system.

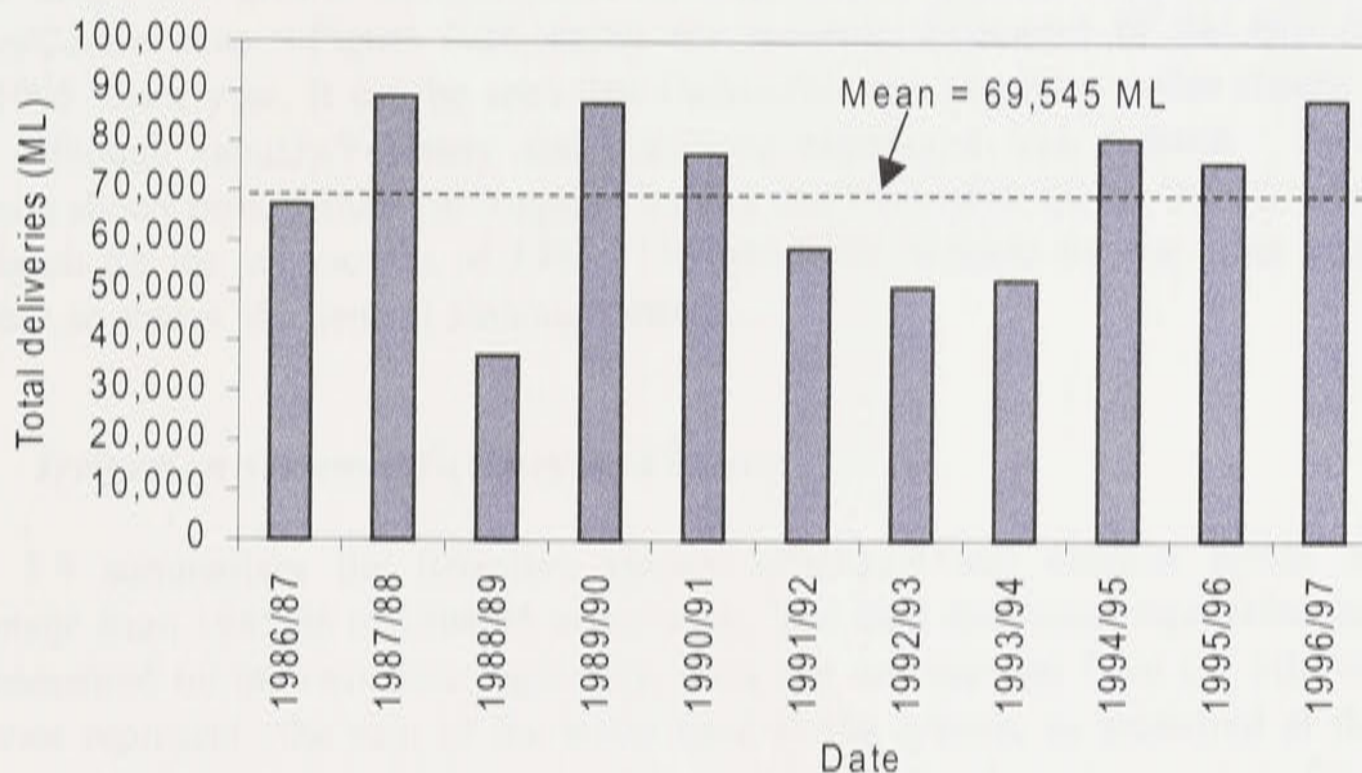


Figure 3.27: Historical water deliveries from the Jemalong Weir (Department of Land and Water Conservation, unpublished).

Table 3.8. Distribution of water usage along main channels.

Channel Name	Channel line*	Usage (ML)			
		1991/92	1992/93	1993/94	1994/94
Cadow Channel	A-B-C-D	5,300	4,300	5,400	7,000
Cadow No.2	B-E-F	2,500	2,200	2,600	3,200
Warroo No.2	E-G	3,400	2,100	3,200	3,700
Warroo Channel	B-H-I	10,700	8,200	9,300	11,800
Warroo No. 1	H-J	4,000	3,300	2,700	4,200
Jemalong Channel	A-K-L-M	8,900	8,200	8,100	10,100
Jemalong No.2	K-N-O-P	4,300	4,900	5,300	7,300
Total		39,100	33,200	36,600	47,300

* See Figure 3.25 for locations.

Source: Lyall and Macoun Consulting Engineers (1995).

The distribution and temporal pattern of irrigation usage varies substantially from year to year according to the weather and farm practice. Typically some 12,000 to 20,000 ha are irrigated with an average application rate of about 4 ML ha⁻¹ yr⁻¹ (400 mm yr⁻¹) (Coffey and Partners International Pty Ltd, 1994).

Winter crops are grown in the Jemalong area while summer crops predominate in the Warroo/Cadow area. Figure 3.28 shows the monthly diversions of the two divisions for 1994/1995 water year. It can be seen that Cadow/Warroo require a rather steady demand for water, although January/February and May/June experience less demand. The pattern for Jemalong shows peak demand in August, October and December for the last six months of 1994 and March for the six months of 1995. Unfortunately, records for the other years were not available to assess the general seasonal pattern.

3.5.4. Irrigation system efficiency and losses

Table 3.9 summarises the irrigation system efficiency and channel losses expressed in percentage from 1985/86 to 1994/95 water years. The total diversions represents the sum of the flow measured by the two flow regulators, each just downstream from the bifurcation. Total deliveries represent the sum of the water used in the system, as measured at the Dethridge outlets at the farms gates. The average channel losses for the entire system for the 10-year period is about 12%. This compares favourably with an average channel loss of about 14% for the period 1962/65 to 1994/1995 (Lyall and Macoun Consulting Engineers, 1995). The average irrigation system efficiency for 10 year period which is computed as total irrigation deliveries over total irrigation diversion is about 88%. Comparing the losses between Cadow/Warroo and Jemalong channels, it has been observed that Cadow/Warroo has higher losses (12.6%) than Jemalong (9.6%) using the 1994/1995 irrigation diversions deliveries data for the two divisions (Table 3.10).

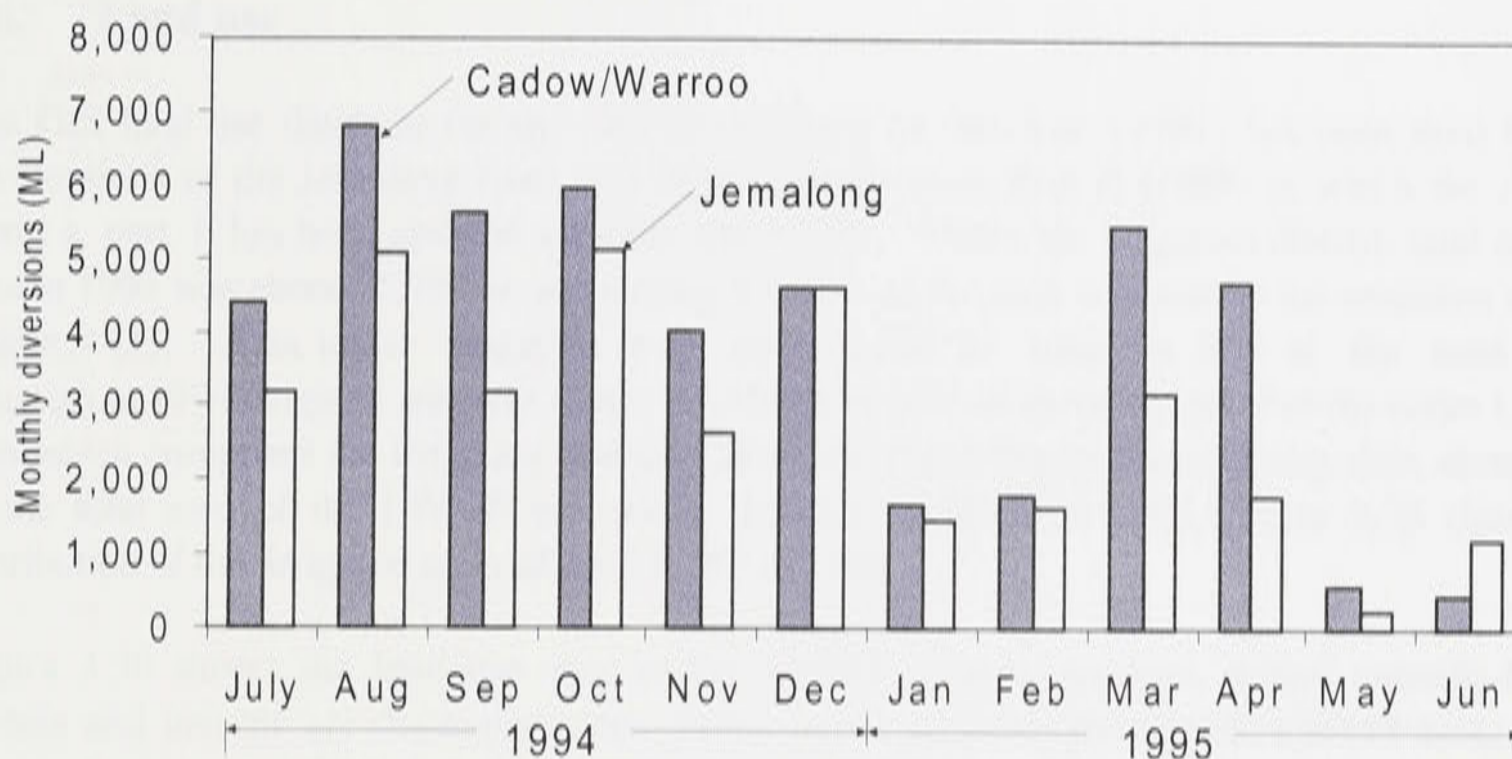


Figure 3.28: Monthly diversions for the 2 main channels (Cadow/Warroo and Jemalong) for 1994/1995 water year. Diversions refer to total water supply and include system losses.

Table 3.9: Channel diversions, deliveries and losses.

Water year*	Total diversions (ML)	Total deliveries (ML)	Losses (%)	Irrigation delivery efficiency (%)
1985/86	83,000	78,000	6.0	94.0
1986/87	77,000	67,000	13.0	87.0
1987/88	99,000	89,000	10.1	89.9
1988/89	44,000	37,000	15.9	84.1
1989/90	100,000	87,000	13.0	87.0
1990/91	87,000	77,000	11.5	88.5
1991/92	67,000	59,000	11.9	88.1
1992/93	58,000	51,000	12.1	87.9
1993/94	59,000	52,000	11.9	88.1
1994/95	79,000	70,000	11.4	88.6

* Water year is from June to May.

Source: Lyall and Macoun Consulting Engineers (1995).

Table 3.10: Diversions, deliveries and losses at Cadow/Warroo and Jemalong main channels during 1994/95 water year .

Division	Total diversions (ML)	Total deliveries (ML)	Channel losses (%)
Cadow/Warroo	46,025	40,229	12.6
Jemalong	33,315	30,119	9.6

Source: Lyall and Macoun Consulting Engineers (1995).

3.6. Land use

The GIS land use database for the JWPID prepared by McGrath (1997) has been used for the development of the Jemalong Land and Water Management Plan (LWMP) in which the JWPID forms a part. It has been updated annually since 1992. Within the irrigation district, total dryland area in 1995 was about 76,789 ha accounting for 82% of the total area within the irrigation district (Table 3.11). Area under irrigation was only 16,334 ha which is 18% of the total area, although in 1994 irrigated area was about 23,348 ha or 25% of the total area. For the entire LWMP area which comprises the irrigation district, Lake Cowal and Bogandillon Swamp area, about 86% of the total area of the LWMP was under dryland condition in 1996. Figure 3.29 shows the distribution of the irrigated areas of the LWMP in 1996.

Figure 3.30 shows the land use map in the LWMP. Natural pasture, winter cereals, annual pasture and lucerne are the major crops grown in the dryland areas in the LWMP area. In the irrigated areas, annual pasture, lucerne and winter cereals are widely grown.

In the Bland creek area, land use data has been compiled through various studies by the Department of Land and Water Conservation. Predominant land uses in the Bland creek catchment include cropping and grazing land. Grain and fodder crops, native and improved pasture are also scattered throughout the area (Department of Land and Water Conservation, 1996a).

3.7. Wetlands

The GIS database of wetlands in the JWPID is available at the NSW Department of Agriculture in Forbes (Mc Grath, 1997). This database is the result of the study undertaken the Department of Land and Water Conservation to map the extent and ecological significance of wetlands within the JWPID area of operations. The inventory of wetlands in the District was undertaken to nominate wetland priorities for conservation, review surface drainage management plan with specific reference to wetland management, evaluates possible compensatory wetland sites for water storage and sets broad recommendation for storage basin (Department of Land and Water Conservation, 1997). These wetlands are almost entirely on private lands.

Wetlands in the irrigation district (Figure 3.31) are classified into good, moderate and degraded conditions. This classification was determined by the current quality of the existing values and wetlands' potential to be restored. The irrigation district contains about 10,626.33 ha of wetland areas, of which 29% is assessed as being in good condition, 40% in moderate condition and 31% in degraded condition (Table 3.12). The results of this study are currently under review by the Department of Land and Water Conservation (McGrath, 1997).

The details of wetland management in the irrigation district have yet to be finalised by the Department of Land and Water Conservation. Although the DLWC listed a series of options for the preservation of wetlands, no recommendations has been made yet about which options are applicable to particular wetlands. Further work on a Wetlands Management Plan is proposed which will identify wetlands on each property and recommend a management plan based on the options listed below. The Wetlands Management Plan will recommend appropriate management options for specific wetlands. Options which may be applicable include: (1) maintain wetland in current state; (2) partial restoration; and (3) full restoration.

Table 3.11: Land use in the dryland and irrigated areas of the Jemalong and Wyldes Plain Irrigation District (JWPID) and the Land and Water Management Plan (LWMP) area in hectares.

Land use	JWPID				LWMP	
	1992	1993	1994	1995	1995	1996
DRYLAND						
Annual pasture	11,933	10,815	8,195	12,687	18,719	16,311
Fallow	3,748	2,227	9,297	3,916	5,146	6,254
Grain legume	160	53	166	140	163	357
Lucerne	5,493	6,396	7,271	8,157	10,459	13,044
Natural pasture	34,833	32,063	32,483	32,863	68,040	58,340
Oilseed	168	790	1,025	2,317	2,439	1,149
Perennial pasture	783	1,534	1,540	2,435	2,910	2,727
Summer cereal	75	90	76	82	68	29
Summer forage	152	25	366	105	105	0
Trees	562	607	445	114	2,629	2,643
Winter cereal	12,960	15,668	8,543	13,675	19,115	28,389
Flood	500	464	0	0	0	0
Miscellaneous	368	368	368	298	453	479
Water	-	-	-	-	10,642	9,963
Total Dryland	71,735	71,100	69,775	76,789	140,887	139,685
% of total area	77%	76%	75%	82%	87%	86%
IRRIGATED						
Annual pasture	7,998	7,583	5,901	3,586	4,587	5,158
Fallow	0	90	200	235	253	280
Grain legume	48	27	0	0	0	372
Lucerne	4,138	4,680	5,008	4,712	5,483	4,275
Natural pasture	2,427	2,185	2,407	1,406	1,931	888
Oilseed	978	1,084	1,891	682	653	1,459
Perennial pasture	2,119	2,064	1,976	1,429	2,206	1,522
Summer cereal	274	333	826	735	809	1,579
Summer forage	359	571	1,379	375	1,288	119
Winter Cereal	3,047	3,406	3,760	3,174	3,412	6,171
Total Irrigated	21,388	22,023	23,348	16,334	20,621	21,823
% of total area	23%	24%	25%	18%	13%	14%
TOTAL AREA	93,123	93,123	93,123	93,123	161,508	161,508

Source: McGrath (1997).

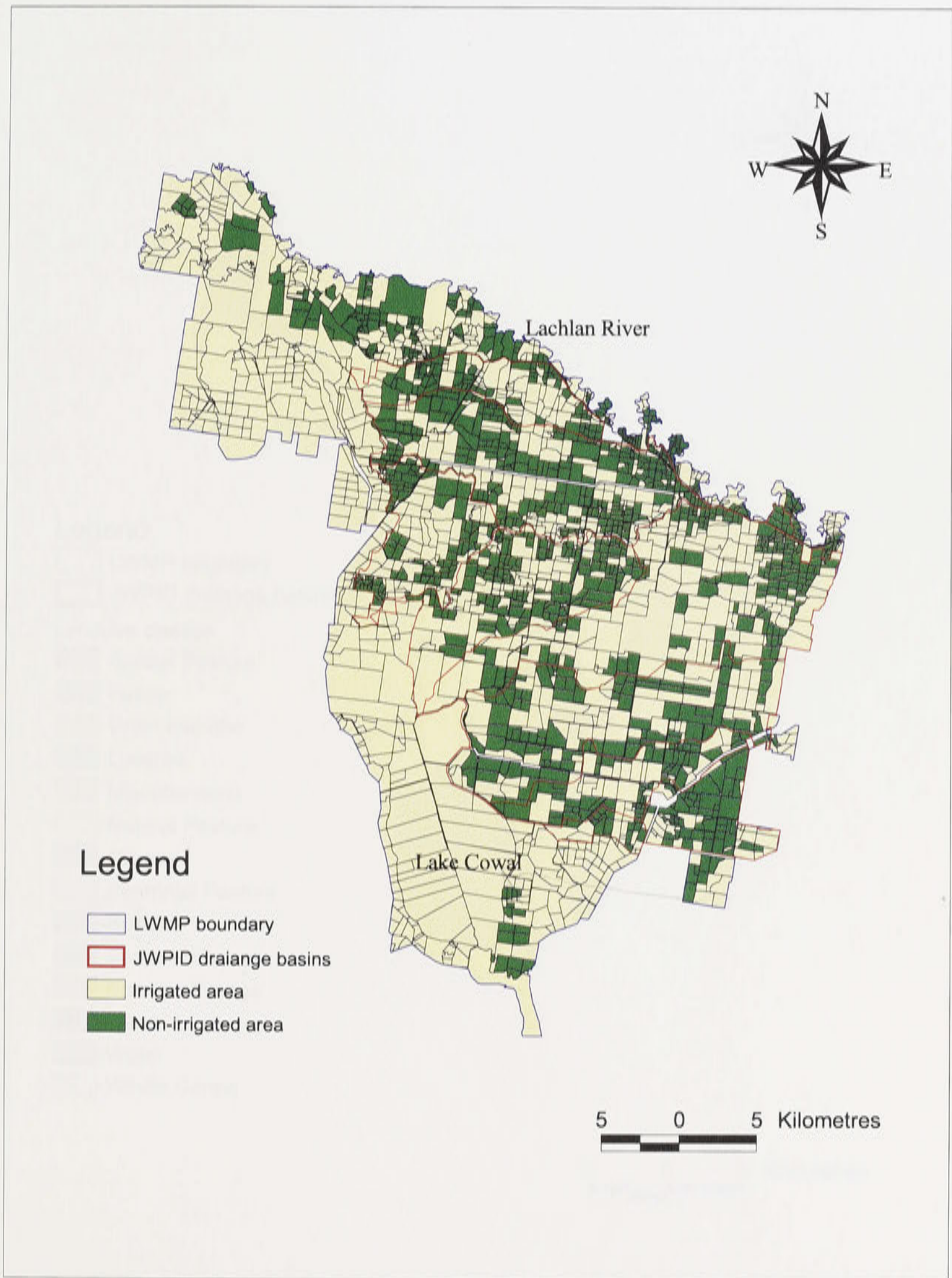


Figure 3.29: Irrigated and non-irrigated areas of the Land and Water Management Plan (LWMP) area (Source of data: Mc Grath, 1997).

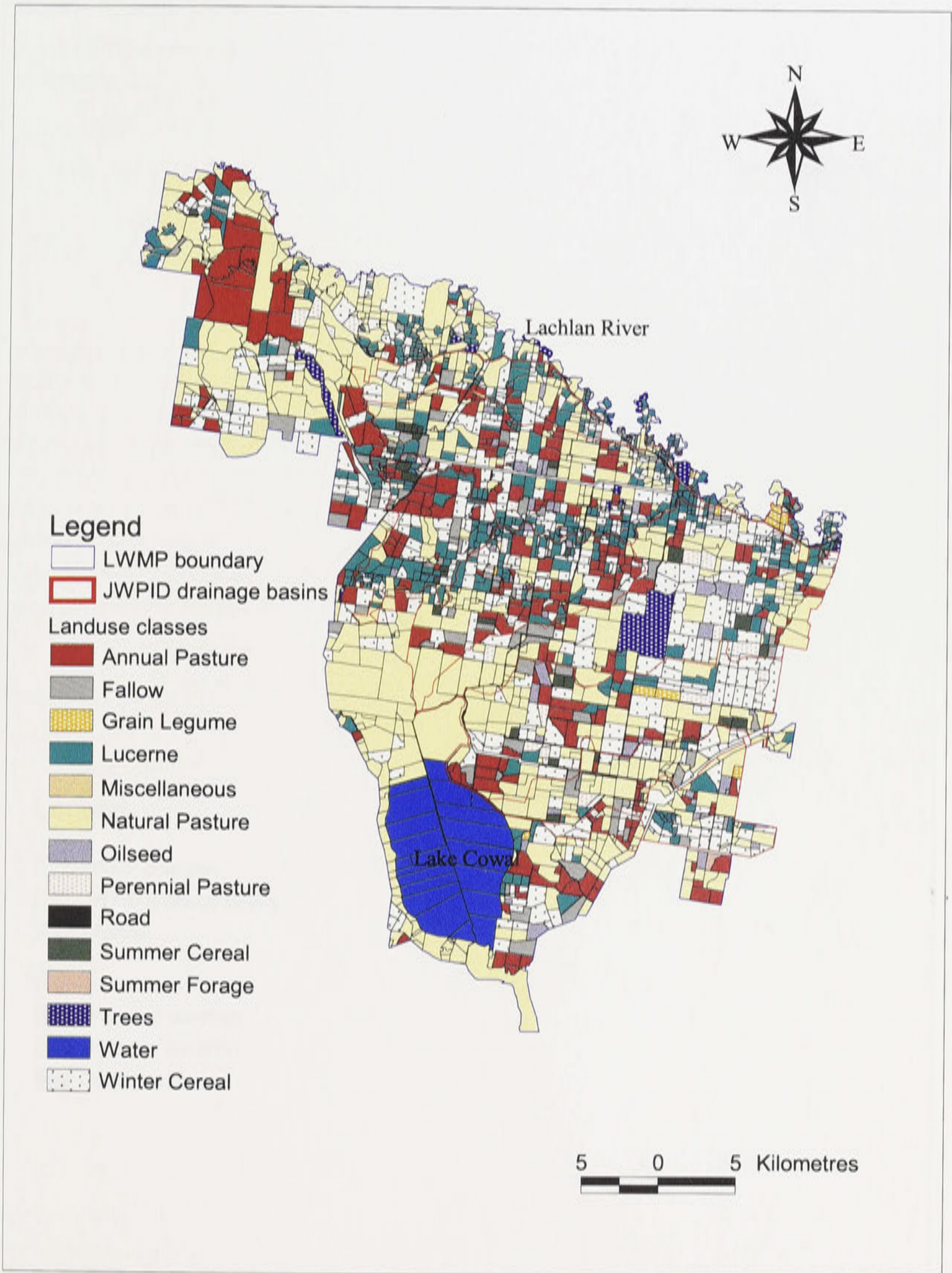


Figure 3.30: Landuse map of the Land and Water Management Plan (LWMP) area in 1996. (Source of data: Mc Grath, 1997).

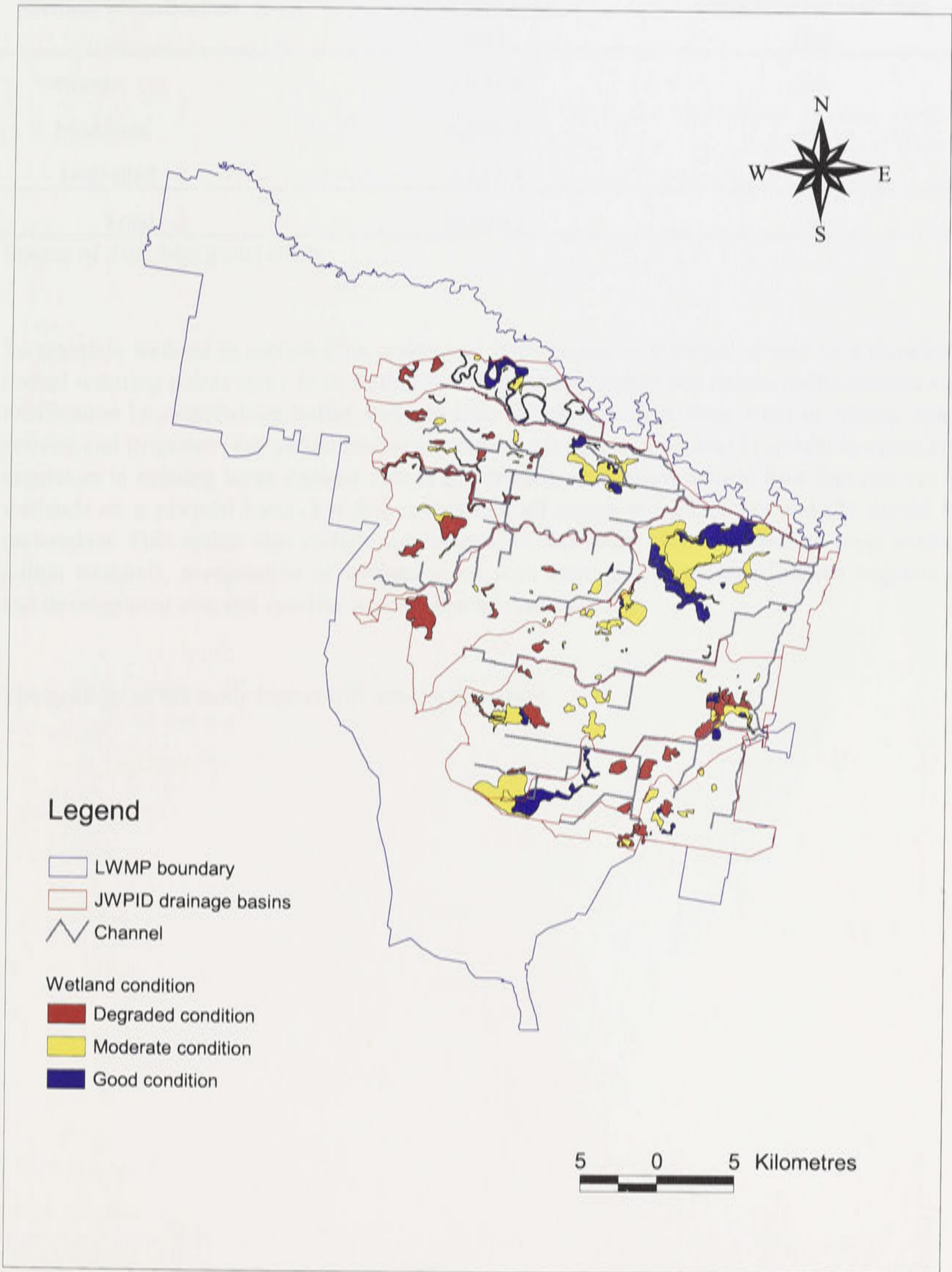


Figure 3.31: Classification of wetlands in the Land and Water Management Plan (LWMP) area. (Source of data: Mc Grath, 1997).

Table 3.12: Classification of wetland areas in the Jemalong and Wyldes Plains Irrigation District.

Wetland classification	Wetland area (ha)	Percent of the total area (%)
Good	3,074.6	29
Moderate	4,293.8	40
Degraded	3,257.9	31
Total	10,626.3	100

Source of data: McGrath (1997).

To maintain wetland in current state, control of stock access to wetlands should be undertaken, formal watering points away from wetlands should be established and reduce sedimentation and nitrification by establishing buffer strips to interdict surface flow from areas of intense stock activity and irrigation. For partial restoration option, all points in option (1) should be taken and regulators in existing levee systems should be constructed to allow natural flow into and out of wetlands on a planned basis. For full restoration, all points in options (1) and (2) should be undertaken. This option also include the removal of any water control structure, weed control within wetlands, revegetation of wetland areas with appropriate species of native vegetation, and development of a site specific wetland management plan.

The geology of the study region will now be discussed.

CHAPTER 4

GEOLOGY

4.1. Structural geology

Hard rocks in the Lachlan River Valley are structurally subdivided into several discrete north-south trending zones which belong to Lachlan Fold Belt. The Jemalong, Lake Cowal and Bland Creek catchment lies within the Bogan Gate Synclinal zone (Figure 4.1).

Within the Jemalong and Wyldes Plains Irrigation District, the Tullamore Syncline (Figure 4.2) exists as a result of the gentle deformation of the Late Devonian rocks. The Jemalong Range represents the exposed eastern limb of the syncline. On the western side is the Manna Anticline where the Manna Range represents the western limb and the outcrop at the Dog Kennel Hill is a remnant of its eastern limb (Anderson *et al.*, 1993).

The Gilmore Fault (Figure 4.2) is a well defined north-northwesterly trending feature extending for several hundred km and is well shown in the 1: 250,000 Forbes (Brunker 1968) and Cootamundra (Warren *et al.*, 1996) Geological Map Series. Other approximate and inferred geological structures in the study area are described in detail in the 1:250,000 Cootamundra Geological Map (Warren *et al.*, 1996).

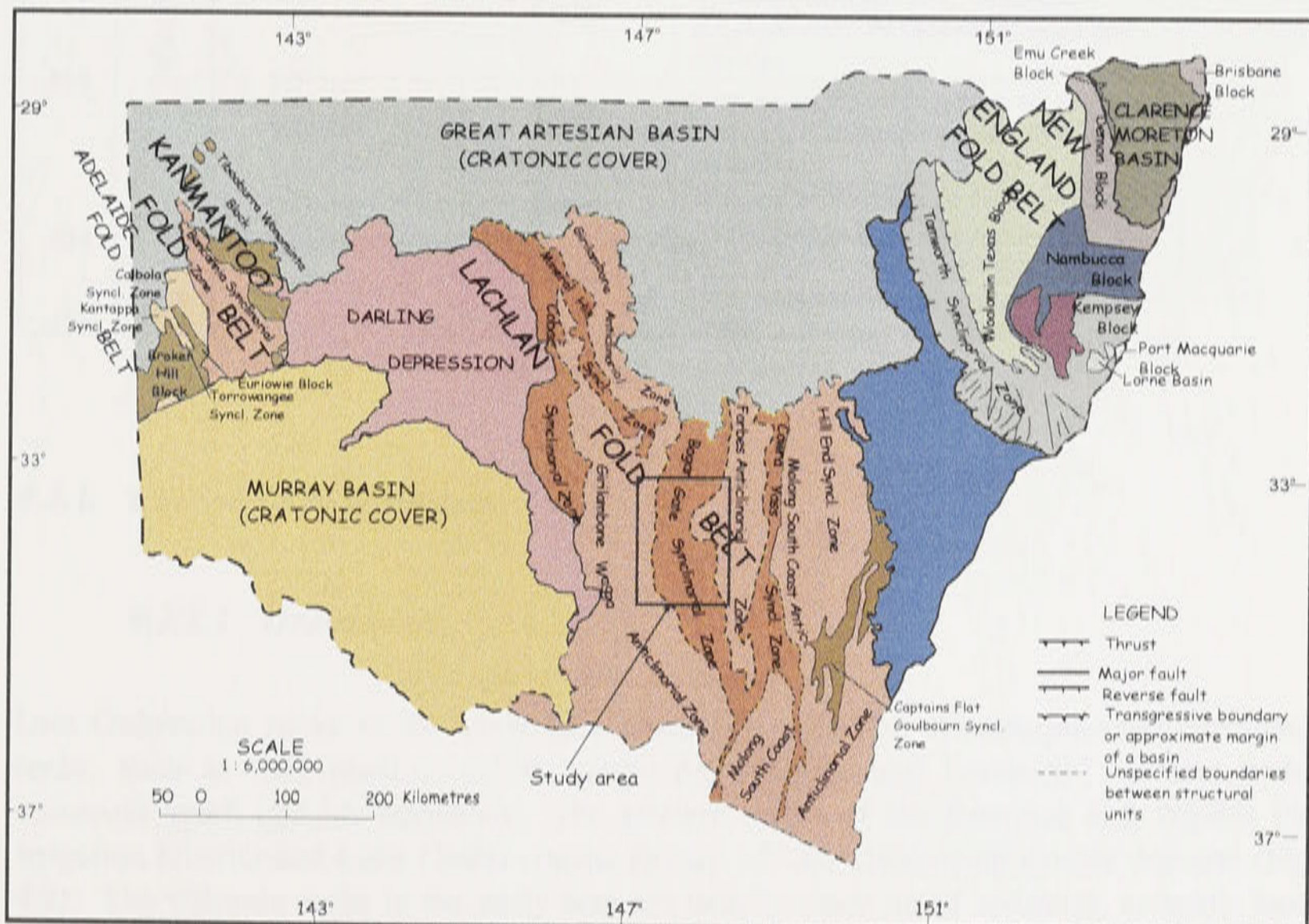


Figure 4.1: Structural units of New South Wales (modified from Pogson, 1972).

4.2. Stratigraphy

The stratigraphic units in the study area are presented in Table 4.1 which include Ordovician, Silurian, Devonian, Tertiary and Quaternary. The distribution of these units is shown in Figure 4.2 with consolidated units cropping out mainly in distinct ridges and forming the boundaries of the unconsolidated Quaternary sediments.

Table 4.1: Stratigraphic units of the study area.

Age (M y)	Era	Period	Division	Lithology
1.8	Cainozoic	Quaternary	Recent	Cowra Formation (gravel, sand, silt and clay)
			Pleistocene	
		Tertiary	Pliocene	Lachlan Formation (gravel, sand, silt and clay); laterite; consolidated sandstone; conglomerate
5				
354	Palaeozoic	Devonian	Late	White, red and green sandstone; conglomerate; green and white siltstone
Middle			Granite; granodiorite	
Early			Andesite; rhyolite; tuff; limestone; conglomerate; red sandstone; shale and siltstone	
410		Silurian	Late	Granite; argillaceous sandstone; shale; slate; phyllite; conglomerate; acid lava; limestone.
			Early	Monzodiorite; gabbroic diorite; volcanics (rhyolite, rhyodacite, dacite and quartz)
434		Ordovician	Late	Tuff; phyllite; schist; sandstone; siltstone; limestone; andesites; basalt; trachyandesite; latite.
490				

4.2.1. Consolidated sediments

4.2.1.1 Ordovician

Late Ordovician rocks in the study area consist of volcanic, metamorphic and sedimentary rocks, such as tuff, phyllite, schist, sandstone, siltstone and limestone. It also includes numerous small igneous intrusions. The western ridges of the Jemalong and Wyldes Plains Irrigation District and Lake Cowal consist mostly of Late Ordovician marine deposits (Figure 4.2). The volcanic rocks in the study area are usually made up of andesites, andesitic basalt, trachyandesite, and latite. Most of these rocks are locally interbedded with siltstones, sandstones and conglomerates. The Ordovician rocks are cropped out or are overlain by quaternary sediments in some areas in Bland creek catchment.

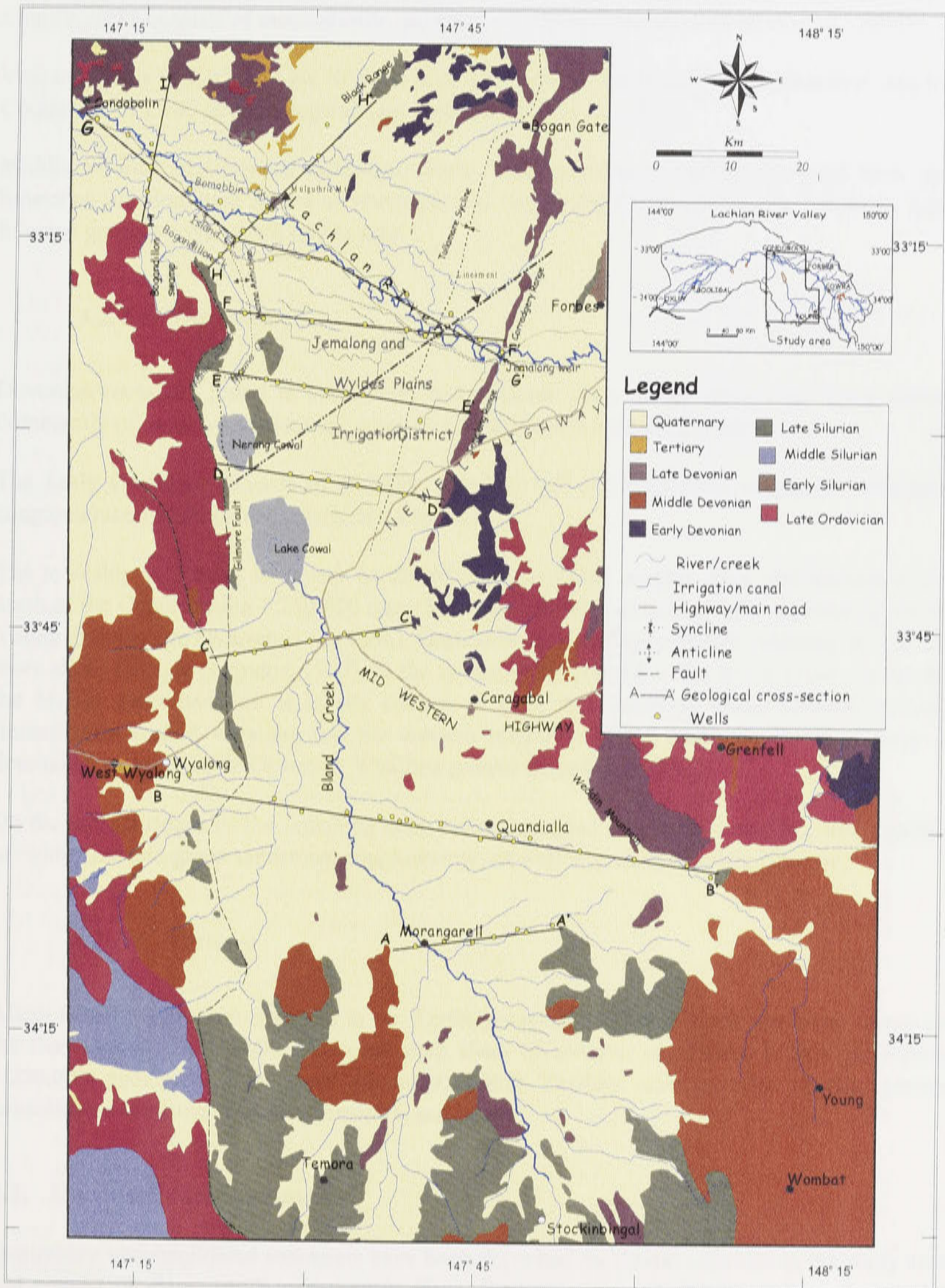


Figure 4.2: Geological map of the study area and locations of cross-sections.

4.2.1.2. Silurian

Silurian units are mostly found at the headwaters of the Bland Creek catchment. The Early Silurian rocks consists of monzodiorite, gabbroic diorite and volcanics (Warren *et al.*, 1996).

Volcanic rocks of Early to Late Silurian units are found in the Bland Creek catchment (see the Cootamundra 1:100 000 geological map sheet: Basden *et al.*, 1975).

Middle Silurian argillaceous sandstone, shale, slate, phyllite, conglomerate, acid lava, and limestone are dominant in the southern part of the Bland Creek catchment. Likewise, Late Silurian granites cover much of this area.

4.2.1.3. Devonian

Devonian rocks are found in the eastern and northern parts of the study area. They consist dominantly of massive sandstones, quartzites, shales and thin beds of limestone.

The Early Devonian consists of andesite, rhyolite, tuff and tuffaceous sediments, limestone conglomerate, red sandstone, shale, and siltstone.

The township of Young is mostly on the Middle Devonian granite. This unit extends to the north of the Cootamundra 1:250 000 map. The long and wide strip of granite is presently called Young granodiorite (Warren *et al.*, 1996). Granodiorite is similar to granite, although it contains more alkali feldspar (Lapidus, 1987). In the township of Grenfell in the Bland Creek catchment the Middle Devonian unit is mostly consist of what is collectively called Grenfell granite. Immediately around Wyalong (on the western boundary of the study area), the geology is dominated by the Middle Devonian Wyalong granite (Brunker, 1968).

On the eastern ridges of the Jemalong area, rocks deposited during the Late Devonian consists of white, red and green sandstone, conglomerate, as well as green and white siltstone.

4.2.1.4. Tertiary

Alkali basalt magmatism occurred in the Tertiary, mainly restricted to the southeast corner on the Cootamundra 1:250 000 geological map sheet (Warren *et al.*, 1996). Within the Forbes 1:250,000 geological map sheet (Brunker, 1968) Tertiary unit includes laterite, poorly consolidated sandstone and conglomerate, and basalt.

4.3. Unconsolidated sediments

Quaternary unconsolidated sediments have been deposited by fluvial activities in the study area and consist of clays, sands and gravels. Two distinct groups of alluvial sediments namely: Lachlan and Cowra formation (from the Pliocene and Pleistocene to Quaternary, respectively) have been identified infilling the valley between Jemalong Gap and Condobolin (Anderson *et al.*, 1993).

Along the Bland Creek catchment, Williams (1988) has also divided the infilled sediments into two units, the Upper and Lower Zones. The Lower Zone in the Bland Creek area has been described as equivalent to Lachlan Formation and the Upper Zone corresponds to the Cowra Formation.

During the course of exploratory drilling, remnants of a third, older unit were observed in some sites (Anderson *et al.*, 1993) which was deposited on the Palaeozoic basement during the Miocene. With the erosion and subsequent deposition, little of this unit remains. For the purpose of this study, this third formation has been included in the Lachlan Formation which is taken to be the basal sediment sequence.

4.3.1. Geological history and mode of deposition

The Murray-Darling system was in its early phase of development during the Eocene to early Miocene period. During this period, Australia had already separated from Antarctica and had commenced its northward drift (Anderson *et al.*, 1993).

The Lachlan River carved its way through the Jemalong and Manna Ranges during this early period of development. The infilling of the valley commenced about Middle Miocene, however renewed erosion and downcutting in the Late Miocene removed most of these sediments and only a small amounts of Middle Miocene deposits remain (Anderson *et al.*, 1993). Major infilling of the valley with sediment started during the Pliocene when the Lachlan Formation was deposited. After a period of non-deposition, the Cowra Formation was deposited during the Pleistocene to the recent period. The Lachlan and Cowra Formations are both interpreted to have been deposited by meandering river systems (Anderson *et al.*, 1993).

4.4. Geological cross sections

Figure 4.2 shows the location of the wells and the cross-sections that have been used in the geological interpretation of the unconsolidated sediments. The nine geological cross-sections (A-A' to I-I') are shown in Figures 4.3 to 4.11. These cross-sections illustrate the nature of the alluvial deposits encountered in exploration wells across the study area. It must be stressed that these cross-sections are interpretive, and suggests conditions of the alluvial environment based on the data available. Extrapolation of geological information has been done in some cases between wells of several kilometres apart.

There are approximately 1915 wells drilled in the study area at different depths by the Department of Land and Water Conservation, other government agencies, private companies and individual farmers (Table 4.2). Of these wells, 52 % lie in the alluvial part of the study area and the rest were drilled in the fractured basement rocks that serve as the boundaries of the alluvial sequence. Table 4.3 shows the number of wells classified according to depths and ownership within the alluvial region. Only about 301 wells are deeper than 50 m and out of these wells, only 95 close to the cross-sections have been used for preparation of the cross-sections (Appendix B).

Table 4.2: Number of bores and wells in the study area (including bores in the basement rocks).

Depth (m)	Ownership				Total
	DLWC*	Private	Other	Unknown	
151 and above	0	22	0	1	23
101-150	15	175	6	0	196
51-100	27	439	3	0	469
25-50	43	478	2	3	526
Less than 25	164	528	5	4	701
Total	249	1642	16	8	1915

* Department of Land and Water Conservation.

Table 4.3: Number of bores and wells in the alluvial part of the study area.

Depth (m)	Ownership				Total
	DLWC*	Private	Other	Unknown	
151 and above	0	7	0	1	8
101-150	9	72	2	0	83
51-100	10	199	1	0	210
25-50	26	259	0	1	285
Below 25	135	275	0	1	411
Total	180	811	3	3	997

* Department of Land and Water Conservation.

4.4.1. Geological cross-section A-A'

The A-A' cross-section (Figure 4.3) is located in the southernmost part of the Bland Creek catchment. Seven wells with the deepest at 123 m at Well no. 14994, have been used in preparation of this section. There is a drop of the topographic surface along this section from 252 m AHD on the eastern side at Well no. 30675 to 227 m AHD to the west at Well no. 36630. The alluvium in this section is dominated by clay sediments with minor lenses of sand. At the top 50 m of the cross-section, clay sediments are mostly grey clays with little sand lenses. Layers of multicoloured and greyish clay sediments dominate the lower depths of the alluvium.

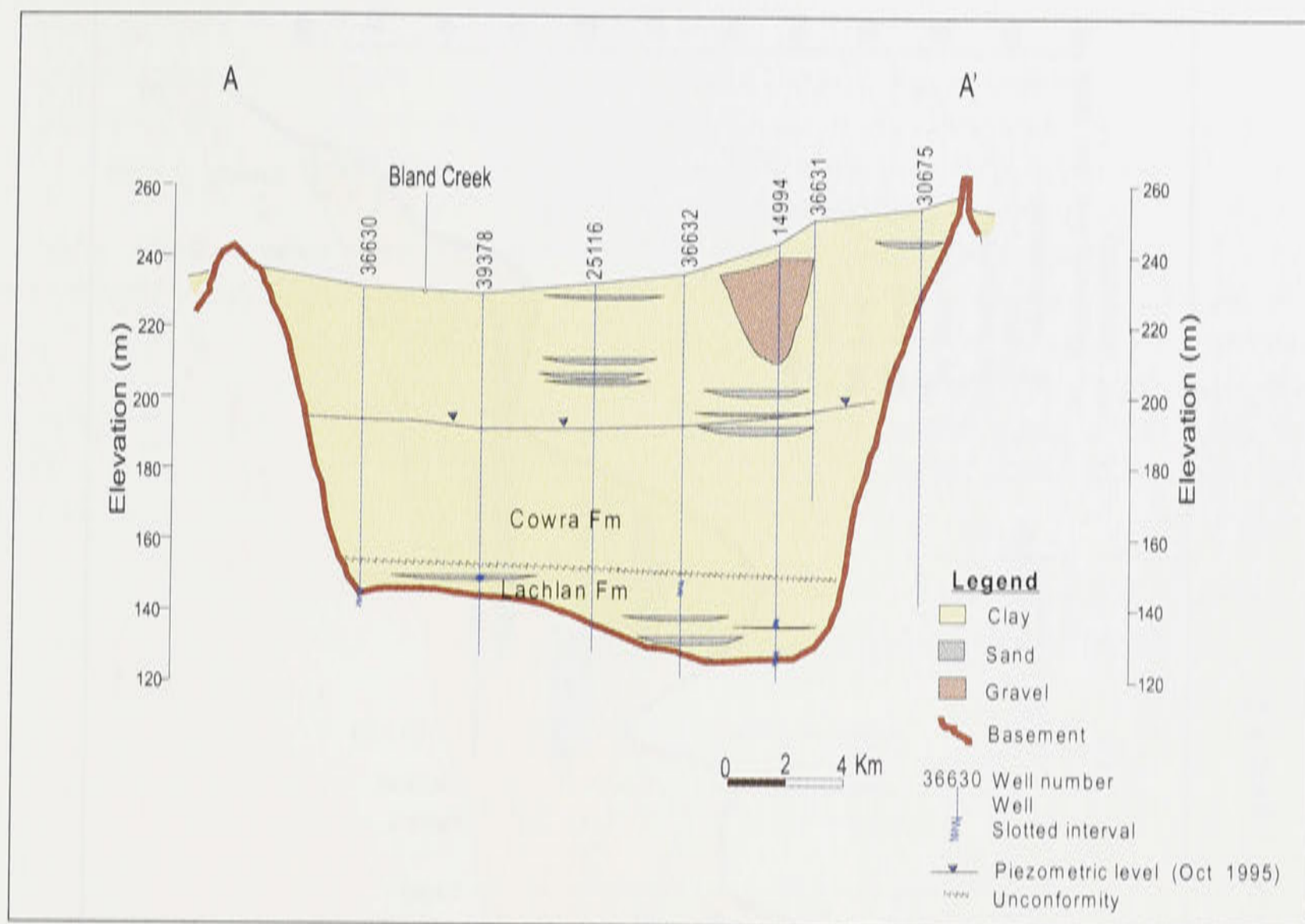


Figure 4.3: Geological cross-section A-A' (see Figure 4.2).

4.4.2. Geological cross-section B-B'

Cross-section B-B' (Figure 4.4) is the longest geological cross-section in the study area and is located in the alluvial area of the Bland Creek catchment (Figure 4.2). This cross-section transverses from Wyalong to north side of Young, slightly below Weddin Mountain. About 18 wells were used in the interpretation of the Quaternary geology at this section (Appendix B). The general slope trend of the basement rock is from east to west, which is also along the general slope of the land surface. The broad channel like basement structure between Well nos. 1232 and 2990 defines the Bland Creek Paleochannel that transverses at this section. Although clay sediments dominate especially in the shallower alluvial section, sand has largely infilled the depressions between Well nos. 36603 and 36606. Likewise, the depression at the upper reach of the cross-section between Wells nos. 27739 and 25704 contains relatively high proportion of sand lenses. Clays within the top 50 m depth are mostly grey clays, while mixture of multicoloured and grey clays are found below 50 m depth. The maximum thickness of sediments in this section is about 120 m found at Well no. 29481.

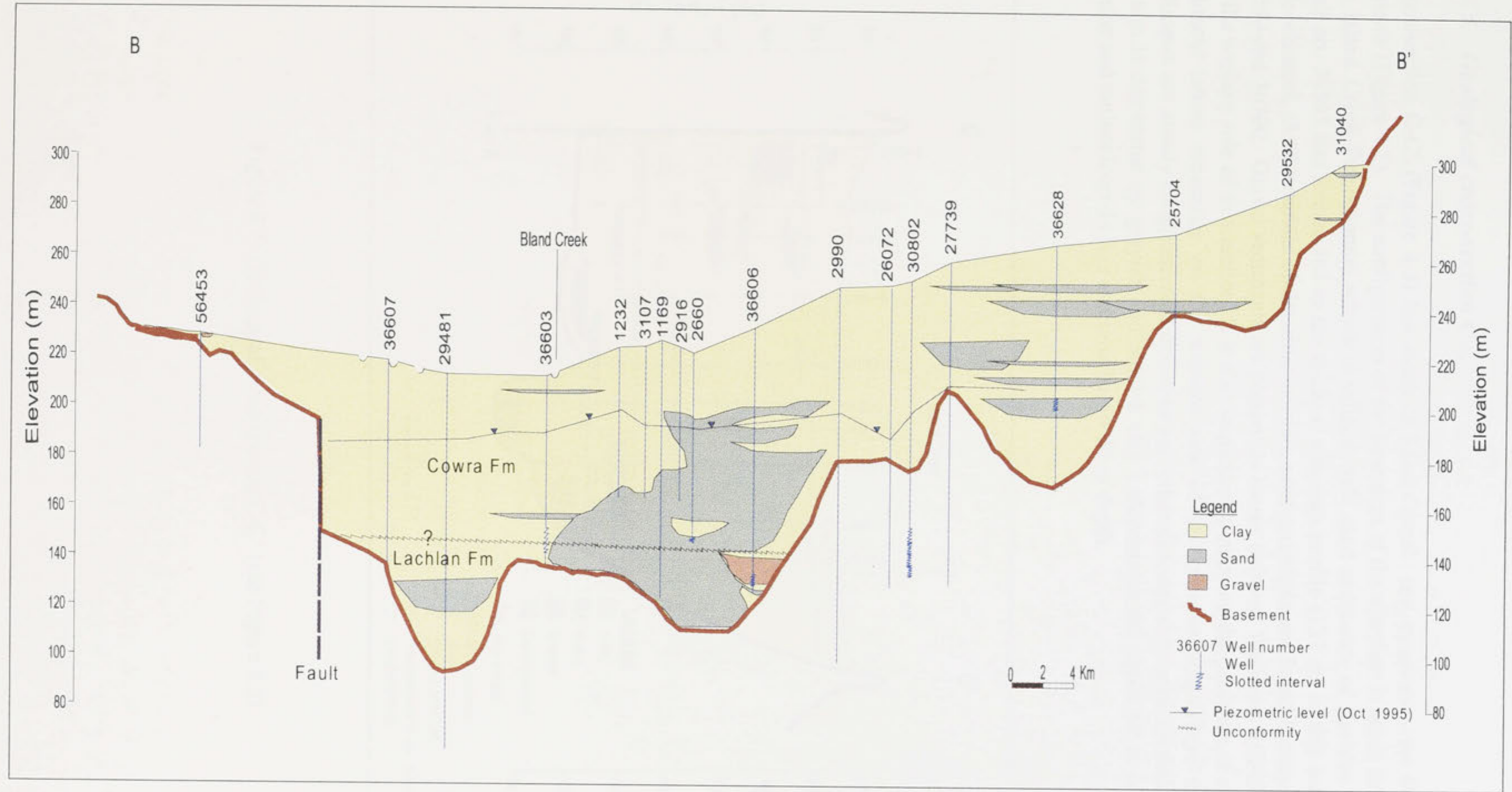


Figure 4.4: Geological cross-section B-B' (see Figure 4.2).

4.4.3. Geological cross-section C-C'

Cross-section C-C' (Figure 4.5) lies south of Lake Cowal and transverses the Bland Creek systems (Figure 4.2). The configuration of the basement of the alluvium is again influenced by the Bland Creek Paleochannel which is infilled with sand sediments of Lachlan Formation. Well no. 36595 has intersected to the thickest alluvium profile (127 m) in this section in the Paleochannel. At the middle of the cross-section, sand sediments are found between Well nos. 36597 and 36700. Gravel sediments are present as lenses between Well nos. 26045 and 36597 on the western side of this section. It is also important to mention the presence of consolidated sediment lenses especially on the western side of the cross-section. These consolidated sediments are mostly conglomerated ironstone and other decomposed rocks. Overall, the cross-section is dominated by greyish and reddish clay sediments in the upper 50 m of the cross-section and multicoloured clays and sand below 50 m depth.

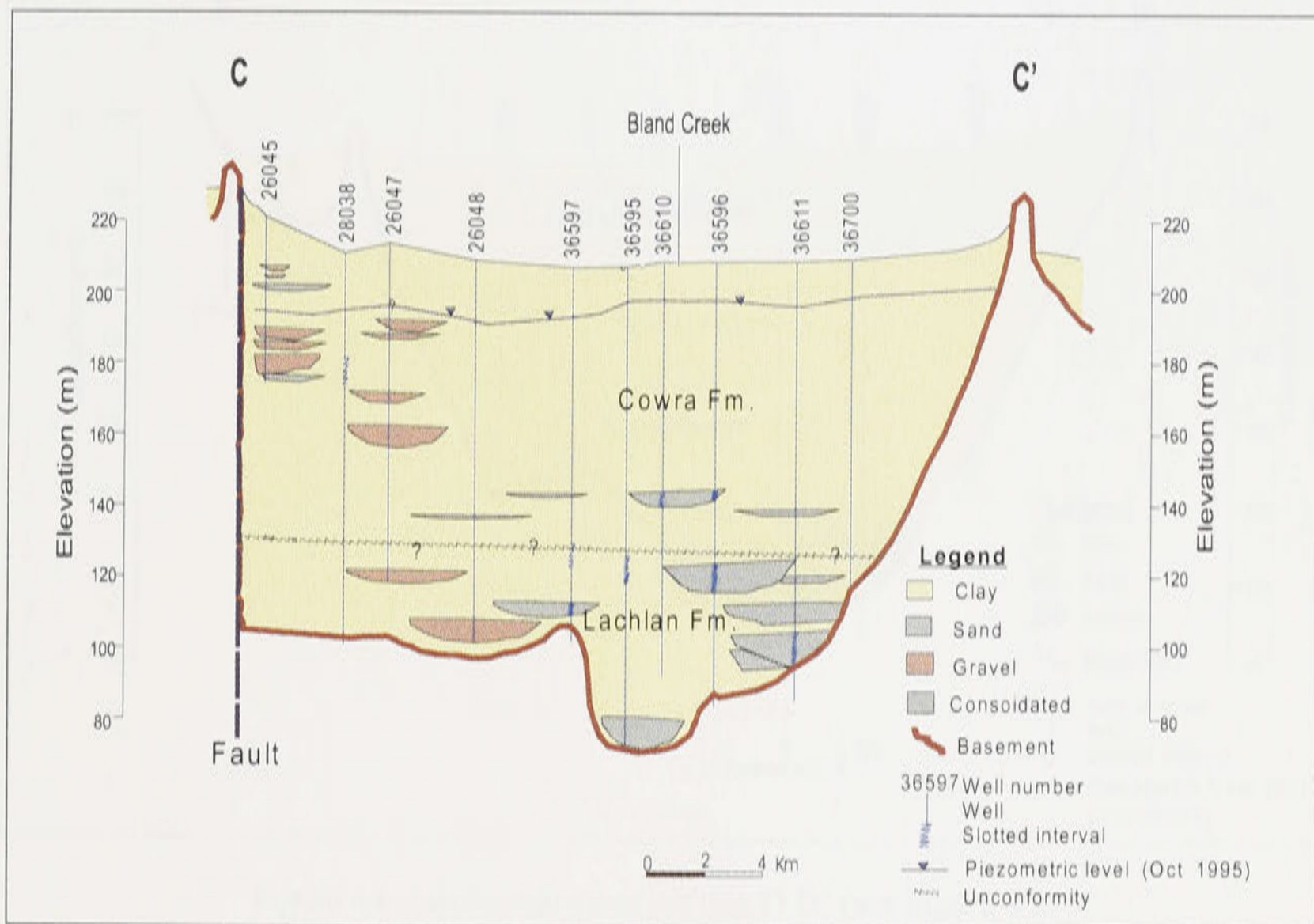


Figure 4.5: Geological cross-section C-C' (see Figure 4.2).

4.4.4. Geological cross-section D-D'

Cross-section D-D' (Figure 4.6) runs along the southern part of the Jemalong and Wyldes Plains Irrigation District and at the northern limit of the Lake Cowal (Figure 4.2). Six wells have been used in preparation of this section and all of them have penetrated the underlying basement. This cross-section displays a similar pattern to cross-section C-C'. Sand deposits of Lachlan Formation with a thickness of about 30 m has infilled the entrenched portion of the valley. Thin lenses of sand and gravel are also found in the upper zone of the cross-section corresponding to the Cowra Formation.

Clay sediments encountered in the section are mostly grey and multicoloured clays found in some layers within the top 50 m depth of the cross-section. The deeper profile of the section (> 50 m) is dominated by sand and yellow, brown and multicoloured clay sediments.

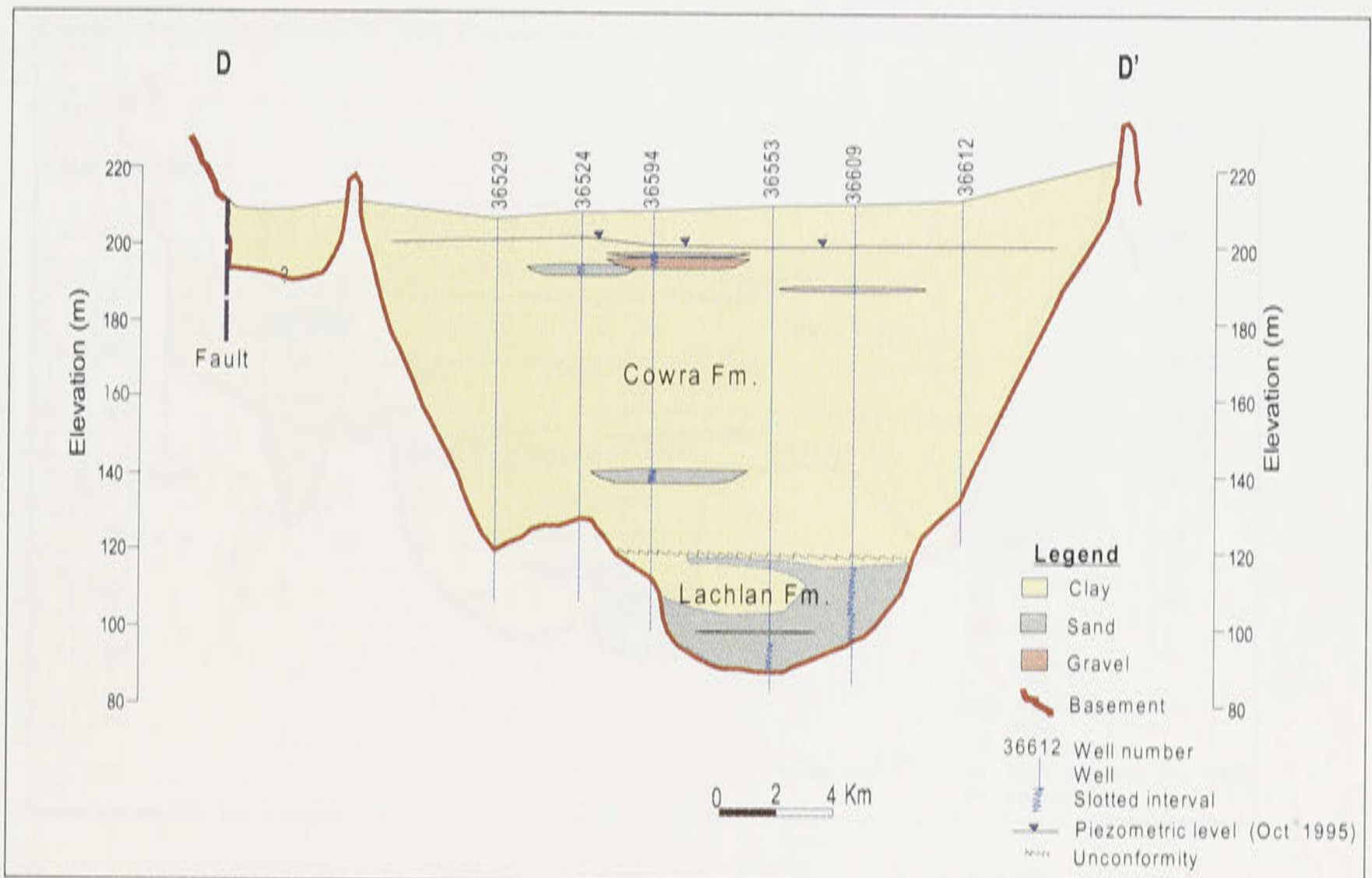


Figure 4.6: Geological cross-section D-D' (see Figure 4.2).

4.4.5. Geological cross-section E-E'

Cross-section E-E' (Figure 4.7) stretches from Manna Mountain to the Jemalong Range (Figure 4.2). Nine wells have been used in preparation of this cross-section and almost all of them have reached the basement rock during the drilling operation. The most deeply entrenched part of the cross-section is infilled with Lachlan Formation sands with a thickness of about 24 m in Well no. 36523. It is dominated by pink, grey, cream and white sands, in addition to a significant cream-white quartz gravel zone in Well no. 36552.

Comparing with cross-section D-D' and other cross-sections further south, cross-section E-E' has increased quantities of sand and gravel present as lenses. According to Anderson *et al.*, (1993), the relative position of the individual lenses indicates the changes in the river course during deposition. Sand and gravel are quite significant at the middle of the cross-section. Most of the sand and gravel lenses have been defined to be productive in terms of water supply. Clay sediments at the upper 50 m of the cross-section are grey clays, although some layers within this depth have reddish, yellowish and light brown clays. Clay sediments at the deeper part of the section are sticky in general and colours vary from one layer to another.

The extent and nature of the alluvium in the Dog Kennel Hill is defined by Well no. 36555 in this section. Drilling at this well encountered clay sediments and intersected decomposed sandstone at 50 m depth below the surface. No major productive sand and gravel were intersected in this well. Between the Dog Kennel Hill and the edge of the Manna Mountain, an entrenchment has been identified at Well no. 31309.

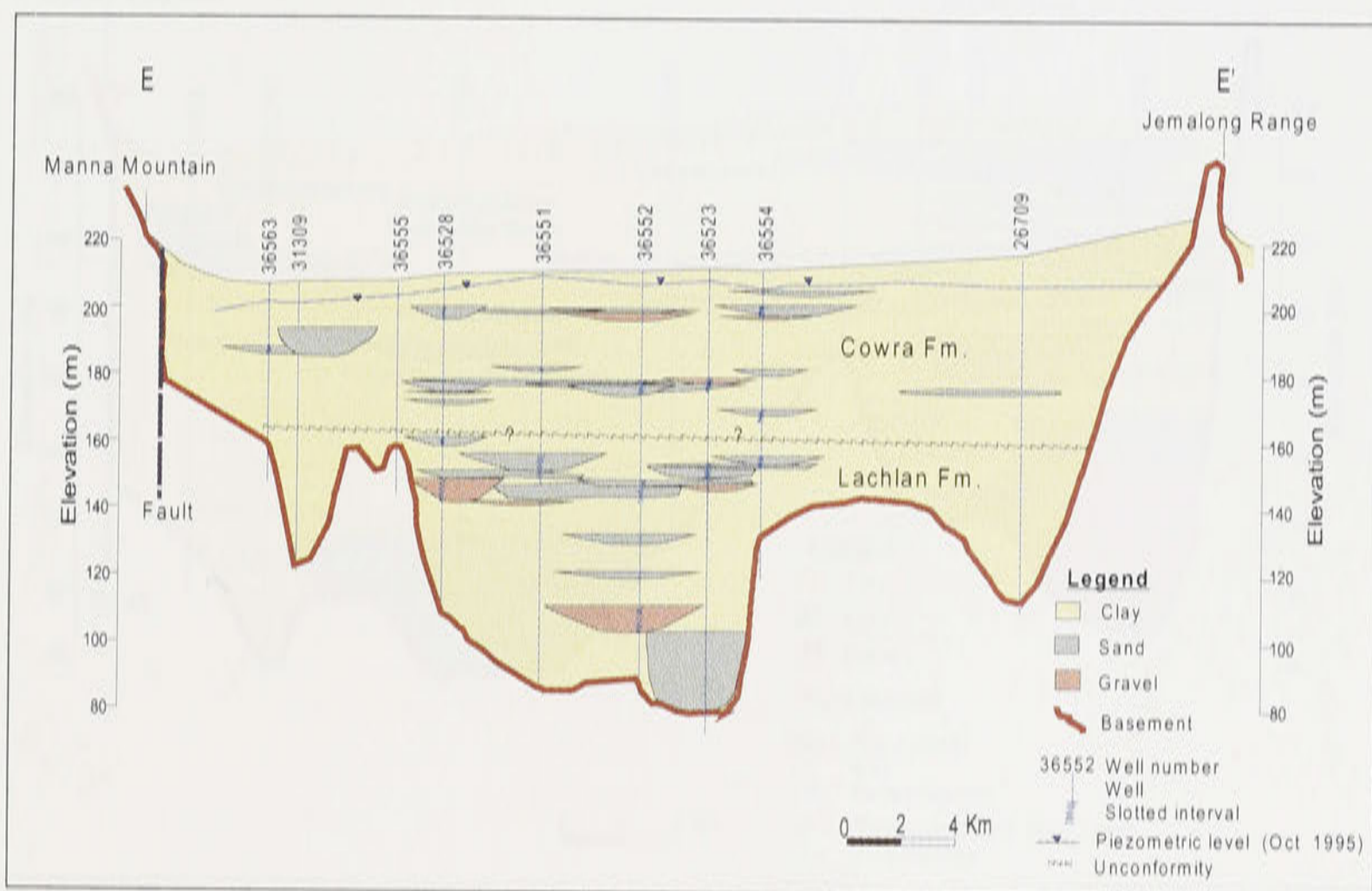


Figure 4.7: Geological cross-section E-E' (see Figure 4.2).

4.4.6. Geological cross-section F-F'

Further north and cutting the Lachlan River, cross-section F-F' (Figure 4.8) stretches from Manna Mountain on the west to the Corradgery Range on the east (Figure 4.2). Eight wells, mostly deep enough to reach the basement have been used in preparation of this cross-section. Two entrenchments were encountered in this cross-section which correspond to the Lachlan Paleochannel on the eastern side and the Warroo Paleochannel on the western side of the cross-section.

The entrenched valley at Well no. 28743 shows the path of the Warroo Paleochannel in this cross-section. Sand occupies the deepest part of this entrenchment. Within this well, lenses of sand were also found at the middle and upper part of the profile. Between Well nos. 21276 and

39307, clay sediments dominate the Cowra Formation, although lenses of gravels are present in Well no. 36085. The clay sediments are yellow to yellow sticky clays at Well no. 21276 and clay sandy at Well no. 28743 within the upper 50 m depth of the cross-section. At the deeper depth (> 50 m), layers of reddish yellow, grey, dark brown, red, pink and multicoloured clays are found.

The entrenched alluvial section underlying the Lachlan River provides high quantities of sand and gravel. In the area around Jemalong Gap, sedimentation was dominated by a high energy meandering stream system which deposited the coarse gravel fraction of its sediment load at the foot of the Corradgery Range. Well no. 36525 encountered strata with very high percentages of sand and gravel.

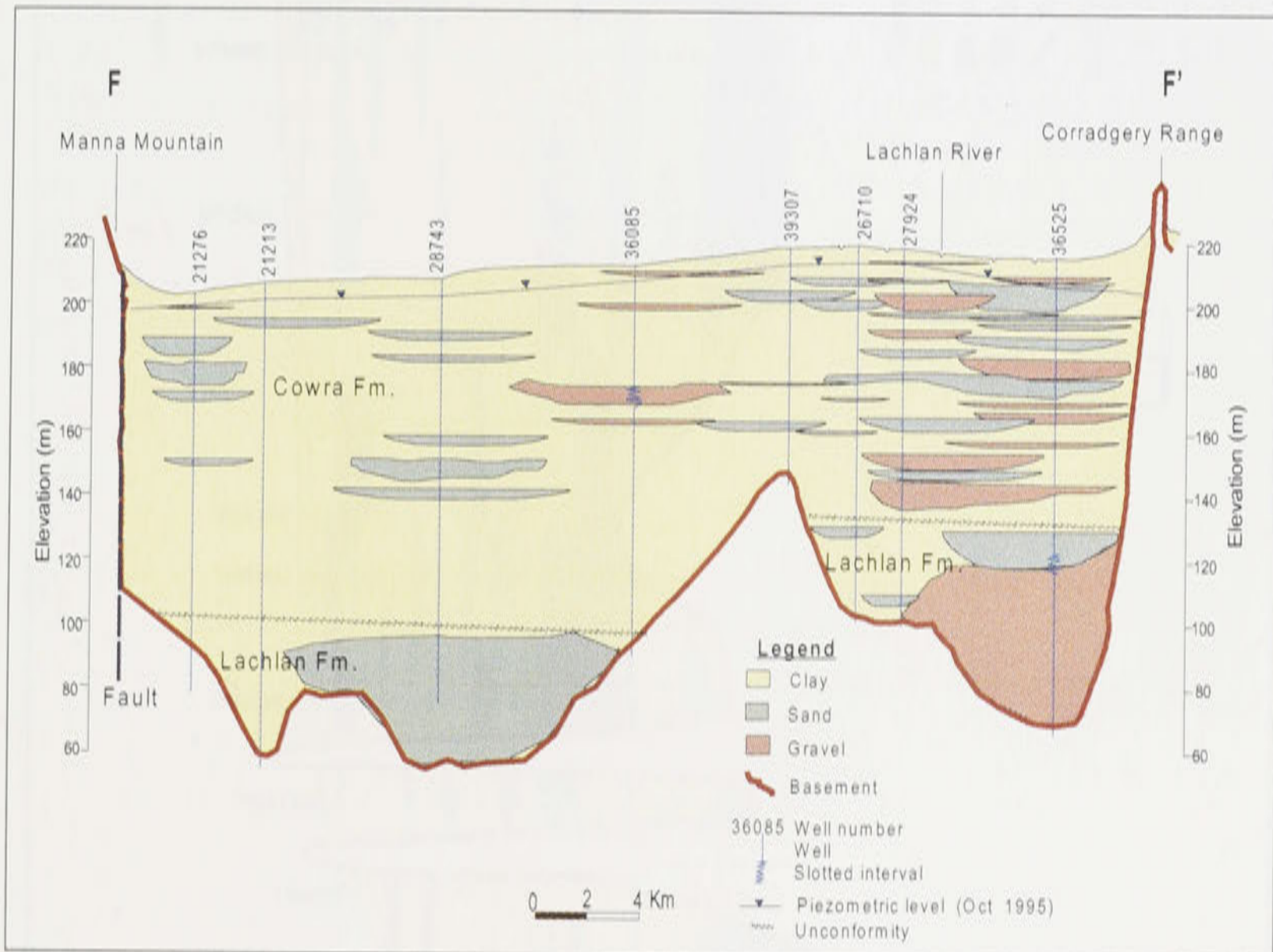


Figure 4.8: Geological cross-section F-F' (see Figure 4.2).

4.4.7. Geological cross section G-G'

Cross-section G-G' (Figure 4.9) is a longitudinal cross-section which extends from the Jemalong Gap to Condobolin at Well no. 53668 in the northwest (Figure 4.2). This cross-section runs approximately along the Lachlan River and defines the strata within or near the river system. Fourteen wells have been used to interpret the nature of the strata and most of these wells have reached the basement.

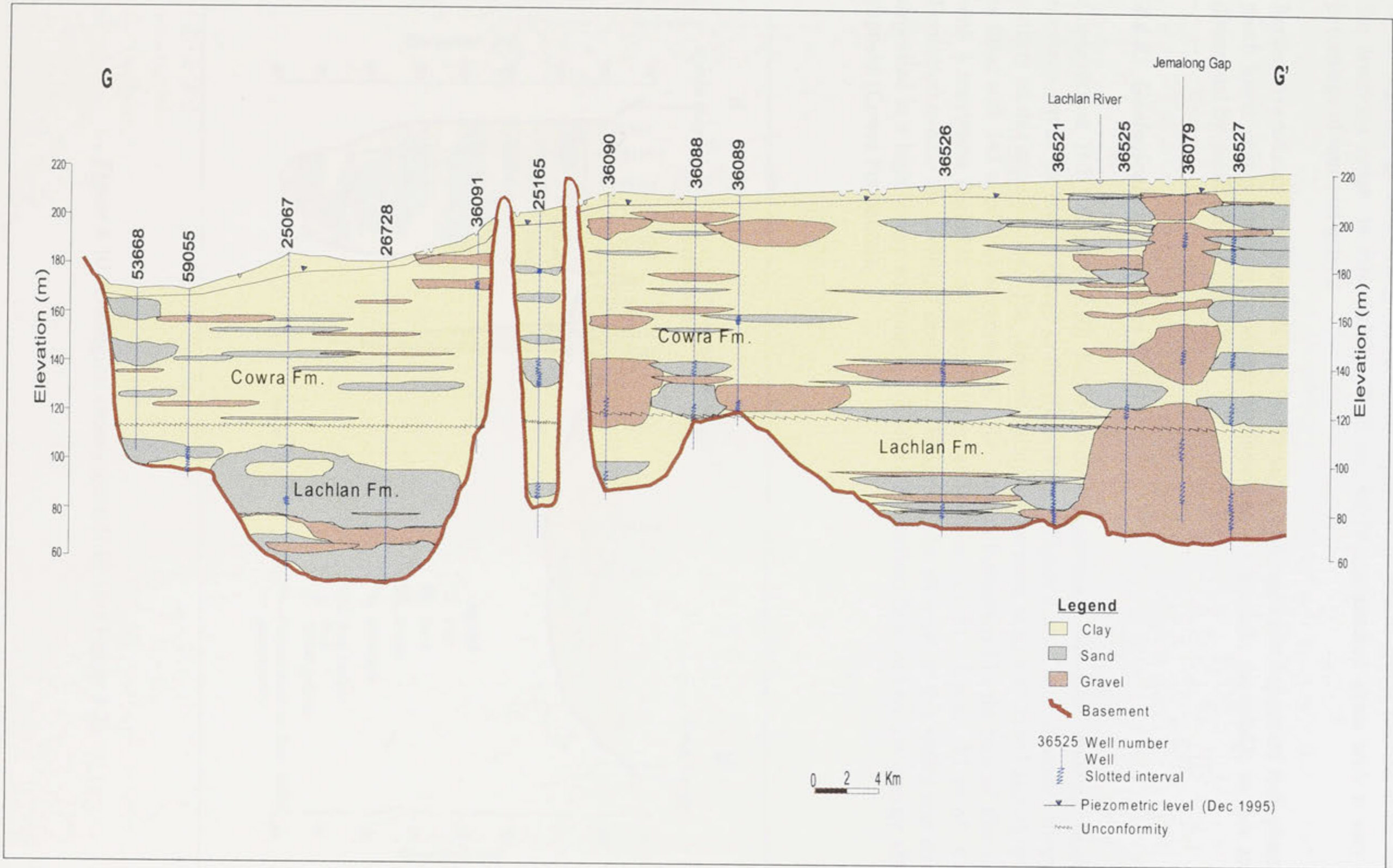


Figure 4.9: Geological cross-section G-G' (see Figure 4.2).

Sedimentation at the upstream area of the cross-section around the Jemalong Gap is dominated by the high energy meandering stream which deposited the coarse gravel fraction at the foot of the Jemalong range. In this vicinity, Well no. 36079 encountered strata with a very high percentage of sand and gravel.

Further downstream between Well nos. 36091 and 53668, sediment deposition took place in a much lower energy meandering stream environment. As a result, the profile in this area is dominated by sand, silt and clay.

4.4.8. Geological cross section H-H'

Cross-section H-H' (Figure 4.10) has a southwest-northeast direction spanning from the northern part of the Manna Range to the Black Range (Figure 4.2). Three discrete valleys are evident on this cross-section. The deepest valley lies between Well nos. 25163 and 25165 and is filled with 142 m of alluvial sediments. The Lachlan Formation fills the base of this valley, with a maximum thickness of about 65 m at Well no. 25151. Up to 77 m of Cowra Formation overlie the Lachlan Formation. Evidently, the alluvium in this valley was initially deposited in a high energy environment (Lachlan Formation) followed by low energy alluvial deposits (Cowra Formation).

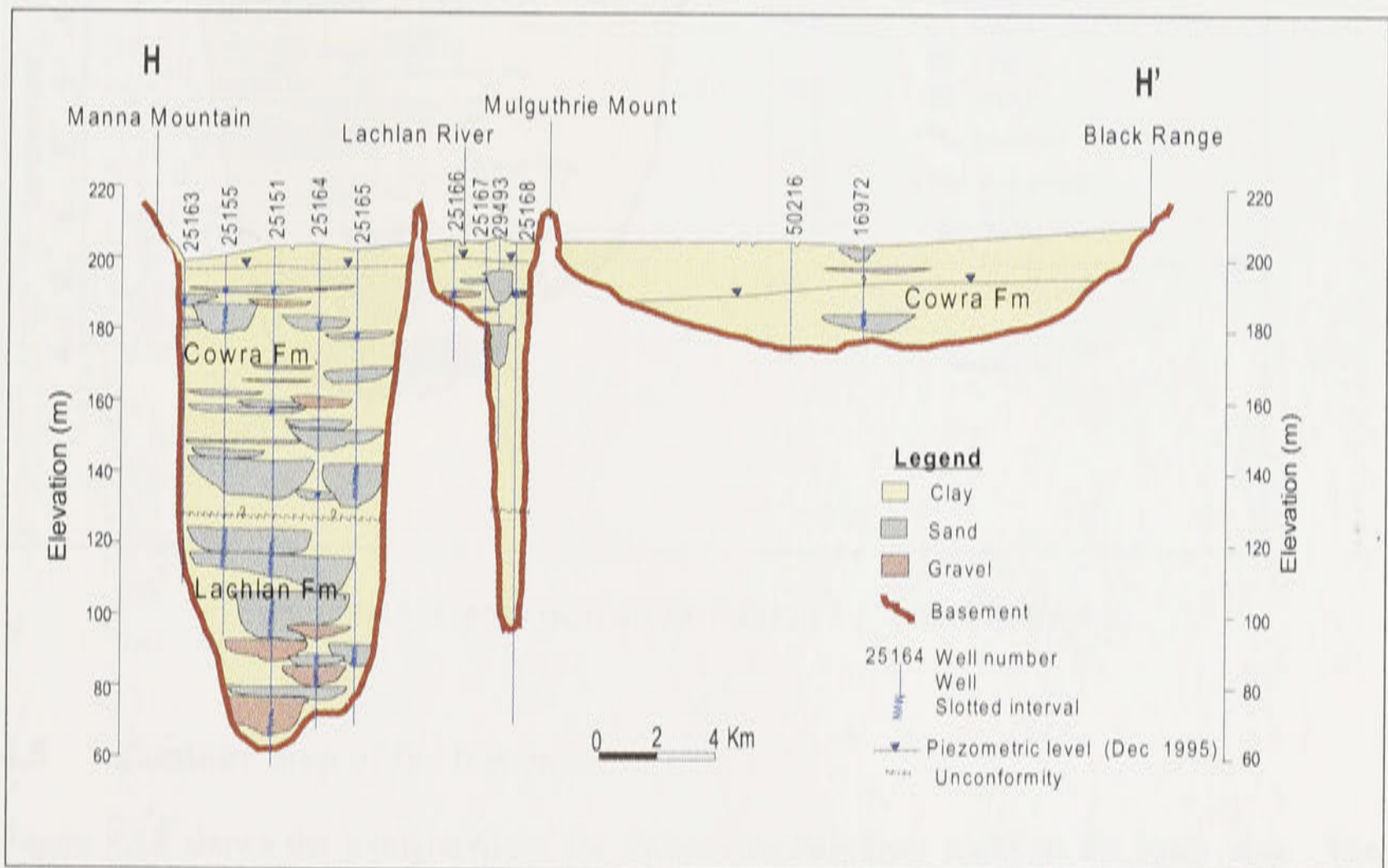


Figure 4.10: Geological cross-section H-H' (see Figure 4.2).

The narrowest valley lies between the two outcrops and underlies the present path of the Lachlan River. The maximum depth of the alluvium recorded at this valley is 106 m at Well no. 25168. Sand and gravel are only minor components of the alluvial infill.

Between Mulguthrie Mount and Black Range, the alluvium has a maximum thickness of 30 m in Well no. 50216. Although lenses of sand have been found in Well no. 16972, the aquifer is not productive.

4.4.9. Geological cross section I-I'

Cross-section I-I' (Figure 4.11) consists of 35 m of Lachlan Formation at Well no. 25067, overlain by up to 95 m of Cowra Formation. The distinct shape of the basement is similar to the deepest valley mentioned in cross-section H-H'. Concentration of sand and gravel have been found in the southern part of the Lachlan River.

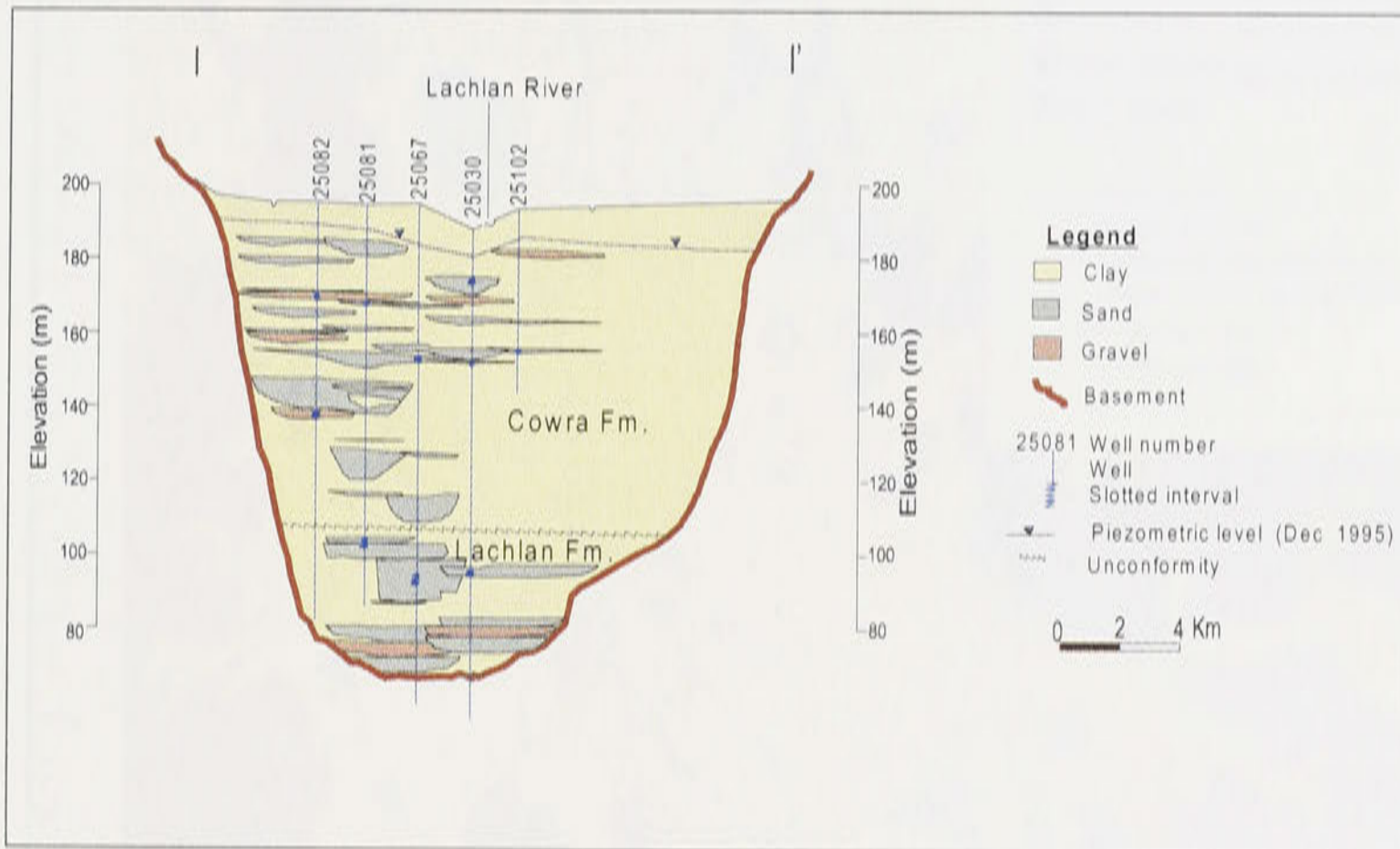


Figure 4.11: Geological cross-section I-I' (see Figure 4.2).

4.5 Contour map of the basement

Figure 4.12 shows the topography of the Palaeozoic basement rocks in the study area. The interpretation of the basements has been derived from the geological well logs and cross sections, and topographic data of the study area. Contours of the basement rocks at 20 m intervals have been derived using the ANUDEM (Hutchinson, 1996) package. ANUDEM is a spatial modelling tools which accurately interpolates topographic data sets of irregularly spaced data points.

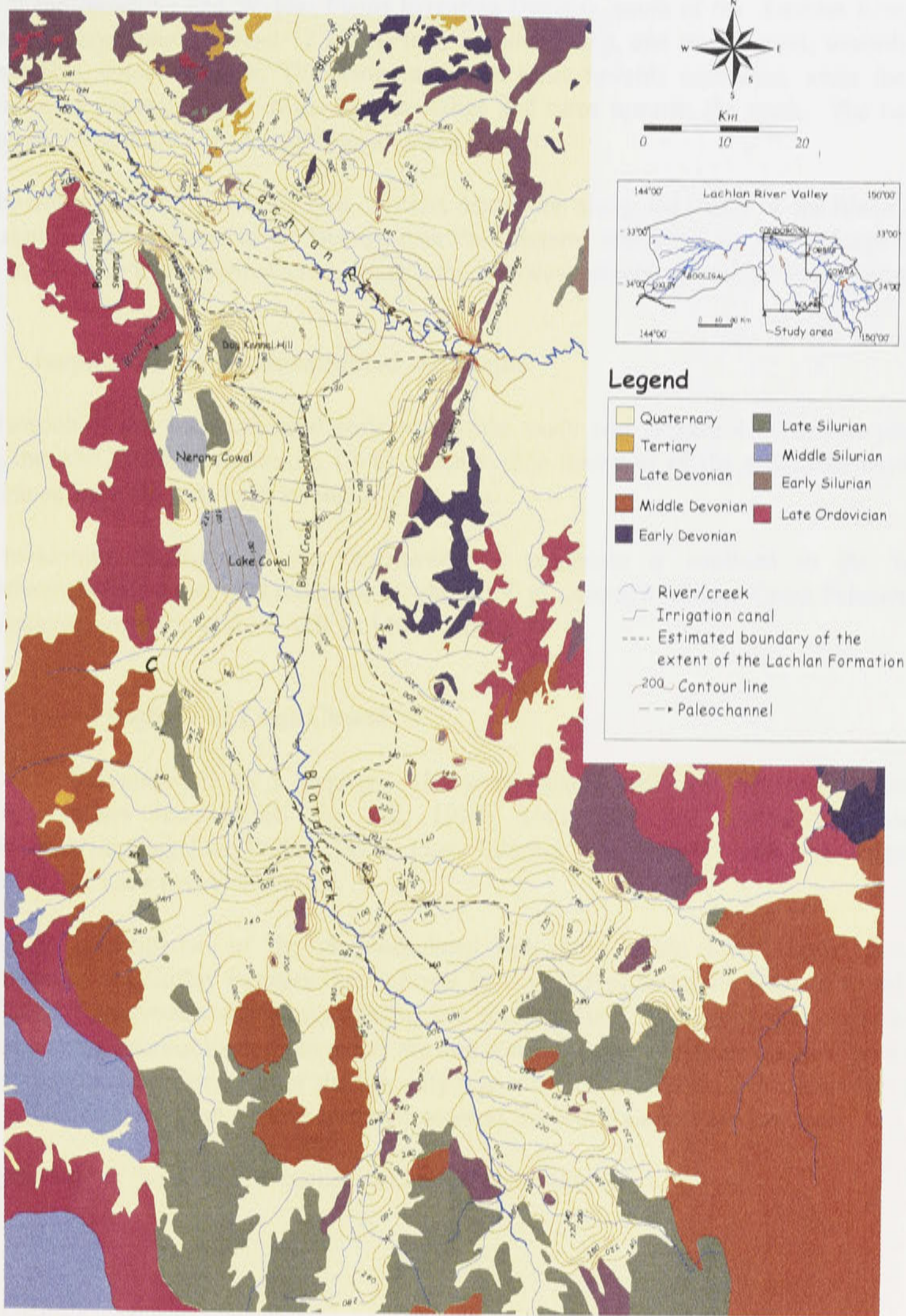


Figure 4.12: Topography of the Palaeozoic basement (contour intervals in m AHD).

Elevations of the basement rock gradually decreases towards the middle of the alluvial area. The lowest recorded elevation from the geological well logs is about 57.61 m AHD at Well no. 36550. The well is drilled in the so-called Warroo Paleochannel which is on the northwestern side of the Jemalong and Wyldes Plains Irrigation District, south of the Lachlan River. The Warroo Paleochannel is about 12 km west of Jemalong Gap, and travels west, towards Dog-Kennel Hill, where it splits. The northern branch turns towards northwest, while the other continues on through a gap in the Manna Range and turns towards the north. The two join further to the north, via Manna and Bogandillon Creeks.

On the southern part of the study area, distinct depression along the valley in the Bland Creek area signifies the presence of the Bland Creek Paleochannel which passes east of Lake Cowal, joins the Warroo Paleochannel and intercepts the east-west orientated Lachlan Paleochannel.

4.6 Isopach of the unconsolidated sediments

The isopach of the unconsolidated sediments in the study area (Figure 4.13) is also prepared using the ANUDEM (Hutchinson, 1996) package. The thickness of the sediments have been determined from the well logs available in the area.

The maximum thickness of the unconsolidated sediments is confined to the Warroo Paleochannels with a recorded thickness of about 150 m. Along the Bland Creek Paleochannel, the thickness ranges from about 110 to 140 m AHD.

4.7. Local geology of Lake Cowal

Lake Cowal is underlain by a sequence of unconsolidated sediments of variable thickness (Coffey Partners International Pty Ltd, 1996). Underlying the alluvial sequence are northwesterly dipping Late Ordovician to Early Silurian volcanoclastics and lavas commonly known as the Lake Cowal volcanics.

Geological investigation of the unconsolidated sediments within Lake Cowal area was undertaken by the Coffey Partners International Pty Ltd (1996) using the Department of Land and Water Conservation and North Mining Ltd drilling data. The geological cross-sections showed that the unconsolidated sediments are dominated by clay to a depth ranging from 40-60 m from the ground surface. Minor shallow silty lenses are also found at the southern part of the Lake, with increasing sand content eastward, towards the Bland Creek Paleochannel.

The hydrology of the alluvial sequences will now be considered.

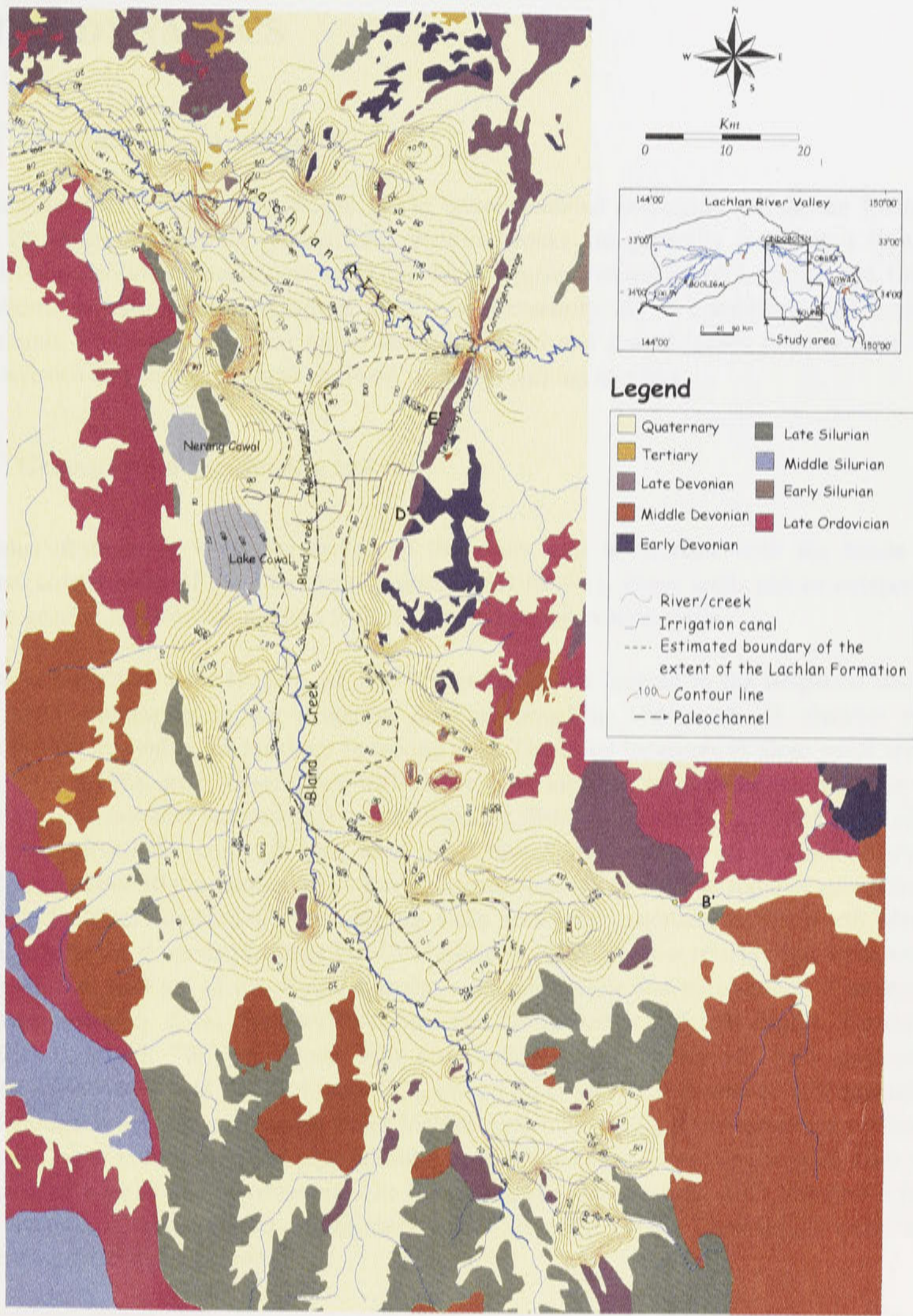


Figure 4.13: Isopach of the unconsolidated sediments.

CHAPTER 5

HYDRODYNAMICS

5.1. Groundwater environment

Groundwater in the study area occurs in the unconsolidated sediments and in the fractured rocks. However, groundwater yields from fractured rocks are generally less than 1 litre per second. Unconsolidated sediments form the main aquifer consisting of Lachlan and Cowra Formations. In hydrogeological terms, these two formations act in combination as a single aquifer unit, however on a local scale, individual sand and gravel lenses display their own characteristics and behave as local confined or semi-confined aquifers.

5.2. Groundwater monitoring system

Numerous observation wells are drilled in the study area to monitor both the heads and electrical conductivity of the groundwater system (Figure 5.1). These wells can be categorised into two groups, shallow observation wells and regional observation wells.

Shallow observation wells (Figure 5.2 and Appendix C) are located in the irrigation district. Water level monitoring in the irrigation district started in 1944 with 43 shallow wells predominantly located in the northern Jemalong area. The exact locations of these wells are not known. Since 1968, more observation wells have been installed to examine comprehensively the shallow groundwater environment of the irrigation district. Currently, more than 100 single or nested observation wells with long-term groundwater level records are available. Around Lake Cowal, about 30 monitoring wells have been installed since 1994 to monitor groundwater level and electrical conductivity. Monitoring wells were also installed by the North Mining Limited around the proposed Lake Cowal Gold Mine in 1994. Shallow observation wells within the irrigation district are of two types, namely: watertable wells and piezometers. Piezometers are constructed with 5 cm diameter PVC pipe and are drilled at different depths. Watertable wells (denoted with "W" on Figure 5.2) are shallow (3 to 10 m) and fully perforated. Piezometers (denoted with "P" on Figure 5.2), on the other hand, are deeper (10-20 m) and are located alongside with the watertable wells. Unlike watertable wells, piezometers are perforated only at the lower end of the PVC pipe (about 1 m long). To date, there are about 26 sites with both watertable wells and piezometers. The remaining sites have mostly with watertable wells alone. Records of groundwater levels since 1968 for most of the observation wells have significant gaps in their record.

Regional observation wells are maintained at about 75 sites in the study area by the DLWC (Figure 5.3). These bores are screened or slotted at depths usually at the water bearing lenses (Appendix D).

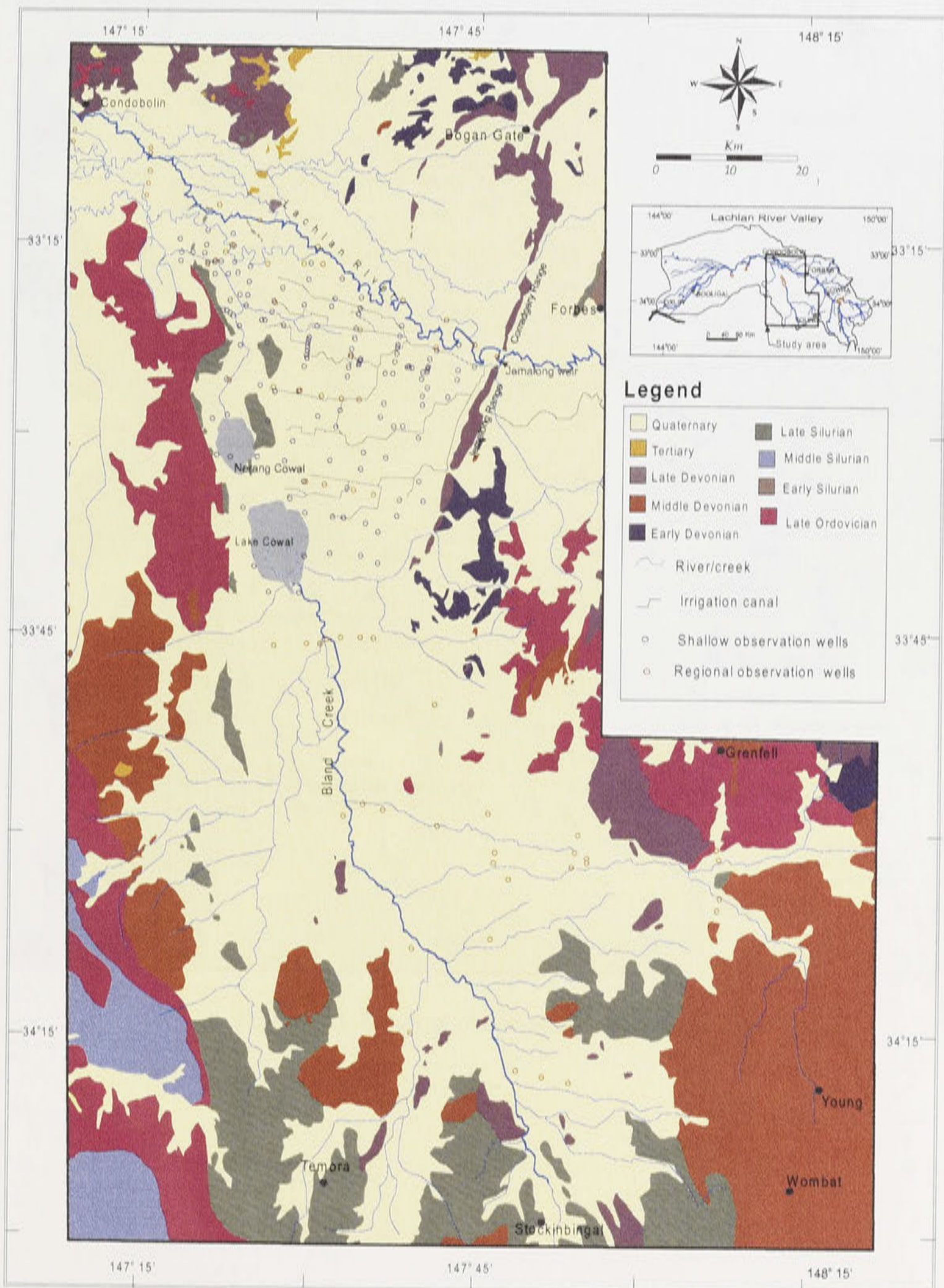


Figure 5.1: Locations of monitoring wells in the study area.

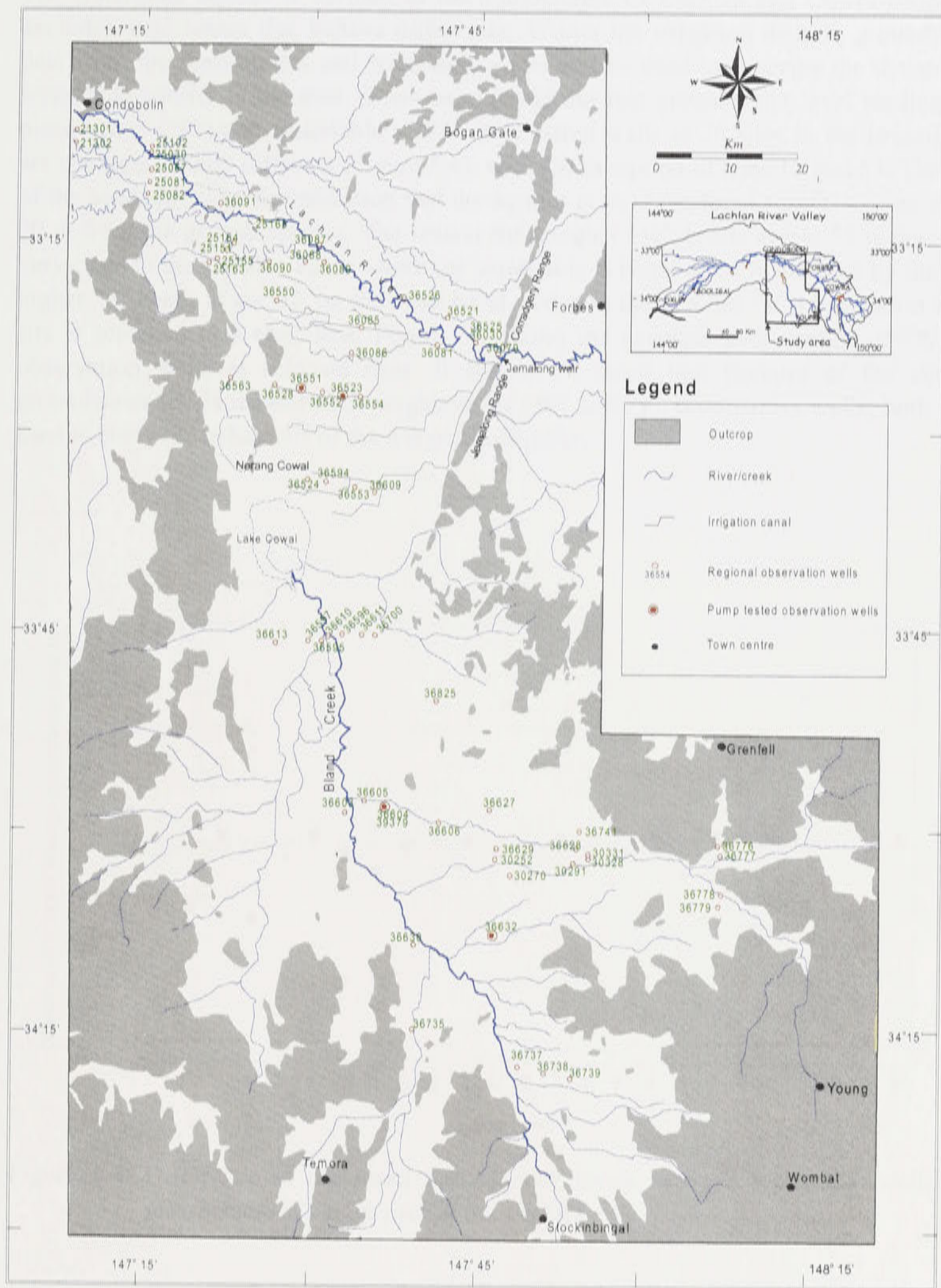


Figure 5.3: Distribution of the regional observation wells in the study area.

5.3. Watertable aquifer

The watertable aquifer is defined as the combination of Lachlan and Cowra formations and excludes sand lenses that behave differently. Within the irrigation district, groundwater level data from the piezometers and watertable wells can be used to describe the dynamics of the watertable aquifer in the area. It has been found out that groundwater level readings between piezometers (“P”) and watertable (“W”) observation wells at 26 sites in the irrigation district are not significantly different (Figure 5.4), with the exception of sites 12 and 53. The similarity of the heads provides an indication that the aquifer is an unconfined aquifer system even below 20 m from the ground surface. The reason for a higher “W” heads at site 53 is that this site is very close to the Lachlan River where the watertable is being directly affected by the river. The higher “P” heads at site 12, on the other hand, is due to the fact that “P” observation well at this site is screened in a sand lens. Figure 5.5 shows the example hydrographs of “W” and “P” observation wells at selected sites. It should be noted that because of the similarity of groundwater levels measured in neighbouring “W” and “P” observation wells, both have been used to study the behaviour of the watertable aquifer.

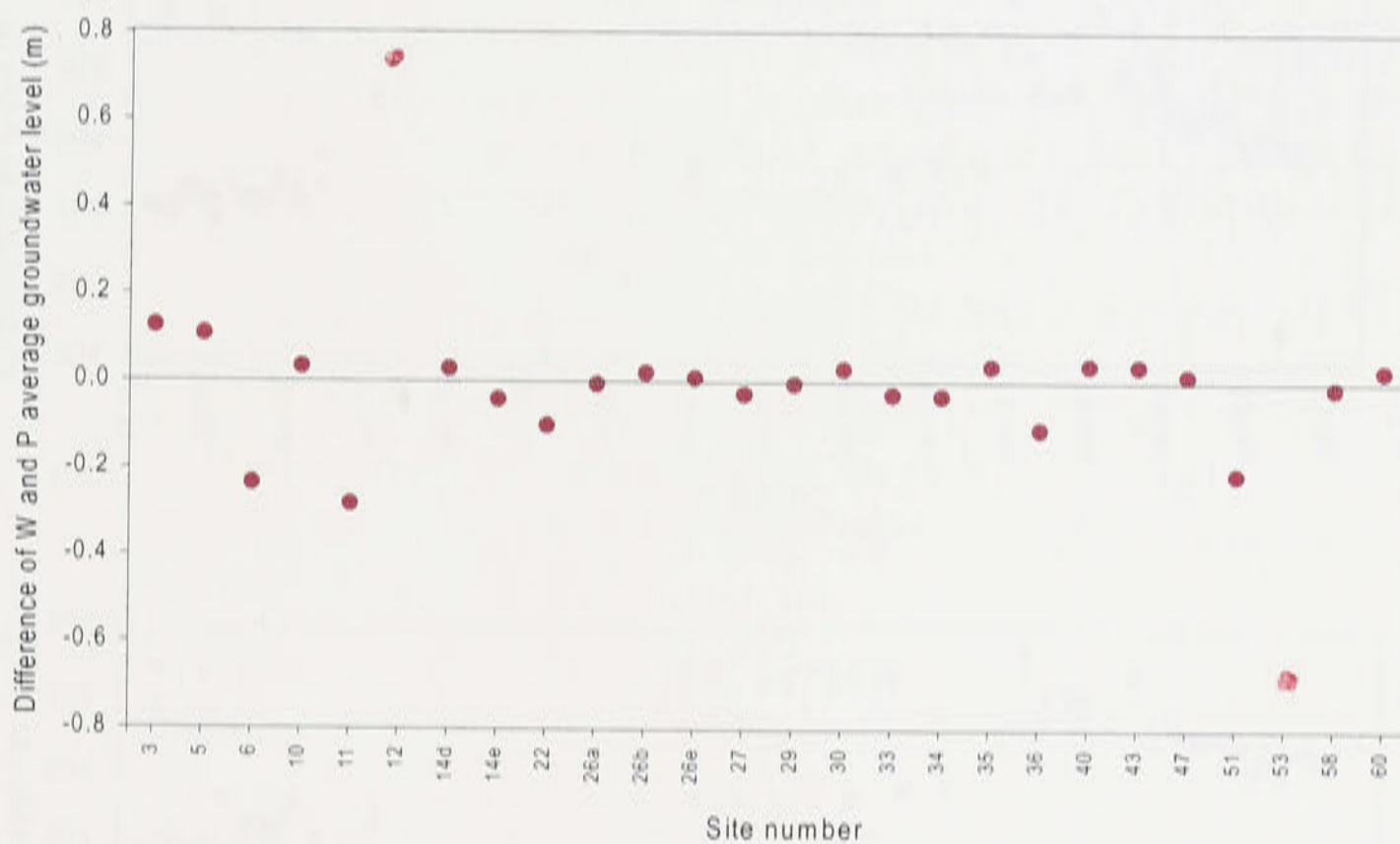


Figure 5.4: Difference of the mean groundwater levels between watertable wells (W) and piezometers (P) at 26 sites in the JWPID.

In the Bland Creek area, wells for monitoring watertable dynamics are very limited. The intensive shallow groundwater monitoring wells are concentrated in the irrigation district. Although regional observation bores are available, only a few of them are used to monitor the dynamics of the shallow aquifers. Most regional observation bores located in this area are used to monitor the piezometric heads of the deep sand and gravel lenses. Due to this limitation, it is not possible to prepare maps for the watertable aquifer in the Bland Creek area and this is an issue that needs to be addressed.

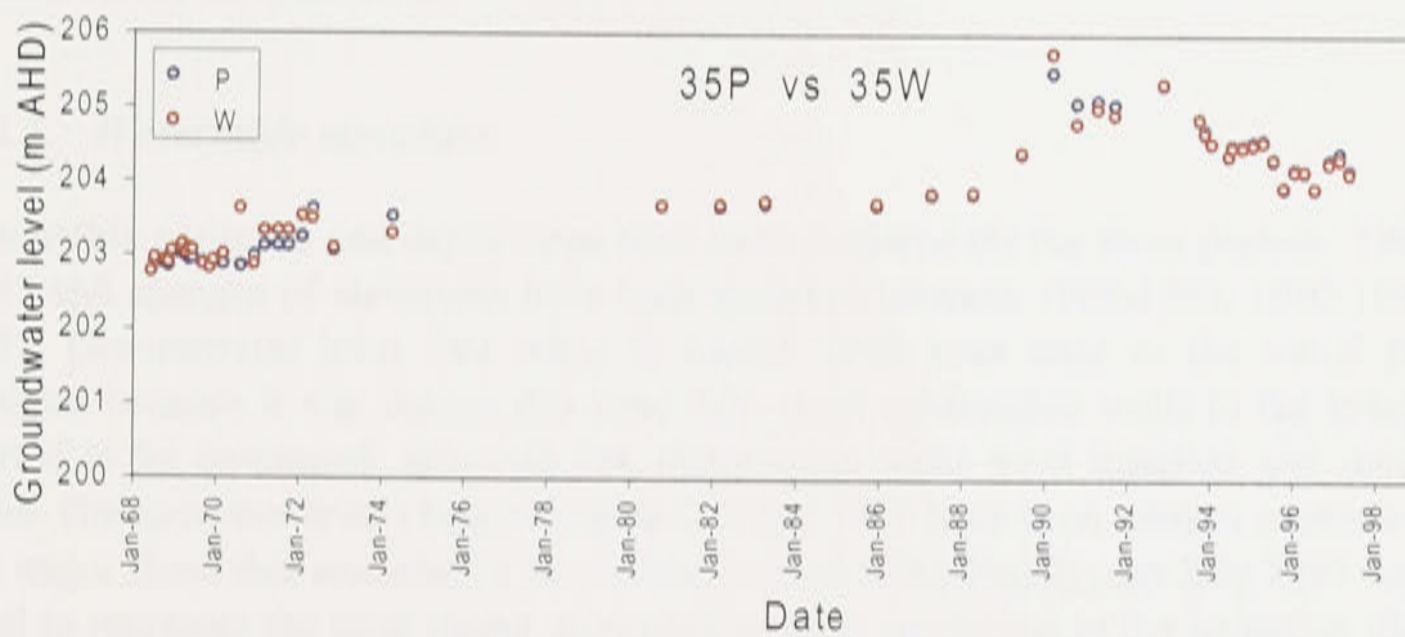
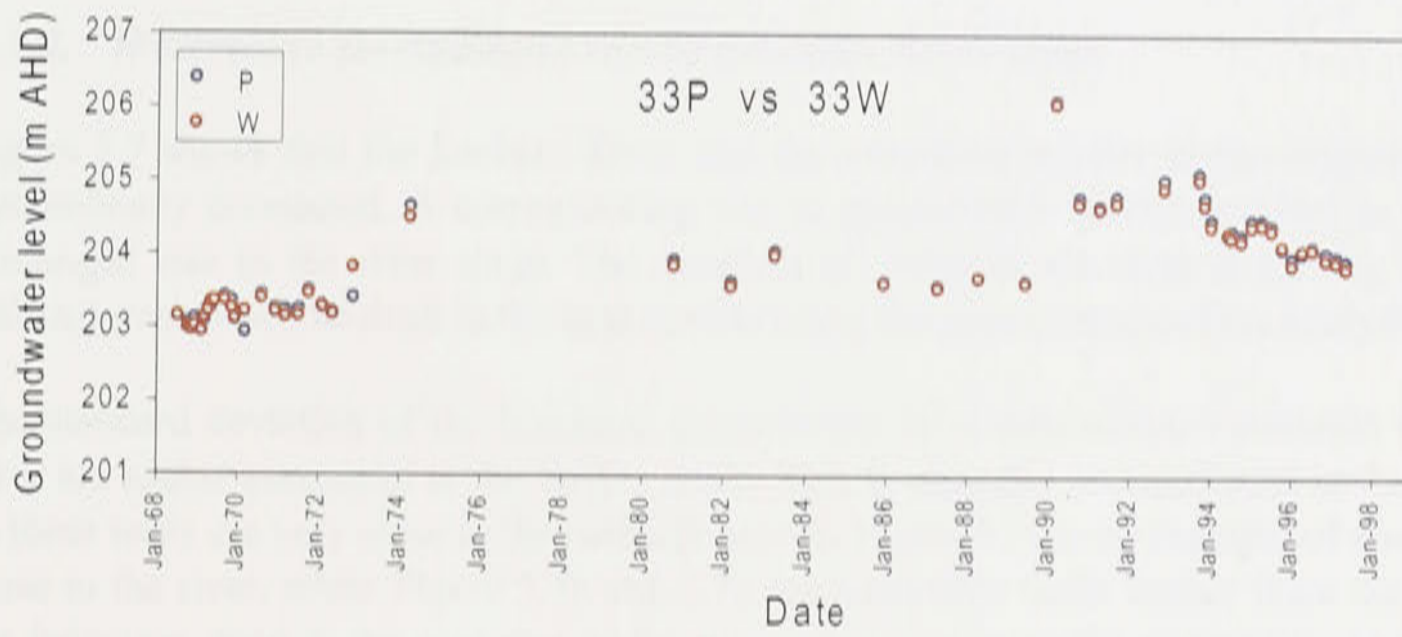
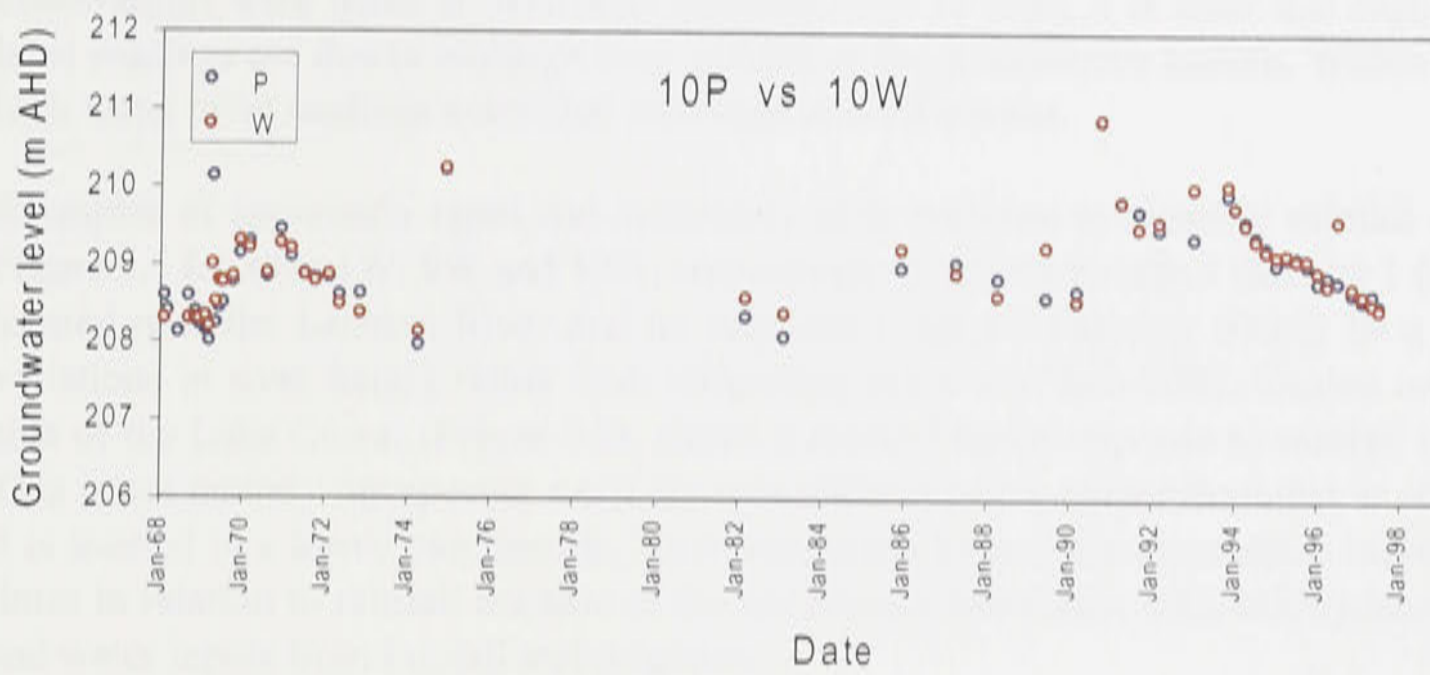


Figure 5.5: Hydrographs of W (Watertable) and P (Piezometer) observation wells at sites 10, 33 and 35 (see Figure 5.2 for locations).

5.3.1. Watertable fluctuations versus rainfall

Watertable level fluctuations are correlated with rainfall (see Figure 5.6 and Appendix E). Although recording of water levels was very irregular from 1968 to 1973, and almost no observations were made at most sites between 1975 to 1983, it is clear that high groundwater level readings are due to recharge from rainfall to the groundwater system. Within a given year, high water level readings coincided with high rainfall months.

Examples of apparently rapid and apparently slow response to monthly rainfall are shown in Figure 5.6 for sites 1W, 9W and 50W, respectively. It should be noted that site 1 (Figure 5.2) is located near the Lachlan River and its response (Figure 5.6a) may simply be a reflection of variations in river height rather than infiltrating rainwater. Site 50W, located on the western side of the Lake Cowal (Figure 5.2), shows a marked lag in response to rainfall (Figure 5.6b). This is not entirely unexpected since the watertable is much deeper than that at site 1, and also it is located in a heavy clay profile. No attempts has been made to examine individual site lag times in relation to rainfall because of the uncertainty associated with soil hydraulic properties and water inputs from rainfall and irrigation.

5.3.2. Watertable fluctuations versus Lachlan River stage

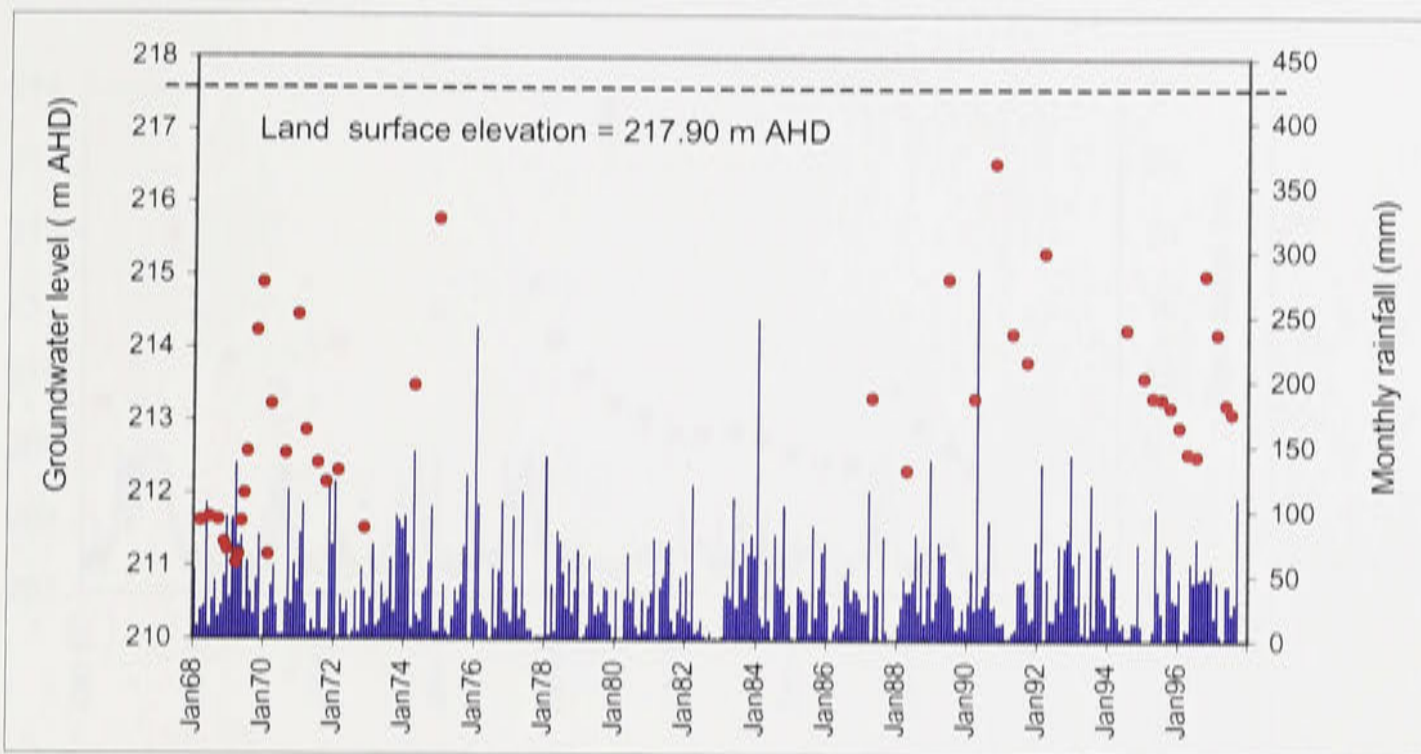
Figure 5.7 shows that the Lachlan River and the watertable aquifer in the irrigation district are hydraulically connected. A corresponding rise in groundwater level is evident as a response to prolonged rise in the river stage. The question of whether the river is serving as effluent or influent stream will be dealt in the next section using the piezometric surface analysis.

The standard deviation of the historical groundwater level data of the watertable wells near the river are higher compared to the farther wells. This is expected as mentioned in the section 5.3.1 as these wells are very close to the recharge source. Figure 5.7a is an example of a watertable well close to the river, while Figure 5.7b and 5.7c are watertable wells farther from the river. Within the irrigation district, the response of the watertable aquifer to the river stage declines with the distance away from the river.

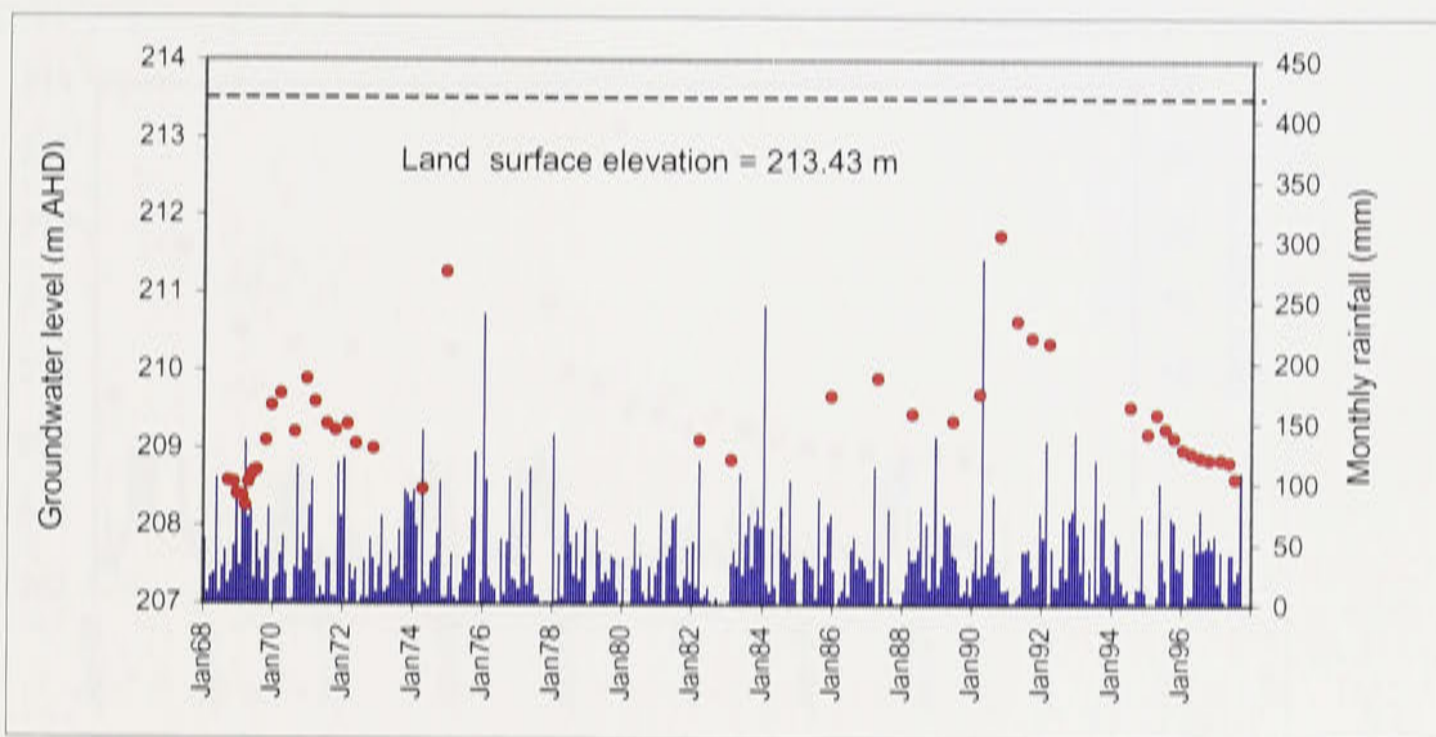
5.3.3. Watertable elevation

Watertable elevation and depth maps have been prepared for the three periods: 1969; 1990 and 1997 and changes of elevations have been analysed between 1969-1990, 1990-1997 and 1969-1997. Groundwater level data taken in March 1969 were used as the initial period of the analysis because it was during this time that most observation wells in the irrigation district started to be monitored, although few observation wells were installed and monitored since 1968. Groundwater level observations in October 1990 have been used to evaluate the effect of the major flood that occurred in the second half of 1990. Finally, the July 1997 data have been used to represent the most recent groundwater level conditions in the irrigation district. Figure 5.8, 5.9 and 5.10 show the watertable elevations and movement of the shallow groundwater in 1969, 1990 and 1997, respectively.

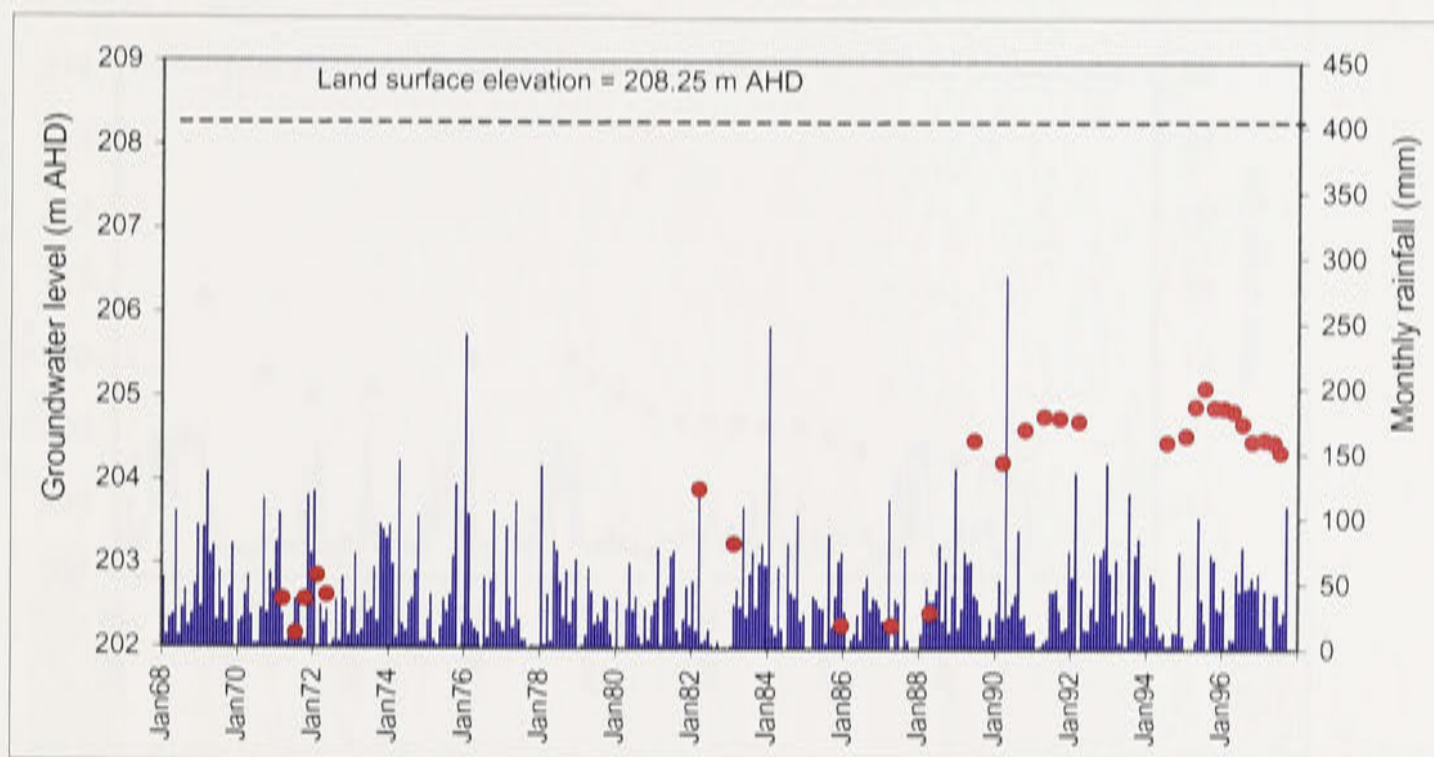
The watertable elevation map of the March 1969 (Figure 5.8) shows a relatively regular gradient from around 216 m AHD at Jemalong Gap to less than 200 m AHD near Lake Cowal. Notable features of this map are the dominant influence of the Lachlan River on the aquifer



(a) Site 1W

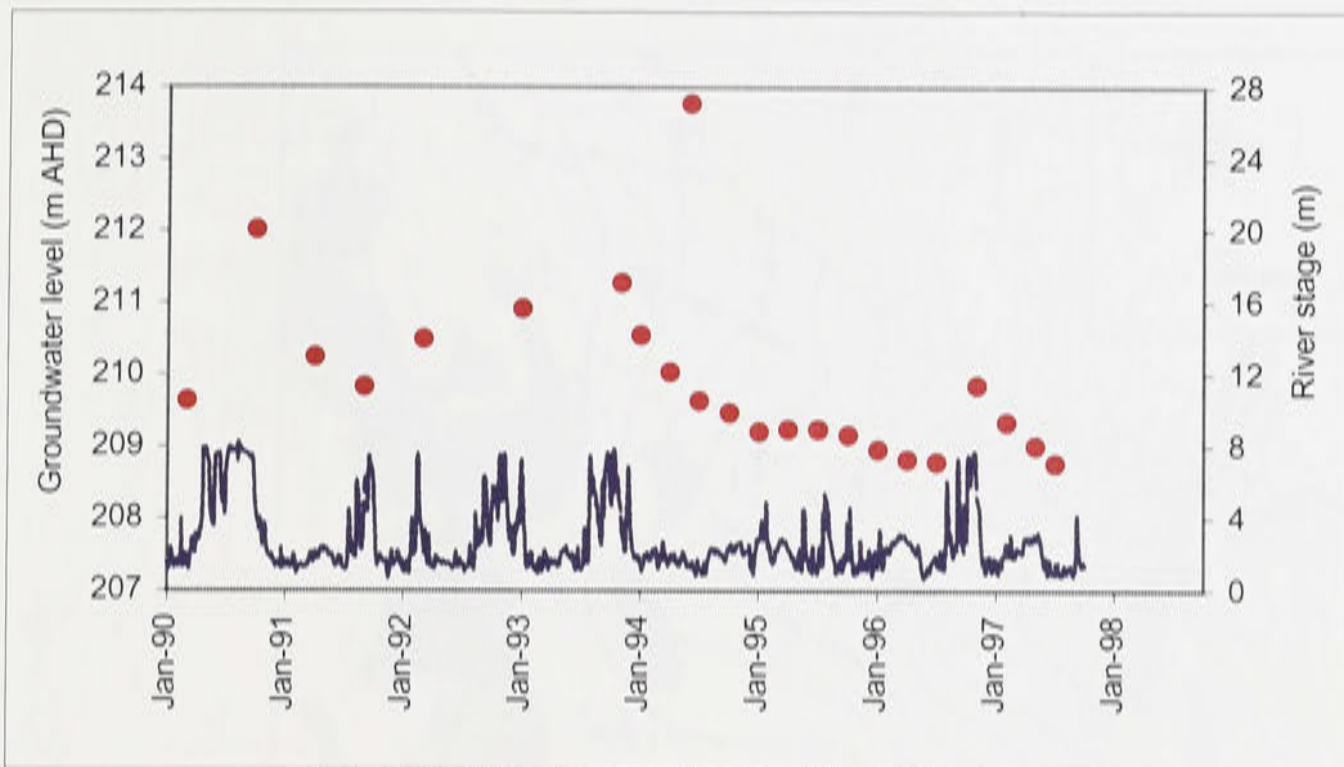


(b) Site 9W

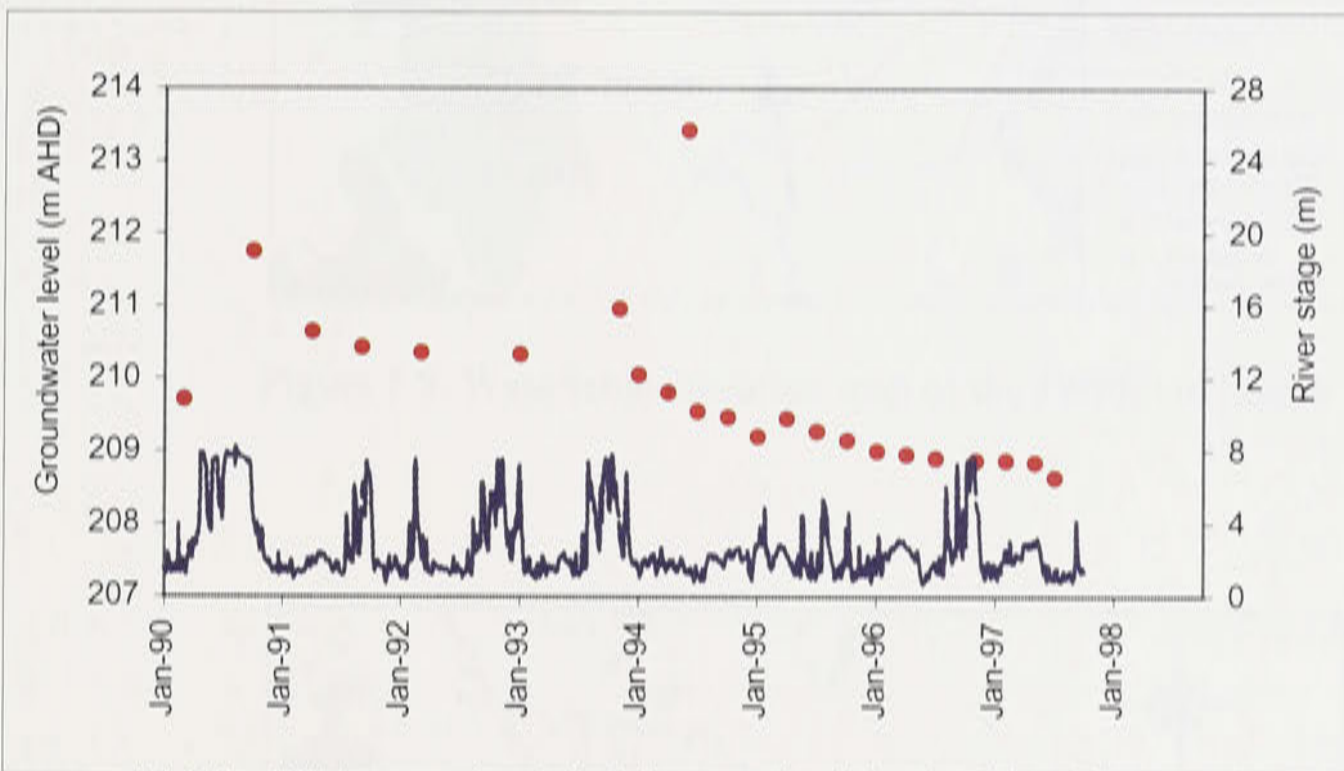


(c) Site 50W

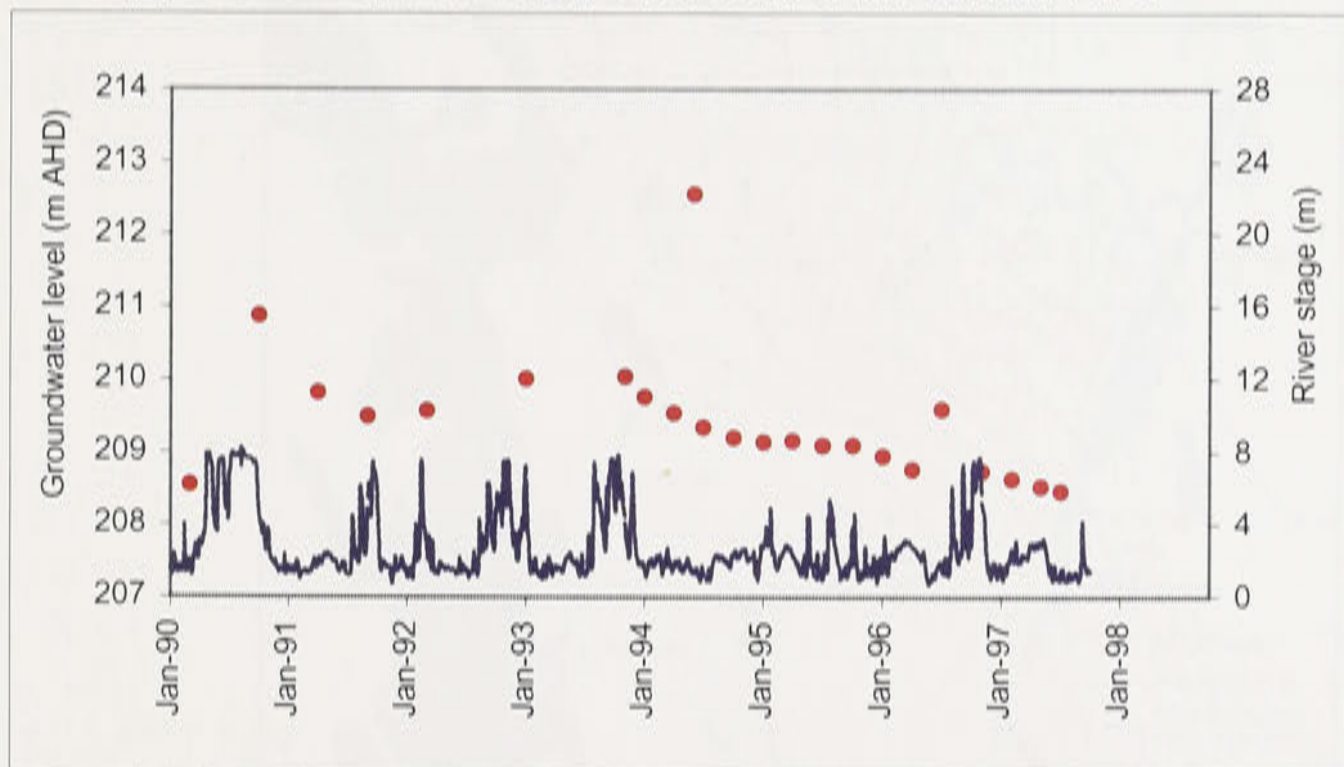
Figure 5.6: Effect of rainfall on watertable elevation at sites 1W, 9W and 50W (see Figure 5.2 for locations).



(a) Site 8W close to the Lachlan River



(b) Site 13W approximately 8 km south of the Lachlan River



(c) Site 43W approximately 19 km south of the Lachlan River

Figure 5.7: Effect of the variations of the Lachlan River stage (solid line) on the watertable elevation (dots) at sites 8W, 13W and 43W.

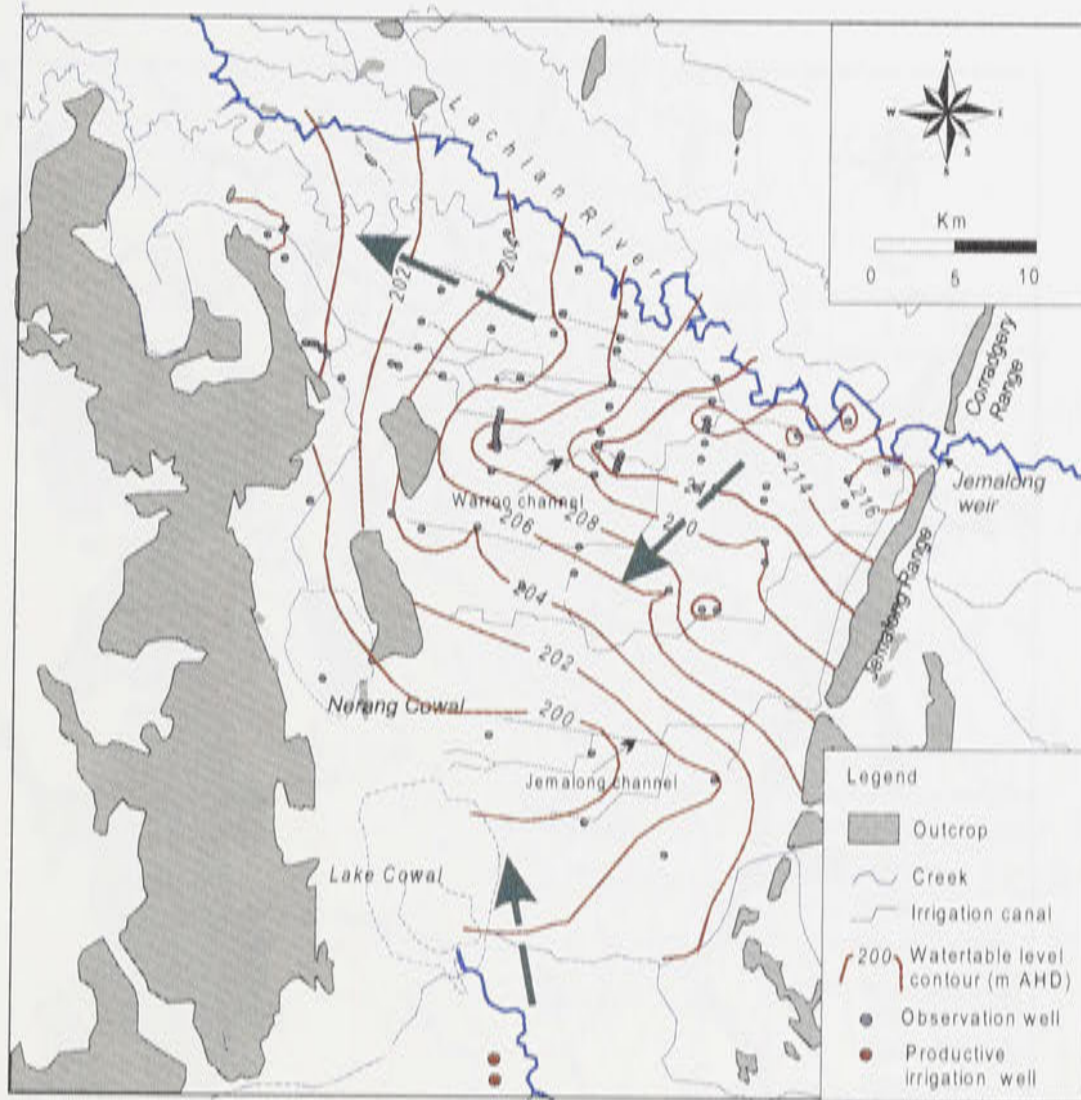


Figure 5.8: Watertable elevation map of the JWPID in March 1969.

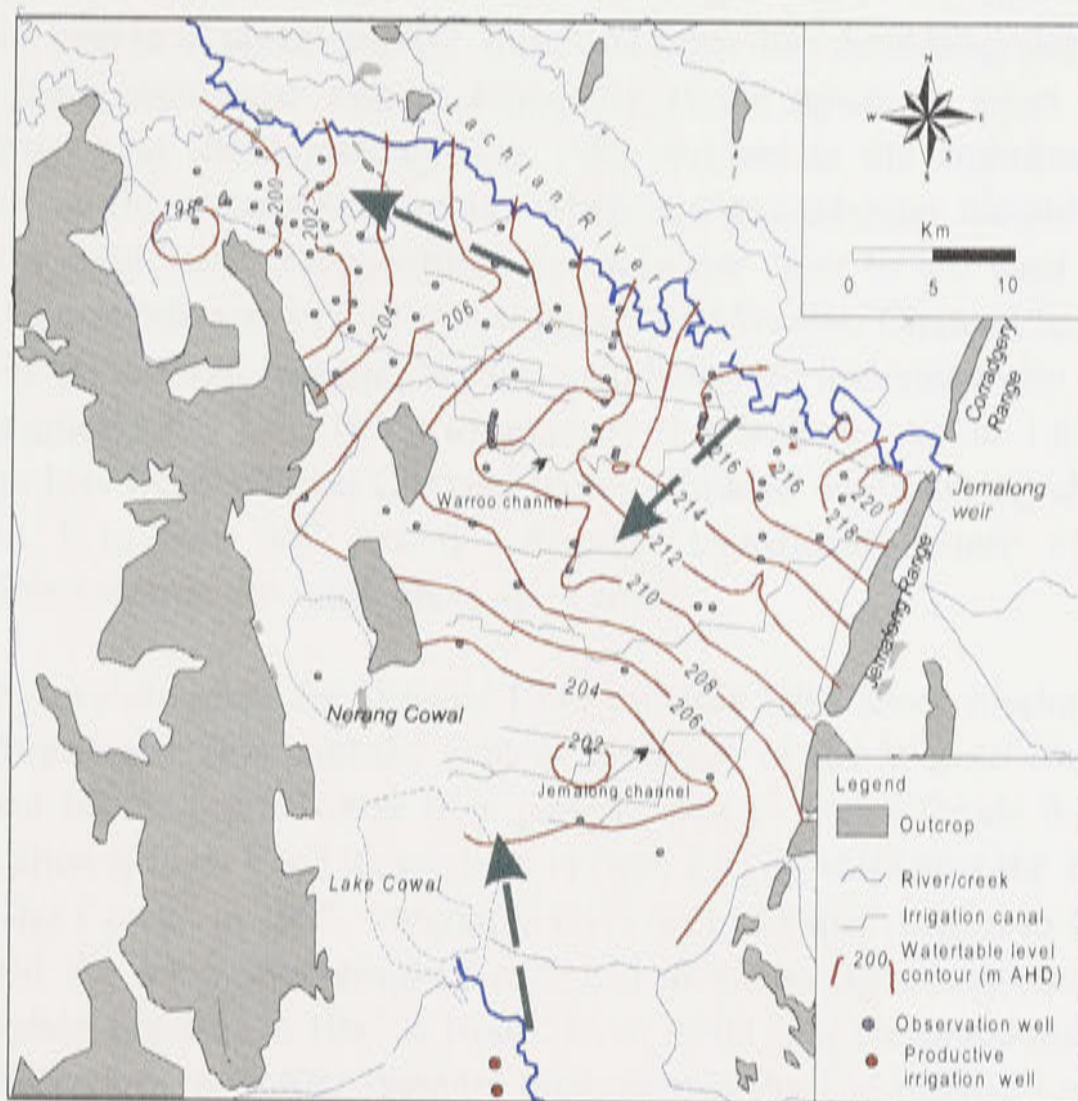


Figure 5.9: Watertable elevation map of the JWPID in October 1990.

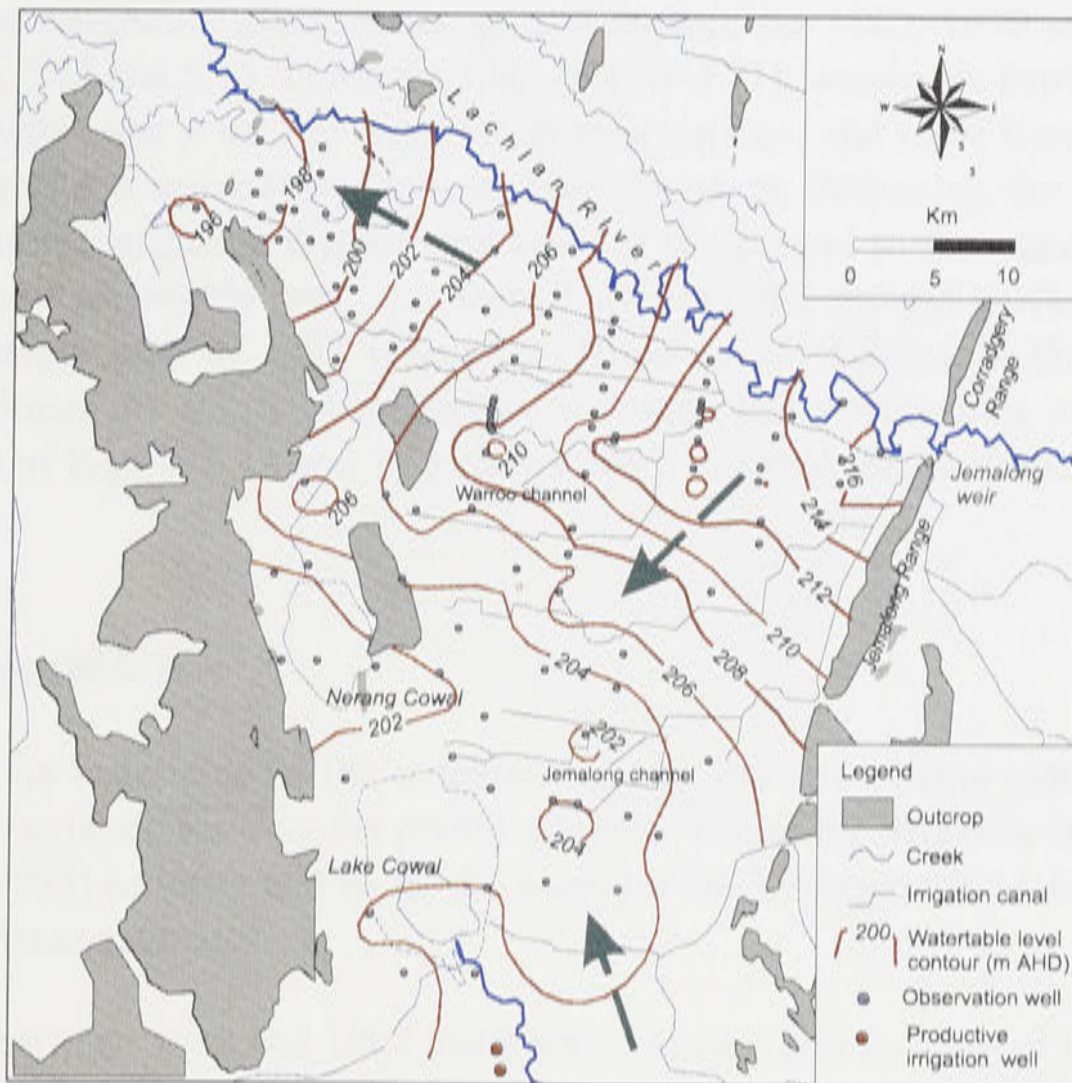


Figure 5.10: Watertable elevation map of the JWPID in July 1997.

system along its course in northwesterly direction from the Jemalong Gap. The Lachlan River is recharging the groundwater system especially at the upstream areas as indicated by the convex contours near the Jemalong Gap. Also evident is the significant influence of the Warroo channel on the watertable contours wherein a groundwater mound has been developed and generated a significant component of groundwater flow to the west and southwest. The behaviour of the groundwater in this area suggests that Warroo Channel has contributed a large amount of recharge through leakage. Separate studies were undertaken by van der Lely (1993) and Kinhill Engineers Pty Ltd (1995) to quantify this leakage. About 1,600 to 3,000 ML per year of seepage loss from Warroo Channel were estimated with varying channel seepage rates from less than 1 to over 300 mm d⁻¹. Another significant feature of Figure 5.8 is the groundwater flow towards the south and Lake Cowl.

The watertable elevation maps for October 1990 and July 1997 show similar features such as the direction of groundwater flow and the evident influence of the Warroo Channel and the Bland Creek catchment on the groundwater flow pattern. Due to major floods that occurred in 1990, watertable elevation is higher and its gradient is from 220 m AHD near the Jemalong Gap to 202 m AHD near Lake Cowl. In 1997, watertable level declined with respect to 1990 level. However, near Lake Cowl, the watertable remained high and shows no significant decline since 1990. The watertable elevation gradient in 1997 is from 216 m AHD near the Jemalong Gap to 204 m near Lake Cowl. According to Coffey Partners International Pty Ltd (1996), Lake Cowl has a bed level of approximately 204 m AHD, this means that Lake Cowl bed and watertable elevation were the same in 1997.

5.3.4. Watertable depth below ground surface

Maps of the watertable depth below ground surface for 1969, 1990 and 1997 are shown in Figure 5.11, 5.12 and 5.13. In March 1969 (Figure 5.11), watertable depth in the vicinity of the Warroo channel was 2 to 4 m from the ground surface, and more than half of the irrigation district area had a watertable depth of less than 6 m. Following the major flood in 1990, watertable in the irrigation district rose close to the ground surface, and in almost half of the irrigation area watertable was less than 2 m from the ground surface (Figure 5.12). The watertable depth map of 1997 (Figure 5.13) shows an increase in the depth to watertable. However, almost the whole of the irrigation district had a watertable of less than 6 m deep. Comparison of Figures 5.11 and 5.13 shows that watertable was shallower in 1997 compared to 1969.

5.3.5. Watertable rise

In general, the watertable in the irrigation district has been rising since 1944. Kelly (1988) estimated watertable rise over the period of 1944-1968 in the irrigation district to be 4 m while Williams' (1993) estimate is 6 m for the same period. Unfortunately data were not available to us to verify these estimates.

The period between 1968 and 1997 had a series of rises and declines of the groundwater levels evidently due to floods and droughts that occurred in the study area. In general, watertable rose between March 1969 and October 1990 (Appendix E and Figure 5.14), while it declined between October 1990 and July 1997 (Figure 5.15). The average rise of watertable between March 1969 and October 1990 is about 2.6 m. A rise of over 3 m occurred during this period in the vicinity of Lake Cowal and Lake Nerang Cowal. On the other hand, the average decline between October 1990 and July 1997 is about 2.0 m. An important feature of this decline is that areas near the Lachlan River have the highest decline and reduces progressively towards the south near Lake Cowal. This shows that the shallow groundwater near Lake Cowal has been trapped and the watertable continues to rise even during non-flood periods. On the average, watertable in the irrigation district has risen by 0.8 m between March 1969 and July 1997 with larger rises in the areas near Lake Cowal and Lake Nerang Cowal (Figure 5.16). The rise of watertable around the lakes has also a significant effect on land salinisation which will be discussed in the next section.

5.3.6. Recharge-discharge area

According to Anderson *et al.* (1993), in the past, groundwater from the Bland Creek had a natural gradient towards the Lachlan River but it appears that the direction of the groundwater flow has changed and now the Bland Creek sub-catchment has a much lower contribution to the groundwater system of the JWPID. Our analysis here indicates that this concept is not correct. We believe that the groundwater flow regime in the Irrigation District has always been the result of two conflicting flow systems from the Lachlan River and Bland Creek catchments towards the Lake Cowal area with the dominant flow from the Lachlan River. Recharge areas are located close to the Jemalong Gap and in the northern part of the Bland Creek (south of Lake Cowal), while the discharge area consists of Lake Cowal, Lake Nerang Cowal and Bogandillon Creek, all on the western side of the District. Fine sediments (Figure 4.6), groundwater flow directions (Figure 5.8, 5.9 and 5.10) and high level of groundwater salinity (Figure 6.1 in the following chapter) confirm this concept. However, it should be noted that the

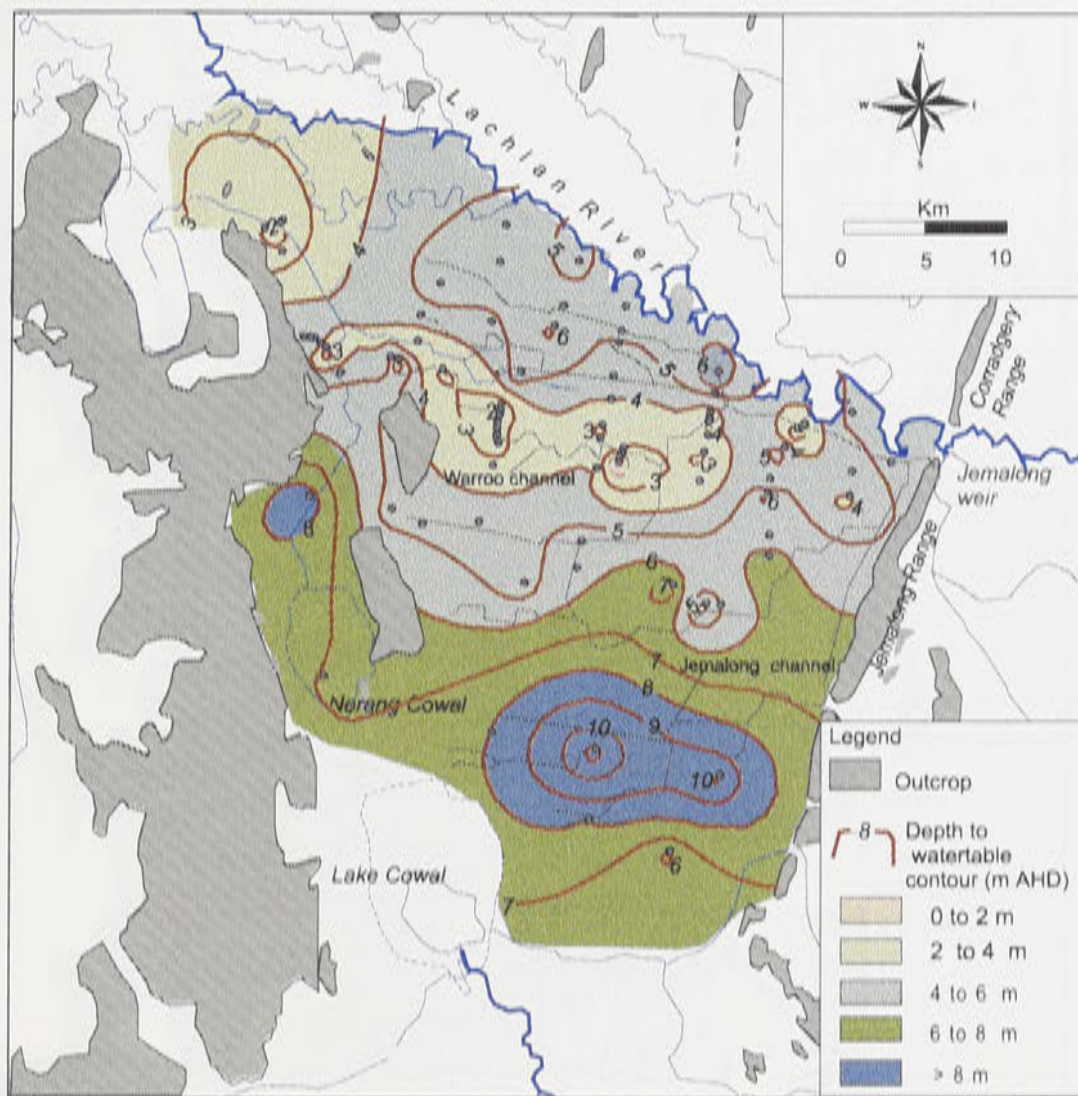


Figure 5.11: Map of watertable depth below ground surface of the JWPID in March 1969.

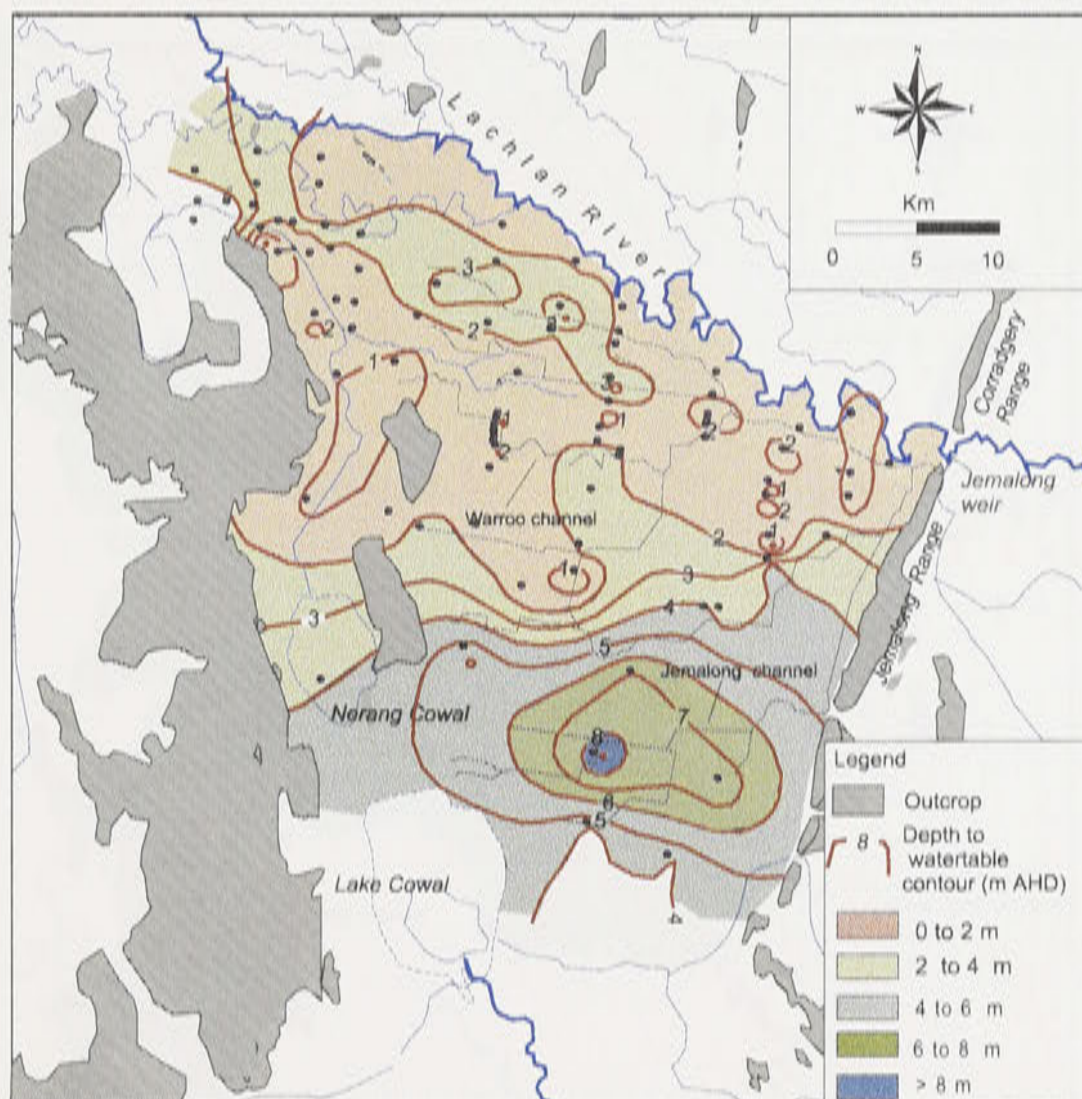


Figure 5.12: Map of watertable depth below ground surface of the JWPID in October 1990.

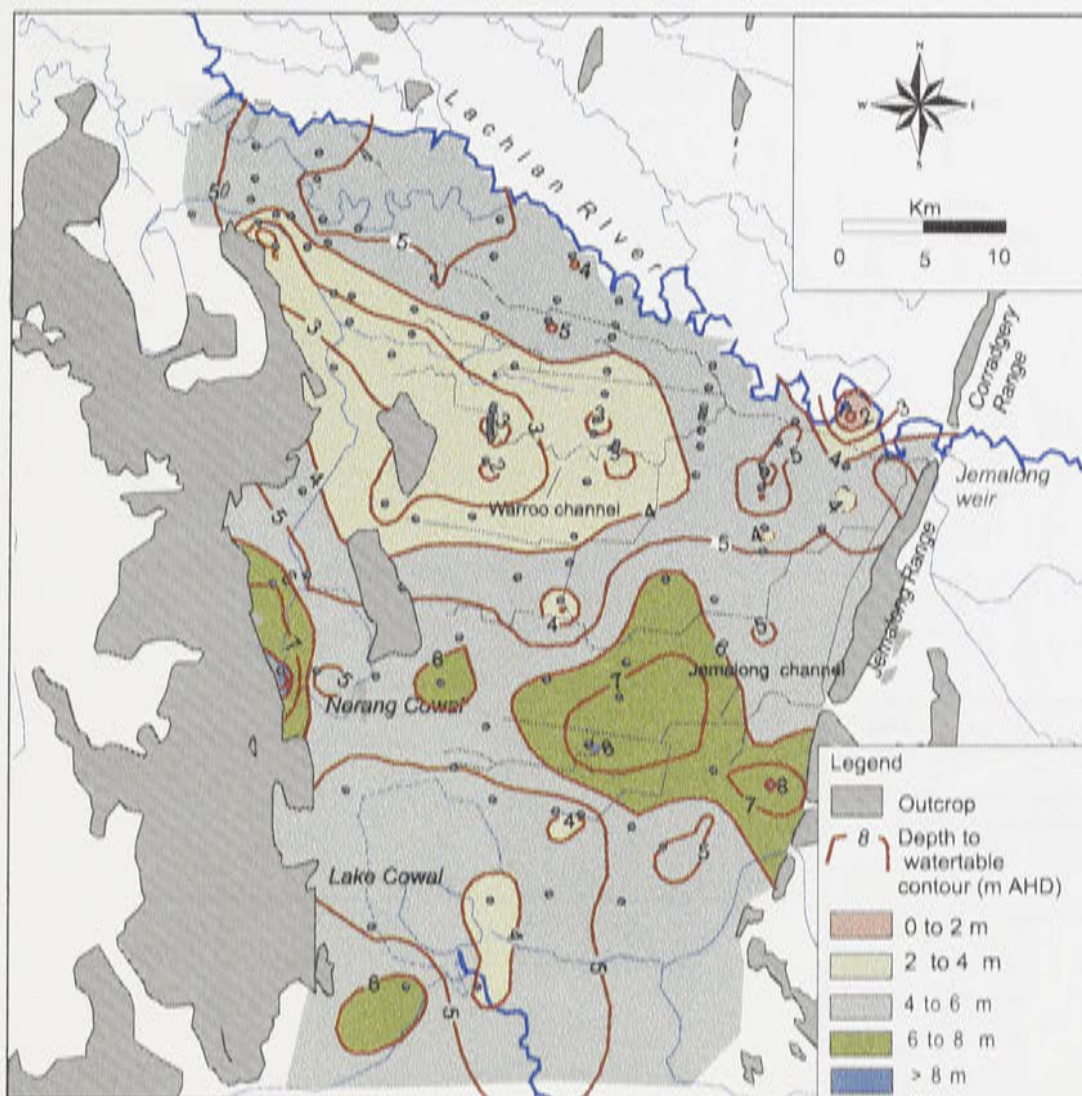


Figure 5.13: Map of watertable depth below ground surface of the JWPID in July 1997.

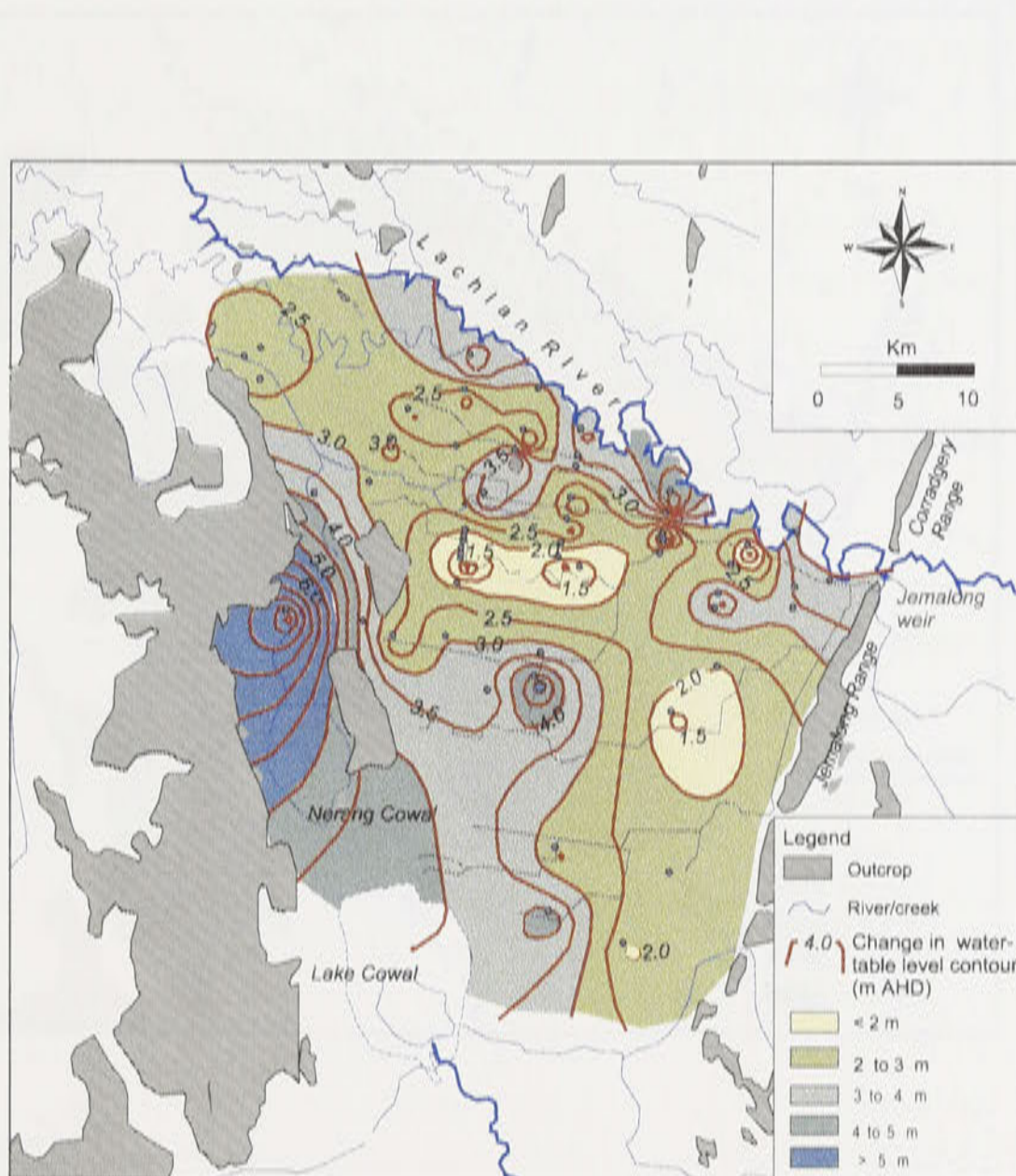


Figure 5.14: Changes in watertable levels between March 1969 and October 1990.

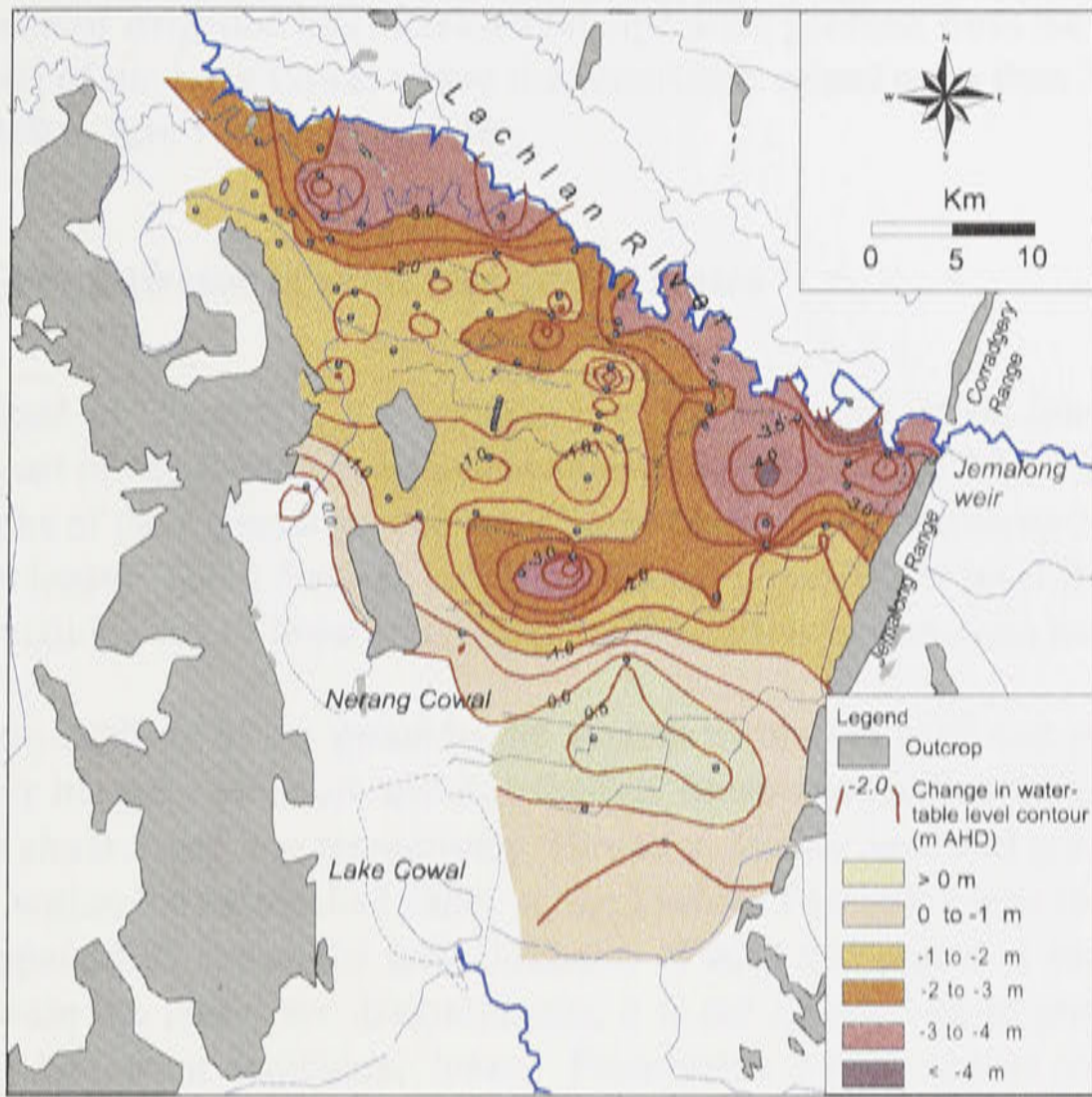


Figure 5.15: Changes in watertable levels between October 1990 and July 1997.

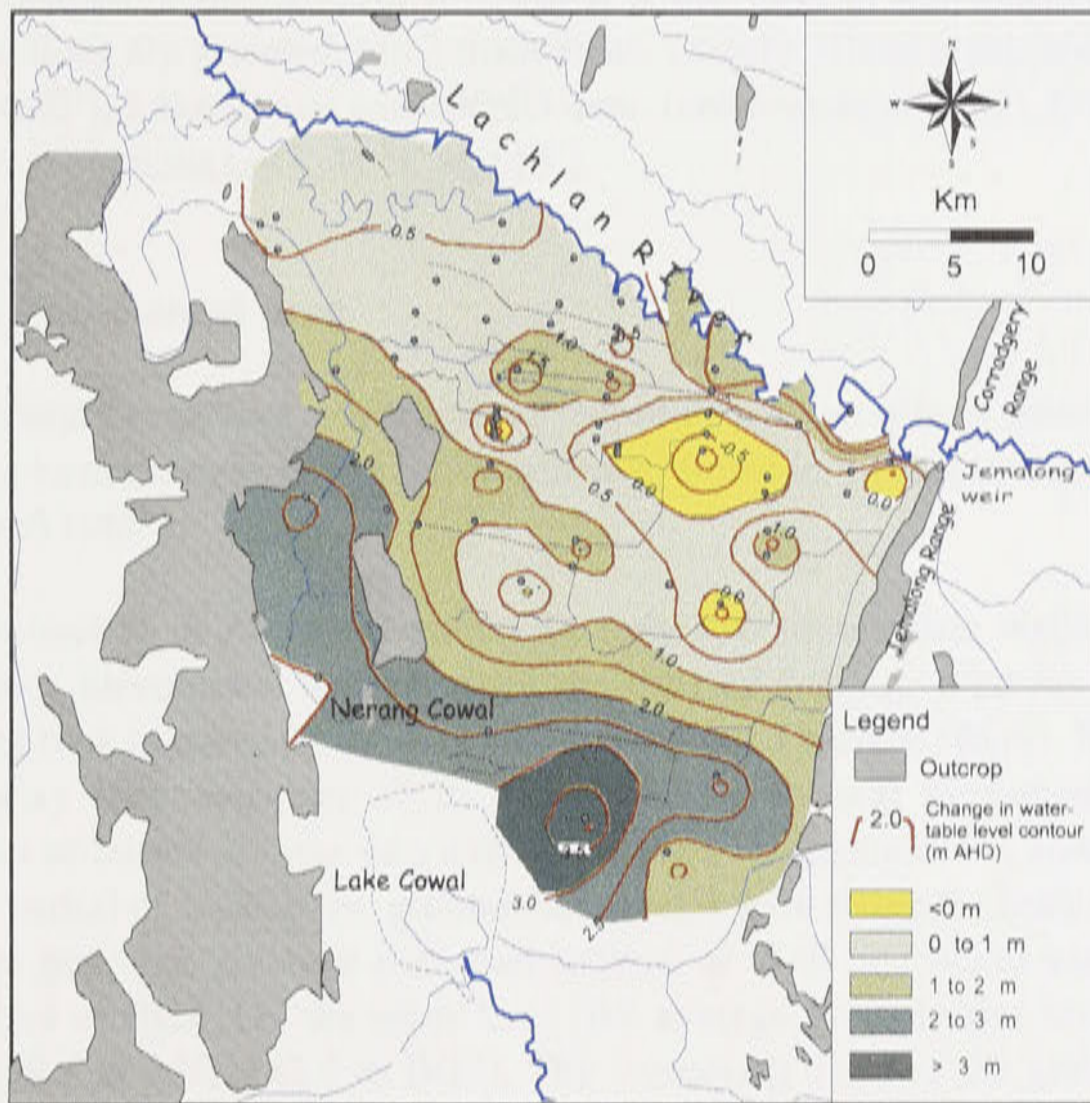


Figure 5.16: Changes in watertable levels between March 1969 and July 1997.

development of irrigation has increased the hydraulic gradient from the Gap towards the north-eastern side of the Lake Cowal where the watertable raised more than 3.5 m over the period of March 1969 to July 1997 (Figure 5.16).

5.4. Groundwater in sand and gravel lenses

As described in Chapter 4, the frequency of the sand and gravel lenses increases from the southern part of the Bland Creek subcatchment towards the Lachlan River. The analysis of the hydrographs of the regional groundwater bores (Appendix F) illustrated the features of the sand and gravel lenses. These features include: seasonal groundwater level fluctuations; groundwater level fluctuations due to flood and drought; and relationship between lenses.

Piezometric analysis of the groundwater system within the sand and gravel lenses is complex due to their irregular structure and distribution. Mean and median thickness of sand and gravel lenses are about 5 and 3 m respectively. However, thicker sand and gravel lenses of 10 to 50 m are found within the entrenched valley of the Lachlan Formation near the Lachlan River (Figure 5.17). Appendix G shows the total thickness of sand and gravel at various bores in the study area. Because the lenses are discontinuous, it is not appropriate to prepare a piezometric map using the data from individual lenses. Piezometric heads appear to be influenced by the thickness of the individual lenses, proximity to the recharge and discharge zones and the thickness of the clay layers that separate the lenses. To better describe the characteristics of the lenses in the study area, piezometric data of the selected regional observation wells found in the nine geological cross-sections in Chapter 4 are used in the succeeding sections. These nine cross-sections are grouped into 3 main areas, namely: Bland creek area (cross-sections A-A', B-B' and C-C'); Lake Cowal and JWPID area (cross-sections D-D', E-E' and F-F'); and Lachlan area (cross-sections G-G', H-H' and I-I').

5.4.1. Bland creek area

In the Bland Creek area, the length of record of hydrographs is generally insufficient to show any long term changes in groundwater levels. Bores in the Bland Creek area were only installed in the mid 1980's.

At cross-section A-A' (see Figure 4.3), only two observation wells (36630 and 36632) have continuous piezometric records since the time of drilling. Well no. 36630 is screened at the fractured rock between 86 to 89 m below the ground surface (BGS). Well no. 36632 is screened at the clay layer between 87 to 91 m BGS. Historical piezometric level fluctuations and thickness of lenses of these two wells are shown in Appendix F.1 and Appendix D respectively. For the period of 1986-1996, groundwater levels were rising for both wells at a rate of about 3.5 to 4 mm per year. Average piezometric level at Well no. 36630 was about 204.2 m AHD or about 26.4 m BGS. On the other hand, the average groundwater level at Well no. 36632 was about 199.3 m AHD (42.6 m BGS). The increasing trend of the groundwater levels indicate a potential gradient of groundwater in the fractured rock system to move upward in this part of the study area. Further south of cross-section A-A', four observation wells (36735, 36737, 36738, and 36739) are installed to monitor the piezometer heads of the upstream area of the Bland Creek. Hydrographs of these wells are also shown in Appendix F.1. Piezometric heads within Bore 36735 are measured at clay (26-32 m BGS) and sandstone (41-46 m BGS) layers. At this site, piezometric head within the fractured rock rose steadily from 1987 to 1997, with a net upward increase of about 0.15 m per year. On the contrary, piezometric head at the upper

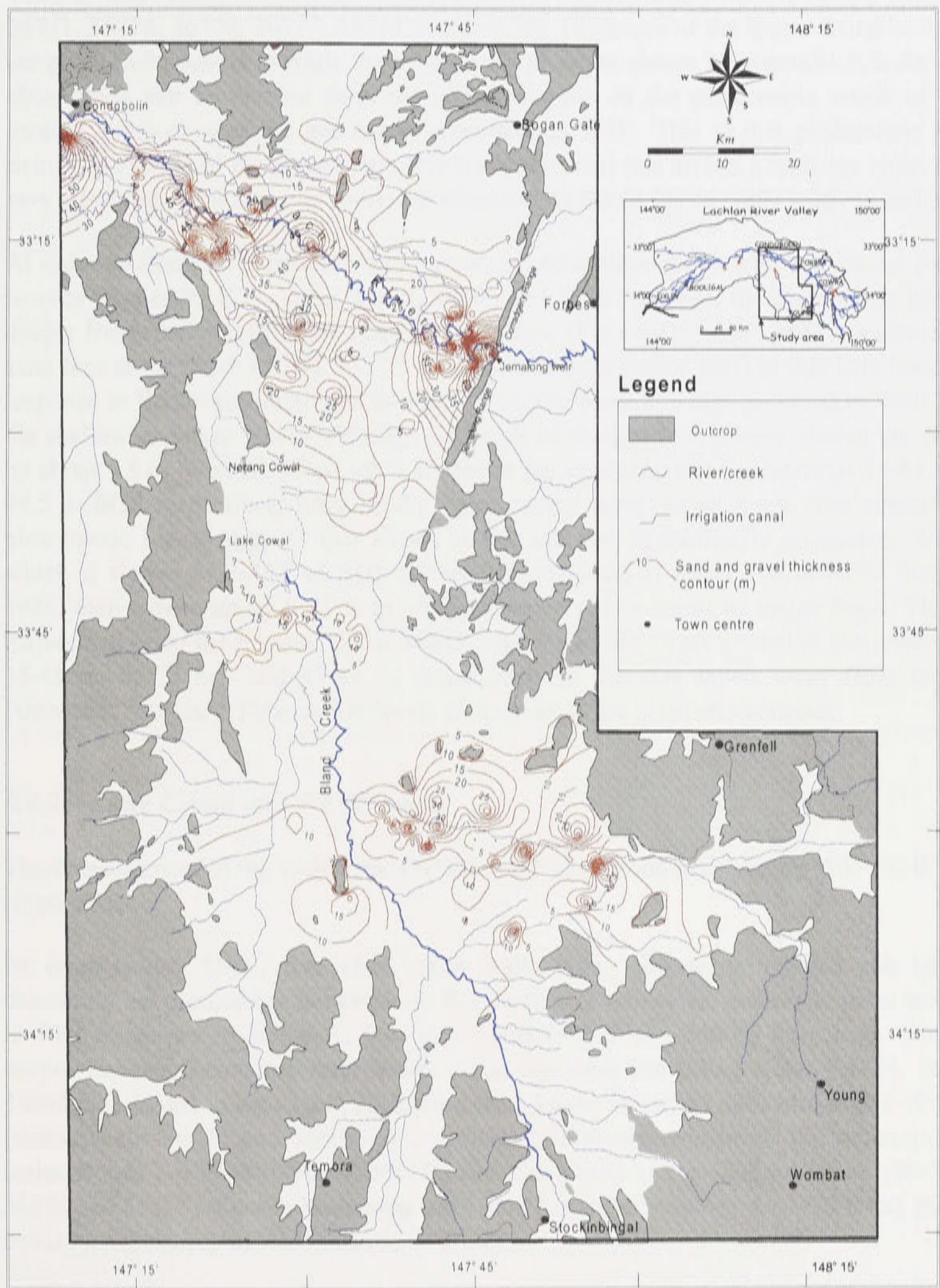


Figure 5.17: Total thickness of sand and gravel in the study area.

clay layer decreased by about 0.12 m per year. In Bore 36737, piezometric head at the gravel lens (46-51 m BGS) is also decreasing. The other two remaining bores (36739 and 36738) show constant piezometric heads.

At cross-section B-B', there are only three observation wells (36603, 36606, 36628) with piezometric level records. However, in the vicinity of this geological cross-section, there are other 15 observation wells (30270, 30291, 30328, 30331, 36604, 36605, 36627, 36628, 36629, 36741, 36776, 36778, 36777, 36779, and 39379). Thickness of the lenses found in these wells are given in Appendix D while the piezometric plots are shown in Appendix F.2. An important observation can be derived from the historical plots of the piezometric levels of the wells located along or near the geological cross-section B-B'. This is that piezometric levels are rising. The rising of the piezometric levels suggests that this area is a recharge zone. In fact, of very steep rise of piezometric levels are observed in Bores 36776, 36777, 36778 and 36779.

At cross-section C-C', there are seven regional observation wells with continuous piezometric records (Appendix F.3). Wells 36611, 36596 and 36597 measure the piezometric heads of the deeper lenses belonging to the Lachlan Formation (Figure 4.5). Bore 36611 is screened in the sand lens at the depth of 106.5-112.5 m BGS. The piezometric level in this lens fluctuates as a response to floodwater input and drought. A similar pattern is also observed in Well 36596 for the shallow and deep lenses, although the heads of shallow lens always exceed the deeper lens by about 1.5 m. Well 36597 which is slotted in the sand lenses at the intervals 78-84 m and 95-98.5 m BGS respectively have similar piezometric heads at all times. The similarity of the piezometric heads suggests that lenses at this site are hydraulically connected. Well 36595 which is slotted 84.7-86.5 m BGS shows a steady head of about 199 m AHD from 1985 to 1989, then it rose up by 0.75 m in 1990, apparently as a result of major flood. This level is maintained up to the present. Wells 36613, 36700 and 36825 are slotted at shallower depths of 35-45 m, 65-75 m, and 43-49 m, respectively in the clay layers away from the Lachlan Formation boundary. Piezometric levels at these wells are relatively constant.

5.4.2. Lake Cowal and JWPID area

The cross-sections lying within the JWPID and Lake Cowal sections are D-D', E-E' and F-F' (Figure 4.2).

At cross-section D-D', five observation wells with piezometric records can be used in describing the piezometric behaviour at this section. Piezometric records in these wells started in 1985 as shown in Appendix F.4. Two wells (36553 and 36609) have been slotted at the deeper Lachlan Formation sand lenses while the three remaining wells (36524, 36594, and 36563) are slotted in the Cowra Formation sand lenses. Based on the hydrographs of the deeper lenses (Wells 36553 and 36609), it is evident that piezometric heads did not respond to the major floods occurred in the 1990s. Piezometric heads at the shallow lenses (Wells 36525, 36594 and 36523) show an increasing trend, and particularly during the 1990 flood, piezometric heads raised sharply in wells 36524 and 36563.

At all sites along the cross-section E-E' (Appendix F.5), the shallowest lenses tends to show more fluctuations than the deeper ones indicating that they were influenced by the recharge events. The deeper lenses in bores 36528 and 36554 have a piezometric level above the shallow watertable aquifer by up to 2 m. This indicates a net upward pressure in these lenses. The deepest lenses at bores 36552 and 36523 are the only lenses with piezometric levels are at or below the shallow lenses. Water levels at all sites in cross-section E-E' peaked in 1991, in

association with the 1990 flood. Watertable at these sites typically lies at 3-6 m BGS, during non-flood times.

Along the cross-section F-F', both shallow and deeper lenses are influenced by the recharge events particularly from the Lachlan River (Appendix F.6). As previously discussed, the Lachlan River is recharging the groundwater system near the Jemalong Gap. However, it is also obvious that some lenses at this section are hydraulically connected. The slight difference of piezometric head between the shallow and deep lenses (shallow lenses are higher) at this section indicates a slow downward leakage of groundwater from shallow to deeper lenses.

5.4.3. *Lachlan area*

The observation well hydrographs of cross-section G-G' (Appendix F.7) show considerable variation in the relationship between the deep and shallow lenses.

Well 36079, downstream of the Jemalong Weir, has been slotted at five different lenses. The shallowest lens is the most responsive to flooding, and at the peaks in the hydrograph there is a tendency for this watertable aquifer to exceed all others (in general groundwater level at slot $1 > 2 > 3 > 4$, where 1 is the shallowest lens and 4 is the deepest). Following flood event, the recharge pulse dissipates quickly in the shallowest lens, but more slowly in the deeper ones. Thus, in post-flooding times there is a net upward pressure at the site since the piezometric head at Slot $4 > 3 > 2 > 1$. Well 36083 shows a similar pattern with the piezometric head of the deep aquifers equalling the shallowest at peaks, and exceeding the shallowest at other times. Observation wells 36526, 36087 and 36089 display a similar net upward pressure. The greatest difference in head occurs in 36087, in which slotted zones 2 and 3 (with similar piezometric behaviour) have a piezometric level of more than 2 m above the shallow lenses. In Wells 36088, 36550, 36081 and 36080, piezometric heads in the deep lenses are generally lower than in the shallow ones, indicating potential for downward movement of recharging water.

The observation well hydrographs within the cross-section H-H' (Appendix F.8) generally show that intermediate and deep piezometric levels are higher than the water level in the shallow lenses (Wells 25151, 25155 and 25164). This indicates that there is a potential gradient upwards.

Appendix F.9 shows hydrographs of the wells in cross-section I-I'. Except at 25030, the piezometric levels of the moderately deep lenses exceed those of the deeper ones. This indicates the potential for the downward dissipation of shallow groundwater. The hydrographic pattern is similar for all lenses in this section. It is evident that peaks in these hydrographs generally reflect high rainfall years. The wet periods that show the strongest reflection in the observation well hydrographs are those of 1973-74, and 1990-1991. At most sites in this section, the hydrographs show a marked rise with a peak in late 1974. The hydrographs show a gradual drop in levels since 1974, but they do not appear to have completely returned to the 1973 pre-flood levels. Other peaks correspond to above average rainfall in 1969-70, 1983-84 and 1990-91. Hydrographs in this section do show slight rises in the base level over the period of record 1968-1995.

5.5. Hydrodynamic parameters of the aquifer

Pumping test at the shallow (30 m depth) observation wells have been carried out in the JWPID in 1994 at sites A, B, and C (Figure 5.2). The test includes stage pumping to assess well capacity and 7 day pumping of each pumping well. The results of the pumping test indicate that transmissivity values at sites A, B and C range between 60 to 300 $\text{m}^2 \text{d}^{-1}$. Storativity also varies from site to site, ranging from 0.0025 to 0.004. It should be noted that the low values of storativity (which are not representative of a watertable aquifer) are due to the fact that pumping tests were undertaken in the sand lenses. Figure 5.18 shows the hydrodynamic parameters for the sites A, B, and C.

During the 1968 investigation undertaken by the Water Resources Commission of NSW (currently Department of Land and Water Conservation), a number of wells were pump tested to determine their transmissivity and yields. Figure 5.3 shows the observation wells that were pump tested. The estimated transmissivity values (Table 5.1) ranged from 113 to 780 $\text{m}^2 \text{d}^{-1}$ for the Cowra Formation and 587 to 1160 $\text{m}^2 \text{d}^{-1}$ for the Lachlan Formation, respectively. However, specific problems associated with the pumping test procedure during those times should be carefully considered. As mentioned by Williamson (1986), the smaller diameter of the test bore (usually 203 mm) introduced a 'well-loss' component to the drawdown level during pumping. In addition, the interval tested was usually only part of an aquifer or one of a number of lenses encountered in the well, reducing the possible true assessment of the potential of the well.

At Lake Cowal, pump test was conducted at sites on the western margin of the lake to determine the hydrodynamic parameters of the tested intervals within the alluvial deposits and fractured rocks. The result of the test indicated that transmissivity values ranged from 10 $\text{m}^2 \text{d}^{-1}$ to 70 $\text{m}^2 \text{d}^{-1}$. Storage coefficient varied between 0.0012 and 0.00086. Transmissivity values for the fractured volcanic rocks at the mine site ranged from 12 $\text{m}^2 \text{d}^{-1}$ to 65 $\text{m}^2 \text{d}^{-1}$ while storage coefficients ranged from 0.0045 to 0.000056.

The salinity and chemistry of groundwater in the alluvial sequence will now be discussed.

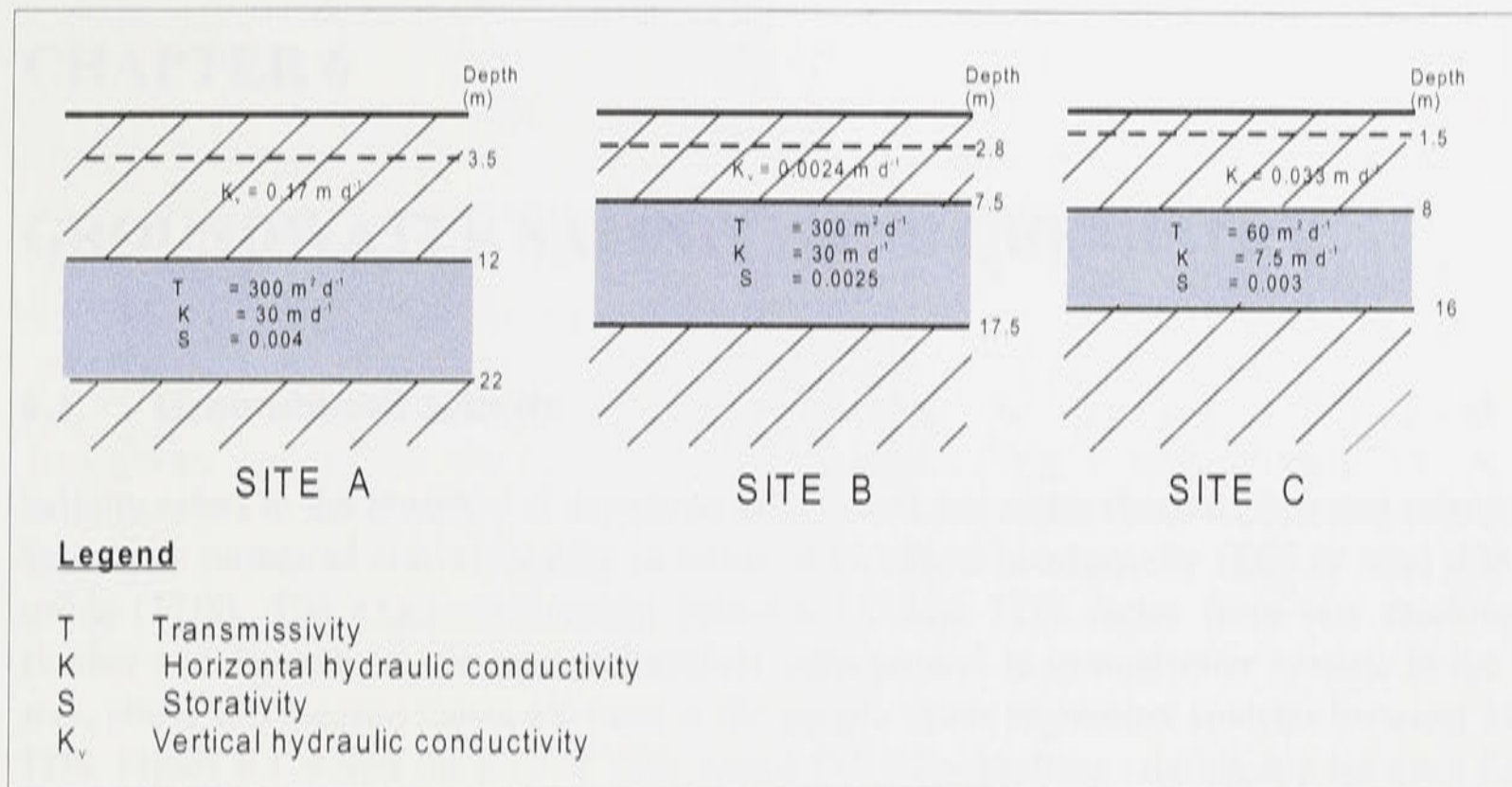


Figure 5.18: Hydrodynamic parameters at sites A, B and C (Figure 5.2) in the JWPID (modified from Coffey Partners International Pty Ltd, 1994).

Table 5.1: Transmissivity values of the selected regional observation wells.

Well number*	Screened zone(m) Interval	Thick-ness	Geological unit	Pump- ing rate (L s ⁻¹)	Transmi- ssivity (m ² d ⁻¹)	Hydraulic conductivity x 10 ⁻³ (m d ⁻¹)
36551	60.47 - 63.76	3.3	Cowra Formation	?	780	236
36523	119.6 - 112.6	3.0	Lachlan Formation	42.75	1160	387
36604	97.8 - 102	4.2	Lachlan Formation	22.2	1150	274
39379	73.9 - 75.6	1.7	Cowra Formation	9.7	113	66
	94.6 - 99.8	5.2	Lachlan Formation	28.5	652.6	125
36632	87.74 - 91.74	4.0	Lachlan Formation	24.9	587	147

*see Figure 5.3 for locations.

Source: Williams (1988).

CHAPTER 6

GROUNDWATER SALINITY AND CHEMISTRY

6.1. Groundwater salinity

Salinity refers to the presence of dissolved salts in soil and water (both surface and subsurface). Salinity is measured conventionally in terms of electrical conductivity (EC) or total dissolved solids (TDS). The exact relationship between EC and TDS varies from one catchment to another and depends on the type of dissolved salts present in groundwater system. In the study area, about 160 measurements are used in the simple linear regression analysis between EC and TDS. Figure 6.1 shows the plot of TDS versus EC. The resulting relationship between EC and TDS for the study is approximated as $TDS (mg L^{-1}) = 0.64 \times EC (\mu S cm^{-1})$. The slope of the linear relationship of EC and TDS within the Murray-Darling Drainage Division is standardised as 0.6 (Mackay *et al.*, 1988).

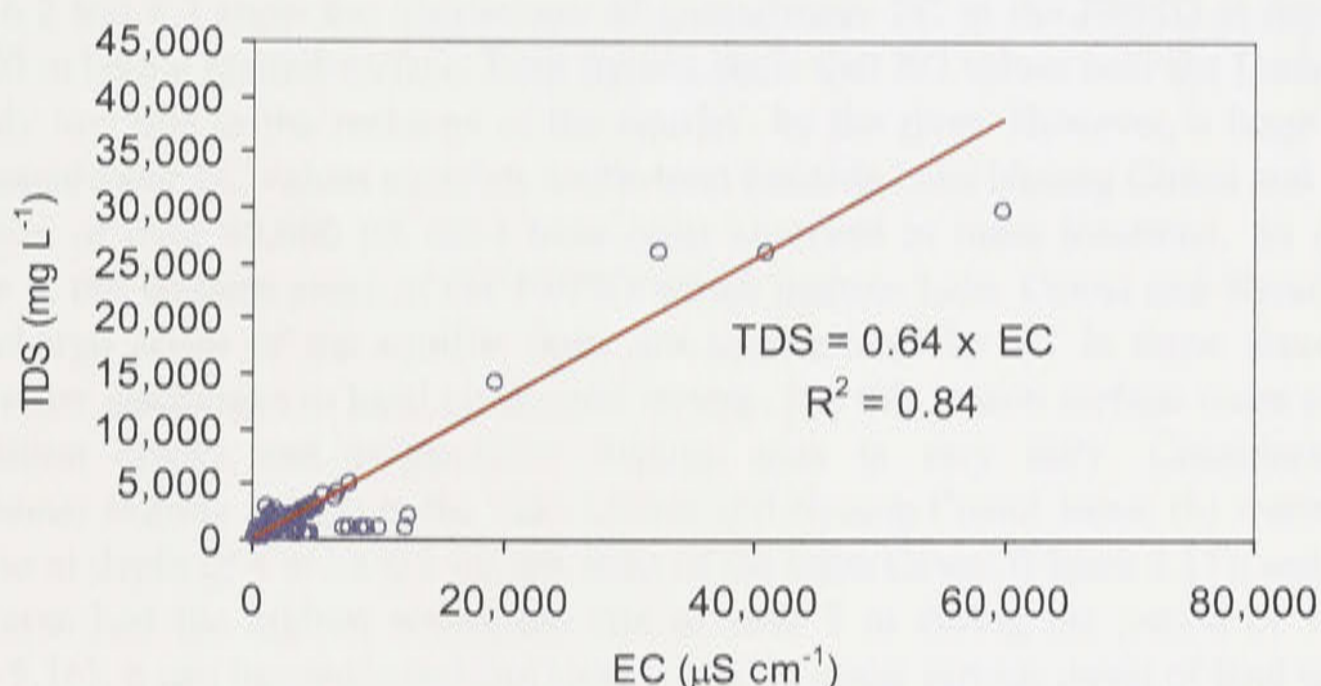


Figure 6.1: Relationship between electrical conductivity (EC) and total dissolved solids (TDS) in the study area (number of measurements = 160).

Traditionally, groundwaters are classified on their TDS content. A TDS range of 0-500 $mg L^{-1}$ is classified as fresh, 500-1,500 $mg L^{-1}$ as marginal, 1,500-5,000 $mg L^{-1}$ as brackish, and greater than 5,000 $mg L^{-1}$ as saline (Department of Primary Industries and Energy, 1985).

Salts originate from the weathering of the earth's primary rock minerals. Lloyd and Heathcote (1985) reported that waters acquire salinity as a result of chemical and biochemical interactions between waters and the material through or over which they flow, and to a lesser extent because of the contribution from the atmosphere. The origin of the salinity can easily be recognised through certain chemical signatures present in the groundwater.

There are various ways in which salt can be introduced into the groundwater system. In Australia, where groundwater salinity is a major problem, salt is derived from a number of

sources such as cyclic (Hingston and Gailitis, 1976; Martin and Harris, 1982; van Dijk, 1969; Blackburn and McLeod, 1983) and connate (O'Reilly, 1994; Lloyd and Heathcote, 1985) salting. Cyclic salting is the term applied to salt input to the ground by atmospheric precipitation. These salts are carried from the ocean and deposited inland. On the other hand, connate salts are salts which have been deposited in shallow marine environment and later mobilised into groundwater systems.

In the study area, groundwater salinity will be discussed under sections 6.1.1, 6.1.2 and 6.1.3 for the watertable aquifer, sand and gravel lenses and the fractured rock aquifers. The available groundwater salinity data are collected in terms of electrical conductivity in $\mu\text{S cm}^{-1}$. However, it should be noted that significant gaps exist in salinity data (both spatially and temporally) and this has complicated the analysis of the available data.

6.1.1. Salinity of the watertable aquifer

About 120 shallow observation wells have EC records since 1968, with additional 19 and 22 observation wells since 1983 and 1994, respectively. Plots of EC values at observation wells installed before 1994 are shown in Appendix H. EC measurements before 1990 are irregular with a 10 year record gap between 1975 to 1985.

Figure 6.2 and 6.3 show the distribution of groundwater EC in the JWPID at depths of 0-8 m and 8-20 m below ground surface. Both figures show that EC values near the Lachlan River are relatively low due to the recharge of the aquifer by the river. However, a large area of very high groundwater EC values stretches south-west towards Lake Nerang Cowl and Lake Cowl. EC values of over 40,000 $\mu\text{S cm}^{-1}$ have been observed in these locations. As mentioned in Chapter 5, the western areas of the JWPID which include Lake Cowl and Nerang Cowl are the discharge zones of the aquifer. Salts are accumulated by ET in these areas, and saline groundwater discharges to local creeks and swamp. For this reason surface water at the Manna-Bogandillon creeks and Bogandillon Swamp area is very salty. Considering that: (a) groundwater salinity is high in the Lake Cowl and Nerang Cowl areas; (b) watertable in July 1997 was at depth of 4 m on the eastern edge of the Lake Cowl (Figure 5.13); and (c) the Lake Cowl area had the highest watertable rise of over 3 m during the period of 1969 to 1997 (Figure 5.16), it can be concluded that Lake Cowl is under serious threat of land salinisation.

Salinity variations around or near Lake Cowl in piezometers 1 to 22 (refer to Figure 5.2 in Chapter 5) from July 1994 to May 1997 are plotted in Figure 6.4 and summarised in Table 6.1. These piezometers were installed in 1994 by the Department of Land Water Conservation (DLWC) to monitor the quarterly groundwater behaviour and salinity levels around the lake. Salinity has also been recorded in nested piezometers screened at the shallower horizon at the proposed Lake Cowl Gold mine (see Figure 5.2). Groundwater salinity results collected between February to December 1994 (Coffey Partners International Pty Ltd, 1995a and 1995b) at the western shore of Lake Cowl are given in Table 6.2. Groundwater salinity variation for the DLWC piezometers is within the range of 3,000 $\mu\text{S cm}^{-1}$ to 55,000 $\mu\text{S cm}^{-1}$.

Salinity plots from July 1994 to May 1997 (Figure 6.4) suggest that most piezometers had a reasonably consistent salinity, though there are some exceptions over this period. Large groundwater salinity increases of 30,470 and 30,500 $\mu\text{S cm}^{-1}$ are recorded at piezometers 12 and 20 respectively (Table 6.1). Both are located on the western side of the Lake Nerang Cowl. Piezometers 15 and 16 show a salinity increase of 25,360 $\mu\text{S cm}^{-1}$ and decrease of 5,600

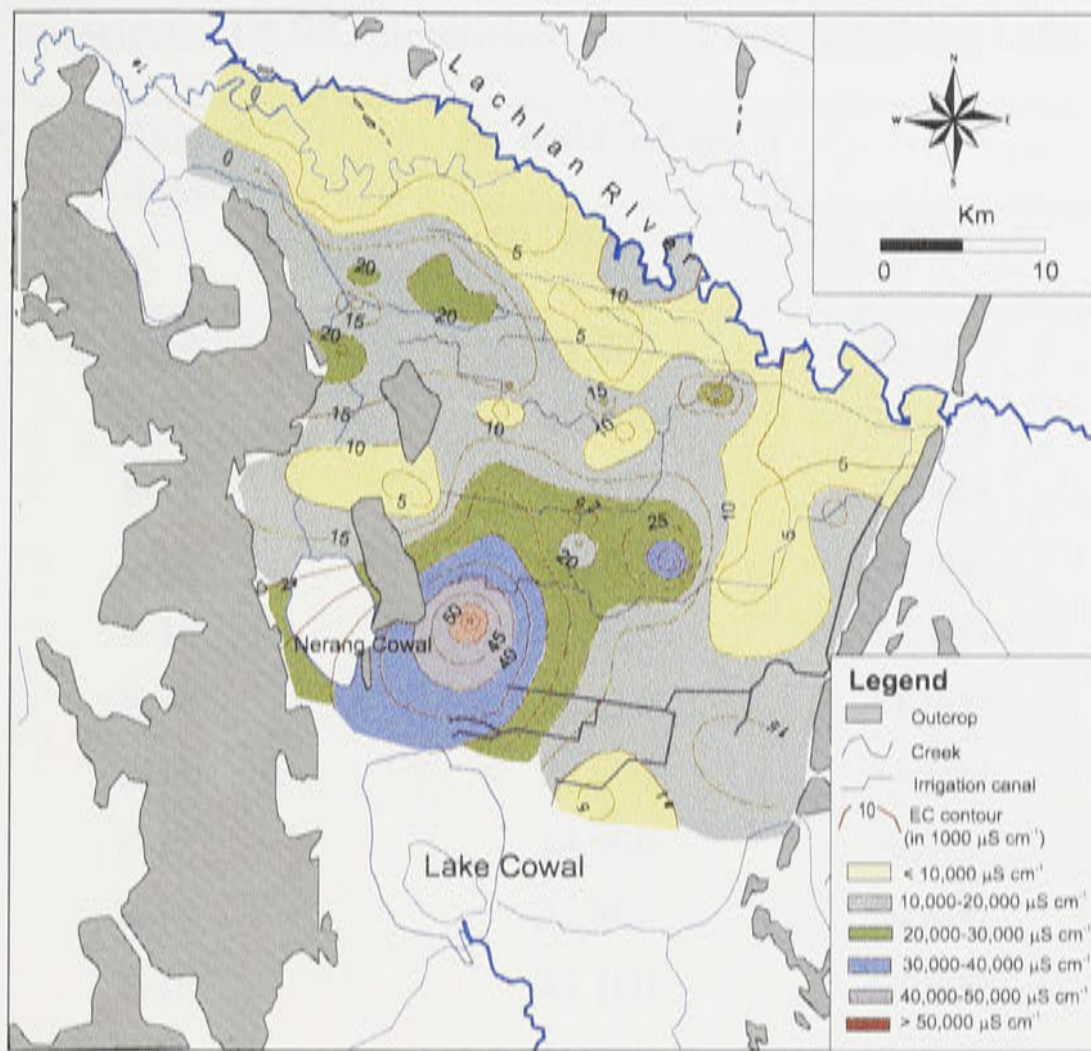


Figure 6.2: Groundwater electrical conductivity (EC) of the JWPID watertable aquifer in February 1997 at the depth of 0-8 m.

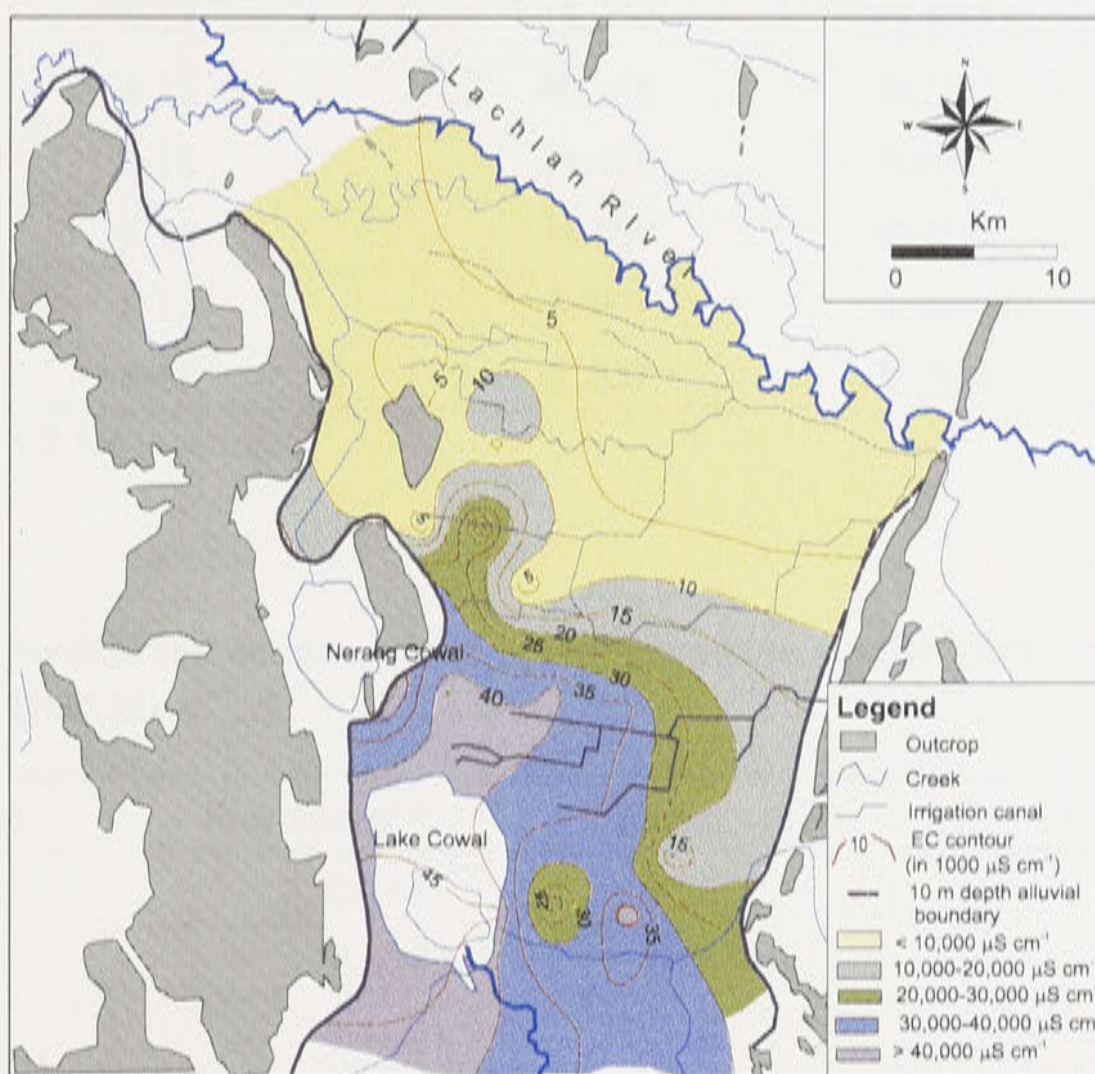


Figure 6.3: Groundwater electrical conductivity (EC) of the JWPID watertable aquifer in February 1997 at the depth of 8-20 m.

Table 6.1: Change of electrical conductivity (EC) values between July 1994 and May 1997 at the selected DLWC piezometers in the Lake Cowal and Lake Nerang Cowal areas.

Piezometer*	Slotted depth (m)	EC level ($\mu\text{S cm}^{-1}$)		Difference
		July 1994	May 1997	
1	8-18	42,500	42,600	100
2	8-18	45,500	43,500	-2,000
3	8-18	47,400	44,800	-2,600
4	8-18	45,500	44,400	-1,100
5	8-18	13,330	17,100	3,770
6	8-18	36,100	41,900	5,800
7	8-18	29,900	18,600	-11,300
8	8-18	34,900	32,800	-2,100
9	8-18	31,800	34,800	3,000
10	8-18	43,100	41,800	-1,300
11	8-18	41,800	40,800	-1,000
12	8-18	14,630	45,100	30,470
13	8-18	15,330	11,300	-4,030
14	8-18	40,000	42,700	2,700
15	8-18	15,970	41,600	25,630
16	8-18	40,100	34,500	-5,600
17	8-18	14,450	9,400	-5,050
18	8-18	34,500	40,800	6,300
19	8-18	3,580	6,000	2,420
20	8-18	8,200	38,700	30,500

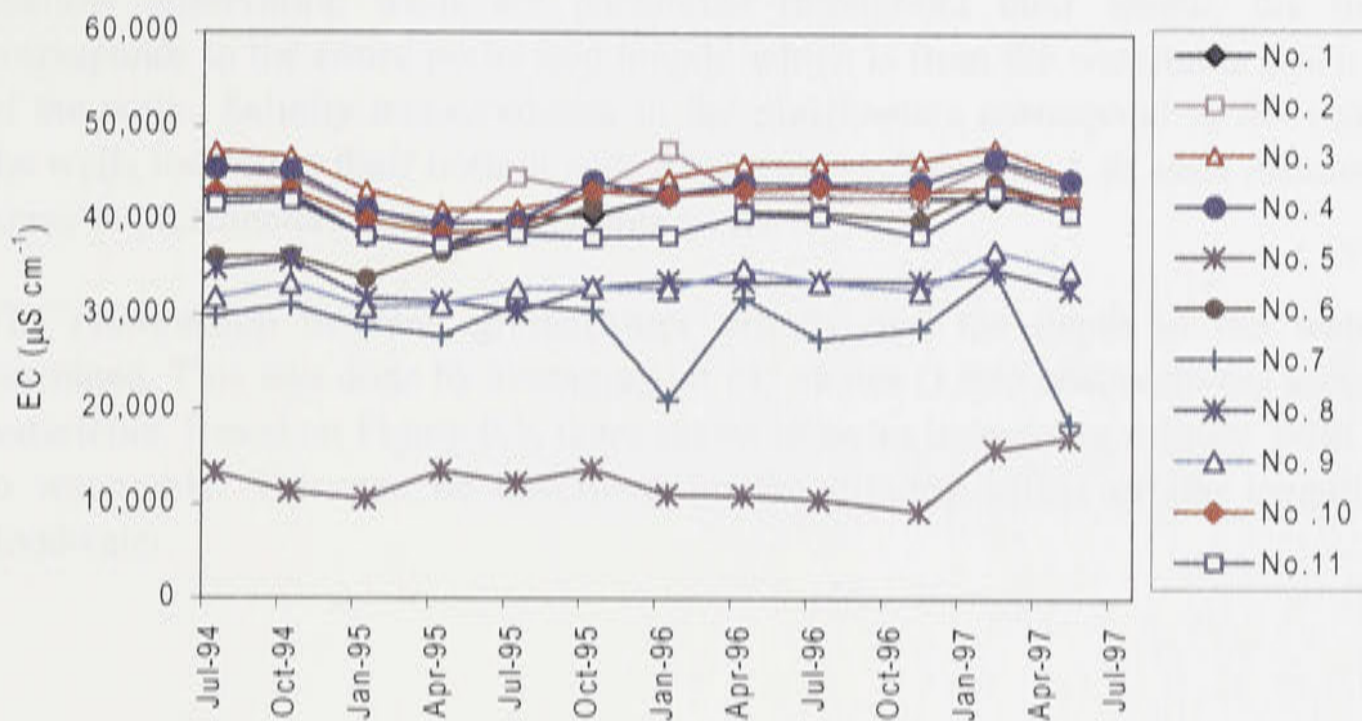
*See Figure 5.2 for locations.

Table 6.2: Groundwater salinity of the upper watertable aquifer at the proposed Lake Cowal Gold Mine.

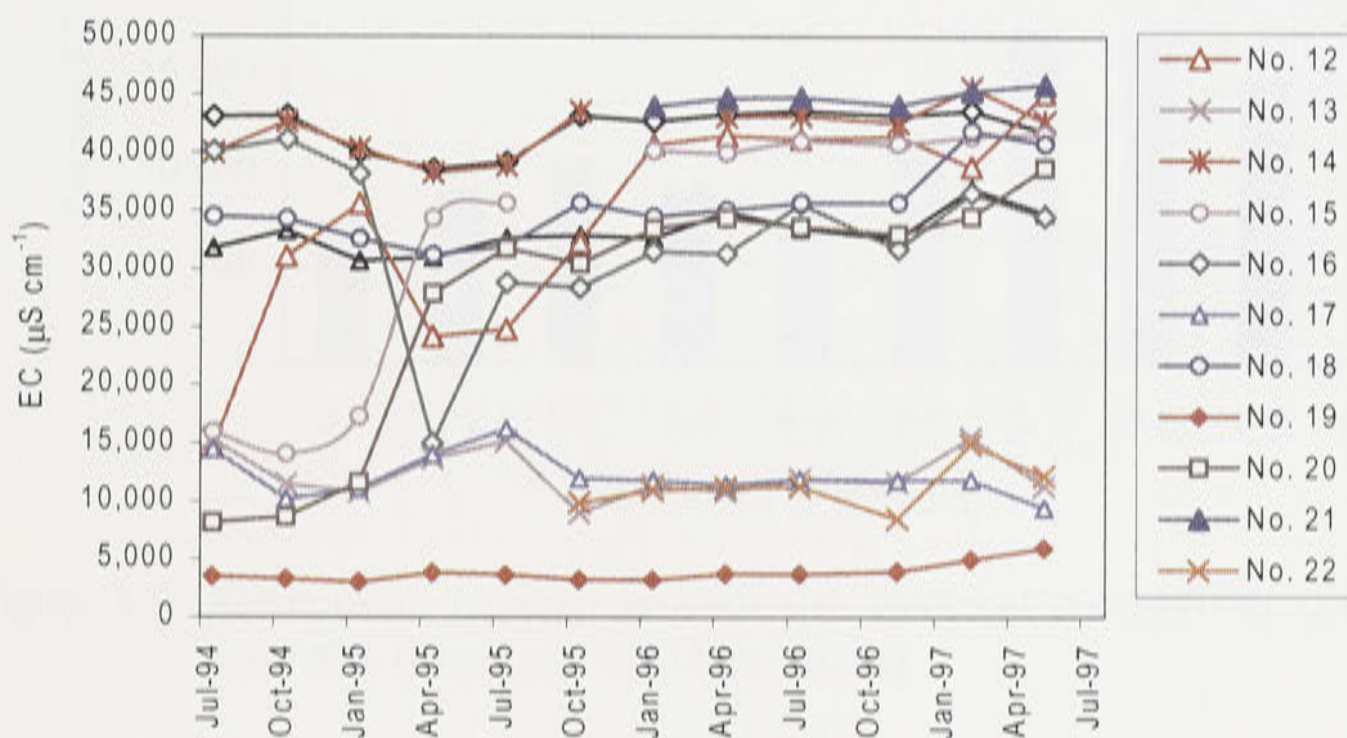
Date sampled	Piezometer *	Depth (m)	EC level ($\mu\text{S cm}^{-1}$)
8-Feb-94	RA341	14-22	63,500
8-Feb-94	RA342	18-25	54,900
9-Dec-94	P415B	10-16	26,600
10-Dec-94	P416B	10-16	41,800
9-Dec-94	P418B	10-16	44,400

Source of data: Coffey Partners International Pty Ltd (1996).

* See Figure 5.2 for locations.



(A) Piezometer number 1 to 11



(B) Piezometer number 12 to 22.

Figure 6.4: Plots of electrical conductivity (EC) measured from piezometers 1 to 22 at the southern part of the JWPID and around lakes Cowal and Nerang Cowal areas from July 1994 to May 1997.

$\mu\text{S cm}^{-1}$ respectively over the period considered. Piezometers around the Lake Cowal periphery (piezometer 1, 2, 3, and 4) have EC values almost consistently above 40,000 $\mu\text{S cm}^{-1}$.

Piezometers located further from the lakes Cowal and Nerang Cowal (piezometer 5, 13, 17, 19, 22) have EC values of 5,000 to 15,000 $\mu\text{S cm}^{-1}$. Groundwater salinity measurements at the western shore of Lake Cowal indicate that salinity in this area has a high degree of variability ranging from 26,600 $\mu\text{S cm}^{-1}$ to 72,000 $\mu\text{S cm}^{-1}$ (Table 6.2).

Appendix I compares the dynamics of the electrical conductivity between the shallow observation wells and relatively deeper piezometers located at the same sites. Since the shallow observation wells are perforated throughout their length, the measured salinity corresponds to the entire perforated length which is from the watertable down to the lower end of the wells. Salinity measurements in the piezometers correspond to the screened portion of the wells located at their bottom end. As shown in Appendix I, at each location, EC values are lower in piezometers than in watertable wells.

The relationship between groundwater salinity and the depth to the watertable are now examined. This was done by averaging all EC values (1,863 observations) according to depth to watertable. Based on Figure 6.5, there seems to be an increase in salinity with increasing depth to watertable. This can be described by the diluting effect of the irrigation, rainfall and floodwater.

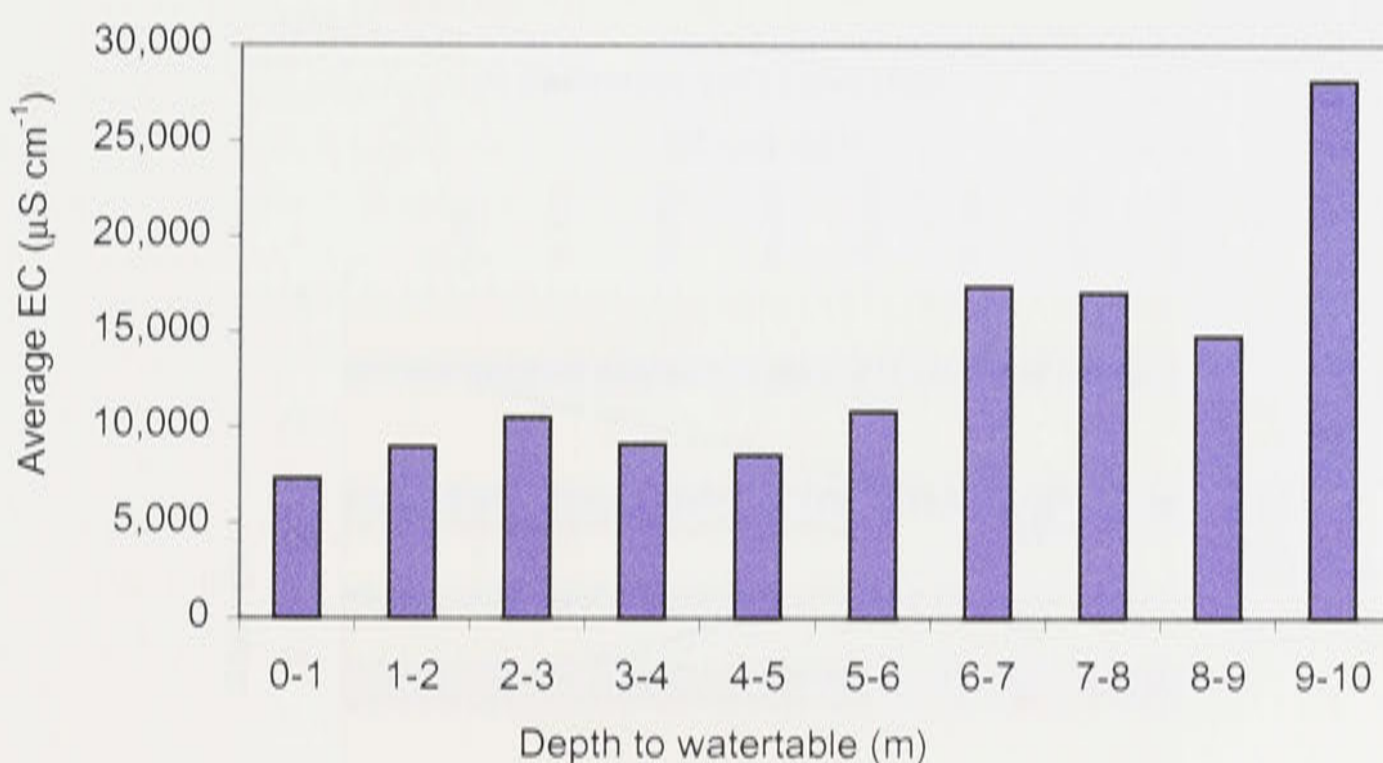
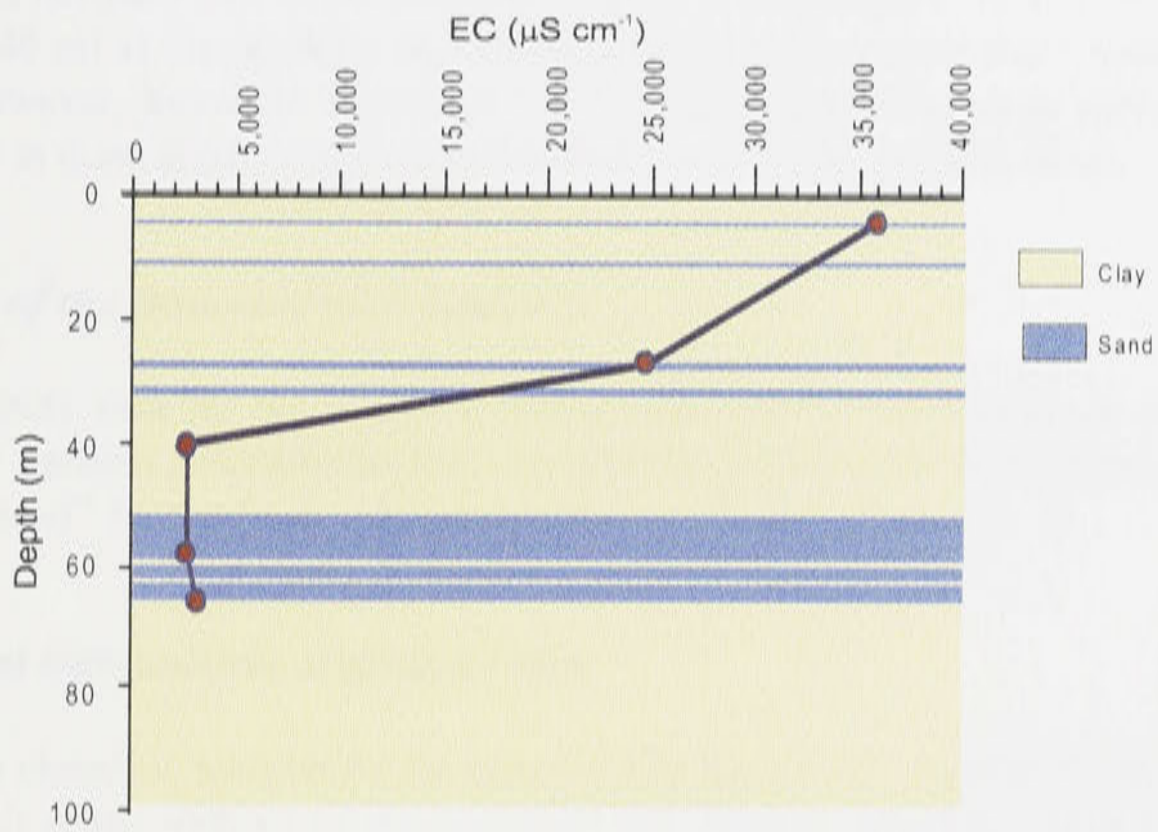


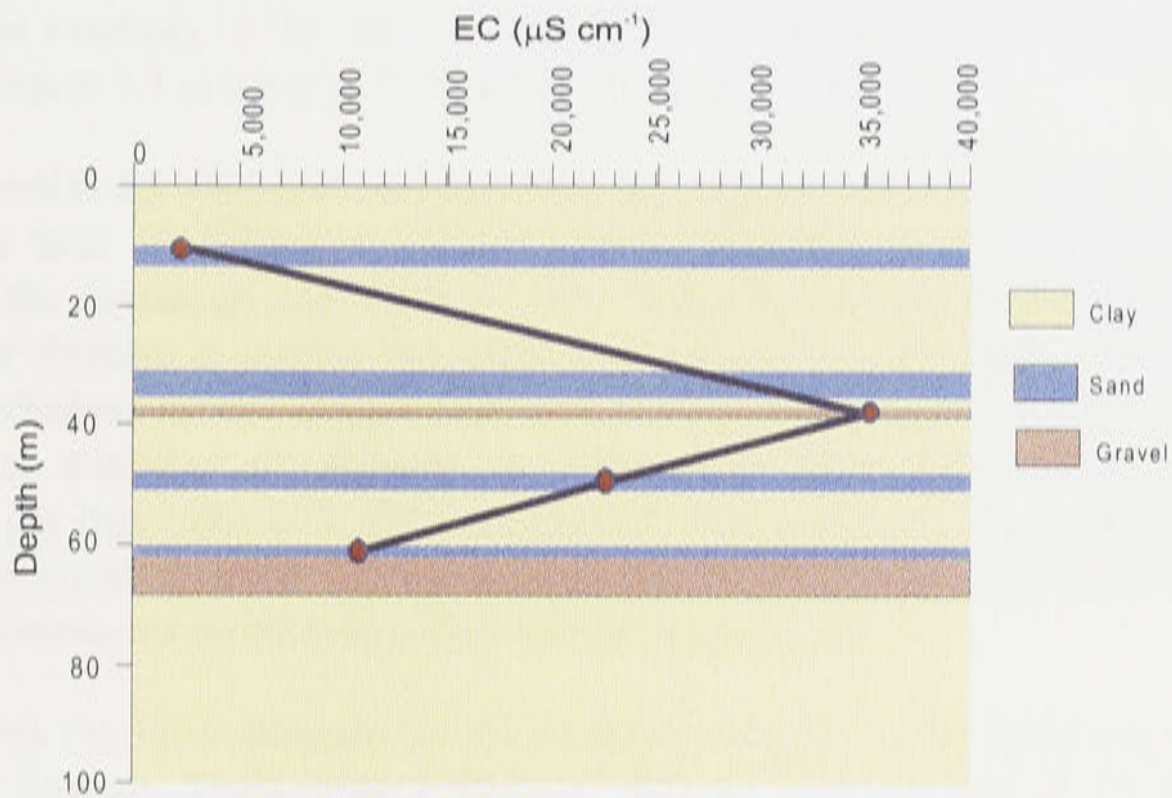
Figure 6.5: Relationship between groundwater electrical conductivity (EC) and depth to watertable (based on 1863 observations).

6.1.2. Salinity of sand and gravel lenses

Electrical conductivity measurements at the regional observation bores were taken mostly during the period of their drilling which commenced in 1968. Plots of EC measured at the regional observation bores are shown in Appendix J. Although historical EC data for these observation wells are very limited, EC values clearly vary with depth. However, the variation is different from one location to another depending on the characteristics of the sand and gravel lenses and the thickness of the clay layers between sand and gravel lenses. Figure 6.6 shows examples of EC variation with depth for observation wells 36551 and 36528 which are both located in the irrigation district and about 5 km apart from each other (see Figure 5.3). At observation well 36551, EC values decreases from $35,000 \mu\text{S cm}^{-1}$ near the surface (at the depth of 4 m) to about $3,160 \mu\text{S cm}^{-1}$ at the deeper lens (67 m below ground surface). This is because of the thicker clay matrix that separates the deeper lenses from the highly saline watertable aquifer. On the other hand, at observation well 36528, the EC value at the shallow watertable



(A) Observation well number 36551.



(B) Observation well number 36528.

Figure 6.6: Variations of EC values with depth in observation well number 36551 and 36528 (see Figure 5.3 for locations).

(at the depth of 10 m below ground surface) is relatively low ($2,270 \mu\text{S cm}^{-1}$), but at the lens located approximately 38 m from the surface EC value is about $35,100 \mu\text{S cm}^{-1}$. Farther down the aquifer system at observation well 36528, EC value decreases to about $10,570 \mu\text{S cm}^{-1}$ at the lens below 60 m from the ground surface.

Using the limited data from all the regional observation wells in the irrigation district, groundwater salinity maps at four depths (40, 60, 80 and 100 m below the ground surface respectively) have been prepared by interpolation and are shown in Figures 6.7, 6.8, 6.9 and 6.10. In general, groundwater found in the deeper lenses have lower EC values compared to the shallower ones. There are larger areas of $\text{EC} < 2,000 \mu\text{S cm}^{-1}$ at 60m, 80m and 100m than at the

40 m depth in the northern half of the irrigation district. Unfortunately, DLWC EC data in the deeper lenses (>40 m) at the southern part of the irrigation district and near Lake Cowal are very limited. However, based on Figures 6.7 to 6.10, it appears that deep groundwater EC values are higher in these areas compared to the areas closer to the Lachlan River.

6.1.3. Salinity of the fractured rock aquifers

Groundwater salinity data for the fractured rock aquifers in the study area are very limited. However, Coffey Partners International Pty Ltd (1995b) reported a salinity range of 50,900 $\mu\text{S cm}^{-1}$ to 63,700 $\mu\text{S cm}^{-1}$ for the fractured rock aquifer beneath Lake Cowal.

6.2. Chemical composition of groundwater

The results of the chemical analysis for the numerous bores (DLWC regional observation wells and private bores) in the vicinity of the Jemalong and Wyldes Irrigation District and Bland Creek area have been analysed and reported by Anderson *et al.* (1993) and Williams (1988) respectively. The summary of the results of the chemical analysis for the regional observation wells shown in Figure 5.3 in Chapter 5 are shown in Appendix K.

Groundwater samples for chemical analyses from the regional observation wells were mostly sampled at the time of drilling at various depths. Anderson *et al.* (1993) classified the groundwater in the Jemalong and Wyldes Plains Irrigation District hydrogeochemically by means of a Piper diagram to display the major ions present in groundwater. Williams (1988) used the same technique for the Bland Creek area. Using this technique, major ions are plotted in the two base triangles of diagram as cation and anion percentages measured in milliequivalents per litre (meq L^{-1}). Total cations and total anions are each considered as 100 per cent. The respective cation and anion locations for an analysis are projected into the rectangle which represents the total ion relationships (Piper, 1944).

Figure 6.11 shows the Piper diagram for all available samples in the Jemalong and Wyldes Plains Irrigation District. There were a total of 410 chemical analysis and because of the number and spread of data points, Anderson *et al.* (1993) simplified the interpretation by dividing the data set into Lachlan Formation groundwater and Cowra Formation groundwater for the regional groundwater wells (Figure 6.12 and 6.13).

6.2.1. Chemical composition of groundwater in the Lachlan Formation

As mentioned by Anderson *et al.* (1993), there is a linear distribution of chemical types along the flow path of the deep Lachlan Formation (Figure 6.12) from Jemalong Gap to the bores of the cross-section H-H' (Figure 4.2). The most distinct change is from a bicarbonate (HCO_3^-) dominance at Jemalong Gap to a chloride (Cl^-) dominance further downstream. This pattern is typical of the change from recharge to discharge waters. Sulphate (SO_4^{2-}) is a minor component of the deep groundwater especially in vicinity of Jemalong Gap. Unlike the anions, there is no change in cation dominance in the deep groundwater, with sodium (Na^+) being dominant throughout. Calcium (Ca^{2+}) and magnesium (Mg^{2+}) are minor component of the groundwater. There is little spatial variation in Ca^{2+} concentration, although it tends to be slightly higher near Jemalong Gap. Magnesium shows a gradual decrease along the flow path from Jemalong Gap to the cross-section H-H'.

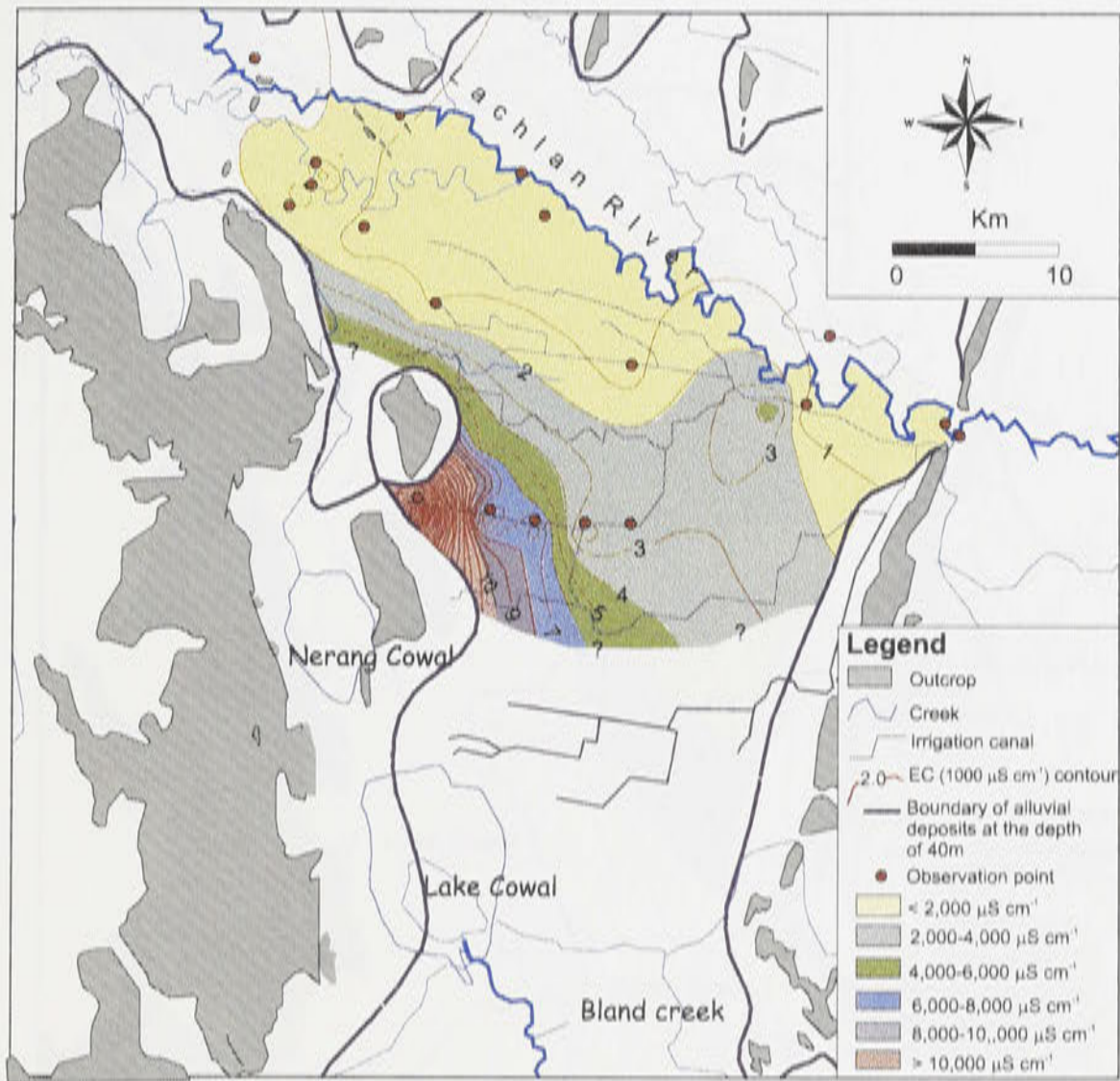


Figure 6.7: Groundwater electrical conductivity (EC) of the JWPID at the depth of 40 m.

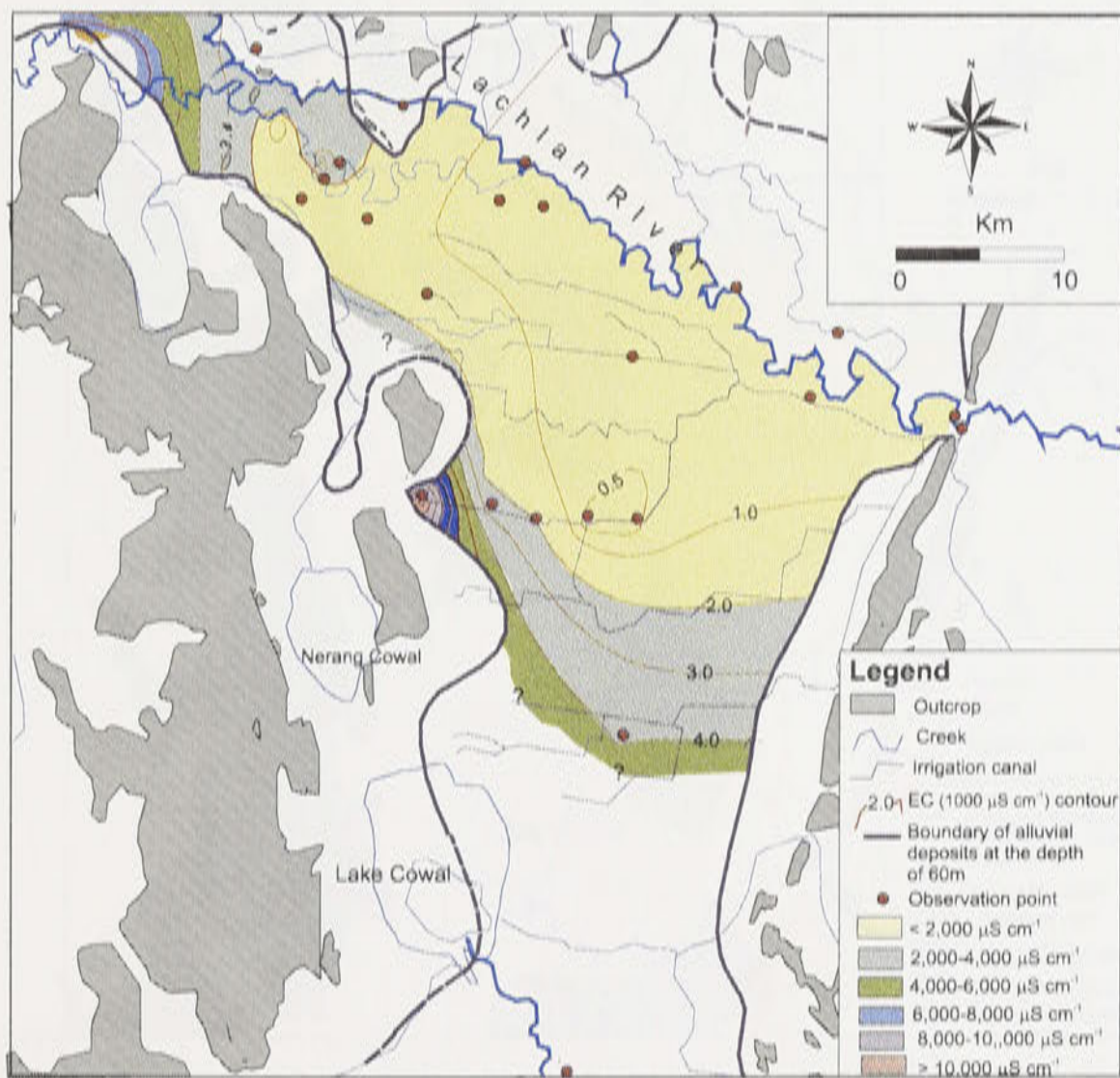


Figure 6.8: : Groundwater electrical conductivity (EC) of the JWPID at the depth of 60 m.

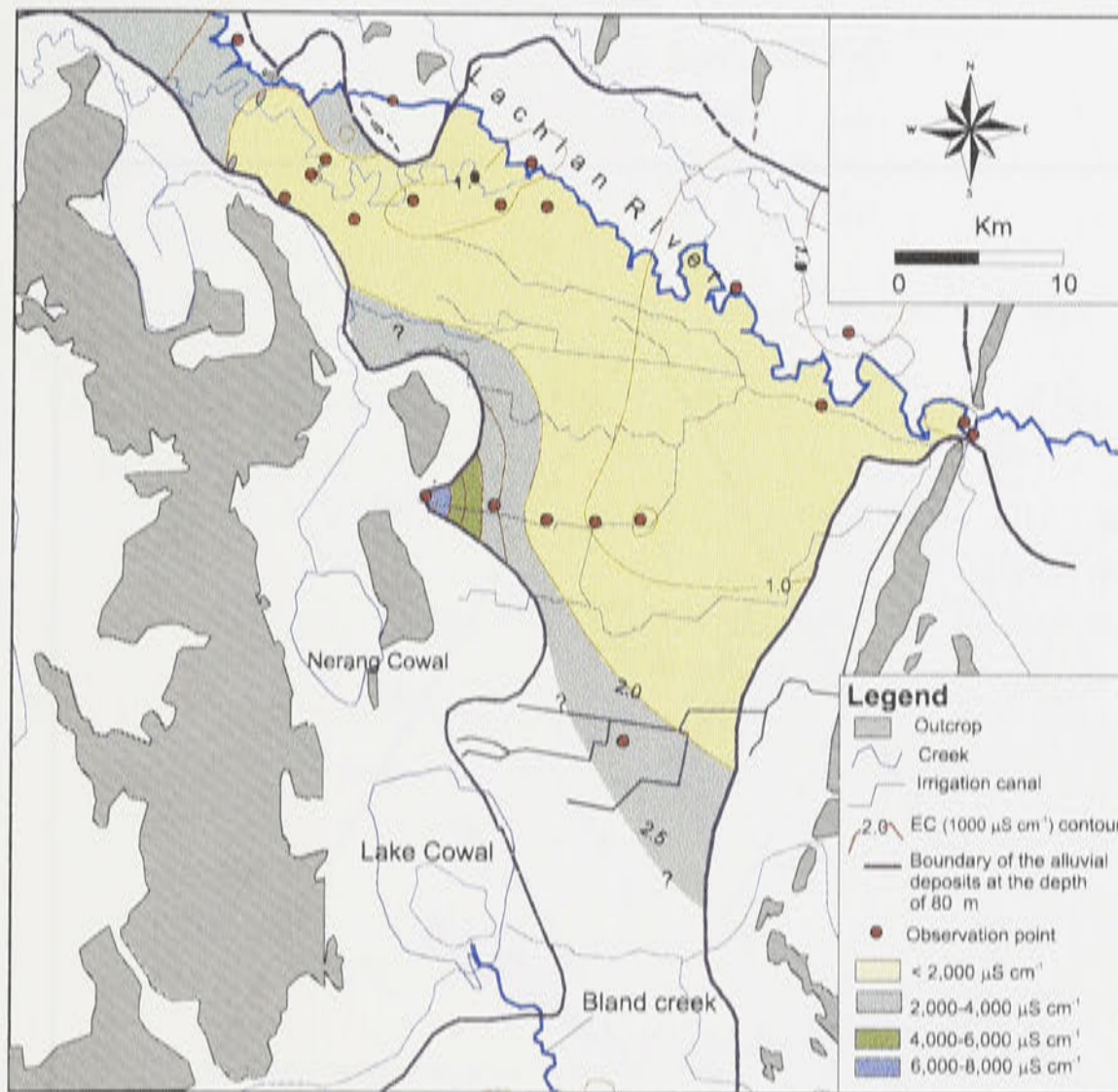


Figure 6.9: Groundwater electrical conductivity (EC) of the JWPID at the depth of 80 m.

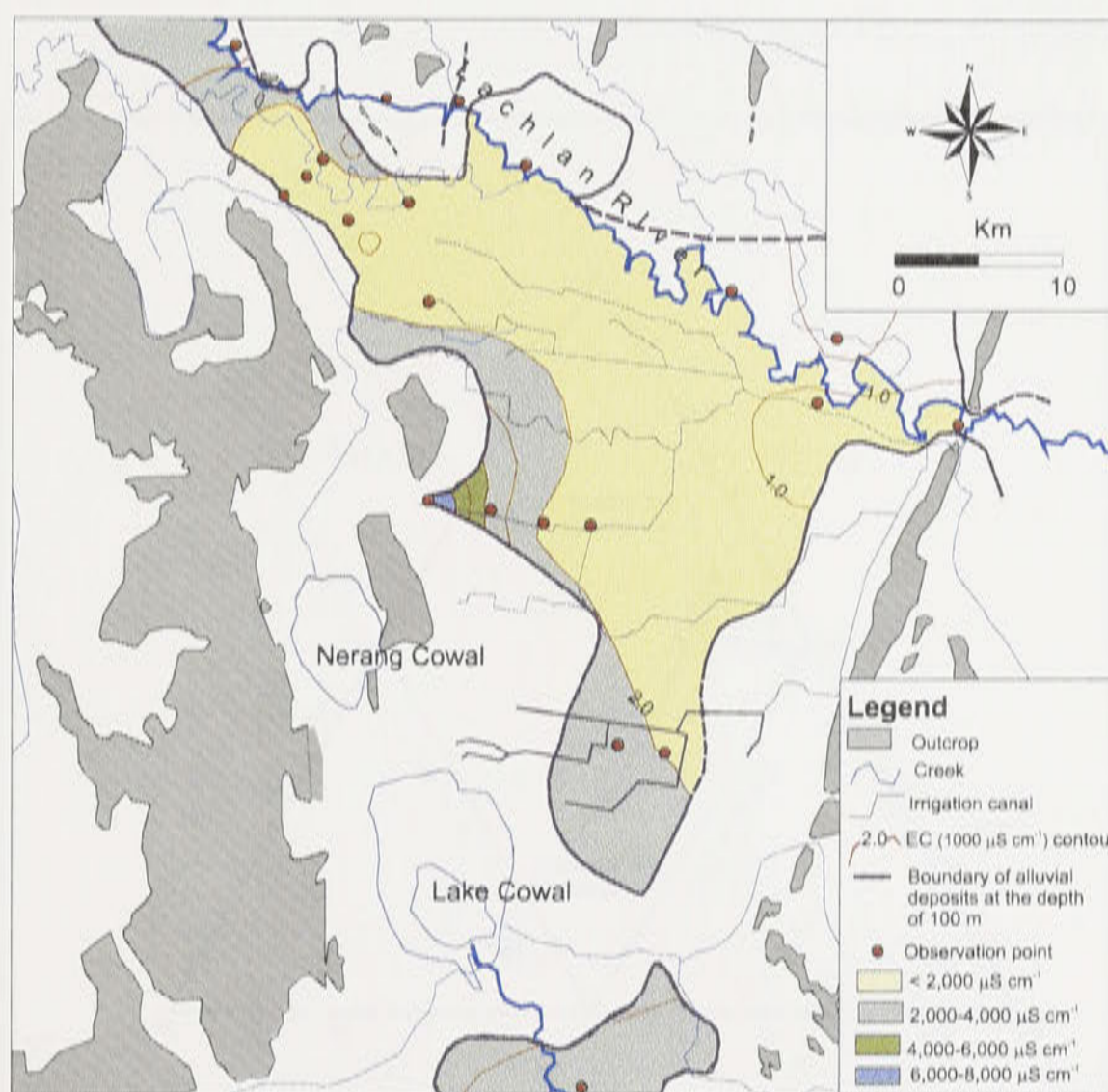


Figure 6.10: Groundwater electrical conductivity (EC) of the JWPID at the depth of 100 m.

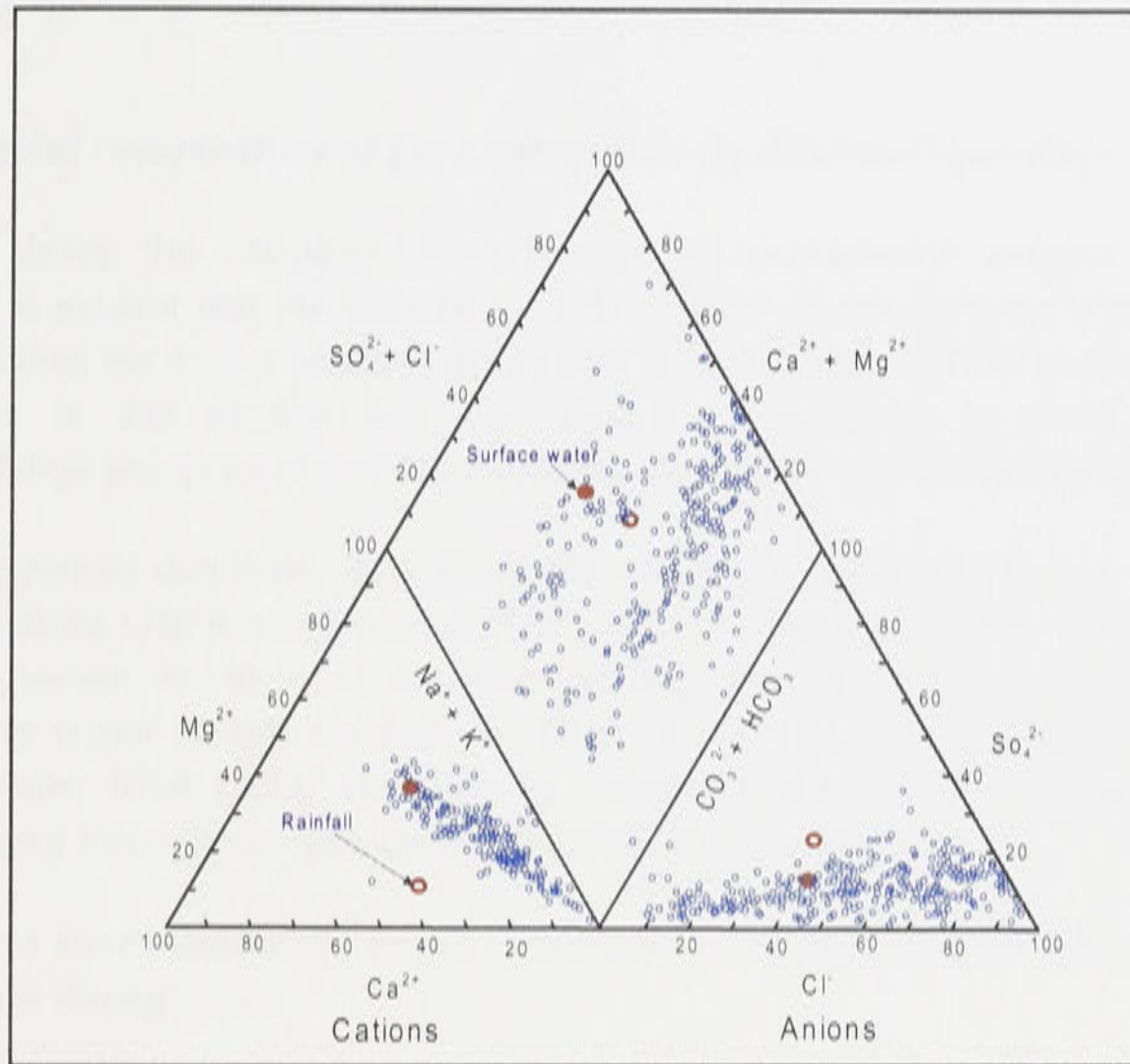


Figure 6.11: Piper diagram of the 410 groundwater samples in the JWPID (modified from Anderson *et al.*, 1993).

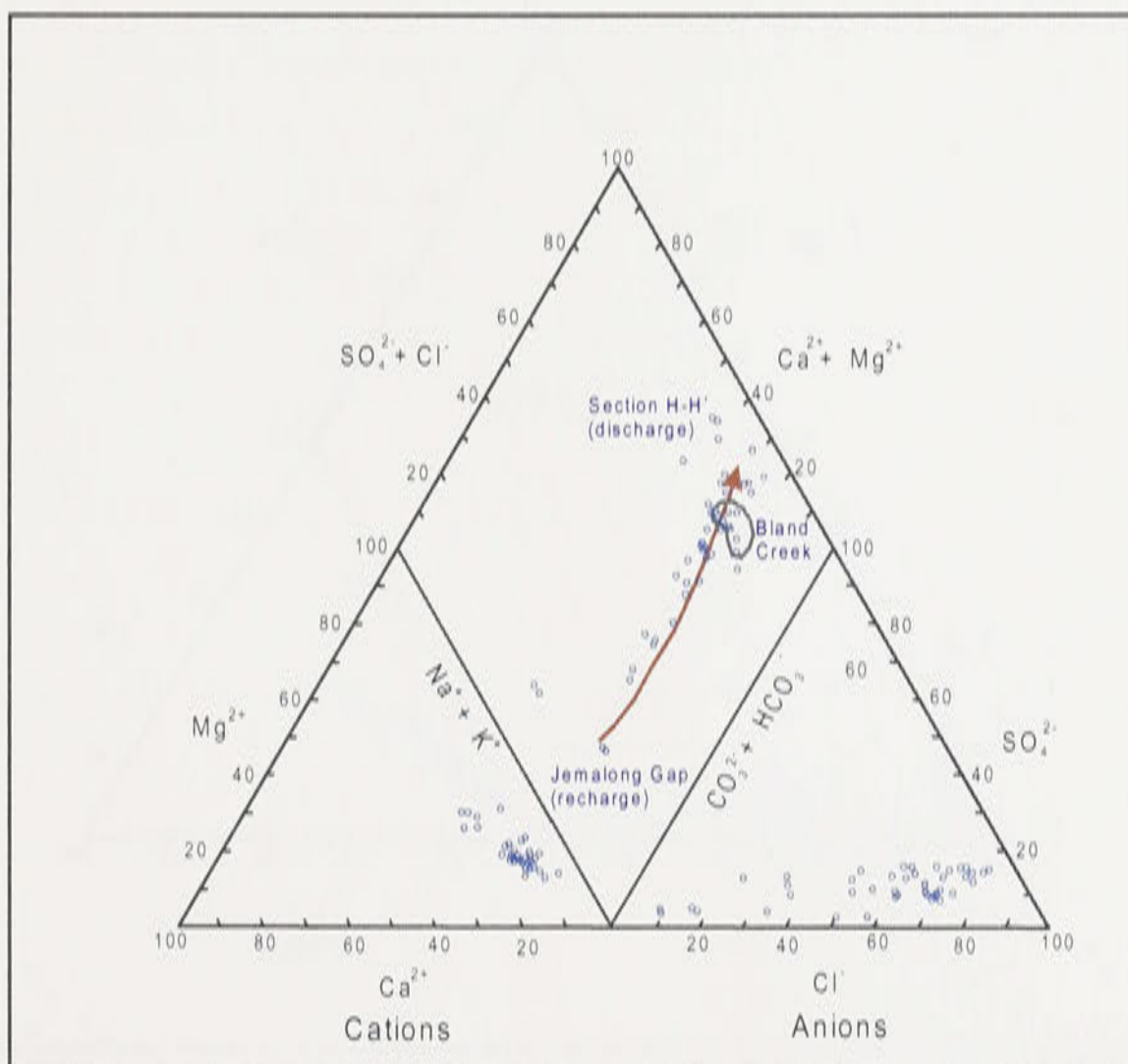


Figure 6.12: Piper diagram of the 46 groundwater samples of Lachlan Formation (modified from Anderson *et al.*, 1993).

The samples from the Bland Creek portion of the Lachlan Formation plot very close together on Figure 6.12. These samples show a Cl^- anionic dominance and a Na^+ cation dominance, typical of late stage or discharge waters (Anderson *et al.*, 1993) and are therefore older waters.

6.2.2. Chemical composition of groundwater in the Cowra Formation

Figure 6.13 shows the chemical characteristics of groundwater samples for the Cowra Formation. It is evident that the chemistry of the shallow samples from Cowra Formation are more variable than the deeper samples from Lachlan Formation, and the patterns are much less definite. This is due to the fact that shallow groundwater is more vulnerable to recharge/discharge processes and of concentration changes along the flow path.

Sodium (Na^+) cations dominate throughout the shallow groundwater system. Along the flow path from Jemalong Gap to cross-section H-H', there is a tendency for the Na^+ concentration to increase. Magnesium, and to the lesser extent calcium, decrease in the direction of flow but are in general only minor cations throughout. There is a change of cation dominance along the direction of flow, from HCO_3^- dominant at Jemalong Gap, to Cl^- dominant downstream. Sulphate is minor throughout, constituting less than 20% of total anions.

Similar patterns are evident in the Bland Creek portion of the Cowra Formation. Sodium is the dominant cation throughout.

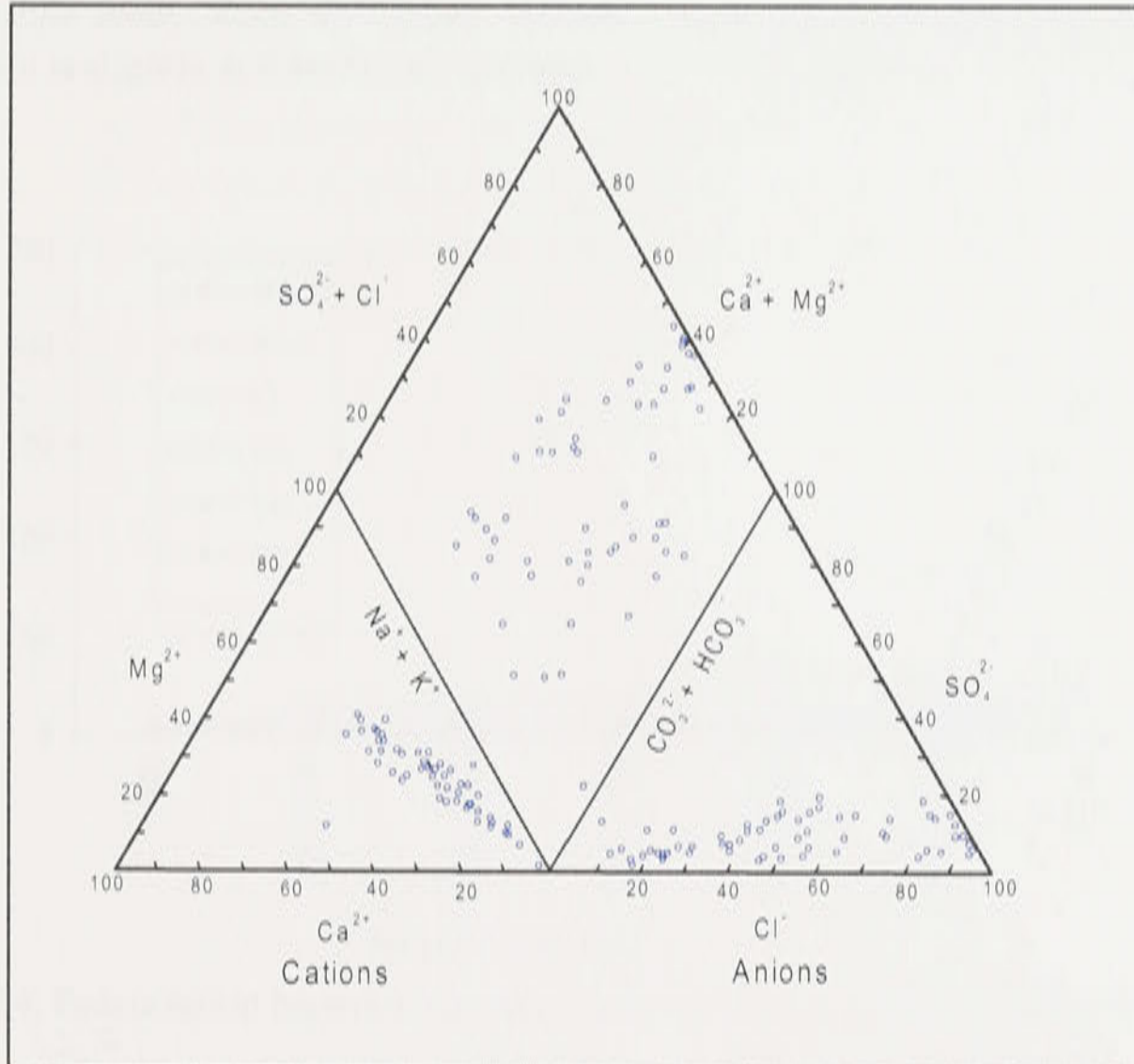


Figure 6.13: Piper diagram of 61 groundwater samples of Cowra Formation (modified from Anderson *et al.*, 1993).

6.2.3. Chemical composition of rainfall and surface water components

The chemistry of the rainfall and surface water are also shown on Figure 6.11. Bicarbonate is the dominant ion in the surface water, although its concentration is only slightly greater than that of chloride. Sulphate constitutes less than 20% of the total anions. Of the cations, sodium is dominant, but calcium and magnesium are also significant, together constituting approximately 60%.

The rainfall chemistry is very similar to surface water, with bicarbonate only slightly dominant over chloride. In this case sulphate contributes a greater fraction of over 25% of the total anions. Once again sodium is dominant and constitute over 50% of the cations. Calcium is also significant, but magnesium makes only a minor contributions to the total cations.

6.2.4. Major ion-TDS relationship

The relationship between major dissolved ions and TDS is shown in Figure 6.14. Based on this figure, sodium and chloride dominate and their concentrations are generally similar in all ranges of TDS values indicating that dominant process is simple dissolution of NaCl. Bicarbonate concentrations (Table 6.3) exceed calcium by about two folds indicating processes other than simple carbonate dissolution, are controlling bicarbonate ions.

6.2.5. Major ion-chloride relationship

Chloride is considered to be conservative ion and not affected by other reactions except simple dissolution. The flux of chloride from rainwater is insignificant since the Lachlan catchment is long distance away from the coast. Rainfall chemistry is shown in Figure 6.11, where bicarbonate is slightly dominant over chloride.

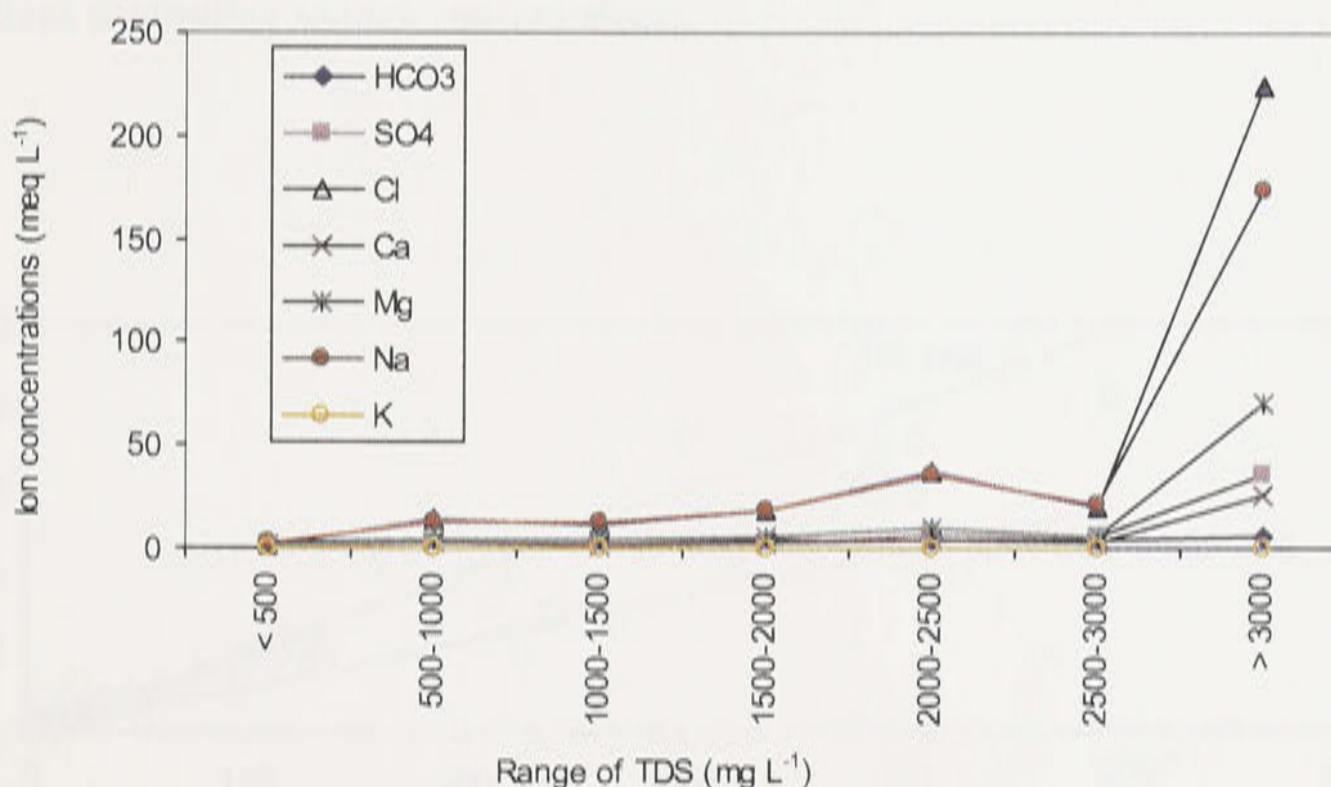


Figure 6.14: Relationship between ion concentrations and ranges of TDS in the study area.

Table 6.3: Concentrations of major ions at different levels of TDS.

TDS range (mg L ⁻¹)	Concentration of major ions (meq L ⁻¹)						
	HCO ₃ ⁻	SO ₄ ²⁻	Cl ⁻	Ca ²⁺	Mg ²⁺	Na ⁺	K ⁺
< 500	2.53	0.38	1.97	0.77	1.08	2.61	0.07
500-1000	4.44	2.73	13.72	2.48	4.76	13.38	0.26
1000-1500	4.84	2.18	11.66	2.14	4.06	12.75	0.11
1500-2000	4.64	3.27	18.27	2.76	5.26	18.00	0.13
2000-2500	4.76	7.81	36.92	3.99	10.29	35.75	0.22
2500-3000	4.48	5.35	20.18	2.86	5.66	21.48	0.18
> 3000	6.34	35.59	223.94	2.12	70.91	173.79	0.32

Figure 6.15 shows that at higher chlorine concentration, there is a deficit of Na⁺ versus Cl⁻ in the irrigation district. Sodium and chloride concentration of the groundwater samples which plot close to 1:1 line are dominated by dissolution of halite. Deviation from 1:1 line indicates addition or removal of sodium from the solution by water-rock interactions. The more possible reactions are ion-exchange on clay minerals and Na-feldspar weathering. The average seawater trend line is also shown on Figure 6.15 to identify the effect of marine sediments on the water chemistry. The groundwater samples from the JWPID plot mainly along the 1:1 line or below it. This indicates dissolution of halite and reverse-ion exchange as the dominant reactions controlling sodium concentrations.

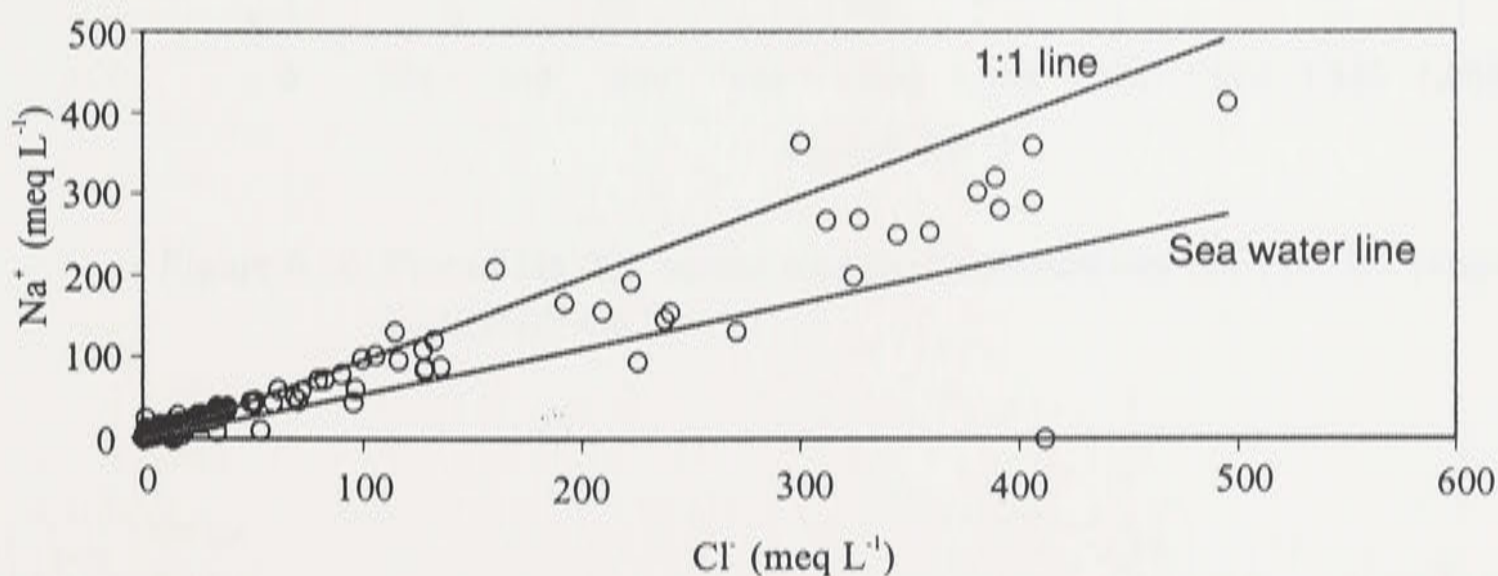


Figure 6.15: Plot of sodium (Na⁺) versus chloride (Cl⁻) for the JWPID and Bland creek groundwater samples.

The relationship between Na^+/Cl^- ratio versus EC is shown in Figure 6.16 and 6.17 for EC range 0-2,000 and 2,000-60,000 $\mu\text{S cm}^{-1}$, respectively. At lower EC concentration ($<2,000 \mu\text{S cm}^{-1}$) (Figure 6.16) show very high Na/Cl ratio, indicating stronger effect of reverse ion-exchange and weathering of Na-feldspar minerals. Na^+/Cl^- ratio varies in the range of 0.3 to 9.4 for EC between 190 to 2,000 $\mu\text{S cm}^{-1}$. However at higher EC concentration ($>2,000 \mu\text{S cm}^{-1}$) Na/Cl ratio is low, ranging from 0.2 to 1.7 (see Figure 6.17).

Figure 6.18 shows Ca^{2+} versus Cl^- relationship for the groundwater samples in the irrigation district. Calcium concentration show great range of variation particularly in higher values, indicating different reactions controlling its concentration. Most of the calcium originates from the dissolution of calcite in the rocks, particularly calcareous sandstone. Some calcium can be released by alteration of anorthite, but the most likely source is the dissolution and ion-exchange process.

Magnesium concentration in most of the groundwaters in the study area show linear relationship with chloride concentration (Figure 6.19) indicating that chloride weathering is taking place regularly along groundwater flow path. Magnesium is usually delivered from the weathering of chloride which is abundant in metamorphic rocks.

There is no clear relationship between potassium and chlorine concentration (Figure 6.20) where the K^+ and Cl^- ratio is below the seawater line.

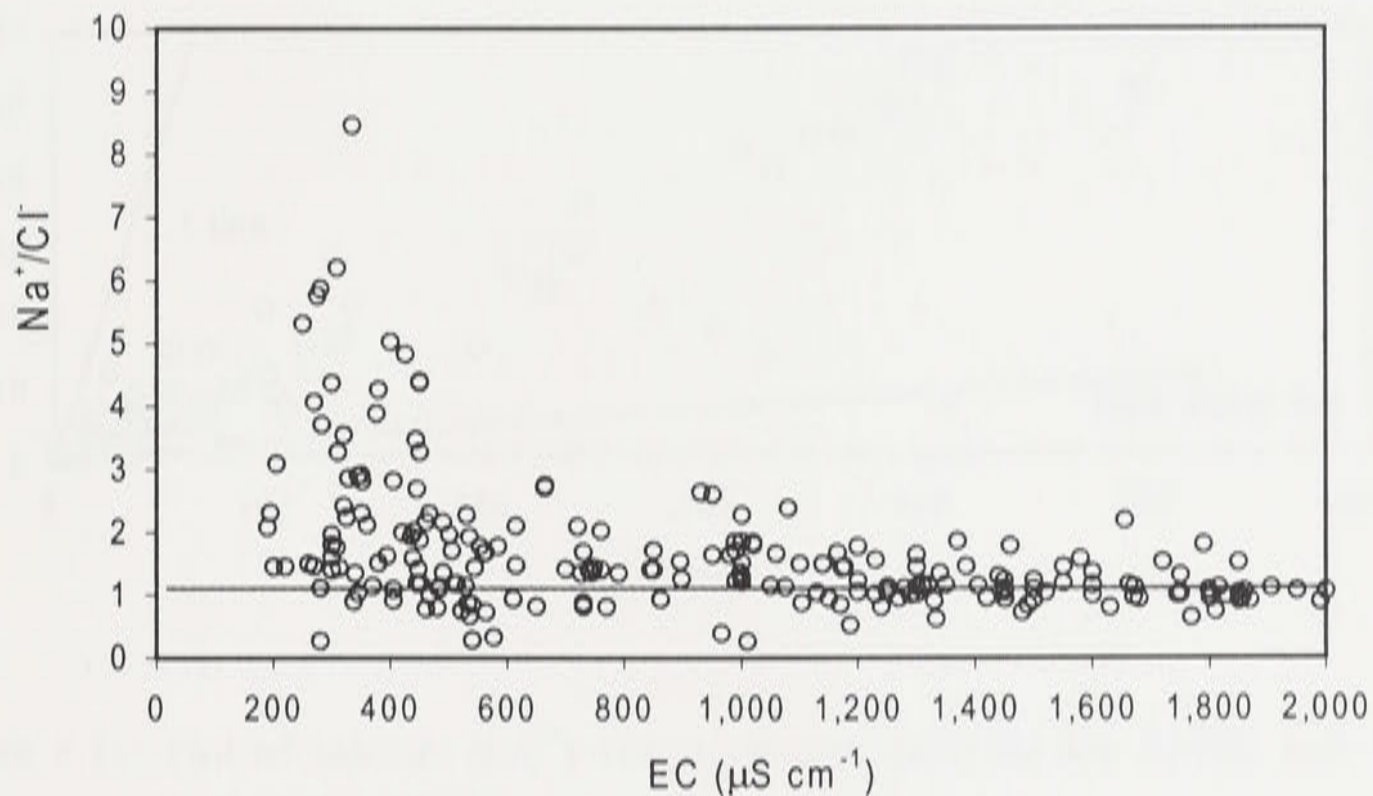


Figure 6.16: Plot of Na^+/Cl^- versus electrical conductivity (EC) for EC range of 0-2,000 $\mu\text{S cm}^{-1}$.

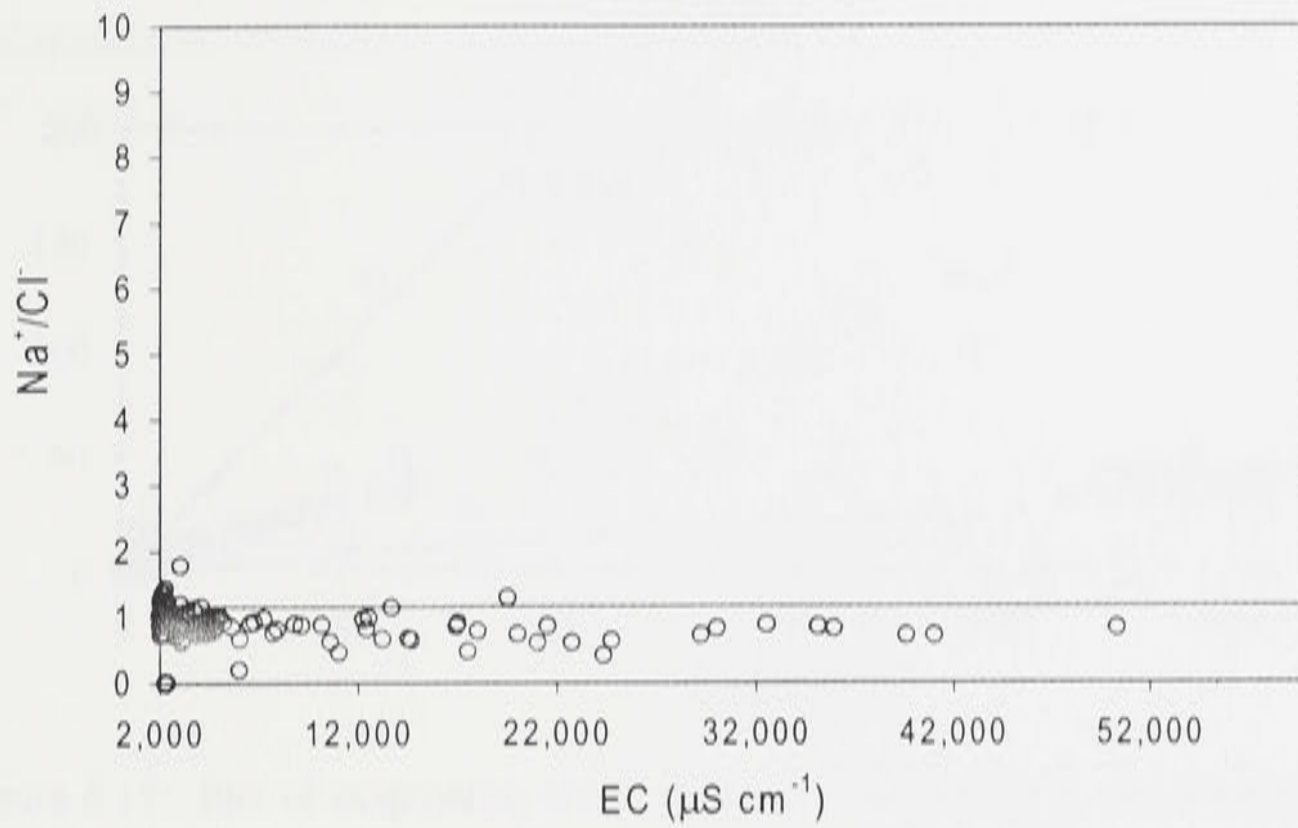


Figure 6.17: Plot of Na^+/Cl^- versus electrical conductivity (EC) for EC range of 2,000-60,000 $\mu\text{S cm}^{-1}$.

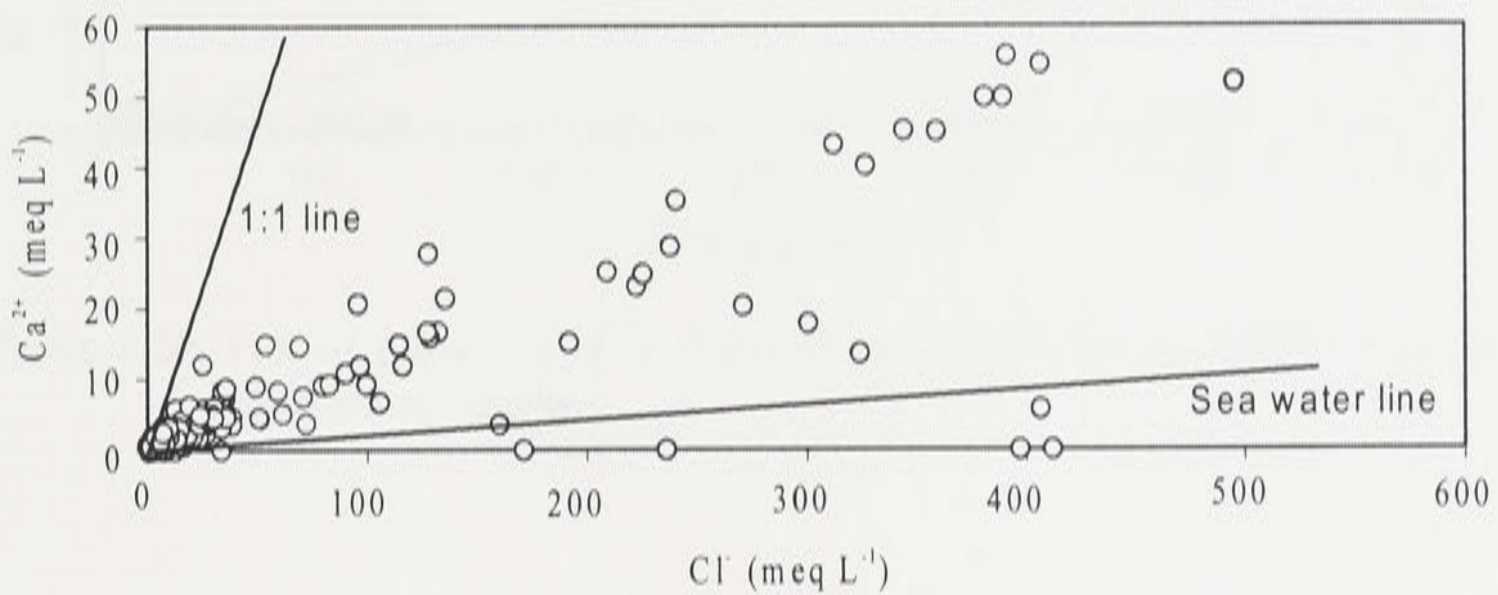


Figure 6.18: Plot of calcium (Ca^{2+}) versus chloride (Cl^-) for the JWPID and Bland Creek groundwater samples.

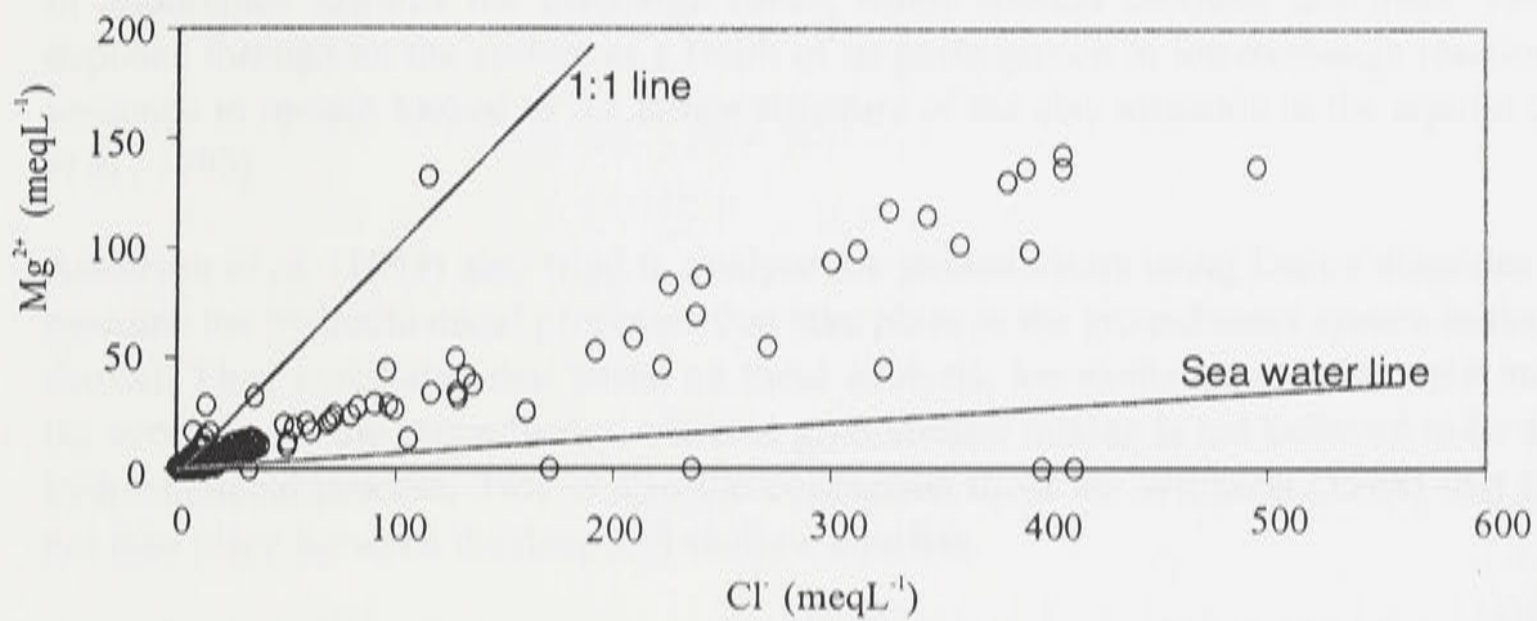


Figure 6.19: Plot of magnesium (Mg^{2+}) versus chloride (Cl^-) for the JWPID and Bland Creek groundwater samples.

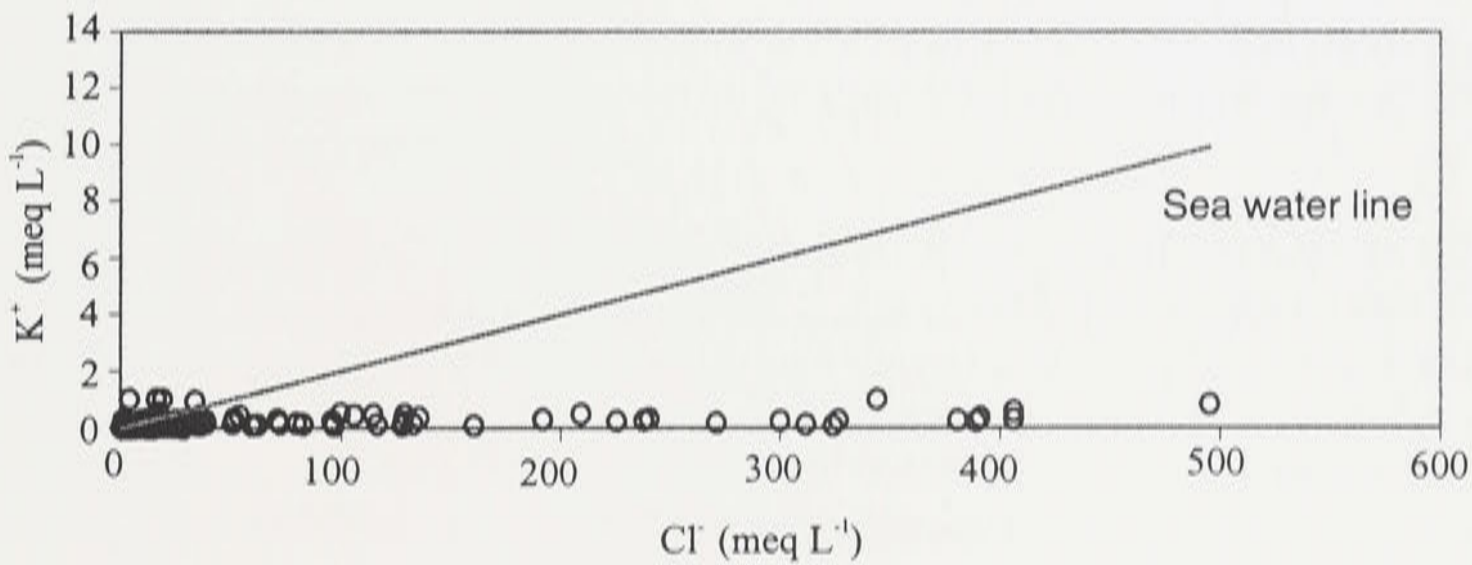


Figure 6.20: Plot of potassium (K^+) versus chloride (Cl^-) for the JWPID and Bland Creek groundwater samples.

6.2.6. Hydrochemical types

Anderson *et al.* (1993) analysed the hydrochemical types of the groundwaters of the JWPID using a system of classification by Szczukariew and Priklonski (Alekin, 1970). The hydrochemical types of the selected observation wells are given in Appendix K.

As reported by Anderson *et al.* (1993), when spatial distribution of the chemical types is examined, the groundwater can be seen to evolved through a sequence of anionic dominance:

$HCO_3^- > Cl^- > SO_4^{2-}$ (recharge waters, eg. Well 36079)

$Cl^- > HCO_3^- > SO_4^{2-}$

$Cl^- > SO_4^{2-} > HCO_3^-$ (discharge waters, eg. Well 25030)

The sequence of cationic dominance is not clear, but there is a tendency for calcium to decrease in importance towards the discharge zones, where sodium becomes dominant. Potassium is depleted throughout the system as a result of its participation in ion-exchange reactions, and its tendency to remain locked in the lattice structure of the clay minerals in the aquifer (Anderson *et al.*, 1993).

Anderson *et al.* (1993) also tried to analyse the groundwaters using Durov diagrams to further examine the hydrochemical processes that take place in the groundwater system in the irrigation district. They concluded that based on these analysis, ion-exchange reactions are important in the evolution of the groundwater, whereas groundwater mixing is not believed to be a dominant hydrochemical process. This is also the conclusion made by Williams (1988) that mixing did not take place between the deep and shallow aquifers.

Based on the chemistry data of the groundwater in the study area, it is therefore concluded that the groundwater evolves along its flow path through concurrent processes of dissolution, ion-exchange, evaporative concentration and mineral precipitation (Anderson *et al.*, 1993).

The groundwater flow modelling and model set-up of the study area will now be considered.

CHAPTER 7

GROUNDWATER FLOW MODELLING AND MODEL SET-UP OF THE STUDY AREA

7.1. Introduction

Groundwater flow models are simplified representations of groundwater flow systems. They provide quantitative assessment of flow and water level changes. Generally, modelling is undertaken to quantify the impacts of various management options and natural changes on the groundwater system.

Over the past 40 years, mathematical models have been widely used in solving various hydrogeological problems. More recently, digital computers have become highly advanced and numerical analysis techniques have been developed that take full advantage of their capabilities. With these tools, groundwater numerical models, and their applications in groundwater management have become commonplace. Finite-difference and finite-element groundwater model techniques are routinely applied to localised and large scale or basin-wide comprehensive groundwater management problems.

The current accessibility of computerised groundwater models means they can be used early in the overall groundwater system investigation. Previously, groundwater models were used only in basins where geologic structures were well defined and the hydrology was well understood. These days, groundwater models are often applied in basins where aquifer structure and hydrogeology are only approximately known. In these cases, the models are used as a tool to guide groundwater analysts to better understand the aquifer system and its behaviour.

The purpose of this chapter is to provide an overview to the use of standard groundwater modelling procedures and then setting up of the three-dimensional numerical model of the study area.

7.2. Groundwater models – a review

No model can exactly reproduce all the characteristics and behaviour of a real groundwater system and it is of some value to recognise how good the model may be for the intended purpose. Different objectives will lead to different models. Selection of the appropriate model will therefore depend on the objectives of the study and availability of resources (Bear, 1991; van der Molen and Pinder, 1993).

The history of the development of mathematical groundwater models has been well described and documented by Gomboso (1995). Simple models have been used since the development of Darcy's Law in 1856. Subsequently, analytical and numerical solutions were developed and applied to various groundwater flow problems. Sand tanks were used to portray groundwater movements. Electric analog techniques were also used long before digital computers became available (Thomas, 1973; ASAE, 1987). Early use of electrical analog simulation techniques resulted from the similarity between Darcy's law and Ohm's law. The network of resistors and capacitors were analogous to aquifer transmissivities and storativities. The bulk of the literature

on application of groundwater analog models is concerned with resistor-capacitor models. Walton (1970) describes some interesting applications. The advantage of analog techniques is that they force the modeller to physically create the model which may ultimately a better feel for the physical system being studied. The disadvantages are that in real-life, analog groundwater model will be bulky, difficult to modify, and incapable of simulating complex transient multi-layered aquifer systems (ASAE, 1987).

Analytical solutions to flow equation, in the form of a partial differential equation, provide ideal insights. Unfortunately, when the boundary conditions are complex, analytical solutions may not exist. Analytical models have limited applications requiring sweeping assumptions and are only applied to aquifers with relatively simple geometry and uniform parameters. A detailed list of differences between the numerical and analytical methods is presented in Ameratunga (1993).

Through the 1950's, groundwater literature was dominated by the advances in analytical modelling, while in the 1960's and 1970's, the focus was shifted to numerical modelling techniques with the aid of digital computers (Walton, 1979). As groundwater modelling techniques have advanced, many different solution techniques have been developed to solve the systems of equations.

Of the numerous available numerical modelling techniques, the two most commonly used are the finite-difference (Gray, 1982) and the finite-element methods (Lewis, 1982; Zienkiewicz, 1991). The finite-difference method was one of the earliest numerical techniques used successfully (Rushton and Redshaw, 1979). However, both methods have approximately the same range of applications. Finite-element methods can employ more general meshes which allows better matching of the system's geometry at the expense of time consumed in setting up the mesh (Ameratunga, 1993).

7.3. Model formulation

The basis for most groundwater flow models is a partial differential saturated flow equation that relates the hydraulic conductivity, hydraulic head, storativity, and source-sink term in the following form for three dimensional flow:

$$\frac{\partial}{\partial x} \left(K_x \frac{\partial h}{\partial x} \right) + \frac{\partial}{\partial y} \left(K_y \frac{\partial h}{\partial y} \right) + \frac{\partial}{\partial z} \left(K_z \frac{\partial h}{\partial z} \right) = S_s(x, y, z) \frac{\partial h}{\partial t} + Q(x, y, z, t) \quad (7.1)$$

where K is the hydraulic conductivity (LT^{-1}), h is the hydraulic head (L), S_s is the specific storativity of the porous material (L^{-1}), Q is the source/sink term (T^{-1}), $(x, y, \text{ and } z)$ are the cartesian coordinates, and t is time (T). The above equation defines the three-dimensional movement of groundwater of constant density through porous material and is the basis of simplified equations for one- and two-dimensional systems. The derivation of this equation through Darcy's Law and continuity equation is presented in Rushton and Redshaw (1979). Under steady-state conditions, the derivative $\partial h/\partial t$ is zero.

Since analytical solutions of the above equation are rarely possible, numerical methods must be employed to obtain an approximate solution. One such method is the finite-difference method, wherein the continuous system is replaced by a finite set of discrete points in space and time, and the partial derivatives are replaced by their finite-difference approximations. By considering

the boundary and the initial conditions of the system, the process will lead to a set of linear equations whose solution yields values of head at specific points and times. These values constitute an approximation of the time-varying head distributions.

7.4. MODFLOW, Visual MODFLOW, and PEST

MODFLOW is a finite-difference groundwater code in FORTRAN 77 (McDonald and Harbaugh, 1988). It is widely used on mainframe, mini and desktop computers. The structure of the code consists of a main program and a series of highly independent subroutines called modules, each dealing with a specific feature of the groundwater system. It simulates groundwater flow in two and three dimensions. Layers can be simulated as confined, unconfined, or a combination of both. Various source-sink terms such as flow to wells, areal recharge, evapotranspiration, flow to drains and flow through riverbeds can be simulated.

Visual MODFLOW (Waterloo Hydrogeologic Inc, 2000) is a fully-integrated package which combines MODFLOW, MODPATH (a particle-tracking model), MT3D (modular three-dimensional transport model) and PEST (Parameter ESTimation) with the most intuitive and powerful graphical interface available. The innovative menu structure allows an easy dimensioning of the model domain and select units, conveniently assigns model properties and boundary conditions, runs model simulations, and visualises the results with line contours or colour shading. Visual MODFLOW was first released in August 1994 and currently is widely used by consulting firms, research institutions and government agencies worldwide.

Groundwater models are traditionally calibrated via a tedious and frustrating trial and error method. PEST is a model-independent and non-linear parameter estimator which is expected to facilitate the task of model calibration. Theoretically, PEST should adjust the model parameters until the fit between the model output and the observed values is optimised in the weighted least squares sense. It uses the Gauss-Marquardt-Levenberg algorithm which is described in detail in the PEST User's manual published by Watermark Computing (1994). The recent version of PEST program has already a windows interface and is incorporated in the Visual MODFLOW. The capability of PEST in calibration of a complex three-dimensional model will be tested in this research.

7.5. Previous modelling exercise in the study area

Two groundwater modelling studies were conducted in the Jemalong and Wyldes Plains study area by Coffey Partners International Pty Ltd. The first model was set up in the irrigation district in 1994 to assess the effectiveness of subsurface drainage measures for the control of groundwater levels in the JWPID and to make recommendations on the location on such measures (Coffey Partners International Pty Ltd, 1994). The second model that covers a much smaller area was set up within the Lake Cowal area for a proposed mine dewatering project (Coffey Partners International Pty Ltd, 1995b). These two models will be briefly described in the following sections.

7.5.1. Groundwater model for JWPID

The three dimensional groundwater model for the irrigation district was set up and calibrated in steady-state using a finite-element program called COFSEEP developed by Coffey and

Partners, Inc. The finite-element mesh consisted of 359 nodes and 344 rectangular and triangular elements in plan view of the top layer.

For this modelling exercise, the aquifer system was divided into six layers which consisted of three separate aquifers, an aquitard which overlay the top aquifer, and two aquitards that separated the upper, middle and lower aquifers, respectively. Figure 7.1 shows a typical cross-section of the system with six layers used in this modelling exercise. This cross-section is located in the northern part of the model domain (Figure 7.2). Hydraulic boundaries of the aquifer system included a no-flow boundary on the eastern side along the Jemalong Range; and another no-flow boundary on the western side along Manna Range except for a 5 km section at the northern limit of the model which was treated as a constant head boundary. The northern and the southern limit of the modelled area were simulated as constant head boundaries.

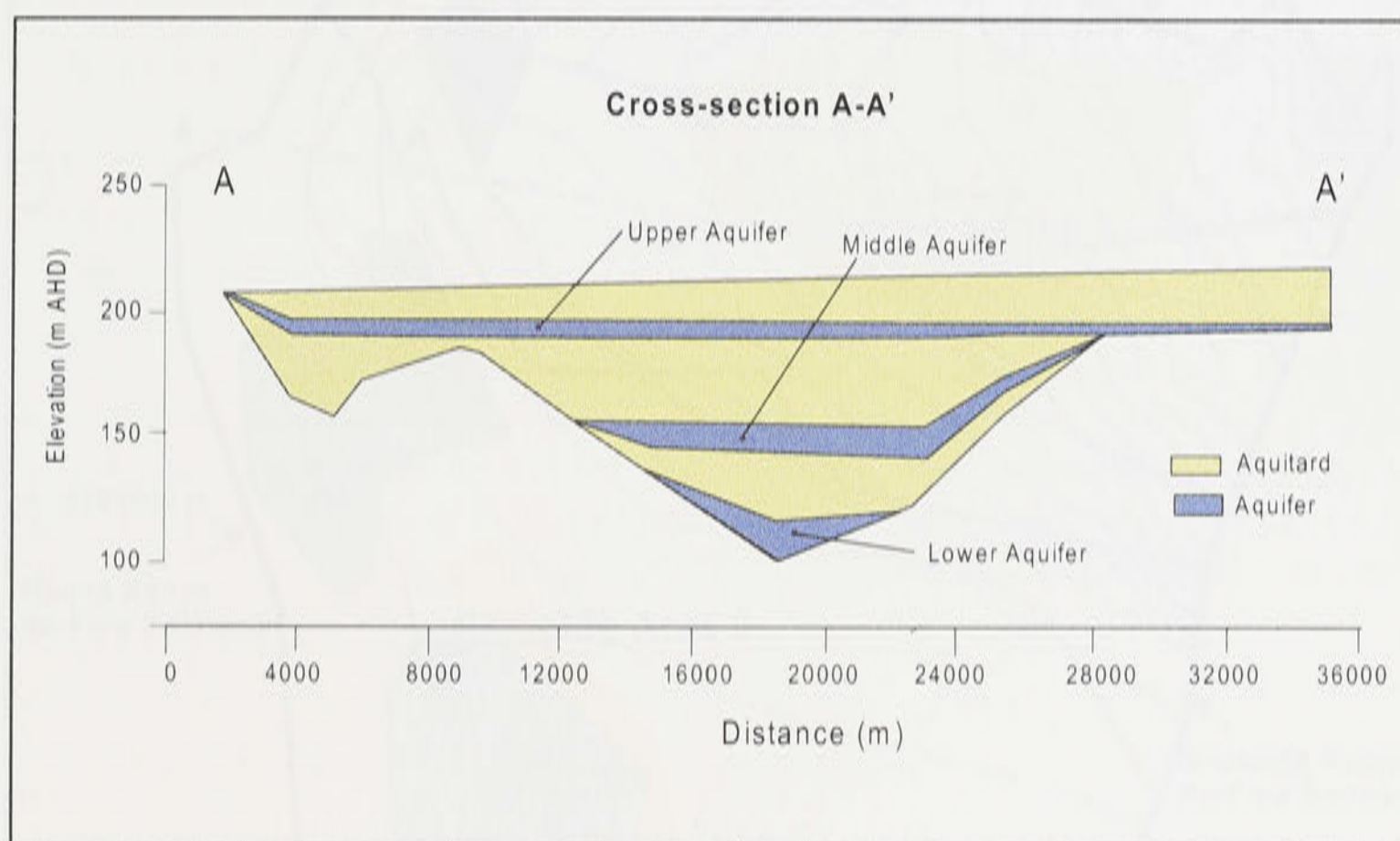


Figure 7.1: A typical cross-section (see Figure 7.2 for the location) of the aquifer system (modified from Coffey Partners International Pty Ltd, 1994).

The modelled area was divided into four zones (A, B, C and D) where separate hydraulic properties were assigned to each zone, based on the regional geological characteristics and pump test results. Accordingly, groundwater accessions had been assumed to be concentrated in zones A (18 mm yr^{-1}), B (18 mm yr^{-1}) and C (3.6 mm yr^{-1}) only. Assumed accession rates were based on the analyses that were carried out for a range of rates that provides a reasonable match between groundwater level. The model was only calibrated in steady-state conditions.

Figure 7.2 shows the computed and the observed groundwater contours for 1992 in the upper aquifer. The model was in general agreement in the northern half of the study area while in the southern half, there was a large discrepancy of about 6 m between the observed and computed heads. In spite of this problem, the calibration was regarded as successful and the model was used for simulations of three groundwater extraction options in the study area. Option A was to

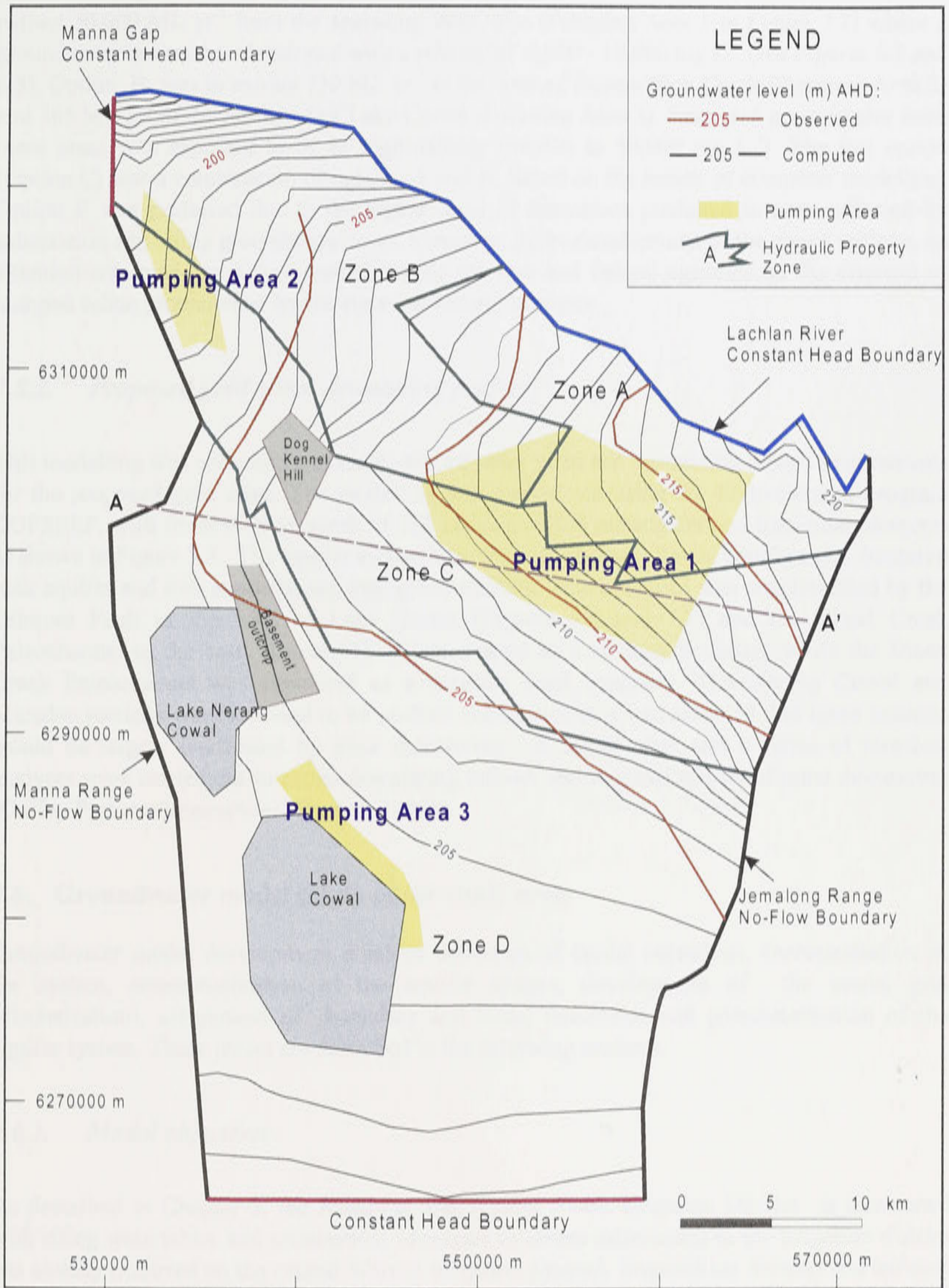


Figure 7.2: Computed and observed groundwater levels for the JWPID in 1992 (modified from Coffey Partners International Pty Ltd, 1994).

extract 30,000 ML yr⁻¹ from the Jemalong West area (Pumping Area 1 in Figure 7.2) where a groundwater mound has developed with a salinity of 5,000 - 10,000 mg L⁻¹ (see Figures 6.2 and 6.3). Option B was to extract 730 ML yr⁻¹ at the west of Bogandillon Creek (Pumping Area 2) and 365 ML yr⁻¹ at the northeast of Lake Cowal (Pumping Area 3). Extracted groundwater from these areas was expected to be of high salinity (30,000 to 50,000 mg L⁻¹). The last option (Option C) was a combination of options A and B. Based on the results of computer modelling, Option B was preferred due to the higher level of drawdown predicted in areas affected by salinisation and rising groundwater level. However, in the development of the above options, no attention was made to severe restrictions by the state and federal agencies on the disposal of pumped saline groundwater by the state and federal agencies.

7.5.2. Proposed gold mine dewatering project

This modelling was undertaken to assess groundwater yield and dewatering design requirements for the proposed gold mine. The modelling was carried out using the finite-element program COFSEEP, with finite-element mesh of 213 nodes and 208 rectangular and triangular elements as shown in Figure 7.3. The aquifer system was divided into two alluvial aquifers, one fractured rock aquifer and four aquitards separating the aquifers. The modelled area was bounded by the Gilmore Fault to the west of Lake Cowal (Figures 4.2 and 7.3) and the Bland Creek Paleochannel to the east. Gilmore Fault was treated as a no-flow boundary while the Bland Creek Paleochannel was simulated as a constant head boundary. The Nerang Cowal and Marsden sections were assessed to be no-flow boundaries as it was assumed that these sections would be largely unaffected by mine dewatering. A steady-state and a series of transient analyses were carried out to assess dewatering inflows and regional effects of mine dewatering (Coffey Partners International Pty Ltd, 1995b).

7.6. Groundwater model set-up of the study area

Groundwater model development involves definition of model objectives, characterisation of the system, conceptualisation of the aquifer system, development of the model grid (discretisation), assignment of boundary and initial conditions and parameterisation of the aquifer system. These issues are described in the following sections.

7.6.1. Model objectives

As described in Chapter 5, the Jemalong and Wyldes Plains Irrigation District is threatened with rising watertables and salinisation. Moderate to severe salinisation in the irrigation district has already occurred on the central Warroo irrigation channel, Bogandillon Swamp and isolated sections along the irrigation channel systems. Management of this irrigation area and salinisation occurring on its western part requires that the contributions of all processes impacting on the groundwater dynamics and salinisation be clearly identified. The objectives of the groundwater model, which will be calibrated in steady and transient conditions, will be to examine the watertable rise, interactions between the aquifer system and surface water as well as the irrigation system. This will assist the development of management strategies to minimise the risk of land salinisation.

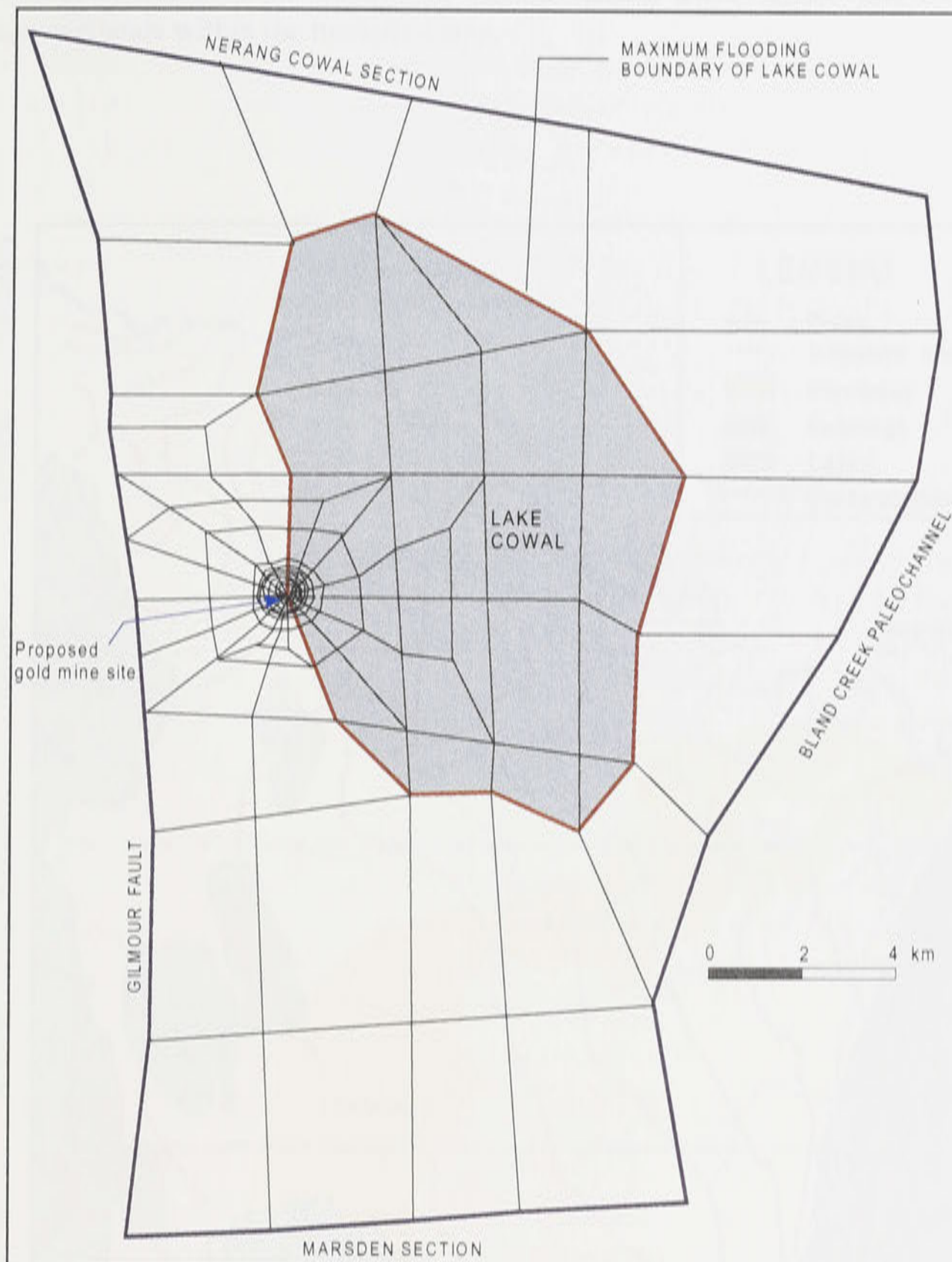


Figure 7.3: Boundary conditions and elements for the proposed Gold Mine Dewatering Project (modified from Coffey Partners International Pty Ltd, 1995b).

7.6.2. *Characterisation of the aquifer system*

Physiographic, geologic and hydrogeologic characteristics of the study area have been comprehensively described in Chapters 3, 4 and 5 of this thesis. The information contained in these chapters set out background information for the modelling study.

7.6.3. *Geometry of the modelled domain*

Figure 7.4 shows the modelled domain which extends approximately 45 km from east to west and 66 km from north to south. The eastern side of the area is defined by the Jemalong Range, while the western side is bounded by the Manna Range. To the north, Lachlan River defines the

boundary of the modelled area, while the southern limit is an arbitrary boundary between the JWPID and Bland Creek catchment. The ephemeral lakes Cowal and Nerang Cowal are the major wetlands within the modelled area.

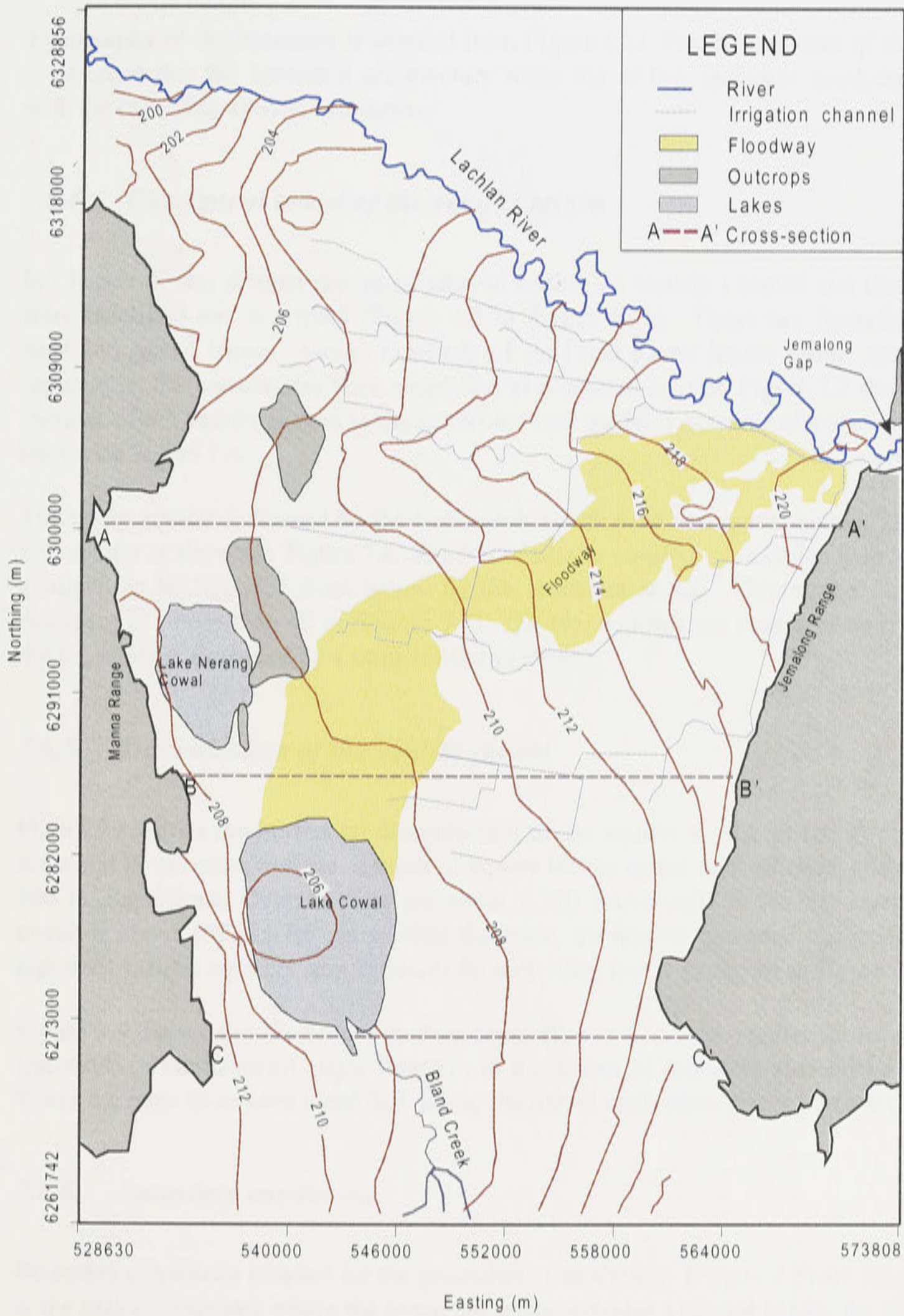


Figure 7.4: Land surface elevation contours of the modelled area in m AHD and locations of three cross-sections of the aquifer system (see Figure 7.5).

A geological fault known as Gilmore Fault (Figure 4.2) along the edges of the Manna Range in western side of the model area is believed to drain the aquifer system.

Land surface elevation of the modelled area based on the Department of Land and Water Conservation's watertable and piezometric wells elevation data is shown in Figure 7.4. Surface elevations ranges from 220 m AHD near the Jemalong Gap to less than 206 m AHD in the Lake Cowal area.

Topography of the basement is adopted from Figure 4.12. For the purposes of the modelling, it is assumed that the basement sedimentary rocks are of low hydraulic conductivity compared with the overlying alluvial sediments.

7.6.4. Conceptual model of the aquifer system

In Chapter 4, two distinct groups of alluvial sediments namely Lachlan and Cowra formations were identified and described (Figure 4.3 to Figure 4.11). These two formations consists of sand and gravel lenses. Since hundreds of sand and gravel lenses could not be simulated separately, the system has been simplified as a layered aquifer. Figure 7.5 shows three cross-sections of the aquifer system in the conceptualised model. Locations of these cross-sections are shown on Figure 7.4.

The upper aquifer is formed by the Cowra Formation sand and gravel lenses. The thickness of this aquifer is shown in Figure 7.6. The lower aquifer consists of Lachlan Formation which is assumed to be bounded from below by the basement rocks. This aquifer has a maximum thickness of more than 40 m (Figure 7.7). The two aquifers are separated by a clay layer and the top aquifer is covered by a semi-confining layer.

7.6.5. Discretisation of the aquifer system

Figure 7.8 shows the horizontal discretisation of the aquifer system in the study area into 123 rows and 84 columns to form a mesh of square blocks called cells of equal sizes with 500 m x 500 m dimensions. Overall, there are about 6,789 active cells in the top layer of the model covering about 169,725 ha. In vertical direction, the aquifer has been discretised in a way to represent various aquifers and aquitards by individual layers as shown in Figure 7.5.

Figure 7.9 shows the discretised bottom layer (Layer 4) of the aquifer system in plan view. Locations of the assumed major fractures in the basement rocks are also shown on this figure. These fractures have been identified during the model calibration processes (see Chapter 8).

7.6.6. Boundary conditions

Boundary conditions adopted for the groundwater modelling (Figure 7.8) are no-flow boundary at the eastern boundary where the Jemalong range provides a natural barrier for the groundwater flow. No-flow boundary is also adopted for the western boundary except for a 5 km section at the northern limit of the model which is treated as a flow boundary similar to that of Coffey Partners International Pty Ltd (1994).

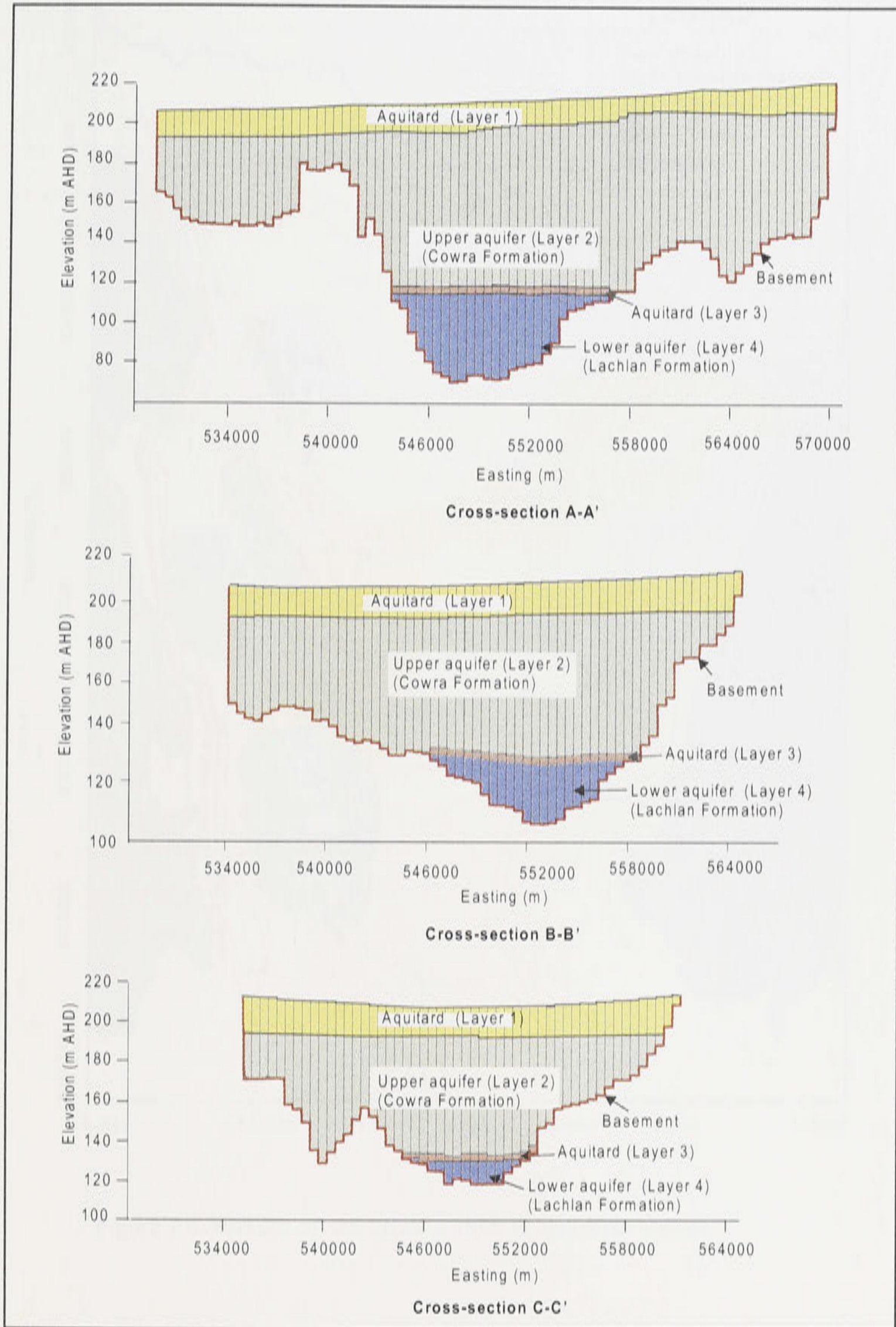


Figure 7.5: Selected cross-sections of the modelled area showing the aquifer systems (see Figure 7.4 for locations).

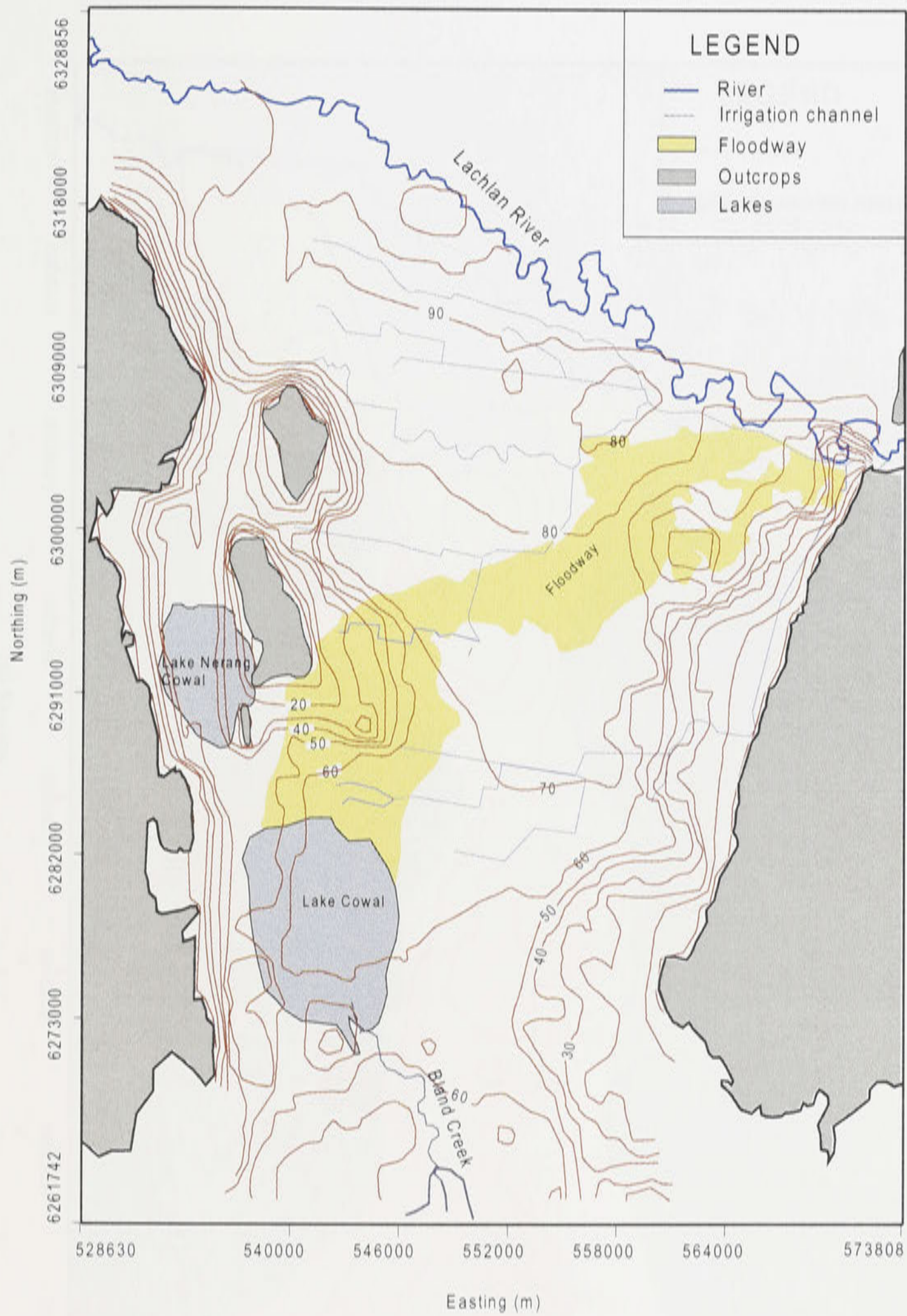


Figure 7.6: Isopach of the upper aquifer (Layer 2) in metres.

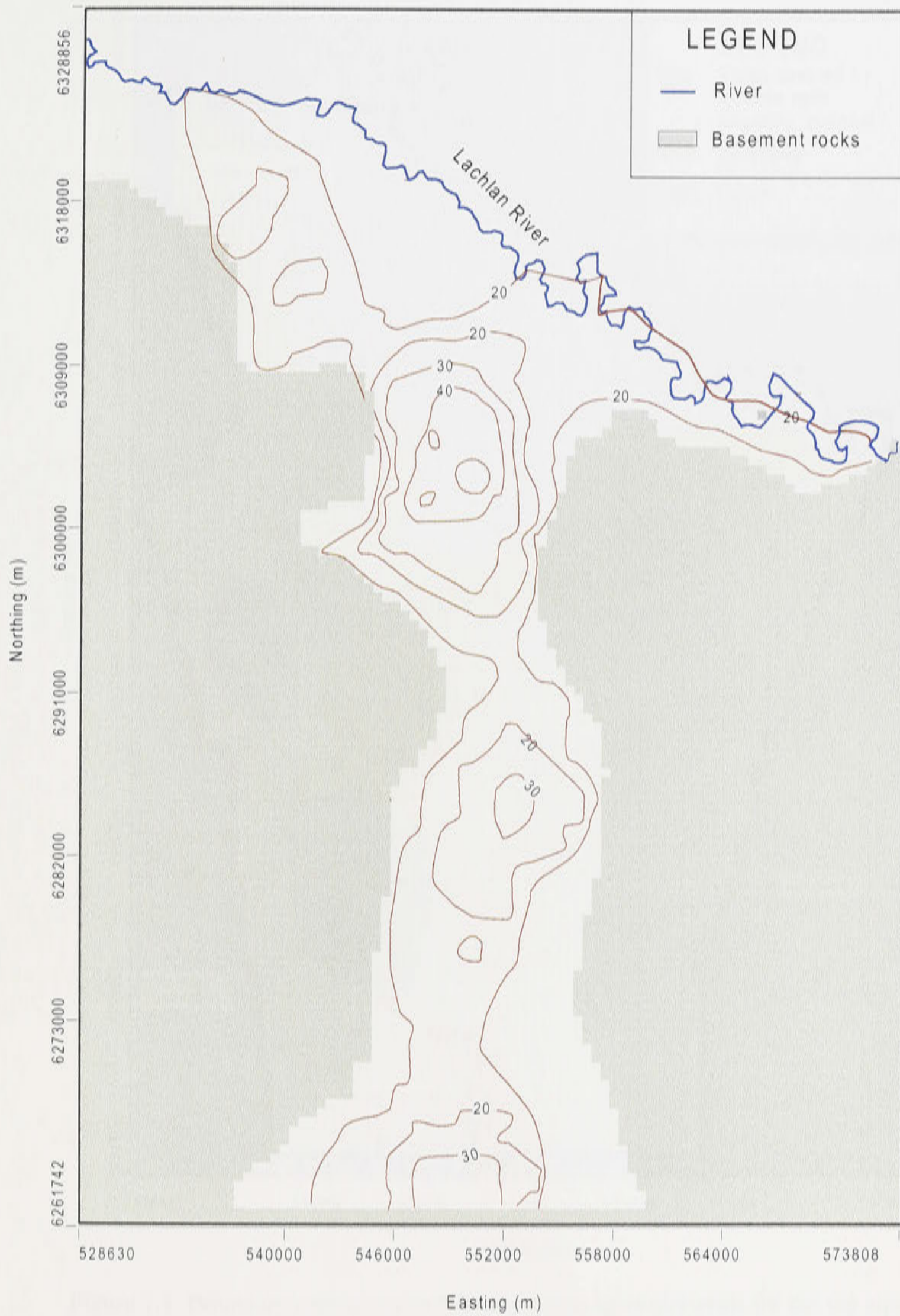


Figure 7.7: Isopach of the lower aquifer (Layer 4) in metres.

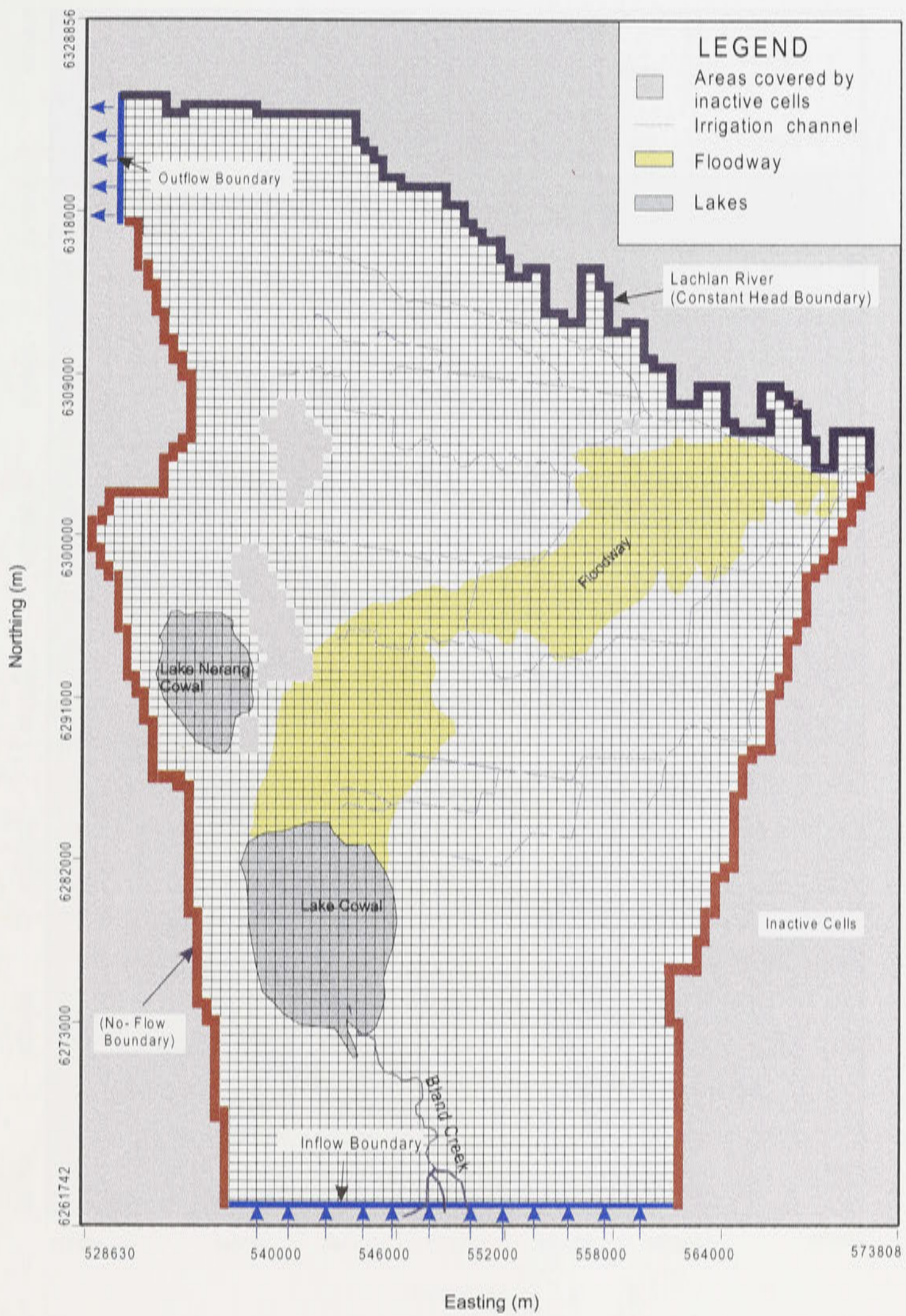


Figure 7.8: Boundary conditions and discretisation of model grids for the top aquifer.

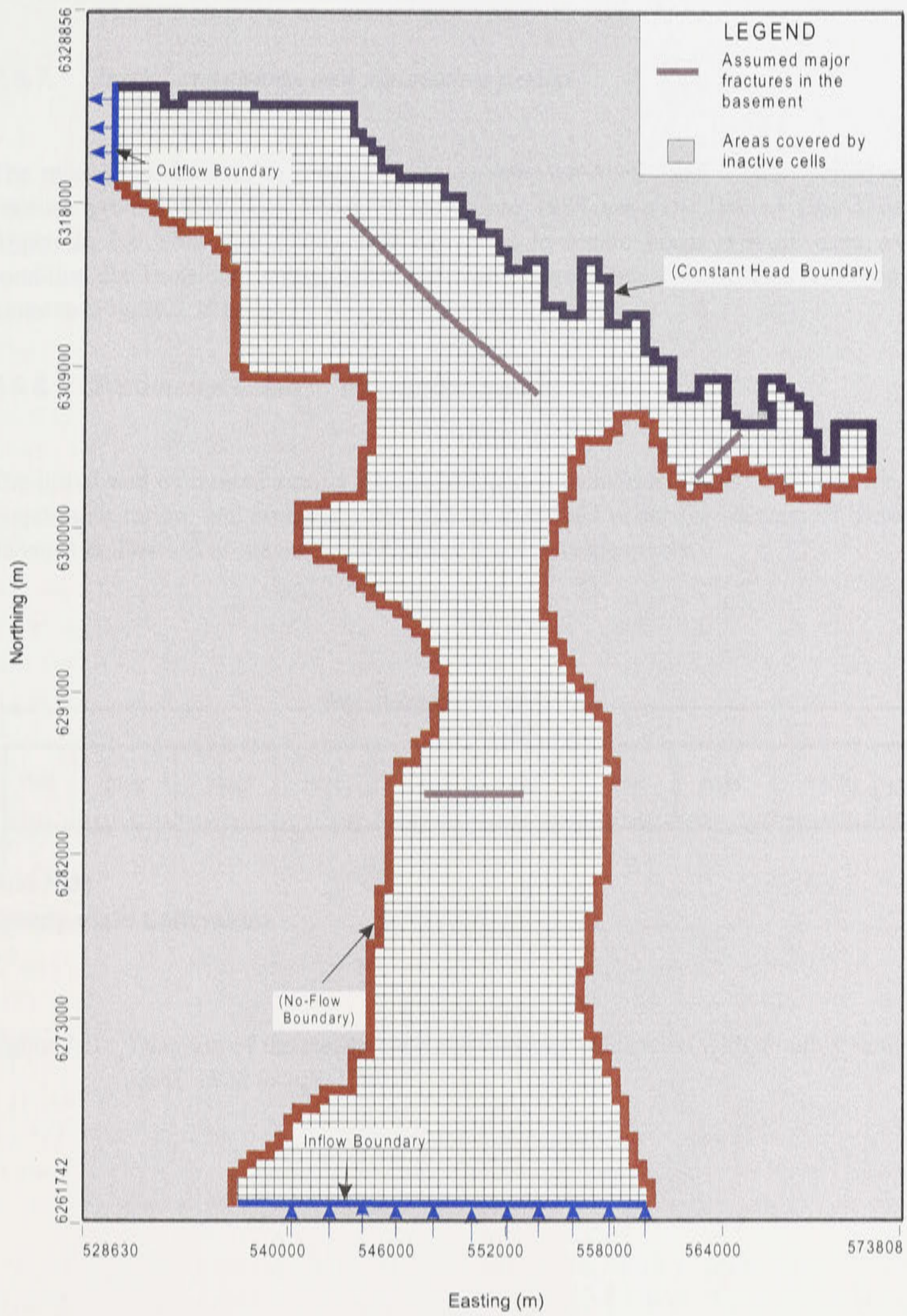


Figure 7.9: Boundary conditions and the model grids for lower aquifer.

The northern limit of the modelled area is treated as constant head boundary. The southern boundary is assumed to be an inflow boundary where groundwater flow from the Bland Creek sub-catchment enters the modelled area.

7.6.7. *Initial conditions and simulation period*

The model will be first calibrated in steady-state for April 1988. This period was selected because groundwater level observations before 1988 are very limited (see Figure 5.6 and Appendix E). Then the steady-state calibrated hydraulic heads will be used as the initial condition for transient calibration of the model from May 1988 to July 1997 on a monthly timestep (Figure 7.10).

7.6.8. *Parameterisation of the aquifer system*

The initial and calibrated aquifer parameters which include hydraulic conductivity, storativity, evapotranspiration, and recharge rates will be described under the sections of steady-state and transient calibration of the model in Chapter 8 and 9, respectively.

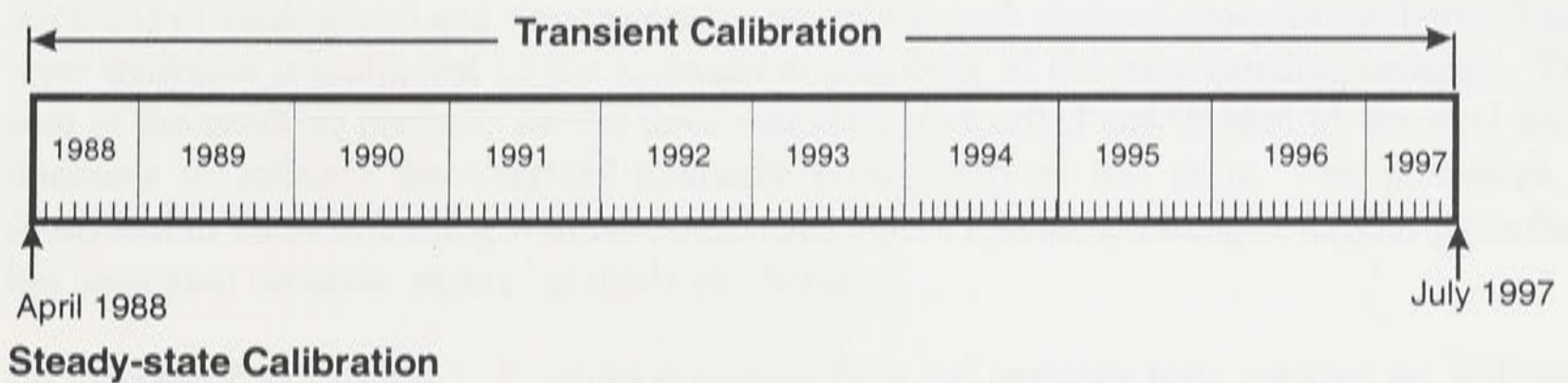


Figure 7.10: Diagram of the steady-state and transient calibration with monthly timesteps from April 1988 to July 1997.

CHAPTER 8

STEADY-STATE CALIBRATION

8.1. Introduction

The first stage following establishment of the model set-up consists of the steady-state calibration of the model. As part of this process, the initial boundary conditions, hydraulic conductivities, recharge rates and possible upward or downward leakages will be applied from values obtained from the Department of Land and Water Conservation and from previous studies in the modelled area. These parameters will be adjusted until the best fit between the computed and observed piezometric heads is reached. To a limited extent, this process was facilitated by the PEST software. Since PEST can only optimise selected parameters, most parameters are adjusted through trial and error method and then optimised by PEST.

8.2. Hydraulic conductivity

Figures 8.1 and 8.2 show the optimised hydraulic conductivity (K) zones for the upper and lower aquifers (Layers 2 and 4, Figure 7.5) and the corresponding initial estimates are presented in Table 8.1. For each aquifer, initial K values were estimated by calculating the aggregate thickness of sand, gravel and clay materials available at each regional groundwater bores. Then layer thickness is multiplied by the hydraulic conductivity of the corresponding material. The sum of the resulting products for the three materials are totalled and divided by the total layer thickness to estimate the weighted hydraulic conductivity at this point. This procedure is illustrated in Table 8.2, using well no. 36523 (see Figure 5.3) as an example. Similar procedure has been used for other regional groundwater bores.

As mentioned in Chapter 5, K values estimated from the pumping tests reported by Williams (1988) seems extremely high for these aquifer materials, while pumping test conducted by Coffey Partners International Pty Ltd (1994) in the shallow groundwater system shows a more reasonable range of K values from 7.5 to 30 m d⁻¹. In this research, the assumed K values of 60, 15, and 0.5 m d⁻¹ for gravel, sand, and clay materials respectively, were found to be adequate. To identify zones of similar hydraulic conductivities, a contouring technique using SURFER (Golden Software Inc, 1995) was used. The resulting zones conform to the geological characteristics of the alluvial deposits. As expected, zones along the Lachlan river have higher K in the both aquifers (Layers 2 and 4).

The distribution of the hydraulic conductivity values for the upper aquitard (Layer 1) was estimated using the surface soil classification map of the area (Figure 8.3). Initial hydraulic conductivity values used for each zone of this layer are 0.01, 0.5, 1.0 and 2.0 m d⁻¹ for clay, clay loam, sandy loam and sandy soils, respectively (Table 8.3). For the lower aquitard (Layer 3), a uniform hydraulic conductivity value of 0.1 m d⁻¹ was adopted.

The initial estimates of the hydraulic conductivity are for the horizontal flow direction (x-direction). For the three dimensional aquifer system, hydraulic conductivity (K) for the y and z directions are estimated by assuming that $K_x = K_y$ and $K_z = 0.1 K_x$ (Waterloo Hydrogeologic Inc, 2000).

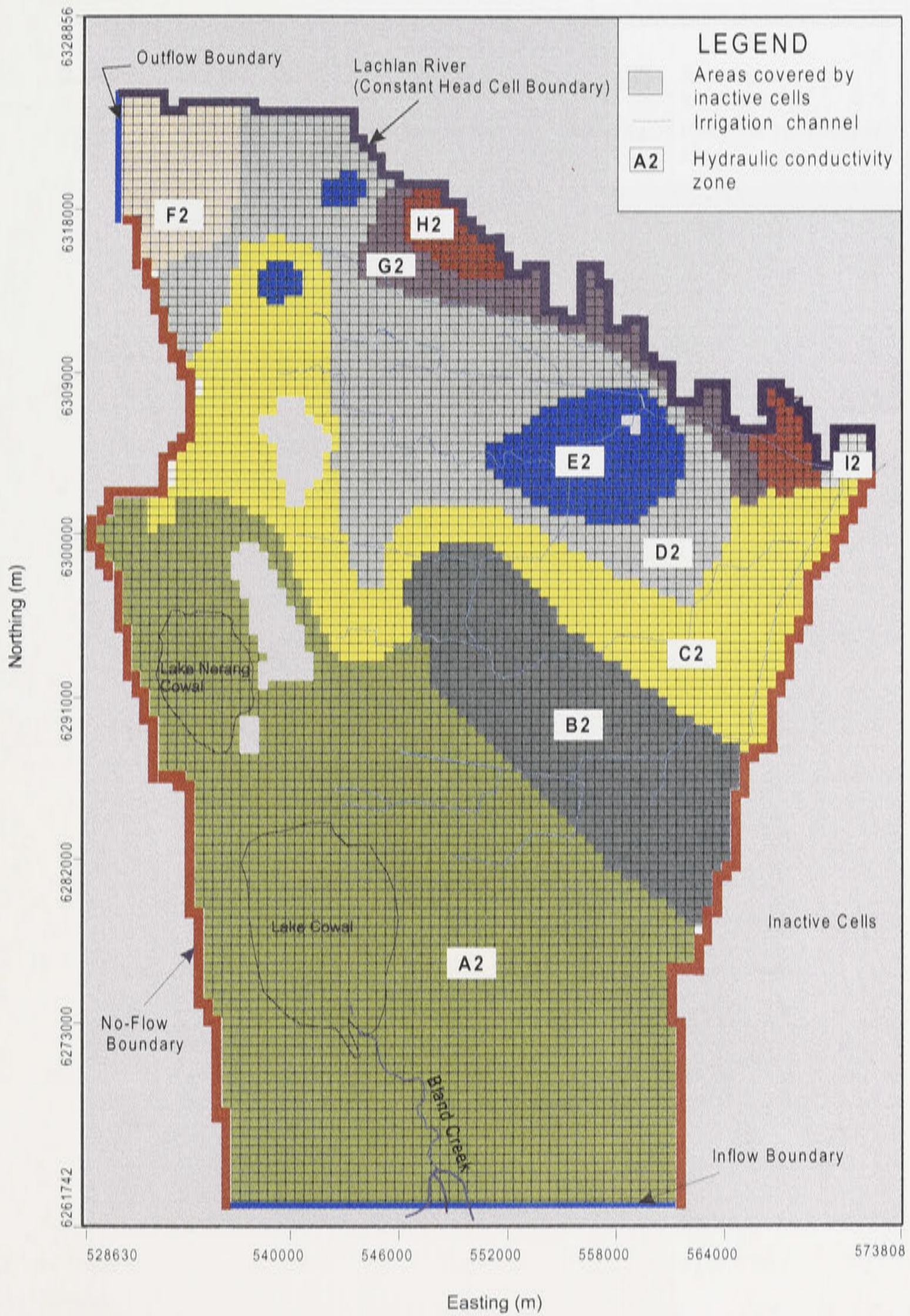


Figure 8.1: Distribution of hydraulic conductivity zones for the upper aquifer or Layer 2 of Figure 7.5 (see Table 8.1 for respective K values).

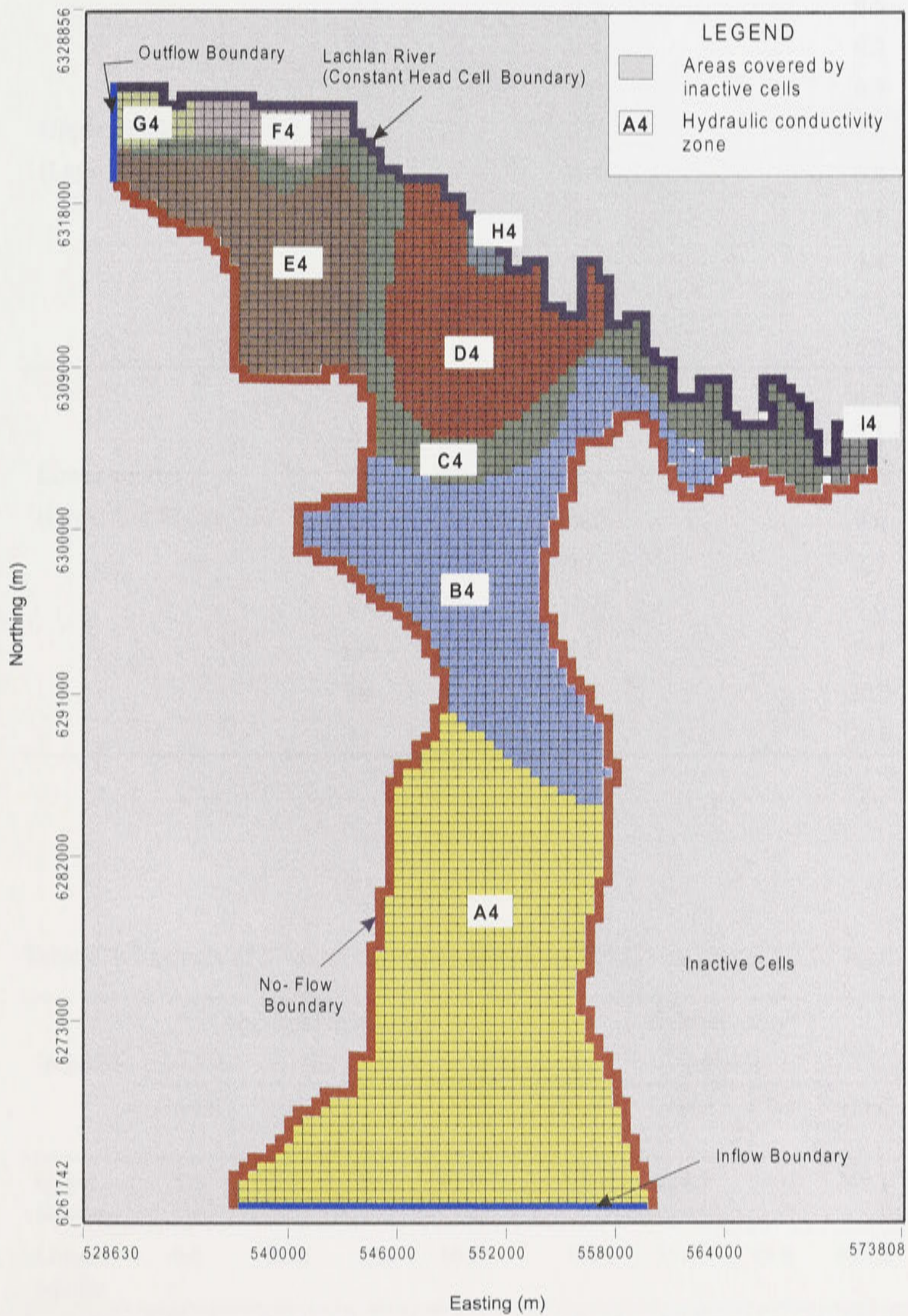


Figure 8.2: Distribution of hydraulic conductivity zones for the lower aquifer or Layer 4 of Figure 7.5 (see Table 8.1 for respective K values).

Table 8.1: The initial and the calibrated hydraulic conductivity (K) values (see Figure 8.1 and 8.2 for locations of zones).

Aquifer	Zone	Initial K values (m d ⁻¹)	Calibrated K values (m d ⁻¹)
Upper aquifer (Layer 2 of Figure 7.5)	A2	0.5	0.5
	B2	0.4	0.2
	C2	1.0	0.7
	D2	3.0	1.6
	E2	0.5	0.9
	F2	4.0	0.7
	G2	6.0	5.4
	H2	10.0	5.4
	I2	20.0	6.5
Lower aquifer (Layer 4 of Figure 7.5)	A4	5.0	2.4
	B4	1.0	2.1
	C4	5.0	5.0
	D4	10.0	9.0
	E4	1.0	2.7
	F4	10.0	7.6
	G4	1.0	0.4
	H4	20.0	20.0
I4	20.0	20.0	

Table 8.2: Example of K values estimation at well no. 36523 (see Figure 5.3 for location).

Aquifer	Aggregate thickness (m)				Transmissivity* (m ² d ⁻¹)				Weighted K ** (m d ⁻¹)
	Gravel	Sand	Clay	Total	Gravel	Gravel	Clay	Total	
Upper aquifer	3.5	8.3	69.2	81.0	210.0	124.5	34.6	369.1	4.6
Lower aquifer	0.0	23.8	27.0	50.8	0.0	357.0	13.5	370.5	7.3

* Assumed K values for gravel, sand and clay are 60, 15 and 0.5 m d⁻¹, respectively.

** The estimated K value for each aquifer is the total weighted transmissivity value divided by total weighted thickness.

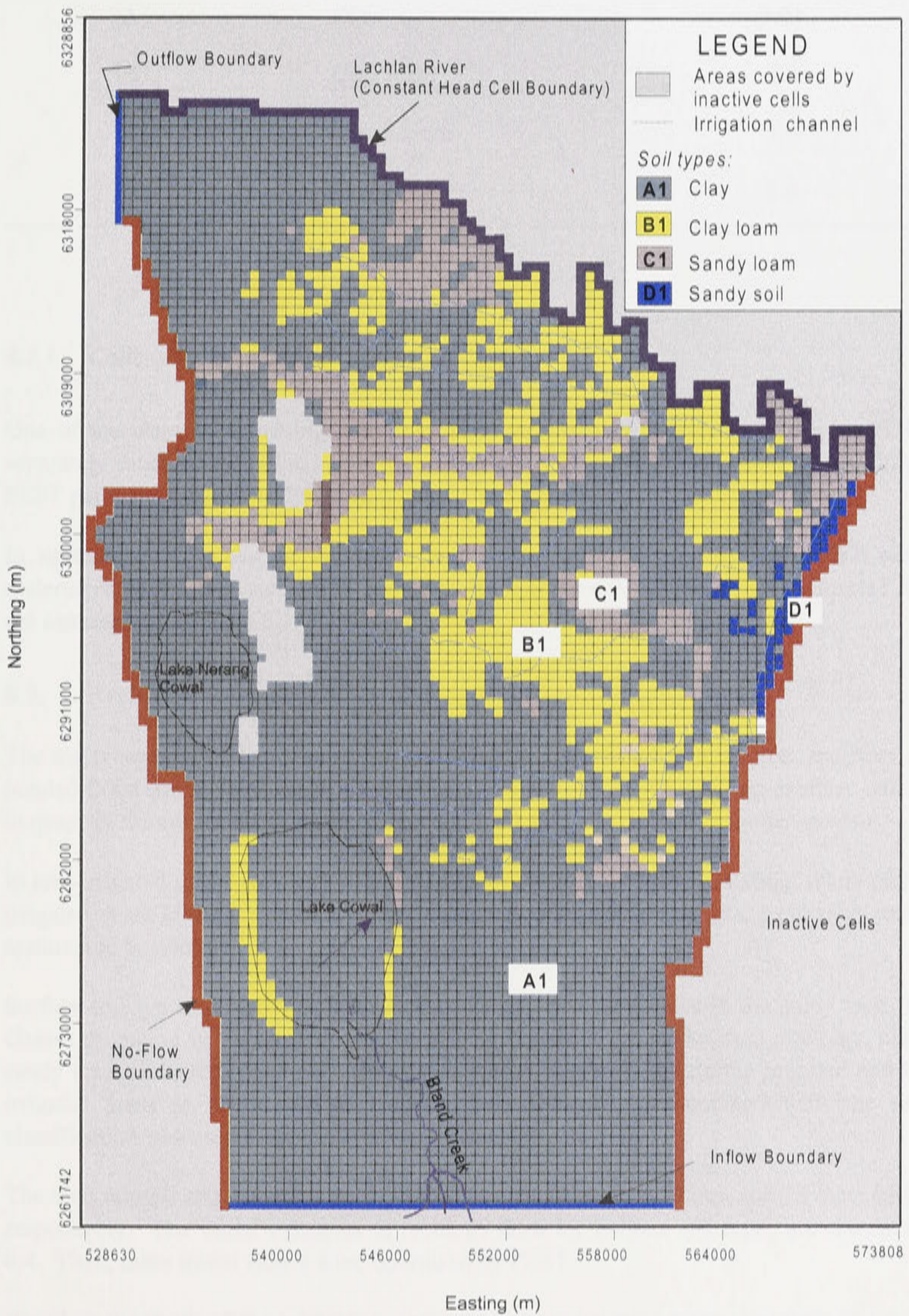


Figure 8.3: Distribution of hydraulic conductivity zones for the upper aquitard or Layer 1 of Figure 7.5 (see Table 8.2 for respective K values).

Table 8.3: Hydraulic conductivity values for upper aquitard or Layer 1 (see Figure 8.3 for location of zones).

Zones	Soil types	K (m d ⁻¹)
A1	Clay	0.01
B1	Clay loam	0.5
C1	Sandy loam	1.0
D1	Sandy	2.0

8.2.1. Calibration of K values using PEST software

One of the ways of achieving a successful optimisation of parameter values by PEST is to separately estimate hydraulic conductivity and recharge for the steady-state model. In general, PEST performs better with fewer parameters to estimate.

In optimising K values of the upper and lower aquifers, two separate PEST runs were undertaken. After each run, PEST provided the optimised K values. These calibrated K values are summarised in Table 8.1.

8.3. Recharge from rainfall and irrigation

The major sources of recharge to the groundwater system in the study area are from rainfall, ponded flood water, farm irrigation and channel seepage. This modelling exercise will attempt to quantify the contribution of each source to the total recharge of the aquifer system.

In non-irrigated areas, recharge is assumed to be from rainfall and flooding, while recharge in irrigated areas is due to rainfall, irrigation and flooding. Recharge due to channel seepage is assumed to be confined to the Warroo channel.

Surface soil type information was used to identify recharge zones in the study area. The soil classes discussed in Figure 3.17 for the irrigation district are reclassified into clay, clay loam, sandy loam and sand. Land use information is also used to delineate the irrigated and the non-irrigated areas in the modelled domain. This information combined with the new soil classification was used to identify recharge zones (Figure 8.4).

The total rainfall and irrigation water used for April 1988 were 37 mm and 22 mm (4,862 ML), respectively. The initial estimates of recharge rates for various soil types are shown in Table 8.4. Then, these initial values were optimised by PEST.

Based on the result of the calibration, recharge rates in irrigated areas vary from as low as 0.01 mm yr⁻¹ in clay soils to about 123 mm yr⁻¹ in sandy soils. In non-irrigated areas, an expected lower recharge rates have been optimised with almost negligible recharge in clay soil areas. High recharge rate occurred in the vicinity of the Warroo channel where coarse textured soils are abundant.

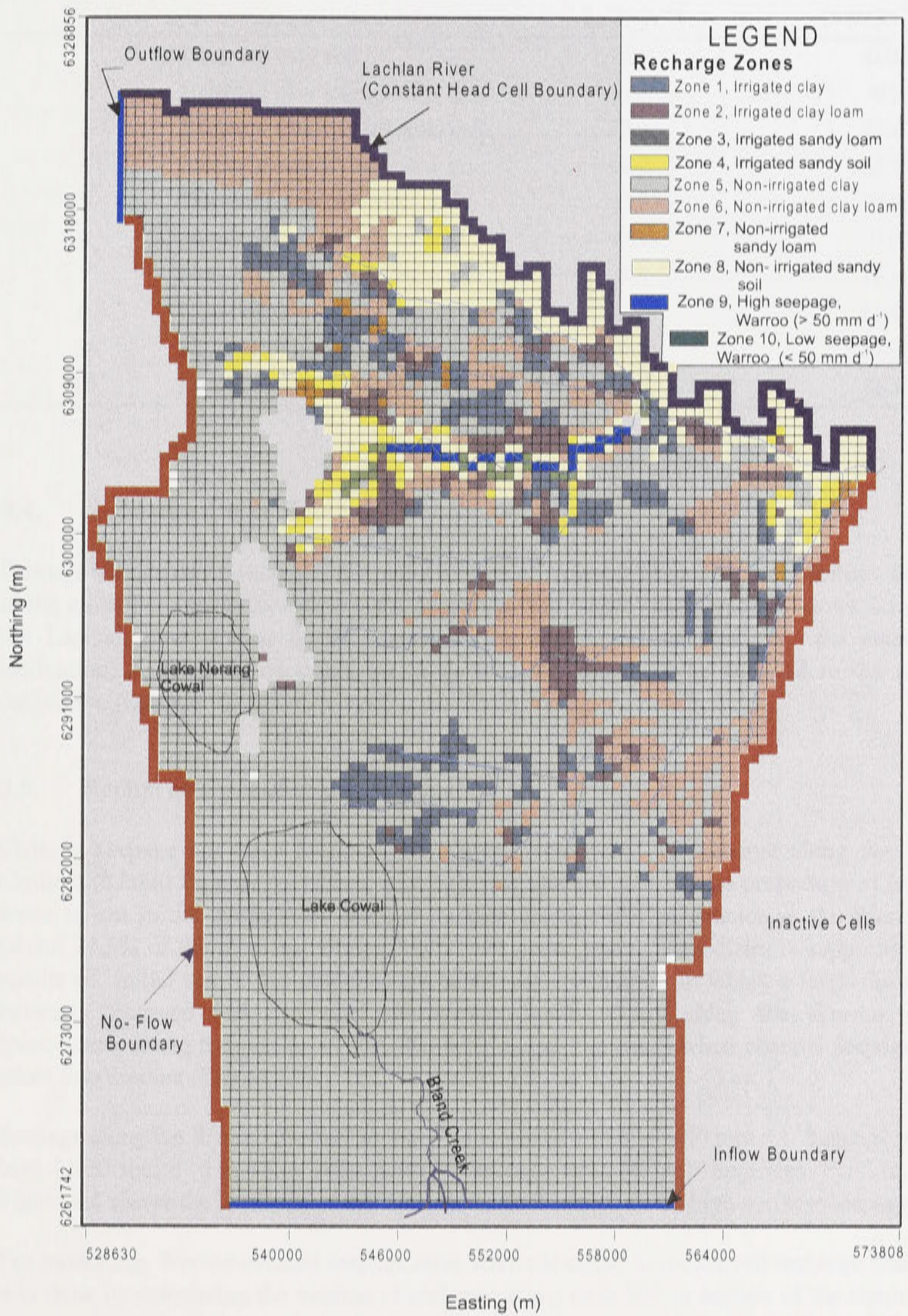


Figure 8.4: Distribution of recharge zones in the modelled area (see Table 8.4 for the recharge values).

Table 8.4: Initial and calibrated recharge values for the modelled area (see Figure 8.5 for locations)

Zone no.	Soil type	Initial recharge rates (mm yr ⁻¹)	Calibrated recharge rates (mm yr ⁻¹)
1	Irrigated clay soil	0.1	0.07
2	Irrigated clay loam soil	0.5	0.2
3	Irrigated sandy loam soil	20.6	22.4
4	Irrigated sandy soil	41.2	122.7
5	Non-irrigated clay soil	0.03	0.0005
6	Non-irrigated clay loam soil	0.16	0.07
7	Non-irrigated sandy loam soil	6.6	16.4
8	Non-irrigated sandy soil	13.2	17.0
9	High seepage Warroo	360.0	300.0
10	Low seepage Warroo	80.0	86.0

8.4. Recharge due to flooding

Farmers believe that flooding is the major source of recharge in the irrigation district. Flooding in the modelled area occurs below the Jemalong Gap where large overbank flows occur from the Lachlan river during floods. However, for the period selected for the steady-state calibration, no flooding occurred. Recharge from flooding will be assessed in the transient calibration (Chapter 9).

8.5. Recharge from channel seepage

Channel seepage has been found to be a major component of recharge along the Warroo Channel (Kinhill Engineers Pty Ltd, 1995). It was claimed that a large proportion of irrigation water is lost in the conveyance channel through seepage and percolation in the Warroo area (about 21.5% of the diversion during 1993/1994 water year). This claim is supported by the results of initial run of the model in the steady-state condition in which a large discrepancy between observed and computed piezometric heads occurs along the Warroo channel (particularly along the portion of the channel close to the river) when channel seepage is not taken into account (Figure 8.5).

Seepage along the Warroo channel sections which from 1 to over 300 mm d⁻¹. Seepage was into high (>50 mm d⁻¹) and low (<50 mm d⁻¹) seepage rates (Kinhill Engineers Pty Ltd, 1995). Figure 8.6 shows the locations of the Warroo channel sections with high and low seepage rates.

For modelling, Warroo channel seepage rates were converted to model cell recharge rates. This was done by calculating the volume of recharge along each 500 m section of the channel with an average width of 10 m and distributing this recharge over a model cell of 500m x 500 m. For

example, at the low seepage rate channel section ($<50 \text{ mm d}^{-1}$), the equivalent recharge rate in the model cell for channel seepage rate of $4,300 \text{ mm yr}^{-1}$ (11.8 mm d^{-1}) is calculated as:

$$R_c = \frac{4,00 \text{ mm yr}^{-1} \times 10 \text{ m} \times 500 \text{ m}}{500 \text{ m} \times 500 \text{ m}} = 86 \text{ mm yr}^{-1} \quad (8.1)$$

where R_c is the equivalent recharge rate in the model cell. The PEST calibrated equivalent recharge rates are 86 and 300 mm yr^{-1} in low and high seepage Warroo channel sections, respectively (Figure 8.6).

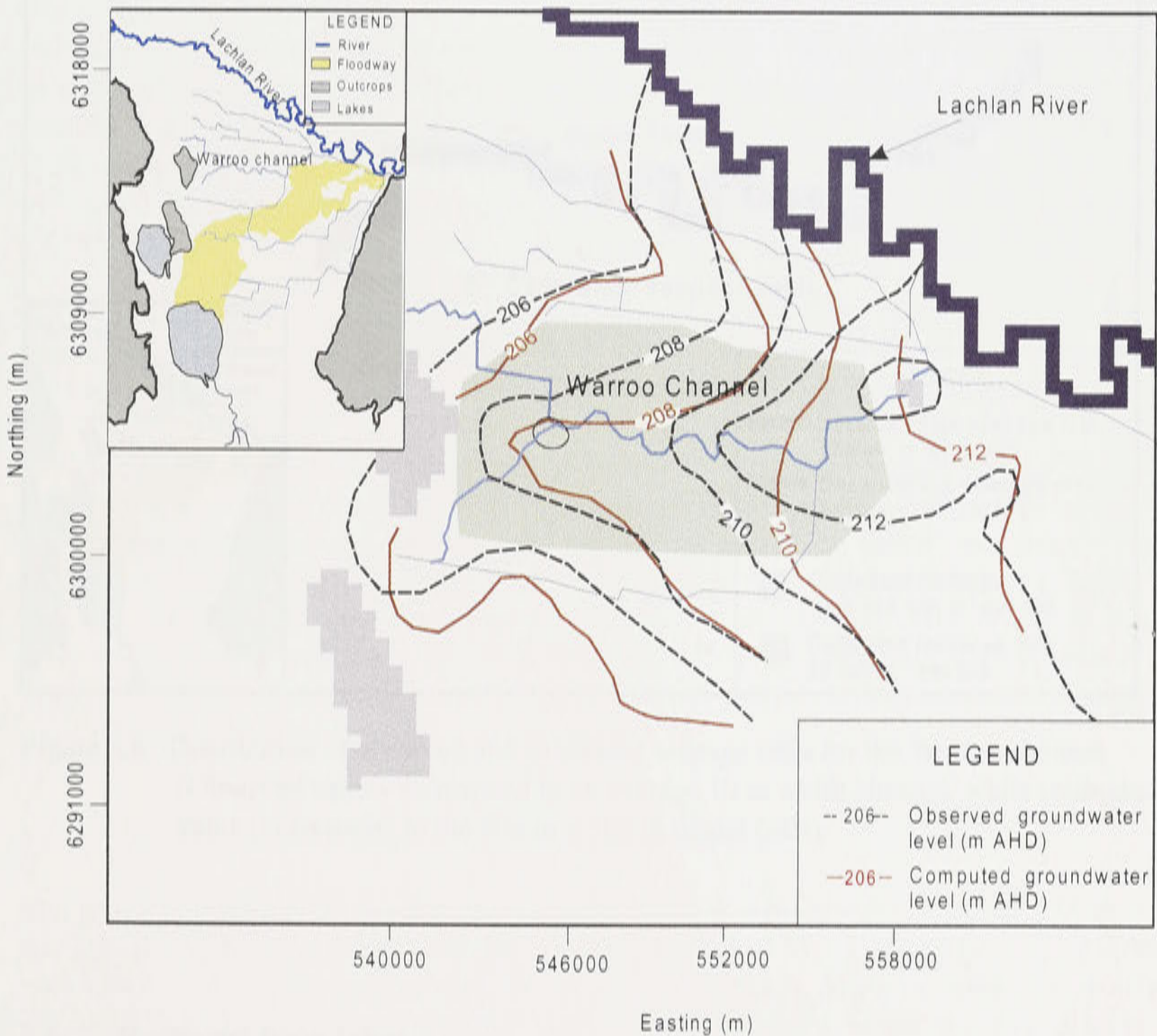


Figure 8.5: Comparison of observed and computed piezometric head distributions along Warroo channel without considering the channel seepage for April 1988.

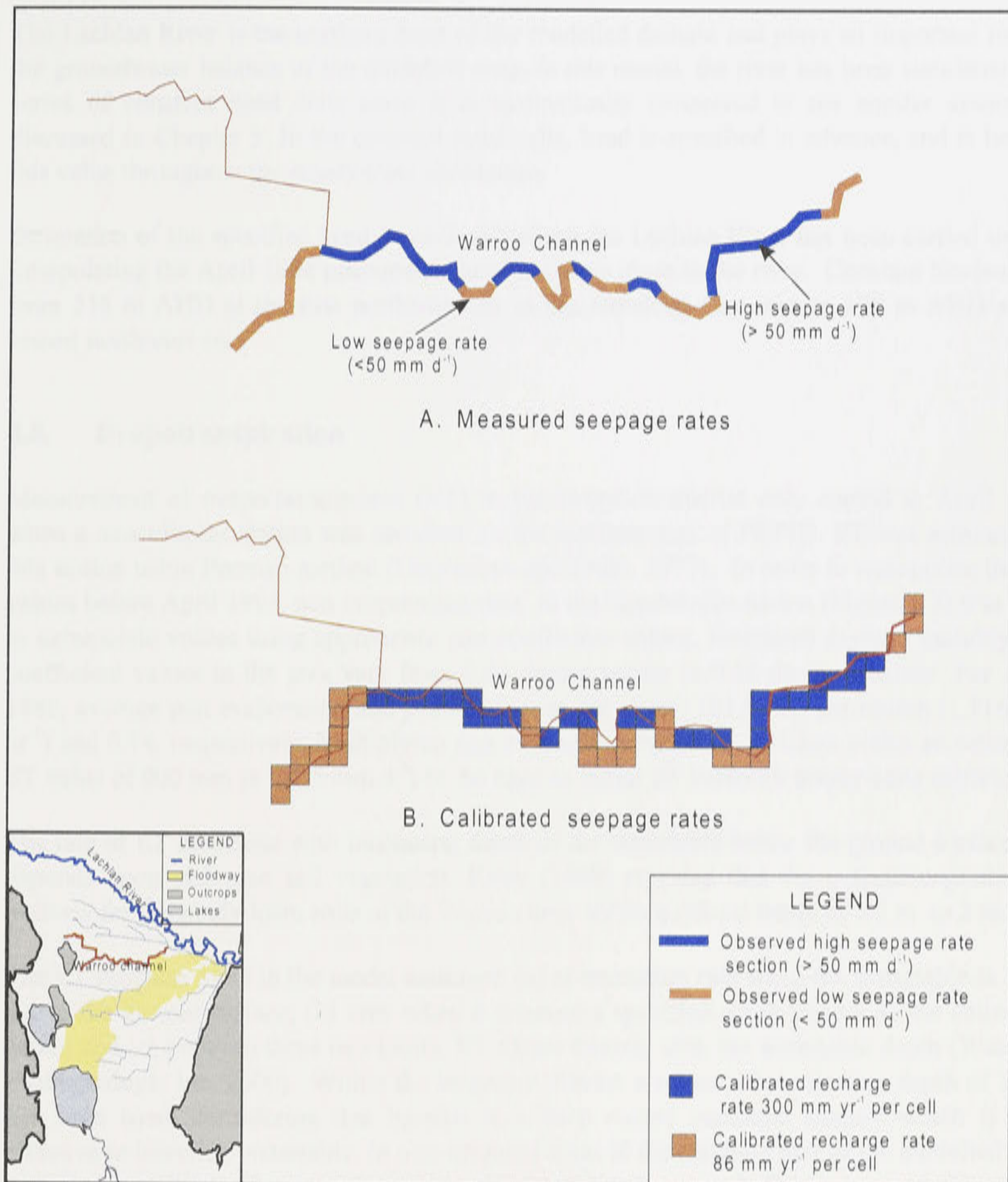


Figure 8.6: Distribution of observed and calibrated seepage rates for the Warroo channel. (Observed values correspond to an average 10 m width channel, while calibrated values correspond to the 500 m x 500 m model cells).

8.6. Recharge from lakes

Since the unconsolidated sediments in Lakes Cowal and Nerang Cowal area are dominated by a very thick clay layer (see Chapter 4), it has been assumed that surface water from the lakes is not recharging the groundwater system. This assumption has been substantiated by comparing the outputs of the model with and without recharge from the lakes.

8.7. Constant head cell boundary

The Lachlan River is the northern limit of the modelled domain and plays an important role in the groundwater balance of the modelled area. In this model, the river has been simulated as a series of constant head cells since it is hydraulically connected to the aquifer system as discussed in Chapter 5. In the constant-head cells, head is specified in advance, and is held at this value throughout the steady-state simulation.

Estimation of the specified head in each cell along the Lachlan River has been carried out by interpolating the April 1988 piezometric head contours close to the river. Constant heads range from 218 m AHD at the first northeast cell in the Jemalong Gap area to 198 m AHD at the lowest northwest cell.

8.8. Evapotranspiration

Measurement of evapotranspiration (ET) in the irrigation district only started in April 1995 when a new climate station was installed in the northern part of JWPID. ET was estimated at this station using Penman method (Doorenbos and Pruitt, 1977). In order to extrapolate the ET values before April 1995, pan evaporation data at the Condobolin station (Figure 2.2) was used to extrapolate values using appropriate pan coefficient values. Estimated average monthly pan coefficient values in the area vary from 0.66 during winter to 0.78 during summer. For April 1988, average pan evaporation and pan coefficient are about 101.3 mm per month (1,216 mm yr⁻¹) and 0.74, respectively. Multiplying pan evaporation by pan coefficient yields an estimated ET value of 900 mm yr⁻¹ (2.5 mm d⁻¹) to be used as initial ET value for steady-state calibration.

The rate of ET decreases with increasing depth of the watertable below the ground surface and depends upon soil type and vegetation. Kelly (1988) reported that the evapotranspiration is uniform for the sandy loam soils of the Warroo area within a critical depth of 1.5 m to 2 m.

The ET function used in the model assumed: (a) at maximum rate when the watertable is at or above the ground surface; (b) zero when it exceeds a specified depth known as the extinction depth; and (c) between these two limits, ET varies linearly with the watertable depth (Waterloo Hydrogeologic Inc, 2000). Within the irrigation district, a reasonable extinction depth of 2.5 m has been used, considering that lucerne is a deep rooted perennial pasture which is very effective in lowering watertable. In non-irrigated areas in the southern part of the modelled area, however, a calibrated lower extinction depth of 2 m has been used. This is because this area is mostly grown with natural pasture.

8.9. Inflow and outflow across aquifer boundaries

The inflow boundary of the southern part of the study area was simulated by a series of injection wells along this boundary with injection rates ranging from 0.5 to 60 m³ d⁻¹ per cell. High rates correspond to the middle of the boundary where the thickness of the sediments is maximum (Figure 8.7a). The rates were initially estimated using Darcy's Law but were adjusted in the calibration process. Outflow at the Manna Gap was similarly simulated using a series of pumping wells at each cell of the outflow boundary. Pumping rates were also initially estimated using Darcy's Law and were eventually adjusted during the calibration. A constant pumping rate of 0.5 m³ d⁻¹ for each well at the outflow boundary proved to be suitable (Figure 8.7).

0.7	1	1	1	1	1.5	2	3	4	4	5	13	18	18	20	20	20	20	40	60	60	60	60	60	60	60	60	60	60	60	60	60	60	15	15	15	12	12	12	12	8	8	6	3	2	2	1.5	1.5	1	0.8	0.8	0.5	0.5	0.5
-----	---	---	---	---	-----	---	---	---	---	---	----	----	----	----	----	----	----	----	----	----	----	----	----	----	----	----	----	----	----	----	----	----	----	----	----	----	----	----	----	---	---	---	---	---	---	-----	-----	---	-----	-----	-----	-----	-----

(A) Flow rates ($\text{m}^3 \text{d}^{-1}$) at each cell of the inflow boundary.

-0.5
-0.5
-0.5
-0.5
-0.5
-0.5
-0.5
-0.5
-0.5
-0.5

(B) Flow rates ($\text{m}^3 \text{d}^{-1}$) at each cell of the outflow boundary.

Figure 8.7: Distribution of flow rates at each cell of the inflow (A) and outflow (B) boundaries (see Figure 7.8).

8.10. Leakages through the basement's fractures

The output of the initial runs of the steady-state model showed that results were unsatisfactory unless leakages into the fractured basement rocks were taken into account. As shown on Figure 8.8, major differences between the computed and observed piezometric heads are in the areas near Manna Gap (Fracture line A), Jemalong Gap (Fracture line B), and to the north-east of Lake Cowal (Fracture line C).

In order to simulate the assumed leakages, three series of pumping wells have been placed in the lower aquifer close to the basement along the estimated three fracture lines A, B and C in Figure 8.8. Fracture lines A and B have been assigned with uniform leakage rate of $200 \text{ m}^3 \text{ d}^{-1}$ per cell, while a lower leakage rate of $23 \text{ m}^3 \text{ d}^{-1}$ per cell has been adequate for the two adjacent rows of 11 cells (44 cells in total) for the fracture line C.

8.11. Drainage of the system by the Gilmore Fault

The Gilmore Fault (see Figure 4.2) which lies along the edges of the Manna Range has been believed to be a conduit for groundwater drainage in this area (Coffey Partners International Pty Ltd, 1994). Here, the Gilmore Fault has been simulated as a drain (Figure 8.9). In simulating the drainage through the fault, it has been assumed that the drain removes water from the aquifer at a rate proportional to the difference between the head of the aquifer and the fixed head or elevation of the drain. Also it has been assumed that the drain has no effect if the head in the aquifer falls below the fixed head of the drain. Drain elevation and conductance have been defined for each cell of the drain. A range of drain elevations of 205 m AHD at the southernmost region to about 198.1 m AHD in the northernmost area has been used, while a conductance value of $30 \text{ m}^3 \text{ d}^{-1}$ were adopted for all drain cells.

8.12. Results of the steady-state calibration

8.12.1. Observed versus computed piezometric heads

After a series of adjustments of the initial values of parameters with the support of PEST, and taking into account vertical leakages to the basement rocks, the observed and the computed piezometric head values became reasonably close (Figure 8.10).

The relation between computed versus observed heads for the 88 observation points mostly located between the Lake Cowal area and the Lachlan River (see Figure 5.2) is shown in Figure 8.11. The number of observation points are limited in the southern part of the modelled area. Figure 8.11 provides a graphical representation of the quality of the fit between the observed data and the computed results. Calibration statistics (see Appendix L for definition) such as the mean error (-0.21 m), mean absolute error (0.67 m), the standard error of estimate (0.09 m), the root mean squared error (0.9 m), and the normalised root mean squared error (4.4%) shown in Figure 8.11 indicate that the model is well calibrated.

A comparison of the results of this calibration against that of Coffey's model (Figure 7.2) shows that the present work has achieved significantly better agreement. Coffey's model did not assume leakage and therefore was not able to assess its impact on the behaviour of the aquifer. Coffey's model heads are more than 3 metres higher than the observed heads in the northeast of the Lake Cowal.

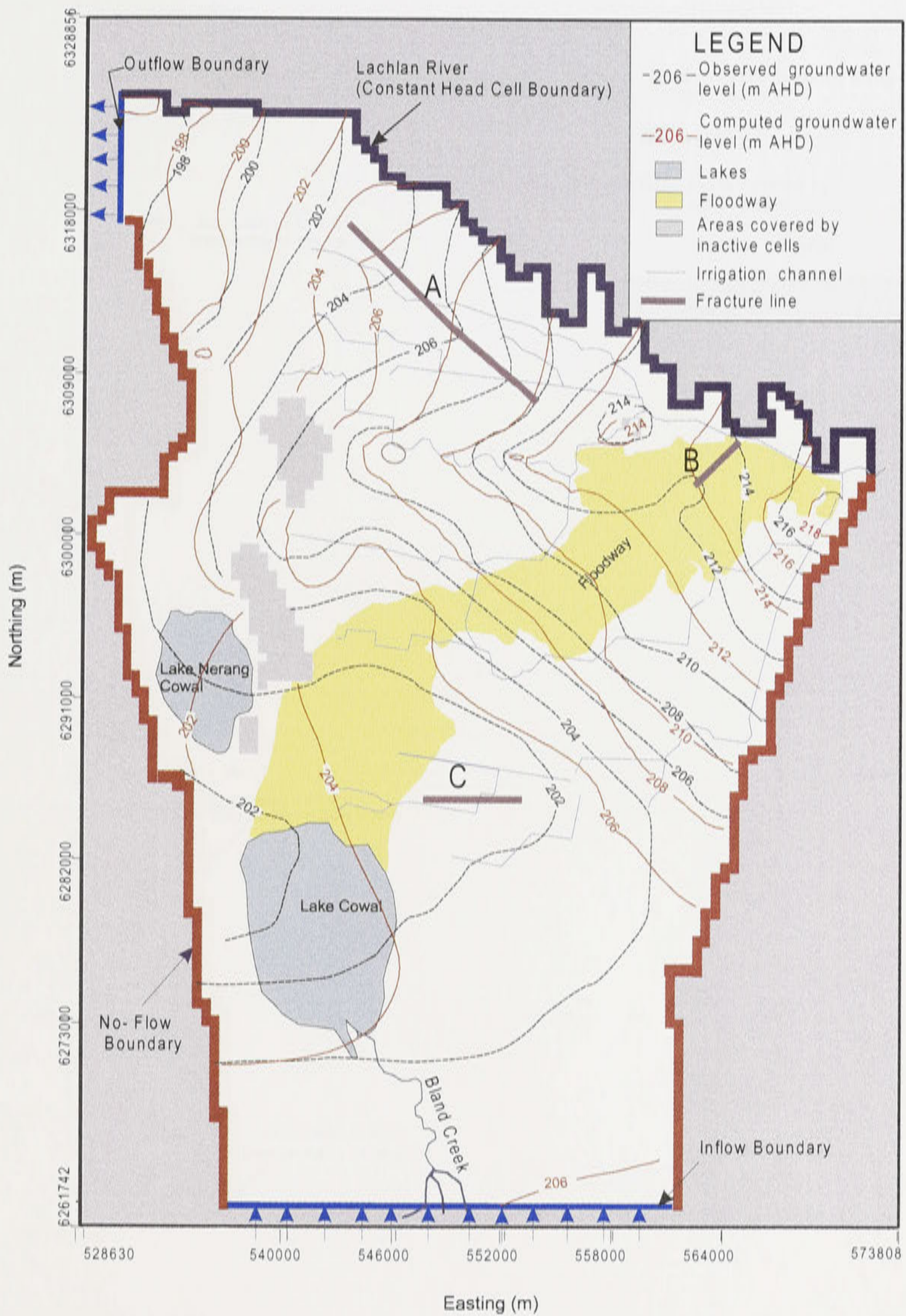


Figure 8.8: Distribution of computed piezometric heads for April 1988 in the modelled area without leakage through the basement.

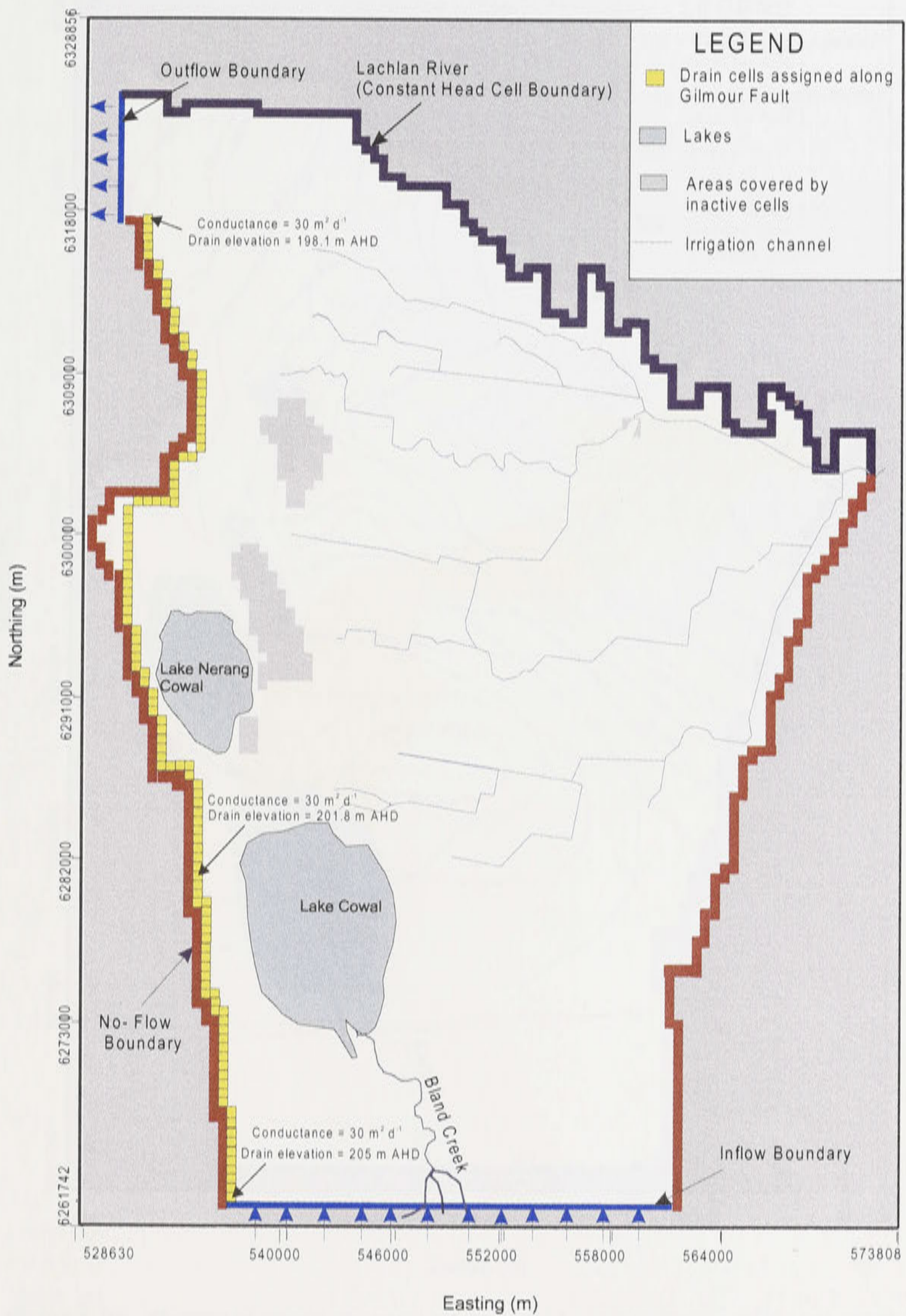


Figure 8.9: Distribution of drain cells along the Gilmore Fault in the western side of the modelled domain.

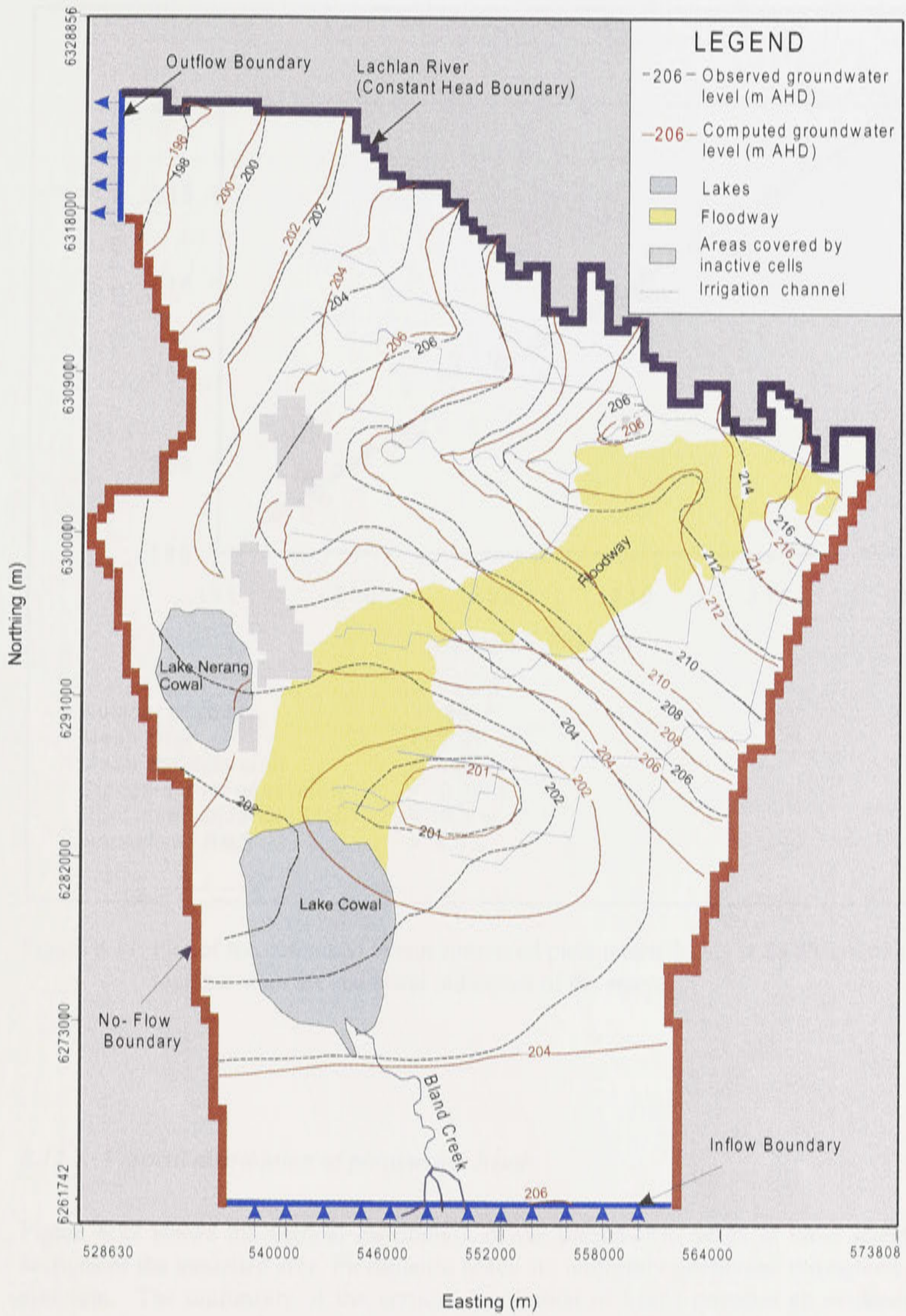


Figure 8.10: Computed versus observed piezometric head distribution of the top aquifer for April 1988.

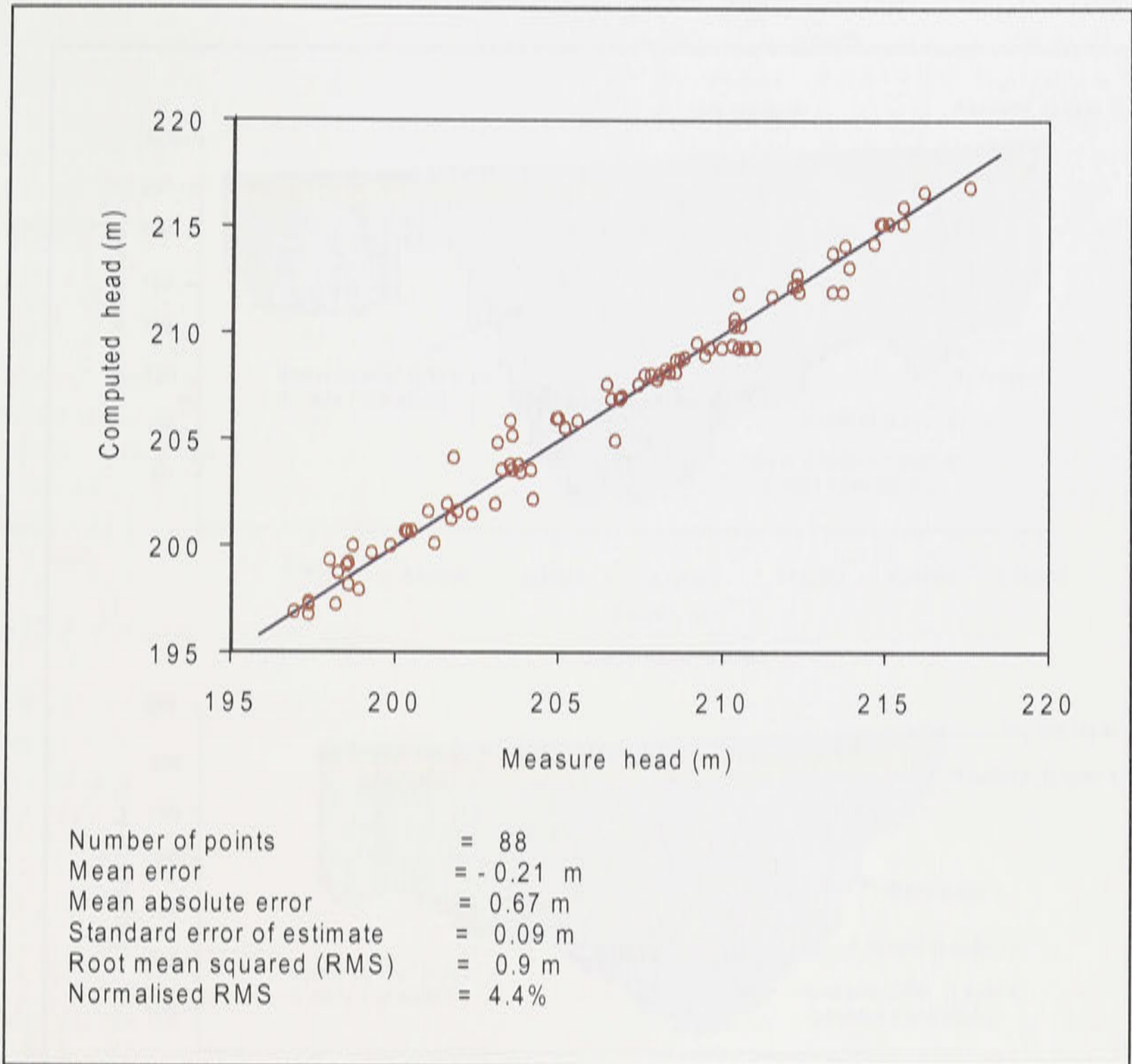


Figure 8.11: Plot of the computed versus measured piezometric heads at 88 observation points together with the statistical indicators of the errors.

8.12.2. Vertical distribution of piezometric heads

Figure 8.12 shows the vertical distribution of the piezometric heads in three selected cross-sections of the modelled area. Piezometric heads are uniformly distributed throughout the entire alluvium. The uniformity of the vertical distribution of heads provides an evidence that the upper and lower aquifer are behaving as a single unconfined aquifer system, although as mentioned in Chapter 5, local scale individual sand and gravel lenses may display their own characteristics as local confined or semi-confined aquifers.

Piezometric head variation across the southern cross-section C-C' is very low, ranging from 203.8 to 203.9 m AHD. This is due to the fact that this cross-section is parallel with the piezometric contour of 204 m.

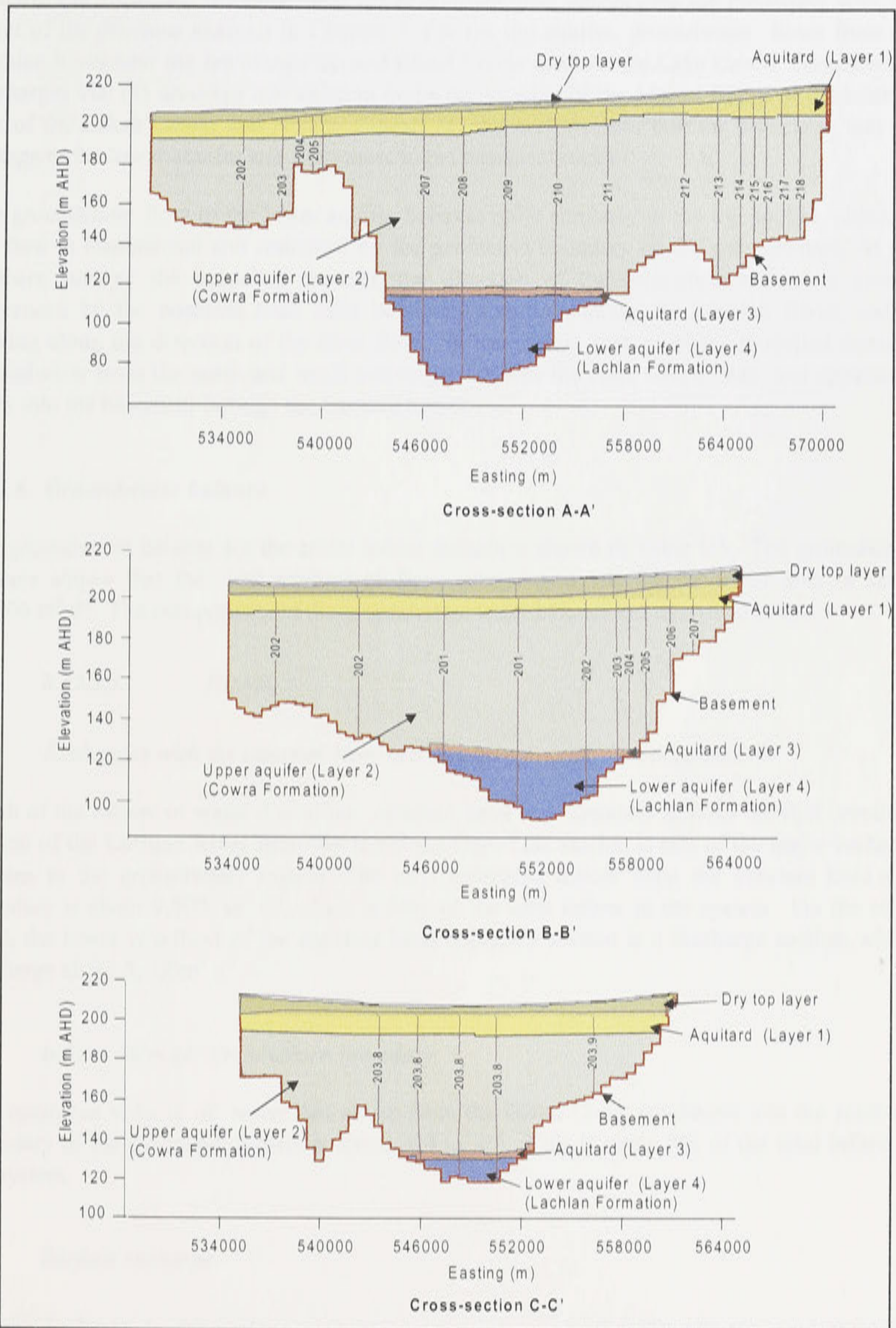


Figure 8.12: Vertical distribution of the piezometric heads in three selected cross-sections of the modelled domain.

8.12.3. *Direction of groundwater flow*

Figures 8.13 and 8.14 show the computed piezometric head distribution and direction of groundwater flows for the upper and lower aquifers. The movements are consistent with the result of the previous analysis in Chapter 5. For the top aquifer, groundwater flows from the Lachlan River near the Jemalong Gap and Bland Creek towards the Lake Cowal. Groundwater discharges via: (1) drainage into existing faults on the edge of the Manna Range at the western part of the Lakes Cowal and Nerang Cowal; (2) the northwestern outflow boundary; and (3) leakage to the lower aquifer and from there to the basement rocks.

The groundwater flow in the lower aquifer behaves quite similarly to the top aquifer, although the flow is channelised and restricted by the geometric boundary of the paleochannel. At the northern part of the modelled domain, the direction of the groundwater flow is greatly influenced by the constant head cells boundary condition along the Lachlan River, and is moving along the direction of the river flow. In the middle section of the modelled domain, groundwater from the north and south converges towards the Lake Cowal area, and apparently leaks into the basement through the fracture line C.

8.12.4. *Groundwater balance*

The groundwater balance for the entire model domain is shown in Table 8.5. The groundwater balance shows that the total amount of flow entered and left the modelled area is about 30,000 m³ d⁻¹. The components of the groundwater water balance are described below:

8.12.4.1. *Inputs*

a. *Exchanges with the constant head cell boundary along the Lachlan River*

Much of the inflow of water due to the constant head cell boundary is from the first one-third section of the Lachlan River from the Jemalong Gap. This section is one of the major recharge sources to the groundwater system. The total estimated inflow from the constant head cell boundary is about 9,900 m³ d⁻¹. This is 34% of the total inflow to the system. On the other hand, the lower two-third of the constant head boundary section is a discharge section, which discharge about 5,100m³ d⁻¹.

b. *Inflow through the southern boundary*

The estimated volume of water that enters from the Bland Creek catchment into the southern boundary of the modelled domain is about 914 m³ d⁻¹. This is about 3% of the total inflow to the system.

c. *Surface recharge*

Surface recharge is the main contributor to the inflows to the groundwater system in the modelled area. For the steady-state simulation in April 1988, the total amount of recharge is about 19,500 m³ d⁻¹ (7,100 ML yr⁻¹) which is about 66% of the total inflow (Table 8.5). This simulated recharge is close to the recharge estimate of 8,000 ML yr⁻¹ by Williams (1993) for the study area and is equivalent to 4.2 mm yr⁻¹ if spread uniformly throughout the modelled domain.

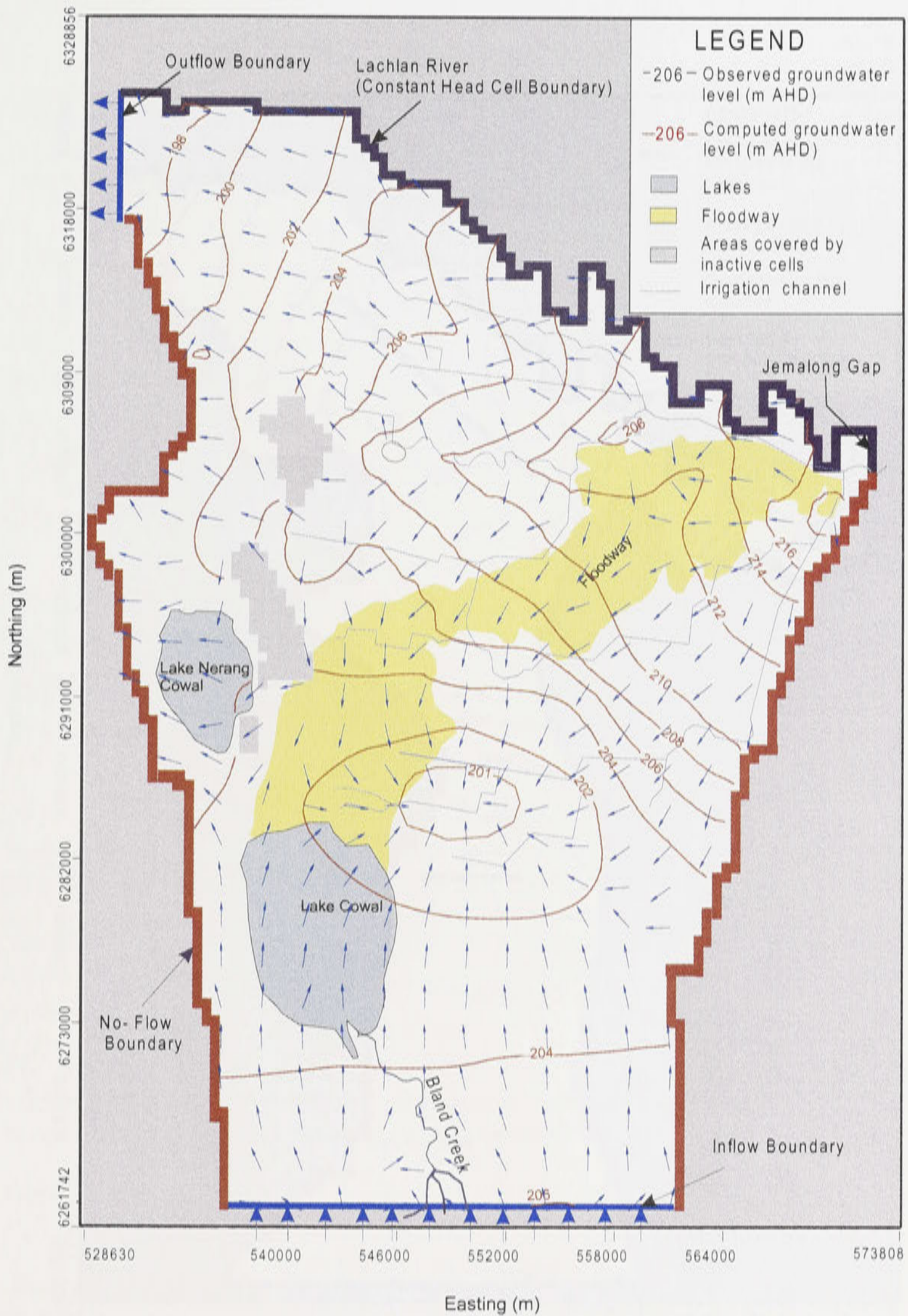


Figure 8.13: Computed piezometric heads and direction of groundwater flow for the upper aquifer in April 1988.

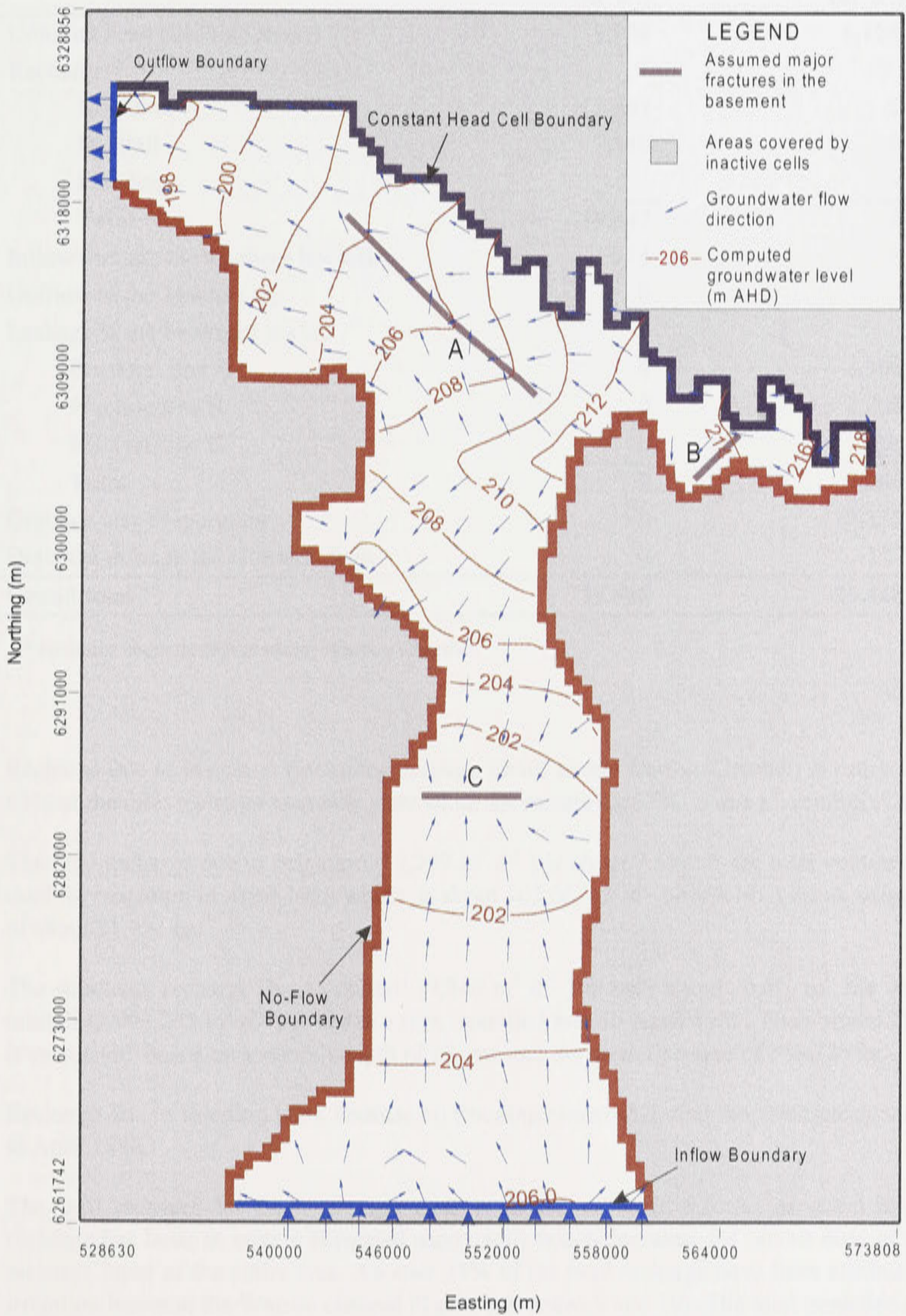


Figure 8.14: Computed piezometric heads and direction of groundwater flow for the lower aquifer in April 1988.

Table 8.5: Steady-state groundwater balance of the modelled area.

Component	Input (m ³ d ⁻¹)	Output (m ³ d ⁻¹)
Constant head (Lachlan River)	9,908	5,125
Recharge:		
Irrigation*	12,207	0
Rainfall	7,240	0
Flooding	-	-
Total	19,447	0
Inflow through the southern boundary	914	0
Outflow in the Manna Gap	0	7
Leakage to the basement rocks:		
Fracture line A	0	5,300
Fracture line B	0	1,200
Fracture line C	0	506
Total	0	7,006
Groundwater evaporation	0	17,183
Drainage through the Gilmore fault	0	127
Grand total	29,448	29,448

* Includes seepage losses along Warroo Channel.

Recharge due to irrigation (including seepage losses along Warroo Channel) is estimated to be 63% of the total recharge as steady state while the remaining 37% is due to rainfall (Table 8.5).

The total recharge due to irrigation (12,207 m³ d⁻¹) is about 7.5% of the total volume of water used for irrigation in April 1988 which is about 162,067 m³ d⁻¹ (4,862 ML) for an irrigated area of about 21,731 ha.

The simulated recharge due to rainfall (7,240 m³ d⁻¹) is only about 0.4% of the volume of rainfall (2,093,275 m³ d⁻¹) over the entire modelled area in April 1988. The volume of rainfall is calculated based on a rainfall depth of 37 mm and the modelled area of 169,725 ha.

Recharge due to flooding is nil because no flooding occurred during the steady-state simulation in April 1988.

The total recharge for each recharge zone is shown in Table 8.6. As expected the highest recharge has been in zone 4 (irrigated sandy soil) which accounts for about 40% of the total recharge input of the entire area. Another 35% of the total recharge have been attributed to the irrigation losses at the Warroo channel (Table 8.6, zones 9 and 10). The total modelled recharge due to irrigation losses at the Warroo channel of 6,850 m³ d⁻¹ (2,500 ML yr⁻¹) is close to the seepage loss estimate of 5,480 m³ d⁻¹ (2,000 ML yr⁻¹) for the Warroo channel by van der Lely (1993).

Table 8.6: Total recharge rate at each recharge zone in the modelled domain.

Zone no.*	Soil type	Total Recharge (m ³ d ⁻¹)	Percent of total recharge (%)
1	Irrigated clay soil	41	0.2
2	Irrigated clay loam soil	38	0.2
3	Irrigated sandy loam soil	16	0.1
4	Irrigated sandy soil	7749	39.9
5	Non-irrigated clay soil	41	0.2
6	Non-irrigated clay loam soil	259	1.3
7	Non-irrigated sandy loam soil	4188	21.5
8	Non-irrigated sandy soil	260	1.3
9	High seepage section, Warroo Channel	5414	27.9
10	Low seepage section, Warroo Channel	1432	7.4
Total		19438	100

* See Figure 8.4 for locations.

8.12.4.2. *Outputs*

a. *Outflow at the Manna Gap and the constant head boundary*

Outflow at the Manna Gap is relatively low (7 m³ d⁻¹). A major proportion of the outflow through the constant head cells boundary (5,125 m³ d⁻¹) takes place along the lower third part of the Lachlan River.

b. *Leakage to the basement rocks*

Calibration of the steady-state model showed that without assuming a leakage component into fractured basement, modelling results give unsatisfactory agreement with measured heads. As shown in Table 8.5, the total amount of leakage is about 7,000 m³ d⁻¹, where a major part of this (about 93%) occurs near the Lachlan River (Fracture lines A and B). The total leakage constitutes 23% of the total outflow in the system. On the other hand, only about 506 m³ d⁻¹ is estimated to be lost in the basement along Fracture line C. It should be noted that the fracture lines A, B and C appear to have helped in preventing the watertable from rising significantly. This could lower the rate of land salinisation expansion.

c. *Drainage to Gilmore Fault*

Calibration of the steady-state model has also estimated the volume of groundwater which drained by the to Gilmore Fault. The Gilmore Fault (see Figure 4.2) lies along the edges of the Manna Range and is believed to be the major conduit of groundwater in this area. The result of

the calibration shows that only about $125 \text{ m}^3 \text{ d}^{-1}$ is drained through the Fault. It does not appear to be a major conduit.

d. Evapotranspiration

Evapotranspiration provides the major output component of the groundwater balance in the modelled area. As shown in Table 8.5, about $17,200 \text{ m}^3 \text{ d}^{-1}$ (58% of the total output) is lost from the groundwater system. This is equivalent to 3.7 mm yr^{-1} over the entire modelled area.

Transient calibration will now be discussed.

CHAPTER 9

TRANSIENT CALIBRATION

9.1. Introduction

Following steady-state calibration, groundwater models should be calibrated in transient condition because groundwater systems are dynamic and their pressures fluctuate over time, mainly due to changes of recharge, discharge and extraction.

Here, the transient calibration is undertaken in the period between May 1988 and July 1997, in which major floodings and droughts occurred. The simulation period is divided into monthly stress periods. A stress period is defined as a period in which all the stresses on the system are constant. Stress periods can in turn be divided into timesteps. In this modelling study, each stress period is assigned a single timestep. Overall, 111 monthly timesteps (or stress periods) were generated for the entire transient simulation period (Appendix M).

Transient calibration was performed by adjusting the spatially-distributed and time-dependent parameters. The spatially-distributed parameters are hydraulic conductivities, and storage coefficients, while time-dependent parameters include: recharge, evapotranspiration, constant potentiometric heads along the Lachlan River, leakages to the basement's fractures, drainage through Gilmore Fault, and inflows and outflows through the flow boundaries.

9.2. Hydraulic conductivity

Optimisation of K values for transient condition was also undertaken using PEST software. The calibrated K values in the steady-state model (Table 8.1 and 8.2) were used as initial values for the optimisation process. The results showed K values calibrated in steady-state were adequate.

9.3. Storage coefficients

The range of storage coefficients for each aquifer (Table 9.1) have been estimated by trial and error method based on specific storage coefficients. Specific storage coefficient of 0.00005 m^{-1} was estimated for Layer 2, while a lower specific storage coefficient value of 0.000005 m^{-1} has been estimated for Layer 4. The model uses specific storage coefficient as input, however storage coefficient can be estimated by multiplying specific storage coefficient by the aquifer thickness. This means that storage coefficient at Layer 2 (upper aquifer) ranges from 0.002 to 0.0045, since a large portion of this layer has a thickness of 40 to 90 m (see Figure 7.6). For Layer 4 (lower aquifer) with a thickness of 20 to 40 m, storage coefficient ranges from 0.001 to 0.002. The calibrated storage coefficients are comparable with the pumping test results at the three sites in the irrigation district (Figure 5.18) by Coffey Partners International Pty Ltd (1994).

The storage coefficient for Layer 1 has also been estimated by trial and error method. The distributions of storage coefficient zones for this layer are identical to the hydraulic

conductivity zones (Figure 8.3). Storage coefficients of Layer 1 in Table 9.1 range from 0.01 to 0.04, with higher values assigned to sandy loam and sandy soils zones.

Table 9.1: Calibrated storage coefficients.

Layer*	Storage coefficient
Layer 1:	
zone A1 (clay soil)	0.01
zone B1 (clay loam soil)	0.01
zone C1 (sandy loam soil)	0.03
zone D1 (sandy soil)	0.04
Layer 2	0.002-0.0045
Layer 4	0.001-0.002

* See Figure 7.5. and 8.12.

9.4. Recharge due to rainfall and irrigation

The steady-state calibration showed that the amount of recharge to the aquifer from rainfall and irrigation varies from one part of the study area to another, mainly due to differences in soil types and land uses. As a result, eight recharge zones (excluding the Warroo channel) were identified to represent these variabilities (see Chapter 8). Based on the result of the steady-state calibration, an initial recharge factor (percentage of the calibrated recharge with respect to the volume of available rainfall or irrigation water) has been derived for each zone.

In transient modelling, calibration of recharge factor for each zone was undertaken by trial and error method. Monthly rainfall and delivered irrigation water for 1988 to 1997 are shown in Figures 9.1 and 9.2. Higher recharge factors of 2 to 7.5 % have been used in sandy soils, while very low recharge factors (0.15 to 0.5%) have been used for clay soils (Table 9.2).

9.5. Recharge due to flooding

Flooding has a major impact on the piezometric levels of the groundwater system in the irrigation district. Major floodings in 1990 raised the groundwater levels in the vicinity of Lakes Cowal and Nerang Cowal and along the Warroo area (Figure 5.14) to more than 3 m from the 1969 levels. As mentioned earlier, flooding in the area occurs below the Jemalong Gap where large overbank flows occur from the Lachlan River and floodwaters spread over a large area. A large proportion of the floodwaters enters the area through the 17 mile and 21 mile breakouts (Figure 3.18). Generally, the 17 and 21 mile breakouts commence to flow when the gauge height at the Jemalong Weir reaches a relative level of 7.53 m and 7.31 m, respectively. Figure 9.3 shows the daily water level at the Jemalong Weir gauging station, and

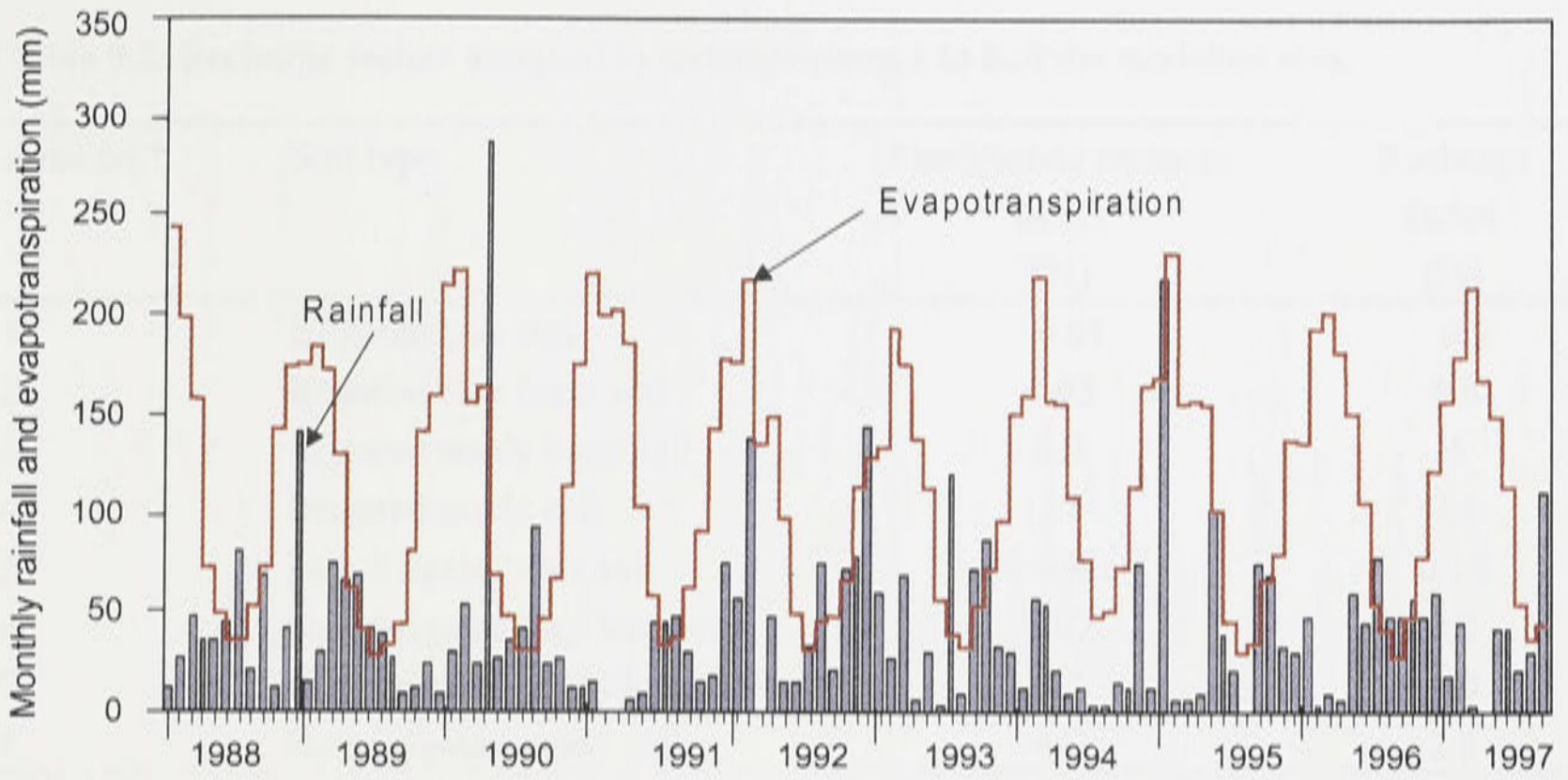


Figure 9.1: Monthly rainfall and evapotranspiration in the modelled area from 1988 to 1997.

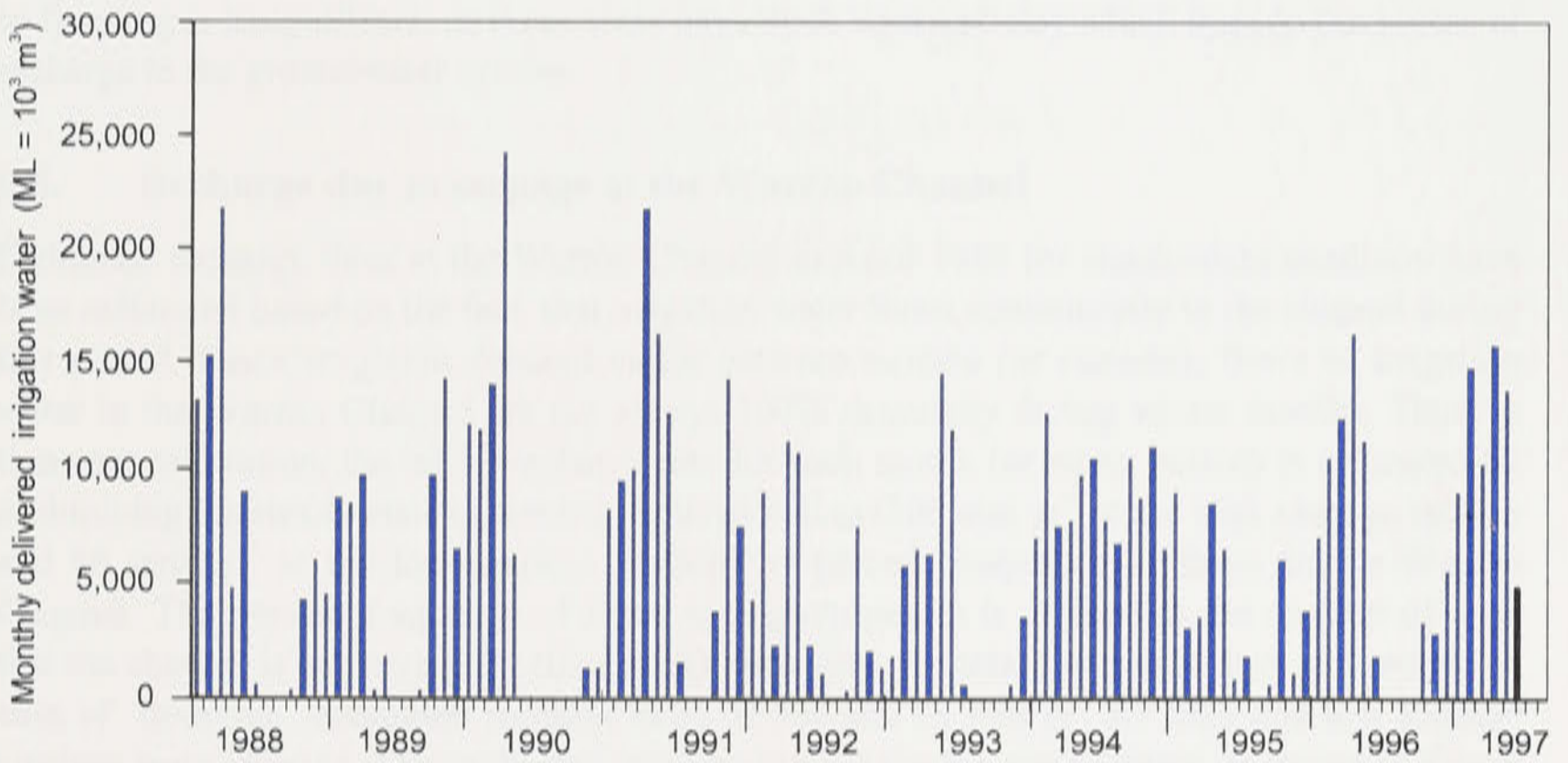


Figure 9.2: Monthly delivered irrigation water in the modelled area from 1988 to 1997.

Table 9.2: Recharge factors assigned to recharge zones 1 to 8 of the modelled area.

Zone no.*	Soil type	Steady-state recharge factor (%)	Recharge factor (%)
1	Irrigated clay soil	0.01	0.5
2	Irrigated clay loam soil	0.03	0.8
3	Irrigated sandy loam soil	3.2	4
4	Irrigated sandy soil	17	7.5
5	Non-irrigated clay soil	0.0001	0.15
6	Non-irrigated clay loam soil	0.02	0.2
7	Non-irrigated sandy loam soil	3.7	1.0
8	Non-irrigated sandy soil	4.0	2.0

*Recharge zone 9 and 10 are discussed in section 9.6.

the period of overflows at the 21 mile breakout between 1988 to 1997. Based on this gauging record, the 1990 flood was considered to be the longest flood event that occurred in the study area during this period. Calibrated recharge rates due to flooding at the floodway ranged from 100 mm yr⁻¹ to about 300 mm yr⁻¹ in flooded clay soils to sandy soils, respectively (Table 9.3). However, in the southern part of the modelled area and areas around Lake Cowal, recharge due to flooding is insignificant, as these areas have thick layers of clay which impede the access of recharge to the groundwater system.

9.6. Recharge due to seepage at the Warroo Channel

Estimated recharge rates at the Warroo Channel in April 1988 for steady-state condition have been calibrated based on the fact that irrigation water flows continuously in the channel during this period. Since irrigation demand varies between months (or seasons), flows of irrigation water in the Warroo Channel are not always 100% especially during winter months. Thus, in transient calibration, the initial recharge rate for each month (or stress period) is estimated by multiplying the steady-state calibrated recharge values (300 mm yr⁻¹ at the high seepage section and 86 mm yr⁻¹ at the low seepage section) by percent frequency of flows in the Warroo Channel. The percent frequency of flows in a given month is defined as the number of days that the channel is conveying (or filled with) water over the total number of days in a month. In case of flooding, maximum recharge rates of 300 and 86 mm yr⁻¹ for high and low seepage sections were adopted. The calibrated recharge rates at the Warroo Channel is shown in Figure 9.4.

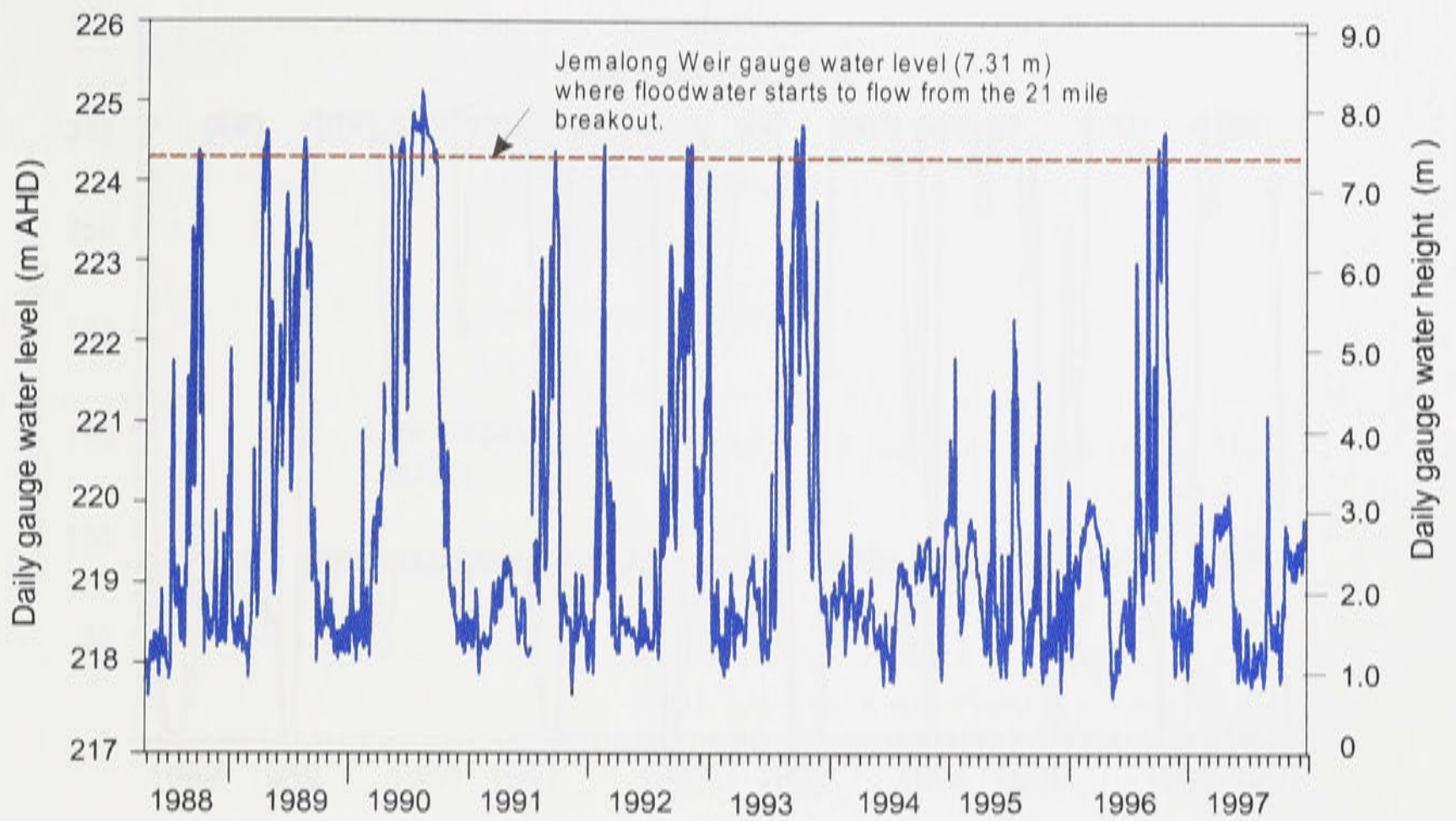


Figure 9.3: Lachlan River water level at the Jemalong Weir gauging station.

Table 9.3: Calibrated recharge at the floodway during flooding events from May 1988 to July 1997.

Zone no.*	Soil type	Calibrated recharge (mm yr ⁻¹)
1	Irrigated clay soil	100
2	Irrigated clay loam soil	150
3	Irrigated sandy loam soil	250
4	Irrigated sandy soil	300
5	Non-irrigated clay soil	150
6	Non-irrigated clay loam soil	150
7	Non-irrigated sandy loam soil	250
8	Non-irrigated sandy soil	300

* see Figure 9.4 for locations.

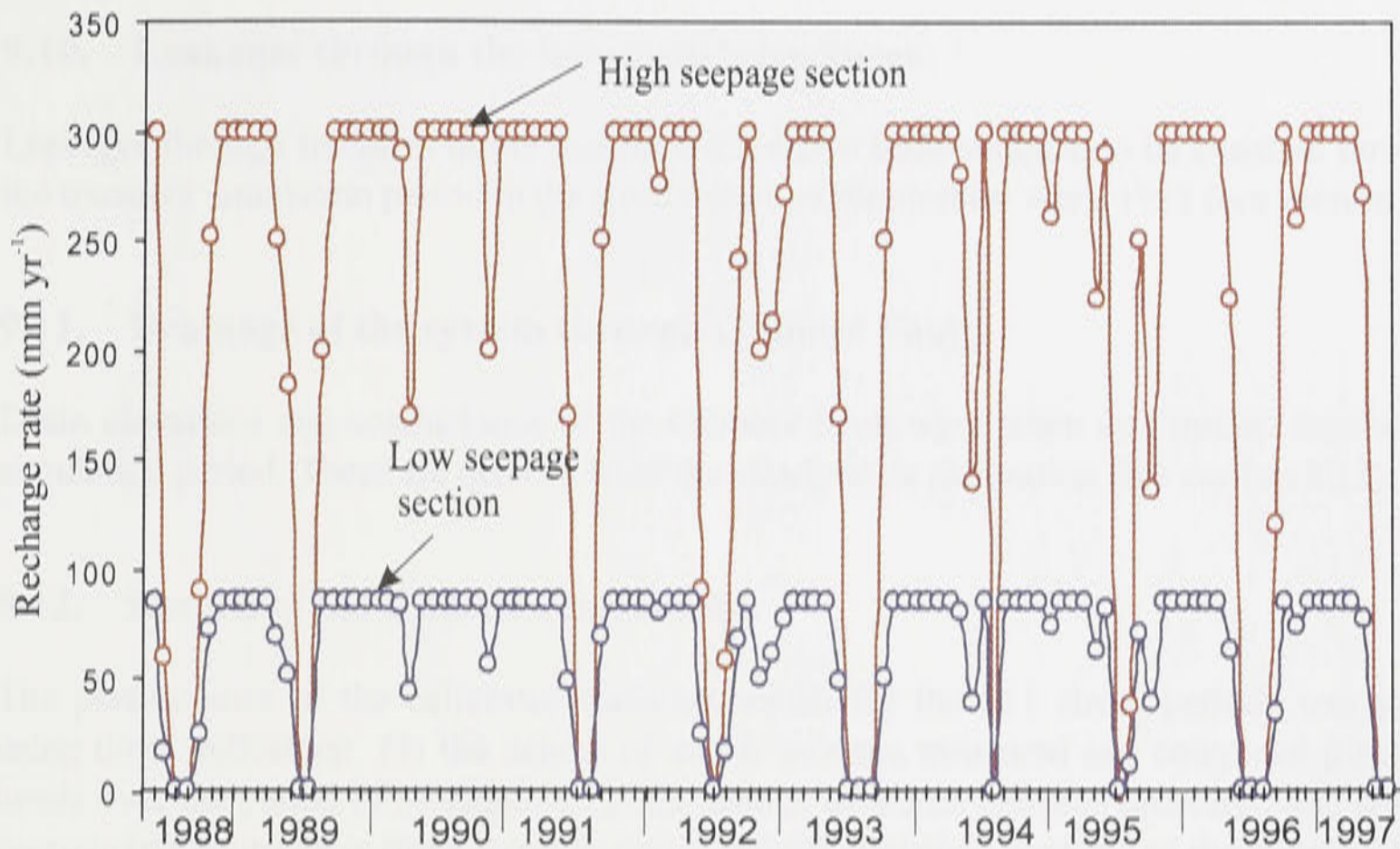


Figure 9.4: Recharge rates in the high and low seepage sections of the Warroo channel.

9.7. Constant head cell boundary

In the original USGS MODFLOW package (McDonald and Harbaugh, 1988) constant head boundaries could not be changed during transient simulations. However, Visual MODFLOW includes the time-varying constant head in the package. Values of the constant head cells along the Lachlan River in each stress period during the transient calibration have been estimated by using measured piezometric heads close to the Lachlan River. Constant heads have been interpolated for the periods with no piezometric head measurements.

9.8. Evapotranspiration

Figure 9.1 shows the evapotranspiration (ET) used for transient modelling. Monthly ET values for the entire period ranged from 26 mm during winter months to 240 mm during summer months. The computation of ET from the shallow watertable has already been explained in section 8.8.

9.9. Inflow and outflow across aquifer boundaries

The inflow rates from the steady-state simulation for the southern boundary of the modelled area (Figure 8.7) have been adopted for the transient simulation, and are assumed to be constant throughout the simulation period. On the other hand, the constant flow rates per cell used in the outflow boundary had been increased from 0.5 to $2 \text{ m}^3 \text{ d}^{-1}$ for all timesteps during the calibration process.

9.10. Leakages through the basement's fractures

Leakages through fractures in the basement have also been assumed to be constant throughout the transient simulation period in the steady-state calibration for April 1988 (see section 8.10).

9.11. Drainage of the system through Gilmore Fault

Drain elevations and conductance of the Gilmore Fault were taken as constant for the whole simulation period. These are derived from the steady-state calibration (see section 8.11).

9.12. Results of the transient calibration

The performance of the calibrated transient model for the 111 stress periods was assessed using three indicators: (1) the degree of match between measured and computed piezometric heads over the period of simulation; (2) the degree of match between measured and computed piezometric contours at three stress periods; and (3) statistical analysis of the degree of match between the measured and computed heads. These are described in detail in the following sections.

9.12.1. Match between measured and computed heads over the period of simulation at selected observation wells

During the calibration process, the match between measured and computed heads was checked at 16 selected observation wells (Figure 9.5). Comparisons between measured and computed heads at the selected observation wells are shown in Figures 9.6a to 9.6d. In general, computed heads show a good match with the measured heads for the period of simulation at all observation wells.

9.12.2. Match between measured and computed head contours at three selected stress periods

The match between the piezometric head contours interpolated from computed and measured piezometric heads for October 1990 (timestep 30), October 1994 (timestep 78) and July 1997 (timestep 111) are shown in Figures 9.7 to 9.9. Figure 9.7 represents the period of high groundwater level as a result of the major flood that occurred in the area in 1990, while Figure 9.8 represents the period of decline in groundwater heads. Figure 9.9 depicts the final time step for the calibrated model. In general, there is a good match between computed and the measured heads, except in areas around Lake Cowal where the measured head contours are not very accurate due to limited number of piezometers.

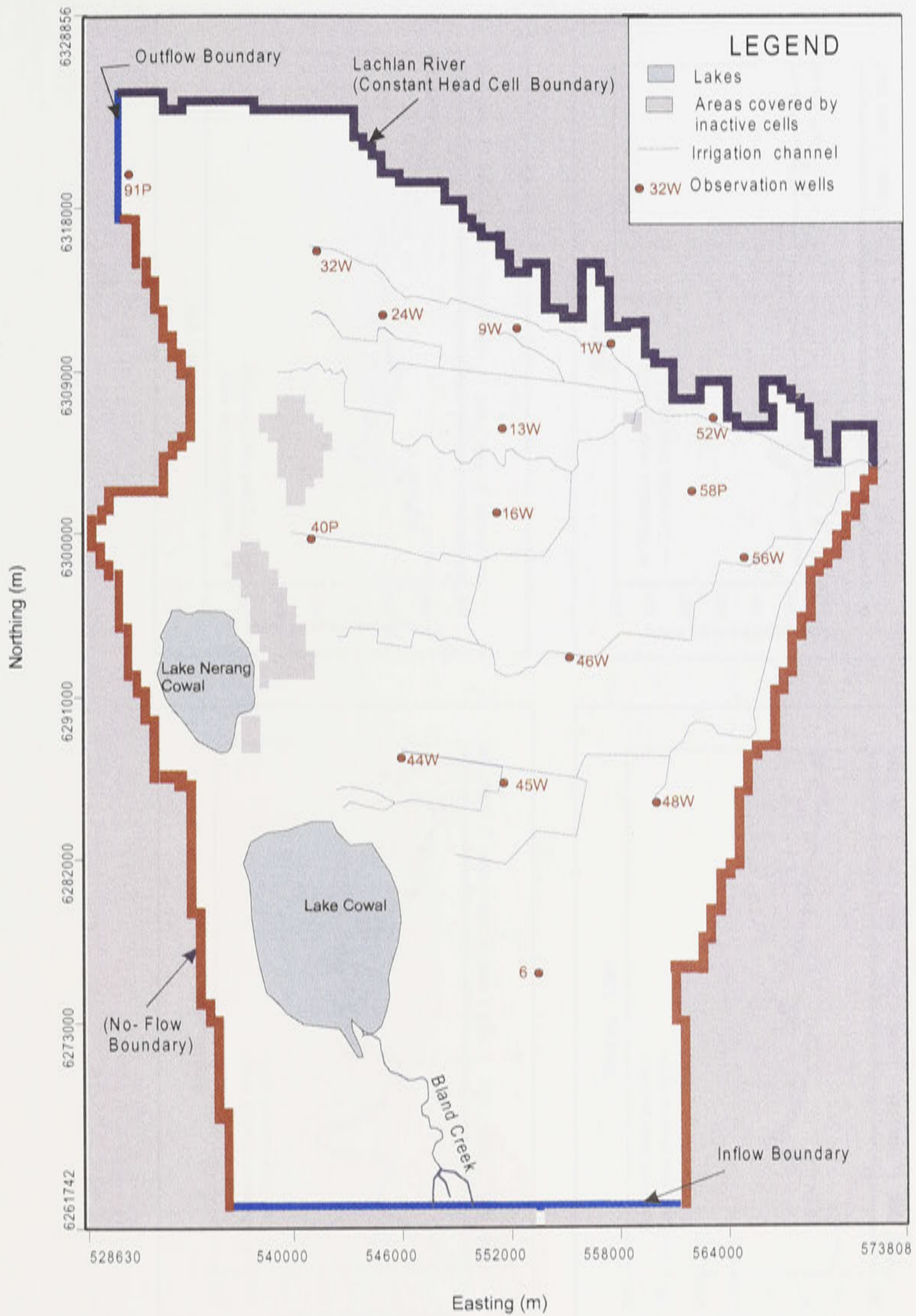


Figure 9.5: Location of the selected observation wells used to check the match between measured and computed heads for transient calibration.

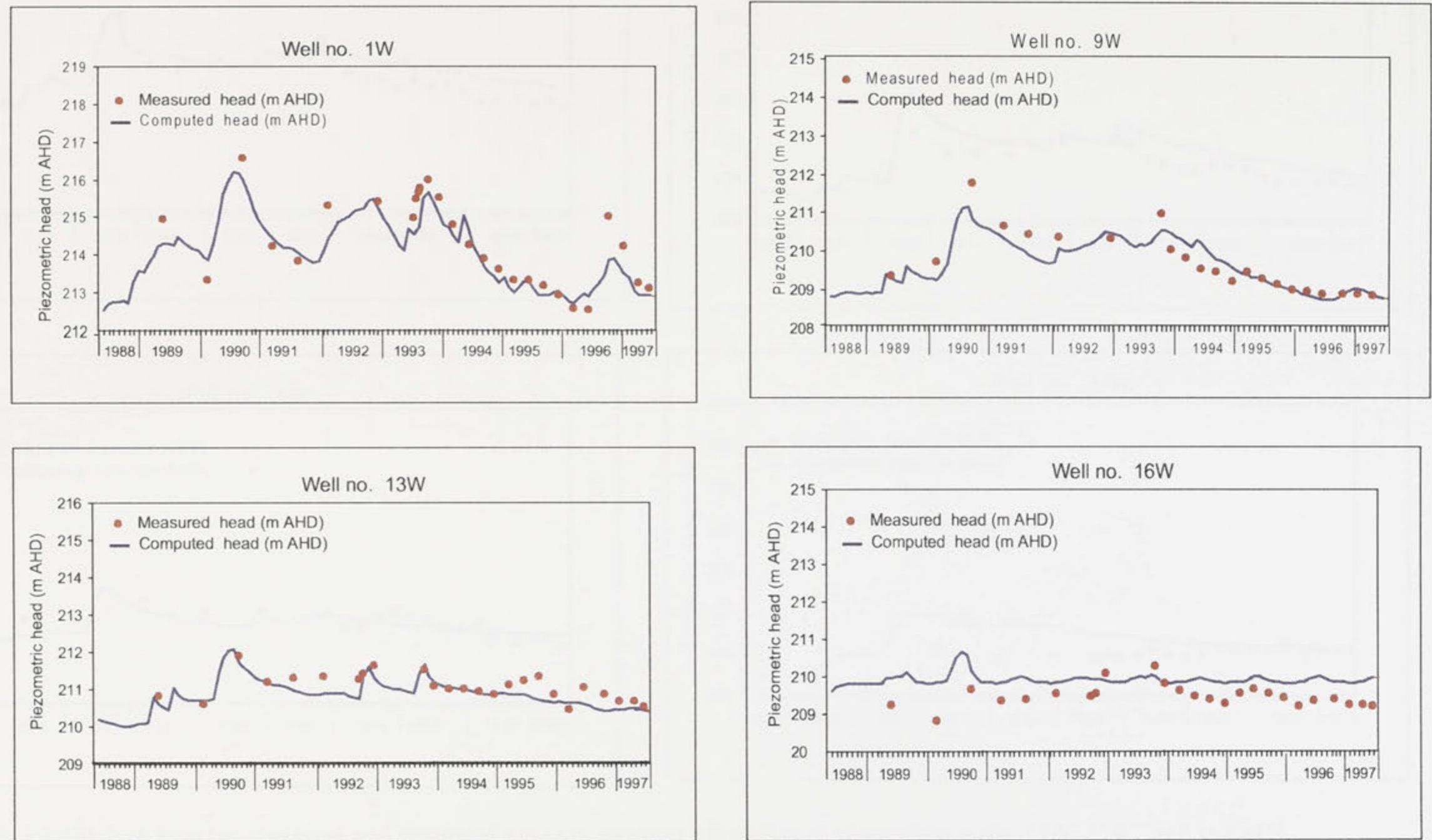


Figure 9.6a: Comparison between measured and computed heads in transient simulation at observation wells 1W, 9W, 13W and 16W for 1st May 1988 to 31st July 1997 (see Figure 9.5 for locations).

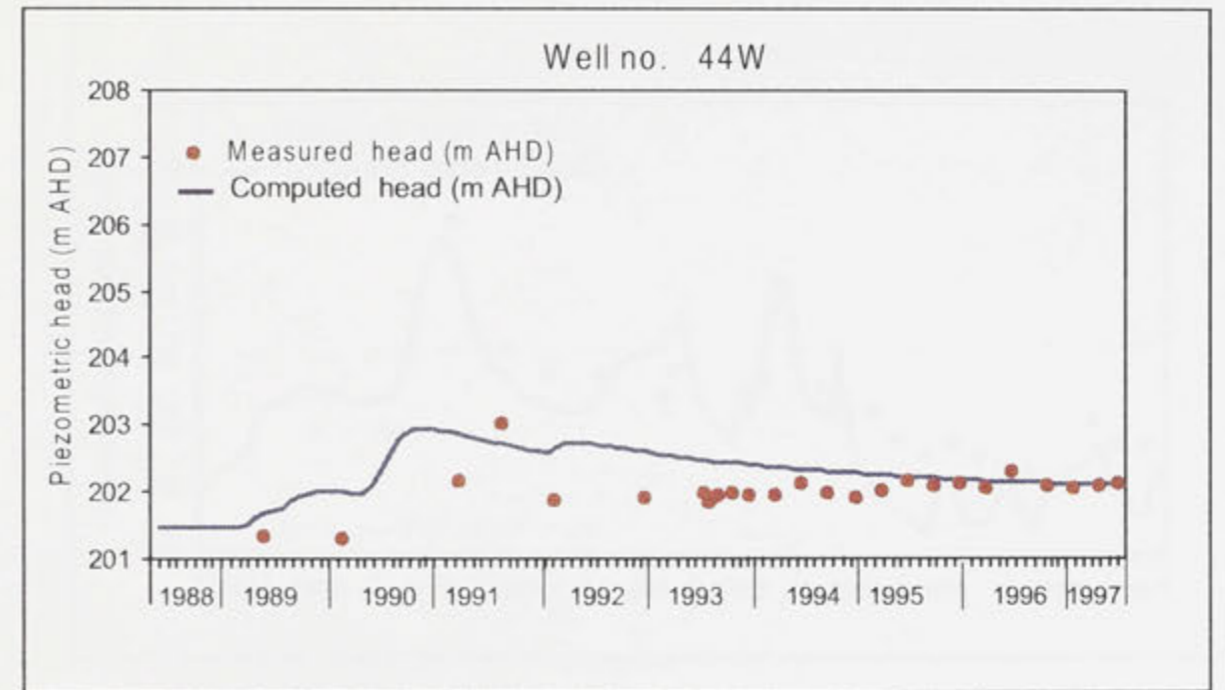
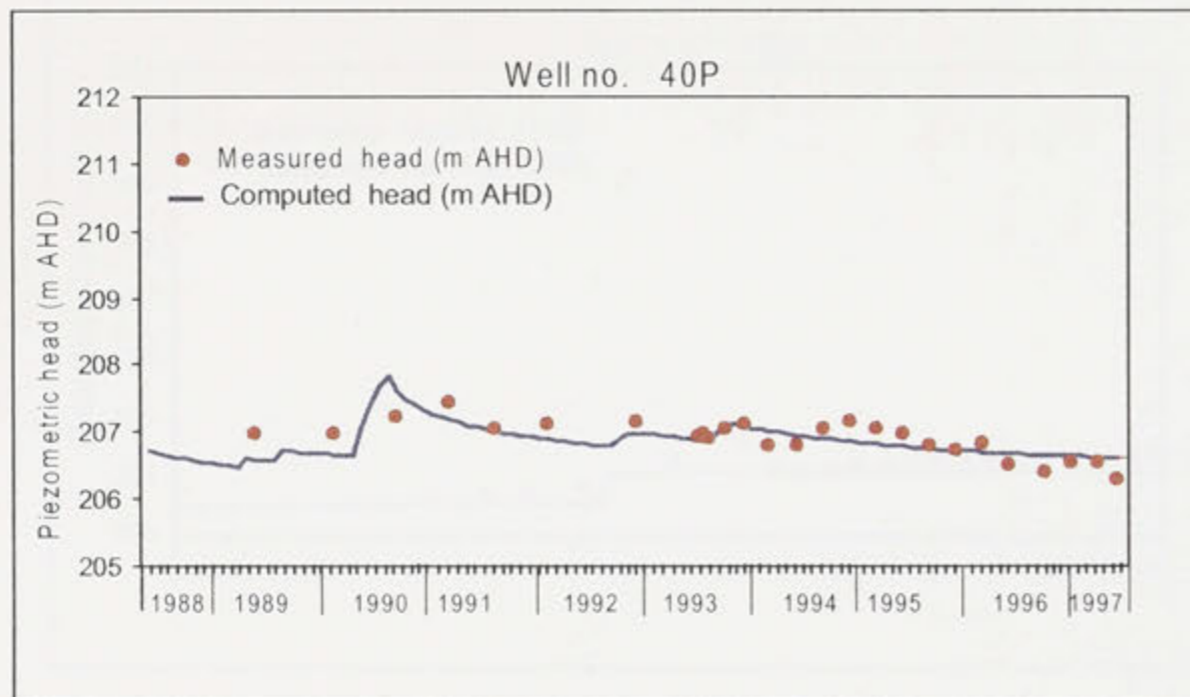
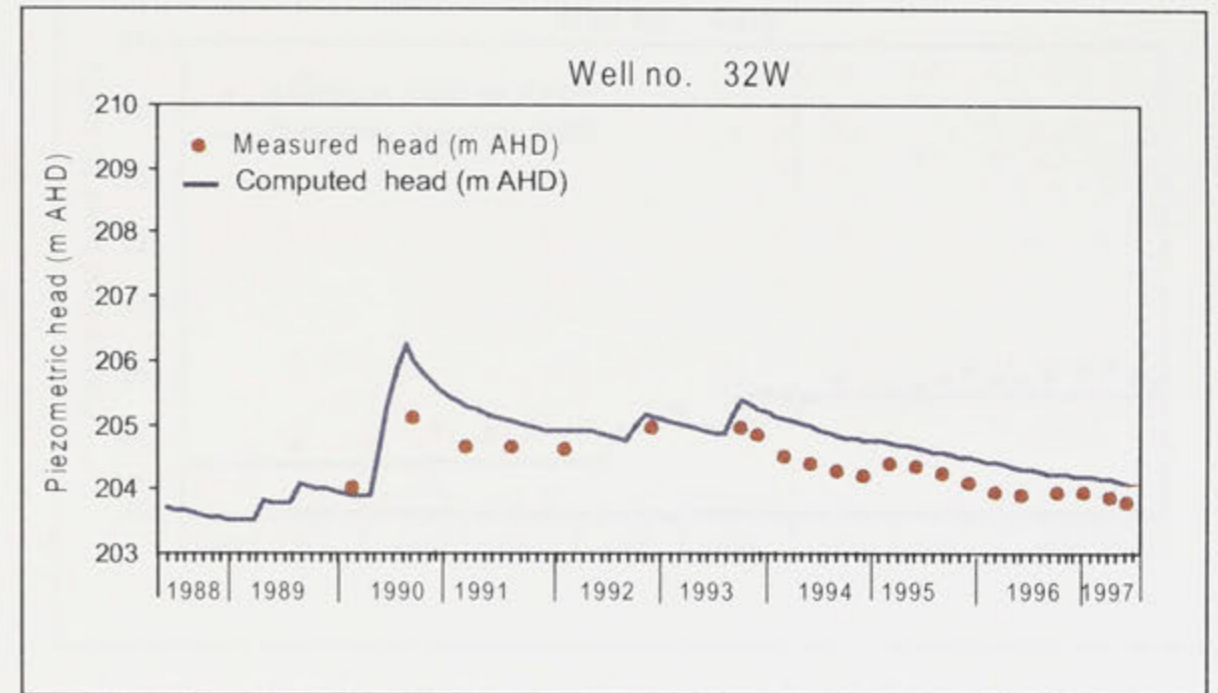
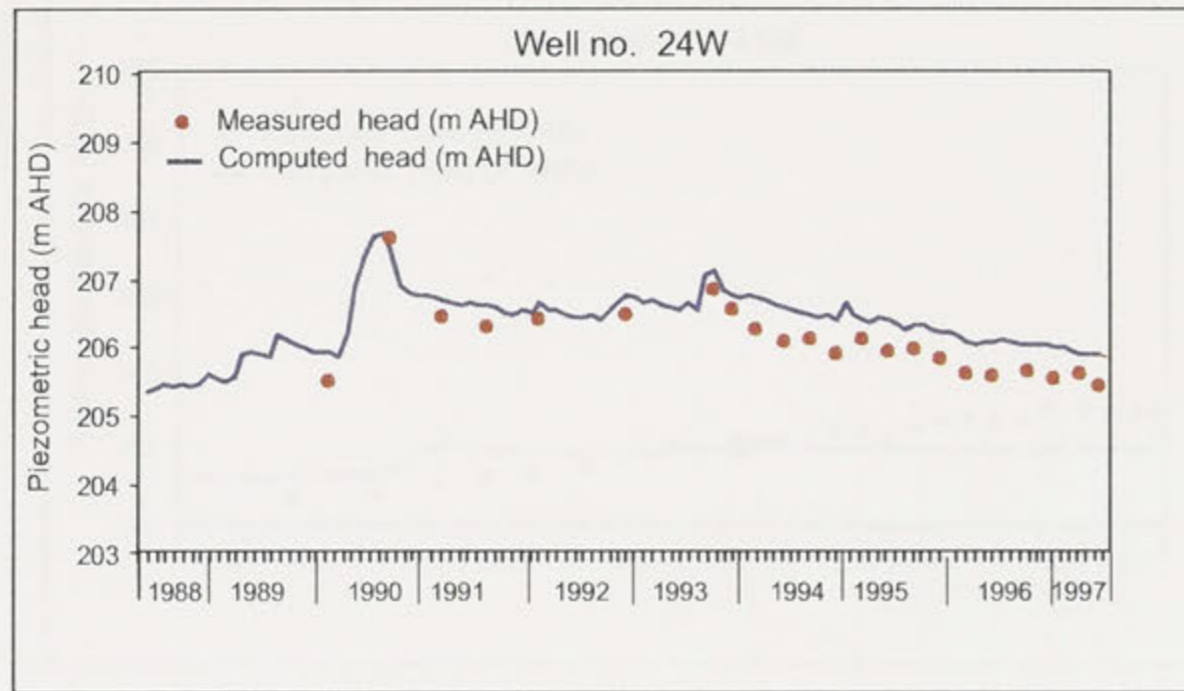


Figure 9.6b: Comparison between measured and computed heads in transient simulation at observation wells 24W, 32W, 40P and 44W for 1st May 1988 to 31st July 1997 (see Figure 9.5 for locations).

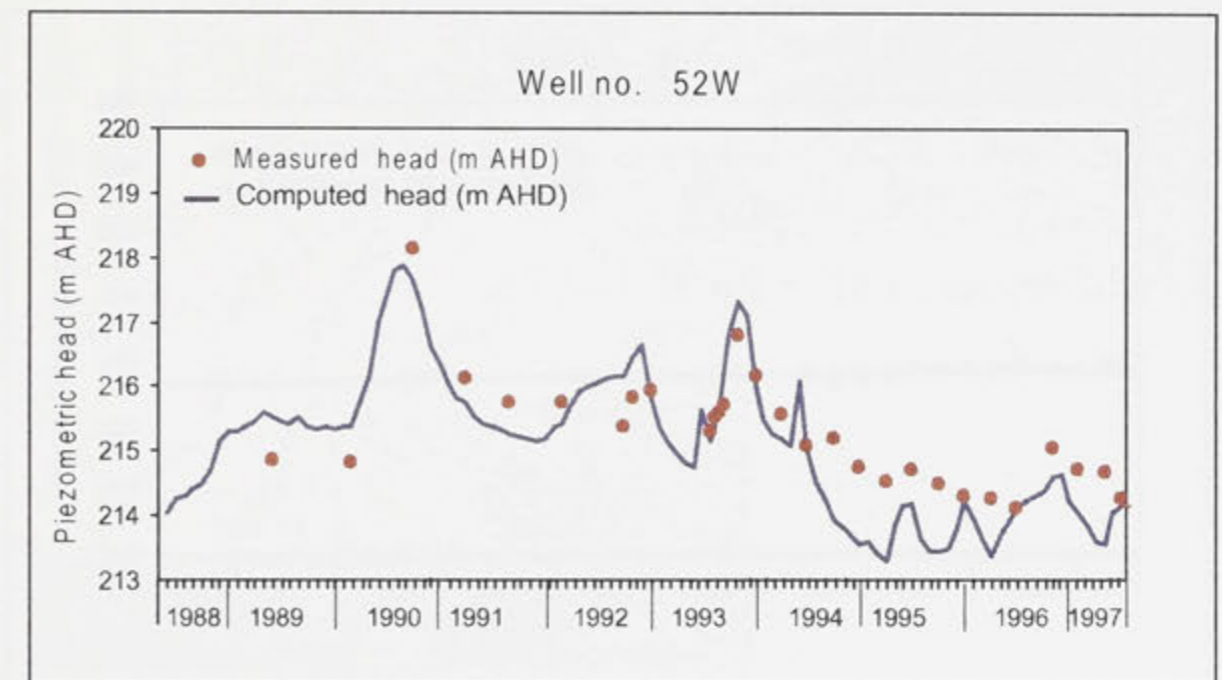
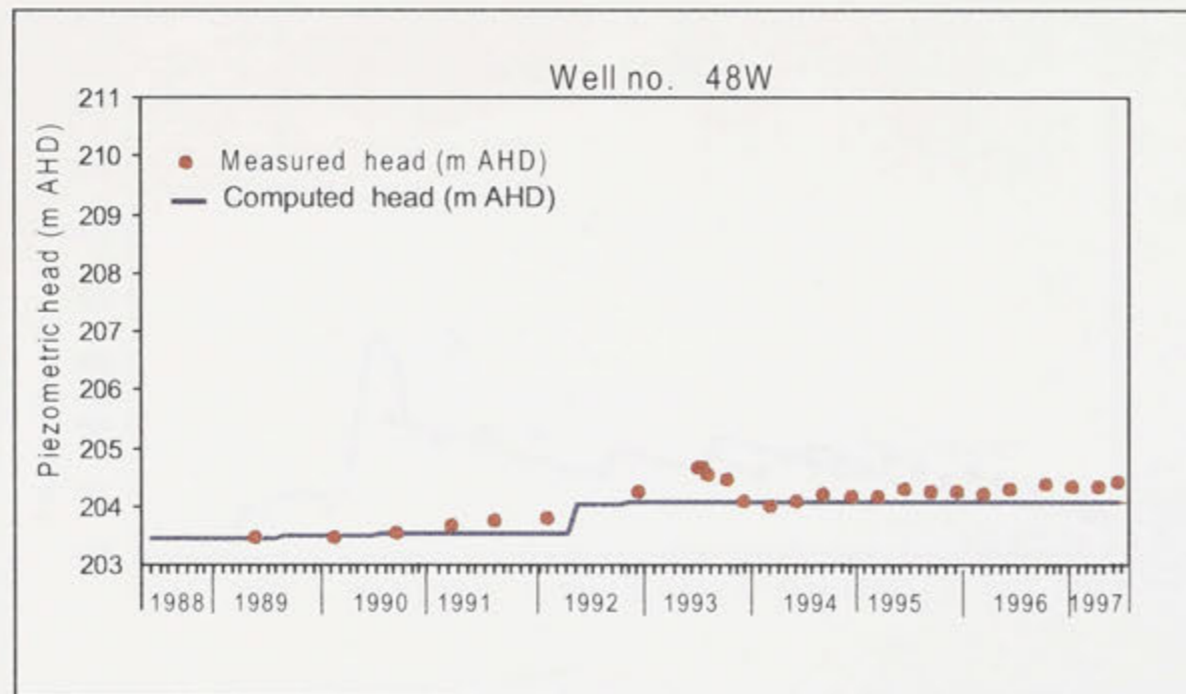
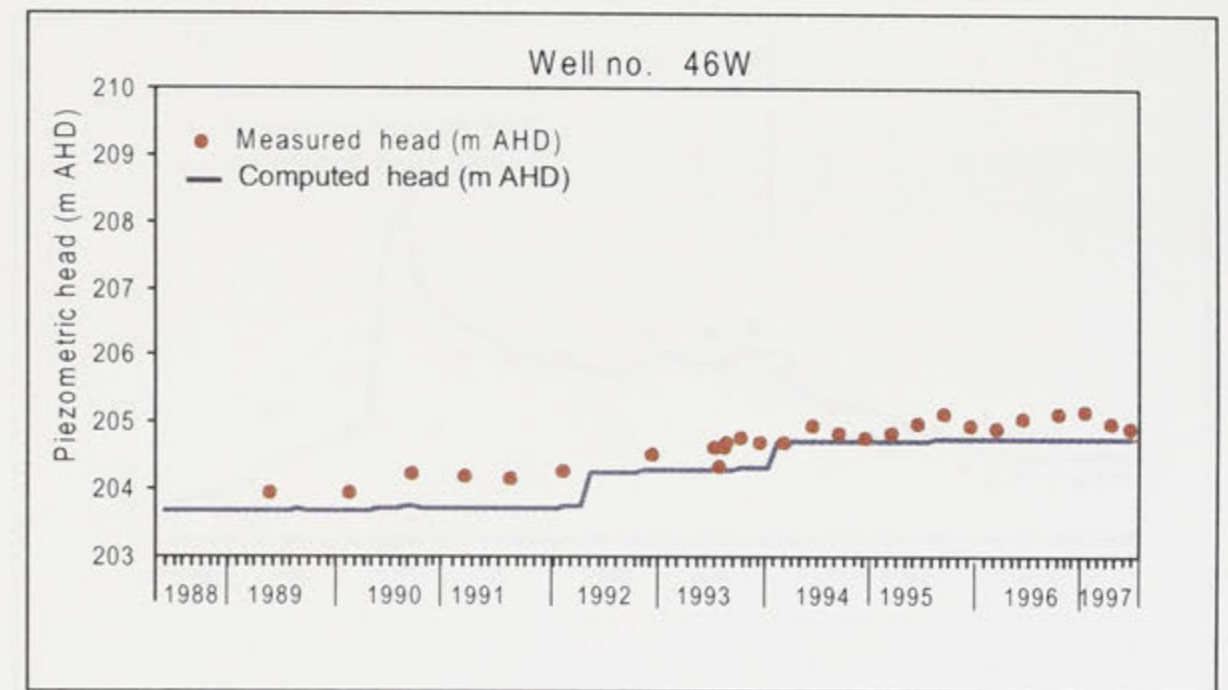
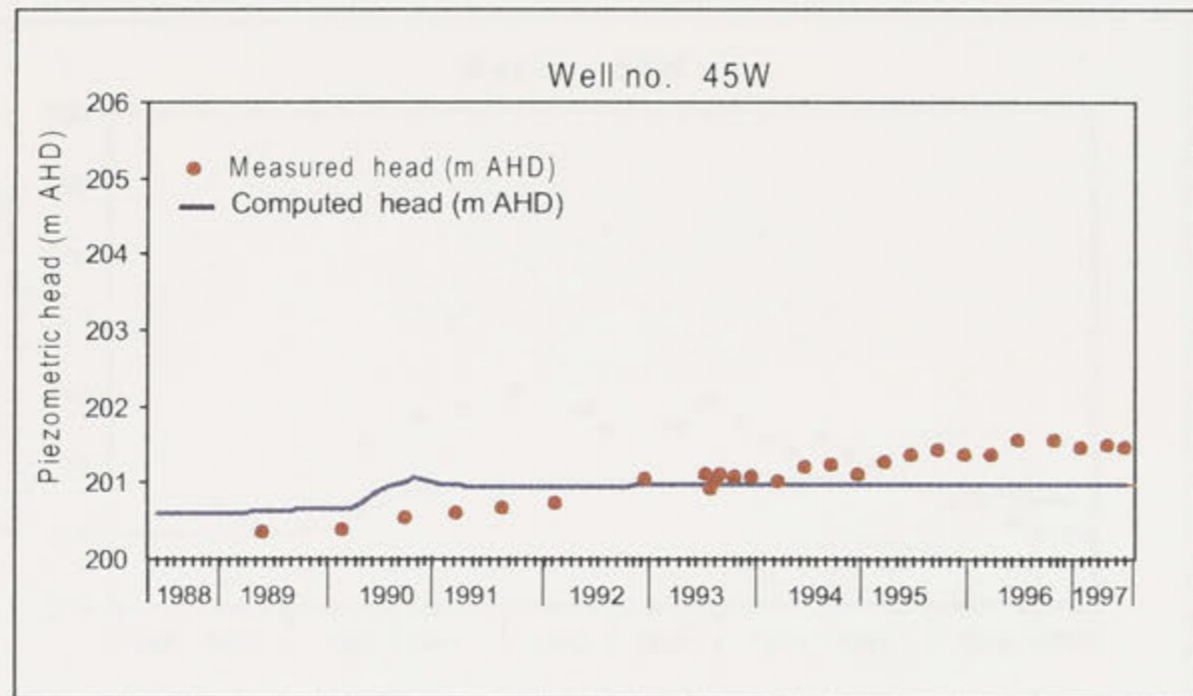


Figure 9.6c: Comparison between measured and computed heads in transient simulation at observation wells 45W, 46W, 48W and 52W for 1st May 1988 to 31st July 1997 (see Figure 9.5 for locations).

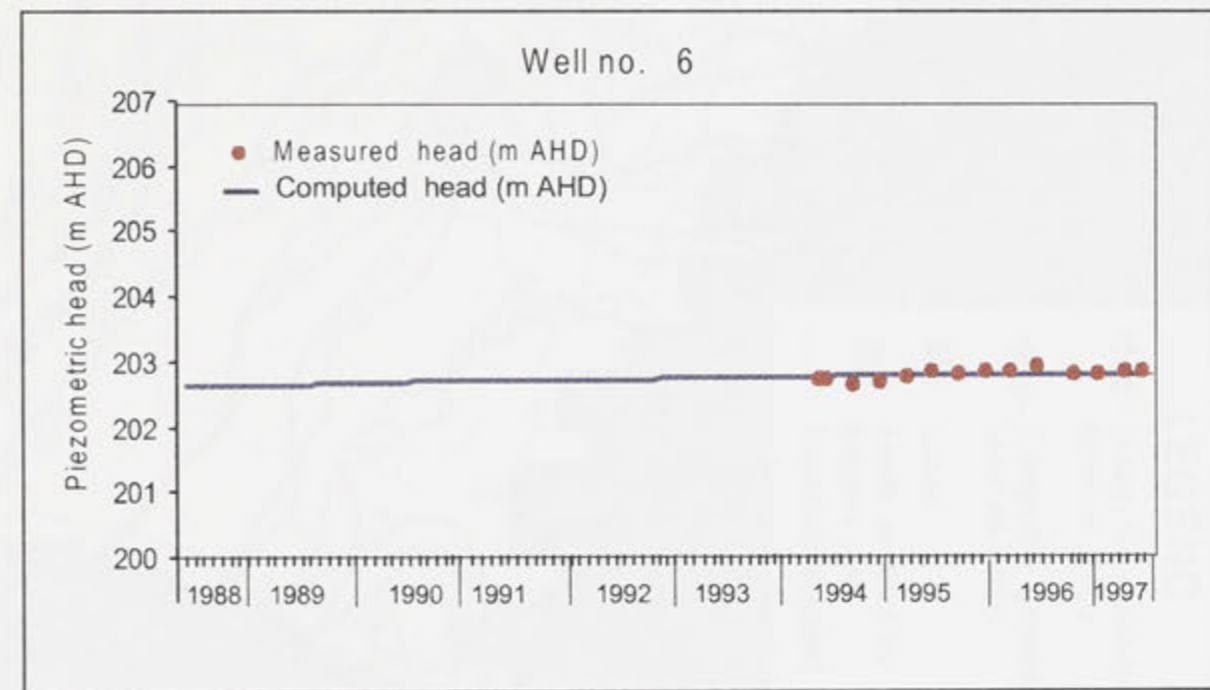
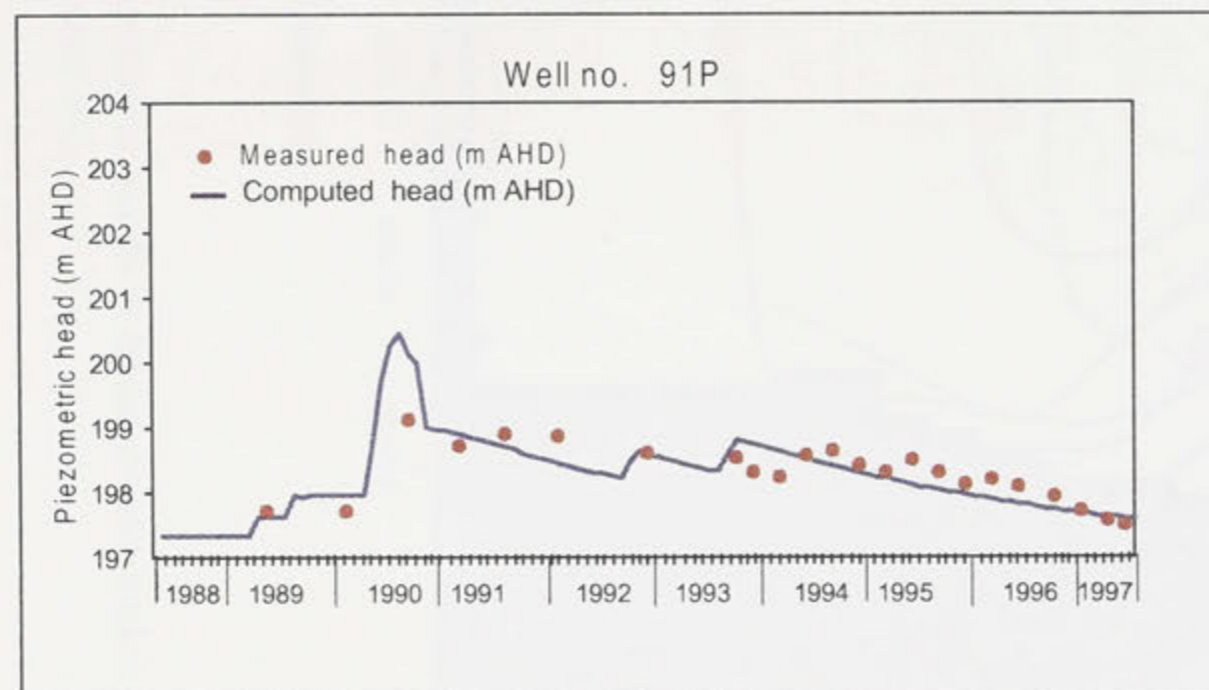
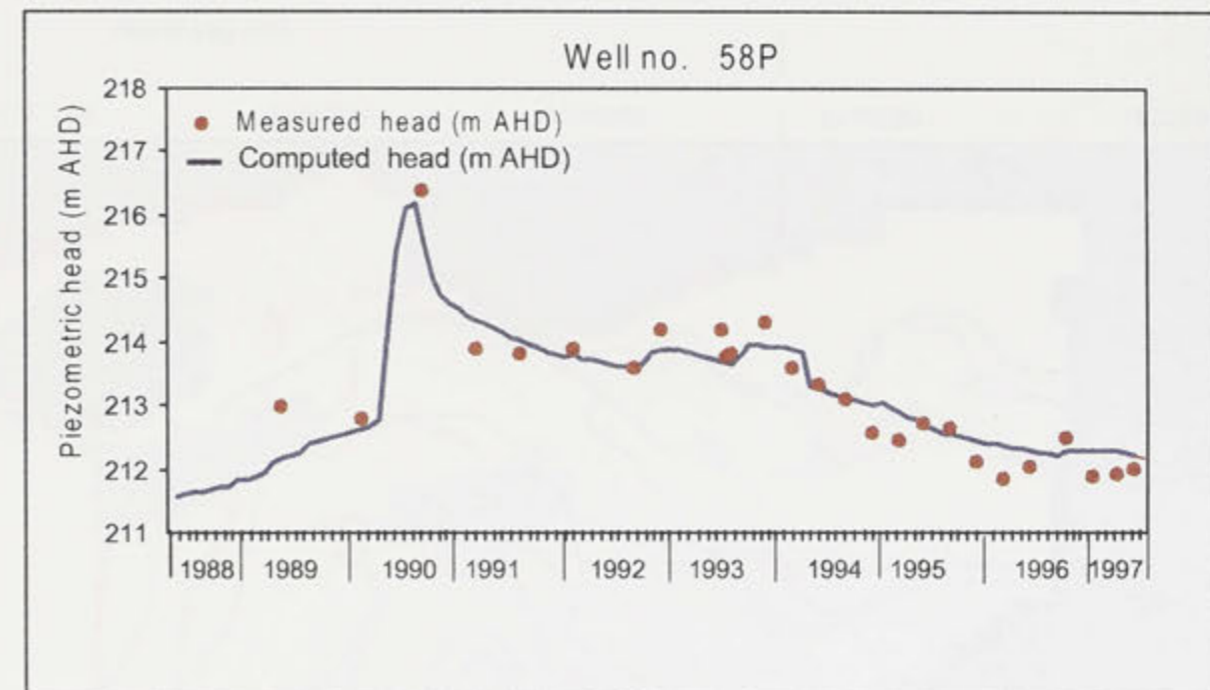
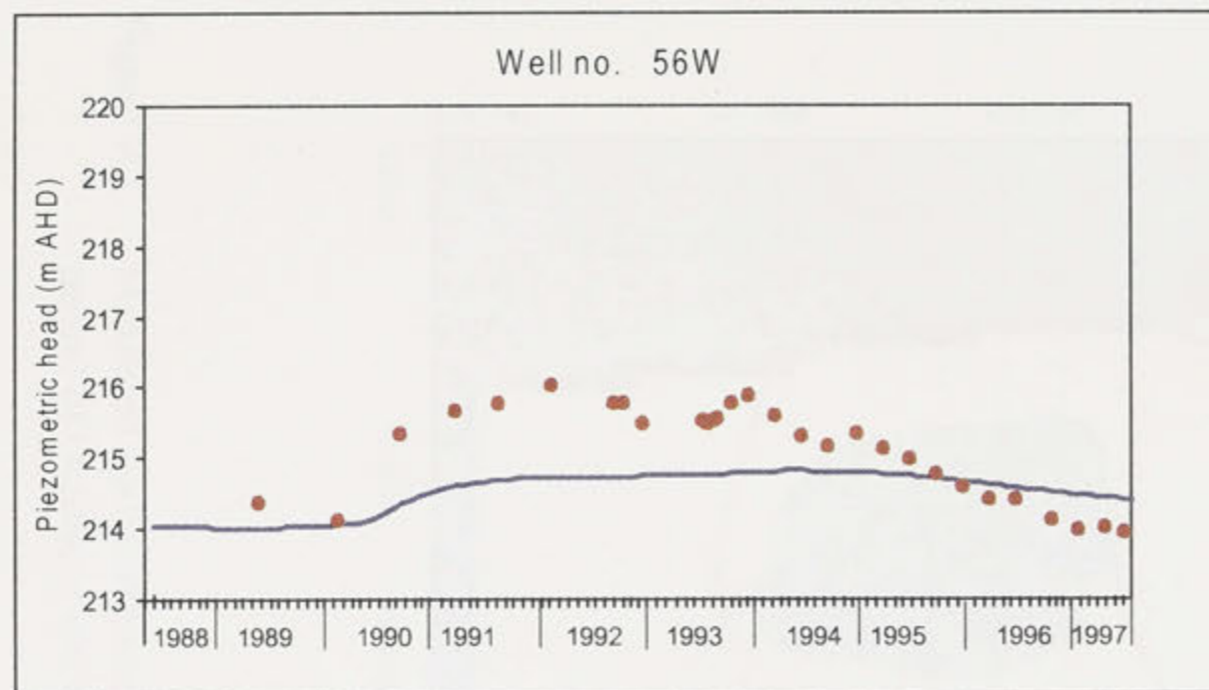


Figure 9.6d: Comparison between measured and computed heads in transient simulation at observation wells 56W, 58P, 91P and 6 for 1st May 1988 to 31st July 1997 (see Figure 9.5 for locations).

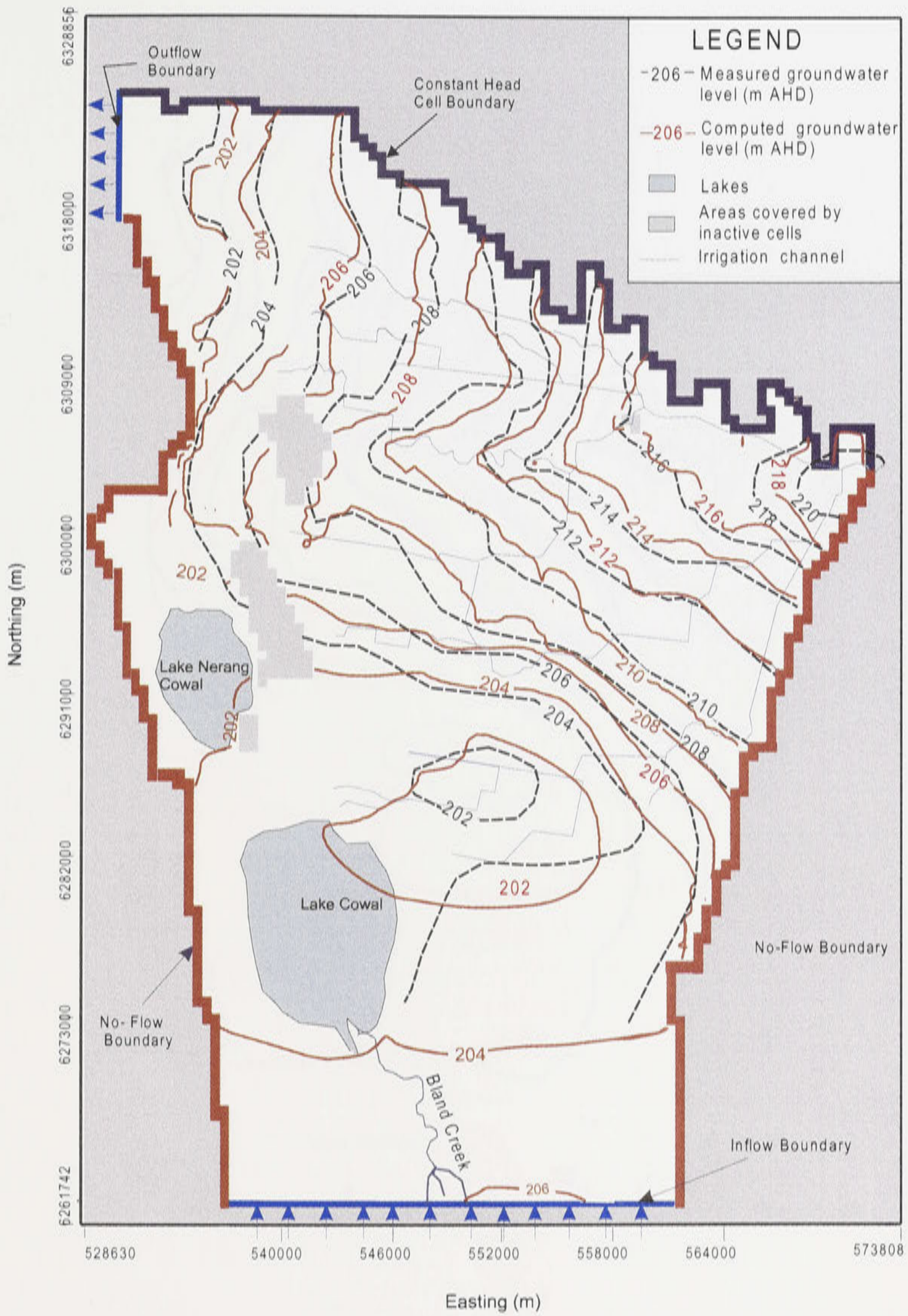


Figure 9.7: Measured and computed piezometric heads in transient simulation for the flood period of October 1990 (timestep 30).

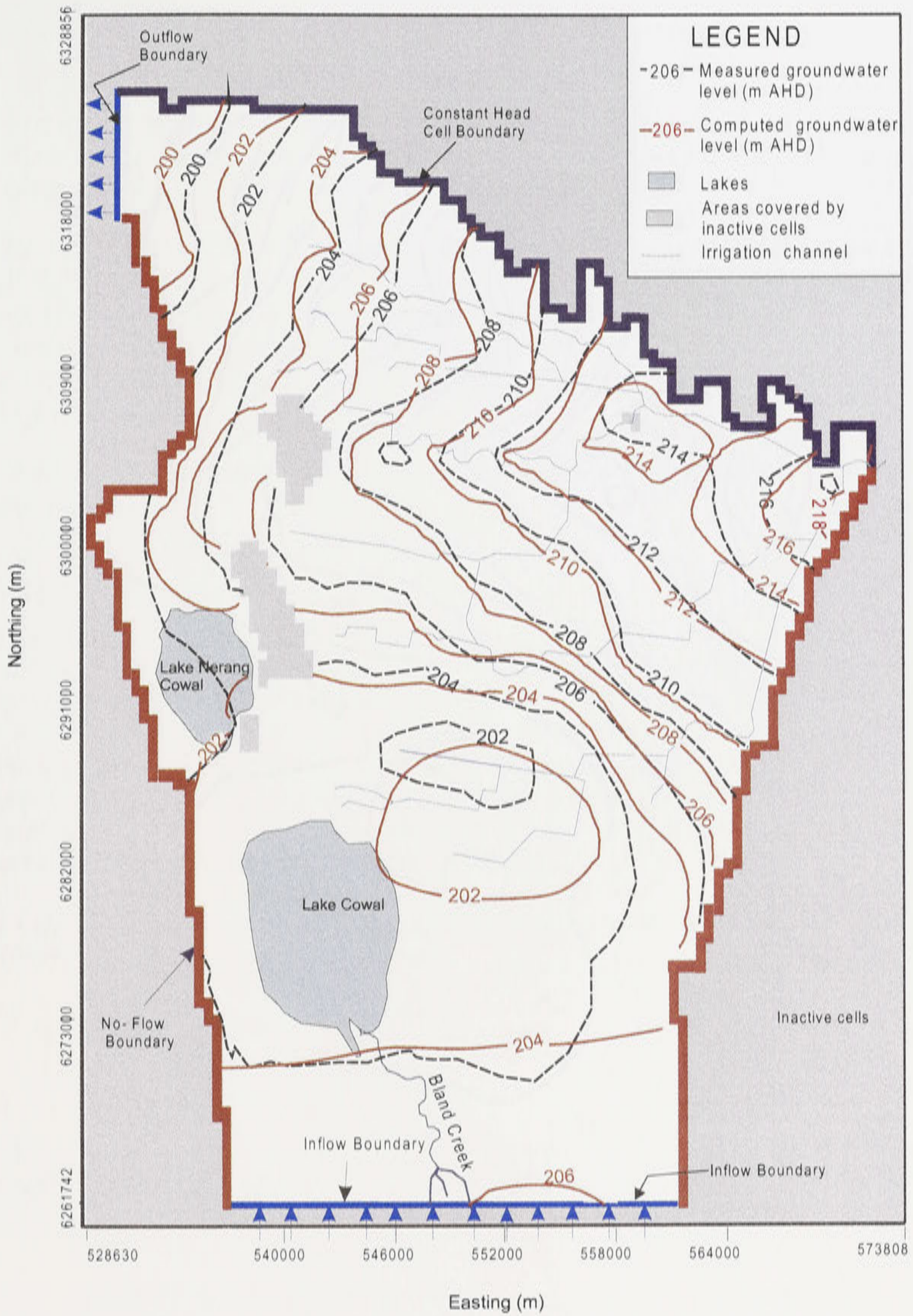


Figure 9.8: Measured and computed piezometric heads in transient simulation for October 1994 representing a period of low groundwater levels (timestep 78).

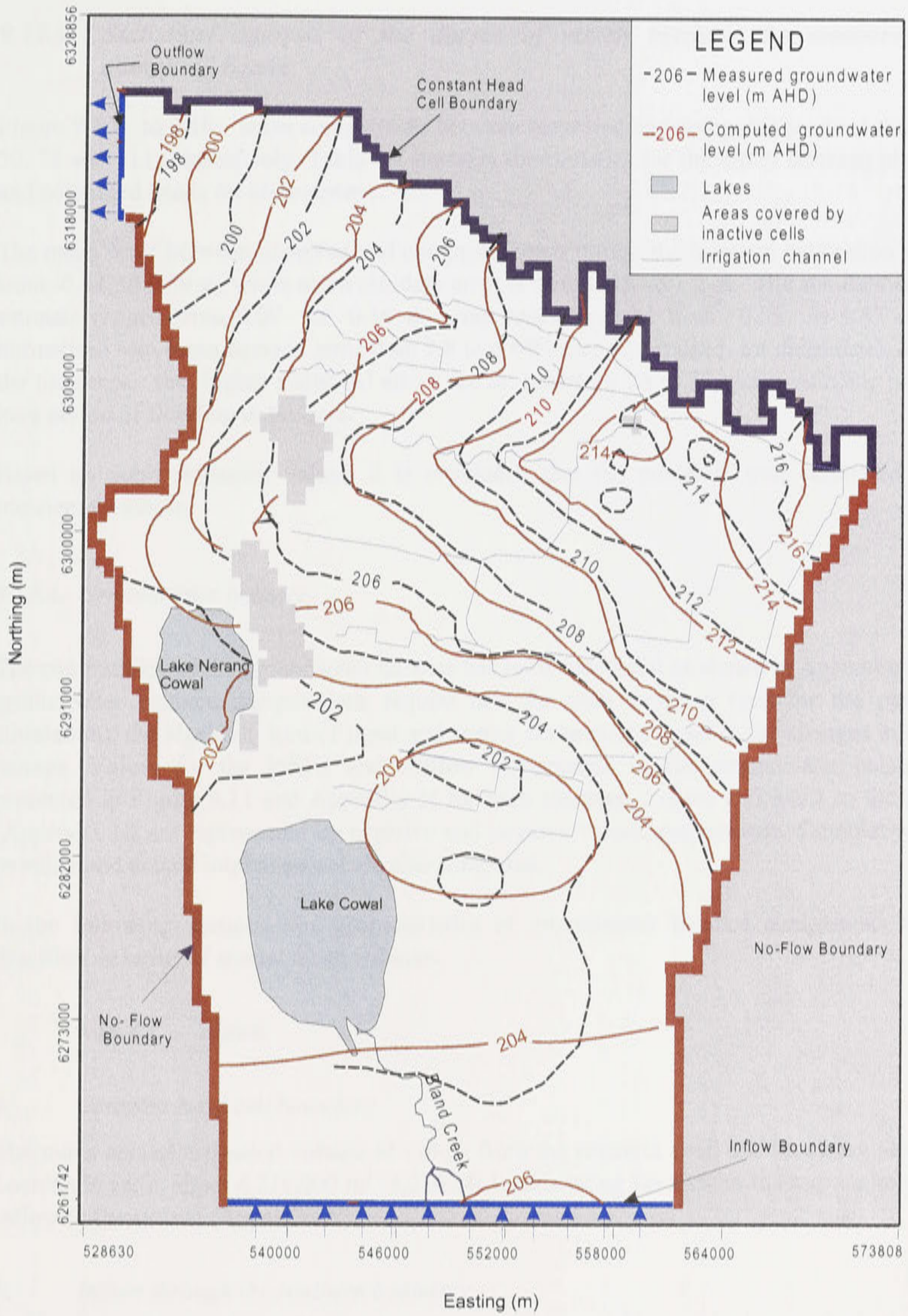


Figure 9.9: Measured and computed piezometric heads in transient simulation for July 1997 representing the end of the period of simulation (timestep 111).

9.12.3. Statistical analysis of the degree of match between the measured and computed heads

Figure 9.10a to 9.10c show comparisons between measured and computed heads at timesteps 30, 78 and 111, respectively. Table 9.4 presents the statistics for the errors between observed and computed heads for all timesteps.

The mean error between observed and computed heads during the transient calibration ranged from -0.42 to 0.69 m, while mean absolute error is from 0.65 to 1.2 m. The standard error of estimate ranged from 0.09 to 0.16 m, root mean squared from 0.85 to 1.57 m, and normalised root mean squared error from 3.8 to 6.44% (see Appendix L for definition). Among the timesteps, the higher statistical errors are at timesteps 26 to 29 which coincide with the long period of flooding in the area.

Based on these statistical values, it is concluded that the model is well calibrated under transient condition.

9.12.4. Groundwater balance

The computation of the groundwater balance has been successful as shown in Appendix N. The groundwater balance computations require that for each timestep (and for the period of simulation), the algebraic sum of input and output components equal to the changes in aquifer storage. Values for the inflow and outflow components of the groundwater balance are presented in Figure 9.11 and Appendix N for each timestep. Losses and gains to the aquifer (Appendix N) are represented by negative and positive values, respectively. Cumulative total, monthly and annual total averages are also computed.

In the following sections, the characteristics of groundwater balance components will be described in terms of annual mean volumes.

9.12.4.1. Inputs

a. Constant head cell boundary

The mean annual estimated volume of inflow from the constant head cell boundary along the Lachlan River is about 4,216,000 m³ (4,216 ML), accounting for 23% of the mean annual total inflow to the system (Appendix N).

b. Inflow through the southern boundary

Only about 1.8% (334,000 m³) of the average annual total inflow of the model is coming from the Bland Creek catchment. Since inflow rates through the southern boundary were held constant throughout the transient simulation period, the average flow rate of 915 m³ d⁻¹ is equal to the computed flow rate in the steady-state model.

Table 9.4: Statistical indicators of the errors for all timesteps in transient simulation.

Time-step	Indicators of the errors*				
	Mean error (m)	MAE (m)	SEE (m)	RMS (m)	NRMS (%)
1	-0.37	0.72	0.09	0.99	4.60
2	-0.38	0.75	0.10	1.00	4.70
3	-0.39	0.78	0.10	1.05	4.90
4	-0.42	0.80	0.11	1.10	5.00
5	-0.40	0.80	0.11	1.07	4.90
6	-0.37	0.76	0.10	1.02	4.80
7	-0.31	0.72	0.10	0.97	4.51
8	-0.24	0.71	0.10	0.95	4.40
9	-0.23	0.69	0.10	0.93	4.30
10	-0.21	0.69	0.10	0.92	4.27
11	-0.17	0.69	0.10	0.91	4.20
12	-0.01	0.69	0.10	0.90	4.22
13	-0.01	0.71	0.10	0.92	4.30
14	-0.05	0.74	0.10	0.95	4.40
15	-0.08	0.75	0.10	0.97	4.50
16	0.12	0.77	0.10	0.97	4.50
17	0.10	0.72	0.10	0.91	4.17
18	0.10	0.69	0.09	0.87	4.02
19	0.10	0.69	0.09	0.86	3.90
20	0.09	0.67	0.09	0.86	3.90
21	0.09	0.67	0.09	0.85	3.87
22	0.10	0.67	0.09	0.85	3.90
23	0.01	0.65	0.09	0.85	3.80
24	-0.03	0.75	0.09	0.92	4.04
25	0.31	0.87	0.12	1.12	4.80
26	0.55	1.03	0.13	1.30	5.70
27	0.69	1.20	0.14	1.53	6.40
28	0.62	1.17	0.16	1.57	6.44
29	0.25	1.18	0.16	1.50	6.06
30	0.16	1.10	0.15	1.39	5.70
31	0.05	1.02	0.14	1.29	5.38
32	0.06	0.94	0.13	1.21	5.14
33	0.09	0.88	0.12	1.15	4.98
34	0.13	0.84	0.12	1.11	4.89
35	0.17	0.82	0.12	1.09	4.86
36	0.15	0.82	0.12	1.08	4.84
37	0.13	0.82	0.11	1.07	4.83
38	0.12	0.84	0.12	1.08	4.89
39	0.05	0.88	0.11	1.10	5.03

Table 9.4: Continued.

Time-step	Indicators of the errors*				
	Mean error (m)	MAE (m)	SEE (m)	RMS (m)	NRMS (%)
40	-0.01	0.90	0.12	1.12	5.14
41	-0.01	0.87	0.12	1.09	4.97
42	-0.01	0.84	0.12	1.07	4.86
43	-0.02	0.84	0.11	1.06	4.81
44	-0.01	0.84	0.11	1.07	4.81
45	0.00	0.84	0.11	1.06	4.77
46	0.03	0.85	0.12	1.08	4.82
47	0.03	0.81	0.11	1.05	4.69
48	0.04	0.81	0.11	1.04	4.64
49	0.04	0.80	0.11	1.03	4.60
50	0.01	0.82	0.11	1.04	4.67
51	-0.03	0.84	0.11	1.06	4.78
52	-0.04	0.85	0.11	1.07	4.83
53	-0.02	0.83	0.11	1.04	4.70
54	0.10	0.84	0.11	1.06	4.80
55	0.18	0.86	0.12	1.09	4.90
56	0.11	0.84	0.11	1.07	4.84
57	0.06	0.83	0.11	1.06	4.80
58	0.04	0.81	0.11	1.04	4.70
59	0.02	0.82	0.11	1.04	4.70
60	-0.01	0.81	0.11	1.03	4.70
61	-0.01	0.82	0.11	1.03	4.70
62	0.00	0.81	0.11	1.02	4.70
63	-0.04	0.86	0.11	1.06	4.90
64	-0.10	0.86	0.11	1.08	5.03
65	0.02	0.94	0.12	1.17	5.28
66	0.08	0.98	0.13	1.23	5.30
67	0.09	0.89	0.12	1.14	5.05
68	0.13	0.84	0.11	1.11	5.03
69	0.13	0.82	0.11	1.09	4.96
70	0.15	0.82	0.11	1.09	4.97
71	0.17	0.84	0.11	1.10	5.04
72	-0.17	0.84	0.11	1.10	5.04
73	-0.17	0.88	0.12	1.10	5.44
74	0.17	0.88	0.12	1.15	5.44
75	0.13	0.87	0.12	1.16	5.24
76	0.11	0.85	0.11	1.10	5.14
77	0.12	0.83	0.11	1.07	4.98
78	0.12	0.85	0.12	1.08	5.08

* MAE = mean absolute error; SEE = standard error of estimate; RMS = root mean squared error; NRMS = normalised root mean squared (see Appendix L for definitions).

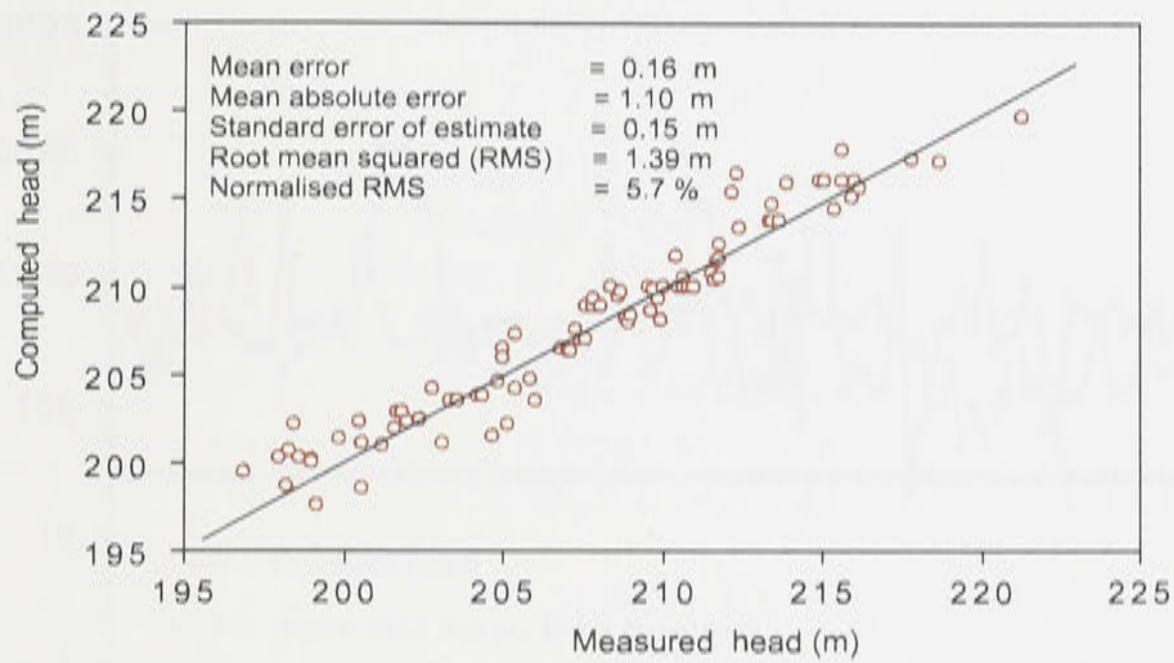
Table 9.4: Continued.

Time- step	Indicators of the errors*				
	Mean error	MAE	SEE	RMS	NRMS
	(m)	(m)	(m)	(m)	(%)
79	0.11	0.88	0.12	1.13	5.35
80	0.08	0.90	0.13	1.20	5.70
81	0.15	0.88	0.12	1.12	5.38
82	0.14	0.83	0.11	1.06	5.12
83	0.15	0.79	0.10	1.00	5.00
84	0.13	0.78	0.10	1.02	4.94
85	0.13	0.79	0.11	1.03	5.01
86	0.12	0.79	0.11	1.03	5.03
87	0.05	0.82	0.11	1.05	5.14
88	-0.01	0.83	0.11	1.06	5.20
89	0.02	0.80	0.11	1.02	5.06
90	0.03	0.80	0.10	1.02	5.01
91	0.08	0.77	0.10	0.99	4.85
92	0.13	0.76	0.10	0.98	4.70
93	0.16	0.77	0.10	0.99	4.80
94	0.17	0.78	0.10	1.00	4.84
95	0.19	0.80	0.10	1.01	4.90

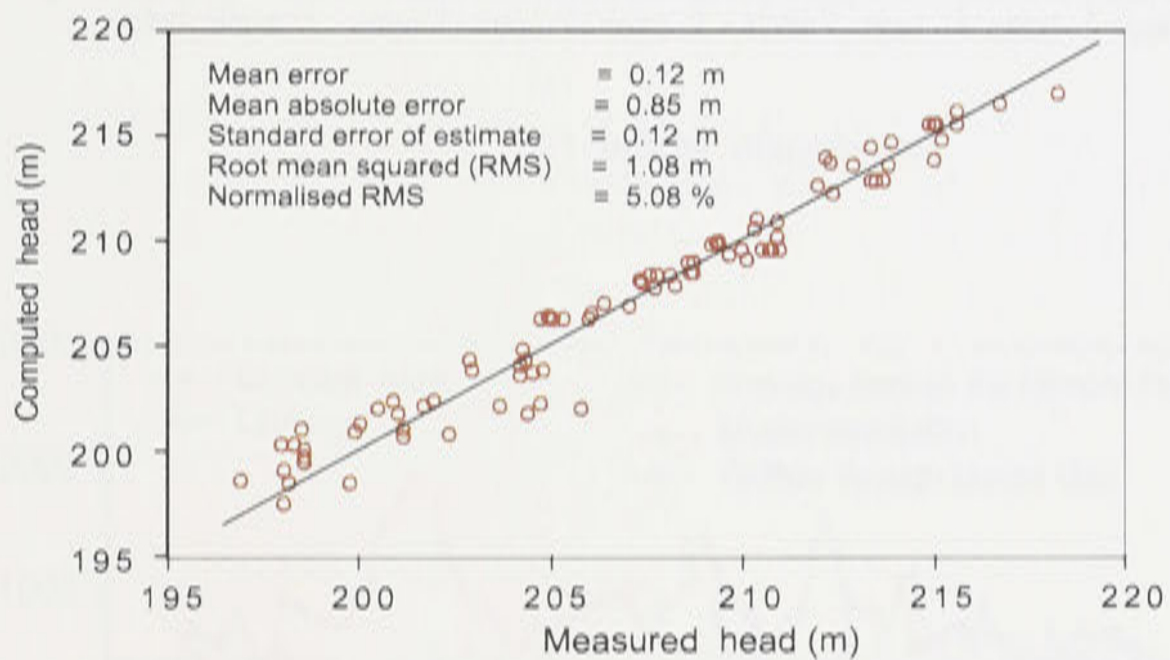
Table 9.4: Continued.

Time- step	Indicators of the errors*				
	Mean error	MAE	SEE	RMS	NRMS
	(m)	(m)	(m)	(m)	(%)
96	0.19	0.79	0.10	1.00	4.90
97	0.19	0.80	0.10	1.01	4.90
98	0.13	0.83	0.11	1.04	5.19
99	0.09	0.86	0.11	1.06	5.23
100	0.03	0.87	0.12	1.08	5.23
101	0.00	0.85	0.11	1.07	5.12
102	0.05	0.82	0.11	1.04	4.95
103	0.09	0.79	0.10	1.01	4.76
104	0.13	0.79	0.10	0.99	4.67
105	0.16	0.79	0.10	0.99	4.60
106	0.16	0.79	0.11	0.99	4.65
107	0.14	0.80	0.11	1.00	4.70
108	0.12	0.79	0.10	1.00	4.70
109	0.12	0.78	0.10	0.98	4.70
110	0.07	0.85	0.12	1.13	5.11
111	0.04	0.84	0.11	1.09	5.40

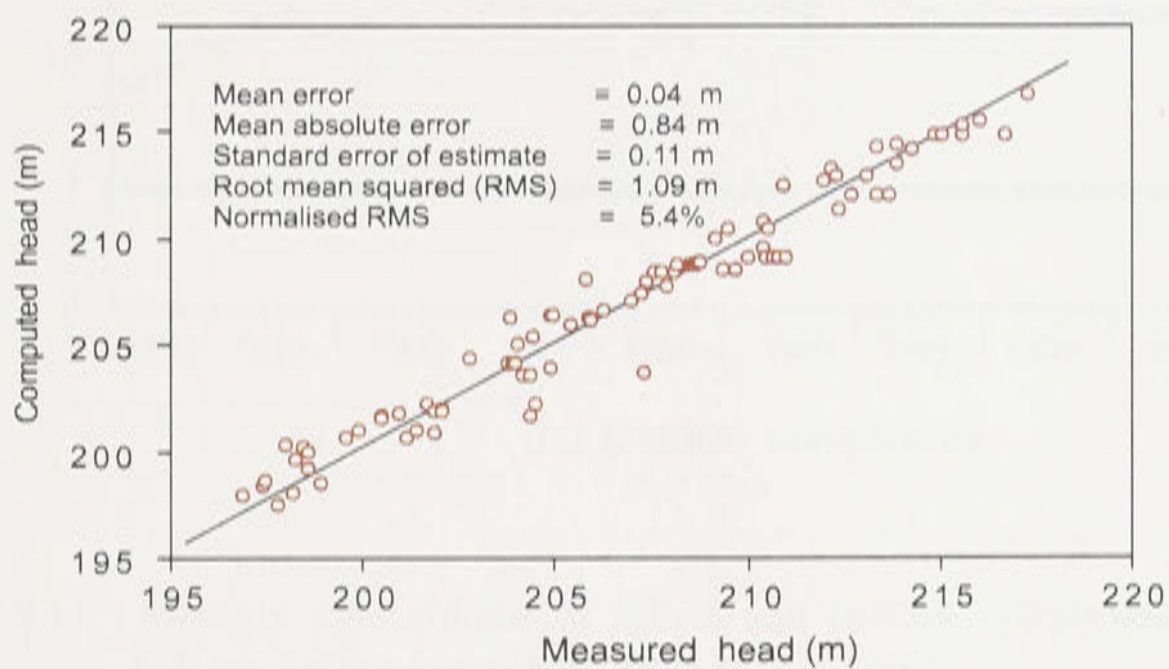
* MAE = mean absolute error; SEE = standard error of estimate; RMS = root mean squared error; NRMS = normalised root mean squared (see Appendix L for definitions).



(a) Time step number 30

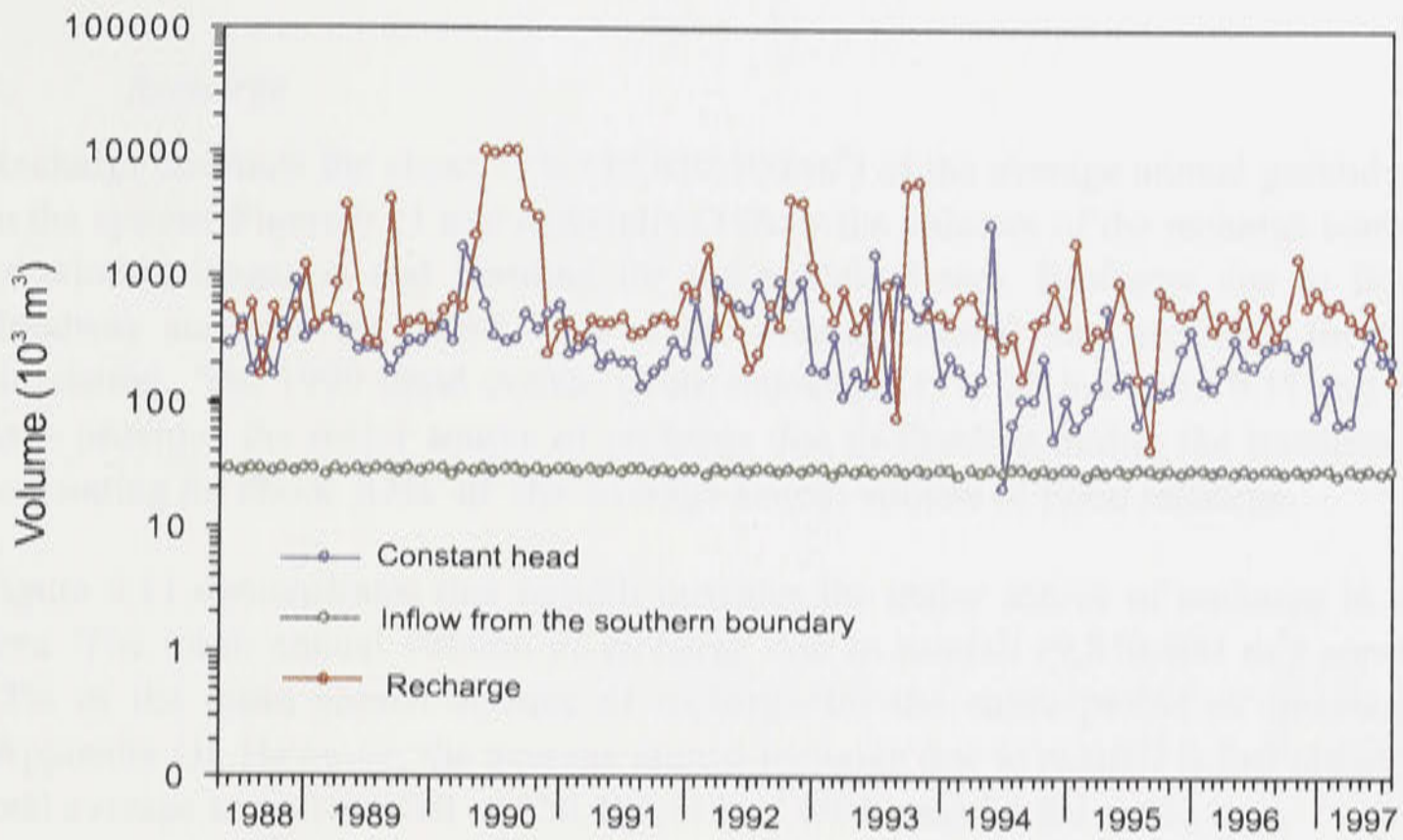


(b) Time step number 78

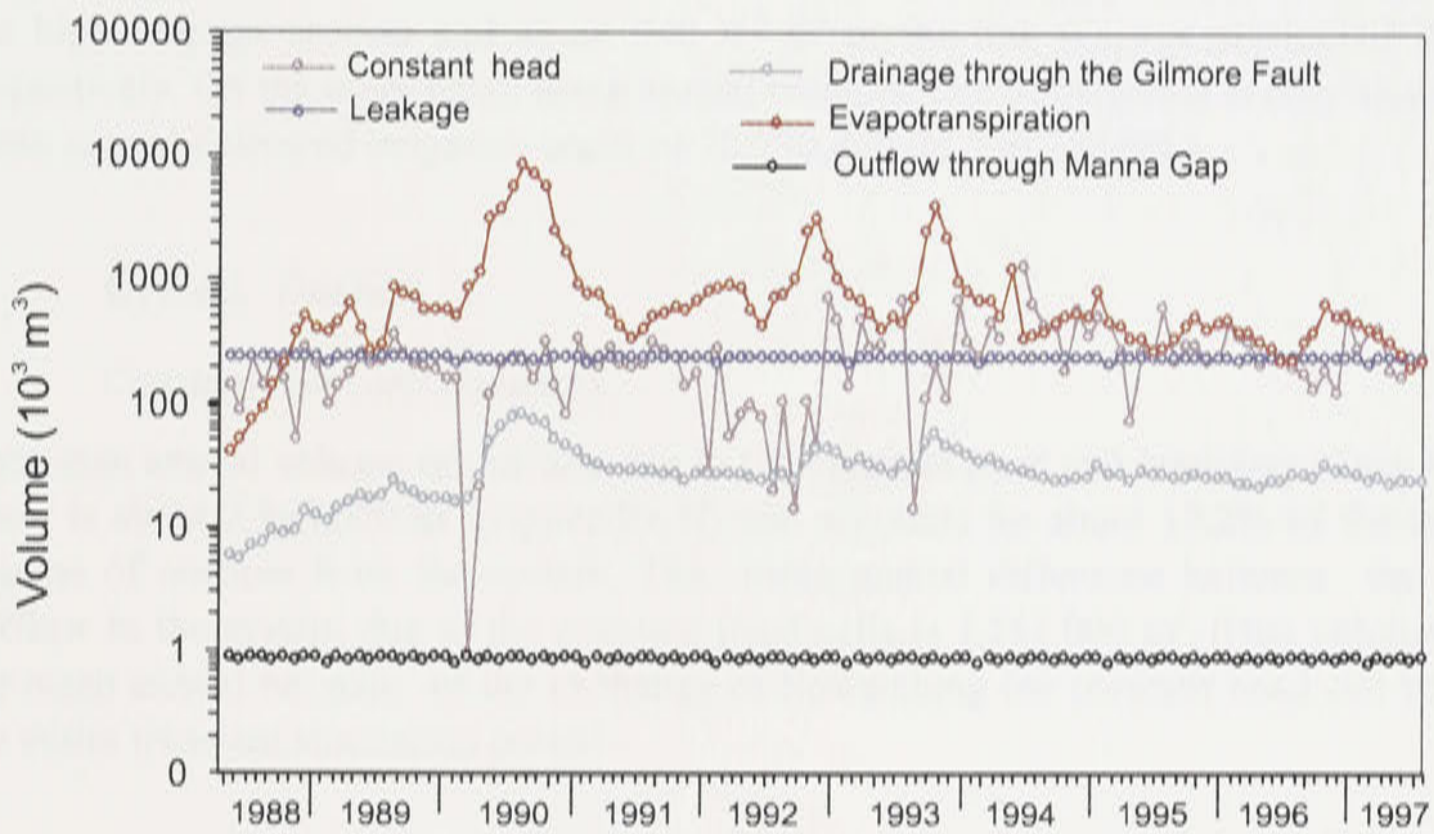


(c) Time step number 111

Figure 9.10: Comparison of computed versus observed piezometric heads and statistical indicators of the errors in transient simulation for timesteps number 30,78 and 111.



(A) Inflow components



(B) Outflow components

Figure 9.11: Monthly total volume of inflow and outflow components of the groundwater balance for the period May 1988 to July 1997.

c. *Recharge*

Recharge accounts for about 75% (13,630,500 m³) of the average annual groundwater inflows in the system. Figure 9.11 and Appendix O show the volumes of the recharge components such as rainfall, irrigation and flooding for the modelled area. Recharge due to flooding at the floodway accounts for about 11% of the average annual total recharge for the period of simulation. The 1990 flood events (from timesteps 25 to 30 in Figure 9.11 and Appendix O) have provided the major source of recharge due to flooding during the transient simulation, accounting for about 87% of the average annual volume of flood recharge.

Figure 9.11 demonstrates that rainfall provides the major source of recharge in the modelled area. The mean annual volume of recharge due to rainfall (9,850,400 m³) constitutes about 72% of the mean annual volume of recharge for the entire period of transient simulation (Appendix O). However, the average annual recharge due to rainfall is just about 1.2 % of the total average annual rainfall of 850,407,113 m³ (501 mm) for the entire area.

Mean annual recharge due to irrigation accounts for about 16% (2,226,700 m³) of the total volume of recharge for the entire transient simulation period. However, about 80% of this volume has been recharged around the Warroo Channel area. Average recharge rate due to irrigation losses at the Warroo Channel for the entire simulation period is about 3,898 m³ d⁻¹ at the high seepage section and about 940 m³ d⁻¹ at the low seepage section of the channel, respectively. On the other hand, mean annual recharge due to irrigation is only about 3% of the mean annual delivered irrigation water of 70,730,440 m³ (70,730 ML).

9.12.4.2. *Outputs*

a. *Constant head cell boundary*

The mean annual volume of outflow due to the constant head cell boundary along the Lachlan River is about 2,963,000 m³ (Appendix N) and accounts for about 17.2% of the mean annual volume of outflow from the system. The mean annual difference between the inflow and outflow to the system due to the constant head cells is 1,253,000 m³. This volume represents the mean annual net gain of the exchange of flows along the constant head cell boundary for the entire transient simulation period.

b. *Leakage to the basement rocks*

The mean annual volume of leakage into the fractured basement of 2,768,500 m³ (2,768 ML) accounts for 16.2% of the mean annual volume of outflow from the system for the entire transient simulation period. As shown in Appendix O, about 77.6% (2,154,600 m³ yr⁻¹) of the mean annual leakage occurred in Fracture line A, while 15.8% and 6.6% were leaked along Fracture lines B and C, respectively. It should be noted that leakage rates assigned in Fracture lines A, B, and C were held constant throughout the simulation period.

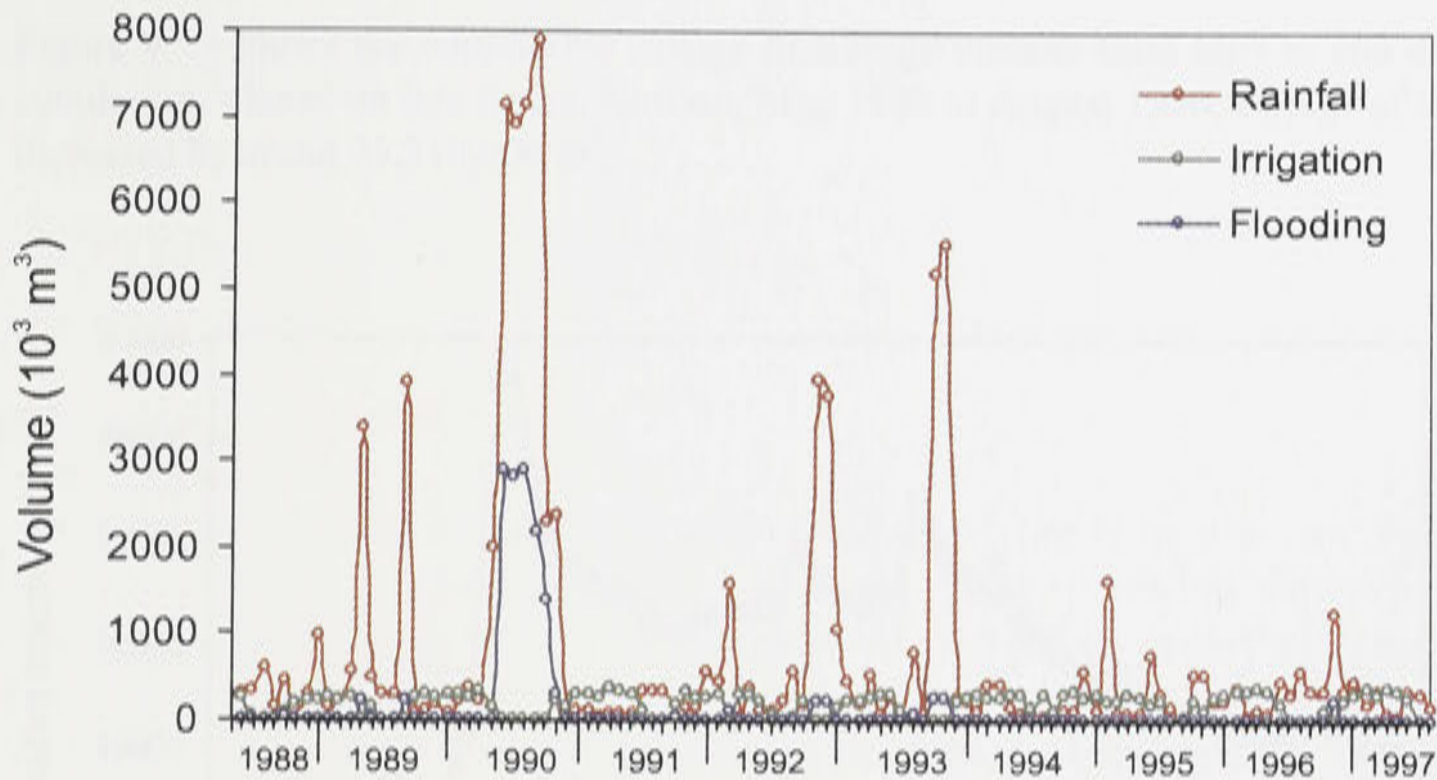


Figure 9.12: Monthly total volume of recharge components for the period May 1988 to July 1997.

c. Drainage through the Gilmore Fault

The contribution of drainage through the Gilmore Fault to the total volume of outflow for the entire transient simulation period is only 2%. About 339,600 m³ (Appendix N) have been drained through the fault annually for the period of simulation.

d. Evapotranspiration

Evapotranspiration is a major source of groundwater outflow from the system, accounting for about 64.5% (11,056,000 m³) of the mean annual total volume of outflow. On the average, groundwater is lost through ET at a rate of 30,274 m³ d⁻¹ during the transient simulation period. Larger volume of groundwater is lost through evapotranspiration when groundwater is near the ground surface especially during flooding events (Figure 9.11).

e. Outflow through Manna Gap

The mean annual volume of outflow through the Manna Gap is 10,200 m³ or about 0.01% of the mean annual total volume of outflow from the system. As mentioned earlier in section 8.12.4.2, the low volume of outflow through the Manna Gap is due to the fact that the majority of the outflow occurs at the constant head cells boundary along the lower third part of the Lachlan River.

9.12.4.3. Change in groundwater storage

The change of groundwater storage indicates net gain between inflows and outflows, with positive values indicating a rise of groundwater level, while negative values signifying a fall of groundwater level (Appendix N). The transient simulation shows a mean annual positive net gain of 1,043,100 m³ (1,043.1 ML) of groundwater in the system for the period of simulation..

Figure 9.13 shows the cumulative change in storage volume from start to end of the transient simulation. Based on this figure, between May 1988 to August 1990, storage of the aquifer has increased by about 29,310,000 m³.

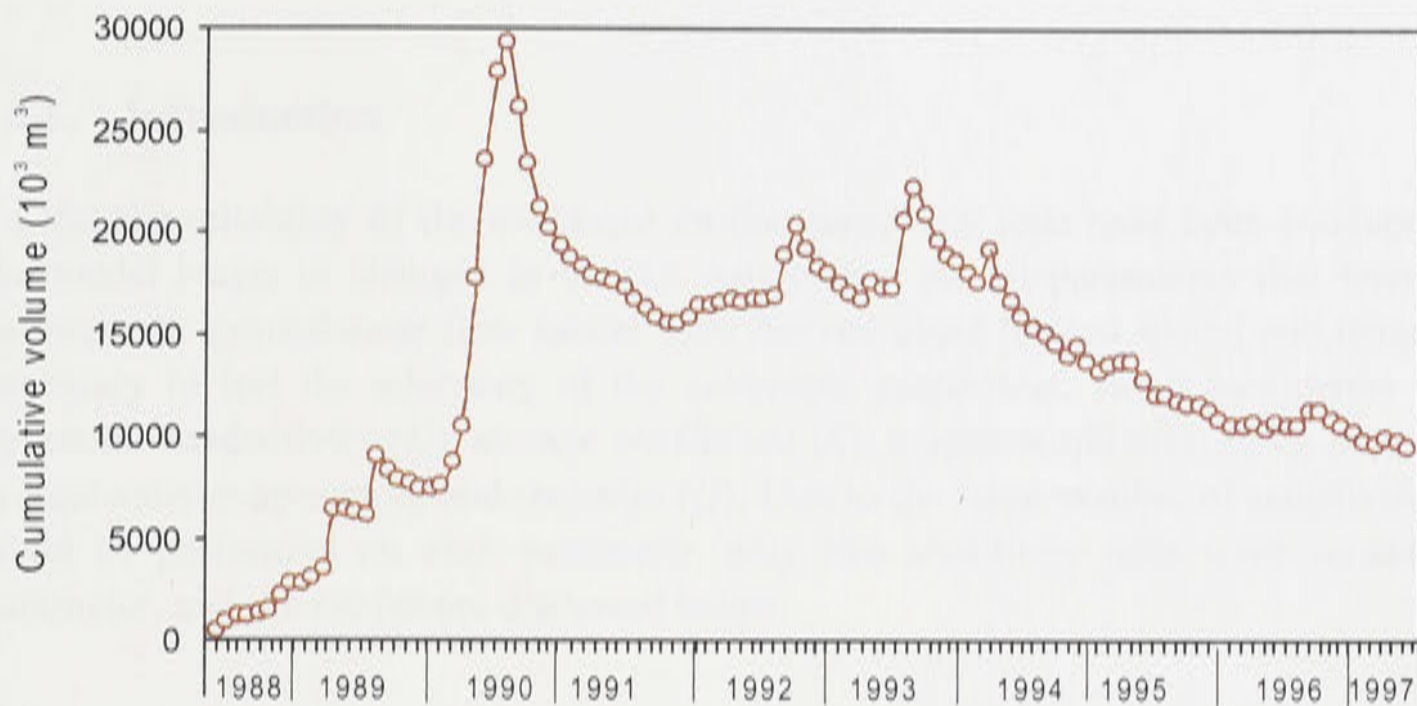


Figure 9.13: Cumulative volume of change in storage for the entire transient simulation period of May 1988 to July 1997.

9.13. General comments on PEST software

Due to the complexity of the groundwater system of the modelled area, the application of PEST in the calibration process has been limited. In general, PEST has efficiently optimised aquifer parameters in the steady-state calibration over a short period of time. However, in transient calibration with over 100 stress periods, optimisation process proved very time consuming, especially for optimising the time-dependent parameter such as recharge.

With our experience, application of PEST in the parameter optimisation process is advisable only in a simple aquifer system, with fewer stress periods (or timesteps) and parameters to optimise.

CHAPTER 10

SENSITIVITY ANALYSIS

10.1. Introduction

To test the reliability of the calibrated model, sensitivity tests have been conducted to see how the model reacts to changes in various parameters. As all parameters that were employed to calibrate the groundwater flow model were derived using limited spatial and temporal data, it is necessary to test the adequacy of the calibrated parameters. Here, parameters tested include hydraulic conductivity (K), storage coefficient (S), evapotranspiration (ET), extinction depth of groundwater evaporation, and recharge (Q). Due to the large number of sensitivity analyses that could be performed on each parameter, only two sensitivity tests were considered for each parameter, and the results are discussed below.

10.2. Hydraulic conductivity

As discussed in Chapter 8, hydraulic conductivity values were estimated using the weighted thickness of sand, gravel and clay materials at the available bores in the study area. Due to the limited number of pumping tests, the accuracy of K distribution is uncertain. To take into account for the possible overestimation and underestimation of K values, sensitivity analyses on K were performed to determine the effects of changes in K on the spatial and temporal distribution of the computed piezometric heads throughout the study area.

As a result of the positive or negative biases that may have occurred, the calibrated values shown in Tables 8.1 and 8.3 were doubled and halved to test the sensitivity of the K values. Therefore, a uniform increase in calibrated K values of 100% and a decrease of 50% throughout the study area were compared to those piezometric distribution generated by the calibrated transient model.

The measured and computed piezometric heads were compared for the 16 observation wells as shown in Figures 10.1a to 10.1d. The observation wells are relatively evenly distributed throughout the study area, thus providing an indication of the responsiveness of changes in hydraulic conductivity on piezometric heads throughout the study area.

Overall, the response of the piezometric heads with the increase and decrease of K values are relatively small, although at some locations piezometric heads tend to be more responsive. Observation wells that are most sensitive to changes in hydraulic conductivity are wells 1W, 13W, 45W, 58P and 91P. In these observation wells, the maximum change of heads as a result of increasing K by 100% ranges from 0.4 to 1.4 m. The maximum change when K is decreased by 50% ranges from 0.1 to 1.4 m. Most of these wells are located in high recharge areas, except for 45W and 91P which are located in low recharge zone areas. Well 45W is situated close to the fracture line A near Lake Cowal, while 91P is close to the outflow boundary.

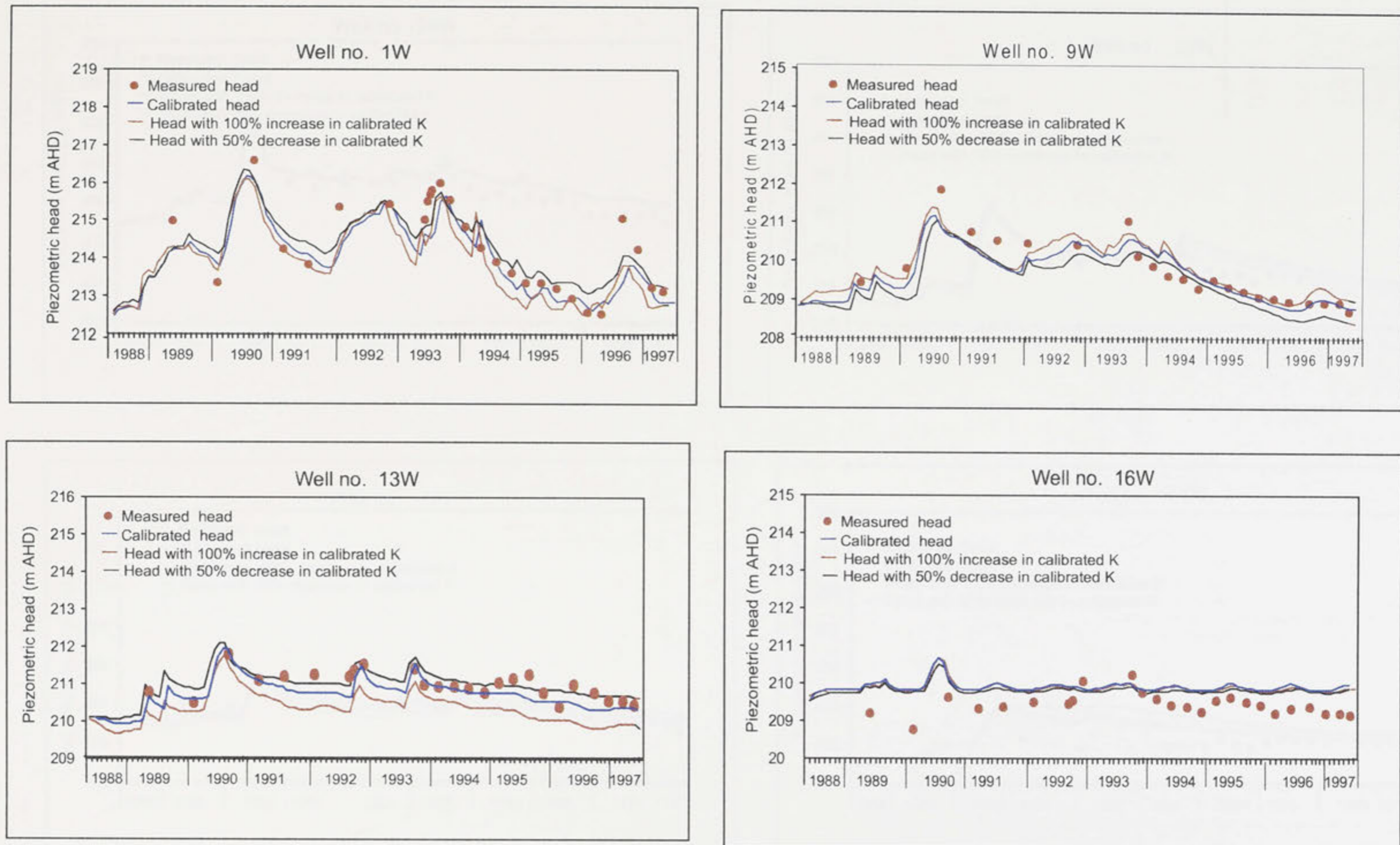


Figure 10.1a: Comparison between measured and computed heads at observation wells 1W, 9W, 13W and 16W with respect to changes in hydraulic conductivity (see Figure 9.7 for locations).

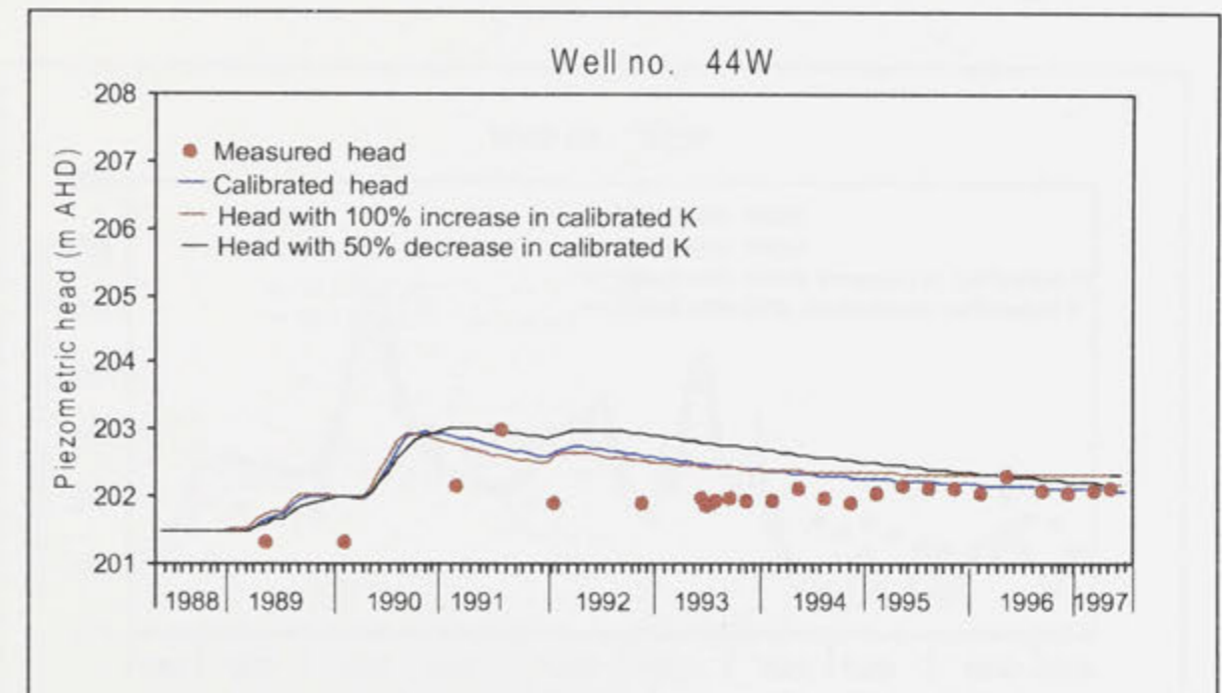
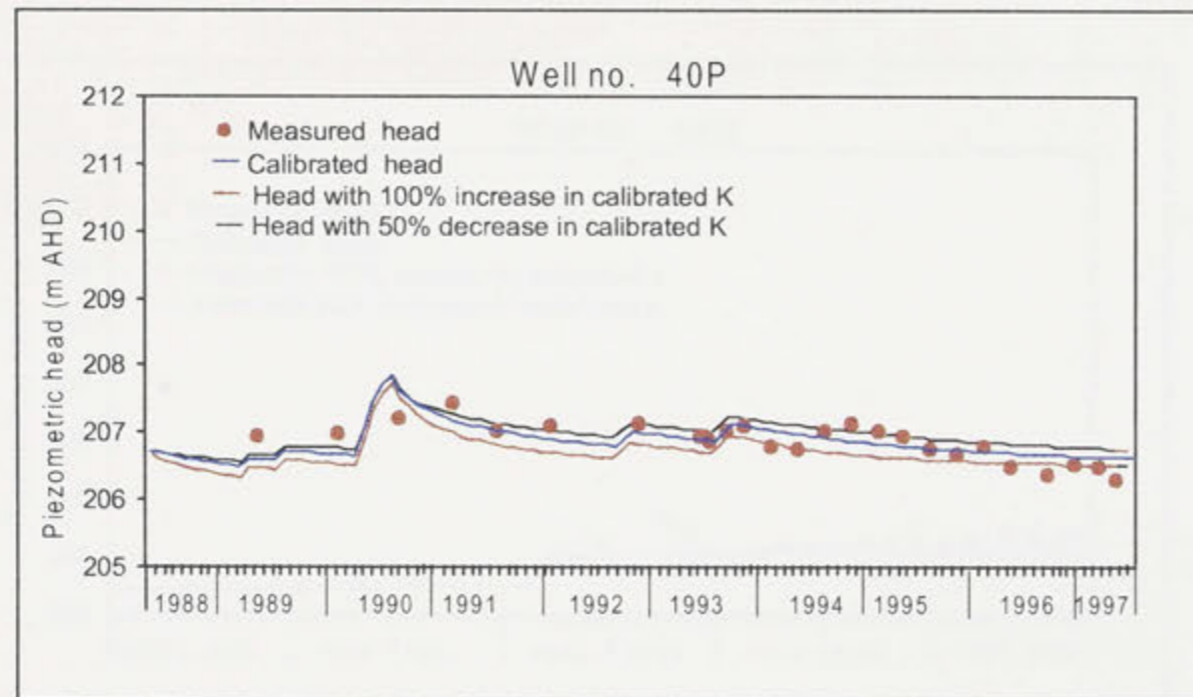
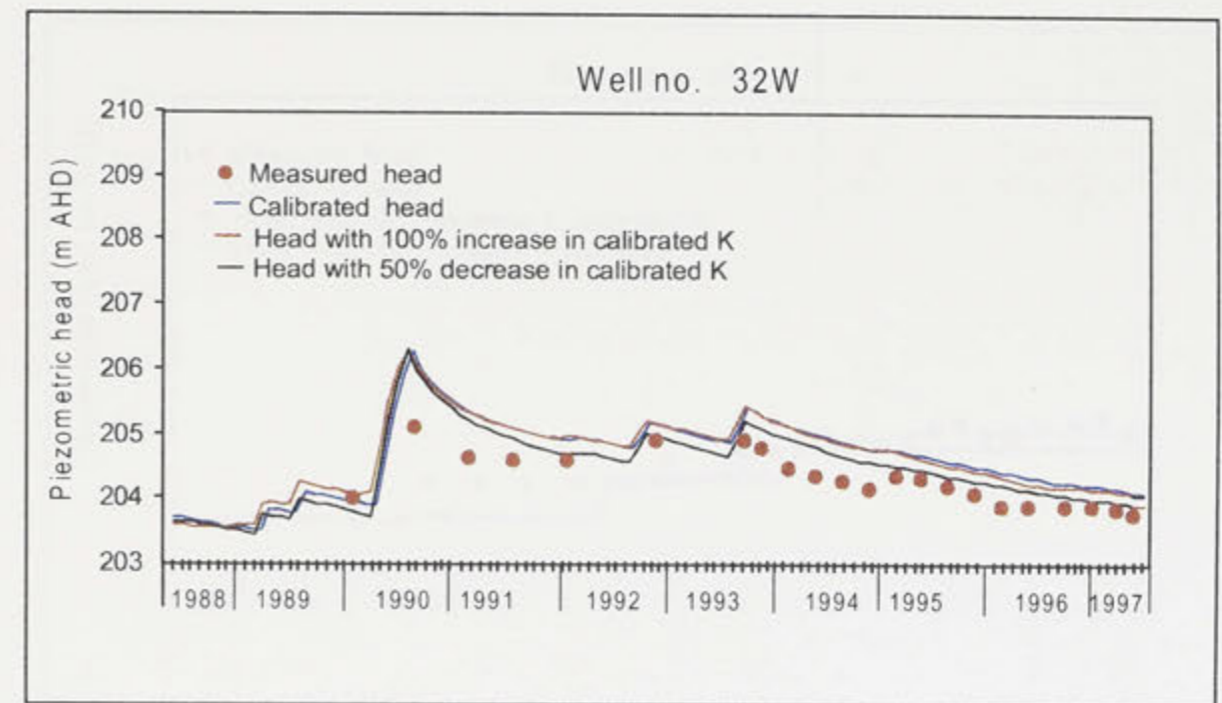
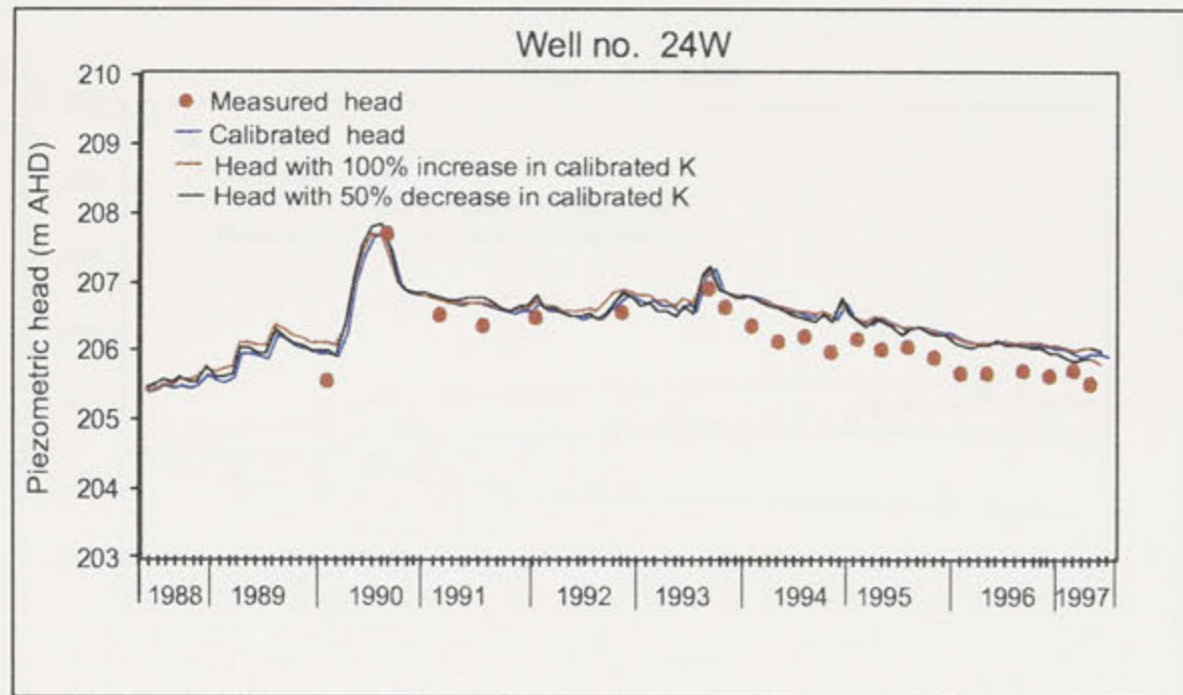


Figure 10.1b: Comparison between measured and computed heads at observation wells 24W, 32W, 40P and 44W with respect to changes in hydraulic conductivity (see Figure 9.7 for locations).

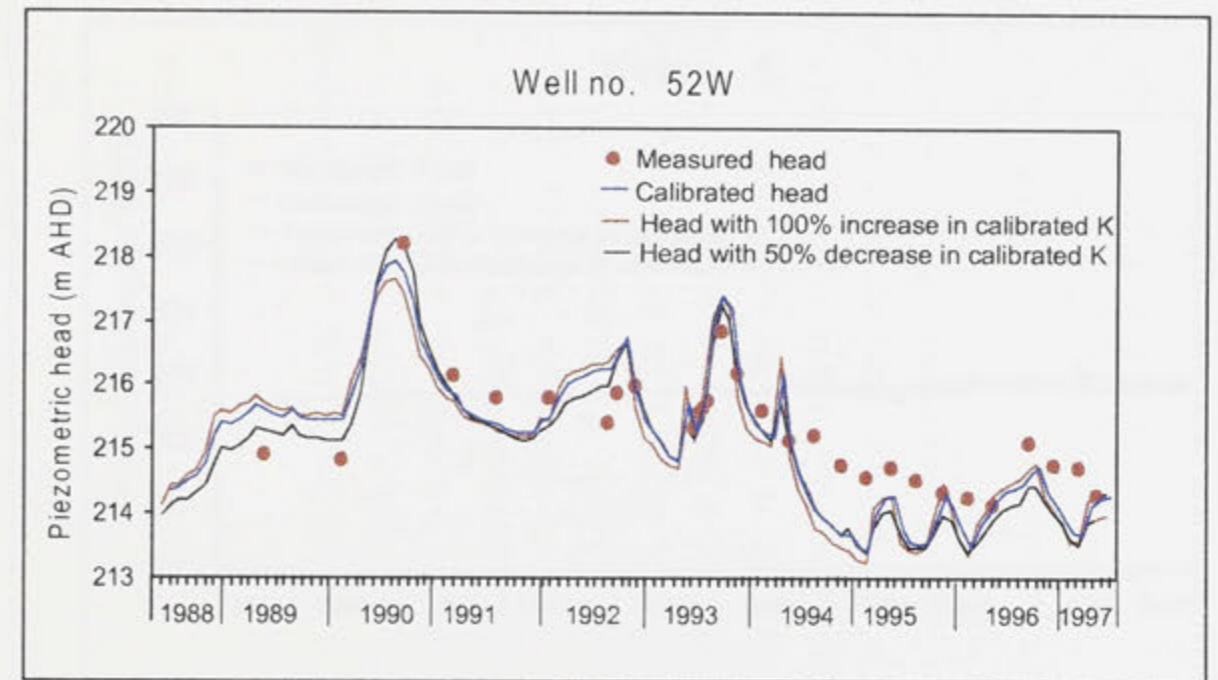
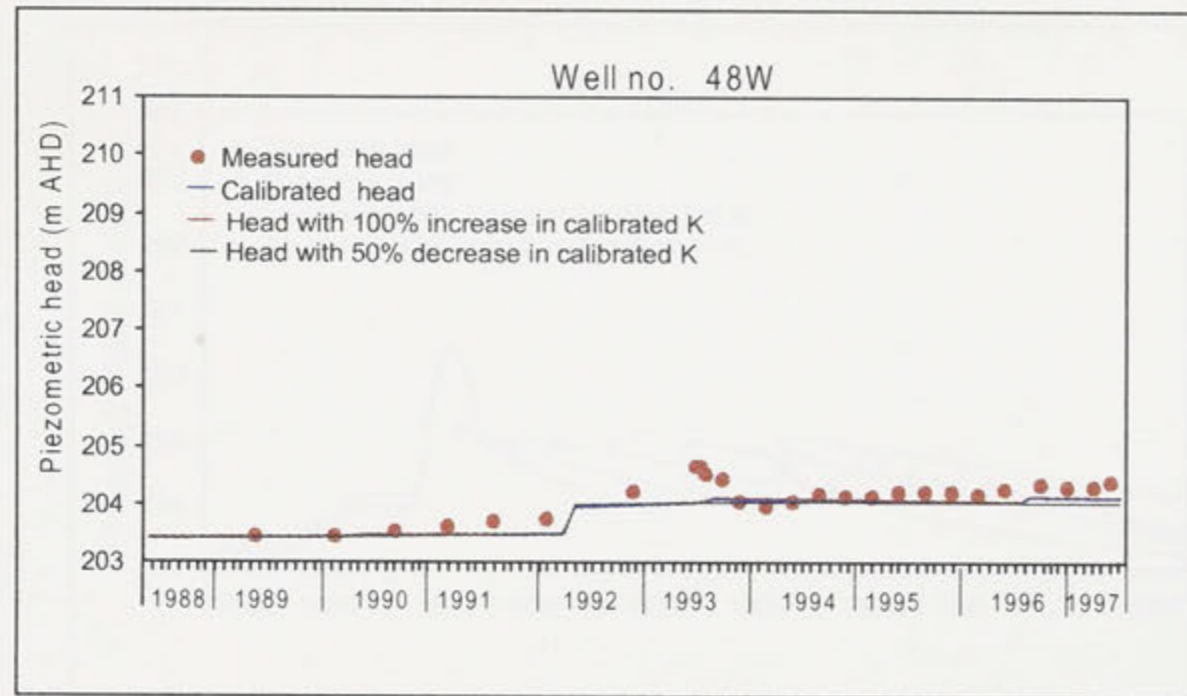
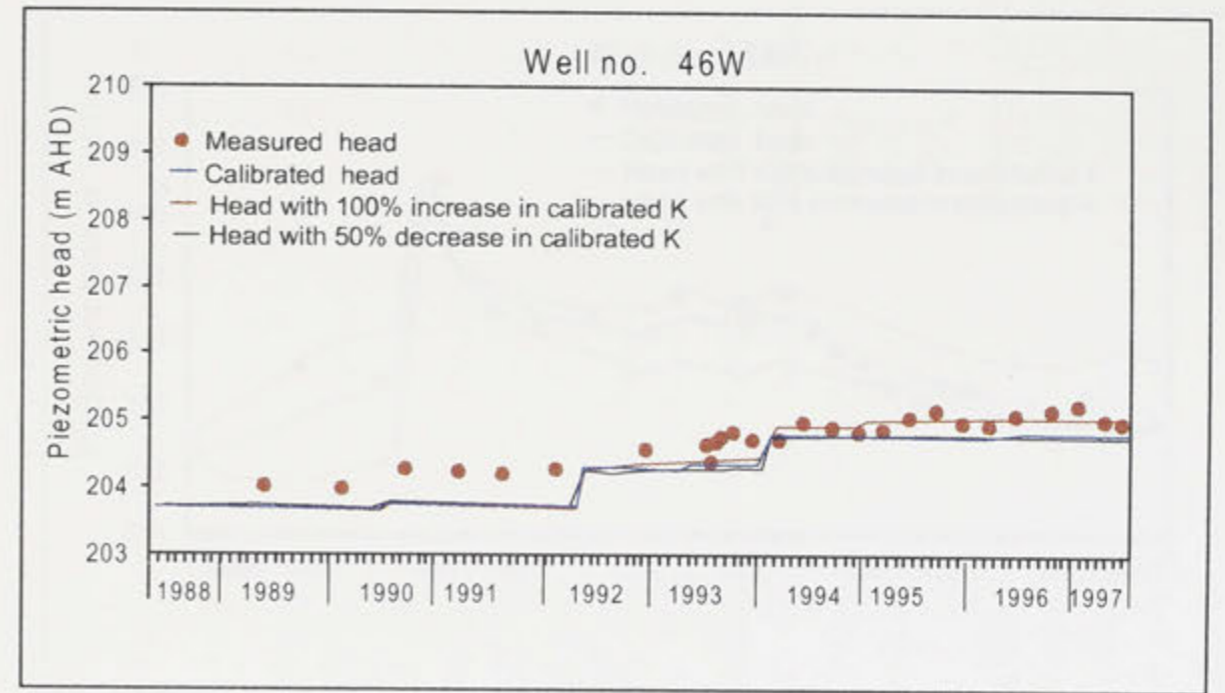
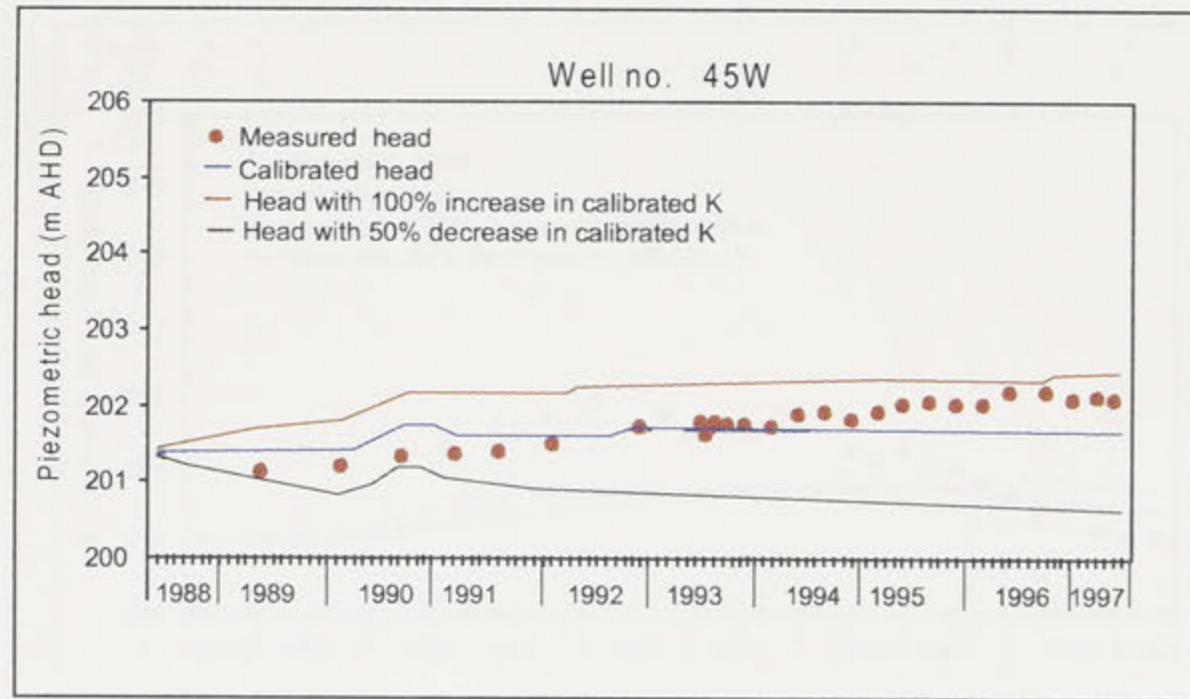


Figure 10.1c: Comparison between measured and computed heads at observation wells 45W, 46W, 48W and 52W with respect to changes in hydraulic conductivity (see Figure 9.7 for locations).

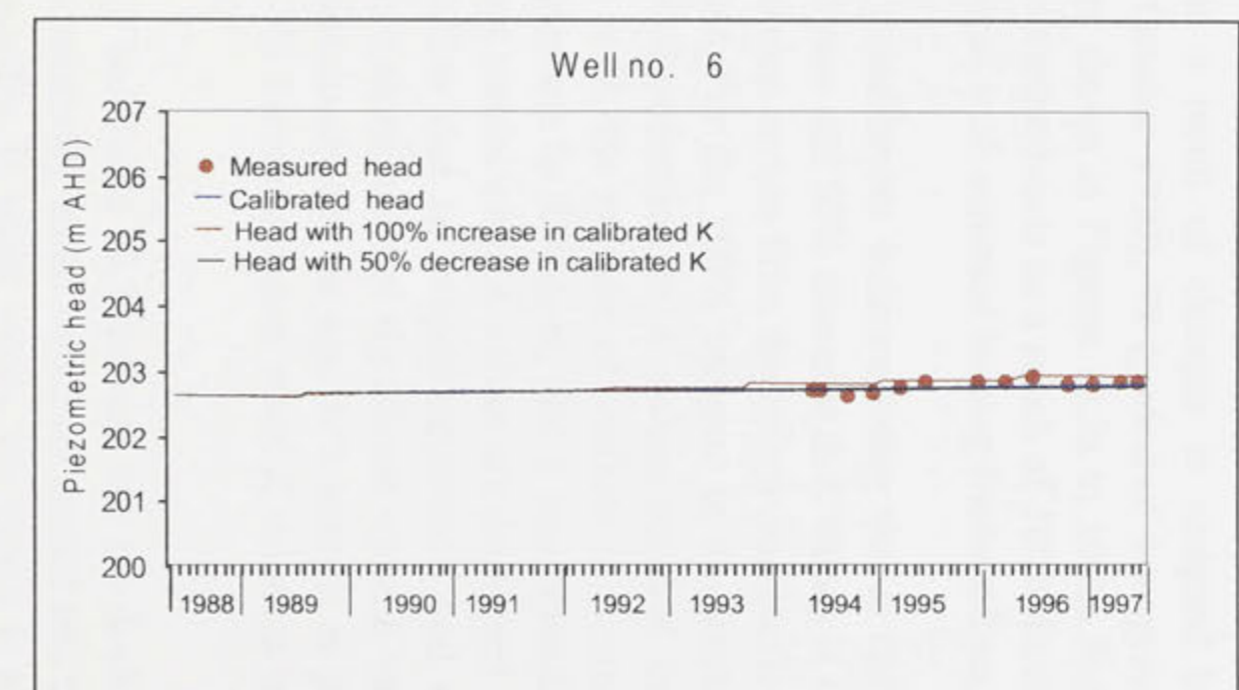
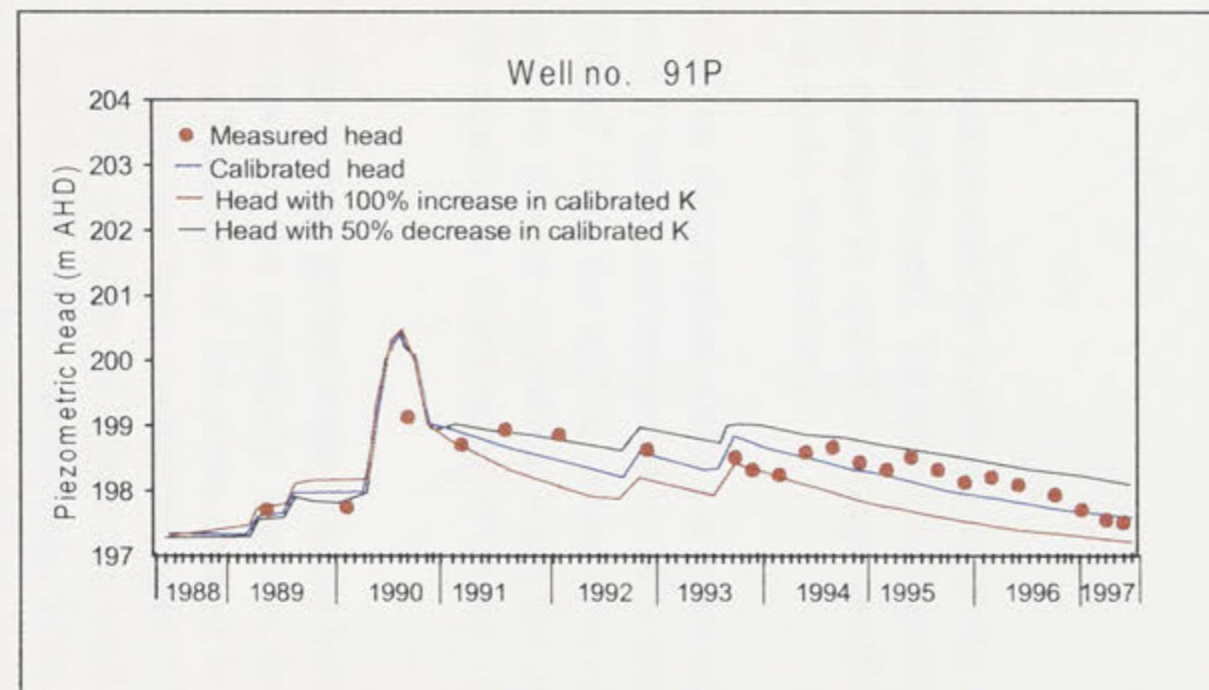
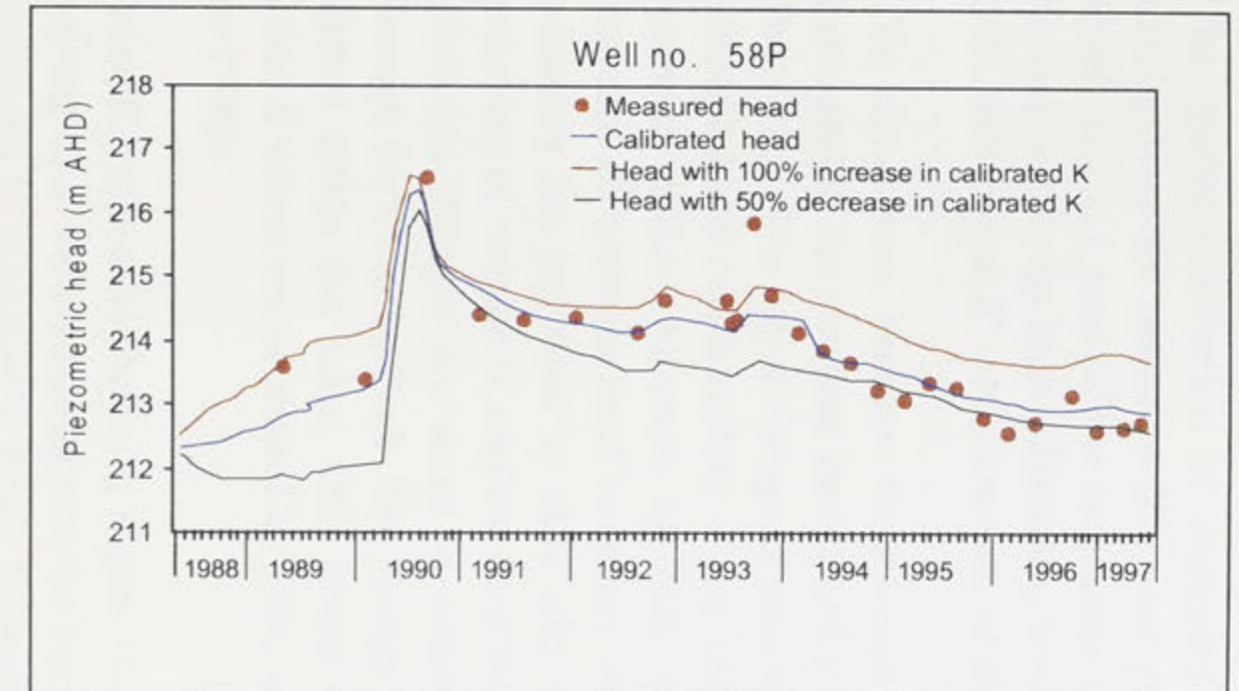
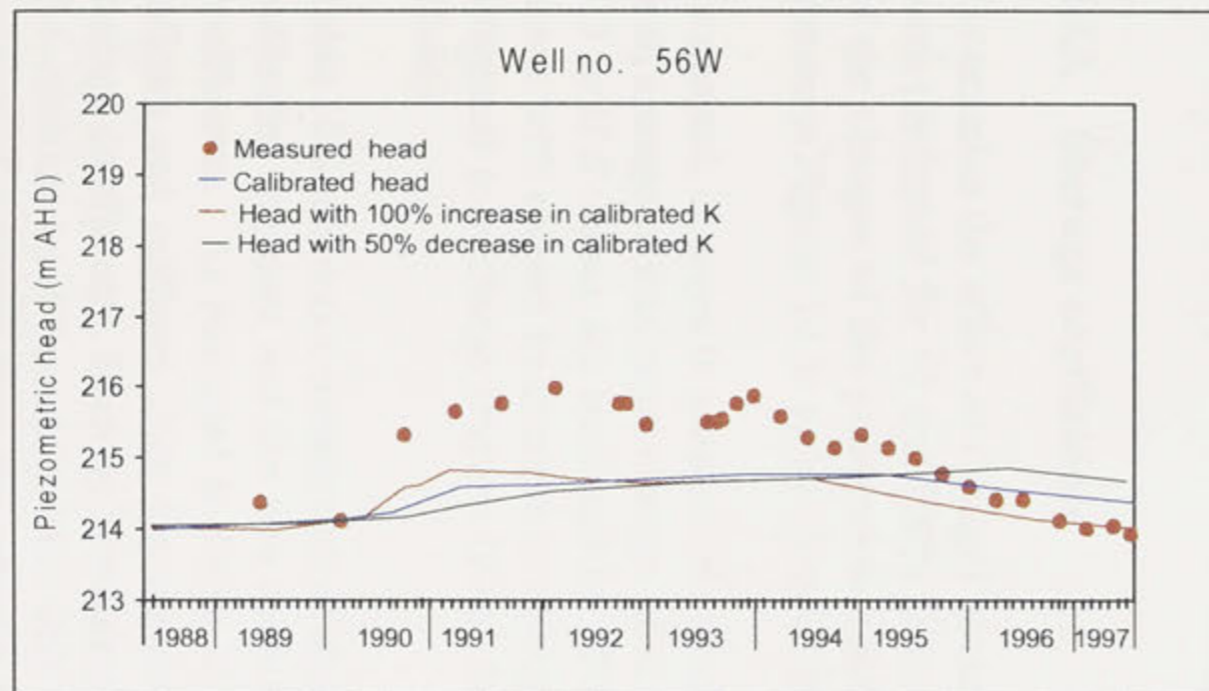


Figure 10.1d: Comparison between measured and computed heads at observation wells 56W, 58P, 91P and 6 with respect to changes in hydraulic conductivity (see Figure 9.7 for locations).

The spatial distribution of computed heads as a result of changes in assigned hydraulic conductivity for timesteps 30 (flood period of October 1990), 78 (period of low groundwater level) and 111 (end of the simulation period) are shown in Figures 10.2a to 10.2c. From these figures, relatively high differences between piezometric heads as a result of 100% increase and 50% decrease in K values are centred along the areas with assumed leaking fracture lines.

The comparison between the average annual groundwater balance using the K distribution calibrated in the transient model, and a 100% increase and 50% decrease in K values is shown in Table 10.1. The major change in groundwater balance occurs from the inflow and outflow of the constant head cell boundary at the Lachlan River. For the 100% increase in K , constant head boundary inflow increases by 78%, while a 50% reduction in K values resulted in a 45% decrease of constant head boundary inflow. As well, the volume of outflow at constant head boundary has increased by 60% with a 100% increase in K values, and a corresponding 33% reduction of volume of outflow from this boundary results when K values are decreased by 50%. Moderate changes are noted in volume of outflow due to evapotranspiration and drainage through the Gilmore Fault. The change in aquifer's storage is not significant when K values are altered within this range. Only about 1% increase in change in aquifer's storage is produced when K values are decreased by 50%, and about 3% decrease occurs when K values is increased by 100%.

Overall, the results shown in Figure 10.1 and 10.2 and Table 10.1 indicate that the doubling and halving of K values throughout the aquifer has a relatively small effect on spatial and temporal variations in piezometric heads throughout the aquifer. In other words, the model is relatively insensitive with respect to modest changes in assigned hydraulic conductivities.

10.3. Storage coefficients

To examine the effect of changes in storage coefficients across the aquifer, sensitivity analyses were performed for 50 and 100% increases in storage coefficients. Temporal and spatial results of the changes of the piezometric heads due to the changes in specific storage coefficient are shown in Figures 10.3a to 10.3d and Figures 10.4a to 10.4c, respectively.

In general, changes in piezometric heads for most of the observation wells are relatively small, with a range of maximum change of 0.04 to 0.8 m if S values are increased by 50% and 0.10 to 1.3 m if S values are increased by 100%. From Figure 10.4, the spatial changes in computed heads with respect to changes in storage coefficients are greater in periods when the aquifer is subjected to recharge (Figure 10.4a) than when the aquifer is discharging (Figures 10.4b and 10.4c).

Table 10.2 presents a comparison of changes in average annual groundwater balance between the calibrated transient and the two models which incorporate the sensitivity analysis on storage coefficients. As indicated in Table 10.2, only a small change of the mean annual volume of inflows and outflows from the constant head boundary has been computed after increasing storage coefficients. Even by increasing S values by 100%, volumes of inflow and outflow from the constant head boundary have only increased by 9% and 19%, respectively. Mean annual volume of outflows from groundwater evaporation and drainage decrease with an increase in S due to drop of piezometric heads, thus also reducing the overall total volume of outflow in the system. With 50% increase in S values, the corresponding decrease of volume of outflow from groundwater evaporation and drainage are about 11% and 6%, respectively.

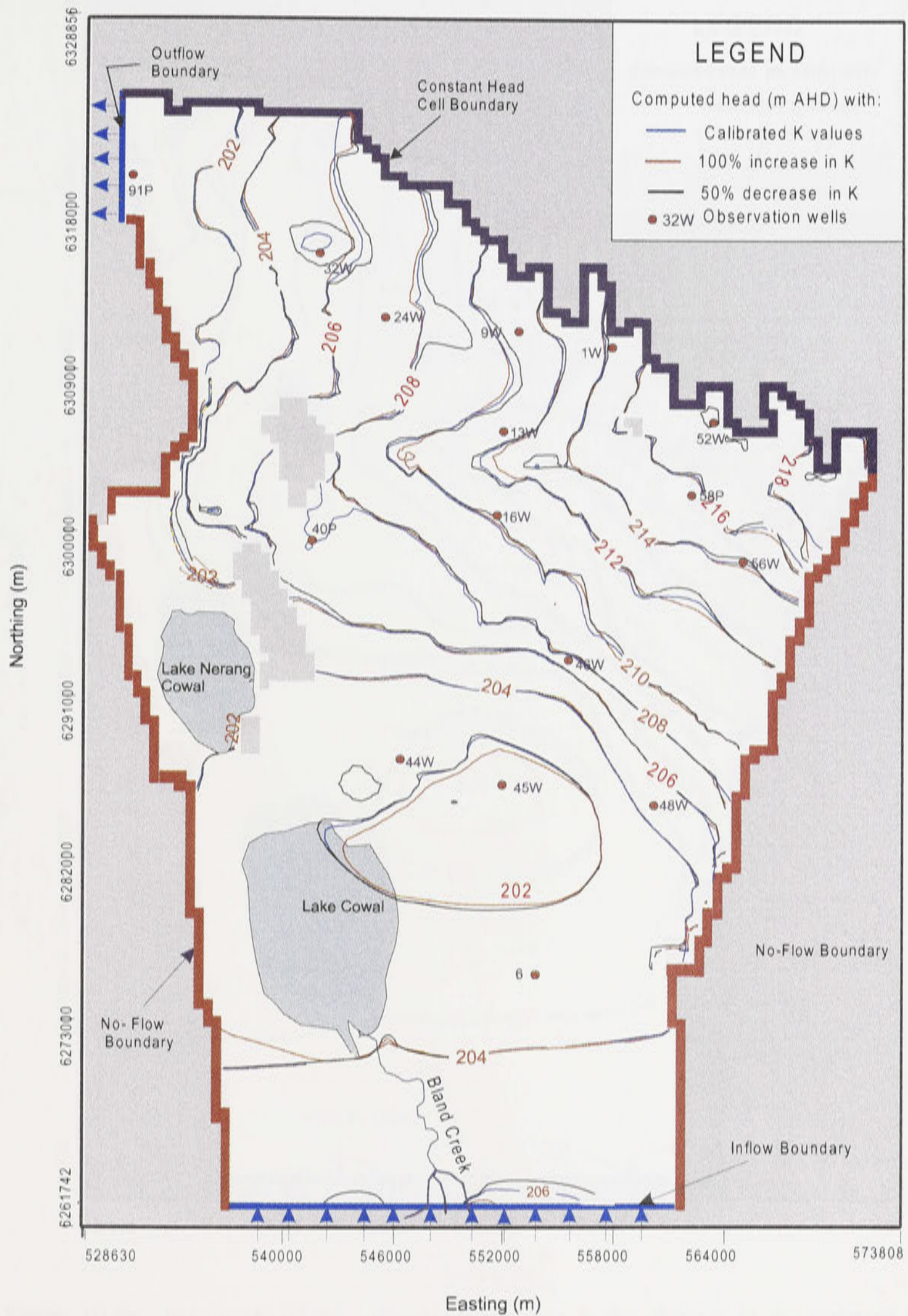


Figure 10.2a: Sensitivity of the computed heads due to the changes in the assigned hydraulic conductivity for the flood period of October 1990 (timestep 30).

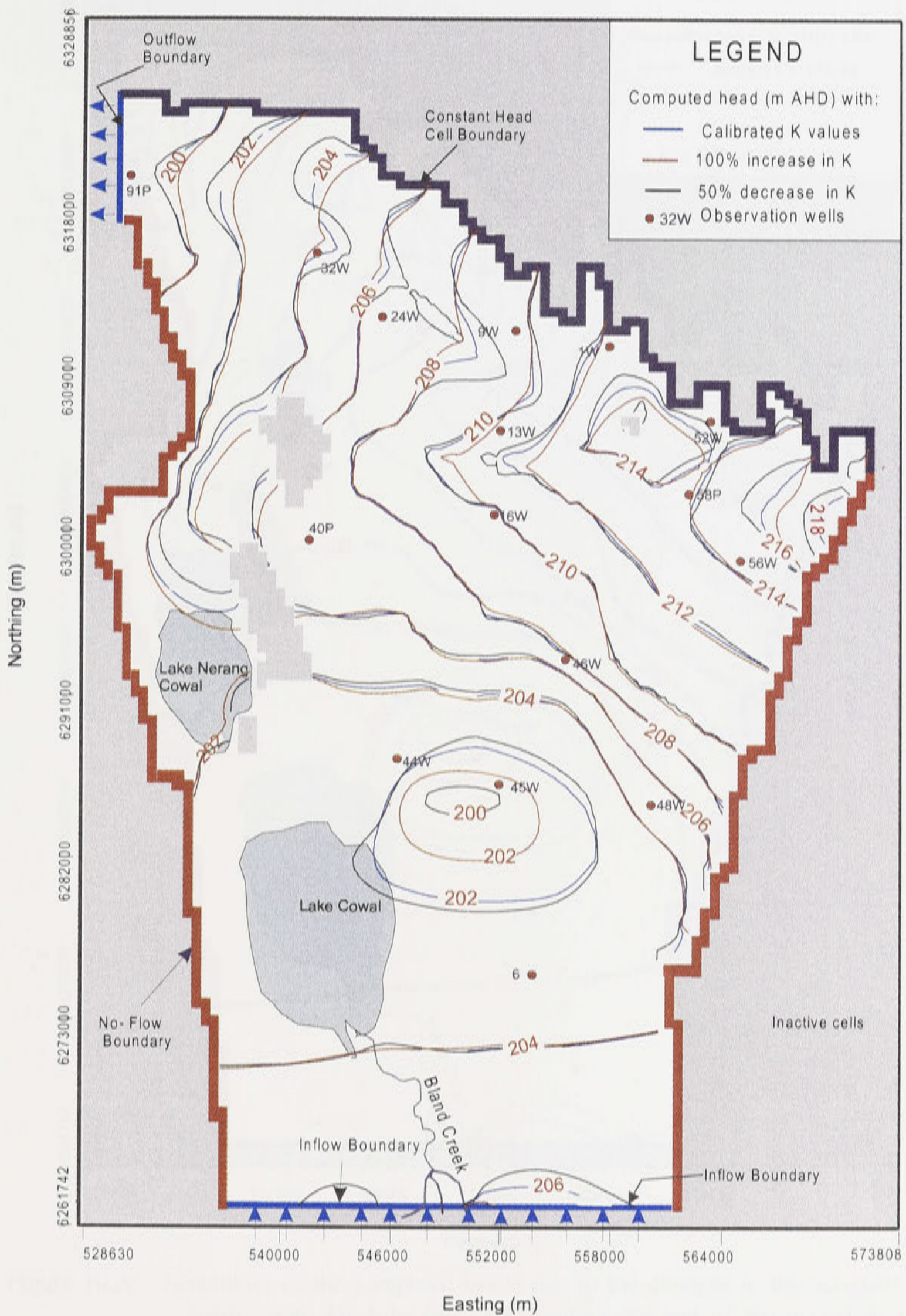


Figure 10.2b: Sensitivity of the computed heads due to the changes in the assigned hydraulic conductivity for October 1994 representing a period of low groundwater levels (timestep 78).

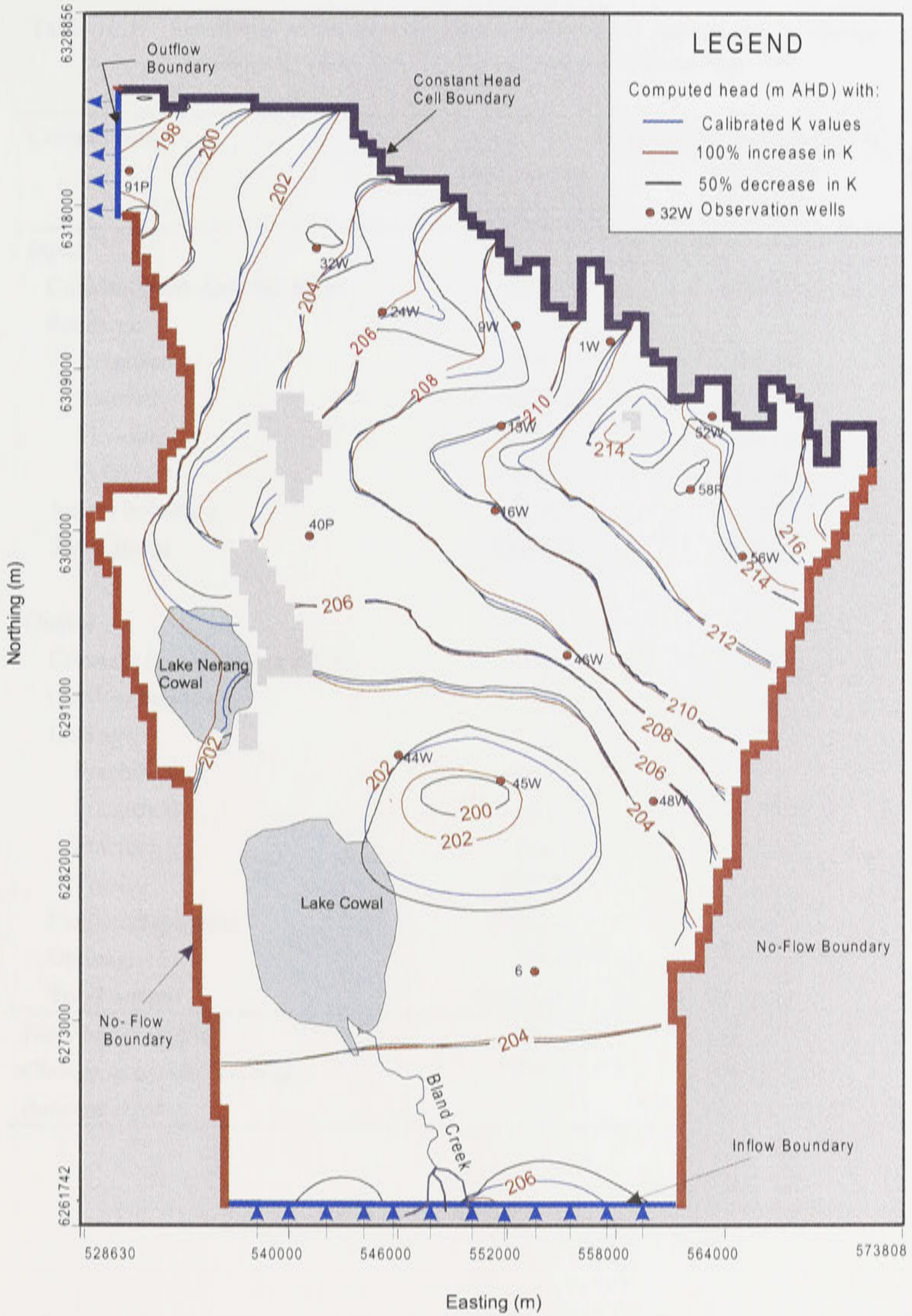


Figure 10.2c: Sensitivity of the computed heads due to the changes in the assigned hydraulic conductivity for July 1997 representing the end of the period of simulation (timestep 111).

Table 10.1: Sensitivity of the average annual groundwater balance due to changes in hydraulic conductivity (K) values for the period May 1988 to July 1997.

Components	Mean annual volume (10^3 m^3)		
	50% decrease in K values	Calibrated model	100% increase in K values
<i>Input</i>			
Constant head-Lachlan River	2322.0	4216.0	7502.4
Recharge:			
Irrigation	2226.7	2226.7	2226.7
Rainfall	9850.4	9850.4	9850.4
Flooding	1553.4	1553.4	1553.4
Total	13630.5	13630.5	13630.5
Inflow boundary	334.0	334.0	334.0
Total input	16286.5	18180.5	21467.0
<i>Output</i>			
Constant head-Lachlan River	1970.2	2953.9	4740.1
Outflow boundary	10.2	10.2	10.2
Leakage:			
Fracture A	2154.6	2154.6	2154.6
Fracture B	438.2	438.2	438.2
Fracture C	184.7	184.7	184.7
Total	2777.5	2777.5	2777.5
Evapotranspiration	10222.6	11056.0	12488.7
Drainage	250.8	339.6	435.4
Total output	15231.4	17137.3	20451.9
<i>Total input- output</i>	<i>1055.1</i>	<i>1043.2</i>	<i>1015.1</i>
<i>Change in aquifer's storage</i>	<i>1054.8</i>	<i>1043.1</i>	<i>1014.7</i>
<i>Balance error</i>	<i>0.3</i>	<i>0.1</i>	<i>0.4</i>

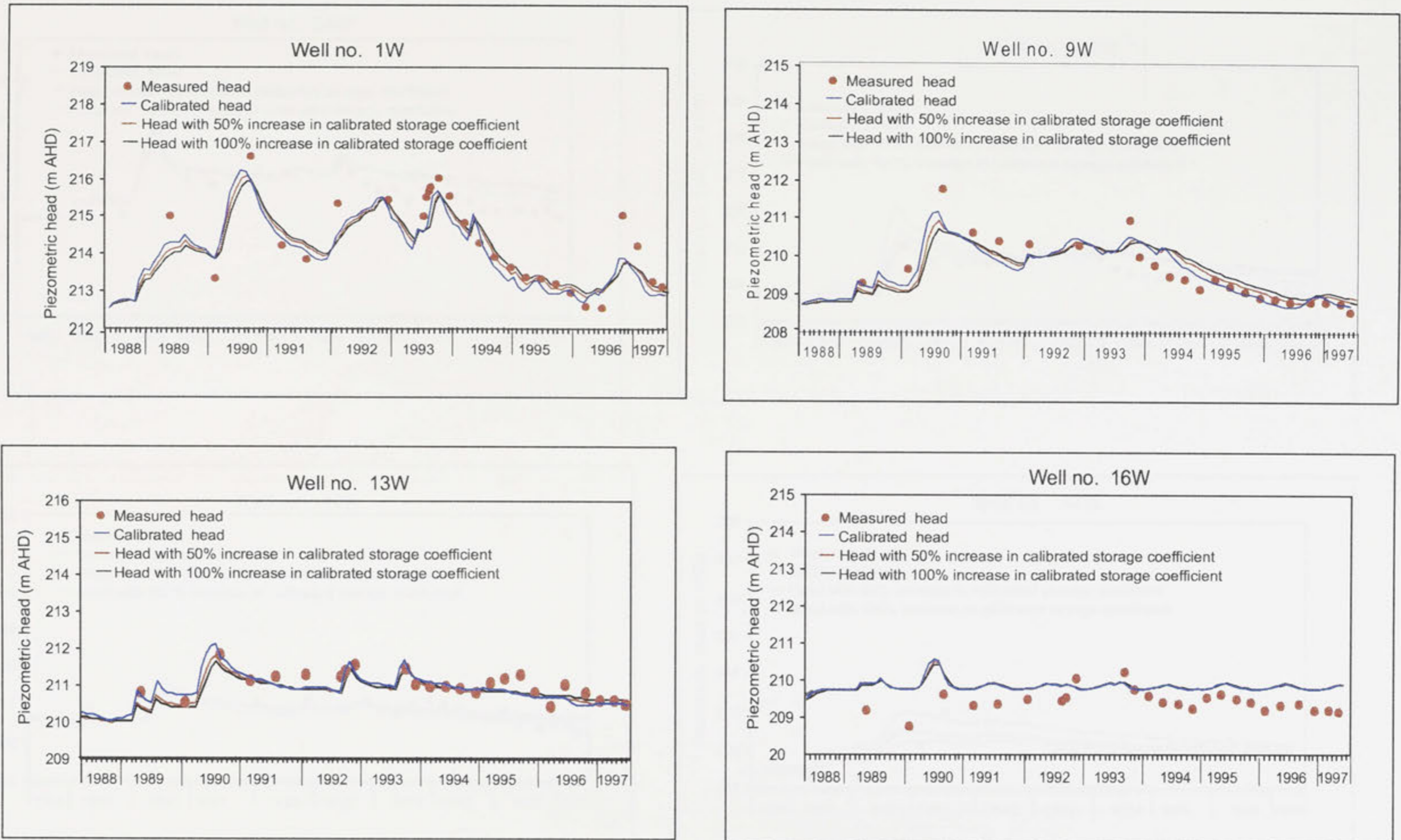


Figure 10.3a: Comparison between measured and computed heads at observation wells 1W, 9W, 13W and 16W with respect to 50% and 100% increase in storage coefficient (see Figure 9.7 for locations).

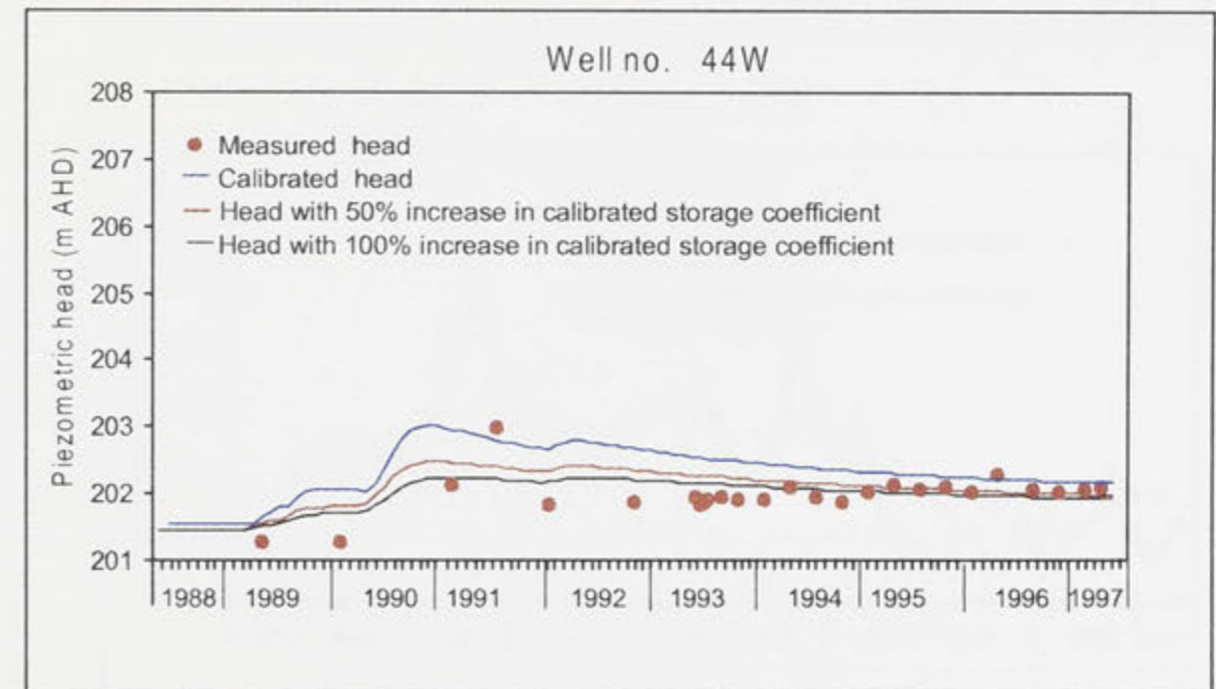
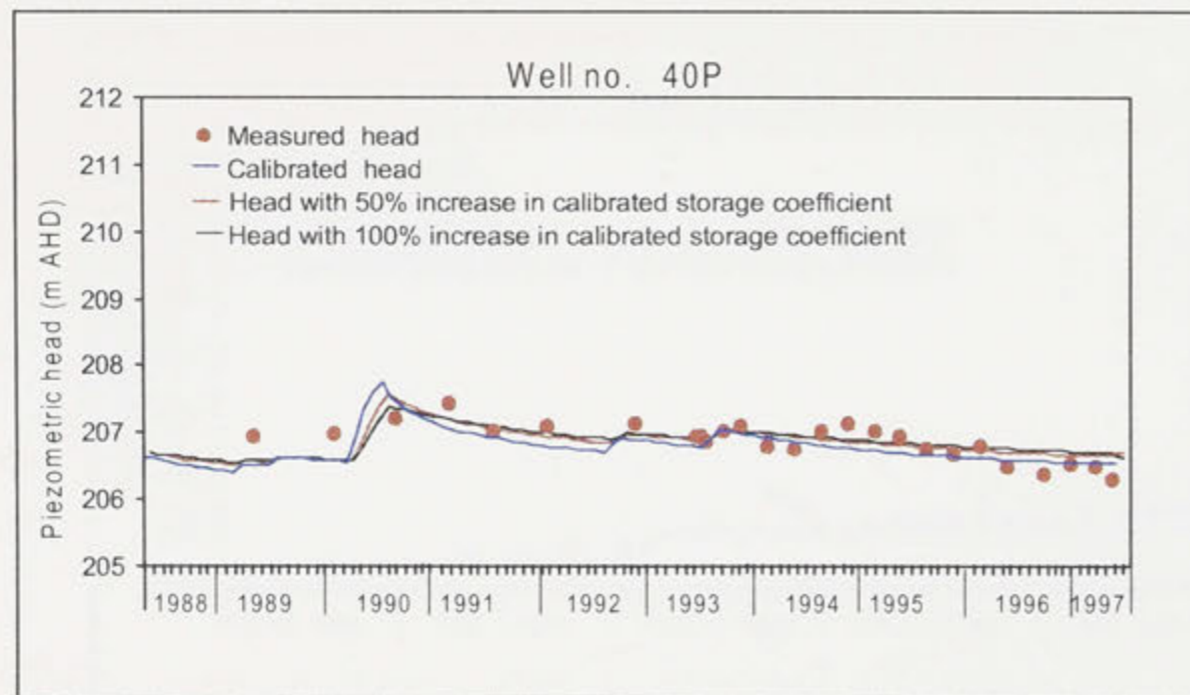
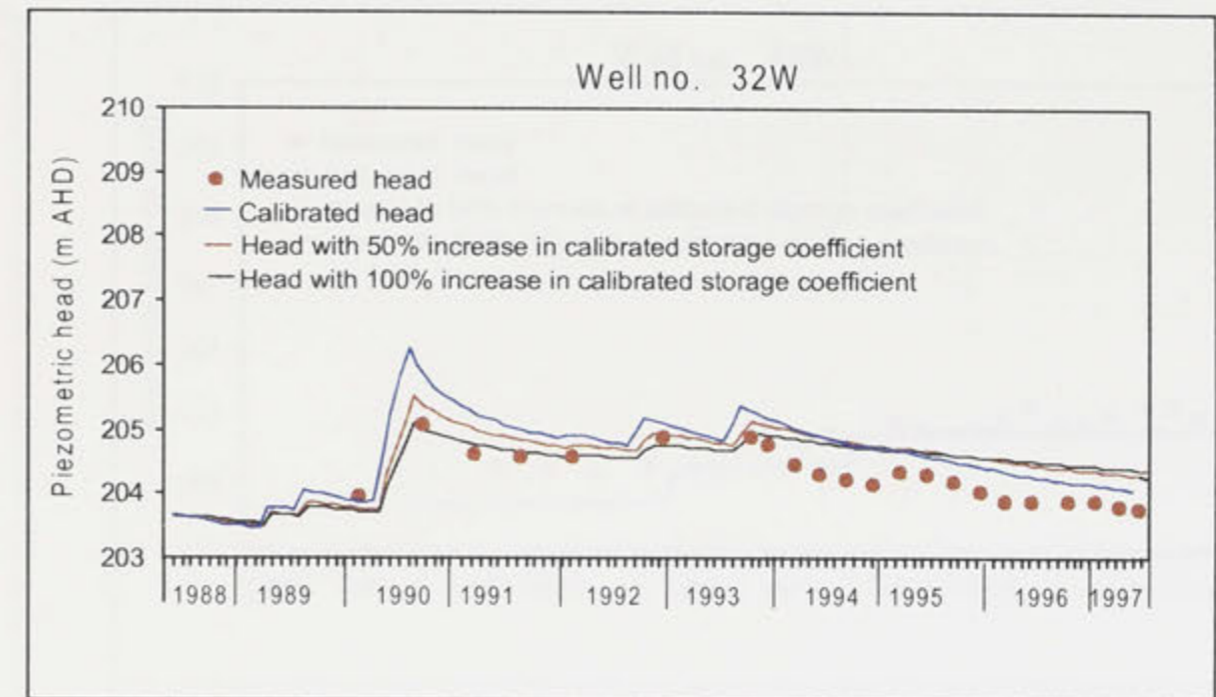
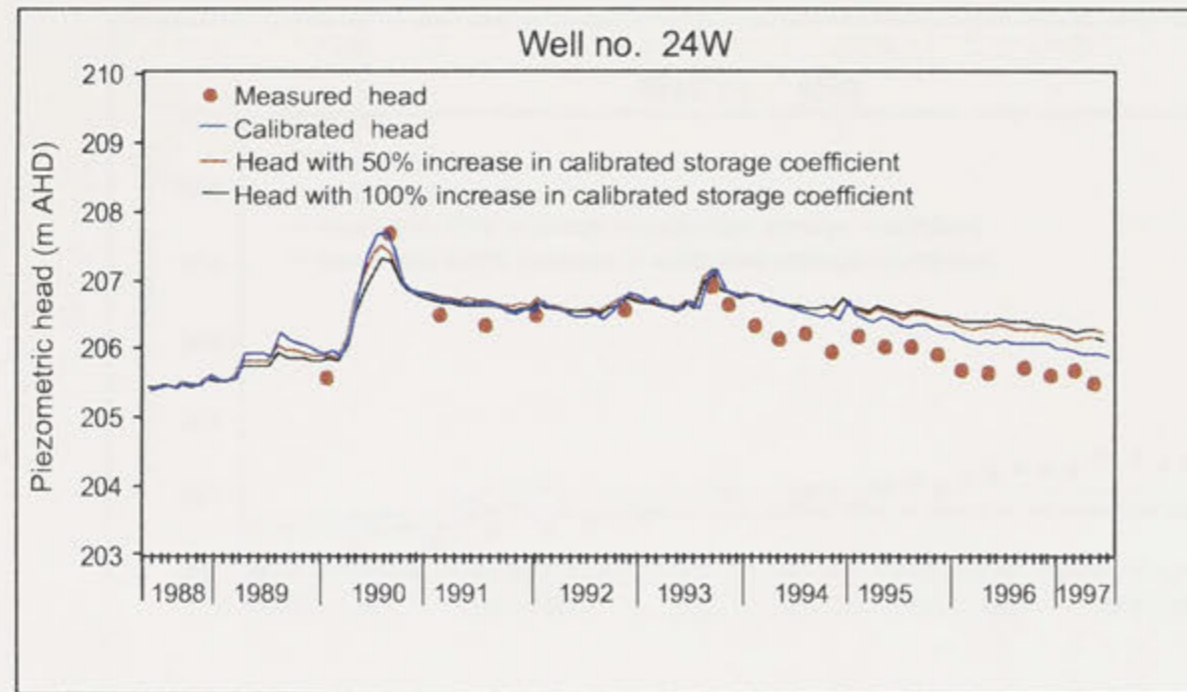


Figure 10.3b: Comparison between measured and computed heads at observation wells 24W, 32W, 40W and 44W with respect to 50% and 100% increase in storage coefficient (see Figure 9.7 for locations).

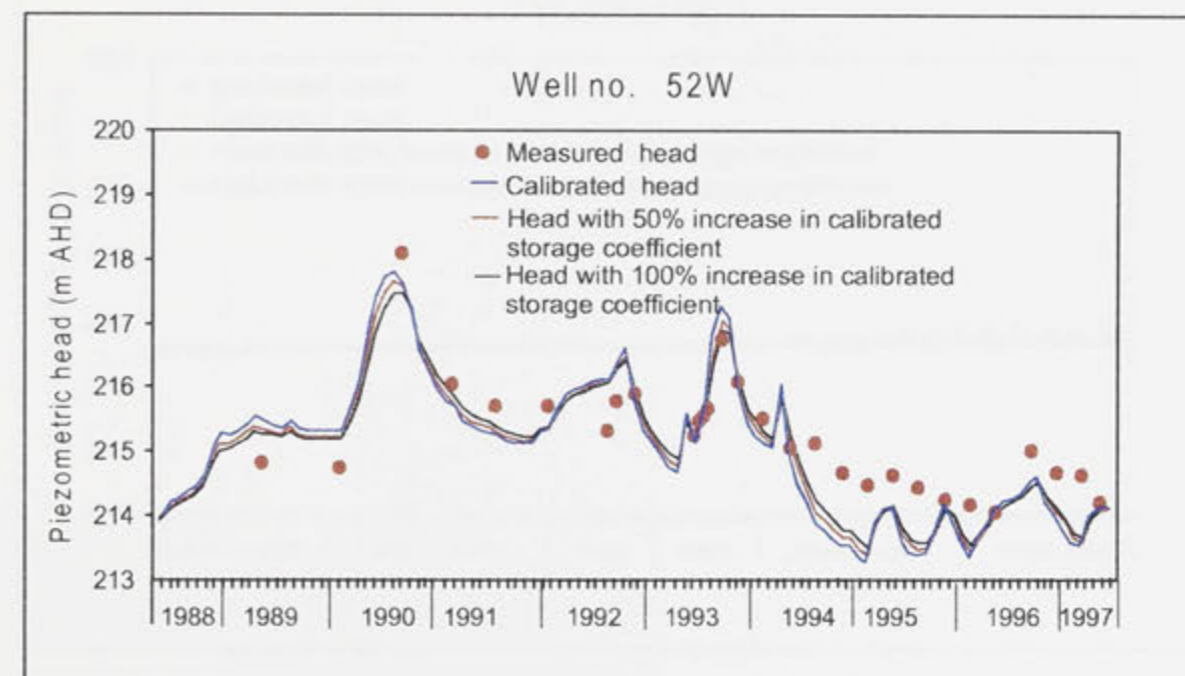
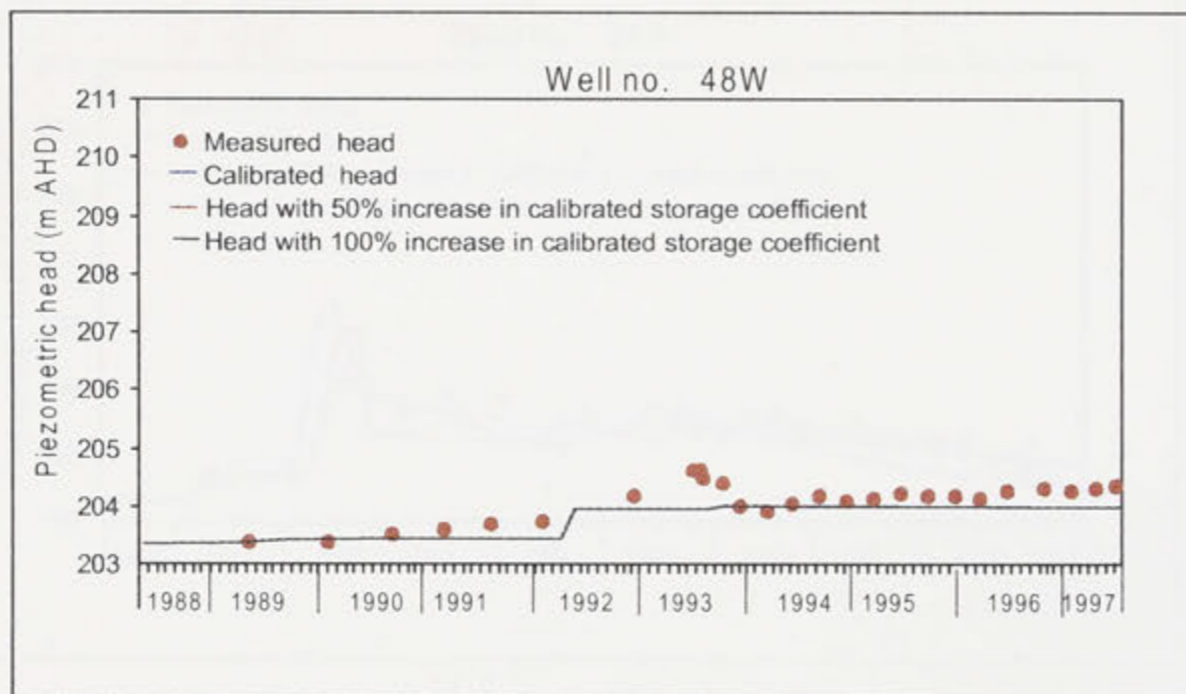
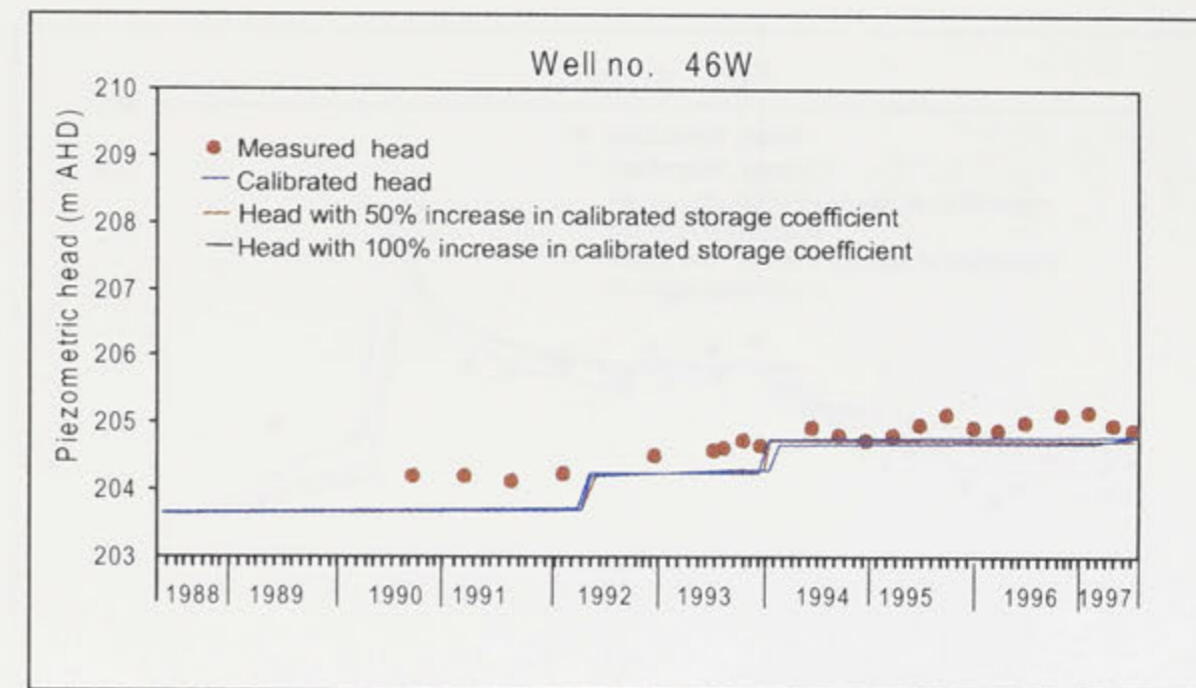
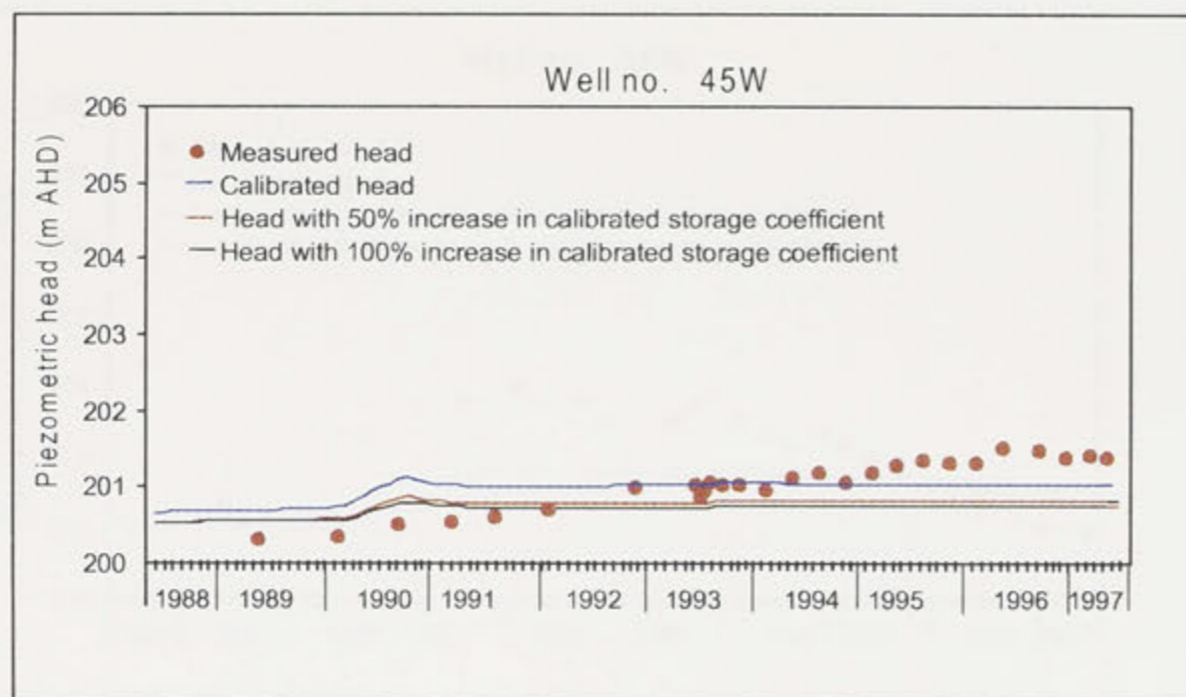


Figure 10.3c: Comparison between measured and computed heads at observation wells 45W, 46W, 48W and 52W with respect to 50% and 100% increase in storage coefficient (see Figure 9.7 for locations).

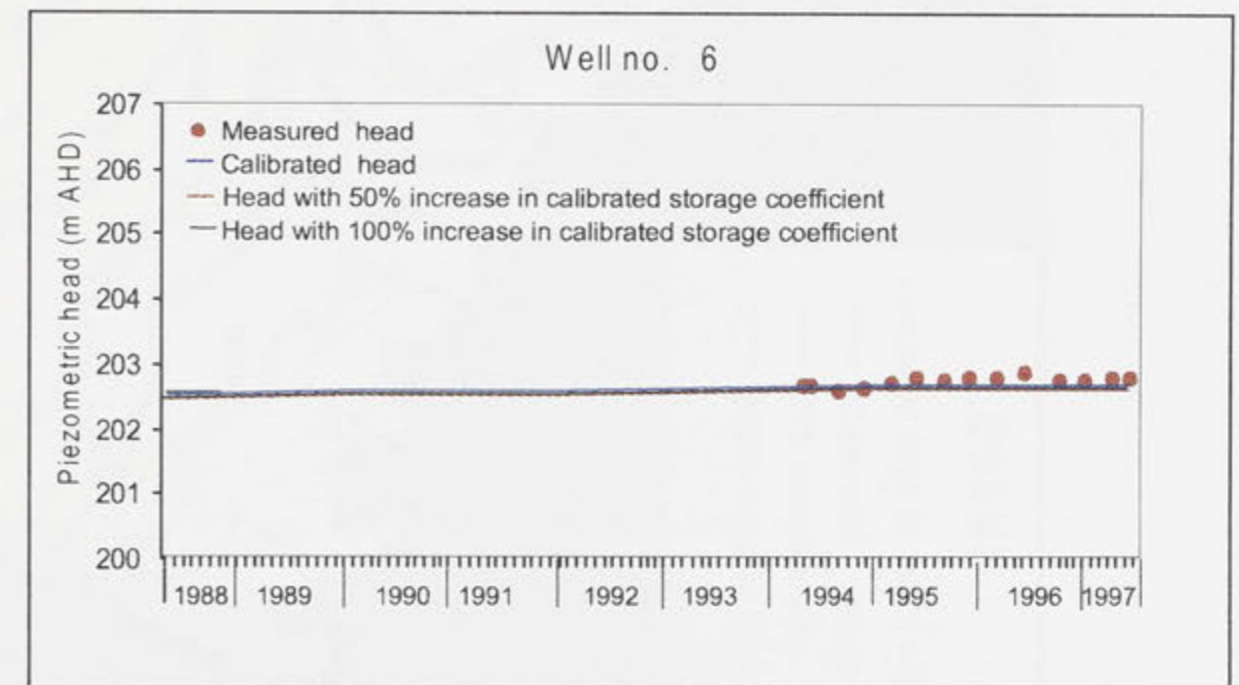
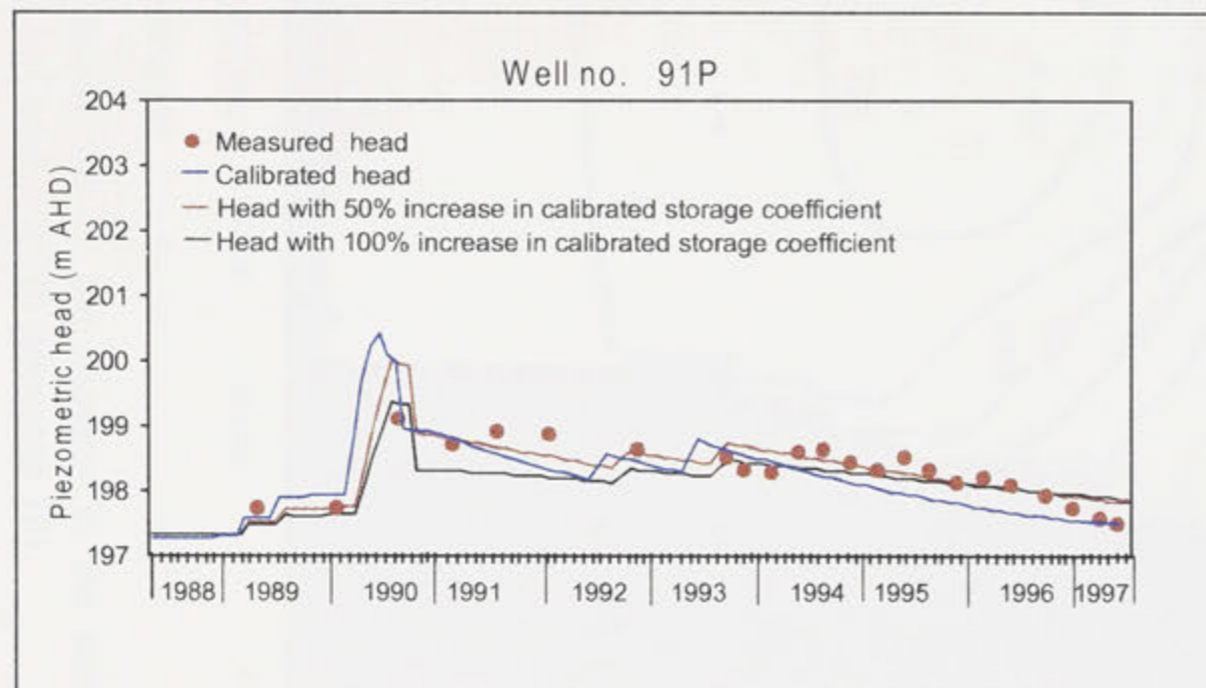
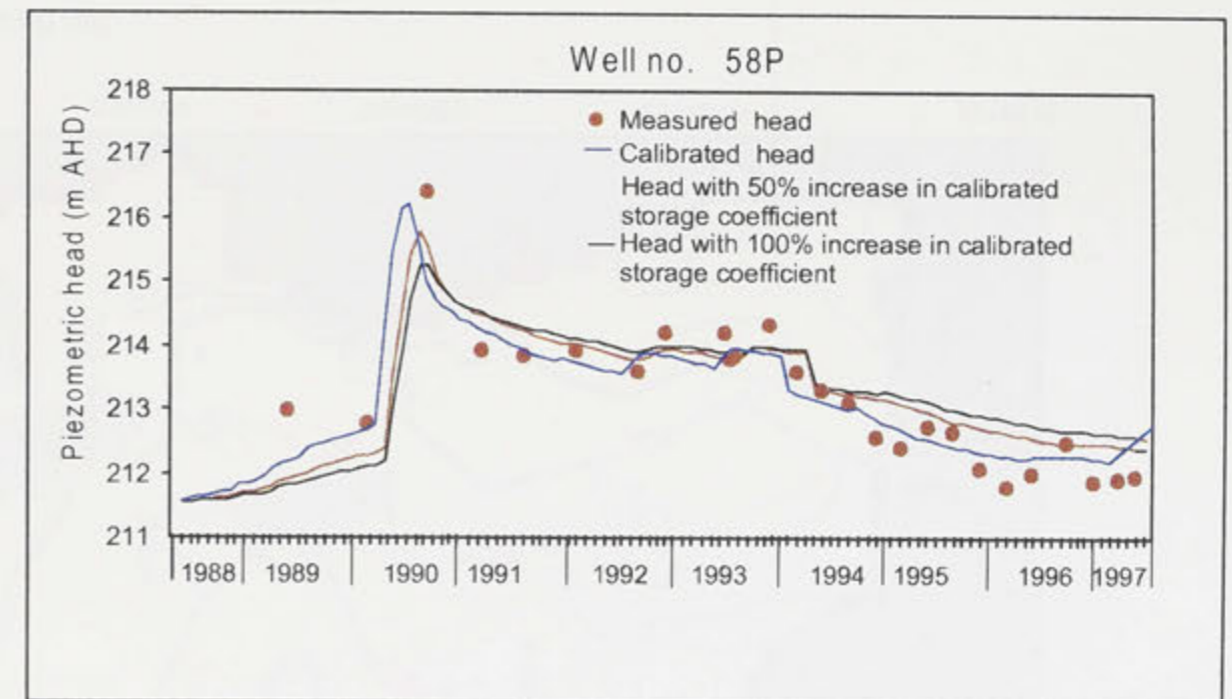
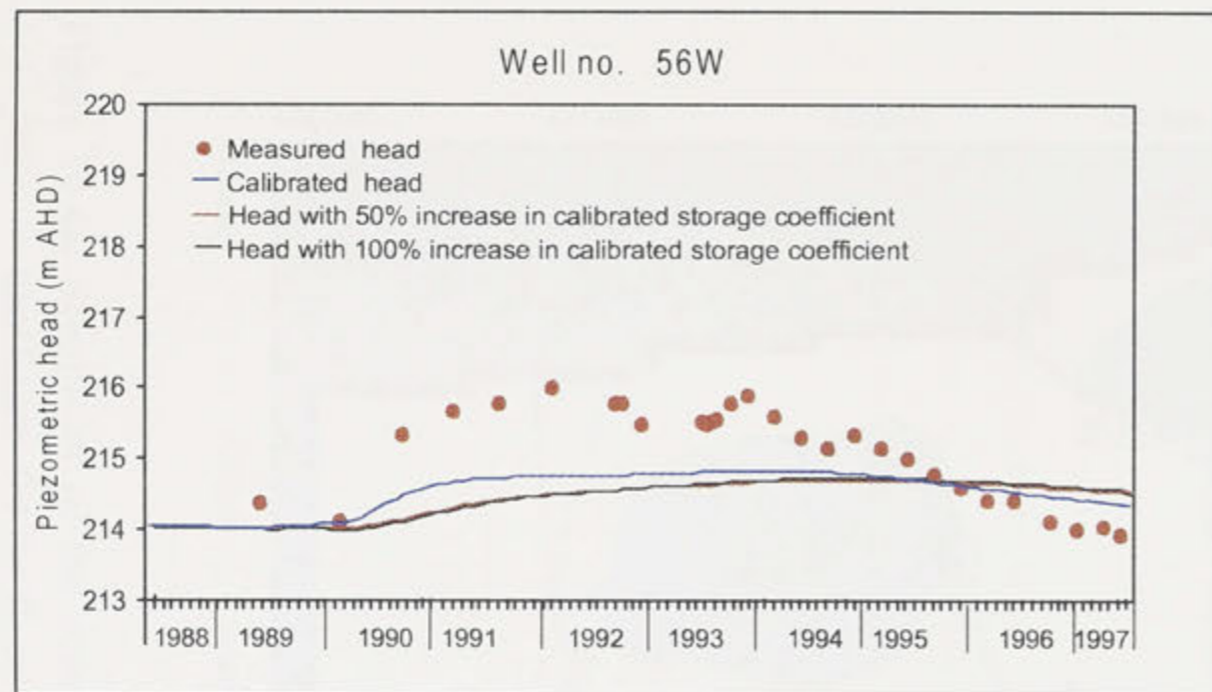


Figure 10.3d: Comparison between measured and computed heads at observation wells 56W, 58P, 91P and 6 with respect to 50% and 100% increase in storage coefficient (see Figure 9.7 for locations).

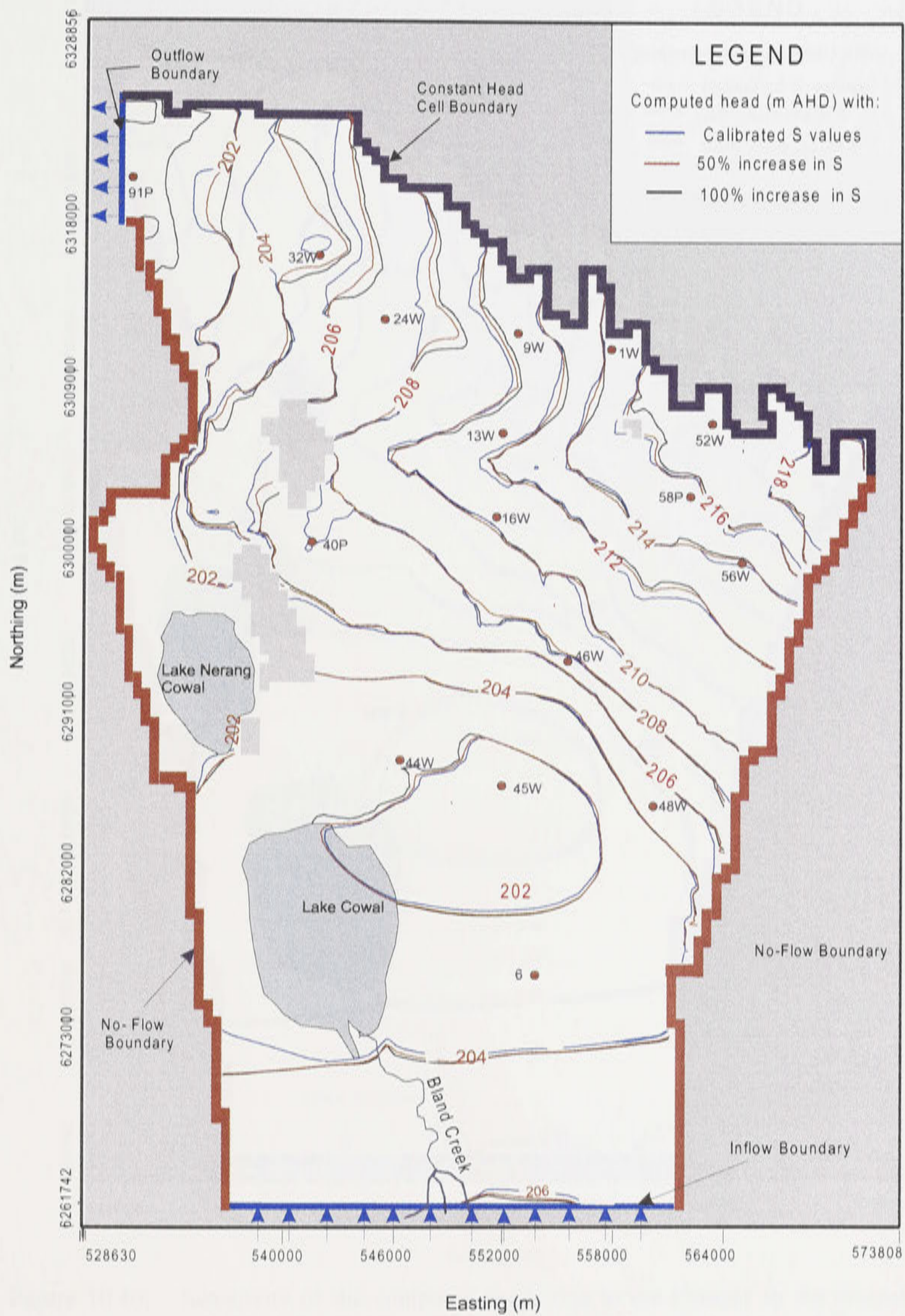


Figure 10.4a: Sensitivity of the computed heads due to the changes in the assigned storage coefficient for the flood period of October 1990 (timestep 30).

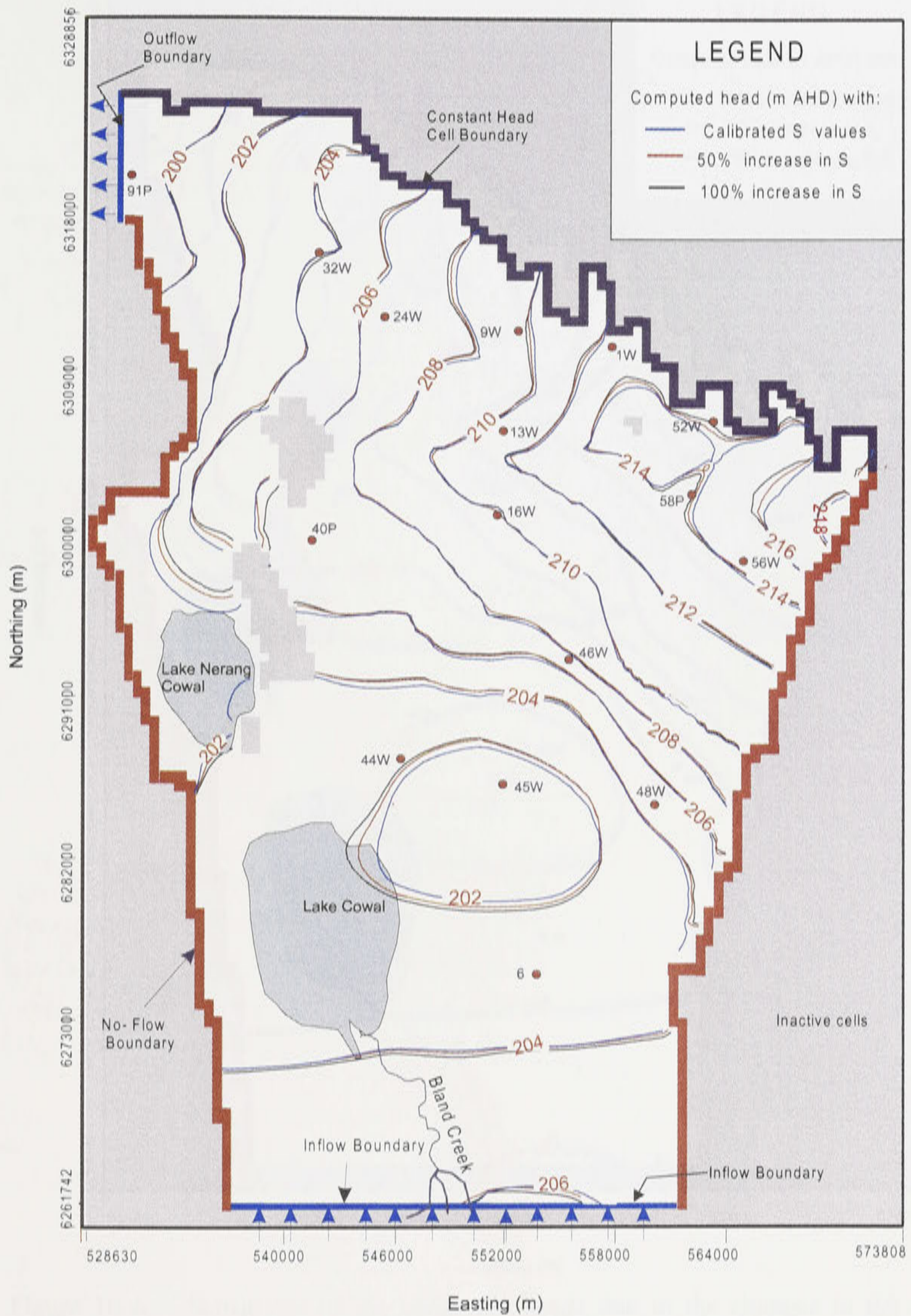


Figure 10.4b: Sensitivity of the computed heads due to the changes in the assigned storage coefficient for October 1994 representing a period of low groundwater levels (timestep 78).

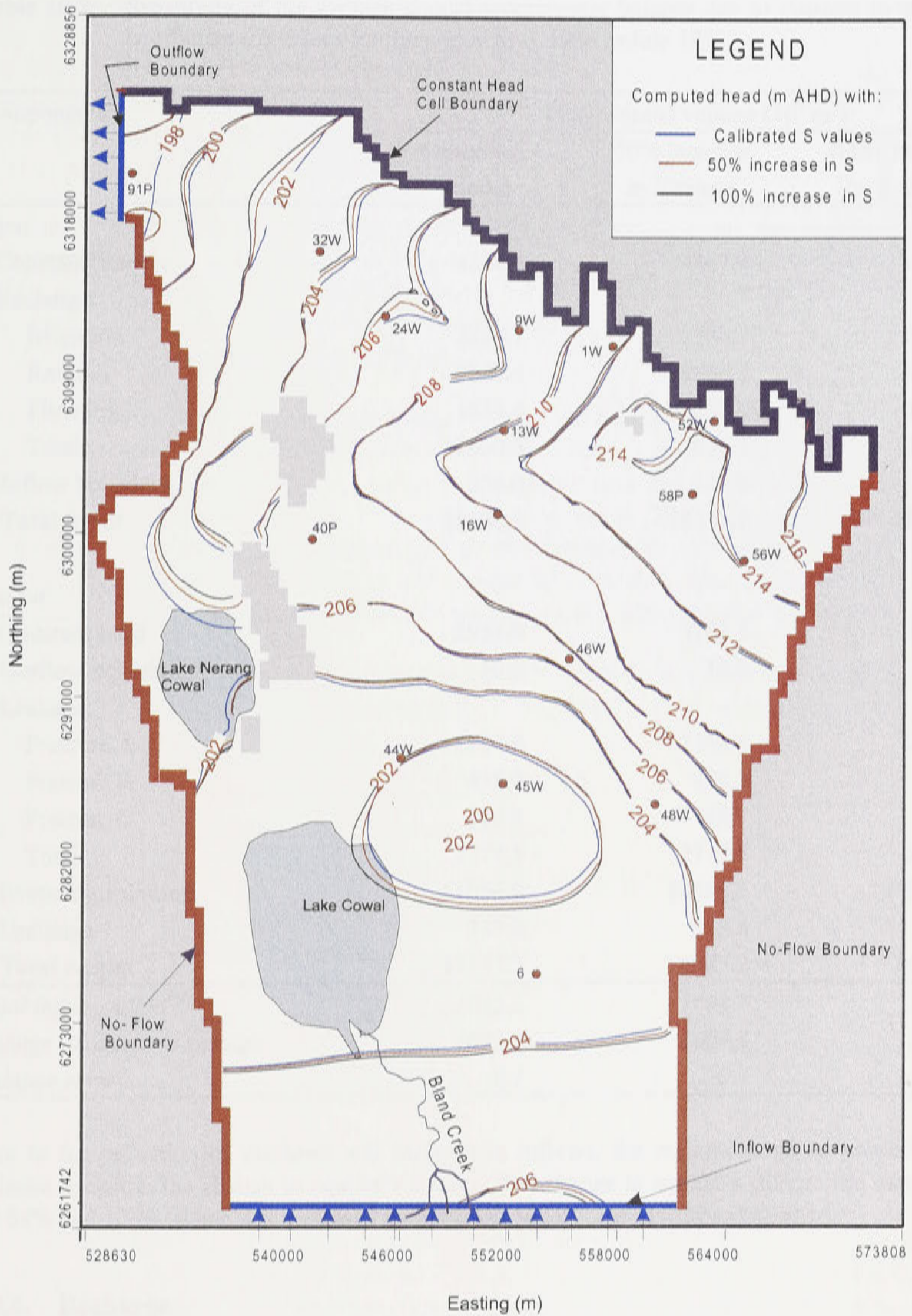


Figure 10.4c: Sensitivity of the computed heads due to the changes in the assigned storage coefficient for July 1997 representing the end of the period of simulation (timestep 111).

Table 10.2: Sensitivity of the average annual groundwater balance due to changes in storage coefficient (*S*) values for the period May 1988 to July 1997.

Components	Mean annual volume (10^3 m^3)		
	Calibrated model	50% increase in <i>S</i> values	100% increase in <i>S</i> values
<i>Input</i>			
Constant head	4216.0	4407.4	4601.6
Recharge:			
Irrigation	2226.7	2226.7	2226.7
Rainfall	9850.4	9850.4	9850.4
Flooding	1553.4	1553.4	1553.4
Total	13630.5	13630.5	13630.5
Inflow boundary	334.0	334.0	334.0
Total input	18180.5	18371.9	18566.1
<i>Output</i>			
Constant head	2953.9	3262.5	3505.1
Outflow boundary	10.2	10.2	10.2
Leakage:			
Fracture A	2154.6	2154.6	2154.6
Fracture B	438.2	438.2	438.2
Fracture C	184.7	184.7	184.7
Total	2777.5	2777.5	2777.5
Evapotranspiration	11056.0	10383.5	9808.9
Drainage	339.6	333.4	320.4
Total output	17137.3	16767.2	16422.1
<i>Total input- output</i>	<i>1043.2</i>	<i>1604.7</i>	<i>2144.0</i>
<i>Change in aquifer's storage</i>	<i>1043.1</i>	<i>1604.3</i>	<i>2143.6</i>
<i>Balance error</i>	<i>0.1</i>	<i>0.4</i>	<i>0.4</i>

Due to the reduction of outflows and increase in inflows, the major change in groundwater balance occurs in the change in aquifer's storage. The change in aquifer's storage has increased by 54% and 106% when *S* is increased by 50% and 100%, respectively as expected.

10.4. Recharge

The sensitivity of the calibrated model due to rainfall, irrigation and flooding has been tested by increasing and decreasing recharge factors by 20% for eight recharge zones (Table 9.3) in the area. In addition, the calibrated recharge in the high and low seepage sections (Figure 9.4) along the Warroo channel has also been altered by $\pm 20\%$.

The comparison of piezometric heads due to $\pm 20\%$ changes in recharge at 16 observation wells is shown in Figures 10.5a to 10.5d. Based on these figures, it is evident that some of the observation wells are more sensitive than others. For example, five observation wells (13W, 32W, 44W, 58P and 91P) show higher variation of piezometric heads than the remaining 11

observation wells. These five wells are located in high recharge zones in the modelled domain. With 20% increase of recharge, the increase in piezometric heads range from 0.3 m to 0.5 m for the five sensitive observation wells, and 0.02 to 0.20 m for the remaining 11 observation wells during timestep 30 (when the aquifer was recharging due to flooding). Similarly, with 20% reduction of recharge, reduction in piezometric heads during timestep 30 ranges from 0.30 m to 0.54 m in the five sensitive wells, and 0.02 to 0.2 m for the remaining 11 wells.

The spatial distribution of the piezometric heads (Figure 10.6a to 10.6c) also show that larger change in heads have been observed in high recharge zones after altering the recharge values by $\pm 20\%$. Comparing piezometric head distributions between timestep 30, 78 and 111, it is evident that variations of piezometric heads are also higher during high recharge events (timestep 30) than in low recharge periods (timestep 78 and 111).

Table 10.3 shows a comparison in mean annual groundwater balance for the calibrated transient model and for 20% increase and decrease in the overall recharge. Among the recharge components, the major changes in volume in the groundwater balance are in recharge due to rainfall followed by recharge due to irrigation and recharge due to flooding. Mean annual volume of outflow due to evapotranspiration has also increased by $2,030,000 \text{ m}^3 \text{ yr}^{-1}$ (18%) as a result of 20% increase of total recharge, and reduced by 19% when recharge is reduced by 20%. Changes are also noted in the inflow and outflow components of the constant head boundary.

The change in aquifer's storage has increased by 14% when the total recharge is increased by 20%. Change in aquifer's storage decreases by 16% when the total recharge is decreased by 20%.

10.5. Evapotranspiration

As described in section 8.8, the ET function used in the model assumed that ET would be a maximum when the watertable is at the groundwater surface and is zero when it is lower than the extinction depth. Between these two limits varies linearly with depths. Because of these assumptions, two types of sensitivity tests for ET were performed. These are: (a) increasing the ET rate by 25 and 50%; and (b) altering the extinction depth from 2.5 m to 2 m and 4 m. This section only discusses the sensitivity results with respect to changes in ET rate. The sensitivity analyses of piezometric heads with respect to changes in extinction depth is discussed in the next section 10.6.

Figures 10.7a to 10.7d show that piezometric heads in all observation wells have not significantly changed as a result of 25% and 50% increase in ET rate. Figures 10.8a to 10.8c showed the comparison of the piezometric head distributions if ET rate is increased by 25 and 50%. Based on these figures, the 25 and 50% increase of ET has no significant impact on the piezometric heads during low recharge periods and in areas with relatively deeper watertables. The effect of increasing ET becomes apparent during high recharge periods where watertables are close to the ground surface. An example of the effect of increase in ET on the piezometric head distributions during high recharge periods is shown in Figure 10.8a for timestep 30. Around Warroo area in the irrigation district where watertable depth ranges from 0-2 m

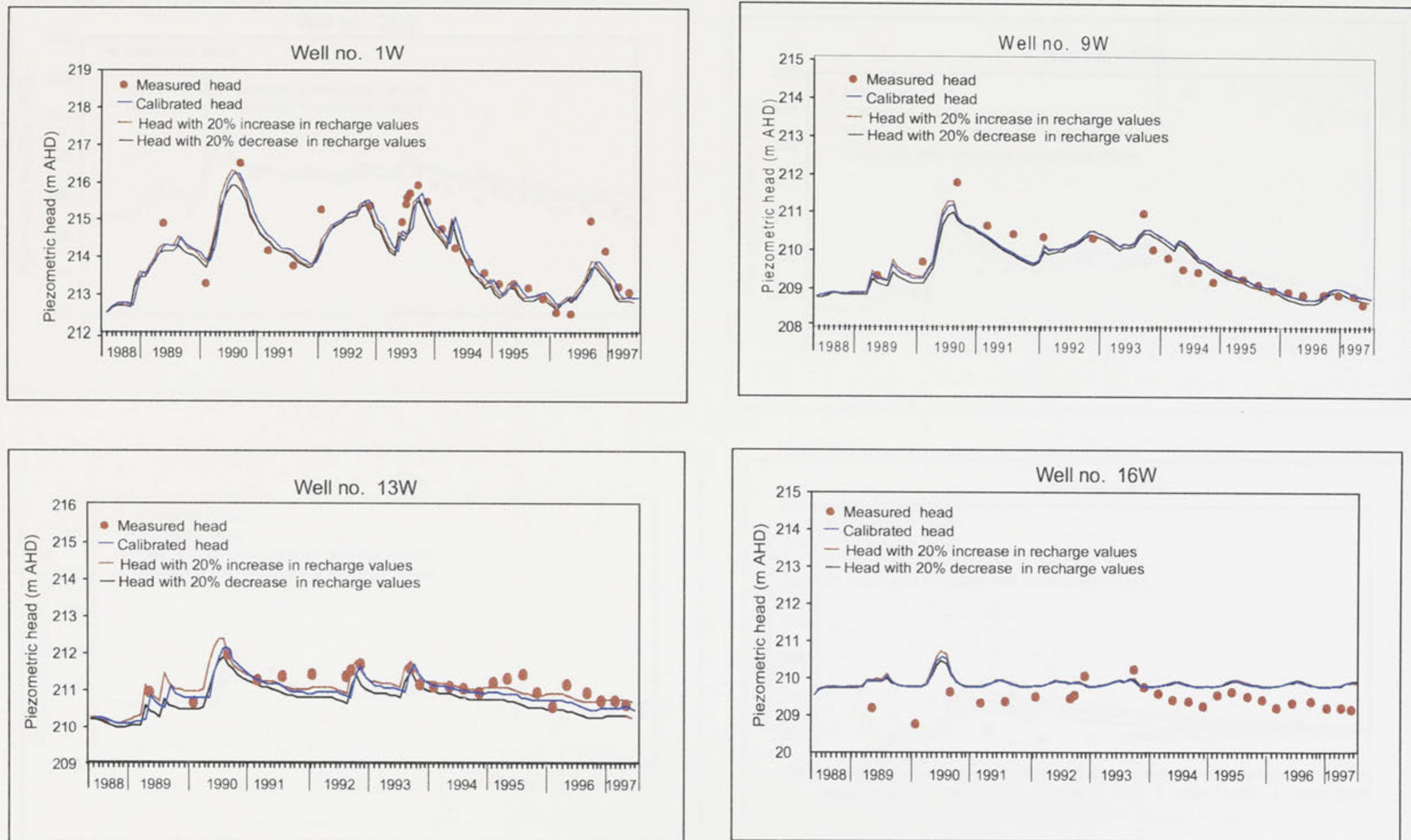


Figure 10.5a: Comparison between measured and computed heads at observation wells 1W, 9W, 13W and 16W with respect to $\pm 20\%$ changes in recharge values (see Figure 9.7 for locations).

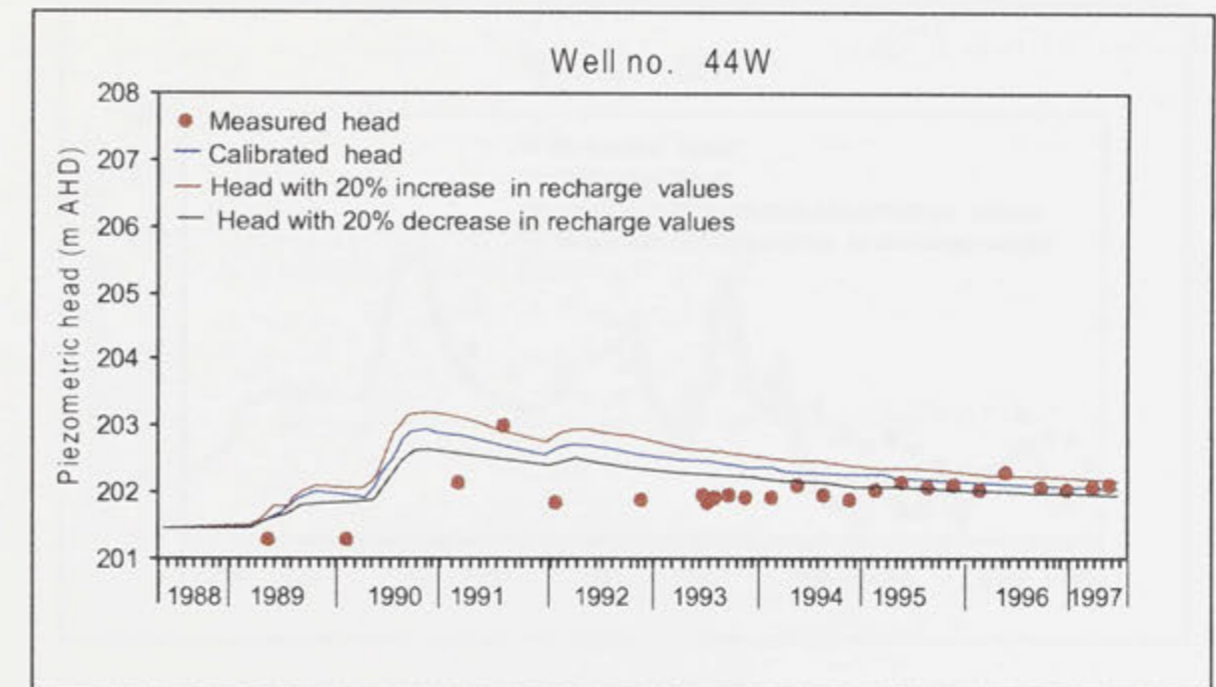
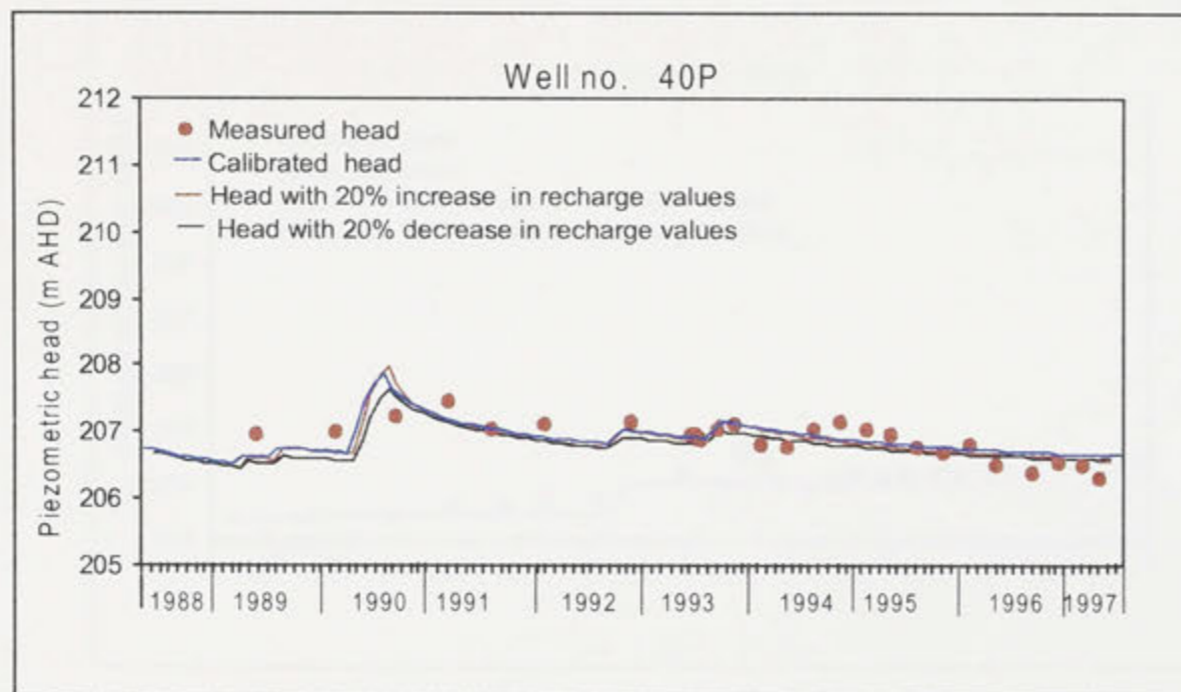
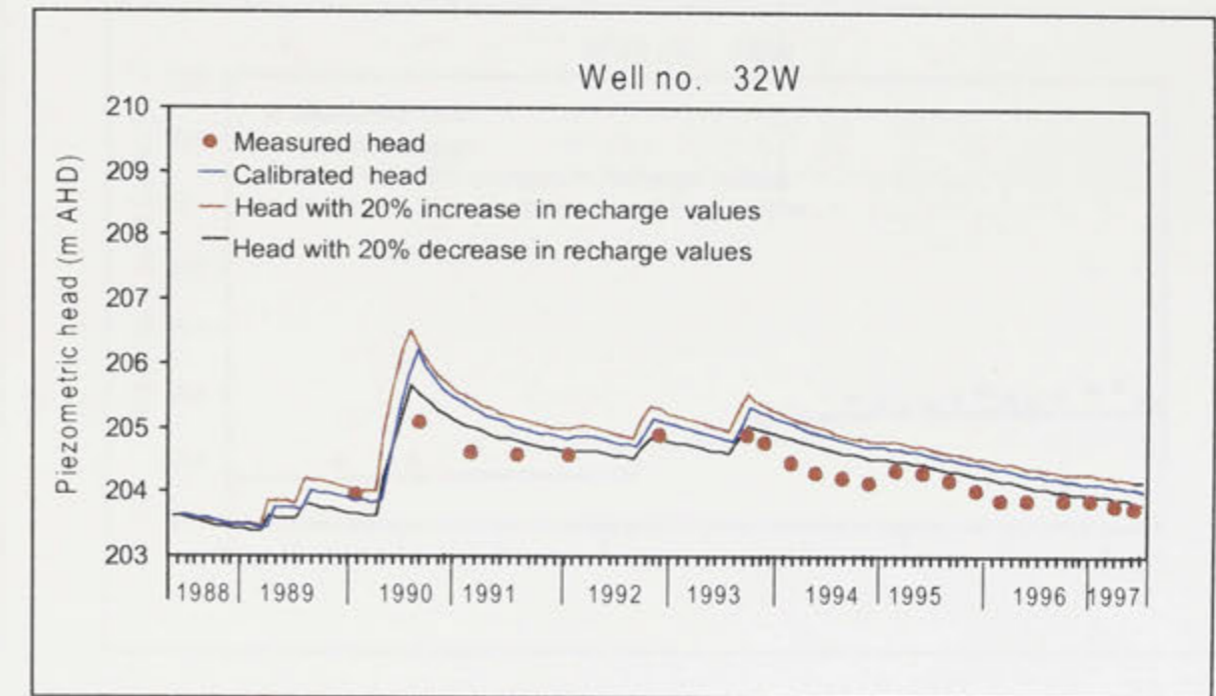
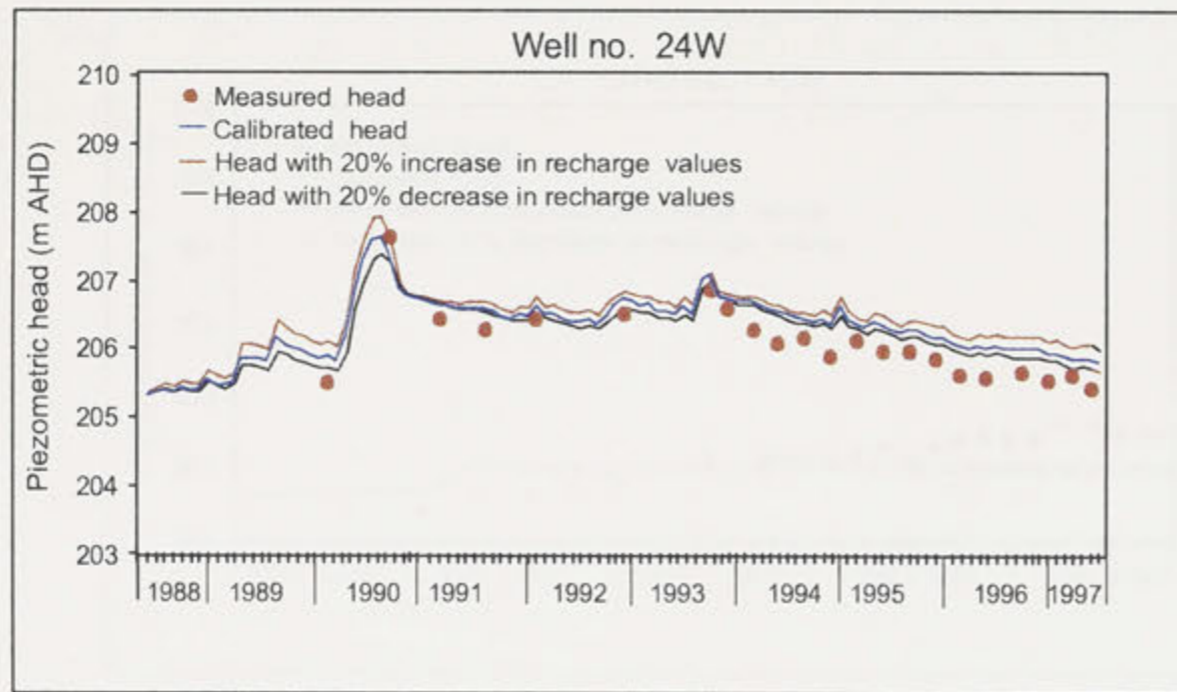


Figure 10.5b: Comparison between measured and computed heads at observation wells 24W, 32W, 40P and 44W with respect to $\pm 20\%$ changes in recharge values (see Figure 9.7 for locations).

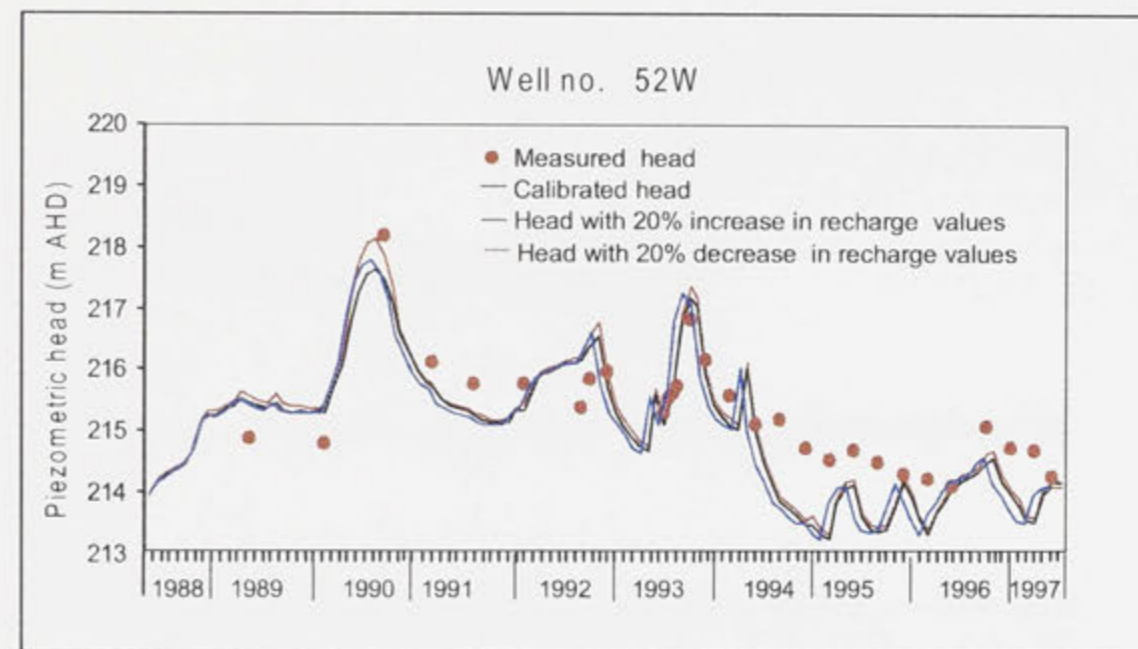
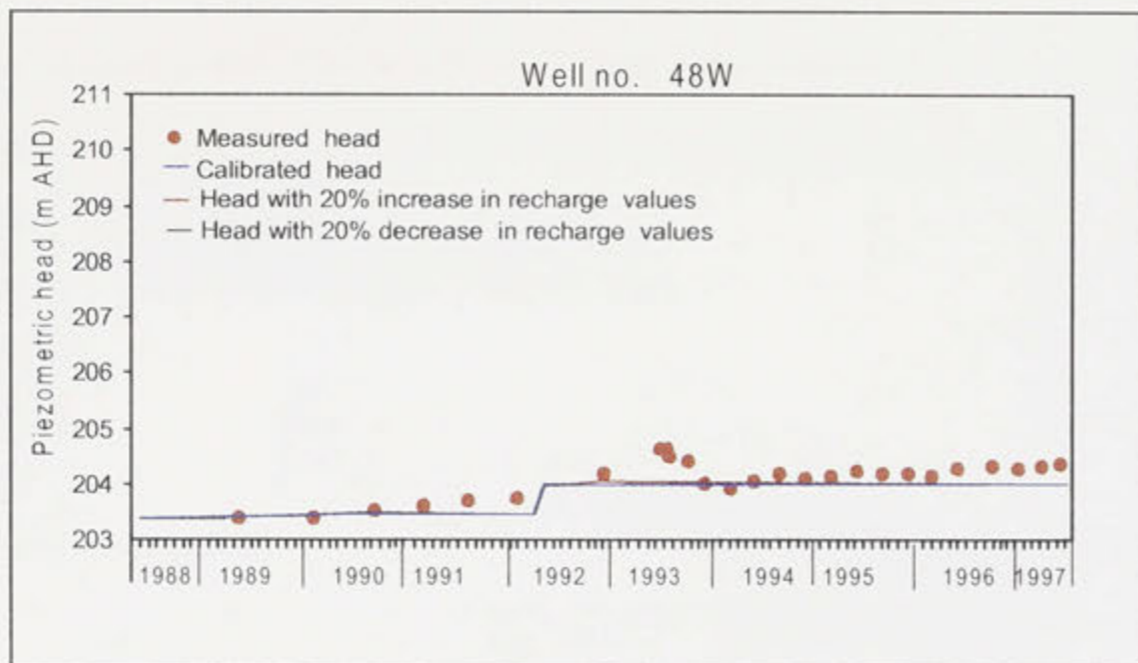
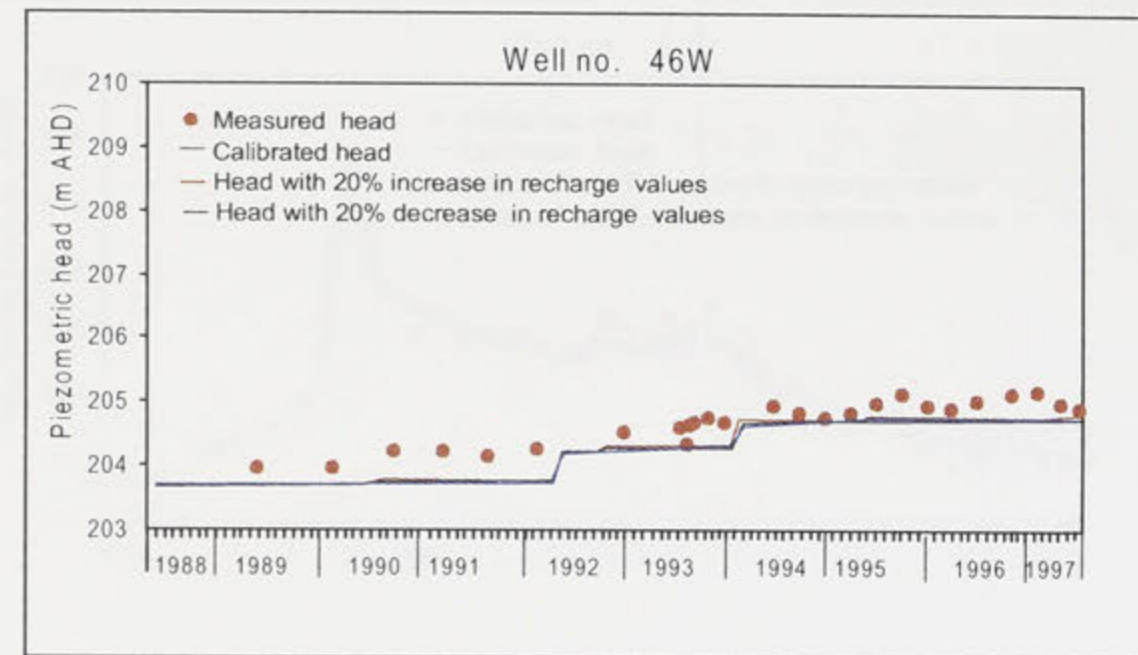
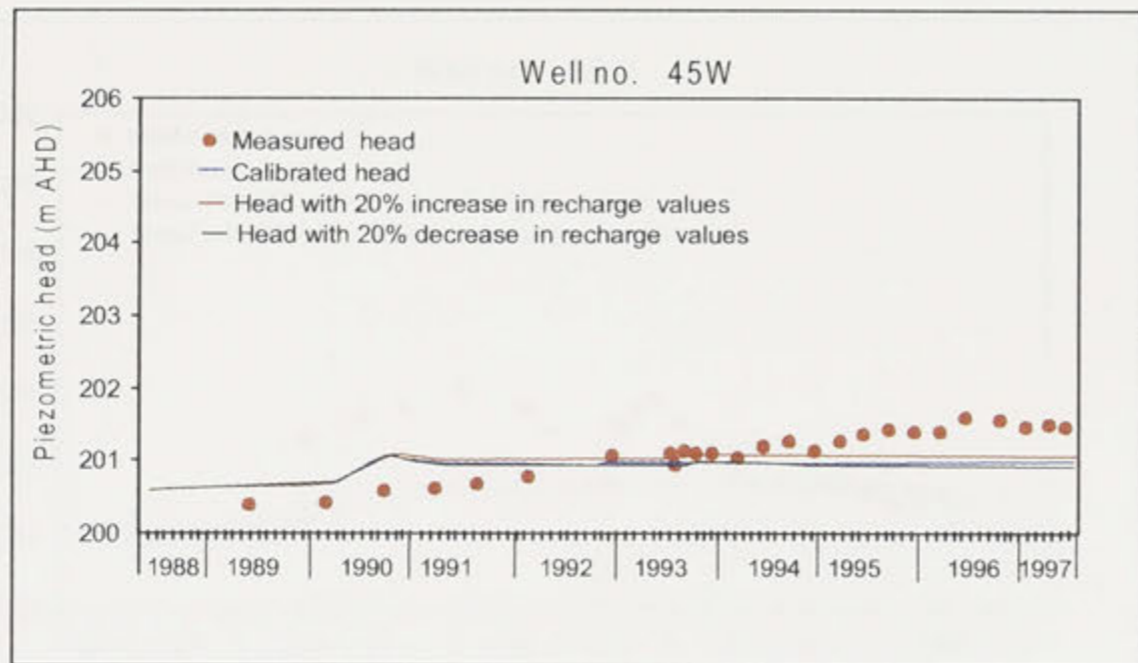


Figure 10.5c: Comparison between measured and computed heads at observation wells 45W, 46W, 48W and 52W with respect to $\pm 20\%$ changes in recharge values (see Figure 9.7 for locations).

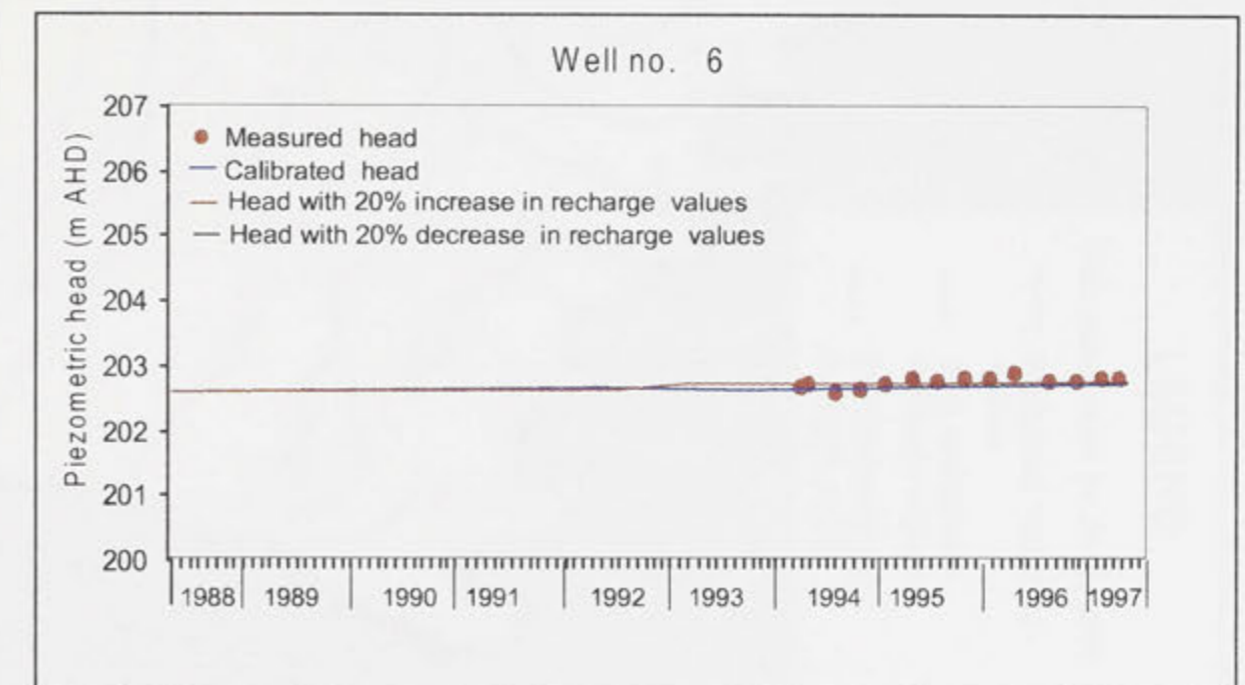
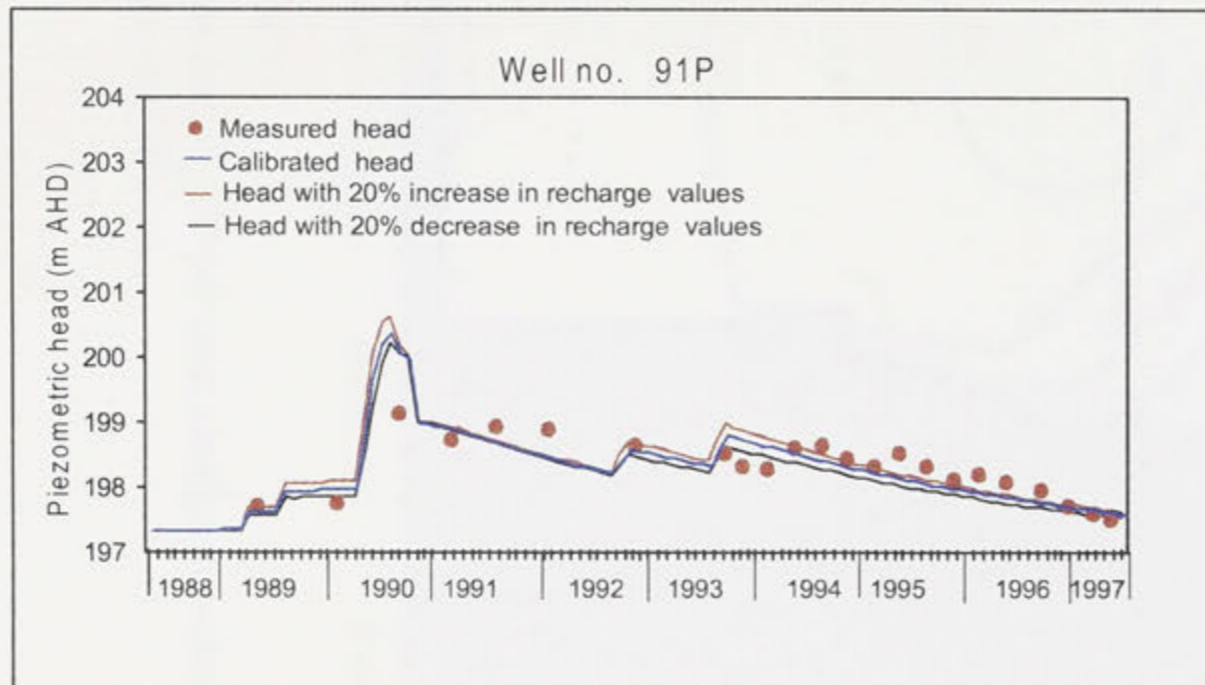
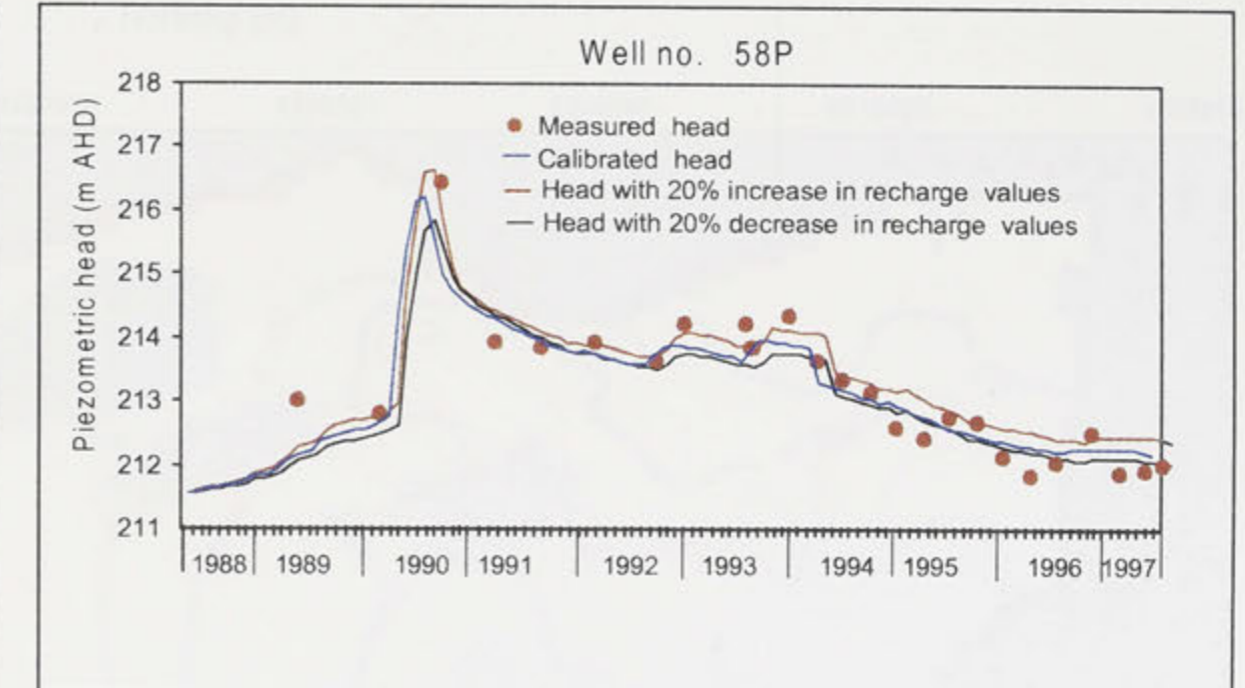
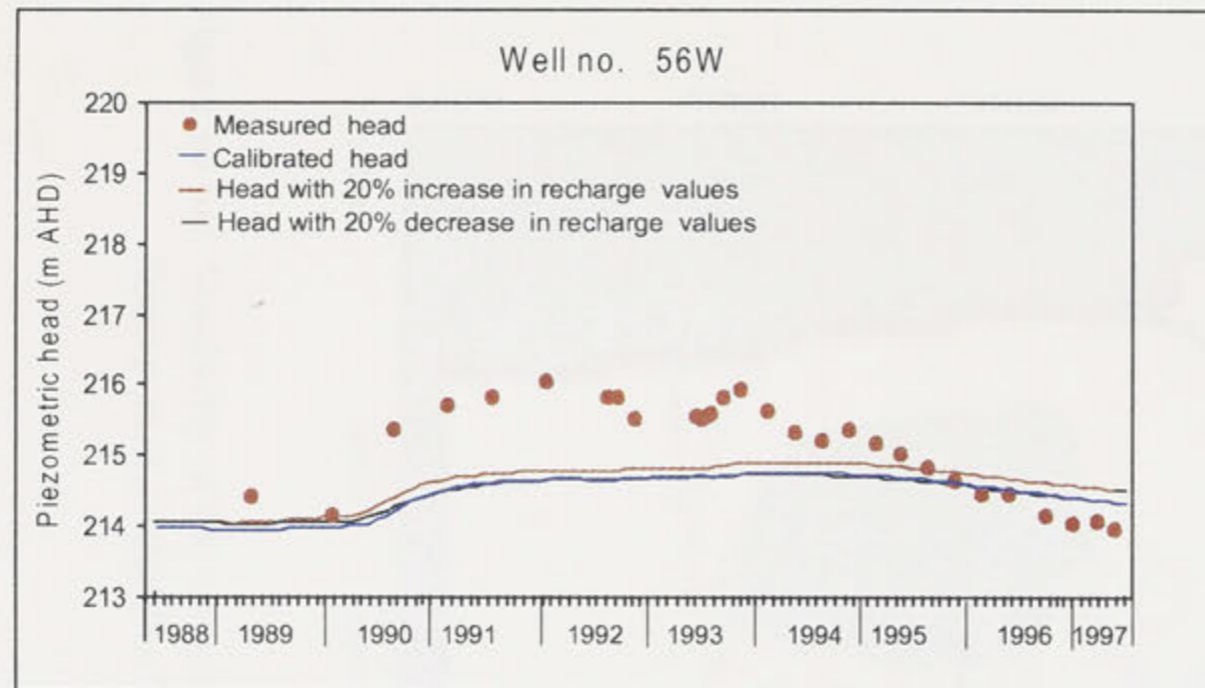


Figure 10.5d: Comparison between measured and computed heads at observation wells 56W, 58P, 91P and 6 with respect to $\pm 20\%$ changes in recharge values (see Figure 9.7 for locations).

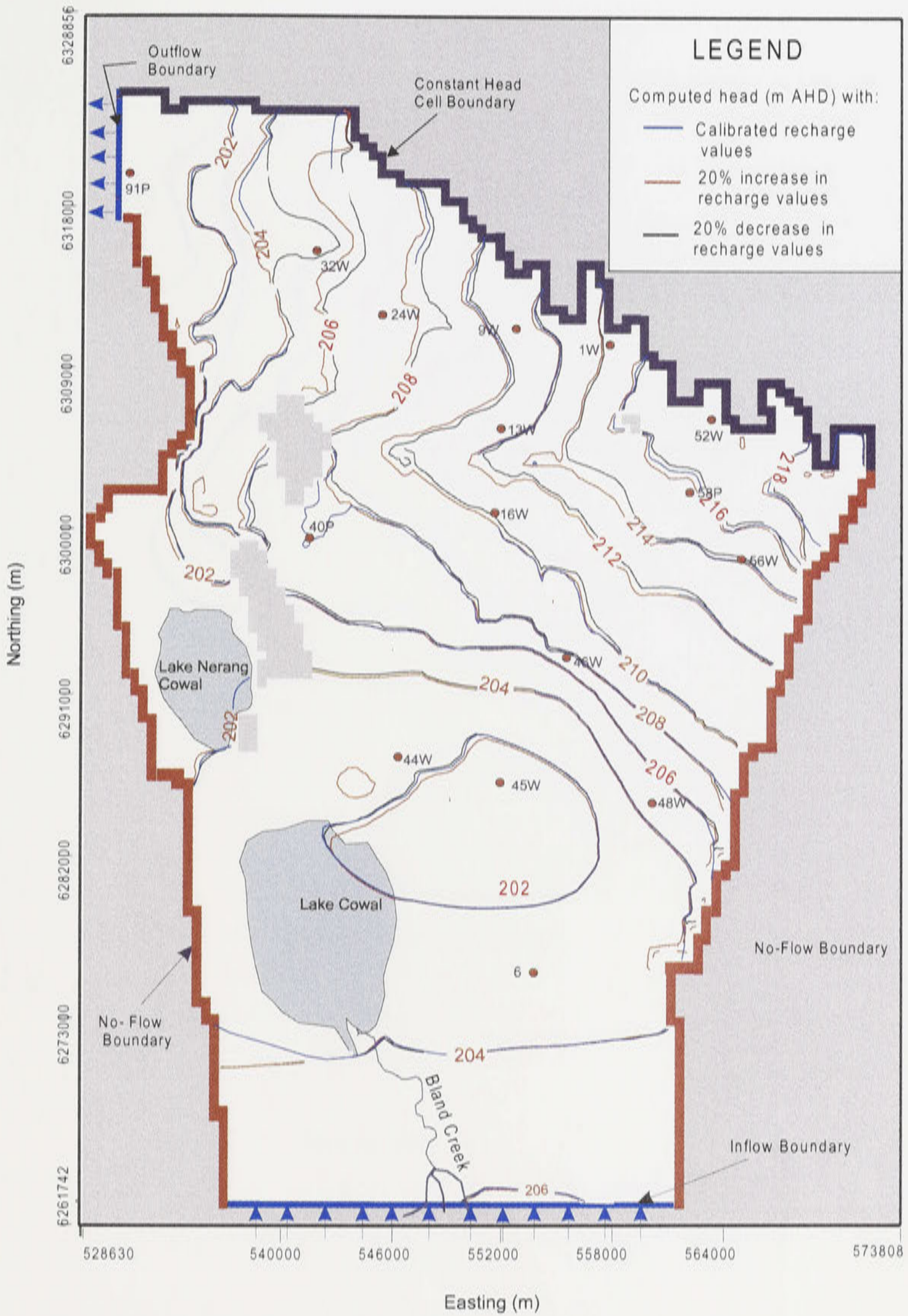


Figure 10.6a: Sensitivity of the computed heads due to ± 20 per cent change in recharge for the flood period of October 1990 (timestep 30).

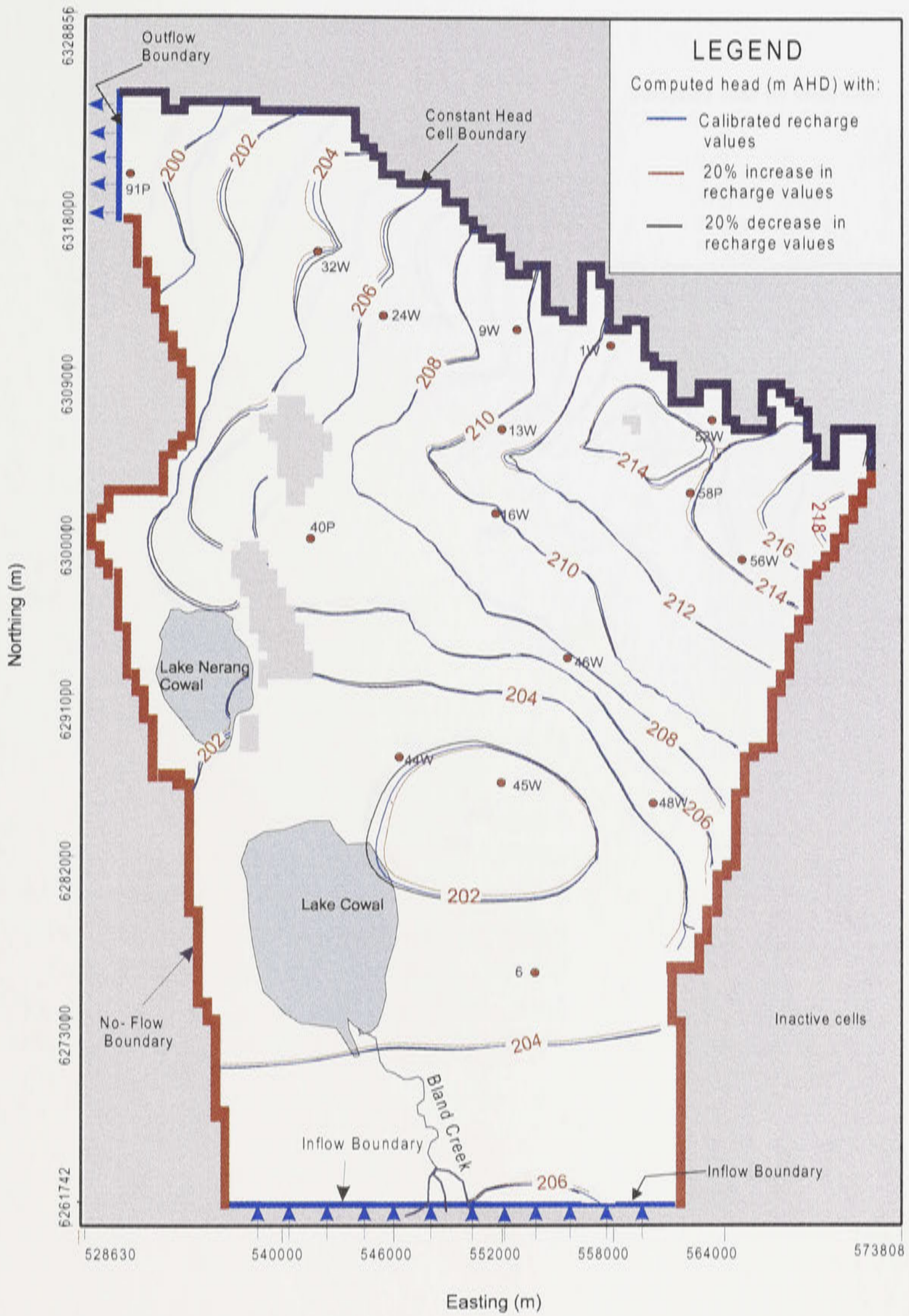


Figure 10.6b: Sensitivity of the computed heads with due to ± 20 per cent change in recharge for October 1994 representing a period of low groundwater levels (timestep 78).

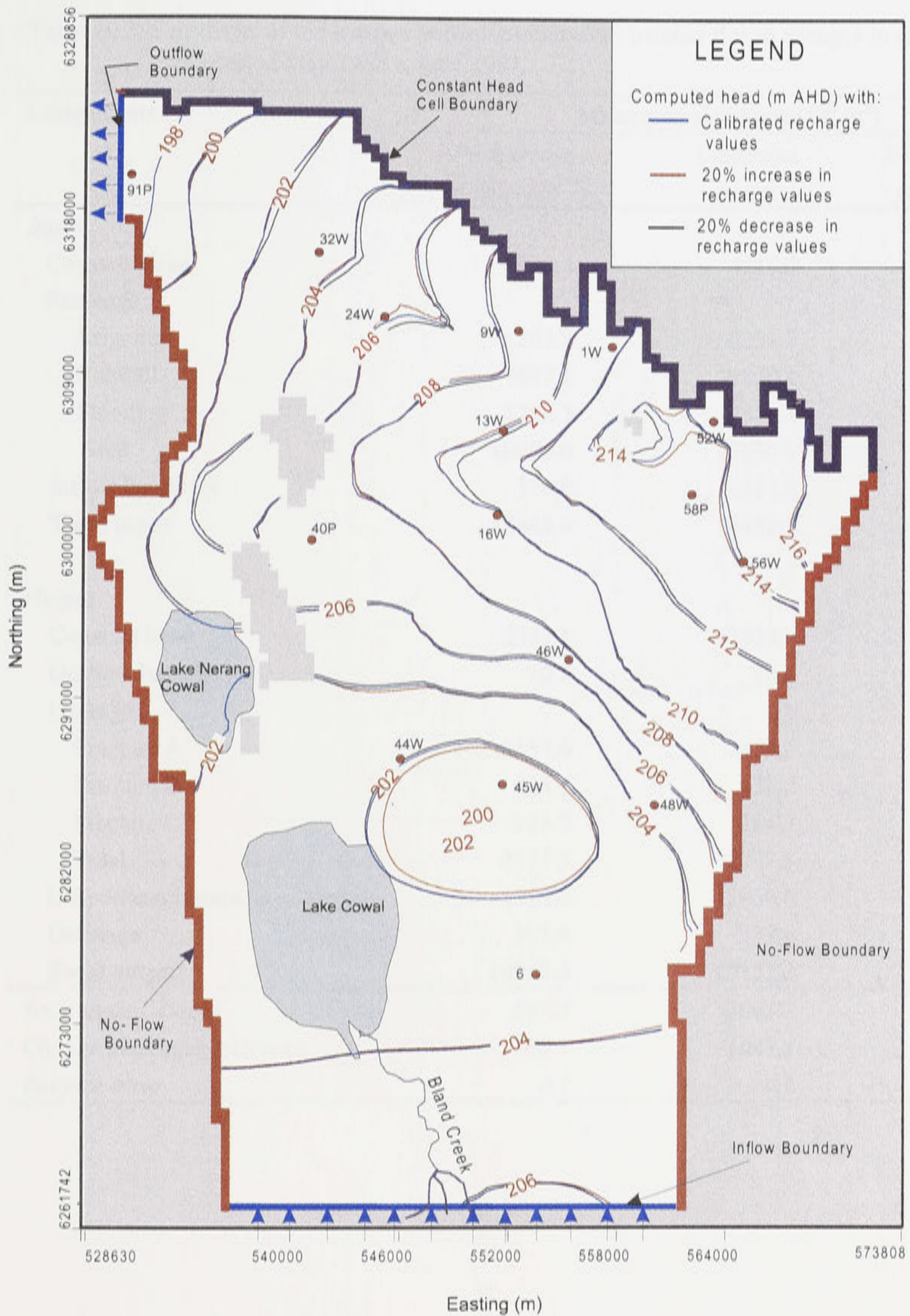


Figure 10.6c: Sensitivity of the computed heads with due to ± 20 per cent change in recharge for July 1997 representing the end of the period of simulation (timestep 111).

Table 10.3: Sensitivity of the average annual groundwater balance due to changes in recharge for the period May 1988 to July 1997.

Components	Mean annual volume (10^3 m^3)		
	20% decrease in recharge	Calibrated model	20% increase in recharge
<i>Input</i>			
Constant head	4408.8	4216.0	4056.4
Recharge:			
Irrigation	1202.3	2226.7	3016.5
Rainfall	7687.1	9850.4	11401.1
Flooding	1202.3	1553.4	1767.8
Total	10900.8	13630.5	16185.5
Inflow boundary	334.0	334.0	334.0
Total input	15643.6	18180.5	20576.0
<i>Output</i>			
Constant head	2745.1	2953.9	3148.2
Outflow boundary	10.2	10.2	10.2
Leakage:			
Fracture A	2154.6	2154.6	2154.6
Fracture B	438.2	438.2	438.2
Fracture C	184.7	184.7	184.7
Total	2777.5	2777.5	2777.5
Evapotranspiration	8924.6	11056.0	13085.4
Drainage	305.4	339.6	368.6
Total output	14762.8	17137.3	19390.0
<i>Total input - output</i>	<i>880.8</i>	<i>1043.2</i>	<i>1186.0</i>
<i>Change in aquifer's storage</i>	<i>880.1</i>	<i>1043.1</i>	<i>1185.0</i>
<i>Balance error</i>	<i>0.7</i>	<i>0.1</i>	<i>1.0</i>

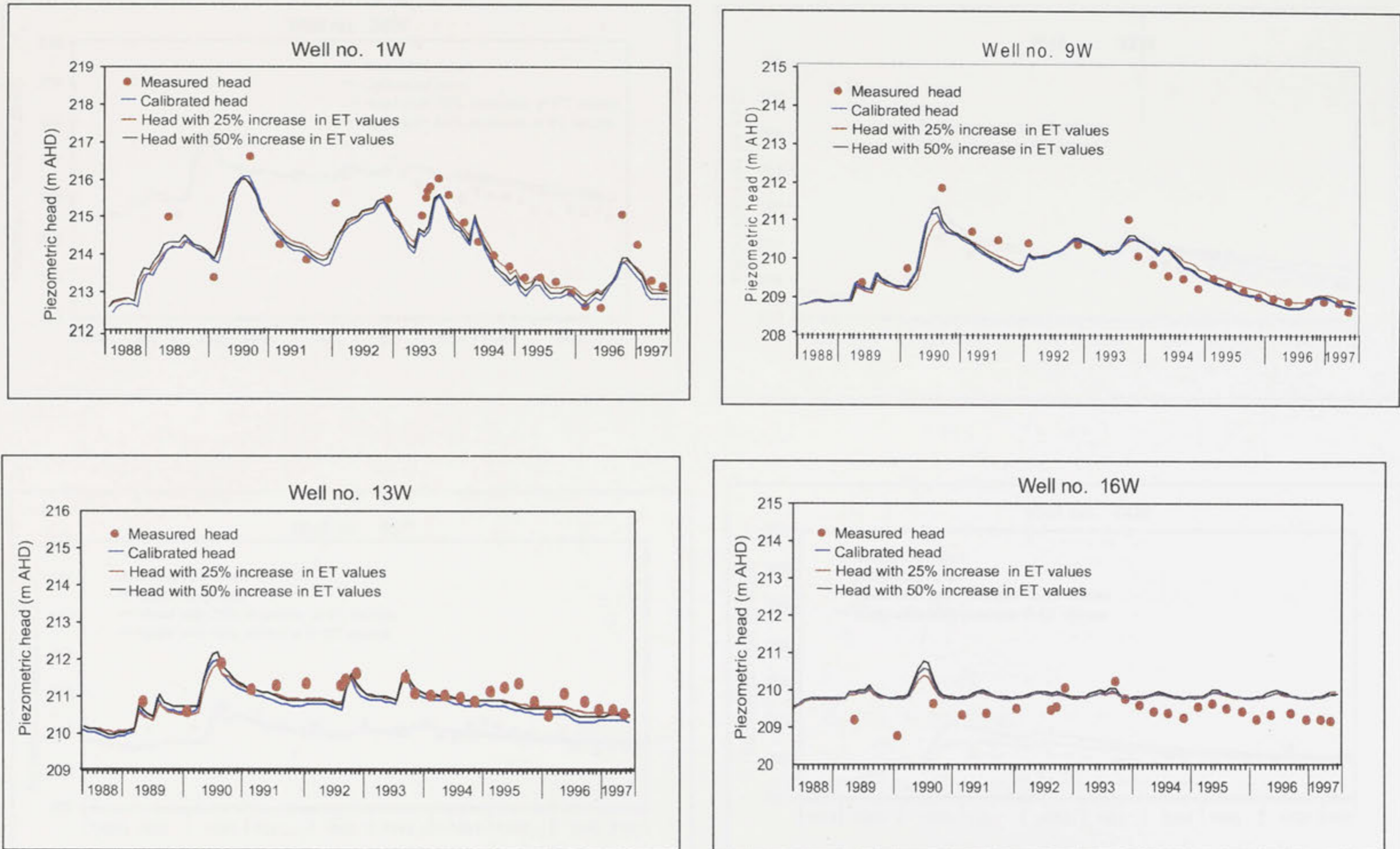


Figure 10.7a: Comparison between measured and computed heads at observation wells 1W, 9W, 13W and 16W with respect to 25% and 50% increase in evapotranspiration rate (see Figure 9.7 for locations).

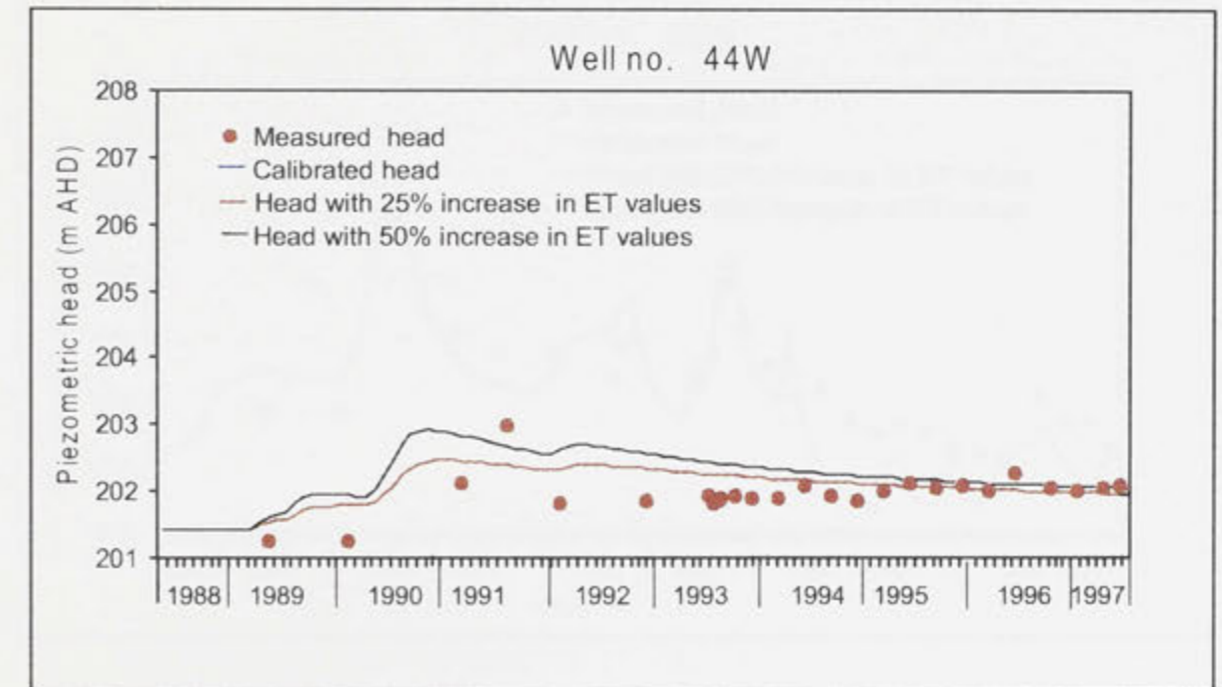
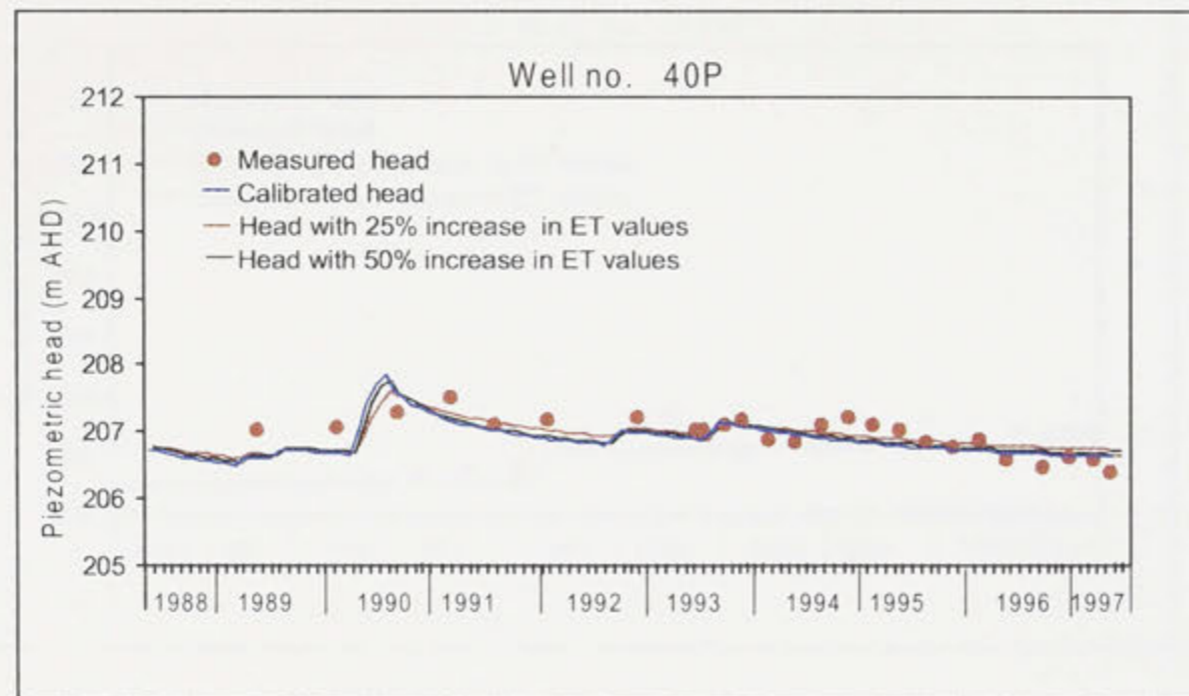
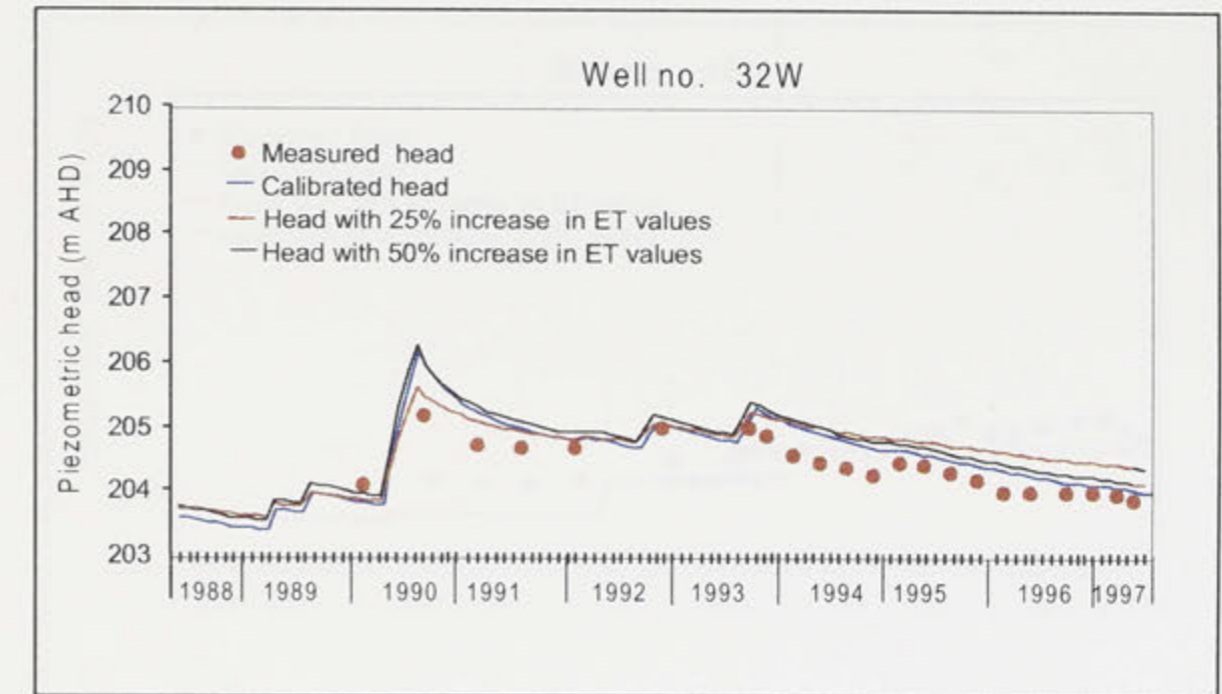
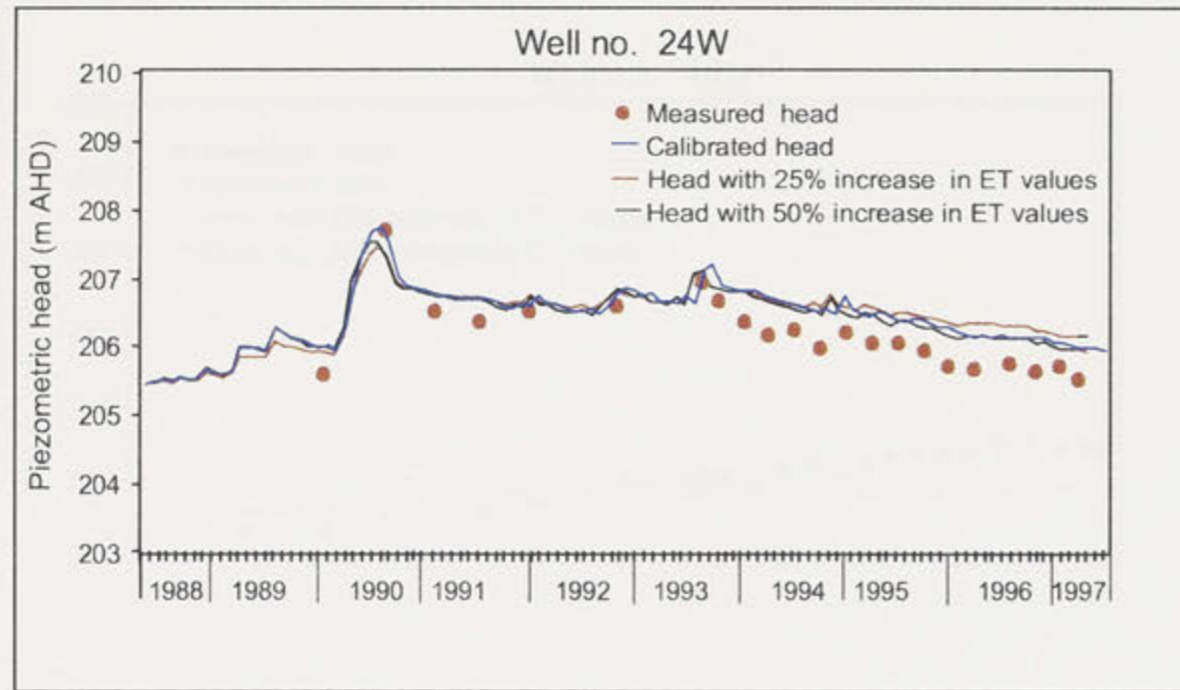


Figure 10.7b: Comparison between measured and computed heads at observation wells 24W, 32W, 40P and 44W with respect to 25% and 50% increase in evapotranspiration rate (see Figure 9.7 for locations).

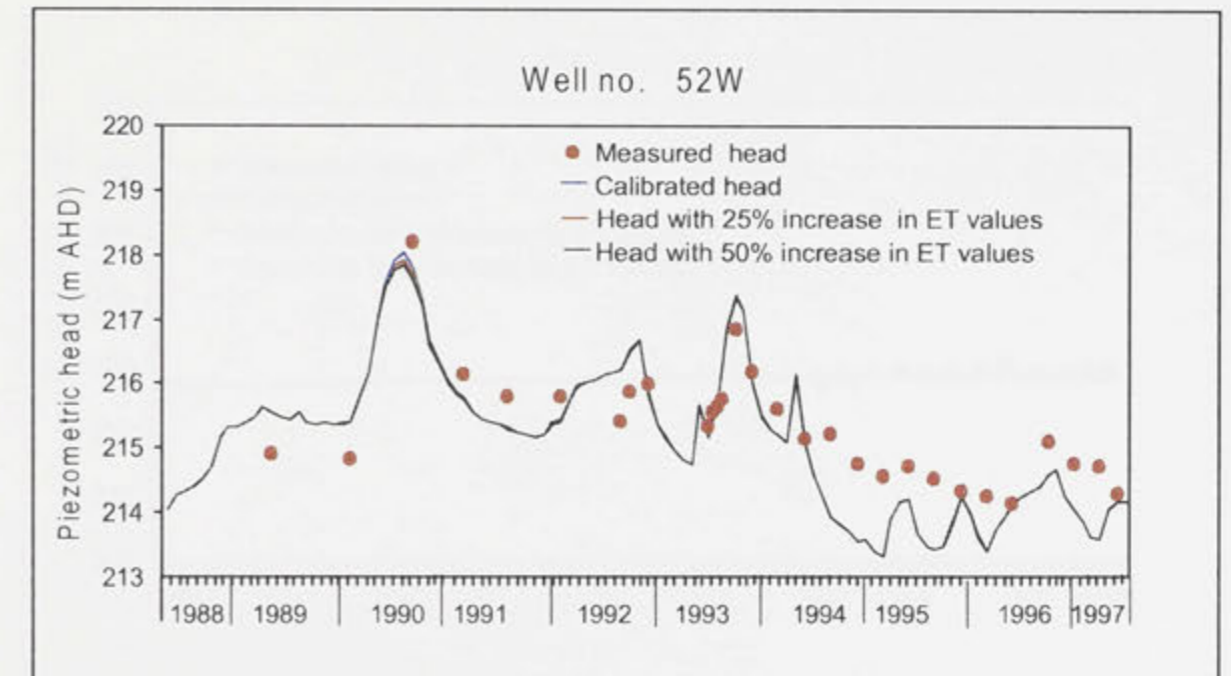
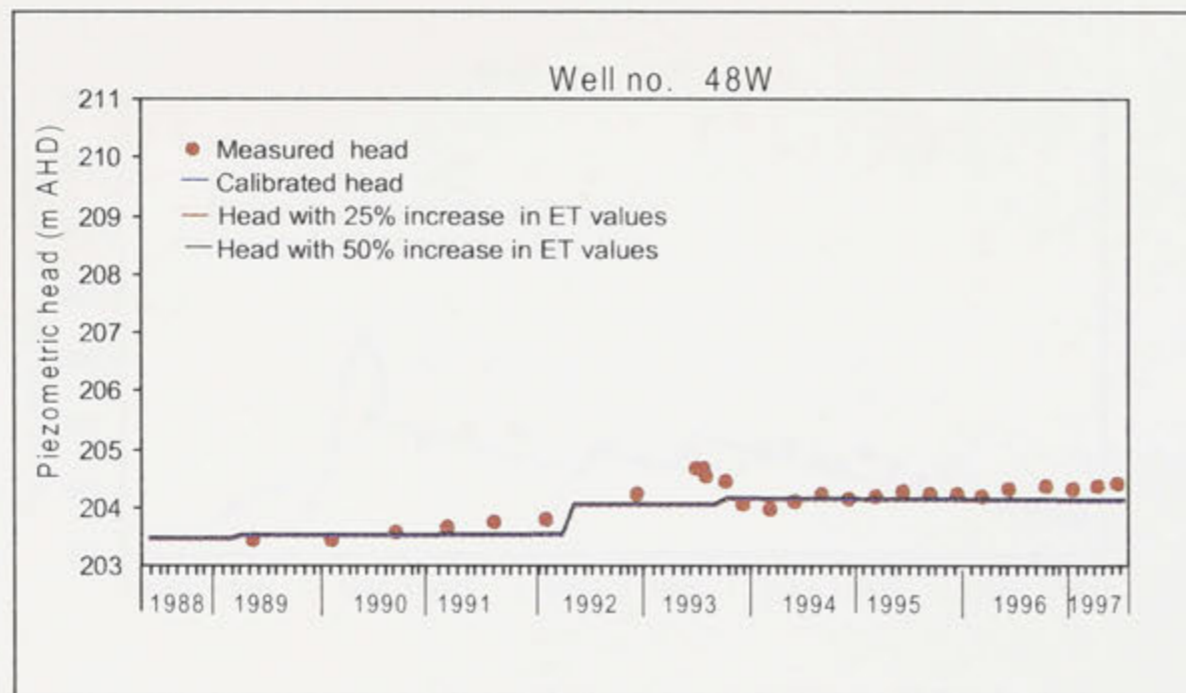
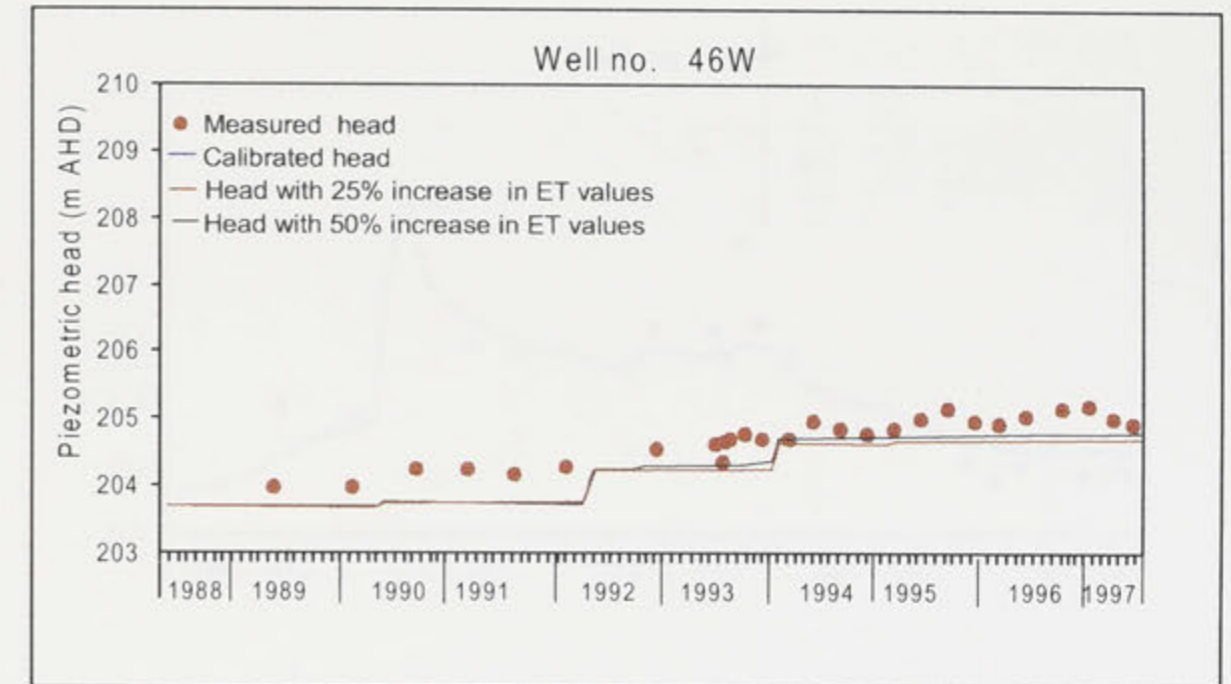
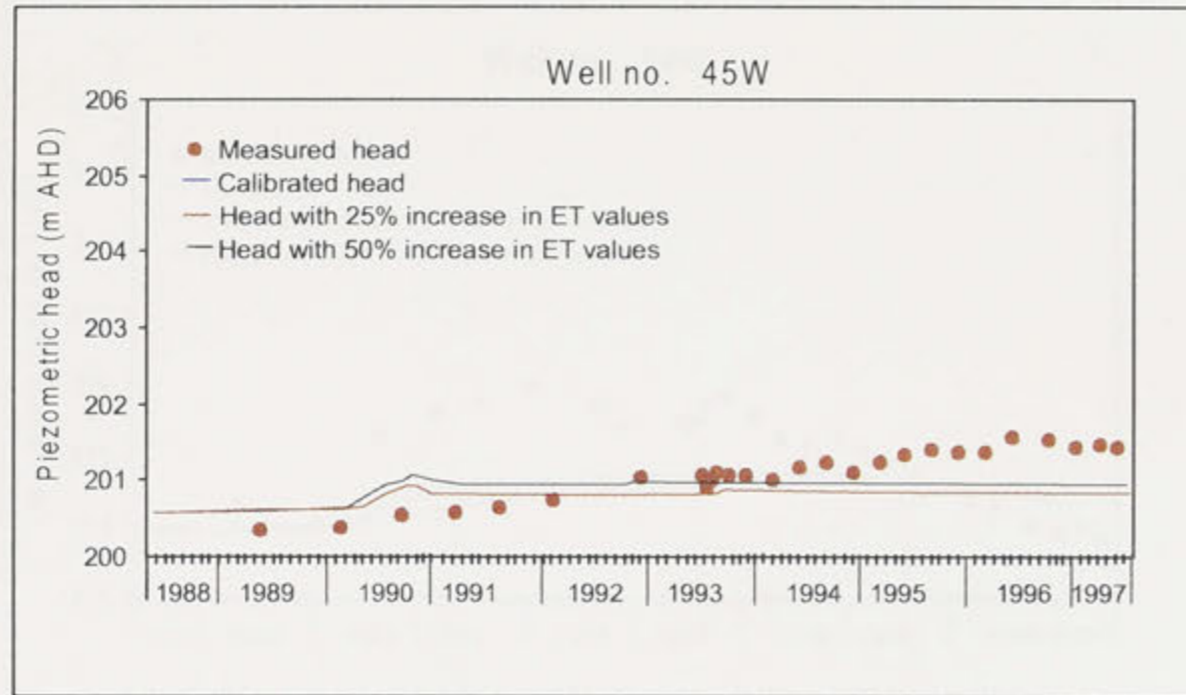


Figure 10.7c: Comparison between measured and computed heads at observation wells 45W, 46W, 48W and 52W with respect to 25% and 50% increase in evapotranspiration rate (see Figure 9.7 for locations).

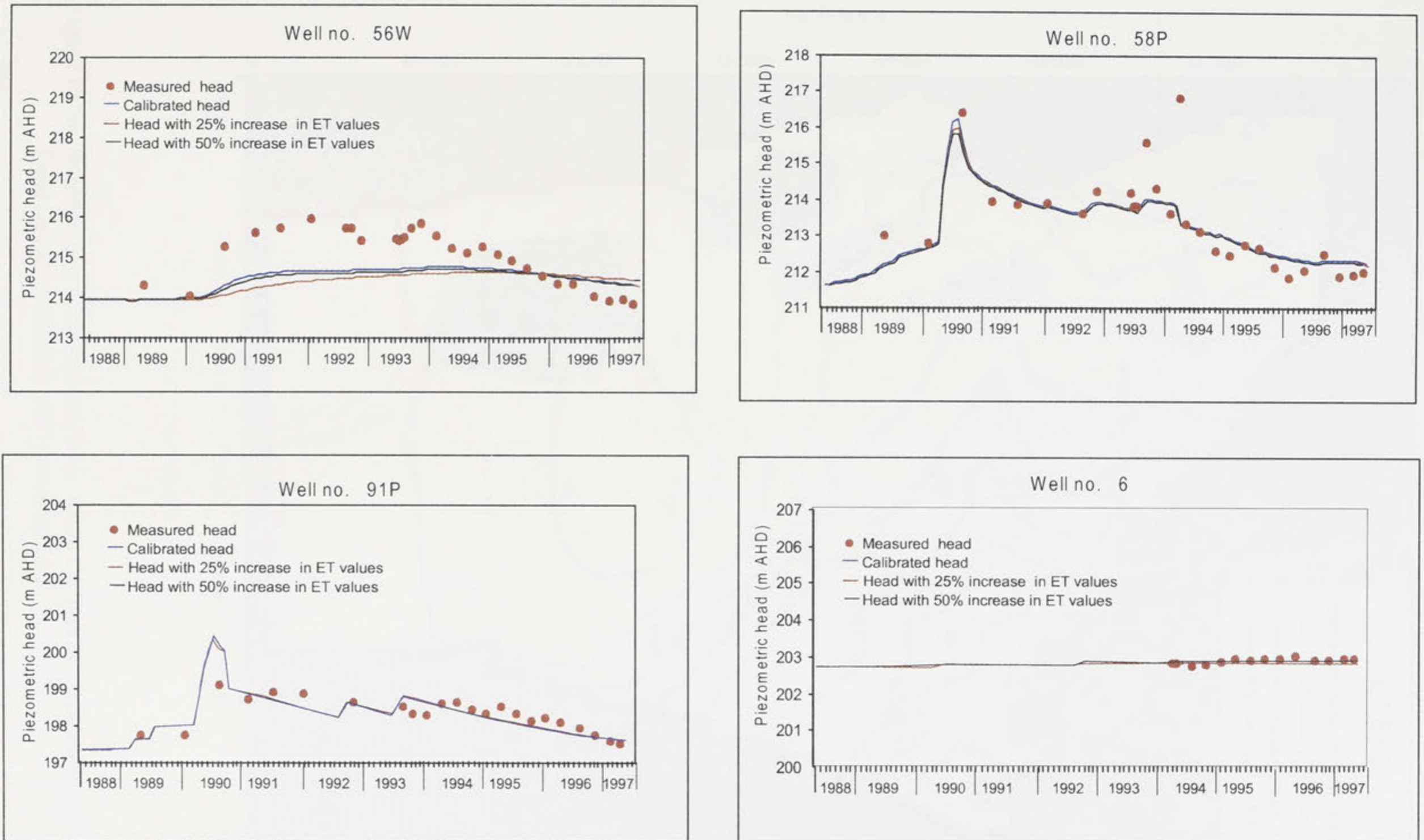


Figure 10.7d: Comparison between measured and computed heads at observation wells 56W, 58P, 91P and 6 with respect to 25% and 50% increase in evapotranspiration rate (see Figure 9.7 for locations).

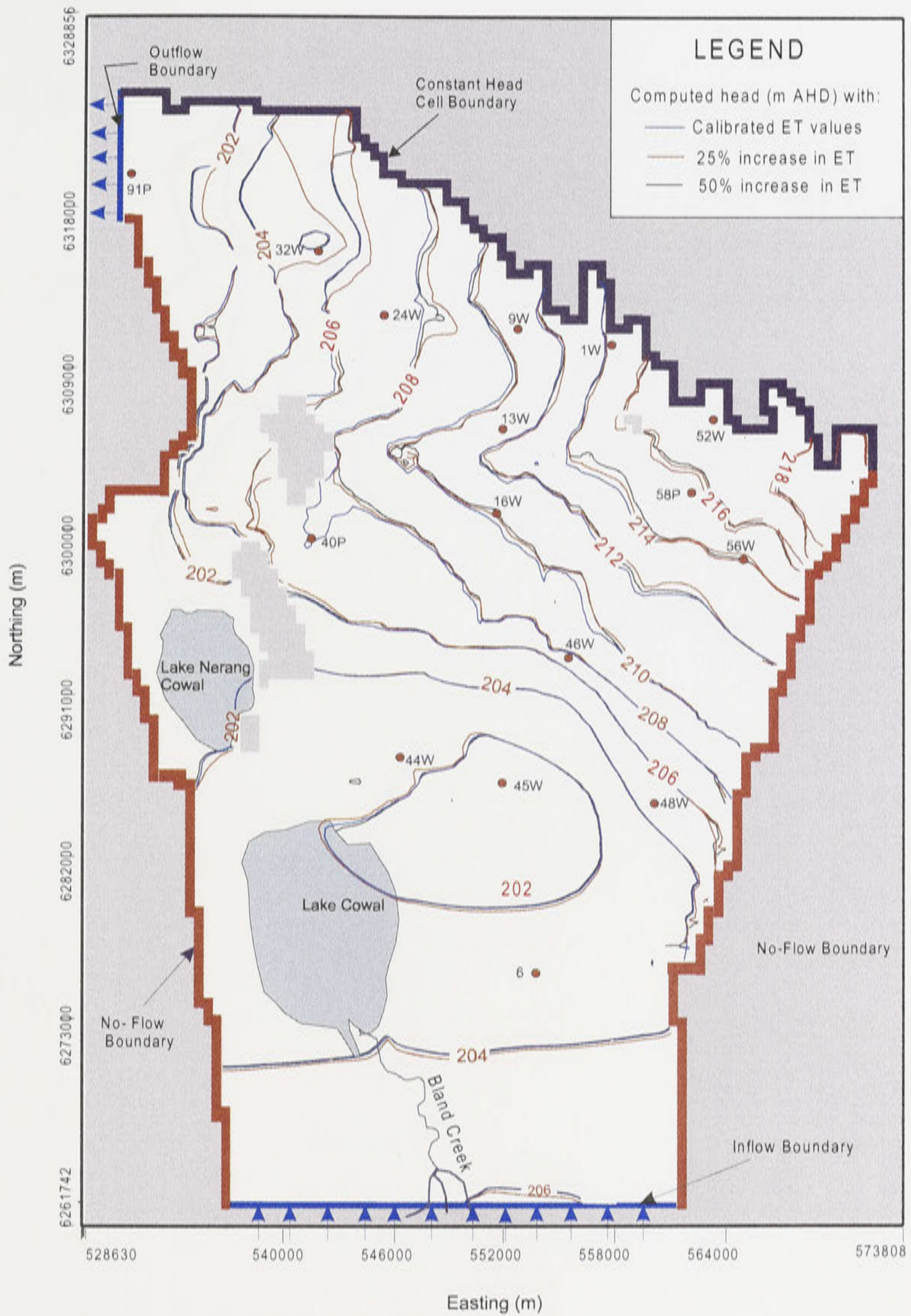


Figure 10.8a: Sensitivity of the computed heads due to changes in evapotranspiration rate for the flood period of October 1990 (timestep 30).

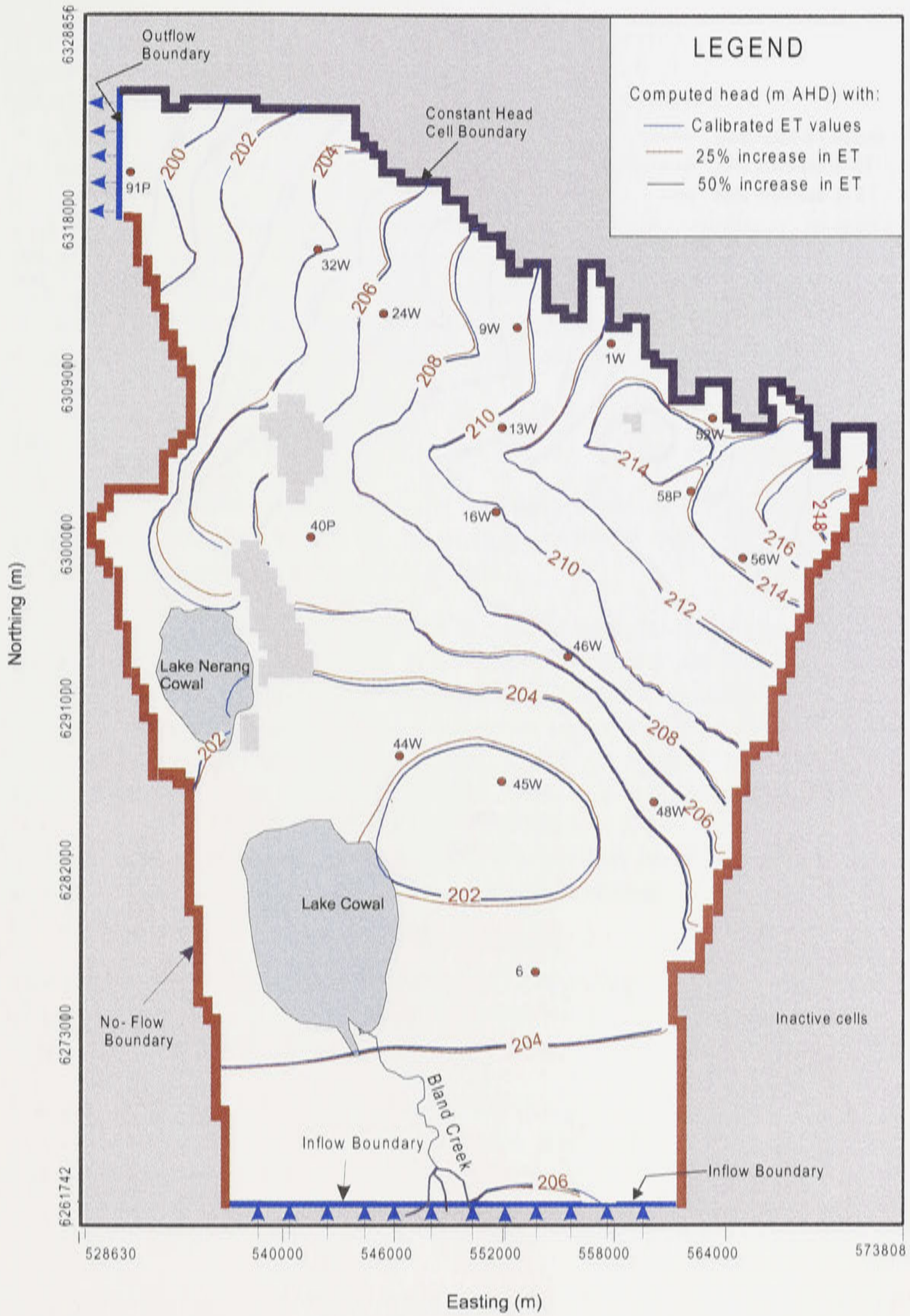


Figure 10.8b: Sensitivity of the computed heads due to changes in evapotranspiration rate for October 1994 representing a period of low groundwater levels (timestep 78).

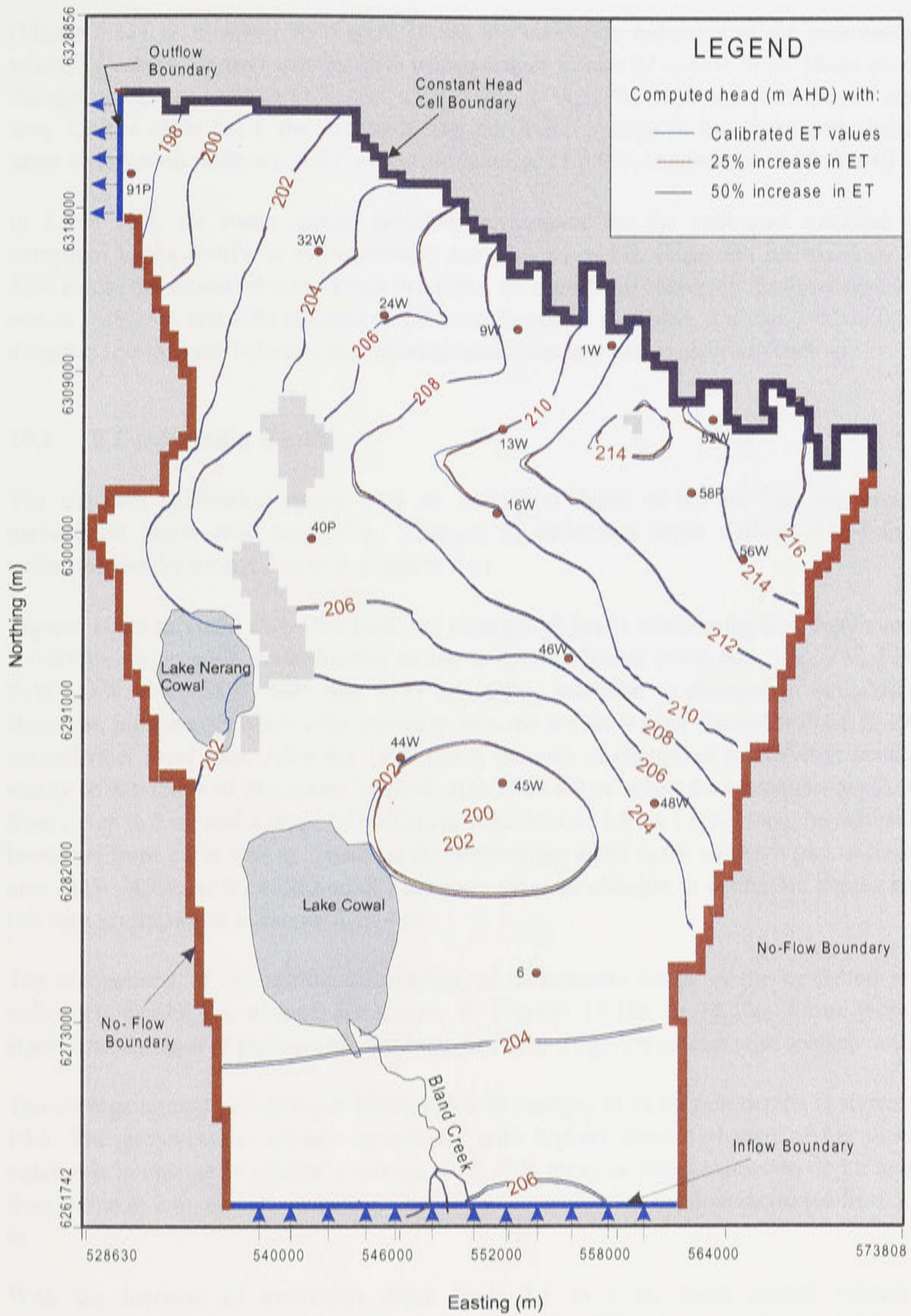


Figure 10.8c: Sensitivity of the computed heads due to changes in evapotranspiration rate for July 1997 representing the end of simulation (timestep 111).

(Figure 5.12), at timestep 30 (Figure 10.8a) the maximum reduction of the piezometric heads when ET values are increased by 25% values ranges from 0.07 m to 0.70 m. These are based on the eight observation wells (1W, 9W, 13W, 16W, 24W, 32W, 52W and 58P) located around this area. On the other hand, the corresponding maximum change in the piezometric heads in the same observation wells when ET values are increased by 50% ranges from 0.05 to 0.40 m.

In Table 10.4, the mean annual groundwater balance for the calibrated transient model is compared to the results of the sensitivity analyses when ET values are increased by 25% and 50% across the modelled area. From this table, no significant change in the groundwater balance occurs with 25% and 50% increase in ET rates. Based on this table, it is also evident that there is dynamic equilibrium between the constant head boundary and evapotranspiration.

10.6. ET extinction depth

The transient calibration model uses an extinction depth of 2.5 m. The sensitivity of the piezometric heads with respect to changes in extinction depth will be tested by altering extinction depths from 2.5 m to 4 m and to 2 m.

Figures 10.9a to 10.9d show the temporal changes of heads when extinction depths are altered. Evidently, observation wells located in the irrigation district (well nos. 1W, 9W, 13W, 16W, 24W, 32W, 40P, 56W, 58P, and 91P) are highly sensitive to changes in extinction depths. However, piezometric heads only started to become sensitive after the major flood in 1990 when groundwater level rose. After the 1990 flood, the rate of change of piezometric heads become steady with a range of maximum increase of 0.37 to 1.0 m when the extinction depth decreased from 2.5 m to 2 m, and a range of maximum reduction of 1.2 to 1.8 m when the extinction depth increased from 2.5 m to 4 m. Heads at the observation wells in the southern part of the modelled area (44W, 45W, 46W, 48W, and 6P) are insensitive to changes in extinction depths because in this area groundwater is deeper than 4 m.

The comparison of the spatial distribution of piezometric heads in the modelled area when extinction depths are altered are shown in Figures 10.10a to 10.10c. From these figures, significant changes of piezometric heads occur in the irrigation district with shallow watertables.

The average annual groundwater balance due to changes in extinction depths is shown in Table 10.5. The groundwater balance component with highest percent change of the mean annual volume is in change in aquifer's storage, with 40% increase when extinction depth is decreased from 2.5 m to 2 m, and about 224% reduction when extinction depth is increased from 2.5 m to 4 m.

With the increase of extinction depth from 2.5 to 4 m, mean annual volume due to evapotranspiration has also significantly increased by 88%. As a result, the total volume of output exceeded the total volume of input by 1,298,800 m³ yr⁻¹. Meanwhile, significant changes in mean annual volumes of inflows and outflows in the constant head boundary, and drainage are also observed with the change in extinction depths.

Table 10.4: Sensitivity of the average annual groundwater balance due to changes in evapotranspiration (ET) rates for the period May 1988 to July 1997.

Components	Mean annual volume (10^3 m^3)		
	Calibrated model	25% increase in ET values	50% increase in ET values
<i>Input</i>			
Constant head	4216.0	4380.0	4542.0
Recharge:			
Irrigation	2226.7	2226.7	2226.7
Rainfall	9850.4	9850.4	9850.4
Flooding	1553.4	1553.4	1553.4
Total	13630.5	13630.5	13630.5
Inflow boundary	334.0	334.0	334.0
Total input	18180.5	18344.5	18506.8
<i>Output</i>			
Constant head	2953.9	2950.9	2857.9
Outflow boundary	10.2	10.2	10.2
Leakage:			
Fracture A	2154.6	2154.6	2154.6
Fracture B	438.2	438.2	438.2
Fracture C	184.7	184.7	184.7
Total	2777.5	2777.5	2777.5
Evapotranspiration	11056.0	11300.0	11512.8
Drainage	339.6	328.7	330.6
Total output	17137.3	17317.4	17489.7
<i>Total input-total output</i>	<i>1043.2</i>	<i>1027.1</i>	<i>1017.1</i>
<i>Change in aquifer's storage</i>	<i>1043.1</i>	<i>1027.0</i>	<i>1016.6</i>
<i>Balance error</i>	<i>0.1</i>	<i>0.1</i>	<i>0.5</i>

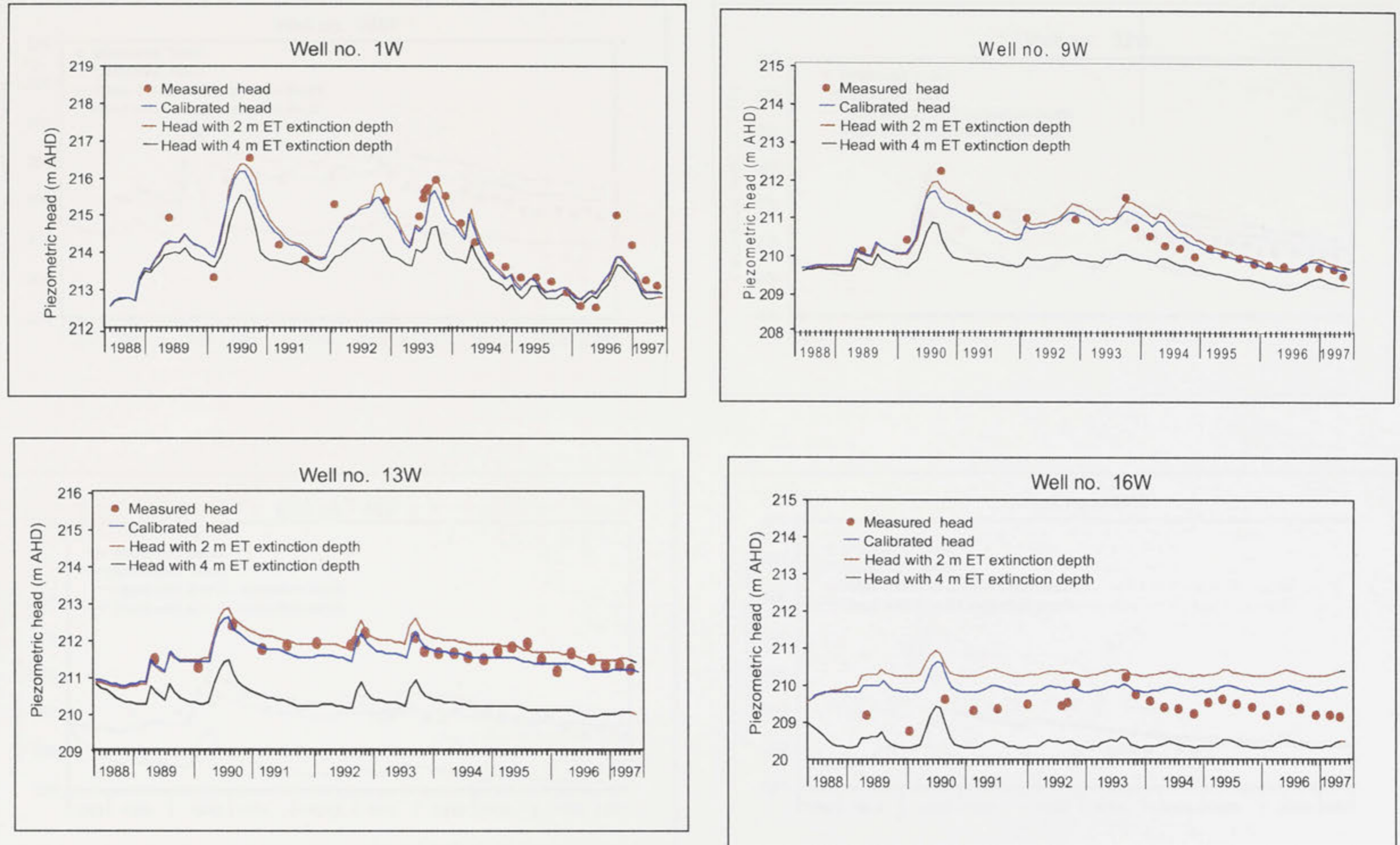


Figure 10.9a: Comparison between measured and computed heads at observation wells 1W, 9W, 13W and 16W with 2 m and 4 m ET extinction depths (see Figure 9.7 for locations).

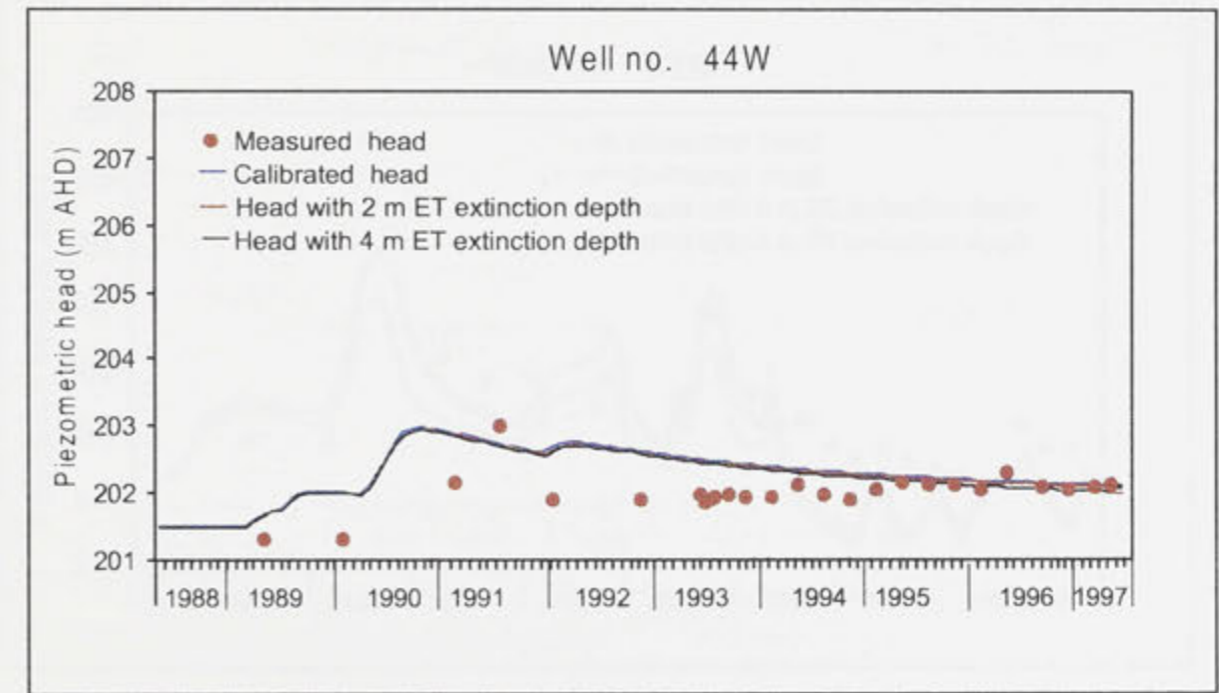
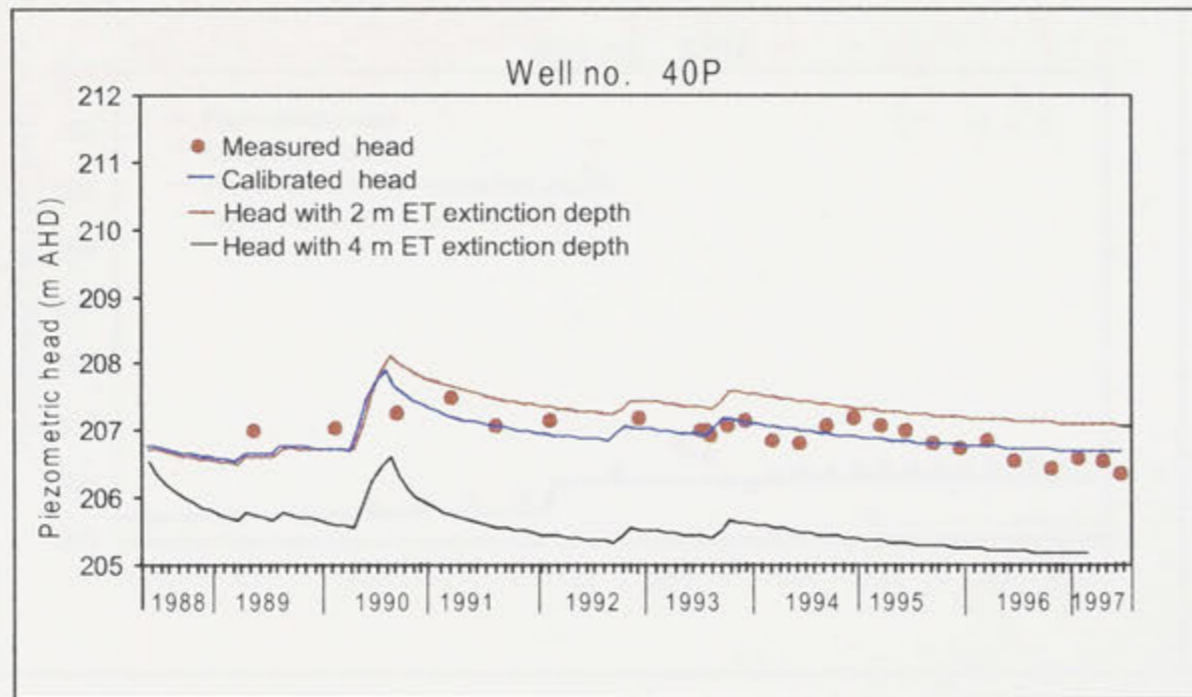
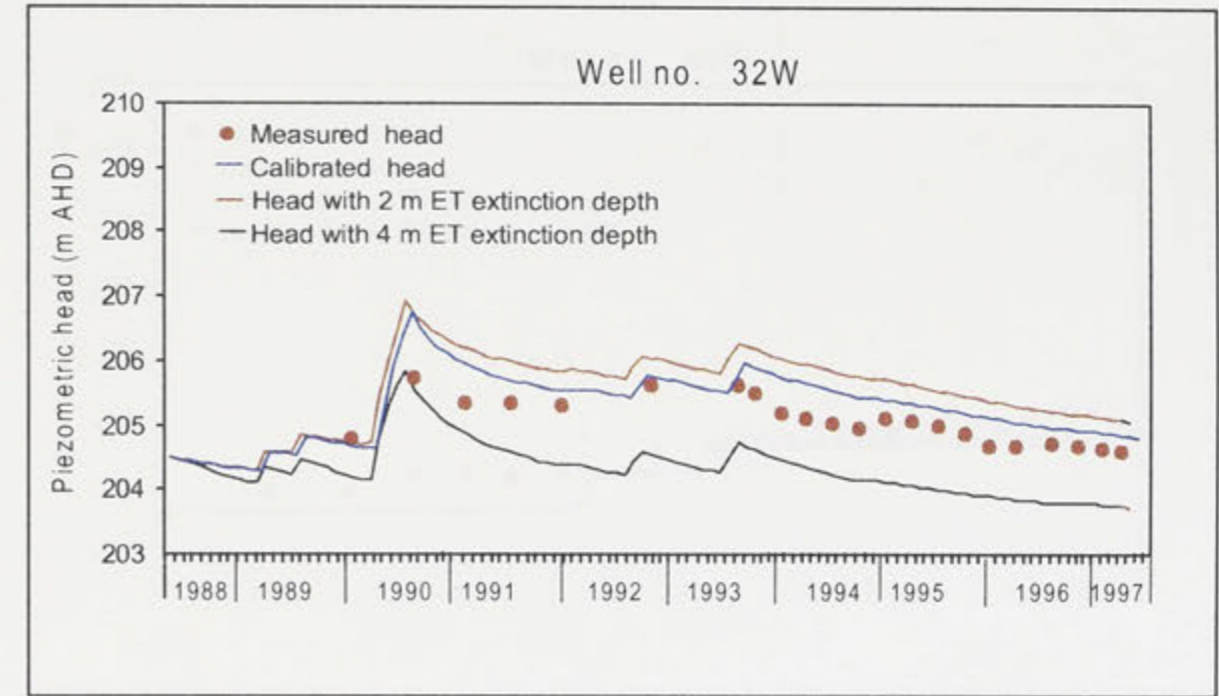
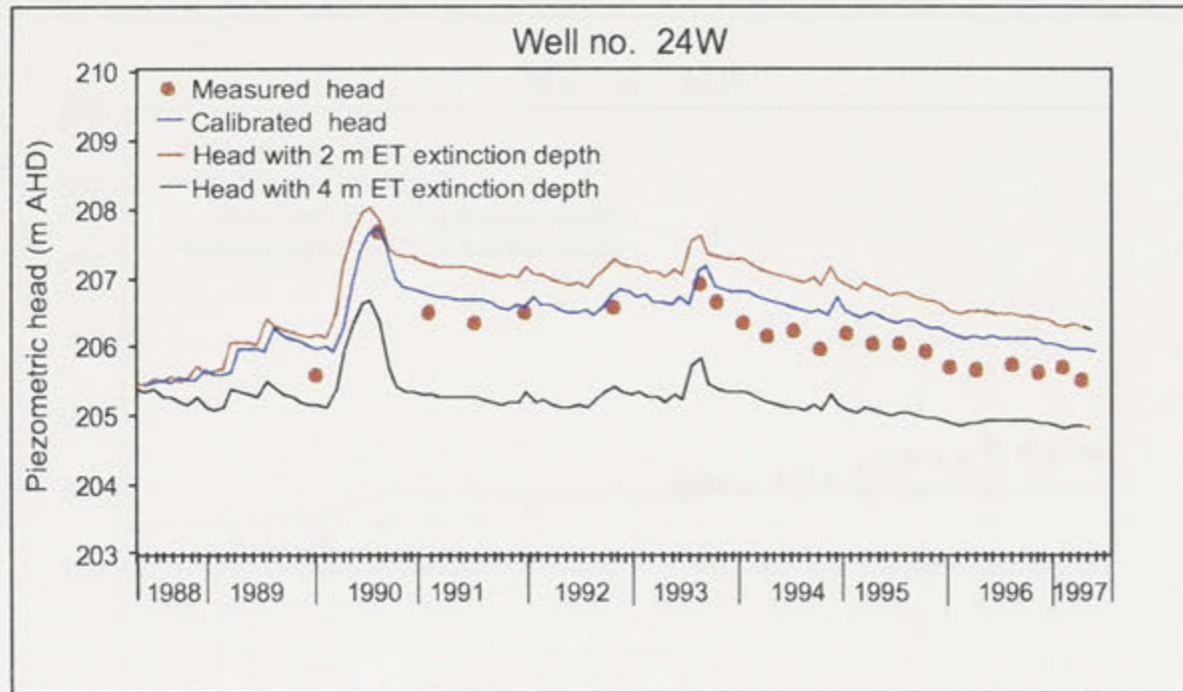


Figure 10.9b: Comparison between measured and computed heads at observation wells 24W, 32W, 40P and 44W with 2 m and 4 m ET extinction depths (see Figure 9.7 for locations).

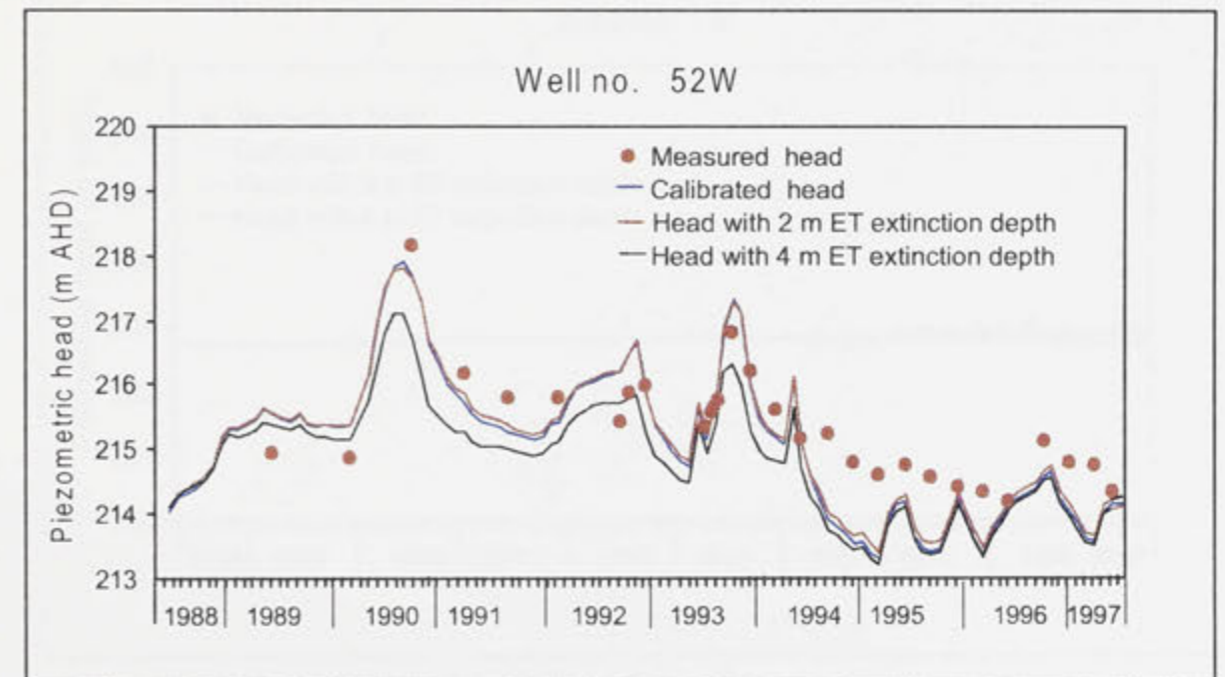
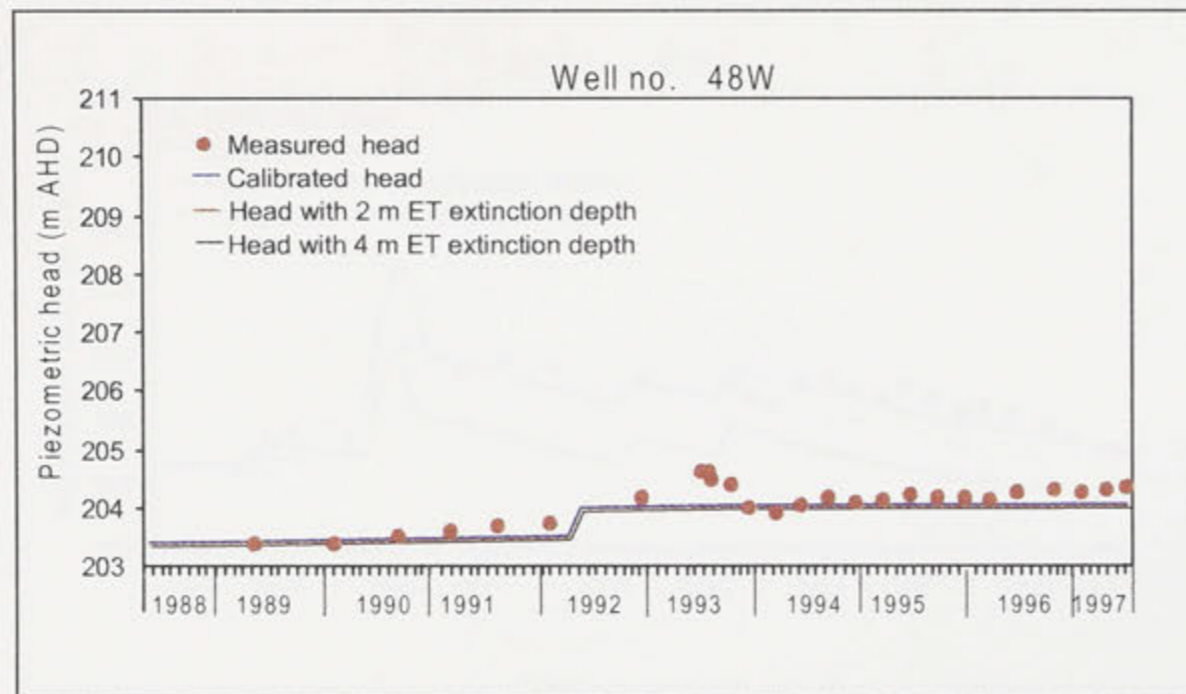
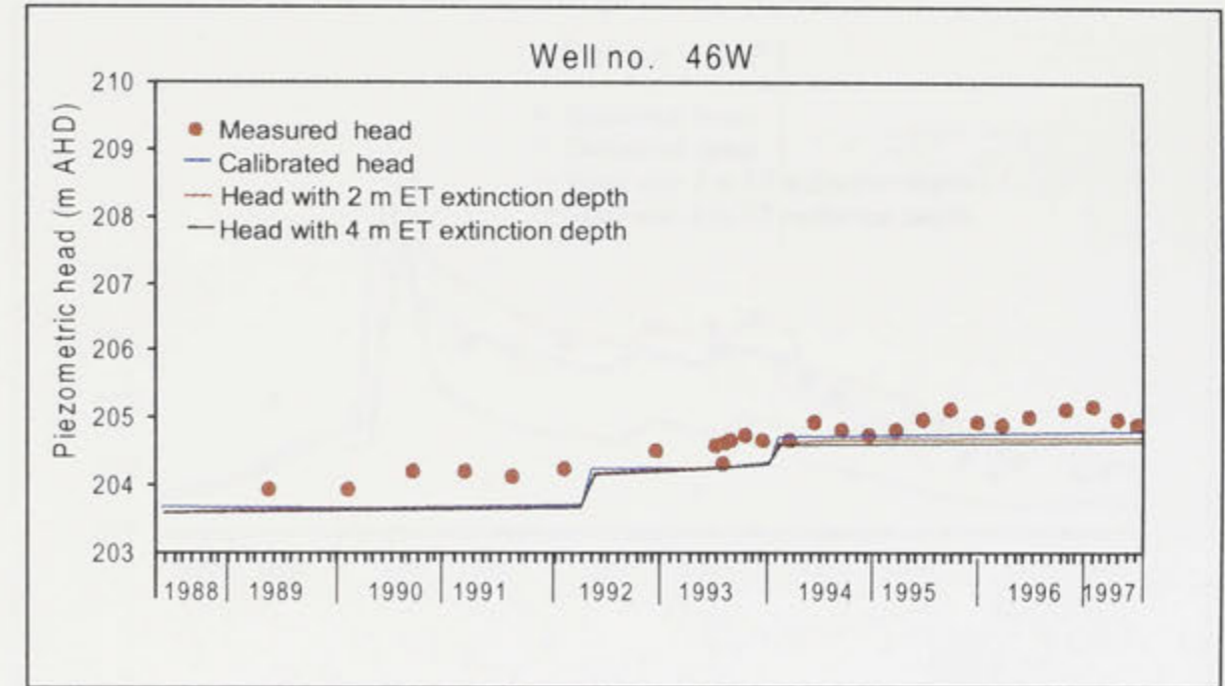
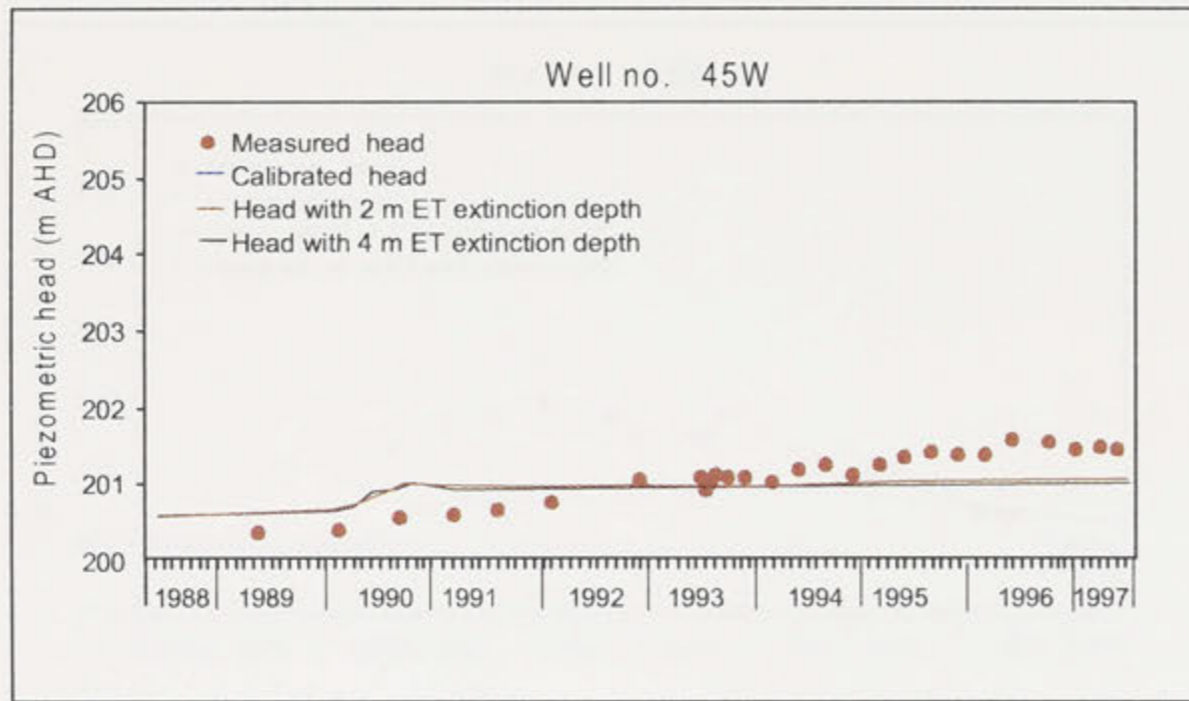


Figure 10.9c: Comparison between measured and computed heads at observation wells 45W, 46W, 48W and 52W with 2 m and 4 m ET extinction depths (see Figure 9.7 for locations).

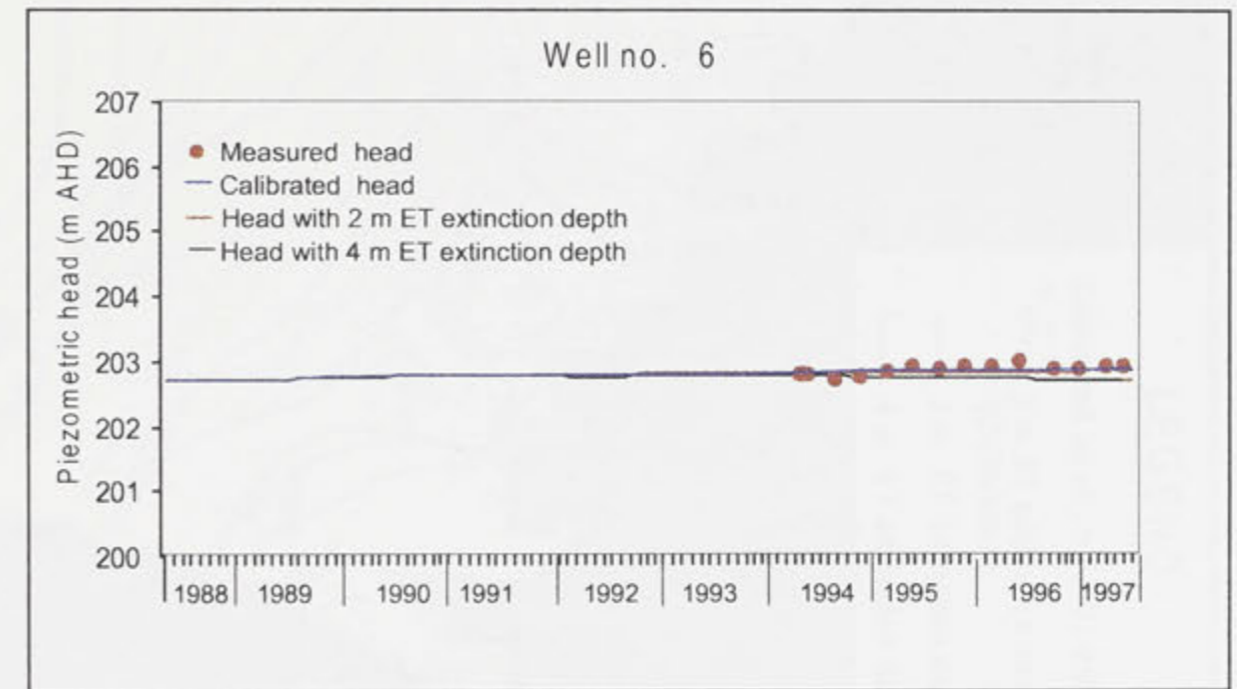
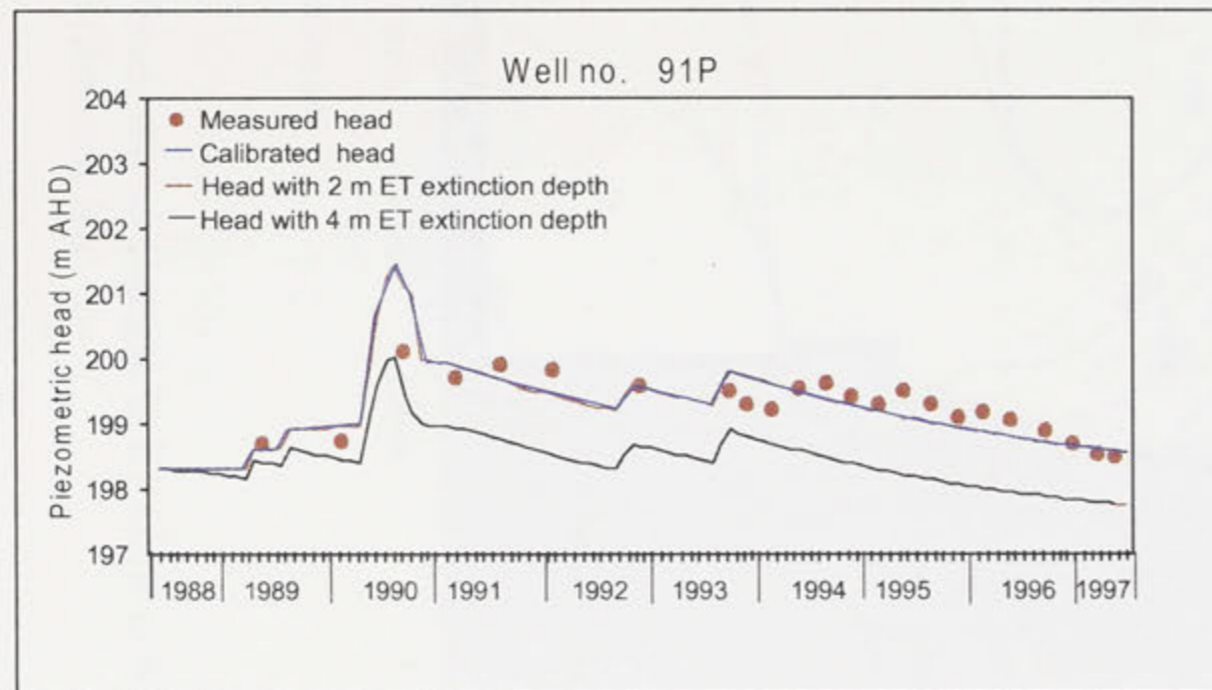
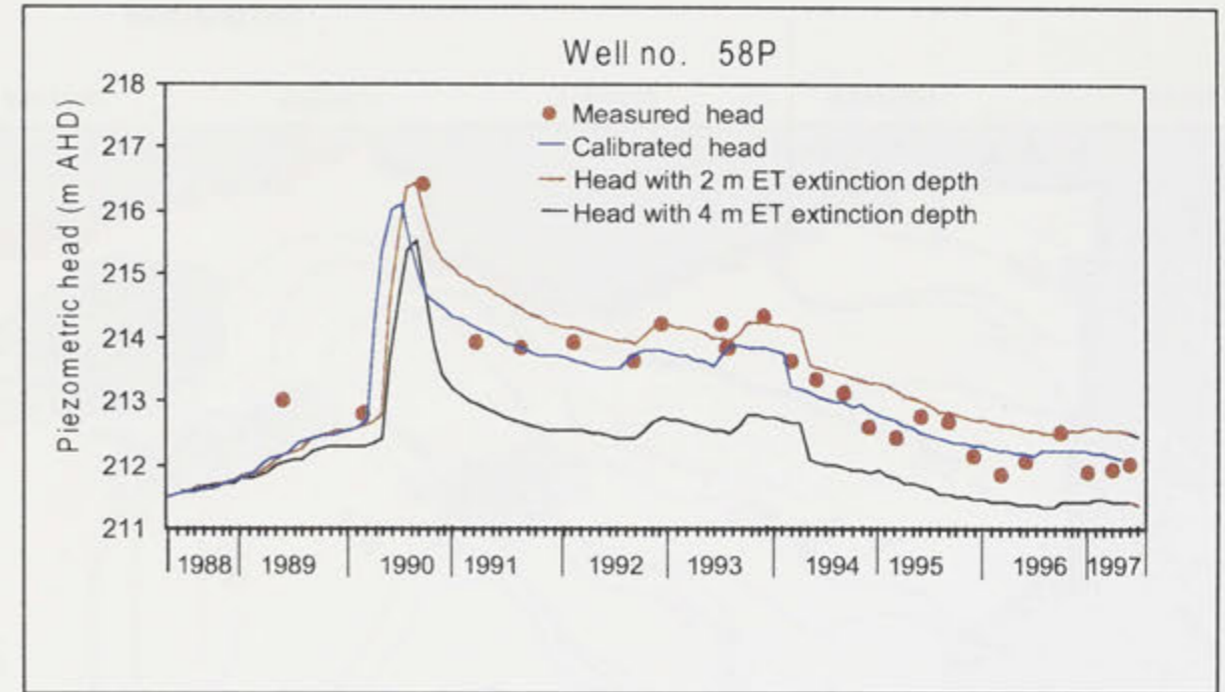
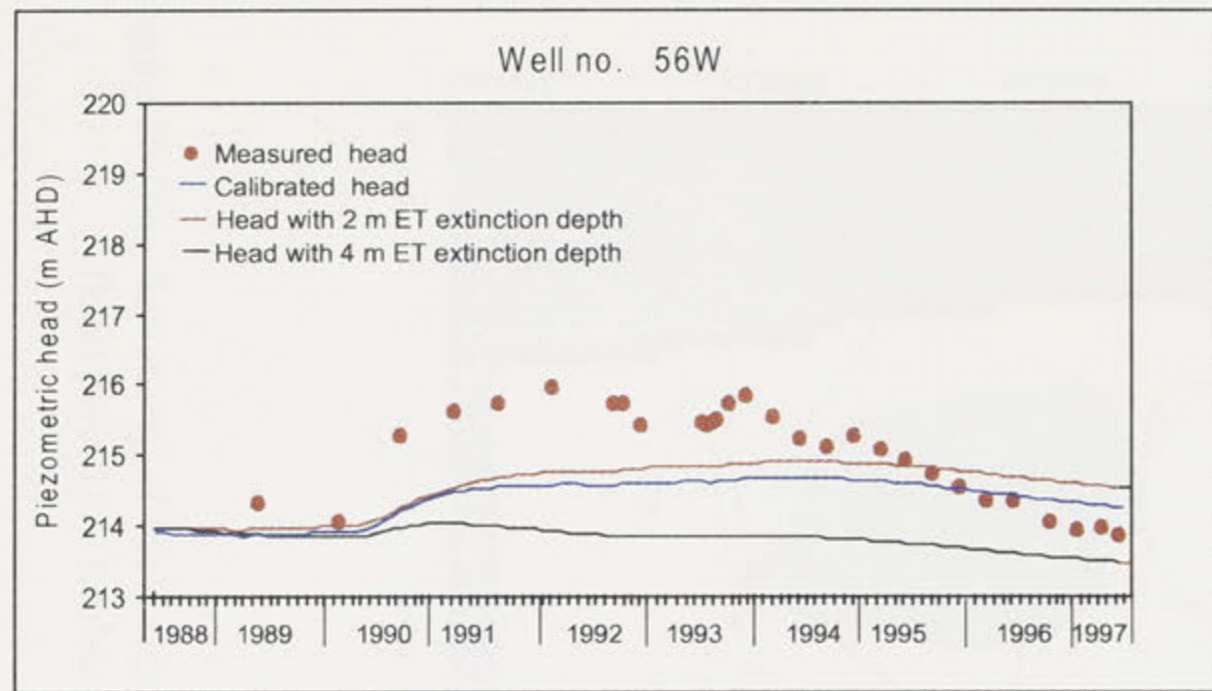


Figure 10.9d: Comparison between measured and computed heads at observation wells 56W, 58P, 91P and 6 with 2 m and 4 m ET extinction depths (see Figure 9.7 for locations).

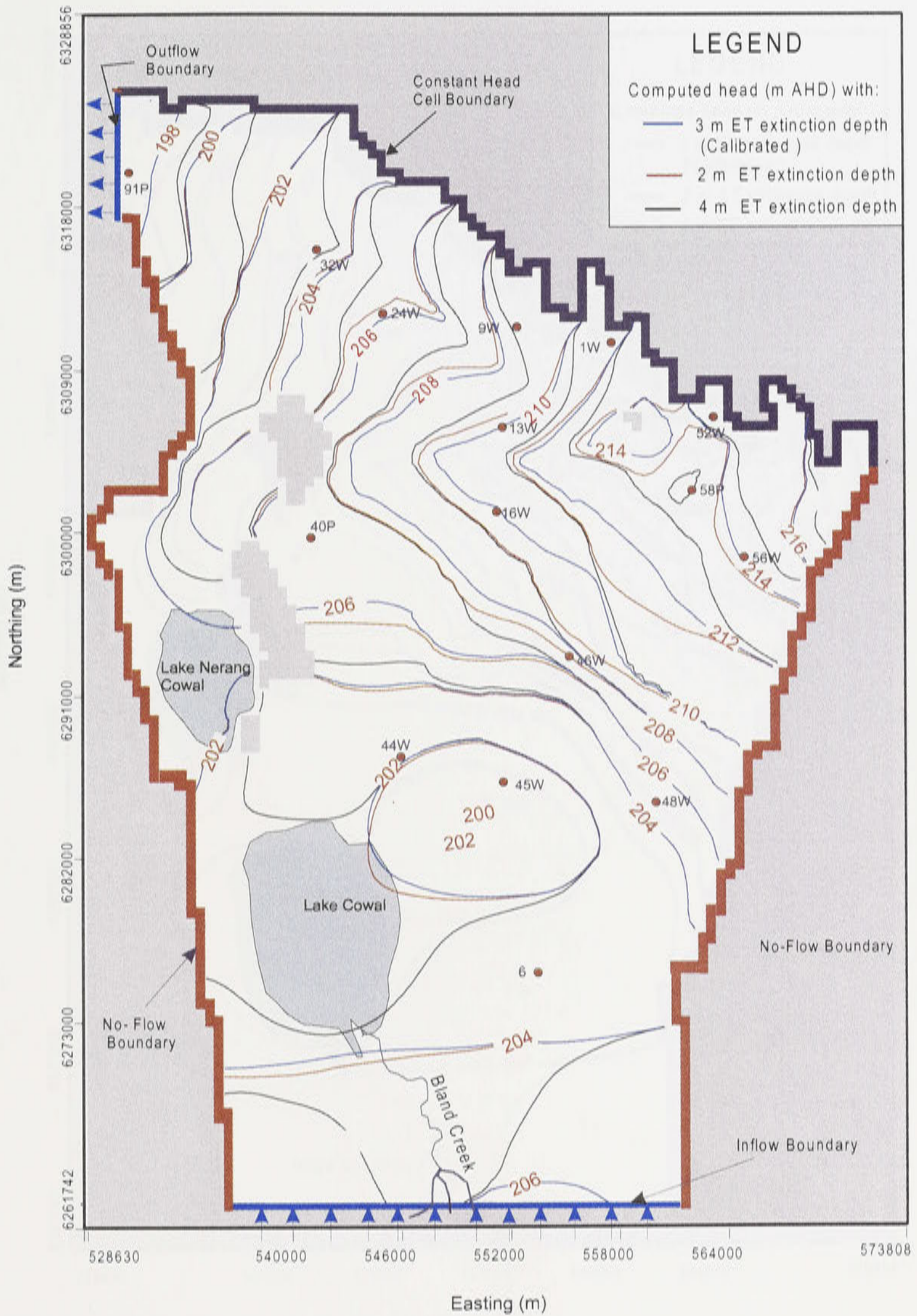


Figure 10.10a: Sensitivity of the computed heads due to changes in ET extinction depth for the flood period of October 1990 (timestep 30).

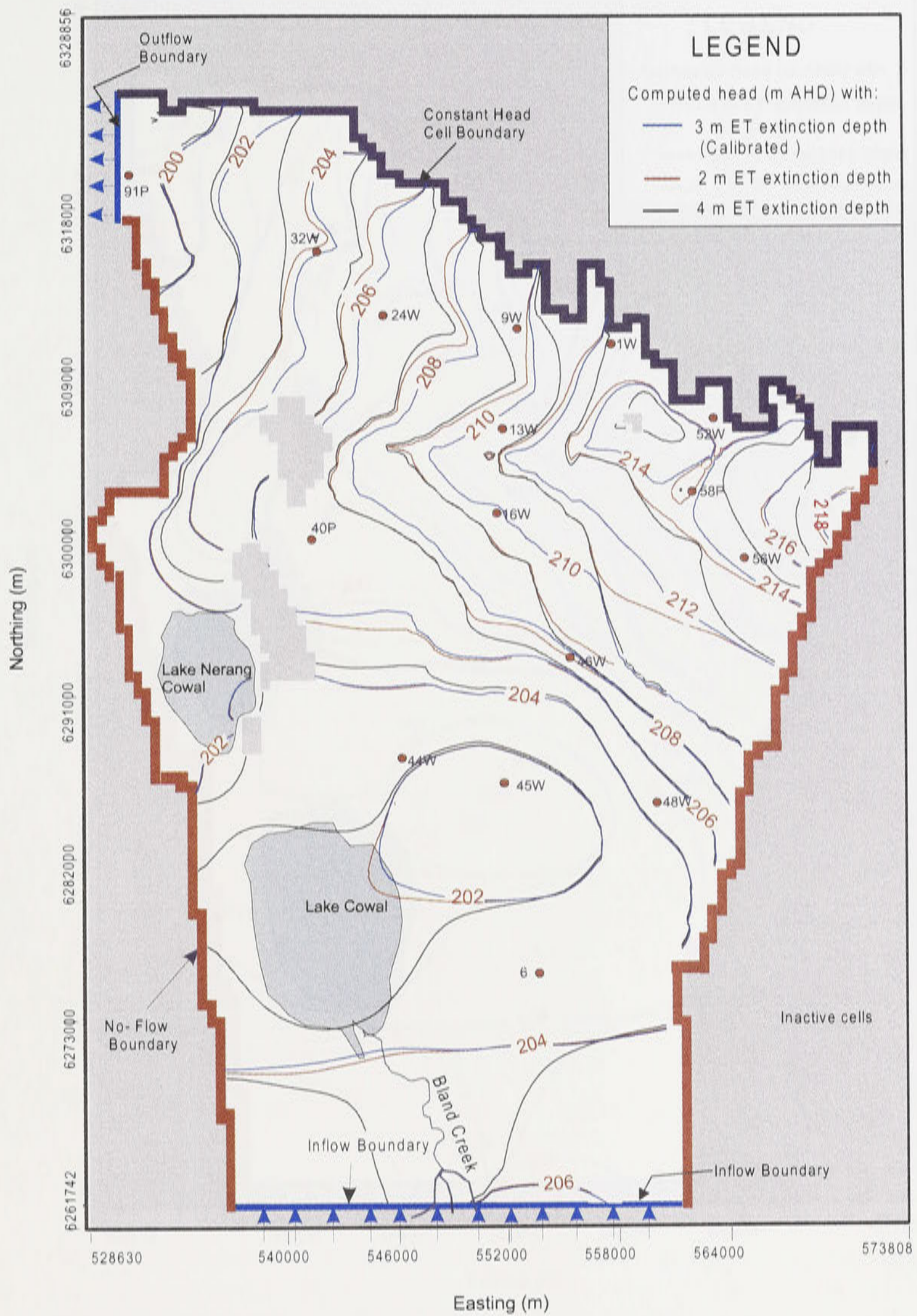


Figure 10.10b: Sensitivity of the computed heads due to changes in ET extinction depth for October 1994 representing a period of low groundwater levels (timestep 78).

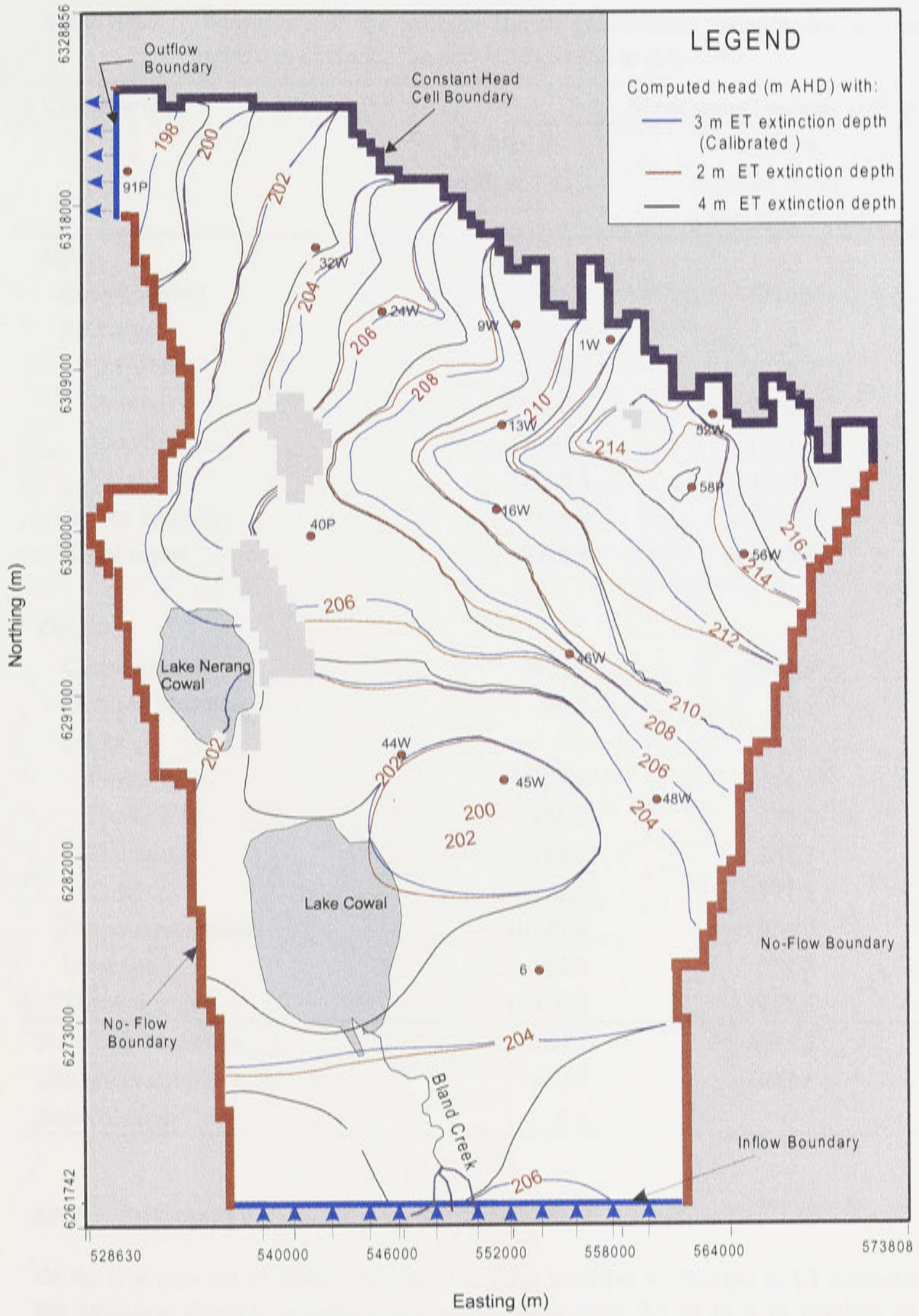


Figure 10.10c: Sensitivity of the computed heads due to changes in ET extinction depth for July 1997 representing the end of the period of simulation (timestep 111).

Table 10.5: Sensitivity of the average annual groundwater balance due to changes in ET extinction depth for the period May 1988 to July 1997.

Components	Mean annual volume (10^3 m^3)		
	Extinction depth of 2 m	Extinction depth of 2.5 m (calibrated model)	Extinction depth of 4 m
<i>Input</i>			
Constant head	4406.4	4216.0	9664.3
Recharge:			
Irrigation	2226.7	2226.7	2226.7
Rainfall	9850.4	9850.4	9850.4
Flooding	1553.4	1553.4	1553.4
Total	13630.5	13630.5	13630.5
Inflow boundary	334.0	334.0	334.0
Total input	18370.9	18180.5	23628.8
<i>Output</i>			
Constant head	3423.6	2953.9	1175.1
Outflow boundary	10.2	10.2	10.2
Leakage:			
Fracture A	2154.6	2154.6	2154.6
Fracture B	438.2	438.2	438.2
Fracture C	184.7	184.7	184.7
Total	2777.5	2777.5	2777.5
Evapotranspiration	10721.6	11056.0	20828.4
Drainage	343.0	339.6	136.4
Total output	16910.4	17137.3	24927.7
<i>Total input-total output</i>	<i>1460.5</i>	<i>1043.2</i>	<i>-1298.8</i>
<i>Change in aquifer's storage</i>	<i>1460.0</i>	<i>1043.1</i>	<i>-1298.9</i>
<i>Balance error</i>	<i>0.5</i>	<i>0.1</i>	<i>0.1</i>

10.7. Summary

Of the five parameters tested, the model is most sensitive to changes in ET extinction depth. In the irrigation district, increasing extinction depth from 2.5 m to 4 m resulted in significant reduction in piezometric heads and aquifer's net storage. The model is also sensitive to changes in storage coefficients and recharge values, but less sensitive to changes in evapotranspiration rates and hydraulic conductivity values. Based on the results of the sensitivity analyses, it is concluded that the calibrated values of parameters are reasonable.

Simulation of management options will now be presented.

CHAPTER 11

SIMULATION OF MANAGEMENT OPTIONS

11.1. Introduction

A wide range of management options is available to control salinity and waterlogging on irrigated and dryland agricultural areas and watercourses. Salinity management options may be broadly classified as engineering options, biological options and policy options which are described comprehensively by Ghassemi *et al.* (1995). Examples of engineering options include surface and subsurface drainage, conjunctive use of surface and groundwater, interception scheme, dilution flow, and improving irrigation efficiency. Biological options, on the other hand, involve modification of agricultural practices and revegetation of salt-affected lands and agroforestry, while policy options include water pricing, transferrable water entitlement, and integrated catchment management. However, choice of options depends on the particular circumstances. Technical, economic, social and political considerations are the major influences on the implementation of management options.

In the Jemalong and Wyldes Plains Irrigation District, not all options are applicable in addressing the land salinisation issues, as some options are site specific. For example, pumping of groundwater for conjunctive use of surface and groundwater even in the narrow strip along the Lachlan River where the groundwater is relatively less saline is not viable. This is mainly due to the fact that extraction of groundwater in this area will cause a northward movement of more saline groundwater towards the river and gradually will increase salinity of the pumped water. Also, groundwater pumping with the objective of lowering groundwater levels can not be considered because no option is available for the disposal of pumped saline groundwater without jeopardising the water quality of the Lachlan River.

Improvement of irrigation and drainage efficiency in the study area and tree-planting strategy are the applicable options. In this chapter, these options are assessed using the calibrated groundwater flow model developed for the area.

11.2. Model scenarios

The following scenarios have been simulated to assess the behaviour of the aquifer system:

- 'Average/no change' scenario;
- Reduce recharge through improved irrigation and drainage efficiency; and
- Reducing recharge through partial area tree-planting.

The three management strategies are simulated over a 23-year period from 1998 to 2020 (hereafter referred to as the 'forecasting period'). The assumptions and the hydrogeological impacts of the above management strategies are presented in the succeeding sections.

11.3. The 'average/no change' scenario

11.3.1. Data used and assumptions

The 'average/no change' scenario assumes that general land use practices remains unaltered until 2020. In this approach, input time-dependent parameters such as recharge, constant head boundary, inflow and outflow boundaries, drainage and leakages are assumed to be constant over the simulation period. Input values are prepared as the annual values to run the model in annual timesteps using the calibrated July 1997 piezometric heads as the initial condition. Overall, 23 timesteps are required to complete the simulation.

Recharge due to rainfall and irrigation has been estimated as described in section 9.4, and based on long term average data of each component available for the study area. Mean annual rainfall value of about 434 mm (Figure 3.14) for the period 1889-1997 has been used, while an average annual irrigation water delivery of $70 \times 10^6 \text{ m}^3$ (70,000 ML) from 1986 to 1997 (Figure 3.27) over an average irrigated area of 19,308 ha has been considered. Annual recharge values due to seepage along the Warroo Channel used in the prediction are 220 mm and 63 mm, for high and low seepage sections, respectively. These values were derived using average values of May 1988 to July 1997 in transient calibration (section 9.5).

Values of the constant head cells along the Lachlan River have been similarly computed by averaging the values used in the transient calibration for each cell. This means that a uniform constant head value for each cell along the river is assumed to forecast groundwater condition up to year 2020. Since piezometric heads in the aquifer system along the Lachlan River fluctuates due to stresses (flooding and drought) during the transient calibration period, this assumption is a valid representation of an average hydrogeological condition along the constant head boundary.

The annual evapotranspiration value used in the simulation is 1,387 mm (3.8 mm d^{-1}) which is an average value from 1974 to 1997. Inflows and outflows across aquifer boundaries, leakages through the basement's fractures and drainage of the system through the Gilmore Fault are based on the transient calibration values described in sections 9.9, 9.10 and 9.11, respectively.

11.3.2. Results and discussion

Figures 11.1 and 11.2 show maps of watertable depths in the modelled area during the initial condition (July 1997) and at the end of forecasting period (year 2020). Based on these two maps, major differences are observed in Warroo Channel area and northeast of Lake Cowal. In the Warroo Channel area, watertable has declined by almost 1 m at the end of year 2020, which is the continuation of the gradual piezometric heads decline observed in the area following the major flood in 1990 (see observation wells 9W, 13W and 24W in Figure 9.6a and 9.6b). On the other hand, groundwater depths in year 2020 at the northeast of Lake Cowal is shallower than in July 1997 as groundwater is continuously rising in this area (see Figure 9.6c for well numbers 45W, 46W and 48W).

Figure 11.3 shows piezometric head distribution for the year 2020. Comparing this Figure with Figure 9.9 for July 1997, there is an apparent increase in heads along the northeast side of Lake Cowal.

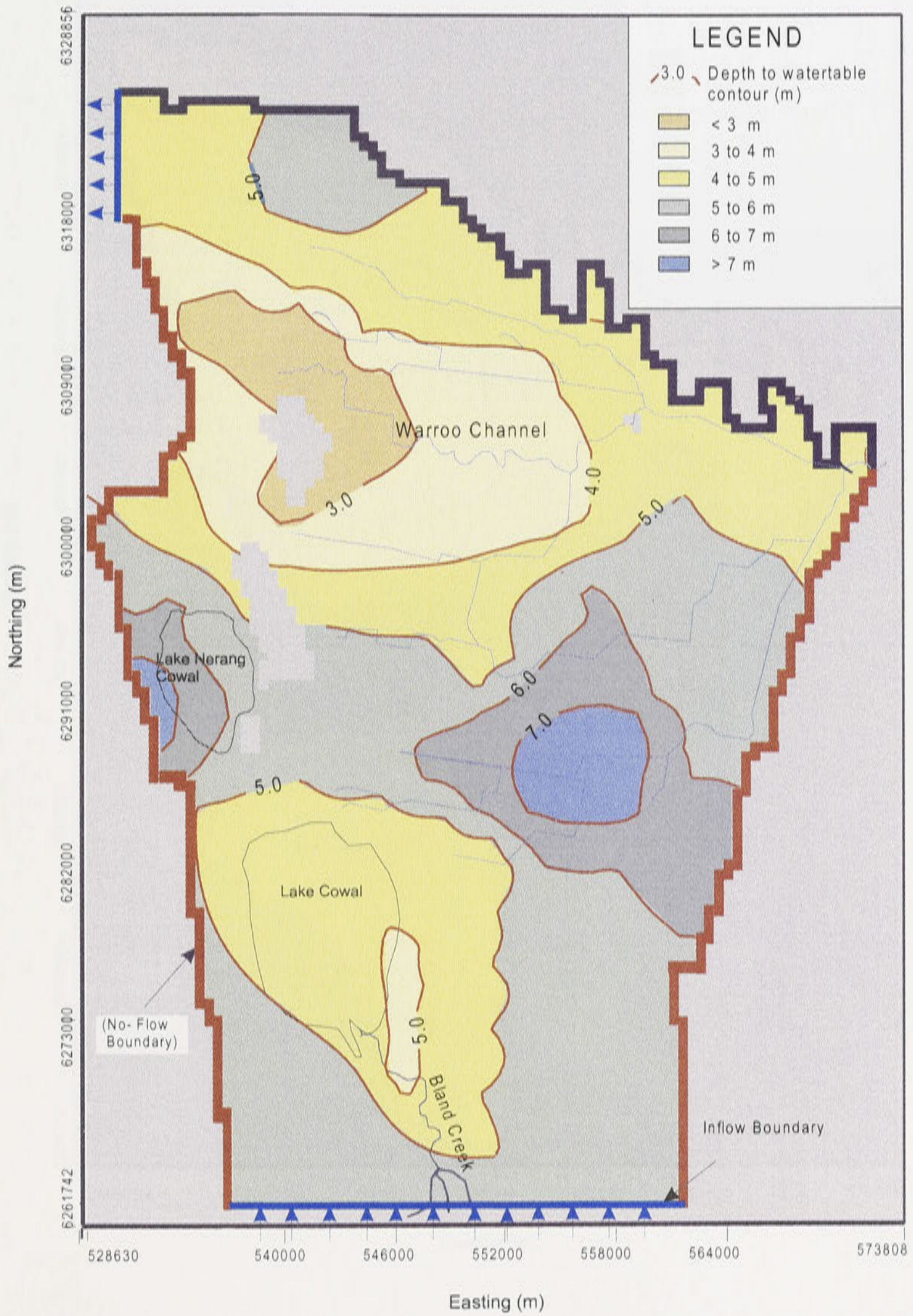


Figure 11.1: Computed watertable depth map of July 1997.

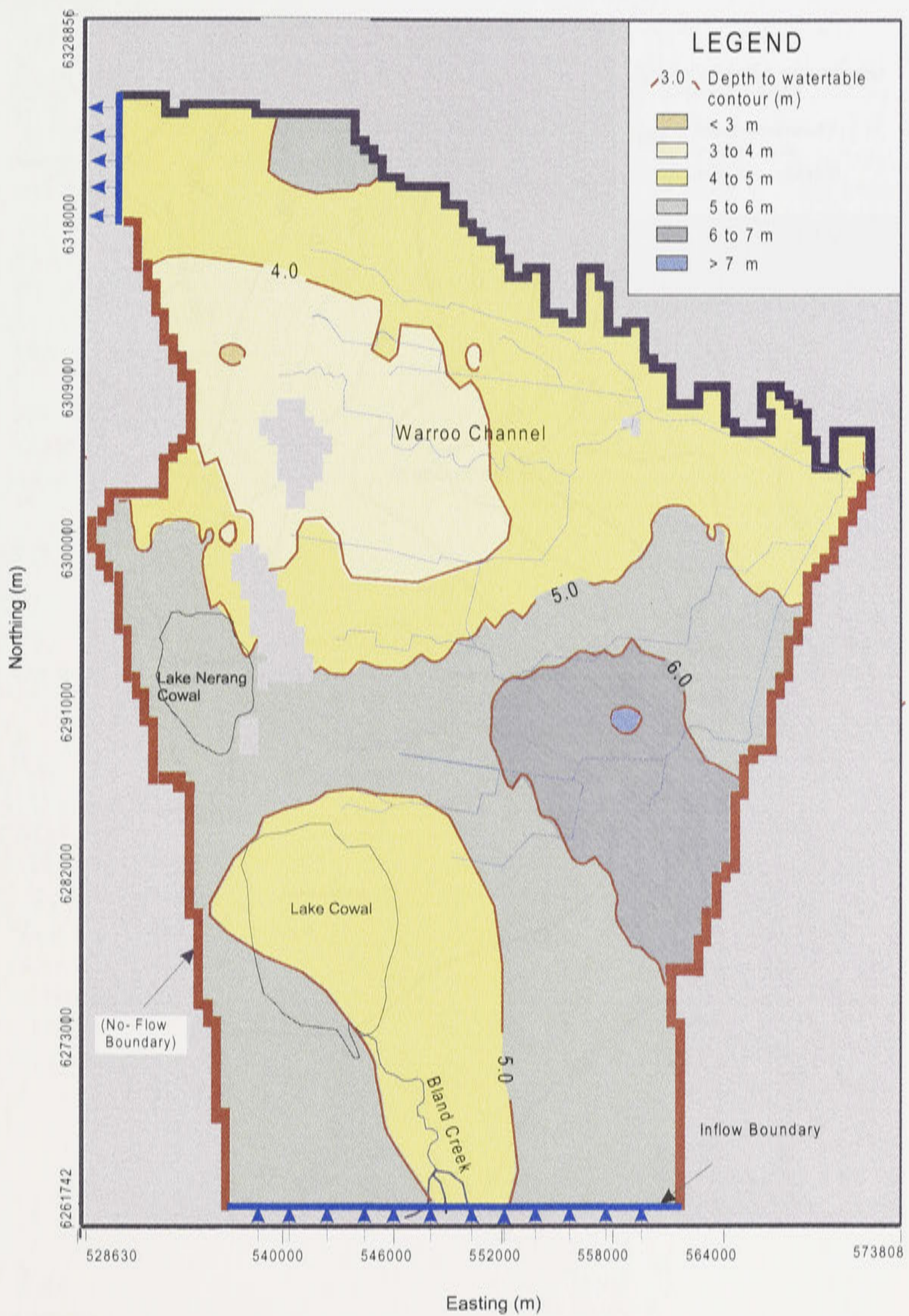


Figure 11.2: Computed watertable depth map for year 2020 with 'average/no change' scenario.

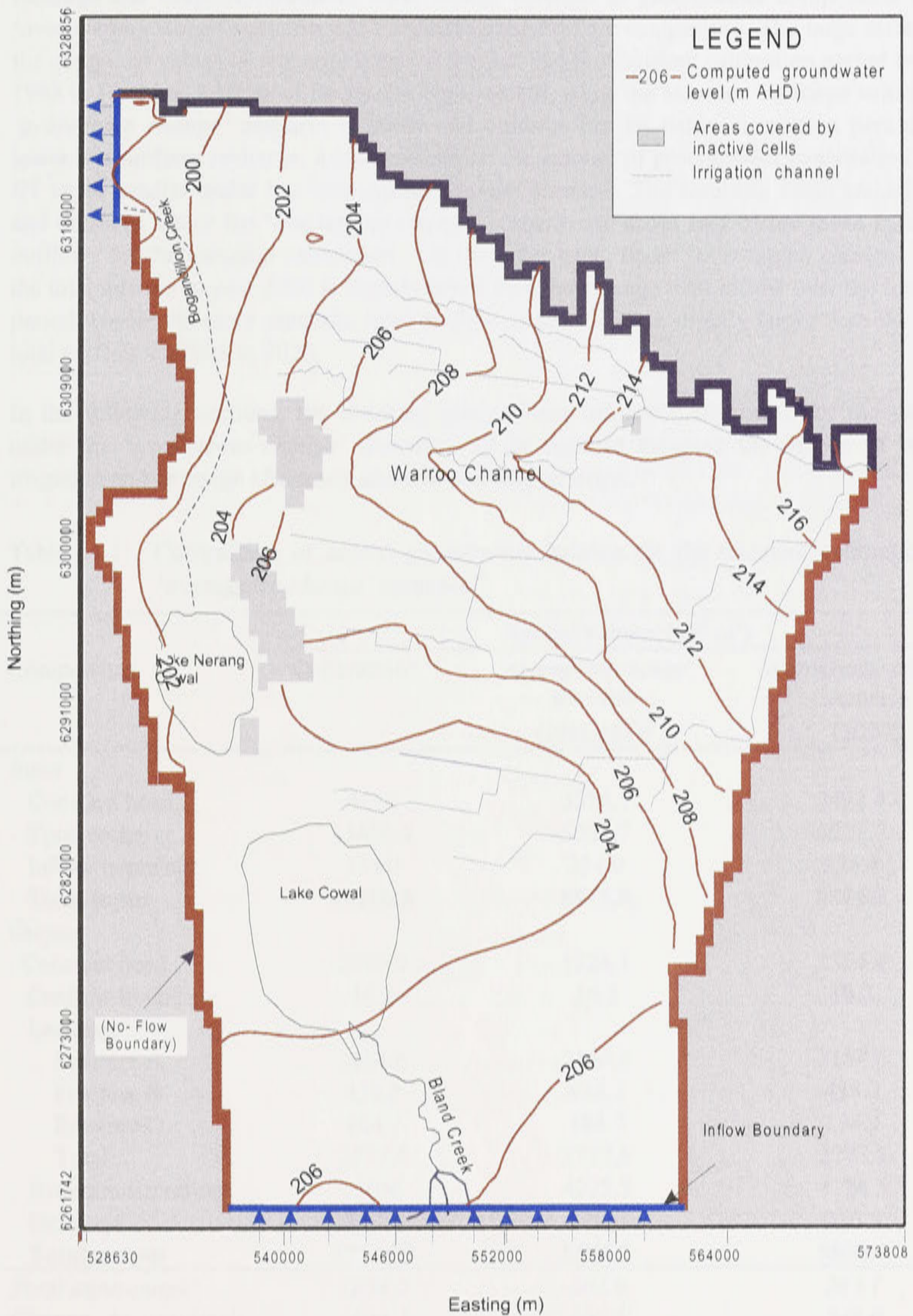


Figure 11.3: Computed piezometric head distribution for year 2020 under the 'average/no change' scenario.

Table 11.1 shows the mean annual groundwater balance for the period 1998 to 2020 under the 'average/no change' scenario and compares the water balance components for this period with the corresponding values for the year 2020 and for the period of calibration. Except for recharge and evapotranspiration, mean annual volumes of groundwater components between 'average/no change' scenario and transient calibration are comparable. The large difference in the computed values of recharge is due to the fact that the transient calibration period from May 1988 to 1997 had a series of floods and high rainfall, while the assumed recharge values for the 'average/no change' scenario is lower and uniform for the entire simulation period. With lower and uniform recharge, it is expected that the amount of groundwater evaporation through ET to be smaller under the 'average/no change' scenario. The resulting mean annual inflows and outflows under the 'average/no change' scenario are about half of the mean inflows and outflows for the transient calibration. On the other hand, under 'average/no change' scenario the total inflows in year 2020 is slightly lower than the average total inflow over the forecasting period. Under the same scenario, total outflow in year 2020 is slightly larger than the average total outflow for 1998 to 2020.

In the following sections, the resulting groundwater balance components for the year 2020 under the 'average/no change' scenario will be used to compare the impact of improved irrigation and drainage efficiency and tree-planting strategy.

Table 11.1: Comparison of annual groundwater balance for the transient calibration, and 'average/no change' scenario.

Components	Annual volume (10^3 m^3)		
	Calibration*	'Average/no change' scenario (1998-2020)	'Average/no change' scenario (2020)
<i>Input</i>			
Constant head	4216	3516.3	3478.4
Total recharge	13630.5	5021.7	5021.7
Inflow boundary	334.0	334.0	326.4
Total input	18180.5	8872.0	8826.5
<i>Output</i>			
Constant head	2963.0	1324.1	1354.4
Outflow boundary	10.2	10.2	10.2
Leakage:			
Fracture A	2154.6	2154.6	2154.6
Fracture B	438.2	438.2	438.2
Fracture C	184.7	184.7	184.7
Total	2777.5	2777.5	2777.5
Evapotranspiration	11056	4222.7	4224.5
Drainage	339.6	229.6	216.8
Total output	17146.3	8564.1	8583.4
<i>Total input-output</i>	<i>1034.2</i>	<i>307.9</i>	<i>243.1</i>
<i>Change in aquifer's storage</i>	<i>1034.1</i>	<i>307.1</i>	<i>243.0</i>
<i>Balance error</i>	<i>0.1</i>	<i>0.8</i>	<i>0.1</i>

*Results of transient calibration in Chapter 9 (see Appendix N).

11.4. Reduced recharge by improving irrigation and drainage efficiency

11.4.1. Data used and assumptions

Results of transient calibration (Chapter 9) showed that about $2.141 \times 10^6 \text{ m}^3$ (2,141 ML) per year of recharge comes from seepage losses of irrigation water in the Warroo Channel. These losses account for approximately 5% of the total delivered irrigation water in the Warroo Channel and about 2.5% of the total delivery for the entire irrigation district. Also, as mentioned in Chapter 9, rainfall is the major source of recharge for the aquifer system in the study area especially when rainwater is ponded on farms for a longer period of time. For example during the 1990 floods, ponding occurred on a large number of properties, and a duration of ponding of 7 months was typical for most of the properties within the study area. As a result, about $36 \times 10^6 \text{ m}^3$ (36,000ML) of flood recharged the aquifer system during this 7-month period. This is equivalent to about 28% of the total accumulated volume of recharge for the entire period of simulation of 111 months (9 years and 3 months). Within the irrigation district, model calibration has estimated that about 31% of the total rainfall has reached the watertable during this period. Floodwaters from the Lachlan River contributed 11% to the total recharge of the aquifer system during the period of transient calibration. Therefore, one feasible option to be considered is lessening flooding and improving the drainage facilities.

Under this scenario, three options have been evaluated to determine the impact of improving irrigation and drainage efficiency in the study area. Results of these options will be compared with the 'average/no change' scenario. These options are:

Option A : Sealing of Warroo Channel

Option B : Reducing recharge rates due to ponded rainwater and river flooding by 50 percent.

Option C : Combining options A and B

Option A assumes that engineering works such as channel lining will be carried out to seal off seepage losses. As a result, recharge due to seepage along the Warroo Channel has been assumed to be zero. Option B, on the other hand, assumes that recharge due to ponded rainwater and river flooding is reduced by 50% by improving drainage facilities and flood prevention structures along the appropriate sections of the Lachlan River. The details of the design and implementation of these drainage system are presented in "Jemalong Land and Water Management Plan - Surface Drainage Management Study" prepared by Lyall Macoun Consulting Engineers (1995).

11.4.2. Results and discussion

11.4.2.1: Option A

Figure 11.4 and Figure 11.5 show the piezometric head distribution and watertable depths, respectively, for year 2020 assuming zero seepage for Warroo Channel. As a result of this option, a decline of watertable depths of over 1 m of watertable depths (Figure 11.6) has been computed for the Warroo Channel area compared to the 'average/no change' scenario. Also, a

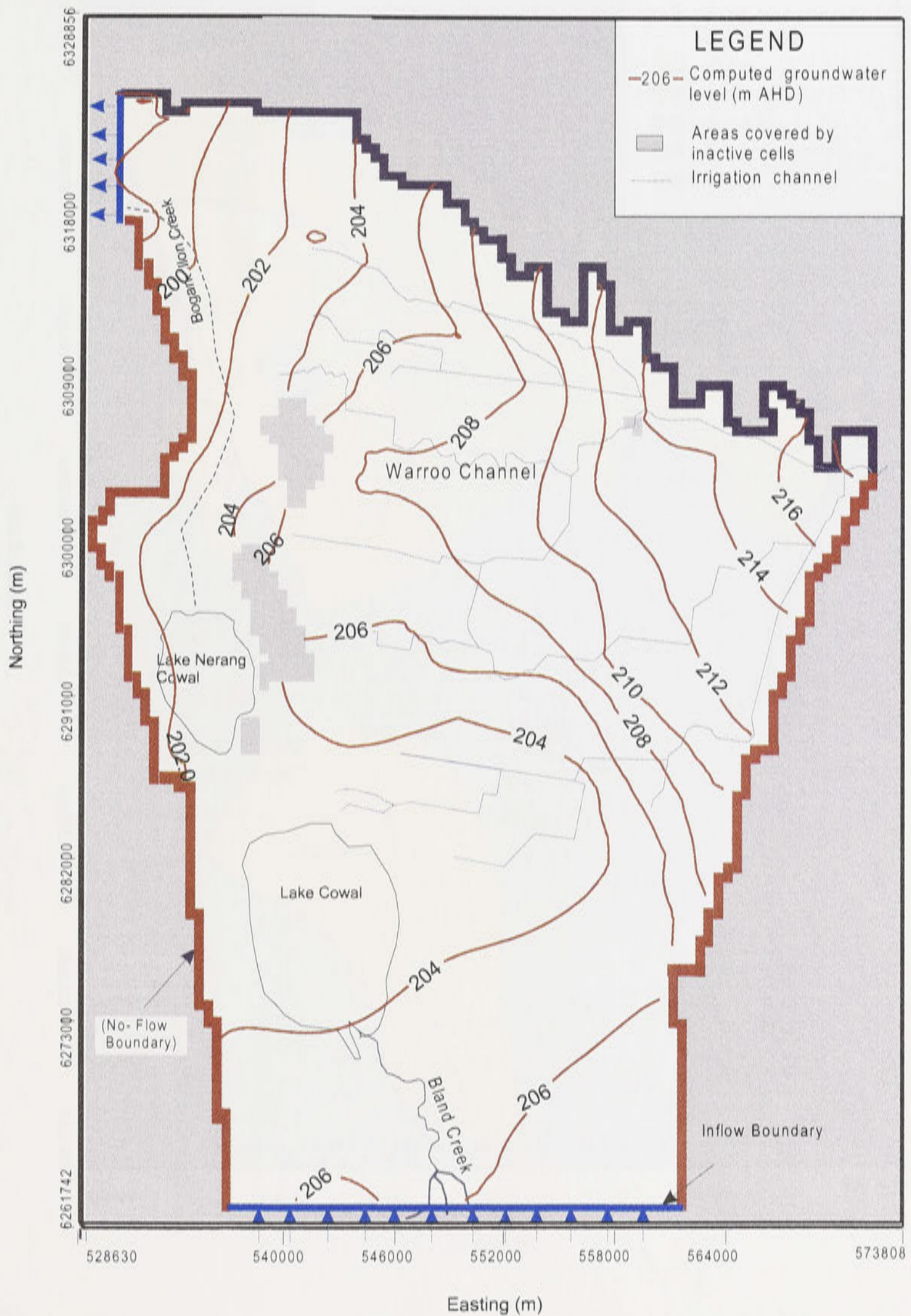


Figure 11.4: Piezometric head distribution under 'sealing of Warroo Channel' (Option A) in year 2020.

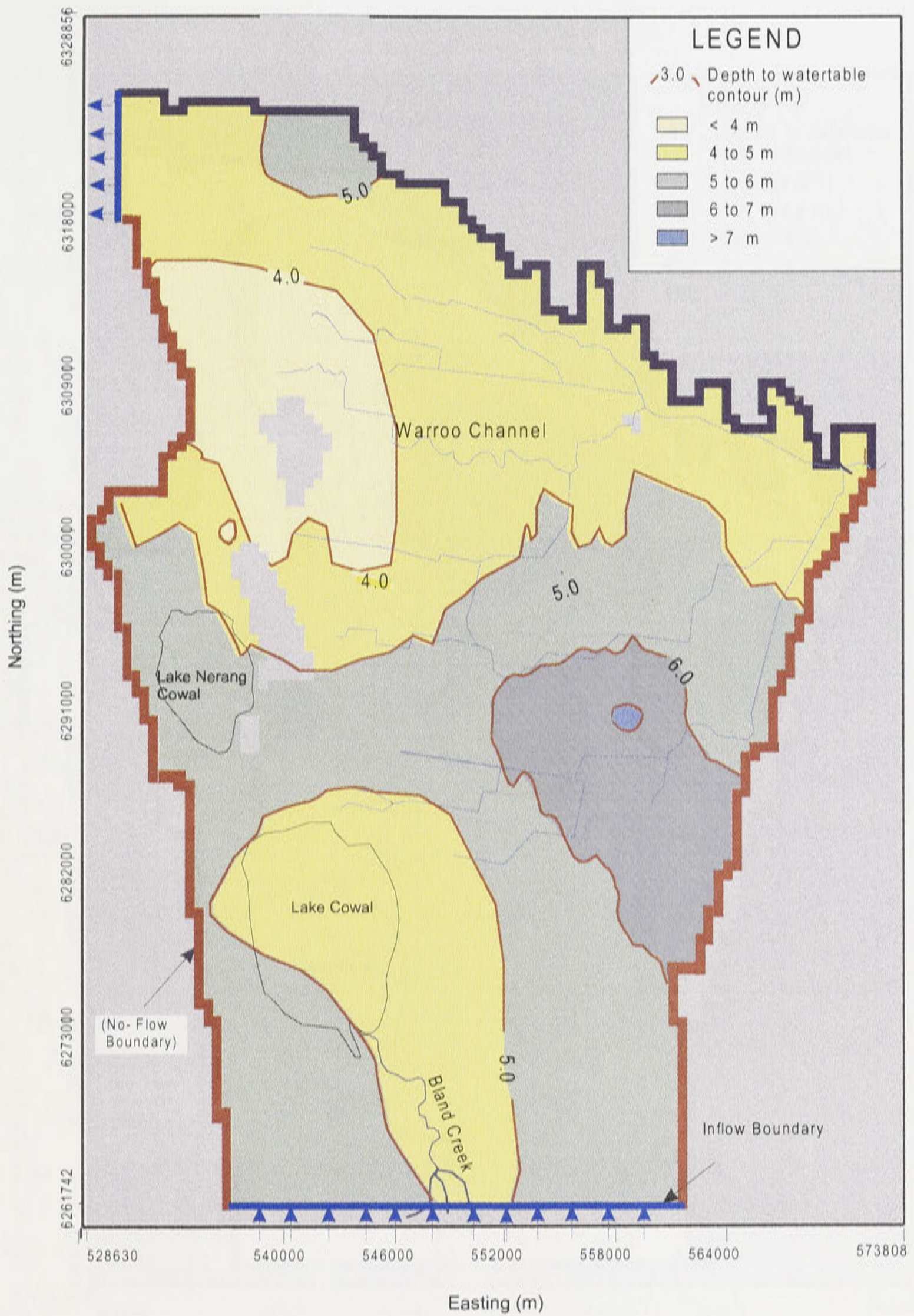


Figure 11.5: Watertable depths under 'sealing of Warroo Channel' (Option A) in year 2020.

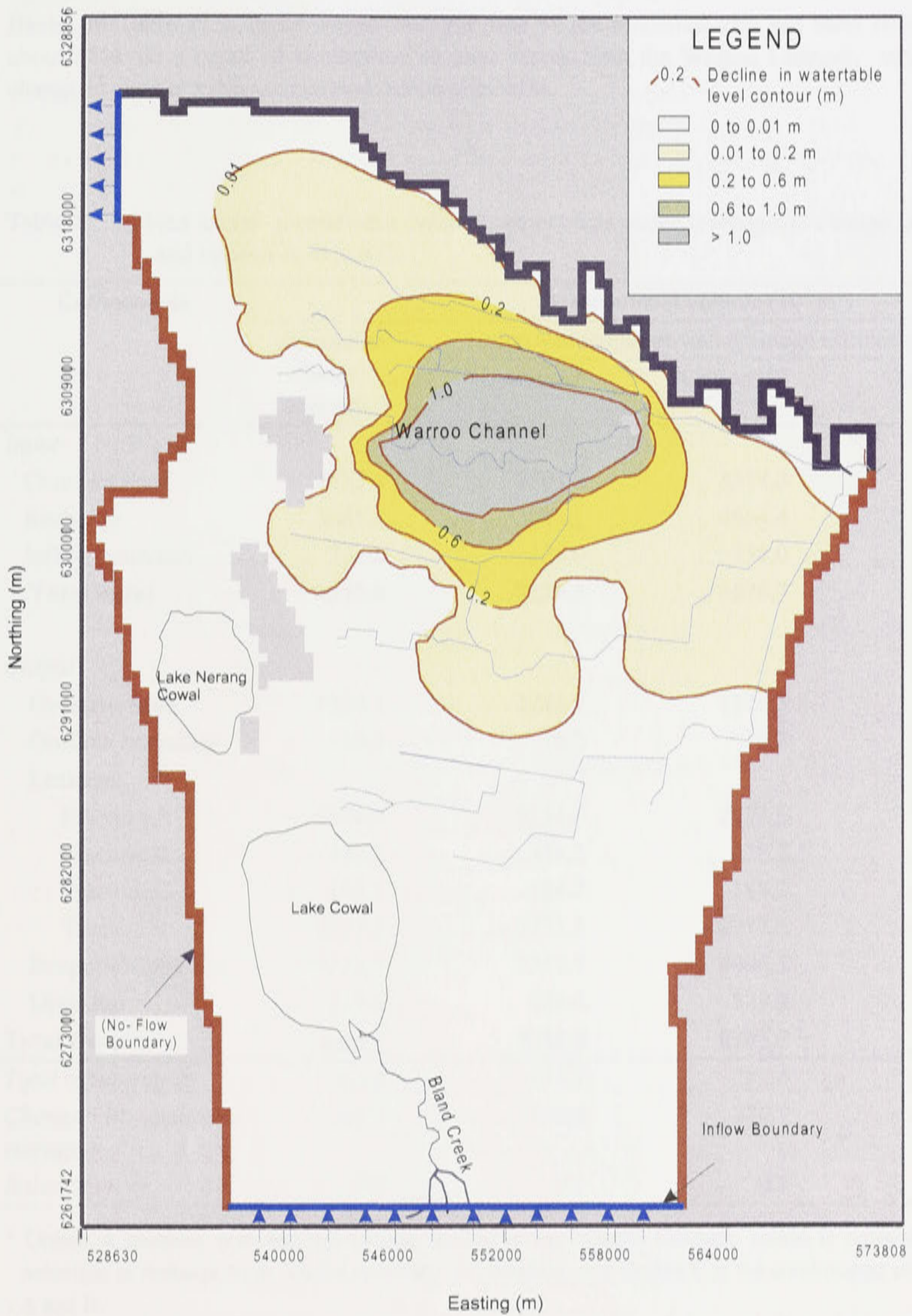


Figure 11.6: Decline in watertable depths for year 2020 due to Option A as compared with the 'average/no change' scenario.

reduction of watertable depths of up to 0.2 m extends over a large part of the irrigated area (Figure 11.6). As expected, the southern and western part of the model domain are not influenced at all by the effect of zero seepage from the Warroo Channel.

Based on Table 11.2, mean annual recharge rate of the modelled area has been reduced by about 38% as a result of eliminating seepage losses from the Warroo Channel, while the change in aquifer's storage has been reduced by 62%.

Table 11.2: Mean annual groundwater balance components under 'average/no change' scenario and options A, B and C.

Components	Mean annual volume (10^3 m^3)			
	'Average/no change' scenario	Improved irrigation and drainage efficiency		
		Option A*	Option B*	Option C*
<i>Input</i>				
Constant head	3516.3	3701.2	3578.3	3783.7
Recharge	5021.7	3094.1	4664.4	2736.8
Inflow boundary	334.0	334.0	334.0	334.0
Total input	8872.0	7129.3	8576.7	6854.5
<i>Output</i>				
Constant head	1324.1	1243.7	1272.5	1189.3
Outflow boundary	10.2	10.2	10.2	10.2
Leakage:				
Fracture A	2154.6	2154.6	2154.6	2154.6
Fracture B	438.2	438.2	438.2	438.2
Fracture C	184.7	184.7	184.7	184.7
Total	2777.5	2777.5	2777.5	2777.5
Evapotranspiration	4222.7	2757.7	4006.5	2599.8
Drainage	229.6	229.5	229.2	229.1
Total Output	8564.1	7018.6	8295.9	6805.9
<i>Total input-output</i>	<i>307.9</i>	<i>110.7</i>	<i>280.8</i>	<i>48.6</i>
<i>Change in aquifer's storage</i>	<i>307.1</i>	<i>110.6</i>	<i>280.9</i>	<i>48.5</i>
<i>Balance error</i>	<i>0.8</i>	<i>0.1</i>	<i>0.1</i>	<i>0.1</i>

* Option A assumes zero seepage through sealing of the Warroo Channel; option B represents 50% reduction in recharge from ponded rainwater and flooding; and Option C is the combination of Options A and B.

11.4.2.2. Option B

Figures 11.7 and 11.8 show the piezometric and watertable depth maps, respectively, under option B for the year 2020. The decline in watertable depths in year 2020 between option B and the 'average/no change' scenario (Figure 11.9) shows that changes in watertable depths in the modelled area are confined in the high seepage areas located at the northern part of the irrigation district and in the northeast of Lake Cowal as expected. However, the maximum decline is only about 0.15 m, which is much lower than decline in option A. Based on the mean annual total groundwater balance (Table 11.2), change in aquifer's storage has been decreased by only 9%.

11.4.2.3. Option C

Piezometric and watertable maps for year 2020 under option C are shown in Figures 11.10 and 11.11, respectively. The decline in watertable depths with option C (combined options A and B) is shown in Figure 11.12. This option is slightly more effective than option A. Option C has decreased the watertable depths more than 1.4 m in Warroo area. The mean annual groundwater balance using option C (Table 11.2) shows 82% reduction of change in aquifer's storage as a result of reduction of the total recharge by 46%.

Hydrogeologically, Option C is the best among the three options as it lowers the piezometric heads more effectively over a much larger area. However, surface drainage facilities (which are required for Option A and C) are generally expensive. Thus, economically, option A which is the sealing off of the Warroo Channel seepage seems to be most cost-effective alternative.

11.5. Partial area tree-planting strategy

Reforestation and farm tree establishment have been included as control measures in salinity management plans for the Australian catchments, based on an expectation that evapotranspiration from forests or woodlands will be greater than crops and pastures in the same location (Clifton *et al.*, 1993). The potential value of trees for reducing recharge to groundwater, particularly in upper catchment areas with shallow soils and high rainfall, is relatively well established. Their effectiveness in discharge areas, as means of lowering watertables by direct uptake of groundwater, is less certain (Morris and Thomson, 1983; Marcar *et al.*, 1995).

One of the reforestation strategy that has recently received increased attention in Australia is alley farming. Alley farming is a technique in which crops and pastures are grown between parallel belts of trees (Lefroy and Scott, 1994). Alley farming has other advantages in addition to its higher water use: it provides shelter which will substantially reduce wind erosion and can lead to increase pasture, livestock, and crop production (Bird *et al.*, 1992). In the higher rainfall areas ($>500 \text{ mm yr}^{-1}$) 2 to 12 rows of commercial trees are planted between 30 to 200 m alleys. The narrow alleys usually support grazed pastures with *Eucalyptus globulus* while the wider spacings have been used for *Pinus radiata* windbreaks and alley cropping systems (George and Bennet, 1992). In the lower rainfall areas ($280\text{-}500 \text{ mm yr}^{-1}$), non-commercial eucalypts are used. The degree of profitability of the alley farming system depends on the effectiveness of the trees in lowering watertables and increasing agricultural options in the treated paddocks (George and Bennet, 1992).

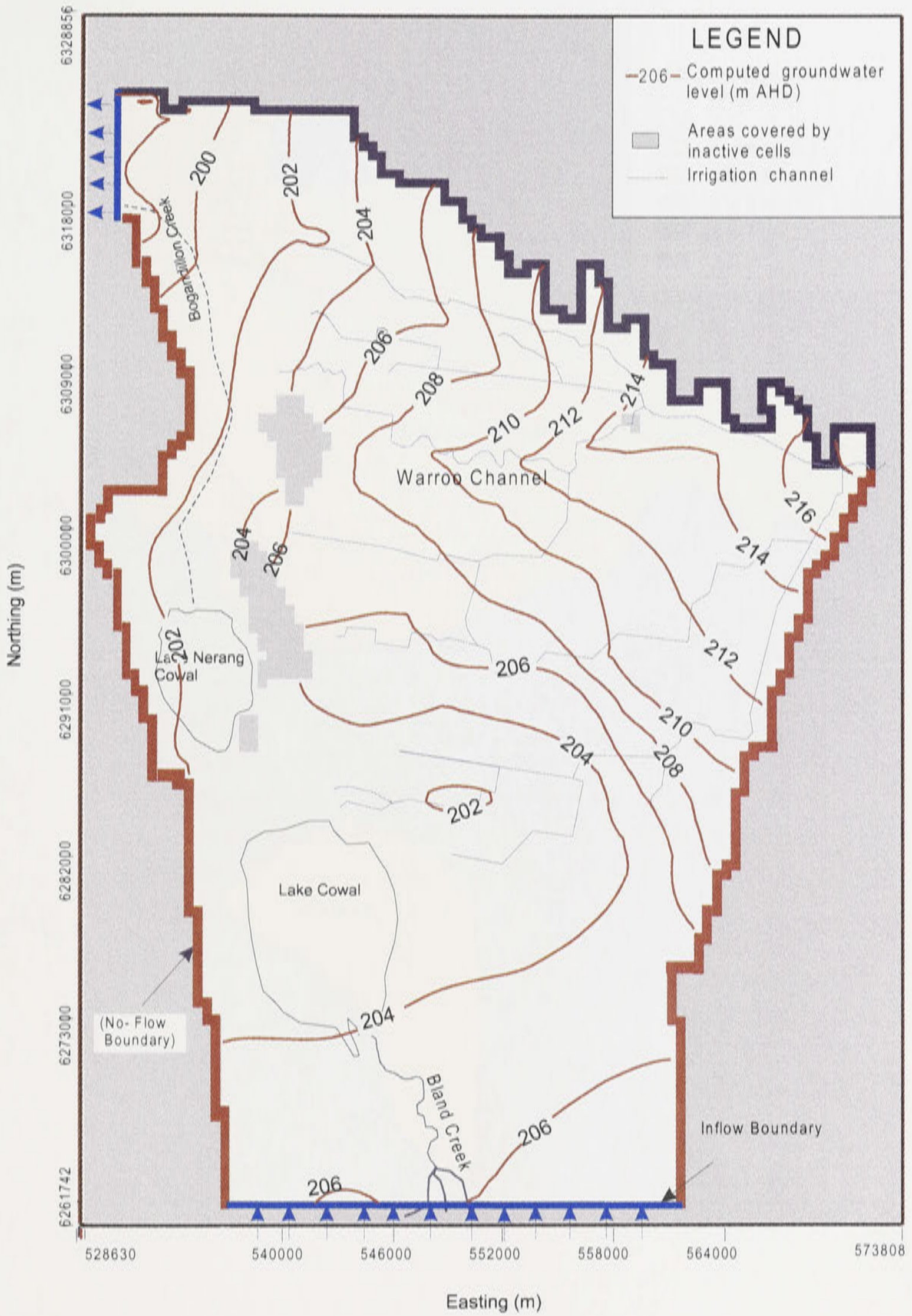


Figure 11.7: Piezometric head distribution under Option B in year 2020.

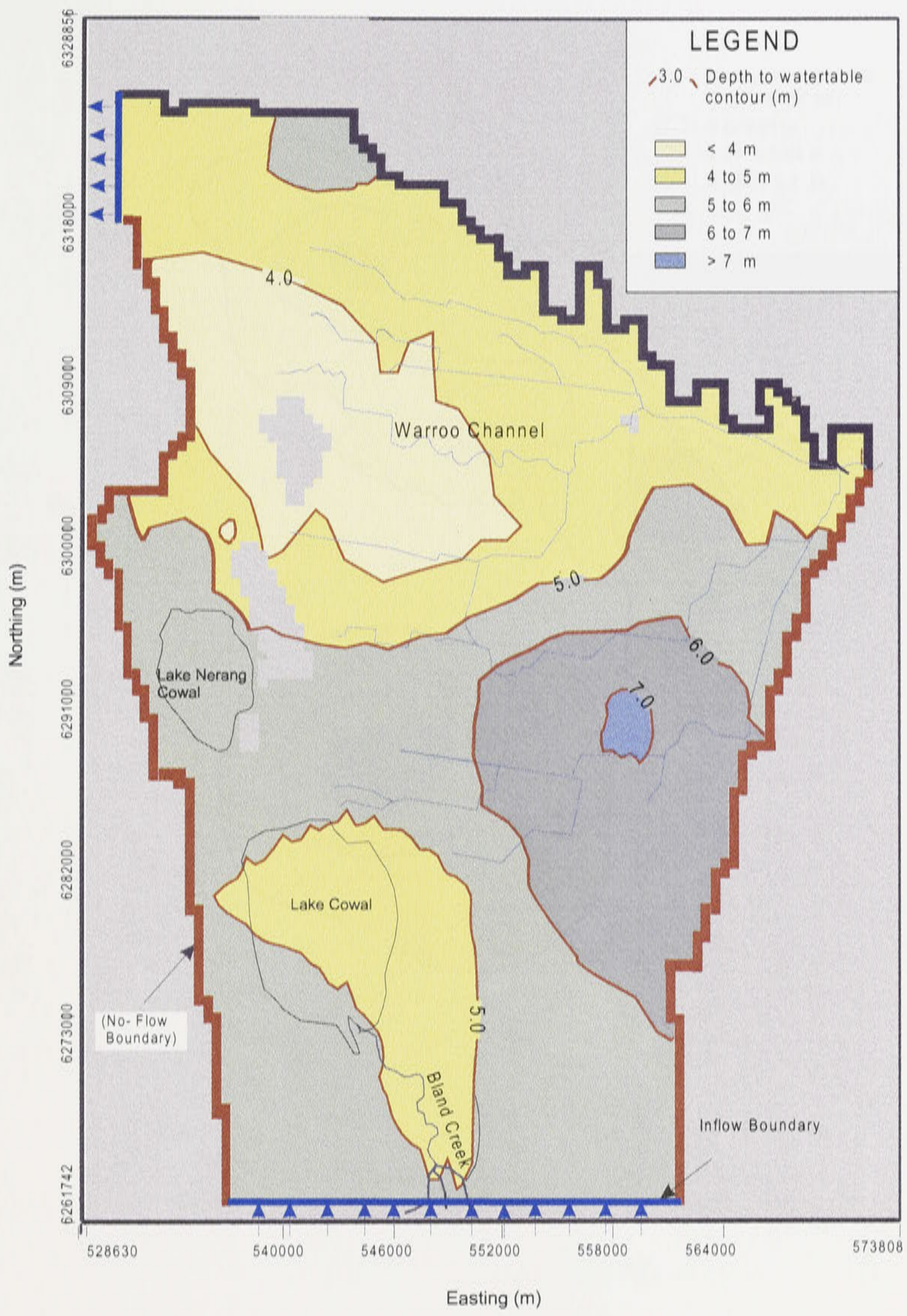


Figure 11.8: Watertable depths under Option B in year 2020.

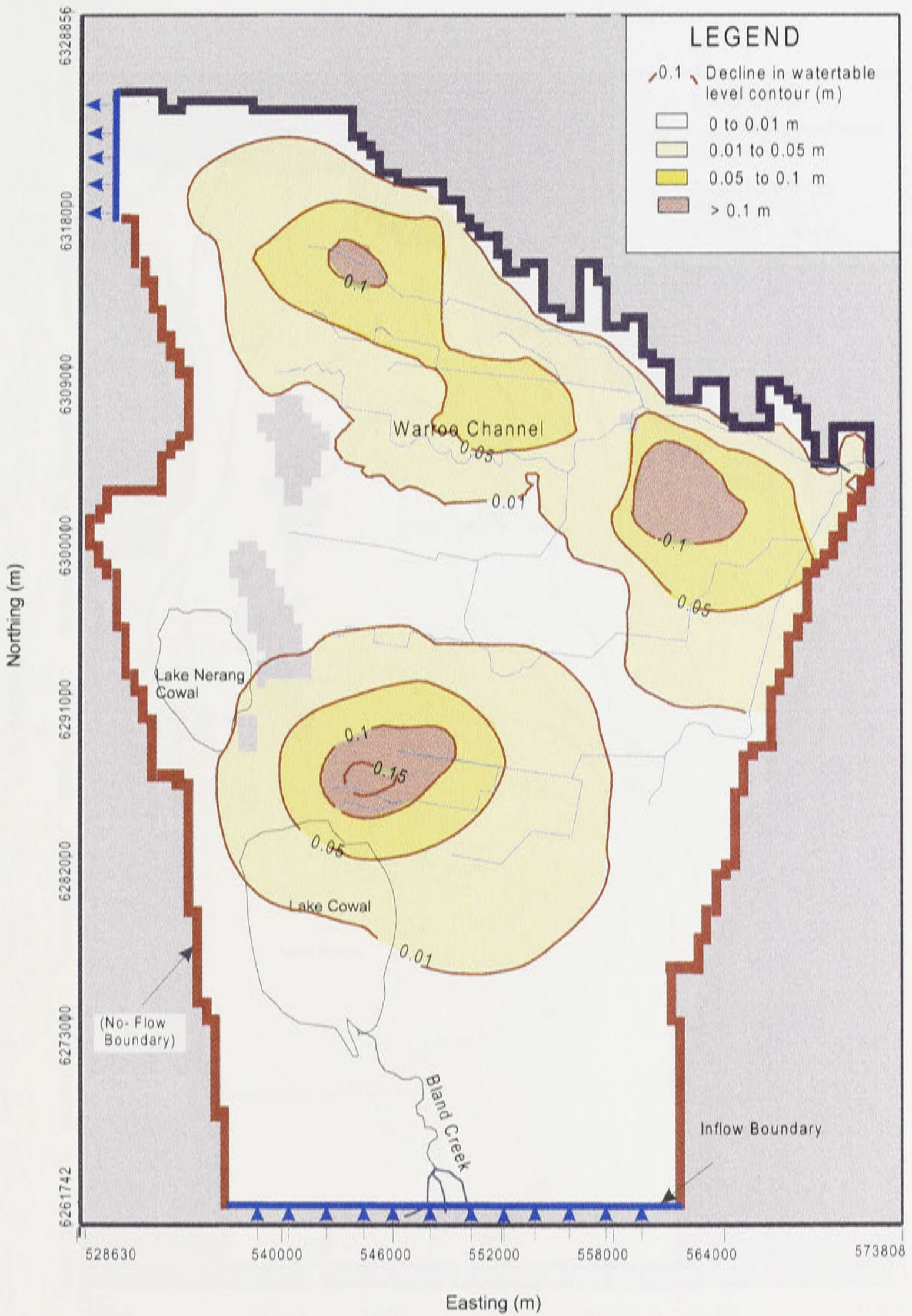


Figure 11.9: Decline in watertable depths for year 2020 due to Option B as compared with the 'average/no change' scenario.

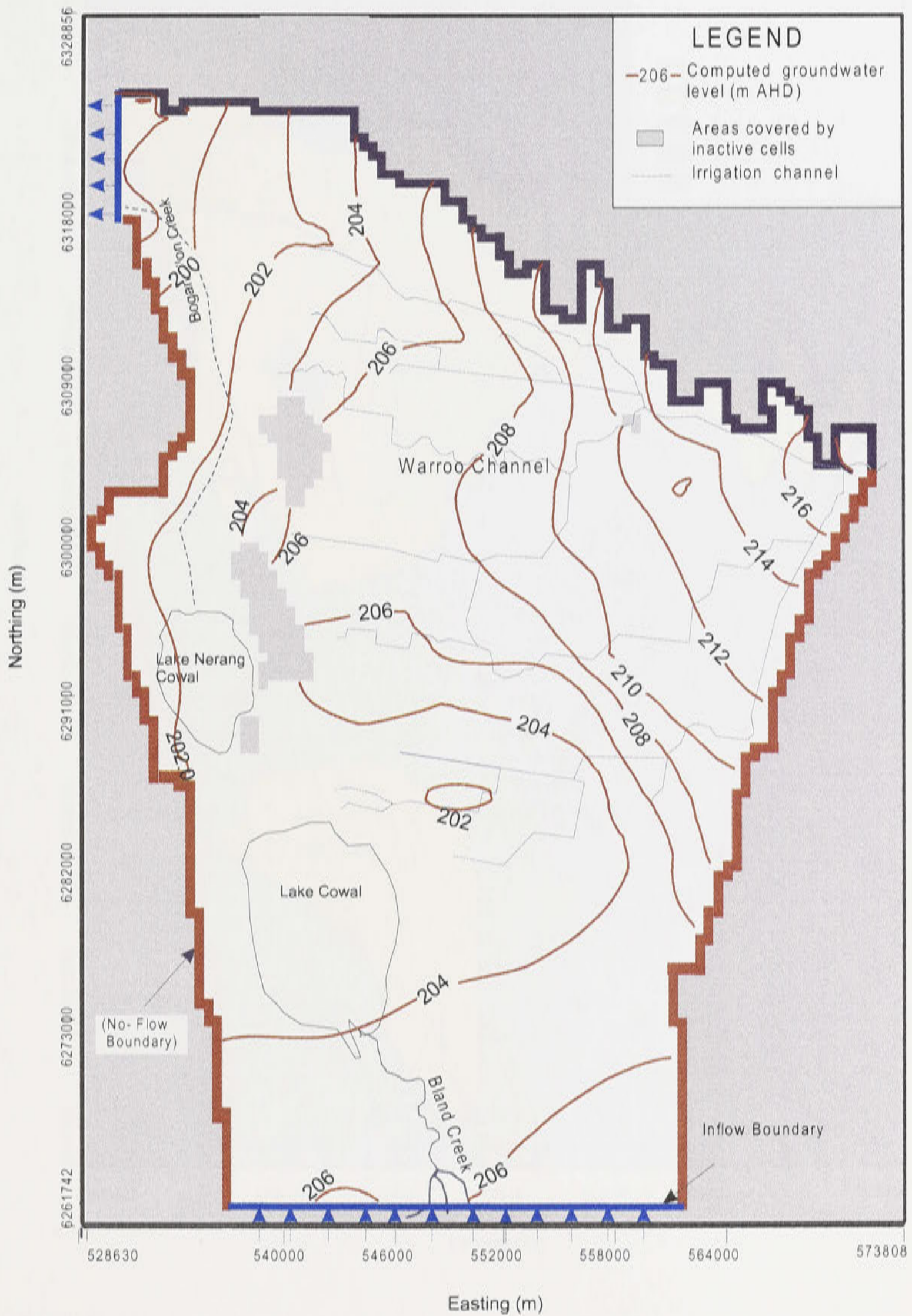


Figure 11.10: Piezometric head distribution under Option C in year 2020.

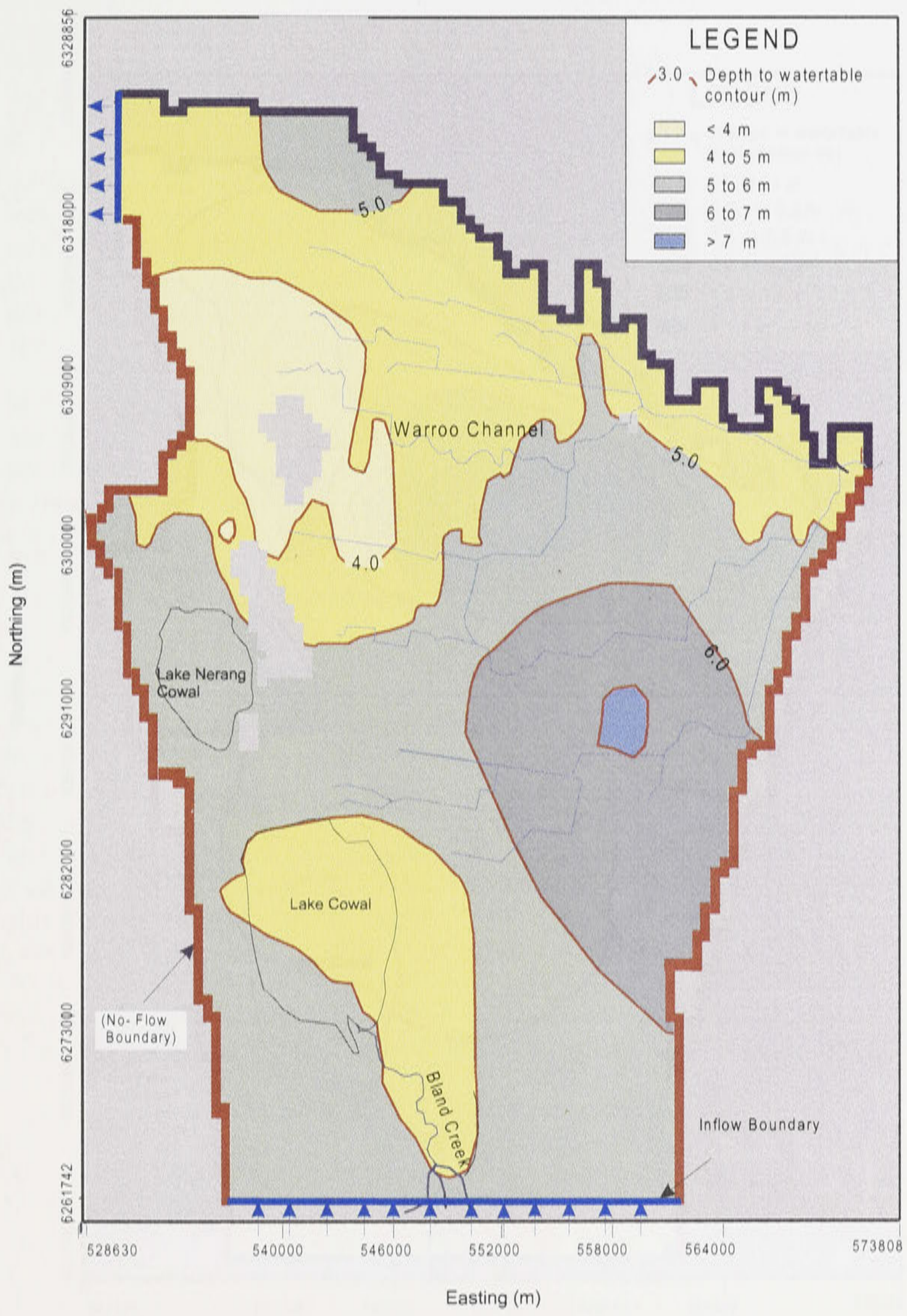


Figure 11.11: Watertable depths under Option C in year 2020.

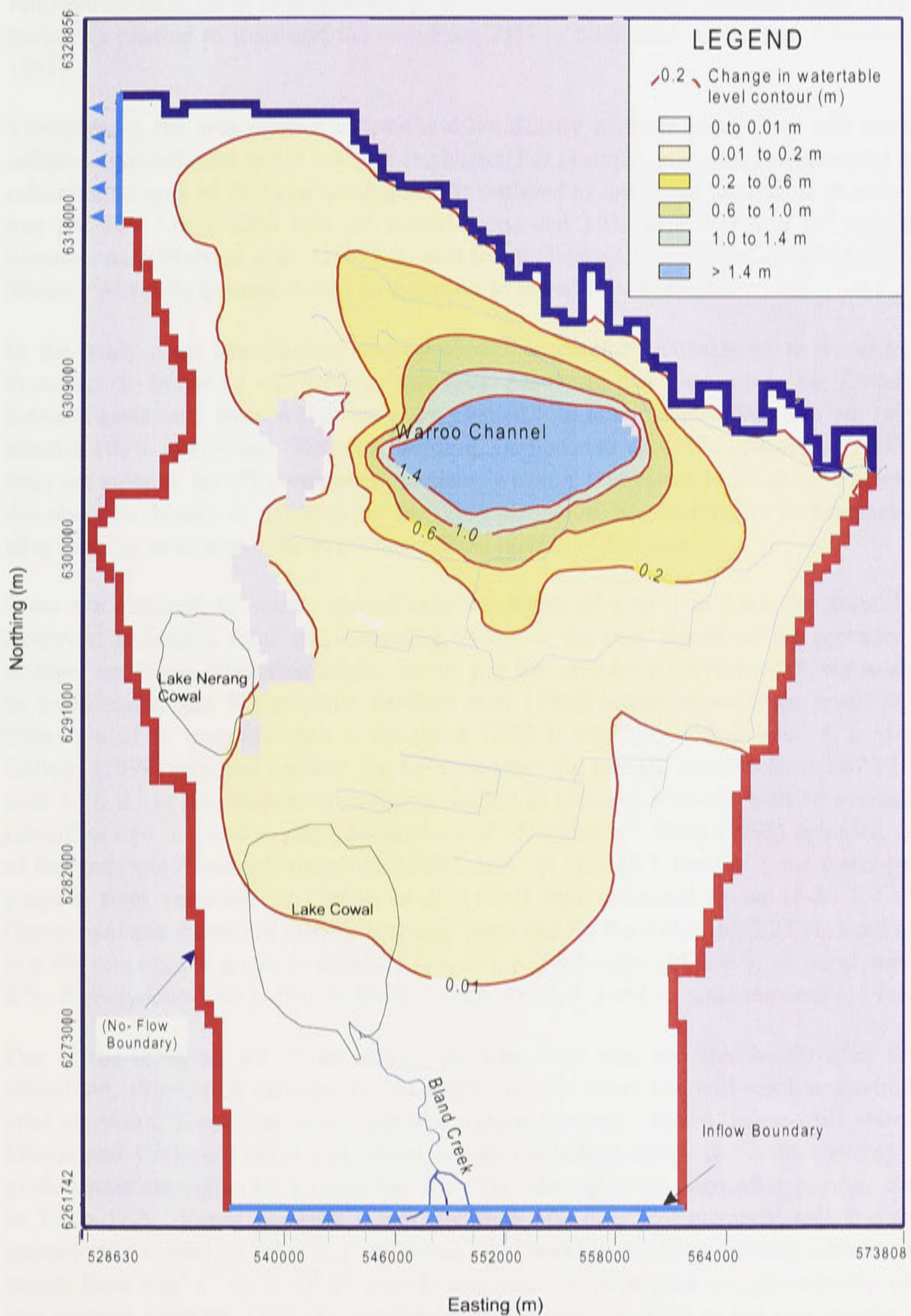


Figure 11.12: Decline in watertable depths in year 2020 due to Option C, as compared with the 'average/no change' scenario.

Planting density varies depending on the tree species. For example, in North Stirling Land Conservation District, Western Australia, where annual rainfall ranges from 490 to 510 mm, a suggested alley farming approach involved planting a double row of trees (covering about 8 m), followed by 20 to 30 m of cropping or pasture. Using this strategy, approximately 25% of each hectare is planted to trees and the remaining 75% to traditional agriculture (Gomboso *et al.*, 1997).

Variations in the area planted to trees and the density of those plantations will significantly influence groundwater levels within a catchment. For example, according to Schofield (1990), a reforestation area of 29 % of a catchment is required to lower the watertable at a rate of 200 mm per year in a 1200 mm yr⁻¹ rainfall zone and 18% in a 750 mm yr⁻¹ rainfall zone. Simulations by Salama *et al.* (1993) showed that replanting 25% of the Cuballing catchment in Western Australia to trees, would be sufficient to lower the watertable.

In the study area, tree-planting density should be carefully considered to avoid too much disruption to irrigation and farming activities. Assuming that trees are to be planted at 5 m between rows, and trees within rows are planted 5 m apart, about 400 trees are required to attain a 100% plantation. For alley farming, Gomboso *et al.* (1997) reported that 80 to 200 trees are suitable for alley cropping practices, which is equivalent to 20 to 50% plantation. In this study, a density of 80 trees per ha (20% plantation) are assumed to be reasonable for an alley farming in an area with an average annual rainfall of 434 mm.

Trees are assumed to extract groundwater to depths of 4 to 8 m from the ground surface. However, extraction rates vary according to age of the tree. Based on the previous studies, younger eucalypts, when tree height, canopy and leaf area are relatively small, water use would be considerably less. For example, Eastham *et al.* (1993) estimated water use levels in a young plantation of *E. camaldulensis* to be about 7,000 L tree⁻¹ yr⁻¹ (19 L tree⁻¹ d⁻¹). Morris and Collopy (1999) reported a water use for a six-year old tree (*E. camaldulensis*) of 10 L d⁻¹ to over 30 L d⁻¹ in the Shepparton irrigation region in northern Victoria with an average annual rainfall of 480 mm and average evaporation of 1350 mm yr⁻¹. Scott (1993) recorded water use of four-year old *E. camaldulensis* of 7,000 L tree⁻¹ yr⁻¹ (or 19 L tree⁻¹ d⁻¹) and water use by six year-old trees recorded by Clifton *et al.* (1993) was estimated to be 18-34 L tree⁻¹ d⁻¹. Greenwood and Beresford (1979), recorded water use for the following 2.25 year-old eucalypts in a 420 mm rainfall zone: *E. wandoo* (21 L d⁻¹), *E. caldocalyx* (21 L d⁻¹), *E. occidentalis* (20 L d⁻¹), *E. loxophleba* (20 L d⁻¹), *E. kondininensis* (17 L d⁻¹) and *E. camaldulensis* (17 L d⁻¹).

Due to the levelling out of the canopy diameter, leaf area and tree height after five years (Schofield, 1984), it is assumed in this study that tree water use will reach a maximum level after six years. Thereafter, water use will remain constant. Based on reported water use by Morris and Collopy (1999) and others, in the modelling study, the annual average rate of groundwater extraction by a single tree from one year up to six years after planting are shown in Table 11.3. Based on these values, for each 500 m x 500 m model cell, the computed groundwater extraction rates by trees (about 2000 trees) under alley farming scheme plantation ranges from 4 m³ d⁻¹ to 36 m³ d⁻¹ from first to year six. After year six, groundwater extraction rate remains constant. Here, *E. camaldulensis* has been assumed as the tree species for tree-planting strategy because this species could tolerate higher levels of groundwater salinity in the range of 4,000 – 5,000 µS cm⁻¹ (Thomson *et al.*, 1987).

Evapotranspiration in the plantation area is from trees and from the natural vegetation. In this modelling, groundwater extraction by trees in the Visual MODFLOW will be simulated as pumping wells. The estimation of ET (other than trees) in the forested area is calculated by

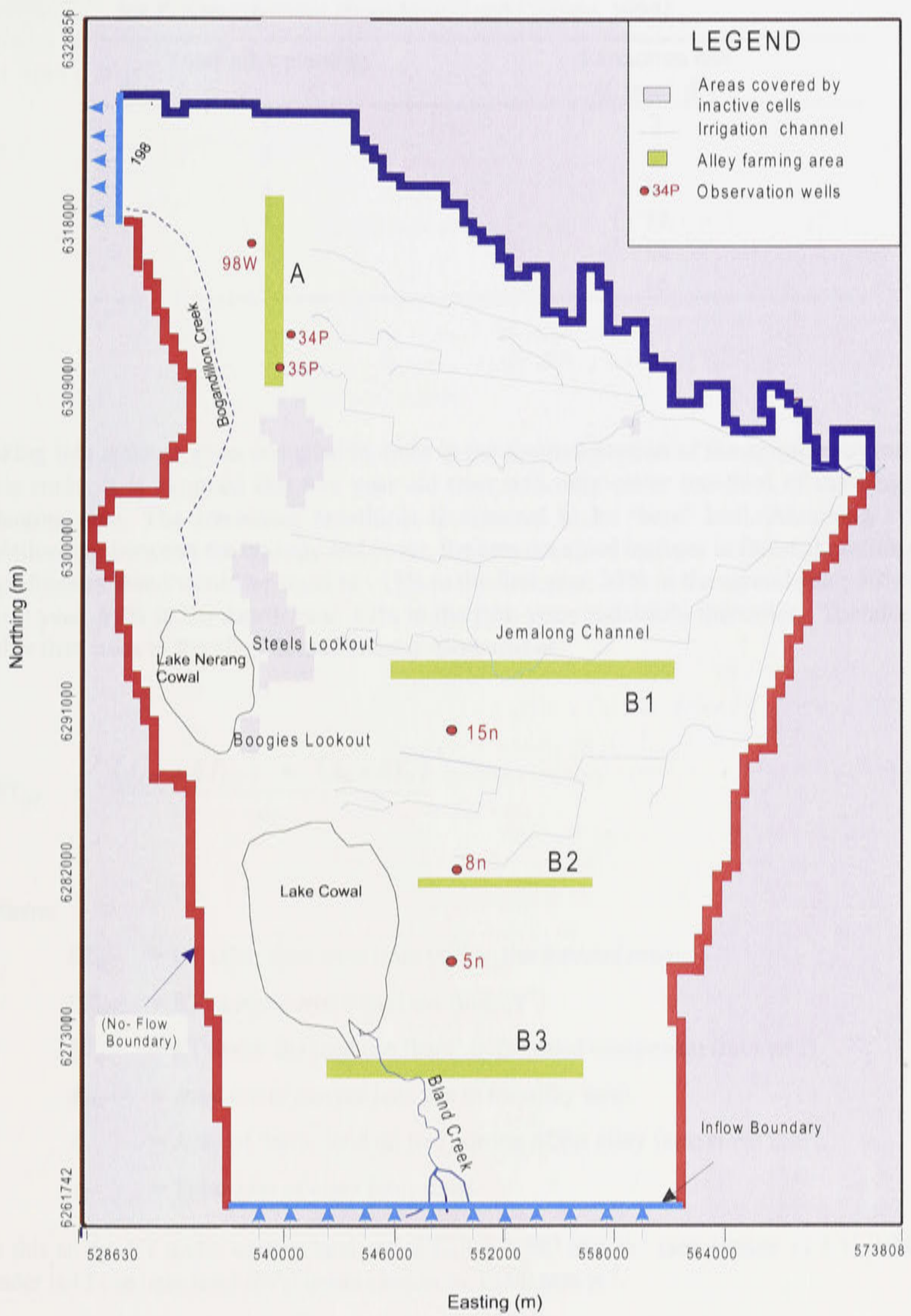


Figure 11.13: Location of plantation areas under tree-planting strategy.

Table 11.3: Assumed rate of groundwater extraction per tree from 1 to 6 years after planting for *E. camaldulensis* (from Morris and Collopy, 1999).

Years after planting	Extraction rate (L tree ⁻¹ d ⁻¹)
1	2
2	5
3	10
4	12
5	14
6	18

taking into account areas occupied by trees in the forested portion of the agroforestry stand. In this study, it is assumed that two year old trees will only cover one-third of the designated planting area. The remaining two-thirds is assumed to be 'bare' land. Assuming a linear relationship between the tree age and cover, the area occupied by trees in forested portion of the agroforestry stand would be equal to : 17% in the first year; 33% in the second year; 50% in the third year; 67% in the fourth year; 83% in the fifth year; and 100% thereafter. Therefore, ET other than trees in the alley farmed areas is computed as:

$$ET_{OT} = \frac{(A_{LU} \times ET_{LU}) + (A_b \times ET_b)}{A_T} \quad 11.1$$

Where:

- ET_{OT} = ET other than trees (mm yr⁻¹) in the forested area
- ET_{LU} = ET under current land use (mm yr⁻¹)
- ET_b = ET under the land use 'bare' in the treed component (mm yr⁻¹)
- A_{LU} = Area under current land use in the alley farm.
- A_b = Area of 'bare' land on tree portion of the alley farm stand (ha)
- A_T = Total area of alley farm stand.

In this study, ET under current land use (ET_{LU}) is 1,387 mm yr⁻¹ (see section 11.3.1), while ET under land use bare land (ET_b) is assumed to be 1,000 mm yr⁻¹.

Two options were simulated under the tree-planting strategy. The first option involves alley farming on the western part of the irrigation district above Dog Kennel Hill (designated as area A in Figure 11.13). As groundwater flow is moving towards the salt-affected Bogandillon Creek area, tree plantation above Dog Kennel Hill is aimed to partially intercept this flow and thus lowering the watertable in the Bogandillon Creek area.

The second option involves alley farming in southern part of the study area. The aim of this option is to simulate the impact of tree planting on the continually increasing watertables in this area which in long term will cause severe land salinisation as well as increasing the salinity of

Lake Cowal's water. Under this option, three designated areas are assumed to be under alley farming. These are labelled as B1, B2 and B3 areas (Figure 11.3). Area B1 is located below and parallel to the Jemalong Channel, while Areas B2 and B3 are situated on the eastern side and southern part of Lake Cowal, respectively.

11.5.1. Results and discussion

11.5.1.1. Tree plantation above Dog Kennel Hill (Area A)

A series of model runs has been undertaken to identify the optimal extent of the area above the Dog Kennel Hill for tree planting under alley farming strategy. As shown in Figure 11.13, the assumed extent of the area for alley farming under 20% plantation is about 10.5 km x 1 km (1,050 ha), comprising of about 42 model cells.

The piezometric head distribution in year 2020 under this option is shown in Figure 11.14. Comparing this figure with Figure 11.3 for 'average/no change' scenario, an evident decline in head of about 2 m is observed in the tree plantation area. Figure 11.15 shows the watertable depth map, while Figure 11.16 presents the magnitude of decline in watertable when this option is adopted. There is a significant reduction in watertable depth of the order of 0.5 to 2.0 m in year 2020 over the plantation area and in the Bogandillon Creek.

Three observation wells (wells 34P, 35P, 98W) shown in Figure 11.13 were used to evaluate the characteristics of the decline in watertable within and near the plantation area. As presented in Figure 11.17, a sharper decline of watertable depth can be observed from year 1998 to 2005 for the three observation wells, followed by gradual stability towards the year 2020.

Table 11.4 shows the mean annual groundwater balance components of the area from 1998 to 2020 due to 'average/no change' scenario and alley farming strategy. The volume of inflow from the constant head boundary along the Lachlan River has been increased by only 2%, and volume of outflow from the same boundary has been reduced by 4% under alley farming strategy. With tree plantation, total ET is about 6% more than ET under the 'average/no change' scenario. The average annual groundwater extraction by trees for the entire period of simulation is about 494,100 m³.

The simulations of alley farming options above the Dog Kennel Hill (Plantation A) indicates the potential of this strategy in halting the land salinisation process around these areas. Since rise in local and/or regional watertable is a key component of dryland salinity, planting of trees is an effective means of lowering watertables. Obviously, extending the area of alley farming to the west of the simulated area will increase the effectiveness of this option. Also, planting trees along the gaps between Dog Kennel Hill and Steels Lookout, and on the southern part of Lake Nerang Cowal would further increase the effectiveness of this option.

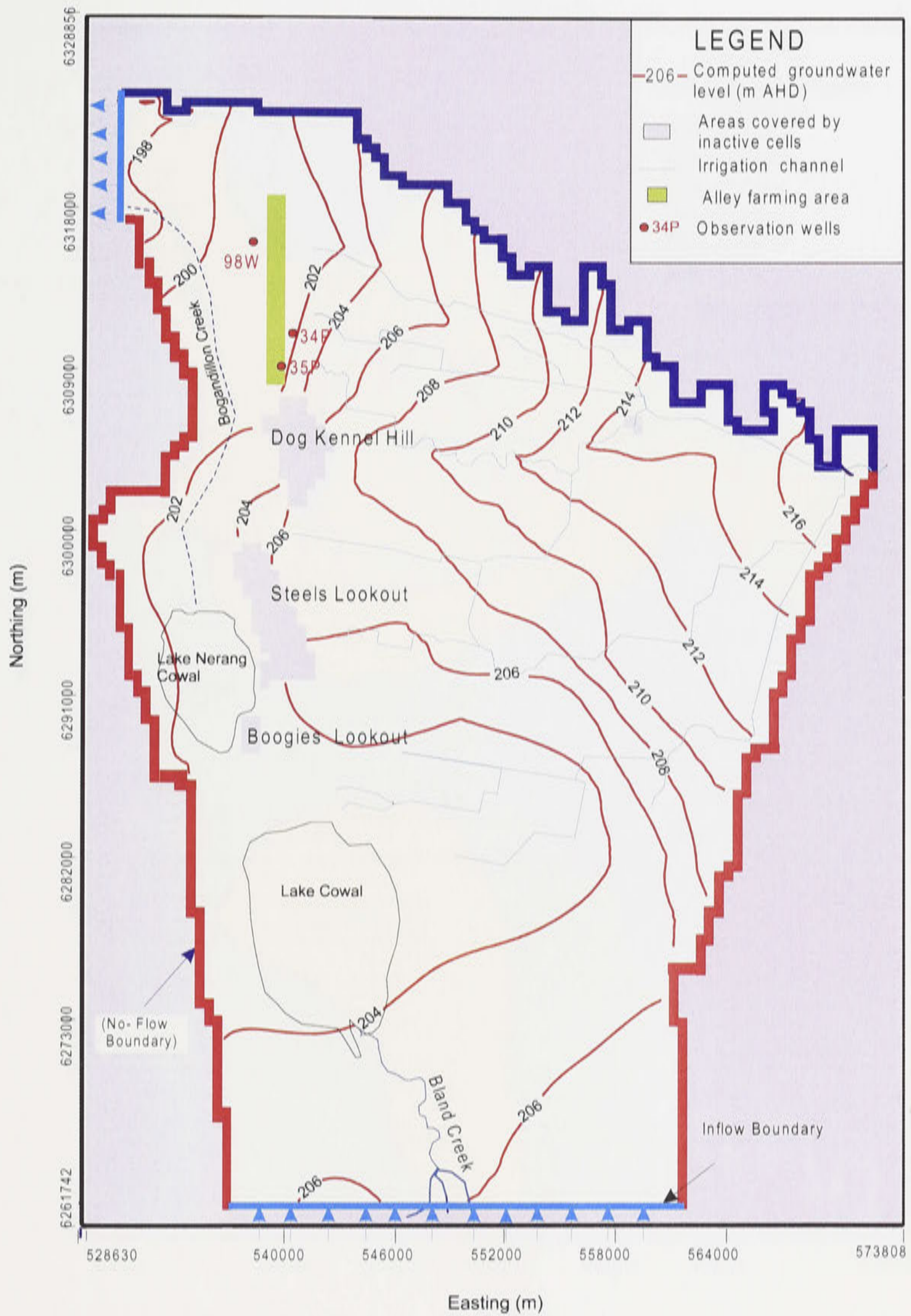


Figure 11.14: Piezometric head distribution due to tree plantation above Dog Kennel Hill in year 2020.

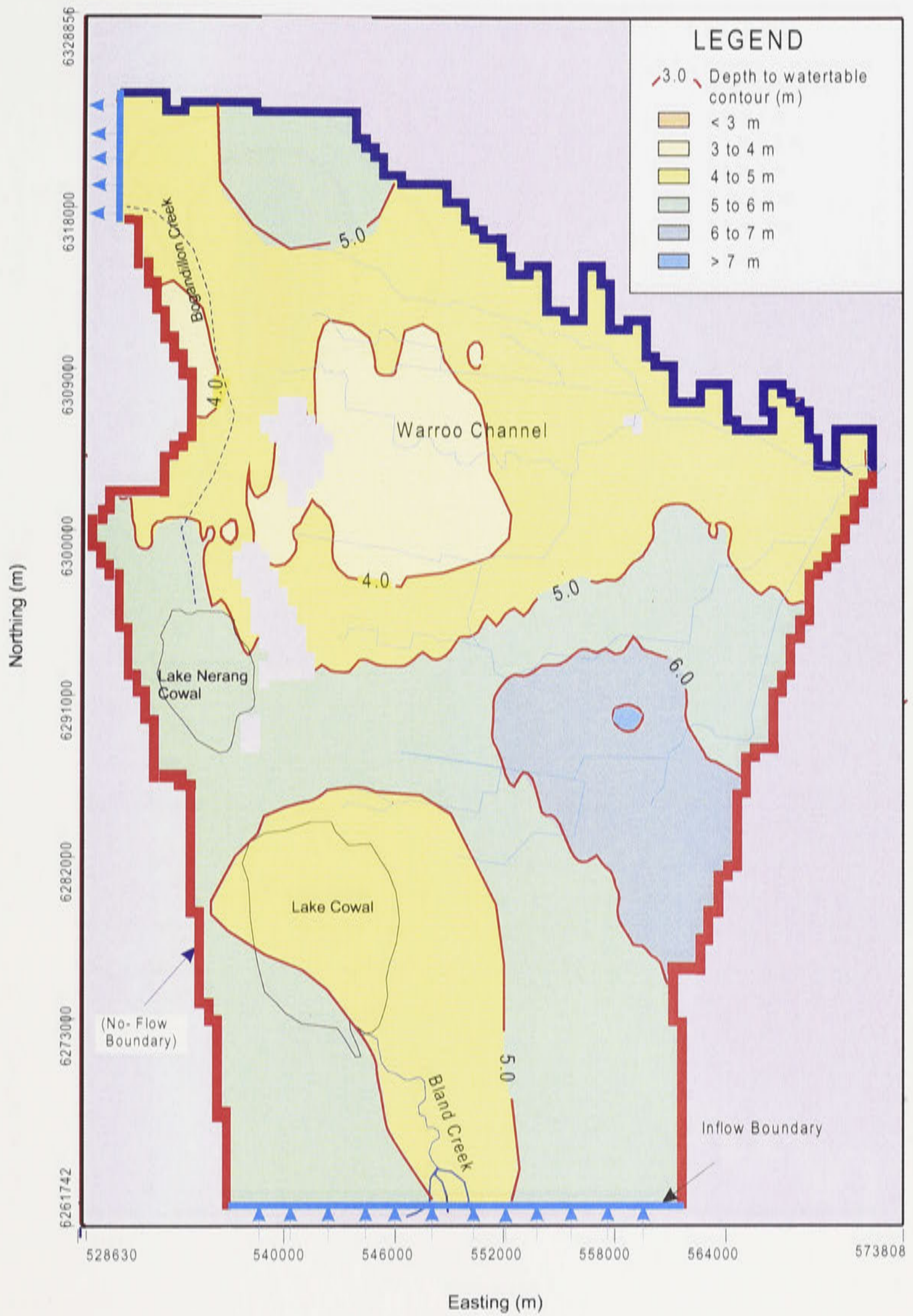


Figure 11.15: Watertable depths in year 2020 under tree-planting strategy (Area A).

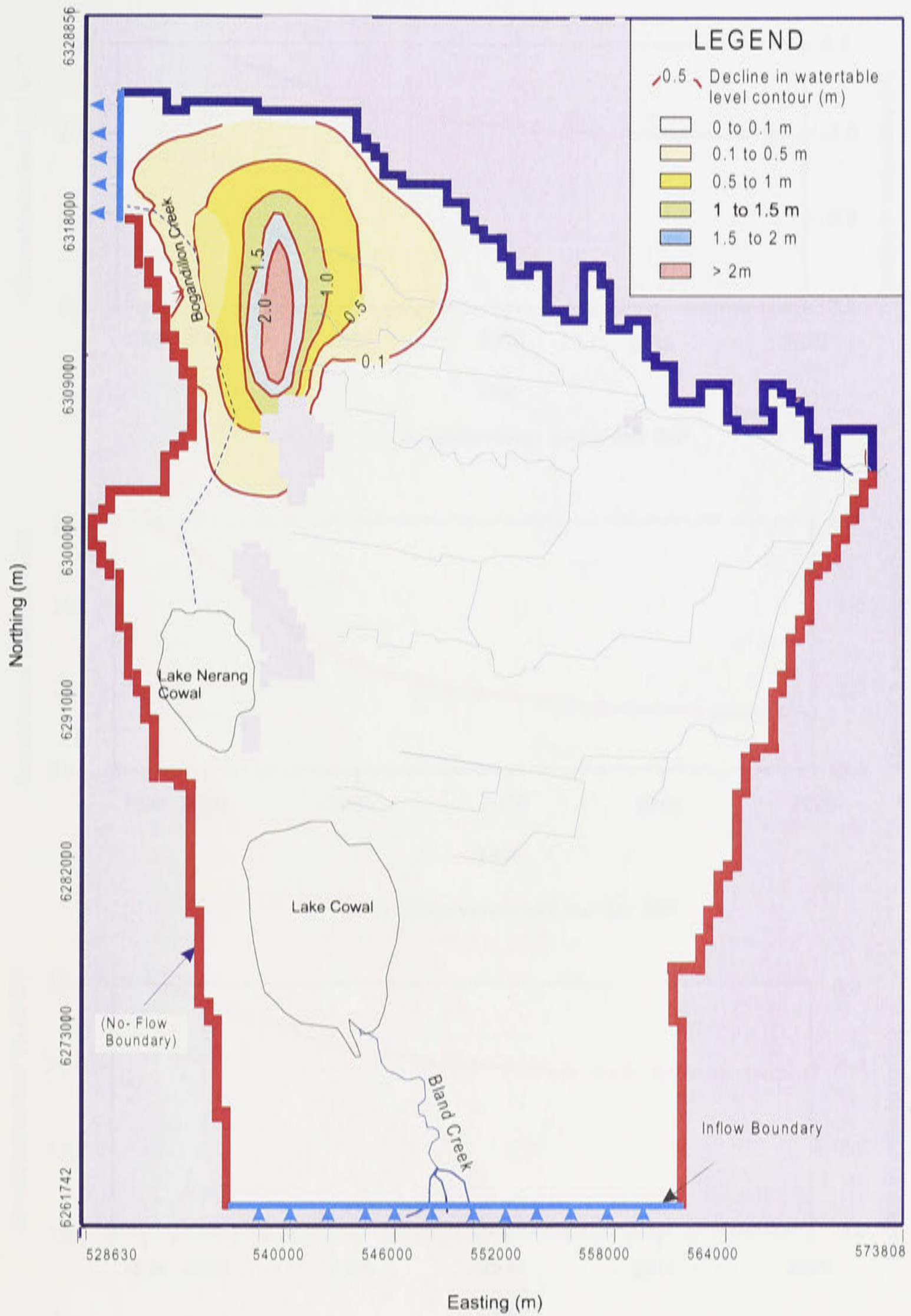
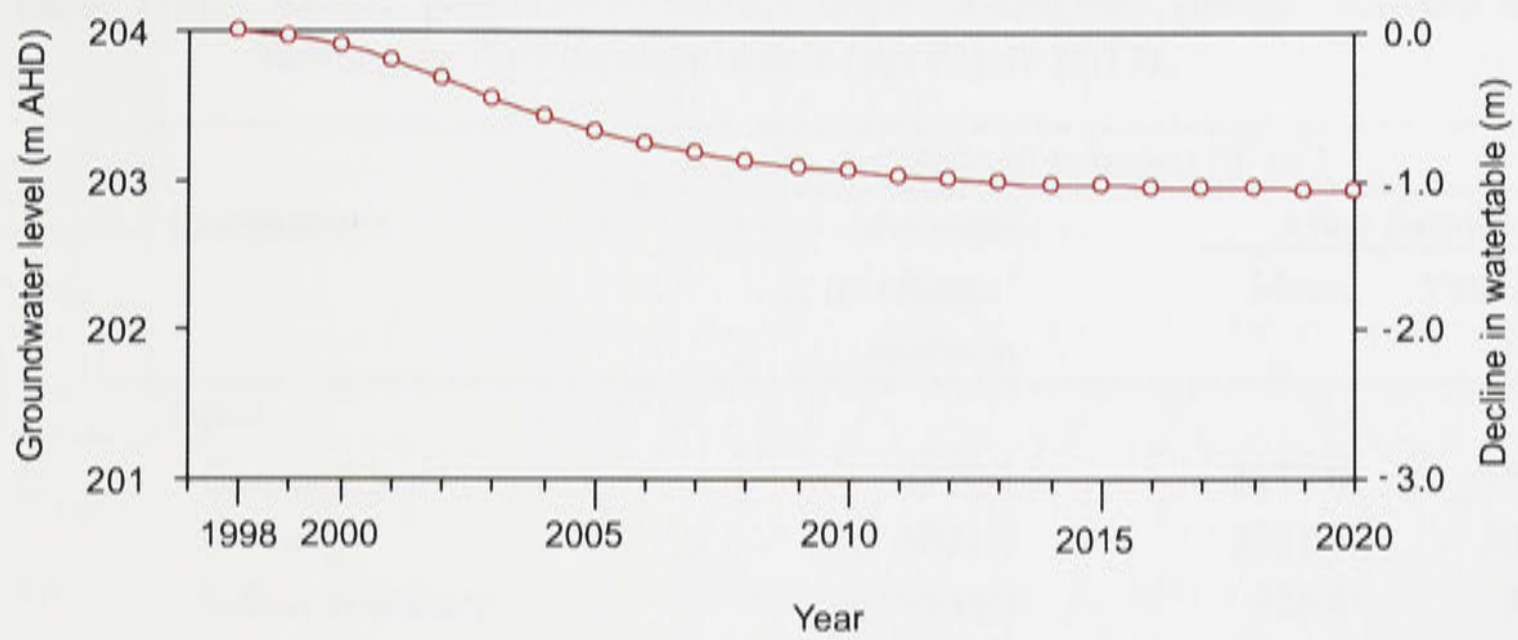
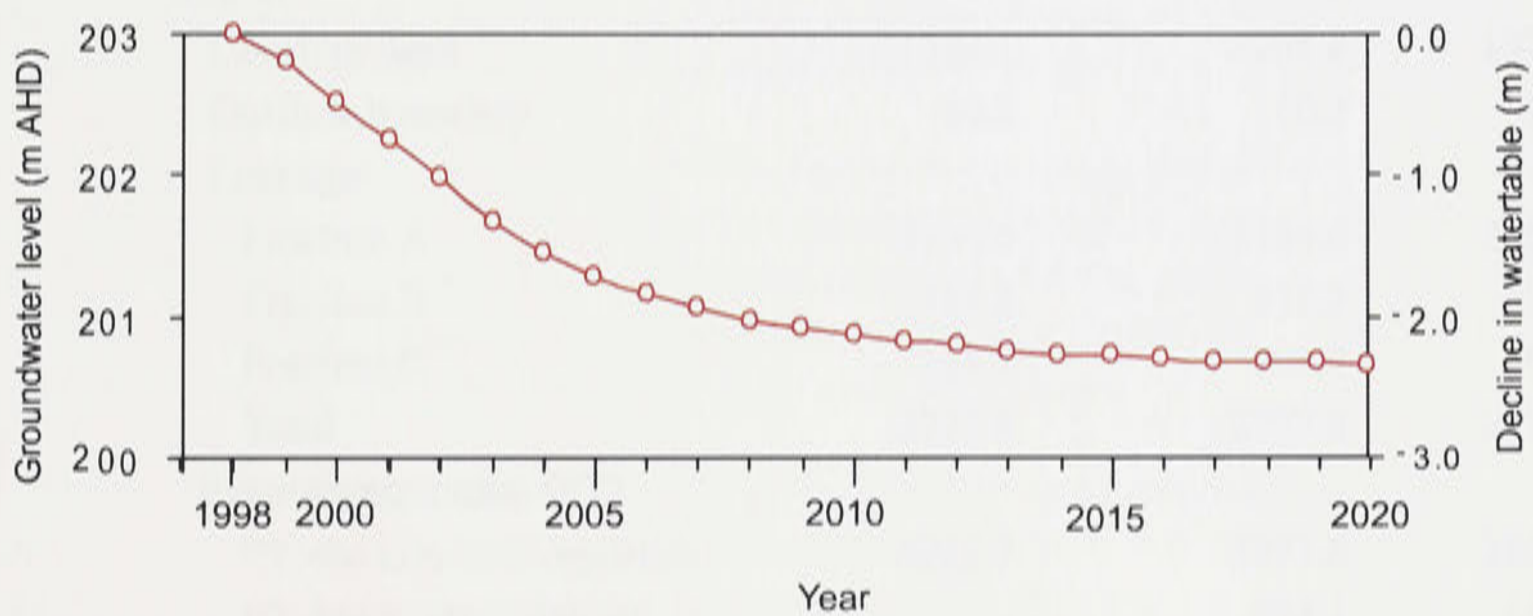


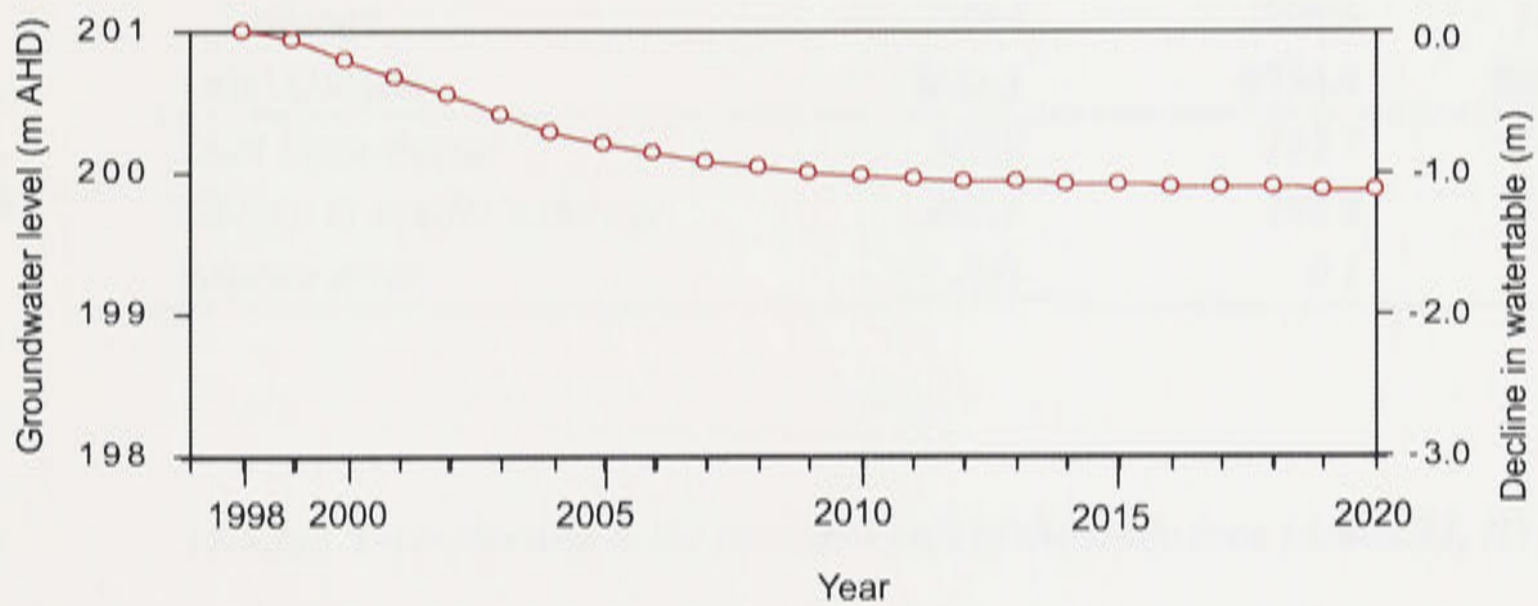
Figure 11.16: Decline in watertable depths in year 2020 due to tree-planting strategy (Area A), as compared with the 'average/no change' scenario.



A. Observation well number 34P



B. Observation well number 35P



D. Observation well number 98W

Figure 11.17: Decline in watertable depth at three observation wells (wells 34P, 35P and 98W) in the alley farmed areas A (see Figure 11.13).

Table 11.4: Annual groundwater balance under 'average/no change' scenario and alley farming for the Plantation area A (see Figure 11.13).

Components	Annual volume (10^3 m^3)		
	'Average/ no change' scenario	Mean	Year 2020
<i>Input</i>			
Constant head	3516.3	3577.0	3573.3
Recharge	5021.7	5021.7	5021.7
Inflow boundary	334.0	326.4	326.4
Total input	8872.0	8925.1	8831.4
<i>Output</i>			
Constant head	1324.1	1268.4	1275.3
Outflow boundary	10.2	10.2	10.2
Leakage:			
Fracture A	2154.6	2154.6	2154.6
Fracture B	438.2	438.2	438.2
Fracture C	184.7	184.7	184.7
Total	2777.5	2777.5	2777.5
Evapotranspiration (ET)			
ET due to natural vegetation	4222.7	3977.6	3890.8
ET due to groundwater extraction by trees	-	494.1	557.4
Total	4222.7	4471.7	4448.2
Drainage	229.6	206.6	180.0
Total Output	8564.1	8734.4	8691.2
<i>Total input-output</i>	<i>307.9</i>	<i>190.7</i>	<i>140.2</i>
<i>Change in aquifer's storage</i>	<i>307.1</i>	<i>190.6</i>	<i>140.3</i>
<i>Balance error</i>	<i>0.8</i>	<i>0.1</i>	<i>0.1</i>

11.5.1.2. Tree-planting at the southern part of the study area (Areas B1, B2 and B3)

As mentioned earlier (section 11.3.2), groundwater level in the southern of the study area is continuously rising even during non-flood periods. This behaviour could become critical in the future when the watertable becomes closer to the land surface causing land salinisation and increase salinity in the Lake Cowal. Therefore, this trend should be stopped and preferably reversed. In this regard, the tree plantation option provides a good management option.

Approximation of the optimal size of plantations at each designated plantation areas under this option was also carried out through series of model runs. Initially, a single plantation area (B1) has been strategically selected parallel to the Jemalong Channel to intercept the groundwater

flow from the irrigation district towards the south. However, a single plantation area was found to be insufficient in lowering down the watertable. As a result, two additional plantation areas (B2 and B3) were added to effectively lower the watertable. As presented in Figure 11.13, the approximated plantation size at area B1 is 15.5 km x 1 km (1,550 ha), while B2 and B3 are 9.5 km x 0.5 km (475 ha) and 14 km x 1 km (1,400 ha), respectively.

The piezometric head distribution in the study area in year 2020 presented in Figure 11.18 which shows a remarkable decline of heads in the vicinities of the plantation areas. Comparing the heads in these areas with that of Figure 11.3 under the '*average/no change*' scenario, a decline of over 4 m can be observed.

The distribution of the computed watertable depths in year 2020 is shown in Figure 11.19, while Figure 11.20 shows the decline in watertable depths during this period due to tree-planting strategy in this part of the study area as compared with the '*average*' option. Based on these figures, a significant decline in watertable depths of over 4.0 m in year 2020 has been calculated between the tree-planting strategy and the '*average/no change*' scenario. A larger portion of the simulated area has a watertable decline of about 1.0 m.

The decline in groundwater level under this option for the three selected observations wells 5n, 8n and 15n (Figure 11.13) is presented in Figure 11.21. Based on Figure 11.21, it can be seen that for the first few years after plantation, groundwater level continues to rise. When trees become relatively mature, groundwater levels decline. A decline of 1.2 m to 2 m can be observed at the end of year 2020 for the three observation wells.

Table 11.5 shows the annual groundwater balance components with respect to alley farming on the southern part of the study area. From this table, it can be seen that the average annual outflow exceeds inflow by about 824,000 m³. Groundwater extraction by trees constitutes about 16% of the total groundwater outflow from the aquifer system. As a result, the volume of outflow due to ET is 27% higher than in the '*average/no change*' scenario.

11.6. Summary

In summary, three scenarios have been simulated by the model to evaluate groundwater behaviour in the study area until year 2020, which include: (a) '*average/no change*' scenario; (b) reducing recharge through improved irrigation and drainage efficiency; and (c) reducing recharge through partial area tree-planting.

The '*average/no change*' scenario assumes that general land use practices remain unaltered over the forecasting period. Values of the input parameters are historical average data for the area. The results of the simulation under this scenario indicate that groundwater level in the southern part of the study is continuously rising over the period of simulation. The rise is due to the groundwater flow moving from the irrigation district towards this area.

The second scenario (reduced recharge through improved irrigation and drainage efficiency) is divided into three options: (a) sealing of Warroo Channel; (b) reducing recharge rates due to ponded rainwater and river flooding by 50 percent; and (c) combinations of options A and B. Compared with the '*average/no change*' scenario, the results of the simulation indicated that by eliminating seepage along Warroo channel, watertables would decline by over 1.0 m along the Warroo Channel area at the end of year 2020. Simulation of option B, on the other hand, has only resulted in lower watertable decline of about 0.15 m at the end of year 2020. Finally, option C (combination of options A and B), provided the largest decline in watertables depths

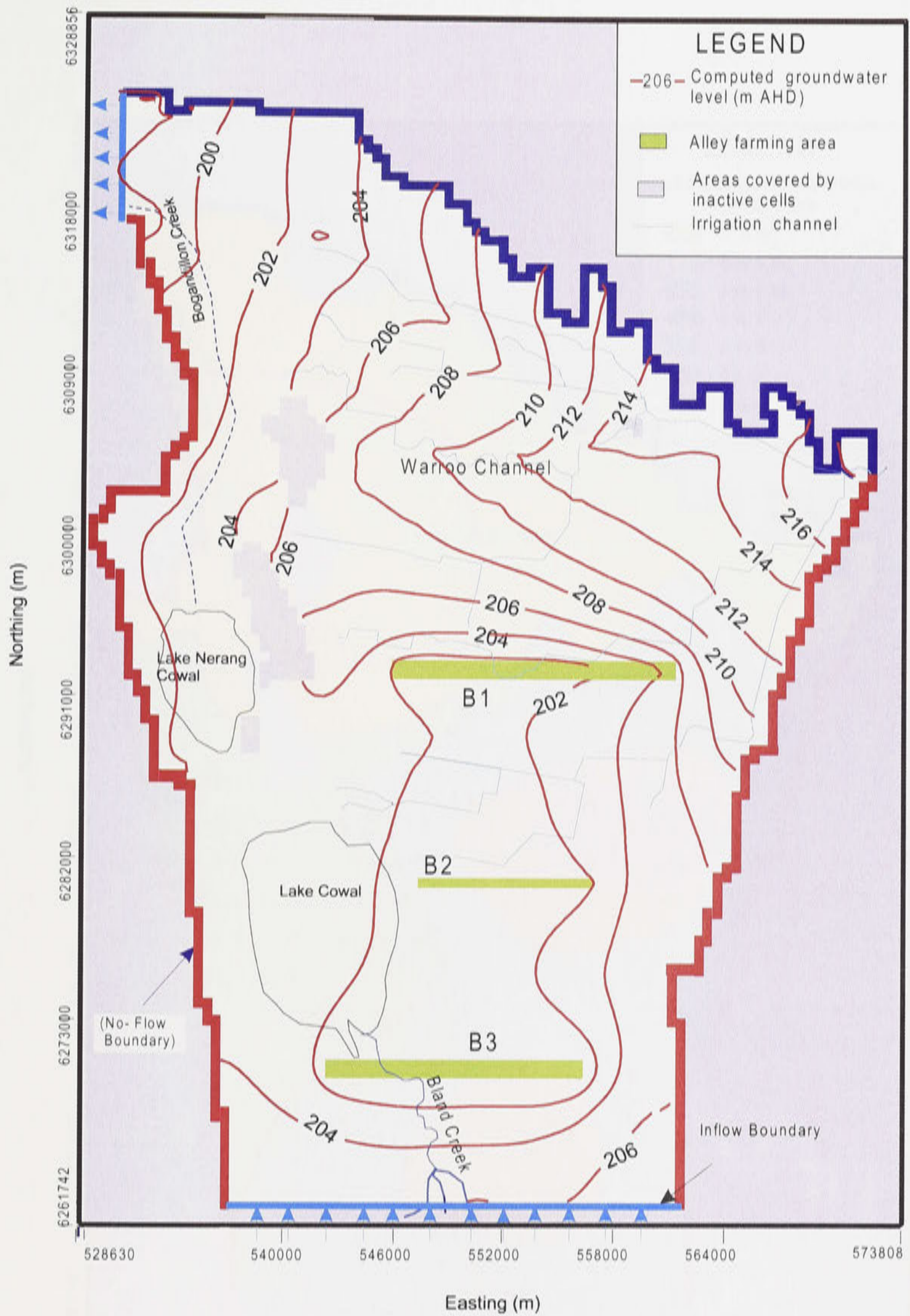


Figure 11.18: Piezometric head distribution in year 2020 under the tree-planting strategy in the southern part of the study area.

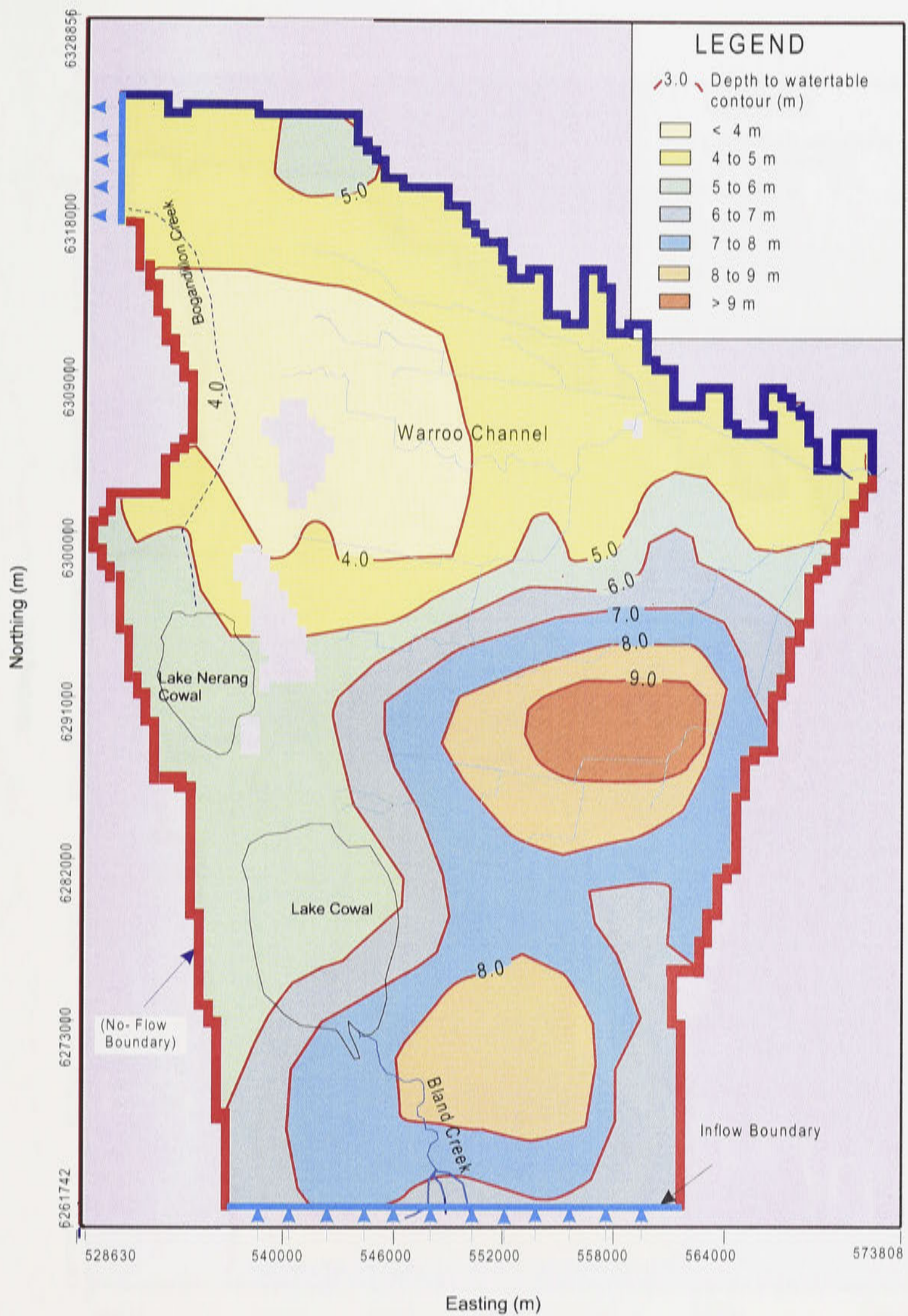


Figure 11.19: Watertable depths under the tree-planting strategy in the southern part of the study area in year 2020.

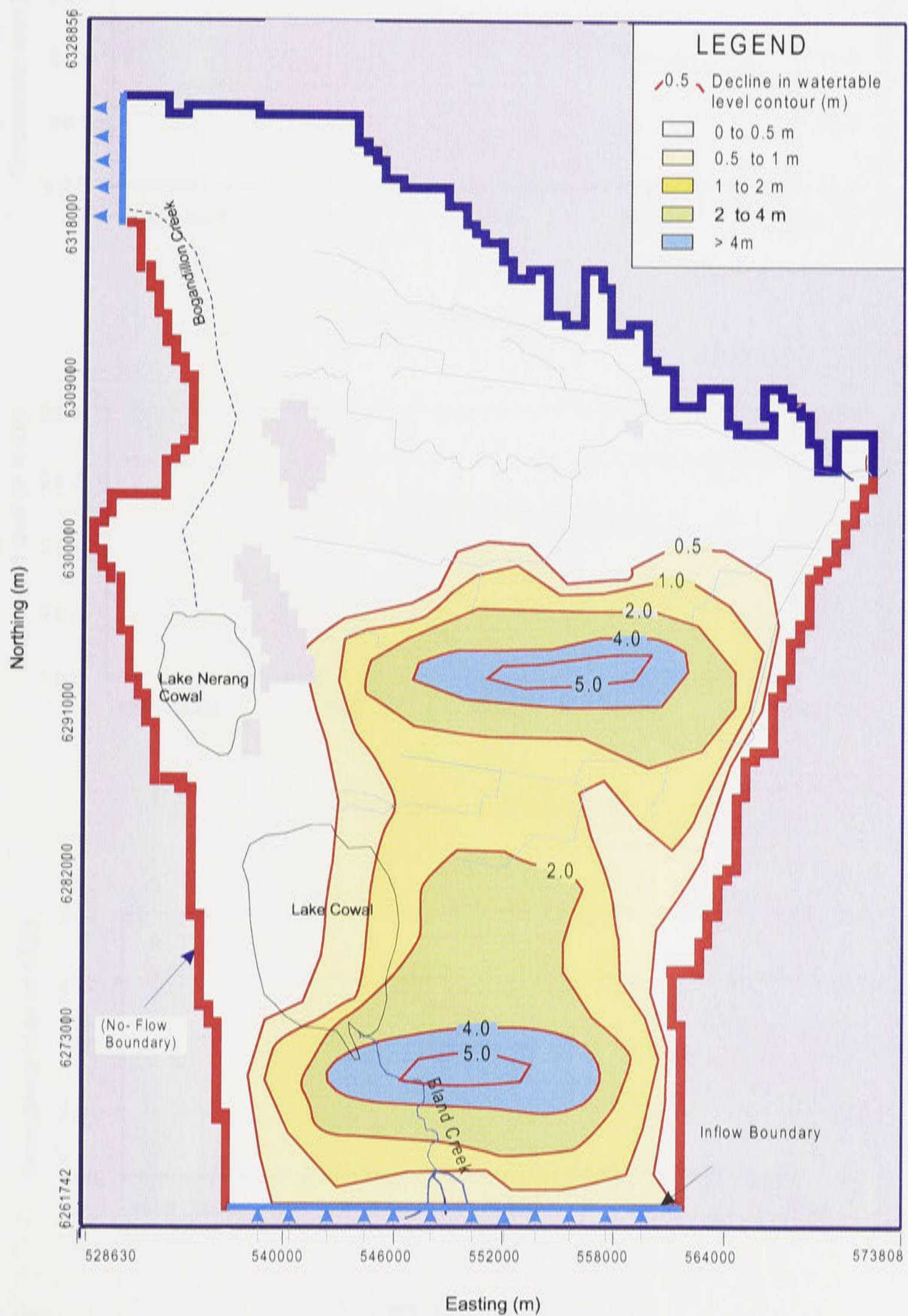
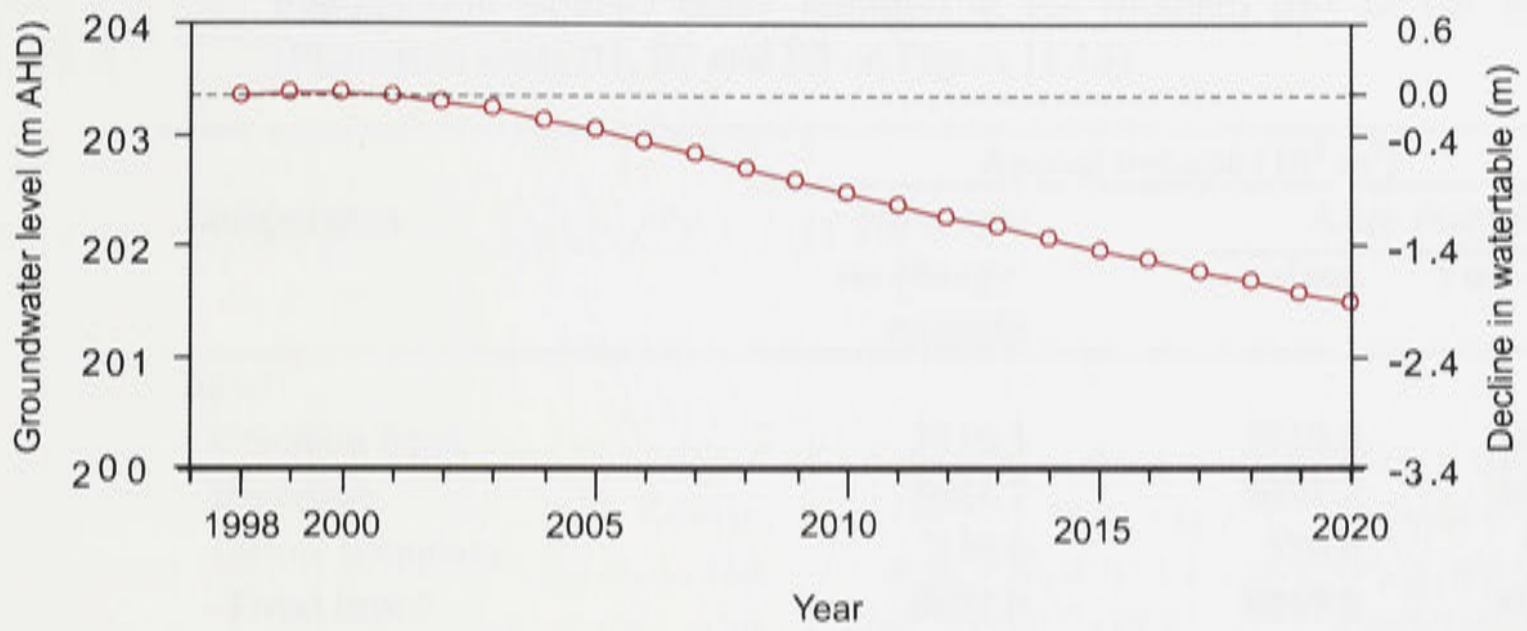
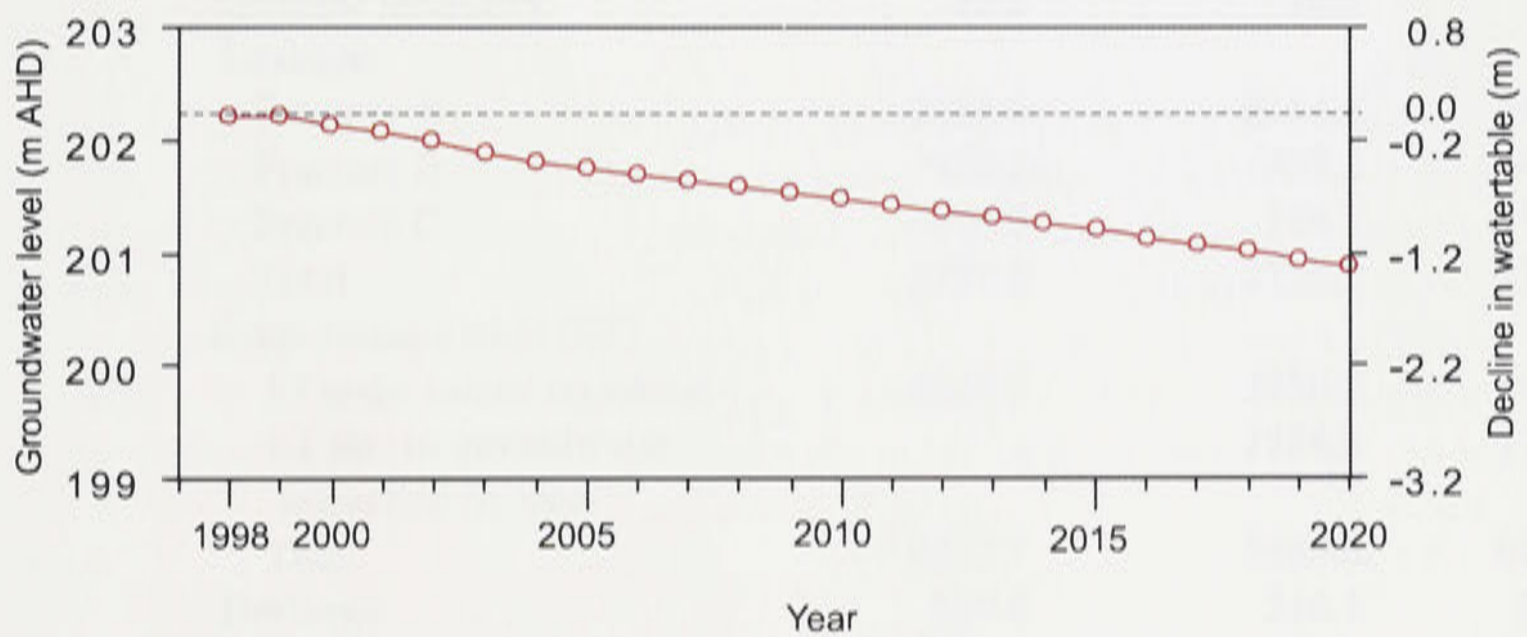


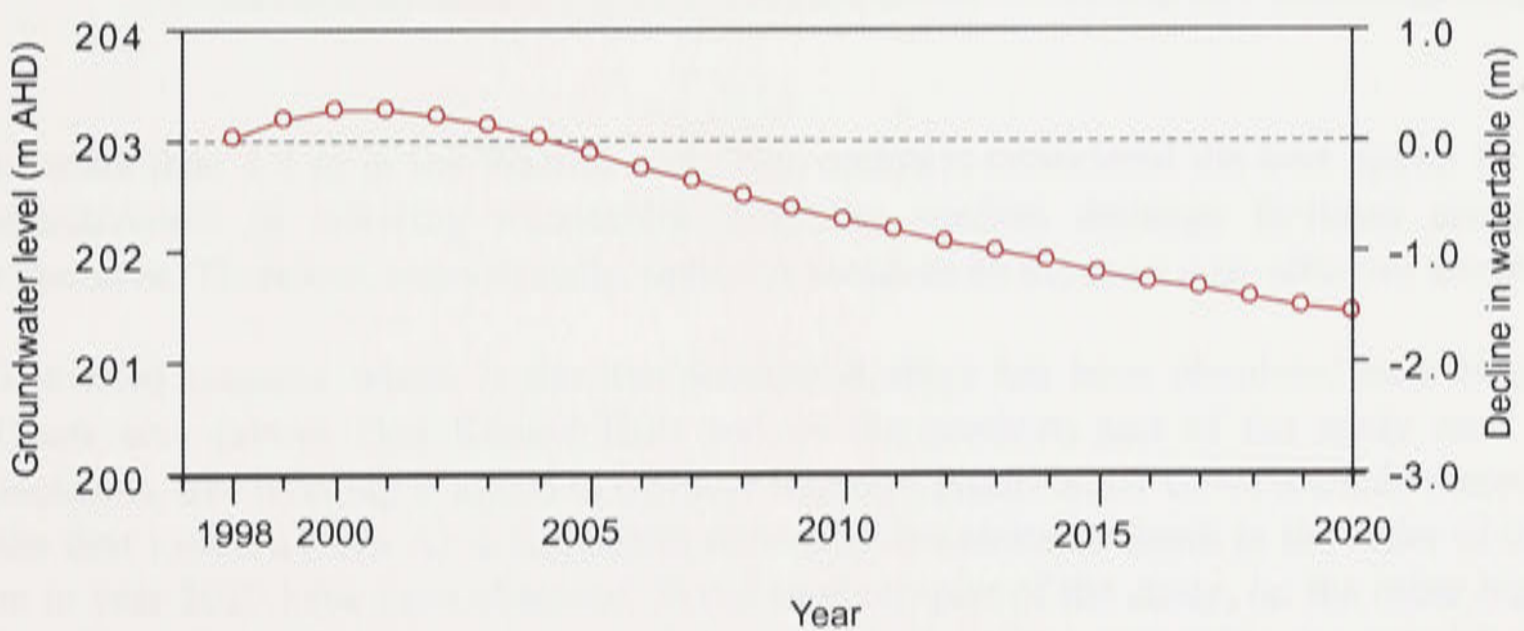
Figure 11.20: Decline in watertable depths in year 2020 due to tree-planting strategy in the southern part of the study area as compared with the 'average/no change' scenario.



A. Observation well number 5n



B. Observation well number 8n



C. Observation well number 15n

Figure 11.21: Decline in watertable depths at three observation wells (5n, 8n and 15n) in the southern part of the study area.

Table 11.5: Annual groundwater balance components under 'average/no change' scenario and tree-planting strategy (alley farming) at the southern part of the study area (Plantation areas B1, B2 and B3 on Figure 11.13).

Components	Annual volume (10^3 m^3)		
	'Average/ no change' scenario	Mean	Year 2020
<i>Input</i>			
Constant head	3516.3	3518.9	3487.2
Recharge	5021.7	5021.7	5021.7
Inflow boundary	334.0	326.4	326.4
Total input	8872.0	8867.0	8835.3
<i>Output</i>			
Constant head	1324.1	1322.2	1348.7
Outflow boundary	10.2	10.2	10.2
Leakage:			
Fracture A	2154.6	2154.6	2154.6
Fracture B	438.2	438.2	438.2
Fracture C	184.7	184.7	184.7
Total	2777.5	2777.5	2777.5
Evapotranspiration (ET)			
ET under natural vegetation.	4222.7	3780.8	3505.0
ET due to groundwater extraction by trees	-	1584.2	1787.0
Total	4222.7	5365.0	6292.0
Drainage	229.6	216.1	184.0
Total Output	8564.1	9691.0	9612.4
<i>Total input-output</i>	307.9	-824.0	-777.1
<i>Change in aquifer's storage</i>	307.1	-823.9	-777.0
<i>Balance error</i>	0.8	0.1	0.1

of more than 1.4 m in the Warroo area. This option is considered the best option in terms of effectiveness in lowering watertables. However, surface drainage facilities are generally expensive. Therefore, economically, option A seems to be the most cost-effective alternative.

The third scenario which is the tree-planting strategy has been simulated near Bogandillon Creek area (above Dog Kennel Hill) and on the southern part of the study area. In both locations, tree planting is aimed to partially intercept groundwater flows towards these areas. In the first location (area A), a significant reduction in watertable depth in the order of 0.5 to 2.0 m in year 2020 have been observed. In the southern part of the study, on the other hand, three locations of tree plantations were needed to effectively reduce watertables by over 1.0 m over a larger area.

In general, adoption of alley cropping as a tree-planting strategy is a good management option in stopping or reversing the rising trend of watertables in the study area.

CHAPTER 12

SUMMARY AND CONCLUSIONS

Understanding the hydrodynamic behaviour of the aquifer system in the Jemalong and Wyldes Plains Irrigation District and Lake Cowal area is a critical strategy for successful long-term environmental management of the area. The study area is threatened with a rising watertable and salinisation. Previous studies in the area, however, had conflicting conclusions about the contribution of irrigation to groundwater recharge and salinisation processes. While some researchers assumed that irrigation significantly contributes to the degradation of the area, many farmers maintained that periodic flooding of the Lachlan River accounts for watertable rise and expansion of salinity.

The present study has reviewed the state of knowledge on water resources and related land resources of the Lachlan River Valley in order to put the issues within the larger context, and has investigated the groundwater systems in the study area. A numerical groundwater flow model has also been developed and calibrated to examine watertable rise, interactions between aquifers, surface water and the irrigation system and to quantify various components of the recharge and discharge of the groundwater balance. This model can be used to investigate management strategies and options in order to minimise the risk of land salinisation.

12.1. Summary

The following highlights the findings of the study and is presented in three sub-sections.

12.1.2. Lachlan River Valley

The Lachlan River Valley covers an area of about 84,700 km². About 75% of the Valley is flat, with slopes less than 3 degrees. The Valley is an important agricultural areas in New South Wales. About 14% of the total agricultural production in NSW comes from the Valley. Lucerne, pasture and winter cereals are the major crops grown in the area.

Rainfall in the Valley is generally distributed evenly throughout the year, but varies widely from year to year. The upper region receives up to 1000 mm per year, and this drops to 500 mm and 300 mm in the middle and lower parts of the catchment, respectively. Analysis of the rainfall data indicates a cyclic pattern of changes in annual rainfall since the last century. The most widespread change occurred around 1945-1946. The long-term average annual rainfall in Forbes and Cowra after 1945-1946 is almost 90 mm more than the average long-term annual rainfall prior to 1945-1946. Potential evaporation exceeds the annual rainfall over the entire Valley, rising from less than 1250 mm yr⁻¹ in the east up to 1,750 mm yr⁻¹ to the west. During summer months, pan evaporation exceeds rainfall by up to sixfold.

Runoff in the Valley comes from the 20% of the Valley upstream of Mandagery Creek confluence near Eugowra, with little contribution from the flat plains west of Condobolin. The average annual runoff in the Valley appearing in stream channels after losses due to evaporation, transpiration and deep seepage is about $1.3 \times 10^9 \text{ m}^3$ (1,300 gigalitres), which is approximately 4% of the annual rainfall over the entire valley. Streamflows in the Lachlan River are mainly regulated by Wyangala Dam which has a maximum capacity of $1.2 \times 10^9 \text{ m}^3$ (1,200 gigalitres). Other major structures along the river include diversion weirs and enroute storages (such as Lakes Cargelligo and Brewster) which permit re-regulation of flows in the Lower Lachlan. River regulation and water abstraction have substantially lessened the seasonality of the river flows. Stream salinity levels in the Lachlan River are normally in the medium range (between 300 and $800 \mu\text{S cm}^{-1}$), however salinity gradually increases downstream. There is also an increasing time trend of stream salinity in the Lachlan River at a rate of about $5 \text{ to } 8 \mu\text{S cm}^{-1} \text{ yr}^{-1}$ from Cowra and further downstream over the period of measurement. Phosphorus concentrations are moderately high (between 30 and $100 \mu\text{g L}^{-1}$), and algal blooms are already a major problem in Carcoar Dam and Lake Cargelligo.

Surface water usage is influenced by seasonal irrigation demands and water availability. Irrigation is the greatest user of surface water, accounting for approximately 93% of all surface water used in the area. Over 80,000 ha of land is irrigated along the Lachlan River.

Groundwater storage for the Lachlan Valley is approximately $300 \times 10^9 \text{ m}^3$ (300,000 gigalitres) with 98% stored in the alluvial deposits, and the estimated potential annual yield is about $1.2 \times 10^9 \text{ m}^3$ (1,200 gigalitres) per year. Groundwater is used basically for irrigation (47%), stock and domestic (37%) and town water supply (16%). Much of the water within the alluvial sediments has low salinity (EC less than $1000 \mu\text{S cm}^{-1}$), however EC increases with distance away from recharge areas.

In general, groundwater levels in the Valley have increased over a period of time, although trend analysis of groundwater levels are quite limited and at best localised to a few intensively studied areas. As a result, in recent years there has also been an increasing incidence of dryland salinity identified throughout the Valley. The exact area affected by dryland salinity is unknown, although at the headwaters, an estimated 19% of the area is at immediate risk of dryland salinisation. This study has found that the management of groundwater is limited by the availability of long term time series piezometric data.

12.1.2. The Jemalong and Bland creek study area

The study area includes the Jemalong and Wyldes Plains Irrigation District (JWPID) and part of the alluvial area of the Bland Creek catchment. The irrigation district has a total area of 93,123 ha with water for irrigation diverted from the Lachlan River at the Jemalong Weir. Average annual streamflow of the Lachlan River at the Jemalong weir gauging station is about $1.2 \times 10^9 \text{ m}^3$ (1,200 gigalitres) with salinity level ranging from 210 to $640 \mu\text{S cm}^{-1}$. Irrigation for cropping and grazing started in 1944. In any one year, the area irrigated ranges from 12,000 to 20,000 ha. Annual pasture, lucerne and winter cereals are widely grown and up to 1000 ha of rice. The average annual irrigation delivery for the whole irrigation system is about $70 \times 10^6 \text{ m}^3$ (70,000 ML), with 63% of this is delivered along the Cadow and Waroo main irrigation channels.

Mean annual rainfall in the study area varies spatially from 680 mm at Wombat (east of Bland Creek catchment) to about 440 mm at the Warroo area in the JWPID. Average daily potential evapotranspiration during summer months is about 6.6 mm d^{-1} , while during winter months mean potential evapotranspiration is about 1.3 mm d^{-1} .

The JWPID is divided into ten drainage basins which generally drain in westerly or southwesterly directions towards Lake Cowal, Nerang Cowal, Manna Creek and Bogandillon Creek. Flood breakouts provide significant groundwater recharge for the district, with floodwaters confined to the floodway in all but the wettest years. Bland creek and its tributaries, at the southern part of the JWPID drain northward discharging into Lake Cowal. Lake Cowal also receives flood runoff from the Lachlan River through the floodway. Flood is the major recharge source for Lake Cowal. When Lake Cowal is full, floodwater begins to fill Lake Nerang Cowal by flowing across the intervening saddle. Once filled to capacity the overflow from the Lake Cowal system ultimately discharges to the Lachlan River. The Lake has a maximum storage capacity of $194 \times 10^6 \text{ m}^3$ (194,000 ML) and the frequency of partial inundation of the Lake is approximately 50% (31 out of 64 years from 1930 to 1994).

The quality of the irrigation water diverted for the irrigation district is good, with EC values ranging from $210 \mu\text{S cm}^{-1}$ to $640 \mu\text{S cm}^{-1}$. An average of about 50 t d^{-1} of salt are transported to the irrigation district. Surface water at Bogandillon creek is already saline, with the highest recorded EC value of $39,000 \mu\text{S cm}^{-1}$ in October 1994. Surface water in Lake Cowal is still relatively fresh with EC less than $1,500 \mu\text{S cm}^{-1}$.

A large proportion of the area is covered by unconsolidated (Tertiary and Quaternary) sediments. Two distinct groups of unconsolidated sediments, the Lachlan and Cowra Formations, infill the paleochannels and floodplain. The Lachlan Formation is the older and deeper unit consisting of clays, silts, sands and gravels in varying admixtures. This formation is confined to the paleochannels and is believed to be of Pliocene age. The Cowra Formation, deposited since the Pleistocene, overlies unconformably the Lachlan Formation. It consists of moderately well sorted sand and gravel with inter-bedded clays. Maximum thickness of the unconsolidated sediments is confined to the paleochannels.

Groundwater in the area occurs in the unconsolidated sediments and in the fractured rocks, but the latter yields only less than 1 L s^{-1} . Unconsolidated sediments form the main aquifer consisting of Lachlan and Cowra Formations. In hydrogeological terms, these two formations act in combination as a watertable aquifer. However, on a local scale individual sand and gravel lenses display their own characteristics as local confined or semi-confined aquifers.

Monitoring of the groundwater level in the irrigation district started in 1944 at a limited number of sites. However, additional monitoring wells were drilled from 1968 to 1994 to examine watertable dynamics and groundwater quality of the entire irrigation district. Unfortunately, monitoring of these wells has been spasmodic. Regular measurement of piezometric heads would assist analysis and management enormously. Results of analysis indicate that an average rise of 2.6 m has been observed between March 1969 and October 1990. The highest rise of over 3 m occurred during this period in the vicinity of Lake Cowal. The major flood in 1990 resulted in the watertable in the irrigation district rising close to the ground surface. In almost half of the irrigation area the watertable was less than 2 m below the ground surface. After the 1990 flood, groundwater levels gradually declined by about 2.0 m between October 1990 and July 1997.

However, near Lake Cowal, the watertable has continued to rise, even during non-flood periods. Periodic major floods have a clear and enormous influence of watertable heights.

The Lachlan River has a dominant influence on the aquifer system in the irrigation district along its course from Jemalong Gap. The river recharges the aquifer in the upstream areas, while further downstream, groundwater discharges to the river. An evident groundwater mound coinciding with the Warroo Channel generates a significant component of groundwater flow to the west and southwest. The groundwater flow regime in the irrigation district has always been the result of two flow systems, one from the Lachlan River and the other from Bland Creek towards Lakes Cowal and Nerang Cowal. The dominant flow is that from the Lachlan River. Recharge areas are located close to the Jemalong Gap and along the Lachlan River, while discharge areas are on the western side of the District.

Groundwater salinity measurements in the study area near the Lachlan River are relatively low, as expected. However, a large mound of very high salinity groundwater occurs in the south-west around Lakes Cowal and Nerang Cowal. Groundwater salinity also varies with depths. Around Lake Cowal, groundwater EC is extremely high (32,400-72,000 $\mu\text{S cm}^{-1}$). However, the lake sits on a 7 to 10 m of thick laterally continuous clay with very low vertical hydraulic conductivity which so far has protected the lake from the underlying saline aquifer.

12.1.3. Groundwater flow modelling

A major component of this thesis has been the development of a three dimensional groundwater flow model for the study area. The model is made up of 4 layers with uniform grid size of 500 m x 500 m, covering the irrigation district, Lake Cowal and the northern part of the Bland Creek catchment. The model has been calibrated in steady-state for April 1988 and transient condition for the period May 1988 to July 1997. One of the findings during the calibration process is the proposed groundwater leakages, apparently through fractures in the basement along the northern side of the Warroo area, near Jemalong Gap, and at the northeastern side of the Lachlan River. Leakage through these proposed fractures appears to explain why major watertable rise and the expansion of land salinisation have not occurred in the area.

Mean annual volume of various components of the groundwater balance were quantified from the model. Rainfall provides the major source of recharge in the aquifer system. Seepage along the Warroo channel also provides a significant contribution to the recharge to the system. The major source of outflow is by groundwater evaporation through ET. The model suggests that groundwater drainage into the Gilmore Fault, however, is not a major source of groundwater outflow as previously thought. The model also predicted a continuous rise of watertable along the northeastern side of Lake Cowal which in long term could cause salinisation of a large tract of land as well as salinisation of Lake's water.

The model has been used to simulate a number of management scenarios to evaluate their impact to the groundwater system in the study area. The scenarios include the '*average/no change*' scenario, reduced recharge through improved irrigation and drainage efficiency and tree-planting strategy. Under the '*average/no change*' scenario, there is a potential risk of watertable rise and land salinisation expansion on the 'hot spot' areas such as in Warroo Channel area, and in the vicinities of Bogandillon Creek and Lake Cowal. Within the Warroo Channel area, the sealing off

of Warroo Channel seepage effectively lowers watertable in this area by more than 1 m over a relatively large area .

The simulation of 20 percent tree plantation strategy above Dog Kennel Hill to partially intercept groundwater flow towards Bogandillon area indicated a promising outcome. The watertable was lowered by over 0.5 m in the salt-affected areas in Bogandillon creek. On the southern part of the study area where a continuous watertable rise has been observed, tree-planting in three locations lowered the watertable depth by more than 1 m over a very large tract of land. These results showed that judicious tree-planting is an effective alternative for groundwater management in the region.

12.2. Conclusions

Based on the analysis and on the literature cited in the thesis, there is an increasing concern about the unsatisfactory state of health in land, water and environmental resources throughout the Lachlan Catchment region. Land and water salinisation are already prevalent throughout the catchment and Lachlan river salinity is apparently increasing over time at a rate of 5 to 8 $\mu\text{S cm}^{-1}$ per year. However, there is still large information gaps regarding groundwater quality and sustainability in the Valley.

The development of the three-dimensional model has contributed to a much better understanding of the complex interaction between aquifers, surface water and the irrigation within the Jemalong and Wyldes Plains Irrigation District and Lake Cowal aquifer systems. Recharge and discharge terms of the groundwater balance components have been quantified. When farmers argued that irrigation is not a major source of recharge and groundwater level rise in the irrigation district is mainly attributed to periodic flooding and high rainfall, their argument was proven correct. With current rate of irrigation water used throughout the district, irrigation is not posing a serious treat to the groundwater system in the short-term. The cap will mean there can be no expansion in irrigation. However, if the irrigation area expands and adoption of water-dependent crops such as rice increases, recharge components of the groundwater balance will be greatly altered.

The effectiveness of the identified management options in the study area in lowering the watertable has been evaluated through the model. Groundwater management options such as improvement of the irrigation efficiency through Warroo Channel lining and tree-planting in strategic areas proved to be viable options in lowering watertable depths.

12.3. Future research recommendations

There are various knowledge gaps in the study area that need to be addressed in the future. Since the results of the simulations for the selected options are indicative, various other scenarios can be evaluated using the model. As periodic flooding is the major driving process for watertable rise in the area, dynamic simulation in which rainfall is chosen stochastically for a wetter-than-average and drier-than-average period could be simulated. In addition, the impact of rice growing in the study area could be examined.

Understanding of hydrogeochemical processes in the study area is very limited. To gain more insight on the groundwater salinisation processes especially in the Lake Cowal area,

chlorofluorocarbons (CFCs), heavy water isotopes, age-dating of groundwater and radiogenic strontium isotope analyses can be employed. Since leakages into the proposed basement's fractures are just based on the results of the model calibration, further field investigations and hydrogeochemical analysis are required to substantiate this important issue.

The economics of sealing the Warroo Channel should be investigated and the impact of the water saved on environmental flows in the Lachlan or on alternative use should be researched. It is also recommended that this type of study should be extended to other regions in the Lachlan.

13. REFERENCES

- AATSE. (1999). *Water and the Australian Economy*. Australian Academy of Technological Sciences and Engineering. April 1999. 127p.
- Alekin, O.A. (1970). *Osnovy hydrokhimii (Principles of Hydrochemistry)*. Hydrometeorologicheskoe Izdat., Leningrad, 443 p.
- Allan, J. and Lovett, S. (1997). *Impediments to managing environmental water provisions*. Bureau of Resource Sciences, Canberra, Australia.
- Alvarez, K. (1982). *Lachlan-Murrumbidgee confluence wetlands surface water resources*. Hydrology Section Report 82/46, Water Resources Commission (unpub).
- Ameratunga, J. (1993). *Introduction to groundwater modelling*. In: *Computer Applications for Groundwater Assessment and Management*. Water Resources Series No. 73. United Nations, New York.
- Anderson, J., Gates, G. and Mount, T.J. (1993). *Hydrogeology of the Jemalong and Wyldes Plains Irrigation Districts*. Department of Water Resources, New South Wales.
- Andrews, E.C. (1910). *The Forbes-Parkes goldfield geological survey*. NSW Mineral Resources Report no. 13.
- ASCE (1987). *Groundwater Management*. 3rd edition. Prepared by the Subcommittee on Groundwater Management of the Committee on Groundwater of the Irrigation and Drainage Division of American Society of Civil Engineers. 263 p.
- Australian Bureau of Statistics. (1996). *Integrated national database. version 2*. Commonwealth of Australia.
- Australian Bureau of Statistics. (1997). *NSW regional statistics*. Commonwealth of Australia.
- Australian Nature Conservation Agency (1996). *A Directory of Important Wetlands in Australia*, Second edition. ANCA, Canberra, Australia.
- Australian Water Resources Council. (1975). *Groundwater Resources of Australia*. v.1, 53 p. Aust. Govt. Publ. Service, Canberra.
- Bari, M.A. and Schofield, N.J. (1992). *Lowering of a shallow, saline watertable by Extensive Eucalypt Reforestation*. *Journal of Hydrology*, v. 1, no. 33, p 273-291.
- Barnett, G. (1994). *Farm forestry to ameliorate dryland salinity in the Lachlan headwaters*. Honours Thesis, The Australian National University, Australia.
- Basden, H., Adrian, J., Clift, D.S.L. and Winchester, R.E. (1975). *Cootamundra 1:100,000 Geological Sheet*. Geological Survey of NSW, Sydney.

- Bear, J. (1991). Eight lectures on mathematical modelling of transport in porous media. In: *Modelling and Applications of Transport Phenomena in Porous Media*, eds Bear, J. and Buchlin, J-M., Kluwer Academic Publishers, Dordrecht, The Netherlands, p. 1-194.
- Bird, P.R., Bicknell, D., Bulman, P.A., Burke, S.J.A., Leys, J.F., Parker, J.N., van Der Sommen, F.J. and Voller, P. (1992). The role of shelter in Australia for protecting soils, plants and livestock. *Agroforestry Systems* v. 20, p. 59-86.
- Bish S. and Gates, G. (1991). Groundwater reconnaissance survey Forbes-Condobolin-Cargelligo, Department of Water Resources, Report No. TS91.033.
- Bish, S. and Williams, R.M. (1994). Review of groundwater use and water level behaviour in the Upper Lachlan Valley 1986-1994, Status Report No.2. TS 94.078. Department of Water Resources, Technical Services Division.
- Bjerknes, J. (1966a). Survey of El Nino 1957-58 in its relation to tropical Pacific meteorology. *Inter-American Tropical Tuna Commission Bulletin*, v. 12, p. 1-62.
- Bjerknes, J. (1966b). A possible response of the atmospheric Hadley circulation to equatorial anomalies of ocean temperature. *Tellus*, v. 18, p. 820-829.
- Bjerknes, J. (1969). Atmospheric teleconnections from the equatorial Pacific. *Monthly Weather Review*, v. 97, p. 163-172.
- Blackburn, G. and McLeod, S. (1983). Salinity of atmospheric precipitation in the Murray Darling Drainage Division, Australia. *Australian Journal of Soil Research*, v. 21, no. 4, p. 411-434.
- Bradd, J.M., Turner, J.V. and Waite, T.D. (1991). Final report of the application of hydrogeochemical and isotope techniques in relation to dryland salinisation and waterlogging at Williams Creek Yass, New South Wales. Australian Nuclear Science and Technology Organisation, ANSTO/C210.
- Brunker (1968). Forbes 1:250,000 Geological sheet. geological survey New South Wales, Sydney, Australia.
- Bureau of Meteorology. (1997). Rainfall and evaporation data. Prepared by Climate and Consultancy Section in the NSW Regional Office of the Bureau of Meteorology.
- Bush, O. (1994). Mapping local groundwater recharge areas using remote sensing and geographic information systems. Honours Thesis, The Australian National University, Australia.
- COAG. (1994). *Report of the Working Group on Water Resource Policy*, Communique, Department of Primary Industries and Energy, Canberra.
- Clifton, C.A., Miles, P., Harvey, W., Trebilcock, B. and Morris J. (1993). Evaluation of the growing strategies for reducing groundwater recharge in the Hill Country of Northern Victoria. Paper presented to the National Conference on Land Management for Dryland Salinity Control, La Trobe University, Bendigo, Victoria, September 1993.

- Coffey Partners International Pty Ltd. (1994). Groundwater modelling study, Jemalong Wyldes Plains. report no. G375/2-AB. Department of Water Resources, New South Wales.
- Coffey Partners International Pty Ltd. (1995a). Hydrogeological study of tailings dams area. North Group. Report No. G255/21-AD.
- Coffey Partners International Pty Ltd. (1995b). Lake Cowal project hydrogeological modelling and dewatering study. North Group. Report No. G255/28-AF.
- Coffey Partners International Pty Ltd. (1996). Hydrogeological assessment Lake Cowal for the Land and Water Management Plan. Report No. G415/1-AC. Department of Land and Water Conservation.
- Conservation and Land Management. (1992). Yass water supply catchment dryland Salinity abatement program. Final Report for the National Soil Conservation Program.
- Dam Safety Committee – NSW (1995). Prescribed dams in NSW. Schedule 1 of the Dam Safety Act as amended.
- Debashish, P., Williams, R.M. and Hamilton, S. (1996). Wagga Wagga urban salinity: implication for groundwater pumping. NSW Department of Land and Water Conservation. Technical Services Division. TS 96.071.
- Department of Land and Water Conservation. (1996a). Lachlan Valley strategic management plan 1996-2000 (draft). Compiled and edited by Catherine Travers. Department of Land and Water Conservation, Forbes, NSW.
- Department of Land and Water Conservation. (1996b). Lachlan regulated system irrigated crop details. Department of Land and Water Conservation, Central West Region, unpublished.
- Department of Land and Water Conservation. (1996c). Window on water. The state of water in NSW 1994/1995. Compiled by Daly, H., Bowling, L., Royal, M., Deal, R., and Mitrovic, S. Water Quality Services Unit. Department of Land and Conservation, Parramatta.
- Department of Land and Water Conservation. (1997). Jemalong Wyldes Plains Irrigation District wetland evaluation. Final draft, Department of Land and Water Conservation, New South Wales, Australia.
- Department of Land and Water Conservation. (1998). Lachlan catchment: state of the rivers report – 1997. New South Wales Department of Land and Water Conservation.
- Department of Land and Water Conservation. (undated). Line diagram of the Lachlan River. Department of Land and Water Conservation, Forbes, NSW.
- Department of Land and Water Conservation. (2001). Sustainable use of the Great Artesian Basin. Media Release-Department of Land and Water Conservation, Central West Regional Office, Orange.

- Department of Primary Industries and Energy. (1985). *1985 Review of Australia's water resources and water use*, volume 1: Water Resource Data Set. Australian Government Publishing Service, p. 12.
- Department of Water Resources. (1989). Water resources of the Lachlan Valley. NSW Department of Water Resources.
- Department of Water Resources. (1990). Water management plan for the wetlands of the Lachlan Valley floodplain (draft). Department of Water Resources, Lachlan Region.
- Department of Water Resources. (1992). Water management strategy for the wetlands of the Lachlan Valley floodplain (draft). Department of Water Resources, Lachlan Region, Forbes.
- Department of Water Resources. (1993). Administration of environmental flows in the regulated Lachlan System. Department of Water Resources, Lachlan Region.
- Department of Water Resources. (1994). Environmental flows in the regulated Lachlan system. Department of Water Resources, Lachlan Region, Forbes.
- Doorenbos, J. and Pruitt, W.O. (1977). Crop water requirements. FAO Irrigation and Drainage Paper 24. Food and Agriculture Organization of the United Nations, Rome. 144 p.
- Eastham, J., Scott, P.R. and Steckis, R.A. (1993). Evaluation of *Eucalyptus camaldulensis* (River Gum) and *Chamaecytisus profiferus* (Tagasaste) for salinity control by agroforestry. *Land Degradation and Rehabilitation*, v. 4, p. 113-122.
- Ellis, M. and Etheridge, A. (1993). Atlas of New South Wales wildlife: monotremes and marsupials. Sydney: NSW National Parks and Wildlife. 42 p.
- Enfield, D.B. (1992) Historical and pre-historical overview of El Nino/Southern oscillation. In: *El Nino : Historical and Paleoclimatic Aspects of the Southern Oscillation*, edited by Diaz, H.F. and Markgraft, V. Cambridge University Press.
- Environmental Research and Information Consortium. (1995). Radiometric soils mapping. Jemalong/Wyldes Plains. ERIC Pty Ltd.
- Fanning, D. (1995). Lake Cowal gold project North Mining Ltd fauna impact statement. In: *Lake Cowal Gold Project Environmental Statement*. NSR Environmental Consultants Pty Ltd., Hawthorn, Victoria, Australia.
- Fleming, P.M. (1982). The water resources of the Murray-Darling Basin, In: *Murray-Darling Basin Project Development Study, Stage 1*. CSIRO working papers, Canberra, Australia, p. 38-54
- Forbes Rigby Pty Ltd. (1996). Jemalong and Wyldes Plains Irrigation District Land and water management plan floodway management study. Prepared on behalf of the Department of Land and Water Conservation, Central West Region. 77 p.
- Gates, G.B. and Williams, R.M. (1988). Dryland salinity study and changes in groundwater levels in Southeast New South Wales. NSW Department of Water Resources. TS 88.010.

- George, R.J. and Bennett, D.L. (1992). Soil moisture characteristics under perennial and annual pastures. Paper presented at the Dryland Salinity Conference, Yass, New South Wales, 28 September 1992. Department of Conservation and Land Management.
- Ghassemi, F., Jakeman, A.J. and Nix, H.A. (1995). *Salinisation of Land and Water Resources - Human Causes, Extent, Management and Case Studies*. University of New South Wales Press Ltd, Sydney 2052 Australia. 526 p.
- Golden Software Inc. (1995). Surfer version 6.01. Surface mapping system. Golden Software Inc, Golden Colorado, USA.
- Goldney, D.C. and Bowie, J.S. (Ed's) (1996). The national trust (NSW) scenic and scientific survey of the Central West Region. v. 1. Draft Report. Mitchell College of Advanced Education, Bathurst.
- Gomboso, J. (1995). A Hydrogeological-economic modelling approach to dryland salinity in the NSLCD, W.A. PhD Thesis, The Australian National University, Canberra ACT, Australia. 606 p.
- Gomboso, J., Ghassemi, F. and Appleyard, S.J. (1997). Dryland salinity in the North Sterling Land Conservation District, Western Australia: simulation of management options. *Hydrogeology Journal*, v. 5, no. 1, p. 80-97.
- Gray, W.G. (1982). Comparison of finite difference and finite element methods. . *NATO/ASI Mechanics of Fluids In Porous Media - New Approach in Research*, University of Delaware, 1982.
- Greenwood, E.A.N. and Beresford, J.D. (1979). Evaporation from vegetation in landscape developing secondary salinity using ventilated-chamber technique I. *Journal of Hydrology*, v. 42, p. 369-382.
- Greenwood, E.A.N., Klein, L., Beresford, J.D. and Watson, J.D. (1985). Differences in annual evaporation between grazed pasture and eucalyptus species in plantations on a saline farm catchment. *Journal of Hydrology*, v. 78, p. 261-278.
- Gromer, M. (1992). Jemalong-Wyldes Plains land and water management plan. NSW Agriculture Working Papers.
- Harris, J.H. and Gehrke, P.C. (eds) (1997). Fish and rivers in stress: The NSW rivers survey. NSW Fisheries and the Cooperative Research Centre for Freshwater Ecology, Cronulla.
- Hatton, P.J. (1991). Water management plan for the Wibertroy/Cowal wetlands (draft). Department of Water Resources NSW Lachlan Region.
- Hayman, G. (1996). Implementation of the Boorowa River salinity catchment plan - final report. Project no. LA0022.93. Report to the National Landcare program. Boorowa Regional Landcare Office, Boorowa, NSW.
- Helsel, D.R. and Hirsch, R.M. (1992) Statistical methods in water resources. *Studies in Environmental Science*, v. 49, 522 p. Elsevier Science Publishers.

- Hingston, F.J. and Gailitis, V. (1976). The geographic variation of salt precipitation over Western Australia. *Australian Journal of Soil Research* v. 14, p. 319-35.
- Hird, C. (1991). Soil Landscapes of the Goulburn 1:250,000 sheet. Soil Conservation Service of NSW, Sydney.
- Hook, R.A. (1992). Rapid appraisal techniques for dryland salinity. Pilot study: Upper Lachlan Catchment. An initiative of the Salt Action Program.
- Hutchinson, M.F. (1996). A locally adaptive approach to the interpolation of digital elevation models. *Third International Conference/Workshop on Integrating GIS and Environmental Modeling*. NCGIA, University of California, Santa Barbara.
- Jolly, I., Dowling, T.I, Zhang, L., Williamson, D.R. and Walker, G.R. (1997a). Water and salt balances of the catchments of the Murray-Darling Basin. Technical Report 37/97. CSIRO Land and Water, Canberra.
- Jolly, I., Morton, R, Walker, G.R, Robinson, G., Jones, H., Nandakumar, N., Nathan, R., Clarke, R. and McNeill, V. (1997b). Stream salinity trends in catchments of the Murray-Darling Basin. Technical Report 14/97, CSIRO Land and Water, Canberra.
- Keenan, C., Watts, R. and Serafini, L. (1996). Population genetics of golden perch, silver perch and eel-tailed catfish within the Murray-Darling Basin. In: *Proceedings MBDC Riverine Environment Research Forum*, October 1995, Attwood Victoria. Murray-Darling Basin Commission.
- Kelly, I.D. (1971). Jemalong and Wyldes Plains Irrigation Districts geomorphology, soils and groundwater conditions. Water Conservation and Irrigation Commission, New South Wales. 70 p.
- Kelly, I.D. (1988). Investigation on the groundwater and salinisation environment in the Jemalong and Wyldes Plains Irrigation Districts, New South Wales. Resource Assessment Group Murrumbidgee Region.
- King, A. (1997). Jemalong Wyldes Plains Irrigation District wetland evaluation – final draft. Ecological Services Unit, Centre for Natural Resources, NSW Department of Land and Water Conservation, Parramatta.
- Kinhill Engineers Pty Ltd. (1995). Selection of channel seepage management options Jemalong and Wyldes Plains Irrigation District – final report. Prepared for the Department of Land and Water Conservation, Lachlan Region, Forbes NSW, Australia.
- Lachlan Catchment Management Committee. (1993). A community strategy for natural resources management in the Lachlan catchment region. Lachlan Catchment Management Committee, Forbes, New South Wales. 26 p.
- Lachlan River Management Committee. (1998) Lachlan environmental flow rules for 1998/98. NSW Department of Land and Water Conservation, Parramatta.
- Lapidus, D.F. (1987). *Dictionary of Geology*. Collins.

- Lawrence, B.W. (1991). Fish management plan. Murray Darling Basin Commission, Canberra.
- Lefroy, T. and Scott, P. (1994). Alley farming: new vision for Western Australian farmland. *Journal of Agriculture, Western Australia*, v. 35, p. 119-26.
- Lewis, R.W. (1982). Finite element models for flow through porous media. *NATO/ASI Mechanics of Fluids In Porous Media – New Approach in Research*, University of Delaware, 1982.
- Lloyd, J.W. and Heathcote, J. (1985). *Natural inorganic hydrochemistry in relation to groundwater: an introduction*. Oxford University Press. 294 p.
- Lyall and Macoun Consulting Engineers. (1995). Jemalong land and water management plan surface drainage management study (draft). Prepared for the Steering Committee.
- Mackay, N., Hillman, T. and Rolls J. (1988). Water quality of the River Murray – review of monitoring 1978 to 1986. Murray Darling Basin Commission Water Quality Report no. 1, 62 p.
- Magrath, M.J.L. (1992). Waterbird study of the Lower Lachlan and Murrumbidgee Valley wetlands in 1990/91. A report prepared for the NSW Department of Water Resources.
- Marcar, N., Crawford, D., Leppert, P., Javanovic, T., Floyd, R. and Farrow, R. (1995). Trees for saltland: a guide to selecting native species for Australia. Division of Forestry, CSIRO, Canberra, p. 72.
- Martin, H. (1969). The palynology of some Tertiary and later deposits in New South Wales. PhD Thesis, UNSW (unpub).
- Martin, H. (1973a). Upper Tertiary palynology in Southern New South Wales. Special Publication, *Geological Society of Australia*. p 33-54.
- Martin, H. (1973b). The palynology of some Tertiary and Pleistocene deposits, Lachlan River Valley, New South Wales. *Australian Journal of Botany*. Suppl. series. 6, p. 51.
- Martin, R.E. and Harris, P.G. (1982). Hydrochemical study of groundwater from an unconfined aquifer in the vicinity of Perth, Western Australia, *Aust. Water Res. Council, Tech. Paper*, v. 67.
- Massey, C. (1997). An assessment of riverine environment health in the Lachlan Catchment draft report. Department of Land and Water Conservation, Forbes, New South Wales.
- Maunsell and Partners. (1986). Jemalong and Wyldes Plains Irrigation District: options for management of salinisation and waterlogging. Water Resources Commission, New South Wales.
- Mc Innes, J.M.L. (1995). The Bland Creek Catchment: state of the catchment. Department of Land and Water Conservation, New South Wales. 113 p.
- McBryde, D.M.A. (1995). A population study of European carp (*Cyprinus carpio* L.) in the Lower Lachlan River, NSW. Dissertation submitted in partial fulfilment of the Bachelor

of Applied Science (Environment Science) Honours Degree, Charles Sturt University, Mitchell.

- McDonald, M.G. and Harbaugh, A.W. (1988). A modular three-dimensional finite difference groundwater flow model. US Geological Survey Open-File Report, National Center, Reston, VA, 83-875, 586 p.
- McGowen, I. (1996). Comments on draft final report – Radiometric soils mapping, Jemalong/Wyldes Plains by ERIC. NSW Department of Agriculture, Orange.
- McGrath, S. (1997). A report on the GIS used in the production and implementation of the Jemalong Land and Water Management Plan. NSW Agriculture, Forbes.
- Megalla M.N. and Kalf, F.R. (1973). Buried channel of the Lachlan River valley from Cowra to Forbes, NSW. Hydrogeological Report, 1973/37. Water Resources Commission, NSW (unpubl.)
- Morris, J.D. and Collopy, J.J. (1999). Water use and salt accumulation by *Eucalyptus Camaldulensis* and *Casuarina Cunninghamiana* on a site with shallow saline groundwater. *Agricultural Water Management*, v. 39, p. 205-227. Elsevier Science.
- Morris, J.D. and Thomson, L.A.J. (1983). The role of trees in dryland salinity control. *Proceeding of Royal Society of Victoria*, v. 95, no. 3, p. 123-131.
- Morton, R. (1996). Statistical methodology for stream salinity trends. CSIRO Biometrics Unit Report, Canberra, 9 p.
- Murray-Darling Basin Commission. (1987). *Salinity and Drainage Strategy – Background Paper*. Murray-Darling Basin Ministerial Council Background Paper no. 87/1. Prepared by the Salinity and Strategy Working Group, Dec 1987. 90 p.
- Murray-Darling Basin Ministerial Council. (1996). *Setting the Cap: Report of the Independent Audit Group*, Executive summary, November 1996. Murray Darling Basin Ministerial Council, Canberra.
- Nicholls, N. (1992). Historical El Nino/Southern oscillation, variability in the Australasian region. In: *El Nino : historical and paleoclimatic aspects of the southern oscillation*, edited by Diaz, H.F. and Markgraft, V. Cambridge University Press.
- Nicoll, S. and Scown, J. (1993). Dryland salinity in the Yass Valley, process and management. New South Wales Department of Conservation and Land Management, Final Technical Report for the Natural Resources Management Strategy. 186 p.
- Northcote, K.H. (1979). A factual key for the recognition of Australian soils. Rellim Technical Publications: Glenside South Australia.
- NSW Government. (1997). Proposed interim environmental objectives for NSW waters – Lachlan Catchment. Environmental Protection Agency, Chatswood.

- NSW Department of Agriculture. (1994). Farmers soils map. Department of Agriculture, Forbes Office.
- O'Reilly, K. (1994). The use of management options in controlling salinity and waterlogging: a review of relevant literature. Department of Land and Water Conservation. 26 p.
- Odins, J.A. (1975). The application of seismic refraction to groundwater studies of unconsolidated sediments, Masters Thesis, University of New South Wales, Australia.
- Panta, K., Mc Mahon, T.A., Milano, H.M. and Turrall, H.N. (1997). Hydrology of Lachlan River Valley: an interim report. Centre for Environmental Applied Hydrology. Department of Civil and Environmental Engineering, The University of Melbourne, Parkville, Victoria, Australia.
- Piper, A.M. (1944). A graphic procedure in the geochemical interpretation of water analysis. *Trans. Am. Geophys. Union*, v. 25, p. 914-923.
- Pittock, A.B. (1975). Climatic change and patterns of variation in Australian rainfall. *Search*, v. 6, no. 11-12, p. 498-504.
- Pogson, D.J. (1972). *Geological map of New South Wales, scale 1:1,000,000*. Geological Survey of New South Wales, Sydney.
- Powell, J. (1992). Dryland salinity control in the Boorowa River catchment. Sydney, Salt Action.
- Preece, R., Robinson, G. and Curry, M. (1997). Key sites program; river water quality trends July 1991 to June 1996 – summary report. Department of Land and Water Conservation, Centre for Natural Resources, Water Quality Services Unit, Parramatta.
- Pressey, R.L., Bell, F.C., Barker, J., Rundle, A.S. and Belcher, C.A. (1984). Biophysical features of the Lachlan-Murrumbidgee confluence, South-western NSW. NSW National Parks and Wildlife Service. Australia.
- Prime Minister's Science and Engineering Council. (1996). *Managing Australia's Inland Waters: Roles for Science and Technology*. Department of Industry, Science and Tourism, Canberra.
- Rankine and Hill Pty Ltd. (1979). Lachlan Valley flood mitigation study. Rankine and Hill Pty Ltd Consulting Engineers report to NSW Water Resources Commission, Parramatta.
- Rankine and Hill Pty Ltd. (1983). NSW inland rivers floodplain management studies – Lachlan Valley. Rankine and Hill Pty Ltd Consulting Engineers.
- Ropelewski, C.F. and Halpert, M.S. (1986). North American precipitation and temperature patterns association with the El Nino/Southern Oscillation. *Monthly Weather Review*, v. 115, p. 1606-1626.
- Ross, J.B. (1982). Interim report on the Water Resources Commission bore network in the Upper Lachlan Valley. Hydrogeological Report. Water Resources Commission, NSW (unpubl.).

- Ross, K.L., Banks, L.W, McKenzie, D.C. and Nicol, H.I. (1992). Survey of irrigation in the Lachlan Valley. Technical Bulletin no. 46, NSW Agriculture, October.
- Rushton, K.R. and Redshaw, S.C. (1979). *Seepage and Groundwater Flow*. John Wiley and Sons, Chichester.
- Sainty, G. and Roberts, J. (1997). *Listening to the Lachlan*. Sainty and Associates Pty Ltd.
- Salama, R.B., Farrington, P., Bartle, G.A. and Watson, G.D. (1993). Salinity Trends in the Wheatbelt of Western Australia. *International Hydrology and Water Resources Symposium*, 2-4 October, 1991, Perth Western Australia, v. 2, p. 386-391.
- Schofield, N.J. (1984). A Simulation Model Predicting Winter Interception Losses from Reforestation Stands in South-west, Western Australia. *Australian Forestry Research*, v. 14, p. 105-127.
- Schofield, N.J. (1990). Determining Reforestation Area and Distribution of Salinity Control. *Hydrological Sciences Journal*, v. 35, no. 1, p. 1-119.
- Scott, D.I. (1991). Rapid appraisal techniques for dryland salinity-Upper Lachlan Catchment hydrogeology and surface hydrology. Department of Water Resources, TS 91.040.
- Scott, P.R. (Ed.). The role of trees in sustainable agriculture – a national conference – reprints of Western Australian papers. Resource Management Technical Report no. 138. Department of Agriculture, Western Australia.
- Shaikh, M., Brady, A.T. and Sharma, P. (1996). Applications for remote sensing to assess wetland inundation and vegetation response in relation to hydrology in the Great Cumbung Swamp, Lachlan Valley, NSW, Australia. Paper presented to the Intercol Conference on Wetlands, Perth, W.A. September 1996.
- Shepherd, M. (1992). Flooding frequency and *Eucalyptus largiflorens* (Black Box): wetland health in the Wah Wah District. Technical Report 92/14. Department of Water Resources, Murrumbidgee Region, Leeton.
- Sivertsen, D. and Metcalfe, L. (1995). Natural vegetation of the southern wheat-belt (Forbes and Cargelligo 1:250,000 map sheets). *Cunninghamia, A Journal of Plant Ecology*. v. 4, no. 1 National Herbarium of NSW, Sydney.
- Sturgess, B.F., Kelly, I.D. and McAuliffe, T.F. (1993). Bogandillon creek salinity report. Department of Water Resources, Lachlan Region-Forbes.
- Sturgess, B.F. (1994). Lake Cargelligo shallow water conditions report (draft). Technical Report LR94/1. Department of Water Resources.
- Thomas, R.G. (1973). *Groundwater Models*. FAO Irrigation and Drainage Paper 21. Food and Agriculture Organization of the United Nations, Rome. 192 p.

- Thomson, L.A.J., Morris, J.D. and Halloran, G.M. (1987). Salt tolerance in eucalypts. Proceedings Conference on 'Afforestation of Salt-affected Soils', Karnal, India, February 1987.
- Togher, C. (1996). A report on the biodiversity and land management of the Abercrombie River catchment. National Parks Association of NSW Inc, Sydney South.
- Total Catchment Management. (1993). Focus on dryland salinity in the headwaters region of the Lachlan River catchment. Lachlan Catchment Management Committee.
- Troup, A.J. (1965). The southern oscillation. *Quarterly Journal of Royal Meteorological Society*, v. 91, p. 490-506.
- van der Lely, A. (1993). Channel seepage from Warroo Main Channel, Jemalong Irrigation District. Technical services, Murrumbidgee Region, Department of Water Resources, Technical Report no. 93/04.
- van Der Molen, D.T. and Pinder, J. (1993). Environmental Model Calibration Under Different Specifications: An Application to the Model SED. In Jorgensen, S.E. (Ed). Theoretical Modelling Aspects. *Ecological Modelling*, v. 68, no. 1-2, p. 1-20.
- van Dijk, D.C. (1969). Relict salt, a major cause of recent land damage in the Yass Valley, Southern Tablelands, New South Wales. *Aust. Geog.* v. 11, p. 439-42.
- Walker, G.R., Jolly, I.D., Williamson, D.R., Gilfedder, M., Morton, R., Zhang, L., Dowling, T., Dyce, P., Nathan, R., Nandakumar, N., Fates, G.W.B., Linke, G.K., Seker, M.P., Robinson, G., Jones, H., Clarke, R., McNeill, V. and Evans, W.R. (1998). Historical stream salinity trends and catchment salt balances in the Murray-Darling Basin. final report – NRMS D5035. Technical Report 33/98. CSIRO Land and Water, Canberra.
- Walker, G.T.(1923). World weather 1. *Memoirs of the Indian Meteorological Department*, v.24, p. 75-131.
- Walker, G.T. and Bliss, E.W. (1932). World weather V. *Memoirs of the Royal Meteorology Society*, v. 4, p. 53-84.
- Walton, W.C. (1970). *Groundwater Resources Evaluation*. McGraw-Hill Book Company, New York.
- Walton, W.C. (1979). Progress in Analytical Groundwater Modelling. In Back, W., and Stephenson, D.A. (Eds). , *Contemporary Hydrogeology – The George Burke Maxey Memorial Volume. Journal of Hydrogeology.* v. 43., p. 149-159.
- Warren, A.Y.E., Gilligan, L.B. and Raphael, N.M. (1996). *Cootamundra 1:250,000 Geological Sheet SI/55-11*. Second edition. Geological Survey of new South Wales, Sydney.
- Water Conservation and Irrigation Commission. (1971). Water resources of New South .Wales. Water Conservation and Irrigation Commission. p. 95-97. Government Printer, Sydney.

- Water Conservation and Irrigation Commission. (1972). Water resources of the Lachlan Valley. Report no. 23 – survey of thirty-two New South Wales River valleys. Water Conservation and Irrigation Commission, Sydney.
- Water Resources Commission. (1984). Groundwater in New South Wales (NSW State Water Plan). Water Resources Commission, New South Wales.
- Water Resources Commission. (1986). Groundwater Resources of the Lachlan Valley and associated tributaries upstream of Lake Cargelligo. Report no. 1. Water Resources Commission.
- Water Resources Commission. (undated). Wyangala dam flood mitigation investigation. New South Wales Water Resources Commission and Addendum.
- Waterloo Hydrogeologic Inc. (2000). Visual MODFLOW user's manual. Waterloo Hydrogeologic Inc., Waterloo, Ontario, Canada.
- Watermark Computing (1994). PEST: model independent parameter estimation.
- Williams, B.G. (1993). The shallow groundwater hydrology of the Jemalong Wyldes Plain Irrigation Districts. Draft report for the Jemalong Wyldes Plain Irrigation Districts Land and Water Management Plan, unpubl.
- Williams, B.G. and Williams, A.F. (1992). Electromagnetic induction survey of the Jemalong Plains area. 15 p.
- Williams, J. (1988). Hydrogeology of the Bland River catchment. BSc (Hons) Thesis. University of New South Wales. Australia.
- Williams, R.M. (1990). Groundwater conditions in the Young (Scenic Road) Landcare Group area. Technical services division, NSW Department of Water Resources.
- Williamson, W.H. (1961). Some Aspects of late Cainozoic Geology of the Lachlan Valley, NSW. ANZAAS, Brisbane (unpub).
- Williamson, W.H. (1964a). The Development of groundwater resources of alluvial formations. In: *Water Resources Use and Management*. Melbourne University Press. Melbourne. p. 195-211.
- Williamson, W.H. (1964b). Evidence of abandoned course of the Lachlan River, NSW. *Australian Journal of Science*. v. 26, no. 4, p. 117-118.
- Williamson, W.H. (1968a). Water- from tank stream to snowy scheme. In : *A Century of Scientific Progress*. (Royal Soc. NSW Centenary Publication) Aust. Medical Publishing Co., Sydney.
- Williamson, W.H. (1968b). The Lachlan Valley. *Journal of the Geological Society of Australia*. 16(1). The Geology of New South Wales. p. 545-548.

- Williamson, W.H. (1970). Groundwater in unconsolidated sediments – recent developments in NSW. In: *Proceeding of Groundwater Symposium 1969*. Report no. 113, p. 1-12, Water Research Lab, University of New South Wales. Australia.
- Williamson, W.H. (1986). Investigation of the groundwater resources of the Lachlan Valley alluvium, part 1: Cowra to Jemalong Weir. Department of Water Resources, Hydrogeological Unit, report No. 1986/12.
- Williamson, D.R., Gates, G.W.B., Robinson, G., Linke, G.K., Seker, M.P. and Evans, W.R. (1997). Salt trends: historic trend in salt concentration and saltload of streamflow in the Murray-Darling Drainage Division. Report to NRMS-MDBC by the Project 5043 Steering Committee. 63 p.
- Willing and Partners Pty Ltd. (1993). Jemalong-Wyldes Plains basin four computer surface drainage model. Project no. 3197, Department of Water Resources. New South Wales. 27 p.
- Zienkiewicz, O.C. (1991). *The Finite Element Method*, 4th ed., McGraw-Hill, London, 1991.

APPENDIX A

List of active meteorological stations in the Lachlan River Valley with at least 50 years of records

Station ID	Station Name	Year Started	Year Ended	Latitude	Longitude
010001	1950	1999	34.50	150.00
010002	1950	1999	34.50	150.00
010003	1950	1999	34.50	150.00
010004	1950	1999	34.50	150.00
010005	1950	1999	34.50	150.00
010006	1950	1999	34.50	150.00
010007	1950	1999	34.50	150.00
010008	1950	1999	34.50	150.00
010009	1950	1999	34.50	150.00
010010	1950	1999	34.50	150.00
010011	1950	1999	34.50	150.00
010012	1950	1999	34.50	150.00
010013	1950	1999	34.50	150.00
010014	1950	1999	34.50	150.00
010015	1950	1999	34.50	150.00
010016	1950	1999	34.50	150.00
010017	1950	1999	34.50	150.00
010018	1950	1999	34.50	150.00
010019	1950	1999	34.50	150.00
010020	1950	1999	34.50	150.00
010021	1950	1999	34.50	150.00
010022	1950	1999	34.50	150.00
010023	1950	1999	34.50	150.00
010024	1950	1999	34.50	150.00
010025	1950	1999	34.50	150.00
010026	1950	1999	34.50	150.00
010027	1950	1999	34.50	150.00
010028	1950	1999	34.50	150.00
010029	1950	1999	34.50	150.00
010030	1950	1999	34.50	150.00
010031	1950	1999	34.50	150.00
010032	1950	1999	34.50	150.00
010033	1950	1999	34.50	150.00
010034	1950	1999	34.50	150.00
010035	1950	1999	34.50	150.00
010036	1950	1999	34.50	150.00
010037	1950	1999	34.50	150.00
010038	1950	1999	34.50	150.00
010039	1950	1999	34.50	150.00
010040	1950	1999	34.50	150.00
010041	1950	1999	34.50	150.00
010042	1950	1999	34.50	150.00
010043	1950	1999	34.50	150.00
010044	1950	1999	34.50	150.00
010045	1950	1999	34.50	150.00
010046	1950	1999	34.50	150.00
010047	1950	1999	34.50	150.00
010048	1950	1999	34.50	150.00
010049	1950	1999	34.50	150.00
010050	1950	1999	34.50	150.00

Appendix A: List of active meteorological stations in the Lachlan River Valley with at least 50 years of records.

Station Number	Station Name	Year start of record	Elevation (m)	Longitude	Latitude
049004	Lake Cargelligo (Booberoi)	1884	165	146.57	-33.67
049012	Eubalong PO	1884	160	146.47	-33.11
049019	Ivanhoe (Ivanhoe Post office)	1884	85	144.3	-32.90
049021	Ivanhoe (Wokabity)	1872	73	144.18	-33.03
049032	Mount Hope (General Store)	1885	223	145.88	-32.84
050004	Bogan Gate Post Office	1894	240	147.80	-33.10
050007	Condobolin (Borambil Park)	1868	215	147.28	-33.17
050008	Peak Hill	1890	275	147.87	-32.77
050014	Condobolin (Condobolin Ret. Vilage)	1881	220	147.15	-33.08
050020	Warroo (Geeron)	1889	210	147.53	-33.27
050031	Peak Hill (Peak Hill Post Office)	1890	267	148.19	-32.72
050036	Trundle Post Office	1899	255	147.71	-32.92
050037	Tullamore Post Office	1914	239	147.57	-32.63
050040	Ungarie Post Office	1896	227	146.97	-33.64
050044	West Wyalong Post Office	1895	255	147.18	-33.93
050045	Yalgogrin North (Roloma)	1887	315	146.83	-33.85
063000	Abercrombie Bridge	1931	435	149.3	-33.95
063007	Binda Post Office	1905	740	149.37	-34.32
063011	Borenor Post Office	1903	800	148.95	-33.25
063022	Cowra Agric. Research Station	1905	-	148.68	-33.78
063023	Cowra (Soil Cons. Service)	1943	381	148.68	-33.80
063029	Mandurama (Homeleigh)	1899	790	149.1	-33.75
063032	Golspie (Aystin)	1897	855	149.66	-34.28
063053	Millthorpe (Pilcher St)	1899	960	149.18	-33.45
063083	Trunkey Creek (Black Stump Hotel)	1890	860	149.32	-33.82
063093	Wombeyan Caves	1942	580	149.95	-34.3
063094	Bigga (Woolbrook)	1890	700	149.12	-34.0
063116	Bigga (Wyoming)	1940	650	149.14	-34.09
063267	Wyangala Dam	1929	351	148.94	-33.98
065006	Canowindra (Canowindra St)	1886	300	148.66	-33.57
065010	Cudal Post Office Agency	1884	440	148.74	-32.29
065013	Eugowra Post Office	1885	270	148.37	-33.43
065016	Forbes (Camp St)	1875	240	148.01	-33.39
065017	Garema	1933	229	147.93	-33.53
065019	Gooloogong Post Office	1889	265	148.43	-33.43
065020	Manildra Post Office	1893	438	148.70	-33.19
065023	Molong (Wellington St)	1884	560	148.86	-33.10
065026	Parkes (Mac Arthur St)	1889	324	148.16	-33.14
073000	Barmedman Post Office	1887	238	147.38	-34.15
073005	Binalong Post Office	1897	470	148.62	-34.67
073008	Caragabal	1916	-	-	-
073009	Cootamundra Post Office	1889	318	148.0	-34.63
073014	Grenfell Post Office	1885	384	148.16	-33.90

Source of data: Bureau of Meteorology (1998).

Appendix A: Continued.

Station Number	Station Name	Year start of record	Elevation (m)	Longitude	Latitude
073016	Harden (Bunaroo St)	1886	431	148.37	-34.55
073017	Green Thorpe (Iandra)	1890	440	148.37	-34.06
073018	Illabo Post Office	1903	268	147.73	-34.8
073021	Koorawatha Post Office	1903	341	148.55	-34.04
073022	Cootamundra (Land grove)	1891	460	148.17	-34.65
073023	Kangiara (Laverstock)	1902	560	148.78	-34.58
073025	Old Junee (Millbank)	1895	270	147.55	-34.78
073029	Murrumburrah (Old Post Office)	1884	370	148.35	-34.53
073032	Quandialla Post Office	1925	250	147.79	-34.01
073033	Bethungra (Retreat)	1896	322	147.68	-34.65
073036	Stockinbingal Post Office	1903	295	147.88	-34.50
073037	Temora (Barmedman Road)	1880	278	147.53	-34.43
073038	Temora (Agric. Research Station)	1934	270	147.53	-34.41
073041	Wombat (Tumbleton)	1888	530	148.18	-34.4
073043	Wallendbeen Post Office	1914	462	148.13	-34.52
073050	Bowning (Wanganui)	1907	560	148.8	-34.75
073054	Wyalong Post Office	1895	245	147.25	-33.93
073091	Oakhurst 1 (Wyalong)	1907		147.5	-33.9
073099	Junee Reefs (Clear Hills)	1898	290	147.62	-34.63
073100	Bumbaldry	1897	450	147.43	-33.91
073114	Sebastopol (Erin vale)	1889	315	147.53	-34.67
075007	Booligal (Belmont)	1890	95	144.91	-33.85
075018	Hat (Coorong)	1877	80	144.45	-34.22
075025	Goolgowi (Goolgowi Shire Council)	1930	123	145.71	-33.98
075027	Gubbata (Cooma St)	1937	192	146.55	-33.63
075030	Lake Cargelligo (Gunniguldrie)	1929	152	146.12	-33.23
075032	Hillston (Hillston Airport)	1881	122	145.52	-33.49
075039	Lake Cargelligo (Lake Cargelligo Apt)	1881	169	146.37	-33.28
075043	Lake Cargelligo (Merri-Merrigal)	1884	140	146.6	-33.4
075044	Merriwaga Post Office	1930	114	145.62	-33.8
075050	Naradhan (Marshall)	1880	192	146.32	-33.62
075057	Rankins Springs Post Office	1887	220	146.26	-33.84
075066	Tullibiguel Post Office	1924	245	146.07	-33.42
075069	Booligal (Ulonga)	1876	84	144.63	-34.08
075132	Lake Cargelligo (Wooyeo)	1906	169	146.3	-33.2

Source of data: Bureau of Meteorology (1998).

Appendix B

Wells used in the preparation of the geological cross-sections A-A' to I-I'.

Well No.	Location	Depth (ft)	Stratigraphic Column	Remarks
Geological cross-sections A-A' to G-G'				
10001	LA 301	100.00	100.00	100.00
10002	LA 302	102.00	102.00	102.00
10003	LA 303	105.00	105.00	105.00
10004	LA 304	110.00	110.00	110.00
10005	LA 305	115.00	115.00	115.00
10006	LA 306	120.00	120.00	120.00
10007	LA 307	125.00	125.00	125.00
Geological cross-sections H-H' to I-I'				
10008	LA 308	130.00	130.00	130.00
10009	LA 309	135.00	135.00	135.00
10010	LA 310	140.00	140.00	140.00
10011	LA 311	145.00	145.00	145.00
10012	LA 312	150.00	150.00	150.00
10013	LA 313	155.00	155.00	155.00
10014	LA 314	160.00	160.00	160.00
10015	LA 315	165.00	165.00	165.00
10016	LA 316	170.00	170.00	170.00
10017	LA 317	175.00	175.00	175.00
10018	LA 318	180.00	180.00	180.00
10019	LA 319	185.00	185.00	185.00
10020	LA 320	190.00	190.00	190.00
10021	LA 321	195.00	195.00	195.00
10022	LA 322	200.00	200.00	200.00
10023	LA 323	205.00	205.00	205.00
10024	LA 324	210.00	210.00	210.00
10025	LA 325	215.00	215.00	215.00
10026	LA 326	220.00	220.00	220.00
10027	LA 327	225.00	225.00	225.00
10028	LA 328	230.00	230.00	230.00
10029	LA 329	235.00	235.00	235.00
10030	LA 330	240.00	240.00	240.00

Appendix B: Wells used in the preparation of the geological cross-sections A-A' to I-I'.

Well ID	Owner Type	Surface elevation AHD (m)	Drilled depth (m)	Alluvium depth (m)
Geological cross-section A - A'				
36630	DLWC	226.90	91.00	86.00
39378	PWD	227.20	102.00	85.00
25116	Private	230.00	105.20	96.93
36632	DLWC	236.80	115.00	107.00
14994	Private	248.10	123.40	122.83
36631	DLWC	248.40	80.00	80.00
30675	Other govt	252.00	112.60	24.38
Geological cross-section B - B'				
56453	Private	227.85	45.70	1.20
36607	DLWC	218.10	85.00	80.00
29481	Private	212.00	150.88	119.88
36603	DLWC	211.85	77.40	75.00
1232	Private	223.90	56.08	90.00
3107	Private	222.50	60.96	98.34
1169	Private	225.95	102.41	105.00
2916	Private	223.10	61.57	110.00
2660	Private	221.00	76.20	108.00
36606	DLWC	232.08	110.60	110.00
2990	Private	248.70	151.18	68.58
26072	Private	248.80	120.40	67.06
30802	Private	251.50	119.00	76.00
27739	Private	258.00	129.54	48.77
36628	DLWC	266.00	98.50	97.00
25704	Private	270.00	60.96	30.48
29532	Private	285.00	122.83	38.00
31040	Private	300.00	60.96	20.00
Geological cross-section C-C'				
26045	Private	221.20	47.20	58.46
28038	Private	211.00	110.10	107.29
26047	Private	213.50	94.50	109.00
26048	Private	209.10	108.20	112.17
36597	DLWC	207.20	106.00	102.00
36595	DLWC	207.25	136.70	127.00
36610	DLWC	207.80	116.00	127.00
36596	DLWC	208.00	124.50	122.00
36611	DLWC	208.30	124.00	114.00
36700	DLWC	209.00	92.00	90.00

Appendix B: Continued.

Bore Number	Owner Type	Surface elevation AHD (m)	Drilled depth (m)	Alluvium depth (m)
Geological cross-section D-D'				
36529	DLWC	205.20	102.00	90.00
36524	DLWC	207.60	104.00	83.00
36594	DLWC	208.45	110.00	96.00
36553	DLWC	209.95	129.00	124.00
36609	DLWC	210.70	128.00	116.00
36612	DLWC	211.36	92.00	80.00
Geological cross-section E-E'				
36563	DLWC	207.40	60.01	47.00
31309	Private	207.50	87.48	85.34
36555	DLWC	208.60	64.00	50.00
36528	DLWC	209.95	100.00	100.00
36551	DLWC	211.00	124.01	124.00
36552	DLWC	210.05	125.00	123.00
36523	DLWC	212.10	140.00	130.00
36554	DLWC	211.90	93.00	80.00
26709	Private	215.80	106.38	104.24
Geological cross-section F-F'				
21276	Private	203.05	126.50	109.42
21213	Private	206.35	152.40	148.74
28743	Private	208.50	134.10	148.00
36085	DLWC	212.95	123.40	122.50
39307	Private	208.40	73.30	69.00
26710	Private	219.50	118.90	118.90
27924	Private	219.00	122.50	122.50
36525	DLWC	215.00	148.50	145.50
Geological cross-section G-G'				
53668	Local govt	168.00	66.40	70.00
59055	Private	168.00	77.40	73.66
25067	DLWC	184.00	135.94	129.84
26728	Private	180.00	132.30	131.06
36091	DLWC	194.00	27.10	83.21
25165	DLWC	202.21	117.30	123.00
36090	DLWC	211.00	126.40	123.80
36088	DLWC	208.65	103.60	89.90
36089	DLWC	209.60	94.40	88.30

Appendix B: Continued.

Bore Number	Owner Type	Surface elevation AHD (m)	Drilled depth (m)	Alluvium depth (m)
36526	DLWC	214.00	144.00	140.50
36521	DLWC	217.00	145.00	142.50
36525	DLWC	218.00	148.50	145.50
36079	DLWC	222.00	140.50	145.00
36527	DLWC	220.00	154.30	150.00
Geological cross-section H-H'				
25163	DLWC	198.60	91.40	87.00
25155	DLWC	200.30	107.60	120.00
25151	DLWC	202.80	146.30	142.04
25164	DLWC	203.60	136.60	131.00
25165	DLWC	201.20	134.10	123.00
25166	DLWC	204.80	34.10	18.29
25167	DLWC	204.30	39.60	23.16
29493	Private	206.20	59.44	59.44
25168	DLWC	204.50	135.60	106.00
50216	Private	206.00	31.40	30.00
16972	Private	206.00	25.90	28.00
Geological cross-section I-I'				
25082	DLWC	194.10	114.30	114.30
25081	DLWC	194.60	108.80	125.00
25067	DLWC	194.90	135.90	129.84
25030	DLWC	188.00	131.70	121.31
25102	DLWC	194.00	50.60	121.00

Appendix C

Shallow observation wells in the JWPID

Well ID	Well Name	Well Type	Depth (ft)	Location	Notes
1-W	10001	Observation	10	10001	
2-W	10002	Observation	15	10002	
3-W	10003	Observation	20	10003	
4-W	10004	Observation	25	10004	
5-W	10005	Observation	30	10005	
6-W	10006	Observation	35	10006	
7-W	10007	Observation	40	10007	
8-W	10008	Observation	45	10008	
9-W	10009	Observation	50	10009	
10-W	10010	Observation	55	10010	
11-W	10011	Observation	60	10011	
12-W	10012	Observation	65	10012	
13-W	10013	Observation	70	10013	
14-W	10014	Observation	75	10014	
15-W	10015	Observation	80	10015	
16-W	10016	Observation	85	10016	
17-W	10017	Observation	90	10017	
18-W	10018	Observation	95	10018	
19-W	10019	Observation	100	10019	
20-W	10020	Observation	105	10020	
21-W	10021	Observation	110	10021	
22-W	10022	Observation	115	10022	
23-W	10023	Observation	120	10023	
24-W	10024	Observation	125	10024	
25-W	10025	Observation	130	10025	
26-W	10026	Observation	135	10026	
27-W	10027	Observation	140	10027	
28-W	10028	Observation	145	10028	
29-W	10029	Observation	150	10029	
30-W	10030	Observation	155	10030	
31-W	10031	Observation	160	10031	
32-W	10032	Observation	165	10032	
33-W	10033	Observation	170	10033	
34-W	10034	Observation	175	10034	
35-W	10035	Observation	180	10035	
36-W	10036	Observation	185	10036	
37-W	10037	Observation	190	10037	
38-W	10038	Observation	195	10038	
39-W	10039	Observation	200	10039	
40-W	10040	Observation	205	10040	

Appendix C: Shallow observation wells in the JWPID.

Shallow observation wells*	EASTING (m)	NORTHING (m)	Elevation top of the well (m AHD)	Elevation natural surface (m AHD)	Depth (m)	Slotted interval (m)
1 W	558972	6308748	218.2	217.9	7.9	
2 W	558720	6307355	218.8	218.4	6.4	
3 P	558467	6306098	219.4	219.1	7.3	
3 W	558467	6306098	219.3	219.1	3.3	
3 AW	558534	6306007	219.5	219.1	3.7	
3B W	558506	6305923	218.7	218.5	7.7	
3C W	558470	6305793	218.4	218.0	7.5	
3D W	558546	6306050	219.8	219.5	4.3	
4 W	558348	6304821	216.9	216.6	7.3	
5 P	558157	6303758	216.8	215.9	19.2	
5 W	558157	6303758	216.8	215.9	3.8	
6 P	557874	6302033	216.1	215.2	26.5	
6 W	557874	6302033	216.0	215.2	5.1	
7 W	556183	6295736	213.7	213.4	10.9	
8 W	553203	6312768	214.1	213.8	6.4	
9 P	553006	6311162	214.2	213.4	12.8	
9 W	553006	6311162	214.1	213.4	7.7	
10 P	552893	6310429	213.3	212.6	14.6	
10 W	552893	6310429	213.3	212.6	4.4	
11 P	552581	6308397	212.8	212.6	12.2	
11 W	552581	6308397	212.8	212.6	4.9	
12 P	552370	6306972	213.2	212.6	16.5	
12 W	552370	6306972	213.2	212.6	6.8	
13 W	551927	6305468	213.4	213.1	4.9	
14 W	551783	6304542	216.6	216.4	4.9	
14A W	552979	6303309	214.2	214.0	4.2	
14B W	553020	6303475	214.4	214.2	2.3	
14C W	553067	6303666	215.0	214.7	4.4	
14D P	553078	6303835	215.5	215.3	8.8	
14D W	553078	6303835	215.5	215.3	3.1	
14E P	553143	6303867	215.8	215.5	6.1	
14E W	553143	6303867	215.9	215.5	5.0	
14F W	553185	6303964	217.0	216.7	6.1	
15 W	551519	6302835	214.3	214.0	5.4	
16 W	551307	6301588	212.6	212.3	5.4	
17 W	550608	6298384	212.4	212.1	9.3	
18 W	550353	6296779	210.7	210.4	6.0	
19 W	550453	6315438	212.2	211.9	6.5	
20 P	549540	6312688	212.3	212.0	6.8	
21 W	548991	6311451	211.3	211.1	6.5	
22 P	546053	6317584	209.2	208.9	12.4	
22 W	546053	6317584	209.2	208.9	5.6	
23 W	545716	6315302	209.4	209.1	6.4	
24 W	545188	6311719	209.7	209.5	8.0	
25 W	546990	6308673	210.8	210.6	6.1	
26 W	545851	6306587	210.1	209.8	5.0	
26A W	545851	6306431	210.1	209.8	3.7	
26B P	545815	6306224	210.2	209.9	6.1	

*W: Watertable wells; P: Piezometers

Appendix C: Continued.

Shallow Observation wells*	EASTING (m)	NORTHING (m)	Elevation top of the well (m AHD)	Elevation natural surface (m AHD)	Depth (m)	Slotted interval (m)
26B W	545815	6306224	210.2	209.9	4.0	
26C W	545790	6306085	210.6	210.2	4.6	
26D W	545765	6305880	211.3	211.0	4.9	
26E P	545739	6305705	211.9	211.6	8.2	
26E W	545739	6305705	211.9	211.6	4.6	
26F W	545717	6305536	211.3	211.0	4.3	
26G W	545685	6305380	212.4	212.0	3.4	
26H W	545636	6305083	211.8	211.5	4.3	
26I W	545608	6304940	212.3	212.0	4.3	
26J W	545603	6304799	213.1	212.8	3.7	
26K W	545583	6304723	214.0	213.7	2.7	
26L W	545572	6304531	214.0	213.7	2.7	
26M W	545553	6304340	212.2	212.0	5.5	
27 P	545590	6304647	213.4	213.1	7.8	
27 W	545590	6304647	213.4	213.1	3.4	
28 W	545322	6302937	211.3	210.9	5.2	
29 P	544522	6299469	208.8	208.5	8.8	
29 W	544523	6299469	208.8	208.5	5.7	
30 P	542252	6308779	207.6	207.3	10.8	
30 W	542252	6308779	207.6	207.3	3.3	
31 W	533319	6317760	202.9	202.6	4.5	
32 W	542074	6314078	209.2	208.9	6.9	
33 P	540886	6312118	207.5	207.2	16.0	
33 W	540886	6312118	207.5	207.2	5.0	
34 P	540747	6310543	207.1	206.1	11.7	
34 W	540747	6310543	207.0	206.1	6.0	
35 P	539538	6309356	206.7	206.5	14.9	
35 W	539538	6309356	206.7	206.5	5.2	
35B P	539101	6309420	206.8	206.5	0.0	
36 P	535140	6310080	202.8	201.6	9.5	
36 W	535140	6310080	202.9	201.6	2.7	
36A W	534829	6310326	205.1	204.8	5.8	
36B W	534414	6310666	205.0	204.6	5.8	
36C W	534203	6310703	204.3	203.6	5.8	
36D W	533789	6310772	205.1	204.7	6.1	
37 W	536037	6308579	205.8	205.5	5.4	
38 W	534198	6301032	207.6	207.3	10.2	
39 W	539161	6300309	208.6	208.4	4.9	
40 P	541051	6299388	210.4	210.1	12.2	
40 W	541051	6299388	210.4	210.1	6.0	
41 W	535011	6290083	206.1	205.8	7.2	
42 W	543750	6292228	209.1	208.8	8.7	
43 P	547283	6295851	208.9	208.5	7.9	
43 W	547283	6295851	208.8	208.5	4.7	
44 W	545329	6286801	207.8	207.5	8.7	
45 W	551568	6285778	210.0	209.6	11.8	
46 W	553730	6290631	212.1	211.8	10.7	

*W: Watertable wells; P: Piezometers

Appendix C: Continued.

Shallow Observation wells*	EASTING (m)	NORTHING (m)	Elevation top of the well (m AHD)	Elevation natural surface (m AHD)	Depth (m)	Slotted interval (m)
47 P	556050	6279565	209.5	209.2	7.0	
47 W	556050	6279565	209.5	209.2	5.9	
48 W	559029	6284144	211.7	211.4	13.5	
50 W	551121	6281522	208.6	208.3	11.7	
51 P	569361	6303122	223.4	223.1	15.2	
51 W	569361	6303122	223.4	223.1	10.4	
52 W	563959	6305331	219.8	219.6	9.7	
53 P	567148	6306213	216.5	216.2	21.0	
53 W	567148	6306213	216.5	216.2	9.8	
54 W	567096	6302590	220.5	220.2	4.6	
55 W	566954	6301246	220.0	219.6	3.7	
56 W	565629	6298756	219.3	219.0	5.2	
57 W	562989	6304058	219.0	218.7	8.5	
58 P	562094	6302213	217.1	216.8	11.0	
58 W	562094	6302213	217.1	216.8	5.1	
59 W	561908	6301271	219.1	218.8	12.6	
60 P	562081	6298889	216.8	215.2	9.5	
60 W	562081	6298889	216.8	215.2	6.3	
61 W	562040	6297507	216.9	216.6	9.6	
62 W	559172	6294512	215.3	215.0	9.5	
63 W	558154	6294597	214.8	214.5	11.0	
64 W	532487	6317865	201.7	201.4	4.3	
64A W	532407	6317745	199.0	198.3	0.0	
65 W	531430	6317439	199.5	199.2	5.0	
65A P	531430	6317439	200.1	199.6	0.0	
66 W	532454	6315915	201.1	200.8	3.4	
91 P	531147	6320073	202.2	201.9	9.8	
91 W	531147	6320073	202.1	201.9	3.0	
92 W	530947	6318811	202.5	202.2	11.5	
93 W	527564	6318985	201.9	201.5	12.5	
94 W	527367	6317854	201.7	201.4	6.0	
95 W	529328	6318987	203.7	203.4	10.2	
96 W	527407	6320875	203.6	203.3	9.0	
97 W	535595	6316167	202.1	202.0	5.5	
98 W	534410	6315913	202.3	202.1	6.0	
99 W	537311	6314908	204.0	203.7	4.5	
100 W	537075	6312937	204.2	203.9	6.5	
101 W	536004	6313055	203.2	202.9	7.5	
102 W	534927	6320038	205.1	204.8	13.0	
103 W	535013	6321634	202.9	202.6	15.0	
104 W	535229	6317581	205.3	204.9	7.5	
105 W	537450	6317084	206.0	205.7	10.0	
106 W	531231	6322056	201.9	201.6	7.5	
107 W	534674	6312237	203.3	203.0	7.5	
108 W	536900	6311350	204.6	204.4	7.0	
1	544935	6271045	208.6	208.1	18.0	8-18
2	540625	6271010	211.0	210.4	18.0	8-18
3	538475	6274650	209.7	209.1	18.0	8-18

*W: Watertable wells; P: Piezometers

Appendix C: Continued.

Shallow observation wells*	EASTING (m)	NORTHING (m)	Elevation top of the well (m AHD)	Elevation natural surface (m AHD)	Depth (m)	Slotted interval (m)
4	545550	6276225	208.3	207.8	18.0	8-18
5	549200	6276625	208.2	207.5	18.0	8-18
6	553575	6276225	208.9	208.4	18.0	8-18
7	554225	6280775	210.1	209.6	18.0	8-18
8	549500	6281750	208.8	208.3	18.0	8-18
9	545700	6282325	208.2	207.7	18.0	8-18
10	543375	6284225	208.6	208.1	18.0	8-18
11	536800	6282925	208.4	207.9	18.0	8-18
12	532875	6290150	209.5	208.9	18.0	8-18
13	538750	6289800	207.3	206.6	18.0	8-18
14	542575	6289400	208.7	208.2	18.0	8-18
15	549075	6289575	209.3	208.8	18.0	8-18
16	553425	6288550	211.1	210.6	18.0	8-18
17	549800	6294450	210.7	210.1	18.0	8-18
18	540075	6295150	209.3	208.7	18.0	8-18
19	534425	6295900	207.2	206.5	18.0	8-18
20	532375	6295450	208.9	208.4	18.0	8-18
21	562282	6283950				8-18
22	558692	6281870				8-18
23	556101	6275250				8-18
24	536221	6305920				8-18
25	539951	6306260				8-18
26	556743	6302060				8-18
27	561647	6292940				8-18
28	556610	6297840				8-18
29	561780	6286740				8-18
30	557023	6290040				8-18
RA341**	537336	6277603				14-22
P331**	537367	6278052				25-27
D323**	537852	6278049				82-94
P414A**	535250	6276498				22-34
P414B**	535247	6276497				10-16

*W: Watertable wells; P: Piezometers

Observation wells 1-30 are piezometers slotted at 8-18 m interval.

** Piezometers installed by the North Mining Ltd.

Appendix D: Regional observation wells in the study area.

Bore no.	Location *	Year installed	Drilled depth (m)	Water bearing zone (m)	Slotted/ screened depth (m)	Slot no.	Elevation (m AHD)	Tested yield (L/s)	Geology
36630	A	1986	91.0	86 - 91	86 - 89	1	230.6		slate
36632	A	1987	115.0	97.5 - 98.5 103 - 105	87 - 91	1	241.9	24.87	sand sand
36735	A	1987	62.0		26-32 41-46	1 2	240.2 240.2		clay + sand sandstone
36737	A	1987	62.0		46-51	1	256.9		gravel
36738	A	1987	86.0		29-33 74-81	1 2	265.4 265.4		sand
36739	A	1987	72.5		22-25	1	276.0		sand
30252	B	1980	109.1	59.1-60 64.9-66.4 71.6-73.1	59.1-60 64.9-66.4 71.6-73.1	1 2 3	246.2 246.2 246.2	0.13 0.63	gravel sand sand
30270	B	1980	110.0	51-5-52.1 57.9-59.4			249.4 249.4	0.00 0.13	sand sand
30291	B	1980	96.0	7.6-8.1	7.3-8.2	1	265.9	0.00	sand
30328	B	1980	18.3	7.9-8.5 11.6-12.5	7.9-8.5 11.6-12.2	1 2	268.3 268.3	0.13 0.19	gravel clay
30331	B	1980	18.3	8.2-9.7	8.2-9.7	1	270.6	0.19	sand
36603	B	1985	77.4	66.4 - 71	67 - 71	1	218.9	0.08	quartzite
36604	B	1985	118.1	96-105	98-100 100-102	1 2	223.3 223.3	22.23	?
36605	B	1985	115.0	80-90	86-102	1	219.9		clay
36606	B	1985	110.6	89 - 106	99 - 105	1	233.3		sand+gravel
36627	B	1986	126.5	118-124	118-124	1	242.5		sand
36628	B	1986	98.5	22 - 28 61 - 68.5	24 - 27 61 - 67	1 2	264.9 264.9		sand sand
36629	B	1986	55.0	38.-40	38-40	1	246.9		clay
36741	B	1987	109.0		29.5-35.5 65-73 76-93	1 2 3	265.1 265.1 265.1	0.50 1.00	sand sand sand
36776	B	1988	100.0	61-65	60-66	1	307.8	0.00	sand
36777	B	1988	102.0		17-22 50-54 62-80	1 2 3	305.3 305.3 305.3		sand sand sand
36778	B	1988	103.0	25-30 60-66 80-85	24-30 60-66 79-85	1 2 3	312.3 312.3 312.3	0.00 0.28 0.33	
36779	B	1988	97.0	52-56 74-89	50-56 70-88	1 2	313.1 313.1	0.33 1.80	sand sand
39379	B	1987	111.0	61-62 73-76 94-100			223.4 223.4	9.60 28.50	
36825	C	1989	89.0		43-49	1	221.0		clay
36610	C	1985	116	64-68	64-68	1	209.3		sand
36611	C	1985	124	105-114	106.5- 112.5	1	209.1		sand

* Letters A to I correspond to the geological cross-sections in Chapter 4

Appendix D: Continued.

Bore no.	Location *	Year installed	Drilled depth (m)	Water bearing zone (m)	Slotted/ screened depth (m)	Slot no.	Elevation (m AHD)	Tested yield (L/s)	Geology
36613	C	1985	84.0	34-45	35-45	1	213.4	0.50	ironstone
36700	C	1987	92		65-75	1	209.0		clay
36595	C	1985	136.7	82-90	84.7-86.5	1	209.3	1.10	ironstone
36596	C	1985	124.5	64-66	64-65.5	1	208.0		sand
				85.5-93	85-87	2	208.0		sand + clay
36597	C	1985	106	78-84	78-84	1	209.8	0.00	clay
				95 - 98.5	95 - 98.5	2	209.8	1.50	sand
36594	D	1985	110.0	11-15	11-15	1	208.8		clay
				69-72	69-71	2	208.8		clay
36524	D	1984	104.0	17-17	15-17	1	207.4		sand
36553	D	1985	129.0	117.5-124	118-126	1	210.0		sand
36609	D	1985	128.0	97-116	106-113	1	210.9		sand
36563	D	1985	60.0	19-21.3	19-21	1	207.6		sand
36551	E	1985	124.0	4-5					sand
				11-12.3					sand
				28.5-30	28-30	1	208.6		sand
				33-34.7					sand
				55-58					sand
				58.1-62.9	60-63	2	208.6	39.43	sand
				64-66.3					sand
				67-70.1					sand
36552	E	1985	125.0	25.1-37.5	32.5-36.5	1	210.4	1.00	clay+sand
				62.3-67.9	64-70	2	210.4	0.38	gravel+clay
				100.5-108.4	101-106	3	210.4	1.26	sand+clay
36554	E	1985	93.0	11-15	12.8-15.2	1	211.8	1.51	sand+clay+gravel
				42-44	43.3-46.3	2	211.8	1.51	sand + clay
				56-59	55.8-59.7	3	211.9	0.36	sand + clay
36523	E	1984	140.0	10.5-11.6					clay
				32.5-36.3	33-36.3	1	212.1		sand
				58-62.3	59-62.3	2	212.1		sand
				108-126.8	112-118	3	212.1	42.90	sand
				127.5-129.8					gravel+sand
				130-131.8					sand
36528	E	1985	100.0	10-13.7	10-13.7	1	210.6		sand
				31.7-33					sand
				38.-39.5					gravel
				49-52	49-52	2	210.6		sand
				60-66.5	62-66.5	3	210.6		sand+gravel
36550	F	1985	122.0	26.3-31.9	26-29	1	207.1	0.31	sand
				44.3-64.5	46.-56	2	207.1	0.35	clay/sand
				105-114	108-114	3	207.1	0.31	clay+sand
36085	F	1977	123.4	38.7-44.8	38.7-44.8	1	213.0	1.50	gravel+clay
36086	F	1975	128.0	45.7-48.7	45.7-48.7	1	216.5	0.40	gravel

* Letters A to I correspond to the geological cross-sections in Chapter 4.

Appendix D: Continued.

Bore no.	Location *	Year Installed	Drilled depth (m)	Water bearing zone (m)	Slotted/ screened depth (m)	Slot no.	Elevation (m AHD)	Tested yield (L/s)	Geology
36525	F	1984	148.5	93-99	93-99	1	222.6	0.63	sand
36030	F	1976	60.9	13.7-19.8	13.7-19.8	1	229.6	1.43	gravel
				27.4-33.5	27.4-33.5	2	229.6	1.30	gravel
36081	F	1975	108.2	28.9-36.6	28.9-36.6	1	219.1	1.58	gravel
				79.2-83.9	79.2-83.3	2	219.2	0.21	clay
				94.5-97.5	94.4-97.5	3	219.2	0.65	clay
36526	G	1984	144.0	72.0-82.5	72.0-82.0	1	216.2	0.37	sand+gravel
				130.0-136.0	131.0-136.0	2	216.2	0.37	sand+wood
36080	G	1976	79.2	3.1-9.1					
				12.2-15.2	12.1-15.2	1	222.2	1.36	
				13.7-16.5					
				18.3-19.5					
				26.2-29.3					
				32-36.3	33.2-35.6	2	222.2	1.11	
				38.1-42.4					
				48.2-50.3					
				59.4-63.1	60.3-62.4	3	222.2	0.91	
36079	G	1976		3.5-4.5					seep clay
				22.0-28.0	22.0-28.0	1	225.5	0.70	gravel
				70.1-79.2	70.1-76.2	2	225.3	1.67	gravel
				91.4-97.5	91.4-97.5	3	225.4	1.67	gravel
				106.6-115.8	106.4-115.4	4	225.3	1.20	gravel
				128.0-137.6	124.5-133.6	5	225.3	1.88	gravel
36082	G	1976	60.9	16.8-17.8	16.7-17.9	1	219.7	1.67	
				25.6-27.7	25.6-27.7	2	219.7	1.88	
				39-41.4	39-41.4	3	219.7	1.50	
36083	G	1976	64.0	12.8-14	12.8-14	1	215.6	1.11	
				36.5-38.4	36.5-42.6	2	215.6	0.48	
				43.5-45.4	43.5-45.4	3	215.8	1.67	
36087	G	1976	138.7	30.4-36.5	30.4-36.5	1	210.2	1.20	
				81.6-87.7	81.6-87.7	2	209.9	1.36	
				121-128	121-128	3	209.9	1.50	
36088	G	1975	103.6	67-73	67-73	1	208.5	1.50	
				85.3-91.4	85.3-91.4	2	208.7	4.55	
36089	G	1975	94.4	50.2-53.1	50.2-53.1	1	210.7	1.50	
				85.3-88.3	85.3-88.3	2	210.8	0.97	
36090	G	1975	126.4	85.3-91.4	85.3-91.4	1	205.9	0.81	gravel
				115.2-121.3	115.2-121.3	2	205.6	1.00	sand
36091	G	1976		20.1-23.4	20.4-23.4	1	201.1		gravel

* Letters A to I correspond to the geological cross-sections in Chapter 4.

Appendix D: Continued.

Bore no.	Location *	Year installed	Drilled depth (m)	Water bearing zone (m)	Slotted/ screened depth (m)	Slot no.	Elevation (m AHD)	Tested yield (L/s)	Geology
36521	G	1984	145.0	16.1-18.0 26.0-28.0 100.0-102.8 121.5-123.5 124.0-142.5					sand sand sand sand sand
21301	G	1968	25.9	7.6-8.2 19.5-22.8 27.7-27.7				0.00 0.13 0.19	sand sand gravel
21302	G	1968		10-10.6 12.8-14.3 15.8-18.2 31.3-40.4 41.7-43.5	24.3-25.8	1	188.3	0.38 0.76 1.52 1.89	clay sand and gravel gravel and sand sand and gravel
25151	H	1969	146.3	41.7-43.5 51.5-56.3 58.8-70.9 74.9-123.9 10.9-13.3 33.8-34.7 38.1-38.7 44.1-46.5 55.1-56.0 80.1-93.5 97.5-111.2	51.8-53.3 53.3-56.3 61.8-70.9 10.9-13.3	1 2 3 1	189.3 189.3 189.3 202.8	0.38 0.38 0.76	gravel and sand sand and gravel sand and gravel sand
				111.1 128.0-138.0	100.5-111.1 130.4-138.0	4 5	202.8 202.8	16.85 24.96	sand sand+gravel sand sand
25155	H	1969	107.6	8.8-10.3 13.4-13.7 13.7-21.3 37.7-38.9 41.7-3.5 55.7-57.8 77.4-88.3	9.1-10.3 14.6-21.3	1 2	200.3 200.3	0.51 0.38 0.51 0.51 0.63 0.76 1.14	sand sand sand sand sand sand sand
25163	H	1969	91.4	9.1-12.1 16.1-19.1	10.3-12.1	1	198.6 198.6	0.63 0.51	sand sand
25164	H	1969	136.6	12.4-13.0 20.7-24.3 53.9-57.5 69.4-71.5 88.0-99.2 115.5-127.9	21.3-24.3	1	203.6 203.6 203.6 203.6 203.6	0.38 0.38 0.76 32.08 41.05	sand sand sand sand sand sand
25165	H	1969	134.1	23.1-25.2 33.2-36.8	23.7-25.2	1	202.1		sand Sand

* Letters A to I correspond to the geological cross-sections in Chapter 4

Appendix D: Continued.

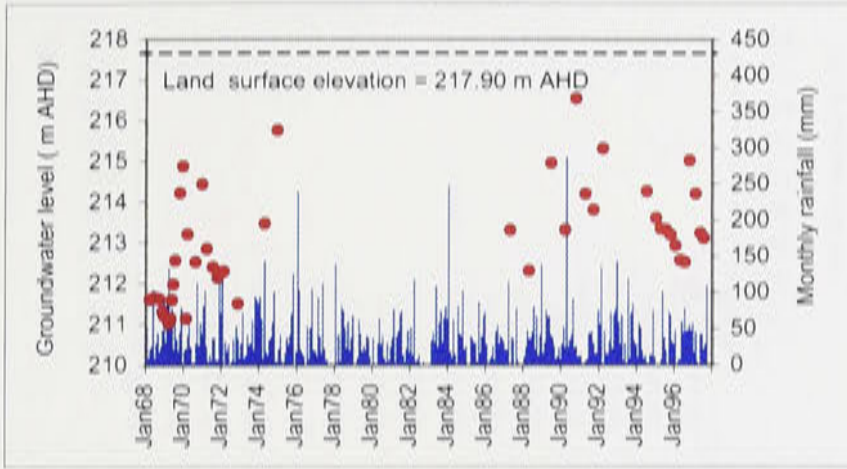
Bore no.	Location *	Year installed	Drilled depth (m)	Water bearing zone (m)	Slotted/ screened depth (m)	Slot no.	Elevation (m AHD)	Tested yield (L/s)	Geology
				60.0-72.4	60.9-70.0	2	202.1	4.96	Sand
				111.2-117.2	110.9-117.9	3	202.1	0.25	Sand
25166	H	1969	34.1	14-16.4	14.16.4	1	204.8	0.76	
25167	H	1969	39.6		10-10.9	1	204.3	0.38	
				18.2-19.4	18.2-19.4	2	204.3		
25168	H	1969	135.6	13.4-14.9	13.4-14.9	1	204.5	1.52	
25030	I	1968	131.7	13.01-14.3	13.1-14.3	1	194.7	0.76	sand
				24.3-26.4					sand
				32.9-37.1	35.9-37.1	2	194.7	0.38	sand
				34.0-66.7					sand and clay
				84.7-85.9					clay
				92.0-94.7	92.9-94.4	3	194.7	0.38	sand
				105.1-110.2					sand and gravel
25067	I	1968	135.9	9.1-14.2					clay
				25.9-26.5					clay
				27.4-8.3					clay and sand
				31.-32.5					sand and gravel
				41.1-42.6	41.1-42.6	1	194.9	0.38	sand and gravel
				67.3-68.5					sand and gravel
				79.2-79.9					sand and gravel
				92.3-119.0	100.5-103.5	2	194.9	0.38	sand and gravel
				115.5-127.9					sand and gravel
25081	I	1968	108.8	8.2-10.0					clay
				17.0-18.2					clay
				26.5-27.4	26.5-27.4	1	194.6	0.38	sand
				33.5-34.4					sand
				48.1-49.6					sand
				56.0-57.2					sand
				64.0-66.1					sand
				70.4-74.6					sand
				89.9-92.9	89.9-92.9	2	194.6	0.76	sand
25082	I	1968	114.3	8.5-9.7					sand
				15.8-17.6					sand
				24.9-27	24.9-27.0	1	195.3		sand
				29.8-31.9					sand
				35.6-38.3					sand+gravel
				41.1-42.6					sand
				49.0-51.7					sand
				56.3-59.9	57.9-60.0	2	195.3	0.38	sand
25102	I	1968	50.6	9.1-10.3					clay
				31.3-31.9					sand
				39.0-39.3	39.0-40.2	1	194.1	0.38	sand
25103	I	1968	90.5	10.6-13.6					
				19.5-21	19.5-21	1	194.8	1.01	

* Letters A to I correspond to the geological cross-sections in Chapter 4.

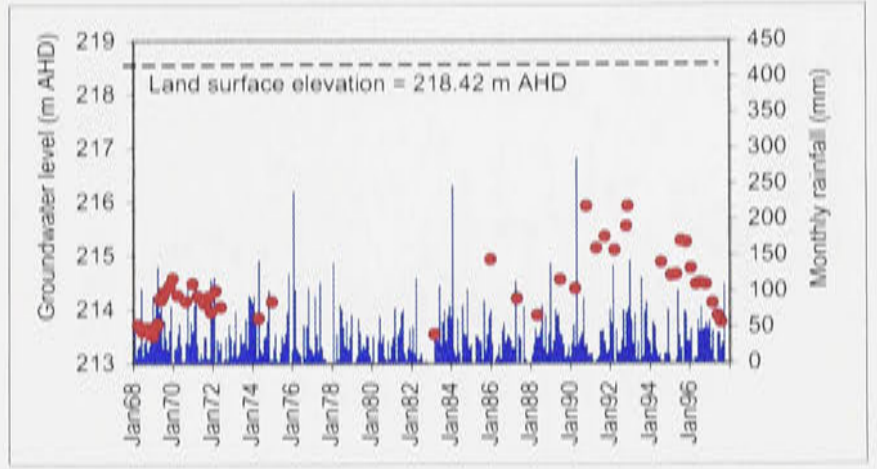
Appendix E

Hydrographs of the shallow observation wells in the JWPID

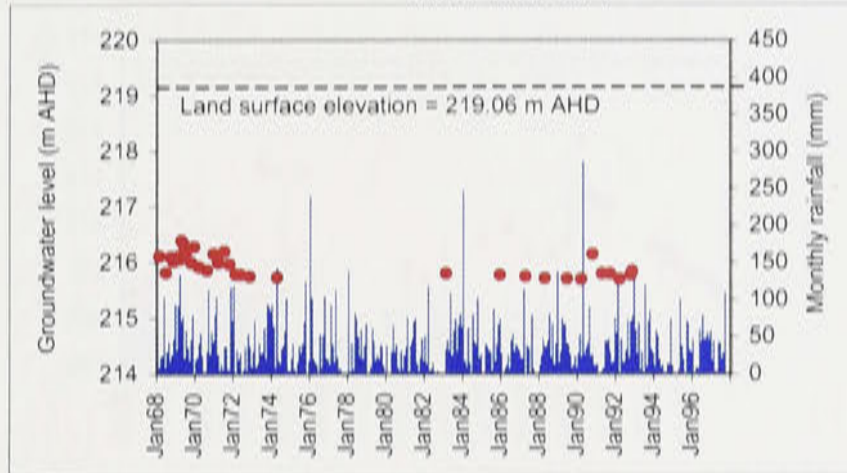
Well no. 1 W



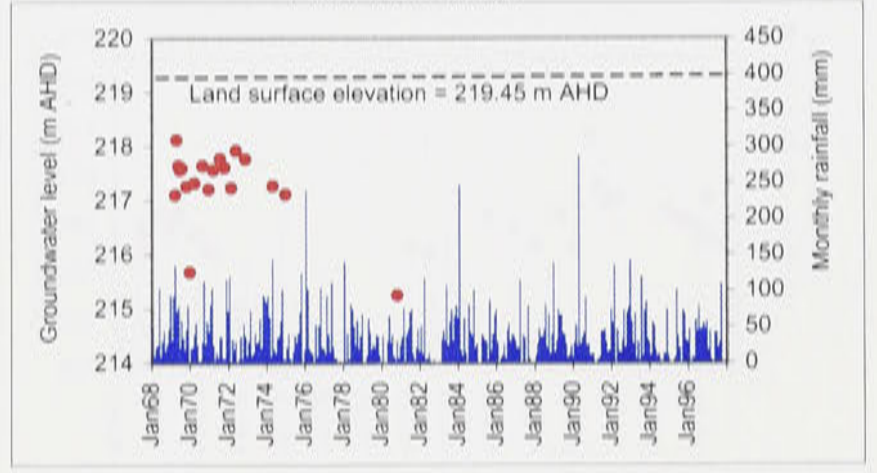
Well no. 2 W



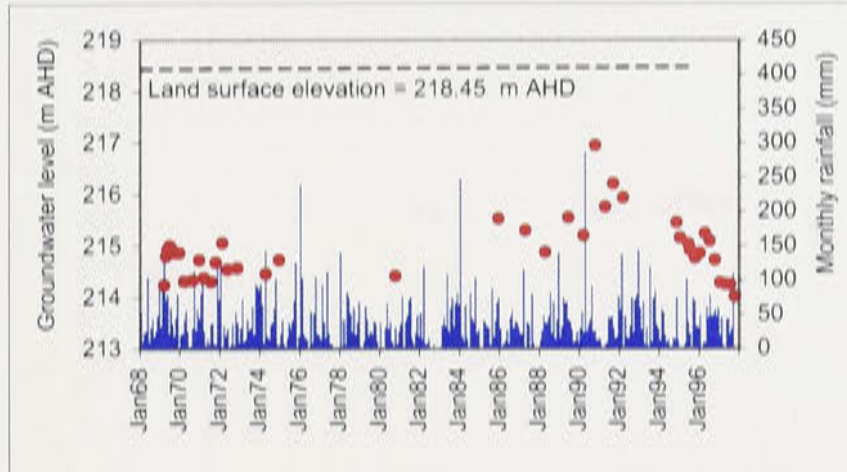
Well no. 3W



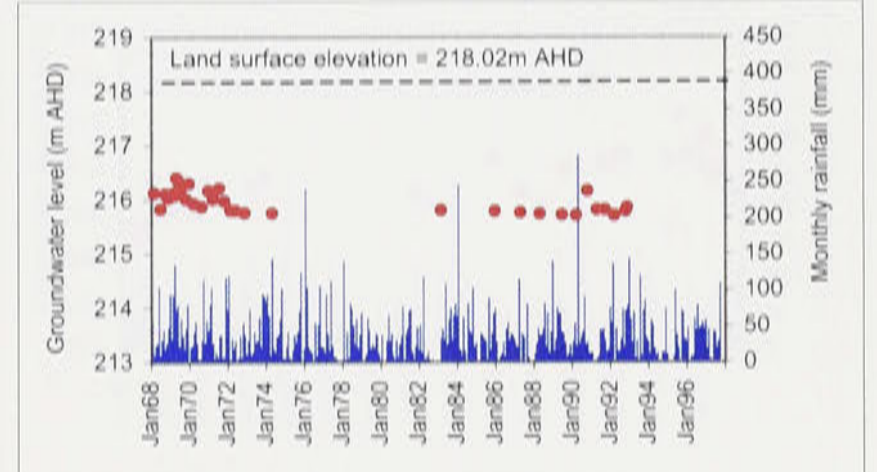
Well no. 3AW



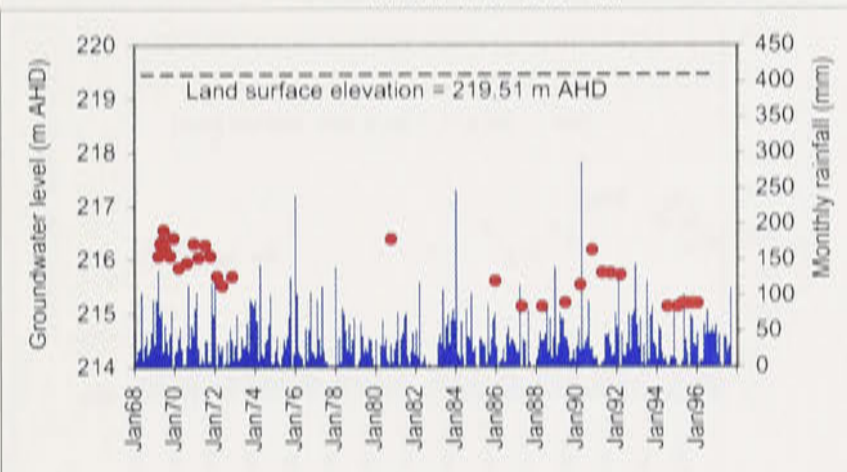
Well no. 3B W



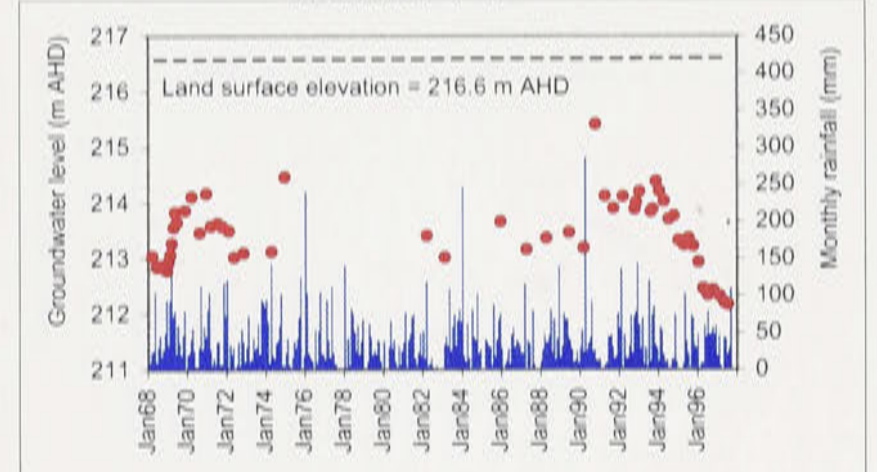
Well no. 3C W



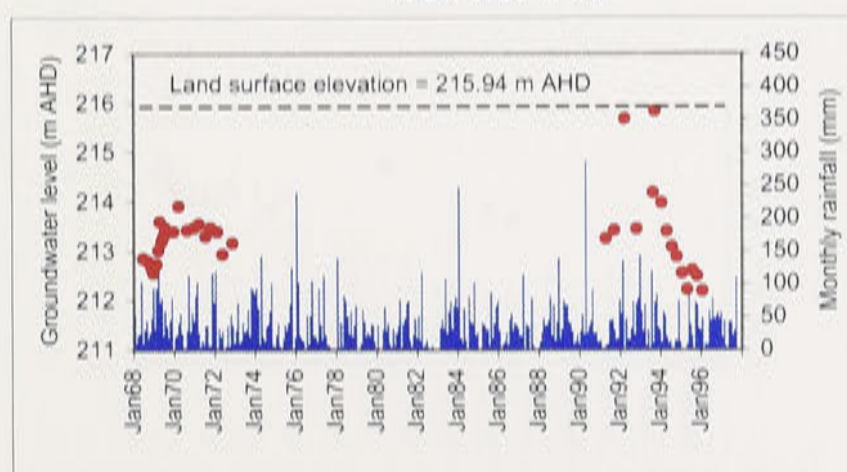
Well no. 3D W



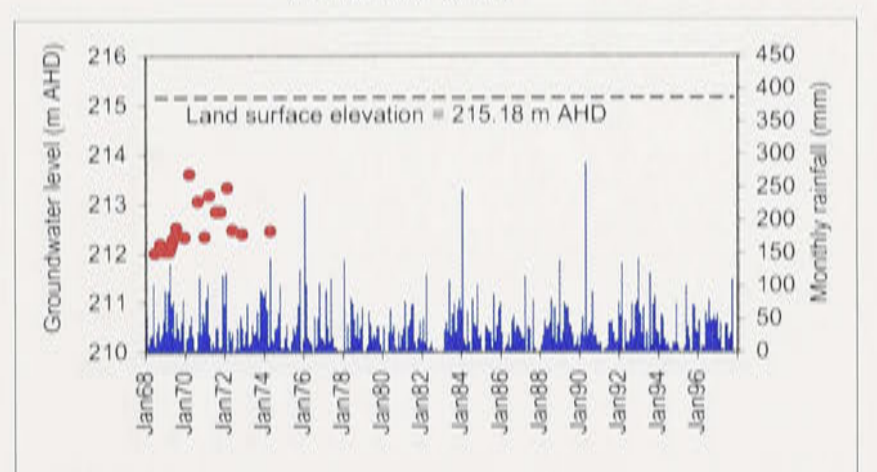
Well no. 4 W



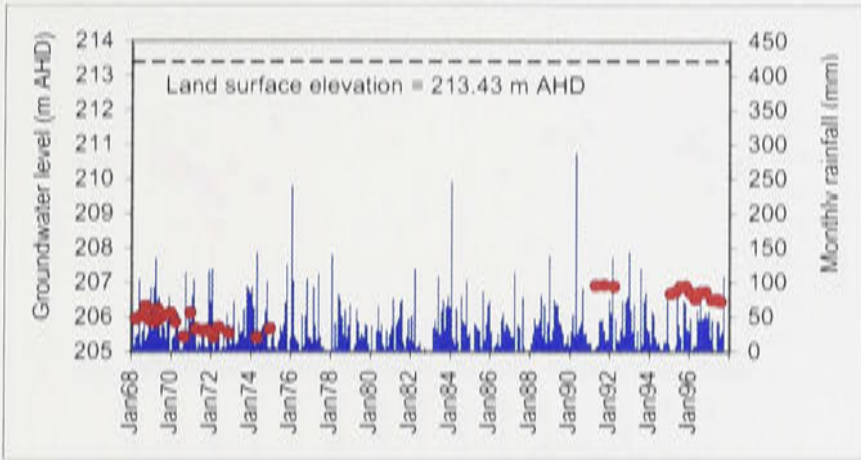
Well no. 5 W



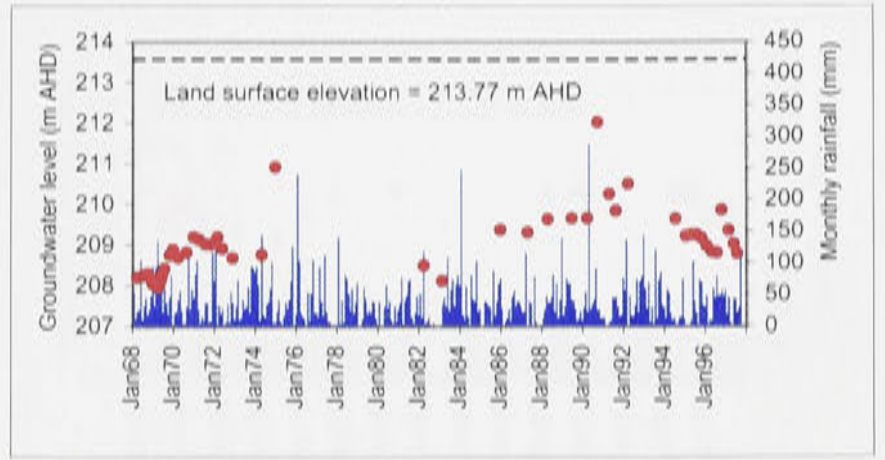
Well no. 6 W



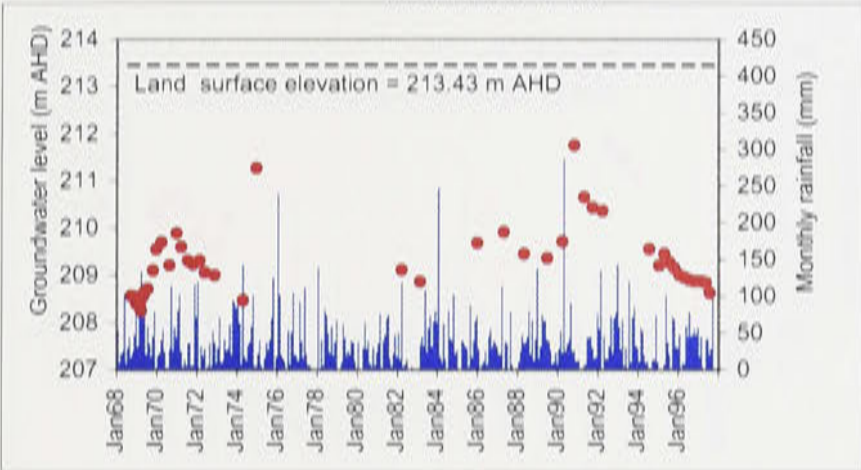
Well no. 7 W



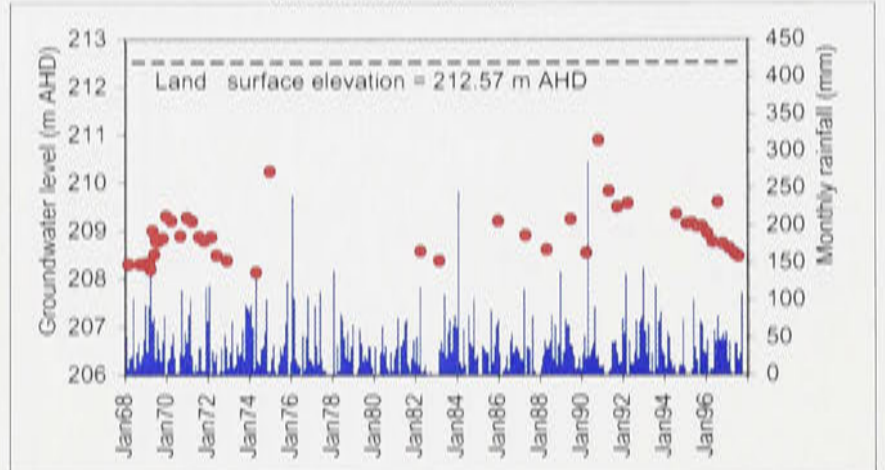
Well no. 8 W



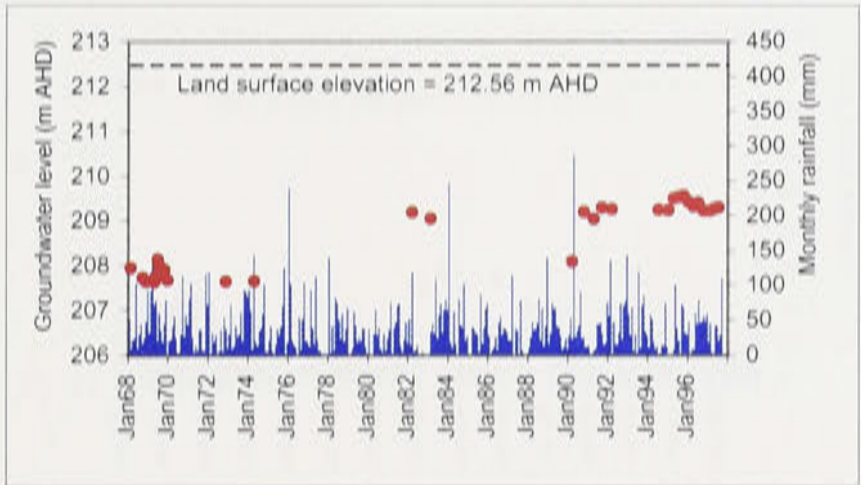
Well no. 9 W



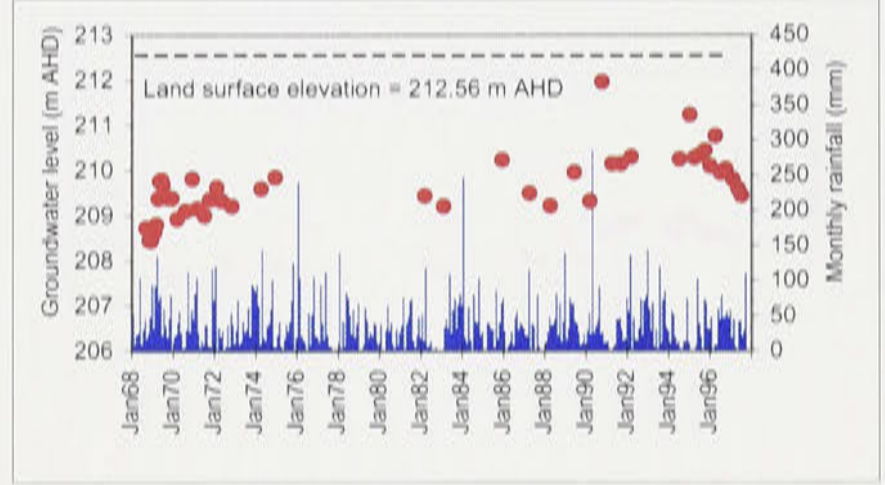
Well no. 10 W



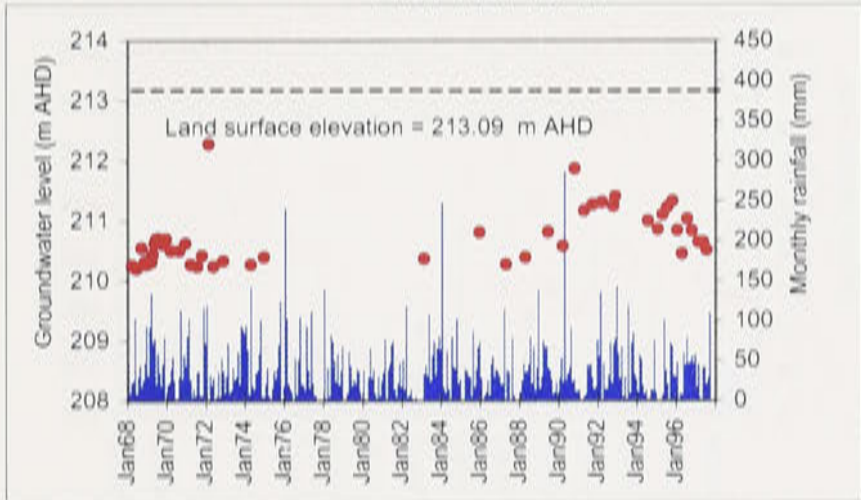
Well no. 11 W



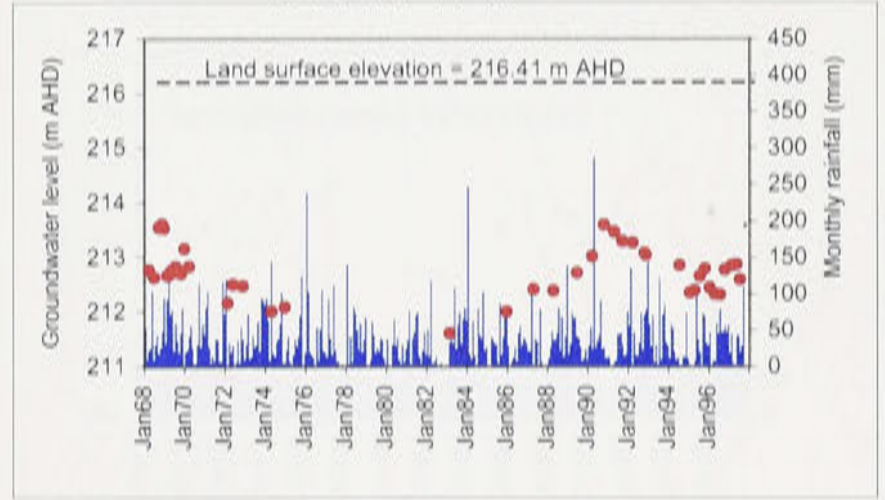
Well no. 12 W



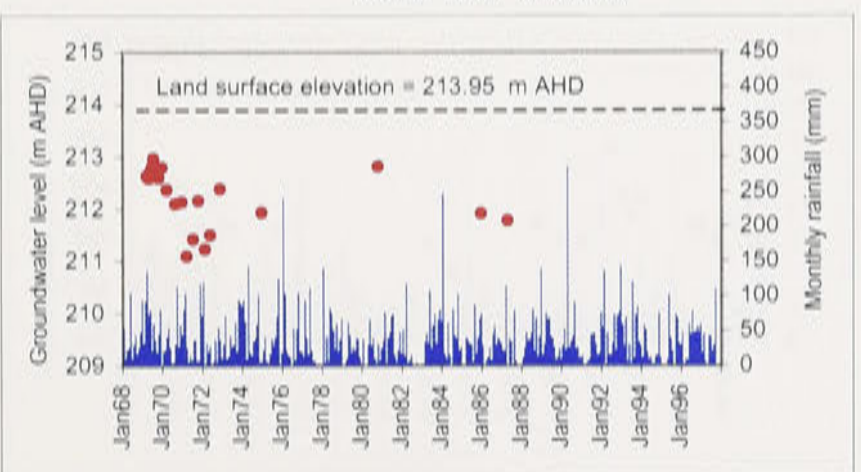
Well no. 13 W



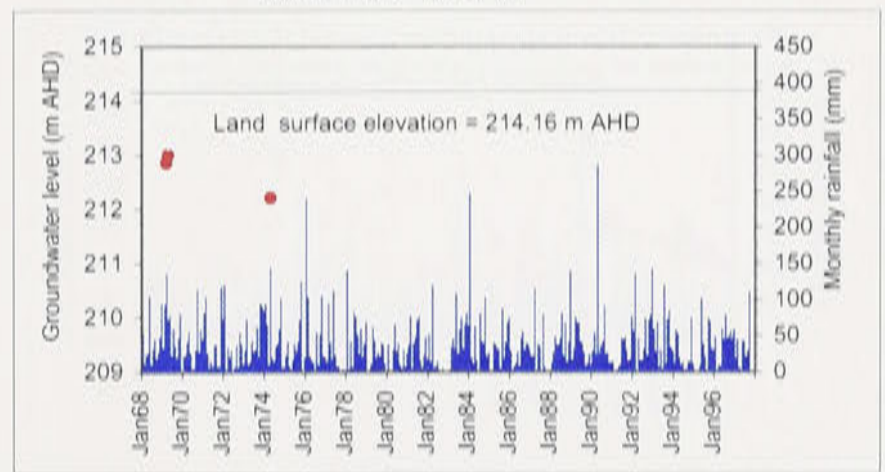
Well no. 14 W



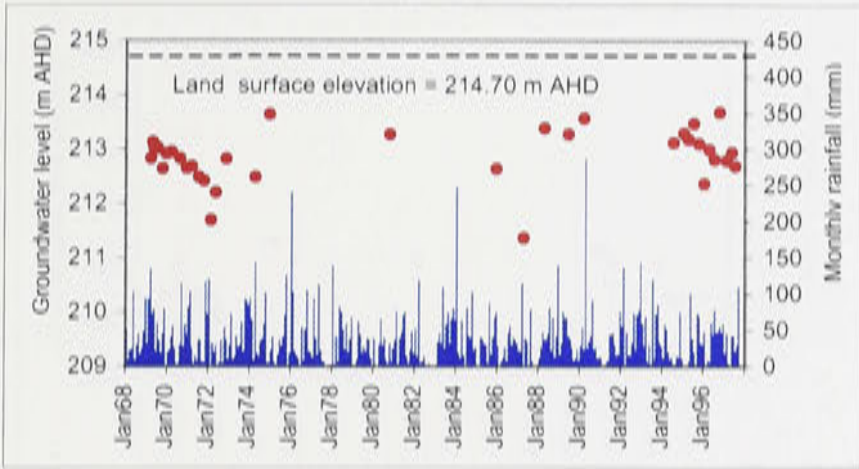
Well no. 14A W



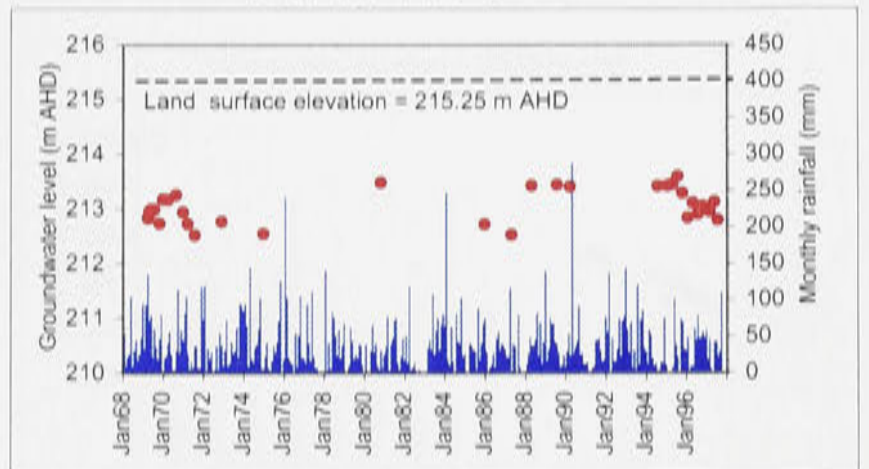
Well no. 14B W



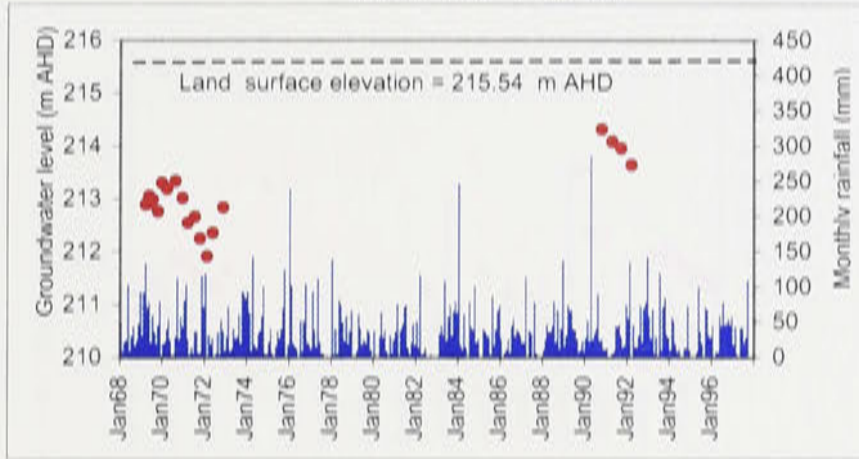
Well no. 14C W



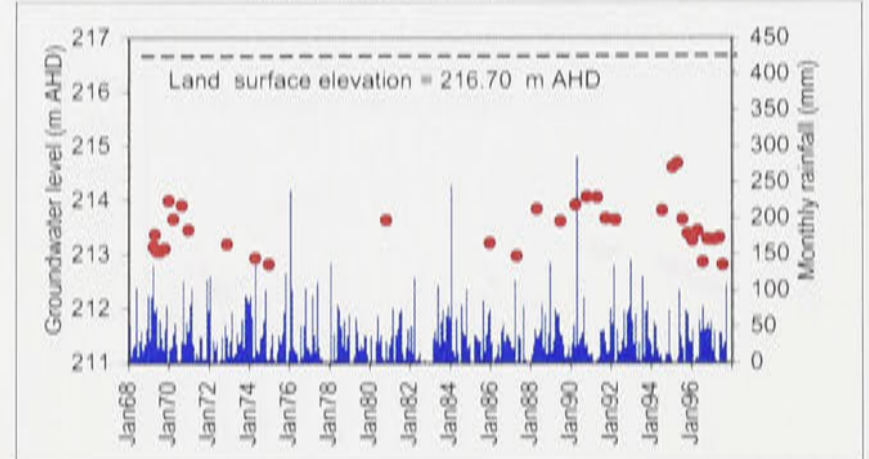
Well no. 14D W



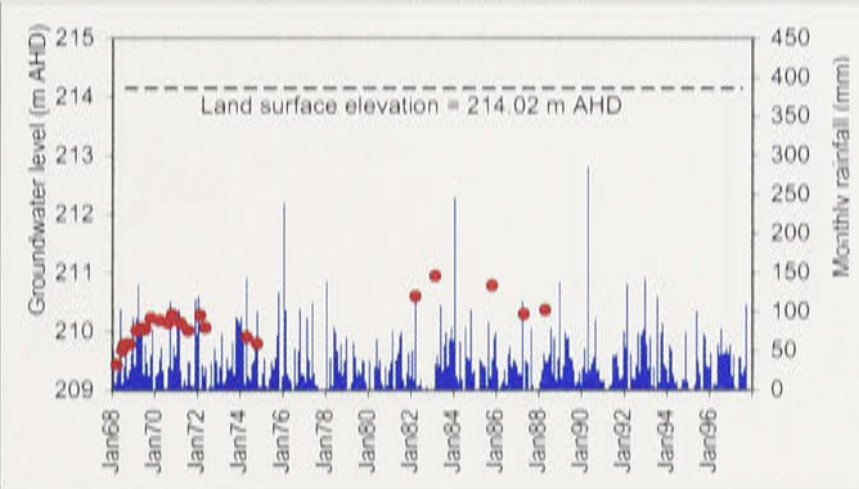
Well no. 14E W



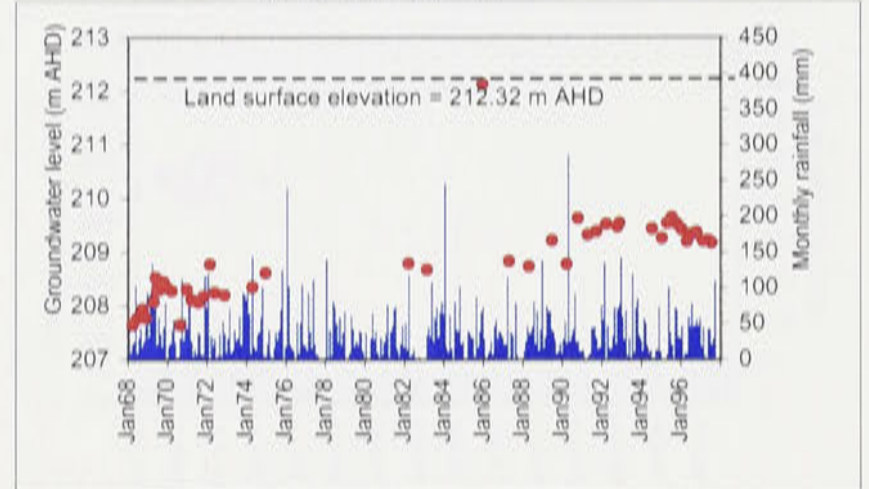
Well no. 14F W



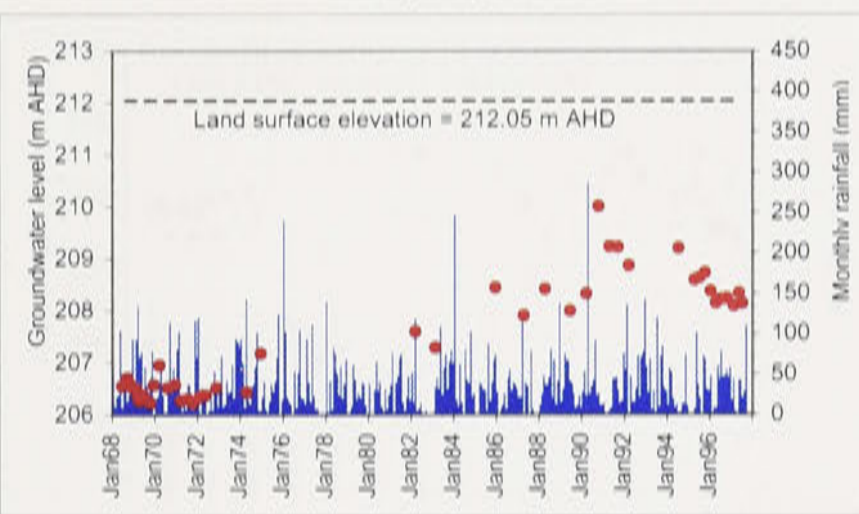
Well no. 15 W



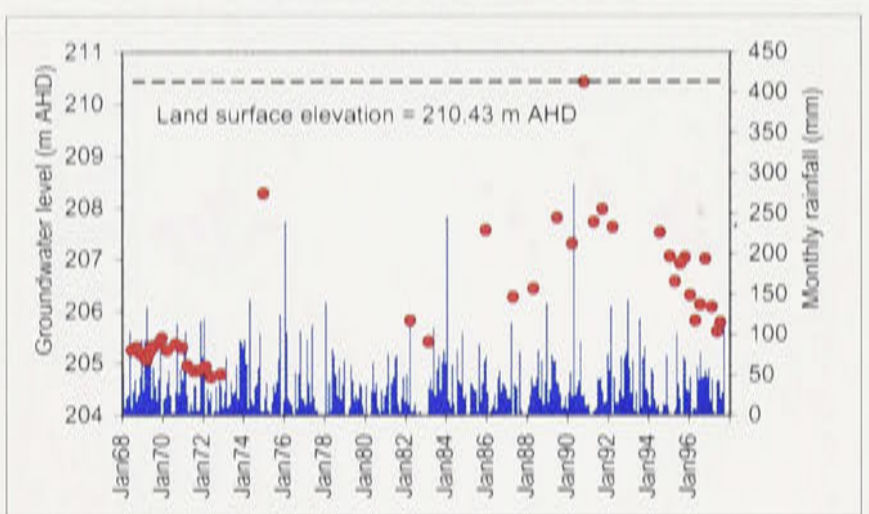
Well no. 16 W



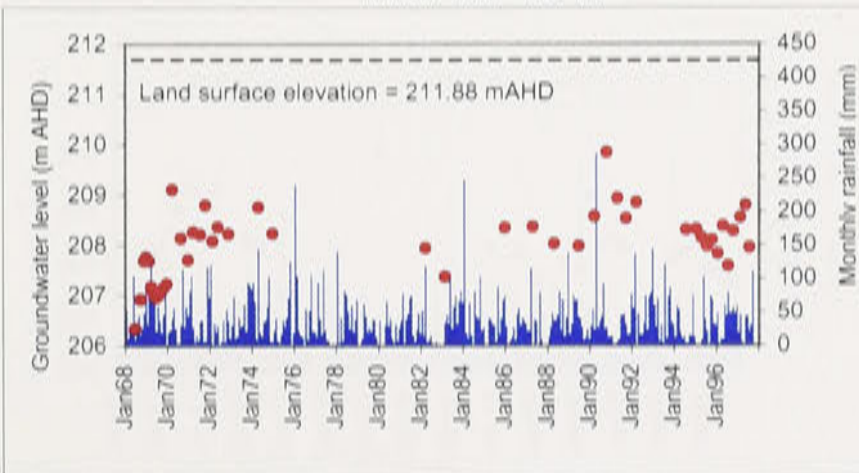
Well no. 17 W



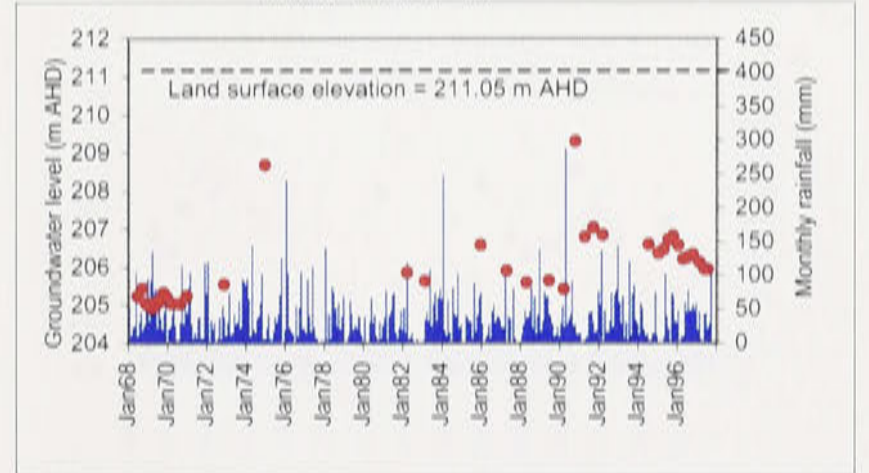
Well no. 18 W

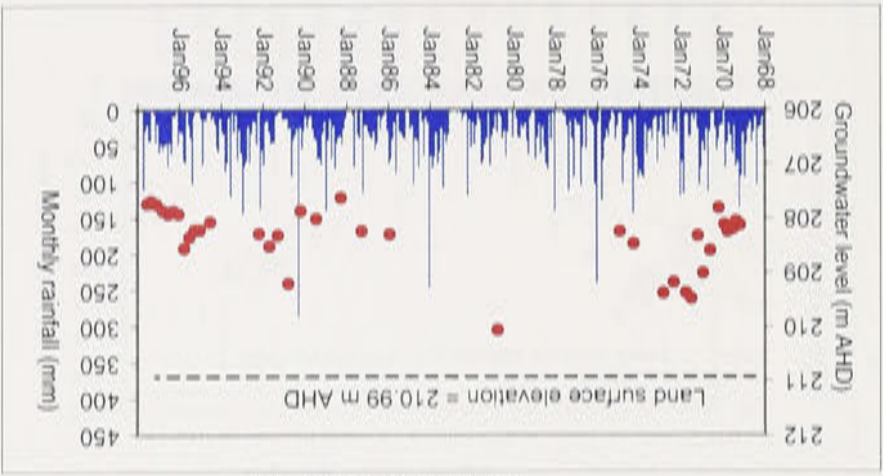


Well no. 19 W

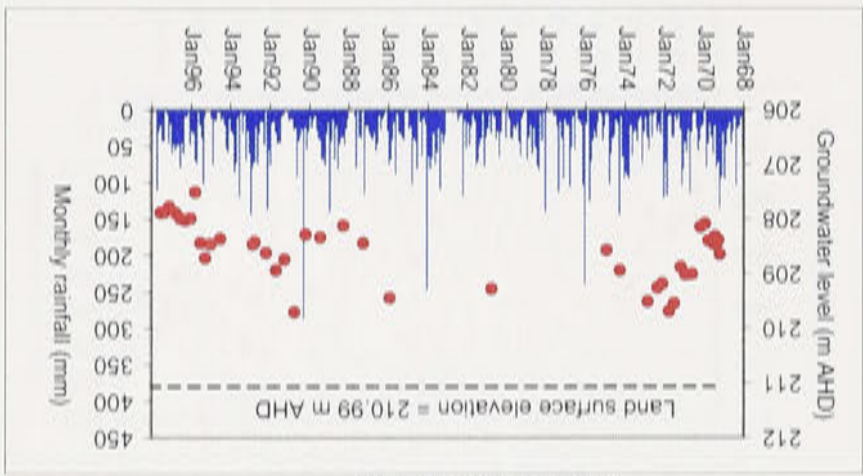


Well no. 21 W

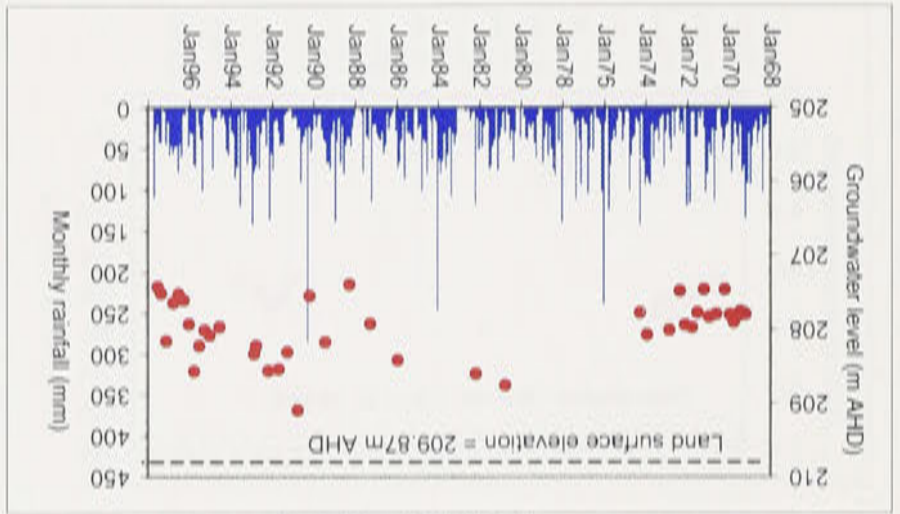




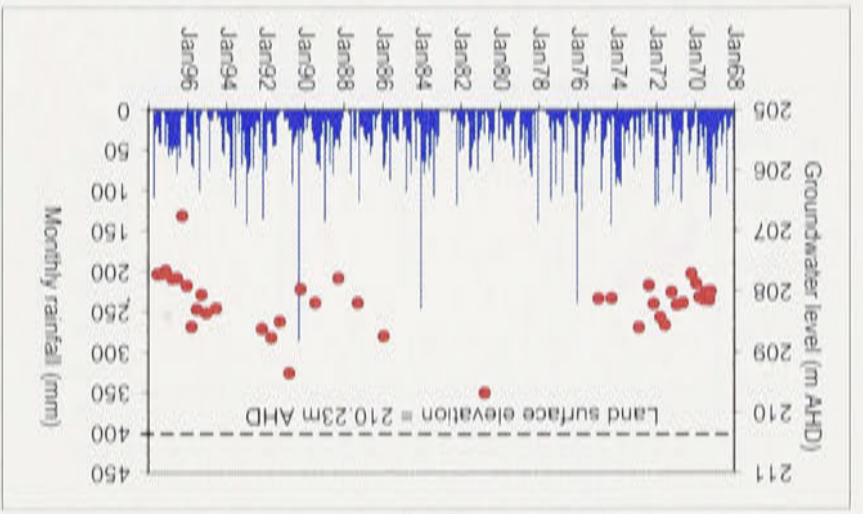
Well no. 26D W



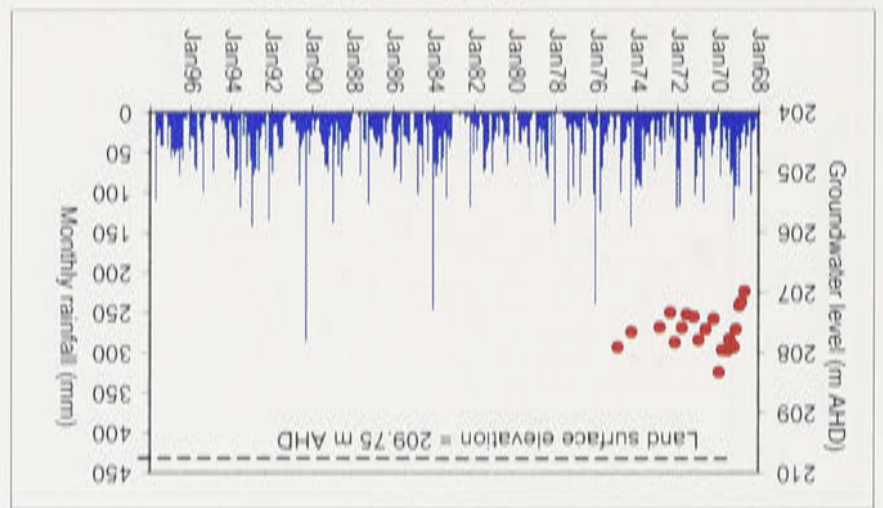
Well no. 26E W



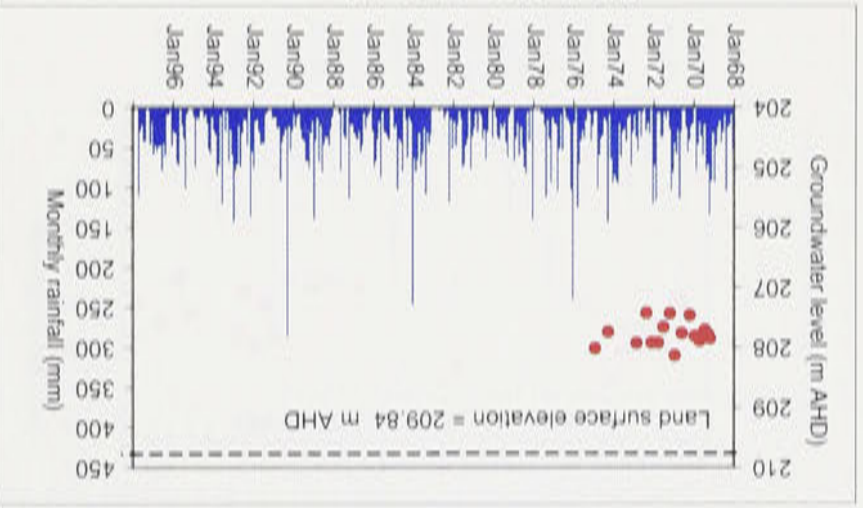
Well no. 26B W



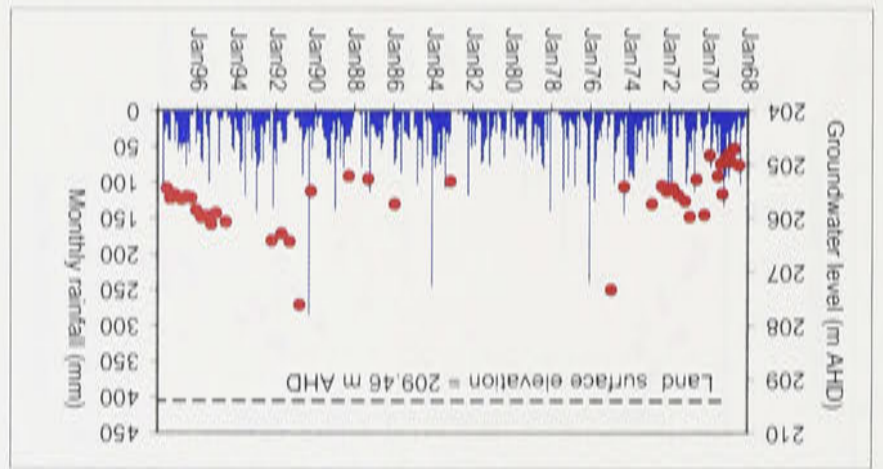
Well NO. 26C W



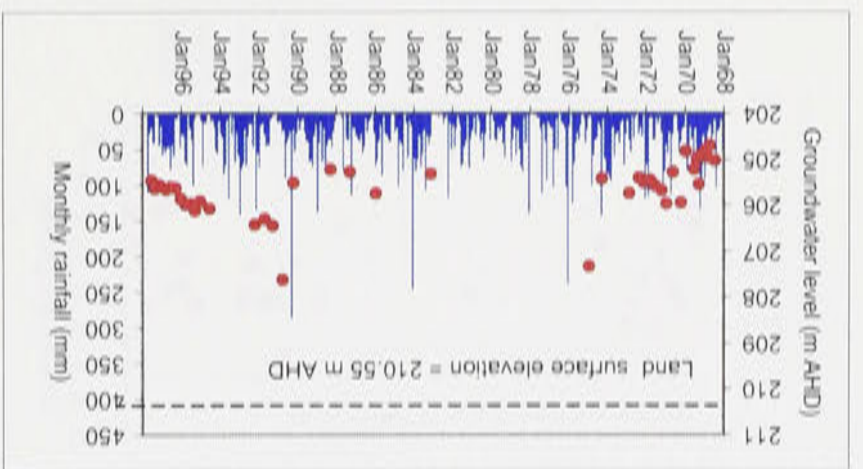
Well no. 26 W



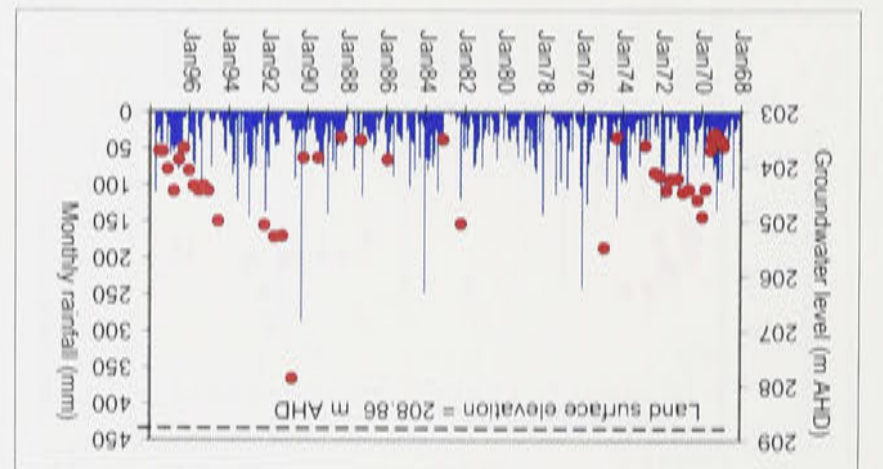
Well no. 26A W



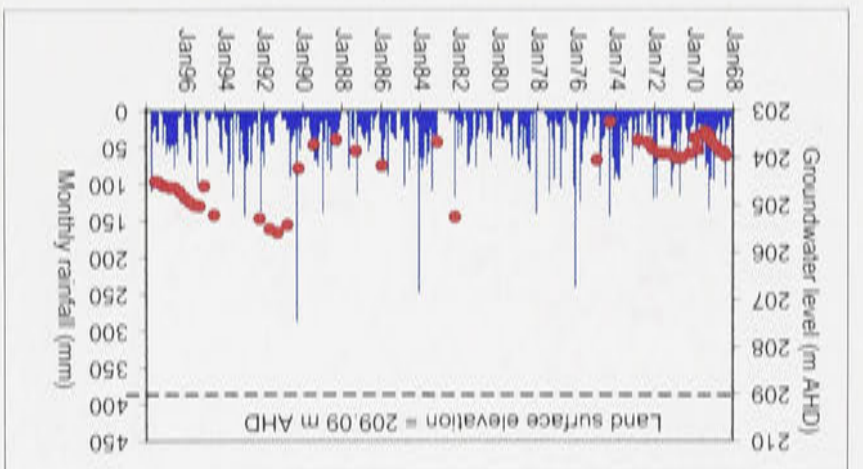
Well no. 24 W



Well no. 25 W

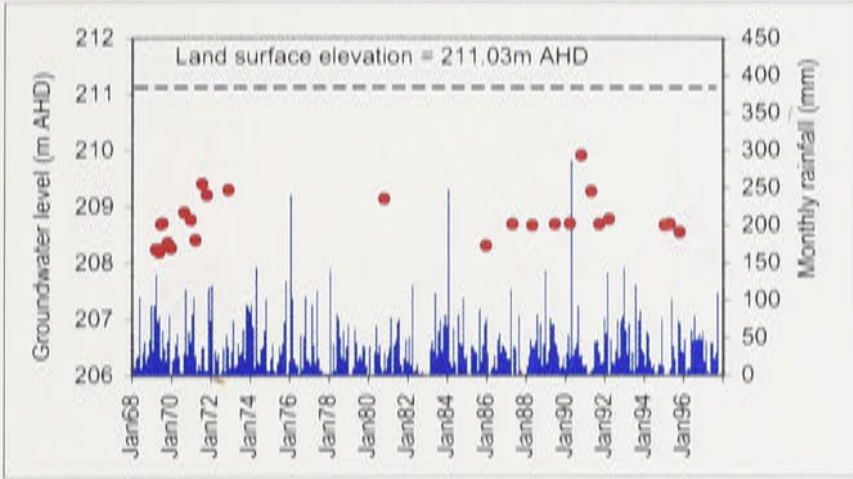


Well no. 22 W

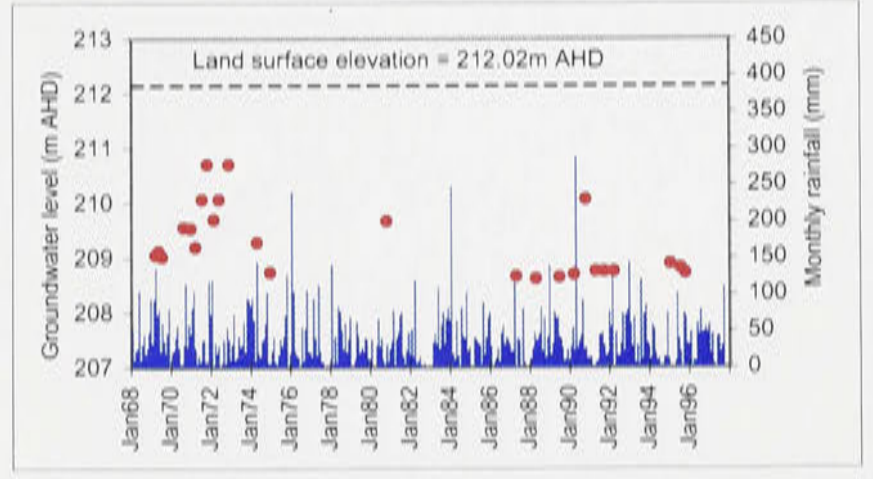


Well no. 23 W

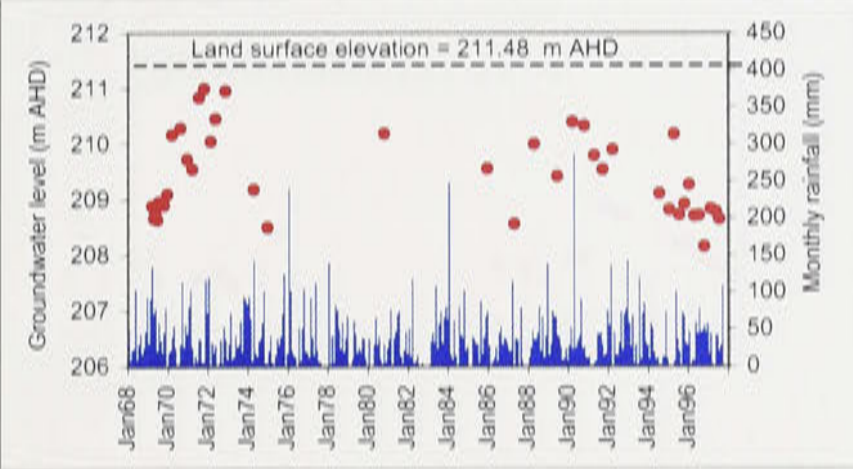
Well no. 26F W



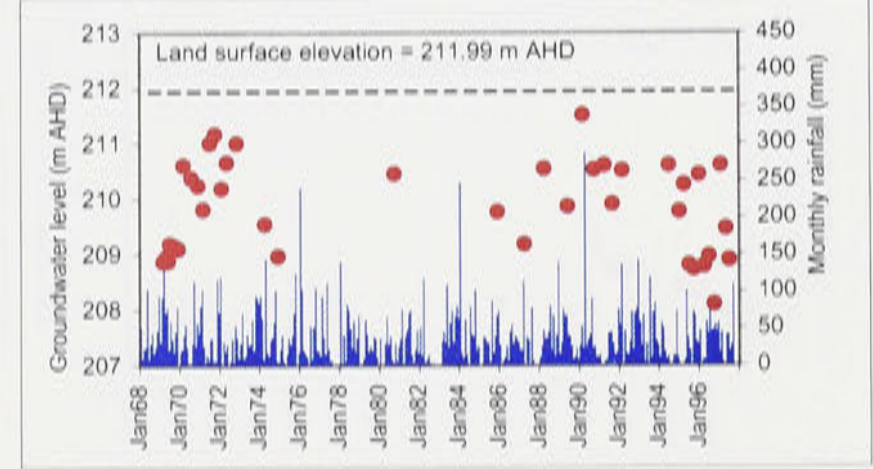
Well no. 26G W



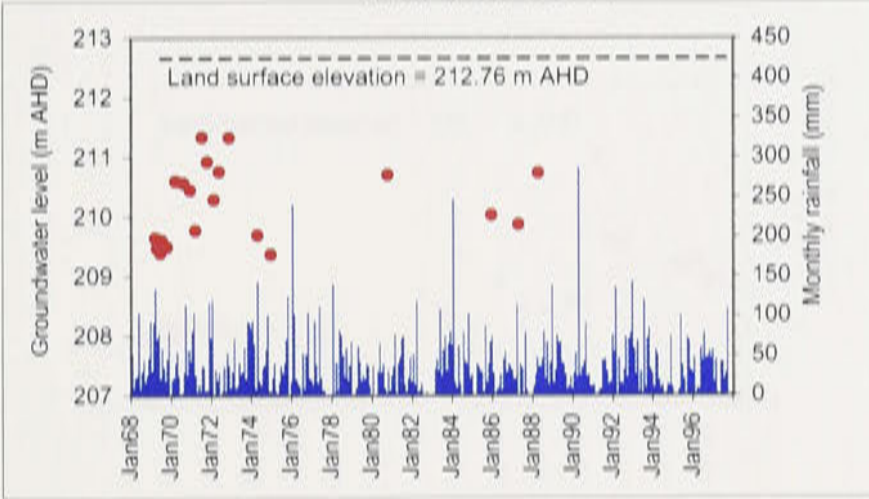
Well no. 26H W



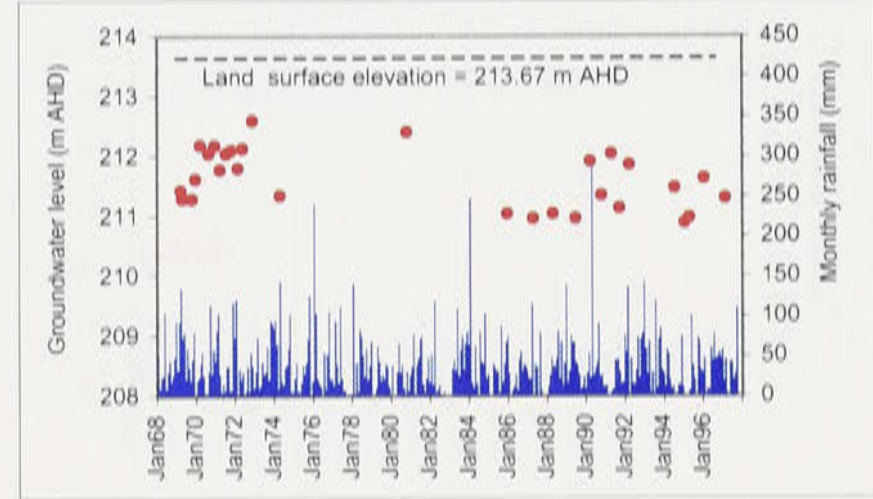
Well no. 26I W



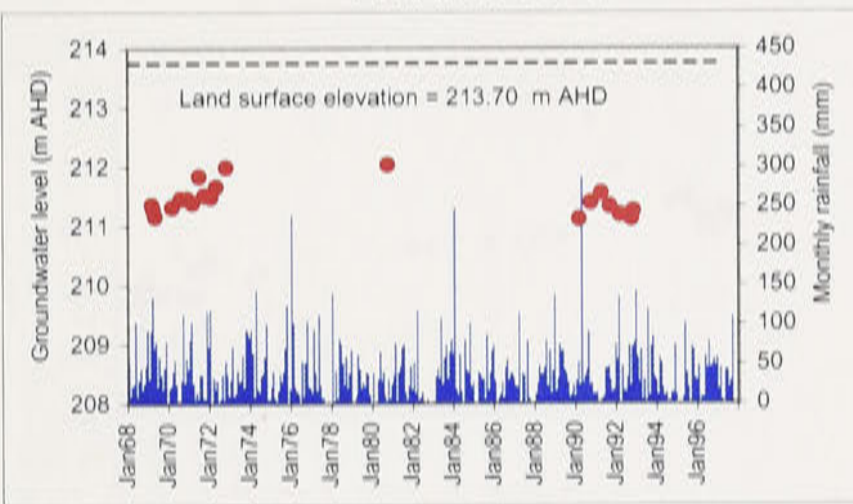
Well no. 26J W



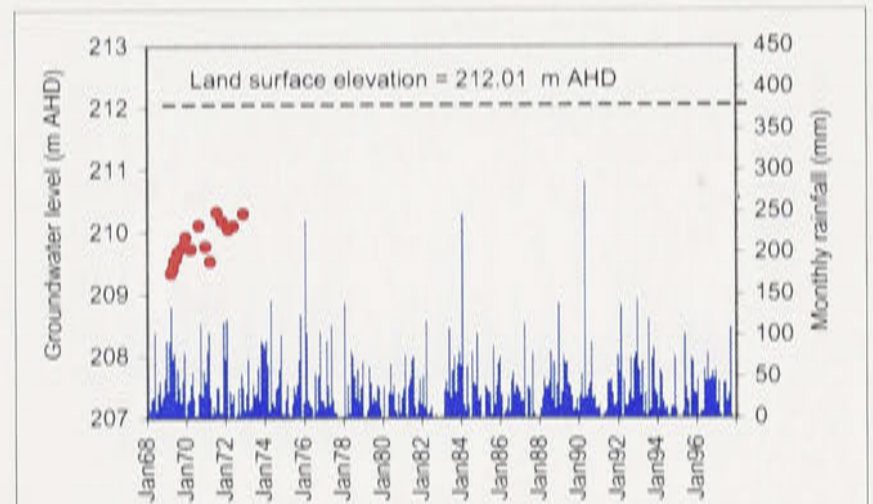
Well no. 26K W



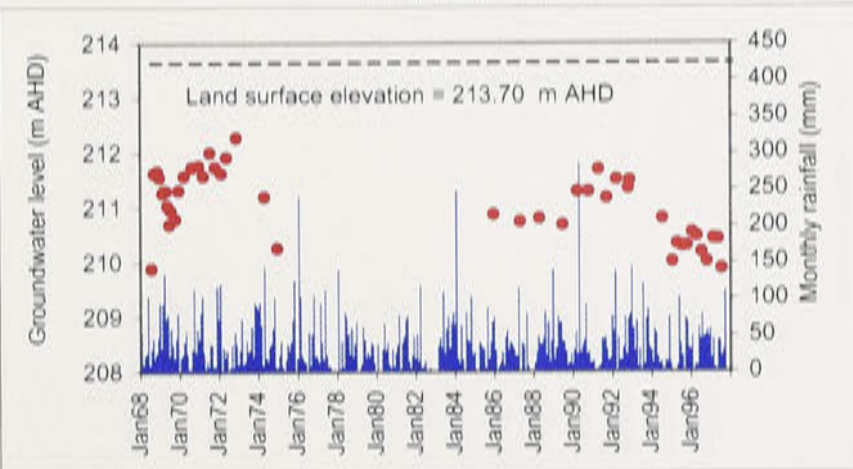
Well no. 26L W



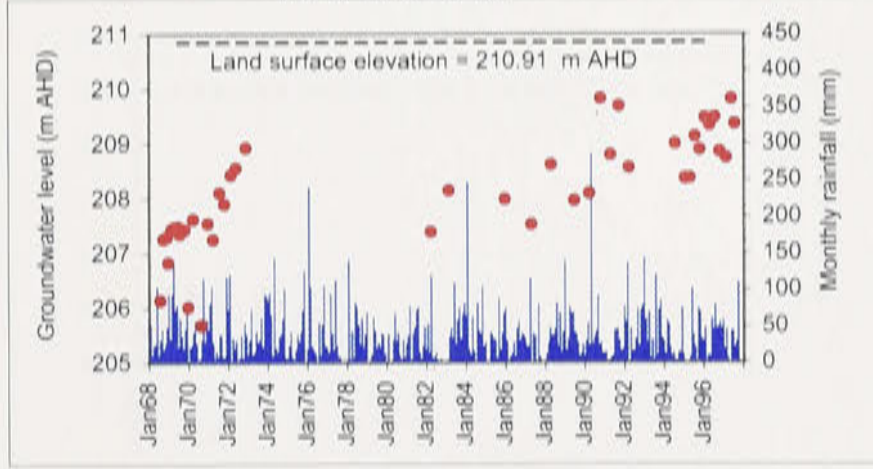
Well no. 26M W



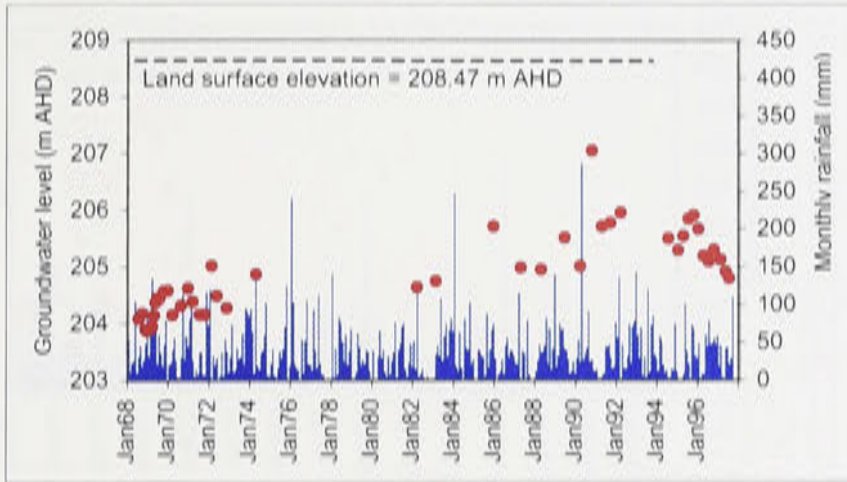
Well no. 27 W



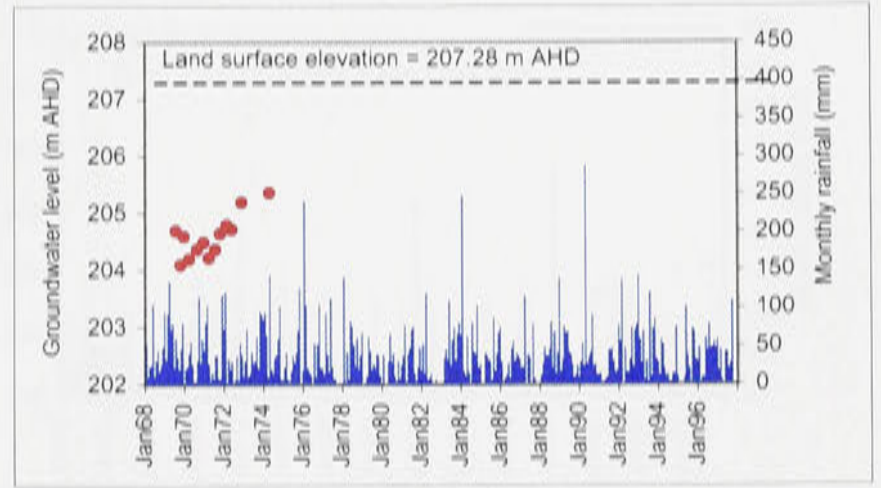
Well no. 28 W



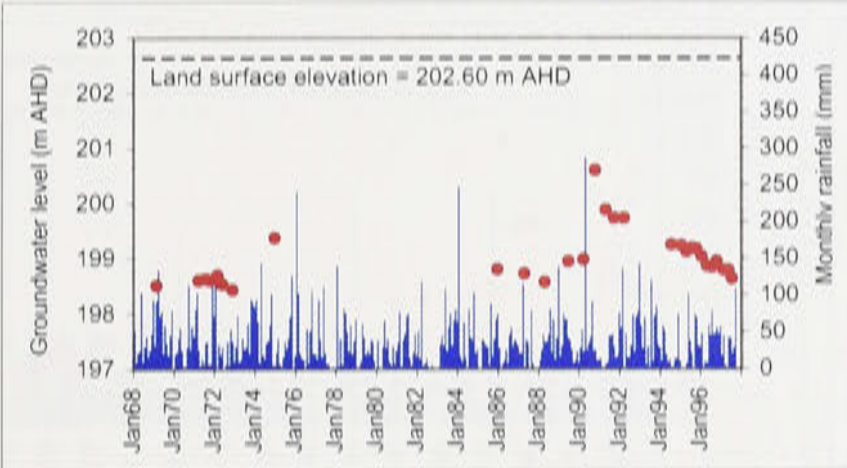
Well no. 29 W



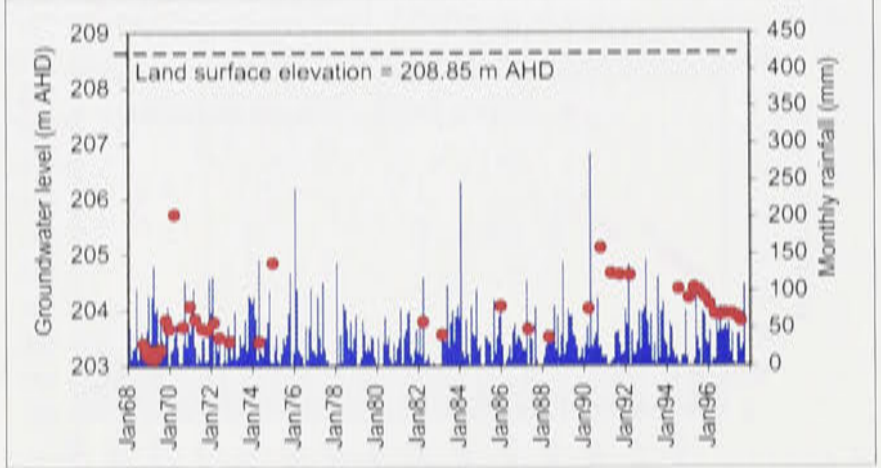
Well no. 30 W



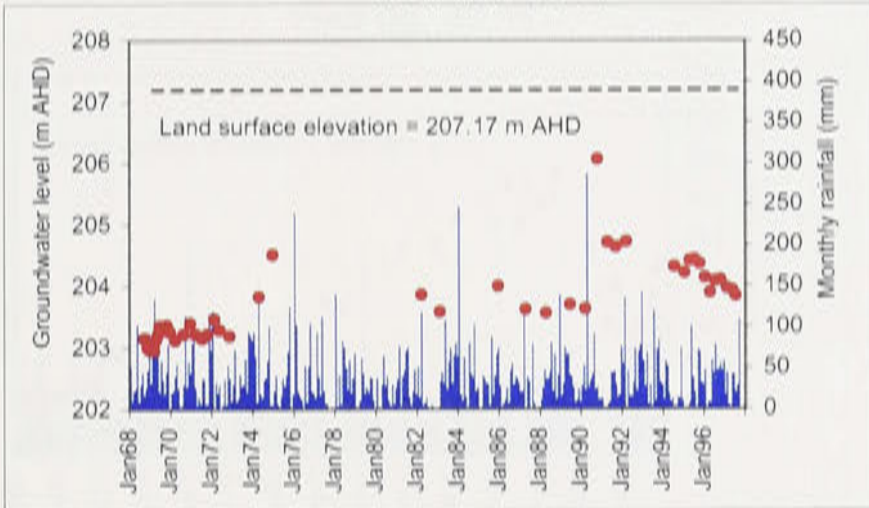
Well no. 31 W



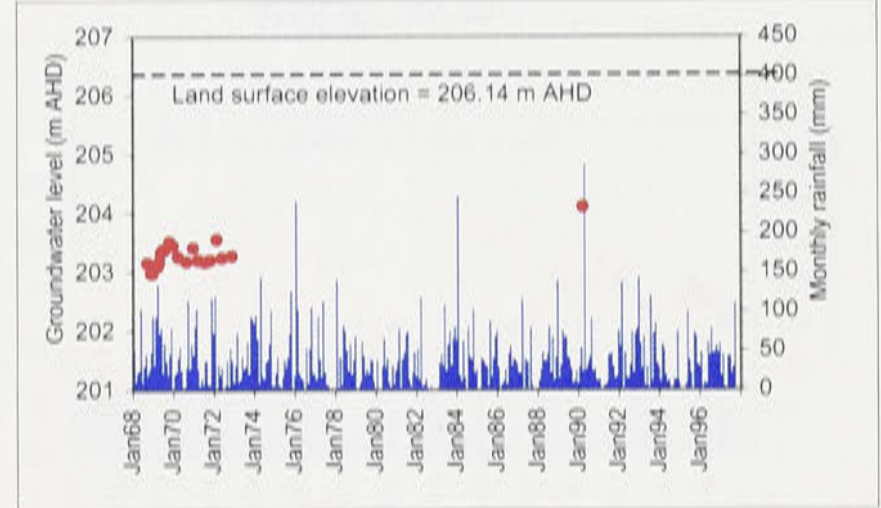
Well no. 32 W



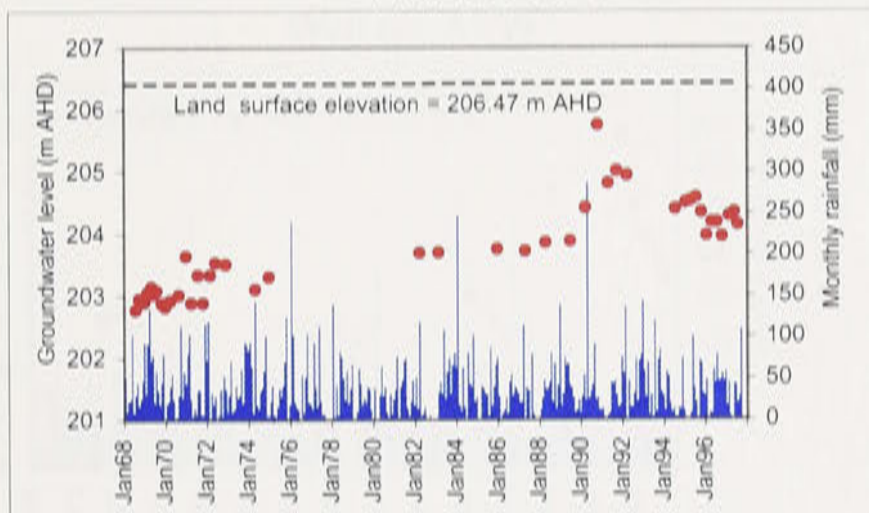
Well no. 33 W



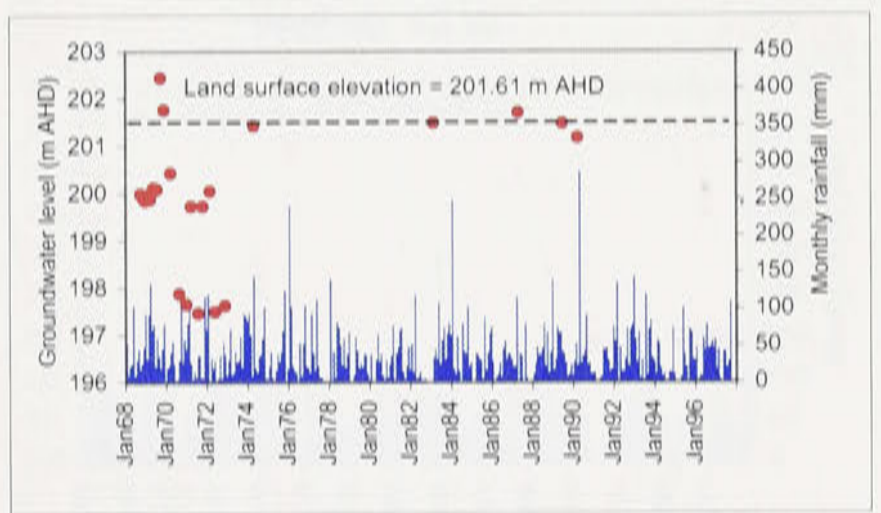
Well no. 34 W



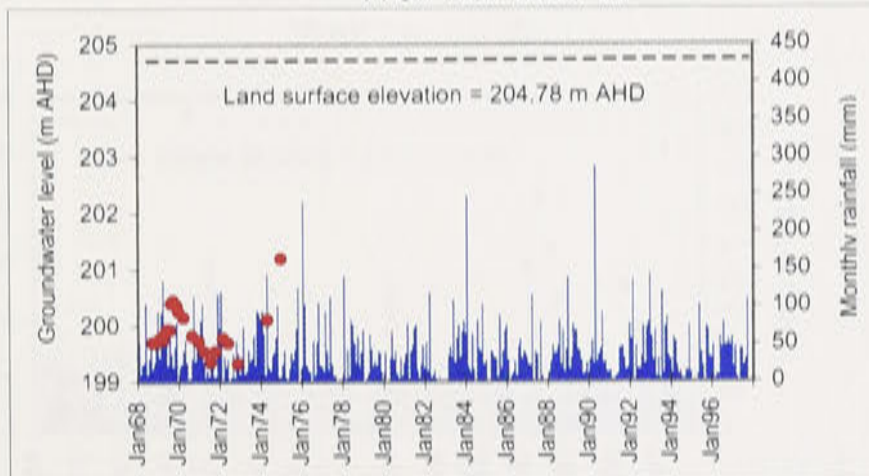
Well no. 35 W



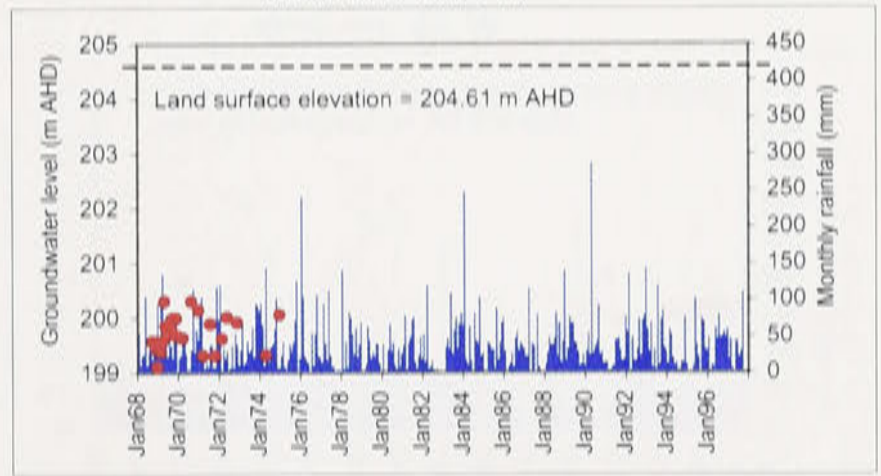
Well no. 36 W



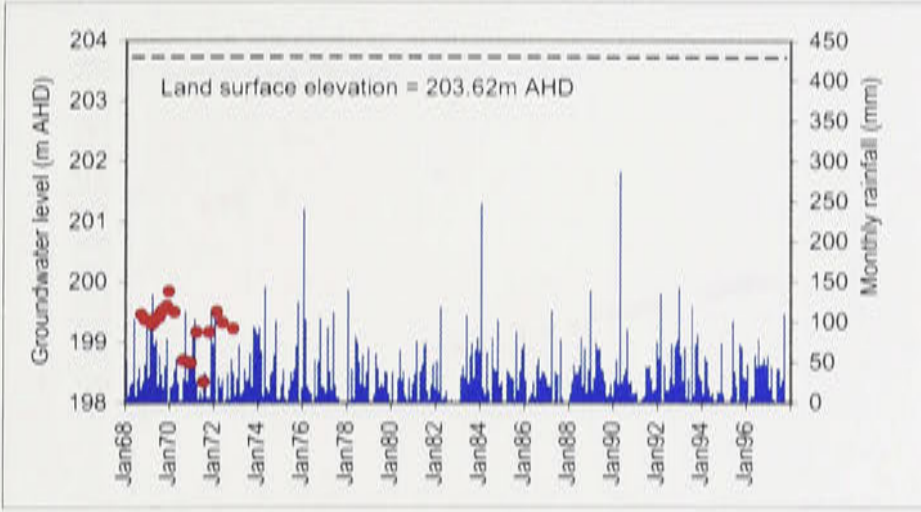
Well no. 36A W



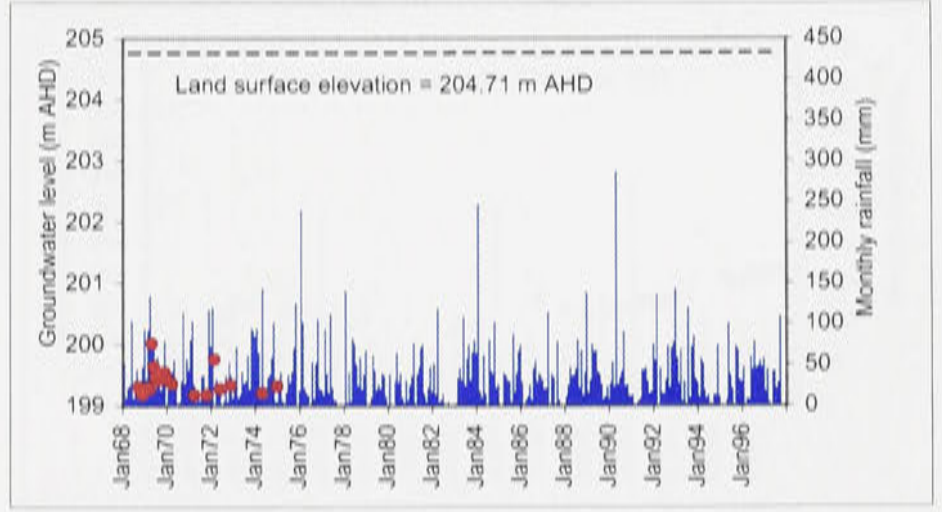
Well no. 36B W



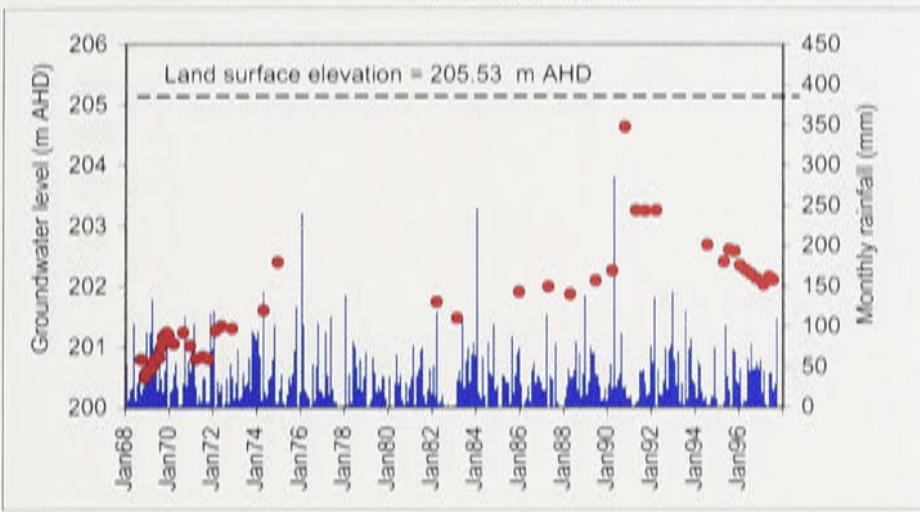
Well no. 36C W



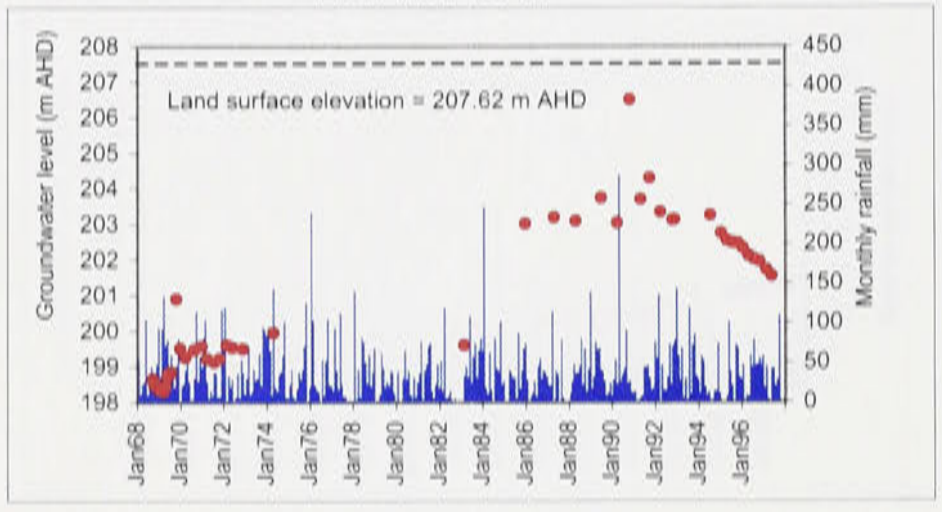
Well no. 36D W



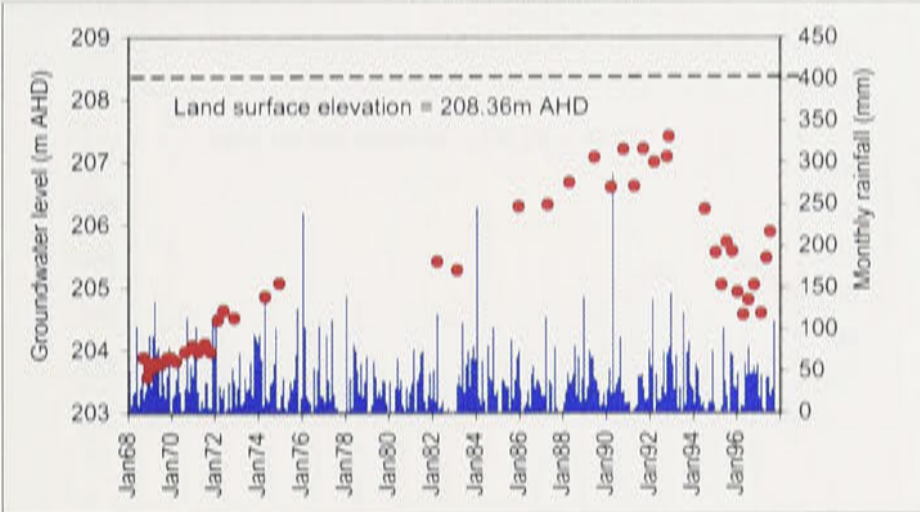
Well no. 37 W



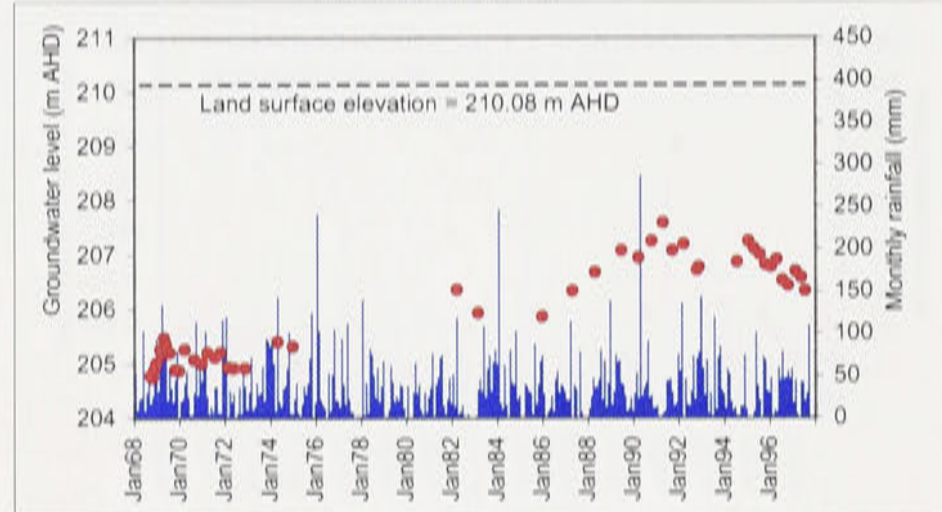
Well no. 38 W



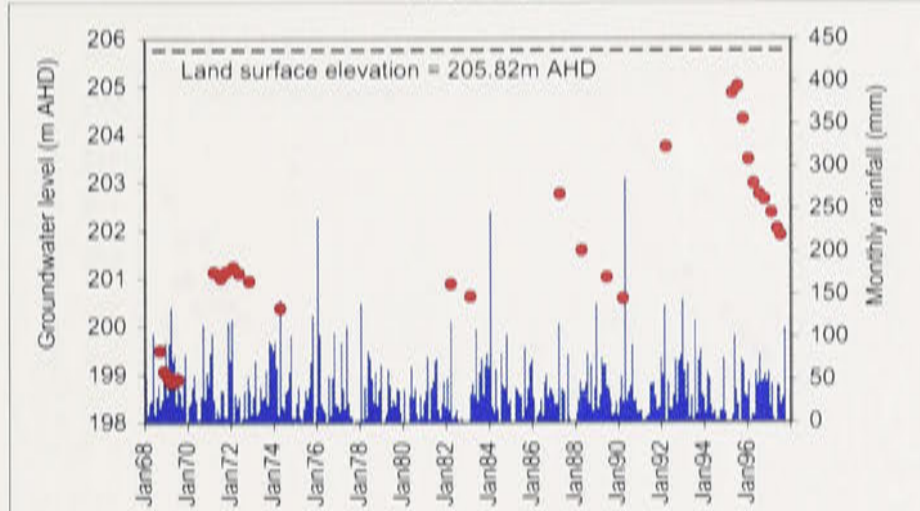
Well no. 39 W



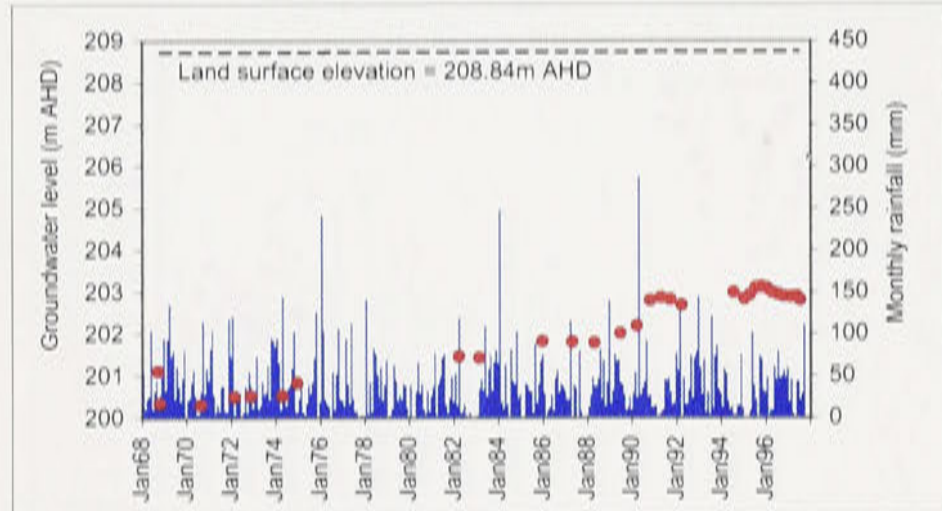
Well no. 40 W



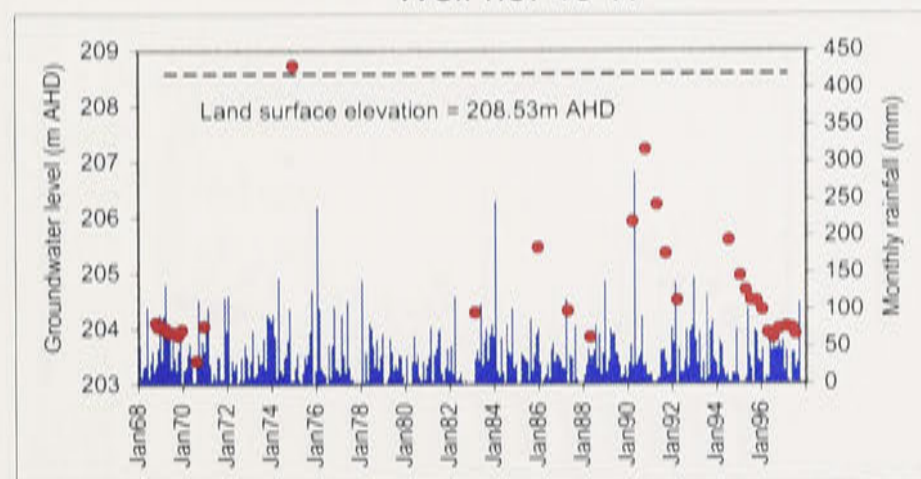
Well no. 41 W



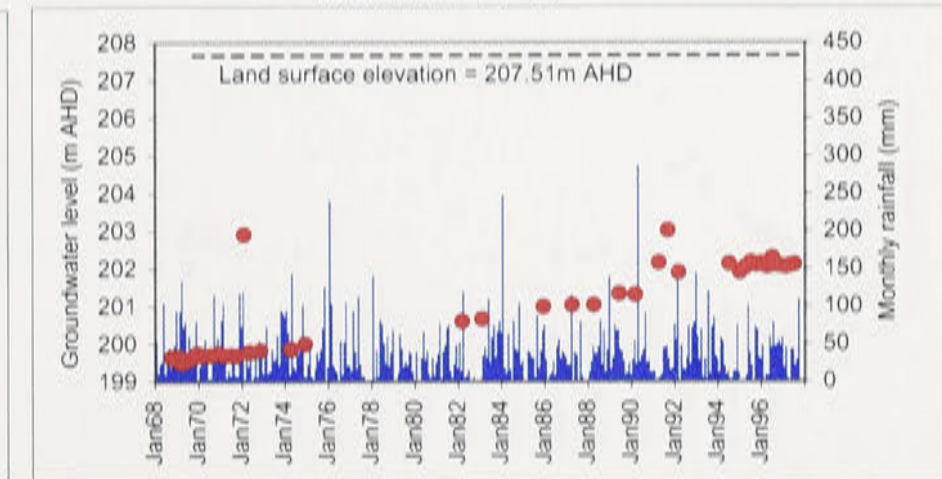
Well no. 42 W



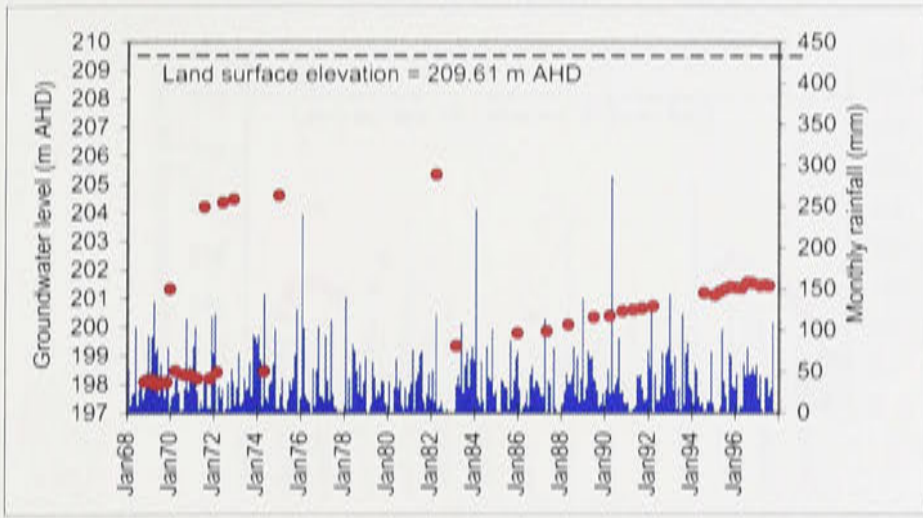
Well no. 43 W



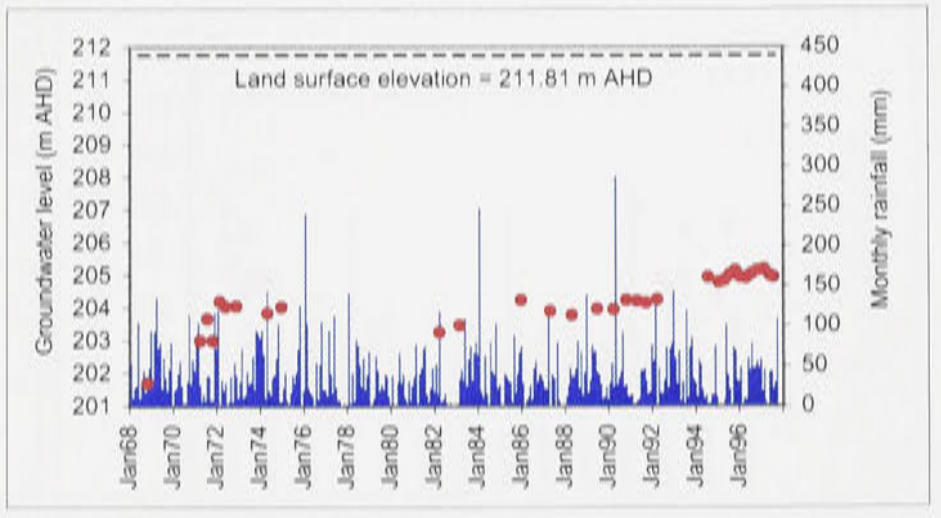
Well no. 44 W



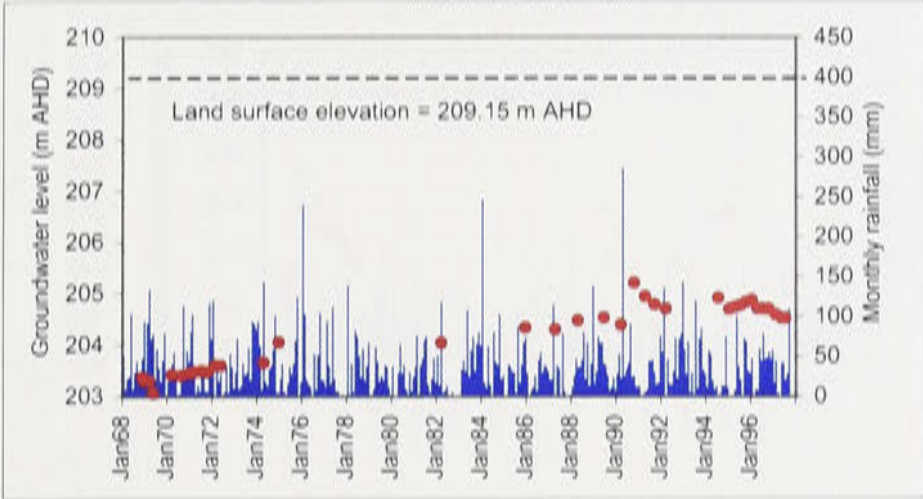
Well no. 45 W



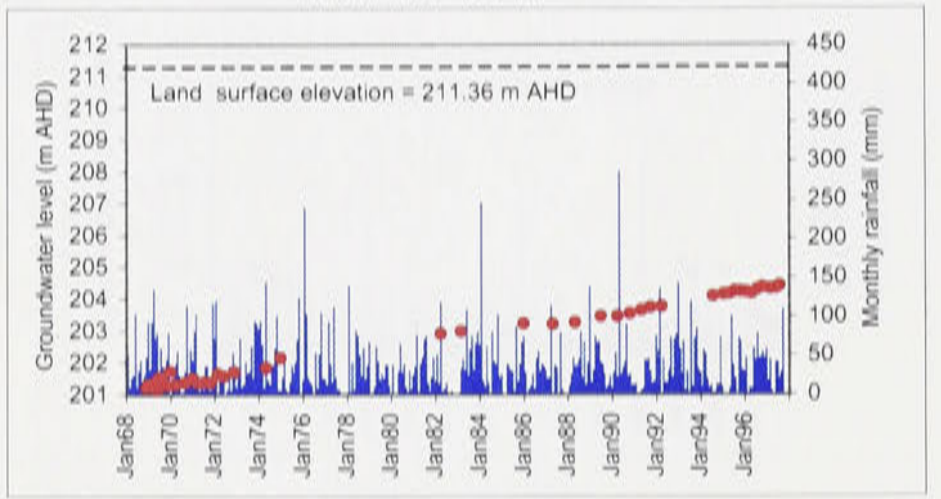
Well no. 46 W



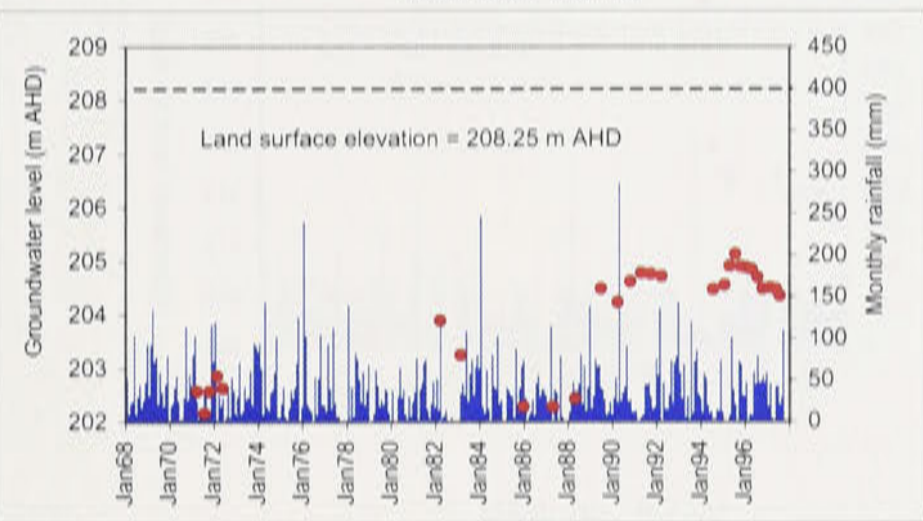
Well no.47 W



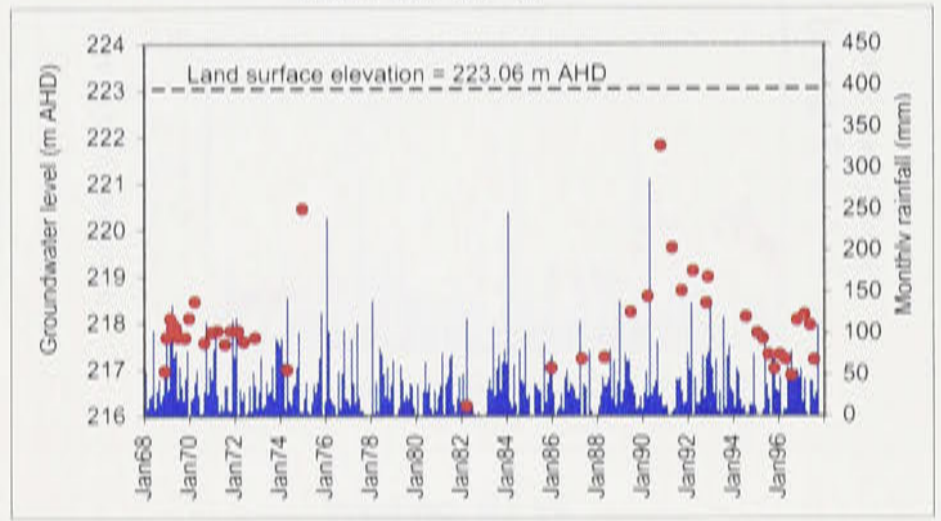
Well no. 48 W



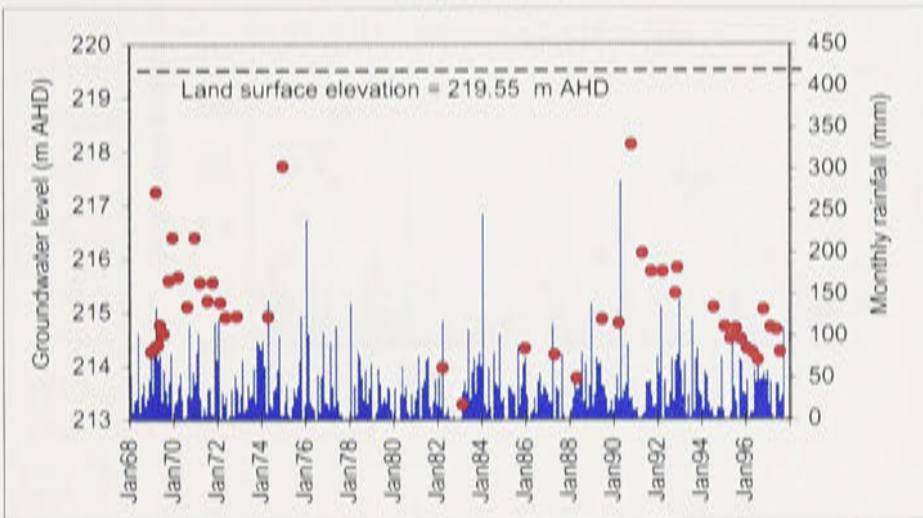
Well no. 50 W



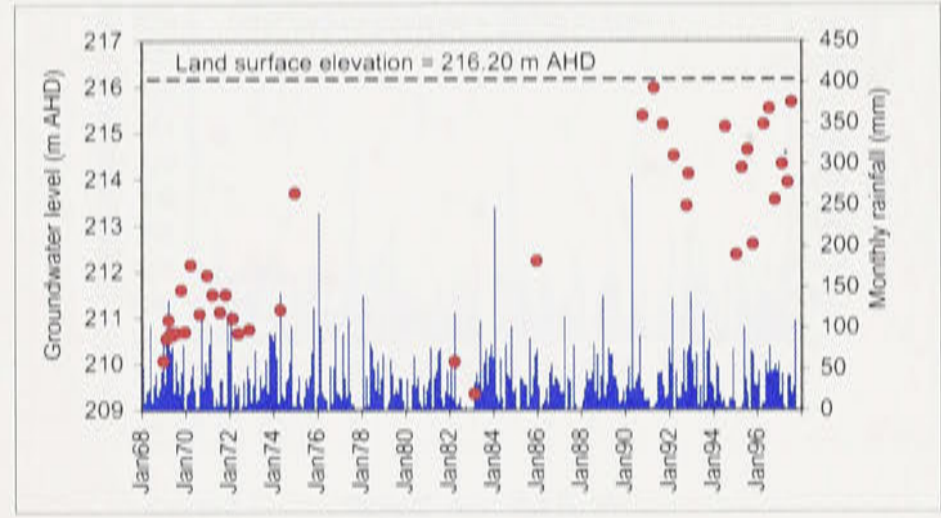
Well no. 51 W



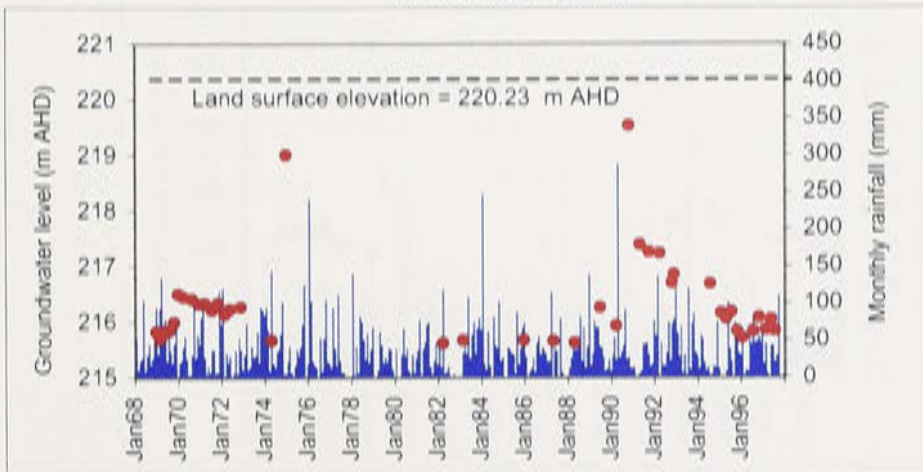
Well no. 52 W



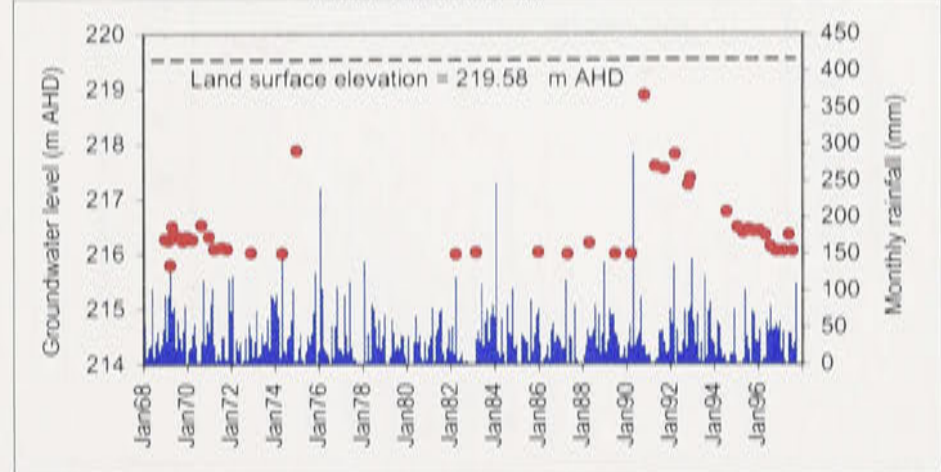
Well no. 53 W



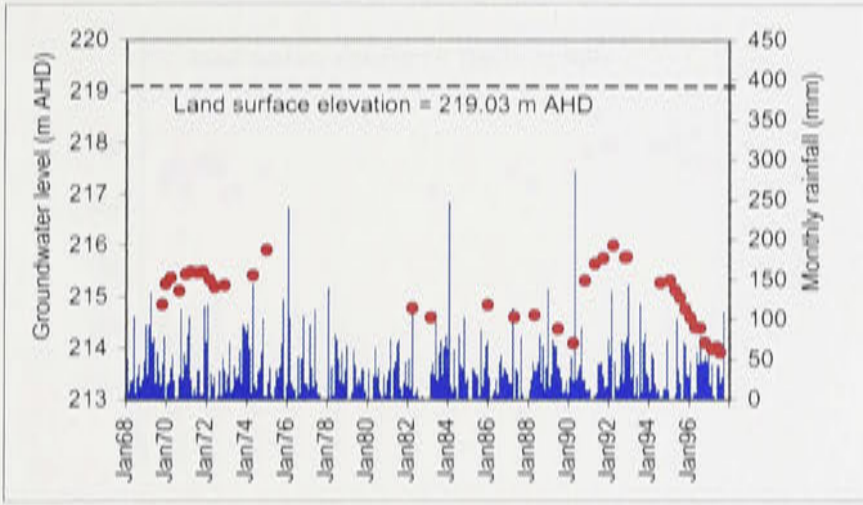
Well no. 54 W



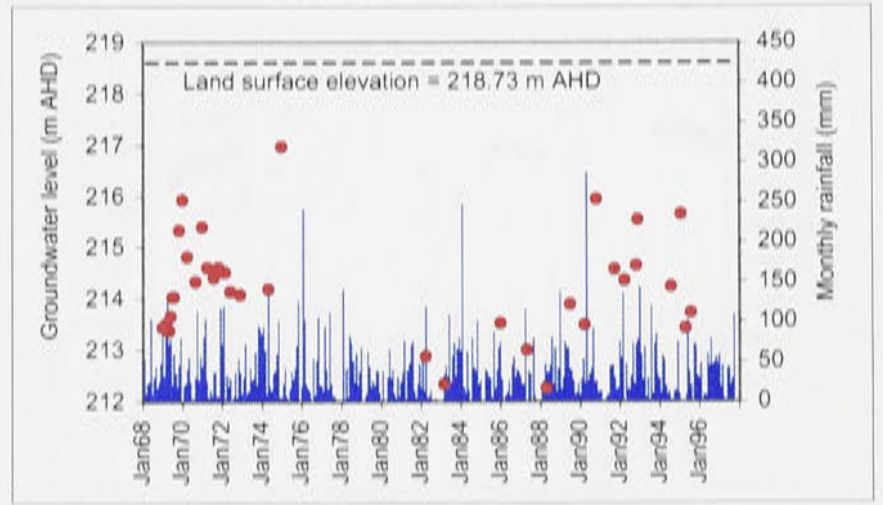
Well no. 55 W



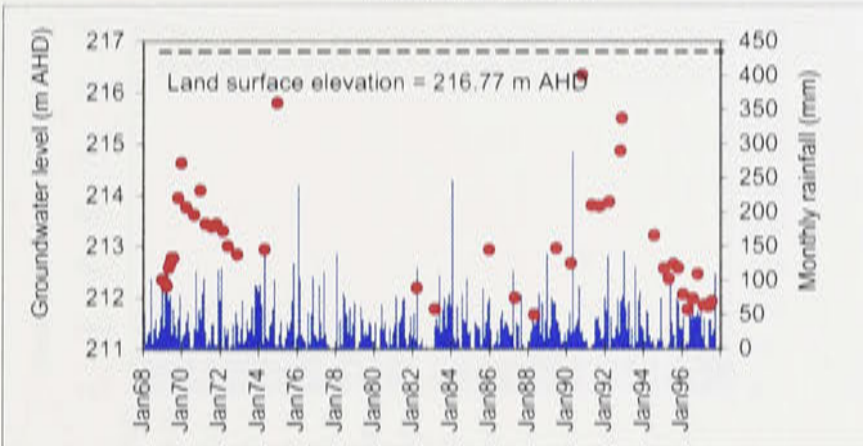
Well no. 56 W



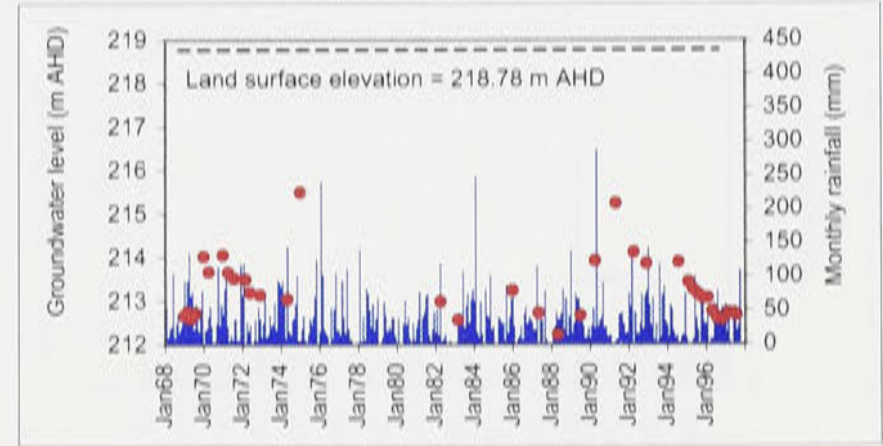
Well no. 57 W



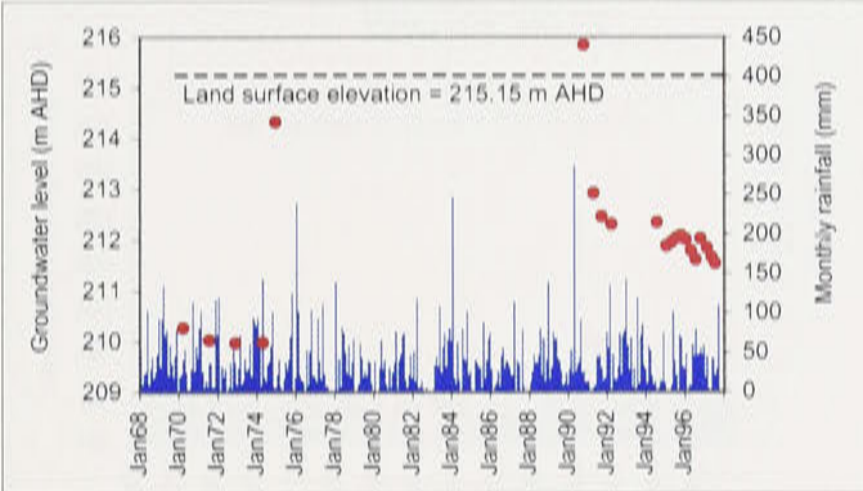
Well no. 58 W



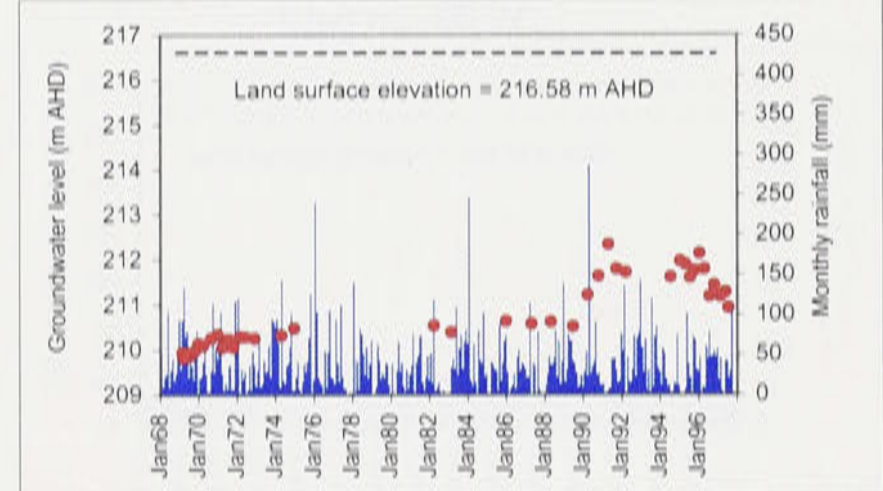
Well no. 59 W



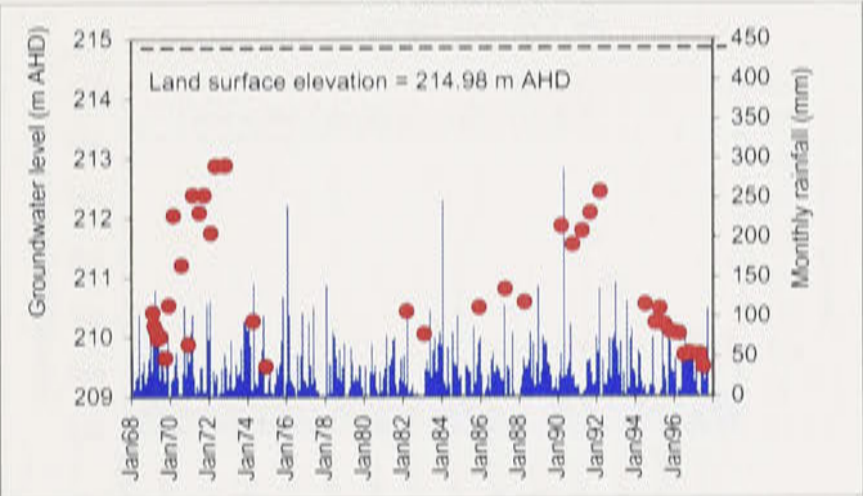
Well no. 60 W



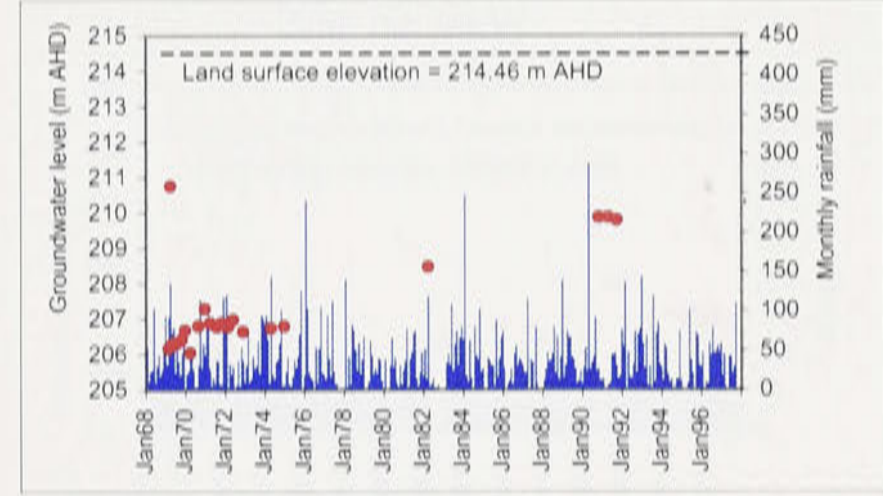
Well no. 61 W



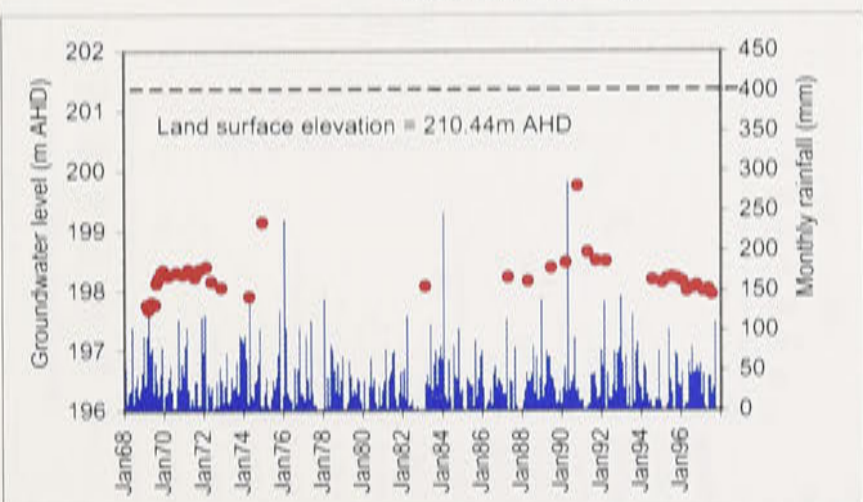
Well no. 62 W



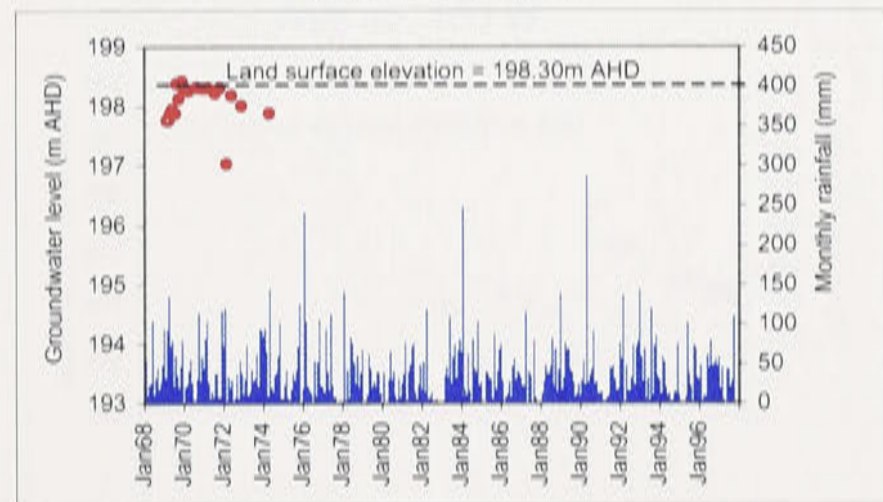
Well no. 63 W



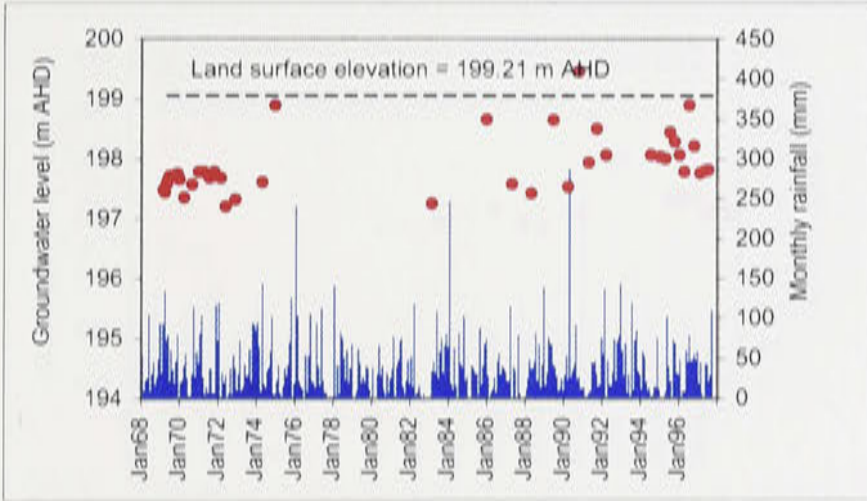
Well no. 64 W



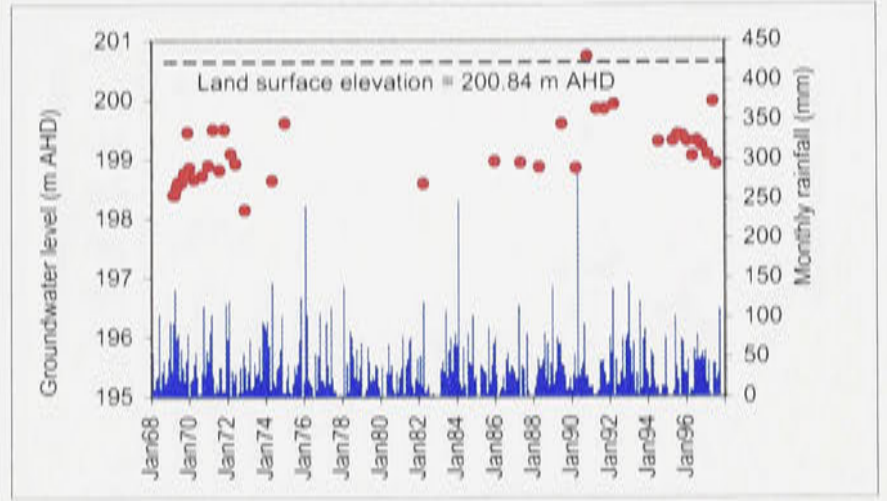
Well no. 64A W



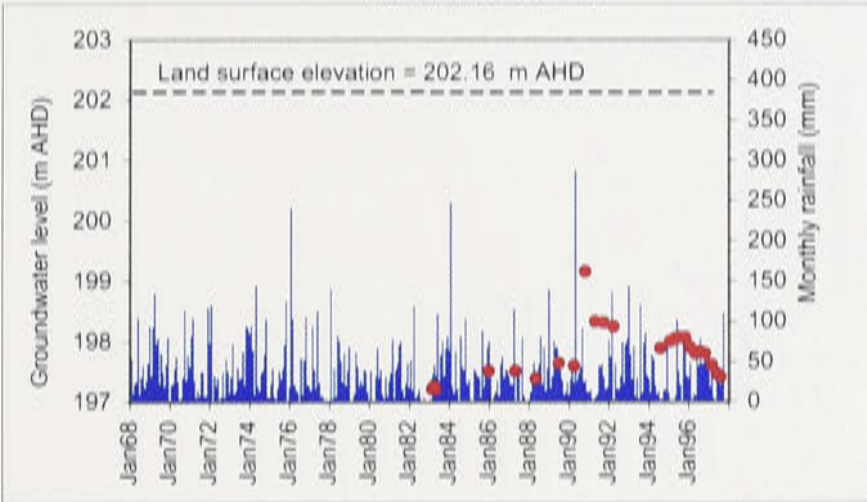
Well no. 65 W



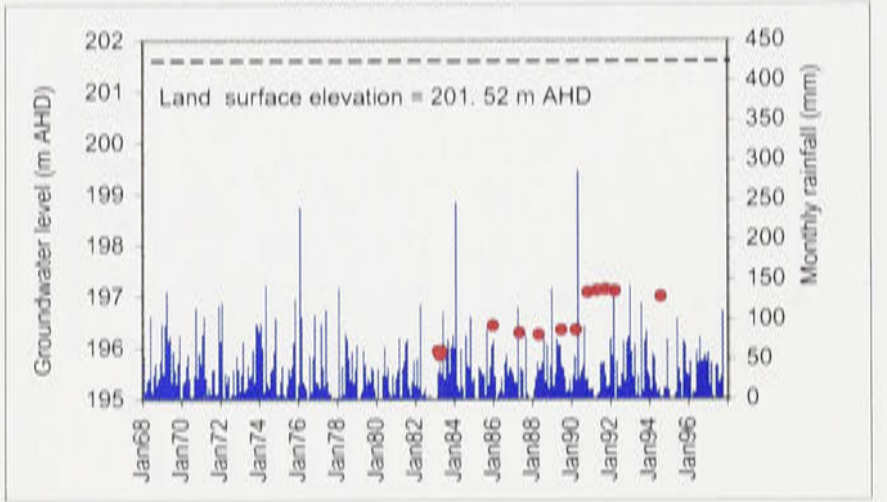
Well no. 66 W



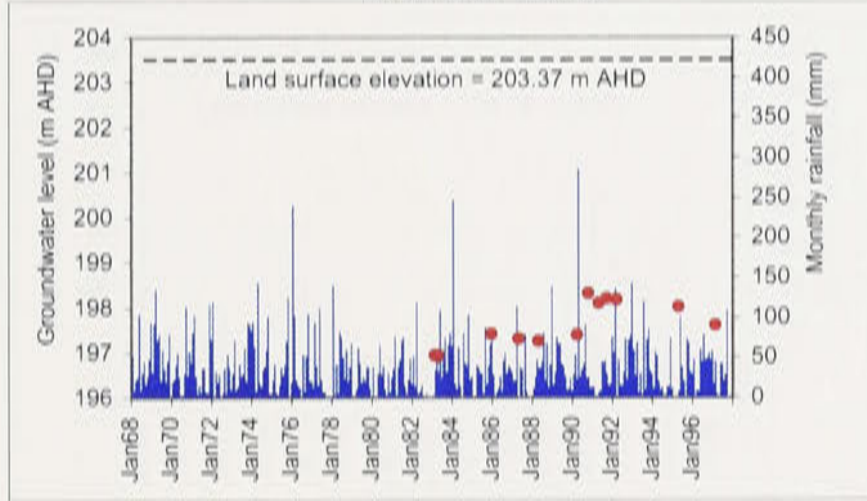
Well no. 92 W



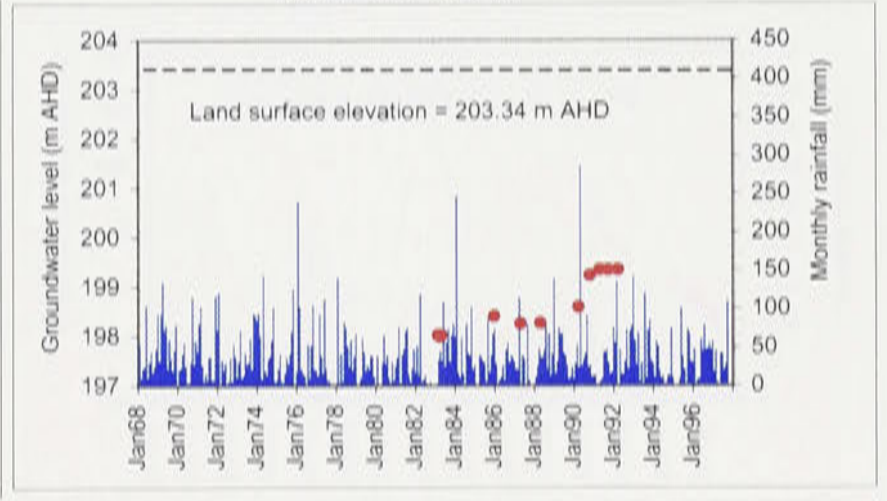
Well no. 94 W



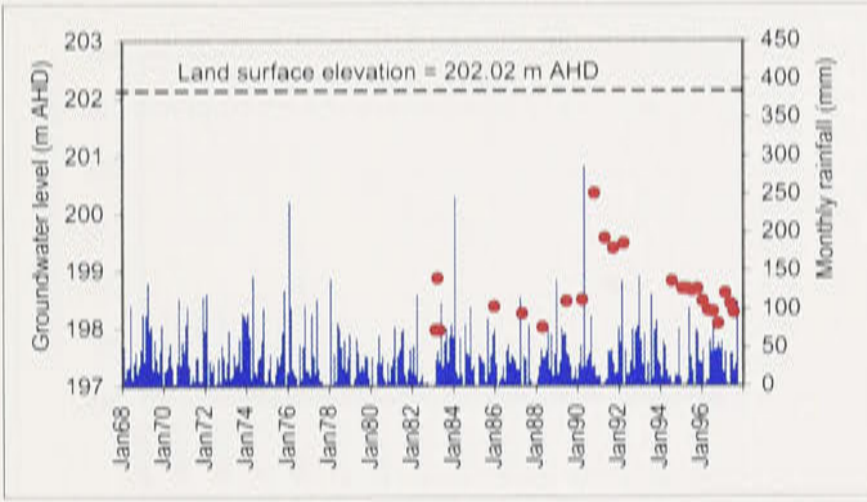
Well no. 95 W



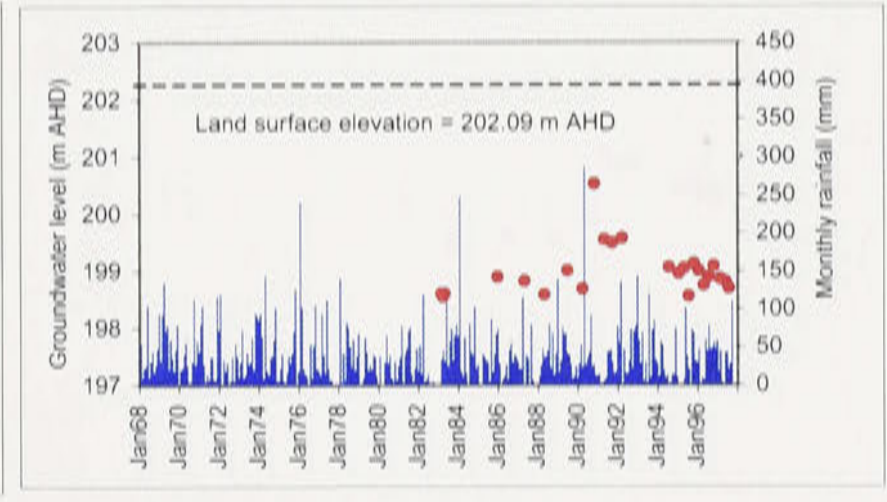
Well no. 96 W



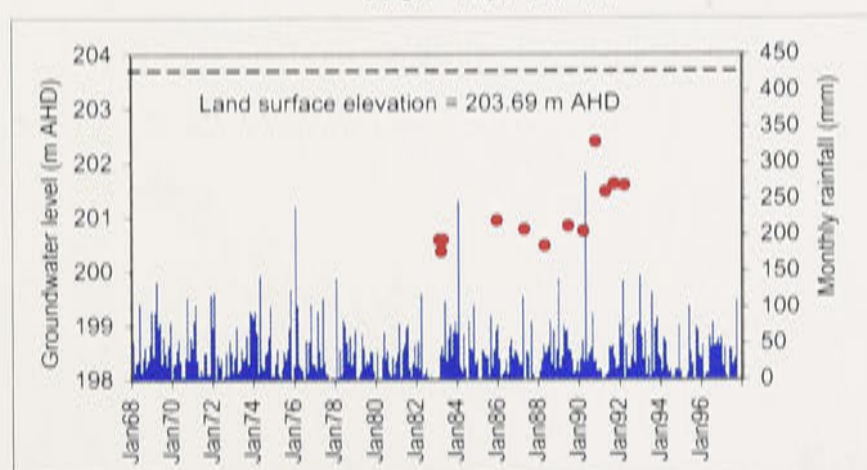
Well no. 97 W



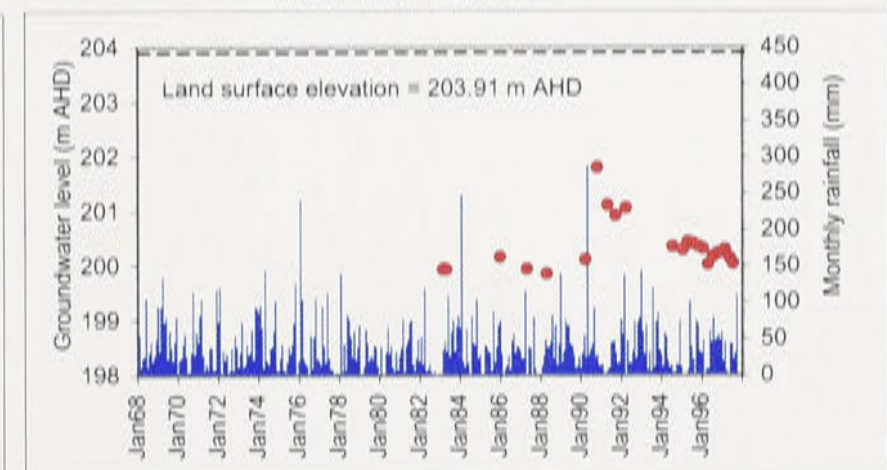
Well no. 98 W



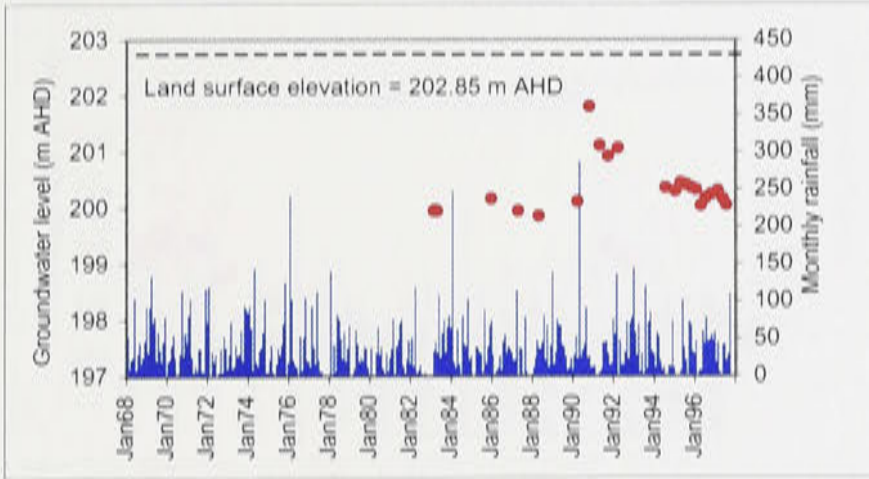
Well no. 99 W



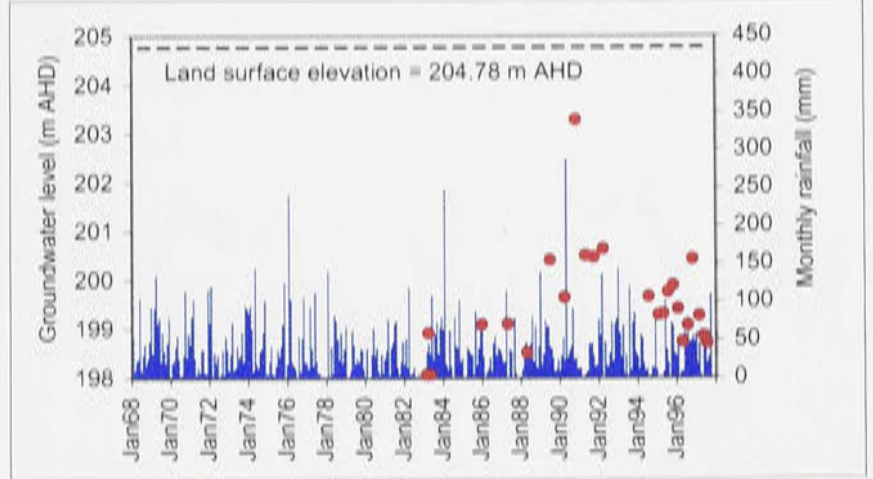
Well no. 100 W



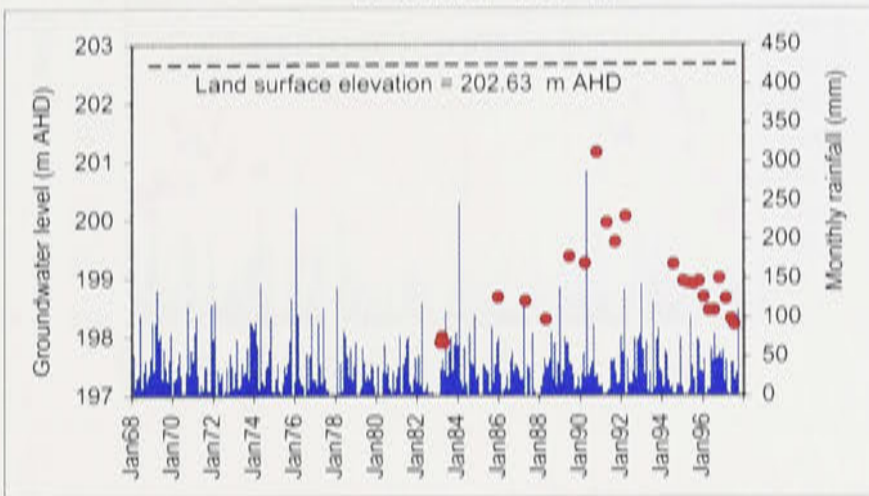
Well no. 101 W



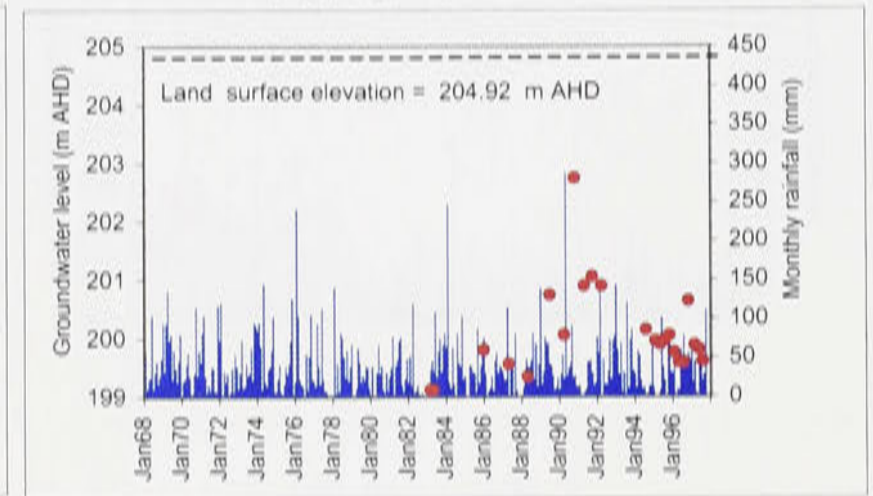
Well no. 102 W



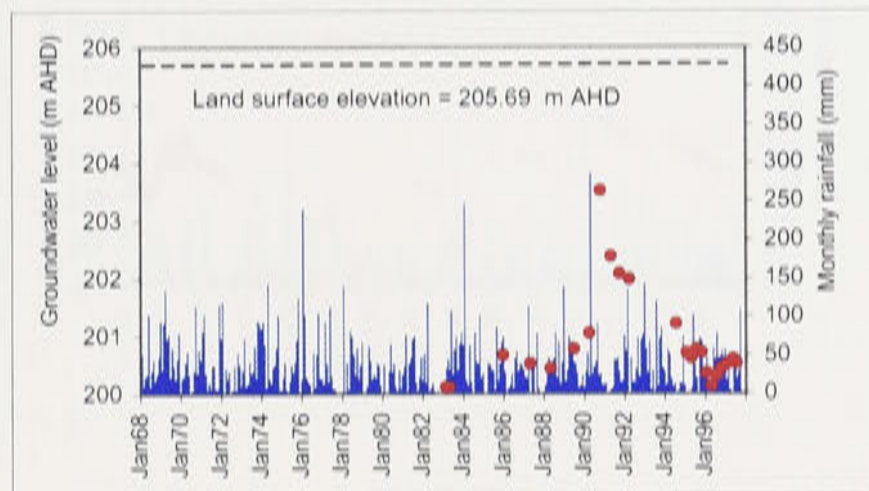
Well no. 103 W



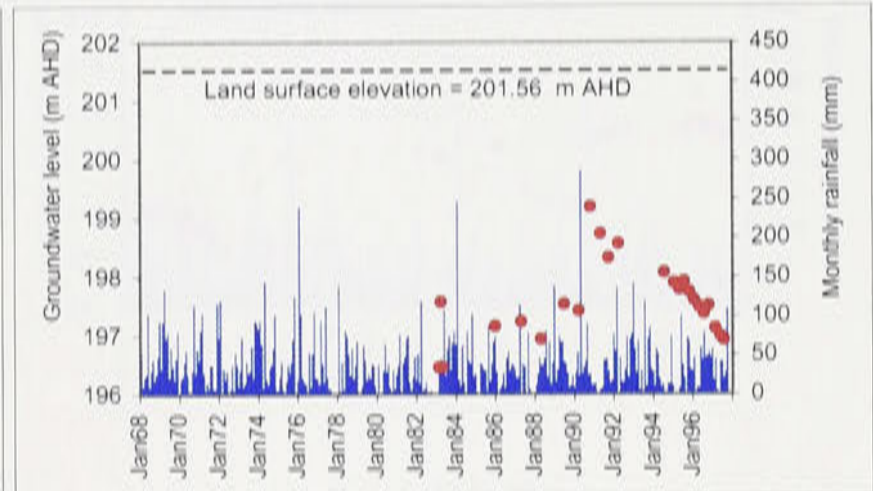
Well no. 104 W



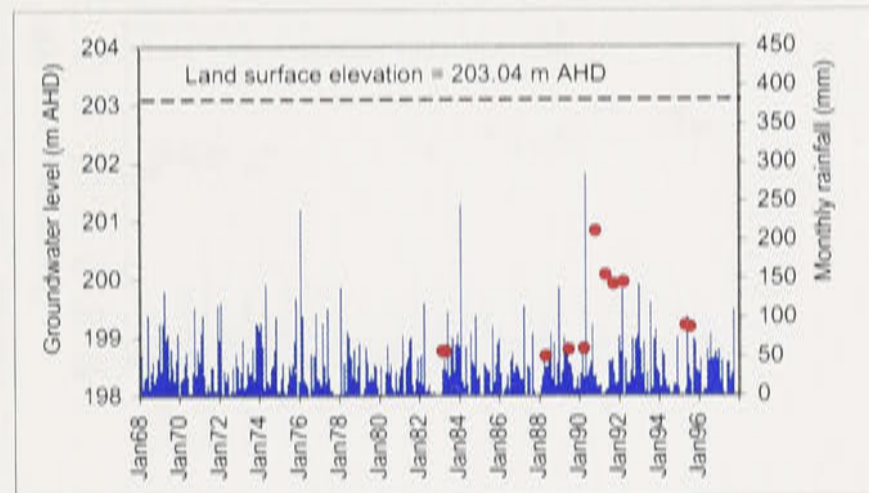
Well no. 105 W



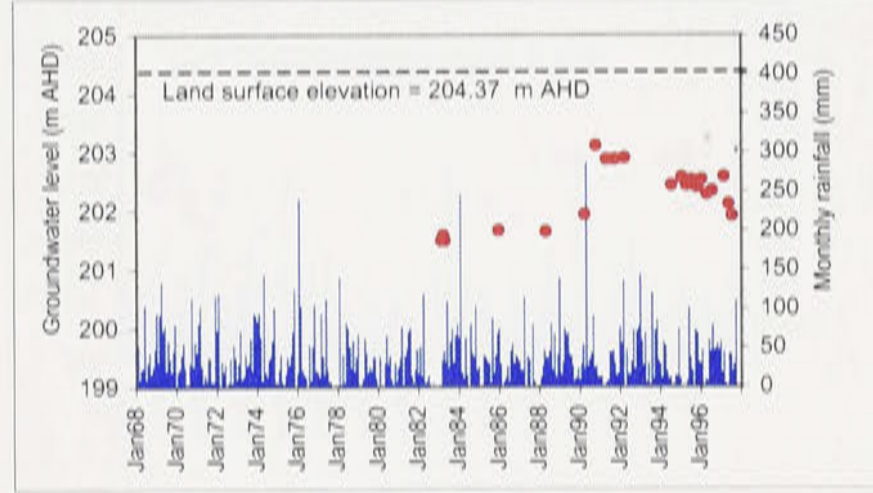
Well no. 106 W



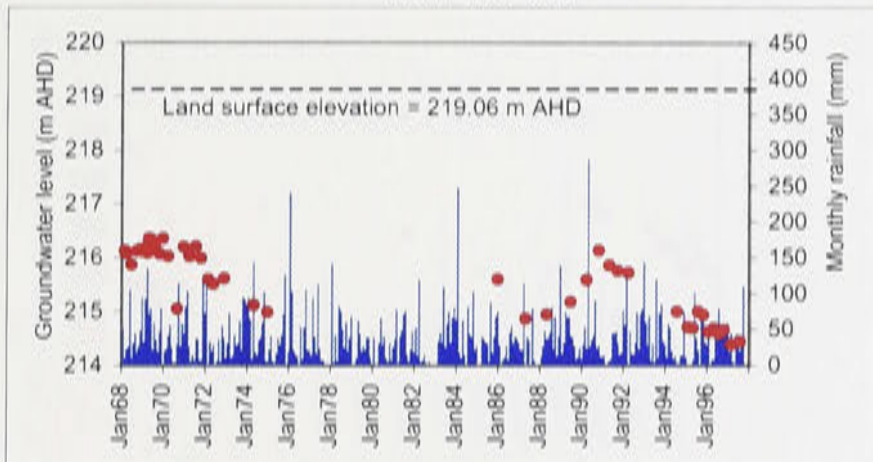
Well no. 107 W



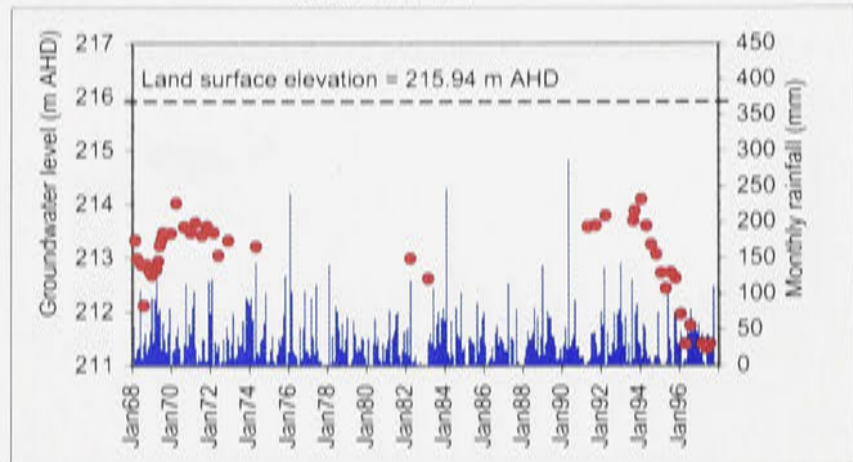
Well no. 108 W



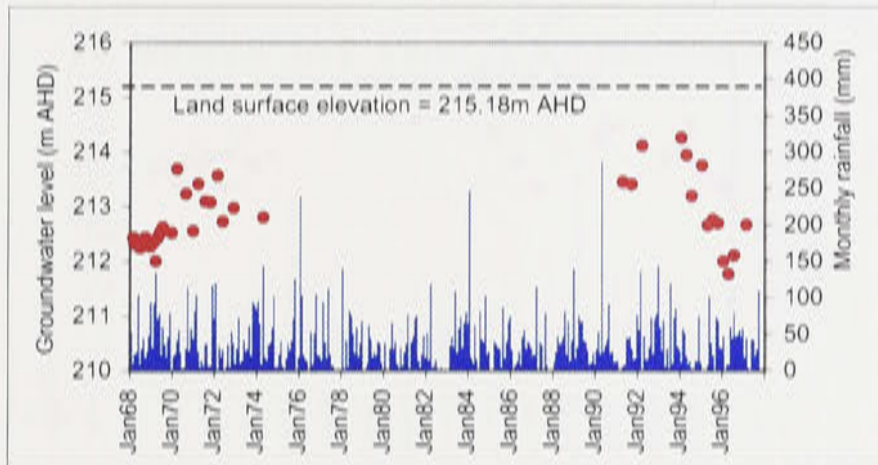
Well no. 3 P



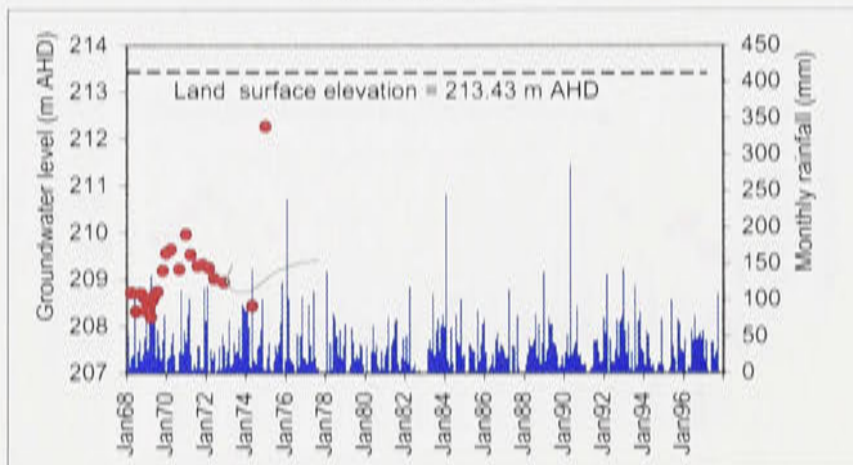
Well no. 5 P



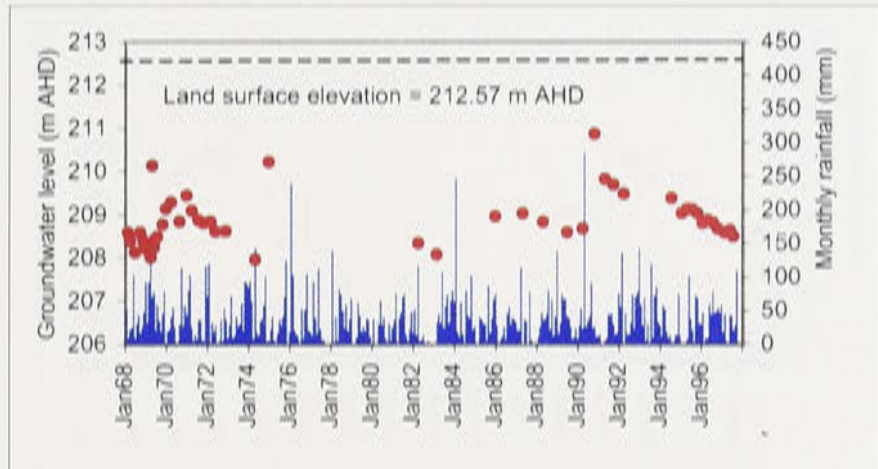
Well no. 6 P



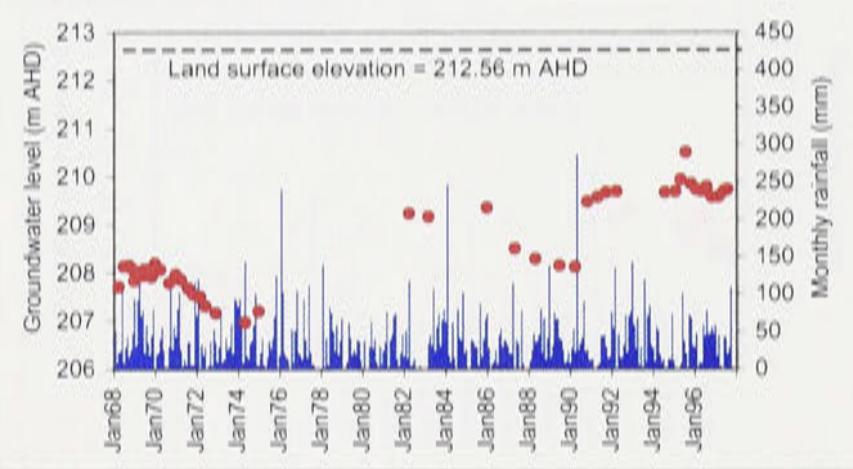
Well no. 9 P



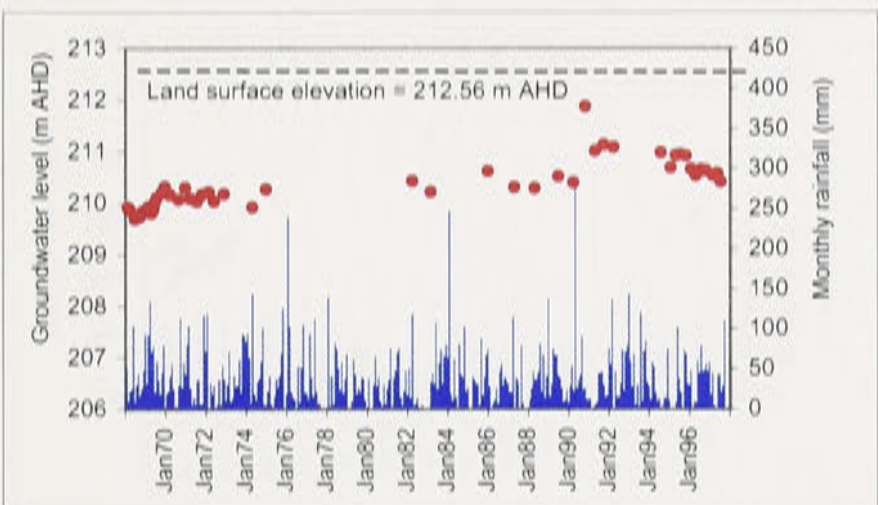
Well no. 10 P



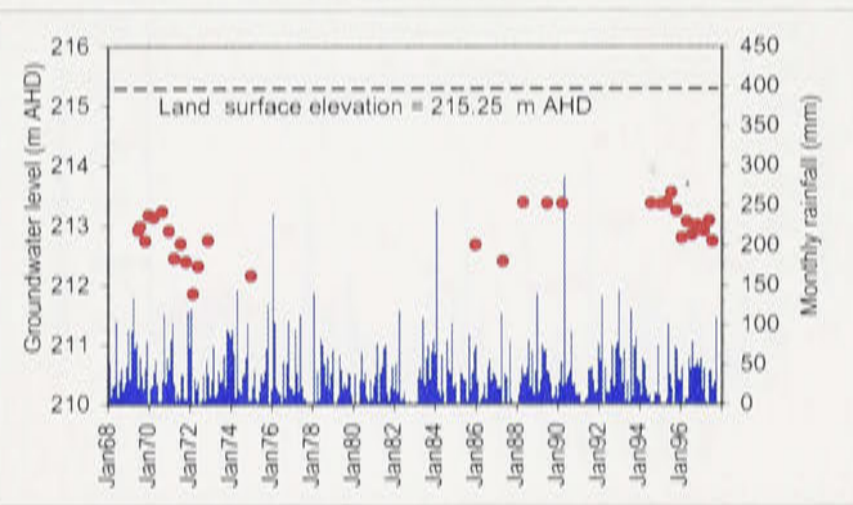
Well no. 11 P



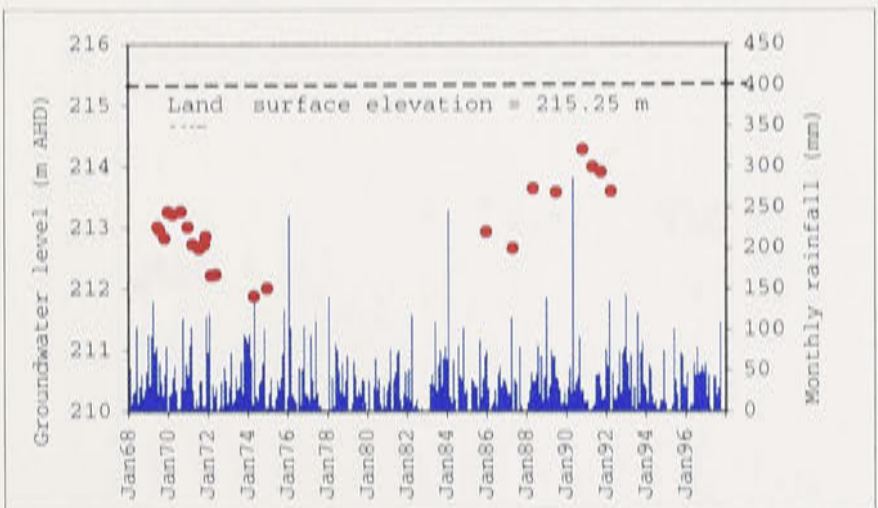
Well no. 12 P



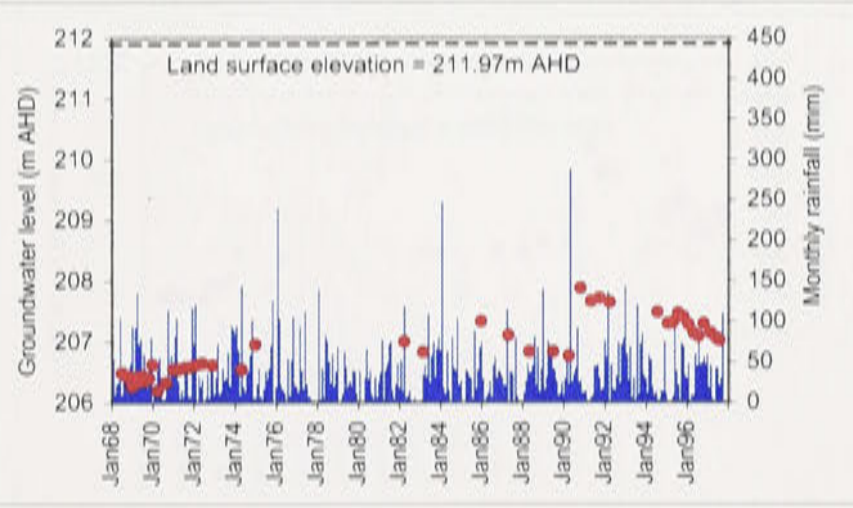
Well no. 14D P



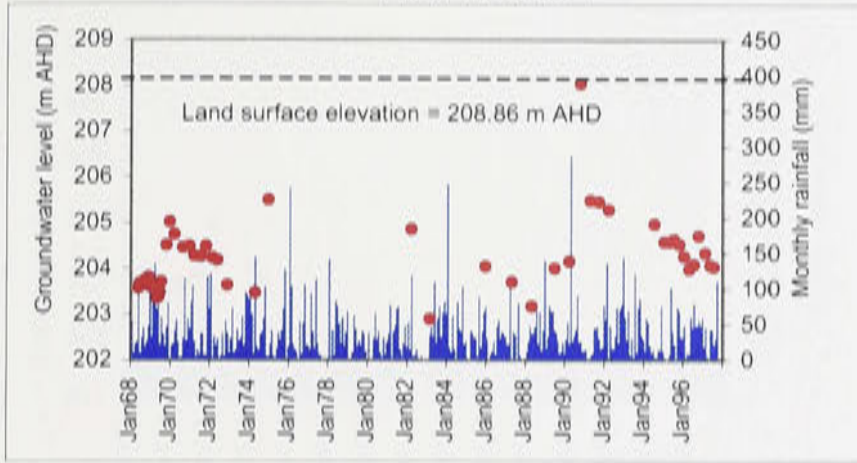
Well no. 14E P



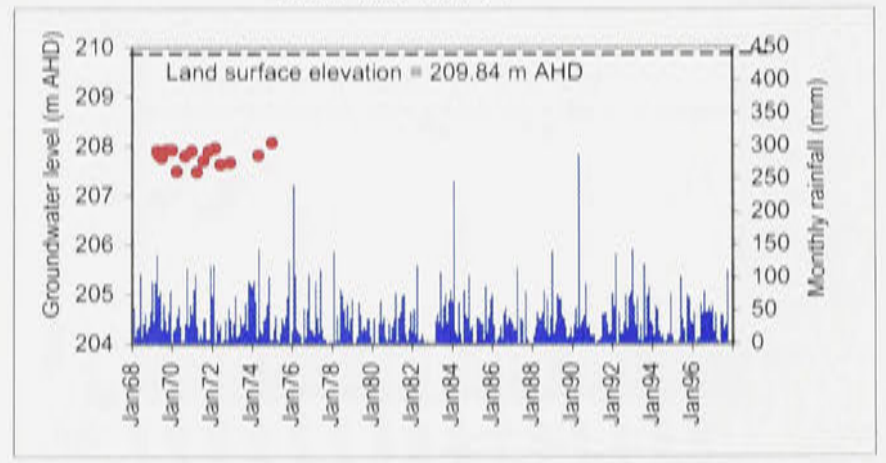
Well no. 20 P



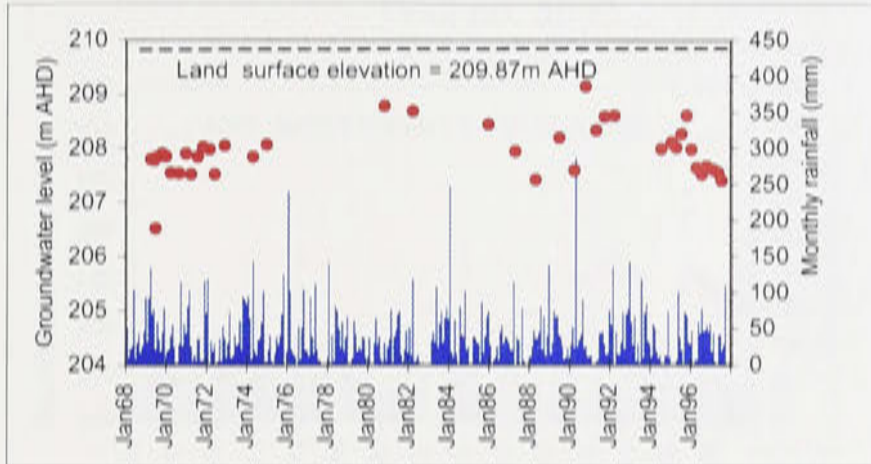
Well no. 22 P



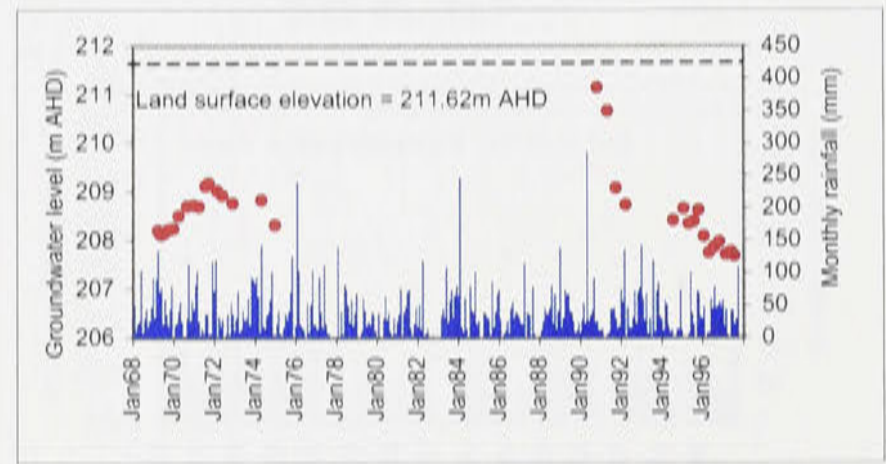
Well no. 26A P



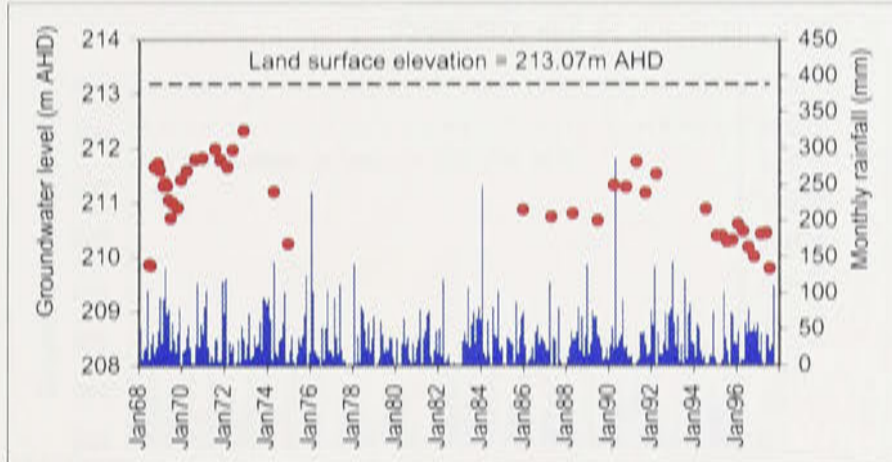
Well no. 26B P



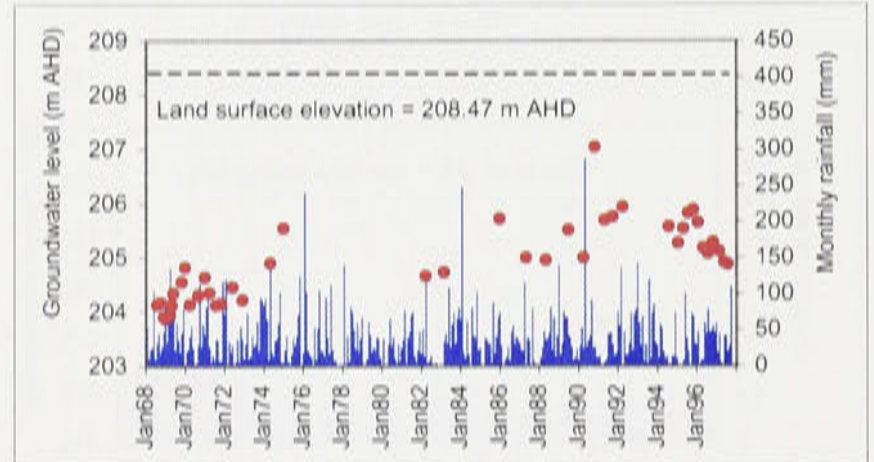
Well no. 26E P



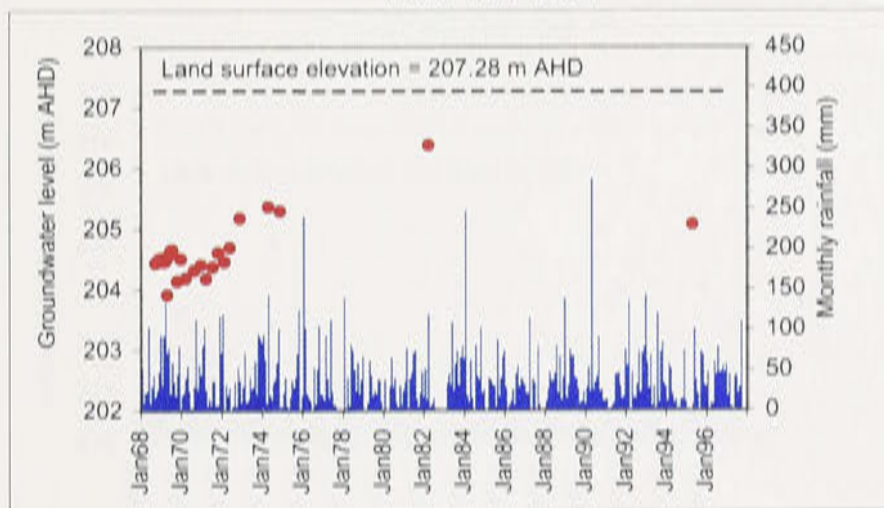
Well no. 27 P



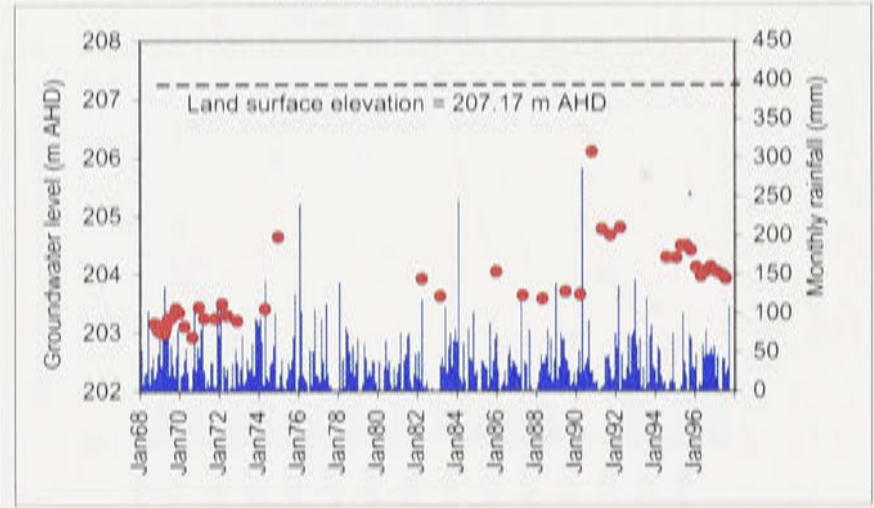
Well no. 29 P



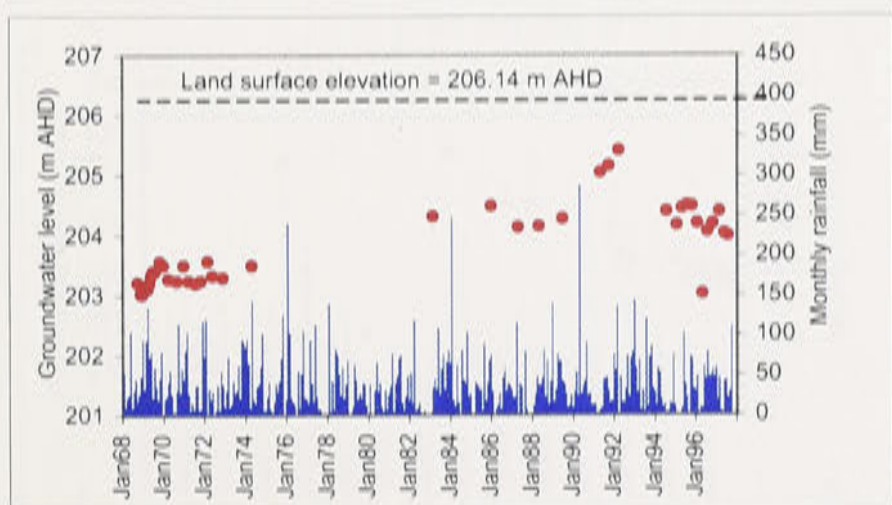
Well no. 30 P



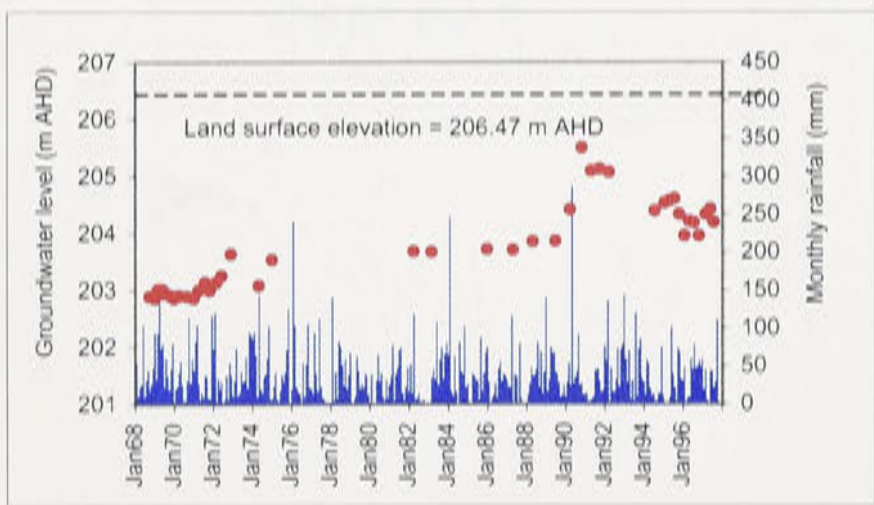
Well no. 33 P



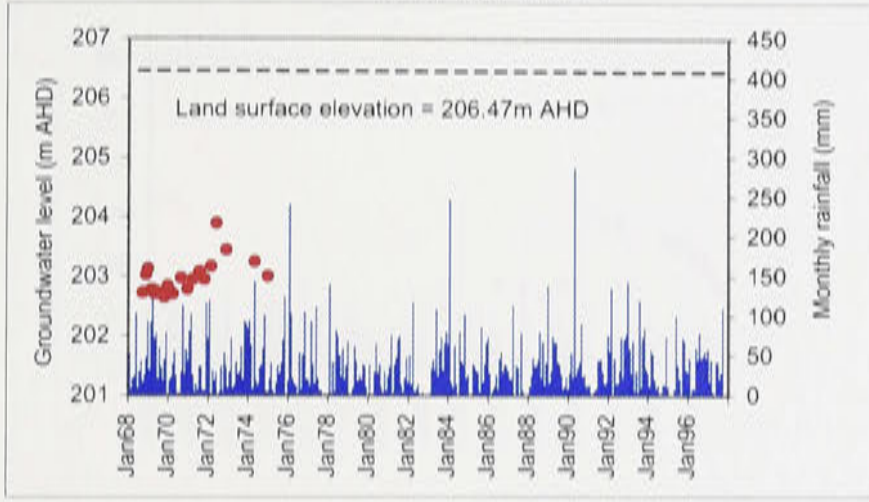
Well no. 34 P



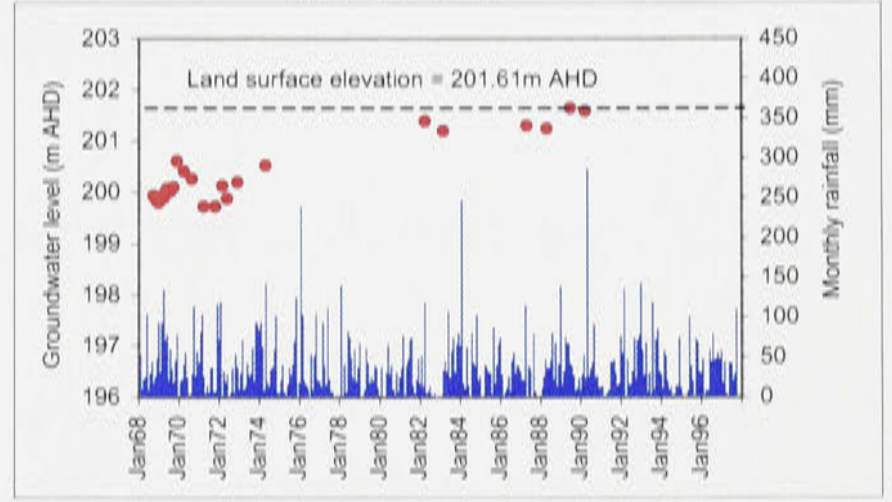
Well no. 35 P



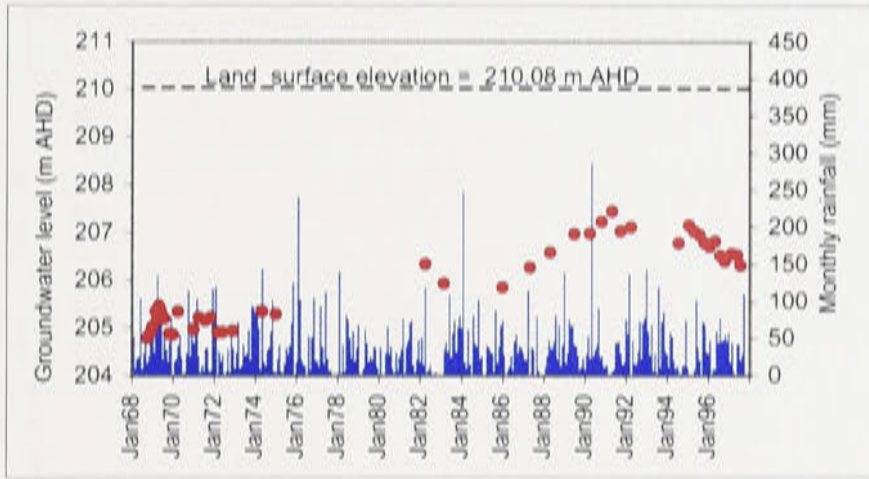
Well no. 35B P



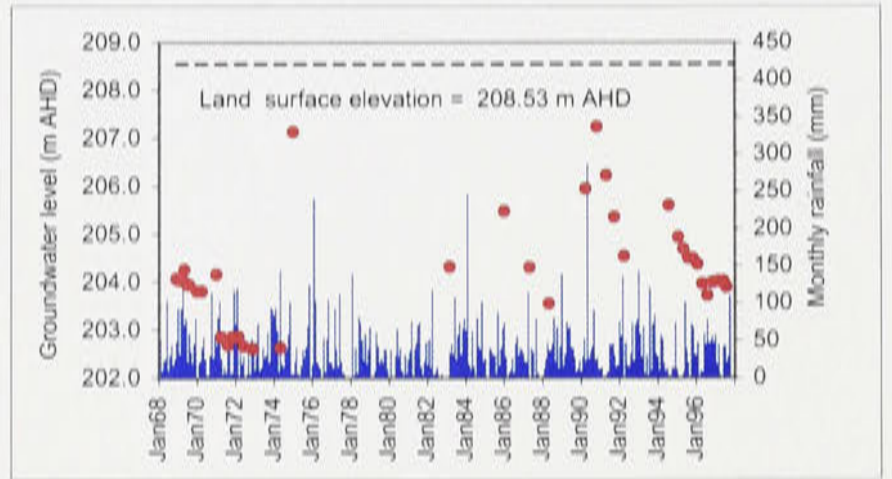
Well no. 36 P



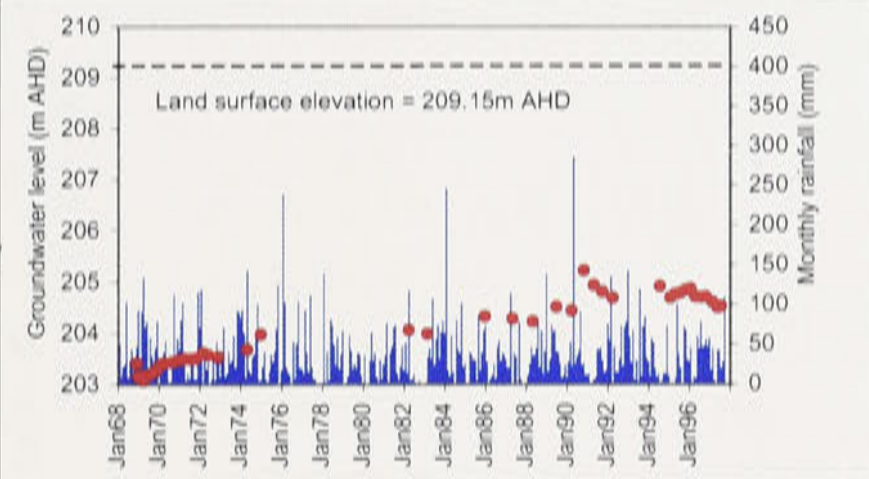
Well no. 40 P



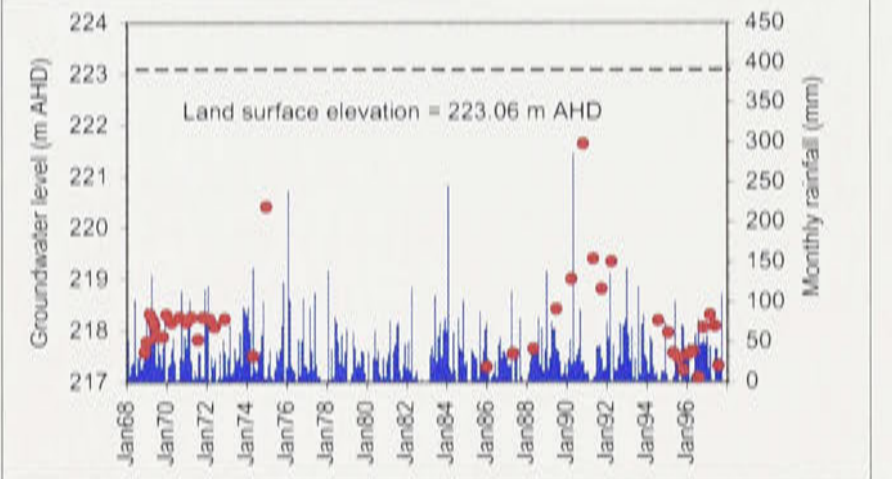
Well no. 43 P



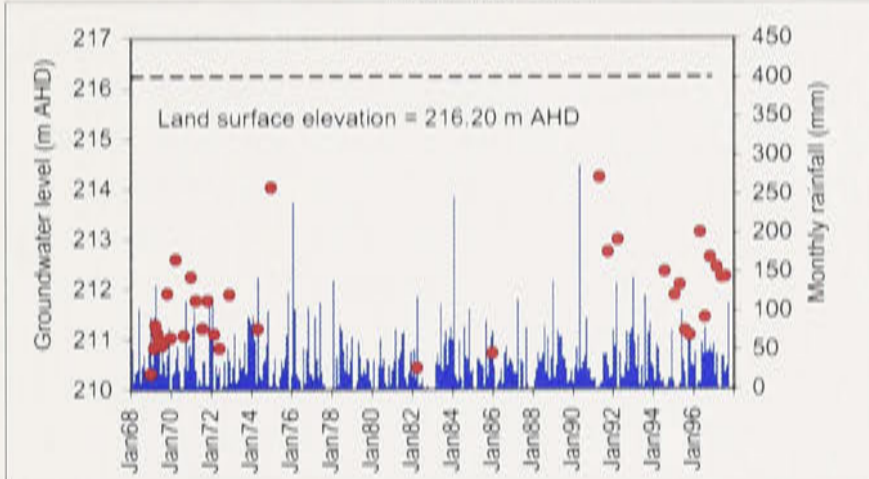
Well no. 47 P



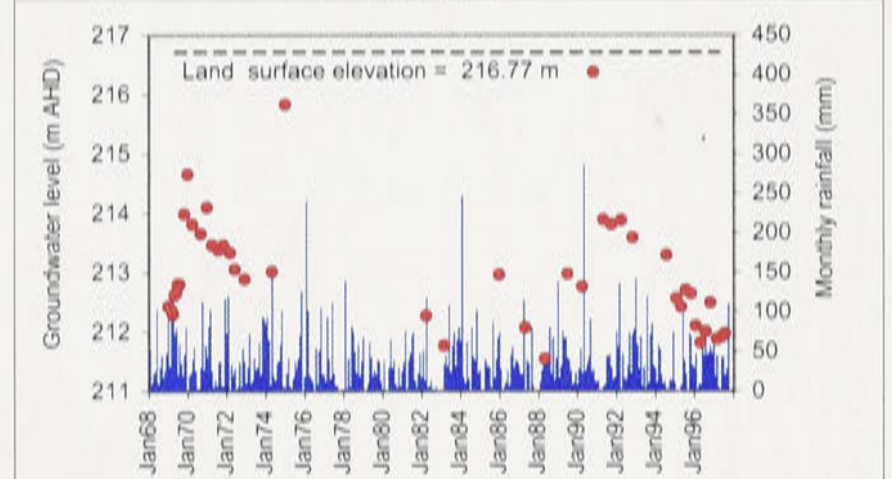
Well no. 51 P



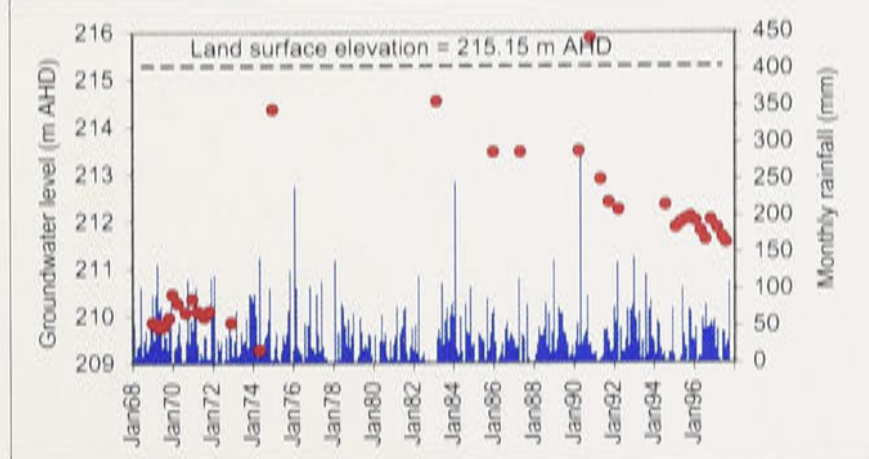
Well no. 53 P



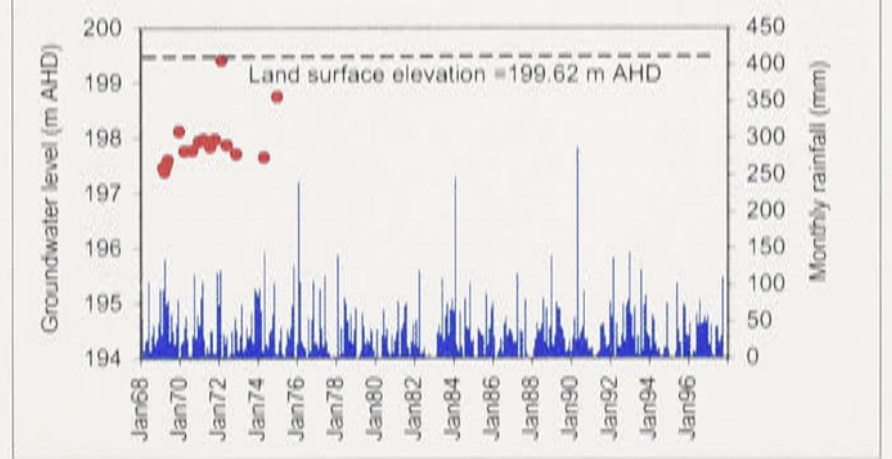
Well no. 58 P



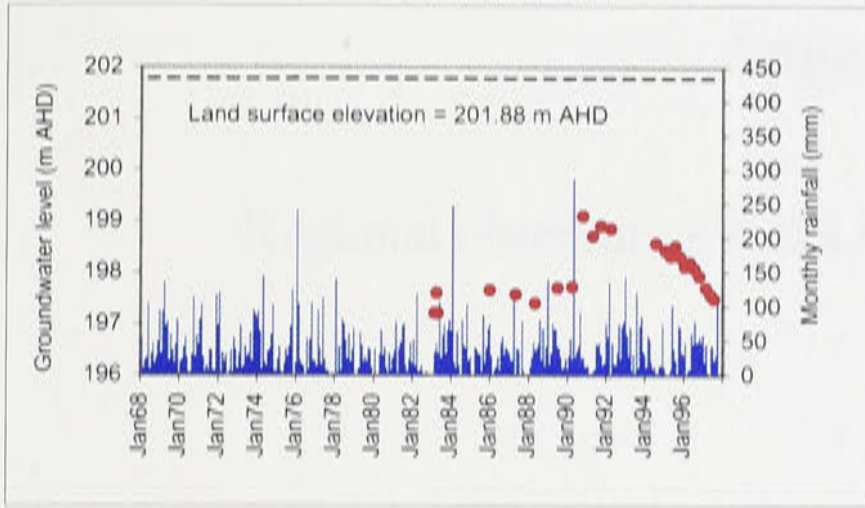
Well no. 60 P



Well no. 65A P



Well no. 91 P



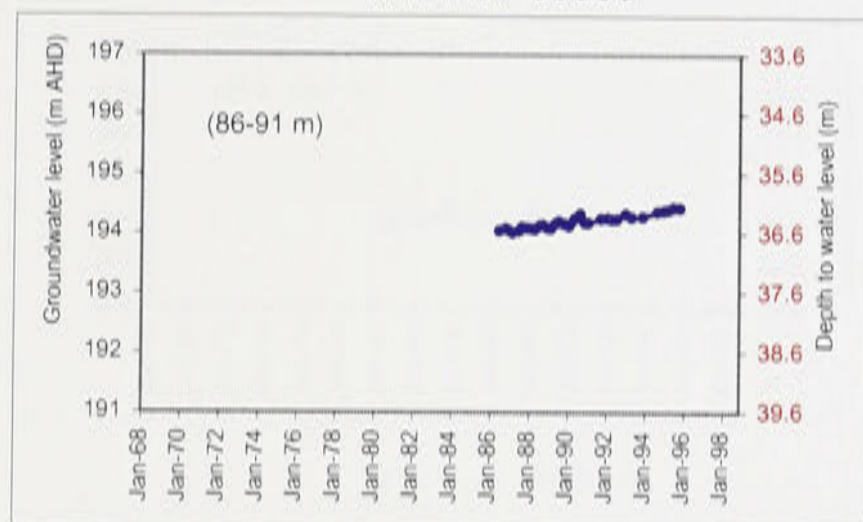
Appendix F

Regional observation wells hydrographs in the study area

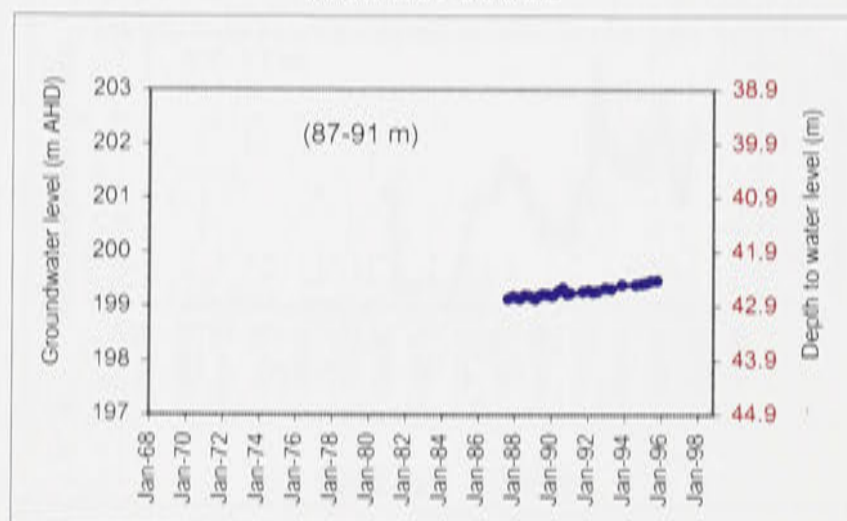


Appendix F.1: Regional observation wells hydrographs at or near cross-section A-A' .
 (see Figures 4.2, 4.3 and 5.3 for locations).

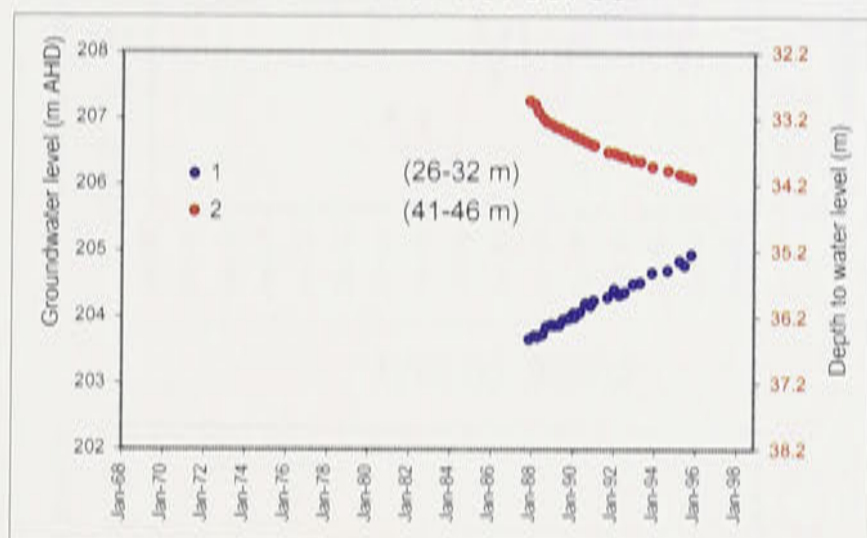
Well no. 36630



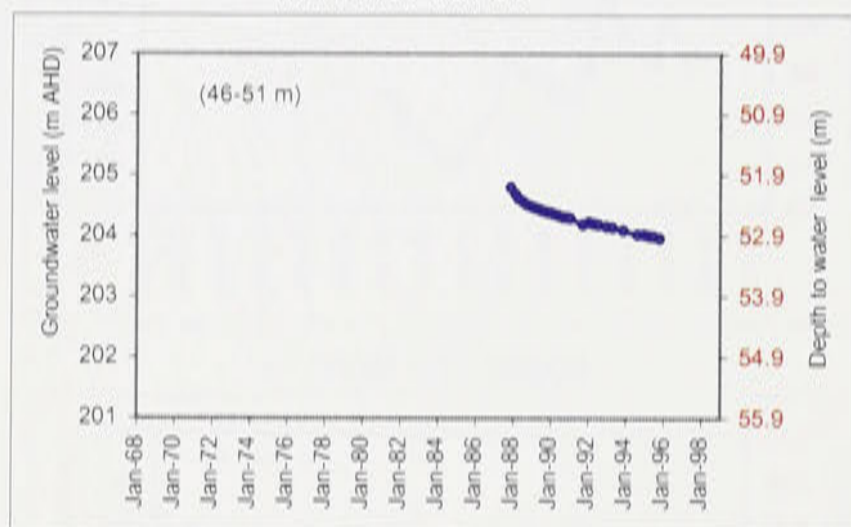
Well no. 36632



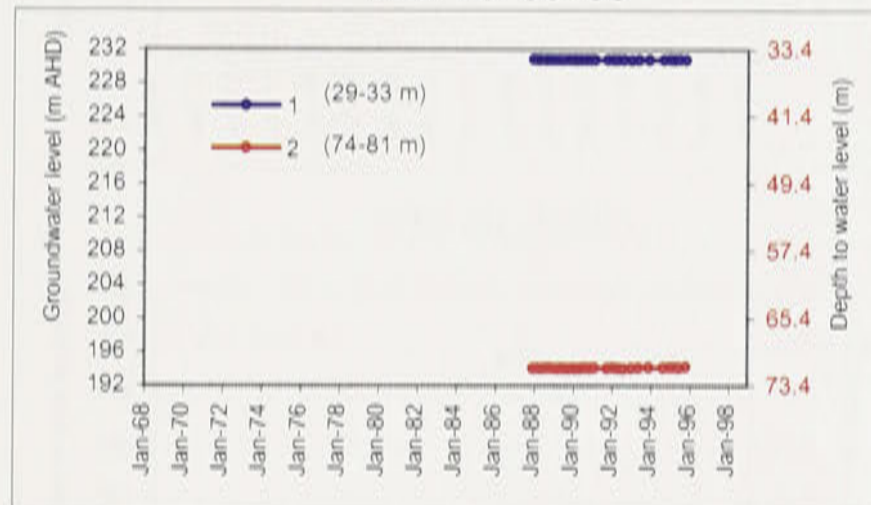
Well no. 36735



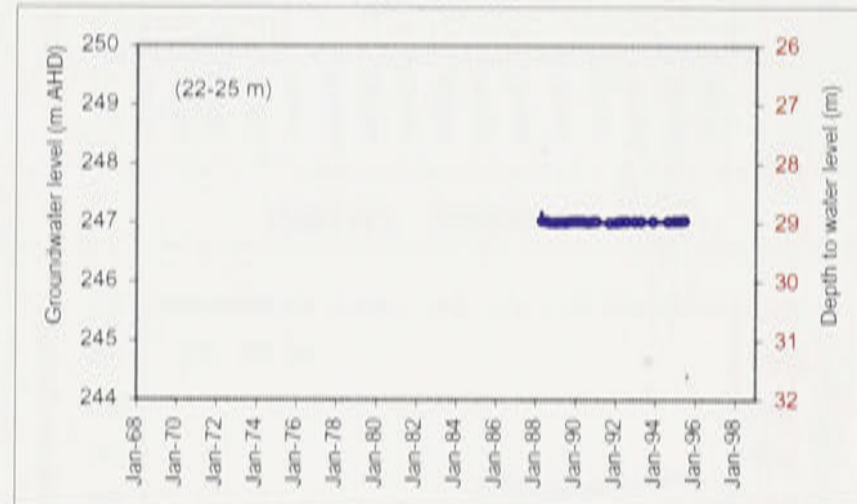
Well no. 36737



Well no. 36738

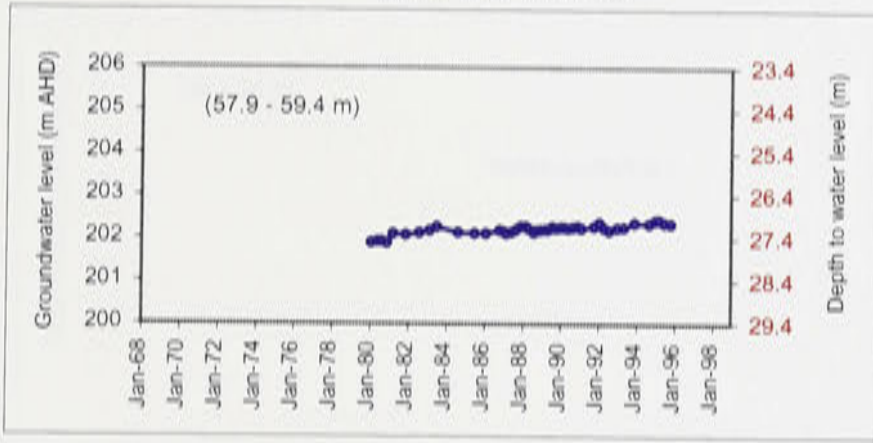


Well no. 36739

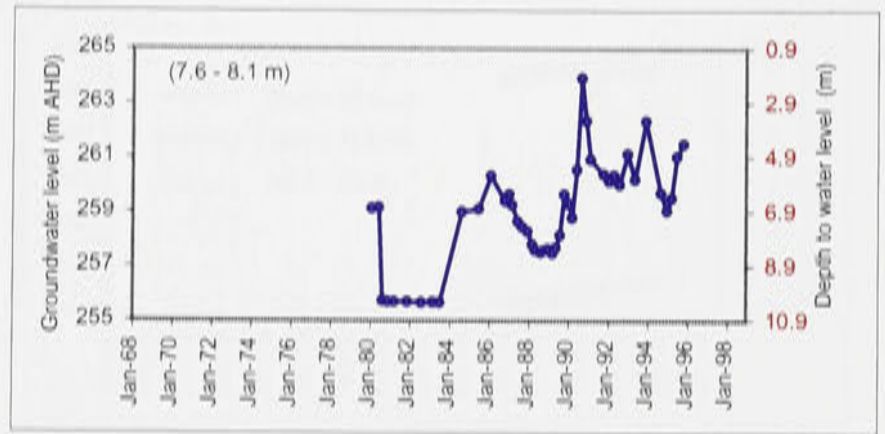


Appendix F.2: Regional observation wells hydrographs at or near cross-section B-B'.
(see Figure 4.2, 4.4 and 5.3 for locations).

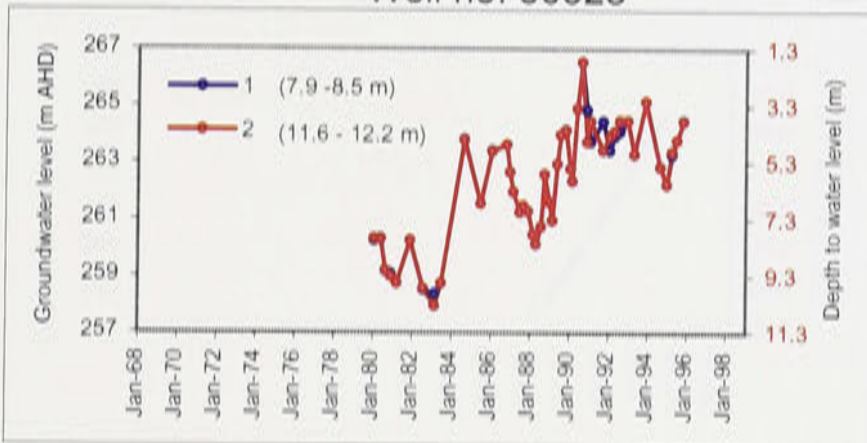
Well no. 30270



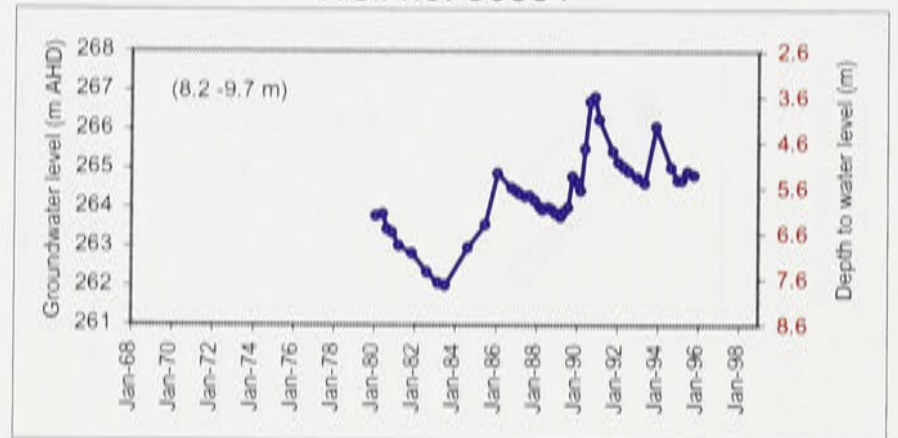
Well no. 30291



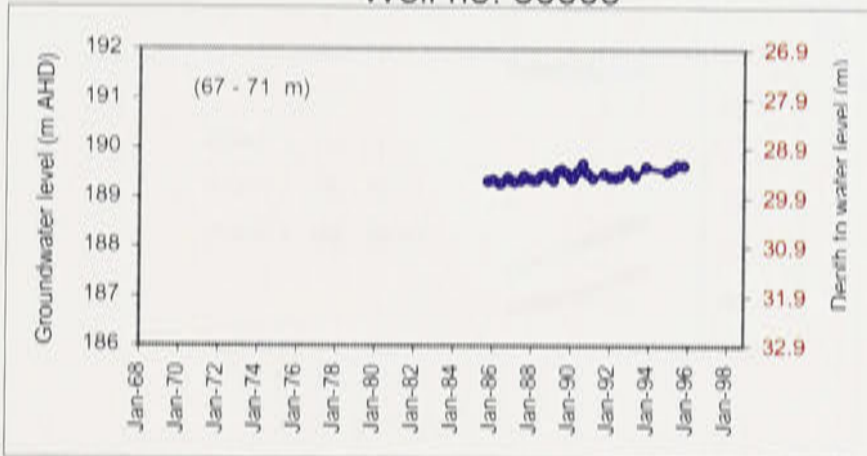
Well no. 30328



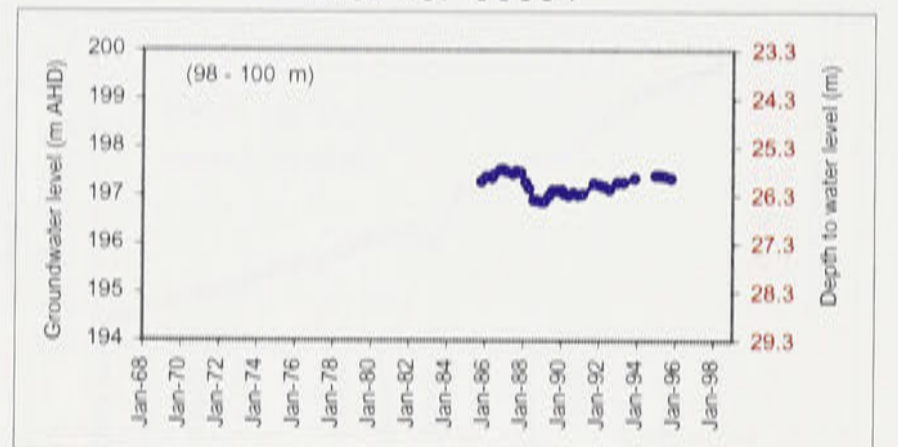
Well no. 30331



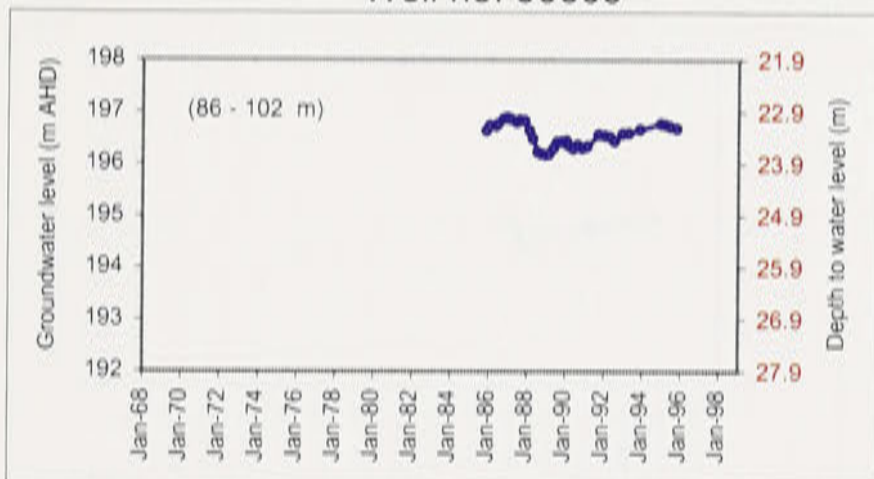
Well no. 36603



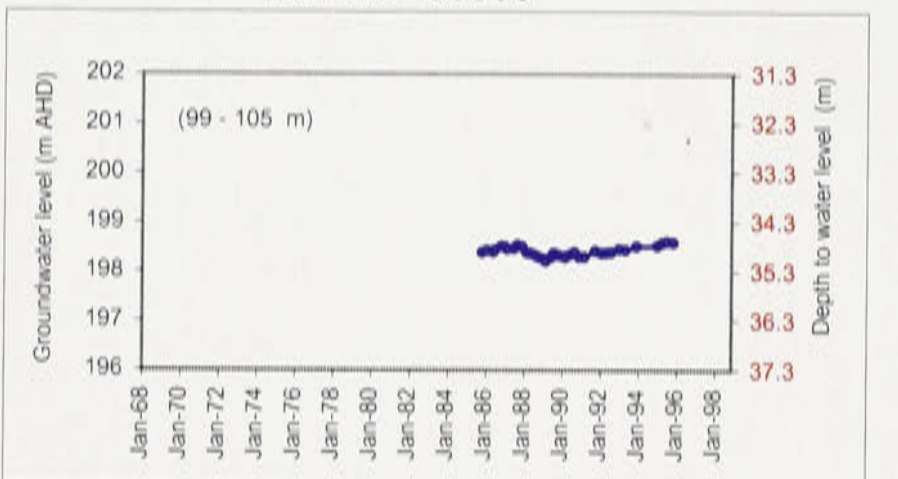
Well no. 36604



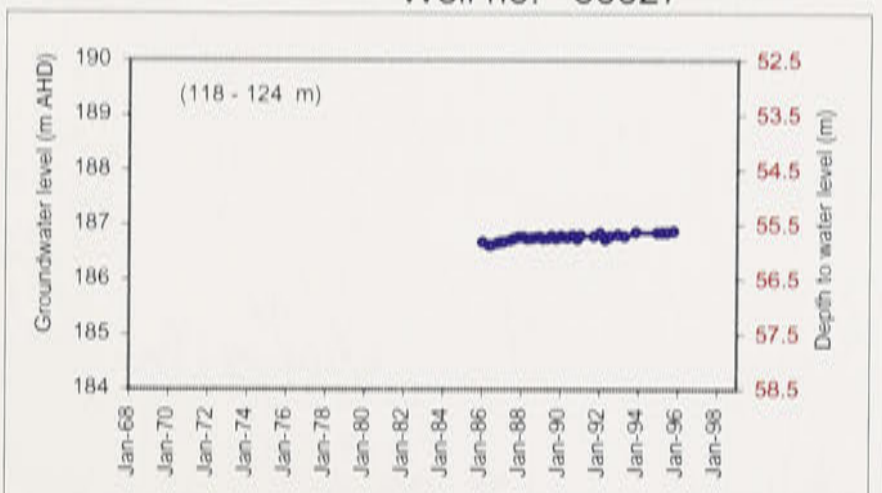
Well no. 36605



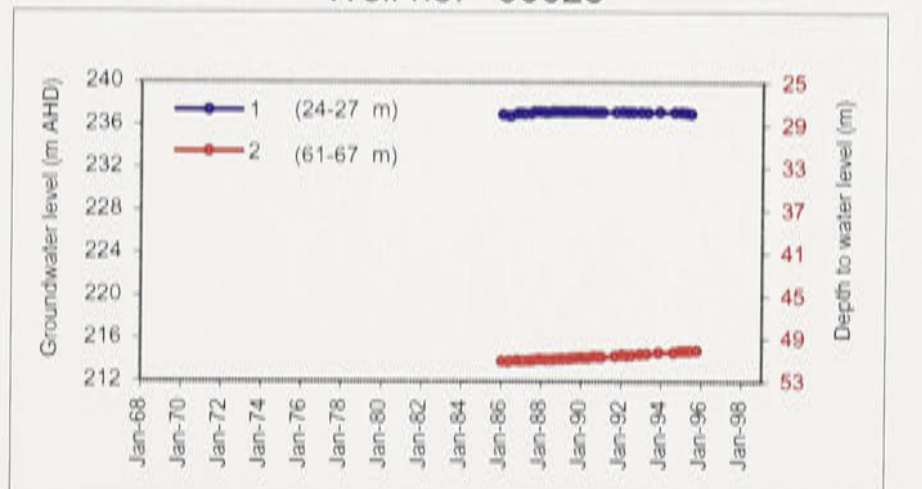
Well no. 36606



Well no. 36627

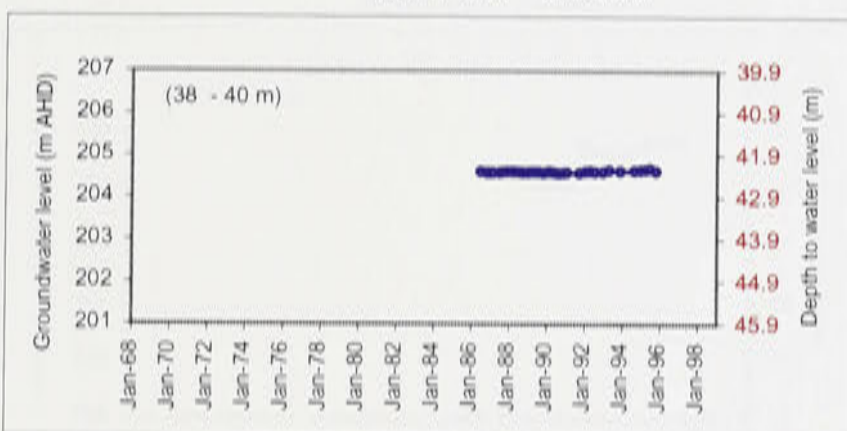


Well no. 36628

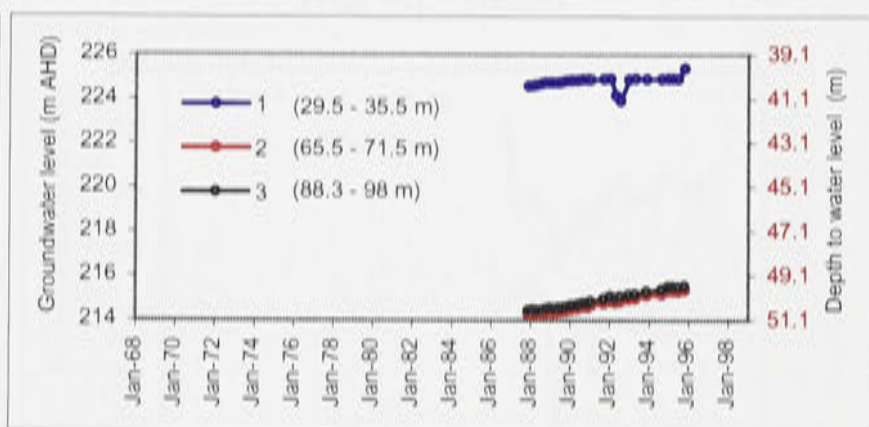


Appendix F.2 (continued).

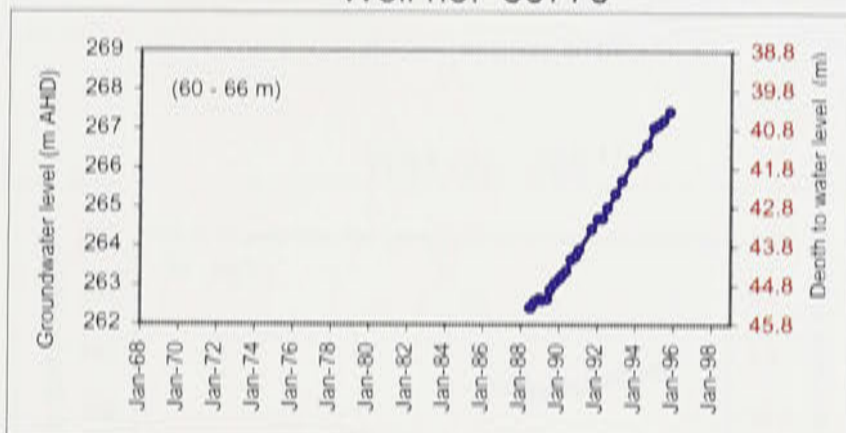
Well no. 36629



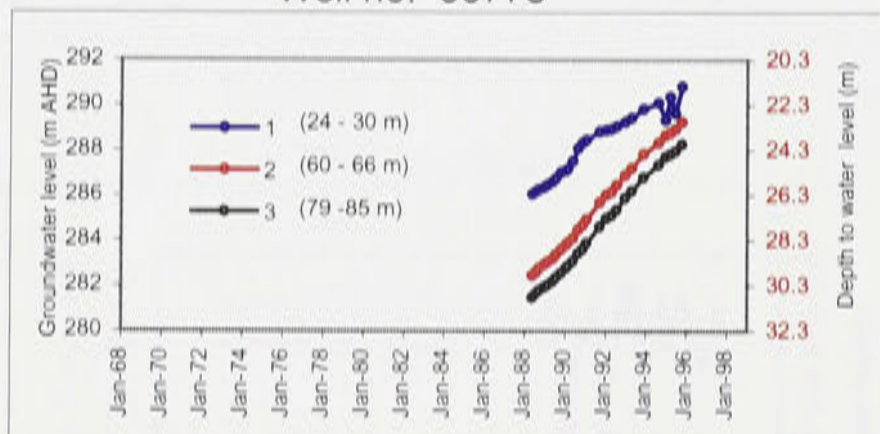
Well no. 36741



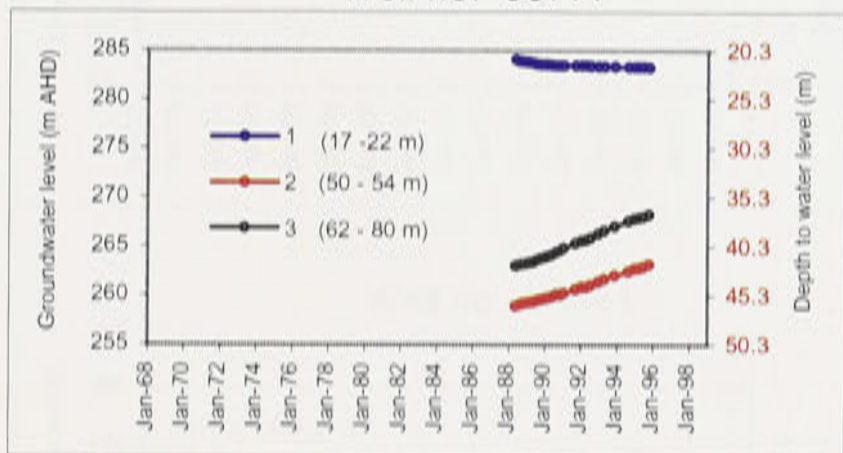
Well no. 36776



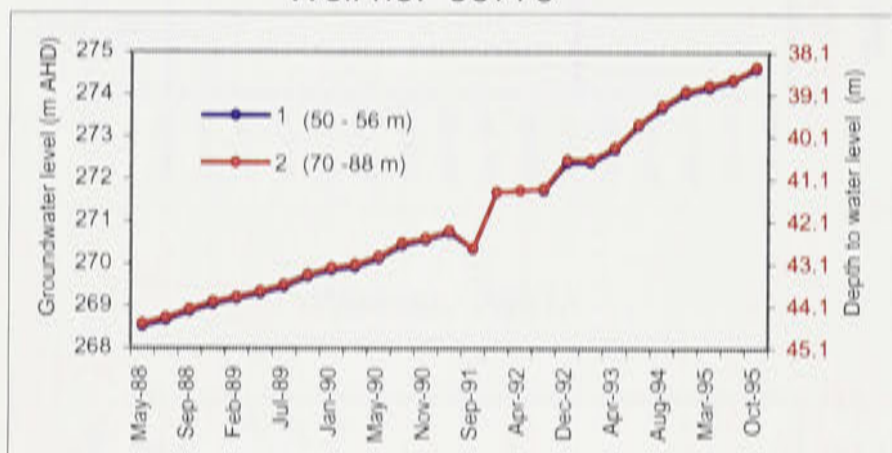
Well no. 36778



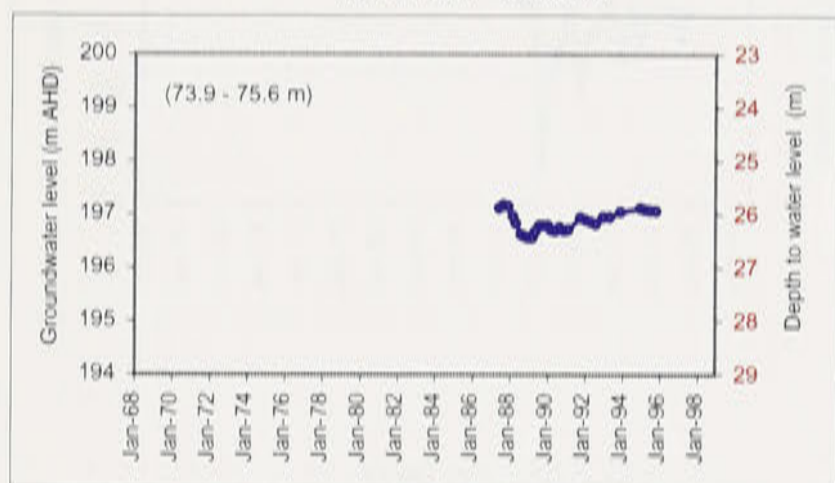
Well no. 36777



Well no. 36779

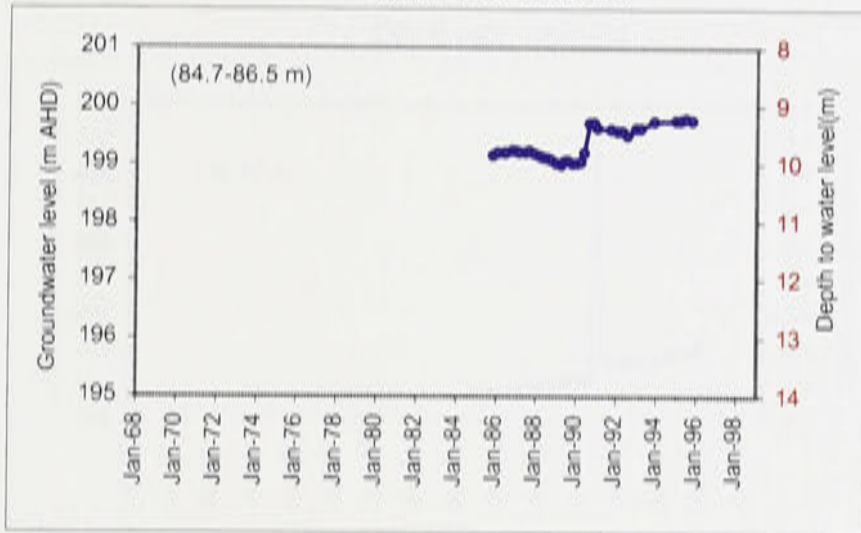


Well no. 39379

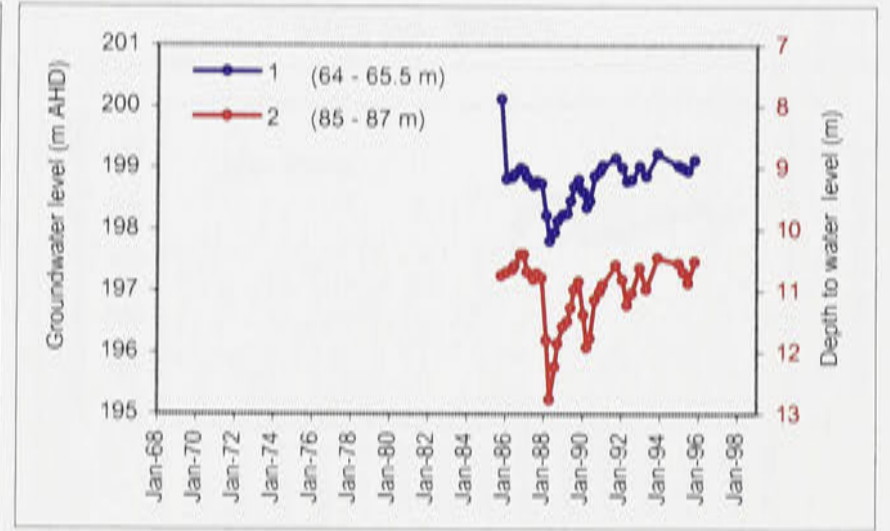


Appendix F.3: Regional observation wells hydrographs at or near cross-section C-C' .
 (see Figures 4.2, 4.5 and 5.3 for locations).

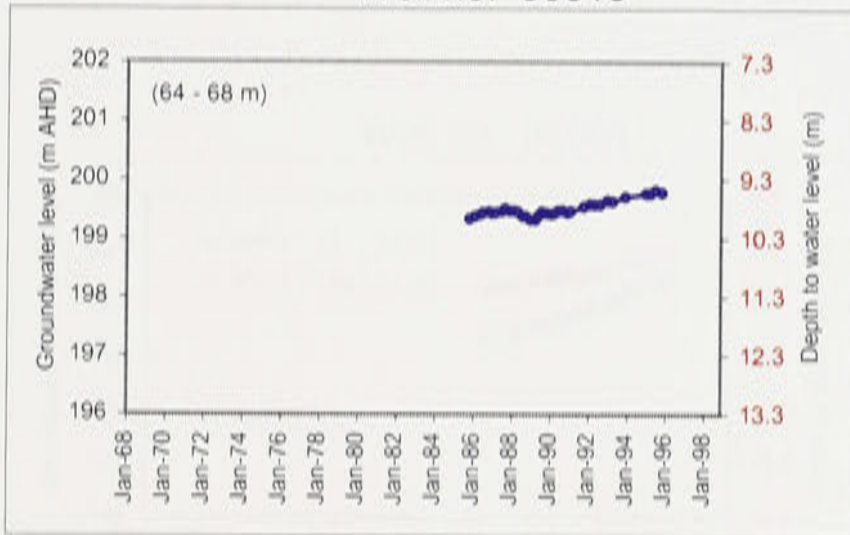
Well no. 36595



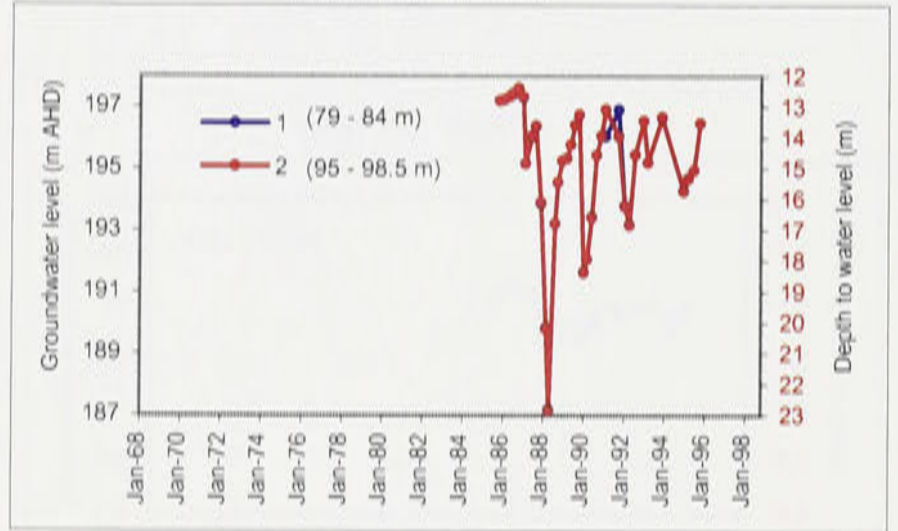
Well no. 36596



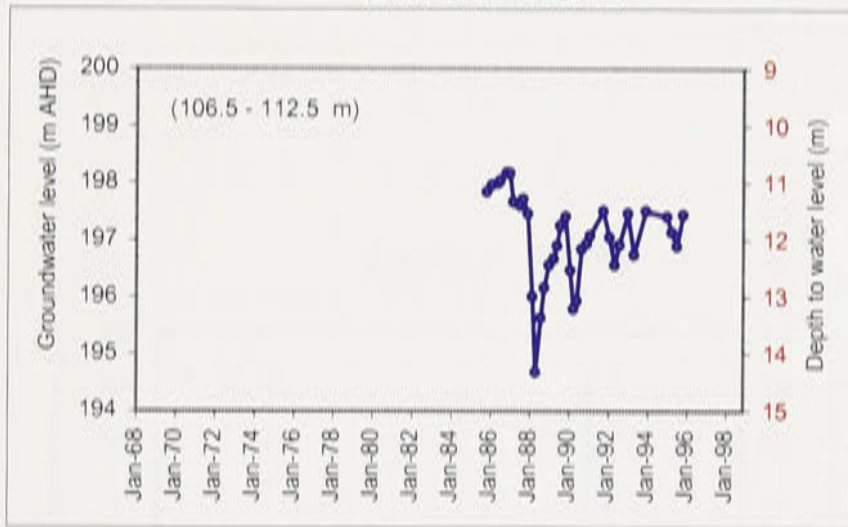
Well no. 36610



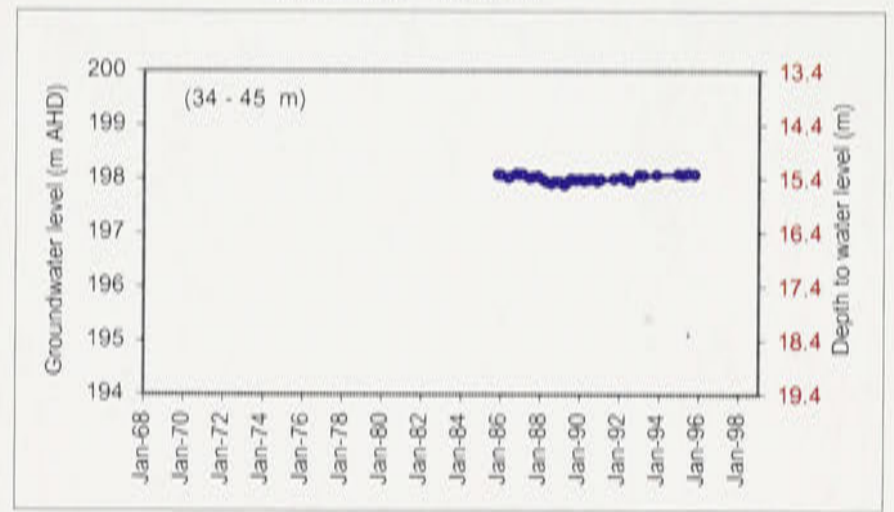
Well no. 36597



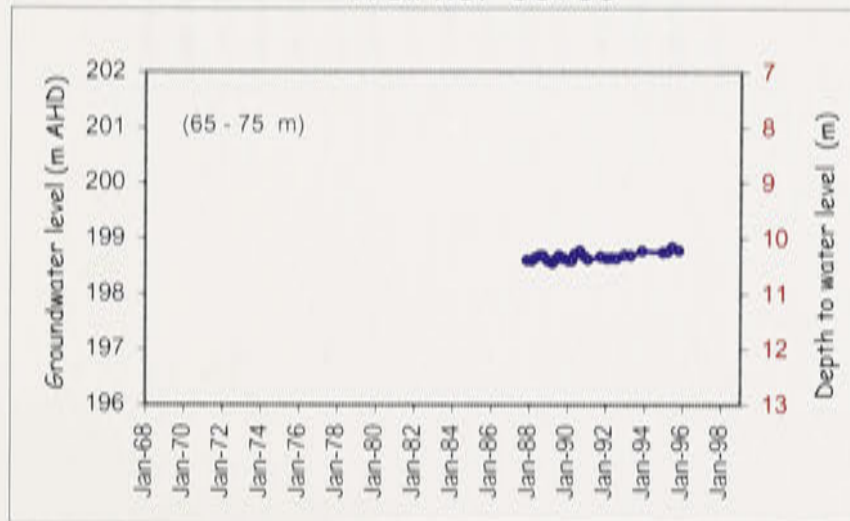
Well no. 36611



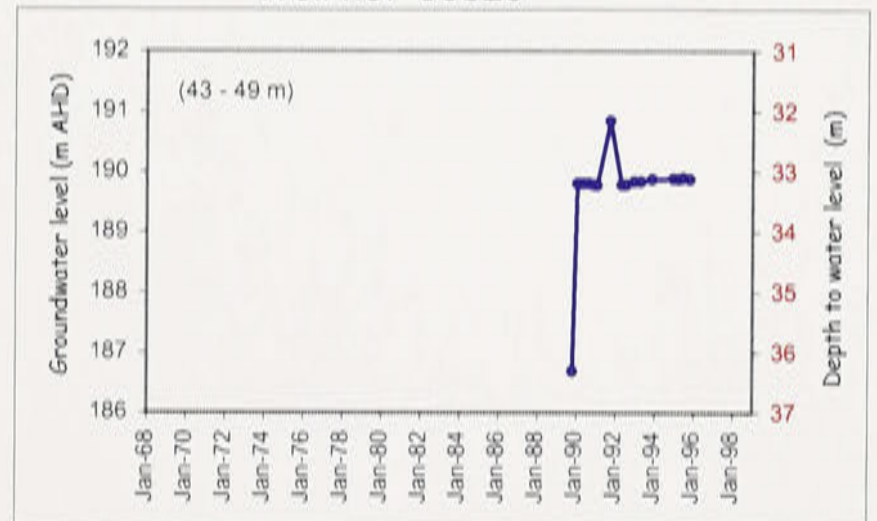
Well no. 36613



Well no. 36700

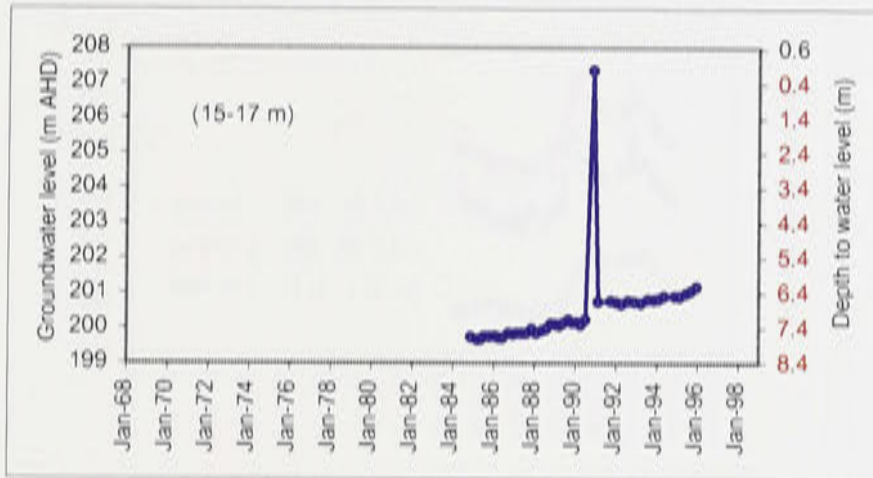


Well no. 36825

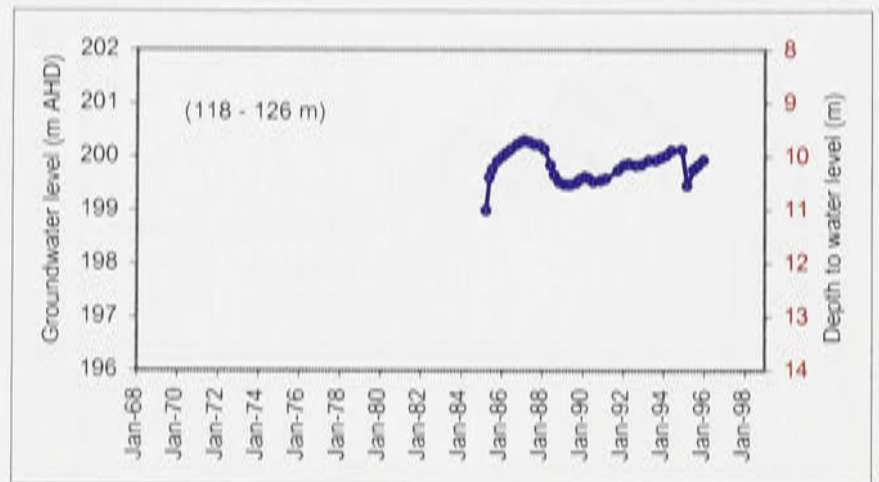


Appendix F.4: Regional observation wells hydrographs at or near cross-section D-D'.
 (see Figures 4.2, 4.6 and 5.3 for locations).

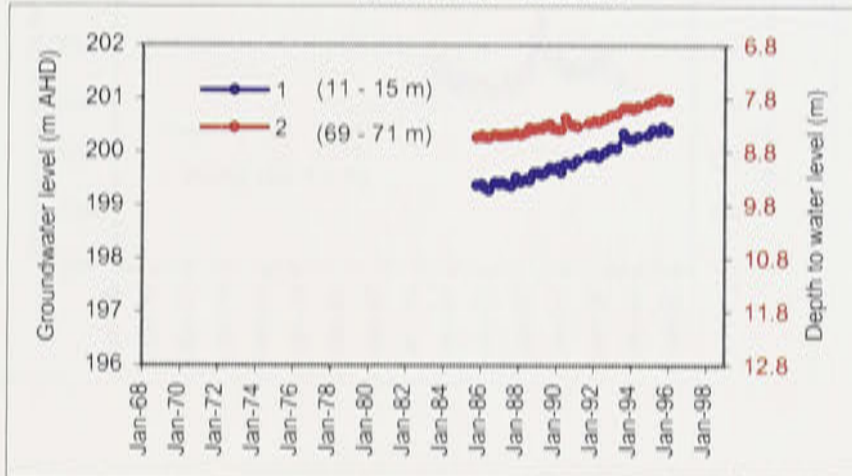
Well no. 36524



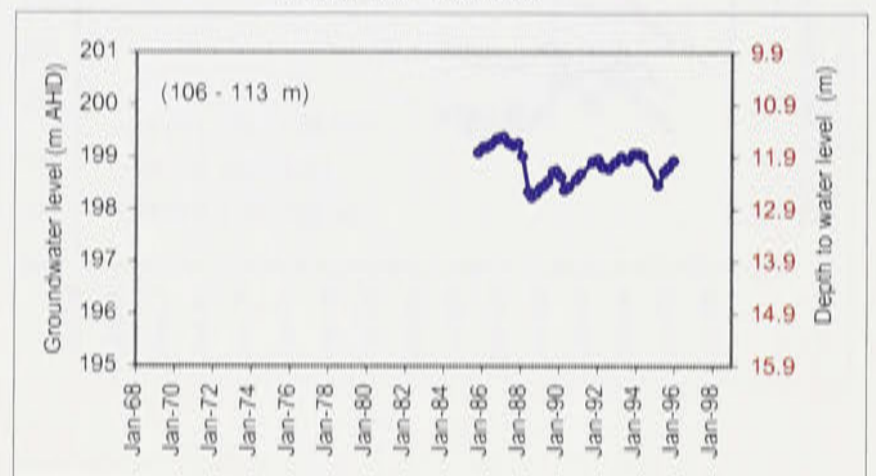
Well no. 36553



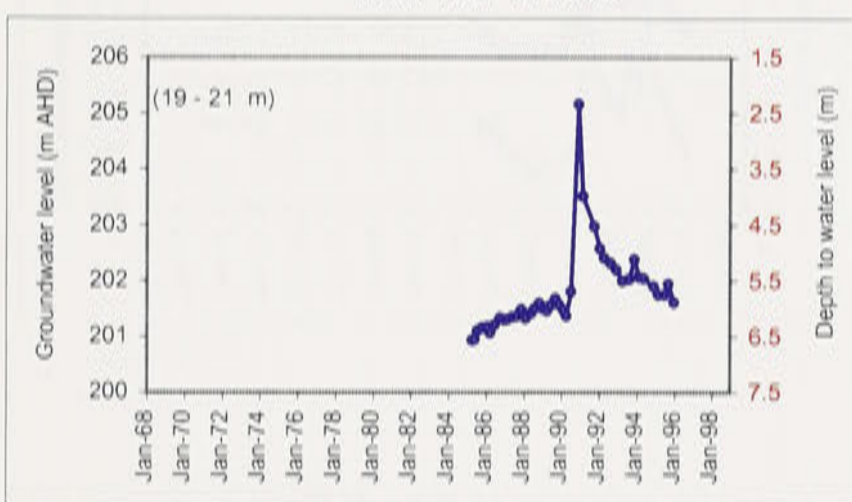
Well no. 36594



Well no. 36609

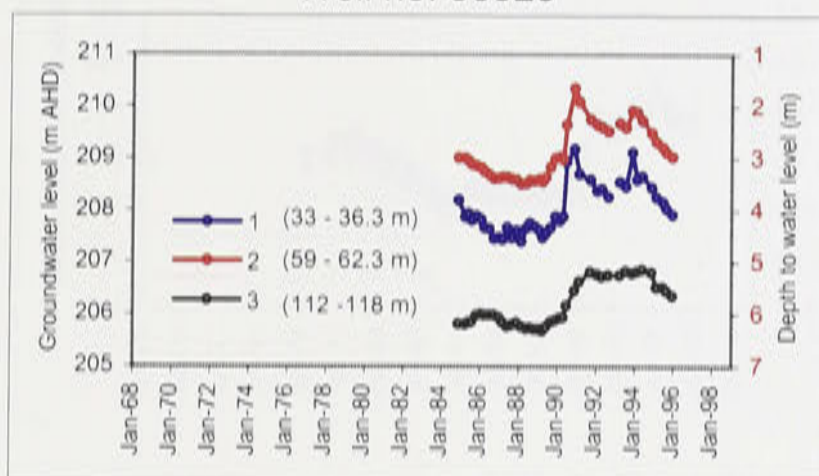


Well no. 36563

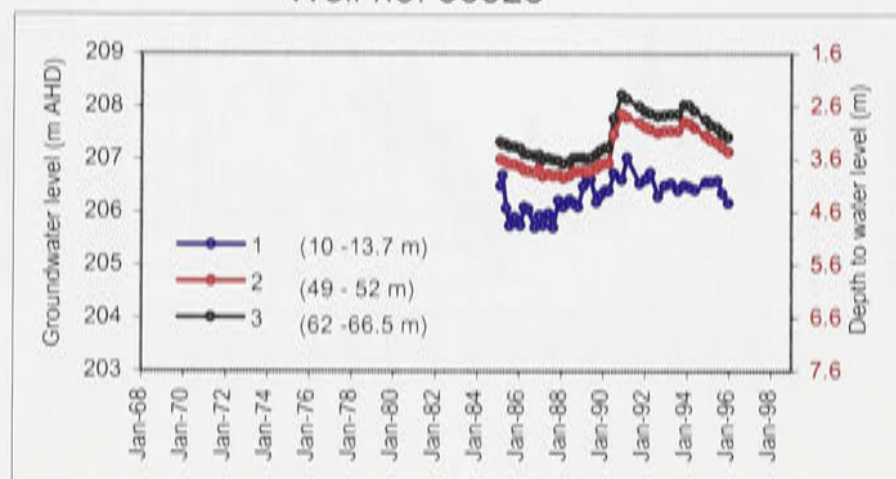


Appendix F.5: Regional observation wells hydrographs at or near cross-section E-E' .
 (see Figures 4.2, 4.7 and 5.3 for locations).

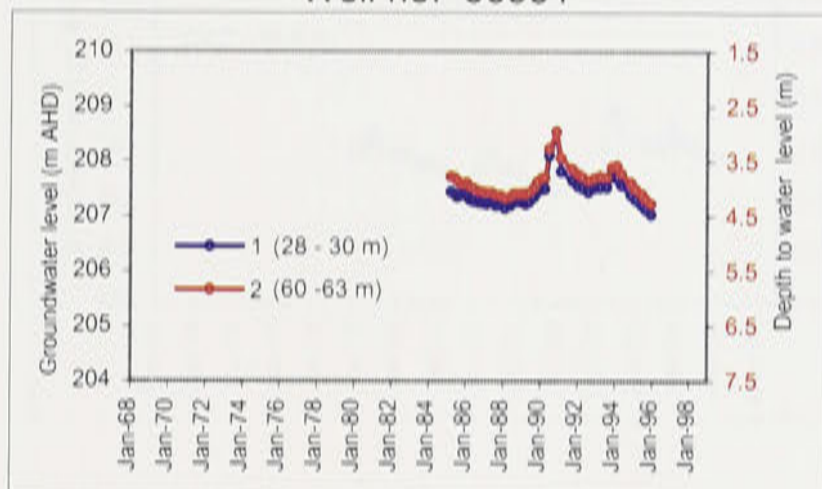
Well no. 36523



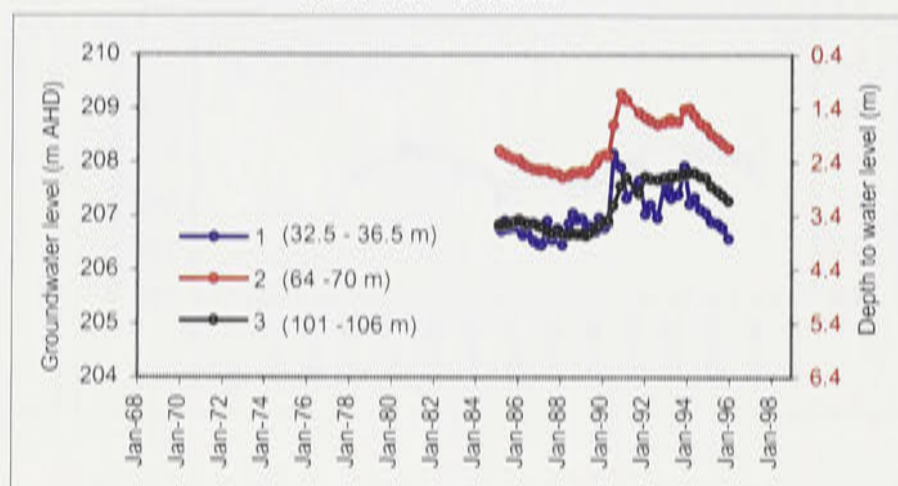
Well no. 36528



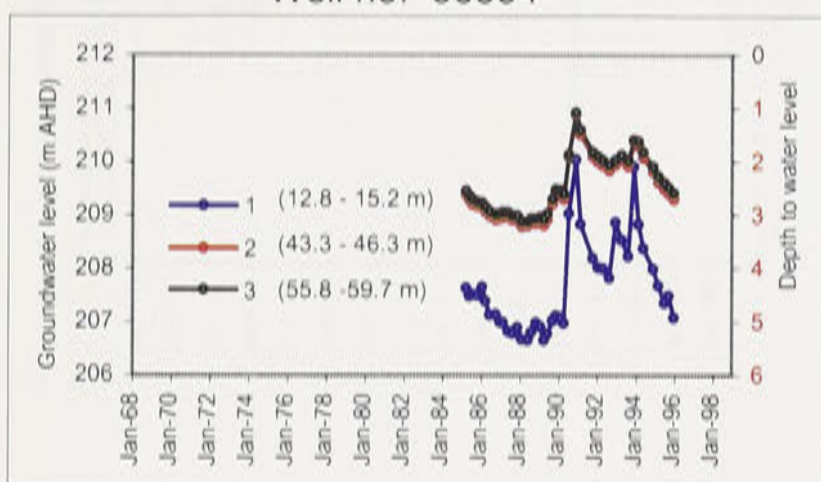
Well no. 36551



Well no. 36552

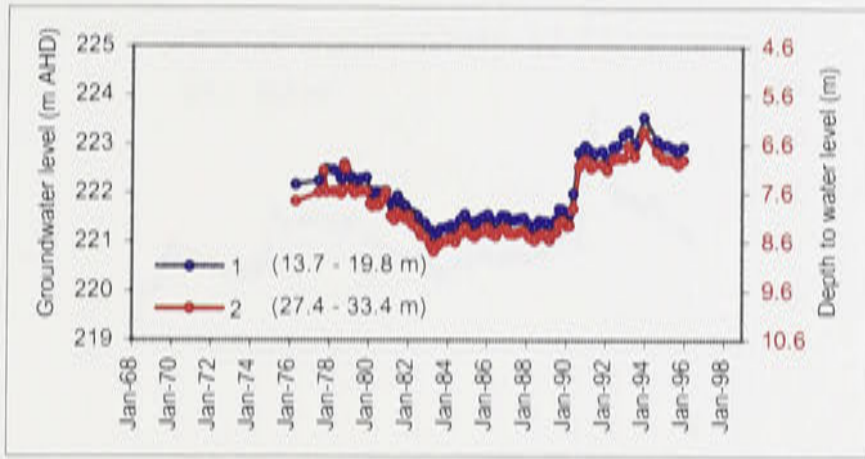


Well no. 36554

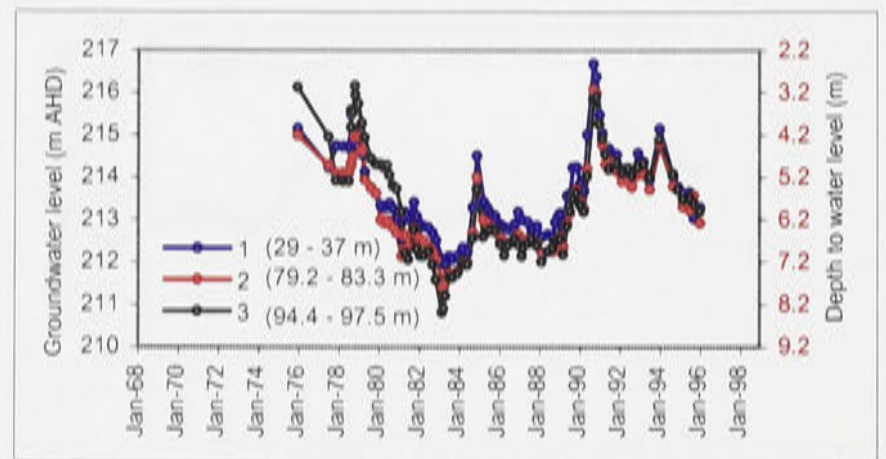


Appendix F.6: Regional observation wells hydrographs at or near cross-section F-F'.
 (see Figures 4.2, 4.8, and 5.3 for locations).

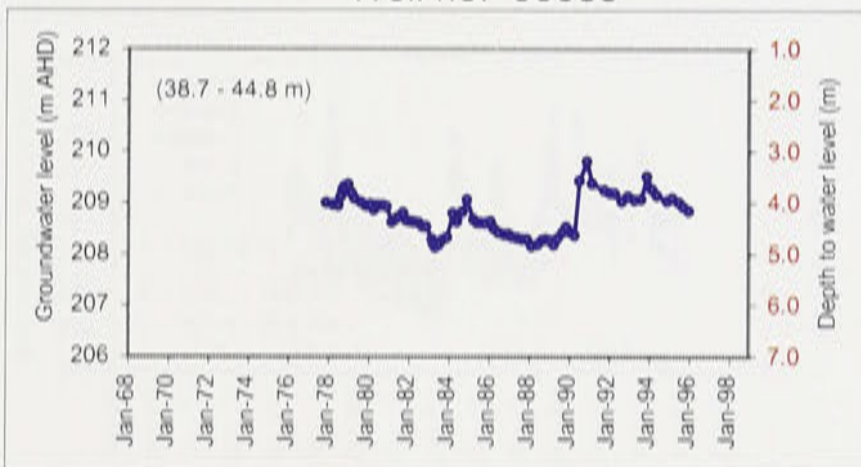
Well no. 36030



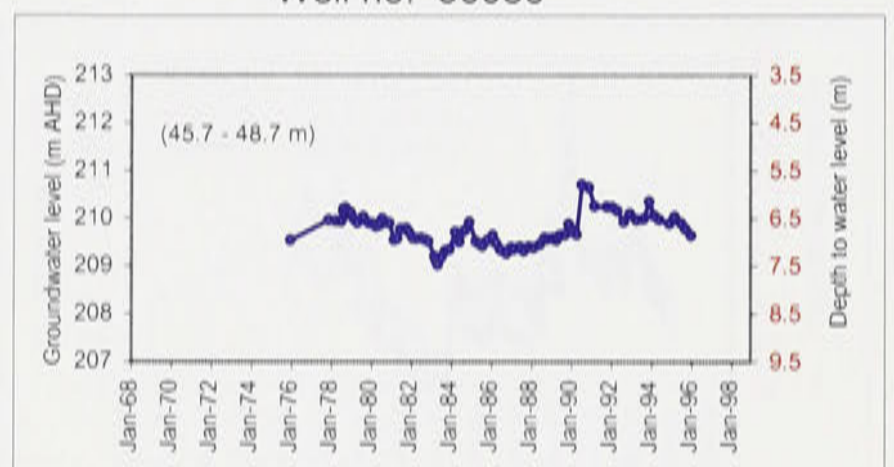
Well no. 36081



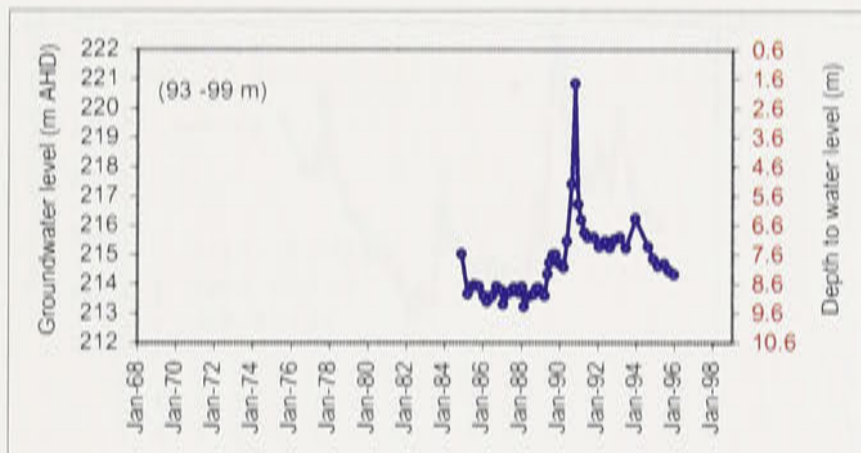
Well no. 36085



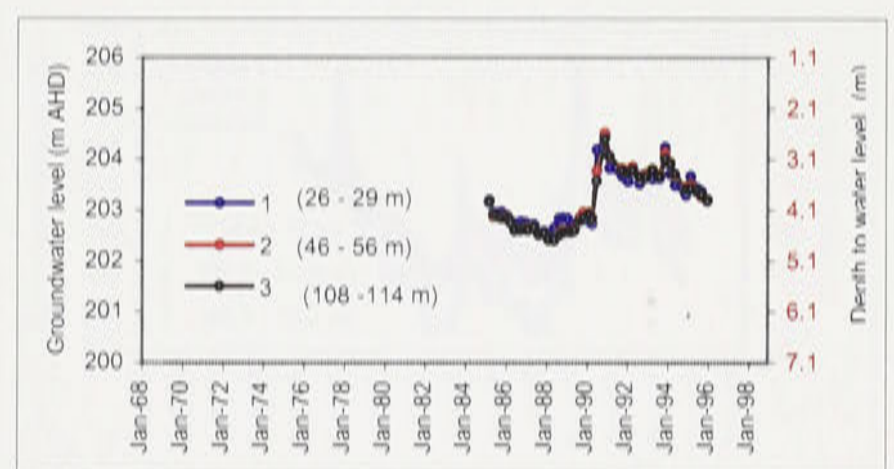
Well no. 36086



Well no. 36525

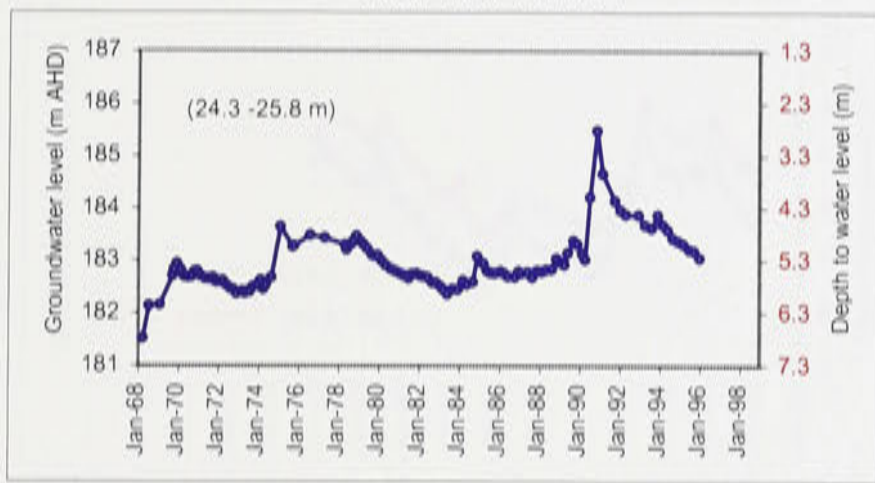


Well no. 36550

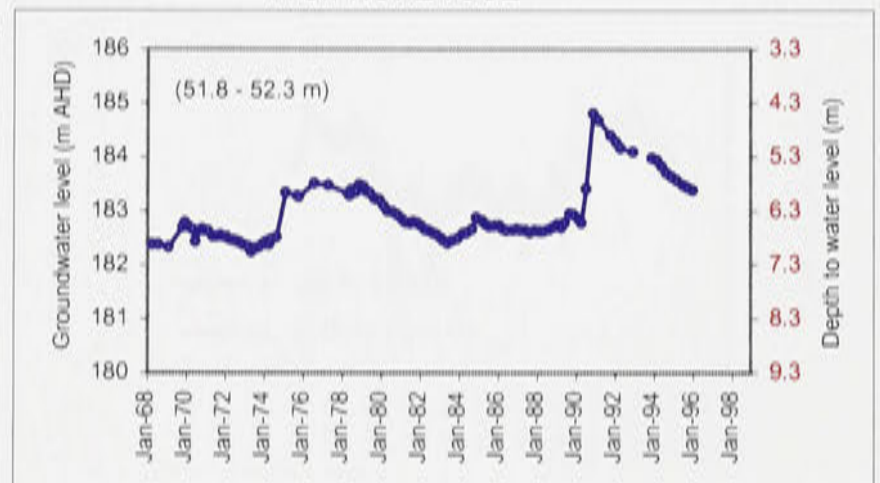


Appendix F.7: Regional observation wells hydrographs at or near cross-section G-G'.
 (see Figures 4.2, 4.9 and 5.3 for locations).

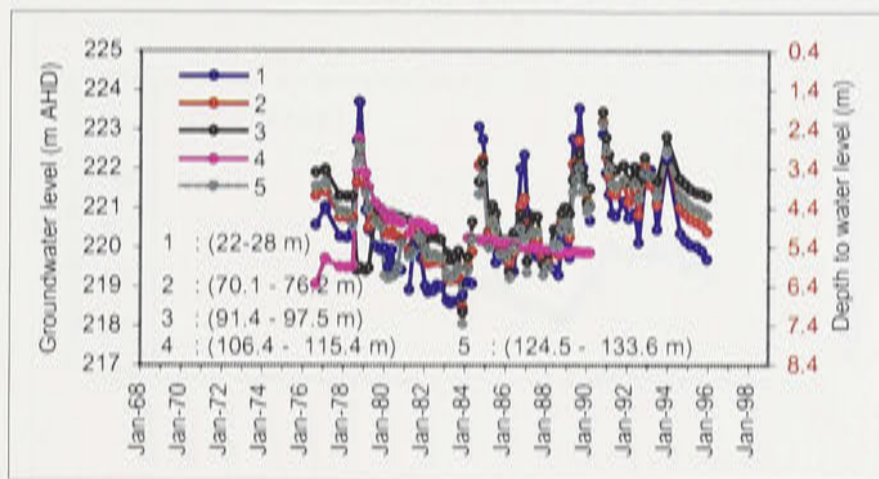
Well no. 21301



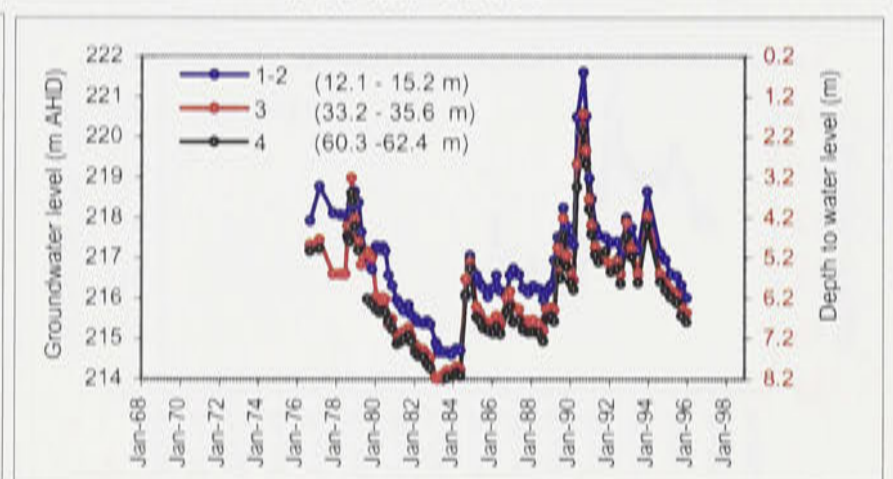
Well no. 21302



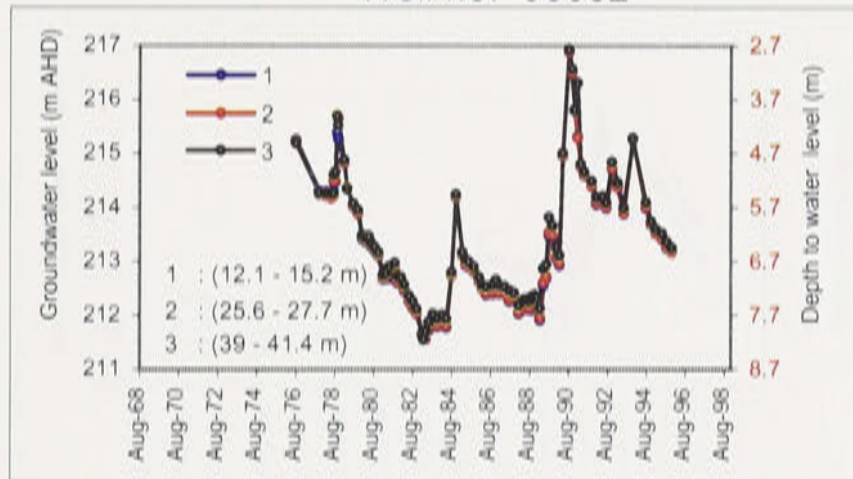
Well no. 36079



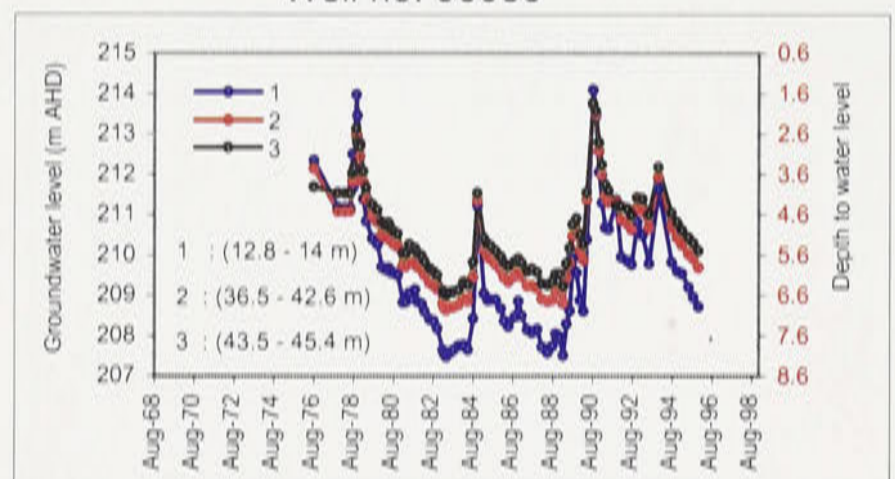
Well no. 36080



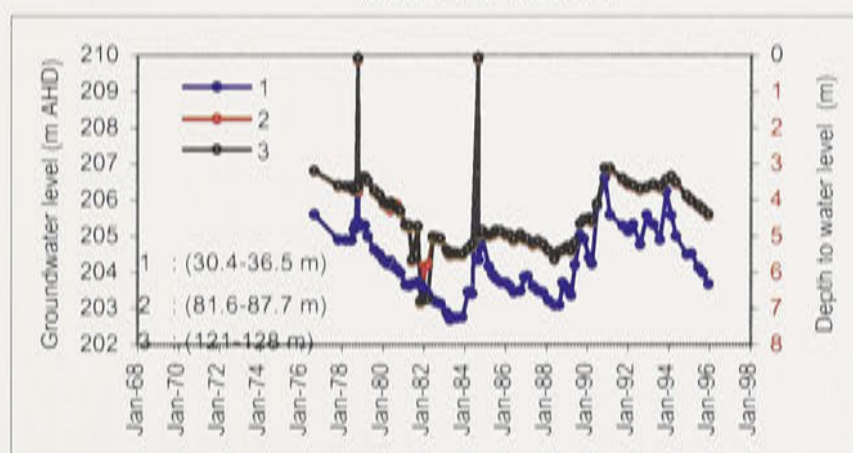
Well no. 36082



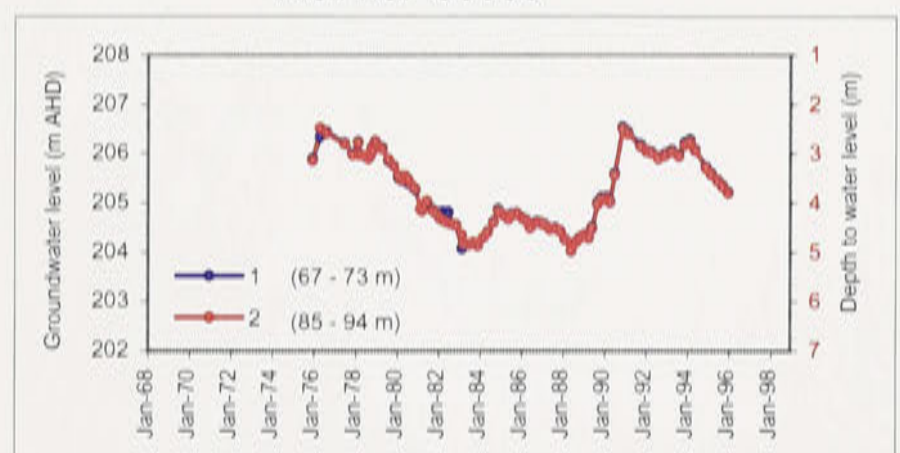
Well no. 36083



Well no. 36087

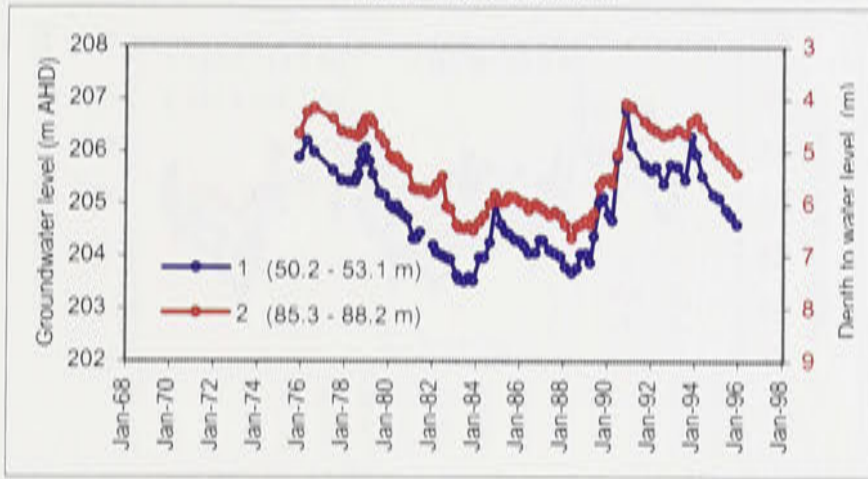


Well no. 36088

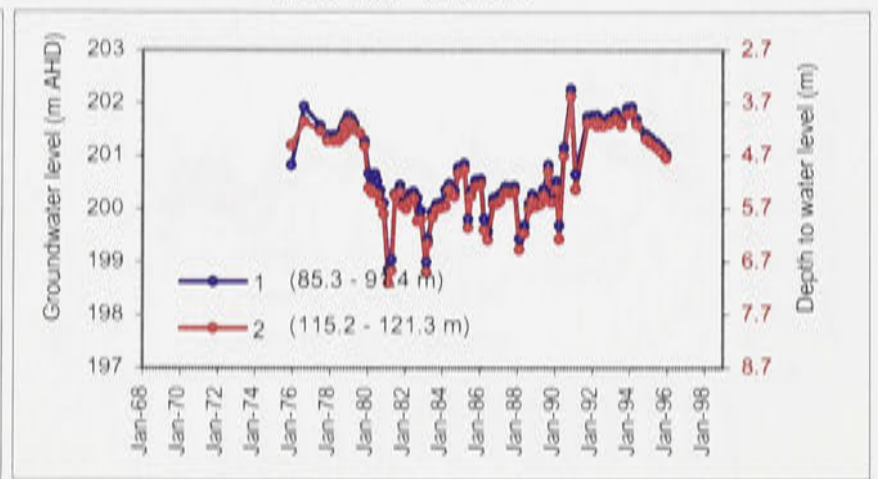


Appendix F.7: (continued).

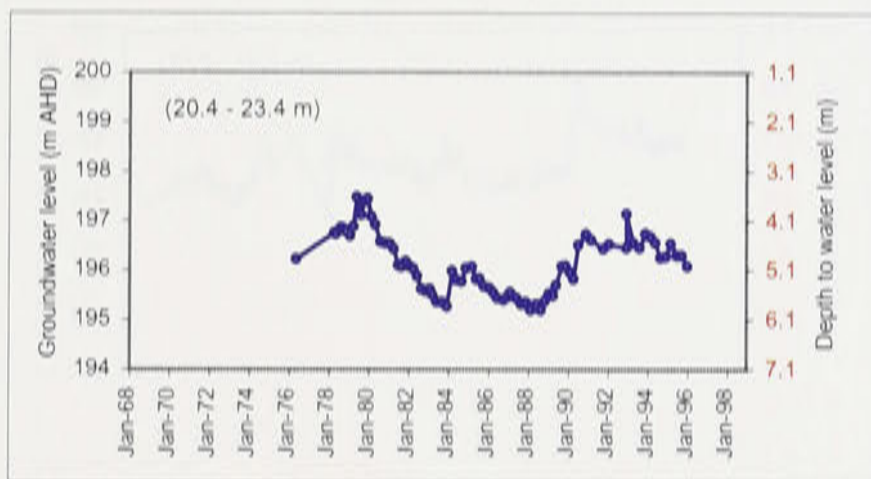
Well no. 36089



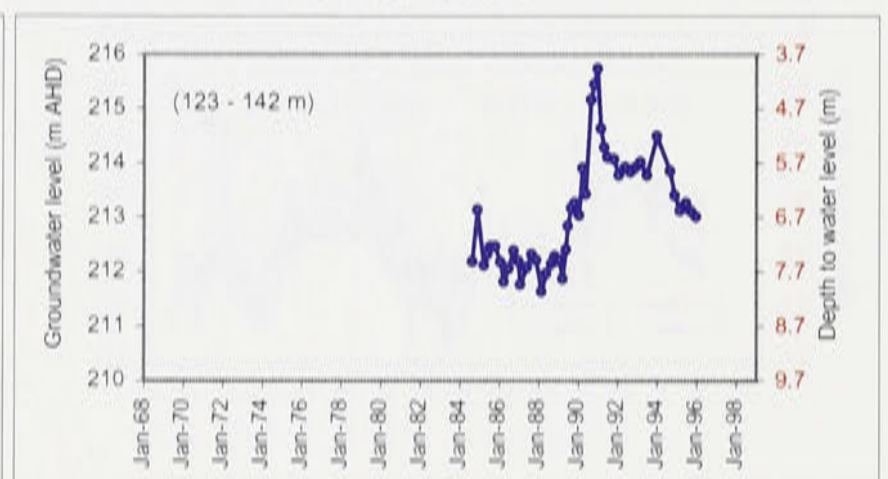
Well no. 36090



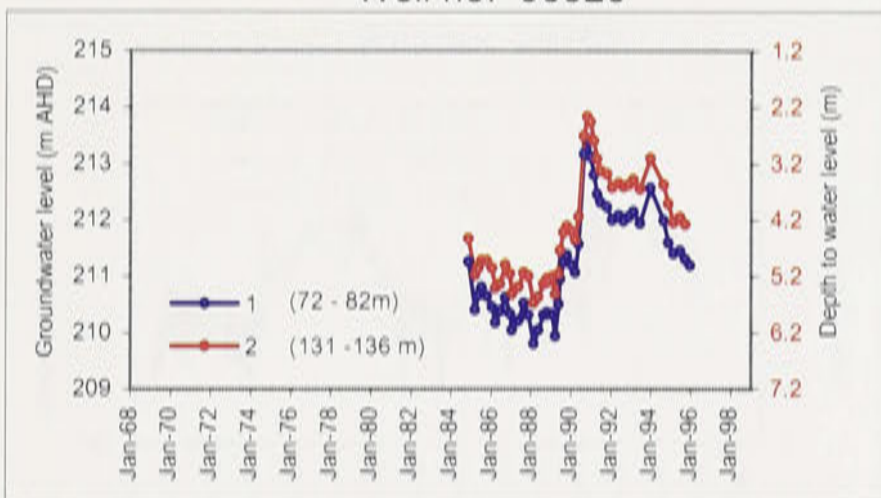
Well no. 36091



Well no. 36521

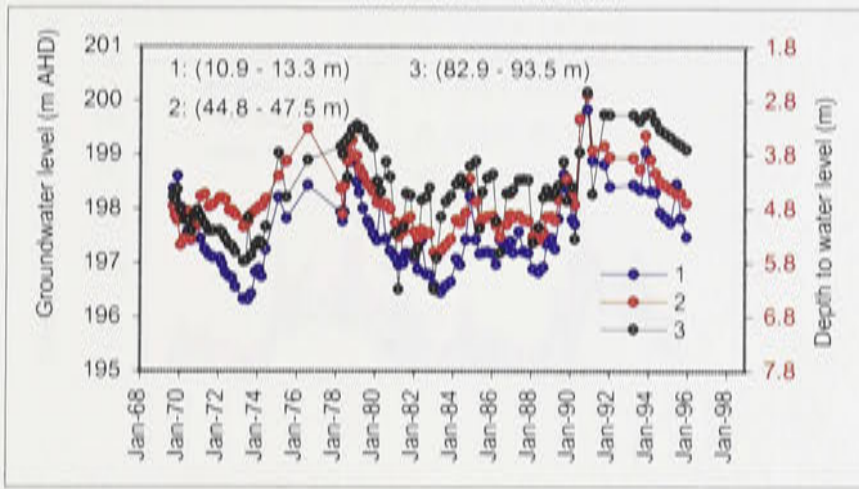


Well no. 36526

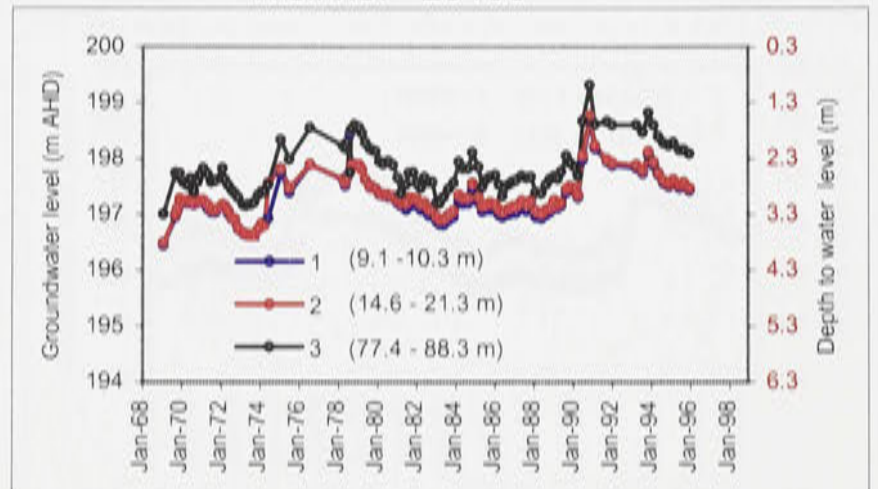


Appendix F.8: Regional observation wells hydrographs at or near cross-section H-H'.
(see Figures 4.2, 4.10 and 5.3 for locations).

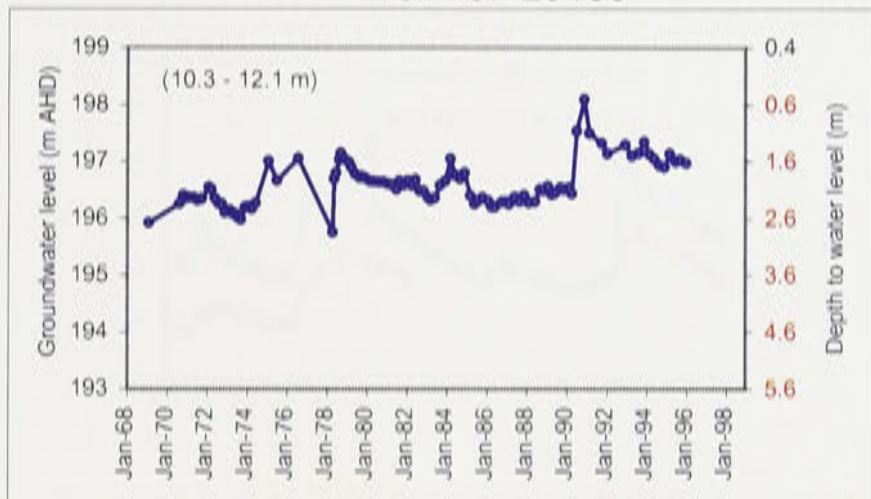
Well no. 25151



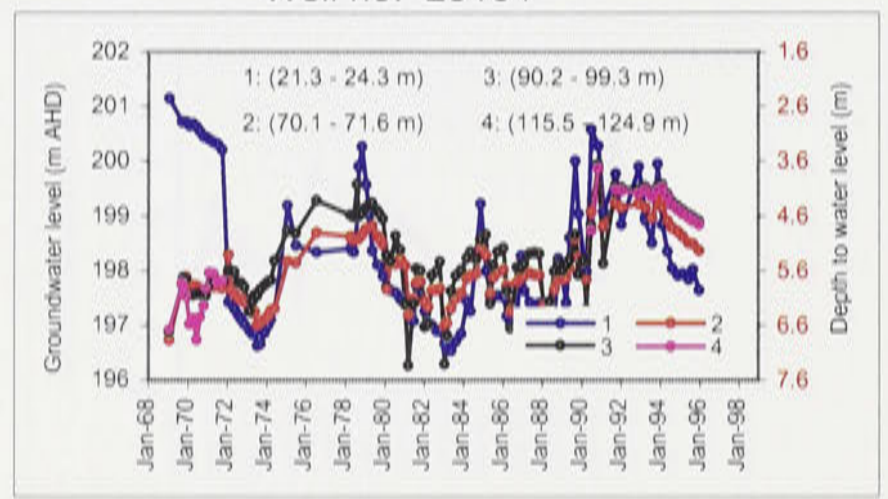
Well no. 25155



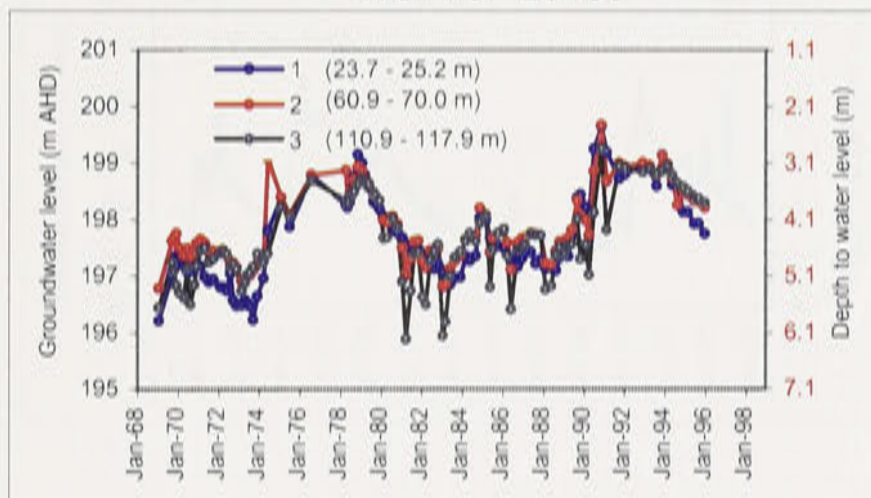
Well no. 25163



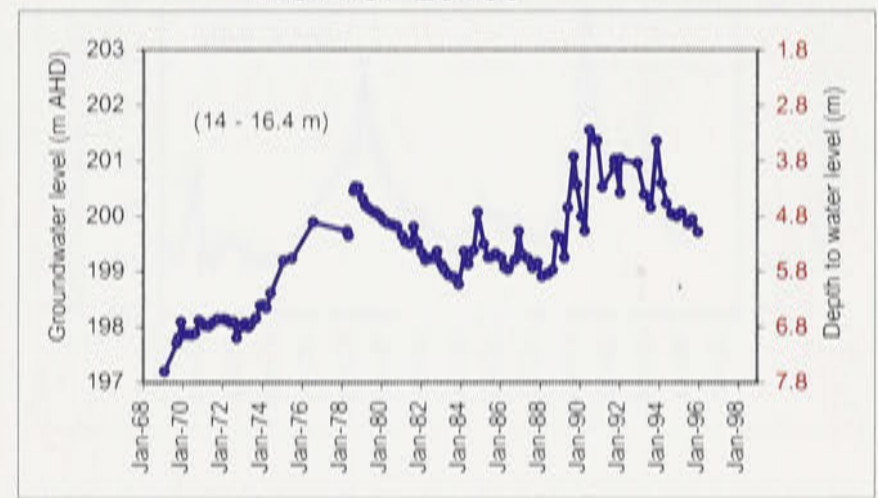
Well no. 25164



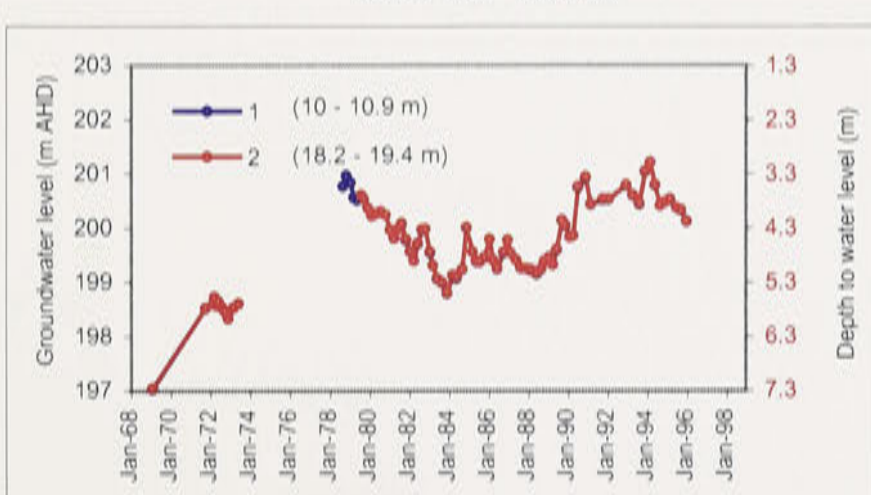
Well no. 25165



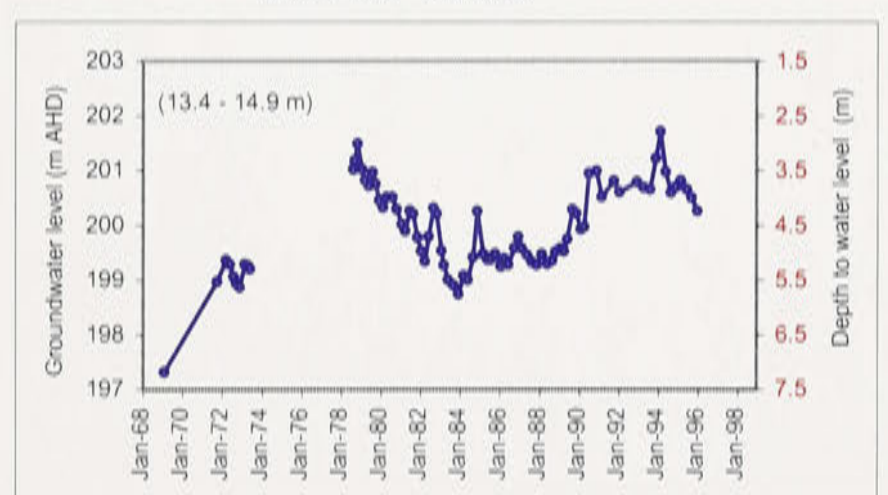
Well no. 25166



Well no. 25167

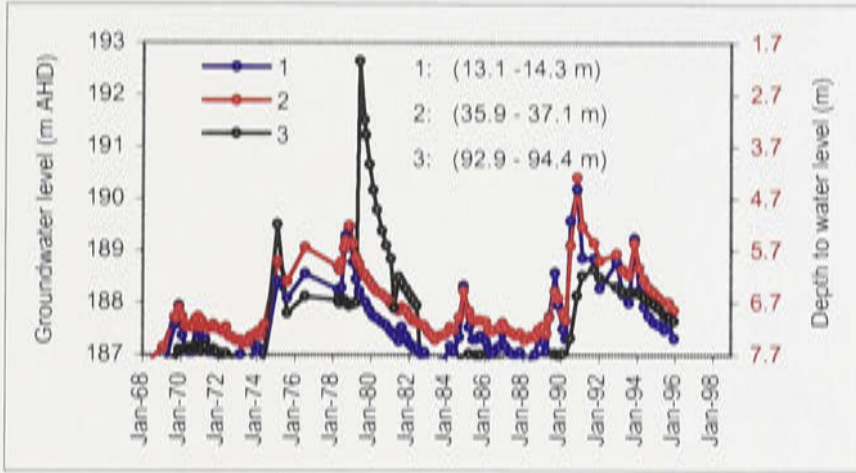


Well no. 25168

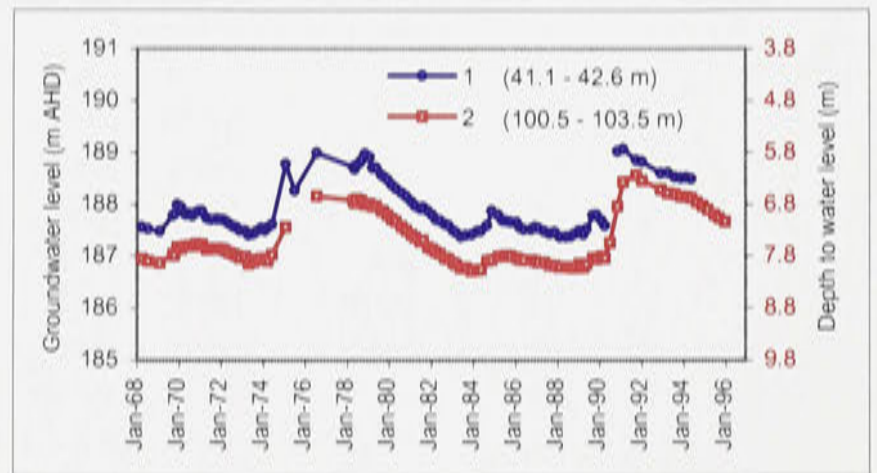


Appendix F.9: Regional observation wells hydrographs at or near cross-section I-I':
 (see Figures 4.2, 4.11 and 5.3 for locations).

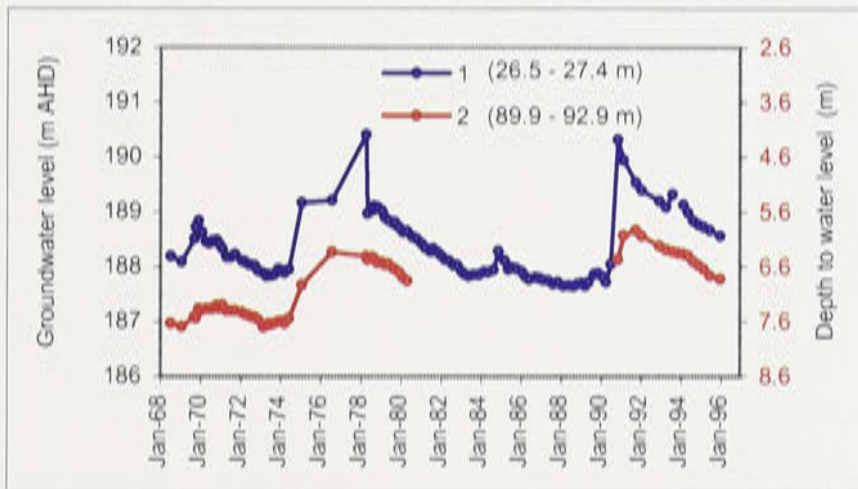
Well no. 25030



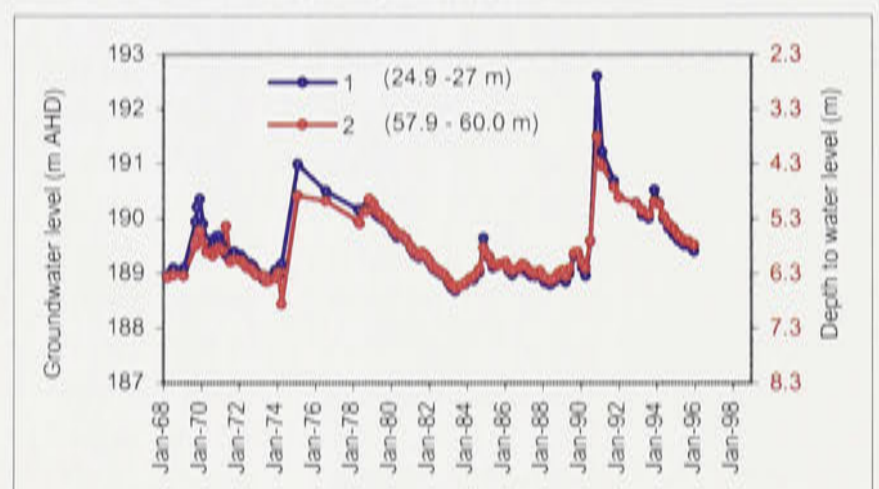
Well no. 25067



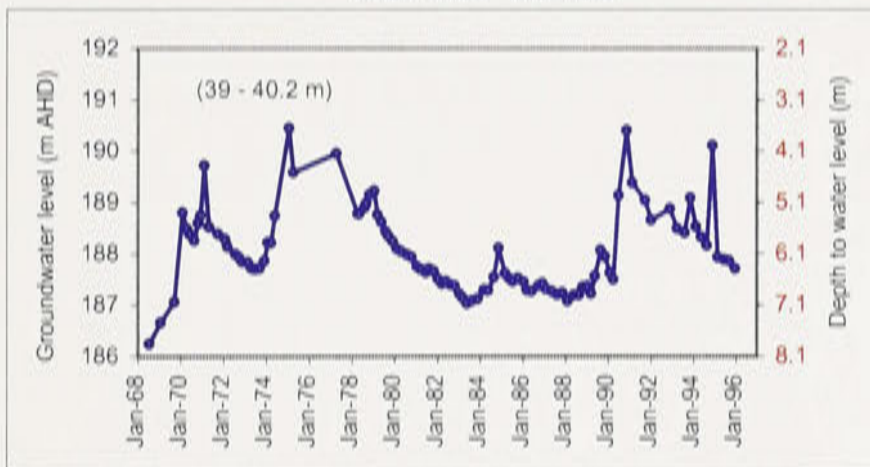
Well no. 25081



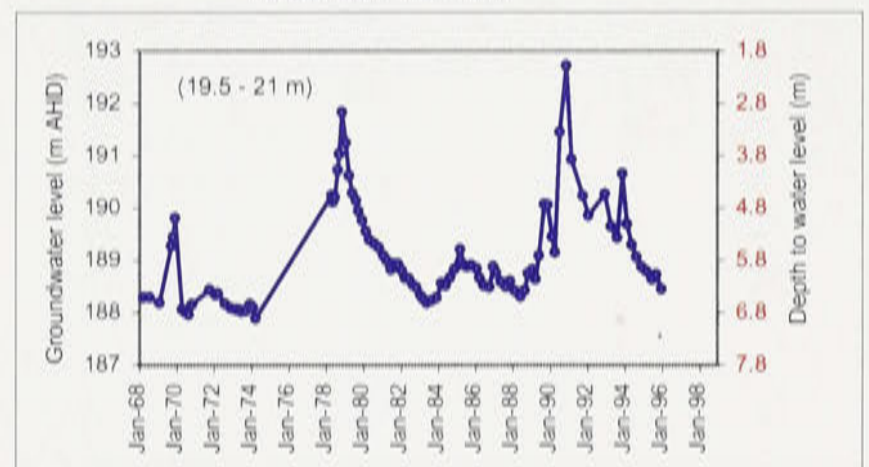
Well no. 25082



Well no. 25102



Well no. 25103



Appendix G

Thickness of sand and gravel lenses at the different wells in the study area

Appendix G: Total thickness of sand and gravel lenses at the different wells in the study area.

Well number	EASTING (m)	NORTHING (m)	Aggregate thickness (m)			Bore number	EASTING (m)	NORTHING (m)	Aggregate thickness (m)		
			Sand	Gravel	Total				Sand	Gravel	Total
495	591437	6195683	0.6		0.6	8362	569687	6307340	7.3		7.3
952	546122	6346048	0.0		0.0	8374	557729	6236972	6.7		6.7
968	566098	6273949	0.0		0.0	8385	566003	6234658	3.4		3.4
989	532738	6337876	0.0		0.0	8411	564605	6235637	5.5		5.5
993	564571	6273698	0.0		0.0	8417	568351	6232038	1.8		1.8
1000	521177	6344537	0.0		0.0	10935	569446	6331503	0.0		0.0
1010	523829	6342378	0.0		0.0	10970	555200	6334976	6.7		6.7
1028	530117	6338496	0.0		0.0	10991	593000	6190440	0.0		0.0
1044	528543	6341915	0.0		0.0	11245	561311	6183265	14.0		14.0
1067	564925	6267575	16.5		16.5	11438	561739	6206271	2.5		2.5
1169	558849	6238306	28.3		28.3	12164	563267	6328485	0.0		0.0
1188	603000	6184070	4.9		4.9	12173	563694	6329725	0.0		0.0
1232	556109	6238955	4.3		4.3	12316	551003	6303114	7.0	1.5	8.5
1322	559335	6236972	5.8		5.8	12329	551493	6304181	0.6		0.6
1349	576412	6240025	0.0		0.0	12352	544603	6301663	0.0	0.3	0.3
1366	580613	6236167	12.5		12.5	13469	568434	6263808	0.0		0.0
1423	585500	6227500	29.3		29.3	14173	577138	6234525	47.3		47.3
1464	574704	6221160	6.7	3.7	10.4	14531	590547	6190464	0.0		0.0
2660	560867	6237849	42.1		42.1	14843	562261	6226957	0.0		0.0
2686	563666	6234962	3.1		3.1	14865	568392	6224786	5.2		5.2
2705	557558	6231532	3.1		3.1	14950	544312	6304047	11.0	1.5	12.5
2842	561539	6239789	0.6		0.6	14994	575625	6223282	5.6	29.9	35.5
2849	564566	6241921	34.8		34.8	16097	568300	6254667	0.0		0.0
2916	559941	6238522	12.2		12.2	16099	572820	6263990	0.0		0.0
2951	558012	6235048	7.0		7.0	16300	574897	6336327	0.0		0.0
2965	569358	6234201	8.5		8.5	16636	560598	6195908	18.2		18.2
2977	571471	6235444	0.0		0.0	16652	564761	6193762	0.0		0.0
2990	570232	6235992	0.0		0.0	16947	562865	6327370	3.7		3.7
3074	562979	6232501	3.1		3.1	16972	547489	6336355	9.2		9.2
3075	559213	6231616	0.0		0.0	17134	562022	6329450	6.1		6.1
3107	557814	6238895	1.5		1.5	17582	565171	6326027	3.4		3.4
3118	567355	6232849	0.0		0.0	17659	535637	6284550	0.0		0.0
3124	532316	6343492	0.0		0.0	18441	552953	6231809	0.0		0.0
3132	529774	6346000	0.0	7.9	7.9	18525	552560	6228198	18.6	3.0	21.6
3135	523682	6346633	0.0		0.0	18832	569806	6306990	5.8	0.9	6.7
3224	568783	6239650	2.4	10.0	12.4	19105	564454	6238937	30.5		30.5
3266	561047	6244453	0.0		0.0	20524	559604	6235718	14.3		14.3
3299	550047	6276928	0.0		0.0	21134	554357	6309184	0.3		0.3
4065	547287	6339874	0.0		0.0	21139	554644	6308935	0.3		0.3
4066	543351	6341464	0.0		0.0	21177	536753	6315985	15.2	4.9	20.1
6919	595250	6199770	0.0		0.0	21213	538810	6308975	2.7	2.7	5.5
6922	595400	6203140	0.0		0.0	21225	588834	6190556	0.0	2.4	2.4
7473	609725	6223700	0.0		0.0	21259	536282	6305755	7.6	0.6	8.2
7715	561377	6236040	2.8		2.8	21274	589022	6186107	0.0		0.0
7803	563809	6235895	3.7		3.7	21276	536141	6309763	17.7	4.9	22.6
8139	577211	6306775	0.0	4.6	4.6	21284	586738	6187147	6.1	6.7	12.8
8358	569082	6307845	1.5	0.9	2.4	21301	512256	6335948	20.1	4.9	25.0

Note: Wells with shadings are the regional observation wells in the study area.

Appendix G: Continued.

Well number	EASTING (m)	NORTHING (m)	Aggregate thickness (m)		
			Sand	Gravel	Total
21302	511948	6334532	76.8	33.5	110.4
21316	589942	6194095	0.0	0.8	0.8
21326	533656	6323706	0.6	1.2	1.8
21333	584552	6188019	0.0		0.0
21342	534264	6327000	9.2	0.0	9.2
21362	591476	6195135	0.0	3.1	3.1
21525	594840	6207260	0.0		0.0
21678	564775	6325175	0.0		0.0
21831	542634	6268539	0.0		0.0
21832	545719	6266413	0.0		0.0
21903	575443	6325552	0.0		0.0
23152	569158	6230533	13.7		13.7
23374	568568	6325472	3.1		3.1
23502	587691	6233927	5.5		5.5
24243	570164	6302303	61.6	14.3	75.9
24313	569552	6308201	12.5	28.9	41.4
24457	547187	6305213	25.0	4.9	29.9
25030	522791	6332034	25.6	5.8	31.4
25060	587669	6195394	0.0		0.0
25062	590918	6192542	0.0	5.8	5.8
25067	522653	6330201	41.5	4.6	46.0
25081	522441	6328468	29.9	2.1	32.0
25082	522165	6326782	13.4	6.1	19.5
25102	522586	6333544	3.7	1.8	5.5
25103	525069	6333642	2.4	2.1	4.6
25109	568025	6224790	3.7		3.7
25116	569359	6221450	4.9		4.9
25149	588800	6200410	0.0		0.0
25151	533848	6319077	59.1	18.6	77.7
25155	532614	6317932	36.6	0.0	36.6
25163	531433	6317342	6.1	0.0	6.1
25164	534964	6320133	40.8	12.8	53.7
25165	535752	6321308	28.4	0.0	28.4
25166	538239	6323392	0.0	2.4	2.4
25167	539100	6324203	3.1	1.2	4.4
25168	539714	6324527	1.5	0.9	2.5
25469	561500	6231910	4.0		4.0
25487	556436	6235337	12.2		12.2
25509	530740	6320991	36.9	38.7	75.6
25682	579841	6232947	3.4		3.4
25699	604375	6226000	0.0		0.0
25704	591900	6233306	4.6		4.6
25741	556141	6328567	6.7	7.3	14.0
25762	601615	6224300	0.0		0.0
25850	603175	6226375	0.3	0.0	0.3
25871	552181	6330889	1.5	2.1	3.7
25963	561604	6317337	2.8	9.2	11.9
25970	569997	6309037	3.7	5.2	8.8
26045	535437	6261638	3.1	12.5	15.6
26046	541805	6263969	0.0	4.9	4.9

Note: Wells with shadings are the regional observation wells in the study area.

Bore number	EASTING (m)	NORTHING (m)	Aggregate thickness (m)		
			Sand	Gravel	Total
26054	538646	6267238	6.7	13.4	20.1
26055	544354	6261880	0.0		0.0
26056	541780	6263631	0.0	0.9	0.9
26057	540063	6258755	0.0		0.0
26067	532299	6322333	13.7	35.0	48.8
25069	588825	6192360	0.0		0.0
26072	572904	6236379	0.0		0.0
26157	531152	6321995	32.6	17.7	50.3
26360	565390	6301696	12.2	18.9	31.1
26394	558986	6333325	0.0		0.0
26442	556004	6310341	20.4	1.5	22.0
26506	528456	6318902	0.0	11.3	11.3
26507	526868	6318991	1.8	14.6	16.5
26644	511315	6336658	7.9	9.5	17.4
26047	539683	6263039	18.6		18.6
26048	542618	6263254	0.0	6.4	6.4
26049	543717	6267581	25.6		25.6
26050	542649	6268698	0.0		0.0
26051	544013	6269642	0.0		0.0
26052	545603	6269842	0.0		0.0
26053	546085	6267827	0.3	11.0	11.3
26645	511793	6337589	0.0	4.3	4.3
26709	561124	6294798	2.4		2.4
26710	561736	6306827	13.7		13.7
26727	599575	6219950	0.0	14.6	14.6
26728	528150	6327193	47.9	9.7	57.6
26769	595580	6202390	0.0		0.0
26771	595830	6204430	6.1		6.1
26812	561774	6306158	17.4	3.1	20.4
26876	578392	6233506	0.0		0.0
26936	564422	6302497	48.5	3.1	51.5
26937	563497	6304312	35.1		35.1
26938	561939	6302150	17.1	0.9	18.0
26940	566964	6305643	49.4	21.3	70.7
27223	517321	6251173	0.3	0.0	0.3
27282	552977	6321237	7.9	6.0	13.9
27294	553137	6321790	0.0	4.0	4.0
27412	568808	6305598	8.5	15.9	24.4
27413	562250	6235425	7.6		7.6
27456	567514	6316019	0.6	9.1	9.7
27457	566819	6310896	14.0	25.9	40.0
27458	566948	6309931	3.4	41.5	44.8
27637	567750	6310345	36.9	11.3	48.2
27662	545854	6303925	20.4	9.1	29.6
27739	577301	6236045	11.9		11.9
27795	563013	6231136	0.0		0.0
27853	579194	6198499	0.0		0.0
27924	563493	6306901	23.2	26.8	50.0
28037	535210	6261464	0.0	3.4	3.4
28038	538151	6261896	0.0		0.0

Appendix G: Continued.

Well number	EASTING (m)	NORTHING (m)	Aggregate thickness (m)		
			Sand	Gravel	Total
28110	588760	6215276	0.0		0.0
28142	530397	6328248	1.8	4.0	5.8
28143	529554	6328350	29.3	13.1	42.4
28144	529294	6326398	17.4	26.2	43.6
28353	574502	6316729	0.0	7.0	7.0
28742	545139	6306784	19.8	0.0	19.8
28743	545679	6308608	38.7	23.5	62.2
28805	545390	6257547	1.8		1.8
28877	592750	6198330	12.5		12.5
28878	592330	6198610	0.0		0.0
28897	545171	6241370	3.4		3.4
28918	575418	6317420	0.0	11.3	11.3
29035	570160	6232200	11.6		11.6
29095	583809	6233325	6.4		6.4
29275	570139	6303153	7.0	22.0	29.0
29277	569977	6303297	5.5	15.9	21.3
29413	586494	6234217	7.0		7.0
29414	587065	6234028	6.7		6.7
29481	544982	6239532	13.4		13.4
29492	588088	6214554	0.0		0.0
29493	539189	6324787	16.5	22.0	38.4
29494	539799	6324254	25.6	0.0	25.6
29507	583100	6199637	3.1		3.1
29519	602275	6221325	21.3		21.3
29574	553235	6273005	0.0		0.0
29575	556224	6270486	4.0		4.0
29736	548732	6268745	0.0		0.0
29825	540192	6252667	0.0	1.5	1.5
29972	572624	6313518	0.0	2.5	2.5
30252	572791	6233019	25.3		25.3
30270	574961	6230773	1.8		1.8
30291	583942	6232510	2.1		2.1
30292	584155	6233454	0.0		0.0
30293	584212	6234512	0.0		0.0
30328	585977	6233073	1.5	0.6	2.1
30331	585935	6233698	5.2		5.2
30333	586155	6234584	0.0		0.0
30572	570600	6232225	3.7		3.7
30578	560726	6255964	0.0		0.0
30594	592430	6208620	0.0		0.0
30627	547898	6299348	16.8	3.1	19.8
30630	571460	6230260	7.0		7.0
30675	580513	6223961	1.5		1.5
30683	556436	6235337	5.0		5.0
30802	574917	6235730	0.0		0.0
31028	542400	6302140	3.0	1.5	4.6
31110	566974	6225615	3.1		3.1
31121	559048	6261198	0.0		0.0

Note: Wells with shadings are the regional observation wells in the study area.

Bore number	EASTING (m)	NORTHING (m)	Aggregate thickness (m)		
			Sand	Gravel	Total
31122	552612	6266062	1.7		1.7
31309	535785	6301413	0.0		0.0
31341	551368	6267359	13.7		13.7
31614	589298	6235435	0.0		0.0
31760	575160	6249890	0.0		0.0
32338	571699	6323371	0.0		0.0
33533	580352	6235112	1.5		1.5
33534	569855	6236794	0.0		0.0
33720	532633	6329821	0.0	2.4	2.4
33722	533060	6329703	2.4	2.4	4.9
33723	532627	6329232	3.7	2.7	6.4
34084	563537	6235384	62.2		62.2
34096	587423	6232352	64.9		64.9
34224	522713	6329844	5.5	0.0	5.5
34235	584517	6215057	6.1		6.1
34548	569260	6310451	4.0	0.0	4.0
34585	558871	6233436	2.1		2.1
34790	592800	6188770	0.0		0.0
34900	585695	6232956	9.1		9.1
35104	590171	6203373	14.6		14.6
35930	587638	6186073	0.0		0.0
36079	572539	6304535	0.0	115.0	115.0
36081	563934	6305718	13.7	7.7	21.4
36083	559098	6312552	0.0	15.7	15.7
36085	553144	6308243	0.0	10.6	10.6
36087	547072	6319976	24.4	45.8	70.1
36088	545070	6317630	24.3	13.9	38.2
36089	547707	6317508	3.1	19.8	22.9
36090	539838	6317558	9.2	44.3	53.5
36091	532537	6325475	0.0	9.2	9.2
36522	577000	6305885	8.0	6.0	14.0
36523	550673	6298555	31.9	3.5	35.4
36524	545810	6286580	3.0	0.0	3.0
36525	569390	6306215	31.5	81.0	112.5
36526	559098	6312552	34.5	12.0	46.5
36527	575275	6302250	43.9	24.8	68.6
36528	540969	6299942	12.5	8.8	21.3
36529	542865	6287070	0.0	0.0	0.0
36551	544680	6299570	16.6	1.1	17.7
36552	547856	6298828	11.3	6.8	18.0
36553	552420	6285560	14.5		14.5
36554	553027	6298288	11.0	0.0	11.0
36555	539280	6300460	0.0		0.0
36563	534610	6300890	2.3	0.0	2.3
36594	548280	6286190	0.0		0.0
36595	547800	6263665	0.0		0.0
36596	550825	6264615	3.5		3.5
36597	545925	6263580	8.0		8.0

Appendix G: Continued.

Well number	EASTING (m)	NORTHING (m)	Aggregate thickness (m)		
			Sand	Gravel	Total
36603	551440	6239500	3.0		3.0
36606	564770	6238070	43.0	2.0	45.0
36607	541180	6241340	0.0		0.0
36608	572590	6237375	0.0		0.0
36609	555400	6285100	20.5		20.5
36610	549040	6264360	4.0		4.0
36611	553590	6264625	18.4		18.4
36612	559075	6284315	0.0		0.0
36613	541460	6263500	6.0		6.0
36629	573000	6234440	0.0		0.0
36627	571875	6240000	41.0		41.0
36630	561300	6220750	0.0		0.0
36631	576830	6222940	0.0		0.0
36632	572330	6222210	3.0		3.0
36700	555500	6264570	0.0		0.0
36735	561400	6208860	0.0	8.0	8.0
36737	576300	6203580	0.0	8.0	8.0
36738	579770	6202575	36.5	3.0	39.5
36739	583785	6201850	3.0	0.0	3.0
36741	584700	6236940	44.0		44.0
36745	583500	6230070	6.0		6.0
36825	564425	6255225	0.0		0.0
37286	569158	6309800	4.3	0.6	4.9
37676	603280	6221525	0.0		0.0
38239	558507	6232188	1.8		1.8
38782	539743	6253217	0.6		0.6
39307	559110	6307570	6.1	0.5	6.6
39311	566575	6302790	2.0	16.0	18.0
39316	573500	6303920	58.0	24.0	82.0
39317	565425	6302710	10.0	0.0	10.0
39378	565375	6221550	1.0		1.0
39379	557150	6240250	19.0	7.0	26.0
43578	557013	6320211	0.0	2.7	2.7
43907	570856	6325017	0.0		0.0
44819	616440	6214525	0.0		0.0
44903	559525	6323775	0.0		0.0
45418	566578	6309486	1.2	0.0	1.2
50216	546310	6332040	0.0		0.0
50713	555595	6345730	0.0		0.0
50717	554611	6244938	0.0		0.0
50988	530464	6340473	0.0		0.0
51682	585075	6225525	0.0		0.0
51907	573300	6226950	0.0		0.0
52185	584660	6225307	0.0		0.0
52367	584800	6215925	0.0		0.0
42945	586709	6231716	0.0		0.0

Note: Wells with shadings are the regional observation wells in the study area.

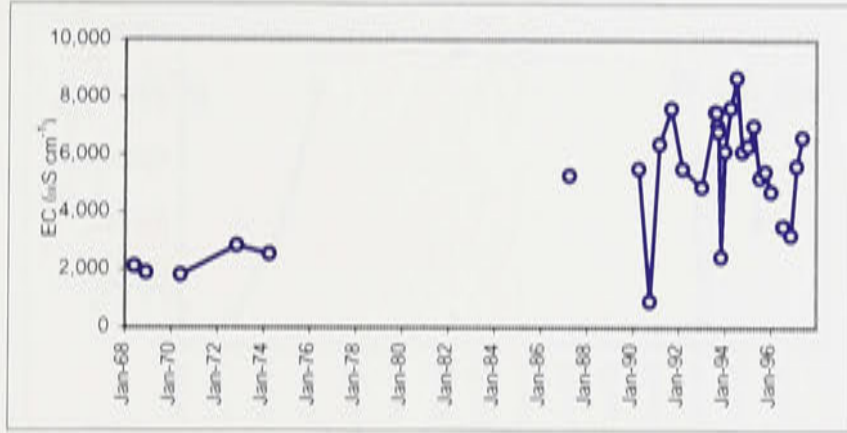
Well number	EASTING (m)	NORTHING (m)	Aggregate thickness (m)		
			Sand	Gravel	Total
53668	514840	6337030	23.0	3.2	26.1
53669	514850	6337360	2.9	9.2	12.1
56453	529090	6244610	0.0	0.9	0.9
55001	580940	6232640	0.3		0.3
55545	601860	6218390	0.0		0.0
56120	586070	6229800	4.7		4.7
56169	574280	6224820	0.0		0.0
57265	601625	6221095	0.0		0.0
57348	572160	6232220	0.0		0.0
57860	535746	6318887	16.5	0.5	17.0
57861	535180	6319925	28.5	0.0	28.5
57974	547060	6267850	0.0	14.0	14.0
58010	572995	6234740	0.0		0.0
58420	589560	6198160	0.0		0.0
58858	566865	6306485	24.5	0.0	24.5
59055	519250	6334770	5.4	4.3	9.7
59370	513260	6335700	11.3	0.0	11.3
59566	567740	6305350	9.7	0.0	9.7
60738	551750	6210050	0.0		0.0
63797	550780	6207930	5.0		5.0
63798	552635	6207625	24.0	13.0	37.0

Appendix H

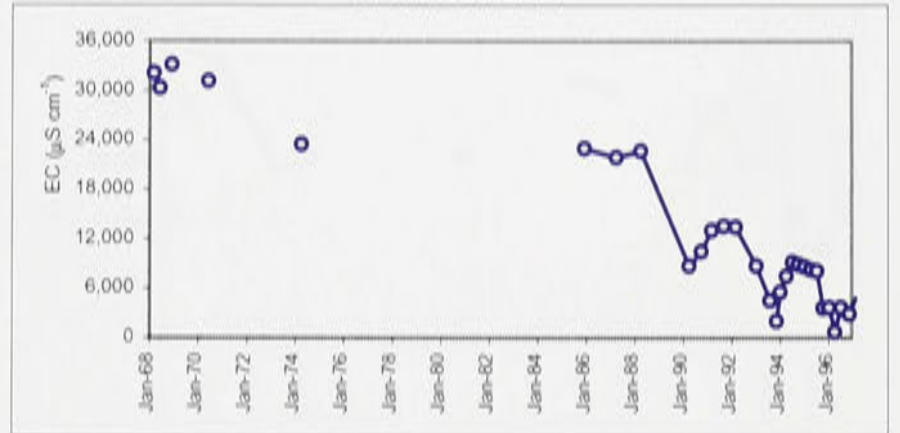
Plots of electrical conductivity (EC) monitored at the shallow observation wells at the JWPID

Appendix H: Plots of electrical conductivity (EC) at the shallow observation wells at JWPID.

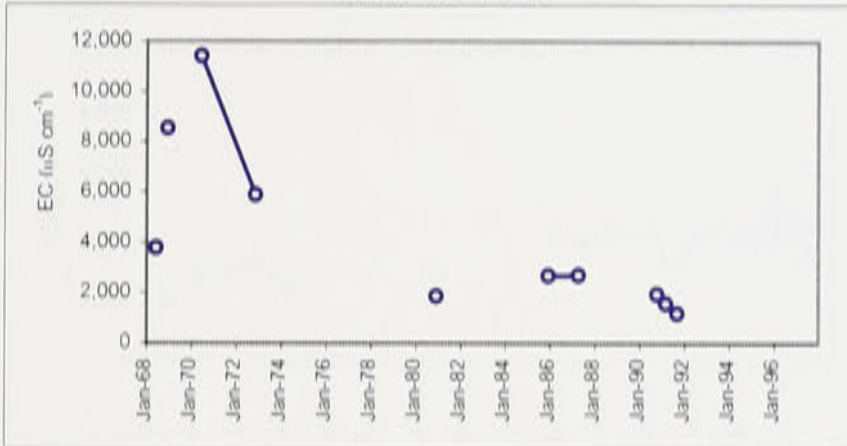
Well no. 1 W



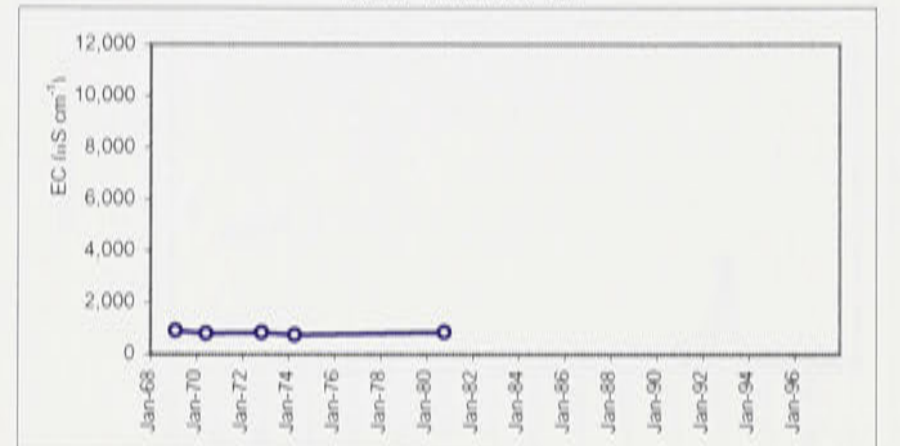
Well no. 2 W



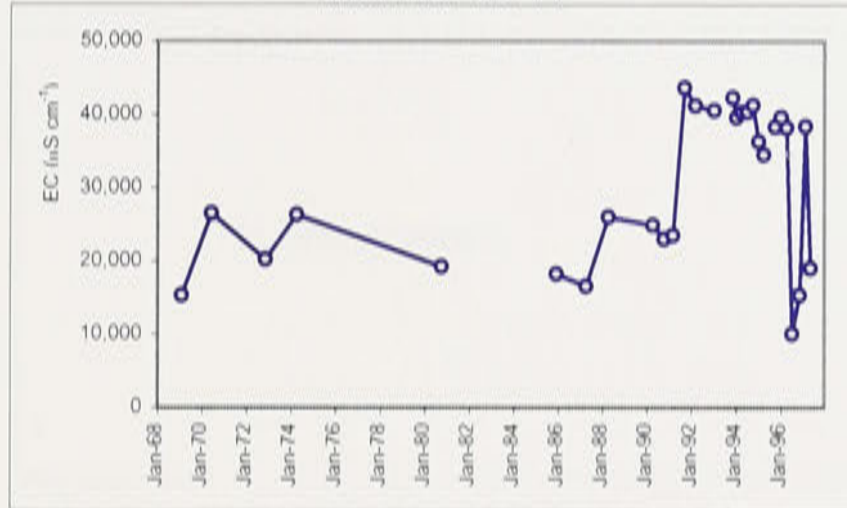
Well no. 3 W



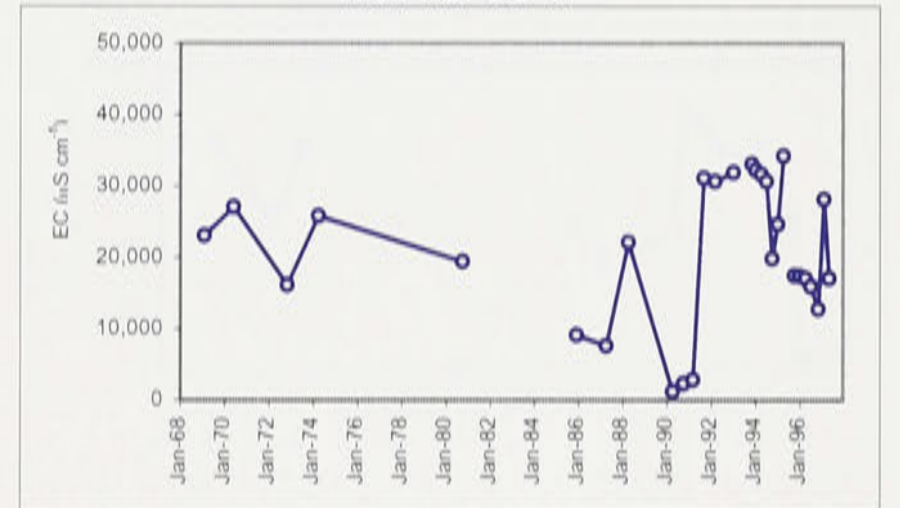
Well no. 3A W



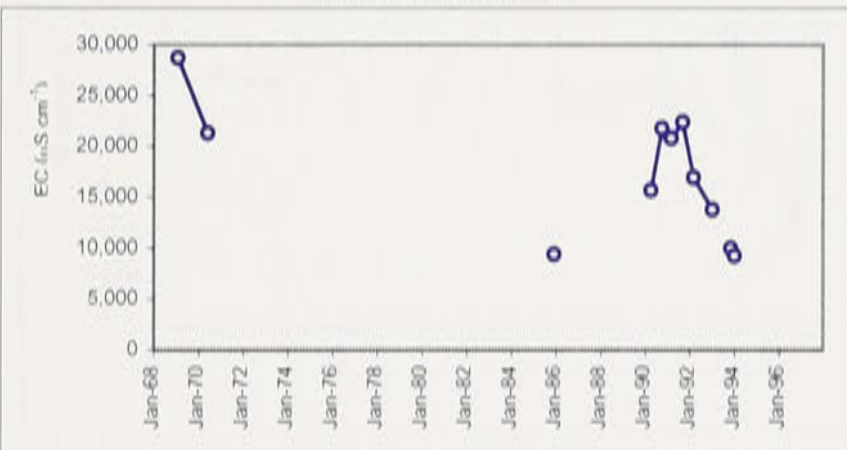
Well no. 3B W



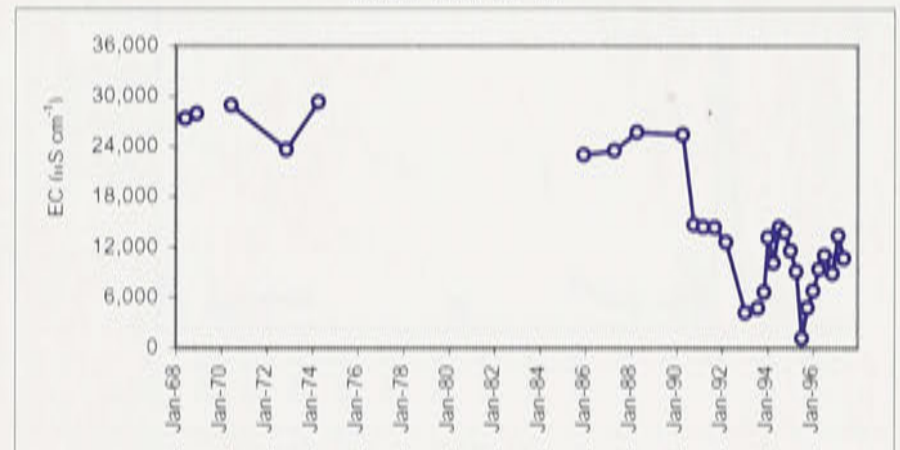
Well no. 3C W



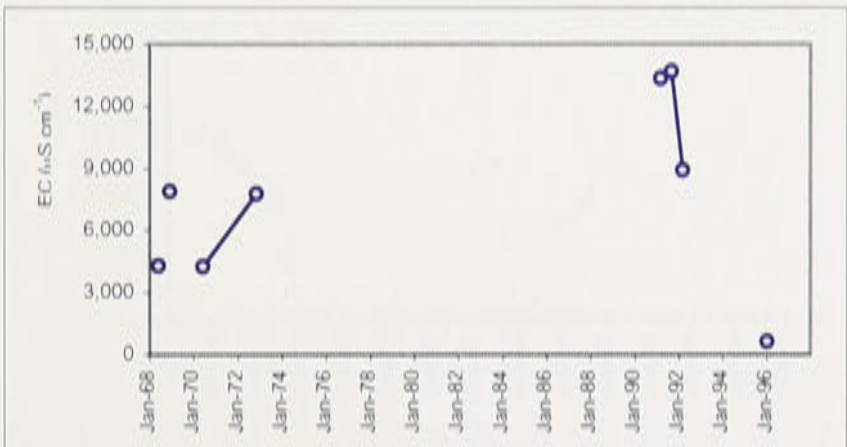
Well no. 3D W



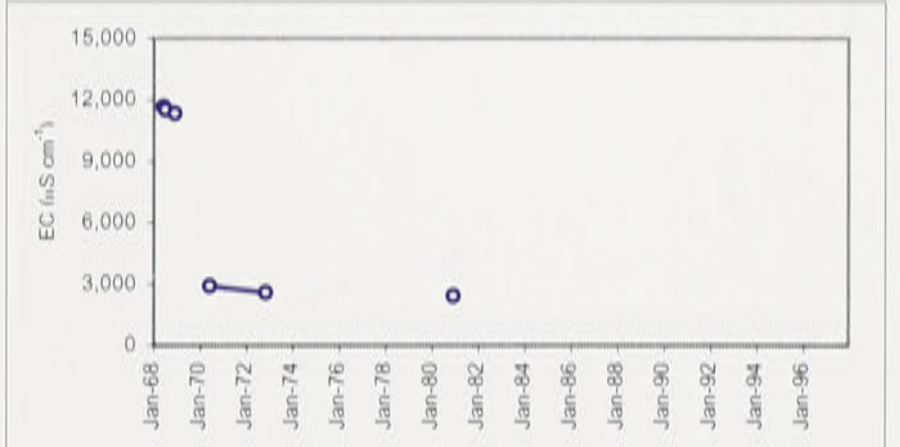
Well no. 4 W



Well no. 5 W

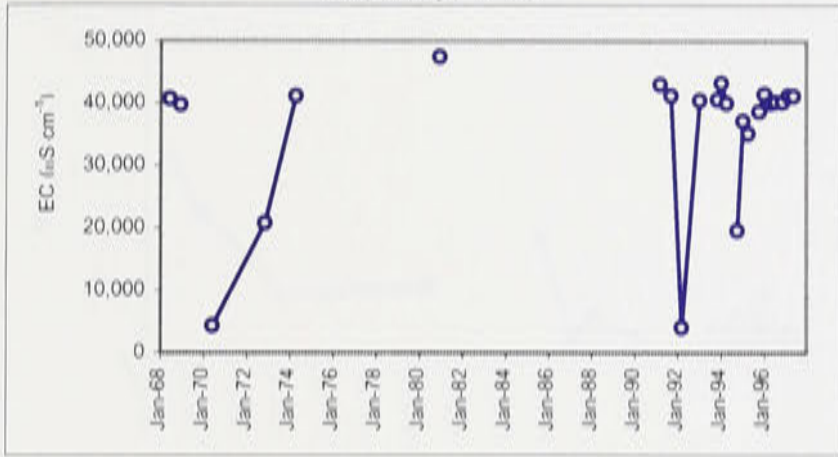


Well no. 6 W

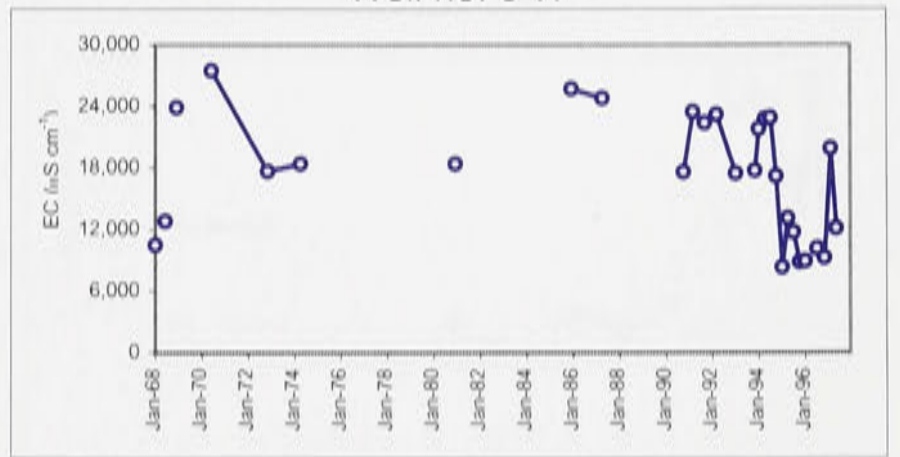


Appendix H: Continued.

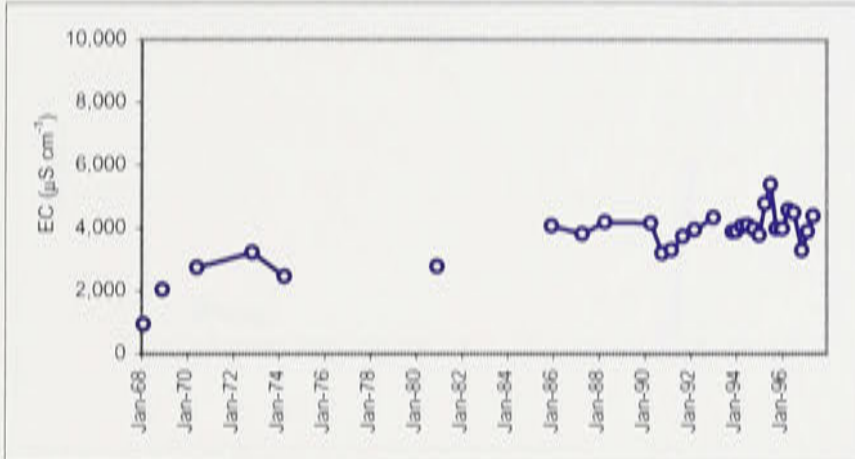
Well no. 7 W



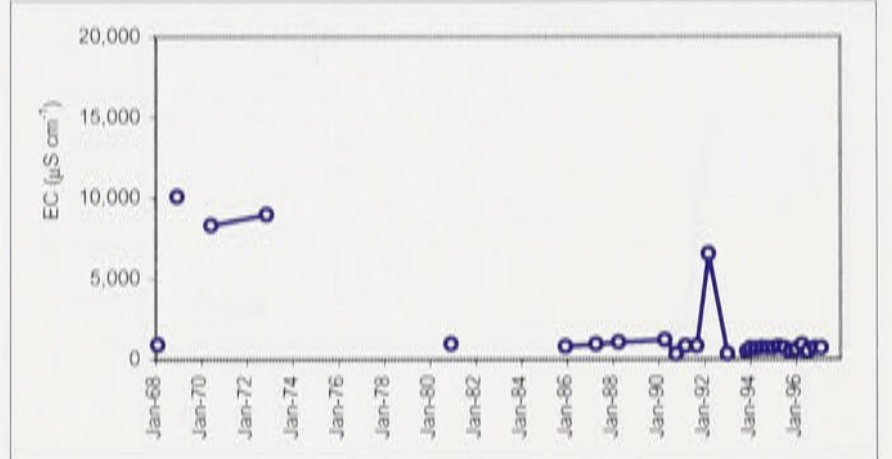
Well no. 8 W



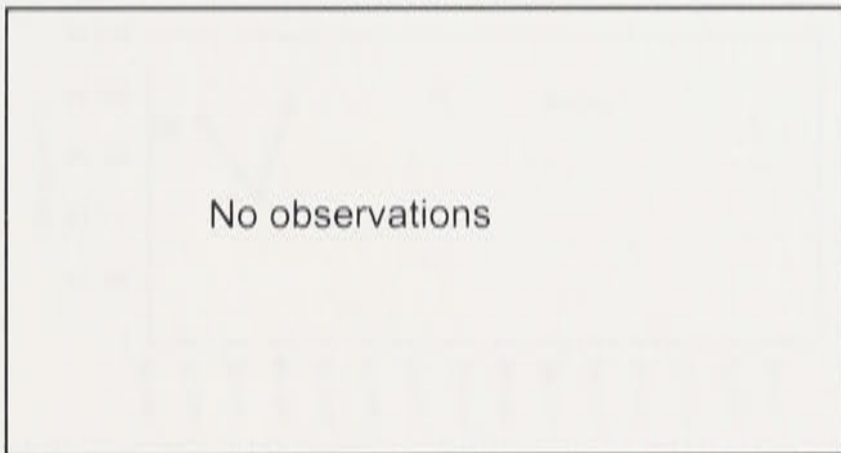
Well no. 9 W



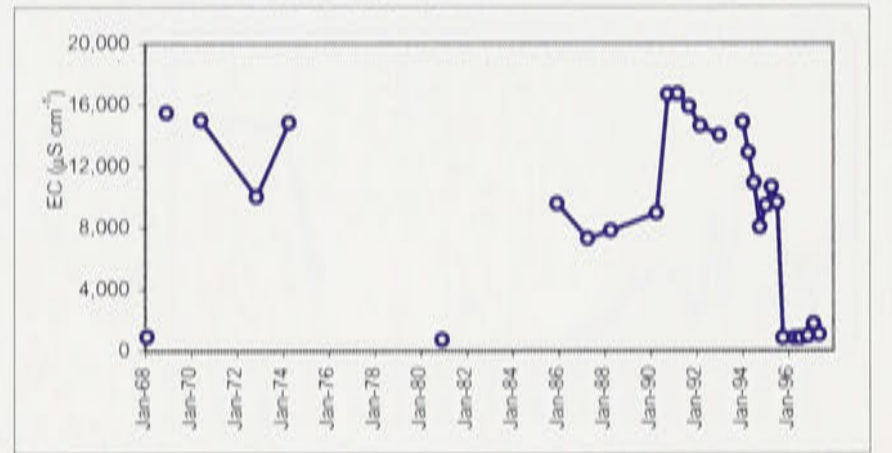
Well no. 10 W



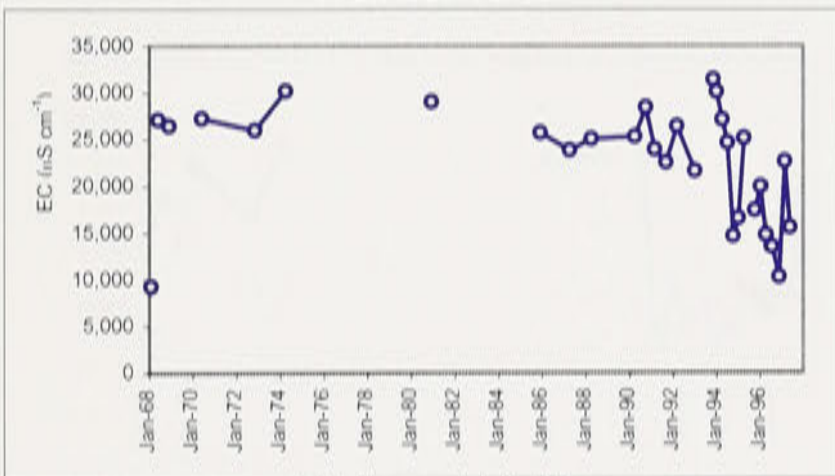
Well no. 11 W



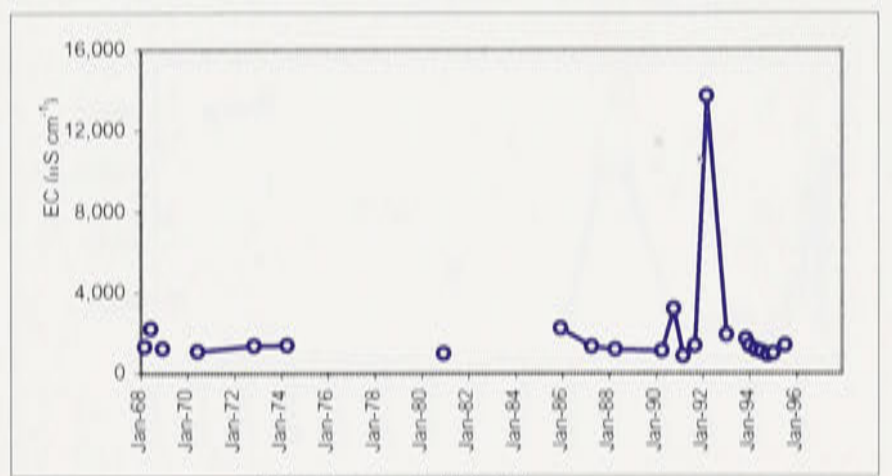
Well no. 12 W



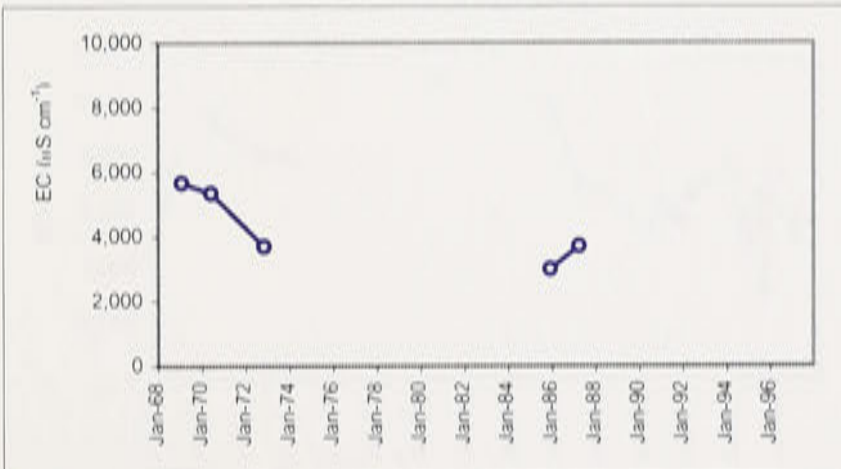
Well no. 13 W



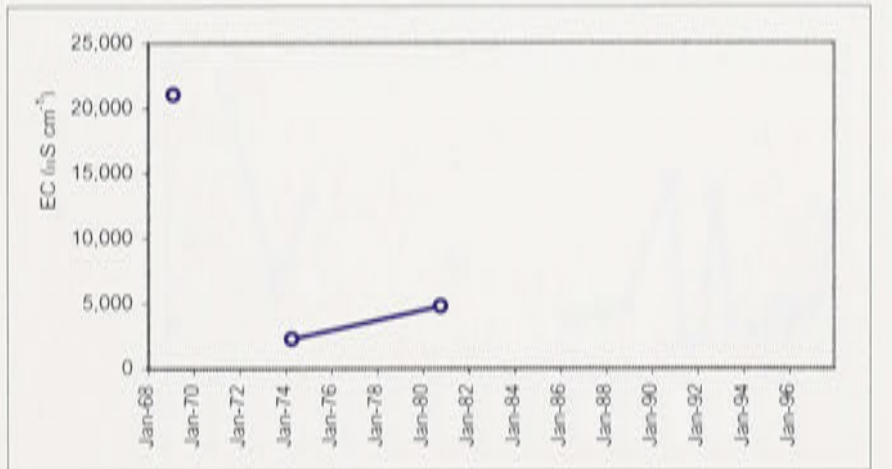
Well no. 14 W



Well no. 14A W

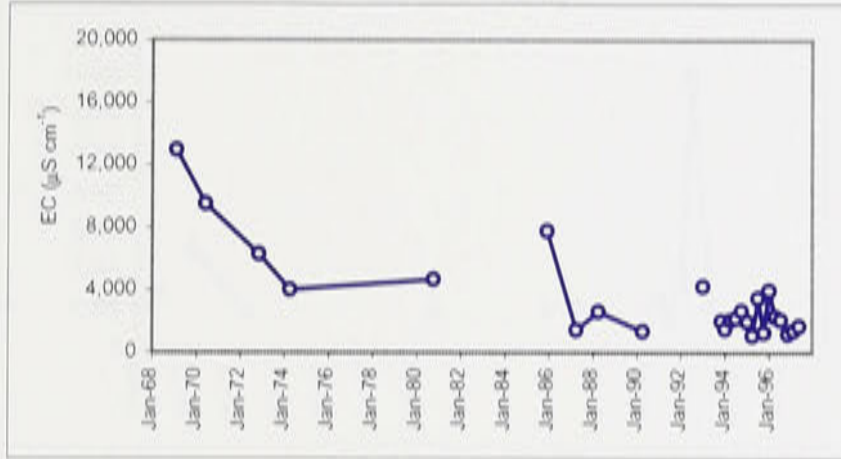


Well no. 14B W

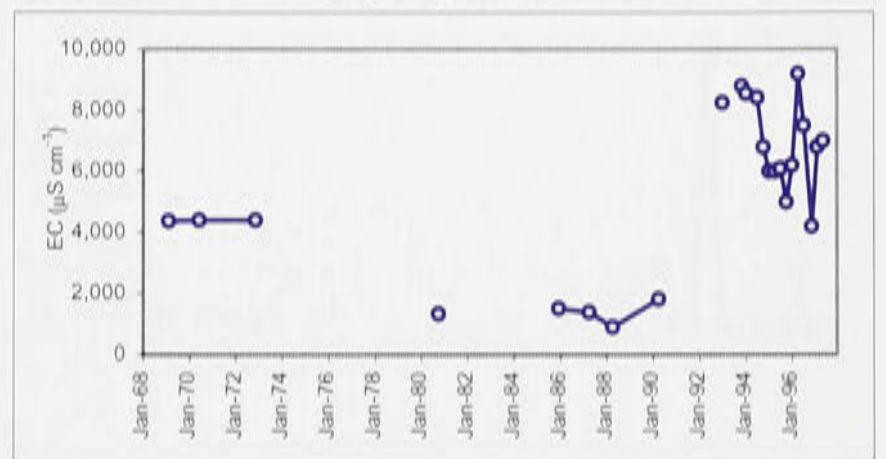


Appendix H: Continued.

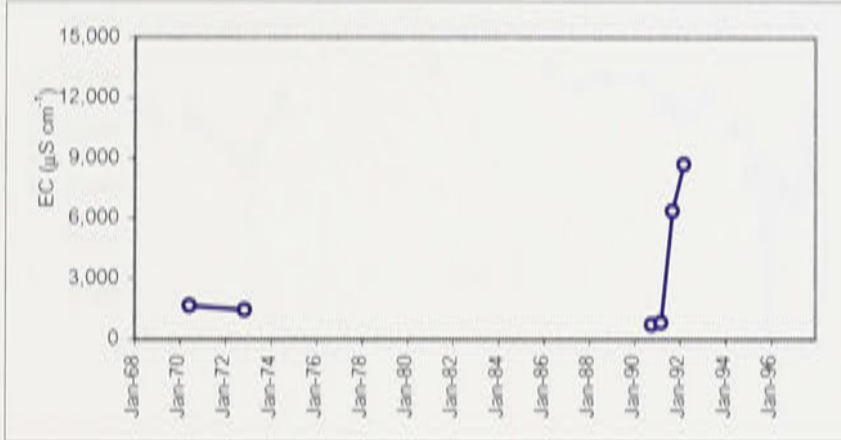
Well no. 14C W



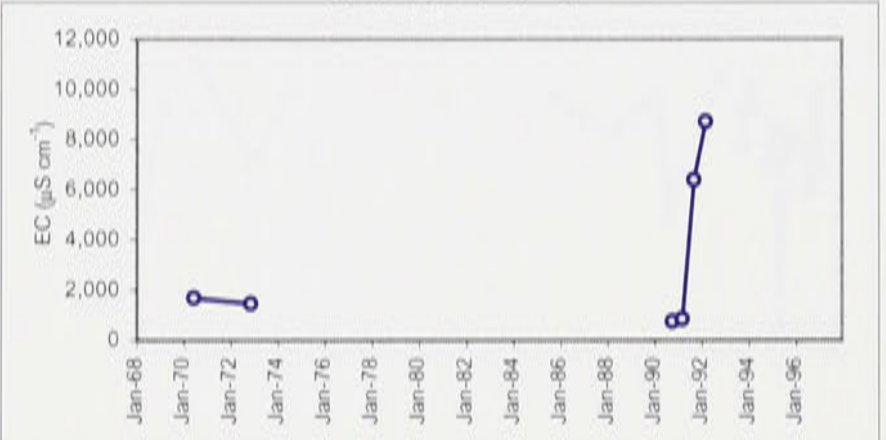
Well no. 14D W



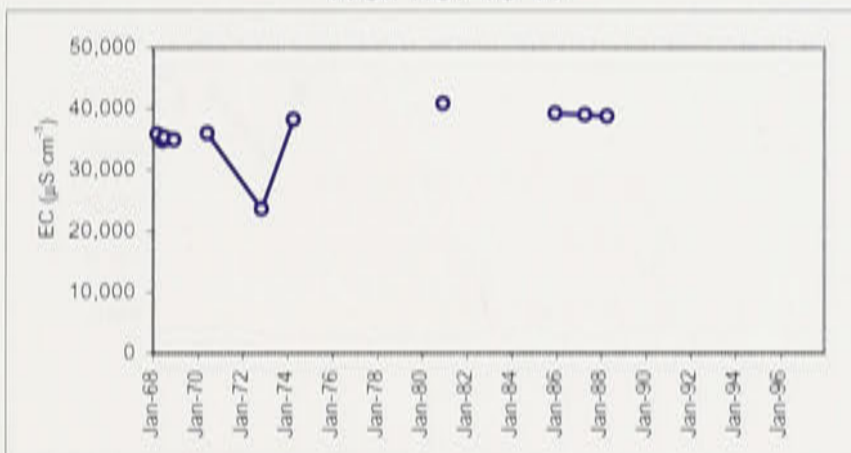
Well no. 14E W



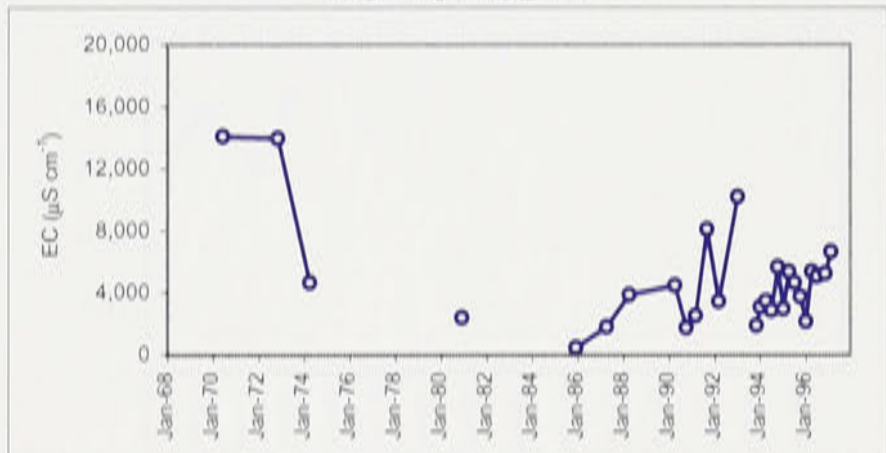
Well no. 14F W



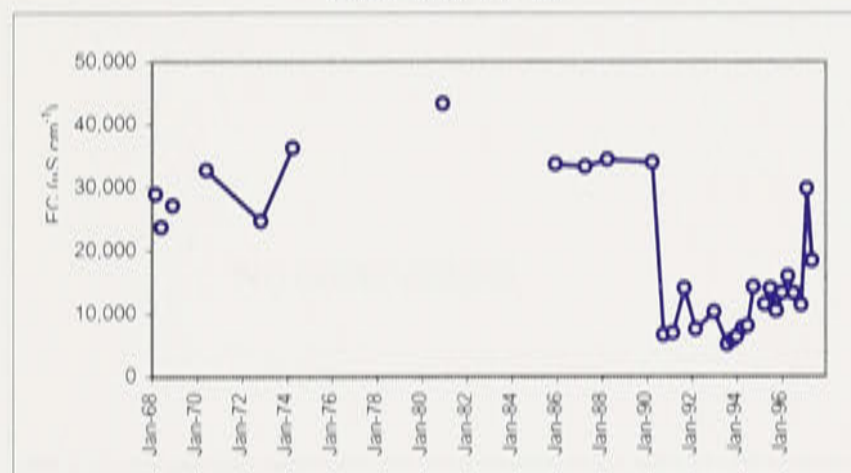
Well no. 15 W



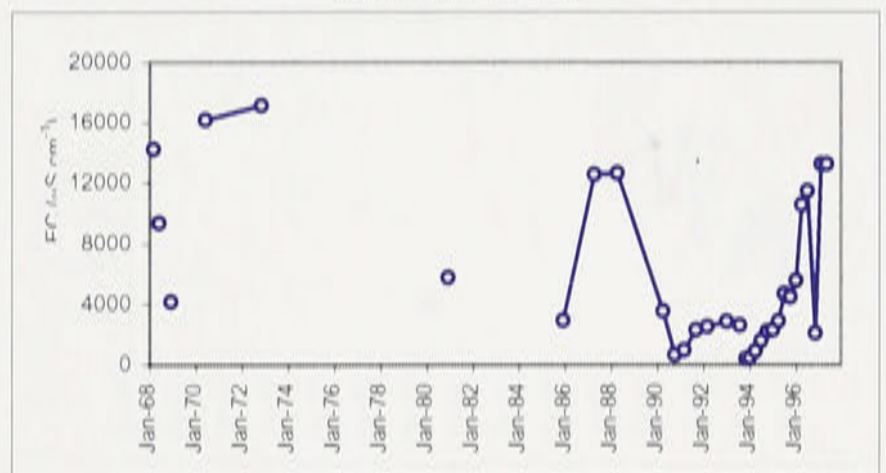
Well no. 16E W



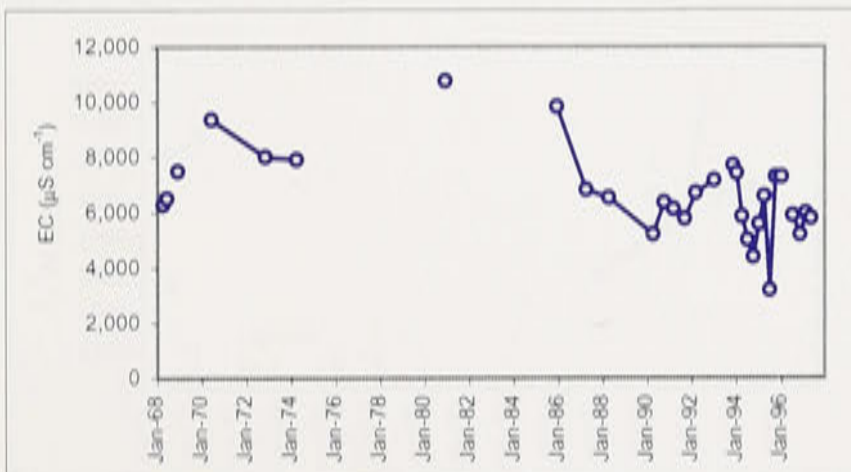
Well no. 17 W



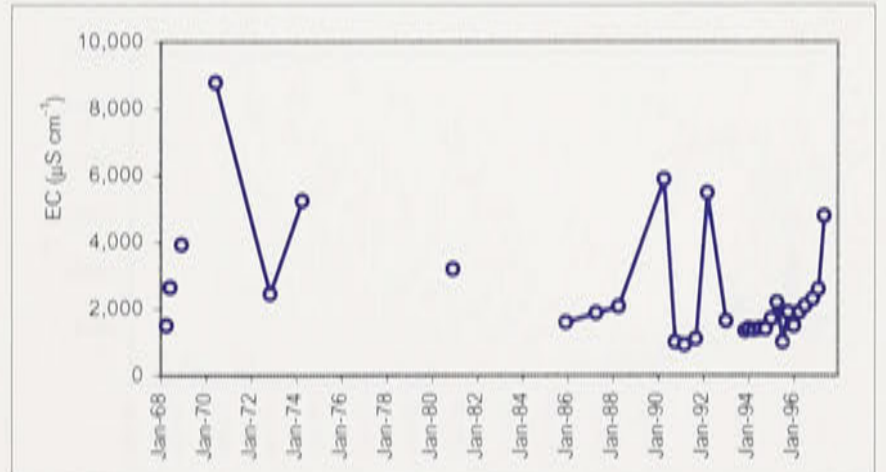
Well no. 18 W



Well no. 19 W

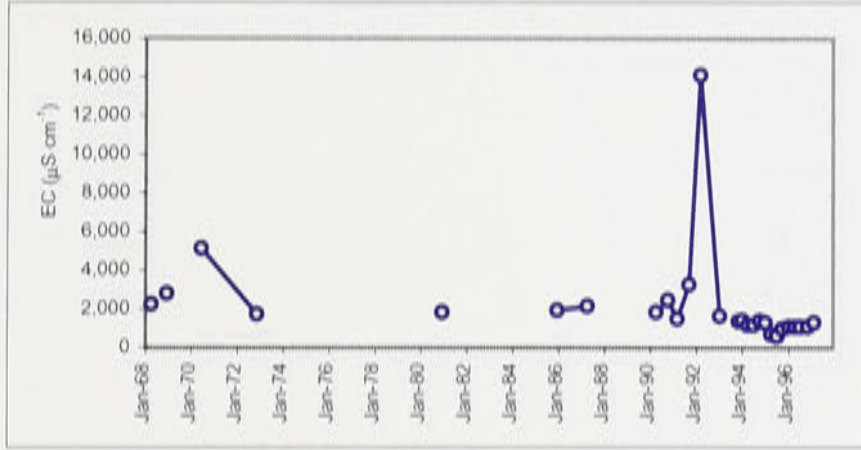


Well no. 21 W

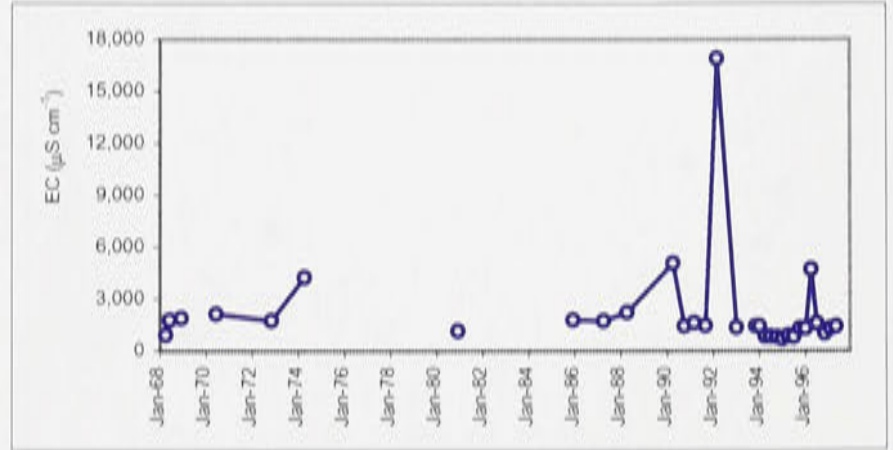


Appendix H: Continued.

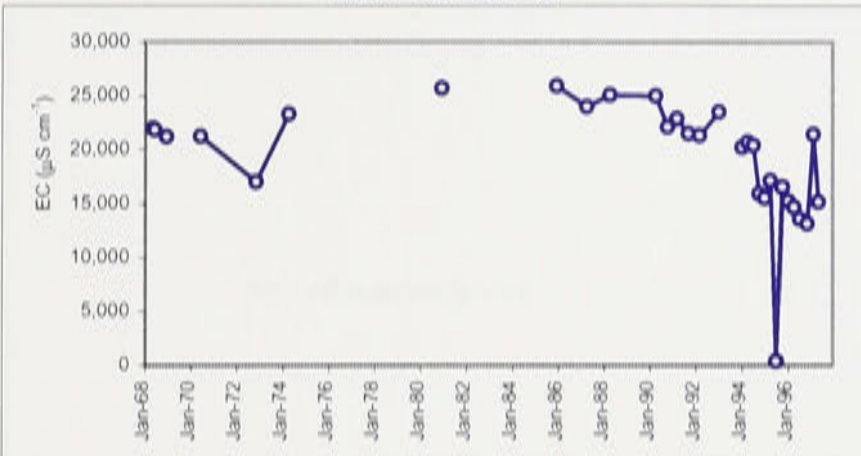
Well no. 22 W



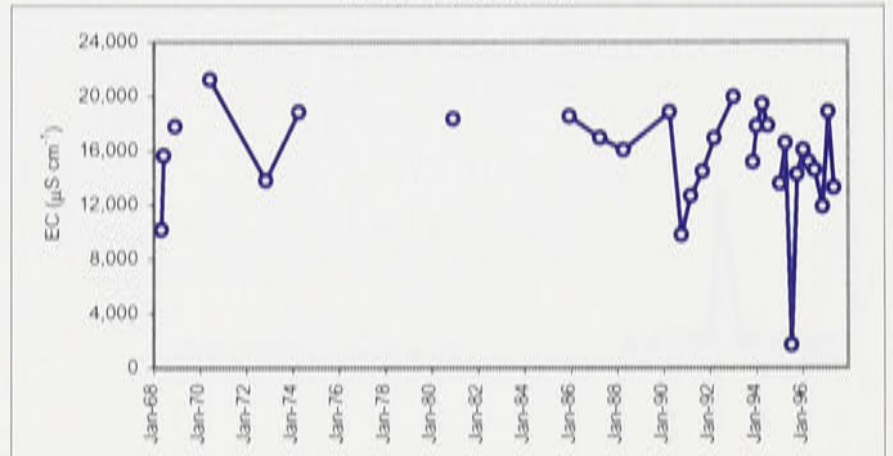
Well no. 23 W



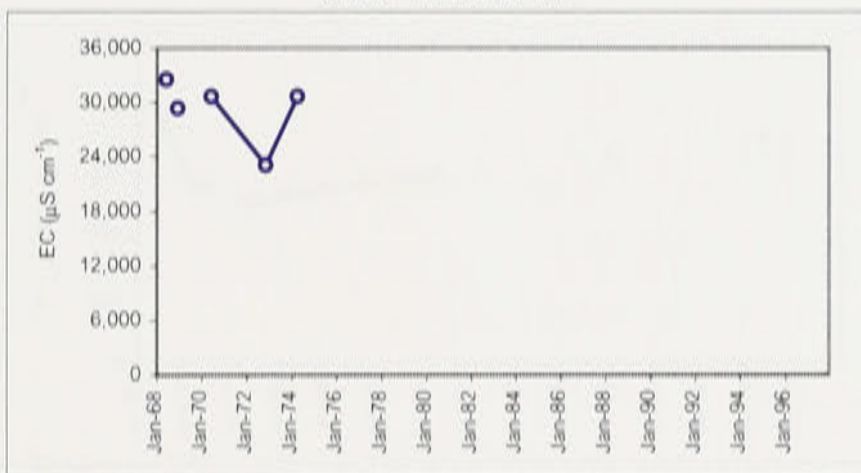
Well no. 24 W



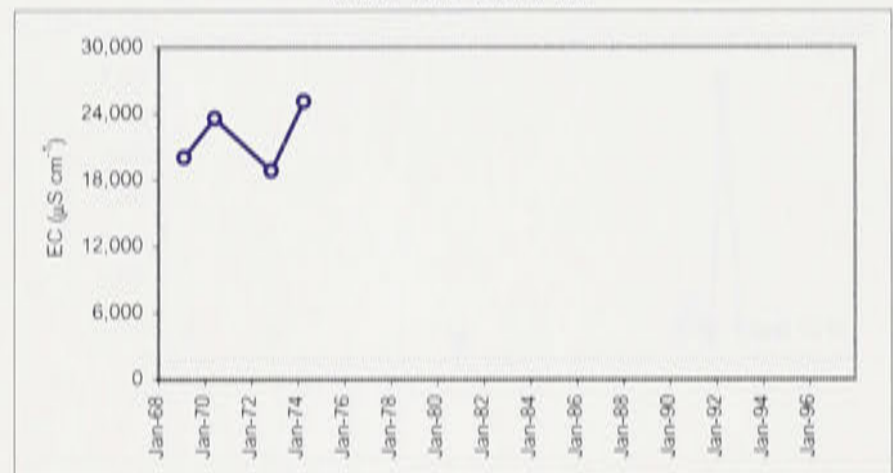
Well no. 25 W



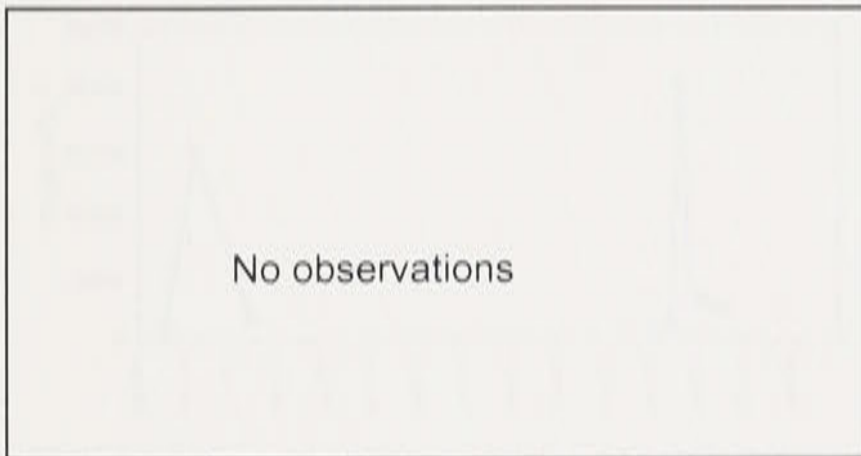
Well no. 26 W



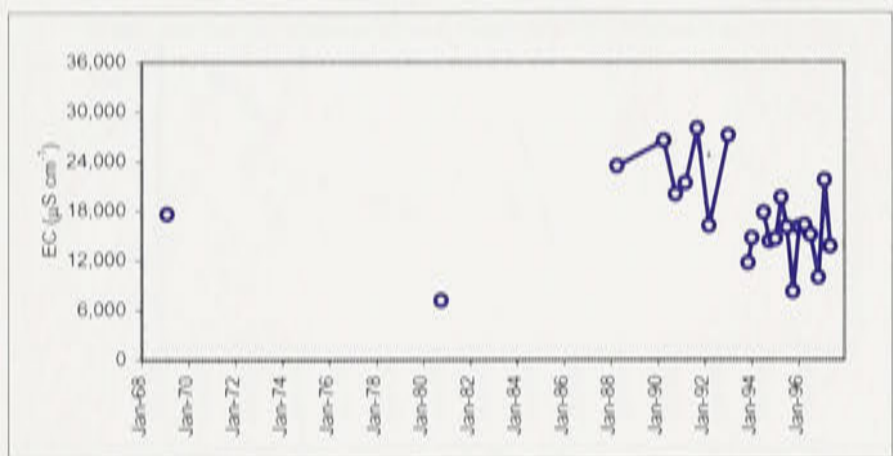
Well no. 26A W



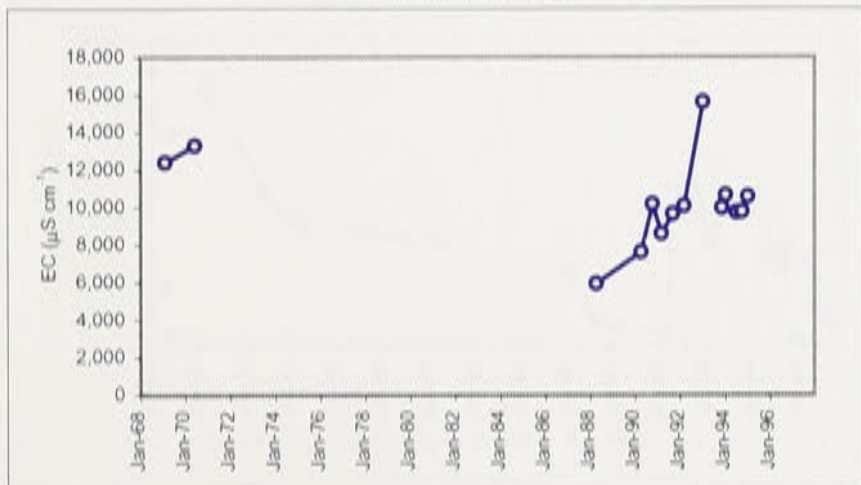
Well no. 26B W



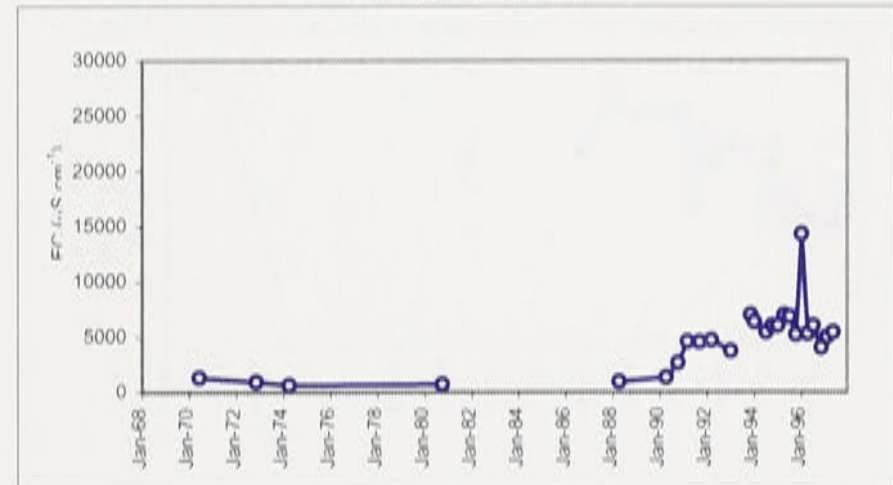
Well no. 26C W



Well no. 26D W

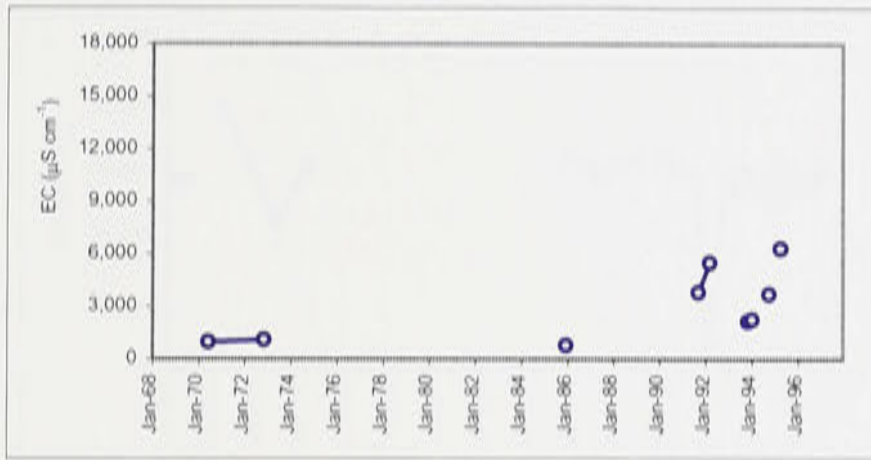


Well no. 26E W

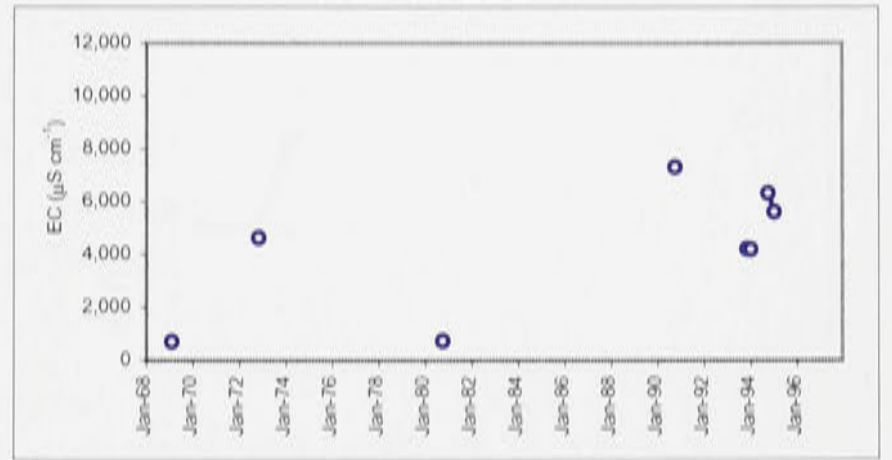


Appendix H: Continued.

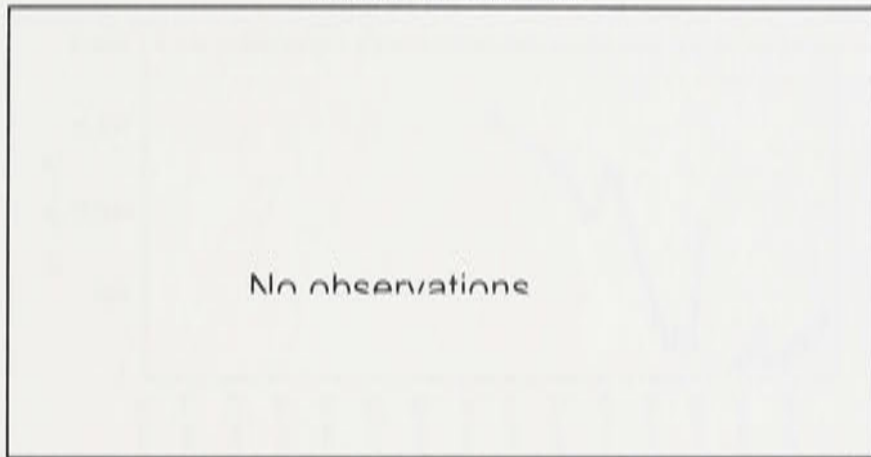
Well no. 26F W



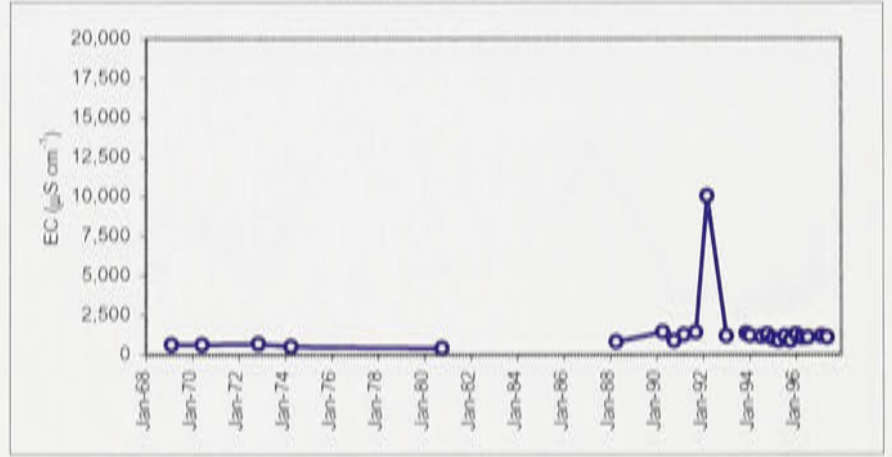
Well no. 26G W



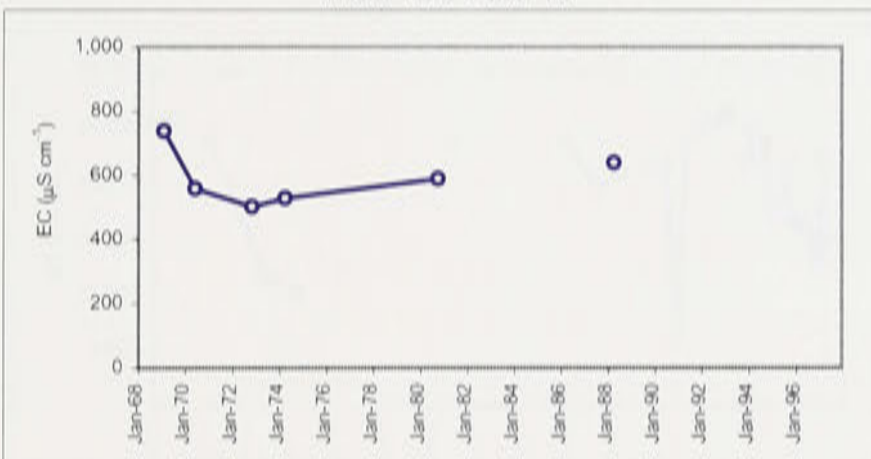
Well no. 26H W



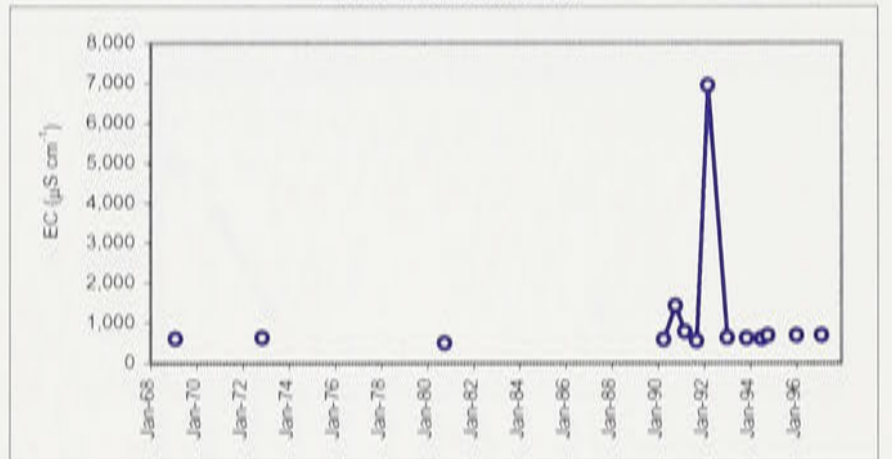
Well no. 26I W



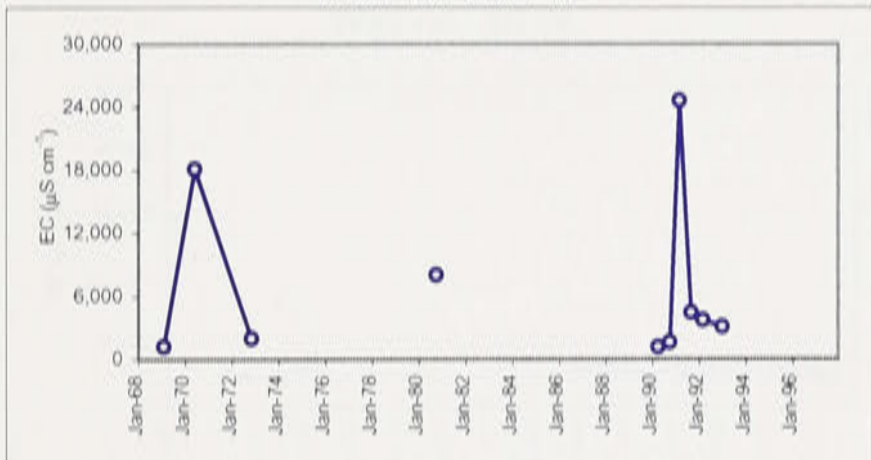
Well no. 26J W



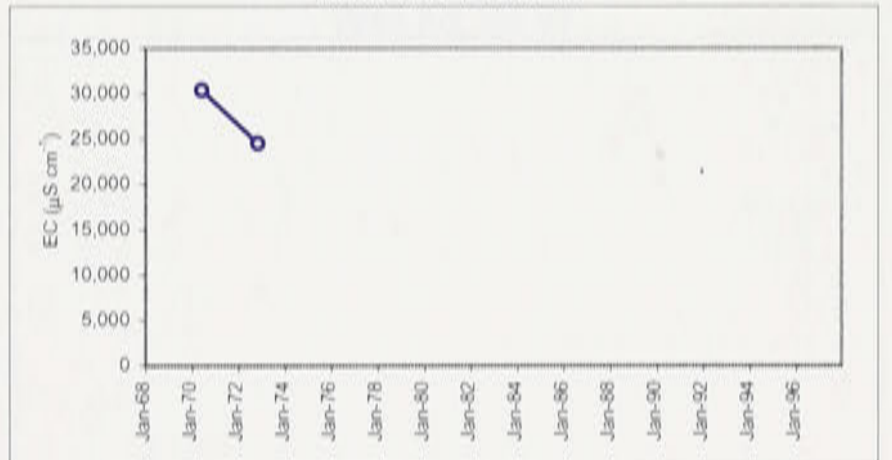
Well no. 26K W



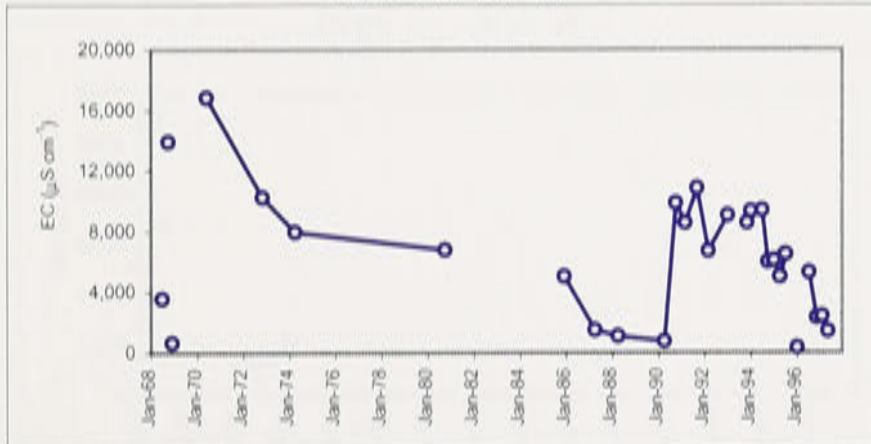
Well no. 26L W



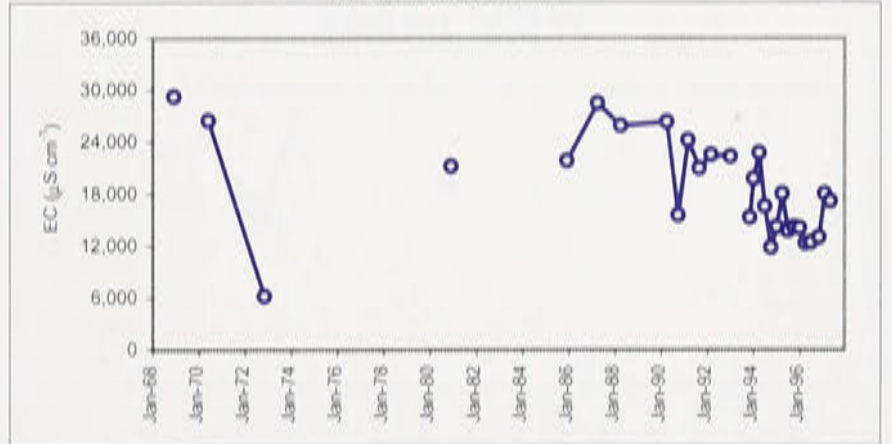
Well no. 26M W



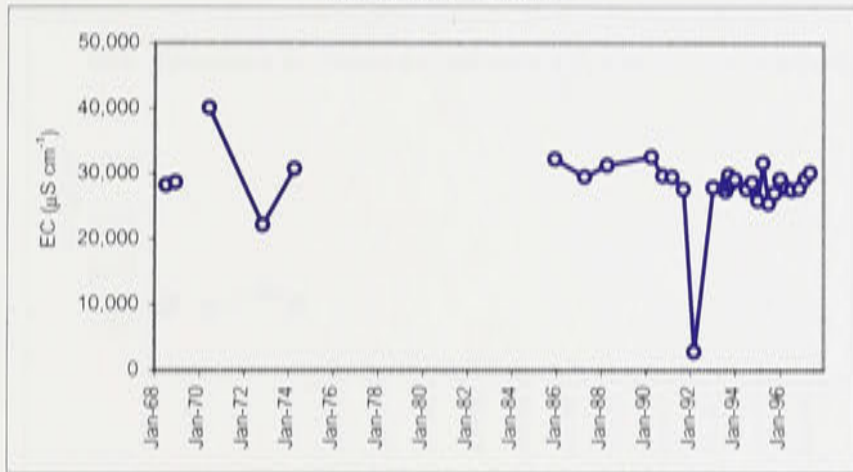
Well no. 27 W



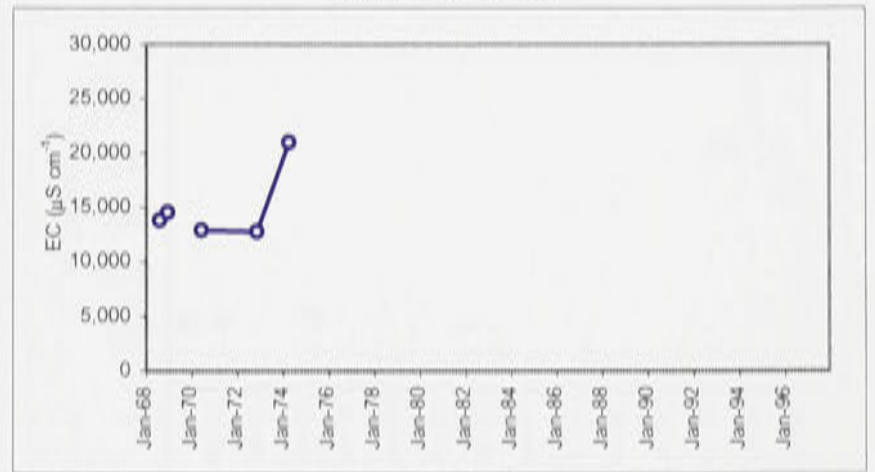
Well no. 28 W



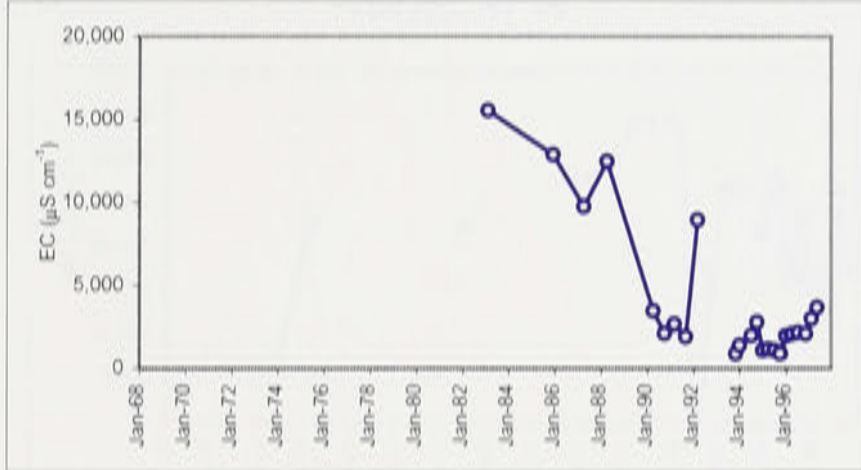
Well no. 29 W



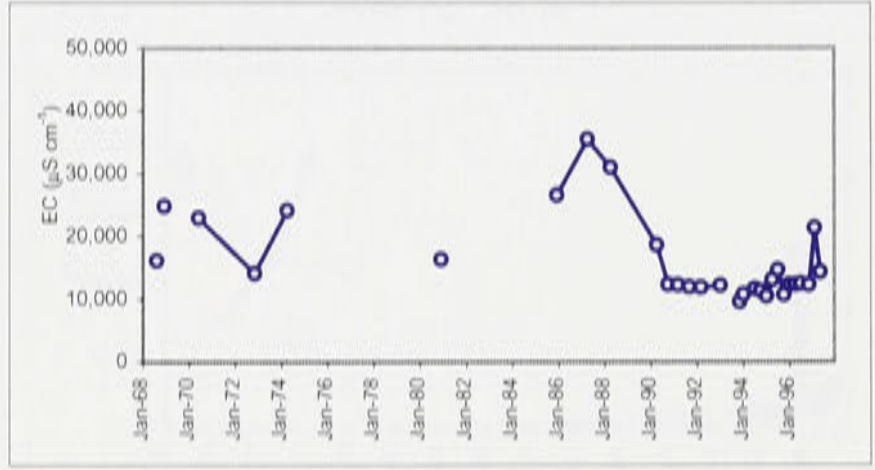
Well no. 30 W



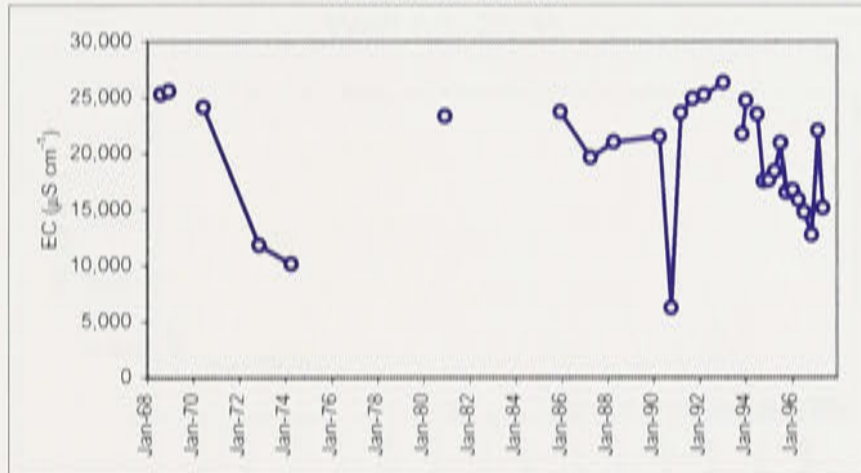
Well no. 31 W



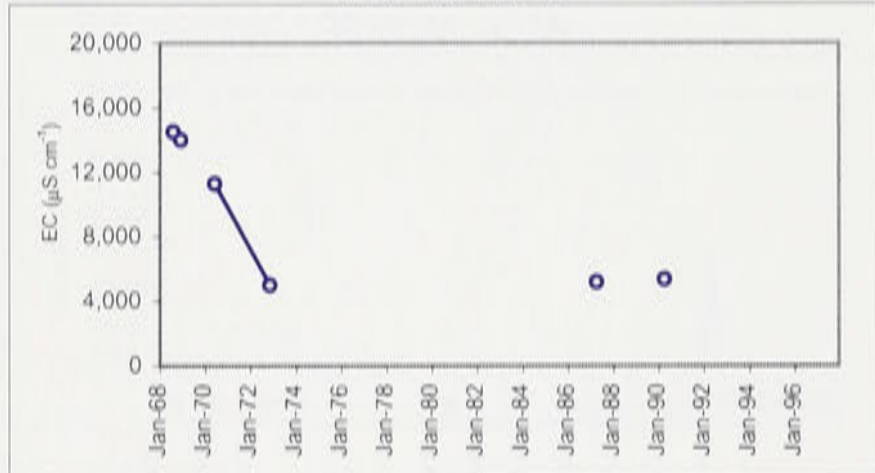
Well no. 32 W



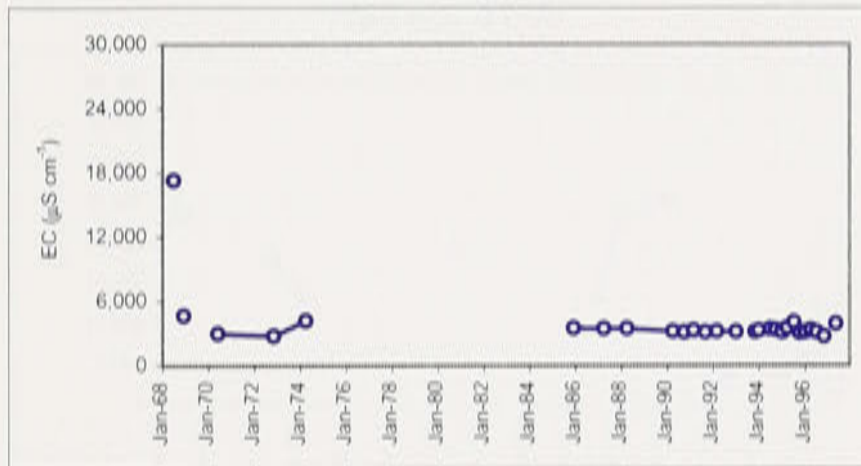
Well no. 33 W



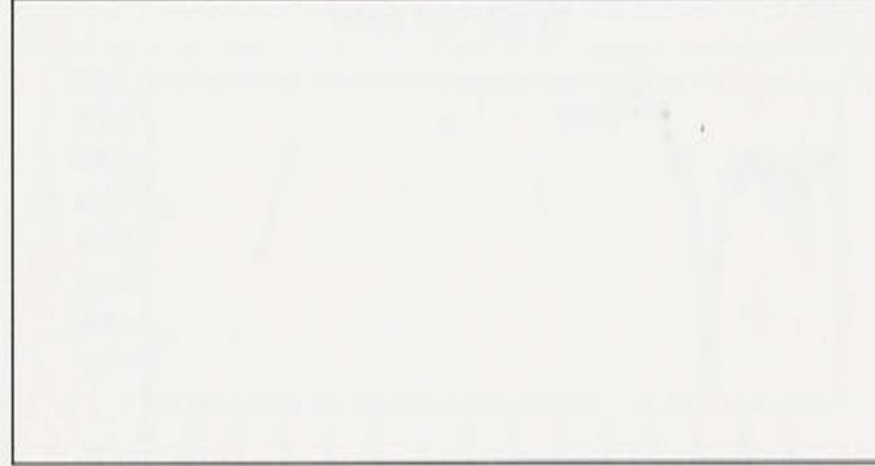
Well no. 34 W



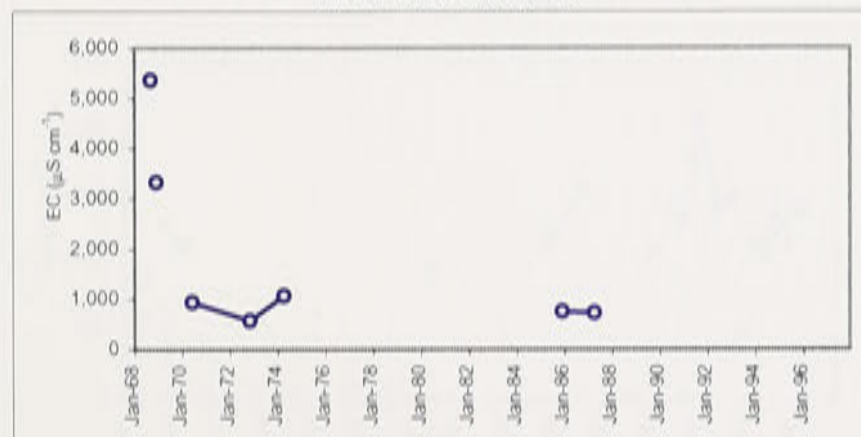
Well no. 35 W



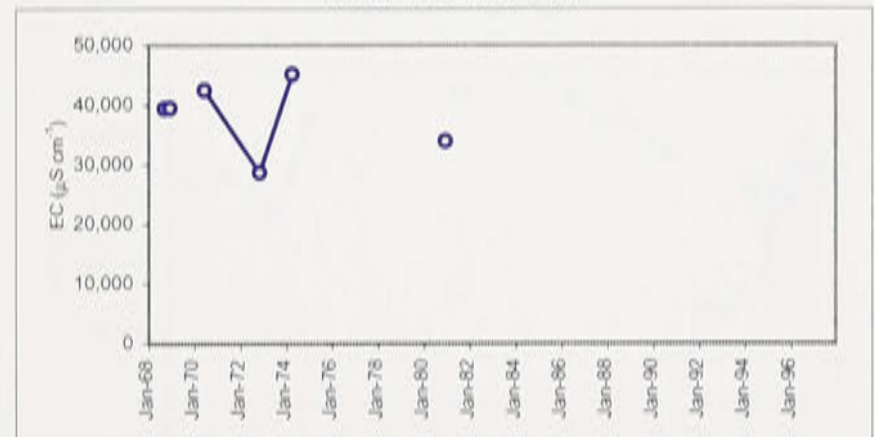
Well no. 36 W



Well no. 36A W

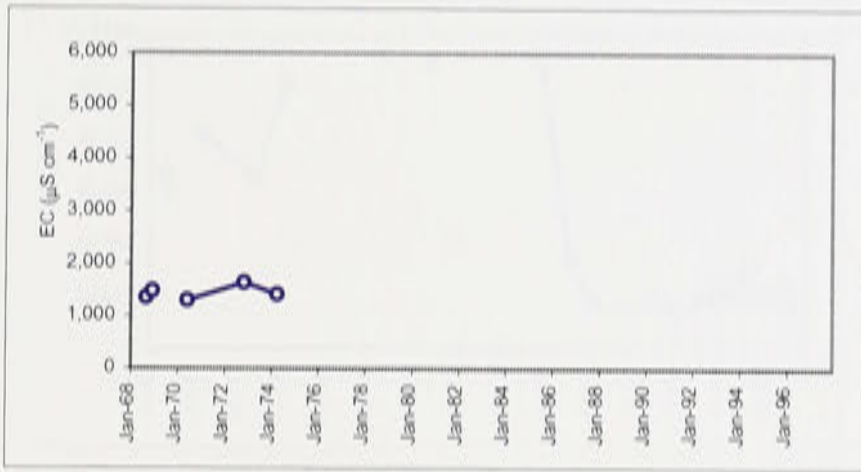


Well no. 36B W

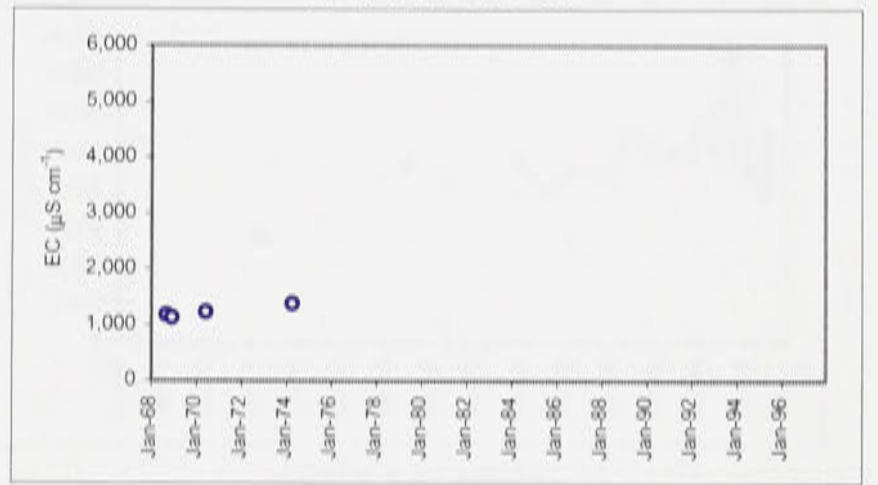


Appendix H: Continued.

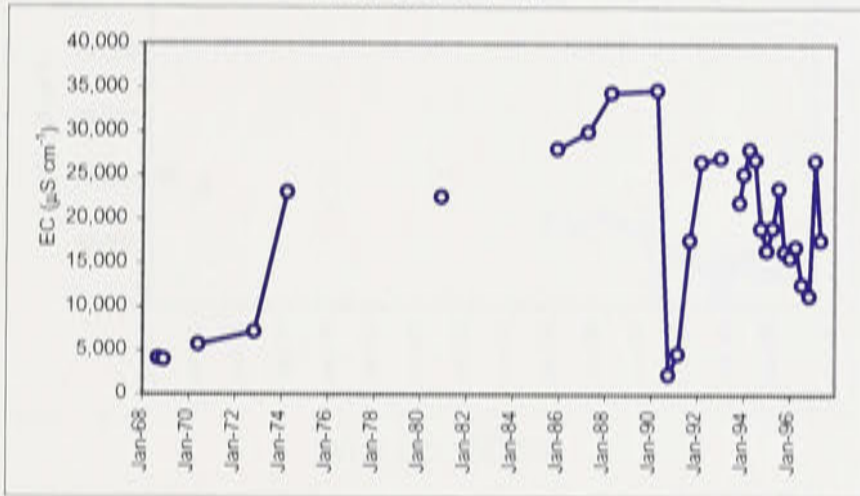
Well no. 36C W



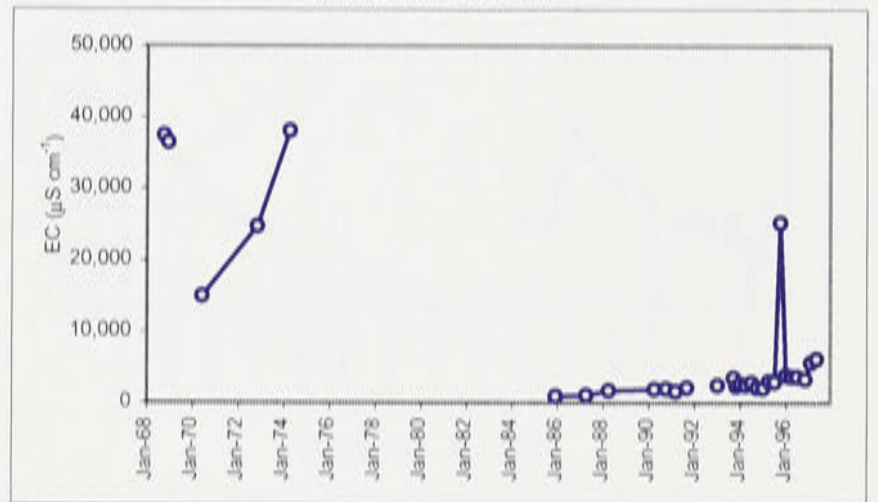
Well no. 36D W



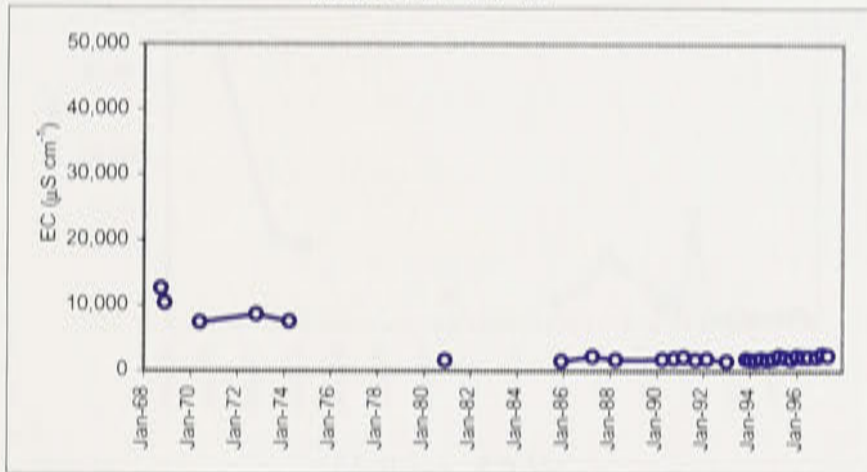
Well no. 37 W



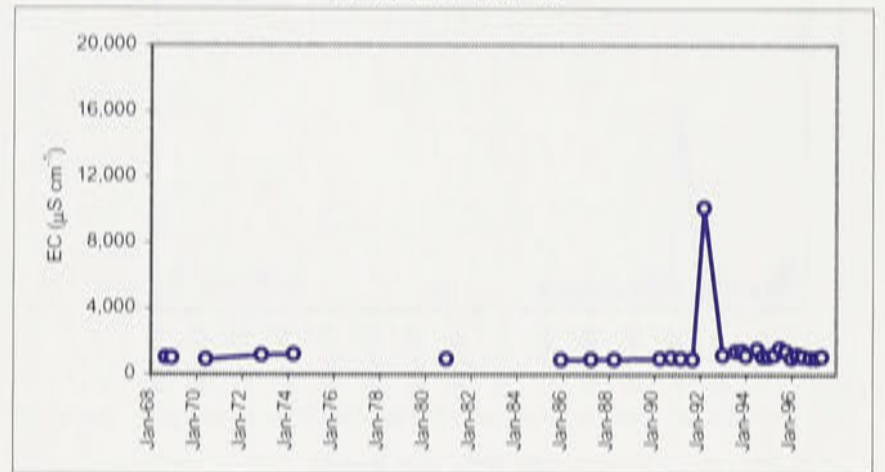
Well no. 38 W



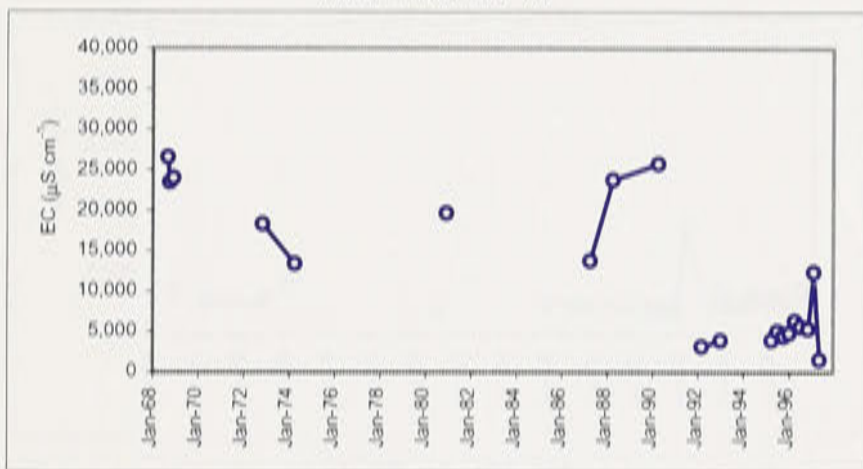
Well no. 39 W



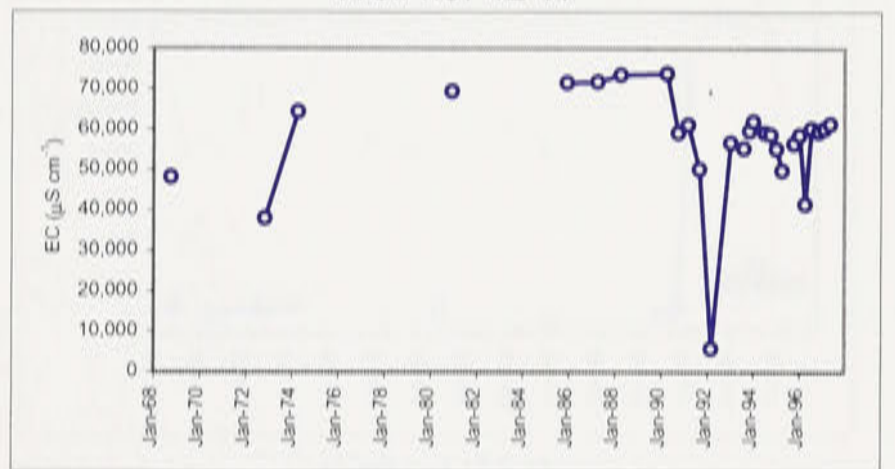
Well no. 40 W



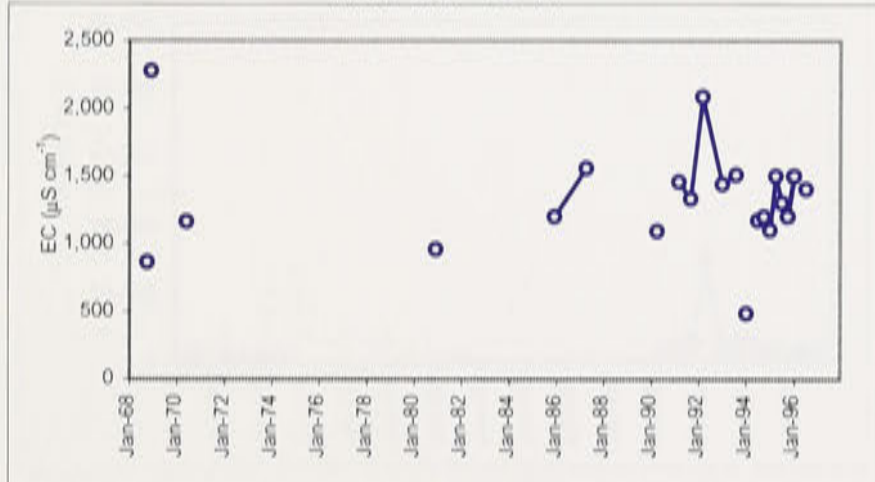
Well no. 41 W



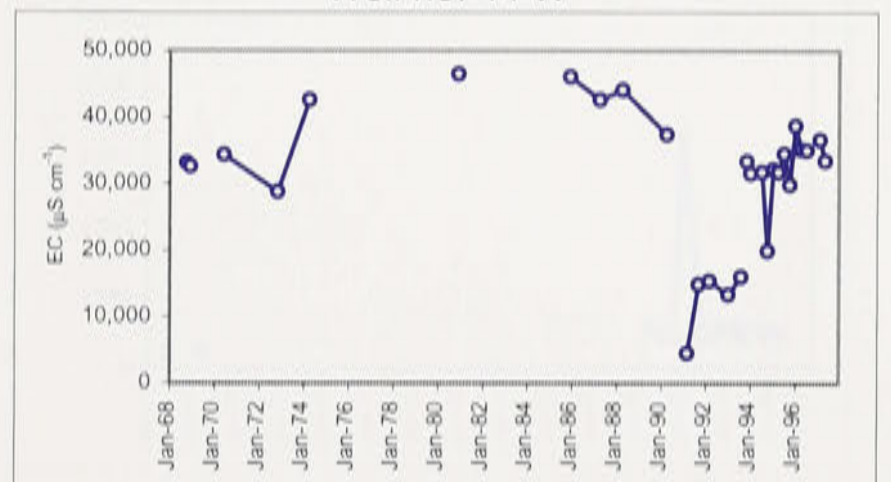
Well no. 42 W



Well no. 43 W

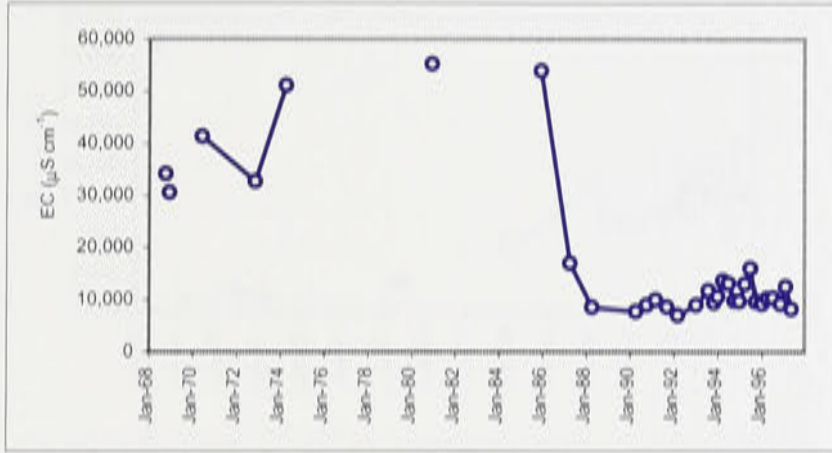


Well no. 44 W

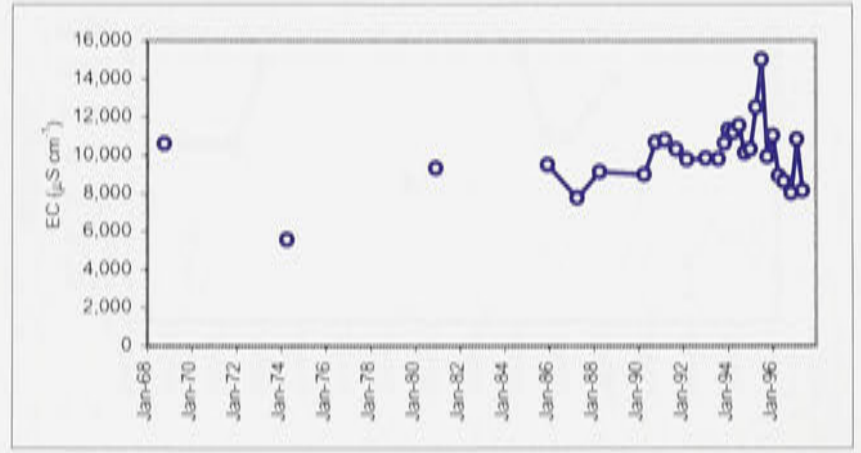


Appendix H: Continued.

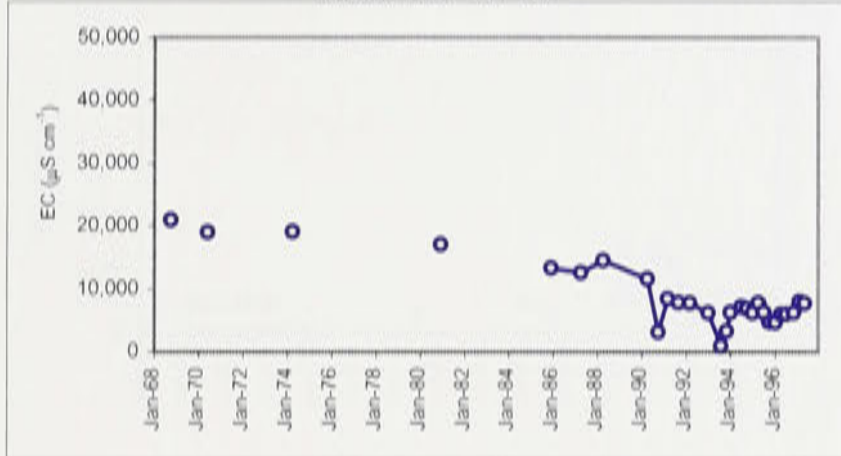
Well no. 45 W



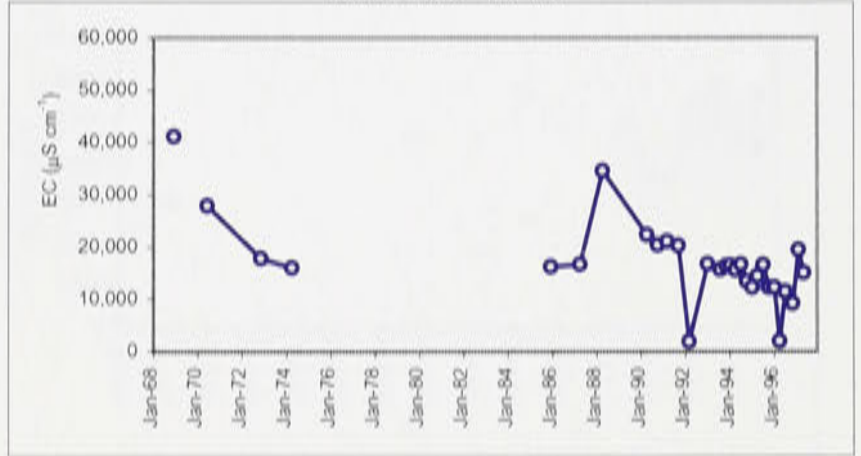
Well no. 46 W



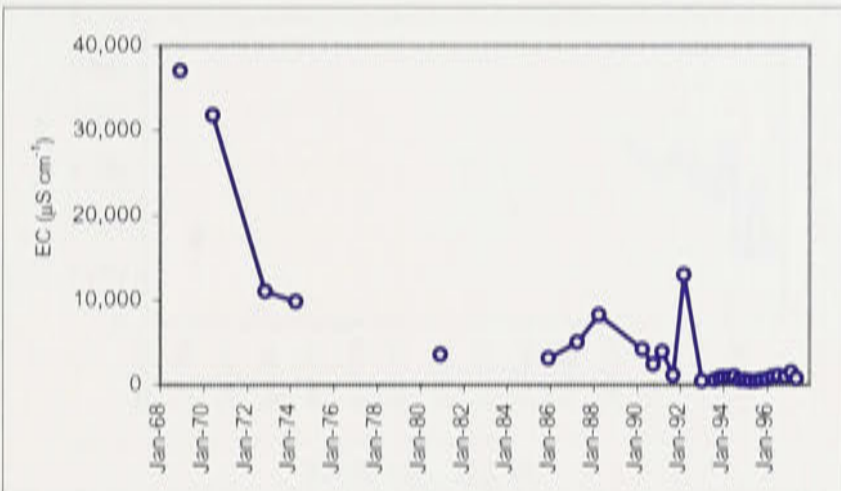
Well no. 47 W



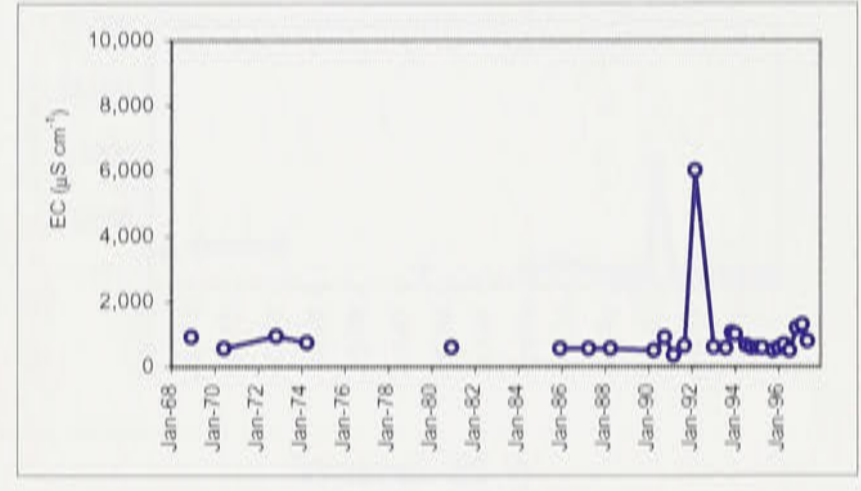
Well no. 48 W



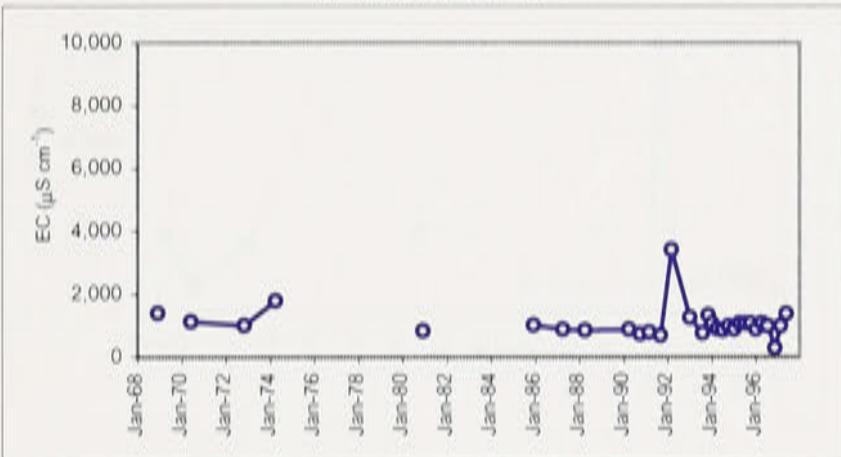
Well no. 50 W



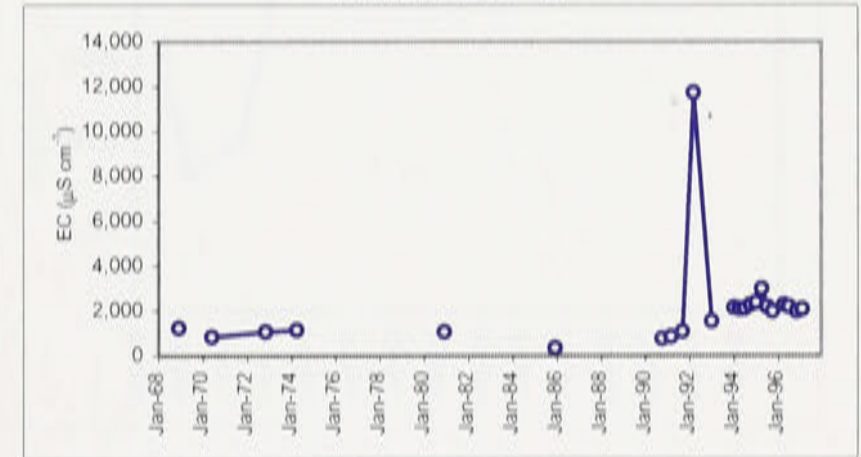
Well no. 51 W



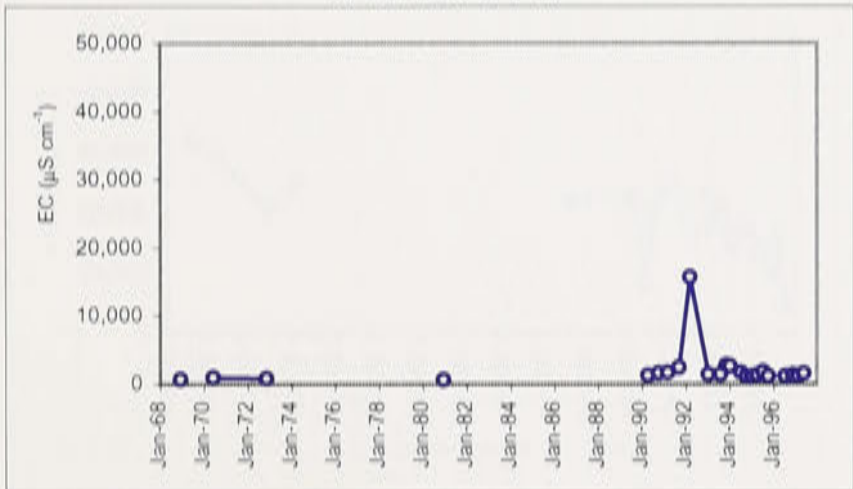
Well no. 52 W



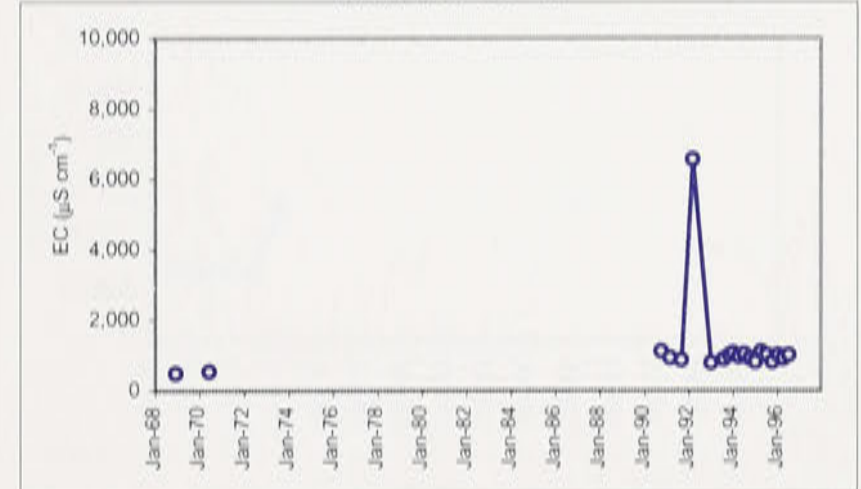
Well no. 53 W



Well no. 54 W

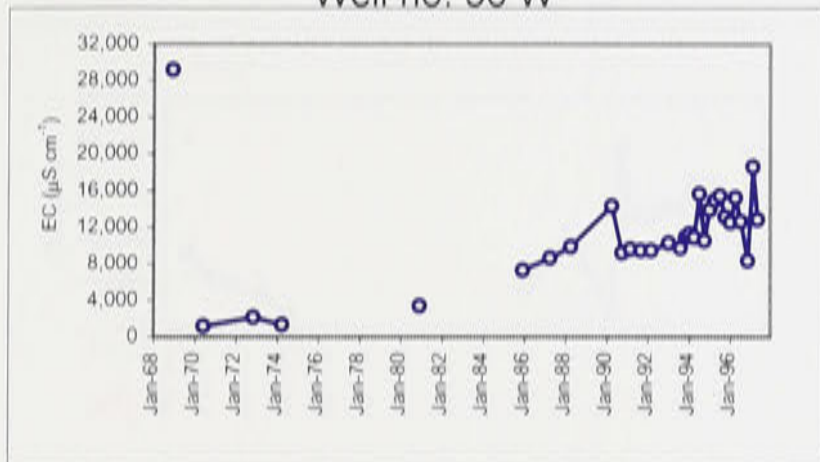


Well no. 55 W

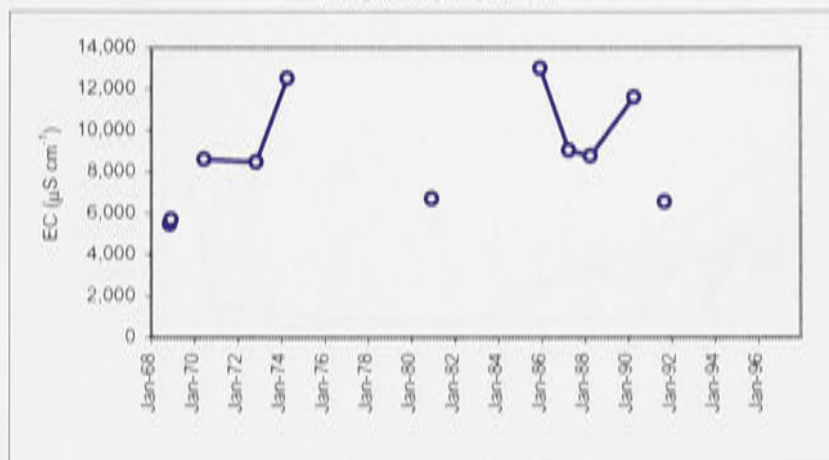


Appendix H: Continued.

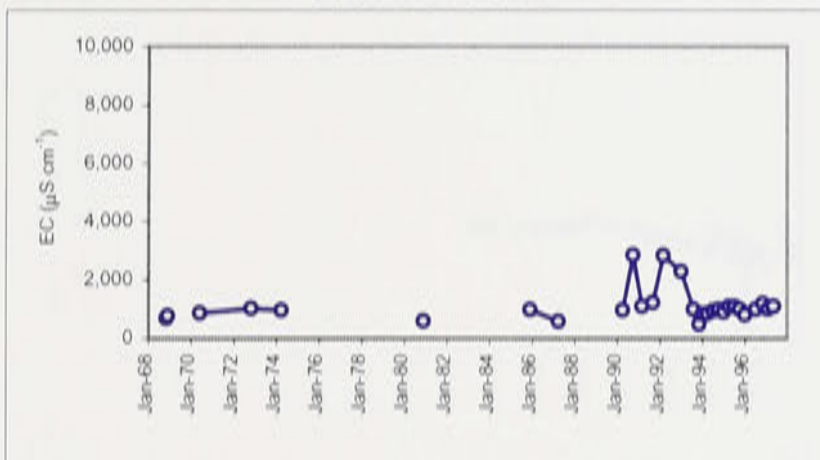
Well no. 56 W



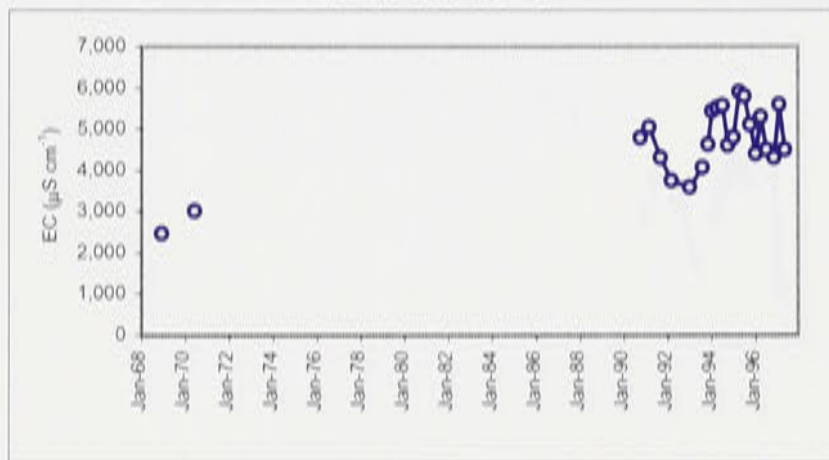
Well no. 57 W



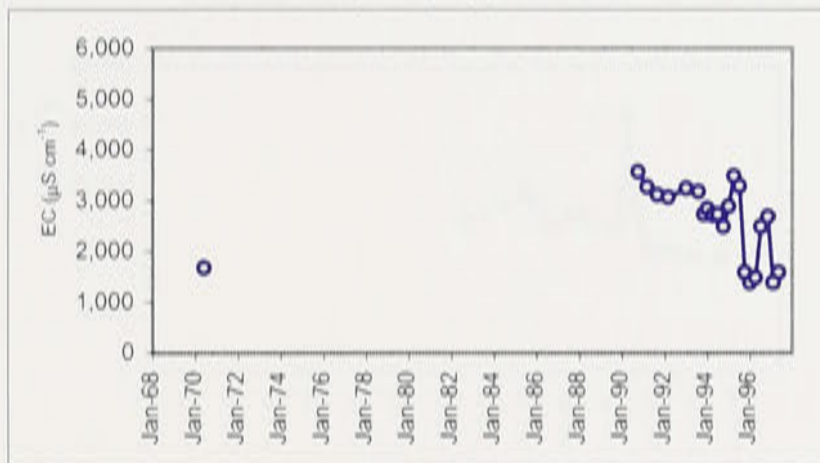
Well no. 58 W



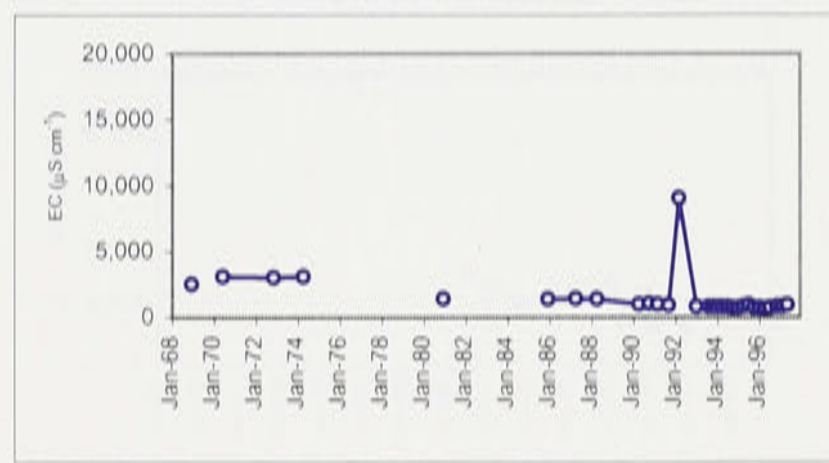
Well no. 59 W



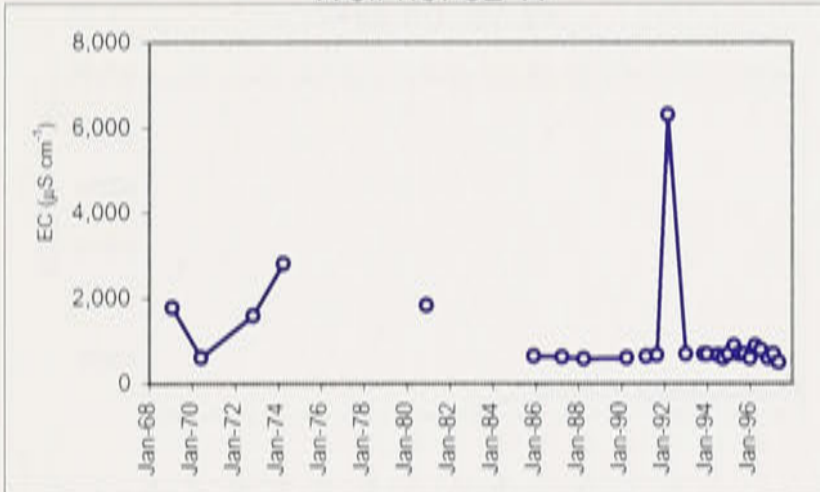
Well no. 60 W



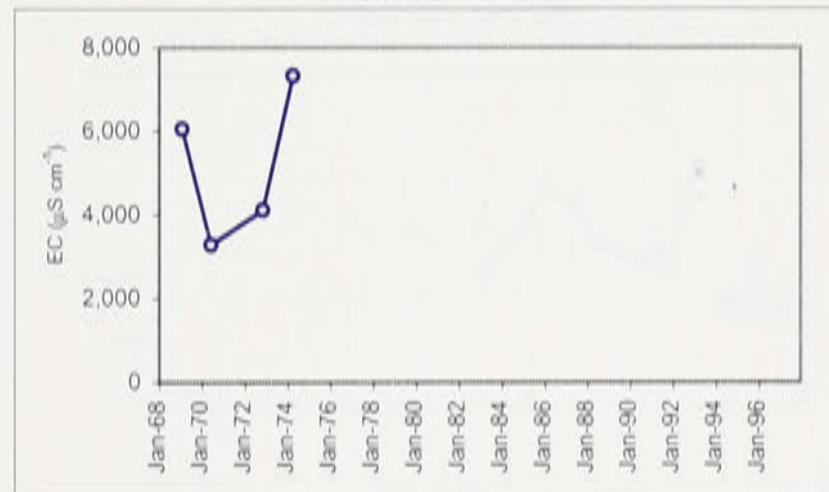
Well no. 61 W



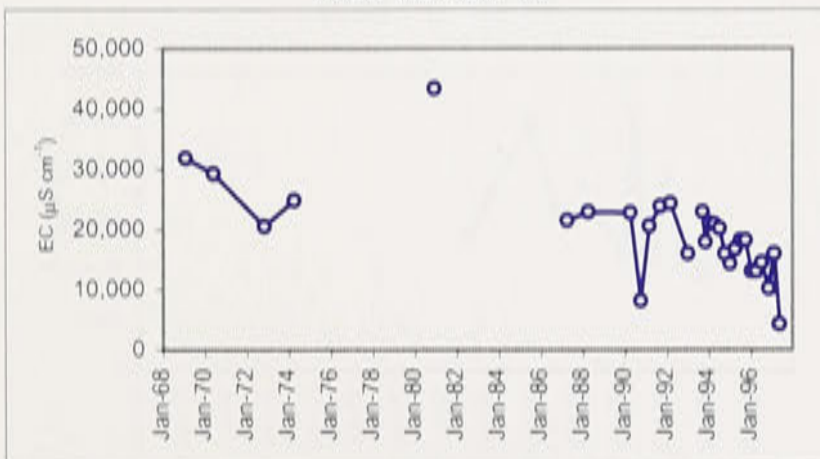
Well no. 62 W



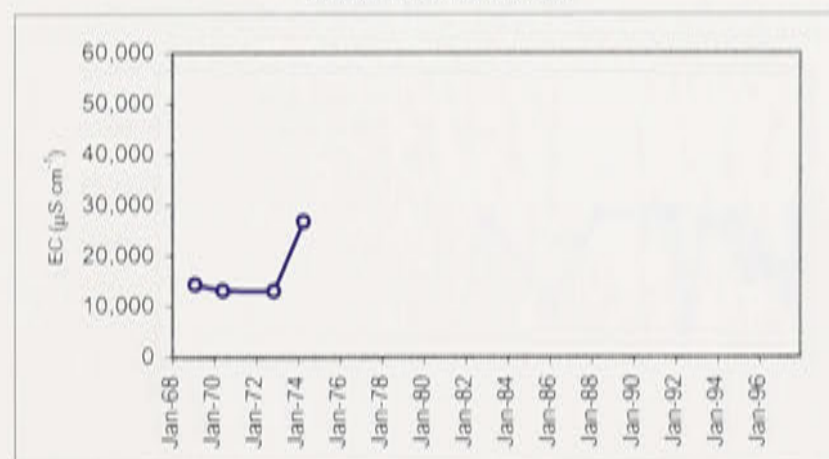
Well no. 63 W



Well no. 64 W

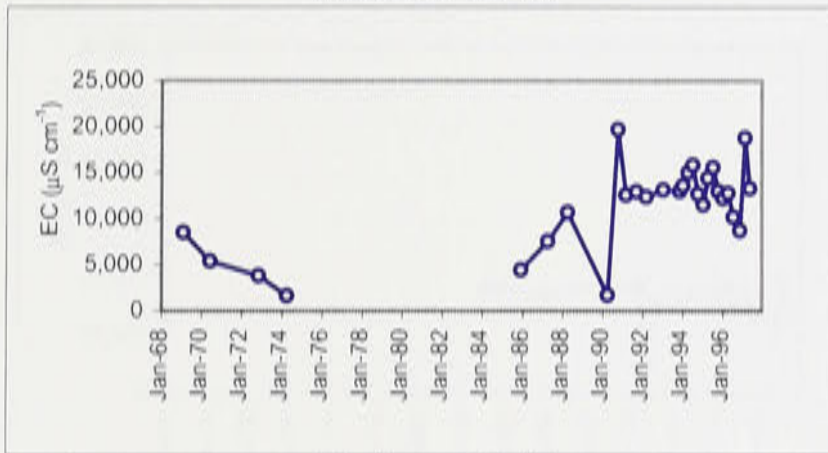


Well no. 64A W

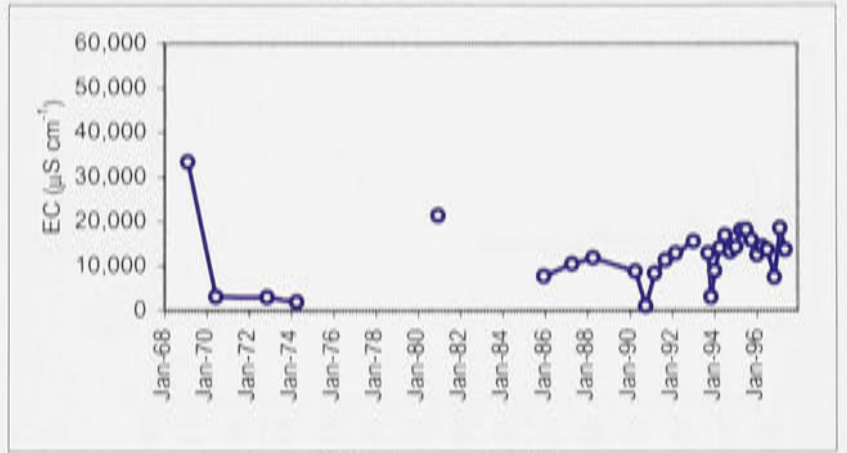


Appendix H: Continued.

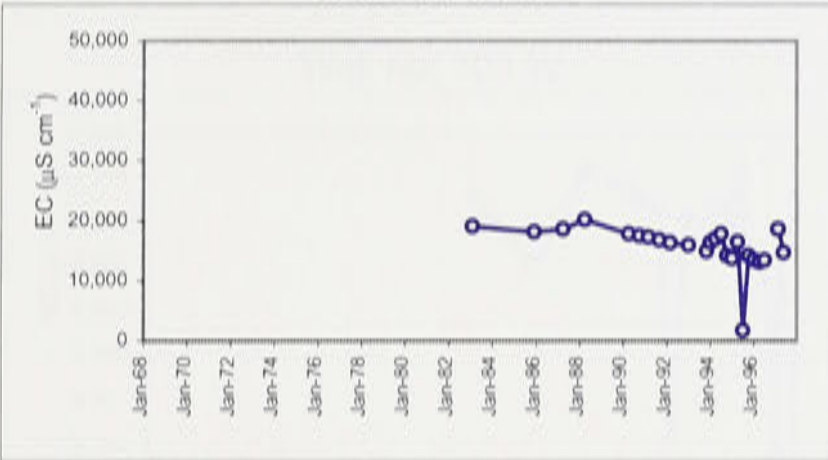
Well no. 65 W



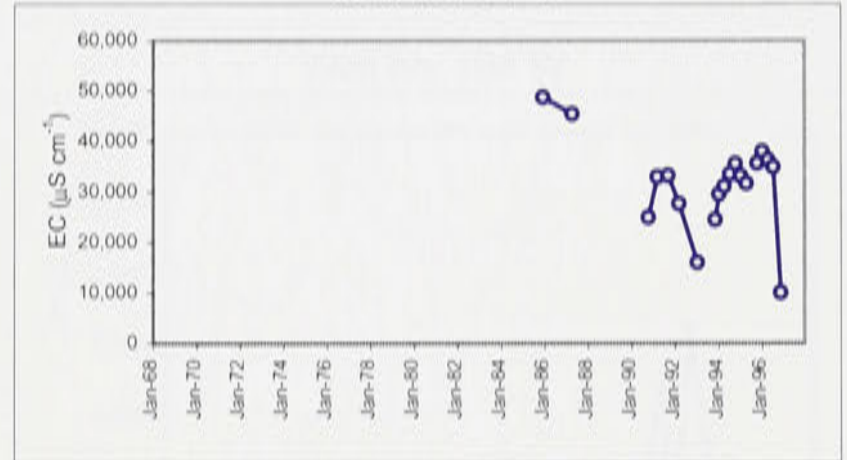
Well no. 66 W



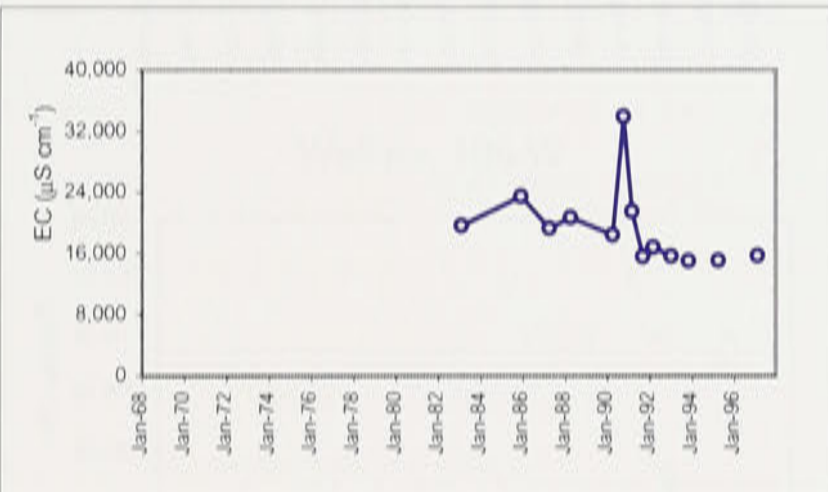
Well no. 92 W



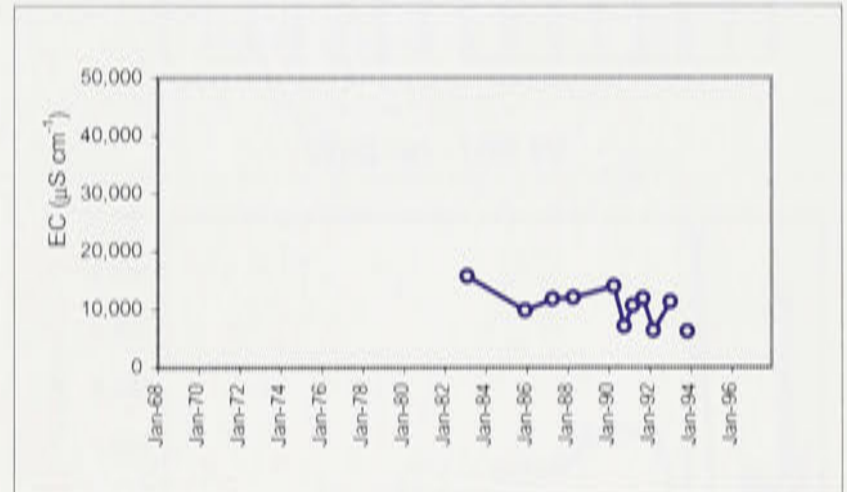
Well no. 94 W



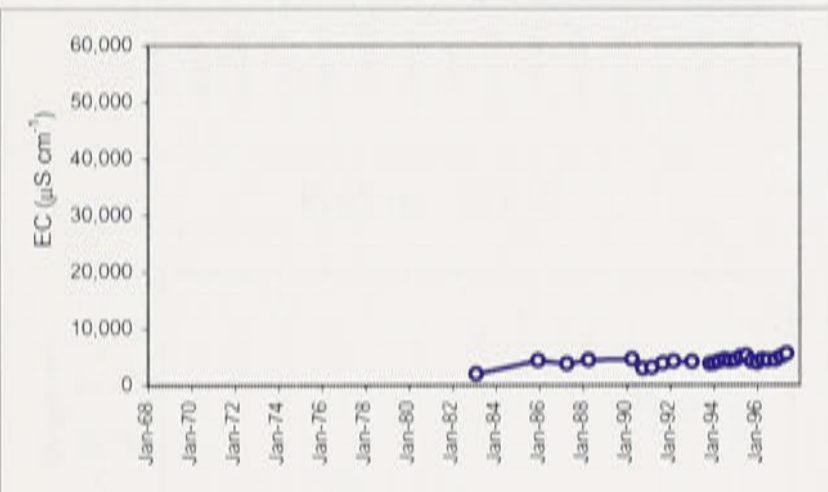
Well no. 95 W



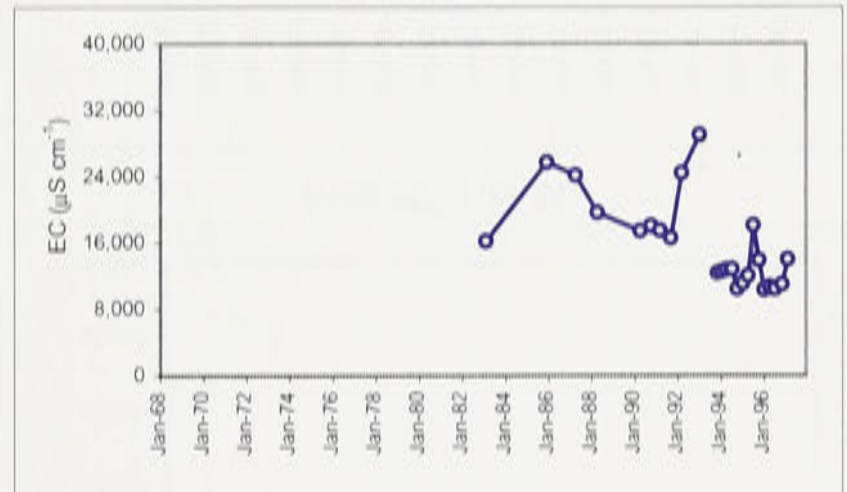
Well no. 96 W



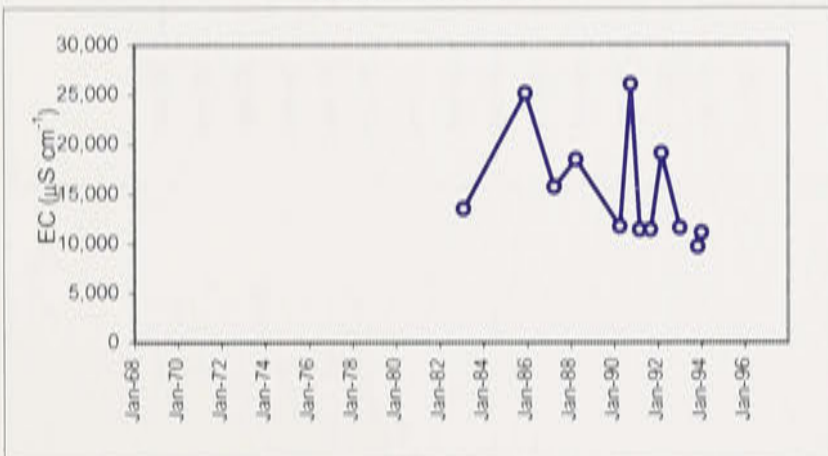
Well no. 97 W



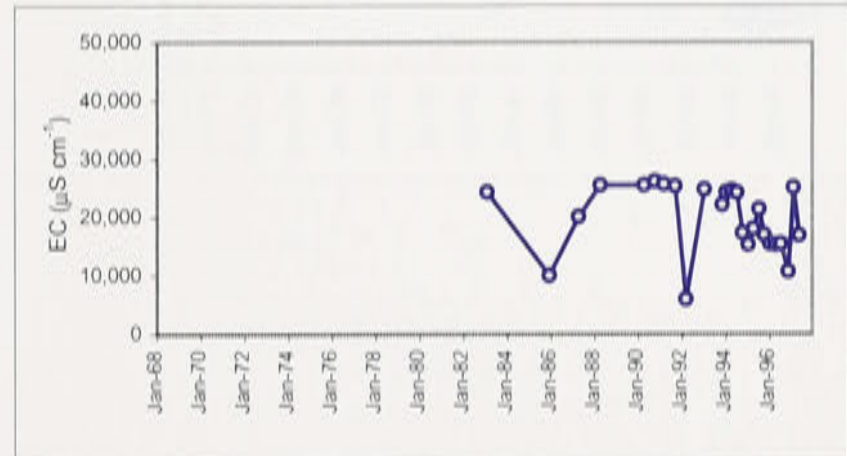
Well no. 98 W



Well no. 99 W

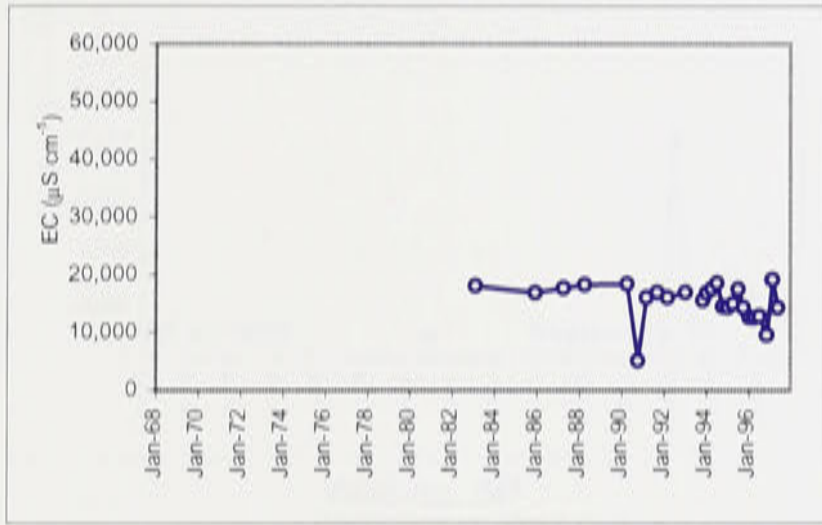


Well no. 100 W

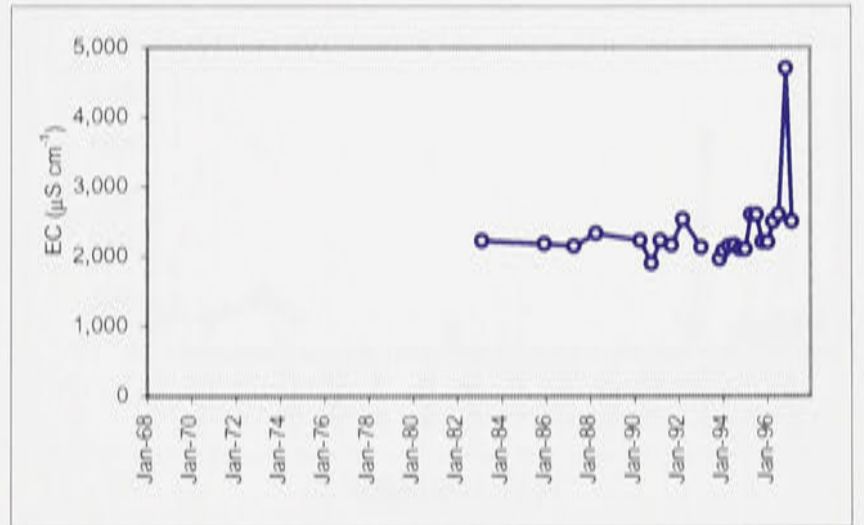


Appendix H: Continued.

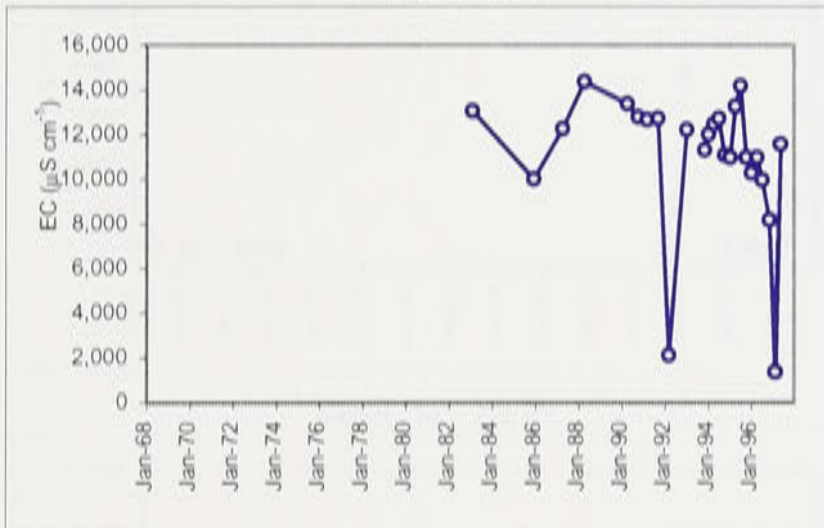
Well no. 101 W



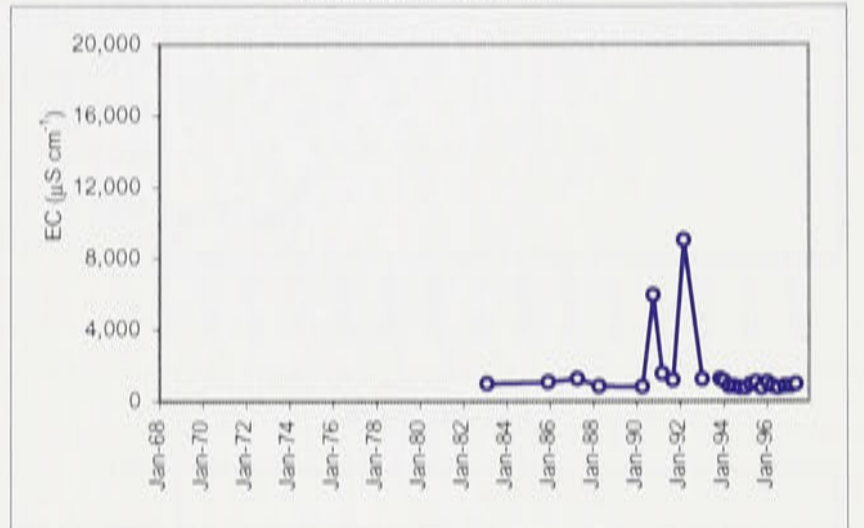
Well no. 102 W



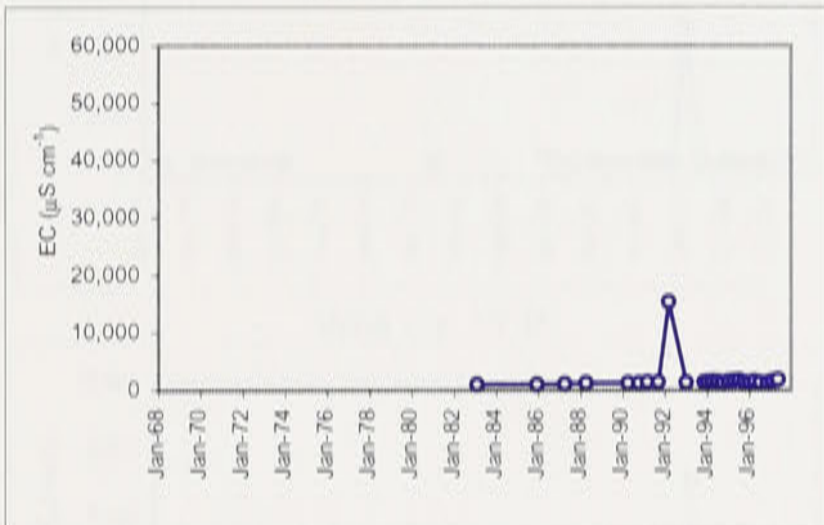
Well no. 103 W



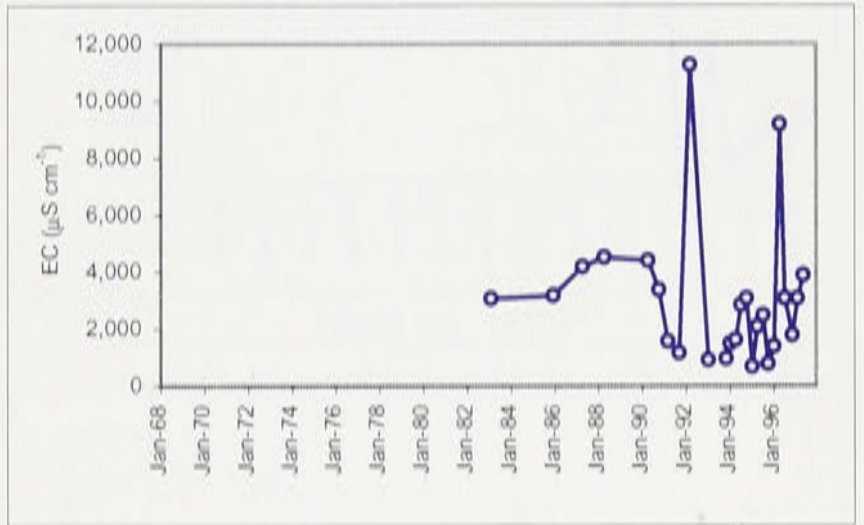
Well no. 104 W



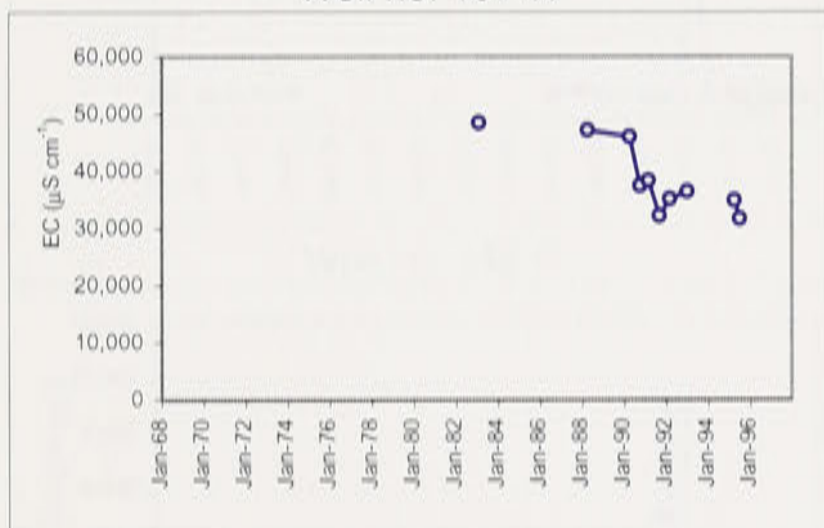
Well no. 105 W



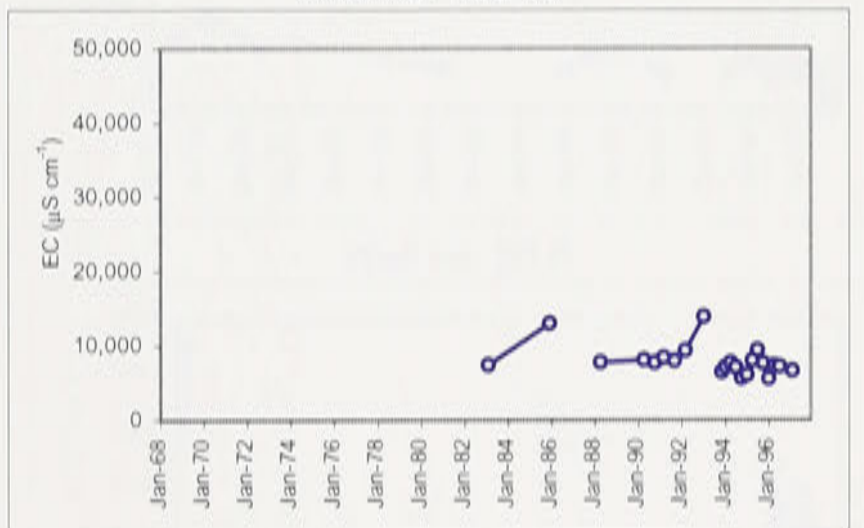
Well no. 106 W



Well no. 107 W

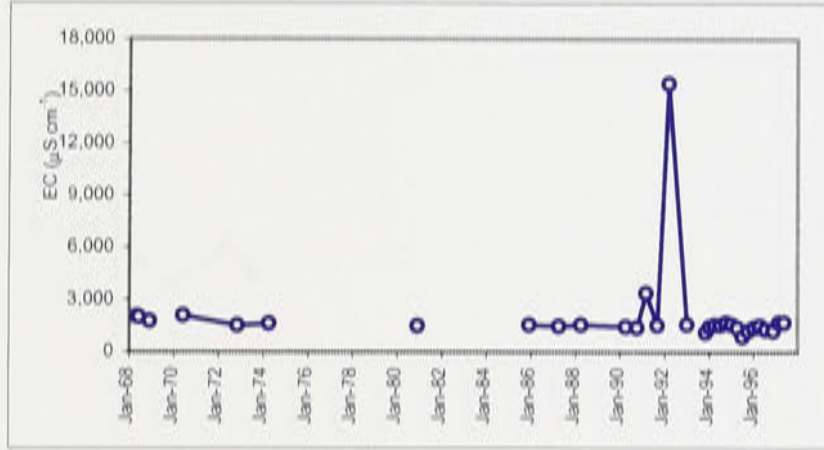


Well no. 108 W

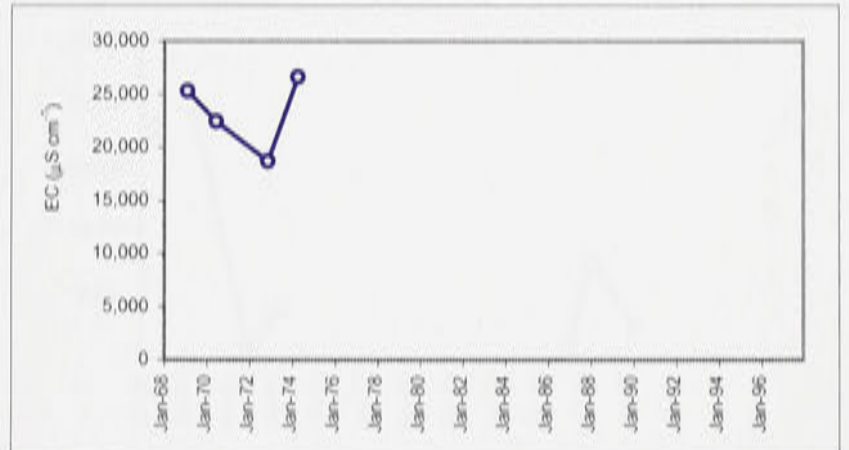


Appendix H: Continued.

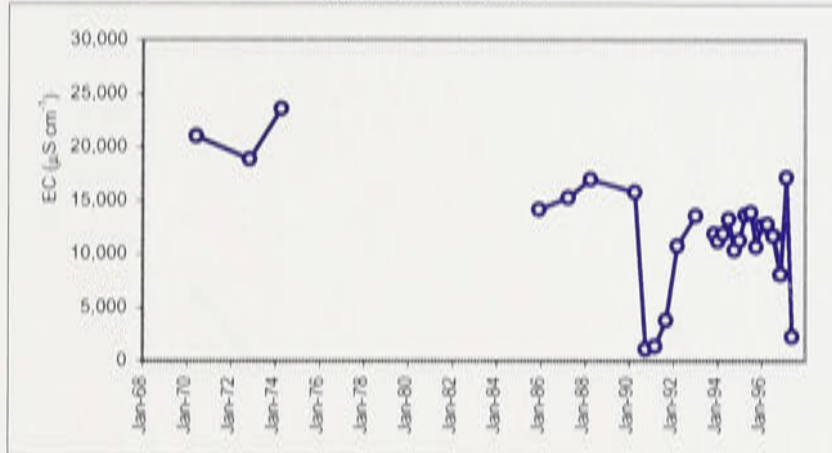
Well no. 22 P



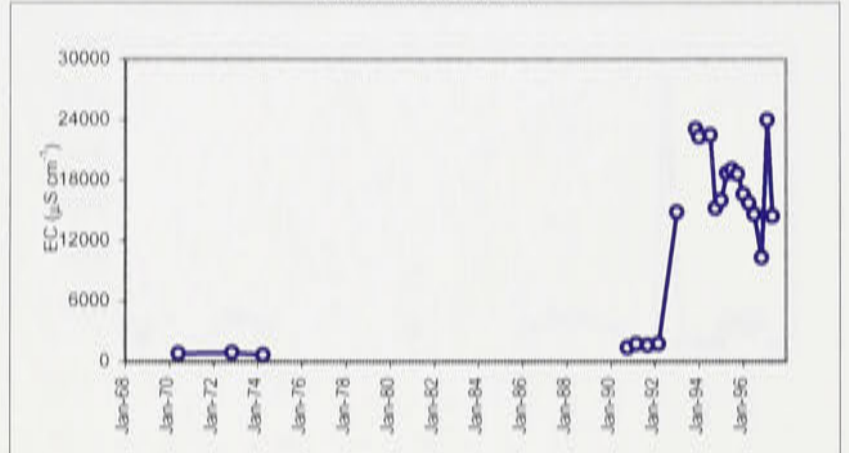
Well no. 26A P



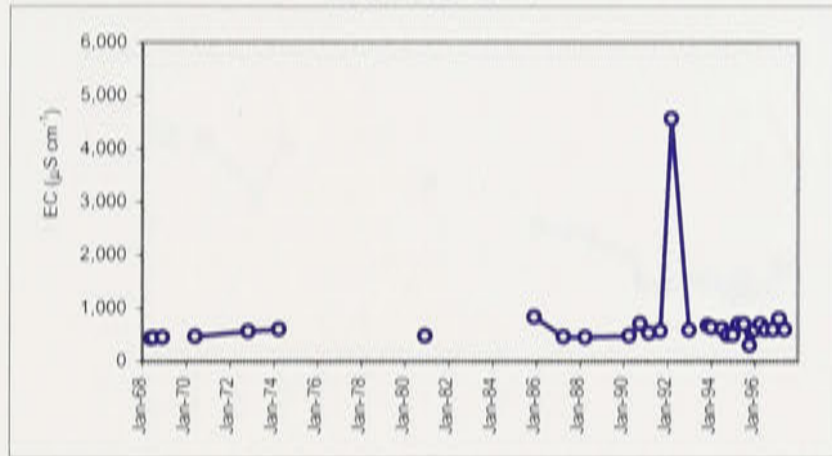
Well no. 26B P



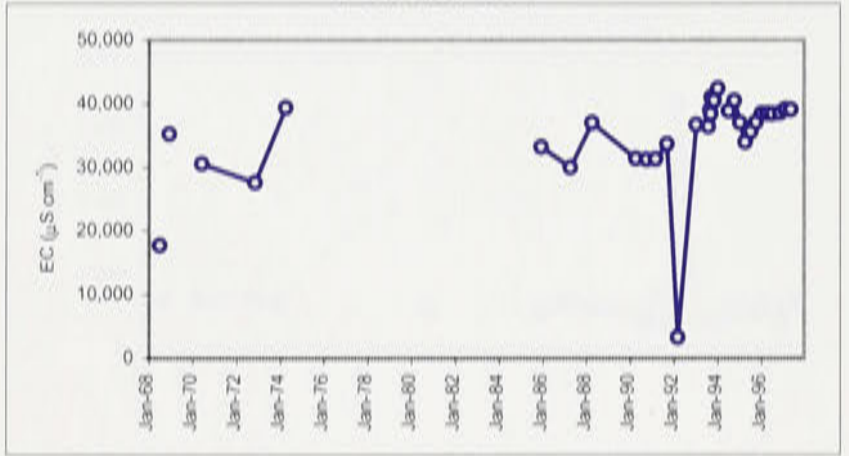
Well no. 26E P



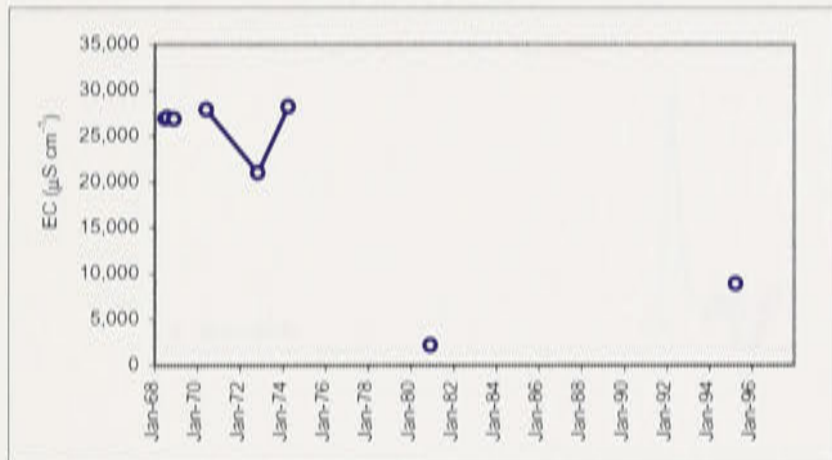
Well no. 27 P



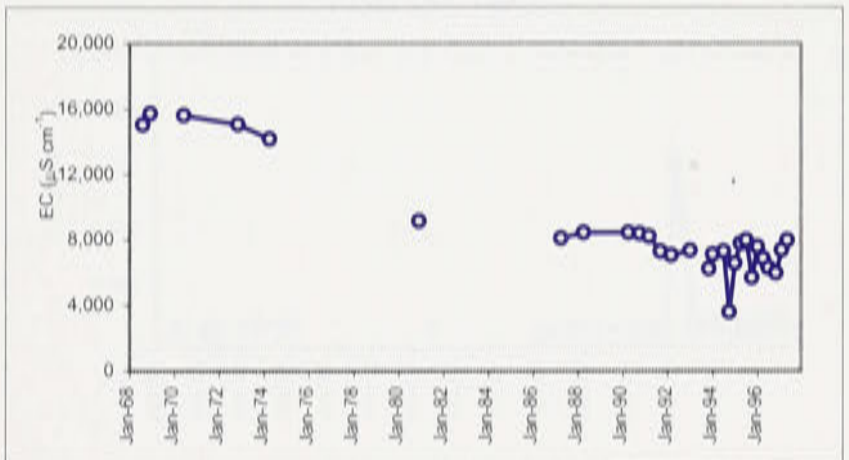
Well no. 29 P



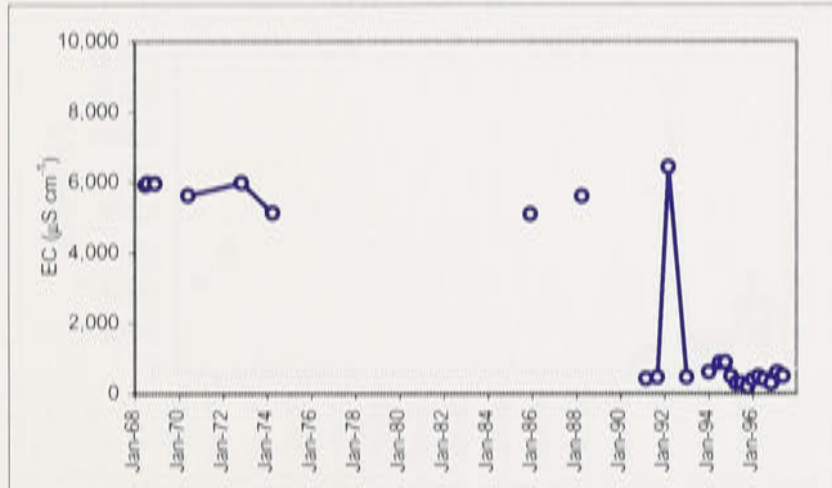
Well no. 30 P



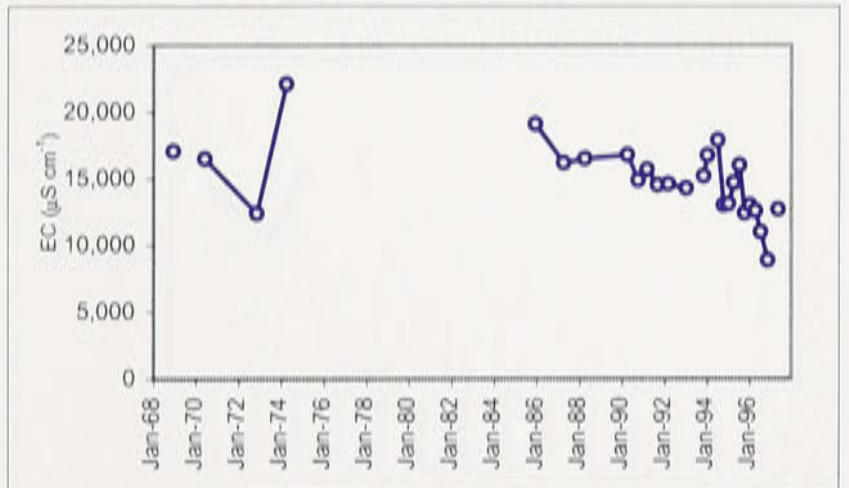
Well no. 33 P



Well no. 34 P

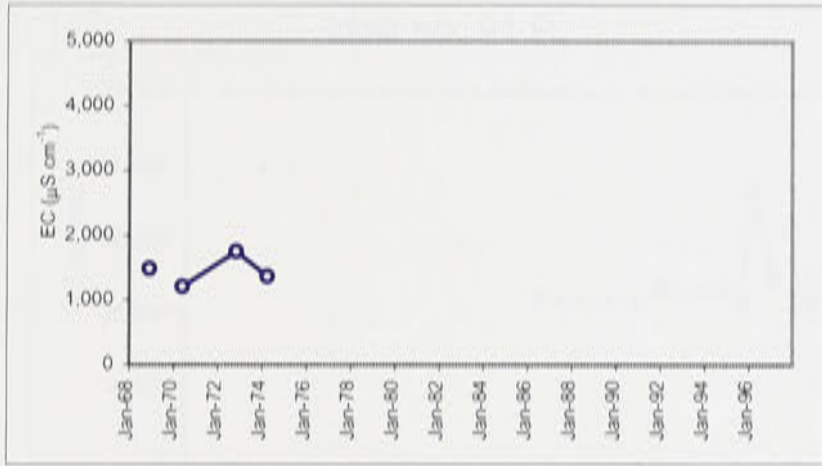


Well no. 35 P

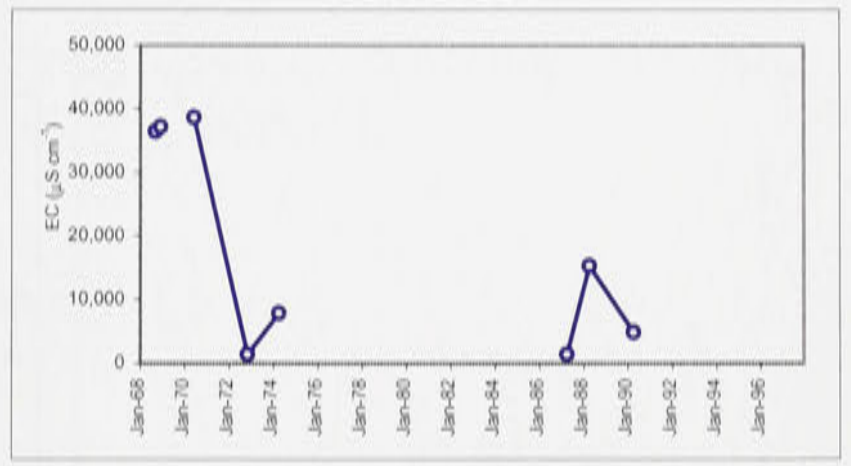


Appendix H: Continued.

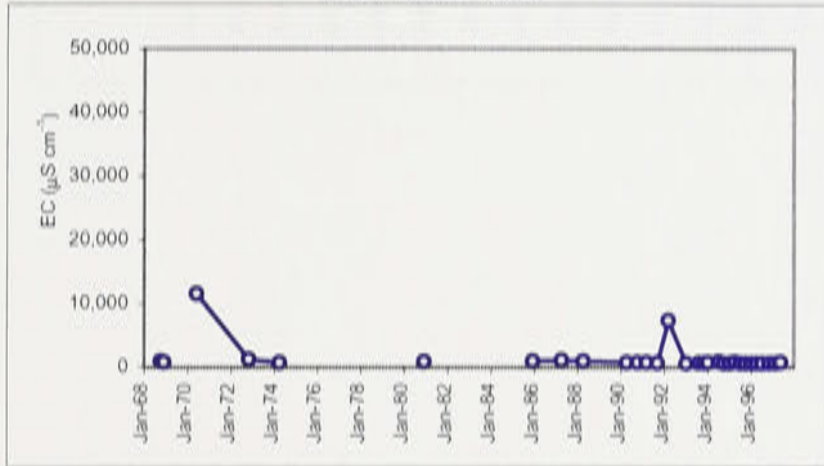
Well no. 35B P



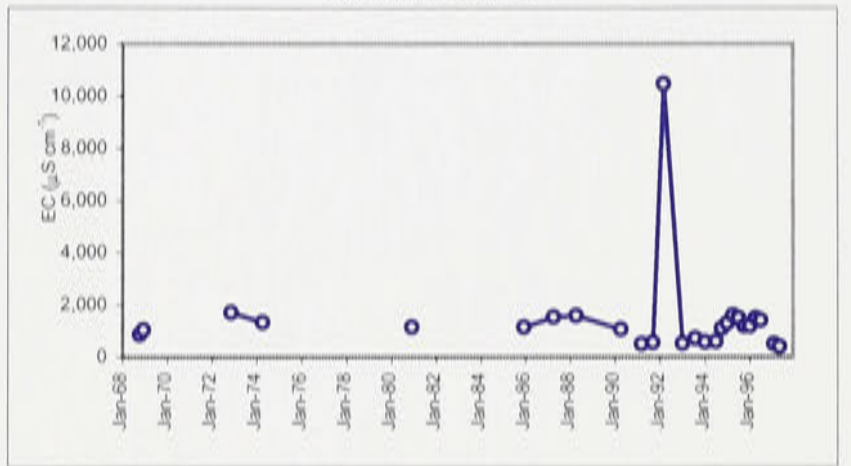
Well no. 36 P



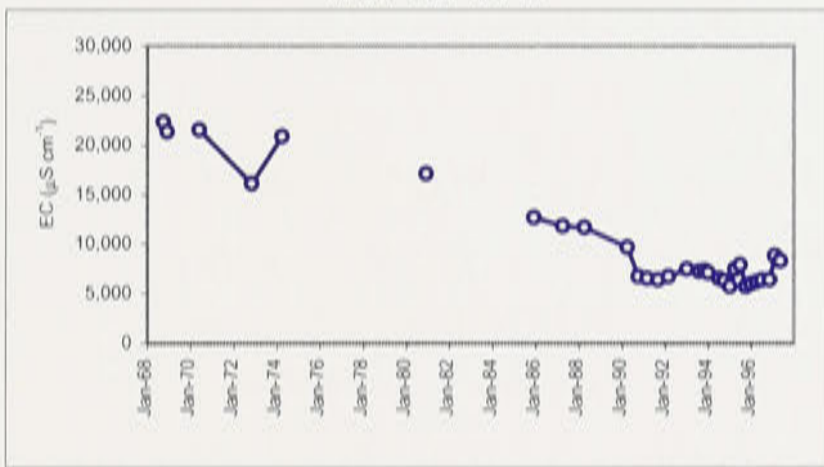
Well no. 40 P



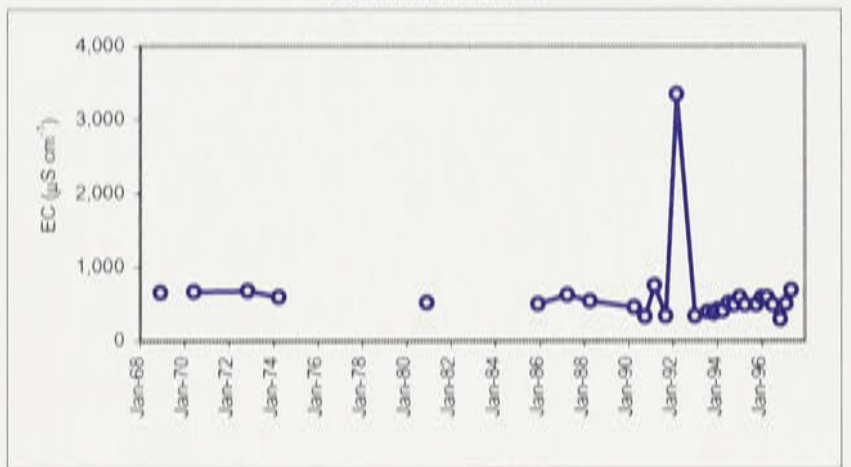
Well no. 43 P



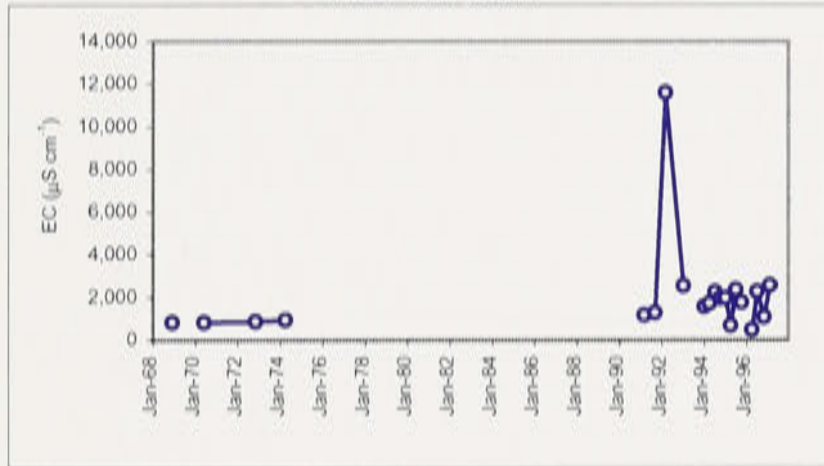
Well no. 47 P



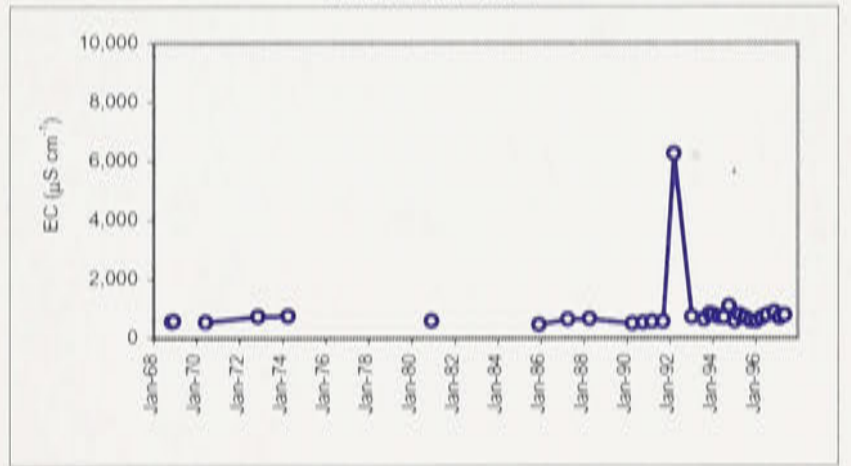
Well no. 51 P



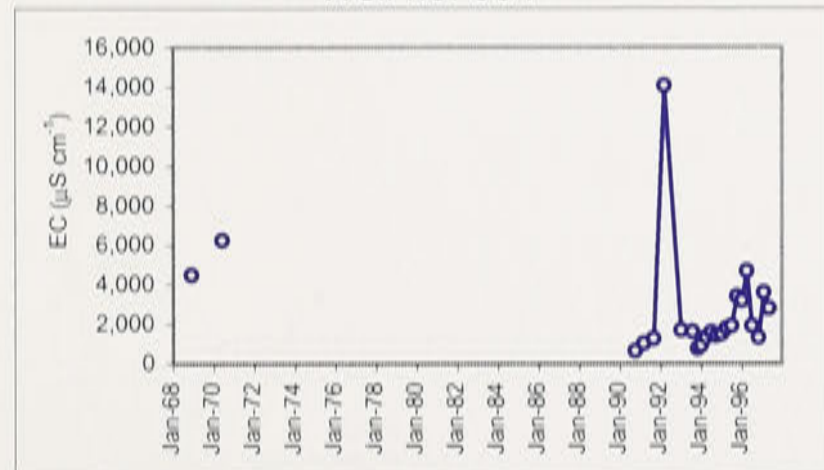
Well no. 53 P



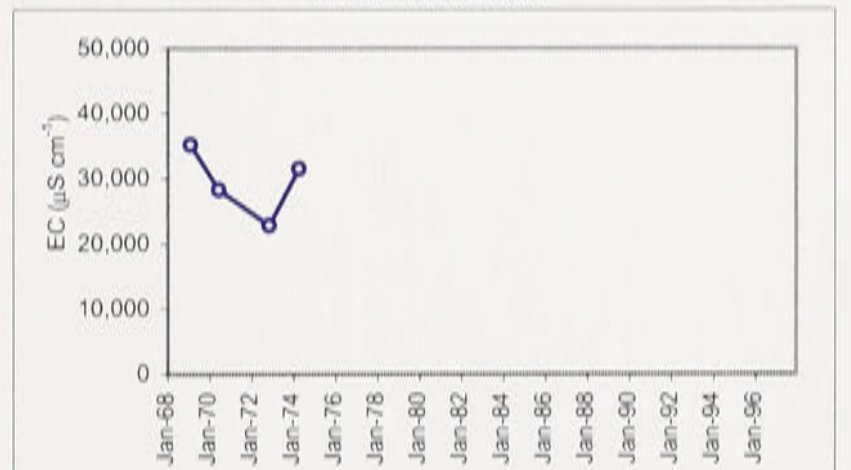
Well no. 58 P



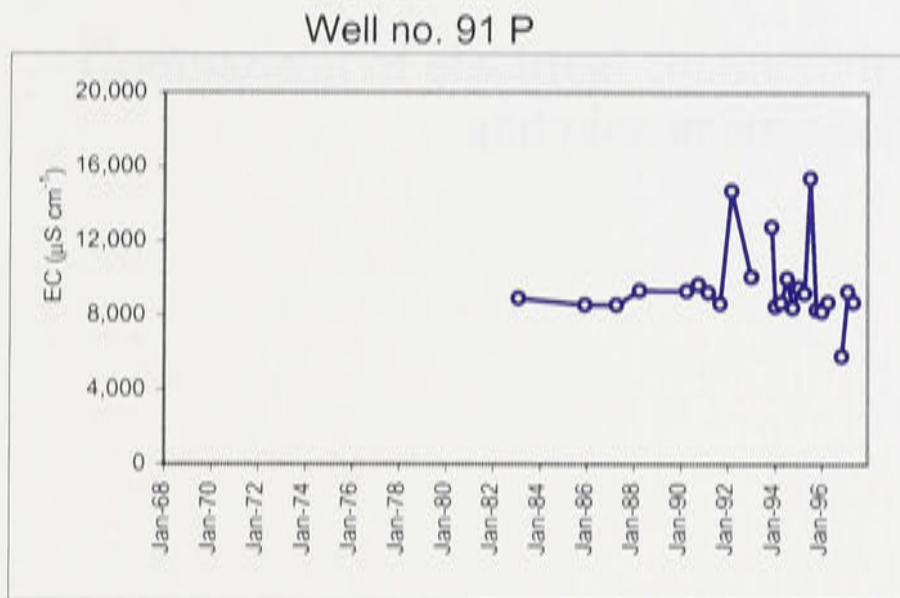
Well no. 60 P



Well no. 65A P



Appendix H: Continued.



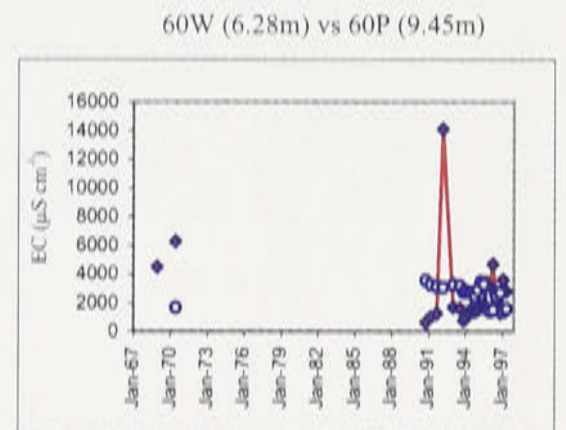
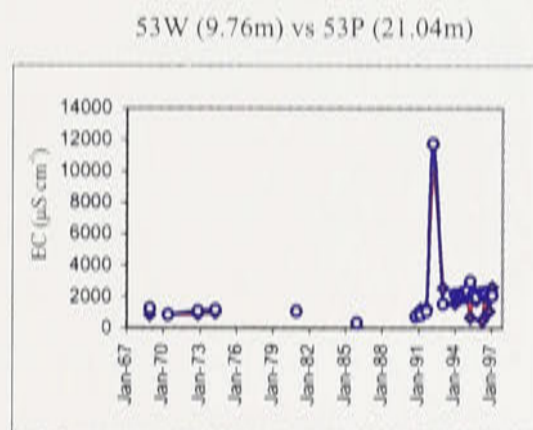
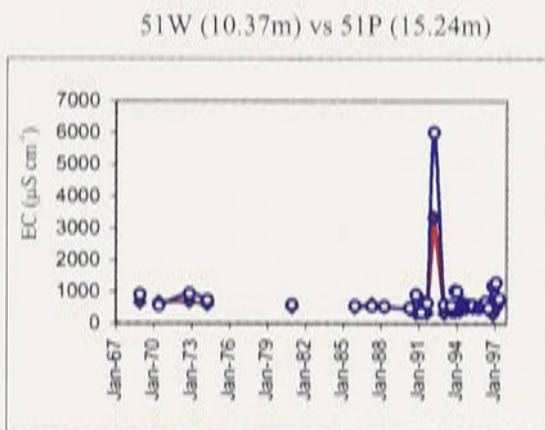
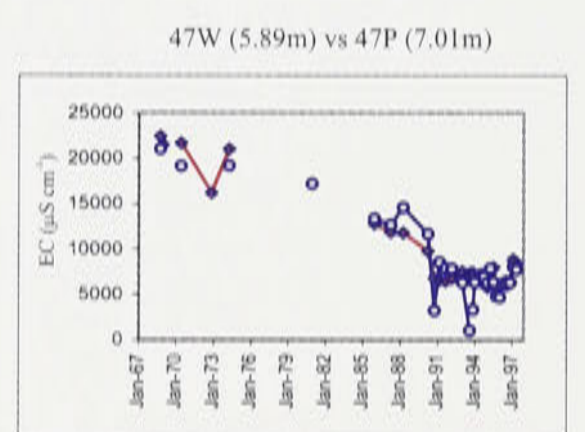
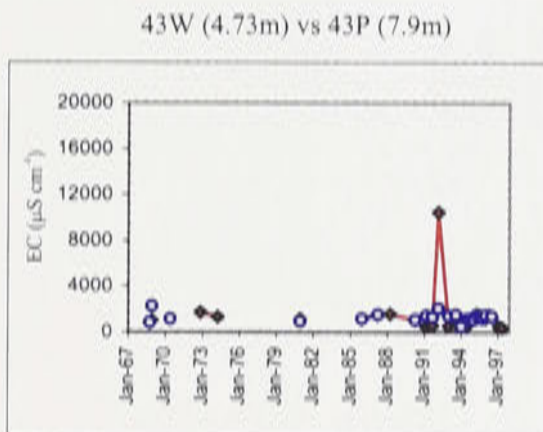
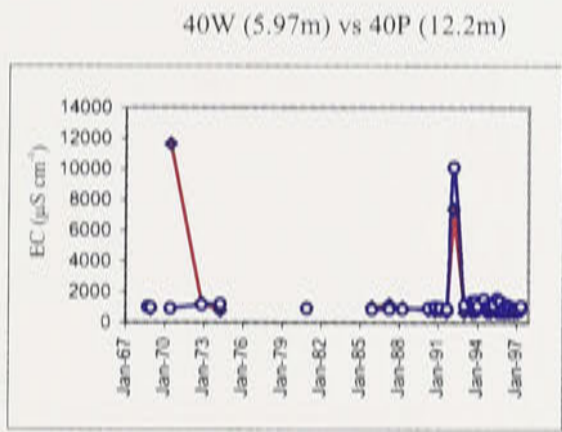
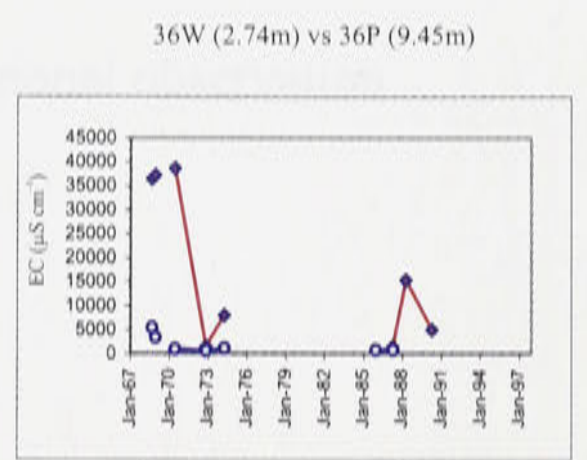
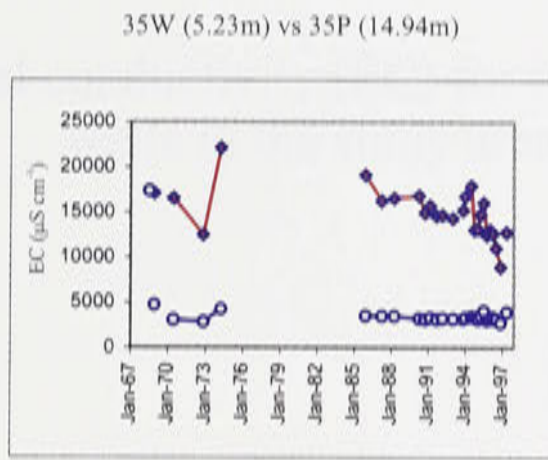
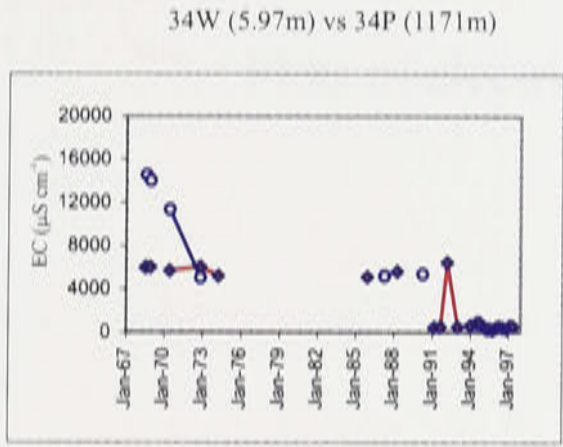
Appendix I

Comparison of electrical conductivity (EC) values between watertable and piezometric wells at the JWPID

Appendix I: Comparison of electrical conductivity (EC) values between watertable and piezometric wells in the study area.



Appendix I: Continued.

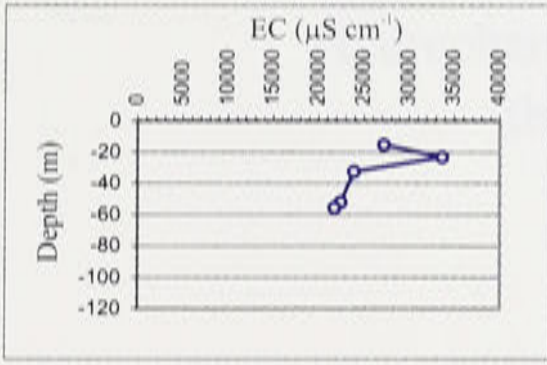


Appendix J

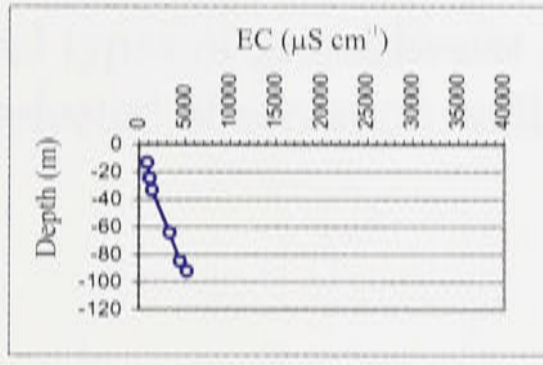
Plots of electrical conductivity (EC) for regional observation wells in the study area

Appendix J: Continued.

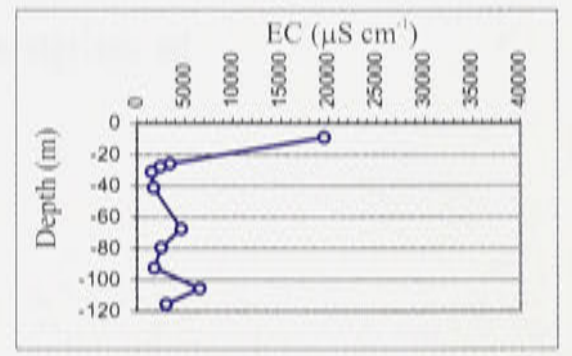
Well 21276



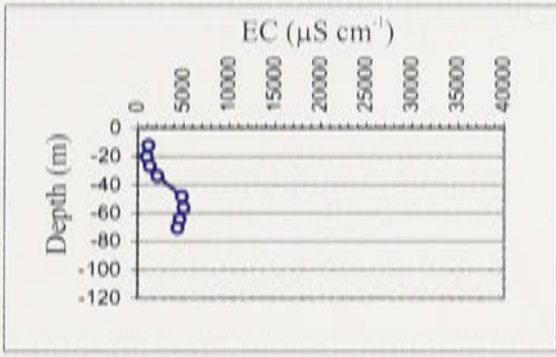
Well 25030



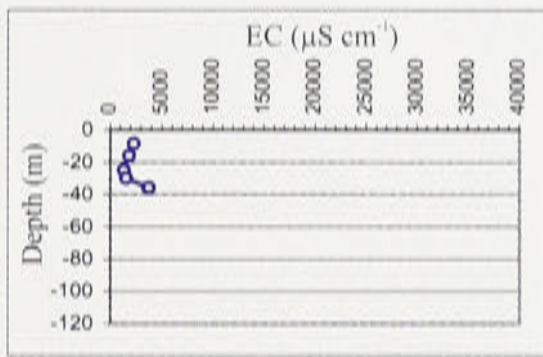
Well 25067



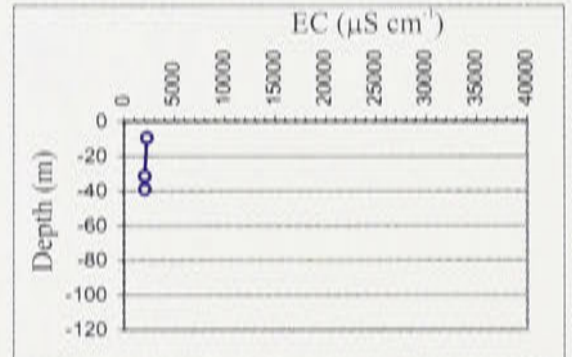
Well 25081



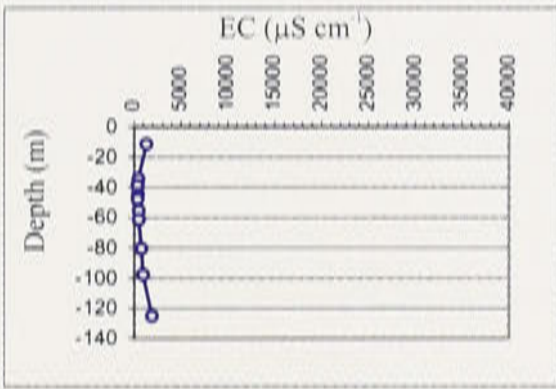
Well 25082



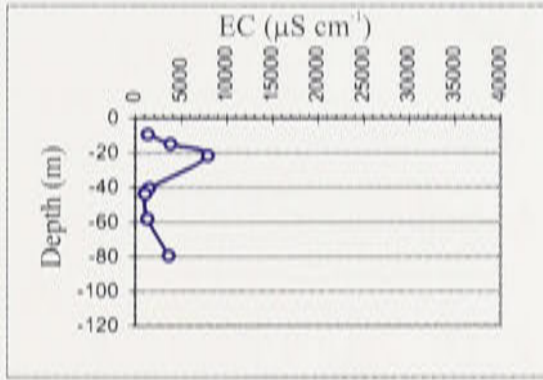
Well 25102



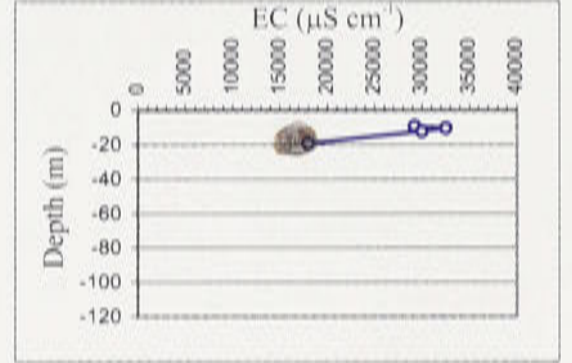
Well 25151



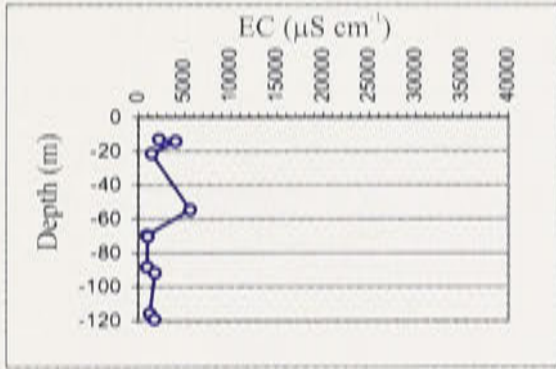
Well 25155



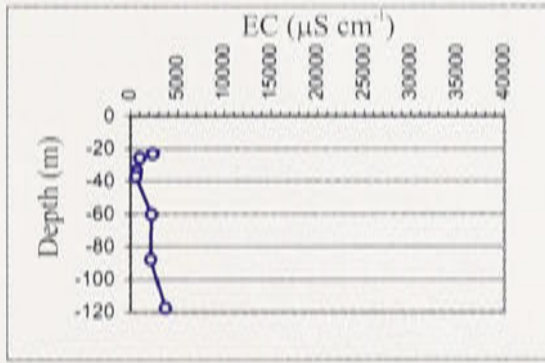
Well 25163



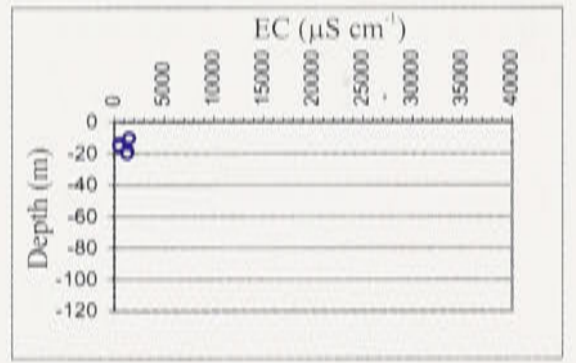
Well 25164



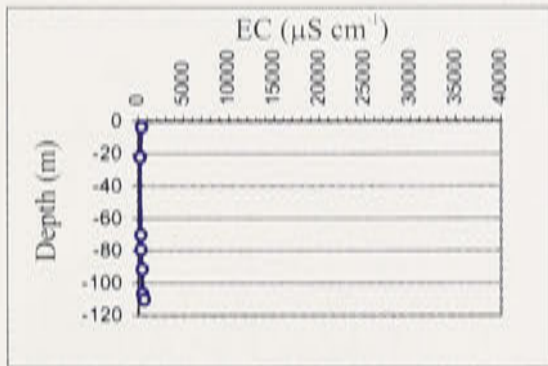
Well 25165



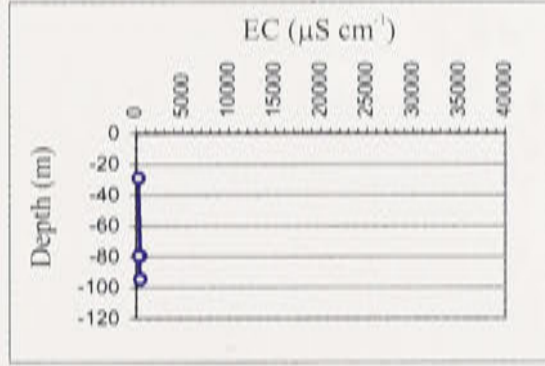
Well 25168



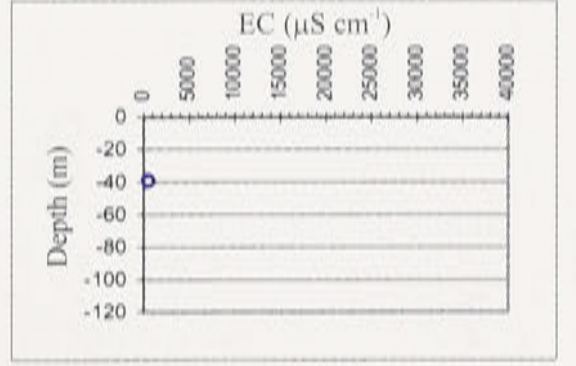
Well 36079



Well 36081



Well 36085



Appendix K

Hydrochemical types of groundwater samples at the selected observation wells.

Well No.	Sample No.	Ca	Mg	Na+K	Cl	SO ₄	CO ₃ +HCO ₃	Total Hardness	Hydrochemical Type
2004	210	28	12	57	12	10	21	103	Ca-Mg-Cl-SO ₄
2005	211	25	10	55	10	10	20	100	Ca-Mg-Cl-SO ₄
2006	212	24	11	56	11	11	21	104	Ca-Mg-Cl-SO ₄
2007	1001	25	10	55	10	10	20	100	Ca-Mg-Cl-SO ₄
2008	201	22	9	53	9	9	18	91	Ca-Mg-Cl-SO ₄
2009	202	21	8	52	8	8	17	88	Ca-Mg-Cl-SO ₄
2010	203	20	7	51	7	7	16	85	Ca-Mg-Cl-SO ₄
2011	204	19	6	50	6	6	15	82	Ca-Mg-Cl-SO ₄
2012	205	18	5	49	5	5	14	79	Ca-Mg-Cl-SO ₄
2013	206	17	4	48	4	4	13	76	Ca-Mg-Cl-SO ₄
2014	207	16	3	47	3	3	12	73	Ca-Mg-Cl-SO ₄
2015	208	15	2	46	2	2	11	70	Ca-Mg-Cl-SO ₄
2016	209	14	1	45	1	1	10	67	Ca-Mg-Cl-SO ₄
2017	210	13	0	44	0	0	9	64	Ca-Mg-Cl-SO ₄
2018	211	12	0	43	0	0	8	61	Ca-Mg-Cl-SO ₄
2019	212	11	0	42	0	0	7	58	Ca-Mg-Cl-SO ₄
2020	213	10	0	41	0	0	6	55	Ca-Mg-Cl-SO ₄
2021	214	9	0	40	0	0	5	52	Ca-Mg-Cl-SO ₄
2022	215	8	0	39	0	0	4	49	Ca-Mg-Cl-SO ₄
2023	216	7	0	38	0	0	3	46	Ca-Mg-Cl-SO ₄
2024	217	6	0	37	0	0	2	43	Ca-Mg-Cl-SO ₄
2025	218	5	0	36	0	0	1	40	Ca-Mg-Cl-SO ₄
2026	219	4	0	35	0	0	0	37	Ca-Mg-Cl-SO ₄
2027	220	3	0	34	0	0	0	34	Ca-Mg-Cl-SO ₄
2028	221	2	0	33	0	0	0	31	Ca-Mg-Cl-SO ₄
2029	222	1	0	32	0	0	0	28	Ca-Mg-Cl-SO ₄
2030	223	0	0	31	0	0	0	25	Ca-Mg-Cl-SO ₄
2031	224	0	0	30	0	0	0	22	Ca-Mg-Cl-SO ₄
2032	225	0	0	29	0	0	0	19	Ca-Mg-Cl-SO ₄
2033	226	0	0	28	0	0	0	16	Ca-Mg-Cl-SO ₄
2034	227	0	0	27	0	0	0	13	Ca-Mg-Cl-SO ₄
2035	228	0	0	26	0	0	0	10	Ca-Mg-Cl-SO ₄
2036	229	0	0	25	0	0	0	7	Ca-Mg-Cl-SO ₄
2037	230	0	0	24	0	0	0	4	Ca-Mg-Cl-SO ₄
2038	231	0	0	23	0	0	0	1	Ca-Mg-Cl-SO ₄
2039	232	0	0	22	0	0	0	0	Ca-Mg-Cl-SO ₄
2040	233	0	0	21	0	0	0	0	Ca-Mg-Cl-SO ₄
2041	234	0	0	20	0	0	0	0	Ca-Mg-Cl-SO ₄
2042	235	0	0	19	0	0	0	0	Ca-Mg-Cl-SO ₄
2043	236	0	0	18	0	0	0	0	Ca-Mg-Cl-SO ₄
2044	237	0	0	17	0	0	0	0	Ca-Mg-Cl-SO ₄
2045	238	0	0	16	0	0	0	0	Ca-Mg-Cl-SO ₄
2046	239	0	0	15	0	0	0	0	Ca-Mg-Cl-SO ₄
2047	240	0	0	14	0	0	0	0	Ca-Mg-Cl-SO ₄
2048	241	0	0	13	0	0	0	0	Ca-Mg-Cl-SO ₄
2049	242	0	0	12	0	0	0	0	Ca-Mg-Cl-SO ₄
2050	243	0	0	11	0	0	0	0	Ca-Mg-Cl-SO ₄
2051	244	0	0	10	0	0	0	0	Ca-Mg-Cl-SO ₄
2052	245	0	0	9	0	0	0	0	Ca-Mg-Cl-SO ₄
2053	246	0	0	8	0	0	0	0	Ca-Mg-Cl-SO ₄
2054	247	0	0	7	0	0	0	0	Ca-Mg-Cl-SO ₄
2055	248	0	0	6	0	0	0	0	Ca-Mg-Cl-SO ₄
2056	249	0	0	5	0	0	0	0	Ca-Mg-Cl-SO ₄
2057	250	0	0	4	0	0	0	0	Ca-Mg-Cl-SO ₄
2058	251	0	0	3	0	0	0	0	Ca-Mg-Cl-SO ₄
2059	252	0	0	2	0	0	0	0	Ca-Mg-Cl-SO ₄
2060	253	0	0	1	0	0	0	0	Ca-Mg-Cl-SO ₄
2061	254	0	0	0	0	0	0	0	Ca-Mg-Cl-SO ₄

Appendix K: Hydrochemical types of groundwater samples at the selected observation wells.

Well no.	Depth (m)	CO ₃ ²⁻	HCO ₃ ⁻	SO ₄ ²⁻	Cl ⁻	Ca ²⁺	Mg ²⁺	Na ⁺	K ⁺	Hydrochemical type
		meq L ⁻¹	meq L ⁻¹	meq L ⁻¹	meq L ⁻¹	meq L ⁻¹	meq L ⁻¹	meq L ⁻¹	meq L ⁻¹	
25030	13.1	0.1	2.6	0.5	3.4	1.6	2.2	3.0	0.1	Na-Mg-Ca-Cl-HCO ₃
25030	31.0	0.0	3.6	2.4	6.2	0.7	1.2	10.3	0.1	Na-Cl-HCO ₃
25030	92.5	0.3	4.5	6.1	27.5	3.3	7.1	26.9	0.3	Na-Cl
25067	41.1	0.1	4.3	3.4	8.1	1.2	2.1	12.5	0.1	Na-Cl-HCO ₃
25067	100.6	0.0	4.8	4.5	19.0	3.5	6.1	17.8	0.2	Na-Mg-Cl
25081	26.5	0.3	4.9	2.7	7.8	1.2	2.1	12.3	0.1	Na-Cl-HCO ₃
25081	70.4	0.0	6.2	9.4	32.2	4.9	9.2	32.2	0.3	Na-Cl
25082	25.0	0.1	4.2	1.1	9.0	0.7	1.2	12.2	0.1	Na-Cl-HCO ₃
25082	57.9	0.0	8.3	25.0	99.5	9.3	27.0	99.2	0.5	Na-Cl
25102	39.0	0.1	4.7	2.0	8.2	1.3	3.1	10.6	0.2	Na-Mg-Cl-HCO ₃
25103	11.5	1.6	9.6	5.3	15.7	0.6	1.6	28.3	0.1	Na-Cl-HCO ₃
25151	10.9	0.2	4.9	2.1	13.5	4.1	4.4	11.5	0.0	Na-Mg-Cl
25151	82.2	0.0	3.0	0.7	2.0	0.8	1.2	3.6	0.1	Na-Cl-HCO ₃
25155	9.1		4.7	10.2	42.9	6.1	14.5	37.3	4.1	Na-Mg-Cl
25155	77.4	0.0	3.4	4.4	25.4	5.8	10.7	19.7	0.1	Na-Mg-Cl
25163	9.1	0.0	7.5	57.0	375.1	25.5	128.2	305.1	0.8	Na-Mg-Cl
25164	21.3	0.0	4.7	0.4	3.3	0.8	0.9	6.7	0.1	Na-HCO ₃
25164	91.4	0.0	5.3	0.3	5.3	1.1	1.4	8.4	0.2	Na-Cl-HCO ₃
25165	23.8	0.0	3.8	1.8	11.1	2.0	3.7	10.8	0.3	Na-Cl-HCO ₃
25165	110.9	0.0	4.4	6.7	33.8	8.4	12.7	26.6	0.2	Na-Mg-Cl
36079	22.0	0.0	1.7	0.1	0.2	0.5	0.8	0.6	0.0	Na-Mg-Ca-HCO ₃ -Cl
36079	110.0	0.0	3.7	0.3	2.0	0.8	1.1	4.3	0.0	Na-HCO ₃ -Cl
36080	12.2	0.0	2.3	0.4	2.5	1.3	1.9	2.0	0.1	Mg-Na-Ca-Cl-HCO ₃
36080	60.4	0.0	1.5	0.1	0.5	0.5	0.8	0.7	0.0	Mg-Na-Ca-HCO ₃ -Cl
36081	28.9	0.0	1.7	0.1	0.6	0.7	0.9	0.9	0.0	Mg-Na-Ca-HCO ₃ -Cl
36081	94.5	0.0	2.3	0.5	1.4	0.5	0.8	3.0	0.0	Na-HCO ₃ -Cl
36082	16.8	0.0	1.8	0.9	3.7	1.2	2.0	3.1	0.0	Na-Mg-Cl-HCO ₃
36083	12.8	0.0	2.4	0.3	1.1	0.9	1.2	1.6	0.0	Na-Mg-Ca-HCO ₃
36086	45.7	0.0	2.6	1.4	11.0	2.3	4.2	8.7	0.1	Na-Mg-Cl
36087	30.4	0.0	2.9	0.3	1.3	0.7	1.2	2.5	0.1	Na-Mg-HCO ₃ -Cl
36087	121.0	0.0	4.0	1.9	8.4	1.4	2.5	10.2	0.1	Na-Cl-HCO ₃
36088	85.3	0.0	3.0	0.9	3.9	0.9	1.4	5.5	0.1	Na-Cl-HCO ₃
36089	85.3	0.0	3.5	1.8	8.7	1.8	2.6	9.3	0.1	Na-Cl-HCO ₃
36090	115.2	0.0	3.4	1.4	11.3	1.8	2.7	11.4	0.1	Na-Cl-HCO ₃
36091	20.0	0.0	5.0	2.5	5.8	0.6	1.3	10.7	0.1	Na-Cl-HCO ₃
36521	16.0	0.0	1.7	0.7	4.4	1.0	1.6	3.9	0.0	Na-Mg-Cl-HCO ₃
36521	123.5	0.0	4.5	2.4	16.8	2.7	3.7	15.7	0.1	Na-Cl
36523	10.5	0.0	9.6	42.2	225.3	24.9	83.2	94.7	0.3	Na-Mg-Cl

Table 6.4: (continued).

Appendix K: Continued.

Well no.	Depth (m)	CO ₃ ²⁻	HCO ₃ ⁻	SO ₄ ²⁻	Cl ⁻	Ca ²⁺	Mg ²⁺	Na ⁺	K ⁺	Hydrochemical type
		meq L ⁻¹	meq L ⁻¹	meq L ⁻¹	meq L ⁻¹	meq L ⁻¹	meq L ⁻¹	meq L ⁻¹	meq L ⁻¹	
36523	128.0	0.0	3.9	1.3	12.0	1.5	2.3	13.4	0.0	Na-Cl-HCO ₃
36524	15.0	0.0	2.5	0.2	0.3	0.5	0.6	2.1	0.0	Na-HCO ₃
36526	131.0	0.0	4.5	2.2	13.4	2.5	3.3	15.0	0.1	Na-Cl-HCO ₃
36528	10.0	0.0	18.3	3.0	1.2	0.3	0.6	24.3	0.1	Na-HCO ₃
36551	4.0	0.0	9.7	68.7	326.5	40.2	116.9	269.2	0.3	Na-Mg-Cl
36551	67.0	0.0	2.7	1.7	26.4	4.1	8.2	18.3	0.1	Na-Mg-Cl
36552	32.5	0.0	3.9	10.8	95.6	20.8	44.5	45.2	0.3	Na-Mg-Cl
36552	101.0	0.0	3.1	1.1	10.5	1.4	2.7	9.8	0.1	Na-Cl-HCO ₃
36553	111.0	0.0	3.5	1.4	11.9	1.6	2.4	12.3	0.1	Na-Cl-HCO ₃
36554	12.8	0.0	11.2	25.8	132.2	16.8	41.4	121.2	0.2	Na-Mg-Cl
36554	55.8	0.0	2.2	0.3	1.0	0.4	0.6	2.3	0.1	Na-HCO ₃ -Cl
36563	19.0	0.0	4.7	56.7	390.9	55.8	98.3	280.9	0.4	Na-Mg-Cl
36595	84.7	0.0	3.3	17.4	128.3	16.1	32.1	87.6	0.5	Na-Mg-Cl
36596	85.0	0.0	3.1	2.0	20.8	2.1	3.4	21.2	0.1	Na-Cl
36597	18.0	0.0	2.5	0.7	2.1	0.7	1.1	3.0	0.1	Na-Mg-HCO ₃ -Cl
36597	95.0	0.0	3.6	1.8	13.9	2.1	3.1	13.2	0.1	Na-Cl
36609	106.0	0.0	3.1	1.7	13.2	1.8	2.7	11.8	0.1	Na-Cl
36610	64.0	0.0	1.4	11.2	135.2	21.5	37.9	89.2	0.4	Na-Mg-Cl
36611	106.5	0.0	3.2	1.8	9.7	1.8	2.4	9.2	0.1	Na-Cl-HCO ₃

Source of data: Anderson *et al.* (1993).

Appendix L

Statistical

Statistical indicators for errors

Statistical indicators for errors

Statistical indicators for errors

A. Mean Error

The mean error is defined by the equation

$$\text{Mean Error} = \frac{1}{n} \sum_{i=1}^n (A_{i,obs} - A_{i,est})$$

The mean error may be used to assess the accuracy of the model. A positive mean error indicates that the model tends to over-predict, while a negative mean error indicates that the model tends to under-predict. A mean error of zero indicates that the model is unbiased.

B. Mean Absolute Error

The mean absolute error is defined by the equation

$$\text{Mean Absolute Error} = \frac{1}{n} \sum_{i=1}^n |A_{i,obs} - A_{i,est}|$$

This measure of error is useful for assessing the accuracy of the model. It is less sensitive to outliers than the mean error.

C. Standard Error of the Estimate (SEE)

The standard error of the estimate is defined by the equation

$$SEE = \sqrt{\frac{1}{n-2} \sum_{i=1}^n (A_{i,obs} - A_{i,est})^2}$$

The SEE is a measure of the standard deviation of the residuals. It is a useful indicator of the model's accuracy.

D. Root Mean Squared Error (RMSE)

The root mean squared error is defined by the equation

Appendix L: Statistical Indicators of Errors

Assuming:

h_{obs}	=	observed groundwater head
h_{com}	=	computed groundwater head
n	=	number of observation point

Following statistical indicators can be defined as (Waterloo Hydrogeologic Inc, 2000):

A. Mean Error

The mean error is defined by the equation

$$\text{Mean Error} = \frac{1}{n} \sum_{i=1}^n (h_{com} - h_{obs})_i$$

Note that there may be cases where over-calculated and under-calculated values will negate each other and produce a mean error value close to zero. This can lead to false interpretation of the model calibration.

B. Mean Absolute Error

The mean absolute error is the same as the mean error except the absolute values of each computed and observed head difference, are summed. In other words,

$$\text{Mean Absolute Error} = \frac{1}{n} \sum_{i=1}^n |h_{com} - h_{obs}|_i$$

This measures the magnitude of the deviation of the calibration and therefore provides a better indication of calibration than the mean error.

c. Standard Error of the Estimate (S.E.E.)

The standard error of the estimate is expressed by the equation:

$$S.E.E. = \sqrt{\frac{\sum_{i=1}^n (h_{com} - h_{obs})_i^2}{n - 1} - \frac{\left[\sum_{i=1}^n (h_{com} - h_{obs})_i \right]^2}{n}}$$

The error of the estimate is also commonly referred to as the calibration residual.

D. Root Mean Squared (RMS)

The root mean squared error (RMS) is defined by the equation:

$$RMS = \frac{1}{n} \sqrt{\sum_{i=1}^n (h_{com} - h_{obs})^2}$$

E. Normalised RMS

The normalised root mean squared error is the *RMS* divided by the maximum difference between the computed head and the observed head. In other words,

$$\text{Normalised } RMS = \frac{RMS}{(h_{obs})_{max} - (h_{com})_{min}}$$

Appendix M

Dates and length of timesteps in transient model

Date	Start Date	End Date	Length (Days)
1	1/1/1970	1/1/1970	1
2	1/1/1970	1/1/1970	1
3	1/1/1970	1/1/1970	1
4	1/1/1970	1/1/1970	1
5	1/1/1970	1/1/1970	1
6	1/1/1970	1/1/1970	1
7	1/1/1970	1/1/1970	1
8	1/1/1970	1/1/1970	1
9	1/1/1970	1/1/1970	1
10	1/1/1970	1/1/1970	1
11	1/1/1970	1/1/1970	1
12	1/1/1970	1/1/1970	1
13	1/1/1970	1/1/1970	1
14	1/1/1970	1/1/1970	1
15	1/1/1970	1/1/1970	1
16	1/1/1970	1/1/1970	1
17	1/1/1970	1/1/1970	1
18	1/1/1970	1/1/1970	1
19	1/1/1970	1/1/1970	1
20	1/1/1970	1/1/1970	1
21	1/1/1970	1/1/1970	1
22	1/1/1970	1/1/1970	1
23	1/1/1970	1/1/1970	1
24	1/1/1970	1/1/1970	1
25	1/1/1970	1/1/1970	1
26	1/1/1970	1/1/1970	1
27	1/1/1970	1/1/1970	1
28	1/1/1970	1/1/1970	1
29	1/1/1970	1/1/1970	1
30	1/1/1970	1/1/1970	1
31	1/1/1970	1/1/1970	1
32	1/1/1970	1/1/1970	1
33	1/1/1970	1/1/1970	1
34	1/1/1970	1/1/1970	1
35	1/1/1970	1/1/1970	1
36	1/1/1970	1/1/1970	1
37	1/1/1970	1/1/1970	1
38	1/1/1970	1/1/1970	1
39	1/1/1970	1/1/1970	1
40	1/1/1970	1/1/1970	1
41	1/1/1970	1/1/1970	1
42	1/1/1970	1/1/1970	1
43	1/1/1970	1/1/1970	1
44	1/1/1970	1/1/1970	1
45	1/1/1970	1/1/1970	1
46	1/1/1970	1/1/1970	1
47	1/1/1970	1/1/1970	1
48	1/1/1970	1/1/1970	1
49	1/1/1970	1/1/1970	1
50	1/1/1970	1/1/1970	1
51	1/1/1970	1/1/1970	1
52	1/1/1970	1/1/1970	1
53	1/1/1970	1/1/1970	1
54	1/1/1970	1/1/1970	1
55	1/1/1970	1/1/1970	1
56	1/1/1970	1/1/1970	1
57	1/1/1970	1/1/1970	1
58	1/1/1970	1/1/1970	1
59	1/1/1970	1/1/1970	1
60	1/1/1970	1/1/1970	1
61	1/1/1970	1/1/1970	1
62	1/1/1970	1/1/1970	1
63	1/1/1970	1/1/1970	1
64	1/1/1970	1/1/1970	1
65	1/1/1970	1/1/1970	1
66	1/1/1970	1/1/1970	1
67	1/1/1970	1/1/1970	1
68	1/1/1970	1/1/1970	1
69	1/1/1970	1/1/1970	1
70	1/1/1970	1/1/1970	1
71	1/1/1970	1/1/1970	1
72	1/1/1970	1/1/1970	1
73	1/1/1970	1/1/1970	1
74	1/1/1970	1/1/1970	1
75	1/1/1970	1/1/1970	1
76	1/1/1970	1/1/1970	1
77	1/1/1970	1/1/1970	1
78	1/1/1970	1/1/1970	1
79	1/1/1970	1/1/1970	1
80	1/1/1970	1/1/1970	1
81	1/1/1970	1/1/1970	1
82	1/1/1970	1/1/1970	1
83	1/1/1970	1/1/1970	1
84	1/1/1970	1/1/1970	1
85	1/1/1970	1/1/1970	1
86	1/1/1970	1/1/1970	1
87	1/1/1970	1/1/1970	1
88	1/1/1970	1/1/1970	1
89	1/1/1970	1/1/1970	1
90	1/1/1970	1/1/1970	1
91	1/1/1970	1/1/1970	1
92	1/1/1970	1/1/1970	1
93	1/1/1970	1/1/1970	1
94	1/1/1970	1/1/1970	1
95	1/1/1970	1/1/1970	1
96	1/1/1970	1/1/1970	1
97	1/1/1970	1/1/1970	1
98	1/1/1970	1/1/1970	1
99	1/1/1970	1/1/1970	1
100	1/1/1970	1/1/1970	1

Appendix M: Dates and length of timesteps
in transient model.

Time- step	Stress period		Date	Dura- tion (days)
	Start (days)	End (days)		
1	0	31	May 1988	31
2	31	61	June 1988	30
3	61	92	July 1988	31
4	92	123	Aug 1988	31
5	123	153	Sep 1988	30
6	153	184	Oct 1988	31
7	184	214	Nov 1988	30
8	214	245	Dec 1988	31
9	245	276	Jan 1989	31
10	276	304	Feb 1989	28
11	304	335	Mar 1989	31
12	335	365	Apr 1989	30
13	365	396	May 1989	31
14	396	426	June 1989	30
15	426	457	July 1989	31
16	457	488	Aug 1989	31
17	488	518	Sep 1989	30
18	518	549	Oct 1989	31
19	549	579	Nov 1989	30
20	579	610	Dec 1989	31
21	610	641	Jan 1990	31
22	641	669	Feb 1990	28
23	669	700	Mar 1990	31
24	700	730	Apr 1990	30
25	730	761	May 1990	31
26	761	791	June 1990	30
27	791	822	July 1990	31
28	822	853	Aug 1990	31
29	853	883	Sep 1990	30
30	883	914	Oct 1990	31
31	914	944	Nov 1990	30
32	944	975	Dec 1990	31
33	975	1006	Jan 1991	31
34	1006	1035	Feb 1991	29
35	1035	1066	Mar 1991	31
36	1066	1096	Apr 1991	30
37	1096	1127	May 1991	31
38	1127	1157	June 1991	30
39	1157	1188	July 1991	31
40	1188	1219	Aug 1991	31

Appendix M: Continued.

Time- step	Stress period		Date	Dura- tion (days)
	Start (days)	End (days)		
41	1219	1249	Sep 1991	30
42	1249	1280	Oct 1991	31
43	1280	1310	Nov 1991	30
44	1310	1341	Dec 1991	31
45	1341	1372	Jan 1992	31
46	1372	1400	Feb 1992	28
47	1400	1431	Mar 1992	31
48	1431	1461	Apr 1992	30
49	1461	1492	May 1992	31
50	1492	1522	June 1992	30
51	1522	1553	July 1992	31
52	1553	1584	Aug 1992	31
53	1584	1614	Sep 1992	30
54	1614	1645	Oct 1992	31
55	1645	1675	Nov 1992	30
56	1675	1706	Dec 1992	31
57	1706	1737	Jan 1993	31
58	1737	1765	Feb 1993	28
59	1765	1796	Mar 1993	31
60	1796	1826	Apr 1993	30
61	1826	1857	May 1993	31
62	1857	1887	June 1993	30
63	1887	1918	July 1993	31
64	1918	1949	Aug 1993	31
65	1949	1979	Sep 1993	30
66	1979	2010	Oct 1993	31
67	2010	2040	Nov 1993	30
68	2040	2071	Dec 1993	31
69	2071	2102	Jan 1994	31
70	2102	2130	Feb 1994	28
71	2130	2161	Mar 1994	31
72	2161	2191	Apr 1994	30
73	2191	2222	May 1994	31
74	2222	2252	June 1994	30
75	2252	2283	July 1994	31
76	2283	2314	Aug 1994	31
77	2314	2344	Sep 1994	30
78	2344	2375	Oct 1994	31
79	2375	2405	Nov 1994	30
80	2405	2436	Dec 1994	31

Appendix M: Continued.

Time-step	Stress period		Date	Duration (days)
	Start (days)	End (days)		
81	2436	2467	Jan 1995	31
82	2467	2495	Feb 1995	28
83	2495	2526	Mar 1995	31
84	2526	2556	Apr 1995	30
85	2556	2587	May 1995	31
86	2587	2617	June 1995	30
87	2617	2648	July 1995	31
88	2648	2679	Aug 1995	31
89	2679	2709	Sep 1995	30
90	2709	2740	Oct 1995	31
91	2740	2770	Nov 1995	30
92	2770	2801	Dec 1995	31
93	2801	2832	Jan 1996	31
94	2832	2861	Feb 1996	29
95	2861	2892	Mar 1996	31
96	2892	2922	Apr 1996	30

Appendix M: Continued.

Time-step	Stress period		Date	Duration (days)
	Start (days)	End (days)		
97	2922	2953	May 1996	31
98	2953	2983	June 1996	30
99	2983	3014	July 1996	31
100	3014	3045	Aug 1996	31
101	3045	3075	Sep 1996	30
102	3075	3106	Oct 1996	31
103	3106	3136	Nov 1996	30
104	3136	3167	Dec 1996	31
105	3167	3198	Jan 1997	31
106	3198	3226	Feb 1997	28
107	3226	3257	Mar 1997	31
108	3257	3287	Apr 1997	30
109	3287	3318	May 1997	31
110	3318	3348	June 1997	30
111	3348	3379	July 1997	31

Appendix N

**Groundwater balance of the modelled area
for May 1988 to July 1997**

Year	Month	Recharge (mm)	Discharge (mm)	Evaporation (mm)	Groundwater storage change (mm)	Change in groundwater storage (mm)	Change in groundwater storage (mm)	Change in groundwater storage (mm)	Change in groundwater storage (mm)
1988	May	100.0	120.0	80.0	0.0	0.0	0.0	0.0	0.0
1988	June	150.0	130.0	70.0	0.0	0.0	0.0	0.0	0.0
1988	July	180.0	140.0	60.0	0.0	0.0	0.0	0.0	0.0
1988	Aug	120.0	150.0	50.0	0.0	0.0	0.0	0.0	0.0
1988	Sep	110.0	140.0	40.0	0.0	0.0	0.0	0.0	0.0
1988	Oct	90.0	130.0	30.0	0.0	0.0	0.0	0.0	0.0
1988	Nov	80.0	120.0	20.0	0.0	0.0	0.0	0.0	0.0
1988	Dec	70.0	110.0	10.0	0.0	0.0	0.0	0.0	0.0
1988	Jan	60.0	100.0	0.0	0.0	0.0	0.0	0.0	0.0
1988	Feb	50.0	90.0	0.0	0.0	0.0	0.0	0.0	0.0
1988	Mar	40.0	80.0	0.0	0.0	0.0	0.0	0.0	0.0
1988	Apr	30.0	70.0	0.0	0.0	0.0	0.0	0.0	0.0
1989	May	40.0	60.0	0.0	0.0	0.0	0.0	0.0	0.0
1989	June	50.0	50.0	0.0	0.0	0.0	0.0	0.0	0.0
1989	July	60.0	40.0	0.0	0.0	0.0	0.0	0.0	0.0
1989	Aug	70.0	30.0	0.0	0.0	0.0	0.0	0.0	0.0
1989	Sep	80.0	20.0	0.0	0.0	0.0	0.0	0.0	0.0
1989	Oct	90.0	10.0	0.0	0.0	0.0	0.0	0.0	0.0
1989	Nov	100.0	0.0	0.0	0.0	0.0	0.0	0.0	0.0
1989	Dec	110.0	0.0	0.0	0.0	0.0	0.0	0.0	0.0
1989	Jan	120.0	0.0	0.0	0.0	0.0	0.0	0.0	0.0
1989	Feb	130.0	0.0	0.0	0.0	0.0	0.0	0.0	0.0
1989	Mar	140.0	0.0	0.0	0.0	0.0	0.0	0.0	0.0
1989	Apr	150.0	0.0	0.0	0.0	0.0	0.0	0.0	0.0
1989	May	160.0	0.0	0.0	0.0	0.0	0.0	0.0	0.0
1989	June	170.0	0.0	0.0	0.0	0.0	0.0	0.0	0.0
1989	July	180.0	0.0	0.0	0.0	0.0	0.0	0.0	0.0
1989	Aug	190.0	0.0	0.0	0.0	0.0	0.0	0.0	0.0
1989	Sep	200.0	0.0	0.0	0.0	0.0	0.0	0.0	0.0
1989	Oct	210.0	0.0	0.0	0.0	0.0	0.0	0.0	0.0
1989	Nov	220.0	0.0	0.0	0.0	0.0	0.0	0.0	0.0
1989	Dec	230.0	0.0	0.0	0.0	0.0	0.0	0.0	0.0
1989	Jan	240.0	0.0	0.0	0.0	0.0	0.0	0.0	0.0
1989	Feb	250.0	0.0	0.0	0.0	0.0	0.0	0.0	0.0
1989	Mar	260.0	0.0	0.0	0.0	0.0	0.0	0.0	0.0
1989	Apr	270.0	0.0	0.0	0.0	0.0	0.0	0.0	0.0
1989	May	280.0	0.0	0.0	0.0	0.0	0.0	0.0	0.0
1989	June	290.0	0.0	0.0	0.0	0.0	0.0	0.0	0.0
1989	July	300.0	0.0	0.0	0.0	0.0	0.0	0.0	0.0

Appendix N: Groundwater balance of the modelled area for May 1988 to July 1997.

Time step	Input			Output					Change in storage (10 ³ m ³)	Balance error (10 ³ m ³)
	Const. Head (10 ³ m ³)	Inflow boundary (10 ³ m ³)	Recharge (10 ³ m ³)	Const. Head (10 ³ m ³)	Leakage (10 ³ m ³)	Drainage (10 ³ m ³)	ET (10 ³ m ³)	Outflow boundary (10 ³ m ³)		
1	273.7	28.3	566.2	-138.1	-235.8	-5.7	-40.4	-0.9	447.6	-0.1
2	423.4	27.4	373.8	-85.5	-228.2	-5.4	-51.5	-0.8	453.4	-0.1
3	169.6	28.3	597.9	-230.7	-235.8	-6.9	-70.5	-0.9	251.1	0.0
4	288.4	28.3	159.9	-134.3	-235.8	-7.3	-94.2	-0.9	4.2	0.0
5	162.3	27.4	551.3	-228.1	-228.2	-9.0	-141.8	-0.8	133.3	-0.1
6	395.3	28.3	310.7	-154.5	-235.8	-8.8	-214.4	-0.9	119.9	0.0
7	897.3	27.4	552.0	-52.1	-228.2	-9.3	-376.8	-0.8	809.7	-0.1
8	322.7	28.3	1230.1	-275.4	-235.8	-13.5	-499.3	-0.9	556.4	0.0
9	369.9	28.3	400.8	-205.7	-235.8	-12.4	-388.7	-0.9	-44.4	0.0
10	460.7	25.6	463.9	-98.6	-213.0	-11.1	-380.8	-0.8	246.0	-0.1
11	416.7	28.3	846.4	-138.8	-235.8	-14.0	-446.7	-0.9	455.5	-0.1
12	349.1	27.4	3597.9	-171.3	-228.2	-16.0	-641.6	-0.8	2916.6	0.0
13	248.4	28.3	650.1	-255.6	-235.8	-17.7	-400.3	-0.9	16.8	-0.1
14	258.9	27.4	297.1	-209.7	-228.2	-16.9	-262.9	-0.8	-135.0	-0.1
15	266.6	28.3	287.7	-217.1	-235.8	-17.2	-294.3	-0.9	-182.6	-0.1
16	172.6	28.3	4144.6	-354.0	-235.8	-24.0	-830.4	-0.9	2900.5	0.0
17	235.2	27.4	347.5	-249.7	-228.2	-19.9	-763.1	-0.8	-651.7	0.0
18	295.5	28.3	417.1	-212.3	-235.8	-18.5	-705.1	-0.9	-431.7	0.0
19	299.6	27.4	437.5	-196.6	-228.2	-17.1	-569.0	-0.8	-247.1	0.0
20	343.6	28.3	380.9	-186.0	-235.8	-16.3	-561.6	-0.9	-247.8	0.0
21	396.1	28.3	530.2	-153.7	-235.8	-16.2	-554.5	-0.9	-6.3	-0.1
22	304.9	25.6	656.7	-154.0	-213.0	-15.3	-493.5	-0.8	110.8	-0.1
23	1704.7	28.3	554.4	-0.9	-235.8	-16.4	-877.4	-0.9	1156.1	0.0
24	997.9	27.4	2131.0	-20.6	-216.4	-25.7	-1137.6	-0.8	1755.3	0.1
25	575.9	28.3	10058.6	-115.5	-223.5	-47.0	-3036.2	-0.9	7239.7	0.0
26	326.2	27.4	9734.2	-209.1	-216.3	-63.5	-3784.9	-0.8	5813.2	0.0
27	304.0	28.3	10058.6	-238.2	-223.5	-78.5	-5449.4	-0.9	4400.5	0.0
28	316.5	28.3	10058.6	-239.7	-223.5	-80.7	-8388.7	-0.9	1470.0	0.0
29	482.4	27.4	3704.0	-157.2	-216.3	-72.0	-6979.2	-0.8	-3211.6	0.0
30	362.6	28.3	2906.4	-312.7	-223.5	-67.9	-5469.6	-0.9	-2777.1	-0.1
31	479.3	27.4	238.8	-139.7	-228.2	-51.6	-2519.3	-0.8	-2194.2	0.0
32	581.3	28.3	394.6	-83.3	-235.8	-45.4	-1597.8	-0.9	-958.9	0.0
33	243.4	28.3	417.8	-333.1	-235.8	-39.9	-903.3	-0.9	-823.4	0.0
34	273.5	26.5	312.3	-219.4	-213.0	-33.2	-744.7	-8.4	-606.3	0.0
35	305.6	28.3	450.8	-195.6	-235.8	-32.2	-742.5	-0.9	-422.1	0.0
36	188.2	27.4	411.2	-274.2	-228.2	-28.9	-531.1	-0.8	-436.5	0.0
37	218.9	28.3	409.0	-214.2	-235.8	-28.1	-432.4	-0.9	-255.1	0.0
38	199.1	27.4	455.8	-200.1	-228.2	-27.6	-337.8	-0.8	-112.1	-0.1
39	205.0	28.3	325.5	-207.1	-235.8	-28.7	-386.7	-0.9	-300.2	-0.1
40	128.0	28.3	343.7	-323.6	-235.8	-28.6	-497.8	-0.9	-586.6	-0.1
41	173.9	27.4	429.9	-258.4	-228.2	-26.7	-533.3	-0.8	-416.1	-0.1

Appendix N: Continued.

Time step	Input			Output					Change in storage (10 ³ m ³)	Balance error (10 ³ m ³)
	Const. Head (10 ³ m ³)	Inflow boundary (10 ³ m ³)	Recharge (10 ³ m ³)	Const. Head (10 ³ m ³)	Leakage (10 ³ m ³)	Drainage (10 ³ m ³)	ET (10 ³ m ³)	Outflow boundary (10 ³ m ³)		
42	203.8	28.3	468.5	-228.9	-235.8	-26.2	-599.0	-0.9	-389.9	0.0
43	291.2	27.4	408.5	-142.3	-228.2	-24.3	-581.1	-0.8	-249.6	0.0
44	236.1	28.3	823.2	-174.4	-235.8	-26.7	-665.7	-0.9	-15.6	-0.1
45	639.8	28.3	722.2	-28.4	-235.8	-26.9	-828.5	-0.9	270.0	0.0
46	205.6	25.6	1664.8	-272.1	-213.0	-27.0	-844.0	-0.8	539.2	-0.1
47	887.9	28.3	342.2	-53.7	-235.8	-27.1	-896.7	-0.9	44.4	0.0
48	657.3	27.4	655.1	-82.8	-228.2	-26.1	-838.9	-0.8	163.2	-0.2
49	574.0	28.3	361.3	-99.7	-235.8	-25.6	-568.1	-0.9	33.6	0.0
50	511.2	27.4	182.1	-76.6	-228.2	-23.8	-414.1	-0.8	-22.8	0.0
51	863.2	28.3	236.4	-20.2	-235.8	-24.5	-721.5	-0.9	125.3	-0.1
52	483.0	28.3	588.9	-103.9	-235.8	-26.2	-738.5	-0.9	-4.9	-0.1
53	935.9	27.4	395.8	-14.2	-228.2	-24.2	-1016.8	-0.8	74.8	0.0
54	570.5	28.3	4181.8	-102.7	-235.8	-36.7	-2396.9	-0.9	2007.6	-0.1
55	930.6	27.4	3975.7	-46.4	-228.2	-42.8	-3165.2	-0.8	1450.2	0.1
56	177.2	28.3	1228.6	-721.0	-235.8	-42.8	-1515.9	-0.9	-1082.1	-0.2
57	169.6	28.3	687.1	-488.6	-235.8	-39.4	-1007.4	-0.9	-886.9	0.0
58	335.0	25.6	437.1	-134.7	-213.0	-32.7	-758.3	-0.8	-341.8	0.0
59	109.3	28.3	787.5	-488.0	-235.8	-35.2	-661.8	-0.9	-496.4	-0.1
60	170.1	27.4	376.2	-282.2	-228.2	-30.9	-522.1	-0.8	-490.5	0.0
61	136.7	28.3	549.4	-294.1	-235.8	-30.6	-391.4	-0.9	-238.2	-0.1
62	1475.1	27.4	147.7	0.0	-228.2	-27.4	-495.5	-0.8	898.4	0.0
63	108.1	28.3	884.4	-691.0	-235.8	-32.0	-439.9	-0.9	-378.8	0.1
64	975.1	28.3	73.4	-13.6	-235.8	-29.5	-699.0	-0.9	98.2	-0.1
65	639.3	27.4	5423.2	-107.8	-228.2	-47.2	-2507.9	-0.8	3197.9	0.1
66	459.1	28.3	5779.4	-208.1	-235.8	-58.1	-4033.0	-0.9	1730.9	0.0
67	648.9	27.4	488.2	-111.3	-228.2	-46.5	-2200.4	-0.8	-1422.6	0.0
68	143.2	28.3	501.8	-660.7	-235.8	-42.5	-982.8	-0.9	-1249.2	-0.1
69	219.3	28.3	425.8	-321.3	-235.8	-37.8	-808.4	-0.9	-730.7	0.0
70	184.3	25.6	654.0	-234.8	-213.0	-32.9	-675.7	-0.8	-293.1	-0.1
71	123.2	28.3	683.8	-460.7	-235.8	-35.1	-656.8	-0.9	-553.9	-0.1
72	150.2	27.4	447.9	-336.2	-228.2	-31.7	-501.1	-0.8	-472.6	0.0
73	2627.1	28.3	378.8	0.0	-235.8	-30.4	-1194.9	-0.9	1572.3	0.0
74	20.2	27.4	267.5	-1283.8	-228.2	-27.9	-335.1	-0.8	-1560.7	0.0
75	64.0	28.3	327.7	-633.4	-235.8	-27.1	-350.2	-0.9	-827.2	0.0
76	105.0	28.3	153.6	-415.8	-235.8	-25.6	-384.8	-0.9	-775.9	0.0
77	102.1	27.4	423.2	-427.0	-228.2	-24.1	-460.4	-0.8	-587.8	0.0
78	225.7	28.3	459.8	-185.8	-235.8	-24.2	-512.5	-0.9	-245.4	0.0
79	50.6	27.4	829.6	-553.4	-228.2	-25.2	-545.4	-0.8	-445.3	-0.1
80	104.6	28.3	421.7	-358.4	-235.8	-24.8	-496.3	-0.9	-561.5	0.0
81	62.9	28.3	1839.4	-495.2	-235.8	-31.5	-789.8	-0.9	377.5	0.0

Appendix N: Continued.

Time step	Input			Output					Change in storage (10 ³ m ³)	Balance error (10 ³ m ³)
	Const. Head (10 ³ m ³)	Inflow boundary (10 ³ m ³)	Recharge (10 ³ m ³)	Const. Head (10 ³ m ³)	Leakage (10 ³ m ³)	Drainage (10 ³ m ³)	ET (10 ³ m ³)	Outflow boundary (10 ³ m ³)		
82	87.2	25.6	285.8	-445.5	-213.0	-26.1	-444.1	-0.8	-730.8	0.0
83	139.8	28.3	371.9	-267.9	-235.8	-26.7	-419.3	-0.9	-410.5	0.0
84	544.1	27.4	350.8	-71.2	-228.2	-24.4	-341.6	-0.8	256.2	0.0
85	133.7	28.3	925.0	-270.6	-235.8	-28.4	-327.4	-0.9	224.1	0.0
86	151.5	27.4	503.4	-262.3	-228.2	-27.0	-256.9	-0.8	-92.7	-0.1
87	64.7	28.3	154.3	-590.1	-235.8	-26.6	-271.8	-0.9	-877.8	0.0
88	151.5	28.3	41.7	-226.2	-235.8	-24.6	-331.2	-0.9	-597.1	0.0
89	112.7	27.4	775.2	-305.2	-228.2	-25.4	-423.4	-0.8	-67.7	-0.1
90	120.2	28.3	619.0	-303.9	-235.8	-27.0	-494.9	-0.9	-294.8	-0.1
91	272.8	27.4	487.8	-217.2	-228.2	-25.3	-405.2	-0.8	-88.6	-0.1
92	369.1	28.3	530.8	-232.4	-235.8	-25.4	-454.7	-0.9	-20.8	0.0
93	144.3	28.3	708.8	-444.9	-235.8	-25.5	-480.4	-0.9	-306.0	-0.1
94	125.5	26.5	365.6	-348.2	-220.6	-22.2	-367.1	-0.8	-441.3	0.0
95	181.6	28.3	491.4	-322.1	-235.8	-22.6	-373.5	-0.9	-253.6	0.0
96	308.0	27.4	406.9	-202.8	-228.2	-21.0	-319.1	-0.8	-29.7	0.0
97	201.2	28.3	630.7	-257.9	-235.8	-23.4	-276.2	-0.9	66.2	-0.1
98	190.0	27.4	317.7	-234.0	-228.2	-23.2	-225.0	-0.8	-175.9	-0.1
99	259.0	28.3	581.3	-192.5	-235.8	-26.1	-222.1	-0.9	191.3	0.0
100	283.7	28.3	341.5	-170.1	-235.8	-25.9	-316.6	-0.9	-95.6	-0.1
101	301.7	27.4	470.3	-127.1	-228.2	-24.9	-382.8	-0.8	35.7	-0.1
102	226.2	28.3	1458.6	-189.0	-235.8	-31.4	-623.9	-0.9	632.4	-0.1
103	283.6	27.4	591.8	-125.0	-228.2	-28.7	-506.8	-0.8	13.4	-0.1
104	76.8	28.3	769.2	-525.1	-235.8	-29.1	-494.3	-0.9	-410.6	-0.1
105	148.7	28.3	539.7	-279.5	-235.8	-27.1	-443.8	-0.9	-270.1	0.0
106	66.9	25.6	620.2	-397.4	-213.0	-24.1	-386.9	-0.8	-309.4	-0.1
107	70.1	28.3	453.7	-398.3	-235.8	-24.7	-364.0	-0.9	-471.5	0.0
108	211.6	27.4	381.1	-188.4	-228.2	-22.2	-317.5	-0.8	-137.0	0.0
109	353.4	28.3	576.6	-169.3	-235.8	-23.6	-253.3	-0.9	275.6	-0.1
110	208.9	27.4	303.6	-224.0	-228.2	-23.3	-194.5	-0.8	-130.8	-0.1
111	216.1	28.3	149.5	-222.1	-235.8	-23.3	-215.4	-0.9	-303.5	0.0
Total	38998	3089	126083.5	-27407.8	-25608	-3142	-102267	-94.6	9648.4	
Monthly mean	351.3	27.8	1135.9	-246.9	-230.7	-28.3	-921.3	-0.9	86.9	
Annual mean	4216	334.0	13630.5	-2963.0	-2768.5	-339.6	-11056	-10.2	1043.1	

Appendix O

Volume of recharge components and leakages
through the basement rocks.

Station	Recharge	Leakage	Net	Recharge	Leakage	Net
1	171.0	15.2	155.8	171.0	15.2	155.8
2	188.8	14.7	174.1	188.8	14.7	174.1
3	182.6	15.1	167.5	182.6	15.1	167.5
4	175.0	15.2	159.8	175.0	15.2	159.8
5	182.9	15.2	167.7	182.9	15.2	167.7
6	182.9	15.1	167.8	182.9	15.1	167.8
7	182.9	15.2	167.7	182.9	15.2	167.7
8	182.9	15.2	167.7	182.9	15.2	167.7
9	182.9	15.2	167.7	182.9	15.2	167.7
10	182.9	15.2	167.7	182.9	15.2	167.7
11	182.9	15.2	167.7	182.9	15.2	167.7
12	182.9	15.2	167.7	182.9	15.2	167.7
13	182.9	15.2	167.7	182.9	15.2	167.7
14	182.9	15.2	167.7	182.9	15.2	167.7
15	182.9	15.2	167.7	182.9	15.2	167.7
16	182.9	15.2	167.7	182.9	15.2	167.7
17	182.9	15.2	167.7	182.9	15.2	167.7
18	182.9	15.2	167.7	182.9	15.2	167.7
19	182.9	15.2	167.7	182.9	15.2	167.7
20	182.9	15.2	167.7	182.9	15.2	167.7
21	182.9	15.2	167.7	182.9	15.2	167.7
22	182.9	15.2	167.7	182.9	15.2	167.7
23	182.9	15.2	167.7	182.9	15.2	167.7
24	182.9	15.2	167.7	182.9	15.2	167.7
25	182.9	15.2	167.7	182.9	15.2	167.7
26	182.9	15.2	167.7	182.9	15.2	167.7
27	182.9	15.2	167.7	182.9	15.2	167.7
28	182.9	15.2	167.7	182.9	15.2	167.7
29	182.9	15.2	167.7	182.9	15.2	167.7
30	182.9	15.2	167.7	182.9	15.2	167.7
31	182.9	15.2	167.7	182.9	15.2	167.7
32	182.9	15.2	167.7	182.9	15.2	167.7
33	182.9	15.2	167.7	182.9	15.2	167.7
34	182.9	15.2	167.7	182.9	15.2	167.7
35	182.9	15.2	167.7	182.9	15.2	167.7
36	182.9	15.2	167.7	182.9	15.2	167.7
37	182.9	15.2	167.7	182.9	15.2	167.7
38	182.9	15.2	167.7	182.9	15.2	167.7
39	182.9	15.2	167.7	182.9	15.2	167.7
40	182.9	15.2	167.7	182.9	15.2	167.7
41	182.9	15.2	167.7	182.9	15.2	167.7
42	182.9	15.2	167.7	182.9	15.2	167.7
43	182.9	15.2	167.7	182.9	15.2	167.7

Appendix O: Volume of recharge components and leakages through the basement rocks.

Time-step	Source of recharge (10 ³ m ³)				Leakage through fracture lines A,B and C** (10 ³ m ³)			
	Rain-fall	Irrigation*	Flood-ing	Total	A	B	C	Total
1	291.5	274.7	0.0	566.2	-182.9	-37.2	-15.7	-235.8
2	329.5	44.4	0.0	373.8	-177.0	-36.0	-15.2	-228.2
3	597.9	0.0	0.0	597.9	-182.9	-37.2	-15.7	-235.8
4	159.9	0.0	0.0	159.9	-182.9	-37.2	-15.7	-235.8
5	440.1	65.1	46.0	551.3	-177.0	-36.0	-15.2	-228.2
6	104.5	206.2	0.0	310.7	-182.9	-37.2	-15.7	-235.8
7	308.5	243.6	0.0	552.0	-177.0	-36.0	-15.2	-228.2
8	993.3	236.8	0.0	1230.1	-182.9	-37.2	-15.7	-235.8
9	134.1	266.7	0.0	400.8	-182.9	-37.2	-15.7	-235.8
10	224.5	239.4	0.0	463.9	-165.2	-33.6	-14.2	-213.0
11	573.0	273.4	0.0	846.4	-182.9	-37.2	-15.7	-235.8
12	3378.0	0.0	219.9	3597.9	-177.0	-36.0	-15.2	-228.2
13	506.6	143.5	0.0	650.0	-182.9	-37.2	-15.7	-235.8
14	297.1	0.0	0.0	297.1	-177.0	-36.0	-15.2	-228.2
15	287.6	0.0	0.0	287.6	-182.9	-37.2	-15.7	-235.8
16	3917.4	0.0	227.23	4144.6	-182.9	-37.2	-15.7	-235.8
17	76.7	270.8	0.0	347.5	-177.0	-36.0	-15.2	-228.2
18	109.0	308.1	0.0	417.1	-182.9	-37.2	-15.7	-235.8
19	185.8	251.7	0.0	437.5	-177.0	-36.0	-15.2	-228.2
20	85.7	295.2	0.0	380.9	-182.9	-37.2	-15.7	-235.8
21	235.9	294.2	0.0	530.2	-182.9	-37.2	-15.7	-235.8
22	379.7	277.0	0.0	656.8	-165.2	-33.6	-14.2	-213.0
23	207.1	347.3	0.0	554.4	-182.9	-37.2	-15.7	-235.8
24	1977.1	153.9	0.0	2131.0	-177.0	-36.0	-15.2	-228.2
25	7152.8	0.0	2905.9	10058.7	-182.9	-37.2	-15.7	-235.8
26	6922.1	0.0	2812.2	9734.3	-177.0	-36.0	-15.2	-228.2
27	7152.8	0.0	2905.9	10058.7	-182.9	-37.2	-15.7	-235.8
28	7876.3	0.0	2182.4	10058.7	-182.9	-37.2	-15.7	-235.8
29	2297.0	0.0	1406.3	3704.1	-177.0	-36.0	-15.2	-228.2
30	2383.4	228.6	294.2	2906.4	-182.9	-37.2	-15.7	-235.8
31	89.8	149.0	0.0	238.8	-177.0	-36.0	-15.2	-228.2
32	110.8	283.8	0.0	394.6	-182.9	-37.2	-15.7	-235.8
33	124.6	293.3	0.0	417.8	-182.9	-37.2	-15.7	-235.8
34	43.0	268.6	0.0	311.6	-165.2	-33.6	-14.2	-213.0
35	61.7	389.1	0.0	450.8	-182.9	-37.2	-15.7	-235.8
36	75.9	335.3	0.0	411.2	-177.0	-36.0	-15.2	-228.2
37	91.6	317.3	0.0	409.0	-182.9	-37.2	-15.7	-235.8
38	325.0	130.9	0.0	455.8	-177.0	-36.0	-15.2	-228.2
39	325.5	0.0	0.0	325.5	-182.9	-37.2	-15.7	-235.8
40	343.7	0.0	0.0	343.7	-182.9	-37.2	-15.7	-235.8
41	198.2	203.0	28.7	429.9	-177.0	-36.0	-15.2	-228.2

Appendix O:: Continued.

Time-step	Source of recharge (10 ³ m ³)				Leakage through fracture lines A, B and C** (10 ³ m ³)			
	Rain-fall	Irrigation*	Flood-ing	Total	A	B	C	Total
42	139.1	329.5	0.0	468.5	-182.9	-37.2	-15.7	-235.8
43	140.5	268.0	0.0	408.5	-177.0	-36.0	-15.2	-228.2
44	572.1	251.1	0.0	823.2	-182.9	-37.2	-15.7	-235.8
45	432.7	289.5	0.0	722.2	-182.9	-37.2	-15.7	-235.8
46	15969.3	0.0	95.5	1664.8	-165.2	-33.6	-14.2	-213.0
47	37.4	304.9	0.0	342.3	-182.9	-37.2	-15.7	-235.8
48	360.9	294.2	0.0	655.1	-177.0	-36.0	-15.2	-228.2
49	125.3	236.0	0.0	361.3	-182.9	-37.2	-15.7	-235.8
50	110.3	71.8	0.0	182.1	-177.0	-36.0	-15.2	-228.2
51	236.4	0.0	0.0	236.4	-182.9	-37.2	-15.7	-235.8
52	545.4	43.5	0.0	588.9	-182.9	-37.2	-15.7	-235.8
53	175.6	220.1	0.0	395.8	-177.0	-36.0	-15.2	-228.2
54	3955.5	0.0	226.3	4181.8	-182.9	-37.2	-15.7	-235.8
55	3756.8	0.0	218.9	3975.7	-177.0	-36.0	-15.2	-228.2
56	1062.7	165.8	0.0	1228.6	-182.9	-37.2	-15.7	-235.8
57	449.2	237.9	0.0	687.1	-182.9	-37.2	-15.7	-235.8
58	199.0	238.0	0.0	437.1	-165.2	-33.6	-14.2	-213.0
59	524.9	262.6	0.0	787.5	-182.9	-37.2	-15.7	-235.8
60	68.0	308.2	0.0	376.2	-177.0	-36.0	-15.2	-228.2
61	247.2	302.1	0.0	549.4	-182.9	-37.2	-15.7	-235.8
62	25.4	122.3	0.0	147.7	-177.0	-36.0	-15.2	-228.2
63	801.8	0.0	82.6	884.4	-182.9	-37.2	-15.7	-235.8
64	73.4	0.0	0.0	73.4	-182.9	-37.2	-15.7	-235.8
65	5178.0	0.0	245.3	5423.3	-177.0	-36.0	-15.2	-228.2
66	5526.0	0.0	253.4	5779.4	-182.9	-37.2	-15.7	-235.8
67	250.8	237.4	0.0	488.2	-177.0	-36.0	-15.2	-228.2
68	229.4	272.4	0.0	501.8	-182.9	-37.2	-15.7	-235.8
69	109.7	316.2	0.0	425.8	-182.9	-37.2	-15.7	-235.8
70	404.2	249.7	0.0	654.0	-165.2	-33.6	-14.2	-213.0
71	405.3	278.5	0.0	683.8	-182.9	-37.2	-15.7	-235.8
72	163.3	284.6	0.0	447.9	-177.0	-36.0	-15.2	-228.2
73	91.1	287.7	0.0	378.8	-182.9	-37.2	-15.7	-235.8
74	108.8	158.7	0.0	267.5	-177.0	-36.0	-15.2	-228.2
75	41.4	286.3	0.0	327.7	-182.9	-37.2	-15.7	-235.8
76	45.2	108.4	0.0	153.6	-182.9	-37.2	-15.7	-235.8
77	125.5	297.7	0.0	423.2	-177.0	-36.0	-15.2	-228.2
78	128.8	331.0	0.0	459.8	-182.9	-37.2	-15.7	-235.8
79	552.8	276.8	0.0	829.6	-177.0	-36.0	-15.2	-228.2
80	110.1	311.6	0.0	421.7	-182.9	-37.2	-15.7	-235.8
81	1618.0	221.4	0.0	1839.4	-182.9	-37.2	-15.7	-235.8
82	57.8	227.9	0.0	285.8	-165.2	-33.6	-14.2	-213.0

Appendix O: Continued.

Time-step	Source of recharge				Leakage through fracture lines and C				A,B
	(10 ³ m ³)				(10 ³ m ³)				
	Rain-fall	Irrigation*	Flooding	Total	A	B	C	Total	
83	67.2	304.7	0.0	371.9	-182.9	-37.2	-15.7	-235.8	
84	76.3	274.5	0.0	350.8	-177.0	-36.0	-15.2	-228.2	
85	755.5	169.5	0.0	925.0	-182.9	-37.2	-15.7	-235.8	
86	283.4	220.0	0.0	503.4	-177.0	-36.0	-15.2	-228.2	
87	154.3	0.0	0.0	154.3	-182.9	-37.2	-15.7	-235.8	
88	8.0	33.7	0.0	41.7	-182.9	-37.2	-15.7	-235.8	
89	540.3	234.9	0.0	775.2	-177.0	-36.0	-15.2	-228.2	
90	511.9	107.2	0.0	619.0	-182.9	-37.2	-15.7	-235.8	
91	239.9	247.9	0.0	487.8	-177.0	-36.0	-15.2	-228.2	
92	239.7	291.1	0.0	530.8	-182.9	-37.2	-15.7	-235.8	
93	382.2	326.6	0.0	708.8	-182.9	-37.2	-15.7	-235.8	
94	44.0	321.6	0.0	365.6	-171.1	-34.8	-14.7	-220.6	
95	108.3	383.0	0.0	491.4	-182.9	-37.2	-15.7	-235.8	
96	84.2	322.6	0.0	406.9	-177.0	-36.0	-15.2	-228.2	
97	449.9	180.8	0.0	630.7	-182.9	-37.2	-15.7	-235.8	
98	317.7	0.0	0.0	317.7	-177.0	-36.0	-15.2	-228.2	
99	581.3	0.0	0.0	581.3	-182.9	-37.2	-15.7	-235.8	
100	341.5	0.0	0.0	341.5	-182.9	-37.2	-15.7	-235.8	
101	353.0	117.3	0.0	470.3	-177.0	-36.0	-15.2	-228.2	
102	1241.0	0.0	217.6	1458.6	-182.9	-37.2	-15.7	-235.8	
103	353.6	238.2	0.0	591.8	-177.0	-36.0	-15.2	-228.2	
104	458.1	311.1	0.0	769.2	-182.9	-37.2	-15.7	-235.8	
105	172.3	367.4	0.0	539.7	-182.9	-37.2	-15.7	-235.8	
106	327.5	292.7	0.0	620.2	-165.2	-33.6	-14.2	-213.0	
107	75.4	378.3	0.0	453.7	-182.9	-37.2	-15.7	-235.8	
108	36.7	344.5	0.0	381.1	-177.0	-36.0	-15.2	-228.2	
109	330.2	246.4	0.0	576.6	-182.9	-37.2	-15.7	-235.8	
110	303.6	0.0	0.0	303.6	-177.0	-36.0	-15.2	-228.2	
111	149.5	0.0	0.0	149.5	-182.9	-37.2	-15.7	-235.8	
Total	91116.6	20597	14369	126082	-19930.2	-4053.6	-1709.3	-25693.1	
Monthly mean	820.9	185.6	129.4	1135.9	-179.6	-36.5	-15.4	-231.5	
Annual mean	9850.4	2226.7	1553.4	13630.5	-2154.6	-438.2	-184.8	-2278.0	

* Includes seepage losses along Warroo channel.

** See Figure 8.8 and 8.14 for locations.